Under the Auspices of

Saxon State Ministry of Environment and Agriculture

Uranium Mining and Hydrogeology V

14.9.-18.9.2008 Freiberg / Germany

Broder J. Merkel, Andrea Hasche-Berger
(Editors)

in cooperation with

supported by

Forschungszentrum Dresden Rossendorf

Deutsche Forschungsgemeinschaft DFG


Uranium Mining
and Hydrogeology

Contents

Preface

When, in 1789, the German chemist Martin H. Klaproth investigated an ore found in the small mine „Georg Wagsfort“ close to the town of Johann Georgenstadt he did not suspect that this would be the death sentence for the town. He discovered Uranium from the Pechblende mineral and characterized it as distinct element though he did not obtain it in the pure metallic state. As early as from 1819 on this ore was mined in Johann Georgenstadt for the production of dyes. Roughly two third of the ore produced was used for the famous yellow-green Uranium glass. The great Uranium rush started immediately after World War II and within a few years the town of Johann Georgenstadt and other sites in the Erzgebirge were completely devastated by inconsiderate mining through the UDSSR and the WISMUT SDAG. From 1945 to 1989, more than 231.000 tons of U_3O_8 were mined and produced within a very small area of Saxonia and Thuringia. Only the USA and Canada produced more Uranium than the former GDR during that period. After the Reunification of Germany Uranium mining was stopped and the rehabilitation work started. Nearly 20 years later, in 2008, most of this rehabilitation work is done on the one side and we face a completely new situation with respect to Uranium mining on the other side. While the Uranium price has plummeted at the beginning of the 1990s, a Uranium mining renaissance can be observed recently since prices screwed up for two reasons: highly enriched Uranium from dismantling of nuclear weapons is no longer available for “diluting” by means of depleted uranium stored as UF_6 and an increased demand of nuclear fuel due to newly built nuclear power plants in China, India, and other parts of the world.

Therefore the impact of Uranium mining and milling on the environment and in particular on water is still an important issue. Additionally, the intensive use of Phosphate fertilizers containing significant amounts of Uranium and the combustion of coal and oil emits Uranium into the environment.

Although Uranium is an element which was investigated thoroughly during the last six decades we still face enormous gaps in knowledge with respect to the chemical toxicology of Uranium and its behavior in environmental compartments at trace concentrations in particular at the water-rock interface and its interaction with biomass. Thus the fifth International Conference Uranium Mining and Hydrogeology (UMH V) at Freiberg is an excellent opportunity for scientists and engineers to exchange experiences and new scientific results as have been the conferences in 1995, 1998, 2002, and 2005.

Freiberg, September 2008

Broder J. Merkel
Technische Universität Bergakademie Freiberg (TUBAF)


Uranium Mining
and Hydrogeology

Foreword by the Saxon State Minister for Environment and Agriculture

The uranium mining legacy has for decades marked both the landscape and the economy of whole regions in the Erzgebirge mountains. The rehabilitation of the former uranium mining areas is among the most demanding environmental tasks in Saxony and a complex challenge for specialists as well as for authorities. New paths were explored on the search for suitable rehabilitation solutions in the densely populated Erzgebirge regions. New ways had to be found for constructive cooperation of all parties involved. Today, we can say that this has been successful. The rehabilitation measures have progressed far and are a major economic factor now.

This year's conference continues the series of international conferences on uranium mining held by TU Bergakademie Freiberg already in 1995, 1998, 2002, and 2005. The exchanges of knowledge and experience during the past conferences contributed a lot to the decisions finally made by the environmental authorities. UMH V is again focused on crucial issues, such as the long-term performance of land reclamation and renaturation in former uranium mining areas, which is of topical interest after the good progress made in the rehabilitation of the sites of Wismut corporation.

The specialist discussions and talks will surely contribute to expand the already well established international network of science, economy and administration.

Since 2005, due to the international boom and rush for uranium as a raw material for energy, there has been the trend to re-open closed uranium mines or to develop new mines worldwide. The same is true for Saxony where we see more and more interest in new mining activities, although they are not directed to uranium, but to other raw materials such as fluorspar, tin or nickel ore. In the light of the higher radioactive background, natural radionuclides must be taken into account for environmental considerations of mining. Therefore, both the environmental authorities and the site operators face new challenges of how to minimise new contaminations. So it is of topical interest to find best possible solutions for preventing deleterious impacts on the environment.

For your conference, I wish you inspiring discussions and a wealth of forward-looking ideas and thoughts that prove useful in your future scientific, economic and administrative work, as well as a pleasant stay in the mining town of Freiberg.

Freiberg, September 2008

Frank Kupfer
Saxon State Minister for Environment and Agriculture


Uranium Mining
and Hydrogeology

Foreword by the President of the Saxon Mining Authority

Uranium mining had been started by the Sowjet Union´s secret service NKWD immediately after the Word War II in 1946. Until reunification the GDR was the largest uranium producer of the eastern bloc countries and the world's third largest producer after the USA and Canada. The Sowjetisch-Deutsche Aktiengesellschaft (SDAG) Wismut Corporation was solely responsible for production, concentrated especially in the districts of Aue, Erzgebirge 60 km from here, Königstein, Elbsandsteingebirge 70 km from here and Ronneburg, Thuringia 100 km from here. In Hartenstein, Erzgebirge, uranium ore was mined at a depth of over 1,800 m, and with rock temperatures of 67 oC complex air refrigeration was required. In Königstein in the Elbsandsteingebirge, after a conventional setting up of the mine drift, the ore was solution mined. With the aid of sulphuric acid the uranium was separated from the sandstone, which had previously undergone gigantic disintegration blasts to impact a higher permeability. The Thuringian Lichtenberg open pit mine had very steep slopes ad was about. 200 m deep. The uranium which was mined by 45,000 permanent employees was till the end of the GDR delivered exclusively to the Soviet Union. About 231,000 t uranium metal had been produced until 1990.

After reunification, the Soviet Union pulled completely (via treaty) out of the enterprise, and the Federal Republic of Germany took over the Wismut. Since the end of 1991 the Wismut GmbH, as well as outsourcing and privatising former company divisions, is carrying out the scheduled closure, reorganisation and recultivation of the former works with a current workforce of round about 2000. Total estimated costs will be € 6.5 billion. One side-effect of disposing of the sulphuric acid out of the mine drift in Königstein is that the Wismut GmbH produced 30 t. uranium in (2004), a small contribution to supply.

The world market for uranium is a US Dollar-quoted spot market, which had remained stable until 2003. The price for concentrate (Yellow Cake) doubled between March 2003 and November 2004. Reasons for this are considered to be the rise in the price of oil, the weak US Dollar and the CO2 levy. Concomitant to this, stockpiles have been largely exhausted, after production ceased for a period in Canada due to water penetration in an underground mine and in Australia because of a large fire in processing facilities. The price of uranium reached its zenith after the oil crisis in 1979, about twice the current price.

The work to be done includes water treatment, radon management, mine flooding, tailings, land reclamation and remediation, monitoring and more.

Freiberg, September 2008

Glückauf

Professor Reinhard Schmidt
President of the Saxon Mining Authority


Uranium Mining
and Hydrogeology

Uranium ISL Mining Activities at the International Atomic Energy Agency

Jan Slezak

[1] International Atomic Energy Agency, POB 100, Wagramer Strasse 5, A-1400 Vienna, Austria

Abstract. Since the International Atomic Energy Agency's foundation in 1957 the IAEA has had an increasing interest in uranium production cycle issues. The recent activities cover tasks including uranium geology & deposits, uranium resources, production, demand, uranium exploration and uranium mining & milling technologies. All the tasks include environmental issues. In addition, many training courses (also on ISL topics) have been organised and are being prepared. In the past 15 years a lot of emphases have been put on the uranium ISL mining technology in consequence with a depressed development of new mining operations and an increased interest in lower cost operations. Several technical meetings and consultancies were organised and led to publishing of an IAEA technical document (TECDOC-1239) Manual on Acid In Situ Leach Uranium Mining Technology.

Introduction

This paper has been prepared to provide basic information on the activities of the Raw Materials for Nuclear Fuel Cycle Unit of the Nuclear Fuel Cycle and Materials Section of the Division of Nuclear Fuel Cycle and Waste Technology of IAEA and to focus on the fast developing uranium production technology of in-situ leach mining.

The material includes some historical background on meetings held, publications, technical cooperation activities, research and other activities.

Background of the IAEA activities in the field of uranium production cycle

Since its foundation in 1957 the IAEA has had an interest in activities related to uranium geology, exploration and production. The very first expert in uranium prospecting was sent to Myanmar in 1959. In the early years all activities related to uranium were carried out by one professional. From 1968 onwards the staff of the section grew slowly to a peak level of more than six professionals during the 1981-3 period. In the past 15 years the staff has declined to 2.4 and to the lowest number of 1.2 in 2006. The number for 2008 is expected to be 1.8. The present staff covers the fields of uranium geology, exploration, development, mining and ore processing. It also covers many aspects of technical cooperation projects.

Various mechanisms have been developed over the years to fulfil the Agency´s role of gathering and disseminating information on the above mentioned subjects. Amongst these are symposia, technical meetings, consultancy meetings, Training events, technical cooperation and publications. Some of these will be discussed below.

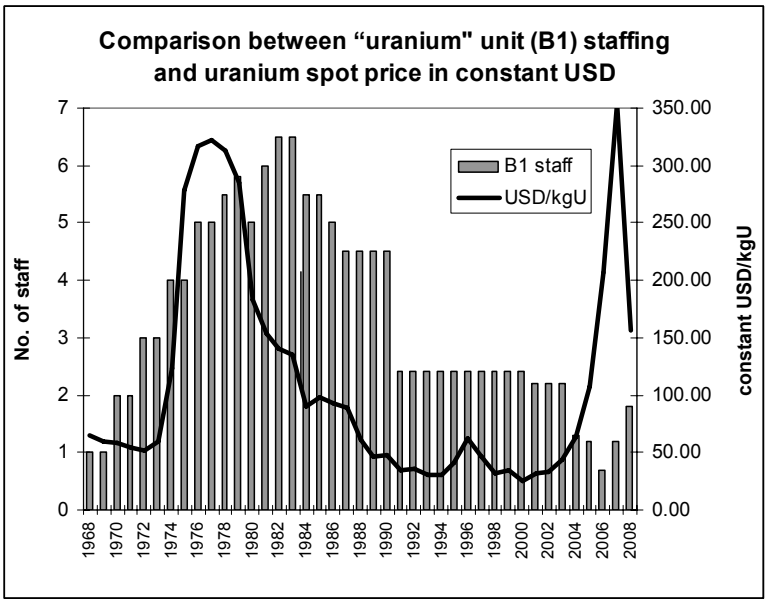

Fig.1. Comparison between “uranium” unit (B1) staffing and uranium spot price in constant USD

Meetings

Several types of meetings have been organized to bring together experts and others interested in various aspects of uranium production cycle activities. These led to important Agency publications before 1990. The first two symposia were: the Athens (Greece) Symposium on the Formation of Uranium Ore Deposits, held in 1974, and the Vienna Symposium on Exploration for Uranium Ore Deposits, in 1976.

Since 2000 two further symposia were organised. The third on the Uranium Production Cycle and the Environment held in Vienna in October 2000 and the fourth one on the Uranium Production Cycle and Raw Materials for the Nuclear Fuel Cycle – Supply and Demand, Economics, the Environment and Energy Security held in Vienna, in June 2005. The fifth symposium "Uranium Production Cycle and Raw Materials for the Nuclear Fuel Cycle" is being prepared for June 2009 in Vienna.

Technical Meetings (TM) and Consultancy Meetings or Consultancies (CS) are other tools used to define, discuss and prepare materials to serve the Member States. Technical Meetings are somewhat larger gatherings of interested participants nominated and financed by their Governments to consider topics of mutual interest. Consultancies are comprised of several (three to six) specialists called by and financed either by the Agency or cost-free, sent by the companies/governments to make recommendations on a particular topic and/or to prepare a document on the topic for publication. A list of recent IAEA TM is provided in Table 1.

Table 1. The Recent IAEA Technical Meetings on the Uranium Production Cycle Topics.

Title	Dates	Venue
Aerial And Ground Geophysical Techniques For Uranium Exploration and Advanced Mining And Milling Methods and Equipment	20-24 March 2006	Singbhum, India
In-Situ Leaching of Uranium Deposits	30 August-1 September 2006	Almaty, Kazakhstan
Uranium Exploration, Mining, Production, Mine Remediation and Environmental Issues	2 - 6 October 2006	Mendoza, Argentina
Uranium Small-Scale and Special Mining and Processing Technologies	19–22 June 2007	VIC, Vienna, Austria
Uranium Exploration, Mining, Production, Mine Remediation and Environmental Issues	1-5 October 2007	Swakopmund, Namibia
Recent Developments in Uranium Exploration, Resources, Production and Demand	1–2 November 2007	VIC, Vienna, Austria
The Implementation of Sustainable Global Best Practices in Uranium Mining and Processing	15–17 October 2008	VIC, Vienna, Austria
Uranium Exploration and Mining Methods	17–20 November 2008	Amman, Jordan

Training events

Training is another tool serving the Member States in spreading information, knowledge and experience. Training events have been held on a variety of topics related to uranium exploration and development since the first, on Uranium Prospecting and Evaluation, which was held in Argentina in 1969. Training events may be regional or inter-regional in scope. They are usually held in an appropriate host country able to provide adequate facilities and some of the teaching staff. Additional course lecturers and facilities are brought by the IAEA to complete the arrangements. Courses are usually of variable duration, providing time for in-depth coverage of the topic and extensive interchange between participants and staff. Participation of selected students has been financed by the IAEA. One of the most extensive and a very useful training programme for young geoscientists was realised in 1990s in Canada and the USA. A list of training courses in uranium production cycle topics is in Table 2. Recently only short-term training events have been provided through the Technical Cooperation programme, typically one week..

Table 2. The IAEA Training Courses on the Uranium Production Cycle Topics

Title	Year	Host country	Region
Uranium Exploration and Evaluation	1969	Argentina	Latin America
Uranium Ore Analysis	1970	Interregional	Spain
Uranium Exploration and Evaluation	1974	India	Asia
Geochemical prospecting for Uranium	1975	Austria	Interregional
Geochemical prospecting for Uranium	1977	Yugoslavia	Interregional
Uranium Exploration and Evaluation	1978	USA	Interregional
Uranium Exploration Methods	1981	Bolivia	Latin America
Uranium Ore Processing	1981	Yugoslavia	Interregional
Uranium Exploration Methods	1982	Madagascar	Interregional
Uranium Deposit Evaluation	1983	Yugoslavia	Interregional
Uranium Ore Processing	1983	Spain	Interregional
Processing of Uranium – from Mining to Fuel Fabrication	1984	France	Interregional
Exploration Drilling and Ore reserves Estimation	1985	Brazil	Interregional
Exploration Drilling and Ore reserves Estimation	1991	India	Asia
Computerized databases in Mineral Exploration and Development	1993	Zambia	Africa
Spatial Data Integration for Uranium Exploration, Resource Assessment and Environmental Studies	1993	China	Asia
Uranium Mining: Its Operation, Safety and Environmental Aspects	1995	France	Middle East& Asia
Uranium In Situ Leaching: Its Planning, Operation and Restoration	1998	USA	Interregional
Uranium Geology, Exploration and Environment	**1990s**	**Canada**	**Interregional**

Technical cooperation

The Technical Cooperation Department of the IAEA helps to transfer nuclear and related technologies for peaceful uses to countries throughout the world. The TC Programme disburses tens of million of USD worth of equipment, services, and training per year in approximately 100 countries and territories which are grouped into four geographic regions. A list of IAEA TC projects on uranium production cycle topics is in Table 3.

Table 3. The Recent and Proposed IAEA TC projects on the Uranium Production Cycle Topics

Country/Region	Title
Argentina	Geology Favourability, Production Feasibility and Environmental Impact Assessment of Uranium Deposits to be Exploited using In Situ Leaching Technology
China	Study of the Key Problems in Prospecting for Sandstone-Type Uranium Deposits and their Amenability to In-Situ Leach (ISL) Mining in the Basins in Northern China
Egypt	Airborne and Ground Gamma-Ray Spectrometry for Radio-element Mapping for Environmental Purposes and for Exploration of Uranium Resources
Pakistan	Uranium geochemistry, mineralogy and host rock uranium deposit description
Latin America	Regional Upgrading of Uranium Exploration, Exploitation and Yellowcake Production Techniques taking Environmental Problems into Account
Algeria	Contribution to the development of activities for the processing of Algerian ores and purification of uranium concentrates
Brazil	Practical guidance tools for nuclear safety analysis of remediation and decommissioning actions of the first uranium ore mining and milling facility in Brazil
China	Techniques And Methods For Optimization Of Uranium Exploration in Both Sedimentary and Volcanic Basins
Egypt	Evaluation of some selected uranium resources in Egypt and production and purification of the yellow cake
Jordan	Uranium exploration
Jordan	Uranium extraction
Africa	Strengthening regional capabilities for uranium mining, milling and regulation of related activities
Venezuela	Exploración de los recursos uraníferos de Venezuela

Publications

The various meetings have led to the publication of a number of volumes of several types. These include Panel Proceedings, Symposium proceedings, Technical Reports and Technical Documents (TECDOCs). In Agency usage the first three of these are "sales publications" and edited while the fourth, the TECDOC is distributed free of charge on request. The Proceedings volumes normally contain the full texts of papers presented at the meeting in the original language with abstracts in English of papers in other languages. Technical Reports are usually guidebooks and manuals and prepared by a group of specialists and are results of Consultancy Meetings. A number of these reports have now been recognized as main references on these subjects. TECDOCs have been used mainly to publish the work of the various working groups on Uranium Production Cycle activities. An example is the TECDOC (IAEA- TECDOC-1239) on "Manual of Acid In Situ Leach Uranium Mining Technology". A list of selected IAEA publications on uranium is presented in Table 4.

Table 4. Some Recent IAEA Publications on the Uranium Production Cycle Topics

Type	Title
IAEA-CSP-10/P, 2002	The Uranium Production Cycle and the Environment. Proceedings of an International Symposium held in Vienna, 2 - 6 October 2000
STI/PUB/1259, 2006	The Uranium Production Cycle and Raw Materials for the Nuclear Fuel Cycle – Supply and Demand, Economics, the Environment and Energy Security, Proceedings series
IAEA-TECDOC-1174, 2000	Methods of Exploitation of Different Types of Uranium Deposits
IAEA-TECDOC-1239, 2001	Manual of Acid In Situ Leach Uranium Mining Technology
IAEA-TECDOC-1244, 2001	Impact of New Environmental and safety Regulations on Uranium Exploration, Mining, Milling and Management of Its Waste
IAEA-TECDOC-1296, 2002	Technologies for the Treatment of Effluents from Uranium Mines, Mills and Tailings
IAEA-TECDOC-1363, 2003	Guidelines for Radioelement Mapping Using Gamma Ray Spectrometry Data,
IAEA-TECDOC-1396, 2004	Recent developments in uranium resources and production with emphasis on in situ leach mining
IAEA-TECDOC-1419, 2004	Treatment of liquid effluent from uranium mines and mills, Report of a CRP 1996-2000
IAEA-TECDOC-1425, 2005	Developments in uranium resources, production, demand and the environment
IAEA-TECDOC-1428, 2005	Guidebook on environmental impact assessment for in situ leach mining projects
IAEA-TECDOC-1463, 2005	Recent developments in uranium exploration, production and environmental issues

Uranium in-situ leach (ISL) mining activity

Conventional mining involves removing ore from the ground, then processing it to remove the minerals being sought. In situ leaching (ISL) involves leaving the ore where it is in the ground and recovering the minerals from it by dissolving them using a leaching solution and pumping the pregnant solution to the surface where the minerals can be recovered from the solution. Consequently there is limited surface disturbance and no tailings or waste rock generated.

Uranium ISL uses the native groundwater in the orebody, which is fortified with a leaching agent and an oxidant. This leaching solution is then injected through the underground orebody to recover the minerals in it by leaching. Once the pregnant solution is returned to the surface, the uranium is recovered in a uranium processing plant using ion exchange resins (or solvent extraction technology).

Basically there are two different chemical concepts used: acid or alkaline. They depend on the ore/host rock composition.

Historically the acid ISL technology has been applied in Ukraine, the Czech Republic, Uzbekistan, Kazakhstan, Bulgaria and recently also in Russia and Australia. The alkaline ISL technology has been used in the USA.

The advantages of this technology are the reduced hazards for the employees from accidents, dust, and radiation; the low cost; no need for large uranium mill tailings and waste rock deposits. The disadvantages are the risk of spreading of leaching solution outside of the uranium deposit, involving subsequent groundwater contamination; the impact of the leaching solution on the rock of the deposit, the limitations of restoration to previous groundwater conditions after completion of the leaching operations.

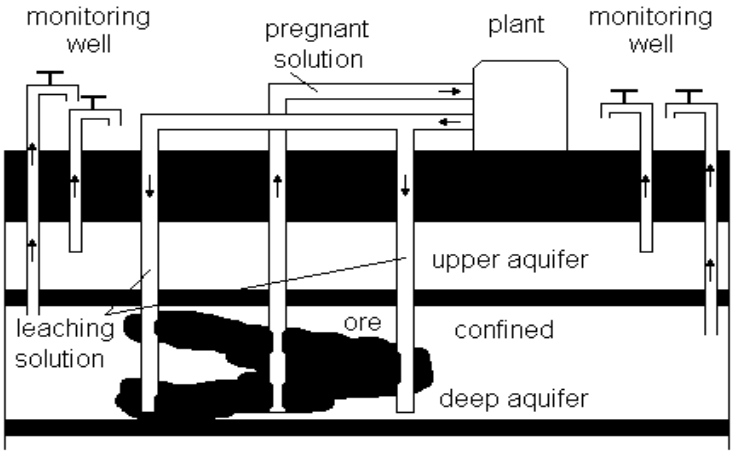

Fig.2. Simplified ISL scheme

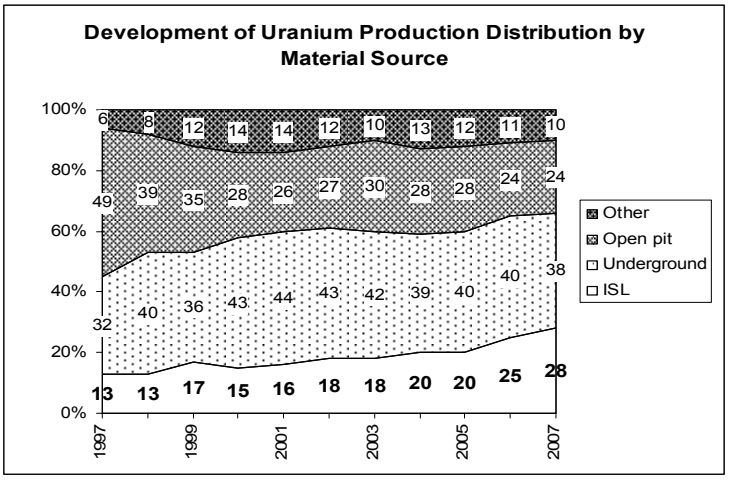

Fig.3. Development of Uranium Production Distribution by Material Source (rounded from sources)

Based on the data presented in the Fig.3., we can easily see that the portion of ISL within all production technologies has doubled in 10 years. Based on the announced and expected development all over the world (mainly Kazakhstan, partially the USA and others) the ratio will continue growing in the near future.

Previous IAEA activities on ISL

Several technical meetings and consultancies have been organized to bring together experts and others interested in ISL mining technology. The very first meeting was organised in Vienna in November 1987. It collected some basic and limited information and experience on this technology and lead to the issue of an IAEA-TECDOC-492 “In Situ Leaching of Uranium: Technical, Environmental and Economic Aspects” in 1989.

The second, much bigger technical meeting was organised in October 1992. Its results are published in an IAEA-TECDOC-720 “Uranium In-Situ Leaching” issued in 1993. The results of the meeting defined a long-term activity on ISL to produce a few documents and to organise some other meetings to document, process and distribute the up-to-date information.

The IAEA-TECDOC-1239 “Manual of Acid In Situ Leach Uranium Mining Technology” issued in 2001 finalised the 7-year long period .

During that period and after, some more documents were produced: An IAEA-TECDOC-979 Environment Impact Assessment for Uranium Mine, Mill and In Situ Leach Projects in 1997, IAEA-TECDOC-1239 “Manual of Acid In Situ Leach Uranium Mining Technology” in 2001, an IAEA-TECDOC-1396 “Recent developments in uranium resources and production with emphasis on in situ leach

mining" in 2004 and an IAEA-TECDOC-1428 "Guidebook on environmental impact assessment for in situ leach mining projects" in 2005.

Different views on ISL

Recently, when looking at the opinions on uranium ISL, we can recognise two, completely different views. One of them is mentioning, that ISL is an environmentally friendly mining method, the other says it is not acceptable at all.

The following chapters give some examples. Many other examples can be found in the literature. Of course, as always, the truth is somewhere between them.

What is ISL mining?

According to the Wyoming Mining Association website, ISL mining is explained in the following manner. (We choose Wyoming because it is the birthplace of "solution mining" as it was originally called.)

"In-situ mining is a noninvasive, **environmentally friendly** mining process involving minimal surface disturbance which extracts uranium from porous sandstone aquifers by reversing the natural processes which deposited the uranium." (Source: http://eziniearticles.com/?What-Is-ISL-Uranium-Mining&id=183880)

An Environmental Critique of In Situ Leach Mining : The Case Against Uranium Solution Mining

The nuclear industry claims that the uranium mining technique of ISL is "a controllable, safe, and environmentally benign method of mining which can operate under strict environmental controls and which often has cost advantages"…..

However, this is simply not borne out by the reality of ISL uranium mines across the world.… The ISL technique is not always controllable, safe, nor environmentally benign, and the hidden costs are usually borne by the underground environment. The process of ISL can lead to permanent contamination of groundwater, which is often used by local people and industries for drinking water supplies, and can also contaminate land which was otherwise good agriculturally productive land. (Source: http://www.sea-us.org.au/isl/islsuks.html)

Future IAEA activities in ISL

Based on what has been shown above, a lot of work has to be done to find answers to questions raised about the ISL technology and to show, that the proper use of this technology in proper conditions and under proper management can give results, which will be acceptable for all involved parties. This is the reason why several activities on ISL are being performed or planned.

The first of them is a preparation of a new IAEA publication on ISL. This publication should include available descriptions (case histories) of all past and present ISL operations, including recent developments in this method.

After this a new coordinated research programme on optimisation of "In Situ Leach (ISL) Mining Technology" to ensure environmentally sound, economic and reliable operations was defined for 2009-11. The ISL technology is relatively new (some 45 years old) and is emerging as an attractive option for permeable sandstone - hosted ore bodies, particularly in the present context when the uranium price is growing. ISL technology has so far been used to depths of 500 m. However, some of the prospective uranium ore bodies are located deeper for which the technology of ISL mining needs to be optimised. Environmental issues and containment of radioactivity, reliability and economics are the major challenges.

Conclusions

Uranium production is expanding, ISL particularly. Besides countries experienced in uranium production, some new countries are involved in uranium exploration and are planning to produce uranium. This requires huge increase in resources (mainly human & financial). There is a very quickly increasing demand from the Member States on information, experience exchange, technical support through the IAEA programmes. All this will require more efforts, broader involvement and closer coordination of all experienced and involved parties (experts, companies, organisations etc.). Quickly developing ISL mining technology will require special attention, because of very controversial experience from the past. Environmental considerations have to become an integral part of any activity in uranium production cycle.

Uranium mining legacies remediation and renaissance development: an international overview

Peter Waggitt

Am Modena Park 12/8, A-1030, Vienna, Austria

Abstract. The uranium mining industry has a record of environmental management that has been very variable over the past 50 years. Although there have been examples of good remediation in some countries, sadly there are many examples of poor or no remediation that remain as a legacy from former times. As the industry is going through a renaissance interest in remediating such legacy sites is increasing significantly. This paper provides a brief overview of some remediation activities at legacy sites in various regions of the world and how international organisations, including the International Atomic Energy Agency, national regulating authorities and the mining companies are working together to address these very important matters in a number of locations.

Introduction

The modern uranium mining industry really began in the late 1940s at a time when there was little thought for protecting the environment. Apart from some laws about protection of water resources there was effectively no environmental protection legislation. As uranium production increased so did the number of locations affected by mining. But in the 1960s there was a decline in activity as major nations fulfilled requirements for weapons programmes. Many uranium mining sites were simply abandoned in these times with no attempt at remediation, thus creating the legacy sites that are still a problem today. Many of these sites have ongoing environmental problems including radiation from discarded tailings and low grade ores or waste rock, or contamination due to seepage from tailings and waste rock, sometimes associated with acid rock drainage from reactive materials.

Concern about these sites and their impacts grew and legislation to control the environmental impacts appeared in many jurisdictions. In Australia, for example,

the Environment Protection (Impact of Proposals) Act came into force in 1974. But these laws were not retroactive, so legacy sites remained untreated.

In the mid 70s the uranium mining industry had a surge of activity meet the demands of a growing nuclear power industry. But not all of these mines were being developed under situations where environmental legislation was applied. In many centrally planned economies of Central Asia, for example, the maintenance of production was all important and environmental and health and safety rules were only a secondary concern at best. As a consequence some of the former legacy sites became larger and new legacies were created in addition.

But the drive for nuclear power stalled and many organisations stockpiled uranium so the demand for new production eased in some quarters. Again sites were abandoned but now there were laws requiring remediation and in some locations such work was done, but only usually where the mining had been recent. Old legacy sites remained untouched for the most part. In Central Asia production continued for some years but as the political tensions eased the strategic need for uranium declined. The result was a large scale closure of mines and processing facilities that now had to compete on the open world market. Few of these mines could achieve the production volumes and efficiencies to do this and so another round of legacy sites was created.

Again the market cycle moved on and in the early days of the 21st century the market for uranium has undergone a renaissance. Uranium production is only about 66% of current market demand. To meet this shortfall` new uranium resources are required and these are being sought all over the world. In many instances developers have turned to former uranium production sites to see if they are likely to be capable of economic production in the new situation. But many of these sites still offer legacy conditions and so in the race for development the need to include legacy remediation has to be borne in mind. For new resources the lessons to be learned from the past must be acknowledged and the creation of new legacies avoided at all costs.

There are many lessons to be learned from the past and this paper sets out some selected examples of good and not so good remediation experiences that the uranium industry should take into account when planning the development and exploitation of resources in this new round of activity.

The history of neglect

Today's legacy problems arose because due to the lack of legislation in earlier times. With no obligation to plan for, or undertake remediation and with no funds having been put aside to carry out the work, remediation did not happen. This last point is a major issue when legacy remediation programmes are discussed or efforts are made to plan work. Mining legacy remediation is a very expensive business, more so when uranium is involved. For example in Germany the cost of remediation of the former uranium mines and associated of the WISMUT company will be about €6.2 billion, a sum of money that few economies could hope to

have available for mine remediation - let alone those recently emerged from years of central planning. Thus, few of the countries most affected by the uranium mine legacy issue have adequate finance or resources and infrastructure in their regulatory networks to plan, develop and manage such programmes. Neither do many of the countries most affected have sufficiently well developed environmental protection laws and resources.

So the diagnosis is one of neglect and lack of resources. The prognosis is not very good at first glance due to the vast amounts of financial support required at a time when there are many other priorities for Governments expenditure in many of the most affected nations. Public health, education and re-building economies are all activities competing for the money available. But all may not be lost if legacy remediation can be incorporated with other development plans.

In today's market this has increased interest in the possibility of re-treating tailings, and perhaps other residues from legacy sites, to extract uranium. A number of proposals are being considered by mining companies and governments in former uranium mining centres around the world. Such plans should only be considered if they are a component of a comprehensive remediation programme. Any new processing scheme should be designed to ensure that the end state of the project will be a remediated site i.e. no new legacy is created.

Case histories

In developing this paper a relatively small number of case histories from around the world were selected to show a cross-section of both the problems being encountered and the solutions being implemented. It will be shown how some options have succeeded and whilst others failed.

Over the past 20 years in Western Europe and North America, there have been significant campaigns undertaking the remediation of uranium mines, especially legacy sites. Such programmes include work at Wismut in Germany, Elliot Lake in Canada, the UMTRA programme in the USA and the work in France at the mines of the Limousin district. All these activities are considered to have had some success and are well been documented in addition to being the main topic of meetings such as those held in Schlema and Gera by Wismut GmbH in 2000 and 2007.

Although uranium mining is a global activity, case histories from only 3 continents are depicted here: Asia, Africa and Australia. There are also legacy sites in Europe and the Americas, both remediated and un-remediated, but space is limited and the histories presented are hopefully some of the more interesting ones.

Case histories from Asia

The former Soviet Union operated a large number of uranium mines throughout Asia, in particular in Kazakhstan, Kyrgyzstan, Tajikistan, Uzbekistan, and Mongo-

lia. Between 1961 and 1995 many of these operations closed down, but rarely was any remediation undertaken, unless sites were close to significant population centres. In Tajikistan for example, the Ghafour waste rock pile, located in an urban area with apartment buildings located less than 50 metres away, was shaped and given a nominal 1 metre soil cover which reduces radon emanation and gamma dose rates considerably; whereas the Degmai tailings repository, located only 2 kilometres from the nearest settlement, has not been covered, has livestock grazing on the pioneer vegetation establishing directly in the tailings and is subject to invasion by persons recovering scrap metal from the tailings.

There appears to have been little or no provision for remediation at many of the former Soviet Union's operations, so there is now no specific funding available to improve the radiological safety situation. The first stage in what is likely to be a long process has been for the International Atomic Energy Agency (IAEA) to provide some suitable equipment and training to enable the local supervising authorities to strengthen their capabilities. In particular to obtain a good set of monitoring and surveillance data to enable authorities to update their characterisation of the wastes contained in the various legacy sites as well as the sites and their surroundings, including ground water. Once obtained, such data will provide a suitable basis for the development of comprehensive remediation plans. Such plans can then be submitted to appropriate funding agencies.

Throughout the four Central Asian countries mentioned above the pattern of abandonment was similar. However, the story since the mid 1990s has differed. Whilst Tajikistan and Kyrgyzstan have no current uranium mining operations, both Uzbekistan and Kazakhstan do. Kazakhstan for example is now the third largest uranium producer in the world and has undertaken a significant amount of remediation work in the former mining areas in the north of the country. Current uranium production in both Kazakhstan and Uzbekistan generally uses in-situ leach technology. Consequently solid waste production is now effectively nil.

Kyrgyzstan had several uranium mining areas, but the sites around Mailuu Suu in the south west of the country have attracted the most attention. In this valley 23 waste rock dumps and 17 tailings piles were left behind with varying degrees of remediation. The relocation of some of these tailings is the focus of a World Bank funded project. Some smaller tailings piles in other parts of Kyrgyzstan have also been remediated e.g. at Kadji Say and Min Kush.

Programmes to plan the remediation and monitoring of these and other sites are in place with assistance from a number of multi-lateral agencies. Again the long term remediation will require considerable finance which is currently beyond the national resources ability to supply.

The area around the former mining and processing site at Taboshar in Tajikistan is another serious example of legacy contamination. Over the years since the abandonment building components and scrap materials have been removed from the site piecemeal to the extent that very little is left that can be easily moved by hand. Much of what is left is in a dangerous state and presents a significant physical safety hazard, and possibly a radiological hazard in some cases. The site is dominated by a pile of yellow process residues (tailings) that are uncontained and continue to erode through wind and rain action. More serious is the use by the lo-

cal population of water contaminated by the seepages as a potable supply and for irrigating food crops. The IAEA, in conjunction with other agencies, is working to improve surveillance and monitoring and to advance plans for remediation.

In Uzbekistan and Kazakhstan the current uranium production operations are aware of their environmental responsibilities and there is a willingness to undertake the monitoring and surveillance that will provide the data necessary for remediation planning. Whilst the current and future operations are looking to provide remediation plans the legacy issues remain to be adequately addressed. A lack of funds for remediation is the major constraint.

In northern Kazakhstan much mine remediation has been done but at sites in the west of the country action much remains to be cleaned up. The centralised tailings storage facility at Stepnogorsk, in the north of the country, remains to be remediated and whilst plans are in hand to deal with this issue, funding remains as the major sticking point.

A similar situation exists in Uzbekistan, which is now the world's seventh largest uranium producer. The former soviet mines were mainly hard rock operations whereas current production is dominated by in-situ leach technology. Some of the former waste rock dumps and mine sites are being remediated but many remain untouched. These materials are at risk of being removed by the local population for use as building materials. The tailings storage facility at Navoi is still used for disposal of gold processing tailings but the uranium mill tailings there still need to be remediated.

In Mongolia, uranium mining was undertaken at Dornod, in the north eastern part of the country. The operation was abandoned in 1995. Since abandonment the railway lines and much of the infrastructure that had been installed to support the mining in a very remote area have been removed.

In 2004 IAEA set up a technical cooperation project to assist in the development of remediation plans for this site. However, by the time field work began in 2006 the renaissance of the uranium market had caused a number of overseas mining companies to begin exploration operations in the vicinity. It now seems likely that these companies will wish to commence uranium mining operations either at new sites or, most likely in the first instance, at the old sites in the Dornod vicinity.

As is commonly the situation in the former Soviet Union states the departure of the original operators has left little experience amongst the staff of regulatory bodies, with no current operations available for these people to observe and learn from, or to help train new personnel. The IAEA is supporting a programme of training and assistance in the development of a suitable regulatory infrastructure

Case histories from Africa

The uranium mining industry has been fairly widespread in Africa with mining taking place in the Saharan region, central Africa, east Africa and in the southern and south western areas. Whilst current operations are making preparations for eventual remediation, the recent renaissance of uranium mining has raised con-

cerns about the creation of new "legacy sites". There are already some legacy sites, in Zambia and the Democratic Republic of Congo for example, but there are also examples of remediation as at Mounana in Gabon.

At Shinkolobwe in the Democratic Republic of Congo (DRC) the uranium mining operation ran from the 1920s until about the mid 1960s when the site was closed out by the operator. There was little remediation and the main structures were left standing, whilst waste rock and tailings piles were abandoned as they stood. The underground workings were sealed off by plugging the shafts with concrete and the open cut was left as it was with some water in the bottom. The site was open to pubic access and many local footpaths criss-cross the site. Since then artisanal miners have returned to the site from time to time. This activity took place most notably in 2003 and 2004 when miners were seeking the cobalt-rich mineral heterogenite, which also contains uranium. Clearly if the current market boom for uranium continues there may well be pressure to re-open the mine on a commercial basis. Should this happen then the issues of managing and remediating the legacy wastes will need to be fully addressed before the new operations start to ensure that both legacy and new waste management will be integrated into a programme that meets international safety standards.

Case histories from Australia

Uranium mining in Australia really became established in the late 1940s with the mine at Rum Jungle. When operations ceased in the 1960s this site was not cleared up. Severe environmental impacts in the nearby Finniss River were blamed on the uranium mine but in fact it was the presence of acid rock drainage from the sulphidic waste rock and the dominance of copper from the poly-metallic ore residues in that seepage that were the main problem. An initial clean up was undertaken by the Federal Government in the 1970s but this was not satisfactory. Thus in 1982 a more comprehensive remediation programme was undertaken. The work has some immediate effects and although it was more than 5 years for the benefits of the work to be fully apparent all seemed to be well. Unfortunately by the late 1990s the performance of the covers in restricting rainfall infiltration had begun to degrade significantly with a consequent increase in acid drainage emissions. Problems also arose with the sustainability of the non-native and agricultural species used for revegetation ands weed invasion was very widespread on the site. A report has been prepared on the need for remedial works. Remediation regarded as a "leading edge technology" solution less than 25 years ago has shown itself to be unsustainable. It should be stressed that much valuable information has been gained from this experience which is being applied to other remediation programmes, in particular in the wet-dry tropics.

The mines of the South Alligator Valley dated from the 1960s when over a few years about 850 t of uranium was produced from 13 small deposits. Again, at the end of the mining work, the sites were abandoned. In the late 1980s the area was incorporated into Kakadu National Park (KNP), a World Heritage National Park, and then the land ownership was returned to the Aboriginal Traditional Owners

(TOs). As part of the KNP lease-back agreement the TOs required that the 13 mine sites and any other legacy evidence of mining be remediated before 2015. Various studies were carried out in the period 2001 to 2005 involving extensive consultations with the TOs. This was necessary to ensure that the proposed works not only met required international safety standards, but also did not compromise the traditional values and cultural beliefs of the TOs. Also there were some natural heritage issues to manage, such as not collapsing mine tunnels which had become the habitat for endangered bat species. As always finance was an issue and it was not until 2006 that the Federal Government finally agreed to grant $7 million for the works programme. The design work was completed by early 2007 and the first phase of the remediation at some of the sites was completed before the onset of the rains in November 2007. The balance of the work will be completed over the next year or two. The works are uncomplicated as there are few radiological safety issues and much of the effort will be in relocating scrap material and some process residues from a variety of locations to a single, specifically designed, containment.

The resurgence of the uranium mining industry

Since late 2003 the uranium mining industry has shown an ever increasing level of activity. Today as many as 600 companies worldwide seem to be expressing an interest in the exploration and development of uranium resources. In the "quiet times" since the last boom period of the late 70s the industry had been very stagnant in terms of development. Now exploration and mine development are activities that are increasing significantly on a global scale. Projects in Africa, for example, include one new mine in Namibia and one under construction in Malawi and several prospects e.g. in Namibia, South Africa and Zambia. Much of the exploration has begun at "brownfield sites" many of which could also be classified as legacy sites. Abandoned previously as being uneconomic with low ore grades, several of theses sites now appear to offer the possibility of a quick start up to exploit a known resource which could provide cash income to finance further exploration and development in regions associated with uranium mineralization.

Even the re-treatment of tailings is being actively pursued in some locations, particularly at legacy sites. The economics look good at first glance with the cost of milling already taken care of and uranium market prices staying around $55-60/lb U_3O_8. The danger to the environment is that such new activities may not consider the costs of final remediation in their economic analyses as the sites are already "legacy sites". The authorities must be firm in their resolve and allow developments such as these to proceed only if they result in an overall better situation from the aspects of safety and environmental protection. This will require strong regulatory processes and infrastructure, and adequate resources and, above all, sufficient numbers of trained staff.

This last point is very serious. Whilst the industry was in apparent decline few young people were keen to join as they saw little future in an apparently moribund industry. As a result there are frequently 20 year gaps in the staffing profile of uranium mining activities which now need to be filled very quickly. This applies

to both operators and regulators. For example, radiation protection workers are in short supply everywhere, as are uranium exploration geologists. The boom in uranium mining calls for increased numbers of persons with these skills to work for both regulators and operators. Consequently all sides of the industry need to attract new staff and set up comprehensive training systems. This will help to ensure that there will be continuity when the older generation, many of whom are now retiring, are no longer available to provide the knowledge and experience that the situation is demanding today and into the future.

Where to from here?

The major lesson to be learned from all of these case studies is that where uranium mining activity is being undertaken, on new or re-activated sites, there needs to be a suitable legislative regime in place to deal with all these issues and prevent the creation of new legacy sites. So how should the uranium mining industry stakeholders move forward to deal with legacy issues and the development surge?

The question of how to assess liability for existing environmental impact and how to address requirements for remediation are questions that are testing the regulatory systems worldwide. Obviously the existing legacy of environmental degradation cannot be blamed on new operators; equally new operations should do nothing to worsen the situation. In addition new projects' remediation plans should be required from the outset to incorporate an approach that will assist with the improvement of the existing situation to the greatest extent practicable. These plans must include guarantees for the financial resources required for remediation.

The most important point is to ensure that today's uranium mining industry is not allowed to create any new legacy sites for the future. For example, where former mining sites are re-activated, every effort should be made to incorporate the remediation of any associated legacy sites into the remediation of the current operation, to the maximum extent practicable.

The uranium mining industry is taking up a new lease on life and is now commonly seen as one part of the integrated solution to meet future global energy needs. By providing the fuel for nuclear power plants uranium mining may be seen to be contributing positively to the battle to reduce CO_2 production and, consequently, global warming. This may an important objective, but it must not be allowed to distract any of the industry's stakeholders from their responsibility to ensure that uranium is always mined in an environmentally responsible manner.

Understanding Uranium Migration in Hard Rocks

W. Eberhard Falck[1], David Read[2], S. Black[3], D. Thornley[3], M. Markovaara-Koivisto[3] and M. Siitari-Kauppi[4]

[1] Institute for Energy, JRC, European Commission, Petten, The Netherlands
[2] Enterpris and University of Aberdeen, UK
[3] University of Reading, Whiteknights, Reading, Berks., UK
[4] Helsinki University of Technology, PO Box 6200, FIN-02015 TKK, Finland

Abstract. Uranium is a major radioactive constituent of spent nuclear fuel and high-level radioactive waste. However, its migration behaviour in crystalline rocks is still inadequately understood. This paper describes the results of controlled laboratory migration experiments and attempts made to simulate them using numerical models. Initial models employing generic information in "blind predictions" are progressively enhanced by data-supported interpretation. Such an approach is intended to mimic the stages of a site assessment, where conceptual and numerical models are progressively refined.

Introduction

Geological disposal is the preferred management end-point for high-level waste (HLW) and, in some countries, spent fuel (SF). Safety assessment (SA) procedures are intended to demonstrate that any releases of radionuclides that will almost certainly occur at some time in the future have negligible impact. SA is made up of various components that are designed to represent the behaviour of the repository itself and the surrounding geological environment, and to predict its long-term behaviour. Although a large body of information on alternative rock matrices for disposal and on pertinent processes and events has been accumulated over the past 30 years, several potentially important processes have not yet been adequately characterised. In particular, the micro-scale behaviour of uranium in crystalline rocks remains poorly understood.

In the course of a site assessment, increasingly detailed information is collected in order to construct and refine numerical models. The process of developing numerical models, such as those for the transport and retention of radionuclides, helps to better understand the repository system as a whole and to identify those

processes that need to be known with greater precision. Iterative model development is a powerful tool and helps to target resources for further investigations and research. The current paper illustrates this point using a laboratory microcosm of uranium migration through crystalline rock cores.

At the early stages of an investigation very little may be known about water compositions and the reactions taking place. Blind predictions using sparse data sets challenge the modeller to carefully document the assumptions employed in scenario construction (Read, 1991). Assumptions regarding newly formed secondary phases incorporating the radionuclide of interest will have to be made on the basis of earlier experimental evidence, 'analogues', or literature data. The major adjustable variables, in addition to those governing the hydraulic properties, are the nature of solubility-controlling solid phases. The model is refined step-by-step with experimental data, thus arriving at a more realistic input-output estimate. The latter may include estimates of reaction kinetics and assumptions regarding 'active' and 'inert' phases. After termination of the actual experiments and analysis of the solids, these results can be compared with the predictions from the model.

Experimental set-up

Two core sections of Syyry granodiorite from Sievi, Finland (49.5 mm diameter and 47.34 mm length) were placed in a triaxial cell (Figure 1). A disc cut from a depleted uranium (DU) penetrator (armour piercing ammunition) was inserted between the two rock slices. The DU is in the form of 25 mm diameter discs, 0.5 mm in thickness (Trueman et al., 2004). The total surface area is 1021 mm^2 and the uranium mass is 4.688 g.

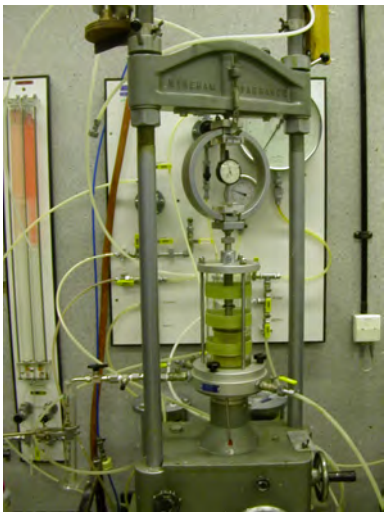

Fig. 1. Experimental set-up.

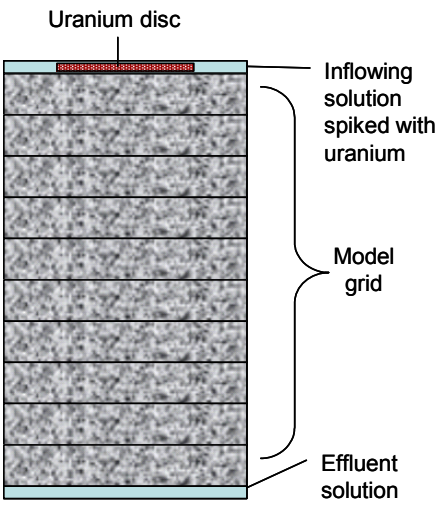

Fig. 2. Conceptual layout of model.

The DU serves only as a well-characterised source of uranium ions and is not meant to mimic exactly the dissolution of SF. Previous studies (Trueman et al, 2003; Baumann *et al*., 2006) demonstrated the rapid degradation of DU under a range of experimental conditions when exposed to excess solution. In the present experiments, rock matrix/aqueous solution ratios are more representative of those found in the field and, in addition, the fate of the radionuclides released is assessed.

In addition to a confining pressure, a slight upward directed flow is imposed on the triaxial cell. The initial volumetric flow rate was 0.017 cm^3/s.

Three basic sets of data will be generated from the experiments : (1) the chemical composition of the effluent as a function of time, (2) evolving alteration products on the disc surface and (3) spatially resolved data from analyses of the rock samples upon termination of the experiment. Together these data will allow a time-resolved (uranium) mass balance for the experiment to be constructed.

Conceptual Model

A one-dimensional ten-cell model (Figure 2) was set up in PHREEQC (Parkhurst & Appelo, 1999). The chemical calculations were performed using the Lawrence Livermore Laboratory thermodynamic database (Version 85 from 02/02/05) that was delivered together with the code (Version 2.12.05).

Initial water compositions

It was assumed that little more 'real data' were available other than that the material in the experiment is a granodiorite from Central Finland. Thus, the first step consisted of modelling the initial water composition (Table 1) based on literature data for comparable material, viz. groundwater from Äspö (quoted in Bruno *et al*., 1999).

Initial calculations showed that the water is close to equilibrium with respect to albite, quartz and several clay minerals, reflecting the main constituents of granitic rock and its weathering products. Subsequent calculations maintained equilibrium with H-saponite, which provides for silicate and pH-buffering in the system. The infiltrating solution was brought into equilibrium with O_2 and CO_2 at their respective atmospheric partial pressures. The resulting water composition was slightly supersaturated with respect to ferric hydroxide and, hence, precipitation of it was allowed, which provides for additional pH-buffering.

Table 1. Calculated (data for Äspö from Bruno et al (1999)) and measured water compositions [mol/dm^3].

Component	Äspö	measured	Component	Äspö	measured
Na^+	$9.13 \cdot 10^{-2}$	$9.27\ 10^{-4}$	HCO_3^-	$1.64 \cdot 10^{-4}$	n.d.
K^+	$2.05 \cdot 10^{-4}$	$5.81\ 10^{-5}$	PO_4^{3-}		$3.13\ 10^{-6}$
Ca^{2+}	$4.73 \cdot 10^{-2}$	$8.85\ 10^{-4}$	Cl^-	$1.81 \cdot 10^{-4}$	n.d.
Mg^{2+}	$1.73 \cdot 10^{-3}$	$1.67\ 10^{-3}$	SO_4^{2-}	$5.83 \cdot 10^{-3}$	$9.12\ 10^{-5}$
Fe^{2+}	$4.30 \cdot 10^{-6}$	$1.33\ 10^{-3}$	pH	7.7	6.64
Mn^{2+}	$5.28 \cdot 10^{-6}$	$8.45\ 10^{-5}$	Eh [mV]	-300	n.d.
H_4SiO_4	$1.46 \cdot 10^{-4}$	$2.75\ 10^{-5}$			

The hydraulic properties of the experimental system

The porosity of the two samples used was 9.1% and 13.6% respectively, by the helium method. An average value of 10% for the total porosity was assumed for the modelling runs and the effect of different effective porosities explored numerically. The mixing cell model in PHREEQC does not allow the effective porosity to be entered explicitly, only implicitly via the average porewater flow velocity.

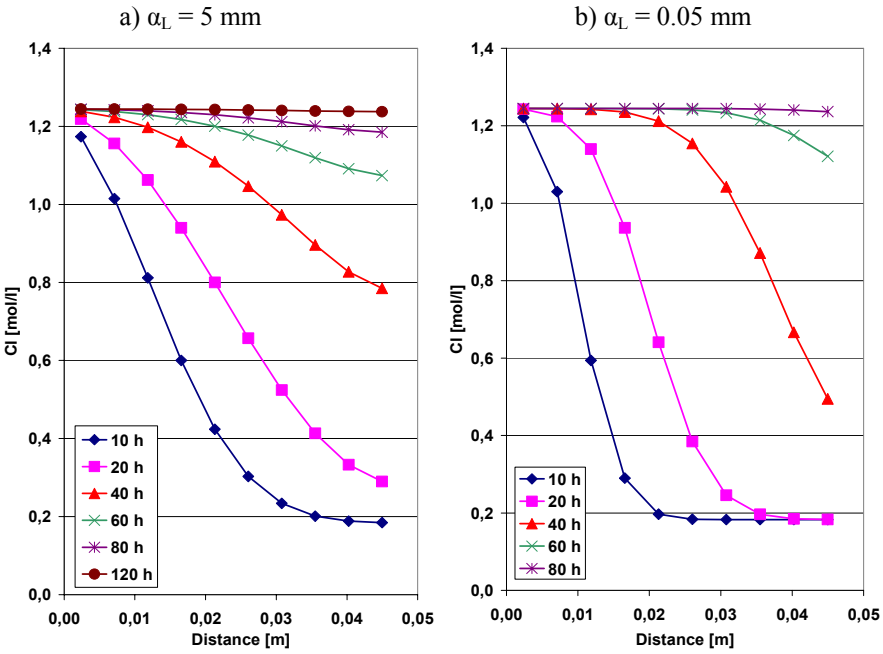

Fig. 3. Sample tracer profiles as a function of dispersion length α_L.

The tortuosity, or length of the stream-tubes within the rock, is defined through the average flow velocities. The cells are modelled as a continuum and as stream tubes so that their length distribution is represented by the dispersivity. A typical choice for the dispersion length is 1/10 of the cell length, here approximately 0.5 mm. In sensitivity calculations this value was varied over several orders of magnitude. Figure 3 exemplifies the effect on the shape of tracer break-through profiles.

For further calculations, a value of 5% for the effective porosity and of 0.5 mm for the dispersion length were chosen, based on the preliminary hydraulic assessment; these correspond to a time step in the PHREEQC model of 18000 s = 5 h.

Safety cases for disposal of HLW and SF in fractured hard rocks rely heavily on the concept of dual porosity and the related concept of matrix diffusion (e.g. SKB, 2006). These assume that, although only the effective porosity takes part in advective-dispersive transport, there will be diffusive exchange between this fraction and the remaining porosity. This exchange lowers peak concentrations and is also responsible for longer tails in concentration distributions. The PHREEQC code allows dual-porosity cases to be formulated for various geometries, which are introduced via a 'shape factor'. Here, a stream-tube geometry embedded in a one-layer deep tube of stagnant cells was considered the most appropriate.

Solubility Controlling Phases for Uranium

Secondary uranium phases that may control solubility were identified by simulating batch experiments with incremental amounts of uranium added. The thermodynamically most stable phases are predicted to be $UO_2(OH)_2$ and $UO_3 \cdot nH_2O$. The latter may actually be polymorphous and have the formula $[(UO_2)_8O_2(OH)_{12}](H_2O)_{12}]$ (Finch *et al*., 1996). The LLNL database contains solubility products for $UO_3 \cdot nH_2O$ with n= 2, 1, 0.9, 0.85, 0.648 and 0.393. $UO_3 \cdot nH_2O$ has been identified as the major corrosion product from the dissolution of DU in soils (Trueman et al. 2003). Considering the persisting uncertainty regarding relevant thermodynamic constants (e.g. Jang *et al*., 2006), schoepite was used as a proxy here.

The uranium source term

Previous experiments (Trueman et al, 2003) have shown that *in extremis* one year is sufficient to completely dissolve a DU disc. Given a total mass of 0.1674 moles of U, an approximate mass loss of $5.4 \cdot 10^{-9}$ mol/s can be calculated. This value has been used as a linear reaction rate. Previous experiments have also shown that not all uranium would move away, but that alteration products accumulate on the surface of the discs (Baumann *et al*., 2006). The instantaneous (equilibrium) precipitation of schoepite as modelled in PHREEQC would constrain aqueous uranium concentration to about $3 \cdot 10^{-5}$ mol/dm^3.

At 5% effective porosity the rock sample contains $4.55 \cdot 10^{-3}$ dm^3 mobile solution. Hence, $2.134 \cdot 10^{-2}$ mol U/time step must be added. With the initial volumetric flow rate of 0.017 cm^3/s, this translates into a concentration of $3.176 \cdot 10^{-4}$ mol/dm^3 in the inflowing solution.

Results of Blind Modelling

Figure 4 shows that the zone where schoepite saturation is reached moves along the column. Steady state effluent uranium concentrations would be attained quickly for an equilibrium model that assumes instantaneous precipitation once saturation is reached. Such a model would cause all precipitation to occur in the first cell, resulting in rapid clogging of the pore space.

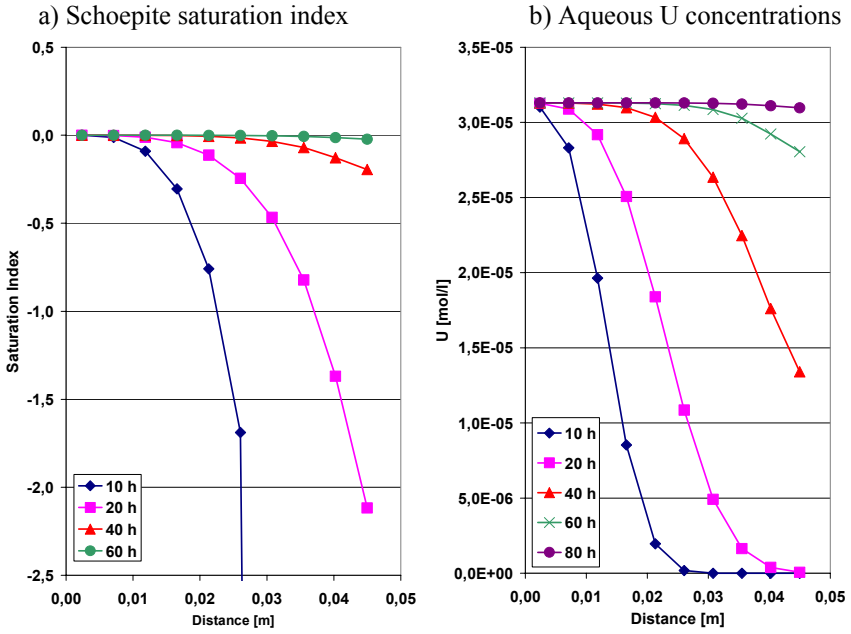

Fig. 4. Flooding the core with a uranium solution of $3.176 \cdot 10^{-4}$ mol/dm^3 while allowing schoepite to precipitate.

Based on a molar volume of 66.61 cm^3/mol, one can calculate a precipitation rate of 0.031 cm^3/day, leading to the total pore volume of 9.6 cm^3 being completely filled within just under 300 days. Of course, with increasing clogging of the pore volume the flow rate and hence the supply of uranium would decline.

In order to model the behaviour of uranium more realistically, precipitation kinetics were assumed in subsequent calculations.

Precipitation Kinetics

PHREEQC allows the definition of different kinetic models and reaction rates for each cell. The data would normally be derived from experiments by curve-fitting. In a blind prediction case no such data are available and modelling of precipitation kinetics is purely conjectural. In order to set up the model for later curve-fitting exercises and to demonstrate the effect of precipitation kinetics, a simple case with arbitrary kinetics was developed. It was assumed that the kinetics of precipitating schoepite would depend on the activity concentration of the uranyl ions in solution with different scaling factors. Figure 5 exemplifies such calculations and the resulting concentration profiles for different (arbitrary) rate constants.

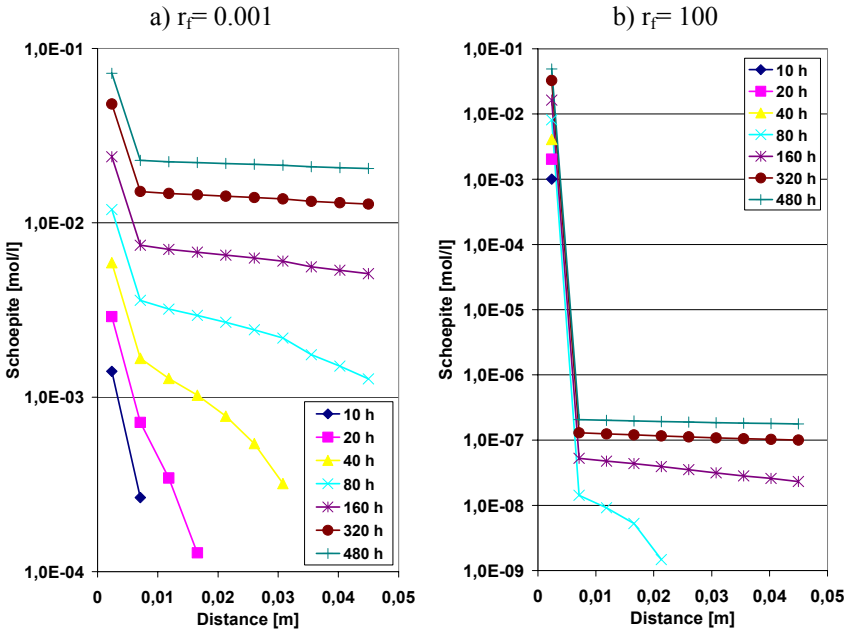

Fig. 5. The effect of different arbitrary precipitation kinetics rate factors r_f on the distribution of total precipitated schoepite along the sample.

Discussion and Conclusions

The first model was constructed solely from the average volumetric flow rate and the total porosity. In the next phase, the actual flow rates will be imposed onto the hydraulic model, as a drop in volumetric flow rates was actually observed. This automatically constrains the degree of freedom for any precipitation kinetics. The

measured bulk chemistry of the effluent will then be compared with that predicted by the model, which helps to identify the various processes that may control pH and redox potential. In addition, those elements that are involved in heterogeneous reactions can be identified on the basis of mass balances. With this information a refined model of the bulk chemical processes will be developed. In turn, better knowledge of the development of the bulk chemistry will help to constrain heterogeneous processes involving uranium. Given the assumed inertness of much of the rock matrix, at least on the time scale of the experiment, and considering the large mass of uranium available, it is quite likely that heterogeneous reactions involving uranium do have a noticeable influence on the bulk pore water chemistry. The modelling study will help to show this.

Blind predictive modelling and subsequent parameterisation of the model with actual experimental data is a valuable process that helps to better understand system behaviour. The blind predictions indicate which system variables are likely to be critical and thus helps to direct priorities for the analytical programme.

References

Baumann N, Arnold T, Geipel G, Trueman E, Black S, Read, D (2006). Detection of U(VI) on the surface of altered depleted uranium by TRLFS. Sci.. Tot Env. 366, 905-909.

Bruno J, Arcos D, Duro L (1999) Processes and features affecting the near field hydrochemistry. Groundwater-Bentonite interaction. SKB Tech. Rep. TR-99-29, 56 p.

Finch R, Cooper M, Hawthorne F, Ewing R (1996) The crystal structure of schoepite $[(UO_2)_8O_2(OH)_{12}](H_2O)_{12}$. Canadian Mineral. 34: 1071-1088.

Jang J-H, Dempsey B, Burgos W (2006) Solubility of schoepite: Comparison and selection of complexation constants for U(VI). Water Res. 40(14): 2738-2746.

Parkhurst D, Appelo C (1999) User's guide to PHREEQC--A computer program for speciation, batch-reaction, one-dimensional transport, and inverse geochemical calculations. U.S. Geological Survey Water-Resources Investigations Report 99-4259.

Read D (1991) CHEMVAL Project: Testing of coupled chemical transport models. CEC Report EUR13675.

Svensk Kärnbränslehantering AB (2006) Long-term safety for KBS-3 repositories at Forsmark and Laxemar - a first evaluation. Main report of the SR-Can project. Report SKB TR-06-09, 613 p.

Trueman E, Black S, Read D, Hodson M (2003). Alteration of depleted uranium metal. Geochim. Cosmochim. Acta, 67, A493.

Trueman, E, Black S, Read D. (2004) Characterisation of depleted uranium (DU) from an unfired CHARM-3 penetrator. Sci. Tot. Env. 327, 337-340.

Detection of hexavalent uranium with inline and field-portable immunosensors

Scott J. Melton[1], Haini Yu[1], Mehnaaz F. Ali[1], Kenneth H. Williams[2], Michael J. Wilkins[2], Philip E. Long[3] and Diane A. Blake[1*]

[1]Dept. Biochemistry, Tulane Univ. Sch. Medicine, New Orleans, LA 70112 USA
[2]Earth Sciences, Lawrence Berkeley Laboratory, Berkeley, CA 94720 USA
[3]Hydrology, Pacific Northwest National Laboratory, Richland, WA 99352 USA

Abstract. An antibody that recognizes a chelated form of hexavalent uranium was used in the development of two different immunosensors for uranium detection. Specifically, these sensors were utilized for the analysis of groundwater samples collected during a 2007 field study of *in situ* bioremediation in a aquifer located at Rifle, CO. The antibody-based sensors provided data comparable to that obtained using Kinetic Phosphorescence Analysis (KPA). Thus, these novel instruments and associated reagents should provide field researchers and resource managers with valuable new tools for on-site data acquisition.

Introduction

The ability to perform quantitative analyses of contaminants in groundwater samples while still in the field has been a long-term goal for environmental scientists. For uranium analysis, samples must be transported off-site for any complex, detailed analysis such as ICP-MS or AAS. Simpler instrumentation like the Kinetic Phosphorescence Analyzer (KPA) is also used primarily in a laboratory setting; in addition, this instrument is useful only for the analysis of uranium and lanthanides (Brina and Miller, 1993). Here we describe two immunosensors that can be adapted for uranium analysis through the use of antibodies that bind to a UO_2^{2+}-chelate complex.

Immunoassays have numerous advantages for quantifying levels of environmental contaminants. Immunoassay methods are rapid and simple to perform. Relatively compact instruments can be designed to quantify antibody binding; such instruments are thus amenable for use in a field setting. Finally, the immunosensors used in the experiments described herein can be modularized such that many different contaminants can be measured using an identical sensor platform;

if an antibody to a specific environmental contaminant can be generated, it can be used with this sensor technology. In the present study, two instruments based on the principle of kinetic exclusion (Blake 1999, Kusterbeck and Blake 2008) were used to assay groundwater samples from a uranium-contaminated site in Rifle, CO. Both immunosensors were able to detect changes in uranium levels during an *in situ* remediation process and thus show promise towards eventual field deployment for a variety of environmental sensing needs.

Methods

Materials

The uranium-selective chelator 2,9-dicarboxyl-1,10-phenanthroline (DCP) was purchased from Alfa Aesar (Ward Hill, MA). 12F6, a mouse monoclonal antibody that binds specifically a UO_2^{2+}-DCP complex, and an immobilized form of chelated uranium (UO_2^{2+}-DCP-BSA conjugate) were available from a previous study (Blake et al. 2004). A Cy5-labeled Fab of goat anti-mouse IgG was obtained from Jackson ImmunoResearch Laboratories (Gaithersburg, MD). Bisacrylamide/azlactone copolymer beads (UltraLink Biosupport), used in the Inline sensor, were a product of Pierce Biotechnology (Rockford, IL). Polystyrene beads, used with the field portable device (FPD), were acquired from Sapidyne Instruments, Inc (Boise, ID). The diameter of both bead types was ~ 98 μm; these beads were coated with the UO_2^{2+}-DCP-BSA conjugate by procedures that have been previously described (Blake et al, 2004; Yu et al, 2005). A UO_2^{2+} standard was made from uranyl acetate obtained from Mallinckrodt (St. Louis, MO). Environmental water samples were obtained in August and September, 2007 from a sampling well (D-02) at the Rifle UMTRA site, Rifle CO. The collected samples (~50 ml each) were filtered through a 0.2 μM IC MILLEX-LG syringe filter (Millipore, Billerica, MA) and refrigerated. All samples were acidified with 8 N HNO_3 to a pH of 2 before analysis. Standard curves were generated using a 1:200 dilution of "Rifle Artificial Ground Water" (RAGW), made from a formulation developed by K.M. Campbell of the U.S. Geological Survey (Menlo Park, CA).

Inline Sensor

The Inline sensor, developed in conjunction with Sapidyne Instruments (Boise, ID) (Fig. 1A) is an instrument designed to be operated in a process line capacity (Yu et al., 2005; Bromage et al., 2007; Kusterbeck and Blake, 2008).

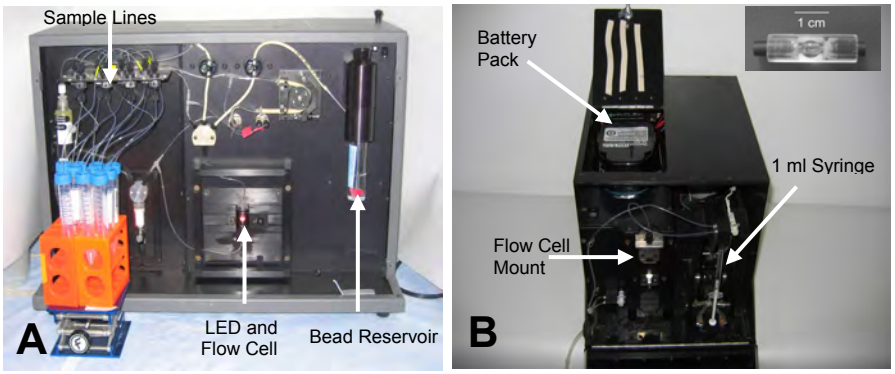

Fig.1. Uranium immunosensors. **A,** The KinExA Inline sensor (footprint, 30x56 cm) autonomously mixes assay components and injects them over a capillary bead column illuminated by an LED. The instrument measures fluorescently labeled antibody bound to the column; multiple samples can be assayed in one experimental run. **B,** The Field Portable Device (footprint, 23.5 x 32 cm) is a self-contained instrument that injects operator-prepared samples from a loaded 1 ml syringe over a pre-filled flow cell (**inset).** The instrument with battery weighs approximately 6 kilograms; a carrying case with room for all necessary accessories (not shown) increases portability.

The Inline sensor required a grounded power source and was able to autonomously mix all components, run a standard curve, and analyze unknowns. Bisacrylamide/azlactone copolymer beads (50 mg) were coated with UO_2^{2+}-DCP-BSA conjugate and loaded into the bead reservoir before the assay sequence was initiated. UO_2^{2+} was spiked into Hepes-buffered saline (HBS, 137 mM NaCl, 3 mM KCl, 10 mM Hepes, pH 7.4) containing 200 nM DCP and a 1:200 dilution of RAGW in order to generate the standard curve. Environmental samples were diluted 1:200 in Hepes-buffered saline containing 200 nM DCP. The pH of the environmental samples after a 1:200 dilution into HBS was between 7.0 and 7.2. All assay mixtures also contained the anti-uranium antibody 12F6 (0.25 nM) and Cy5-Fab (5 nM, used to fluorescently label 12F6). The signals generated by the environmental samples were compared to the standard curve to determine concentrations of UO_2^{2+}. The instrument was programmed (Yu et al, 2005) to generate a five-point standard curve and analyze seven samples in a single experimental run. All data points (standards and environmental samples) were obtained in triplicate.

Field Portable Device

The field portable device (FPD) (Fig. 1B), also developed in conjunction with Sapidyne Instruments (Kusterbeck and Blake, 2008), was designed to be used in the field without the need for a grounded power supply. Instead, the device was powered with a power drill battery available at most hardware stores. The instrument

was completely enclosed in a plastic case and controlled by laptop through a wireless interface. Unlike the re-usable capillary flow cell utilized by other kinetic exclusion instruments (Blake et al., 2004; Yu et al., 2005), the FPD used a disposable flow cell (Fig. 1B, inset) prefilled with polystyrene beads coated with the UO_2^{2+}-DCP-BSA conjugate. Assay components were mixed by the operator; the final concentrations of the reagents were as described for Inline sensor analysis, except the Cy5-Fab concentration was reduced to 2.5 nM. Due to the limited binding capacity of the flow cell, the data points of the standard curve were obtained in singlet, while the environmental sample was analyzed in triplicate.

Kinetic Phosphorescence Analysis

In order to validate the performance of the immunosensors described herein, acidified groundwater samples were also analyzed with a kinetic phosphorescence analyzer (KPA) and Uraplex reagent available from ChemCheck Instruments (Bellingham, WA). Each sample was measured at three dilutions to ensure accuracy.

Results

The Inline sensor and the FPD are both flow fluorimeters that employ the kinetic exclusion method. This method measures the concentration of free, uncomplexed antibody in assay mixtures containing fluorescently-labeled antibody, the contaminant of interest, and antibody-contaminant complexes (Blake et al, 1999). A structural analogue of the contaminant (in this case chelated uranium) was coated onto beads. These beads were subsequently packed into a flow cell and used to capture the free fluorescently-labeled antibody; the fluorescence on the beads was monitored as the assay mixture flowed through the cell.

Typical data traces for the FDP are shown in Fig 2. This instrument recorded the baseline fluorescence 5 seconds prior to injection of the sample. Sample injection was completed in ~50 seconds and the instrument then automatically rinsed the flow cell from a buffer reservoir. The instrument automatically determined the baseline signal from the first 5 seconds of the trace and subtracted that value from the final signal after the rinse to generate a “delta” signal, which was inversely proportional to the amount of UO_2^{2+} in the sample. A delta signal for each sample could be determined in 140 seconds.

In order to generate a standard curve, known amounts of UO_2^{2+} were added to a buffered sample that contained 200 nM DCP chelator and RAGW in the same dilution as that used for the environmental samples. The chelated UO_2^{2+} bound to fluorescently labeled 12F6 antibodies present in the sample; these bound antibodies were therefore not available for binding to the chelated UO_2^{2+} immobilized on the beads. As more soluble UO_2^{2+} was added to the assays, less fluorescently labeled antibody was bound to the beads. This competition for limited antibody

binding sites resulted in a delta signal from the instrument that was inversely proportional to the amount of UO_2^{2+} present in the sample.

A 4-point standard curve was generated using the FPD, as shown in Fig 3.

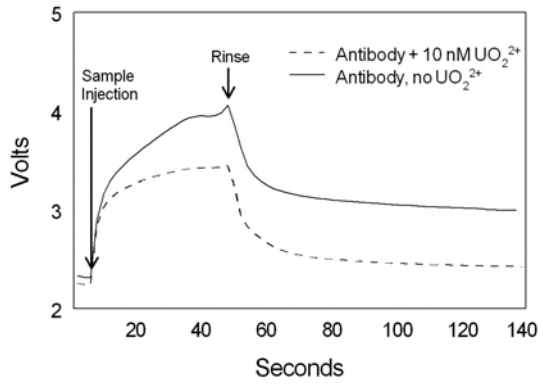

Fig.2. Primary data traces from the FPD. Solid line, sample containing antibody but no UO_2^{2+}. Dashed line, sample containing antibody plus a UO_2^{2+} concentration high enough to fill all antibody binding sites (10 nM).

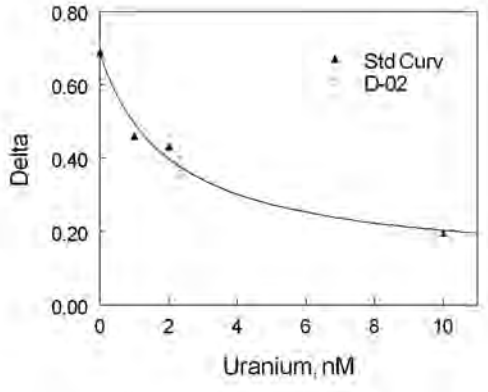

Fig.3. Uranium standard curve developed using the FPD. UO_2^{2+} standards (closed triangles) and a sample from a sampling well in Rifle (well D-02, open circle) were prepared as described in Methods. The concentration of UO_2^{2+} present in the sample after factoring in the dilution was 473.1 +/- 87.9 nM. Points obtained for generation of the standard curve were singlets while the environmental sample was run in triplicate.

The standard curves were fit to the data points using the following equation:

$$Y_A = \frac{a0 - (a1 * x)}{a2 + x} \qquad \text{(Eq 1)}$$

in which Y_A is the delta value at a particular concentration of UO_2^{2+}, a0 is the delta at an infinite concentration, a1 is the magnitude of change in delta from the lowest to the highest UO_2^{2+} concentrations and a2 is the concentration of UO_2^{2+} that results in 50% inhibition of the signal. The a2 is also the equilibrium dissociation constant (K_d) of 12F6 binding to the UO_2^{2+}-DCP complex. Since this value has been determined in a previous study (Blake et al., 2004), the a2 obtained was a reliable indicator of the accuracy of the standard curve. The amount of UO_2^{2+} in an environmental sample was determined by diluting the environmental sample into HBS buffer containing the same reagents used for the standard curve. The sample was then injected over the beads and the resultant data point was fitted onto the standard curve.

Similar analyses were also performed using the Inline sensor. In contrast to the FPD, which used a single bead pack in a disposable flow cell for multiple measurements, the Inline sensor used a fresh set of beads for each measurement. Beads were stored as a slurry in a reservoir bottle (shown in Fig 1A) and the instrument automatically packed a new bead microcolumn at the beginning of each measurement. Typical data traces from the Inline sensor are shown in Fig. 4. The *inset* shows a uranium standard curve prepared by plotting delta versus uranium concentration.

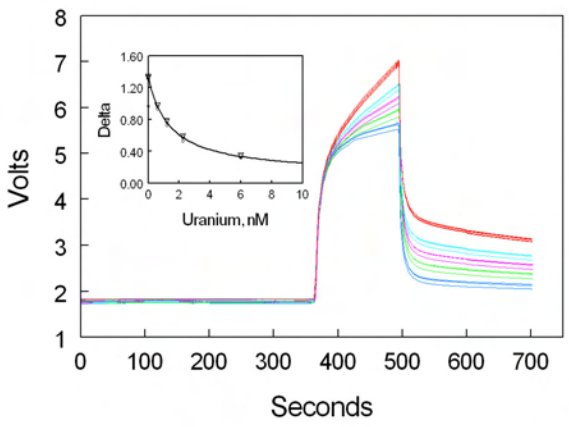

Fig.4. Data traces and uranium standard curve from the Inline sensor. The instrument packed beads into the flow cell, washed sample lines and tubes and mixed experimental samples from stock solutions from 0-359 sec. Sample injection occurred at 360 seconds and was followed by a buffer rinse. *Inset*, Uranium standard curve. All experiments were performed in triplicate.

Finally, both the FPD and the Inline sensor were compared with kinetic phosphorescence analysis for their ability to assess uranium in environmental groundwater samples. These samples were obtained during an *in situ* bioremediation experiment conducted at the Uranium Mill Tailings Remedial Action (UMTRA) site located in Rifle, CO. Detailed descriptions of the history, geology and hydrogeology of this site have been described elsewhere (Anderson, et al., 2003; Vrionis, et al., 2005). Background groundwater concentrations of uranium are approximately 500 to 1000 nM. A series of monitoring wells were installed downgradient of an injection gallery. This injection gallery, installed perpendicular to the groundwater flow, was used to pump acetate into the aquifer. Biostimulation with acetate is thought to initially stimulate the growth of *Geobacter* species, which are able to reduce soluble U(VI) to insoluble U(IV) and decrease the uranium in the water column (N'Guessan et al., 2008). Groundwater samples were collected at intervals after initiation of acetate injection and analyzed for uranium. Fig 5 shows the levels of soluble uranium in a representative downstream well, D-02, during continuous acetate injection from the day 0 to day 35. As reported previously (N'Guessan, 2008) acetate injection caused a relatively sharp decrease in soluble uranium that was detected with all three instruments. Additionally, the data from the two immunosensors correlated well with the data from the KPA.

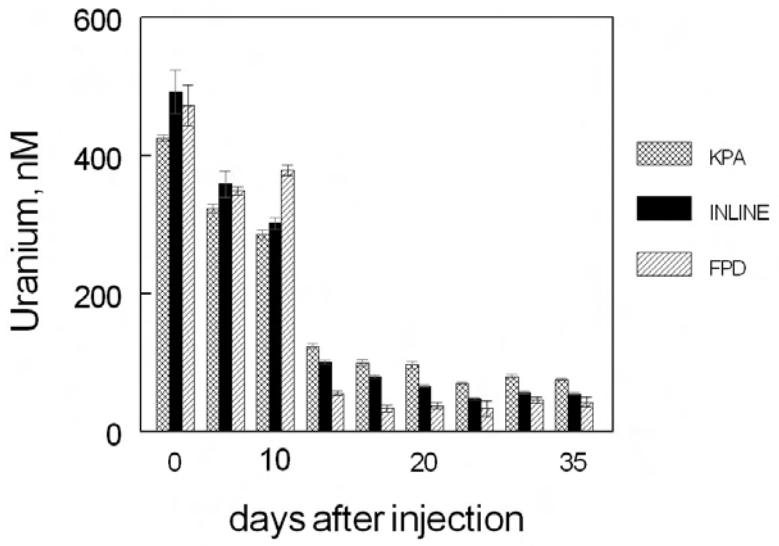

Fig.5. Comparison of KPA, Inline, and FPD analysis. Groundwater samples were collected at the indicated times after the initiation of acetate injection, filtered and acidified. KPA analyses were performed at 3 dilutions; samples were analyzed in triplicate using the Inline Sensor and FPD. The error bars represent the standard error of the mean.

Discussion

Previous work in our laboratory has focused on the isolation/characterization of antibodies that bind to metal-chelate complexes and on the development of antibody-based assays useful for measuring a variety of heavy metals in a given sample (Khosraviani et al., 1998; Delehanty et al., 2003; Darwish and Blake, 2004; Kriegel et al., 2006; Zhu et al., 2007). The work described in this report represents some of the first experiments carried out by our laboratory in a field setting and demonstrates the portability, speed and overall utility of immunosensors for environmental analysis. However, as with all immunoassays, a detailed understanding of the binding properties of the antibody used in the assay is vital for the success of this method.

Monoclonal antibodies that recognize environmental contaminants are typically generated in mice by repeated exposure of the contaminant (or a structural analogue of the contaminant) to the mouse immune system. Metal cations are too small to illicit an immune response and our laboratory has developed a method whereby an immunogen is prepared by immobilizing the metal via a bifunctional chelator to a carrier protein (for a review, see Blake et al., 2007). The antibodies generated from such immunizations recognize metals bound to a chelator, rather than free metals. Since metals in environmental samples almost always exist in a complexed state, an important part of any assay development effort is devising a strategy that removes the metal from its natural complexants and transforms it to a form recognized by the antibody. The antibody used for the uranium analysis, 12F6, recognizes uranium in a complex with DCP (Blake et al, 2004). Thus, the uranium in the environmental samples from the Rifle site had to be dissociated from complexants present in the groundwater samples and subsequently transformed to DCP complexes. While the optimal pre-treatment strategy for Rifle samples (acidification, then neutralization into buffers containing DCP) was not determined until after the field experiment had been completed, future experiments should allow for near real-time quantification of uranium in the field.

The use of the Inline sensor has both advantages and disadvantages for field use. This instrument had a relatively high sample throughput and provided data with minimal effort on the part of the operator. In a typical day at Rifle, we collected and pretreated samples during a day of field work; the Inline sensor was then programmed to analyze them overnight. The instrument's autonomous operation and relatively small footprint (30x56 cm) was advantageous in the cramped conditions that existed in our field laboratory (a converted horse trailer). The Inline sensor provided data that was as precise as larger immunoassay instruments in our laboratory. This superior precision could be attributed to the instrument's ability to prepare a fresh set of reagents (bead column, freshly mixed assay components) for each measurement; however, use of fresh reagents limited the total number of individual samples per run to ~50. The main disadvantage of the Inline sensor was its requirement for a grounded 110 AC power source.

Because of its independent power supply and wireless interface, the FPD could be operated in the absence of a grounded power supply (although the drill batteries

used for operation needed to be recharged either from an automotive battery or a grounded power source). The instrument is comparatively light (6 kg); it was transported in a backpack-like bag that also had room for all necessary reagents and accessories (pipettes, syringes, disposable tubes); thus, this instrument could be used in a remote setting. One of the issues currently being addressed during further FPD development is the binding capacity of the disposable flow cells supplied with the instrument. Unlike the Inline immunosensor, the FPD uses the same bead column for multiple measurements. This ultimately results in a decrease in instrument responsiveness as more and more antibody binds to the UO_2^{2+}-DCP coated on the beads. For the experiments described herein, we responded by limiting the number of standards and experimental samples analyzed on each disposable flow cell. In practical terms, these limitations decreased precision due to fewer replicate measurements. A fresh flow cell was required for every environmental sample, which led to a decrease in sample throughput. New bead coating strategies and sample injection schemes are being explored to optimize instrument performance.

The data obtained with these two new immunosensors compared well that obtained using KPA. As seen in Fig 5, the data from both the Inline and FPD correlated well with the KPA analysis of the D-02 test well, especially at the higher uranium levels seen at the beginning of this study. While the FPD, in particular, was less able to monitor uranium at lower levels, both the Inline sensor and the FPD were able detect the removal of uranium from the groundwater sample collected during experiments performed during the summer of 2007.

The immunosensors described herein can be easily adapted to the analysis of a wide variety of other experimental contaminants. Assays for other heavy metals, PCB's, 2,4-dichlorophenoxyacetic acid, environmental estrogens, organophosphate pesticides, imidazolinone herbicides and TNT have been published using the KinExA™ technology employed by the Inline sensor and FPD (for a review, see Kusterbeck and Blake, 2008). These new field deployable sensors will provide researchers and resource managers with an invaluable tool for generating near real-time data and modifying field experiments already in progress.

Acknowledgments

This work was supported by the Office of Science (BER) of the U.S. Department of Energy, Grant DE-FG98-ER62704 (D.A.B.). The field experiment this work is based on was conducted as part of the U.S. Department of Energy's Integrated Field Challenge Site (IFC) at Rifle, Colorado. The Rifle IFC is a multidisciplinary, multi-institutional project supported by the Environmental Remediation Sciences Division of Biological and Environmental Research, Office of Science, U.S. Department of Energy. The project is lead by Pacific Northwest National Laboratory and includes a number of university and national laboratory partners. The authors thank Kate M. Campbell of the USGS, Menlo Park, CA, for providing the Rifle artificial groundwater formulation.

References

Anderson RT, Vrionis HA, Ortiz-Bernad I, Resch CT, Long PE, Dayvault R, Karp K, Marutzky S, Metzler DR, Peacock A, White DC, Lowe M, Lovley DR (2003) Stimulating in situ activity of Geobacter species to remove uranium from the groundwater of a uranium-contaminated aquifer. Appl Environ Microbiol 69: 5884-5891

Blake, DA, Blake, RC 2nd, Abboud ER, Li X, Yu H, Kriegel AM, Khosraviani M, Darwish IA (2007) "Antibodies to heavy metals: Isolation, characterization and incorporation into microplate-based assays and immunosensors". In *Immunoassay and Other Bioanalytical Techniques* (Ed. J.M. Van Emon), Taylor and Francis, Boca Raton, FL, pp. 93-111

Blake RC 2nd, Pavlov AR, Blake DA (1999) Automated kinetic exclusion assays to quantify protein binding interactions in homogeneous solution. Anal Biochem 272: 123-134

Blake RC 2nd, Pavlov AR, Khosraviani M, Ensley HE, Kiefer GE, Yu H, Li X, Blake DA (2004) Novel monoclonal antibodies with specificity for chelated uranium(VI): Isolation and binding properties. Bioconj Chem 15: 1125-1136

Brina R, Miller AG (1993) Determination of uranium and lanthanides in real-world samples by kinetic phosphorescence analysis. Spectroscopy 8: 25-28

Bromage ES, Lackie T, Unger MA, Ye J, Kaattari SL (2007) The development of a real-time biosensor for the detection of trace levels of trinitrotoluene (TNT) in aquatic environments. Biosensor Bioelectron 22: 232-238.

Darwish IA, Blake DA (2002) Development and validation of a sensitive one-step immunoassay for determination of cadmium in human serum. Anal Chem 74: 52-58

Delehanty JB, Jones RM, Bishop TC, Blake DA. (2003) Identification of important residues in metal-chelate recognition by monoclonal antibodies. Biochemistry 42: 14173-14183

Khosraviani M, Pavlov AR, Flowers GC, Blake DA (1998) Detection of heavy metals by immunoassay: Optimization and validation of a rapid, portable assay for ionic cadmium. Env Sci Technol 32: 137-142

Kriegel AM, Soliman AS, Zhang Q, El-Ghawalby N, Ezzat F, Soultan A, Abdel-Wahab M, Fathy O, Ebidi G, Bassiouni N, Hamilton SR, Abbruzzese JL, Lacey MR, Blake DA. (2006) Serum cadmium levels in pancreatic cancer patients from the East Nile Delta region of Egypt. Environ Health Perspect 114: 113-119

Kusterbeck AW, Blake DA (2008) "Flow immunosensors" in *Optical Biosensors: Today and Tomorrow* (Ed, Ligler FS, Tait CR), Elsevier, New York, pp 243-285

N'Guessan AL, Vrionis HA, Resch CT, Long PE, Lovley DR (2008) Sustained removal of uranium from contaminated groundwater following stimulation of dissimilatory metal reduction. Env Sci Tech 42: 2999-3004

Vrionis HA, Anderson RT, Ortiz-Bernad I, O'Neill KR, Resch CT, Peacock AD, Dayvault R, White DC, Long PE, Lovley DR (2005) Microbiological and geochemical heterogeneity in an in situ bioremediation field site. Appl Environ Microbiol 71: 6308-6318

Yu H, Jones RM, Blake DA (2005) An immunosensor for autonomous in-line detection of heavy metals: Validation for hexavalent uranium. Int J Env Anal Chem 85: 817-830

Zhu X, Hu B, Lou Y, Xu L, Yang F, Yu H, Blake DA, Liu F (2007) Characterization of monoclonal antibodies for lead-chelate complexes: applications in antibody-based assays. J Agric Food Chem 55: 4993-4998

Ground water remediation at the Moab, Utah, USA, former uranium-ore processing site

Donald R. Metzler[1], Joseph D. Ritchey[2], Kent A. Bostick[3], Kenneth G. Pill[2] and Elizabeth M. Glowiak[4]

[1]U.S. Department of Energy Office of Environmental Management, Grand Junction, Colorado, USA
[2]Pro2Serve, Grand Junction, Colorado, USA
[3]Pro2Serve, Oak Ridge, Tennessee, USA
[4]Pro2Serve, Moab, Utah, USA

Abstract. Seepage from the Moab, Utah, USA, former uranium-ore processing site resulted in ammonia and uranium contamination of naturally occurring saline ground water in alluvium adjacent to the Colorado River. An interim ground water remediation system, operating since 2003, is currently being evaluated for design of a long-term remedy. Final design is to minimize ammonia discharge to critical habitat areas.

Introduction

The Moab, Utah, USA, former uranium-ore processing (mill) site encompasses 178 hectares (439 acres), of which 52 hectares (130 acres) is covered by a 30-meter-high (90-feet-high), unlined mill tailings pile. Fig. 1 shows the site location, which is situated on the west bank of the Colorado River and is adjacent to Arches National Park. The processing mill operated from 1956 to 1984 under private ownership. The milling operations created process-related wastes and tailings, a sandlike material containing radioactive and other contaminants. Over time, seepage from the tailings pile resulted in ammonia and uranium contamination in the alluvial ground water beneath the site.

Regulatory framework

Following bankruptcy of the mill owner in 1998, the U.S. Nuclear Regulatory Commission (NRC), which regulates the site, appointed a trustee. Through con-

gressional legislation, title to the site and responsibility for cleanup were transferred to the U.S. Department of Energy (DOE) in 2001. Cleanup, including ground water, was required to be performed in accordance with Title I of the Uranium Mill Tailings Radiation Control Act (UMTRCA) of 1978. The act was instituted to clean up former uranium-ore processing sites across the U.S.; these cleanups were largely completed in the 1980s and 1990s.

Contaminated soils and ground water at the Moab site must be cleaned up to U.S. Environmental Protection Agency (EPA) standards established in Title 40 *Code of Federal Regulations* Part 192 (40 CFR 192).

DOE prepared an Environmental Impact Statement (EIS) to fulfill the National Environmental Policy Act requirement to assess the potential environmental effects of remediating the Moab site. DOE analyzed the potential impacts on surface

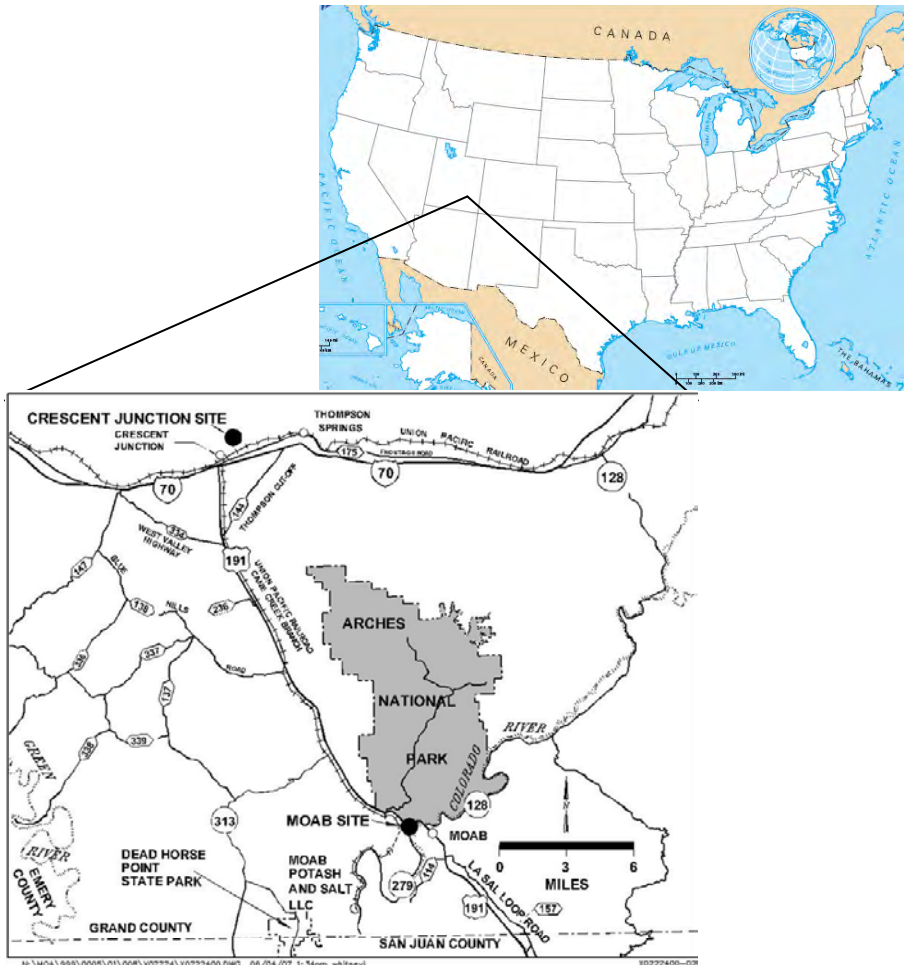

Fig. 1. Location of Moab site.

water and ground water of on-site and off-site remediation alternatives. Uncertainty of river migration and the long-term effects of contaminated ground water entering the Colorado River were expressed as concerns about leaving the contaminated materials on site. Although migration of the river into the tailings pile if left in place were unfounded (DOE 2003a), DOE decided in a 2005 Record of Decision (ROD) to relocate the tailings to a site at Crescent Junction, Utah 48 kilometers (30 miles) north of the Moab site and far away from the Colorado River. The ROD also included actively remediating contaminated ground water at the Moab site.

Final ground water cleanup will be described in a Ground Water Compliance Action Plan (GCAP) that will be submitted to the NRC in 2010 for concurrence. The long-term ground water remedial action must be in place by 2012.

Ground water conditions

The former processing site is underlain by a high hydraulic conductivity alluvium that is connected to the Colorado River (Fig. 2). The alluvium has an anisotropic ratio of 10 to 100. A brine surface occurs beneath saline water. Ground water at the site occurs in alluvial sediments that extend 120 meters (400 feet) below the ground surface. Total dissolved solids (TDS) in ground water vary naturally from slightly saline (1,000 to 3,000 milligrams/liter [mg/L]) to briny (> 35,000 mg/L), usually increasing with depth. The primary source of the slightly saline water, which is found only in the shallowest parts of the saturated zone, appears to be ground water discharge from post-Paradox Salt Formation bedrock that subcrop near the northwest border of the site and north of the tailings pile as shown in Fig. 2. Brine waters dominate the deepest parts of the alluvium and are attributed to chemical dissolution of the underlying Paradox Salt Formation, a large evaporite unit that has deformed to create a salt-cored anticline aligned with and underlying the area.

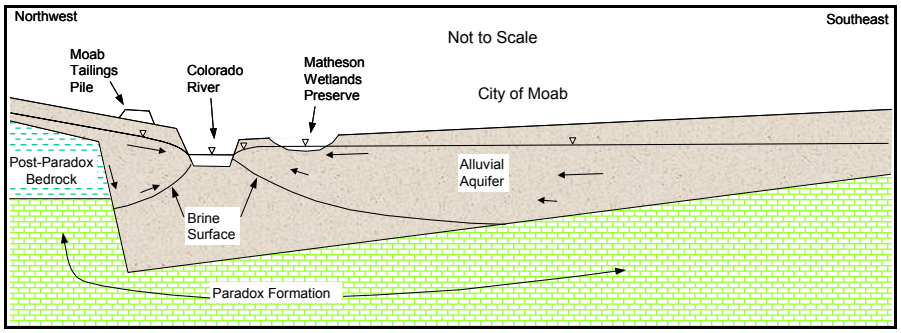

Fig. 2. The conceptual model shows density-dependent ground water flow in alluvium to the Colorado River.

Ground water contamination

During milling operations, the tailings pond contained fluids with TDS concentrations ranging from 50,000 to 150,000 mg/L. In addition, the fluids contained ammonia with concentrations up to 1,500 mg/L and uranium with concentrations up to 10 mg/L (DOE 2007). These fluids had sufficient density to migrate vertically downward through less saline waters and into underlying briny water. This downward migration created a secondary zone of ammonia contamination that may be a long-term source of ammonia in ground water. However, its slow movement, presence within naturally occurring brine, and its likely discharge to the middle of the Colorado River make remediation unnecessary.

Although several other metals are present in alluvial ground water, ammonia and uranium are the primary contaminants of concern.

DOE identified one significant ammonia plume (see Fig. 3) associated with the site. The tailings pile is the source of ammonia seeping into the shallow alluvium, then migrating southwest and discharging into the Colorado River.

EPA has no cleanup standard for ammonia in 40 CFR 192 since it is so prevalent and is an essential part of the nitrogen cycle; however, ammonia is the constituent of greatest ecological concern when it discharges to the Colorado River at levels toxic to aquatic habitat.

When DOE took over the Moab site and began sampling backwater channels of

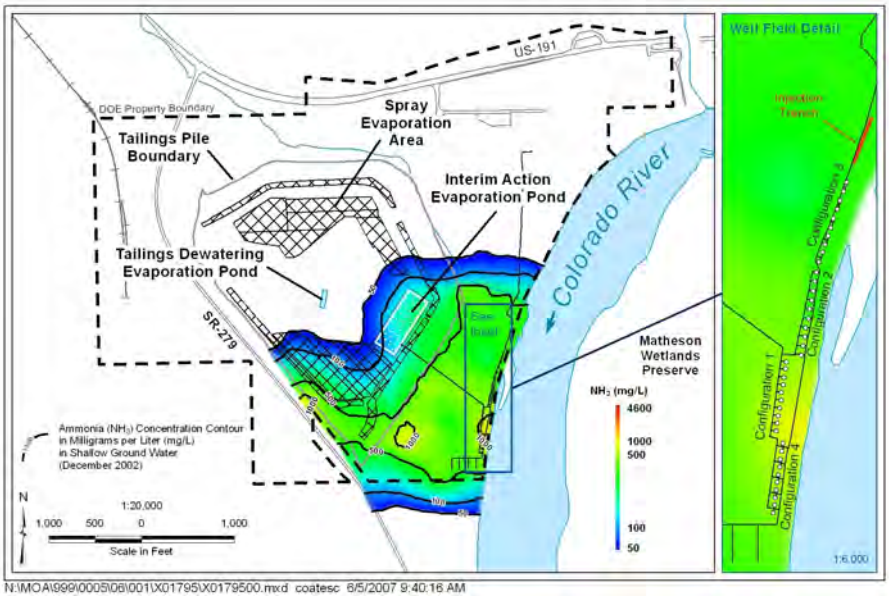

Fig. 3. The distribution of ammonia in shallow alluvial ground water is shown along with a backwater channel.

the Colorado River, ammonia was detected at concentrations that are toxic to certain endangered fish species that inhabit the river, including the Colorado pikeminnow, razorback sucker, bonytail, and humpback chub. Pikeminnow favor slow-moving backwater areas of the river as nursery habitat for young-of-the-year fish.

A plume of uranium in shallow alluvial ground water coincides with the ammonia plume (Fig. 3). A small secondary plume of uranium detected in ground water beneath the ore-processing portion of the site may have been caused by one or more of several sources including former ore storage, process areas, and disposal areas.

As tailings pile and off-pile remediation occur over the next several years, further information regarding the sources of the process area plume will be obtained. Over time, the two uranium plumes have comingled such that elevated concentrations exist within the shallow alluvium beneath a large portion of the site.

Because ground water at the Moab site is not potable, the drinking water standards established by EPA are not applicable. Even though more than 15 million people depend on water from the Colorado River, uranium from the Moab site is not discharged at a sufficient rate to be detectable in the river downstream of the site.

Ground water interim action

In 2003, DOE implemented the first phase of ground water remediation at the Moab site to address concerns regarding elevated ammonia concentration while it evaluates a long-term solution. The ground water interim action system has since been expanded and currently consists of 41 extraction wells, a freshwater injection trench, and an evaporation pond and sprinkler system to evaporate water on top of the tailings pile (Fig. 3).

Four groups of 10 wells, termed configurations, each of which were constructed with similar design features, were installed, with improvements made with every configuration design. In addition, a separate deeper extraction well is often included in Configuration 1 (not shown). Ground water is extracted through the wells from the shallow alluvium and pumped via pipeline to a 1.6-hectare (4-acre) evaporation pond that was constructed outside the 100-year floodplain on top of the tailings pile.

Several extraction wells, particularly in Configuration 2, were screened at shallow depths to minimize drawing up underlying brine during pumping. As a result, these wells have insufficient available drawdown to pump at high enough rates to achieve hydraulic capture of all proximate ground water contamination. Such effectiveness-reducing deficiencies are being evaluated for the long-term ground water remedy.

A 49-meter-long (160-foot-long) infiltration trench was added to the system north of the Configuration 3 wells in fall 2006. This 3-meter-deep (10-foot-deep) trench is designed to inject filtered Colorado River water into the subsurface, thus

creating a hydraulic barrier between the ammonia plume and the backwater areas of the river. The freshwater injection rate using the trench is comparable to the rate attained through a configuration of injection wells.

The impacts of freshwater injection and ground water extraction are based on samples collected from monitoring wells located in and around the well field including in backwater channels of the Colorado River (see Fig. 3). The effectiveness of the well field is evaluated by measuring the contaminant mass removed. Since the inception of well field operations, more than 375 million L (100 million gallons [g]) of ground water has been extracted. Approximately 45,000 kilograms (kg) (90,000 pounds [lbs]) of ammonia and 190 kg (400 lbs) of uranium are removed annually.

A sprinkler system that covers 16 hectares (38 acres) was installed on top of the pile to operate in conjunction with the evaporation pond to maximize the evaporative capacity of the interim action system. Ground water is sprayed at a rate such that it neither runs off nor percolates into the tailings pile cover soils. The site receives 230 millimeters (mm) (9 inches) of precipitation per year and has an annual pan evaporation of 140 mm (55 inches). The sprayed water also provides dust suppression. The extraction rate of the system averages 225 L/minute (60 gpm). Prior to the winter of 2007/2008, extraction was suspended during the colder months because of the reduced evaporation potential. However, to provide maximum protection of a habitat area downgradient of Configuration 1, several of the wells were operated through the majority of this past winter.

The existing interim action will likely be included in the final ground water remedial action. Current site operation and monitoring activities are, in part, designed to provide information for the final action.

Surface water runoff and its effect on aquatic habitat

The Colorado River overflows its banks about every 10 years. The last severe flooding was in 1983 when the river reached the edge of the tailings pile. The winter of 2007/2008 brought above-normal snowfall in the Rocky Mountains that caused concern for high spring runoff. Although the river twice came up to the bank along the well field at the site, no flooding occurred in 2008. Well field operations were suspended during part of May and June as a precautionary measure since flooding of variable-frequency pump motor controllers would have represented a substantial loss of property.

High river flows are known to alter the channel that creates or eliminates backwater habitat. The Moab Wash is an ephemeral intermittent stream that transects the site. Water flow in the wash caused by intense summer storm events carries a high sediment load. The result is a buildup of sediment downstream of the confluence that can add to the backwater habitat area.

Backwater pools form at the edge of the Colorado River as the river rises during normal runoff years. These backwater areas, which serve as fish habitat, may expose endangered fish species to ammonia from the site. As part of the EIS

process, DOE discussed with the U.S. Fish and Wildlife Service the discharge of contaminants to the Colorado River that could have a negative effect on these endangered species. DOE monitors the river water flow each year during spring runoff and is prepared to flush the backwater areas with diverted river water if ammonia concentrations reach an unacceptable level of 3 mg/L.

Long-term ground water remediation strategy

The long-term ground water remediation strategy has to take into account the potential presence of ground water contamination beneath the tailings pile that may remain following pile removal, off-pile sources of contamination such as former process, storage, and disposal areas, and changing habitat areas along the Colorado River.

DOE intends to continue ground water remediation during removal of the tailings pile. Extraction rates and the position of wells will be optimized to more effectively remove ammonia and uranium.

The spray evaporation system will be affected as soon as excavation and conditioning activities on top of the pile begin. Initially, this impact can be addressed by adjusting the location of spray nozzles. Extraction rates will be adjusted to accommodate reduced capacity of the spray evaporation system. Within 10 years, the evaporation pond may have to be eliminated or moved.

If the long-term ground water remediaton system must operate without the benefit of an evaporation system, then an alternative treatment method will be required. Several treatment methods are being considered, including ammonia stripping, recirculation wells, alternating injection and extraction wells, and air sparging with soil vapor extraction.

Conclusions

As the ground water interim action system is further evaluated, tailings removal begins, and the Colorado River channel is mapped following the runoff of 2008, a Final GCAP will be developed and submitted for NRC concurrence. Continued coordination with the U.S. Fish and Wildlife Service will take place to ensure protection of sensitive aquatic species.

Acknowledgment

This work was performed under DOE contract number DE-AC30-07CC60012 for the U.S. Department of Energy Office of Environmental Management, Grand Junction, Colorado, USA.

References

40 CFR 192, U.S. Environmental Protection Agency, “Health and environmental protection standards for uranium and thorium mill tailings”

U.S. Department of Energy (2003a) Migration potential of the Colorado River channel adjacent to the Moab project site, revision 2

U.S. Department of Energy (2003b) Site observational work plan, Moab UMTRA project, GJO-2003-424-TAC

U.S. Department of Energy (2007) 2006 Performance assessment of ground water interim action well field Moab, UT, DOE-EM/GJ1478-2007

Dispersion of uranium in the environment by fertilization

Ewald Schnug and Silvia Haneklaus

Institute for Crop and Soil Science, Federal Research Centre for Cultivated Plants, Julius Kühn Institute (JKI), Bundesallee 50, D-38116 Braunschweig, Germany

Abstract. It was the objective of this contribution to provide a comprehensive synopsis on the significance of the dispersion of uranium in the environment by common fertilizer practices. Recent studies revealed that uranium originating from fertilizers accumulates in soils over time and thereby increases uranium losses to water-bodies. Studies on the uranium content in soils and surface waters in relation to fertilizer practice substantiate such coherence. The most efficient and sustainable solution to the problem is the extraction of uranium from fertilizers.

Toxicological significance of uranium

Uranium (U) is a natural, chemo toxic and radiotoxic heavy metal. With view to the overall level of radioactivity in the environment U is certainly only a minor source of concern (Falck and Wymer 2006). The biochemical toxicity of the heavy metal U is estimated to be six orders of magnitude higher than the radiological toxicity (Milvy and Cothern 1990; NRC 2005). Compared to other heavy metals, the chemical toxicity of U ranges between mercury and nickel, or christoballite and warfarin (Busby and Schnug 2008).

Uranium shows toxic effects on all forms of life: The most common and unspecific one is DNA damage followed by mutations (Envirhom 2005; Henner 2008; Lin et al. 1993; Thiebault et al. 2006). The effect of U on DNA is a sinister combination of the biochemical and radiological toxicology of U. Uranium builds up in living systems inter alia due to its high affinity to phosphorus containing components such as DNA (Busby and Hooper 2007). Once attached to the DNA U amplifies natural background radiation and causes through photoelectron enhancement effects damages to the DNA. This effect occurs to an excess that is obviously much stronger than that from α-radiation of U (Busby, 2005; Schmitz-Feuerhake and Bertell 2008). Bishop (2005) proposed also a signaling from ra-

diated to neighboring cells, which received no direct radiation so that cellular damages are multiplied.

The older an individual is, the higher will be the amount of U that is accumulated. This implies that the risk for contracting damages from U generally increases not only with the amount, but also with the time of exposure and thus with age (WHO 2004).

Mammals have a particularly high sensitivity against U (Fellows et al. 1998). Uranium tends to accumulate in the body, preferentially in kidneys, liver, spleen and bones. Uranium is a popular and long known nephrotoxin (Blantz 1975, Boshard et al. 1992; Flamenboum et al. 1976; Lin and Lin 1988; Lin et al. 1993; Zamora et al. 1998). The most remarkable damage of U coming along with low and medium contaminations is cancer (Linsalata 1994). The studies of Envirhom (2005) revealed that the brain is a target for U toxicity, too. Its sensitivity seems to be similar to that of kidneys (Envirhom 2005).

Uranium in food and uranium uptake by humans

Under non-exposed conditions the daily intake of U from air by humans amounts to about 1 ng U (WHO 2004). Uranium in soils enters the food chain indirectly through plant uptake or directly through consumption of U in drinking waters. The transfer of U from soil to plant is significantly higher for vegetative than for generative plant parts. Concentration factors for U are around 0.05 and similar to that determined for As, Co, Hg and Pb (Schick et al. 2008).

With view to food, lowest U concentrations were found in seeds, leaves and fruits, while approximately three times higher U contents were found in meat. For meat the ranking poultry < pork < beef reflects the animals lifespan and thus accumulation of U. The highest concentrations of U occur in offal and shellfish (Schnug et al. 2005).

A human has an average daily U intake of around 2.5 µg U when a simplified daily diet of 2000 kcal is assumed with 60% cereals and cereal products (1.5 µg/kg U), 20% meat and meat products (5 µg/kg U), 10% vegetables (2 µg/kg U) and 10% fruits (1 µg/kg U) (Schnug et al. 2005; Pais and Benton Jones jr. 1997; WHO 2004). Even a carnivore with a skewed affectation for offal or shellfish might increase this value only to at maximum 4 µg U, while a strict vegan cannot reduce the value below 1 µg U.

In contrast to solid food, the U concentration in drinking water has a distinctly stronger influence on the daily U intake by humans (Cothern and Lappenbusch 1983; Schnug et al. 2005). Water is the most significant factor for the daily amount of U taken up by an individual. The intake of U by water can exceed the intake through solid foods in extreme cases by factor 10 and more if the daily water consumption is 2 L (40 mL/kg body mass according to Heseker (2005)). Thus the evaluation of the U intake by humans requires comprehensive information about U concentrations in drinking waters.

Environmental loads of uranium originating from fertilization

The most likely largest non-point source emitters of U in Germany are agriculture, horticulture and forestry through the use of mineral phosphorus fertilizers. Even under conditions of good agricultural practice (Sharpley and Withers 2004) the annual amount of U unconsciously dispersed in the environment amounts on an average to 10 g/ha (Kratz et al. 2008). Depending on fertilizer type and intensity this U accumulates in soils with rates between 1- 46 µg/ha·yr (Rogasik et al. 2008; Taylor and Kim 2008). Utermann and Fuchs (2008) estimated that in Germany the mean U content in arable soils is 0.15 mg/kg higher than in soils under forestry. This difference can be completely explained by 45 years of cropping with phosphorus fertilization in an agricultural production system operating on a typical intensity level.

Fertilizer derived U in soils is prone to easy leaching, because U is comparatively mobile under pH and redox conditions of typical soils that underlie anthropogenic management (Jaques et al. 2005; Read et al. 2008). Transfer of U originating from fertilizers into water bodies is a fact and was proven in numerous research projects (Azuoazi et al. 2001; Barisic et al. 1992; Conceicao and Bonotto 2000; Hule et al. 2008; Kobal et. al. 1990; Zielinski et al. 1995). Already in 1972 Spalding and Sackett attributed increased U concentrations in North American rivers of ~ 0.7 - 0.9 µg/L U, compared to ~ 0.1 - 0.2 µg/L U in South American rivers (Cothern and Lappenbusch 1983), to the use of phosphate fertilizers in the region. Also Birke and Rauch (2008) found elevated U concentrations in river waters in some regions of Germany. The authors could not fully explain the data by geological factors and assumed that agricultural activities are accountable.

Most recently evidence was provided that, in full accordance with the prognosis of Jacques et al. (2005 & 2008), U originating from fertilizers starts to contaminate groundwater bodies and finally shows up in drinking waters:

Schäf et al. (2007) found a close correlation between U and nitrate in drinking waters from the Rhine-Neckar region. Nitrate is like U easily mobile in soils, increases in ground and drinking water with fertilizer intensity and thus seems to be a suitable indicator for monitoring U transfer from fertilizers to waters.

Schulz et al. (2008) report twice as high U concentrations in drinking waters collected in former West Germany compared to former East Germany. A reasonable explanation is given by the facts that in the former East fertilization intensity was significantly lower and phosphate fertilizer products were employed, which had a lower U content than those used in the West. Consequently Rogasik et al. (2008) determined significantly higher amounts of U that accumulated in long-term phosphorus fertilization experiments in soils of the former East than in West Germany (Rogasik et al. 2008).

Knolle (2008) showed that the variability of boron concentrations explain a significant amount of the U concentrations in German tap waters. Boron is like U applied in significant amounts with phosphorus fertilizers: FAL-PB (2007) reports boron concentrations between 200 and 800 mg/kg B in various phosphorus con-

taining fertilizers, which makes the amount of boron applied with phosphorus fertilizers five times higher than the amount of U applied. Boron is like U easily mobile in soils, which makes it prone to leaching and hence a suitable indicator for monitoring the U transfers from fertilizers to waters.

Finally, leaching of fertilizer derived U from soils to water bodies is expected to increase in the Northern hemisphere in the course of global climate change because of increased rainfall during summer.

Controlling loads of uranium originating from fertilizers

With view to the negative impacts of U on humans and environment the 'Precautionary Principle'[1] should be applied in order to protect water bodies from anthropogenic U contamination. Particularly soils deserve to be protected from U contamination through fertilization, as they are the most vulnerable interface between agriculture and adjacent ecosystems. In this context it is more than surprising that U is the only toxic heavy metal for which no critical or guideline values in soils exist, which address the protection of soils and water bodies, respectively (Ekardt and Schnug 2008). Only Canada released most recently a soil quality guideline value for the protection of both human and environmental health of 23 mg/kg U soil with the restriction that a lower content may need to be considered on sites where drinking water is sourced (CCME 2007).

The most effective measure to limit loads of fertilizer derived U to soils is to regulate U concentrations in fertilizers. Uranium is easy to separate during the manufacturing process of fertilizers (Kratz and Schnug 2006; Hu et al. 2008) and then no longer threat to health and environment, but a source of energy and a resource for chemical processes (Lindemann 2007; Hauser and Meyer 2007; Hu et al. 2008). Regulating U in fertilizers would be a significant contribution to prevent disease in humans through healthy environments (Prüss-Üstün and Corvalán 2006).

References

Azouazi M, Ouahidi Y, Fakhi S, Andres Y, Abbe J C, Benmansour M (2001) Natural radioactivity in phosphates, phosphogypsum and natural waters in Morocco. Journal of Environmental Radioactivity 54: 231-242.

Barisic D, Lulic S, Miletic P (1992) Radium and uranium in phosphate fertilizers and their impact on the radioactivity of waters. Water Research 26: 607-611.

[1] "When an activity raises threats of harm to human health or the environment, precautionary measures should be taken even if some cause and effect relationships are not fully established scientifically" (Montague 2008)

Birke M, Rauch U (2008) Uranium in stream water of the Federal Republic of Germany. In: De Kok, L.J. and Schnug, E. (Eds) Loads and Fate of Fertilizer-derived Uranium. Backhuys Publishers, Leiden, The Netherlands.

Bishop D (ed.) (2005) Compendium of Uranium and Depleted Uranium Research 1942 to 2004. http://www.idust.net/Compendium/Compendium.htm

Blantz R C (1975) The mechanism of acute renal failure after uranyl nitrate. J. Clin. Invest. 55: 621-635.

Bosshard E, Zimmerli B, Schlatter C (1992) Uranium in the diet: risk assessment of its nephro- and. radiotoxicity. Chemosphere 24: 309-321.

Busby C 2005. Does uranium contamination amplify natural background radiation dose to the DNA? Eur. J. Biol. Bioelectromagn. 1: 120-131.

Busby C, Hooper M (2007) Final Report of the UK Ministry of Defence Depleted Uranium Oversight Board (www.duob.org), pp. 51-74.

Busby C, Schnug E (2008) Advanced biochemical and biophysical aspects of uranium contamination. In: De Kok, L.J. and Schnug, E.(Eds) Loads and Fate of Fertilizer-derived Uranium. Backhuys Publishers, Leiden, The Netherlands.

CCME (2007) Canadian Council of Ministers of the Environment Canadian Soil Quality Guidelines for Uranium: Environmental and Human Health. Scientific Supporting Document PN 1371. ISBN 978-1-896997-64-3 PDF http://www.ccme.ca/assets/pdf/uranium_ssd_soil_1.0_e.pdf

Conceicao F T, Bonotto D M (2000) Anthropogenic influences on the uranium concentration in waters of the Corumbatai river basin (SP), Brazil. Revista Brasileira de Geosciecias 30: 555-557.

Cothern C R, Lappenbusch W L (1983) Occurrence of uranium in drinking water in the U.S.. Health Physics 45:89-99.

Ekardt F, Schnug E (2008) Legal aspects of uranium in environmental compartments. In: De Kok, L.J. and Schnug, E. (Eds) Loads and Fate of Fertilizer-derived Uranium. Backhuys Publishers, Leiden, The Netherlands.

Envirhom (2005) Bioaccumulation of radionuclides in situations of chronic exposure of ecosystems and members of the public. Progress Report 2 covering the period June 2003 – September 2005. Report DRPH 2005-07 & DEI 2005-05; DIRECTION DE LA RADIOPROTECTION DE L'HOMME DIRECTION DE L'ENVIRONNEMENT ET DE L'INTERVENTION

FAL-PB (2007) unpublished data of the institutes FAL-PB, deriving from the project: Kördel W, Herrchen M, Müller J, Kratz S, Fleckenstein J, Schnug E, Saring Dr, Thoma J, Haaman H, Reinhold J (2007) Begrenzung von Schadstoffeinträgen bei Bewirtschaftungsmaßnahmen in der Landwirtschaft bei Düngung und Abfallverwertung. Forschungsbericht 202 33 305 und 202 74 271, UBA-FB 001017. UBA-Texte 30/07.

Falck W E, Wymer D (2006) Uranium in phosphate fertilizer production. In: Merkel, B. J. and Hasche-Berger, A. (Eds.) Uranium in the environment. Springer, Berlin Heidelberg 2006, pp. 857-866.

Fellows R J, Ainsworth C C, Driver C J, Cataldo D A (1998) Dynamics and transformations of radionuclides in soils and ecosystem health. Soil Chemistry and Ecosystem Health. Soil Science Society of America. Special Publication No.52, 85-112.

Flamenboum W, Hamburger R J, Huddleston J, Kaufman J S, McNeil J H, Schwartz J H, Nagle R (1976) The initiation phase of experimental acute renal failure: an evaluation of uranyl nitrate-induced renal failure in the rat. Kidney Int. 10: 115-122.

Hauser C, Meyer K (2007) Uranchemie zwischen Phobie und Begeisterung. Nachrichten aus der Chemie 55: 1195-1194.

Henner P (2008) Bioaccummulation aof radionuclides and induced biological effects in situations of chronic exposure of ecosystems – a uranium case study. In: De Kok, L.J. and Schnug, E. (Eds) Loads and Fate of Fertilizer-derived Uranium. Backhuys Publishers, Leiden, The Netherlands.

Heseker H (2005) Untersuchungen zur ernährungsphysiologischen Bedeutung von Trinkwasser in Deutschland. DGE-aktuell 01/2005 vom 12.01.2005. http://www.forum-trinkwasser.de/studien/Studie1/Studie1_Inhalt.htm

Hu Z H, Zhang H X, Wang F, Haneklaus S, Schnug E (2008) Combining energy and fertilizer production – vision for China's future. In: De Kok, L.J. and Schnug, E. (Eds) Loads and Fate of Fertilizer-derived Uranium. Backhuys Publishers, Leiden, The Netherlands.

Hule B, Kummer S, Stadler S, Merkel B (2008) Mobility of uranium from phosphate fertilizers in sandy soils. In: De Kok, L.J. and Schnug, E.(Eds) Loads and Fate of Fertilizer-derived Uranium. Backhuys Publishers, Leiden, The Netherlands.

Jacques D, Šimůnek J, Mallants D, van Genuchten M (2005) Modelling uranium leaching from agricultural soils to groundwater as a criterion for comparison with complementary safety indicators. In: Symposium Proceedings. Scientific Basis for Nuclear Waste Management XXIX, Gent, Belgium, 12-16 September 2005 / SCK•CEN, Warrendale, United States, Materials Research Society, 2006, pp. 1057-1064.

Jacques D, Mallants M, Šimůnek J, van Genuchten M (2008) Modelling the fate of U from inorganic P-fertilizer applications in agriculture. In: De Kok, L.J. and Schnug, E. (Eds) Loads and Fate of Fertilizer-derived Uranium. Backhuys Publishers, Leiden, The Netherlands.

Knolle,F. 2008. Ein Beitrag zu Vorkommen und Herkunft von Uran in deutschen Mineral- und Leitungswässern.PhD thesis, TU Braunschweig, Germany (in press).

Kobal I, Vaupotic J, Mitic D, Kriston J, Ancik M, Jerancic S, Skofljanec M (1990) Natural radioactivity of fresh waters in Slovenia, Yugoslavia. Environmental International 16: 141-154.

Kratz S, Schnug E (2006) Rock phosphates and P fertilizers as sources of U contamination in agricultural soils. In: Merkel, B. J. and Hasche-Berger, A. (Eds.) Uranium in the environment, pp. 57-68. Springer, Berlin.

Kratz S, Knappe F, Schnug E (2008) Uranium balances in agroecosystems. In: De Kok L. J. and Schnug, E. (Eds) Loads and Fate of Fertilizer-derived Uranium. Backhuys Publishers, Leiden, The Netherlands.

Lin R H, Wu L J, Lee C H, Lin-Shiau S Y (1993) Cytogenetic toxicity of uranyl nitrate in Chinese hamster ovary cells. Mutation Research 319: 197-203.

Lin J H, Lin T H (1988) Reanal handling of drugs in renal failure I: Differential effects of uranyl nitrate- and glycerol-induced acute renal failure on renal excretion of TEAB and PAH in rats. J Pharmacol. Exp. Ther. 246: 896-901.

Lindemann I (2007) Futter für Dimona. Strahlentelex 496-497, 6-19. http://www.strahlentelex.de/Stx_07_496_S06-10.pdf

Linsalata P (1994) Uranium and thorium decay series radionuclides in human and animal food chains--A review. J. Environ. Qual. 23 : 633-642.

Milvy P, Cothern C R (1990) Scientific background for the development of regulations for radionuclides in drinking water. In: Radon, Radium and Uranium in Drinking Water (Eds. C. R. Cothern and P. Rebers), Lewis Publishers, Chelsea, Michigan.

Montague P (2008) The precautionary principle in the real world. Environmental Research Foundation. January 21, 2008. http://www.rachel.org/lib/pp_def.htm; Wingspread Statement 2002. Statement on the Precautionary Principle. In: Rampton, S. and Staubner. J. (Eds), Trust us we're experts! Jeremy Putnam Inc., New York.

NRC (2005) The Nuclear Regulatory Commission (NRC) invites comment on petition for rulemaking concerning chemical toxicity of uranium. Docket No. PRM-20-26. Federal Register: June 15, 2005 (Volume 70).

Pais I, Benton Jones jr. J (1997) Uranium. In: The handbook of trace elements. St. Lucie Press, Boca Raton, Florida, pp 143-144.

Prüss-Üstün A, Corvalán A (2006) Preventing disease through healthy environments: Towards an estimate of the environmental burden of disease. ISBN 978 92 4 159420 2. http://www.who.int/quantifying_ehimpacts/publications/preventingdisease/en/index.html

Read D, Black S, Trueman E, Arnold T, Baumann N (2008) The fate of depleted uranium in near surface environments. In: De Kok, L.J. and Schnug, E. (Eds) Loads and Fate of Fertilizer-derived Uranium. Backhuys Publishers, Leiden, The Netherlands.

Rogasik J, Kratz S, Funder U, Panten K, Schnug E, Barkusky D, Baumecker M, Gutser R, Lausen P, Scherer H W, Schmidt L (2008) Uranium in soils of German long-term fertilizer trials. In: De Kok, L.J. and Schnug, E. (Eds) Loads and Fate of Fertilizer-derived Uranium. Backhuys Publishers, Leiden, The Netherlands.

Schäf M, Daumann L, Erdinger L (2007) Uran in Trinkwasserproben im Rhein-Neckar Gebiet. Umweltmed Forsch Prax 12, 315.

Schick J, Schroetter S, Lamas M C, Rivas M C, Kratz S, Schnug E (2008) Soil/plant interface of U. In: De Kok, L.J. and Schnug, E. (Eds) Loads and Fate of Fertilizer-derived Uranium. Backhuys Publishers, Leiden, The Netherlands.

Schmitz-Feuerhake I, Bertell R (2008) Radiological aspects of uranium contamination. In: De Kok, L.J. and Schnug, E. (Eds) Loads and Fate of Fertilizer-derived Uranium. Backhuys Publishers, Leiden, The Netherlands.

Schnug E, Steckel H, Haneklaus S (2005) Contribution of uranium in drinking waters to the daily uranium intake of humans - a case study from Northern Germany. Landbauforsch Völkenrode 55, 227-236.

http://www.fal.de/nn_787874/SharedDocs/01__PB/DE/Downloads/LBF/2005/downloads-pb1900,templateId=raw,property=publicationFile.pdf/downloads-pb1900.pdf

Schulz C, Rapp T, Conrad A, Hünken A, Seiffert L, Becker K, Seiwert M, Kolossa-Gehring M (2008) Elementgehalte im häuslichen Trinkwasser aus Haushalten mit Kindern in Deutschland. Forschungsbericht 202 62 219 UBA-FB 001026. WaBoLu Hefte 04/08. ISSN 1862-4340

Sharpley A N, Withers J A (2004) The environmentally-sound management of agricultural phosphorus. Nutrient Cycling in Agroecosystems 39: 133-146

Spalding RF, Sackett W M (1972) Uranium runoff from the Gulf of

Mexico. Distribution province anomalous concentration. Science 175 : 629-631.

Taylor M, Kim N (2008) The fate of uranium contaminants of phosphate fertilizers. In: De Kok, L.J. and Schnug, E. (Eds) Loads and Fate of Fertilizer-derived Uranium. Backhuys Publishers, Leiden, The Netherlands.

Thiebault C, Carrière M, Milgram S, Gouget B (2006) Cyto and genotoxicity of natural uranium after acute or chronic exposures of normal rat kidney cells in favour of a cell transformation? Toxicology Letters 197: 14-23.

Utermann J, Fuchs M (2008) Uranium contents in German soils. In: De Kok, L.J. and Schnug, E. (Eds) Loads and Fate of Fertilizer-derived Uranium. Backhuys Publishers, Leiden, The Netherlands.

WHO (2004) Uranium in Drinking-water, Background document for development of WHO Guidelines for Drinking-water Quality, World Health Organization.

Zamora M L, Tracy B L, Zielinski J M, Meyerhof D P, Moss M A (1998) Chronic ingestion in drinking water : a study of kidney bieoeffects in humans. Toxicol. Sci. 43: 68-77.

Zielinski R A, Asher-Bolinder S, Meier A L (1995) Uraniferous waters of the Arkansas River valleys, Colorado, USA: A function of geology and landuse. Applied Geochemistry 10: 133-144.

The Potential of Thorium Deposits

Ulrich Schwarz-Schampera

B4.23 Lagerstättenforschung, Bundesanstalt für Geowissenschaften und Rohstoffe, Stilleweg 2, 30655 Hannover

Abstract. Increased uranium prices are continuing to impact uranium resource totals. Many countries have developed ambitious programs for their future energy supply and the use of nuclear energy is regarded a secure option. A number of industrialized and rapidly developing countries lack major uranium resources and the use of thorium as an alternative in the fuel cycle is envisaged. Up to now thorium has had a limited market and there has been little incentive to explore or to develop detailed information on known thorium deposits. This paper presents new data on worldwide thorium resources and potential future use as nuclear fuel.

Thorium Occurrences and Characteristics

Thorium is much more abundant in nature than uranium. Thorium is a naturally-occurring, slightly radioactive metal discovered in 1828 by the Swedish chemist Jons Jakob Berzelius, who named it after Thor, the Norse god of thunder. It is found in small amounts in most rocks and soils, where it is about three times more abundant than uranium. Soil commonly contains an average of around 6 parts per million (ppm) of thorium. Thorium occurs in several minerals, the most common source being the rare earth-thorium-phosphate mineral, monazite, which contains 6-7% in average and up to 12% thorium oxide. A second major source is (urano)thorianite, a suggested name for a mineral intermediate between uraninite and thorianite ($Th,U)O_2$). Monazite and uranothorianite are found in igneous and metamorphic rocks but the richest concentrations are in secondary placer deposits, concentrated by fluviatile, marine and aeolien processes with other heavy minerals. Large thorium enrichments occur in Precambrian metamorphic belts like in southern and eastern Africa, India, Australia and in Scandinavia. Major thorium deposit types include carbonatites, placers, vein-type deposits in metamorphic terranes, and deposits associated with intrusive alkaline rocks. Today, thorium is recovered mainly from monazite as a by-product of processing heavy mineral sand deposits for titanium-, zirconium- or tin-bearing minerals.

When pure, thorium is a silvery white metal that retains its lustre for several months. However, when it is contaminated with the oxide, thorium slowly tarnishes in air, becoming grey and eventually black. Thorium oxide (ThO_2), also called thoria, has one of the highest melting points of all oxides (3300°C). When heated in air, thorium metal turnings ignite and burn brilliantly with a white light. Because of these properties, thorium has found applications in light bulb elements, lantern mantles, arc-light lamps, welding electrodes and heat-resistant ceramics. Glass containing thorium oxide has a high refractive index and dispersion and is used in high quality lenses for cameras and scientific instruments.

Thorium Resources

World monazite resources are estimated to be about 12 million tonnes, two thirds of which are in heavy mineral sands deposits on the south and east coasts of India. There are substantial deposits in several other countries (Table 1). Thorium deposits are found in several countries around the world. The largest thorium reserves are expected to be found in Australia, India, USA, Norway, Canada, and in countries such as South Africa and Brazil. Reserves and additional resources total 6.078 Mio t Th. This number, however, excludes data from much of the world.

Thorium as a Nuclear Fuel

Thorium can be used as a nuclear fuel through breeding to uranium-233 (U-233). Thorium-232 decays very slowly (its half-life is about three times the age of the earth) but other thorium isotopes occur in its and in uranium's decay chains. Most

Table 1. Estimated World thorium resources (RAR + Inferred to USD 80/kg Th) [a].

Country	Tonnes	%
Australia	452 000	17,6
USA	400 000	15,6
Turkey	344 000	13,4
India	319 000	12,4
Brazil	302 000	11,7
Venezuela	300 000	11,7
Norway	132 000	5,1
Egypt	100 000	3,9
Russia	75 000	2,9
Greenland	54 000	2,1
Canada	44 000	1,7
South Africa	18 000	0,7
Other Countries	33 000	1,3
Total	2 573 000	

[a] Uranium 2007: Resources, Production and Demand.

of these are short-lived and hence much more radioactive than Th-232, though on a mass basis they are negligible. Although not fissile itself, thorium-232 (Th-232) will absorb slow neutrons to produce uranium-233 (U-233), which is fissile (and long-lived). Hence like uranium-238 (U-238) it is fertile. In one significant respect U-233 is better than uranium-235 and plutonium-239, because of its higher neutron yield per neutron absorbed. Given a start with some other fissile material (U-235 or Pu-239), a breeding cycle similar to but more efficient than that with U-238 and plutonium (in normal, slow-neutron reactors) can be set up. However, there are also features of the neutron economy which counter this advantage. In particular Pa-233 is a neutron absorber which diminishes U-233 yield. The Th-232 absorbs a neutron to become Th-233 which quickly beta decays to protactinium-233 and then more slowly to U-233. The irradiated fuel can then be unloaded from the reactor, the U-233 separated from the thorium, and fed back into another reactor as part of a closed fuel cycle. When the thorium fuel cycle is used, much less plutonium and other transuranic elements are produced, compared with uranium fuel cycles.

Over the last 30 years there has been interest in utilising thorium as a nuclear fuel since it is more abundant in the Earth's crust than uranium. Also, all of the mined thorium is potentially useable in a reactor, compared with the 0.7% of natural uranium, so some 40 times the amount of energy per unit mass might theoretically be available (without recourse to fast breeder reactors). Basic research and development has been conducted in Germany, India, Japan, Russia, the UK and the USA. Test reactor irradiation of thorium fuel to high burnups has also been conducted and several test reactors have either been partially or completely loaded with thorium-based fuel.

Several reactor concepts based on thorium fuel cycles are under consideration (e.g., the Light Water Breeder Reactor concept). A major potential application for conventional PWRs involves fuel assemblies arranged so that a blanket of mainly thorium fuel rods surrounds a more-enriched seed element containing U-235 which supplies neutrons to the subcritical blanket. As U-233 is produced in the blanket it is burned there. The breeder reactor concept is currently being developed in a more deliberately proliferation-resistant way. The central seed region of each fuel assembly will have uranium enriched to 20% U-235. The blanket will be thorium with some U-238, which means that any uranium chemically separated from it (for the U-233) is not useable for weapons. Spent blanket fuel also contains U-232, which decays rapidly and has very gamma-active daughters creating significant problems in handling the bred U-233 and hence conferring proliferation resistance. Plutonium produced in the seed will have a high proportion of Pu-238, generating a lot of heat and making it even more unsuitable for weapons than normal reactor-grade Pu. A variation of this is the use of whole homogeneous assembles arranged so that a set of them makes up a seed and blanket arrangement. If the seed fuel is metal uranium alloy instead of oxide, there is better heat conduction to cope with its higher temperatures. Seed fuel remains three years in the reactor, blanket fuel for up to 14 years.

Between 1967 and 1988, the AVR (Atom Versuchs Reaktor) experimental pebble bed reactor at Julich, Germany, operated for over 750 weeks at 15 MWe, about

95% of the time with thorium-based fuel. The fuel used consisted of about 100 000 billiard ball-sized fuel elements. Overall a total of 1360 kg of thorium was used, mixed with high-enriched uranium (HEU). Maximum burnups of 150,000 MWd/t were achieved.

Worldwide, the highest activity on thorium as a nuclear energy source is found in India where the Kakrapar-1 and -2 power plants are loaded with 500 kg of thorium blanket. Kakrapar-1 was the first nuclear reactor in the world to use thorium in the blanket, rather than depleted uranium, to achieve power flattening across the reactor core. In addition, the use of thorium based fuel is planned in 4 reactors, which are currently under construction.

India has about 1 % of the world's uranium resources while the thorium resources are one of the largest in the world with about 300 000 tonnes. With about six times more thorium than uranium, India has made utilization of thorium for large-scale energy production a major goal in its nuclear power program, utilizing a three-stage approach:

1. Pressurized Heavy Water Reactors (PHWRs), elsewhere known as CANDUs (CANada Deuterium Uranium) fuelled by natural uranium and Light Water Reactors (LWRs) of the Boiling Water Reactor (BWR) and VVER types. In this stage plutonium is produced.
2. Fast Breeder Reactors (FBRs) that use this plutonium-based fuel to breed U-233 from thorium. The blanket around the core will have uranium as well as thorium, so that further plutonium (ideally high-fissile plutonium) is produced as well as the U-233.
3. Advanced Heavy Water Reactors (AHWRs) that burn the U-233 and plutonium with thorium, getting about 75 % of their power from the thorium.

India's future program on thorium based nuclear power is important for India's long term energy security. Some research and development activities are also carried out on the Compact High Temperature Reactor (CHTR) and on the subcritical Accelerator Driven System (ADS) including the development of a high power proton accelerator.

Since the early 1990s Russia has had a program to develop a thorium-uranium fuel, which more recently has moved to have a particular emphasis on utilisation of weapons-grade plutonium in a thorium-plutonium fuel. The program is based at Moscow's Kurchatov Institute and involves the US company Thorium Power and US government funding to design fuel for Russian VVER-1000 reactors. Whereas normal fuel uses enriched uranium oxide, the new design has a demountable centre portion and blanket arrangement, with the plutonium in the centre and the thorium (with uranium) around it The Th-232 becomes U-233, which is fissile - as is the core Pu-239. Blanket material remains in the reactor for 9 years but the centre portion is burned for only three years (as in a normal VVER). The design of the seed fuel rods in the centre portion draws on extensive experience of Russian navy reactors.

The thorium-plutonium fuel claims four advantages over MOX: proliferation resistance, compatibility with existing reactors - which will need minimal modification to be able to burn it, and the fuel can be made in existing plants in Russia. In addition, a lot more plutonium can be put into a single fuel assembly than with

MOX, so that three times as much can be disposed of as when using MOX. The spent fuel amounts to about half the volume of MOX and is even less likely to allow recovery of weapons-useable material than spent MOX fuel, since less fissile plutonium remains in it. With an estimated 150 tonnes of weapons plutonium in Russia, the thorium-plutonium project would not necessarily cut across existing plans to make MOX fuel.

In 2007 Thorium Power formed an alliance with Red Star nuclear design bureau in Russia which will take forward the program to demonstrate the technology in lead-test fuel assemblies in full-sized commercial reactors.

Much experience has been gained in thorium-based fuel in power reactors around the world, some using high-enriched uranium (HEU) as the main fuel:

The 300 MWe THTR (Thorium High-Temperature Reactor) reactor in Germany was developed from the AVR and operated between 1983 and 1989 with 674,000 pebbles, over half containing Th/HEU fuel (the rest graphite moderator and some neutron absorbers). These were continuously recycled on load and on average the fuel passed six times through the core. Fuel fabrication was on an industrial scale.

The Fort St Vrain reactor was the only commercial thorium-fuelled nuclear plant in the USA, also developed from the AVR in Germany, and operated 1976 - 1989. It was a high-temperature (700°C), graphite-moderated, helium-cooled reactor with a Th/HEU fuel designed to operate at 842 MWth (330 MWe). The fuel was in microspheres of thorium carbide and Th/U-235 carbide coated with silicon oxide and pyrolytic carbon to retain fission products. It was arranged in hexagonal columns ('prisms') rather than as pebbles. Almost 25 tonnes of thorium was used in fuel for the reactor, and this achieved 170,000 MWd/t burn-up. Thorium-based fuel for Pressurised Water Reactors (PWRs) was investigated at the Shippingport reactor in the USA using both U-235 and plutonium as the initial fissile material. It was concluded that thorium would not significantly affect operating strategies or core margins. The light water breeder reactor (LWBR) concept was also successfully tested here from 1977 to 1982 with thorium and U-233 fuel clad with Zircaloy using the 'seed/blanket' concept. The 60 MWe Lingen Boiling Water Reactor (BWR) in Germany utilised Th/Pu-based fuel test elements.

Developing a Thorium-Based Fuel Cycle

The fact that thorium is much more abundant in nature than uranium and the progres in technology still attract countries with limited uranium resources but ambitious programs for the future use of nuclear power. Up to now, production of thorium has been limited due to a lack of demand. Thorium is largely a by-product of the separation of rare earth elements. The production of thorium is presently some hundred tonnes per year. The production reached about 1000 tonnes in the 1970s, and has decreased thereafter due to lack of demand. Owing to its chemical toxicity, radiotoxicity and pyrophoricity, adequate precautions are required in the mining and processing of thorium. However, as a result of the very long half-life of

thorium, limited quantities of pure thorium-232 can easily be handled, while some shielding is required for large amounts. Preparation of thorium fuel is somewhat more complex and more expensive than for uranium. Thorium as a nuclear fuel is technically well established and behaves remarkably well in Light Water Reactors and High Temperature Reactors. It has demonstrated a very good neutron damage resistance due to its excellent chemical and metallographic stability. However, despite the thorium fuel cycle having a number of attractive features, development even on the scale of India's has always run into difficulties.

The main attractive features include (i) the possibility of utilising a very abundant resource which has hitherto been of so little interest that it has never been quantified properly, (ii) the production of power with few long-lived transuranic elements in the waste, (iii) reduced radioactive wastes generally.

The problems include (i) the high cost of fuel fabrication, due partly to the high radioactivity of U-233 chemically separated from the irradiated thorium fuel. Separated U-233 is always contaminated with traces of U-232 (69 year half life but whose daughter products such as thallium-208 are strong gamma emitters with very short half lives); (ii) the similar problems in recycling thorium itself due to highly radioactive Th-228 (an alpha emitter with two-year half life) present; (iii) some weapons proliferation risk of U-233 (if it could be separated on its own); (iv)

the technical problems in reprocessing solid fuels. However, these problems may largely disappear if the fuel is used a Molten Salt Reactor.

Much development work is still required before the thorium fuel cycle can be commercialised, and the effort required seems unlikely while (or where) abundant uranium is available. Nevertheless, the thorium fuel cycle, with its potential for breeding fuel without the need for fast-neutron reactors, holds considerable potential long-term. It is a significant factor in the long-term sustainability of nuclear energy.

References

Thorium based fuel options for the generation of electricity: Developments in the 1990s, IAEA-TECDOC-1155, International Atomic Energy Agency, May 2000.

Thorium as an energy source - Opportunities for Norway. The Thorium Report Committee, 2008, p. 1-150

The role of thorium in nuclear energy, Energy Information Administration/ Uranium Industry Annual, 1996, p.ix-xvii.

Nuclear Chemical Engineering (2nd Ed.), Chapter 6: Thorium, M Benedict, T H Pigford and H W Levi, 1981, McGraw-Hill, p.283-317, ISBN: 0-07-004531-3.

Kazimi M.S. 2003, Thorium Fuel for Nuclear Energy, American Scientist Sept-Oct 2003.

Morozov et al 2005, Thorium fuel as a superior approach to disposing of excess weapons-grade plutonium in Russian VVER-1000 reactors. Nuclear Future?

OECD NEA & IAEA, 2008, Uranium 2007: Resources, Production and Demand.

Mining of Uranium in Kazakhstan

Gulzhan Ospanova[1], Ivan Mazalov[2] and Zhaksylyk Alybayev[3]

[1]Kazakh National Technical University, 22, Satpayev Str., 050013, Almaty, Kazakhstan

Abstract. Approximately one-fifth of the world uranium reserves are found in Kazakhstan. Deposits are divided among six uranium ore provinces according to geological positions, generic features and territorial location. Characteristics of uranium mineralization of deposits are given. In-situ leaching (ISL) technology of uranium recovery from low-grade ore of sand-stone deposits is given and based on selective dissolving of uranium bearing minerals.

Uranium deposits

Uranium deposits discovered in Kazakhstan are different in terms of generic conditions and practical use. Common character of geological positions, generic features and territorial location allow us to divide them into six uranium ore provinces: Chu-Sarysuiskaya, Syrdaryinskaya, North Kazakhstan, Mangyshlakskaya, Kendyktas-Chuili-Betpakdalinskaya, Ilyiskaya.

The first commercial uranium deposit, Kurday, was discovered in 1951 at a location west of Almaty. In the mid 1950s, the first uranium deposit of Kazakhstan was discovered north of Kurday; incorporating several rich and relatively small hydrothermal fields.

The second uranium deposit is in the provice of North of Kazakhstan, and it incorporates many medium- and large-sized hydrothermal fields such as Dzhidely, Grachevskoye, and Kosachinoye. In the mid-1990s, the largest uranium concentrate production plant, Tselinnyi mining and chemical plant, began to operate on the basis of those reserves. The remaining production base allows the use of some of those fields.

The third deposit is in the west of Kazakhstan near the Caspian Sea. The deposit contains rare-earth metals and phosphate. Uranium was produced there along with phosphorites. Aktau (fomer Shevchenko), one of the oil capitals, was established due to the uranium production.

The fourth province is in the east of Kazakhstan along the bank of the Ili river. The deposit comprises two large uranium and coal fields, Kolzhat and Nizhne-Iliyskoye.

At the end of the 1960s, a number of large fields were discovered in the south of Kazakhstan north from the Karatau mountain range. These fields represent the largest reserve of Uranium in the world and are located in the provice of Chu-Sarysu. The deposit includes the unique fields Inkai, Budenovskoye and Mynkuduk.

The ore is located in porous non-watertight deposits and is extracted by the underground leaching method. Some ore bodies are several kilometers long and often form many-tier "shelves" that are a hundred meters deep. Often rhenium, selenium, vanadium and gallium are extracted together with uranium. The Production started in the 1970s, and two plants producing finished uranium concentrate were constructed.

In the Chu-Sarysuiskaya provice uranium mineralization is connected with stratum oxidation zones. Reserves of this province amount to 57% of total reserves of Kazakhstan. Nowadays, Uvanas, Eastern Mynkuduk, Kanzhugan and Southern Moinkum uranium deposits are mined by in-situ leaching method.

North Kazakhstan province uranium deposits are represented by vein-stockwork mineralization in proterozoic and paleozoic folded complexes. Total reserves in this province amount to 18% of total reserves of Kazakhstan.

In the Syrdaryinskaya province uranium mineralization is connected to regional stratum oxidation zones. Reserves in this province amount to 15% of the total reserves of Kazakhstan. Uranium is mined by in-situ leaching method on the Northern Karamurun, Southern Karamurun and Zarechnoye deposits.

Uranium mineralization in the Mangyshlakskaya province is connected to a unique type of deposit associated with fossil fish phosphatized bone detritus conglomeration. The uranium reserves amount to 2% in the whole balance of reserves of Kazakhstan.

In the Kendyktas-Chuli-Batpakdalinskaya province the main type of uranium deposits is endogenous vein-stockwork deposits in land volcanogenous complexes.

Basic reserves of the deposit Ilyiskaya are connected with uranium-coal deposits formed by lignit beds roof ground oxidation. Reserves amount to 7% of total reserves of Kazakhstan.

Uranium mining

Over half of the world's production of uranium occurs in Canada, Australia and Kazakhstan

An increasing proportion is produced by in-situ leaching.

After a decade of falling mine production ending in 1993, output has generally risen since and now comprises 61% of demand for power generation.

Canada produces the largest share of uranium from mines (25% of world supply from mines), followed by Australia (19%) and Kazakhstan (13%). Australian and Canadian production was depressed in 2006. This data is shown in table 1.

Table 1. World uranium production

Country	Year				
	2002	2003	2004	2005	2006
Canada	11604	10457	11597	11628	9862
Australia	6854	7572	8982	9516	7593
Kazakhstan	2800	3300	3719	4357	5279
Niger	3075	3143	3282	3093	3434
Russia (est)	2900	3150	3200	3431	3262
Namibia	2333	2036	3038	3147	3067
Uzbekistan	1860	1598	2016	2300	2260
USA	919	779	878	1039	1672
Ukraine (est)	800	800	800	800	800
China (est)	730	750	750	750	750
South Africa	824	758	755	674	534
Czech Repub.	465	452	412	408	359
India (est)	230	230	230	230	177
Brazil	270	310	300	110	190
Romania (est)	90	90	90	90	90
Germany	212	150	150	77	50
Pakistan (est)	38	45	45	45	45
France	20	0	7	7	5
Total world	36 063	35 613	40 251	41 702	39 429
tonnes U_3O_8	42 529	41 998	47 468	49 179	46 499

Kazakhstan is the third country in the world by uranium production volumes, and state-owned Kazatomprom National Atomic Company is the fourth largest uranium producer in the world (Table 2).

Table 2. World uranium mine production by eight companies in 2006.

Company	Tonnes U	%
Cameco	8249	20.9
Rio Tinto	7094	18.0
Areva	5272	13.4
Kazatomprom	3699	9.4
TVEL	3262	8.3
BHP Billiton	2868	7.3
Navoi	2260	5.7
Uranium One	1000	2.5
Total top 8	33,704	85.5

Table 3. Uranium Production in Kazakhstan.

Year	tonnes U	Year	tonnes U	Year	tonnes U
1997	795	2001	2022	2005	4346
1998	1073	2002	2709	2006	5280
1999	1367	2003	2946	2007	7200
2000	1752	2004	3712		

In 1970 tests on in-situ leaching (ISL) mining commenced in Kazakhstan and were successful, which led to further exploration being focused on two sedimentary basins with ISL potential.

Up to 2000, twice as much uranium had been mined from hard rock deposits than sedimentary ISL. Now almost all production comes from ISL. Uranium production dropped to one quarter of its previous level during the period of 1991 to 1997.

By the 1990s, uranium extraction had shifted from conventional and underground operations around Tselinnyy and Prikaspiyskiy to in-situ leaching operations run by the Stepnoye, Tsentralnoye, and No. 6 Mining Directorates in southern Kazakhstan. Uranium is extracted using a sulfuric acid.

ISL with different amount of technological wells: two wells, scheme-envelop and hexagonal cell with one pump out well and etc. is carried out in Kazakhstan practice. Reagent and oxidizer choosing depends on lithological-geochemical properties of non-useful ore components and character of complex bearing useful elements, such as acidophilic (U, V, Sc, Y, lanthanids), carbonatephilic (U, Sc), or oxiphilic (Re, Mo, Se).

The following characteristics are determined by geotechnological tests: 1) content of technological solutions and concentration of metals; 2) degree of useful components extraction from ores; 3) liquid:solid ratio for maximum extraction of each useful component; 4) specific consumption of leaching solvent, reagent ability of rock. Sometimes, it is possible to determine the proportion coefficient between rates of leaching and filtration processes. This data is the base for ISL.

Rhenium content in samples is 0.5-3.5 g/t. It is necessary to note that the correlation between capacities of rhenium and uranium allows to make prognosis of rhenium content on the base of uranium ores parameters.

90% of selenium reserves are in the uranium ore square.

Vanadium is connected with waterpermeable sandy rocks of uranium deposit. Concentration of V_2O_5 reaches 0.5%.

Calculations of useful components is carried out in rhenium-uranium block. Ore materials of geotechnological tests are used for determination of useful components. The testing section of productive horizon is divided in two parts: i) productive block of rhenium-uranium ores; its roof and foot is determined by calculated capacity of rhenium part (C_{Re}<0.05 g/t); ii) ore and non-ore parts of open-cast.

Data of ecological state of statum water and physico-chemical interaction in the solution-rock system is necessary for detail prospecting. Data of general mineralization; macrocomponents amount (HCO_3^-, CI^-, SO_4^{2-} Cu^{2+}, Mg^{2+}, NO_3^-, K^+, Na^+)

and ore elements; content of microcomponents (heavy metals and other toxic elements) are also necessary.

The value of oxidation-reduction potential of ore Eh-pH depends on water solution content in balance with ore horizon of rock. Changing of electrode potential depends on pH of solution and nature of minerals. The potential value is determined by nature and concentration of ions. Changing of ore potential at pH 6.5-8.0 [+0.48- (-0.42)]V is depending on the ore nature. Eh value reflects oxidation-reduction ability. Oxidation of ore rock was measured too. All these parameters allow to predetermine the presence or absence of ore body.

Depth of uranium ore bedding is 100-700 meters. Kanzhugan and Uvanas deposits are at the minimum depth, whereas Budenovskoye deposit is at the maximum depth. Capacity of permeable to water ore rocks of Kanzhugan, Uvanas and other deposits is lower than 8-20 m. Sand is the basic geotechnological type of rock. Sand filtration coefficient is 7-10 m/day and varies from 2 to 20 m/day. Sand deposits of the top whiting have higher permeability to water than paleogen deposits. Permeability of ore and rock is close. Underground waters of productive horizons are under pressure. Bedding depth of underground waters level of Kanzhugan, Moinkum deposits is 60 m. Underground water salt content of Mynkuduk, Budenovskoye, Uvanas deposits is 2-3 g/L. Salt content of underground water for Zhalpak deposit is 6-7 g/L.

Mineral content of ore sand consists of quartz (40-80%) and feldspar rock (14-28%). Uranium content in lean deposits is 0.03-0.05%. Basic uranium minerals are nasturanium and coffinite. Carbonate content is lower than 1%, basically 0.1-0.4%.

Rhenium content of Kanzhugan, Moinkum, Uvanas deposits is 0.1-0.5 g/t, in some ore parts is higher than 1 g/t.

Scandium content in sand is about 5-6 g/t.

Selenium content is 0.03-0.1%.

Content of scandium, yttrium, cerium and lanthanum in the technological solutions after ISL depends on pH (0.1-10 g/m^3) at average output of pump out wells. Annual output of one well is 3.6-1096 kg.

Thermodynamic calculations of fields for chemical components (U, Mo, Re, Se, V, Sc, Y, some lanthanids) in solid and liquid phases are the theoretical base of ISL. Eh-pH diagrams of C_{Me} – pH (C_{Me} – metal concentration) for standard conditions (T=25°C, P=1-10^5 Pa) are used. Activities of ∑U, ∑Re, ∑Mo, ∑V, ∑Se are $10^{-3.5}$, $10^{-5.8}$, 10^{-3}, $10^{-2.5}$, $10^{-2.5}$ M and correspond to the following concentrations respectively 80, 0.3, 100, 150 and 200 mg/L.

Oxidation of rhenium sulphide proceeds as follows:

$$ReS_2 + 4{,}75O_2 + 2{,}5H_2O \rightarrow ReO_4^- + 2SO_4^{2-} + 5H^+$$

Thermodynamically pH does not influence Re leaching. Rhenium is extracted with U and Mo.

Sulfuric acid with oxidizers is used for uranium extraction by ISL in Kazakhstan. Oxygen, iron (III), manganese dioxide are used as oxidizers. $FeOH^{2+}$, $Fe(OH)^{2+}$ and Fe^+ are used for oxidation of uranium (IY). Oxidation proceeds as multistepped process and is described by the following reactions:

$$UO_2 + Fe(OH)_2^+ \rightarrow UO_2^+ + Fe(OH)_2$$

$$UO_2^+ + Fe(OH)_2^+ \rightarrow UO_2^{2+} + Fe(OH)_2$$

$$Fe(OH)_2 + 2H^+ \rightarrow Fe^{2+} + 2H_2O$$

$Fe^{3+}/Fe^{2+} > 1$ is the optimal ratio at concentration of $Fe^{3+} \geq 0.5$ g/L.

Uranium (YI) oxidation proceeds in acid and carbonate mediums without oxidizers.

Fields of UO_2SO_4 - $UO_2(SO4)_2^{2-}$ and $UO_2(CO_3)_3^{4-}$ in Eh-pH diagrams at sulfuric acid and carbonate uranium leaching respectively are thermodynamically favorable. Thermodynamically uranium extraction by sulfuric acid with oxidizers is possible at pH=6.5-5.0 and without oxidizers at pH<4.5. Content of technological solutions after uranium leaching is (mg/L): 10-500 U; 0.1-0.3 Re; 0.2-1.0 Sc, 2-10 Y; (sometimes 5-50 Y); up to 200 V; 10-100 Mo.

Characteristics of technological solutions and sorbents

UO_2SO_4 anion, $UO_2(SO_4)_2^{2-}$, $UO_2(SO_4)_3^{4-}$ anion complexes are formed at ISL. At pH>2.5 anion complexes are polymerized into the following polynuclear complexes: $U_2O_5(SO_4)_2^{2+}$, $U_3O_8SO_4^{2+}$.

Mo, Re, Sc, V, Y, rare-earth elements (REE) are accompanying useful components of uranium ore after ISL. These elements are the following products: MnO_4^- and ReO_4^-, Sc^{3+},Y^{3+}, REE^{3+}, and vanadium as VO^{2+}, VO_2^+ and VO_3^-.

Carbonate leaching is used at autoclave process in Kazakhstan, as a result $Na_4[UO_2(CO_3)_3]$ or $NH_4[UO_2(CO_3)_3]$ are formed. Mo and Re are found in the technological solution. Average content of components after ISL is given in table 4.

Table 4. Average content of components after ISL for technological solution (g/L)

Component	Technological solution		Component	Technological solution	
	Sulfur acid	Bicarbonate-carbonate		Sulfur acid	Bicarbonate-carbonate
pH	1.2-2	7.5-8.5	Ca	0.3-0.6	0.1-0.3
U	0.015-0.1	0.015-0.1	Mg	0.3-1.6	0.1-0.2
H_2SO_4	1-7	-	AI	0.3-2.5	-
CO_3^{2-}	-	0.01	SO_4^{2-}	10-25	0.9-2
HCO_3^-	-	0.2-2	NO_3^-	0.06-0.6	0.02-0.03
NH_4^+	-	0.06-0.6	Cl^-	0.2-1.7	0.5-0.7
Fe^{2+}	0.2-1.5	-	P	0.02-0.15	-
Fe^{3+}	0.15-0.9	-	SiO_2	0.1-0.5	-

Table 5. Characteristics of some anionites.

Characteristics	Amberlyt IRA-400	Duolite A101D	Permutite S-700	AMP	VP-1p
Active group	$-N^+(CH_3)_3$	$-N^+(CH_3)_3$	$-N^+(CH_3)_3$ $-N^+(CH_2)_2$ $-C_2H_4OH$	$C_5H_9N^+$	$C_5H_9N^+$
Specific surface, m^2/g	-	-	-	-	14-20
Specific volume, sm^3/g	3	3	2.8-3.6	3.3	4
Full exchange capacity to CI^-, mg-equivalent/g	4.2	4.2	3.5-3.7	3.1	4.8
Mechanical hardness, %		50-60		95	95
Size, mm	0.3-1.2	0.3-1.2	0.3-1.2	0.63-1.6	0.63-1.6

Microcomponents content of sulfuric acid solutions is the following (mg/L): Ti 0.2-5; Mn 0.1-20; Zn 0.1-20; Pb 0.006-0.01; Ni 0.1-15; Sr 0.06-0.2; Cu 0.03-5; As about 0.05.

Strong alkaline gel and porous anionites are used for uranium sorption. Sorbents properties are given in table 5.

Commercial anionites are in CI^- form as a rule. At technological processing anionites transfer into SO_4^{2-}, CO_3^{2-} or HCO_3^- forms depends on nature of used reagent and solution.

Sorption proceeds as ion-exchange and complex forming process according to the following equations:

$$(R_4N^+)_2SO_4 + UO_2^{2+} + SO_4^{2-} = (R_4N^+)_2[UO_2(SO_4)_2];$$

$$2(R_4N^+)_2SO_4 + UO_2^{2+} + 2SO_4^{2-} = (R_4N^+)_4[UO_2(SO_4)_3] + SO_4^{2-}$$

$$2(R_4N^+)_2SO_4 + UO_2^{2+} + 2SO_4^{2-} = (R_4N^+)_4[UO_2(SO_4)_3] + 2SO_4^{2-}$$

or if anionite in nitrate form:

$$R_4N^+NO_3 + UO_2^{2-} + 2SO_4^{2-} = (R_4N^+)_2[UO_2(SO_4)_2] + 2NO_3^-$$

Uranium concentration in technological solution after ISL is low ($6\cdot10^{-5}$ – $4.5.10^{-4}$ M). Film kinetics of sorption is prevalent for such solutions. Duration of anionite contacts with solution is 6-8 hours in practice.

The value of U extraction, anionites capacity, anionite characteristics, the content of suphate, nitrate, U distribution coefficient (K_d) are the basic uranium sorption indices. K_d is much higher for low uranium concentration (1-25 mg/L) in comparison with high U concentration (0.1-10 g/L).

Affinity to anionites is the base of depression influence of some anions as the following:

$$SO_4^{2-} < F^- < CI^- < NO_3^- < HSO_4^- < CIO_4^- < PO_4^{3-}$$

Residual uranium concentration is very low (1-2 mg/L).

Uranium desorption is carried out by various chemical reagents (acids, alkilines, salts). U residual capacity of anionite, uranium content in commercial eluate, phisico-chemical characteristics of sorbent are the main desorption indices.

The influence of temperature increasing at uranium desorption was studied. Optimal temperature was determined. At optimal desorption conditions uranium concentration is higher (by 10-15%), process duration is lower (by 20-30%).

Technological solutions after ISL contains U, Re, Sc, REE, Y, V, Mo. Extraction of microelements together with uranium is economically profitable because it includes only exploit expenses (10-15% of cost price of final uranium product).

Strong alkaline ionites are used for sorption extraction of U, Re, Mo, Au, rare elements. AFI-21 and AFI-22 can be used for sorption of U, Sc, Re, and Th from ISL solutions. Vanadium is extracted by VPK amfolite. VP-14KP is effective for rhenium sorption and concentration. Sc, Ca, Vg, AI and rare-earth elements are extracted by using of KU-2, KU-8n, KU-23k ionites.

So, high technico-economical indices of complex processing for uranium ores are obtained due to the achievements in the ISL, ion-exchange and liquid-extraction of metals in Kazakhstan industry practice.

The yellow cake produced by the Mining Groups is converted into natural uranium concentrate (U_3O_8) at he Ulba Metallurgical Plant. It has a variety of functions relevant to uranium, the most basic of which since 1997 is to refine most Kazakhstan mine output of U_3O_8. It also produces beryllium, niobium and tantalum. Since 1973 it has produced nuclear fuel pellets from Russian-enriched uranium which are used in Russian and Ukrainian VVER and RBMK reactors. Other exports are to the USA. It briefly produced fuel for submarines (from 1968) and satellite reactors. Since 1985 it has been able to handle reprocessed uranium. Ulba has secured both ISO 9001 and ISO 14001 accreditation.

Conclusions

Kazakhstan has one-fifth of the world's uranium resources. The Republic has been an important source of uranium for sixty years. Over 2001-2006 production rose from 2000 to 5279 tonnes U per year, and further mine development is aiming for 15,000 t U annual production by 2010 and 30,000 tonnes by 2018.

Kazakhstan produces natural uranium, nuclear fuel for power stations, products and semi-products of beryllium, tantalum, niobium and its alloys. The Republic has a major plant making nuclear fuel pellets and aims eventually to sell value-added fuel rather than just uranium. It aims to supply 30% of the world fuel fabrication market by 2030.

Research findings in-situ leaching, ion-exchange, liquid-extraction of uranium and accompanying useful components U, Mo, Re, Sc, V, Y, rare-earth elements (REE) are given.

Prediction and a new Method of Exploitation of Gold Deposits with Uranium in the Variscian Molass Conglomerate Basins of Germany

Elkhan A. Mamedov

Baku State University. The Scientific-Research Laboratory "Prediction, Search and Economic Estimation of Gold Placer Deposits",. 23, Z.Khalilov str,. Baku AZ 1148, Azerbaijan . http://www.nativegoldau.narod.ru E-mail; elkha-nau@rambler.ru.

Abstract. Gold deposits with uranium in the conglomerate assize belong to the leading Industrial type. They are main suppliers of gold and uranium in the word. The deposits Witwatersrand (South Africa), Blind River (Canada) and so on.

In the history of development of the Earth′s Crust gold deposits with uranium in the molass basins have been formed repeatedly in the periods of revolutionary epoch of orogenesis, mountain building and erosion of auriferous and uranium deposits.

In the territory Germany this Variscian epoch of orogenesis and mountain building, accompanied by forming of gigantic molasses troughs and depressions with thick conglomerate assize. Sudetion, rudnohorian, asturian, zaalian and pfalcian phases of the revolutionary orogenesis and mountain building played an essential role in the forming of thick and extended conglomerate assize in molass basins. On the base of metallogeny of gold and uranium of Germany, the geological criterions, paleohydrology and so on are predictive areas:

- Subvariscian frontal depression.Gold ore province of Ardenn.The High Fenn. Aachenian carbonic basin. Conglomerates of the Upper Carboniferous basins Inda.

- Hessenian depression. Korbakhian gulf. The regions of gold deposits Korbakh and copper-uranium deposits Vreksen. Conglomerates of the Permian age.
- Laakh-Badenian depression.The regiones of the gold and uranium deposits Swartwald {Baden-Baden, Wittiken, Karlsrue and so on} and auriferous placers. Conglomerates assizes of the Carbon- Permian age.
- The Eastern-Thuringenian trough. In the regions of gold deposits Shleits, chamoisite Deposits with ancient auriferous quartzic veins Shvartsburq saddle and Ordovician schist.Conglomerates assizes of the Carbon- Permian age. Auriferous conglomerates of Saxonian of the Saxon-Thuringian zone , and also the western margin of the Czechian massif.
- Molasses troughs of Rudnohorie Mts, Delenian, Olbernhau-Brandov an other troughs in the region of development of Noble quartz formation (Freiberg), gold bearing arsenic pyritic and pyritic ores with native gold in Saxonia.
- Conglomerates assizes of the Carbon- Permian age
- and so on

In the Varision molasses basins conglomerates assizes have a huge thickness, often they clastic rocks of gold and uranium deposits.

The novelty of the exploitation in that the Conglomerates assizes are dissenting rated with water, are probed according to the bearing of Conglomerates with large billow method and are exploitation as placer gold deposits with uranium. Re-estimation of the Varicsian molasses conglomerates basins including carboniferous and cupriferous, on gold with uranium

Thus, the exploitation of Conglomerates assizes of Varisxian molasses basins on gold and uranium with the use of the new method of exploitation allows the create a large and unique mineral- raw base of the Gold-mining Industry with Uranium of Germany.

The Prediction of geodynamic conditions of mining of Elkon uranium field (Eastern Siberia, Russia)

V. N. Morozov[1], E. N. Kamnev[2], I. Y. Kolesnikov[1] and V. N. Tatarinov[1]

[1]Geophysical Center of RAS. 117296, Moscow, GSP-1, Molodeznaja, 3 – Russia
[2]VNIPI Promtechnology 115409, Moscow, Kashirskoje shosse, 33 – Russia

Abstract. The Elkon uranium ore area in Russia as far as geotectonics is concerned is located in the Aldan shield. Like the whole central area of Aldan shield, the Elkon area is characterized by a complicated combination of geological structures including ore-bearing structures forming together a three-level fold-block construction.

For the area a digital map of the relief was processed with the use of algorithm Monolith and modeling stress and strain of rock masses of finite element method.

With account for rock characteristics, the mean intensity of stress in the rock mass unbroken sections is approximately 25 MPa. Being the threshold of analyzing stress distribution in the model, this value is relative. In individual local segments of the rock mass, calculated values σ_i exceed 80 MPa, and in the zones of increased stress, they decrease to 20 MPa and less.

High level of differentiation of σ_I distribution in the model allows us to separate potentially dangerous zones (both the zones of likely destruction of rocks in the dynamic form with increased stresses and rock inrush zones in the areas of rock mass discharge), which are of practical interest in the context of the task we set.

A feature of stress intensity distribution is a thick zone of stress concentration, which is bend-shaped and extends from north to south in the western area. The rest of concentration zones appear to be oriented at angles close to 45° from northeast to southwest and from northwest to southeast. It generally conforms to the ex-

isting stress field and the orientation of uranium ore bodies that are genetically related to fault systems of similar orientation. In the central area of the model the stress level is lower than in boundary parts. Differentiation effect in physical and mechanical characteristics of individual blocks is shown very weakly in the models. Of special interest are zones of concentrations of values τ_{xy}, which would be missing in homogeneous environment with this calculation scheme.

Some approaches to remediation study of the fucoid sandstone in the Straz pod Ralskem site - Nothern Bohemia

Pavel Franta[1], Vaclava Havlova[1], Lukas Kraus[2], Barbora. Drtinova[2], Karel Stamberg[2], Ondra Sracek[3] and Zbynek Vencelides[3]

[1]Nuclear Research Institute Rez plc, Rez near Prague, CZ-250 68.
[2]Department of Nuclear Chemistry, Czech Technical University in Prague, Brehova 7, CZ-115 19 Prague 1.
[3]OPV (Protection of Groundwater) Ltd, Belohorska 31, CZ-16000 Prague 6..

Abstract. The behaviour of acid contaminantion in fucoid sandstone was studied on samples from Straz pod Ralskem, Czech Republic. Long term leaching of solid phase cores of contaminated fucoid sandstone with very low value permeability about 0.6 mD by background groundwater from Cenomanian aquifer was performed and possible chemical reactions were proposed. Results of leaching and modified extraction method divided core samples into two groups, depending on their leaching kinetic parameter (KDM). The KDM is dependent predominantly on pore accessibility for leaching solution and dissolution of secondary minerals. Radioactive ^{35}S and ^{3}H were used to determine effective diffusion coefficients.

Introduction

In the last 40 years of the 20th century uranium mining belonged among the most active sections of Czech mining industry. Uranium ore was exploited either by underground mining (e.g. Rozna, Pribram, Zadní Chodov, Hamr) or *in situ* acid leaching (Straz pod Ralskem). Straz pod Ralskem region is a part of the Bohemian Cretaceous Basin. The geological profile of the site consists of Quaternary alluvial sediments, Turonian and Cenomanian aquifers .The Cenomanian formation is formed by the upper layer of low permeable fucoid sandstone underlied by friable sandstones, which contain uranium bearing minerals. The in-situ leaching of uranium took place for about 30 years and was carried out by the injection of technological solutions with 50-60 g/L of sulphuric acids into the deep layers of the Cenomanian aquifer. The total amount of dissolved matter is estimated as 4 mil-

lion tons. About 40% of contaminants (Al, As, Be, Cd, Co, Cr, Cu, F, Fe, Ni, Mn, Pb, V, Z, SO_4^{2-}, NH_3/NH_4^+) are retained in solid phase. The problem of restoring the groundwater quality in this largest aquifer of North Bohemia is therefore a serious challenge. The study of less permeable "fucoid" sandstones was initiated in order to characterise the potential pathways of contamination and to suggest a remediation approach.

Experimental

Solutions

Two different solutions were used for experiments: background cenomanian water (PCW) sampled from borehole NPV MIPC-18 (Mimon) out of the leaching field area and the acid technology solution (ATS, pH = 1.95) from leaching well No.VP 20-5824 (Table 1).

Rock samples

Dynamic leaching experiment was performed with a solid phase core sample from the borehole VP 13B7051, interval 87 – 119.8 m, characterised by low vertical permeability of 0.597 mD (1 Darcy = $9.64.10^{-6}$ m/s) and lower concentrations of contaminants (1.5 g/L of TDS in pore water). Supplementary batch leaching and diffusion experiments were also performed on the individual samples from a fucoid core, borehole VP 8C 7095, interval 42 - 153m, with TDS 0.3 – 2.3 g/l in pore water. Properties of samples are listed in Table 2 and Table 3.

Table 1. Pure cenomanian water (PCW) and acid technological solution (ATS) composition, used for experiments.

Sol.	pH	Conductivity mS/m	NO_3	PO_4	SO_4^{2-}	H_2SO_4	NH_4OH mg/L	V	Mn
PCW	8.2	26.8	<2.0	0.04	18	-	0.05	0.0001	0.14
ATS	1.95	2000	265	256	26300	261	511	11.2	15
	TDS	Al	As	Ca mg/L	Cr	Fe	K	Mg	Na
PCW	153	-	<0.02	40	<0.002	0.06	1.3	7.7	3.8
ATS	47340	3806	5.13	259	8.7	766	50	51	21

Table 2. Rock sample (a) and pore water (b) properties: fucoid sandstone sample No.48471 (VP 13B 7051, depth 111.5 – 111.8 m). ε = porosity (%), κ_h = horizontal permeability, κ_v = vertical permeability (mD).

a) rock property										
ε %	κ_h mD	κ_v mD	Si wt %	Al wt %	Ca wt %	K wt %	Fe total wt%	Ti wt%	C inorg wt%	C org wt%
21.4	1.803	0.5969	42.8	2.44	0.02	0.126	0.351	0.233	1,86	0,64
b) pore water composition										
pH	Redox absol. mV	Conduct. mS/m		TDS mg/L	NH_4 mg/L		Na mg/L	K mg/L	Mg mg/L	Ca mg/L
3.48	156	158.5		1420	43.6		-	11.7	10.8	63.6
Fe total mg/L	Al mg/L	H_2SO_4 mg/L		SO_4 mg/L						
36.3	115	961		-						

Table 3. Rock sample properties for samples from borehole VP 8C 7095 (depth 143 – 153 m). In bold: data, distinguishing PI group (48541, 48555, 48567) and PII group (48544, 48547, 48550) – see further.

Sample	ε	κ_h	κ_v	Spec. surface	SiO_2	Al_2O_3	Fe_2O_3	CaO	K_2O	TiO_2	C_{org}	C_{inorg}
	%	mD	mD	m^2/g	wt%	wt%	wt%	wt%	wt%	wt%	wt%	wt%
48541	27.3	18.5	6.3	0.65	94.7	2.7	0.67	0.006	0.07	0.23	0.86	0.64
48544	23.2	**1.0**	**0.3**	**1.62**	92.1	4.5	0.66	**0.046**	**0.13**	0.33	0.96	**1.15**
48547	22.8	**0.2**	**0.2**	**1.49**	88.4	6.7	0.82	**0.43**	**0.19**	0.37	1.23	**1.81**
48550	25.6	**7.7**	**-**	**1.32**	93.6	3.7	0.83	**0.027**	**0.09**	0.31	0.71	**1.06**
48555	25.7	31.9	18.2	0.67	93.4	3.7	0.80	0.016	0.09	0.29	0.81	1.00
48567	22.8	90.0	28.4	0.85	96.4	2.0	0.53	0.009	0.05	0.15	0.47	0.64

Column leaching experiments

The column was prepared from unbroken drill core from the cored borehole VP 13B 7051, sample No. 48471 (see Table 2) with a diameter of 130 mm and length 200 mm. Total pore volume of column, PV, was 531 cm^3. Leaching agent, PCW, was injected at the bottom of column with hydrostatic pressure gradient of 17.5 kPa.Linear velocity of effluent was 1.5 cm/day that was near to natural groundwater velocity in uncontaminated Cenomanian aquifer, i.e. fucoid sandstones, which is assumed to be within the range of 1 – 5 cm/day. Experiment was performed for 220 days during which through the column flowed 7919 g of effluent, i.e. about 15

PV. Sampling was carried out about twice a week, concentrations of selected anions and cations were measured by analytical methods and/or AAS and ICP methods in analytical laboratory of NRI Rez. The main part of this contribution deals with the study of behaviour of principal contaminants like SO_4^{2-}, Cl^-, Al, and Fe.

Batch experiments: leaching and modified sequential extraction

Leaching and modified sequential extraction method of six fucoid sandstone samples were performed (Table 3).

Kinetics of leaching

Leaching experiments were carried out applying the batch technique in PE-bottles. The rock samples of the fucoid sandstone (the grain size fraction < 1 cm) were mixed with PCW and also with deionized water for comparison. Sample weight to liquid volume ratio was adjusted to 5 mL/g. The suspensions were shaken at ambient temperature for 1, 5, 24, and 120 hours.

Concentrations of the constituent cations and anions in the leachates were measured using AAS with the aim to assess dominant geochemical processes that could take place during the in situ leaching. Measured concentrations of many minor contaminants (e.g., V, U, Be, Cr) were near to detection limits of used analytical methods.

Sequential extraction

According to Tessier scheme modified three-step sequential extraction (Tessier et al. 1979) was performed as follows:

1. Fraction – water soluble phase: 1g sample + 20 mL deionized water shaking for 1 hour at room temperature.
2. Fraction – adsorbed and exchangeable phases: residual fraction + 20 mL 1 M $MgCl_2$ (pH = 7) for 1 hour at room temperature.
3. Fraction - carbonate phase: residual fraction + 20 mL 1 M NaAc + HAc (pH = 4.8) for 5 hours at room temperature.

Diffusion experiments

Diffusion experiments with ^3H ($T_{1/2}$ = 12.4 years, non sorbing conservative tracer) and ^{35}S ($T_{1/2}$ = 87.4 days; slightly sorbing tracer) were carried out with 6 rock disks (sample 48544 – see Table 3; 10 mm width, 50 mm diameter). Three samples were cut in horizontal direction, three ones were cut in vertical direction in order to determine differences in diffusion in both directions.

The through-diffusion cell set up, experimental procedure and sampling were carried out according to the methodology, widely reported elsewhere (e.g. Skagius and Neretnieks, 1986; Shackelford, 1991).

Table 4. Experimental set up for ^{3}H and ^{35}S diffusion experiments. Sample used: fucoid sandstone (48544, see Table 3).

Sample	Sampling direction	Tracers	Solution in inlet cell	Solution in outlet cell
1	Horizontal	^{35}S	PCW	PCW
2	Horizontal	^{35}S	ATS	PCW
3	Horizontal	^{3}H	PCW	PCW
5	Vertical	^{35}S	PCW	PCW
6	Vertical	^{35}S	ATS	PCW
7	Vertical	^{3}H	PCW	PCW

through-diffusion experiment results also for variable tracer activity in the inlet cell (e.g. Vopalka et al. 2006).

The solutions used were cenomanian water (PCW, composition in Table 1) and acid technology solution (ATS, composition in Table 1). The solution in inlet cell was spiked with radionuclides. The experimental set up is reported in Table 4.

Results

The pH value on the column outlet decreased dramatically (< 1.5) in comparison with pH value of injected PCW (8.2; see Figure 1).

It was almost identical with pH value of acid technological leaching solutions, used for uranium leaching technology. It was interpreted as the transformation of HSO_4^- to SO_4^{2-} and desorption of H^+ from positively charged surface sites initialised after injecting of two pore volumes (PV). Reactions may be expressed:

$$HSO_4^- = SO_4^{2-} + H^+ \quad (1)$$

$$FeOH_2^+ = Fe(OH) + H^+ \quad (2)$$

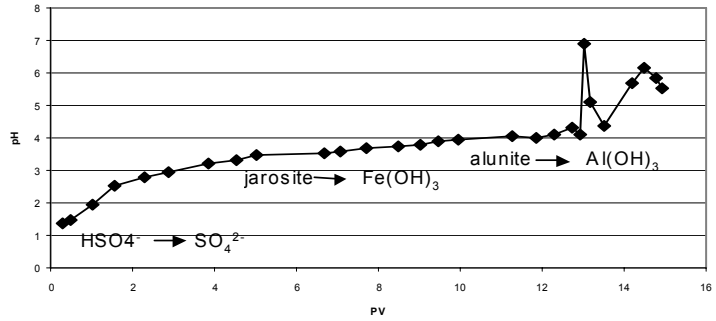

Fig.1. Dependence of pH value on pore volume of leaching cenomanian water.

The acidity presented within rock is massive and causes decrease of pH value at the outlet. The curve presented on Fig. 1 markedly shows periods when the rise pH value is retarded by heterogeneous reactions. At next period (injected 5 – 7 PV) the rise of pH value seems to be retarded as a consequence of the transformation of jarosite to ferric hydroxide.

$$K\,Fe_3\,(SO_4)_2\,(OH)_6 + 3H_2O = K^+ + Fe(OH)_3 + 2\,SO_4^{2-} + 3\,H^+ \quad (3)$$

The pH behaviour around injected 10 PV is characterized by the precipitation of desorbed Al^{3+} as aluminium hydroxide or transformation alunite onto Fe hydroxide.

$$Al^{3+} + 3H_2O = Al\,(OH)_3 + 3\,H^+ \quad (4)$$

$$K\,Al_3\,(SO_4)_2\,(OH)_6 + 3H_2O = K^+ + Al(OH)_3 + 2\,SO_4^{2-} + 3\,H^+ \quad (5)$$

The similar buffering influence on pH value rise can be assigned to the dissolution of alunogene $Al_2(SO_4)_3\,.17H_2O$. This phase was identified by XRF diffraction measurement of dry effluent filtrate, besides copiapite, gypsum, and tschermigite.

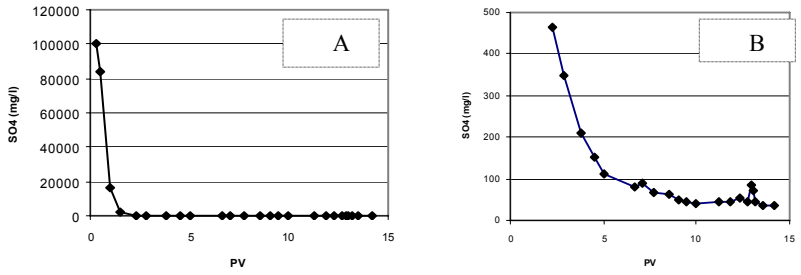

Fig.2 [A],[B]. Development of concentration of sulfates from beginning (A), except first 1.56 PV (B).

Sulphate represents main contaminant in underground leaching area. During experiment the sulphate concentration decreased very fast. This matched the results of batch experiments. The initial value of concentration 100 g/L dropped to 400 mg/L during the first injected two PV of PCW. Next injected PCW leached sulphate from solid phase and after about next 7 PV the sulphate concentration reached the same level as in injected PCW, see Fig.2[A],[B].

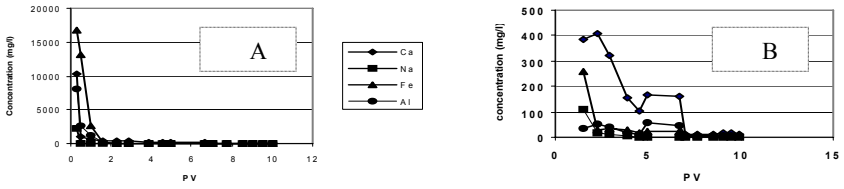

Fig.3 [A],[B]. Development of Ca, Na, Fe a Al concentration from beginning (A), except first 1.56 PV (B).

Concentrations of Ca, Na, Fe and Al dropped fast during injection of the first two PV of cenomanian water, see Fig.3[A],[B]. The most of the element mass was diluted by injected water. Close to 5 – 7 PV injected concentrations of Ca, Na, and Fe temporarily increased, probably due to the dissolution of gypsum ($CaSO_4.2H_2O$) and jarosite ($K\,Al_3\,(SO_4)_2\,(OH)_6$).

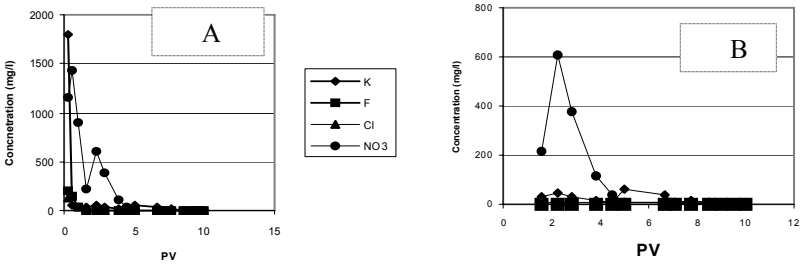

Fig.4 [A],[B]. Development of concentration of K, F, Cl a NO_3 from beginning (A), except first 1.56 PV (B).

In the case of K, F and Cl, their concentrations decreased in the first part of experiment (PV < 2), see Fig.4. Temporary increase of K concentration between 5 – 7 PV was presumably caused by the dissolution of jarosite ($K\,Al_3\,(SO_4)_2\,(OH)_6$).

The majority of studied elements were leached out in the first extraction step of sequential extraction, except for As, K and Na. Differences among results of the sequential extraction for different samples were not significant. The smaller total amounts of Al and Fe obtained by sequential extraction in comparison with longer time leaching by PCW also confirm the dissolution of some characteristic minerals containing Al and Fe (e.g. alunite, jarosite).

From the point of view of kinetic experiment results, the set of samples can be divided into two groups, PI and PII, namely with respect to the rate of leaching of dominant components and of time-dependences on pH. The first group, PI, consists of samples No 48541 (142 m), 48555 (148 m) and 48567 (153 m), the second one, PII, of samples No 48544 (143 m), 48547 (144 m) and 48550 (145 m). It

holds that the rate of leaching is higher in the case of samples PI than in the case of samples PII, see Fig. 5A-C.

The results indicated relatively homogenous region, corresponding to the depths between 143-145 m (samples 48541 – 48567), with respect to the leaching procedure used. After 120 hours leaching the pH of cenomanian groundwater dropped from initially value 8 to 3. This could reflect leaching of contaminants presented within pore space, predominantly sulphate anions and H_4SO_4 and other reactions, e.g., the dissolution of ferric sulphate minerals. The pattern of similar rock properties for mentioned rock groups PI and P II is also consistent with rock characterizing properties (see Table 3, data in grey). The increased values of specific surface, horizontal permeability, CaO, $C_{inorganic}$ and K_2O for PII. group can be assigned to the formation of different types of mineral phases within pore volume (i.e. gypsum, alunite, jarosite, alunogene, copiapite, gypsum, and tschermigite etc. mentioned above). Differences in mineral solubility can than cause difference in leaching kinetics of both rock groups.

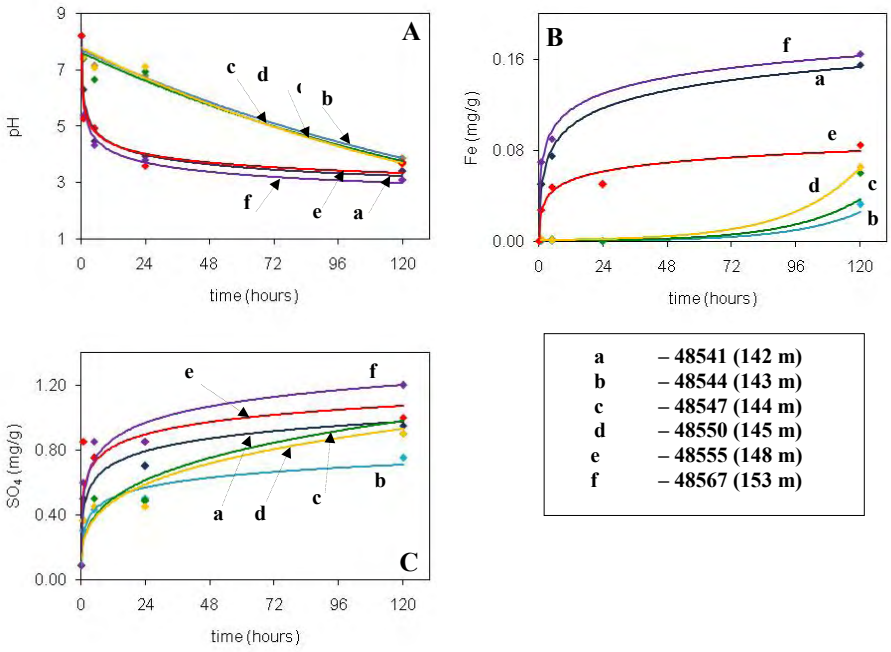

Fig.5. Dependence of pH (A), Fe (B) and SO4 (C) concentration on the leaching time for samples from various depths of the fucoid core.

Furthermore, relative homogeneity of the rock sample in both vertical and horizontal direction are supported by the results of diffusion experiments (sample 48544, PII group). Both ^3H and ^{35}S diffused into the fucoid sandstone saturated with PCW in the similar pattern (see Figure 6). Evaluating experimental result with GOLDSIM diffusion module, effective diffusion coefficient D_e for ^3H in fucoid sandstone was determined as 5.10^{-10} $m^2.s^{-1}$, D_e for ^{35}S was in the range of 2.23^{-10} $m^2.s^{-1}$. ^{35}S diffused through sample No. 1 slightly faster than ^3H (see Fig.

6). This could be caused preferentially by rock heterogeneity. The porosity can vary in 5% range (from 22 to 27 %), depending on mineral composition, intergranular cement content, and presence of organic matter. A straightforward difference is remarkable when using acid solution (ATS) spiked with ^{35}S - much faster penetration through the samples was observed than in the case of cenomanian water spiked with both ^{35}S and ^{3}H. Activity breakthrough was rapid (few hours) indicating processes connected with rock phase dissolution and increase of pore space/preferential transport pathway opening. Acid solution (pH 2) may accelerate the dissolution of Fe + Al minerals mentioned above (e.g. alunite, jarosite) in the pore space and also the dissolution of intergranular cement (kaolinite, illite) and/or carbonate minerals, found even within quartz grains.

Modelling

The differences in kinetic properties of fucoid core samples type of PI and PII were quantified by the means of modelling of sulphate leaching kinetics using six mass transfer models differing in types of the following control processes: so called two-film model (DM), film diffusion (FD), inert layer diffusion (ID), chemical reaction (CR), gel diffusion (GD) and diffusion in reacted layer (RLD) (Stamberg and Cabicar 1980; Stamberg and Plicka 1990). In principle, the results of modelling point to the diffusion character of the leaching of fucoid samples. It seems to be logical because the cenomanian groundwater can be regarded rather as solvent (and the process itself as solvent extraction modelled usually by so called two-film model (DM)), than as classical chemical aggressive leaching agent. With this agree the results of modelling procedure on the basis of which the transfer

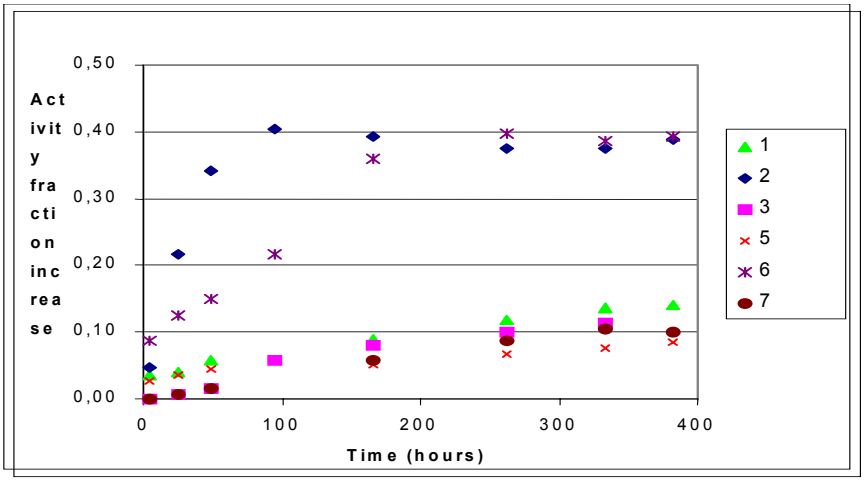

Fig.6. Breakthrough curves for diffusion experiments. See experimental set up and samples identification in Table 3.

model type of DM can be in principle chosen as the best model (see eq. (6):

$$-\frac{dq}{dt} = K_{DM}\left(q - q^{*}\right) \tag{6}$$

where K_{DM} ... kinetic (mass transfer) coefficient, h^{-1},
q ... concentration of a given component in solid phase in time t, mg/g,
q^{*} ... equilibrium concentration of a given component corresponding to the concentration in liquid phase in time t, mg/mL,
t ... time, h.

The values of kinetic coefficients, K_{DM}, characterizing the rate of "leaching" of sulphates from individual fucoid core samples, and the values of quantity *WSOS/DF* (Herbelin and Westall 1996), characterizing the goodness of fit of experimental points (*WSOS/DF* should be smaller than 20) can be found in Table 6. It is evident that the values of K_{DM} belonging to the first group (PI) of core samples re evidently higher than the values of second group (PII) that reflects and proves their different kinetic properties.

Table 6. The results of modelling of kinetic leaching of sulphates

Samples	48541 (PI)	48544 (PII)	48547 (PII)	48550 (PII)	48555 (PI)	48567 (PI)
K_{DM}	1.09e-1 ± 9.49e-4	5.09e-2 ± 1.44e-4	5.08e-2 ± 1.2e-4	5.79e-2 ± 2.78e-2	1.70e-1 ± 9.48e-2	1.43e-1 ± 1.38e-4
WSOS/DF	5.35	8.66	14.0	8.24	8.14	9.77

Conclusions

Contaminants present in fucoid sandstones (predominantly SO_4^{2-}) are leached out relatively fast in the contact with background cenomanian groundwater. The leachate pH value is dependent on SO_4^{2-} release and/or dissolution of Fe-Al-SO_4 minerals (jarosite, alunite, alunogene, copiapite etc.). However, differences in leaching kinetic behaviour were observed. They can be assigned to the rock properties (permeability) and dissolution of secondary mineral phases. Difference in the solubility products of precipitated minerals may contribute to the observed different kinetic patterns. Contaminant transport within fucoid sandstone in contact with background Cenomanian groundwater is driven by diffusion process. This is different from the application of acid solution, when dissolution of rocks and opening of new preferential flow pathways take place.

Acknowledgement

This research was supported by the Ministry of Industry and Trade of the Czech Republic, Grant No. FT-TA3/070.

References

Tessier A, Campbell P G C, Bisson N (1979) Sequential extraction procedure for the speciation of particulate trace metals. Anal Chem 51:844– 50.

Stamberg K, Cabicar J (1980) Models of sorption kinetics in liquid-solid phase system (Modely kinetiky sorpce v systemech kapalina-pevna faze). Acta polytechnica – Technical University of Prague 8 (IV, 1): 107-130.

Stamberg K, Plicka J (1990) The simplified kinetic models describing binary ion exchange systems. Acta Polytechnica– Technic.Univer.of Prague 18 (IV, 3): 5-32.

Herbelin A L, Westall J C (1996) FITEQL – A computer program for determination of chemical equilibrium constants from experimental data, Version 3.2, Report 96-01, Department of Chemistry, Oregon State University, Corvallis, Oregon.

Shackelford Ch.D. (1991) Laboratory diffusion testing for waste disposal – A review. J.Contamin.Hydrology, 7, 177-217.

Skagius K. Neretnieks I. (1998) Porosities and diffusivities of some nonsorbing species in crystalline rocks Water Resources Research 22 3 39 – 398.

Vopalka D., Filipska H., Vokal A. (2006) Some methodological modifications of determination of diffusion coefficient s in compacted bentonite Mat.Res.Soc.Proc Vol 93.

Brenk
Systemplanung

MINING AND ENVIRONMENTAL MANAGEMENT

OUR SERVICES

- Environmental Management
- Radiological Assessments (NORM/TENORM)
- Tailings and Waste Management
- Emergency Response Planning
- Mine Closure and Reclamation
- Design and Planning of Flooding Strategies
- Contaminated Land and Groundwater Remediation

YOUR BENEFITS

- **Sustainable Mining Operations**
- **Cost-Effective and Environmental Sound Solutions**
- **Minimization of Risks and Liabilities**

OUR TOOLS

- Cost-Benefit Analyses
- Geostatistical Analyses
- Geotechnical Engineering
- Surface- and Groundwater Modeling
- Geochemical Modeling
- Air Dispersion Modeling
- Radiological Measurements
- Safety Analyses

Brenk Systemplanung

Heider-Hof-Weg 23
D - 52080 Aachen
Germany

Phone (+49) 24 05 / 46 51 - 0
Fax (+49) 24 05 / 46 51 - 50

www.brenk.com

Permeable Reactive Barriers for Treatment of a Groundwater at a Uranium Mine: Laboratory Evaluation of Reactive Materials

David W. Blowes[1], J.G. Bain[1], S.-W. Jeen[1] and K. Hughes[2]

[1]Department of Earth and Environmental Sciences, University of Waterloo,
[2]Waterloo, Ontario, Canada, N2L 3G1 2AREVA Resources Canada Inc.

Abstract. Oxidation of sulfide minerals has resulted in the release of low quality water from the Claude waste rock storage area at the Cluff Lake Mine in northern Saskatchewan. This low-quality drainage water has been displaced into an underlying aquifer, resulting in the development of a groundwater plume. The principal element of concern in the plume water is dissolved nickel, which occurs in the range of 2 to 14 mg/L. The plume water has low pH (~4.3), is oxidized, contains high concentrations of dissolved sulfate (1000-4750 mg/L), aluminum (up to 45 mg/L), zinc (up to 3 mg/L), cobalt (up to 3 mg/L) and relatively low concentrations of other dissolved heavy metals and iron. A pilot-scale permeable reactive barrier was installed at the site in 2005, to assess the potential for this technology to control the migration. Laboratory experiments are being conducted in conjunction with the field evaluation to assess the treatment performance of three reactive mixtures, which contained organic carbon and varying amounts of zero valent iron (ZVI).

The reactive materials are combined with gravel to maintain adequate permeability. The organic carbon used in the mixtures was obtained from a peat bog near the waste rock storage area. The mixtures include 1) organic carbon mixed with lime and limestone to buffer the pH; 2) organic carbon mixed with 10 vol. % ZVI and 3) organic carbon mixed with 20 vol. % ZVI. The initial results of the column experiments show that all of the mixtures promote bacterially mediated sulfate reduction and removal of dissolved metals through the formation of secondary metal

sulfides. After six months of testing, there was no discernable difference between the two reactive mixtures containing ZVI, and testing of the 20 vol. % mixture was discontinued. Profile sampling indicates that the reactivity of mixture 1, which does not contain ZVI, has declined whereas the reactivity of mixture 2, containing ZVI, has remained constant. The preliminary results of the experiment indicate that the addition of modest amounts of ZVI can increase the longevity of the reactive material. This benefit needs to be weighed against the additional costs associated with the incorporation of ZVI in the reactive mixture.

Depressurising of Deep Underground Workings at McArthur River Mine

Houmao Liu[1], Rashid Bashir[2], Steve Axen[1], James Hatley[2] and Greg Murdock[2]

[1] HCItasca Denver, Inc., Denver, Colorado, USA
[2] Cameco, Saskatoon, Saskatchewan, CANADA

Abstract. The McArthur River mine in northern Saskatchewan is the largest single producer of uranium in the world. Most of the ore is extracted by raisebore mining methods at depths of 530 to 600 m below ground surface where pore pressures in the fractured host sandstone and gneiss are on the order of 5 MPa. Currently, ground freezing is used to isolate the ore from ground-water sources. Localized depressurising of the freezing drifts is being considered to increase their ground-stability.

Cross-hole flow and shut-in tests in eight NQ-size coreholes were conducted in the basement rock that is adjacent to a fault contact with the overlying 500 m thick sandstone unit. The hydrogeologic parameters of basement rock in the vicinity of a freezing drift were obtained. A 15% to 25% reduction of pore pressure over a 25 m distance was observed within a three hour test period.

A detailed three-dimensional ground-water flow model was constructed to replicate the pore pressure measured in the coreholes. The pore pressure distribution simulated from the model provides the hydrogeologic input for geotechnical engineers to evaluate ground-stability and assess whether additional active depressurising should be conducted.


Uranium Mining
and Hydrogeology

Could the calixarenes be a viable solution for radioactive decontamination of mine waters from Romania?

Ioana-Carmen Popescu[1], Florian Aurelian[1], Viorica Ciocan[1], Petru Filip[2] and Zoia Cristu[3]

[1]R&D National Institute for Metals and Radioactive Resources –ICPMRR, Blvd. Carol I no.70, sector 2, 020917-Bucharest Romania, JanePopescu@gmail.com
[2]Institute of Organic Chemistry "C.D.Nenitescu" form Romanian Academy, Spl. Independentei 202B, sector 6, 060023-Bucharest Romania, pfilip@cco.ro
[3]R&D National Institute for Chemistry and Petrochemistry –ICECHIM Bucuresti, Spl. Independentei no. 202, sector 6, 060021-Bucharest Romania, cristu-zoia@yahoo.com

Abstract. The present paper shall briefly overview the past of the Romanian uranium industry and its current state. Then it will present the features of the radioactive contaminated mine waters and the treatment methods used for their decontamination. The advantages and the disadvantages of the decontamination method will be pointed out . The main updates concerning the calixarenic derivatives behavior towards uranium will be presented.

Uranium industry in Romania

Since 1950s the Romanian uranium industry met its top development, when uranium-bearing ores were found by radiometric investigations and aerial gamma prospecting in three main areas, namely Banat, Apuseni Mountains and Eastern Carpathians (Georgescu D., Popescu M. and Aurelian F , 2004).

Since 1952 until 1962, uranium ore was directly extracted and exported to the former Soviet Union, respectively to the Silimäe ore processing plant in Estonia. On 1962, its shipment to the Soviet Union was stopped and it was stockpiled nearby the mining pits. Since 1978 the stockpiled ore beside the new extracted one began to be processed when Feldioara plant was commissioned. Beside that the specific technological researches were tightly related with scientific studies about wastes treatment, mining activities closure and ecological restoration of affected areas by extraction and processing uranium ores (Popescu I.C. et. al., 2005).

Under the complex international context and due to the public concern increasing about the radiological risk and the radioactive contamination threats, the uranium extraction and processing activities were almost closed in Romania, following the European pattern, and the entire scientific interest was shifted towards the environment radioactive decontamination within the areas affected by uranium exploration, exploitation and processing activities.

We have to underline the fact that the information concerning the uranium industrial activity is still classified and protected by the secrecy law.

The main assignments for the research scientist teams were to elaborate extraction flow sheets and projects in order to process the Romanian uranium ores, to purify yellow-cake and to produce nuclear pure uranium dioxide powder.

Main aspects concerning the environmental radioactive pollution and exposure pathways

The environment radioactive pollution is caused mainly by the flow of water on horizontal and vertical direction that enhances the chemical reactions such as leaching processes and rocks' weathering. Other chemical reactions may be initiated either by the microbiological processes or the biofilms occurrence on the surface of the minerals and they are consisting mainly in the minerals' and other elements' oxidation. The most complex chemistry could be observed in cases when the organic compounds are included into the rock mass and the degradation processes will significantly influence the environmental chemistry for the rest of contaminants. Biological contaminants degradation will determine the releases of different gases such as methane,, hydrogen sulfide, carbon dioxide or ammonia.

One of the most important possible exposure pathways is the use of contaminated aquifers or rivers as sources for potable water or for irrigation of crops and watering the livestock.

The air contamination is based on the re-suspension of dust or releases of radon, which may occur. So the inhalation and the contamination of surroundings represent secondary pollution sources.

Radioactive contaminated mine waters features and the decontamination methods used

As it is already known the uranium industry is a significant pollution source, which generated huge amounts of radioactive contaminated wastewaters. A very important part of them is represented by the mine waters, which are a serious threat for the environment and for the people living nearby as well.

The interaction between radioactive contaminated mine waters and environment is very complex because it depends on a lot of factors such as the pH and temperature of water; the uranium ore body geological nature; environmental con-

ditions (aerobic or anaerobic environment); the microorganisms' presence, etc. So to identify the most appropriate and economic feasible solution from the radioactive decontamination viewpoint in order to treat the mine waters contaminated by the radionuclides could be a very difficult challenge.

Before 1989, among the other assignments, in Romania, to recover the uranium from mine waters was a national strategic objective for the research scientists involved in the uranium industrial activity. It was also important to come up with a viable solution using indigenous reagents and substances. Therefore a lot of research studies were performed using different types of ion exchange resins. The most promising one was called VIONIT AT1, a strong basic anionite, fabricated in Romania by the Chemical Plant Victoria from Ramnicu Valcea, which was able to uptake around 100 mg U per 1 mg of resin. Other alternative methods for the recovery of uranium were tested in lab as well.

One of many options was to create a new sort of adsorbent by chemical extraction of the humic acids contained by an indigenous sort of charcoal and to impregnate them into an inert support. Despite the fact that the test results were encouraging respectively the uranium uptake was of about 300 mg / g of humic acids in situ investigations pointed out the inefficiency of this method as the uranium's recovery concerns because only about 3 mg U /g of product were up-taken.

The ionic flotation, uranium precipitation using limestone and iron sulfate, adsorbtion on other adsorbents were also studied as radioactive decontamination methods.

In practice (Popescu I.C., 2005) the methods used for the treatment of radioactive contaminated mine waters could be grouped in:

- Physical methods mainly based on the adsorption, absorption and ion exchanging processes using organic or inorganic compounds;
- Chemical methods that involve redox reactions;
- Biological methods that involve the microorganisms' growth reaction based on electron transfer mechanism.

The control analysis performed out lined the following list of mine water contaminants, which should be removed according to the Romanian specific regulation enforced: solid suspension matter, which proved to contain natural radionuclides, especially uranium and radium; solubilized uranium due to the conjugated action of more favorable factors on the way covered by the underground water through the mine; radium, which is present as an equilibrium element of the radioactive disintegration of uranium.

It has to be underlined the fact that in mine water, all the contaminants listed above have presented content values higher compared to the Romanian safety limits. By time, it has been observed a decrease of this concentration; in fact the variation of this concentration depends on the mining activity intensity and on the quality of the mined ore.

Between 70's and early 80's the concentration of solids in suspension had values higher than 10 g/L, uranium content was frequently higher than 4 mg/L and the radium content was about 0.5 Bq/l. On 1999 mine water analysis showed that ore solid suspension values were less than 5 g/L, uranium content between 1.5-2 mg/L and radium between 0.1-0.3 Bq/lL

Our research scientists' team elaborated a technical flow sheet following the research studies results in order to radioactively decontaminate the mine waters. On its basis a treatment plant was erected and the flow sheet is presented by fig.1.

The other potential contaminants, such as heavy metals, especially mercury and arsenic reached a concentration under the safety limits and thus there will be no need for additional treatment of mine water because of them.

Our most recent chemical analysis of mine water samples showed they have a relative complex composition such as suspended materials ~10 mg/L, uranium present as $Na_4UO_2(CO_3)_3$ ~1.6 mg/L, nitrates ~20 mg/L, sulfates ~0.20 mg/L, chlorides ~0.30mg/L, calcium ~40 mg/L, molybdenum (II) 0.20 mg/L, magnesium ~20 mg/L, $NaHCO_3$ ~ 1000 mg/L. The pH of the water ranges from strong basic to low acidic.

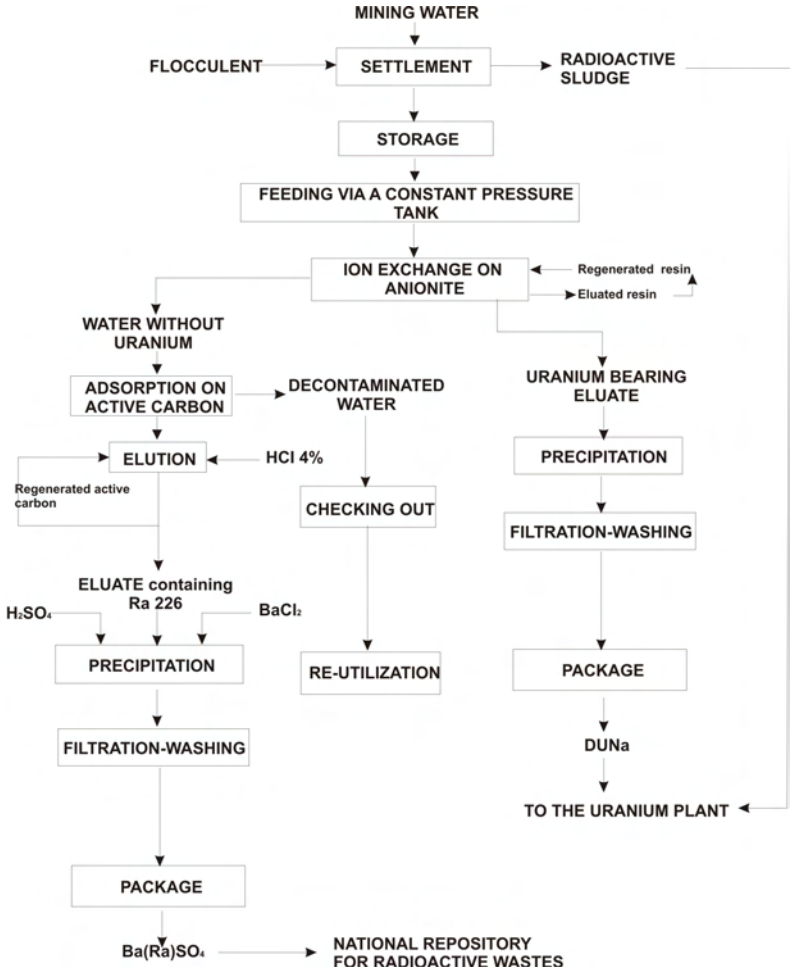

Fig.1. Radioactive mine waters decontamination flow sheet.

Could the calixarenes be a viable solution for the radioactive decontamination of the mine waters?

Despite of their extremely encouraging results each one of the above mentioned procedures presents some weak points such as is the case of the bioremediation processes, where everything is beautiful until the poor micro-organisms die and all the radionuclides accumulated by their bodies return into the natural circuit.

It is important not to ignore the fact that now the science made significant progress in getting to understand intimately the chemical behavior of uranium and his progenitors at molecular level such as in the supramolecular chemistry's case and has reached a point in which is able to filter molecules (see the reverse osmosis units, nano- and ultra-filtration ones as well). Unfortunately the last ones are in many cases too expensive to afford it.

Many research studies have been carried out worldwide in order to synthesize extremely selective organic molecule able to discriminate between the competing ions, to retain uranium and to discriminate the radioactive mine water.

In their quest for the appropriate answer they discovered a very promising class of organic compounds known as calixarenes (Schmeide, K, et. al. , 2002). Calixarenes are macrocyclic molecules formed by 4, 6 ore 8 para-substituted phenolic units linked by methylene bridges ortho to the OH functions (fig.2).

Thus, molecules of different ring sizes are formed. It has been reported recently that the ones especially designed are suitable to separate uranium from aqueous solutions. They have huge potential for industrial applications depending on their structure such as in the case of the uranium detecting sensors (Becker A. et. al., 2005), in determination of uranium contents in the human body fluids (Baglan N., et. al. 2005), separation of cesium and strontium, lanthanides sequestration (Perin R. et. al., 1993), separation of neutral organic molecules, uranium recovery, acce-

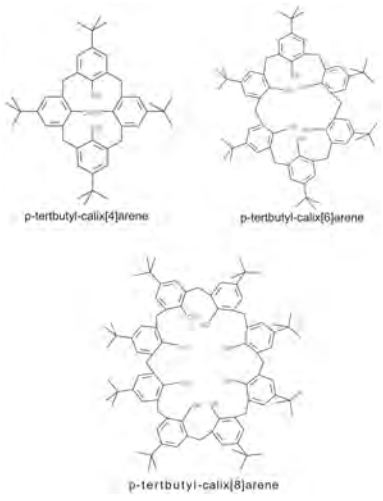

Fig.2. Calix[n]arenas structures (where n=4, 6 or 8).

lerators for instant adhesives, heavy metals separations (Nechifor and so on.

Tests performed on synthetic solutions conducted to recent reports concerning the high selectivity for uranium of the calix[6]arenas functionalized with carboxylic or hydroxamic groups on the lower rim (Schmeide, K, et. al. , 2002).

Conclusions

Romanian uranium mining is a very important source of pollution because it generates is a very important source of pollution because it generates huge amounts of radioactive contaminated wastewaters. The mining water represents a very important part of them and their chemical composition depends on many different environmental factors. The recent research reports' results indicate that the calixarenas could be a very good answer to the potential difficulties in decontaminating radioactive mine waters. Whether they are suitable or not for it, that can be found out only by carrying out new research studies.

References

Georgescu D., Popescu M. and Aurelian F (2004), Assessment of environmental impacts duet o radioactive contamination from uranium mining activities in Romania, 1st International Conference, Advances in Mineral Resources Management and Environmental Geotechology" –AMIREG 2004, 7-9 June 2004, Hania, Crete, Greece.

Popescu I.C. et.al (2005) "Consideration concerning the role played by uranium organometallic complexes during the treatment of radioactive waste waters resulted from uranium mining industry" International Symphosium "Environment and Industry", Bucharest, Romania (2005)

Schmeide, K, et. al. (2002) Complex formation between uranium (VI) and calix[6]arenes studied by time-resolved laser-induced fluorescence spectroscopy, http://www.fjfi.cvut.cz/radchem/formmeet/radchem2002/confprog/session6.html (2002)

Becker A., Tobias H., Porat Z. and Mandler D., Detection of Uranium(VI) in Aqueous Solution by a Calix[6]arene Modified Electrode, (2005) available on the following website address: http://www.forumsci.co.il/chemistry/05/abstracts/P-15.doc (2005)

Baglan N., Cossonnet C., Franck D., Internal exposure of personnel: measurements in an accident situation and expert appraisal in a post-accident situation available on: http://www.irsn.fr/va/09_int/09_int_3_lib/pdf/Ra_sc_tech/143_149.pdf

Perrin R., Lamartine R. and Perrin Monique (1993) , "The potential industrial applications of calixarenes", Pure &App/. Chern., Vol. 65, No. 7, pp. 1549-1559,1993 Printed in Great Britain, @ 1993 IUPAC

Nechifor A., Raicopol M., Serban B., Nechifor G., Josceanu Ana-Maria (2002), "Facilitated Transport of Heavy Metal Ions Through a Magnetic Liquid Membrane Using Azocalix-[4]-Arenes Carriers" Supramolecular Chemistry, Fifth COST D11 Workshop, Singtuna, Sweden, 2002, http://www.orgchem.kth.se/cost/Book%20of%20abstracts%20II.pdf

Treatment of acid drainage in a uranium deposit by means of a passive system

Stoyan Groudev, Irena Spasova, Marina Nicolova and Plamen Georgiev

Department of Engineering Geoecology, University of Mining and Geology "Saint Ivan Rilski", Studenstski grad - Durvenitza, Sofia 1700, Bulgaria

Abstract. Acid mine drainage generated in the uranium deposit Curilo, Bulgaria, with a pH of about 2.5 - 4.0 and polluted with radionuclides (U, Ra), heavy metals (Cu, Zn, Cd, Pb, Ni, Co, Fe, Mn), arsenic and sulphates, were treated efficiently by means of a passive system consisting of a permeable reactive multibarrier and a constructed wetland. The multibarrier consisted of an alkalizing limestone drain and an anoxic section for microbial sulphate reduction, biosorption and additional chemical neutralization. The water flow rate trough the multibarrier varied in the range of 1 - 17 m^3/24 h, reflecting water residence times of about 300 to 18 h.

Introduction

The acid mine drainage waters generated in the uranium deposit Curilo, Bulgaria, are a heavy environmental problem, especially since the end of the mining operations in this deposit sixteen years ago. The fractured ore body and several dumps consisting of mining wastes are, especially after rainfall, the main sources of these waters. The waters have a low pH (usually in the range of 2.5 – 4.0) and contain radionuclides, heavy metals, arsenic and sulphates in concentrations usually much higher than the relevant permissible levels for waters intended for use in the agriculture and/or industry. The solubilization of these pollutants from the residual ore in the deposit is connected mainly with the oxidative activity of the indigenous acidophilic chemolithotrophic bacteria (Groudev et al. 2003).

Since a relatively long period of time a portion of the above-mentioned polluted waters is treated by means of different passive systems such as natural and constructed wetlands, alkalizing limestone drains, permeable reactive multibarriers and a rock filter, used separately or in different combinations. Information about the water treatment carried out by means of these passive systems has been presented in several papers, the most recent of which are these by Groudev et al. (2007a, 2007b). The best results in water clean up were achieved by means of a

complex system involving a permeable reactive multibarrier and a constructed wetland connected in a series. This system was put into operation in the summer of 2004. The present paper summarizes the data obtained during the 42-month operation period and contains the main conclusions based on these data.

Materials and methods

The passive system was constructed in a ravine collecting a portion of the acid drainage waters generated in the deposit. The multibarrier was a pond dug into the ground and its bottom and walls were isolated by an impermeable plastic sheet. The multibarrier consisted of two sections: an alkalizing limestone drain and an anoxic section for microbial dissimilatory sulphate reduction, biosorption and additional chemical neutralization. The alkalizing drain had a volume of about 2.5 m^3 and was filled by a mixture of crushed limestone and gravel pieces (in a ratio of about 1:2 as dry weight) with a particle size less than 12 mm. The second section of the multibarrier had a volume of about 20.4 m^3 (8.0 m long, 1.7 m wide, and 1.5 m deep) and was filled by a mixture of biodegradable solid organic substrates (cow manure, plant compost, straw), crushed limestone and zeolite saturated with ammonium phosphate. This section of the multibarrier was inhabited by a microbial community consisting mainly of sulphate-reducing bacteria and other metabolically interdependent microorganisms (Table 1).

In the spring of 2007 about half of the content of the alkalizing drain and about 30 % of the content of the anoxic section were changed by fresh materials with the relevant initial composition to restore partially the permeability and activity of the multibarrier. The constructed wetland consisted of two sections and was a pond

Table 1. Microorganisms in the acid mine drainage and in the effluents from the permeable reactive multibarrier

Microorganisms	In the acid mine drainage	In the multibarrier effluents
	Cells/ml	
Fe^{2+}-oxidizing chemolithotrophs (at pH 2)	$10^4 – 10^7$	$0 – 10^2$
Aerobic heterotrophs (at pH 2)	$10^1 – 10^4$	$10^1 – 10^3$
$S_2O_3^{2-}$-oxidizing chemolithotrophs (at pH 7)	$0 – 10^3$	$10^1 – 10^4$
Aerobic heterotrophs (at pH 7)	$0 – 10^2$	10^1 - 10^4
Anaerobic heterotrophs (at pH 7)	$0 – 10^1$	10^4 - 10^7
Sulphate-reducing bacteria	$0 – 10^1$	$10^4 – 10^7$
Cellulose-degrading microorganisms	0	$10^3 – 10^6$
Bacteria fermenting sugars with gas production	0	$10^3 – 10^7$
Ammonifying bacteria	0	$10^2 – 10^5$
Denitrifying bacteria	0	$10^2 – 10^5$
Fe^{3+}-reducing bacteria	0	$10^3 – 10^6$
Methane-producing bacteria	0	$10^1 – 10^4$

dug into the ground and its bottom and walls were isolated by an impermeable plastic sheet. The wetland was 12 m long, 2.4 m wide, and 0.8 m deep. Its bottom was covered by a 0.5 m layer consisting of soil rich in organics and mineral nutrients. The wetland was characterized by an abundant water and emergent vegetation and a diverse microflora. *Typha latifolia, Typha angustifolia* and *Phragmites australis* were the main plant species in the wetland but representatives of the *genera Juncus, Eleocharis, Potamogeton, Carex* and *Poa* as well as different algae were also present. The quality of the waters was monitored at different sampling points located at the inlet and the outlet of the alkalizing drain, the anoxic section and the constructed wetland, as well as at different depths within these components of the passive system.

The parameters measured in situ included: pH, Eh, dissolved oxygen, total dissolved solids and temperature. Elemental analysis was done by atomic adsorption spectrophotometry and induced coupled plasma spectrophotometry in the laboratory. The radioactivity of the samples was measured, using the solid residues remaining after their evaporation, by means of a low background gamma-spectrophotometer ORTEC (HpGe – detector with a high distinguishing ability). The specific activity of ^{226}Ra was measured using a 10 l ionization chamber.

Elemental analysis of solid samples from the sediments and the plant biomass was performed by digestion and measurement of the ion concentration in solution by atomic adsorption spectrophotometry and induced coupled plasma spectrophotometry. Mineralogical analysis was carried out by X – ray diffraction techniques. The mobility of the pollutants was determined by the sequential extraction procedure (Tessier et al. 1979). The fraction analysis of the solid organic component in the multibarrier was performed using air dried samples after their prior washing with distilled water to remove the carbonates and the water – soluble organic compounds. The total amount of crystalline polysaccharides (cellulose) and non-crystalline polysaccharides (hemicellulose) was determined by hydrolysis with sulphuric acid (Ryan et al. 1990). The non-crystalline polysaccharides (hemicellulose) were determined by hydrolysis with hydrochloric acid under anaerobic conditions (Lowe 1993). For determination of lignin the samples were initially treated by 1 M HCI for 12 h to remove the solid precipitates from the surface of the organic matrix and to make it well exposed for the subsequent solubilization of the lignin. This solubilization was performed by means of solution containing 2 M NaOH, CuO, $Fe(NH_4)_2(SO_4)_2.6H_2O$ under anaerobic conditions, at 170 ^0C for a period of 4 h in the Soxhlet apparatus (Kögel and Böchter 1985). The suspensions of dissolved organic compounds obtained by the above-mentioned hydrolythic treatments were clarified by centrifugation at 1700 rpm for 30 min. The clarified supernatants were used for determination of the concentration of the respective dissolved organic compounds by their chemical oxidation to CO_2 at high temperature.

The isolation, identification and enumeration of microorganisms were carried out by methods described elsewhere (Karavaiko et al. 1988; Widdel and Hansen 1991; Widdel and Bak 1991; Groudeva and Tzeneva 2001; Hallberg and Johnson 2001).

Results and discussion

An efficient removal of pollutants from the acid drainage waters was achieved by means of the multibarrier (Tables 2). The water flow rate through the multibarrier was changed considerably during the operation period (within the range of about 1 – 17 m^3/24 h, reflecting water residence times of about 300 – 18 hours). These changes were connected mainly with the activity and permeability of the multibarrier.

The activity of the multibarrier was based on three main mechanisms participating in the removal of pollutants: chemical neutralization, biosorption and microbial dissimilatory sulphate reduction. The chemical neutralization was performed by the crushed limestone mainly in the alkalizing drain but also in the second, rich-inorganics section. In the alkalizing drain the pH of the polluted waters was increased to values near the neutral point and as a result of this most of the dissolved iron (present as Fe3+ ions) was precipitated as ferric hydroxides. Portions of the non-ferrous metals and aluminum (usually about 20 – 40 % and about 70 – 80 %, respectively) were also removed in the drain as a result of hydrolysis and subsequent precipitation as well as by sorption by the gelatinous ferric hydroxides. Portions of uranium and arsenic were also removed in this way. The increase in pH in

Table 2. Data about the acid mine drainage and the effluents from the permeable reactive multibarrier

Parameters	Acid mine drainage	Multibarrier effluents	Permissible levels for waters intended for use in agriculture and industry
Temperature ^oC	(+1.2) - (+25.1)	(+1.4) - (+27.5)	-
pH	2.42 – 4.25	6.22 – 7.83	6 – 9
Eh, mV	(+290)-(+597)	(-140)-(-280)	-
Dissolved O_2, mg/l	1.7 – 6.0	0.2 – 0.4	2
TDS, mg/l	930 – 2972	545 – 1827	1500
Solids, mg/l	41 – 159	32 – 104	100
DOC, mg/l	0.5 – 2.1	51 – 159	20
SO_4^{2-}, mg/l	532 – 2057	275 – 1225	400
U, mg/l	0.10 – 2.75	< 0.05	0.6
Ra, Bq/l	0.05 – 0.50	< 0.03	0.15
Cu, mg/l	0.79 – 5.04	< 0.20	0.5
Zn, mg/l	0.59 – 59.8	< 0.20	10
Cd, mg/l	<0.01 – 0.10	< 0.004	0.02
Pb, mg/l	0.08 – 0.55	< 0.02	0.2
Ni, mg/l	0.17 – 1.49	< 0.03 – 0.10	0.5
Co, mg/l	0.12 – 1.22	< 0.03 – 0.10	0.5
Fe, mg/l	37 – 671	0.5 – 9.5	5
Mn, mg/l	2.8 – 79.4	0.5 – 5.2	0.8
As, mg/l	0.05 – 0.32	< 0.01	0.2

the alkalizing drain facilitated the growth of microorganisms in the second section of the multibarrier. The role of chemical neutralization was essential during the cold winter days when the growth and activity of the microbial community in the multibarrier was inhibited or completely ceased. The chemical generation of alkalinity steadily decreased in the course of time because the limestone was armored due to the iron precipitates deposited on its surface. The change of approximately half of the limestone in the alkalizing drain by fresh batch of this material restored to a significant degree the alkalinity production and permeability of this section of the passive system.

The biosorption of pollutants by the dead plant biomass present in the second section of the multibarrier was also an essential mechanism in the water clean up during the warmer but mainly during the cold months of the year (Table 3). Considerable portions of all heavy metals, arsenic and uranium as well as most of the radium were removed in this way. The biosorption, together with the chemical neutralization, was the prevalent mechanism during the first 5 – 6 months since the start of the operation and even later was prevalent in the first 3 – 4 m from the inlet of the anoxic section, especially in the top layers (down to 50 – 70 cm from the surface). The sorption capacity of the dead biomass steadily decreased in the course of time.

The microbial dissimilatory sulphate reduction played an essential role in the water clean up during the warmer months of the year. The anaerobic sulphate-reducing bacteria were a quite numerous and diverse population in the multibarrier (Table 4). The prevalent and most active strains of these bacteria were related to the genera *Desulfovibrio (mainly D. desulfuricans)* and *Desulfobulbus (mainly D. elongatus)* but representatives of the genera *Desulfococcus, Desulfobacter* and *Desulfosarcina* were also well present. As a result of their activity the pH of the waters was stabilized around the neutral point due to generation of hydrocarbonate ions during the microbial sulphate reduction (the role of limestone was also essential as it was mentioned earlier). The non-ferrous metals, iron and arsenic were

Table 3. Content of pollutants in the dead solid plant biomass in the permeable reactive multibarrier

Pollutants	Content, mg/kg dry biomass				
	November 2004	March 2005	March 2006	September 2006	March 2007
Uranium	10-32	17-71	32-114	32-122	30-127
Radium	5-14	10-32	21-53	23-57	23-60
Copper	28-73	37-134	60-225	62-221	64-223
Zinc	14-51	28-82	51-230	59-242	62-248
Cadmium	2-12	6-19	8-41	8-44	9-42
Lead	8-30	7-59	15-73	15-77	16-78
Nickel	8-35	9-62	15-90	19-95	23-99
Cobalt	5-30	11-51	17-82	16-30	18-91
Manganese	32-109	37-135	51-210	55-233	51-230
Arsenic	2-14	6-23	12-44	12-51	12-55

Table 4. Sulphate-reducing bacteria in the effluents from the permeable reactive multibarrier

Sulphate-reducing bacteria	Cells/ml
Desulfovibrio (mainly *D. desulfuricans*)	10^4 - 10^7
Desulfobulbus (mainly *D. elongatus*)	10^2 - 10^7
Desulfococcus (*D. postgatei*)	10^2 - 10^6
Desulfobacter (*D. multivorans*)	10^2 - 10^5
Desulfotomaculum (mainly *D. nigrificans*)	10^1 - 10^4
Desulfosarcina (*D. variabilis*)	10^2 - 10^5
Desulfomonas (non-identified species)	10^1 - 10^4

precipitated mainly as the relevant insoluble sulphides. Uranium was precipitated mainly as uraninite (UO_2) as a result of the prior reduction of the hexavalent uranium to the tetravalent form. All these precipitates were present mainly in the relevant oxidizable mobility fractions.

A relatively long period of time (of about 3 – 4 months) was needed for the sulphate-reducing bacteria to establish a numerous and very active population in the multibarrier. The microbial sulphate reduction was the prevalent mechanisms in the deeply located layers and in the back zones in the multibarrier (at distances longer than 4 – 5 m from its inlet). The microbial sulphate reduction was a function of the concentration of organic monomers dissolved in the waters. These monomers were generated as a result of the biodegradation of the solid biopolymers by the different heterotrophs possessing hydrolythic enzymatic activity. This process resulted in a steady decrease in the concentration of the easily degradable solid biopolymers (cellulose and hemicellulose) present in the mutibarrier (Table 5). At the same time, the precipitation of pollutants caused a negative effect on the permeability of the multibarrier (Table 6). It must be noted that the precipitation of the different pollutants was not homogenous and the different sites in the multibarrier differed considerably from each other with respect to their chemical and mineralogical composition (Table 7). The contents of the different mobility fractions of the pollutants in these solid samples were also different (Table 8). The data from these determinations revealed the relative role of the different mechanisms involved in the water cleanup during the different climatic seasons. The relative portions of the easily leachable mobility fractions (exchangeable and carbonate) in the sediments formed during the cold winter months were much higher than the respective portions in the sediments formed during the warmer months.

The partial change of the solid mixture by fresh material with similar initial composition carried out in the spring of 2007 restored considerably the permeability of the multibarrier and the activity of the anaerobic microbial community. This resulted in an increase of the concentration of dissolved organic substances and the rate of sulphate reduction.

Table 5. Exhaustion of the solid biodegradable organic substrates in the multibarrier during the water clean up

Organic fraction and time of sampling	Sampling points, distance from the inlet					
	1 m top	1 m down	3 m top	3 m down	6 m top	6 m down
	Organic carbon in the sample (percent)					
Crystalline polysaccharides:						
July 2004	8.2	8.2	8.2	8.0	8.2	8.1
November 2005	3.2	4.4	3.5	4.8	3.2	4.3
November 2006	0.5	0.5	0.4	0.8	0.5	0.7
May 2007	2.8	1.0	2.1	0.9	0.8	0.6
Non-crystalline polysaccharides:						
July 2004	37.4	37.1	37.0	37.0	37.4	37.1
November 2005	16.1	21.5	20.3	23.9	20.8	24.0
November 2006	1.4	1.9	1.7	2.8	2.3	3.0
May 2007	6.4	4.1	5.9	3.5	2.1	2.3
Lignin:						
July 2004	5.1	5.1	5.0	5.0	5.2	5.1
November 2005	4.8	5.0	4.7	4.6	4.8	4.8
November 2006	4.6	4.8	4.3	4.1	4.4	4.5
May 2007	5.0	4.6	4.8	4.2	4.1	4.0

Table 6. Data about the changes in the permeability of the main sections of the multibarrier during the treatment of the polluted waters

Section of the multibarrier	Time since the start of the operation, months				
	0 (start)	9	16	22	28
	Filtration coefficient, m/h				
Alkalizing drain	110.4	34.6	10.8	4.7	0.08
Zones in the section for MDSR:					
2 m from the inlet	7.2	3.8	1.5	1.4	0.06
4 m from the inlet	7.2	5.7	3.1	2.6	0.07
6 m from the inlet	7.2	6.6	5.6	5.1	0.08

The microbial activity in the multibarrier markedly depended on the temperature and during the cold winter days was negligible. However, at air temperatures about 0 ^{o}C and water temperatures close to freezing point, the temperatures inside the multibarrier, within the deeply located layers, usually were in the range of about 2 – 6 ^{o}C. Under such conditions the microbial sulphate reduction still proceeded, although at much lower rates. In any case, the water clean up efficiency of multibarrier was much higher during the warmer months of the year (Table 9).

Table 7. Data about the composition of solid samples from the permeable multibarrier

Parameters	Zones in the section for microbial sulphate rduction					
	2 m from the inlet		4 m from the inlet		6 m from the inlet	
	Time since the start of the operation, months					
	16	28	16	28	16	28
pH (KCl)	5.68	7.06	6.35	7.23	7.43	7.45
Ash content, %	71.0	81.9	62.0	70.7	64.0	72.4
Organic content, %	29.0	18.1	38.0	29.3	36.0	27.6
Cu, mg/kg	1211	1950	482	1466	76.4	212
Zn, mg/kg	587	1488	363	921	135	183
Cd, mg/kg	4.9	15.2	2.9	5.2	0.9	1.0
Pb, mg/kg	46.6	41.9	74.9	68.0	36.9	70.7
Ni, mg/kg	269	1565	249	906	20.2	118
Co, mg/kg	298	890	98.4	495	8.8	59
Fe, mg/kg	6204	6632	6512	6804	6468	7120
Mn, mg/kg	473	895	810	2161	459	783
U, mg/kg	60.3	215	45.3	190	11.1	59.6
As, mg/kg	4.96	0.8	0.4	1.1	1.1	1.4
S total, mg/kg	6612	10087	6239	9111	5520	7050

Table 8. Distribution of pollutants in sediments from the permeable reactive multibarrier into different mobility fractions (as % from the total content of the respective pollutant)

Pollutants		Portions in different mobility fractions, %			
		Exchangeable	Carbonate	Oxidizable	Reducible
U	W	7 – 18	3 – 12	60 – 88	2 – 5
	C	21 – 46	8 – 16	41 – 62	2 – 6
Ra	W	68 – 86	3 – 11	2 – 8	5 – 14
	C	71 – 91	3 – 9	2 – 6	4 – 10
Cu	W	7 – 18	4 – 12	54 – 82	5 – 9
	C	12 – 28	10 – 24	32 – 64	4 – 8
Mn	W	21 – 41	19 – 35	15 – 37	5 – 10
	C	28 – 60	23 – 46	10 – 21	5 – 11
Fe	W	7 – 17	14 – 27	44 – 77	8 – 23
	C	14 – 30	25 – 46	14 – 29	19 – 39

Notes: W – during the warmer months; C – during the cold winter months (December – February);

The effluents from the multibarrier were enriched in dissolved organic compounds and in some cases still contained manganese and iron in concentrations higher than the relevant permissible levels (Table 2). These effluents were treated in the constructed wetland where the Mn^{2+} and Fe^{2+} ions were oxidized to Mn^{4+} and Fe^{3+} ions by some heterotrophic bacteria producing peroxide compounds and the enzyme catalase, which degraded the excess of peroxides to molecular oxygen and water. The Mn^{4+} and Fe^{3+} ions precipitated as MnO_2 and $Fe(OH)_3$, respectively. The dissolved organic compounds were efficiently degraded by the different heterotrophs inhabiting the wetland.

Table 9. Removal of pollutants from the acid mine drainage by means of the permeable reactive multibarrier during different climatic seasons

Pollutants	Pollutant removed, g/24 h	
	During the warmer months	During the cold winter months (at 0 – 5 ^{o}C)
Uranium	2.42 – 19.2	0.35 – 2.27
Copper	9.74 – 80.2	1.52 – 7.20
Zinc	6.44 – 114.4	1.40 – 9.72
Cadmium	0.14 – 1.20	0.03 – 0.19
Lead	1.24 – 5.05	0.28 – 1.34
Nickel	2.71 – 11.35	0.60 – 2.84
Cobalt	1.80 – 7.81	0.41 – 2.08
Manganese	23.5 – 194	4.73 – 25.9
Arsenic	0.95 – 2.71	0.27 – 1.04
Iron	594 – 5481	88.4 – 712

Conclusions

The data from this study clearly reveal that complex passive systems consisting of an appropriate combination of units performing processes such as chemical neutralization, biosorption, microbial dissimilatory sulphate reduction, microbial oxidation of manganese and iron ions and degradation of organic substances can be used for an efficient clean up of acidic waters polluted with radionuclides, heavy metals, arsenic and sulphates.

The combination of a permeable reactive multibarrier consisting of an alkalizing limestone drain and an anoxic section for microbial sulphate reduction, biosorption and additional chemical neutralization, with a constructed aerobic wetland for microbial degradation of organic substances and oxidation of the residual concentrations of the bivalent manganese and iron ions is very suitable with this respect.

A passive system of this type can operate even at temperatures close to the water freezing point, although at longer residence times. The application of such passive system is connected with a detailed characterization of the composition and flow rate of the polluted waters, as well as of the climatic conditions and the plant and microbial cenoses in the area, in which the system will be constructed.

Acknowledgements

Parts of this work were financially supported by the European Commission under the project No QLRT – 2001 – 02916 “Multifunctional permeable barriers carrying well-performing microbial biofilms for treatment of mixed polluted plumes” and by the Flemish Government under the project “Improvement of groundwater

protection in Bulgaria using advanced environmental impact assessment (EIA) tools" (CO-9004 1755.01).

References

Groudev S N, Georgiev P S, Spasova I I, Nicolova M V (2007a) Sediments in a natural wetland used to treat acid mine drainage water in a uranium deposit, in Second Annual Meeting of the Society of the Wetland Scientists – Europe, Trebon, Chech Republic, May 30 – June 3, 2007 (ed: L. Krőpfelova) pp 52 – 53 (ENKI, ops: Trebon).

Groudev S N, Georgiev P S, Spasova I I, Nicolova M V (2007b) Bioremediation of acid mine drainage in a uranium deposit, in Biohydrometallurgy: From the Single Cell to the Environment (eds: A Schippers, W Sand, F Glombitza and S Willscher), pp. 248-257 (Trans Tech Publications Ltd: Zurich).

Groudev S N, Spasova I I, Komnitsas K, Paspaliaris I (2003) Microbial generation of acid drainage in a uranium deposit, in Mineral Processing in the 21st Century (eds: L Kuzev, I Nishkov, A Boteva and D Mochev), pp.728-732 (Djiev Trade Ltd: Sofia).

Groudeva V I, Tzeneva V (2001) Biodiversity of sulphate-reducing bacteria (SRB) in anaerobic reactor for removal of heavy metals from polluted water, in: Vocational Training in Biotechnology and Environmental Protection, Module II – Environmental Protection and Biotechnology (ed: A. Kujumdzieva), pp. 95-120 (National Bank of Industrial Microorganisms and Cell Cultures: Sofia).

Hallberg K B, Johnson D B (2001) Novel acidophiles isolated from a constructed wetland receiving acid mine drainage, in: Biohydrometallurgy: Fundamentals, Technology and Sustainable Development (eds: V S T Ciminelli and O Garcia Jr), Part A, pp 433-441 (Elsevier: Amsterdam).

Karavaiko G I, Possi G, Agate A D, Groudev S N, Avakyan Z A (eds), (1988) Biogeotechnology of Metals, Manual, 350 p (Centre for International Projects GKNT: Moscow).

Kögel I, Böchter R (1985) Characterization of lignin in forest humus layers by high-performance liquid chromatography of cupric oxide oxidation products, Soil Biology and Biochemistry, 17:640-673.

Lowe L E (1993) Total and labile polysaccharide analysis of soils, in: Soil Sampling and Methods of Analysis (ed: M R Carter), pp 373-376 (Canadian Society of Soil Science: Boca Raton, Florida).

Ryan M G, Melillo J M, Ricca A (1990) A comparison of methods for determining proximate carbon fractions of forest litter, Canadian Journal of Forest Research, 20: 166-171.

Tessier A, Campbell P G C, Bisson M (1979) Sequential extraction procedure for speciation of particulate trace metals, Analytical Chemistry, 51 (7): 844 - 851

Widdel F, Bak F (1991) Gram-negative mesophilic sulphate-reducing bacteria, in: The Prokaryotes (eds: A Ballows, H-G Trüper, M Dworkin, W Harder and K-H Schleifer), vol IV, 2nd edn, pp 3352 – 3378 (Springer: New York).

Widdel F, Hansen T A (1991) The dissimilatory sulphate and sulphur-reducing bacteria, in: The Prokaryotes (eds: A Ballows, H-G Trüper, M Dworkin, W Harder and K-H Schleifer), vol II, 2nd edn, pp 538 – 624 (Springer: New York).

Uranium fixation by *Cladophora spec.*

Claudia Dienemann[1], Holger Dienemann[2], E. Gert Dudel[1] and C. Schurig[1]

[1]TU Dresden, Institute of General Ecology and Environmental Protection, Pienner Str. 8, 01737 Tharandt
[2]Staatliche Umweltbetriebsgesellschaft Bitterfelder Straße 25, 04849 Bad Düben

Abstract. Shaking and throughput flow column experiments were carried out using different species of filamentous green algae. Only *Cladophora aegagropila* allowed operating a column with live algae for app. 36 hours without blockage. Column experiments resulted in much higher retention of uranium than shaking experiments.

Introduction

Downstream of uranium mining residues (tailings and dumps) very high uranium and radium concentration may occur. In the waters of some of these contaminated sites neutral-alkaline pH-values are measured, on the one hand caused by carbonates added during the conditioning process (Wismut 1999) and on the other hand by the paragenesis of the ore: uranitite in combination with different carbonates (Dahlkamp 1993).

Algae are generally able to accumulate heavy metals inclusive radionuclides compared to the surrounding water (Kalin and Smith 1986; Kalin et al. 2002b; Kalin et al. 2005; Vymazal 1995). This ability is important for the application of algae for waste water treatment, e.g. in Constructed Wetlands or throughput flow reactors. Technical use of filamentous algae for eliminating uranium, however, is almost impossible because of the development of mats, which affect diffusion and may clog the reactor.

At the former Wismut mining site Pöhla Characeae are successfully used (Kalin et al. 2002a; Kiessig et al. 2004), which have been tried efficiently in Canadian wetlands where they grow naturally for waste water treatment, however, they are not endemic in the Saxon ore mountains.

Downstream of the aforementioned former uranium mining sites (Lengenfeld, Helmsdorf, Neuensalz; see Fig. 1), green algae were found, some forming dense mats. Obviously, these algae are well adapted to the chemical conditions of dump and tailing waters (e.g. neutral-alkaline milieu, uranium contents several $\mu g*L^{-1}$ to several $mg*L^{-1}$). Uranium concentrations in algae from these waters vary between

20 and 400 µg*g^{-1} (DM) (Dienemann et al. 2002, Kalin et al. 2005, Vogel et al. 2004).

Cladophora spec. was found main species besides *Ulothrix spec*. (Dienemann et al. 2002). Many Cladophora-species are known to form dense algal mats (Pokorný et al. 2002, Paalme et al. 2002), but some may also appear as bowl-like aggregations, which have been subject to investigation for several decades (Potonié 1912). Nowadays, these bowls are e.g. used to treat the water in aquariums.

Unlike *Cladophora fracta* and *Cladophora glomerata Cladophora aegagropila* does form balls instead of mats, so the working hypothesis was that Cladophora aegagropila may be successfully used in a throughput flow reactors eliminating more uranium from the water than filamentous Cladophora-species without clogging the reactor.

Fig.1. Locations: italics: coal mining residues, other: uranium mining residues

Materials and Methods

Material

Three different species of Cladophora were used: *Cladophora fracta*, *Cladophora glomerata* and *Cladophora aegagropila*. *Cladophora aegagropila* was ordered via aquarium-specialized trade and adapted to laboratory conditions for 3 months.

Cladophora fracta was gathered from water from the cooling towers of Boxberg power station. Before adapting and keeping it in the laboratory it was carefully cleared of all debris.

Cladophora glomerata forms stronger filaments than *Cladophora fracta*. It was collected in the downstream areas of the former uranium mining site Neuensalz and kept for more than 6 months under laboratory conditions.

In all algae uranium contents - measured shortly before the experiments - were less than 1 mg/kg TM.

Methods

Uranium solutions (Uraniumacetate, Fa.Chemapol, p.A.) were adjusted by Na_2CO_3 to pH 7.5 in order to induce the formation of uranium-carbonate-complexes. *Cladophora glomerata* and *Cladophora fracta* were used for batch-experiments (m=6gFM, V=100ml, t=20 min, n=4). Algal material and uranium solution were (slowly) shaken via overhead-shaker (Fa. Heidolph; 5 rpm).

Cladophora aegagropila was used for column experiments. A plexiglass column (Makrolan, Fa. PCH) was filled with *Cladophora aegagropila* and water containing LiCl (Tracer; Fa Merck, p.A.). Uranium concentration of the uranium solu-

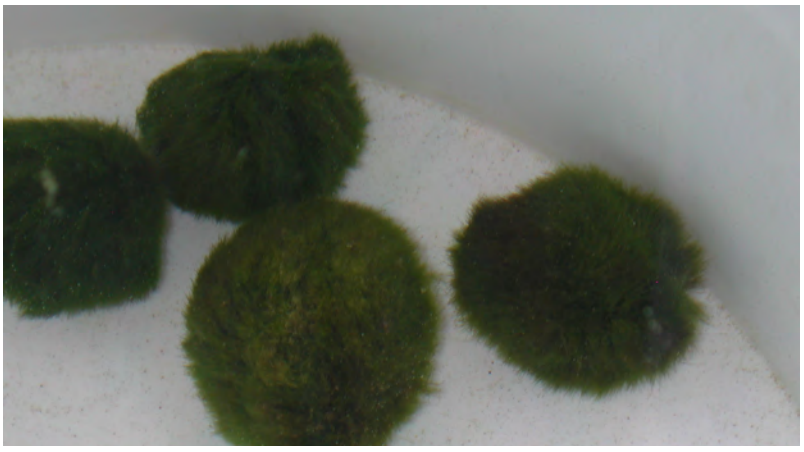

Fig.2. *Cladophora aegagropila*

tion was app. 1700 µg*L^{-1}. Pore volume (250 mL) and exposure time were measured by an extra tracer (KBr (Fa Merck, p.A.)) Flow rate was adjusted to 2ml*min^{-1} (Minipuls, Fa. Gilson)..

Uranium concentration in the uranium solution was measured every 90 minutes, uranium solutions had to be changed after 6 hrs. and after 25 hrs., column outflow was sampled every 30 minutes, all samples were filtrated (0,45µm celluloseacetate, Fa. Sartorius) and concentrations were measured by ICP-MS (Pq2+, Fison/TJA) on isotopes U-238; U-235, Li-7, Br-79 and Br-81.

Results

Fig. 3 shows the results of the batch-experiment with *Cladophora fracta* combined with results from Dienemann et al. 2005 of batch-experiments with the same species and identical experimental design with uranium concentrations of 100 and 250 µg*L^{-1}.

At the end of the experiment, *Cladophora fracta* contained 360 µgU*g^{-1} (DM) (at a water concentration of app. 2700 µgU*l^{-1}).The batch-experiments resulted in no significant difference between *Cladophora fracta* and *Cladophora glomerata* with an average uranium concentration of app. 300 µg*L^{-1}.

Fig. 4 shows the initial concentration (blank values) in the columns for the experiment with *Cladophora aegagropila*. Unfortunately, the necessary re-supply of uranium solution (originally planned to last for 6 hrs.) after 6 and 25 hrs. is clearly marked (arrows).

The application of tracers (Li, KBr) allowed estimating the length of stay in the column (Fig. 5), which is 2 hrs.

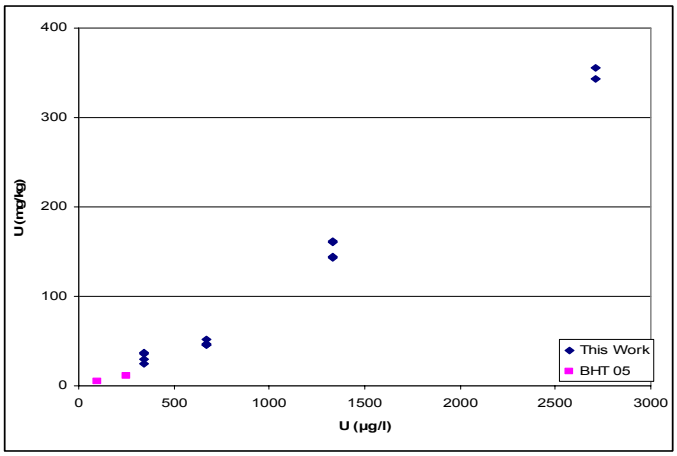

Fig.3. Uranium contents (µg*g^{-1} TM) of *Cladophora fracta* (batch-experiment n=4) of this work combined with results from Dienemann et al. 2005 (r^2 = 0,98)

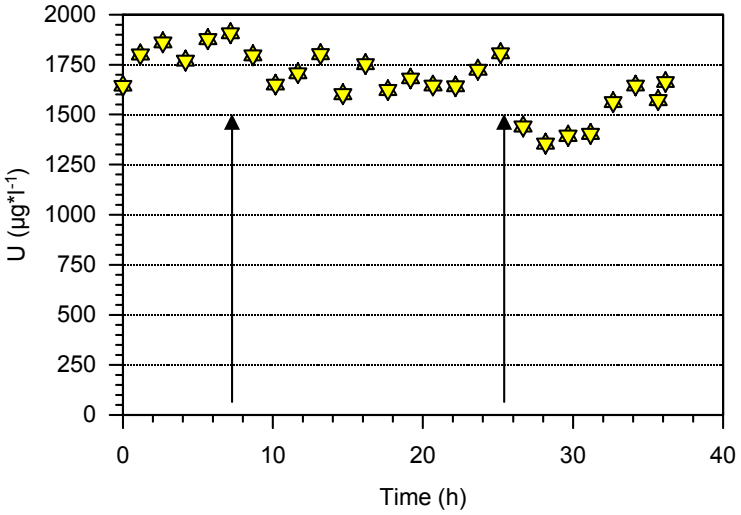

Fig.4. Initial uranium concentrations, experiment with *Cladophora aegagropila*, arrows indicate re-supply of solution

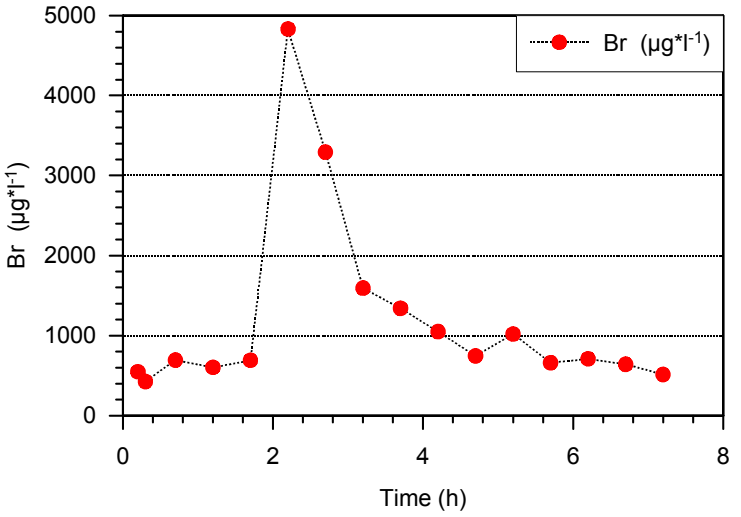

Fig.5. Concentration of tracer for estimation of length of stay in the column (added immediately at the beginning of the experiment) – peak after 2 hrs.

Flow rates were relatively constant (± 10%). Fig. 6 displays differences in uranium concentrations at the column input and output under consideration of the exposure time.

Uranium retention in the column was much higher than expected. Saturation concentration of *Cladophora aegagropila* appears to be app. 800 mg*kg^{-1} DM.

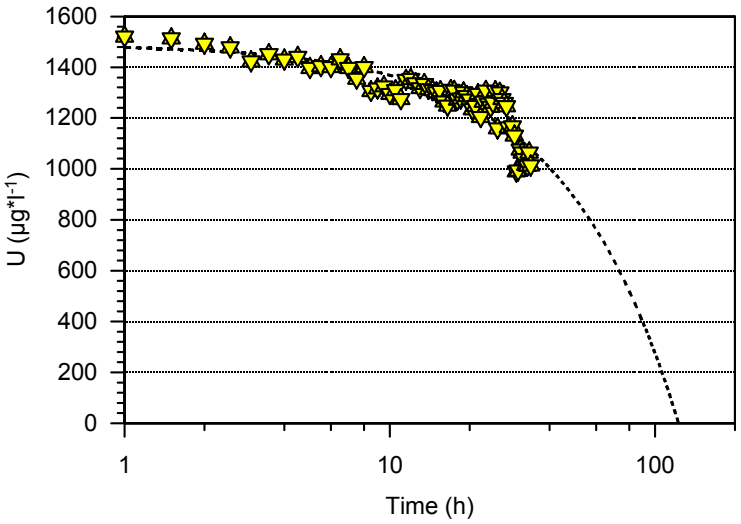

Fig.6. Differences in uranium concentrations at the column input and output under consideration of the exposure time of 2h

Discussion

Batch-experiments show – as expected – relative low uranium retention (see Kalin et al. 2005). Equations comparing the uranium contents in algae of the experiment to those from an artificial flow-path (bypass) in the area of Neuensalz (Vogel and Dudel 2004) correlate.

Differences between filamentous and bowl-like Cladophora species could be explained by differing experiment design, e.g. much longer exposure time in the column experiment. If this were the only reason, it should be possible to find green algae with uranium contents of 700 mg*kg^{-1} DM in the field, which has so far not been the case, although many samples were taken from several former uranium mining sites.

Another difference in the experimental design is the continuous pumping of uranium solution over algae along a column row. It is assumed that at the beginning of the exposition an exchange resp. retention of calcium-ions takes place. Since columns consisted of transparent plexiglass, supposedly live activities of the algae caused CO_2 to be removed from the solution, which would result in a shift of the calcium carbonate-carbonic acid-equilibrium causing carbonate- and calcium concentration to decrease. As these ions are crucial for the uranium speciation, this may result in a change of the uranium species, which increases the sorptive fixation onto the algal material (Dienemann et al. 2005)as well as the probability of reductive fixation (Brooks et al. 2003).

This explanation is also supported by considering the surface of *Cladophora aegagropila*, which appears like a bowl consisting of numerous filaments. So the actual surface is significantly bigger and allows additionally biofilms to grow. Bacteria and fungi may accumulate uranium (Suzuki et al. 2002; Suzuki et al. 2003; Suzuki et al. 2005). Development of biofilms is depending on time.

Algae sampled from the respective ponds usually contained more uranium than found in the water (Dienemann et al. 2002).

Conclusions

Application of *Cladophora aegagropila* allows using conventional throughput flow column reactors for water treatment. Typical problems - like blockage - occuring while using filamentous green algae did not occur. On a larger scale enough light must be provided as well as possibly developing gases considered.

Acknowledgements

Thanks for financial support to BMBF and TU Dresden.
Many thanks for support in keeping all algae and throughout the experiments to K. Hesse, K. Klinzmann and M. Förster. Special thanks to A. Weiske for quick ICP-MS-measurements, even during early morning and late evening hours.

References

Brooks SC, Fredrickson JK, Carroll SL, Kennedy DW, Zachara JM, Plymale AE, Kelly SD, Kemner KM and Fendorf S (2003) Inhibition of bacterial U(VI) reduction by calcium. Environmental Science & Technology 37(9): 1850 -1858

Dahlkamp FJ (1993) Uranium ore deposits. Berlin Heidelberg New York, Springer-Verlag

Dienemann C, Dienemann H, Stolz L and Dudel, EG (2005) Verwendung von Algen und submersen kalzifizierenden Wasserpflanzen zur Aufbereitung neutraler bis basischer Wässer. Behandlungstechnologien für bergbaubeeinflusste Wässer. 56 Berg- und Hüttenmännischer Tag GIS – Geowissenschaftliche Anwendungen und Entwicklungen Wissenschaftliche Mitteilungen 28 B Merkel, H Schaeben, C Wolkersdorfer and A Hasche-Berger Freiberg, TU Bergakademie Freiberg: 27-33

Dienemann C, Dudel EG, Dienemann H and Stolz L (2002) Retention of Radionuclides and Arsenic by Algae Downstream of U Mining Tailings. Uranium Mining and Hydrogeology III B J Merkel, B Planer-Friedrich and C Wolkersdorfer: 605-614

Kalin M and Smith MP (1986) Biological Polishing Agents for Mill Waste Water: An Example Chara. Fundamental and Applied Biohydrometallurgy R W Lawrence, R M R Branion and H G Ebner**:** 491

Kalin, M, Kießig G and Küchler A (2002a) Ecological water treatment processes for underground uranium mine water: Progress after three years of operating a constructed wet-

land. Uranium Mining and Hydrogeology III B J Merkel, B Planer-Friedrich and C Wolkersdorfer: 587-596

Kalin M, Smith M P and Wittrup M B (2002b) Ecosystem restoration incorporating minerotrophic ecology and Stoneworts that accumulate ^{226}Ra. Uranium Mining and Hydrogeology III B J Merkel, B Planer-Friedrich and C Wolkersdorfer**:** 495-504

Kalin M, Wheeler W N and Meinrath. G (2005) The removal of uranium from mining waste water using algal/microbial biomass. Journal of Environmental Radioactivity **78**(2): 151-177

Paalme T, Kukk H, Kotta J and Orav H (2002) "In vitro" and "in situ"' decomposition of nuisance macroalgae *Cladophora glomerata* and *Pilayella littoralis*. Hydrobiologia **475-476**(1): 469-476

Pokorný J, Kvet J, Eiseltová M, Rejmánková E and Dykyjová D (2002) Role of macrophytes and filamentous algae in fishponds. Freshwater wetlands and their sustainable future. - A case study of Trebon Basin Biosphere Reserve, Czech Republic. Kvet J, Jenik J and Soukupová L. Paris New York Boca Raton, UNESCO (United Nations Educational, Scientific and Cultural Organization), The Parthenon Publishing Group **28:** 97-124

Potonié H (1912) Die rezenten Kaustobiolithe und ihre Lagerstätten. Die Humus-Bildungen (2. Teil) und die Liptobiolithe. Berlin, Königlich Preußische Geologische Landesanstalt

Suzuki Y, Kelly SD, Kemner KM and Banfield JF (2002) Nanometer-size products of uranium bioreduction. Nature **419**: 134

Suzuki Y, Kelly SD, Kemner KM and Banfield JF (2003) Microbial populations stimulated for hexavalent uranium reduction in uranium mine sediment. Applied and Environmental Microbiology **69**(3): 1337-1346

Suzuki Y, Kelly SD, Kemner KM and Banfield JF (2005) Direct Microbial Reduction and Subsequent Preservation of Uranium in Natural Near-Surface Sediment. Applied and Environmental Microbiology **71**(4): 1790-1797

Vogel AK and Dudel EG (2004) Zum Einfluss der wasserchemischen Verhältnisse auf die Immobilisierung von Uran und Arsen in submersen Makrophyten (*Chara spec, Microspora spec, Cladophora spec*). Deutsche Gesellschaft für Limnologie (DGL) Tagungsbericht 2004 (Potsdam) Berlin, Weißensee Verlag**:** 486-490

Vymazal J (1995) Algae and Element Cycling in Wetlands. Boca Raton Chelsea Ann Arbor London Tokyo, Lewis Publishers

Wismut (1999) Chronik der Wismut. Chemnitz, Wismut GmbH

Utilization of autochthonous SRB in uranium mine site remediation

Martin Hoffmann[1], Andrea Kassahun[1] and Ulf Jenk[2]

[1]Groundwater research institute GmbH Dresden, Meraner Straße 10, 01217 Dresden, Germany; E-mail: mhoffmann@gfi-dresden.de
[2]Wismut GmbH, Jagdschaenkenstraße 29, 09117 Chemnitz, Germany

Abstract. Closure of uranium mines often result in formation of acid mine drainage (AMD). Usually AMD contains high concentrations of uranium and other heavy metals, which may influence the ambient environment of the mine. To prevent this, restoration measures are required. A feasible way to ensure pollutant immobilization is the utilization of the mine sites natural-attenuation potential, which may be furthermore enhanced by injection of reactive materials. Stimulation of autochthonous sulphate-reducing bacteria would subsequent lead to a reductive reaction zone within the mine.

Introduction

In the former German Democratic Republic intensive uranium mining was performed in different mine sites. Caused by political change, mines were closed in the early 1990's and for the purpose of remediation, flooded today. The aim of the present study was the development of a remediation strategy by using autochthonous microorganisms, most notably sulphate-reducing bacteria, which are widespread in the environment. Our investigations were carried out with material of the Königstein mine, which was operated by acidic in-situ leaching technology, since 1984. Due to the reactions of the used sulphuric acid, the geochemical nature of the deposit was substantially changed. As a result acid mine drainage (AMD) formation occurred by mine flooding. AMD contains high concentrations of uranium, heavy metals and sulphate. A pollutant discharge into the adjacent aquifers has to be prevented by site restoration measures. Currently a conventional pump & treat system is used. However such a system can not be considered as a long term solution.

Site description

Hydro-, geochemical screening

The uranium deposit in Königstein was formed by adsorption and reduction of diluted uranium transported by groundwater flow. The dominating uranium ore, precipitating mainly at sandstone-siltstone boundaries, consists of pitchblende and coffinite. Iron (in part zinc- and lead-) sulphides, hydrated ironoxides and barite were associated minerals (Tonndorf 2000). Uranium production by acidic in-situ leaching and other acidification processes (as a result of anthropogenic induced pyrite oxidation) caused oxidation and therefore mobilization of uranium and heavy metals. The oxidation products remained partly in porewater and ironhydroxide sludge, precipitating by mixing acidified sandstone porewater with neutral groundwater in flooding process. Contaminant concentrations (As, Pb, U, Zn) in mine water (water mixture of acid porewater and neutral groundwater), sandstone, sandstone with siltstone interlayers and ironhydroxide sludge are shown (table 1). They were obtained by hydrochemical analyses and respectively by sequential extraction (Kassahun 2007) as the sum of all fractions. Rock samples were obtained before mine flooding. Sludge samples and mine water were collected from an open drainage canal (march 2007).

Uranium concentrations in rock samples correspond to mean values in the deposits sandstone strata (Tonndorf 2000).

The binding forms of the pollutants were verified by sequential extraction, too (Fig.1).

In the sandstone with siltstone interlayers, which contains clay (14 wt% kaolinite, 2.6 wt% illite), organic carbon (1 wt%) and 0.05 wt% reduced sulphur (Σ monosulphidic+disulphidic) (related to dried matter), pollutants are predominantly in reduced bonds and silicate bonds. Uranium has the same status in sandstone (no clay, 0.02 wt% organic carbon, no reduced sulphur). It seems, that intensive, anthropogenic oxidation has not converted natural pollutant binding forms completely. Nevertheless pollutants are mainly found in oxidized binding forms. Pollutants are either water-soluble or, in case of existing ironhydroxides in the material (sandstone, ironhydroxide sludge), in iron-oxide occluded fractions (incorporated and adsorbed on surface). Reduced zinc and lead in the ironhydroxide sludge sample (10 wt% kaolinite, 8 wt% illite, 0.27 wt% organic carbon, 0.02 wt% acid volatile

Table 1. Pollutant concentrations in mine site samples

	Mine water	Sandstone (siltstone interlayers)	Sandstone	Ironhydroxide sludge
As (mg/kg)	< 0.01	25	92	2000
Pb (mg/kg)	0.24	340	150	180
U (mg/kg)	10	38	52	380
Zn (mg/kg)	14	430	11	190

sulphur) are related to small particles, which contain cement of destabilized sandstone.

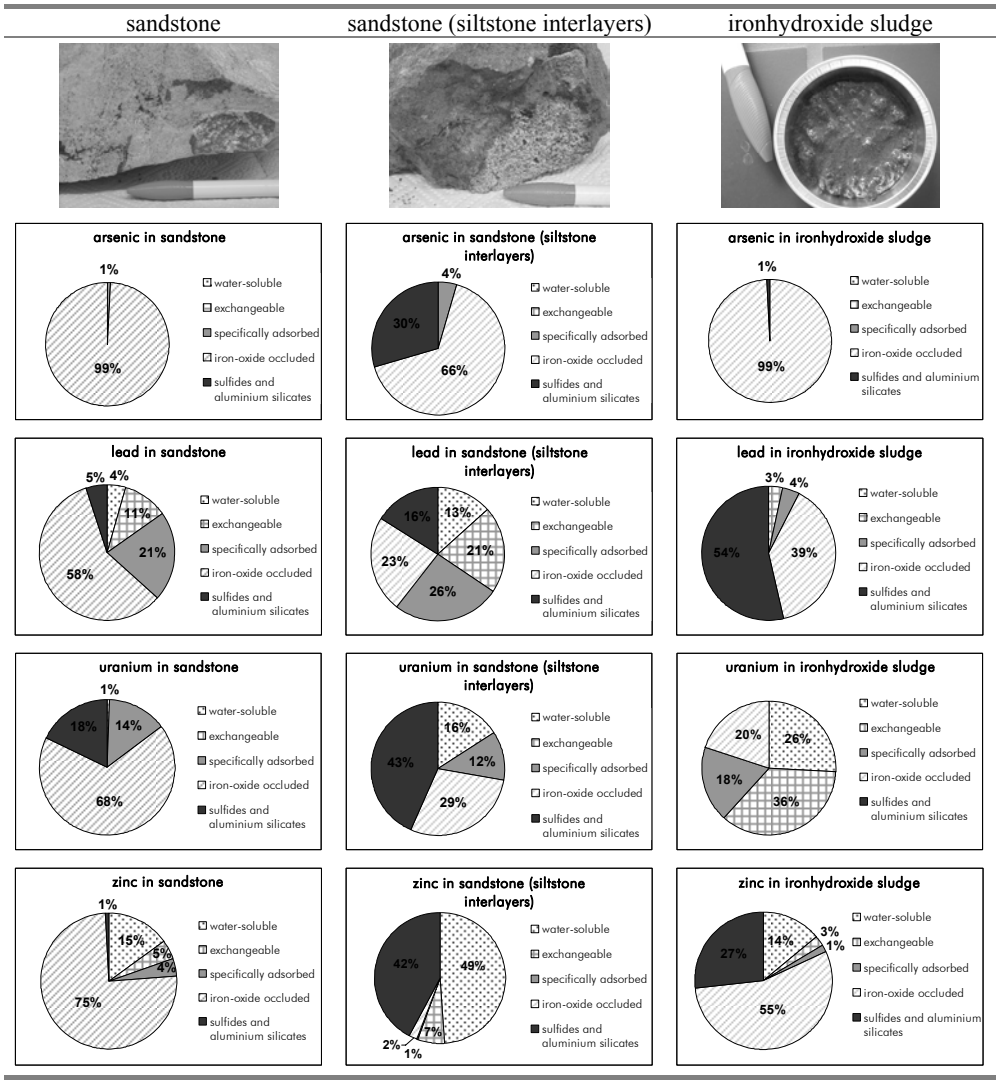

Fig.1. Pollutant binding forms in solid samples

Microbial screening

The characterization of the microbial diversity in the mine site was done, by using molecular genetic methods, like terminal restriction fragment length polymorphism (T-RFLP) (Seifert et al 2008). Furthermore some samples were investigated by bacterial diversity analyses (16S rDNA clone libraries).

The porewater sample of the oxidic ironhydroxide sludge was dominated by an acidophilic, autotrophic, iron oxidizing bacterium (*Ferribacter polymyxa*) and an iron and sulphur oxidizing bacterium (*Acidothiobacillus ferrooxidans*), associated with heterotrophic acidophiles, like *Alicyclobacillus* sp. and *Acidobacteria* sp. In contrast, the sandstone sample was more divers. Unfortunately, most of the sequences were closely related to uncultivated bacteria obtained from diversity analyses of various environmental samples. Major sequence groups belong to the *Deltaproteobacteria* class, like *Desulfovibrio*, *Desulfobacca*, *Desulfomonile* and *Synthrophobacter* species, and to the *Firmicutes* class, like *Desulfosporosinus* and *Desulfitobacterium* species. Thus, next to the commonly accepted presence of acidophilic microbes, autochthonous sulphate-reducing bacteria were detected in different mine site samples.

Development of the remediation technology

Stimulation of sulphate-reducing bacteria metabolism may lead to contaminant remediation. This was widely investigated for heterotrophic bacteria and used in different remediation strategies (Johnson and Hallberg 2005), (Sheoran and Bhandari 2005), (Johnson et al 2004), (Dvorak et al 1992). The injection of an organic carbon source in a uranium mine site will lead to a mobilisation of heavy metals and radionuclides by complexation reactions (Lieser 2001). So heterotrophic bacteria are not useful for remediation technologies within a mine site. In contrast the use of autotrophic sulphate-reducing bacteria, which do not use organic carbon sources, is investigated rarely (Boonstra et al 1999), (van Houten et al 1994), but might be usable for uranium mine site remediation. The autotrophic metabolism may be stimulated by injection of hydrogen or a hydrogen generating agent. Injection of zero-valent iron (ZVI), for example, may lead to hydrogen production due to anaerobic corrosion in the mine water (Eq. 1). This reaction will furthermore change the hydrochemical milieu in the mine water (pH increase, pe decrease). Autotrophic sulphate-reducing bacteria may consume the evolved hydrogen (Eq. 2) and lead to a precipitation of iron sulphide at anodic areas of the ZVI surfaces (Eq. 3).

$$Fe^0 + 2H_2O \rightleftharpoons Fe^{2+} + H_2 + 2OH^- \quad \text{(Eq. 1)}$$

$$SO_4^{2-} + H^+ + 4H_2 \rightleftharpoons HS^- + 4H_2O \quad \text{(Eq. 2)}$$

$$Fe^{2+} + HS^- \rightleftharpoons FeS_{(s)} + H^+ \quad \text{(Eq. 3)}$$

The processes of iron corrosion and subsequent sulphide formation lead to immobilization of diluted heavy metals and radionuclides. Immobilization by reduction on the surfaces of zero valent iron is known for uranium (Gu et al 1998), chromium and lead (Ponder et al 2000). This leads to formation of reduced mineral precipitates (e.g. uraninite). Furthermore sorption on and coprezipitation in ironmono- and -disulphides is known for many elements like arsenic, cadmium, cobalt, chromium, copper, nickel and zinc (Morse and Arakaki 1993), (Bostick and Fendorf 2003), (Farquhar et al 2002).

Therefore usage of zero-valent iron in a autochthonous sulphate-reducing bacteria containing mine site might be a applicable remediation strategy.

First, laboratory experiments were carried out, to demonstrate, that the reaction pathway is feasible for Königstein mine site samples. A mixture of mine site rocks (50 g sandstone, 50 g sandstone with siltstone interlayers), ironhydroxide sludge (17,5 g) and mine water (1070 mL) was put in a glass bottle, covered with a chlorobutyl stopper. As reactive material 3 g zero-valent iron (impure cast powder) were added. Impurities of the reactive material, like carbides or silicides conteracted an early passivation of the iron surface and promoted therefore iron corrosion. The gas phase consisted of nitrogen on the one hand or hydrogen/carbondioxide mix (4:1) on the other hand. The hydrogen/carbondioxide gas phase shall lead to an extensive stimulation of sulphate-reducing bacteria (test named “stimulated” in the following). Storage of the bottles took place at temperatures similar to field conditions (15°C).

Anaerobic iron corrosion induced hydrogen release was detectable by GC-WLD analysis. Values up to 30 vol.% were observed. In consequence of this reaction pe values decreased to -4, while pH increased from 2.8 up to ≈ 7 (Fig.2a).

Sulphate reduction (SR) was observed after a lag-phase of 40 days in the stimulated and 60 days in the non-stimulated system. At first SR was verifiable by a complete blackening of the bottles, which indicates iron sulphide precipitation (Fig.2b). Simultaneous decrease of iron and sulphate concentration occurred. In the stimulated system sulphate was depleted after 197 days. An approximation to describe the time-dependent degree of sulphate consumption is the calculation of sulphate reduction rates. If zero-order kinetics are assumed the rate is represented by the slope of the linear regression line for the relationship between time and sulphate concentrations. Sulphate reduction rates of 17 µmol L^{-1} day^{-1} for the unstimulated and 63 µmol L^{-1} day^{-1} for the stimulated system were observed. These values are very close to the range reported in similar bench-scale experiments (Burghardt et al 2007). There was no detectable sulphide in the aqueous phase, due to ferrous iron excess at any time. However sulphate depletion is led back to microbial sulphate reduction, as accumulation of ^{34}S in residual sulphate was observed (Fig.2d). It is well known, that the light isotope ^{32}S is favoured in metabolism of sulphate-reducing bacteria (Knöller et al 2006).

T-RFLP analysis of the stimulated batch test showed, that the microbial community changed their consistence extremely. After 127 days the mine water was dominated by sulphate-reducing bacteria. Major sequence groups belong to *Desufovibrio sp.*, and *Desulfosporosinus sp*, which were detected in the used sandstone sample, marginally. The former dominating acidophilc, autotrophic, iron oxidizing

bacteria played a minor role. Thus the stimulation of autochthonous autotrophic sulphate-reducing bacteria by iron-corrosion induced hydrogen release was successful.

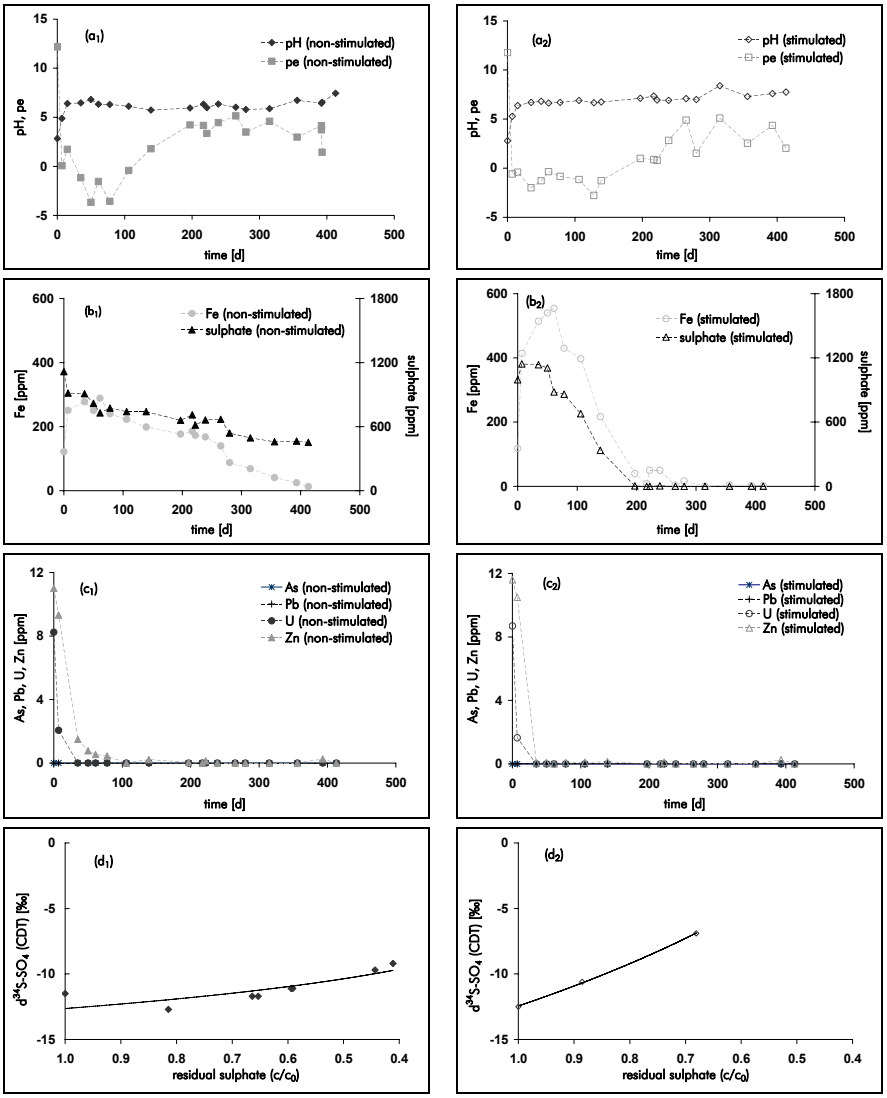

Fig.2. Batch investigations of pollutant immobilization (1-nitrogen gas phase, "non-stimulated"; 2-hydrogen/carbon dioxide gas phase, "stimulated")
(a) pH/pe, (b) Fe- and sulphate-concentration, (c) As-, Pb-, U-, Zn-concentration, (d) sulphur isotope fractionation

As expected sulphate reduction caused pollutant immobilization in all test series (Fig.2c). Dissolved uranium and zinc were depleted in short time scale. Uranium concentration dropped to a quarter of initial concentration within 7 days. A total immobilization of uranium and zinc was observed after 35 days in the stimulated and after 106 days in the non-stimulated system. Arsenic and lead, which were less concentrated in the initial mine water and mainly associated with iron(hydr)oxides in the original solids, remained in the solid phase during the whole test time.

Pollutants were verifiable in batch tests solid phases by SEM-EDX analysis (Fig.3). SEM analysis showed pollutants associated with Fe-precipitates (Fig.4 as example for Pb-rich precipitates). These investigations pointed out, that the proposed immobilization pathway occurred as expected and pollutants were (co)precipitated at parts of the solid phases rich of iron.

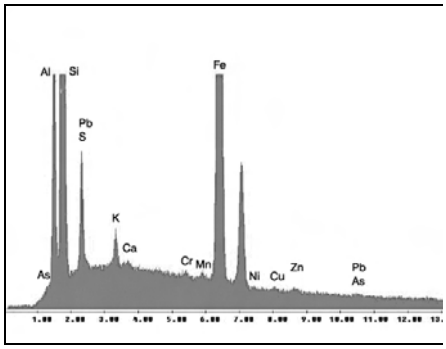

Fig.3. SEM-EDX analysis of batch tests solid phase (various immobilized pollutants detectable)

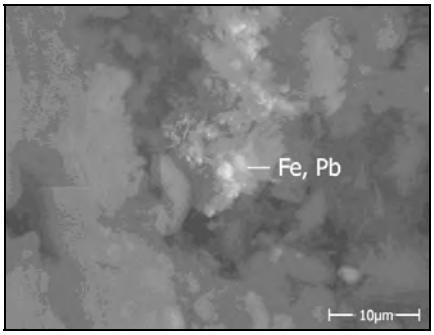

Fig.4. SEM image (BSE imaging mode) of batch sediment (Pb associated with Fe-precipitate)

XPS investigations of the solid phase identified sulphur to occur completely reduced in monosulphidic (50,9%) and disulphidic (49,1%) phases in both systems (data shown for "stimulated" system). This implies, that an alteration of the initially precipitated, iron monosulphides took place quickly. An accelerated pyritization of fresh precipitated monosulphides due to surface oxidation of the precursor iron monosulphide is published (Wilkin and Barnes 1996) and conceivable in the tests, as small amounts of oxygen (up to 4 vol.%) were detected via GC-WLD analysis in the gas phases. Moreover XPS furnished proof, that pollutants immobilized in reduced mineral phases, too. Uranium for example is predominantly tetravalent (80,1% UO_2) and partially immobilized as polysulphide phase (9,1% US_x (x>1)). Only small amounts remained as hexavalent uranium (10,8%) up to the time of XPS analysis (day 237).

The batch-scale experiments showed clearly, that a stimulation of autochthonous autotrophic sulphate-reducing bacteria by iron corrosion induced hydrogen release is possible. In the experimental system this stimulation resulted in a complete change of the composition of the microbial community. Moreover the cou-

pled process of iron corrosion and sulphate reduction led to a conversion of the geochemical conditions. The hydrochemical milieu changed as expected. Sulphur was completely reduced and stayed in solid phase monosulphidic and disulphidic. The pollutants were and stayed immobilized in reduced mineral phases or coprecipitated with iron bearing phases. This means, that the types of bonding changed completely for the pollutants, which were mainly water soluble or coexistent with ironoxides. Applied to the Königstein mine site, the demonstrated pollutant remediation pathway represent a restoration of the original, anthropogenic uninfluenced pollutant binding forms and ensure therefore stable and enduring pollutant retention.

Implementation in field-scale

To establish a reductive reaction zone in a part of the Königstein mine site and thus to prove the reaction pathway in field scale, the reactive material has to achieve more features next to the long-term supply of H_2. To assure a full spread of the material, it is necessary, that the material is injectable and floatable within the convective water flow of the flooded mine, which is induced by the adjacent aquifer.

To realize these features in an iron containing material, zero-valent iron was incooperated in a low density foam glass. Therefore a mixture of glass powder, gray cast powder and Paris white (as blowing agent) was sintered in a conveyor furnace at 830°C. The product was crushed and sieved afterwards. The produced foam glass has a sealed porosity, which makes it floatable. Iron is evenly distributed within the material. Via scanning electron microscopy (SEM) it was detectable on the surface of the material, on the surface of the closed pores and within the glass bulk (Fig.5).

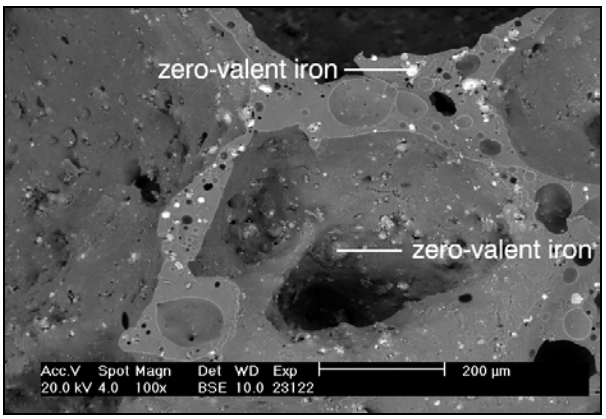

Fig.5. SEM image (BSE imaging mode) of a low density foam glass with zero-valent iron inclusions

Incooperation of the reactive zero-valent iron within the foam glass entailed, that iron corrosion is mainly addicted to the glass dissolution in the water. As a result a long term hydrogen supply occurs, which is regulated by the hydrochemical conditions of this water.

Additionally established protective coatings around the grains of the material (for example soluble glass based, silica coatings) inhibit iron corrosion anymore and thus extend the hydrogen supply in the reaction zone.

Acknowledgement

Funding of this research project was provided by Federal Ministry of Education and Research (Project Management Agency for Water Technology and Waste Treatment). We would like to thank Dr. H. Masuch (SGS Institut Fresenius GmbH) for SEM-EDX, Jochen Albrecht (SGS Institut Fresenius GmbH) for XPS and Prof. Gerhard Franz (TU Berlin) for XRD analyses. Many thanks furthermore to Dr. Kay Knoeller (Helmholtz Centre for Environmental Research) for isotope measurements and Michaela Hache for ICP measurements.

References

Boonstra J, van Lier R, Janssen G, Dijkman H, Buisman C J N (1999) Biological treatment of acid mine drainage. Proceedings of the International Biohydrometallurgy Symposium IBS 1999, Madrid 20-23 June 1999, Series Process Metallurgy, 9: 559-567

Bostick B C, Fendorf S (2003) Arsenite sorption on troilite (FeS) and pyrite (FeS_2). Geochimica et Cosmochimica Acta, 67: 909-921

Burghardt D, Simon, E, Knöller K, Kassahun A (2007) Immobilization of uranium and arsenic by injectible iron and hydrogen stimulated autotrophic sulphate reduction. Journal of Contaminant Hydrology 94: 305-314

Dvorak D H, Hedin R S, Edenborn H M, McIntire P E (1992) Treatment of Metal-Contaminated Water Using Bacterial Sulfate Reduction: Results from Pilot-Scale Reactors. Biotechnology and Bioengineering, 40: 609-616

Farquhar M L, Charnock J M, Livens F, Vaughan D J (2002) Mechanisms of Arsenic Uptake from Aqueous Solution by Interaction with Goethite, Lepidocrocite, Mackinawite, and Pyrite: An X-Ray Absorption Spectroscopy Study. Environ Sci Technol 36: 1757-1762

Gu B, Liang L, Dickey M J, Yin X, Dai S (1998) Reductive precipitation of uranium(VI) by zero-valent iron. Environ Sci Technol 32: 3366-3373

Johnson D B, Rowe O, Kimura S, Hallberg K B (2004) Development of an integrated microbiological approach for remediation of acid mine drainage and recovery of heavy metals. Proceedings of IMWA Symposium Mine Water 2004, University of Newcastle 19-23 Sept 2004, 2: 151-157

Johnson D B, Hallberg K B (2005) Acid mine drainage remediation options: a review. Science of the total environment 338: 3-14

Kassahun A (2007) Methoden zur differentiellen Bestimmung von Abbau, Fällung, Sorption und chemischer Transformation: Sequentielle Extraktion – Bindungsformen anorganischer Schadstoffe und Mineralphasengehalte. KORA-Methodenkatalog: in press

Knöller K, Vogt C, Richnow H-H, Weise S M (2006) Sulfur and oxygen isotope fractionation during benzene, toluene, ethyl benzene and xylene degradation by sulfate-reducing bacteria. Environ Sci Technol 40: 3879-3885

Lieser K H (2001) Nuclear and Radiochemistry. Wiley-VCH, Weinheim

Morse J W, Arakaki T (1993) Adsorption and coprecipitation of divalent metals with mackinawite. Geochimica et Cosmochimica Acta 57: 3635-3640

Ponder S M, Darab J G, Mallouk T E (2000) Remediation of Cr(VI) and Pb(II) aqueous solutions using supported, nanoscale iron. Environ Sci Technol 34: 2564-2569

Seifert J, Schlömann M, Erler B, Seibt K, Rohrbach N, Arnold J, Kassahun A, Jenk U (2008) Characterisation of the microbial diversity in the abandoned uranium mine Königstein. This book

Sheoran A S, Bhandari S (2005) Treatment of mine water by a microbial mat: benchscale experiments. Mine Water and the Environment 24: 38-42

Tonndorf H (2000) Die Uranlagerstätte Königstein. Bergbau in Sachsen Bd. 7, Landesamt für Umwelt und Geologie und Sächsiches Oberbergamt Freiberg.

Van Houten R T, Hulshoff L W, Lettinga G (1994) Biological sulphate reduction using gas-lift reactors fed with hydrogen and carbon dioxide as energy and carbon source. Biotechnology and Bioengineering 44: 586-594

Wilkin R T, Barnes H L (1996) Pyrite formation by reactions of iron monosulphides with dissolved inorganic and organic sulphur species. Geochimica et Cosmochimica Acta, 60: 4167-4179

Elemental Iron (Fe^0) for Better Drinking Water in Rural Areas of Developing Countries

Chicgoua Noubactep[1,2] and P. Woafo[3]

[1] Angewandte Geologie, Universität Göttingen, Goldschmidtstraße 3, D - 37077 Göttingen, Germany
[2] Kultur und Nachhaltige Entwicklung CDD e.V., s/c S.M. Youmbi Peka, Bonhoefferweg 2, D - 37075 Göttingen
[3] Laboratory of Modelling and Simulation in Engineering and Biological Physics, Faculty of Science, University of Yaounde I, Box 812 Yaounde, Cameroon

Abstract. Many of the reasons behind the anthropogenic contamination problems in rural environments of developing countries lie in changes in the traditional way of life and the ignorance on the toxic potential of introduced manufactured products. A generalization trend exists within the international community suggesting that water in developing countries is of poor quality. However, the water quality is rarely analytically determined. Existing potabilization solutions may be prohibitively expensive for the rural populations. Therefore, efficient and affordable technologies are still needed to ameliorate the water quality. In the recent two decades, elemental iron has shown the capacity to remove all possible contaminants (including viruses) from the groundwater. This paper presents a concept to scale down the conventional iron barrier technology to meet the requirements of small communities and households in rural environments worldwide.

Introduction

Water is essential to life and its quality is a major issue in sustainable development (Gadgil 1998). In humid areas of developing countries water problems are currently reported to be related more to quality preservation than to shortages (e.g., Brown 2007, Garcia 2007). Guidelines have been developed for maximum acceptable values for a number of contaminants in drinking water (WHO 2004). Specific guidelines are presented for acceptable concentrations of (i) bacteria, viruses, and parasites; (ii) chemicals of health significance including specific inorganic and or-

ganic constituents, pesticides, disinfectants, and disinfection by-products; (iii) radioactive constituents; and (iv) substances and parameters in drinking water that may give rise to complaints from consumers. Availability of plentiful and safe water for domestic use has long been known to be fundamental to the development process, with benefits spreading across all sectors, such as labour productivity and obviously health sector. It has been shown that the most common and deadly pollutants in the drinking water in developing countries are of biological origin.

The population in the developing world suffers from six main diseases associated with water supply and sanitation (i) Diarrhea, (ii) *Ascaris*, (iii) *Dracunculisis*, (iv) Hookworm, (v) *Schistosomiasis*, and (vi) Trachoma (Gadgil 1998, Sobsey et al. 2008). Many of the poorest people in developing countries must collect water outside the home and are responsible for treating and storing it themselves at the household level. This practice is a serious public health issue and has been addressed in the Millennium Development Goals, which aim to halve, by 2015, the proportion of people without access to safe water in 2000 (UN 2000). Looking toward the future, the water management must involve promoting improved international cooperation (Brown 2007, Micklin 1996).

One of the internationally recommended action to improve water management is water pricing. Water pricing is considered as a key tool: (i) to promote water use efficiency, (ii) to prevent water pollution, and (iii) to make for a more rational allocation of water (Micklin 1996, Sobsey et al. 2008). The idea behind water pricing is that the more one pays for water, the more careful he will use it. The more one must pay to pollute water, the less he will pollute. Economists have long advocated water pricing as helpful key to solve water resource use problems. For water pricing to be effective, water laws and institutions that inhibit formation of open water markets, have been reformed. Comprehensive and accurate water measuring system are currently established where it does not exist. At the end of the chain produced water should be affordable also for poor people, unless the goal of making potable water available could not be achieved. Thus, the question arises how sustainable is water pricing for developing countries?

Rural environments in developing countries have been reported to suffer from aching chemical pollution problems mostly from anthropogenic nature. Many of the reasons behind the chemical anthropogenic problems lie in changes in the traditional way of life and the ignorance on the toxic potential of recently introduced industrially manufactured products (Noubactep 2008a). Frequently, the sole available income generation activities (mining activities, intensive agriculture) are the source of water chemical pollution. Traditionally, there are three main sources of drinking water in rural areas: (i) rain water, (ii) surface water (spring, stream, river), and (iii) shallow groundwater (well). A recent development throughout the world is the installation of drilled wells with mechanic pumps. Drilled wells is considered as the best solution for bringing clean and quality water to surface. But the actual cost (about € 6000 or US$ 9500 each drilled well in Cameroon for example) is prohibitively expensive for many small communities. Therefore, the drinking water problem for developing countries is far from been solved. Ideally, all available water sources (rain water, surface water and shallow groundwater)

should be treated on-side (at the point of use) such that even thirsty farmers, hunters can drink potable water far from their home.

The oldest and simplest method to produce potable water is to filtrate available water through a filter containing a non-toxic material. Ideally the filter material should be able to remove a large spectrum of contaminants (charged/uncharged, organic/inorganic, living/non-living, reducible/non-reducible) and should be cost effective. It is very difficult to find a universal material which can be applied to the removal of a wide range of contaminants due to their very different chemical structures and molecular sizes. Fortunately, elemental iron (Fe^0-bearing materials), a cost-effective and readily available material has shown the capacity to remove all possible contaminants (including biological contaminants – You et al. 2005) from the aqueous solution upon its oxidation (corrosion) during the past two decades. Elemental iron was originally introduced as filling material for subsurface reaction walls for groundwater remediation (Matheson and Tratnyek 1994, O´Hannesin and Gillham 1998).

The present work presents a concept to scale down the conventional iron barrier technology to meet the requirements of households and communities in rural environments worldwide. It is expected that elemental iron may be produced locally by rural communities while using old environmental friendly technologies of blacksmiths. Alternatively, construction steel and other Fe^0-bearing materials (mild steel, cast iron) can be diverted from their intended use to serve as filter material for water treatment. In the following, some information on the quality of water in developing countries is first given. Then a survey of technologies for water treatment is presented, followed by an overview on the iron technology. In the last section, a discussion of the possibility of using the iron technology for ameliorating the quality of drinking water in developing countries is given.

A priori polluted Water

A generalization trend exists within the international community suggesting that water in developing countries is of poor quality (e.g., Zimmerman et al. 2008). Thereby, despite remarkable progress in environmental instrumental analytical chemistry, the water quality is rarely determined. Clearly, the biochemical quality of the water that is drunk by billions of people worldwide is not known. Paradoxically, the western world (i) has developed standards for all known contaminants (nitrates, metals) and groups of contaminants (e.g., pesticides, radioactive species), and (ii) spends a lot of money on preserving wildlife or plant biodiversity in developing countries. The health of indigenous peoples that are currently struggling for survival in a permanently changing environment seems to be less important than that of exotic animals and plants. The majority of these indigenous peoples have shown a great preparedness to cope with the modern world, but have not received the adequate education to be trust to modern environmental challenges (Noubactep 2008a).

The belief that available water is of poor quality has been partly accepted and internalized by the large part of educated people in developing countries who are now seeking solutions to pollution in collaboration with partners worldwide. But how should a solution look like when the nature and the extent of contamination are not known? Another paradox of the belief of "a priori polluted water" is the fact that "Spring Water Companies" are currently supplying "pure", natural spring water (bottled water) to residents of industrialized countries. Thereby, the natural quality of "true flowing" springs, the mineral content, and the "natural taste" are three important features to justify elevated prices. Why should spring waters in the so-called third world be fundamentally of different quality?

The present work considers that the actual water quality is not known and proposes a concept for a safe and affordable technology to ameliorate the water quality in the case it may be polluted (precautionary principle). Before presenting the concept an overview over available treatment technology will be given, followed by a presentation of the elemental iron technology.

Survey of technologies for water treatment

Water supply for human consumption has three primary objectives: (i) the minimisation of contamination of waters to be used as sources for drinking water; (ii) the reduction or removal of contaminants by means of treatment processes; and (iii) the prevention of contamination of the drinking water during distribution, storage and supply (Arnold and Colford 2007, Ram et al. 2007, WHO 2004). In developing countries natural waters are drunk mostly without treatment. These waters are certainly polluted at some sites. In particular in regions where poisonous geogenic species as arsenic are available. For these regions several low-cost point of use technologies have been proposed to protect live of indigenous peoples (Arnold and Colford 2007, Pokhrel et al. 2005, Ram et al. 2007, Ramaswami et al. 2001, Sobsey 2002, Sobsey et al. 2008). The supposedly simple, appropriate and affordable technologies suitable for rural areas with no electricity and no tap water have been mostly proposed in the frame work of international research projects.

The developed countries and international organizations have reported on providing substantial help to the developing world in meeting their pressing water needs (remember that the water quality is unknown as a rule). Technical assistance accompanied by massive infusions of capital is required to ensure universal access to clean drinking water. Beside the use of alternative water sources such as rain water harvesting, two currently proposed solutions are (Ramaswami et al. 2001): (a) On-site treatment in column systems packed with various adsorbents (including activated carbon and metal oxides) and reagents, e.g., iron, lime; (b) In-home treatment with alumina, iron, ferric chloride, and other reagents.

Brown (2007) recently reviewed "point of use" (POU) water treatment and safe storage technologies and their application in developing countries. Physical methods for small-scale water treatment include boiling, heating (using fuel and solar), filtering, settling, and ultraviolet (UV) radiation (solar or ultra violet lamps).

Chemical methods include coagulation-flocculation and precipitation, ion exchange, chemical disinfection with germicidal agents (primarily chlorine), and adsorption. Combinations of these methods simultaneously or sequentially often yield promising results, for example coagulation combined with disinfection. Other combinations or multiple barriers are media filtration followed by chemical disinfection, media filtration followed by membrane filtration, or composite filtration combined with chemical disinfection. The review from Brown (2007) suggested that success of interventions is highly context specific, with no one technology or method representing a universal best solution. Availability of materials, quality of raw water available, cultural factors and preferences, or cost may determine where each of these is most suited to POU water treatment applications in developing countries (Sobsey 2002).

Appropriate point of use technologies for any water of unknown quality must meet certain criteria to be effective: (i) The technology must be effective over a wide range of contaminants, (ii) The technology must be simple to use, should not require running water or electricity, and be easily transferable to the users in their home. (iii) The materials need to be cheap, readily available and/or have a high reuse potential that would further reduce costs. (iv) Finally, any appropriate technology must be assessed to ensure that no other harmful chemicals are introduced into the water while the concerned contaminant is being removed.

Elemental iron is an appropriate material for point of use technologies. It has been already successfully tested in many regions of the world for arsenic removal (Karschunke et al. 2000, Ramaswami et al. 2001). Elemental iron has been successfully used to treat water contaminated with a variety of pollutants including fungicides, nitrates and pesticides. Furthermore, the mechanism of contaminant removal has been shown to be primarily non-specific, this makes Fe^0 an ideal material to treat water of unknown composition. Before presenting a concept to generalize the use of elemental iron as point of use material for rural areas of developing country, an overview on the iron technology will be given.

The elemental iron technology

Permeable reactive barriers (PRBs) are a recent development of a passive system to remediate subsurface waters containing organic or inorganic contaminants. Contaminated groundwater flows under its natural gradient and passes through a permeable curtain (Fig. 1) of treatment medium that either (i) removes the contaminants from the aqueous phase by one ore several mechanisms or (ii) transforms the contaminants into environmentally acceptable or benign species. The most widely adopted treatment medium is elemental iron (Fe^0), a substance that is highly reactive, environmentally acceptable, and is readily available as a manufactured product derived from the recycling of scrap iron and steel. In cores of the reacted treatment media, the most abundant secondary product formed *in situ* is Fe oxyhydroxide (iron corrosion products – iron hydroxides and oxides), but a variety of precipitates has been identified. For example, secondary pyrite, greigite, covel-

lite, chalcopyrite, and bornite have formed in the treatment medium (Jambor et al. 2005, Mackenzie et al. 1999). The secondary sulfides are volumetrically small and are unlikely to impede the permeability of the treatment medium, but the formation of Fe oxyhydroxides and secondary carbonates in the presence of Fe^0 requires further monitoring to determine whether the secondary precipitates and the consumption of Fe^0 will appreciably lessen the effectiveness of such PRBs over the long term. Current indications are that PRBs are both an environmentally effective and a cost-effective technique of remediation (Henderson and Demond 2007, Jambor et al. 2005, Laine and Cheng 2007).

A trend persists in the scientific literature terming iron PRBs as a reduction technology (Kim et al. 2008, Laine and Cheng 2007) although contaminant reduction has not been traceably demonstrated. Elemental iron (Fe^0) is a strong reducing agent (Eq. 1) and the spent agent, Fe^{2+} is environmentally innocuous.

$$Fe^0 \Leftrightarrow Fe^{2+} + 2\ e^- \quad (1)$$

When coupled with the reduction of a compound (e.g. an organic halide - R-X) the reaction should be spontaneous (Eq. 2):

$$Fe^0 + R\text{-}X \Rightarrow Fe^{2+} + RH + X^- \quad (2)$$

Most investigators agree that the mechanism by which Fe^0 remove reducible contaminants is by direct reduction at the iron surface. Other mechanisms have been proposed, including: (i) reduction by hydrogen, (ii) reduction by ferrous iron that is produced during the corrosion process, (iii) adsorption onto in-situ generated iron corrosion products. A few studies have shown that contaminant adsorption onto the Fe^0 surface is an intermediate step towards reduction. The validity of these considerations has been challenged recently (Noubactep 2007, Noubactep 2008b). The major weak point of the "reductive transformation concept" is that it can not explain why non-reducible species (e.g., Zn, viruses) are quantitatively removed in Fe^0-H_2O systems. An alternative concept was proposed considering

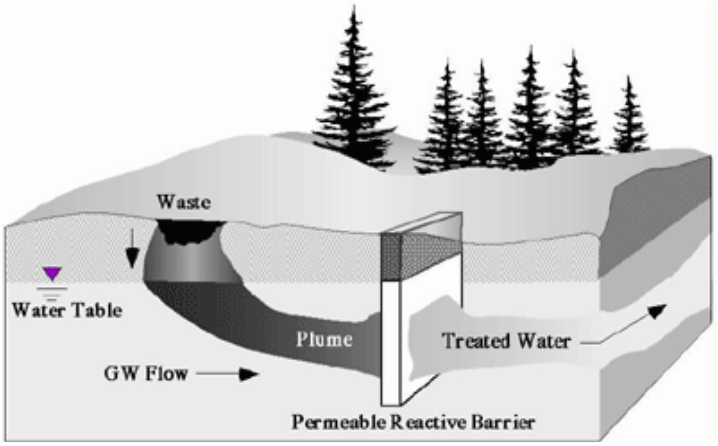

Fig.1. Illustration of a permeable reactive barrier remediating a plume (Source: www.powellassociates.com).

adsorption and co-precipitation as primary mechanism of contaminant removal in Fe^0-H_2O systems (Noubactep 2007).

The new concept takes the dynamic nature of the generation of iron corrosion products into account. Here, contaminant reduction by ferrous iron is an independent reaction path regardless from the external redox conditions and the electronic conductivity of the oxide film on iron. More importantly the new concept explains accurately why non-reducible pollutants and viruses are quantitatively removed in Fe^0-H_2O systems.

The long term feasibility of Fe^0 reactive barriers in the cleanup of contaminated groundwaters has been demonstrated in laboratory column studies and confirmed by field installations. Column studies and fields installations indicate that Fe^0 maintains its reactivity over long periods of time (Jambor et al. 2005). Many forms of iron have been proposed for water treatment. They differ in their size (nm, μm, mm), origin (scrap iron, by-products) and composition (cast iron, carbon steel, bimetallic). The next paragraph discusses how to use this technology to ameliorate the quality of drinking water in developing countries.

Iron technology for developing countries

Considering adsorption and co-precipitation as the primary (initial or first step) removal mechanism of any species (ionic, neutral, organic, inorganic, and living) in the presence of elemental iron (e.g., in Fe^0-H_2O systems), Fe^0 is proposed as reactive medium for filters and small reactive walls for both on-side (well, source, river) and in-home (mostly rain) water treatment. The idea is to scale down reactive barrier for near-surface water treatment. Some features of subsurface reactive walls are still valid, in particular that the oxide-film primarily acts as contaminant scavenger. For reducible contaminants, direct or indirect reduction may still occur. An important difference is the increased availability of molecular oxygen at the surface. Long-term laboratory and field experiments are required to address this specific aspect.

As said above, the idea is not new but filters that had been proposed for water treatment at sites of specific chemical contamination is now proposed for worldwide use with two key differences: (i) the proposition is based on the latest scientific results (contaminant co-precipitation as primary removal mechanism), and (ii) filters and small reactive walls should be available everywhere where water is potentially drinkable even occasionally by hunters or travellers. Moreover biological and chemical contamination are both addressed.

To meet the ambitious goal of worldwide availability and cost-effectiveness, it should be avoided that populations have to buy special manufactured Fe^0 materials. For this purpose potential source of scrap iron should be identified and the material tested for their effectiveness. Alternatively, available Fe^0 materials for other intended purposes can be tested for use as water treatment material. Such Fe^0 materials are abundant in the construction industry (construction steel, reinforcing steel, wire).

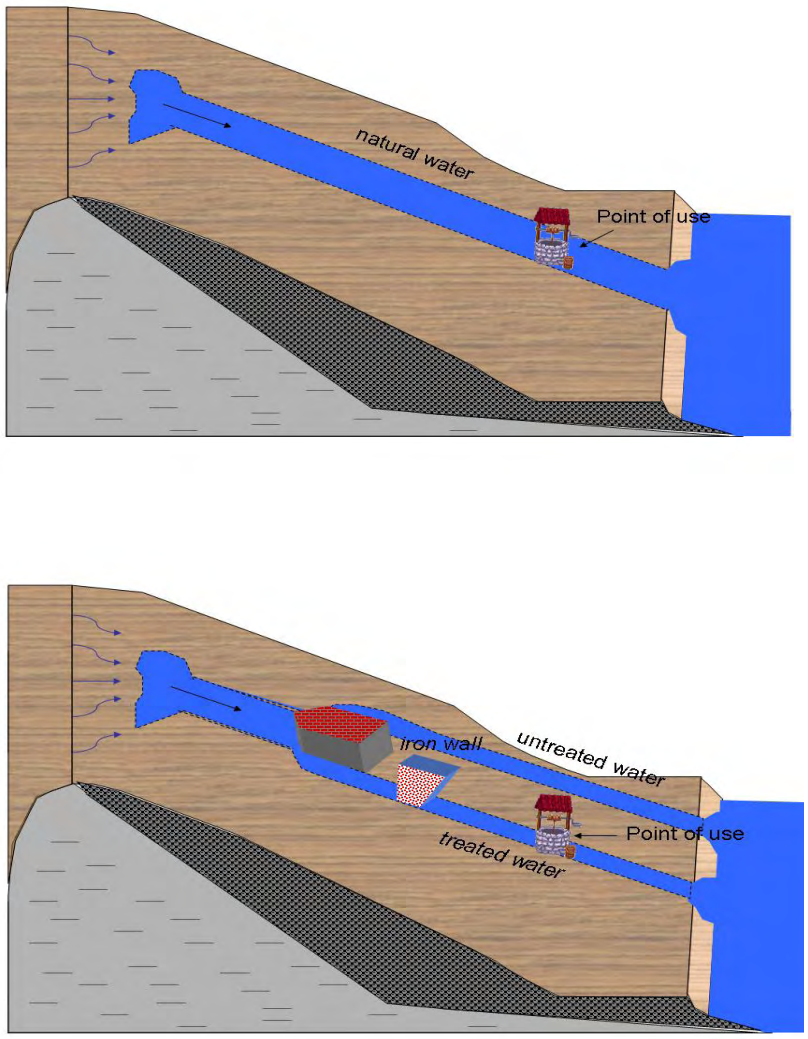

Fig. 2. Illustration of source management options: un-treated (up) and treated in an iron reactive wall (bottom). Whether the whole source flows through the barrier or not depends on the hydrodynamic conditions. The dimensioning of the branch through the reactive barrier will depend on the hydrodynamics, the characteristic of the used Fe^0 material and the wished frequency of Fe^0 replacement (e.g. once or twice a year).

Alternatively: (i) indigenous populations can be encouraged to produce steel by themselves while using environmental friendly technologies of their ancestors; (ii) Governments and NGOs (Non Government Organizations - sponsor) can purchase suitable Fe^0 materials.

The Fe^0 materials mixed with sand should serve as reactive material in in-home filters and in on-site small walls. In both cases layers of available adsorbents can be placed before the layer of Fe^0 to assure long-term reactivity of the filter/wall. On-site treatment units may be installed only on a natural or artificial branch of the available water source for economic purposes (Fig. 2). Intensive laboratory research is needed for a properly dimensioning of these units and to predict the frequency of material change.

The application of the results of these investigations will contribute to ameliorate the health of billions of people worldwide. A potential specific use of this technology is the adequate water supply for population (i) after a natural catastrophes (e.g. earthquake**,** Hurricane**,** Tsunami), (ii) in refugee camps over the world. Therefore, international organizations (FAO, WHO, Red Cross, NGOs) should be interested in the realization of this idea. There is no doubt that the successful application of the proposed concept will help to largely achieve the Millennium Development Goals (halving the proportion of people without access to safe water in 2000 by 2015).

Acknowledgments

Christian Moeck (student research assistant) is kindly acknowledged for technical support. The work was partly supported by the Deutsche Forschungsgemeinschaft (DFG-No 626).

References

Arnold BF, Colford Jr JM (2007) Treating water with chlorine at point-of-use to improve water quality and reduce child diarrhea in developing countries: A systematic review and meta-analysis. Am. J. Trop. Med. Hyg. 6: 354-364.

Brown JM (2007) Effectiveness of ceramic filtration for drinking water treatment in Cambodia. Dissertation, University of North Carolina at Chapel Hill.

Gadgil A (1998) Drinking water in developing countries. Annu. Rev. Energy Environ. 23: 253-286.

Garcia MC (2007) Evaluation of the health risk from water contamination in the city of Tandil, Argentina. GeoJournal 70: 289-296.

Henderson AD, Demond AH (2007) Long-term performance of zero-valent iron permeable reactive barriers: a critical review. Environ. Eng. Sci. 24: 401-423.

Jambor JL, Raudsepp M, Mountjoy K (2005) Mineralogy of permeable reactive barriers for the attenuation of subsurface contaminants. Can. Miner. 43: 2117-2140.

Karschunke K, Gorny M, Jekel M (2000) Arsenic removal by corrosion-induced adsorption. Vom Wasser 95: 215-222.

Kim G., Jeong W., Choe S. (2008): Dechlorination of atrazine using zero-valent iron (Fe0) under neutral pH conditions. J. Hazard. Mater. 155: 502-506.

Laine DF, Cheng IF (2007) The destruction of organic pollutants under mild reaction conditions: A review. Microchem. J. 85: 183-193.

Mackenzie PD, Horney DP, Sivavec TM (1999) Mineral precipitation and porosity losses in granular iron columns. J. Hazard. Mater. 68: 1-17.

Matheson LJ, Tratnyek PG (1994) Reductive dehalogenation of chlorinated methanes by iron metal. Environ. Sci. Technol. 28: 2045-2053.

Micklin PP (1996) Man and the water cycle: challenges for the 21st century. GeoJournal 39: 285-298.

Noubactep C (2007) Processes of contaminant removal in "Fe^0–H_2O" systems revisited. The importance of co-precipitation. Open Environ. J. 1: 9-13.

Noubactep C (2008a) Besseres Trinkwasser an jeder Stelle in ländlichen Gebieten Afrikas. In Afrika & Wissenschaft, Band 1- Heft 3, African Development Initiative, Frankfurt am Main (in Press).

Noubactep C (2008b) A critical review on the mechanism of contaminant removal in Fe^0–H_2O systems. Environ. Technol. (In Press).

O´Hannesin SF, Gillham RW (1998) Long-term performance of an in situ "iron wall" for remediation of VOCs. Ground Water 36: 164-170.

Pokhrel D, Viraraghavan T, Braul L (2005) Evaluation of treatment systems for the removal of arsenic from groundwater. Pract. Period. Haz. Toxic Radioactive Waste Mgmt. 9: 152–157.

Ram PK, Blanton E, Klinghoffer D, Platek M, Piper J, Straif-Bourgeois S, Bonner MR, Mintz ED (2007) Bringing Safe Water to Remote Populations: An Evaluation of a Portable Point-of-Use Intervention in Rural Madagascar. Am. J. Public Health 97 (3), 398–400.

Ramaswami A, Tawachsupa S, Isleyen M (2001) Batch-Mixed iron treatment of high arsenic waters. Wat. Res. 35: 4474-4479.

Sobsey MD (2002) *Managing Water in the Home: Accelerated Health Gains from Improved Water Supply*. Geneva: World Health Organization. Available at http://www.who.int.

Sobsey MD, Stauber CE, Casanova LM, Brown JM, Elliott MA (2008) Point of use household drinking water filtration: A practical, effective solution for providing sustained access to safe drinking water in the developing world. Environ. Sci. Technol. 42 (12), 4261–4267.

UN (United Nations). (2000) *Millennium Declaration*. UN General Assembly: A/RES/55/2, 18 September 2000.

WHO, World Health Organisation. (2004) Guidelines for Drinking-Water Quality, Third Edition: Volume 1 Recommendations. World Health Organisation, Geneva.

You Y, Han J, Chiu PC, Jin Y (2005) Removal and inactivation of waterborne viruses using zerovalent iron. Environ. Sci. Technol. 39: 9263-9269.

Zimmerman JB, Mihelcic JR, Smith J (2008) Global Stressors on Water Quality and Quantity. Environ. Sci. Technol. 42: 4247-4254.

Comparison of three different sorbents for uranium retention from a source water

Karin Popa

'Al.I. Cuza' University, Department of Chemistry, 11 - Carol I Blvd., 700506 – Iasi, Romania

Abstract. A source water from Suceava County with a total salt concentration of 493.5 mg/L was analysed, mainly because of the high content of uranium (5.6 mg/L UO_2^{2+}) in the geological formations were it is coming from. In order to reduce the uranium concentration down to 0.1 mg/L, a natural Callovo-Oxfordian clay, a nano-ETS-10 synthetic titanosilicate and *Azolla caroliniana* Willd. (Pteridophyta) bioaccumulator.

All investigated sorbents were able to decrease the uranium concentration down to the accepted limit. Nevertheless, the price of the sorbents themselves is variable, as well as the price of the considered technological approach. It can be observed that after only 15 min in the sorption system ETS-10 - source water, the final concentration decrease down to the accepted standard for health. For the natural clay, the depollution performance was better, but only after 30 min contact time. For both inorganic ion exchangers the process is temperature independent, the optimum pH is slightly acid and the necessary amount of sorbent of about 1-1.2 mg/mL. This is a disadvantage in the case of the synthetic titanosilicate, which is relatively expensive.

Even if the required contact time in the case of the used biosorption process is of one hour, the performance of the biosorption is the best one and the optimal weigh of sorbent is only 0.25 mg/mL water. The process is slightly temperature dependent, proving the endothermic nature of the biosorption process. A thermodynamic evaluation of the data shows an endothermic heat of sorption and negative free

energy values, indicating that the uranyl ions are preferred in the biosorbent solid phase.

Experience gained from the experimental permeable reactive barrier installed on the former uranium mining site

M. Csővári[1], G. Földing[1], J. Csicsák[2] and É. Frucht[1]

[1]Esztergár L. u. 19 7633 Pécs, Hungary, MECSEK-ÖKO Zrt
[2]Esztergár L. u. 19. Pécs, Hungary MECSEKERC Zrt

Abstract. It is known that uranium exists in groundwater mainly in form of anion complexes. Therefore uranium sorption on soil particles (anion exchange capacity of which is low) is weak. As a result uranium can migrate from the uranium containing waste deposits (waste rock pile, tailings ponds, etc.) causing groundwater contamination. In Hungary in the frame of EU sponsored PEREBAR project a pilot-scale permeable reactive barrier (PRB) was built in 2002 for in situ treatment of uranium contaminated groundwater. The installation still works. The results of the six years' experiment are discussed bellow.

Introduction

Permeable reactive barriers (PRB) provide an efficient technology for passive in-situ groundwater remediation. In the European research project PEREBAR the long-term behaviour of PRBs has been studied. At first step the laboratory and field experiments showed that the elemental **iron in mixture with sand** is an effective material for the removal of uranium from contaminated groundwater as it was demonstrated earlier by some authors. General reviews of the development of research and application of the PRB technology are given among others by Morrison and Spangler 1996, Gavaskar et al. 1998, EPA 1997, 1998, 1999, Meggyes and Simon 2000, Noubactep et al. 2002, Birke et al. 2003, Simon et al. 2003,:Roehl et al. 2005).

The constructed experimental PRB proved to be effective for removing of uranium from the groundwater: the concentration of uranium passed the PRB dropped from app. 2-3 mg/l to app. 0.02 mg/l. The details of the construction and first experimental results are described in some publications (Roehl and Czurda 2002, Csővári et al. 2005, Simon et al. 2003).

Location of the PRB

Among the waste rock piles (WP) obtained during the underground mining activity the most large is the WP3. Major part of the seepage from the WP3 is collected by the cavities of the former mine N1 (because the WP3 is situated practically above the former mine), but some part of it leaves the area in the direction of a drinking water aquifer. Taking into account the possible long-term effect of WP3 (it contains app. 1000 t of uranium), it was important to develop an appropriate method for removing of uranium from the groundwater leaving the area. Therefore the valley cold *Zsid-valley*, collecting the "escaped" contaminated seepage from WP3 was chosen for the test site.

The geological investigations of the site has showed that the upper 1-2.5 m layer consists of clay and clayey sand, under which with thickness of 3-5 m mainly sand and linces of **clayey sand** are present. Over the Pannonian sandstone bedrock a broken sandstone zone (app. 1 m thick) can be found. The site has proved to be ideally suitable for PRB. The average value of the hydraulic conductivity is k_f ~$5x10^{-5}$ m/s. The hydraulic gradient is 0.02 m/m, therefore the groundwater flow velocity is app. 8-9cm/day. Fragment from the wall of the PRB is shown in Fig. 1.

The original groundwater composition can be characterized with high bicarbonate content (600-700 mg/l) with uranium contamination up to 1 mg/l (in 2002).

Based on a detailed site investigation, various approaches towards the possible design of the experimental barrier were considered. The experimental installation was designed with a length of 6.8 m, a thickness of 2.5 m and a depth of 3.8 m. The PRB consists of two zones: zone I is 50cm thick with a low content of coarse elemental iron (12% by volume or 0.39 t/m^3, grain size 1 - 3 mm), and zone II is 1m thick with a higher content of fine elemental iron (41% by volume or 1.28 t/m^3, grain size 0.2 - 3 mm). Sand was mixed with the elemental iron aiming at increasing the porosity of the active zone even in long term. The total mass of elemental iron installed as reactive material was 38 t, of which 5 t was coarser material.

Fig.1. The sediments fragment from the PRB wall on the test site.

On both sides (upstream and downstream) 50cm thick sand layers were placed to allow an even distribution of water inflow and outflow. The PRB is sealed with clay and geosynthetic clay liners at the bottom and with a geomembrane (high density polyethylene - HDPE) at both ends and on the top, and covered over with a layer of clay.

Arrangement of the monitoring wells around the PRB is shown in Fig. 2. Some monitoring wells have been replaced from the starting of the experiment with new ones because of different reasons, so in some cases the numbering of the wells is differs from that of given in the earlier publications. Nevertheless the change of the composition of ground water can be followed using the map of well placement. View on the test site (from North to South) is presented in Fig. 3 together with the location of the main monitoring well Hb1/1.

The principal sketch of design of the experimental PRB installation is displaced in Fig. 4.

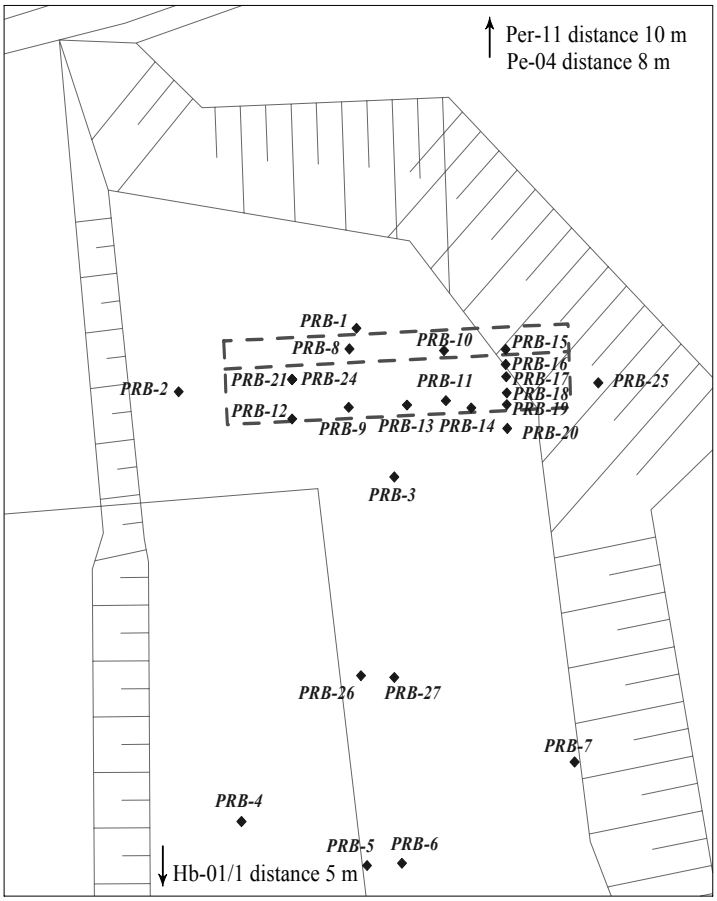

Fig.2. The location of the monitoring wells on PRB test site.

Fig.3. View on the test site (valley) with monitoring wells (May 2008).

Change of the groundwater composition

The first test results were published in the monograph "Long-term Performance of Permeable Reactive Barriers" by Roehl et al. (2005). Some new results have been published by consortium members (Simon et al. 2003, Csővári et al. 2005, Bierman et al. 2006, Meggyes 2007). In this contribution a brief summary for the whole operating period is presented.

The PRB installation is monitored regularly: water samples are collected usually two times per year. Beside the common components (TDS, HCO3, Cl, Na, SO4, Ca, Mg, Fe) the trace elements such as Se, Cr, Zn, As, Mn etc. are also determined in the water periodically. From some wells (built directly in the PRB) only uranium is determined because only small volume of water sample (the monitoring wells in this case are practically tubes only with diameter of 20 mm) was available.

The changing of the most important components (U, TDS, HCO_3^-, SO_4^{2-}, Fe) in the groundwater characterizing the performance of the PRB is presented by graphics in Fig. 6. The data for some selected wells and components for 2007 are presented separately in Fig. 7. For the evaluation of the performance of the PRB the data for Pe-04, PRB-01, PRB-03 and HB1/1 are the most important because the water composition in these wells depends on the processes taking place in the PRB.

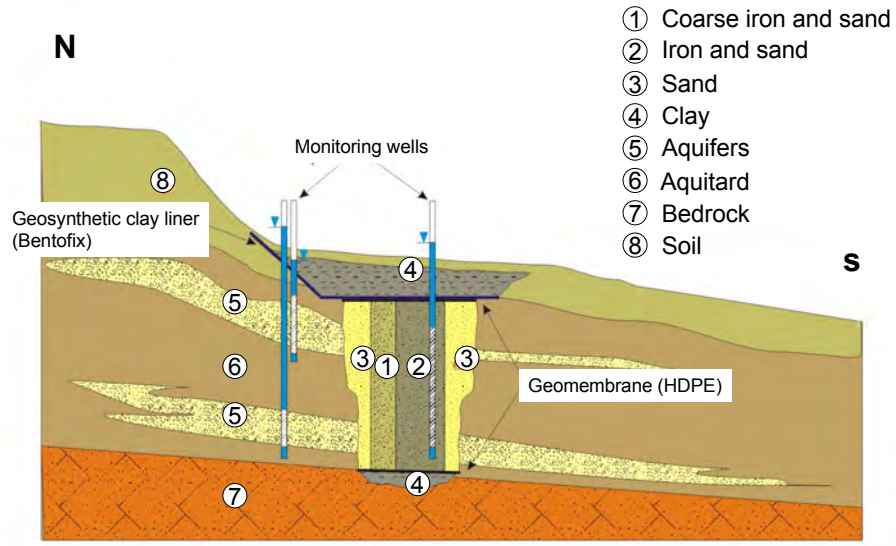

Fig.4. Sketch of the design of the PRB near Pécs (Hungary).

Changing of the uranium concentration

The development of uranium concentration is displaced in the graphics in Fig. 5. It can be seen that the uranium concentration decreases sharply in the reactive wall. The upstream uranium concentration still is growing from 1mg/l to more than 2mg/l in 2007 (well PRB-1, Pe-04), while in the water passed the PRB (well PRB-3) remains on the level of 0.01 mg/l practically over the whole period of observation. Data for 2007 (Fig. 6) also justify that the uranium is still captured by the PRB because its concentration in the reactive zone remains practically on the level of 10 μg/l.

The overall effect of the PRB on the groundwater quality in the valley is shown in Fig. 7. In this figure the uranium concentration in the sample from the monitoring well Hb1/1 (installed in the valley for the monitoring of the water leaving the mining area toward the drinking water catchment area) is presented from 1996 up to 2008. The high performance of the PRB is obvious: uranium concentration in the groundwater decreased sharply (below 0.1 mg/l) immediately after the installation of the PRB and still is on this level.

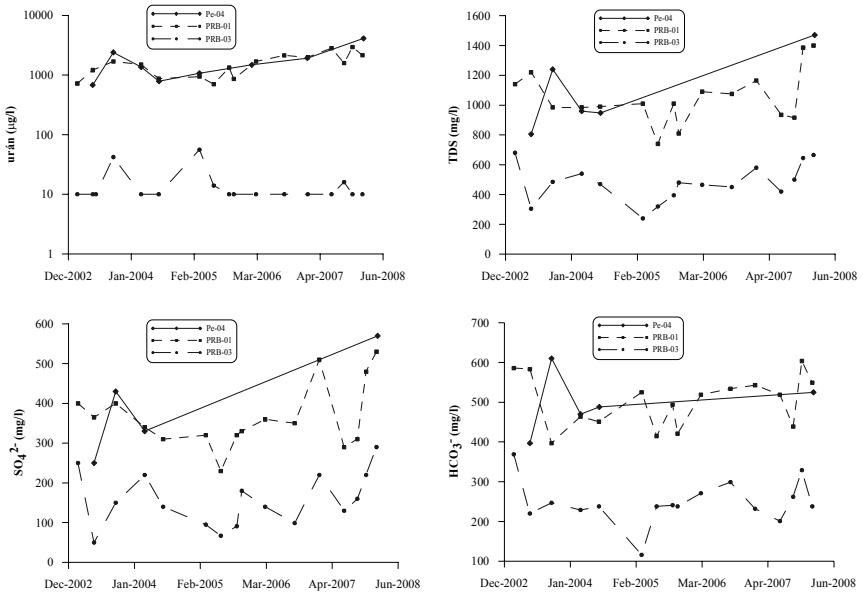

Fig.5. Historical data on the groundwater composition on the test site

Monitoring wells		pH	Eh	U	TDS	HCO_3^{2-}	Ca^{2+}	Mg^{2+}	Fe	SO_4^{2-}
			mV	µg/dm³	mg/dm³	mg/dm³	mg/dm³	mg/dm³	mg/dm³	mg/dm³
PE-04	Upstream	n.d.	-82	1920	n.d.	n.d.	n.d.	n.d.	< 0.002	n.d.
PRB-01		7.2	184	2330	1100	526	158.5	44.6	0.006	398
PRB-15	Fe ~0,39 t/m³		-48	<10					11.000	
PRB-16				32					0.457	
PRB-17	Fe ~1,28 t/m³		46	<10					0.078	
PRB-18			6	13					4.730	
PRB-19			10	13					0.023	
PRB-20			68	<10					0.001	
PRB-03		8.7	-21	<10	536	256	13.4	48.6	0.016	183
PRB-26	Downstream	7.9	-58	14	544	317	25.3	36.6	0.279	135
Hb-01/1		8.2	286	101	626	289	28.9	55.9	0.041	210

Fig.6. Groundwater chemistry for some selected components on the PRB test site in 2007.

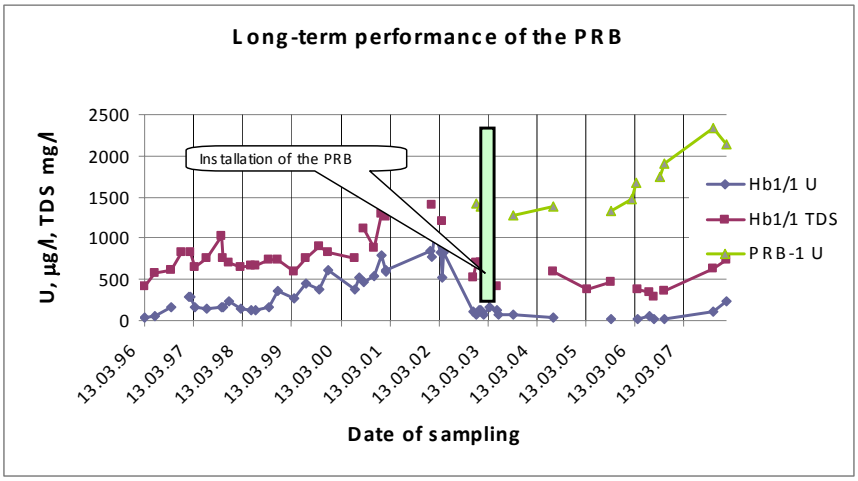

Fig.7. Uranium concentration and the TDS in groundwater prior to the installation and after installation of the PRB on the test site.

Changing of the general composition of the groundwater

It is known that the basic chemical process between the uranium and iron can be described as the reduction of the U(VI) to U(I)V), which precipitates at the elevated pH established in the process of dissolving of the iron:

The concentration ratio of the CO_3/HCO_3 creases at the elevated pH and as a consequence calcium (and in some extent the magnesium too) precipitates presumably in form of carbonates. The resulting effect is the significant decreasing of the TDS in the groundwater.

Practically these processes are observed in the PRB: pH increases from 7.2 to above pH=8, TDS decreases in great extent app. by 50% from the original. The sulfate concentration has dropped to app. half of its original value in the upstream. It is supposed that this is due to anaerobe sulfate reduction process taking place in the PRB body. It is worth mentioning that the dissolving iron is precipitate in the reactive zone with higher pH, there is no sign of its escaping from the reactive zone. In PRB-02 iron concentration is less than 0.1 mg/l.

pH of the groundwater leaving the PRB is higher than that of the upstream, which is an indicator that the PRB is still active from the chemical point of view, i.e. the PRB still works.

Conclusions

The zero-valent iron-based experimental PRB works well after six years of operation, uranium is retarded by the reactive zones with high efficiency (> 99%). Uranium concentration in groundwater passing the installation is on the level of 10 microgram per liter, well below the drinking water limit.
TDS of groundwater decreases by app. 50%, which is explained with the increased pH resulting in the precipitation of calcium carbonate. The considerable decreasing of the sulfate concentration is likely due to the anaerobic sulfate reduction processes enhanced by bacteria.

References

Biermann, V., Simon, F-G., Csővári, M., Csicsák, J., Földing, G., Simoncsics, G. Long-term perfrmance of reactive matarials in PRBs for uranium remediation. In: In: Brodel J. Merkel and Andrea Hasche-Berger (editors) Uranium in the Environment Springer-Verlag Berlin Heidelberg 2006 pp. 275-285

Csővári M., Csicsák J., Földing G., Simoncsics G. (2005) Experimental Iron Barrier in Pécs, Hungary. In: Roehl, K.E., Meggyes, T., Simon, F.-G. & Stewart, D.I.: Long-term Performance of Permeable Reactive Barriers. Elsevier, Amsterdam

EPA (1997) Field demonstration of permeable reactive barriers to remove dissolved uranium from groundwater, Fry Canyon, Utah. EPA 402-C-00-001 november 2000.

EPA (1998) Permeable reactive barrier technologies for contaminant remediation. U.S. EPA Remedial Technology Fact Sheet, EPA 600/R-98/125

EPA (1999) Field applications of in situ remediation technologies: Permeable reactive barriers. U.S. EPA Remedial Technology Fact Sheet, EPA 542-R-99-002.

Franz-Georg Simon, Vera Biermann Mihály Csővari, József Csicsak: Uranium removal using elemental iron and hydroxiapatite in permeable reactive barriers. 8th International Congress on Mine Water and The Environment, Johanesburg, South Africa,19-22 October, 2003 Bublished by IMWA At shaft SinkersCentex Office Park

Meggyes, T. and Simon, F.-G. (2000) Removal of organic and inorganic pollutants from groundwater using permeable reactive barriers. Part 2. Engineering of permeable reactive barriers. Land Contamination & Reclamation, 8 (3), 175-187

Morrison, S.J. and Spangler, R.R. (1996): Subsurface Injection of Dissolved Ferric Chloride to form a Chemical Barrier: Laboratory Investigation, Ground Water, vol. 34, N01, January-February 1996

Noubactep, C., Meinrath, G., Volke, P., Peter, H-J., Dietrich, P., Merkel, B. (2002): Mechanisme of uranium fixation by zero valent iron: The importance of precipitation In: Merkel, J. Planer-Friedrich, B. Wolkersdorfer, C. (2002): Uranium in the Aquatic Environment. Springer 2002

Roehl, K.E. and Czurda, K. (2002) PEREBAR - A European Project on the Long-Term Performance of Permeable Reactive Barriers. In: Prokop, G. (ed.) Proc. 1st IMAGE-TRAIN Cluster Meeting Karlsruhe, November 7-9, 2001, Federal Environment Agency Austria, Vienna, 23-31.

Risk Assessment of Uranium in Selected Gold Mining Areas in South Africa

Peter Wade and Henk Coetzee

Council for Geoscience, Private Bag X112, Pretoria, 0001,
pwade@geoscience.org.za

Abstract. Real and perceived risks due to gold and uranium mining in the West Rand and Far West Rand goldfields of South Africa have led to intense and sometimes heated public debate. In this context, it is critical to present results of such investigations carefully in a neutral format. The format for reporting in the current study was that of a Tier-II risk assessment, as routinely implemented by the US EPA. Sources, release and fate and transport mechanisms have been investigated and integrated with identified pathways to the local communities. An unacceptable level of risk has been identified, primarily due to the chemical toxicity of uranium on ingestion via drinking water.

Introduction

In recent years, environmental degradation due to mining activities in South Africa has become a matter of intense public debate and scrutiny. Political change since 1994 has allowed greater public access to information than was available in the past at the same time as growth in public environmental awareness globally. As often happens in these circumstances, media reports have highlighted extreme negative impacts. In this context, it is critical to present results of environmental investigations carefully in a neutral format and to assess data using an accepted framework. In order to maintain scientific integrity and credibility, it is vital that data are presented in full and without undue delay. Owing to the lack of a broadly accepted integrated environmental risk assessment methodology in South Africa, the United States EPA's guidelines for ecological risk assessment (Environmental Protection Agency 1997) have been employed as a tool for the assessment of risks due to mining.

The West Rand and Far West Rand Goldfields have been mined for gold since the late 19th Century, with the associated uranium having been deposited as mine

waste (primarily tailings) for most of this period, with the exception of a portion of the second half of the 20th Century where uranium was extracted as a by-product of gold mining. The major portion of the mining areas are drained by the Wonderfonteinspruit (See Fig 1), a major tributary of the Mooi River, which is the primary water source for the City of Potchefstroom, downstream of the mining areas. It is estimated that approximately 400,000 people are dependent on the Wonderfonteinspruit as a source of water for, mainly for domestic and agricultural purposes, although some communities use the water for recreational purposes and fishing. A large number of these people live in informal and semi-formal settlements with little or no formal water supply. In these communities, chronic and acute malnutrition and a high incidence of HIV infection are believed to place people at increased health risk and vulnerability to pollution.

Studies by the Department of Water Affairs and Forestry (Institute for Water Quality Studies 1999) have indicated elevated levels of radioactivity in rivers draining the gold-mining areas of the Witwatersrand. A detailed study of the Mooi River system (including the Wonderfonteinspruit) showed radioactivity levels in this system to be elevated, although doses to the public from formal drinking water sources were found to be within acceptable limits at most sites studied.

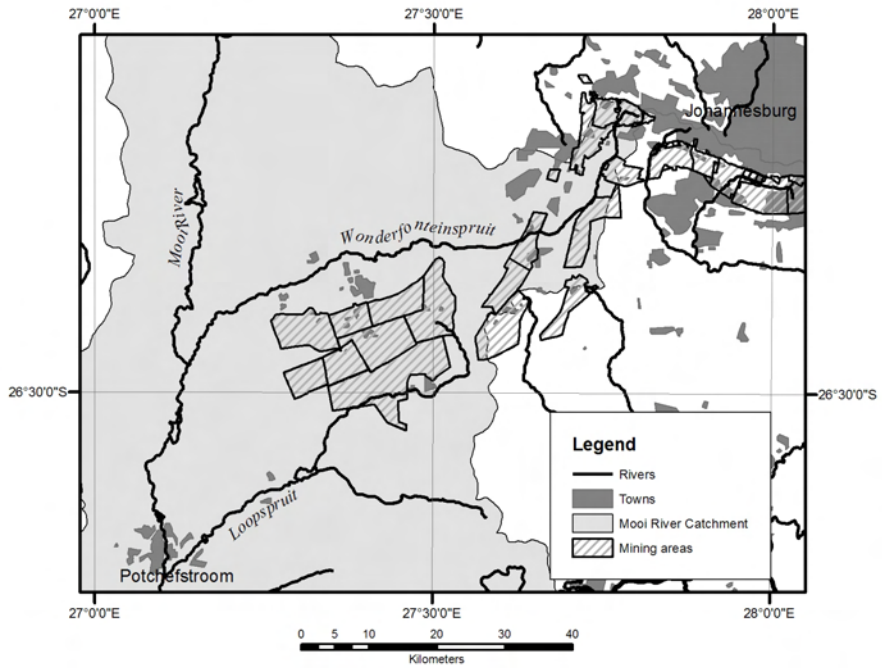

Fig.1. Locality of the Wonderfonteinspruit, showing the Mooi River Catchment, mining areas and local towns.

Risk-assessment methodology

Overview

The process investigated as applicable to a baseline risk assessment in the Wonderfonteinspruit catchment is graphically presented on Fig 2.

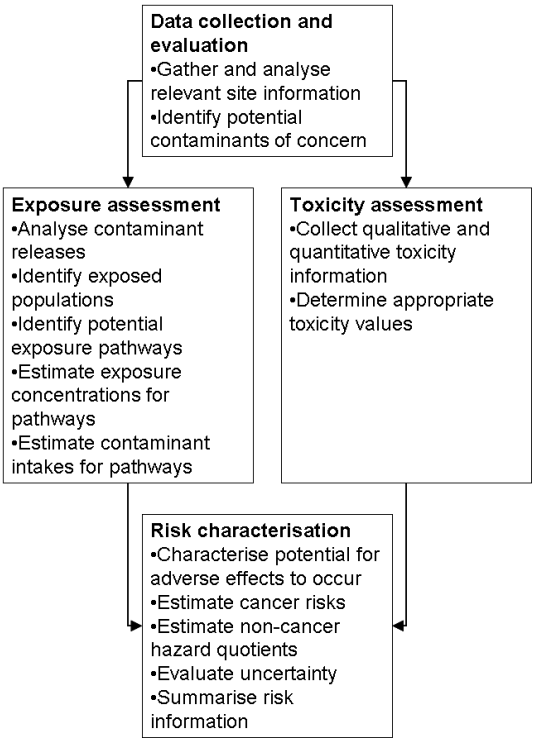

Fig.2. Schematic overview of the RAGS Part A Baseline Risk Assessment.

Site-specific objectives of the risk assessment

The objective of a risk assessment of metals and metalloids in the Wonderfonteinspruit catchment is to provide critical information to the stakeholders in the catchment. The major target group for this study is the authorities responsible for the maintenance of the water supply in the area, i.e. DWAF, regional water-supply authorities, local authorities, particularly the Potchefstroom Municipality.

Furthermore, the major water users in the area, particularly the mining and agricultural industries could utilise the results in their planning processes, while local community members will use the information presented in ordr to make informed choices regarding water use and related activities.

Scope of the risk assessment

The current risk assessment should be viewed as a Tier-II risk assessment, since it builds on the information gathered in previous "Tier-I" risk assessments in the catchment, and adds information about pathways of contaminant transport. The level of detail or depth of the assessment is measured by the amount and resolution of data used, and the sophistication of the analysis employed. Sometimes, as is the current case, the primary limitation is availability of resources. The current assessment will therefore consist of benchmarking measured contaminant concentrations against regulatory limits.

Preliminary conceptual analysis

A conceptual model of the site (in this case the Wonderfonteinspruit catchment) was developed for this study. Conceptual models consist of a set of risk hypotheses that describe predicted relationships among stressor, exposure, and assessment end-point response, along with the rationale for their selection.

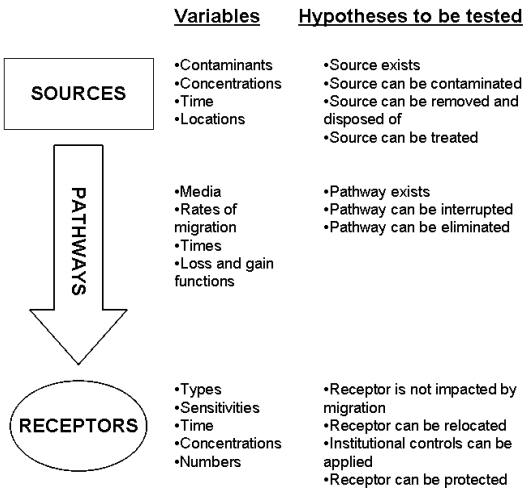

Fig.3. Aid to identifying components of the conceptual model (after Environmental Protection Agency 1989).

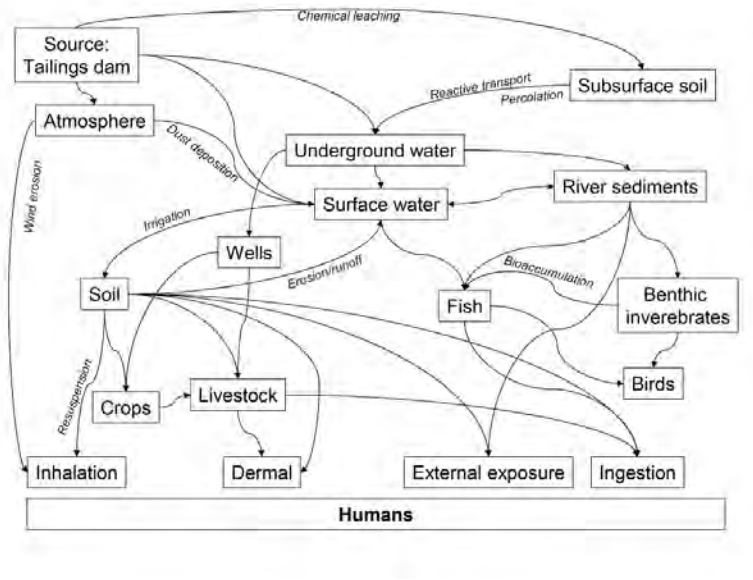

Fig.4. Preliminary graphical conceptual site model (after Servant 2002).

The components of an ecosystem can be divided into several major compartments. None of the environmental compartments exist as separate entities; they have functional connections or interchanges between them (See Fig 4.).

Initial uranium deposition in a compartment, as well as exchanges between compartments (mobility), is dependent upon numerous factors such as chemical and physical form of the uranium, environmental media, organic material present, oxidation-reduction potential, nature of sorbing materials, and size and composition of sorbing particles.

Risk assessment results

Identification of chemicals of potential concern

The following method of selection of contaminants of concern was implemented:

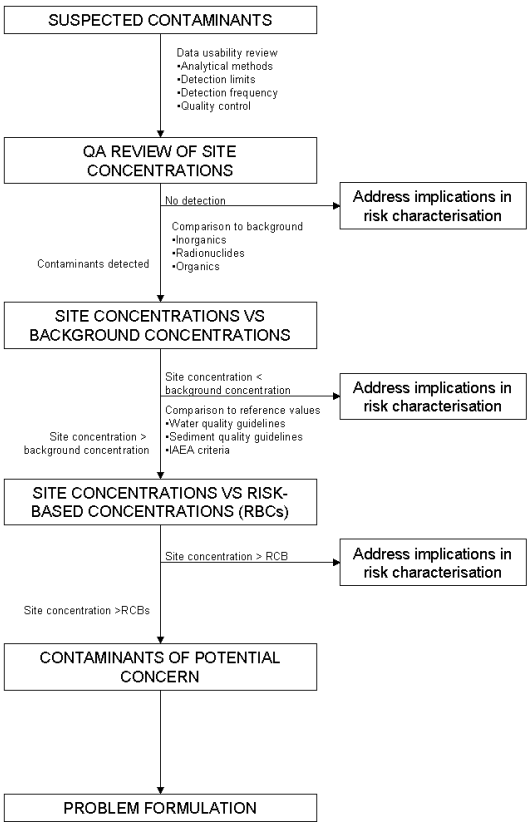

Fig.5. Flowchart for the selection of contaminants of potential concern (COPCs) (after Environmental Protection Agency 1997).

Based on the Tier-1 risk assessment, Cr, Co, Ni, Cu, As, Cd and U were identified as contaminants of potential concern, with U and Cd potentially having the highest environmental impact.

Data compiled from previous studies, combined with analytical data obtained in the scoping phase of the current study, resulted in uranium being selected as the contaminant of greatest concern in terms of surface- and groundwater contamination in the Wonderfonteinspruit catchment.

Environmental chemistry of uranium

Uranium occurs in natural waters in three oxidation states, uranium(IV) (e.g. U^{4+}), uranium(V) (e.g. UO_2^{+}) and uranium(VI) (e.g. uranyl ion UO_2^{2+}). In reducing surface waters, uranium occurs as U^{4+} and UO_2^{+}. Uranium(IV) has a strong tendency to precipitate (e.g. as uraninite, $UO_2(s)$) and to remain immobile, whereas UO_2^{+} forms soluble, but relatively unstable, complexes. Uranium tends to occur in oxi-

dised surface waters as UO_2^{2+} which forms stable, readily soluble, cationic, anionic and/or neutral complexes which are highly mobile.

The speciation of uranium is relatively complex in oxidised fresh surface waters (pH 5−9). Since uranium is a highly charged cation, the redox and complexation reactions of uranium in surface waters are strongly influenced by hydrolysis. Hydrolytic reactions limit the solubility and influence sorption behaviour.

In addition to carbonate, natural organic matter (OM) is a very effective complexing agent of uranium in natural waters. Organic matter may be soluble (dissolved OM, or DOM) or insoluble (particulate OM, or POM), depending on its molecular weight, state of aggregation, degree of protonation, and the extent of metal binding (the ionic strength of the water).

Organic matter may act as a sink for uranium if the uranyl-OM complex is insoluble (as uranyl-POM), or may serve as a mobile phase if the uranyl-DOM complex is soluble, or colloidal.

Sorption plays a dominant role in determining the fate of uranium in freshwater systems. Below pH 5, sorption is generally to clay minerals (e.g. smectite, montmorillonite) and at higher pH, to iron and aluminium (oxy)hydroxides, silica and micro-organisms. This process significantly reduces the mobility of uranium in oxic waters. Sorption of uranium to insoluble organic matter, or organic matter attached to particles (e.g. hydrous iron oxides), also reduces the mobility of uranium.

Oxidation-reduction conditions are important in the geologic transport and deposition of uranium. Oxidised forms of uranium (U(VI)) are relatively soluble and can be leached from the rocks to migrate in the environment. When strong reducing conditions are encountered (e.g. presence of carbonaceous materials or H_2S), precipitation of the soluble uranium will occur.

In addition to the migration of dissolved or suspended uranium due to the movement of water in the environment, the transport and dispersion of uranium in surface water and groundwater are affected by adsorption and desorption of the uranium on surface-water sediments.

Uranium can also be removed from solution by physical adsorption processes, such as adsorption onto oxides of iron or manganese that occur as coatings on the particles of soil and sediment.

Uranium mobility may also be increased owing to the formation of soluble complexes with chelating agents produced by micro-organisms in the soil. Uranium may be transported to vegetation by air or by water. It can be deposited on the plants themselves by direct deposition or resuspension, or it can adhere to the outer membrane of the plant's root system with potential limited absorption. Similarly, uranium deposited on aquatic plants or water may be adsorbed or taken up from the water.

Exposure assessment

Potentially exposed populations

The Wonderfonteinspruit valley is densely populated because of its agricultural value and presence of gold mines. Potchefstroom is located downstream of the Wonderfonteinspruit, from which more than 400 000 people derive their drinking water via the Boskop Dam.

The majority of the inhabitants live in informal settlements, using contaminated ground- and stream water for personal hygiene and drinking. With above-average infection rates of HIV/AIDS and chronic and acute malnutrition, this subpopulation is particularly vulnerable to additional stress of the immune system by contaminants such as uranium.

Identification of exposure pathways

The integration of sources, releases, fate-and-transport mechanisms, exposure points and exposure routes into complete exposure pathways was performed.

Uranium can enter the human via a number of pathways from the source, being largely tailings dams in the catchment, through groundwater, to soil, and to river water. Contaminated groundwater may also be used by humans.

Principal modes of contact are ingestion of water and food products, and inhalation of dust and aerosols.

Toxicity assessment

Key site-related contaminants and key exposure pathways identified

The key contaminant identified in the Wonderfonteinspruit catchment was uranium; for the purposes of this example, the key exposure pathway from stream water to human through the mode of drinking water was chosen.

Types of health risk of concern

Both radiological cancer risk and chemical non-cancer hazards were investigated. The primary organ at risk from uranium chemical toxicity is the kidney, while organs at risk from chronic radiological toxicity include the lymph nodes and the bone. A review of uranium toxicity around the time of the study set minimum derived drinking-water concentrations at 31 µg/l for chemical toxicity, although values as low as 2 µg/l have been identified as a safe limit, and 63 µg/l based on 1 mSv/a, 500 l/a radiological risk, assuming secular equilibrium with its progeny. The World Health Organisation has recently recommended a guideline level of 15 µg/l, based on chemotoxic effects (World Health Organisation 2005). Based on

the recommendation of the United Nations Scientific Committee on the Effects of Atomic Radiation (United Nations Scientific Committee on the Effects of Atomic Radiation 1998) regarding studies of uranium in the environment, the chemical toxicity of uranium formed the basis for the risk assessment in this study. Nuclide-specific analyses were not performed, making a detailed assessment of radiological dose impossible. It should be noted that there is practically no lower limit for acceptable radiological risk, based on a linear dose-response profile, and that recent research suggests that there is also no clear lower threshold for chemical toxicity.

Risk characterisation

Exposed population characteristics

The most-exposed populations are expected to be those of informal settlements.

Magnitude of the carcinogenic and non-carcinogenic risk estimates

In the risk-assessment procedure that was applied, risk quotients are determined by dividing the measured and predicted uranium concentrations in surface water that could be used by communities as a sole drinking-water supply, by the limit or guideline value for the contaminant of concern.

A significant risk is therefore determined where the risk quotient is greater than unity, with higher values indicating higher levels of risk. The carcinogenic risk quotient for uranium in the surface water of the Wonderfonteinspruit is 2.22, based on conservative assumptions regarding secular equilibrium between uranium-series radionuclides. The chemical toxicity risk quotient for this water was calculated as 6.67. Using the more recent guideline level proposed by the World Health Organisation, this figure should be revised to 13.78.

Major factors driving risk

Major factors driving risk are contaminant mobility from tailings dams into the river system, and the practice of drinking from the contaminated streams in the catchment.

Conclusions

The chemical risk quotient associated with drinking river water is 6.67, and the radiological risk quotient is 2.22. Both the numbers are above 1, meaning that there is a risk of ill-health effects by drinking water from contaminated streams in the Wonderfonteinspruit catchment. Studies of the Wonderfonteinspruit catchment

have however established that in the dissolved fraction, uranium is not in secular equilibrium with its progeny, typically displaying activities significantly higher than its radioactive daughters. The assumption of secular equilibrium, used to calculate the radiological risk quotient will therefore lead to an overestimate of the total radiation dose. The radioactive progeny however, have no influence on the chemical toxicity of uranium in solution in water. The recommendation of UNSCEAR (1998) therefore appears to be valid, and it is recommended that the chemical toxicity of uranium be regarded as the primary health risk due to the water in the Wonderfonteinspruit.

Follow-up studies performed by the South African National Nuclear Regulator (National Nuclear Regulator 2007) have confirmed these indications of risk, with a number of sites in the catchment having been identified where the potential radiological dose to the public exceeds the guide level of 1mSv/a, primarily due to pathways relating to the sequestration of radionuclides in sediments. At these sites, uranium is also likely to present a significant hazard due to its chemical toxicity.

References

Environmental Protection Agency (1989) USEPA (1989): Risk assessment guidance for superfund - Volume I: Human health evaluation manual (Part A). , Office of Emergency and Remedial Response. U.S. Environmental Protection Agency, Washington D.C., EPA/540/1-89/002, 289pp.

——(1997) Supplemental ecological risk assessment guidance for superfund, US EPA Region 10 Office of Environmental Assessment Risk Evaluation Unit, Washington D.C., EPA 910-R-97-005, 86pp.

Institute for Water Quality Studies (1999) Report on the radioactivity monitoring programme in the Mooi River (Wonderfonteinspruit) catchment. , Department of Water Affairs and Forestry, Pretoria, N/C200/00/RPQ/2399.,

National Nuclear Regulator (2007) Radiological impacts of the mining activities to the public in the Wonderfonteinspruit Catchment Area, National Nuclear Regulator, Pretoria, TR-RRD-07-0006, 125pp.

Servant, A C. (2002) Methodology to assess the radiological impact of a repository for uranium mill tailings after remediation (short-term impact). In *Uranium in the aquatic environment. - Conference Proceedings 3rd International Conference on Uranium Mining and Hydrogeology 2002, Freiberg, Germany*, edited by B. Merkel, B. Planer-Friedrich and C. Wolkersdorfer, Springer, Heidelberg 907-914.

United Nations Scientific Committee on the Effects of Atomic Radiation (1998) Sources, effects and risks of ionizing radiation. Report to the General Assembly, with annexes. , United Nations Publications, New York, NY,

World Health Organisation (2005) Uranium in Drinking Water - Background document for development of WHO Guidelines for Drinking-water Quality, World Health Organisation, WHO/SDE/WSH/03.04/118, 26pp.

Risk assessment of a landfill for wastes containing naturally occurring radionuclides through infiltration to groundwater

Juan Merino, Jordi Guimerà, Xavier Gaona, Miguel Luna, Anne Delos and Jordi Bruno

Amphos 21, Pg de Rubí 29-31, E-08197 Valldoreix, Spain

Abstract. A risk assessment of a landfill for NORM waste (fertilizer plant process waste) has been carried out. Although some enhanced levels of radionuclides could occur in groundwaters inside the site, the doses potentially received by a hypothetical exposed persons through consumption of water would be lower than the applicable dose limits. Furthermore, dilution in both the aquifer and the Ebro river leads to very low levels of radionuclides in this river, which would be masked by background levels.

Introduction

A fertilizer manufacturer in Flix, Tarragona (Spain) has been disposing process waste in an authorized landfill since 1989. As a result of public concern regarding the enhanced natural radioactivity contained in the wastes, a series of studies were commissioned by the plant owners in order to assess the chemical stability of the wastes, the hydrogeological characterization of the site and the risk posed by the presence of the wastes to the surrounding area. This paper focuses on the radiological impact and risk assessment due to the possible migration of radionuclides to the aquifer through infiltration of water.

Site description

The landfill for NORM (Naturally Occurring Radioactive Materials) wastes is formed by 10 terraces, which are currently closed, and an area under exploitation which is out of the scope of the present study. The site has 5 off-site control piezometers, three on –site wells and two basins for receiving the leachates. Fig. 1

shows an aerial view of the site. The terraces have different altitudes with respect to sea level, with a vertical interval of 37 m between terrace 1 and 10.

The wastes contain relatively high levels of U and Th, as well as Ra, Pa, Pb-210 and Po-210. It is very likely that the source of these radionuclides in the waste is the residual phosphate coming from the recovery process.

Conceptual model

The conceptual model is based on the information gathered in the field work and the information on previous work made available by the landfill managers. Briefly, the waste has been deposited in the 10 terraces consecutively since 1989. Due to infiltration from rain water, leaching of waste can occur. This can lead to a transport of radionuclides to the tertiary basement underlying the landfill, which is linked to an alluvial aquifer discharging to the Ebro river. A well is located 1750 m downstream from the site. In this risk assessment it will be assumed that the well is used for supplying drinking water to a small community (although no uses have been reported for this well). Fig. 2 shows a schematic view of the conceptual model.

Fig.1. Aerial view of the site (from Google Maps).

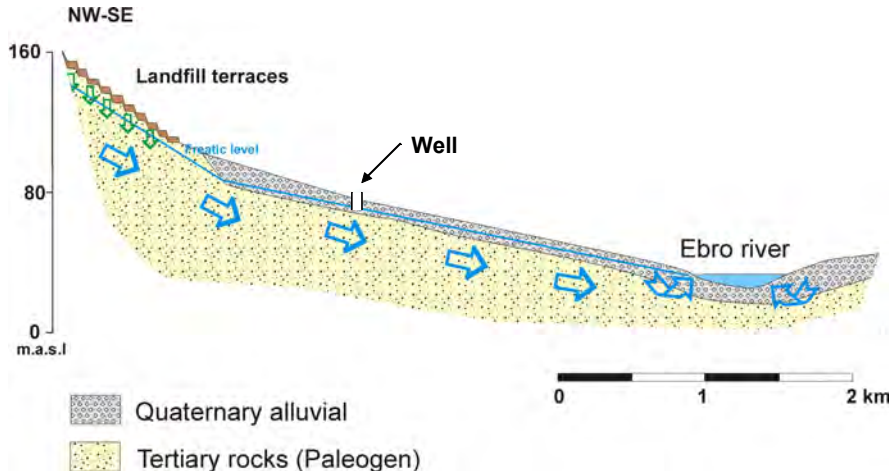

Fig.2. Conceptual model of the system (not at scale)

Exposure pathway

Only the ingestion of well-water pathway is considered to be relevant (irrigation of fields is done with water from the Ebro river).
The effective dose received by an exposed individual will be simply given by:

$$D_{ing} = A_w \cdot I_r \cdot F$$

where

D_{ing}: Dose received by an exponed individual due to consumption of well water (mSv/y)

A_w: Specific activity of each radionuclide in the well water (Bq/l)

I_r: Annual consumption of water by an adult (standard value of 2 l/d)

F Ingestion dose conversión factor for adults (Sv/Bq, tabulated in ICRP 1996).

We have pessimistically assumed that all water consumed by the exposed individual comes from the contaminated well. From the equation above it is necessary to know the specific activity of all radionuclides in the well water. This specific activity has been calculated with the transport model described in the following section.

Transport model

The transport model is based on a one-dimensional flux of groundwater, with advective transport of radionuclides (hydrodynamic dispersion has not been taken into account, although the spatial discretization has led to numerical dispersion). Sorption in the different materials (waste, tertiary host rock and alluvial aquifer) has also been considered, as well as solubility limits in the pore waters of the waste terraces. The box-modelling tool AMBER (Enviros, 2006) has been used to set-up the compartment system and transfers, and to solve the corresponding system of ordinary differential equations. Fig. 3 shows an AMBER window with all the elements of the system:

- 10 compartments for the 10 waste terraces
- 10 compartments for the tertiary host rock underlying the landfill site.
- 100 compartments for the alluvial aquifer (the well abstracts water from compartment number 39).
- 1 compartment for the river, which acts as the sink of the system.
- 10 source term transfers (one transfer per terrace, in order to be able to simulate the different time of closure of the terraces).
- Transfers by infiltration between the terraces and the tertiary host rock.
- Advective transfers between the aquifer compartments.

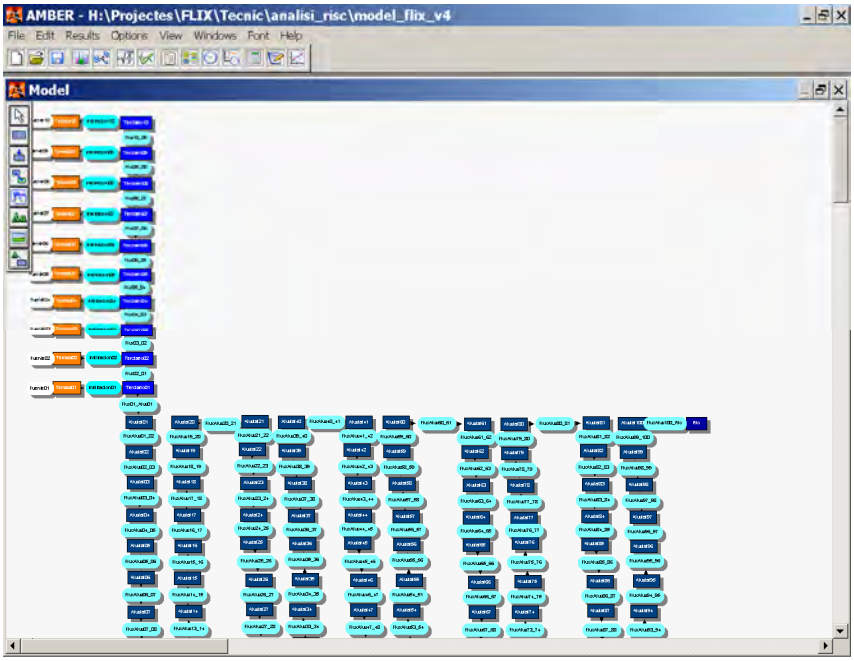

Fig.3. AMBER window showing the box model of the system.

The box-modelling approach is based on the resolution of the following coupled differential equations governing the amount of contaminant in each compartment:

$$\frac{dA_{i,n}}{dt} = -\left[\lambda_i + \sum_m k_{i,nm}\right] A_{i,n} + \lambda_{i+1} A_{i+1,n} + \sum_m k_{i,mn} A_{i,m} + T_{i,n} + S_{i,n}$$

where

$A_{i,n}$: Total amount (in mole) of radionuclide *i* in compartment *n*

$A_{i+1,n}$: Total amount (in mole) of parent radionuclide *i+1* (in the decay chain) in compartment *n*

λ_i: Decay constant of radionuclide *i* (y^{-1})

λ_{i+1}: Decay constant of parent radionuclide *i+1* (y^{-1})

$k_{i,nm}$: Transfer parameter of radionuclide *i* between compartment *n* and *m* (y^{-1})

$T_{i,n}$: Source term of radionuclide i in the compartment *n* ($mol \cdot y^{-1}$)

$S_{i,n}$: Sink of radionuclide i in the compartment *n* ($mol \cdot y^{-1}$)

The transfer parameters are derived from the knowledge of the transport processes taking place between compartments. In particular, the transfer parameter for infiltration between the terraces and the tertiary basement (which gives the leaching rate of the waste) is given by the following formula:

$$k^{\text{inf}\,iltration} = \frac{P \cdot (1-E) \cdot A}{\theta \cdot R \cdot V}$$

where

P: Average annual rainfall ($m \cdot y^{-1}$).

E: Runoff (-).

A: Terrace surface (m^2).

θ: Waste porosity (-).

$R = 1 + \frac{(1-\theta)\rho \cdot K_d}{\theta}$: Retardation factor for each element

ρ: Waste density ($kg \cdot m^{-3}$)

K_d: Distribution coefficient ($m^3 \cdot kg^{-1}$)

V: Volume of terrace (m^3)

On the other hand, the transfer parameter for the advective connections between compartments is given by:

$$k^{advection} = \frac{Flowrate}{\theta \cdot R \cdot V} = \frac{K \cdot \nabla h \cdot A}{\theta \cdot R \cdot V}$$

where

K: Permeability of the material ($m \cdot y^{-1}$).

∇h:	Hydraulic head (-)
A:	Cross-section of each aquifer compartment (m^2)
R:	Retardation factor (defined previously but applied to the aquifer compartments)
θ:	Water filled porosity (-)
V:	Volume of each aquifer compartment (m^3)

All parameters have been populated with data based on experimental or field observations and/or bibliographic sources. In cases where data were scarce or uncertain, a pessimistic approach has been followed in selecting the data.

Results

The AMBER model has been run in a Pentium based PC. Due to the linear behaviour of box-model systems, very short computing time has been needed,. The main results of the transport model and risk analysis are summarized below. It should be pointed out that the model described here is not a predictive model. Instead, it is an assessment of the potential radiological impact to the environment due to the presence of the landfill. On the other hand, all concentrations and activities given in the following sections do not include the natural background, and therefore they should be considered as the concentration and activities that would be added to the background as a consequence of the presence of the landfill.

Tertiary host rock

The specific activities obtained in the tertiary host rock, at the landfill outlet, are shown in Fig. 4. Simulation time has been set to 100 years.

A few years after closure of the landfill uranium isotopes, Ra-226 and Po-210/Pb-210 reach levels high enough to be detected using standard radiometric techniques. Thorium isotopes, being controlled by solubility in pore waters, reach very low levels. This result would confirm that groundwater beneath the landfill could be affected by the presence of the waste, provided that infiltration and waste leaching occur at the rate we have assumed here.

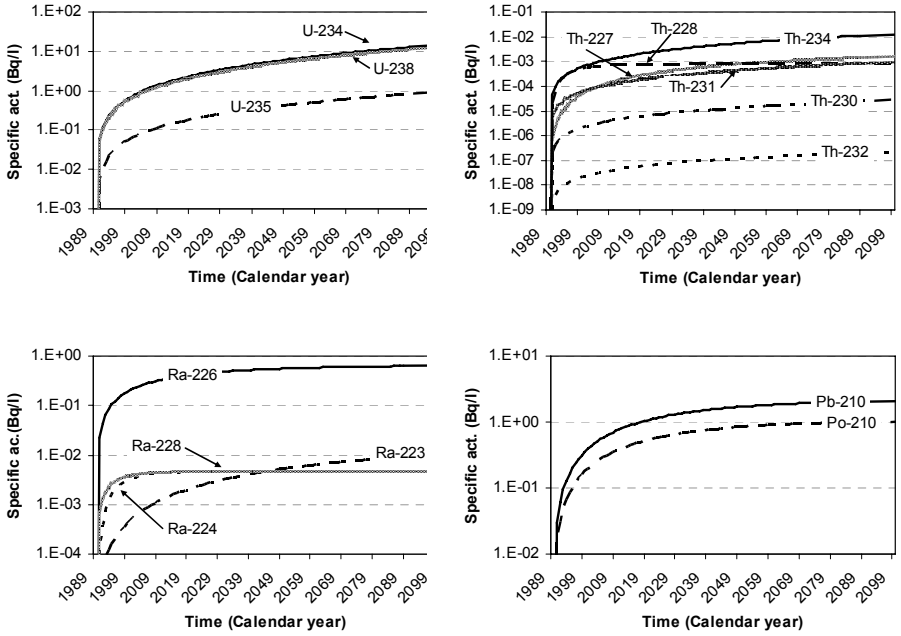

Fig.4. Specific activities of the most relevant radionuclides in the tertiary host rock.

Well

As mentioned previously, the well is located in compartment 39, and therefore the concentrations or specific activities in well water correspond to the concentrations or specific activities of that compartment (it is assumed that abstraction of water does not affect the aquifer dynamics). The specific activities of the most relevant radionuclides in the well water are shown in Fig. 5 Simulation time has been extended to 1,000 years in order to see when the guidelines values for U-238 and U-234 are reached.

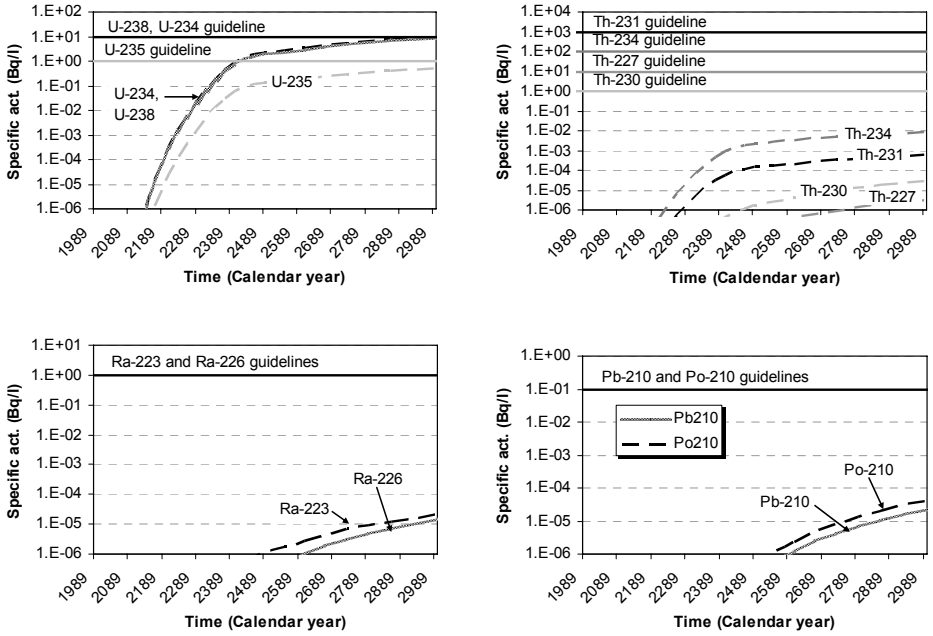

Fig.5. Specific activities of the most relevant radionuclides in the well water. WHO guidelines for drinking water are also given.

However, activities increase with time and eventually the uranium guidance levels established by the WHO (WHO, 2006) are surpassed after 1000 year. The reason why activity levels increase so slowly is that advective transport is retarded by sorption processes in the aquifer matrix, as well as the dilution effect in the aquifer itself.

Doses to the public

The calculated effective dose received by an adult is given in Fig. 6. Also plotted in the graphs are the applicable limits under Spanish regulations, which are 1 mSv/y for the public (Real Decreto 783/2001, BOE 26/07/2001) and 0.1 mSv/y for the Total Indicative Dose for ingestion of water (Real Decreto 140/2003, BOE 45/2003).

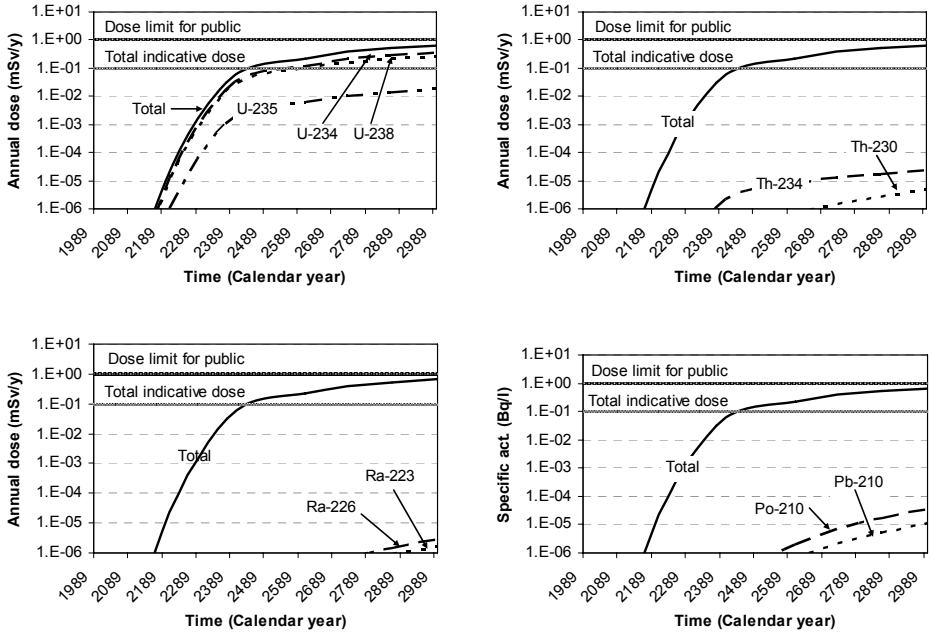

Fig.6. Doses received by an adult due to consumption of well water. The contributions of the most relevant radionuclides are highlighted.

The main contributors to the total dose are the uranium isotopes, reaching the total indicative dose 500 years after the landfill closure. It is worth noting that uranium concentration in the waste pore water is controlled by the solubility of a secondary phase, which we have conservatively assumed to be schoepite. If a more realistic phase is used, such us becquerelite with a lower solubility, then the total indicative dose is not reached in the timeframe of 1,000 years.

Affection to the Ebro river

Finally, the possible affection to the Ebro river as a consequence of discharge of the alluvial aquifer has been assessed. To this end, the mass flux to the river at the end of the aquifer has been multiplied by the river flow rate, giving the "added" concentration of the different radionuclides to the river. The results are given in Fig. 7. In this case it has been necessary to extend the simulation time to 10,000 years to see relevant patterns.

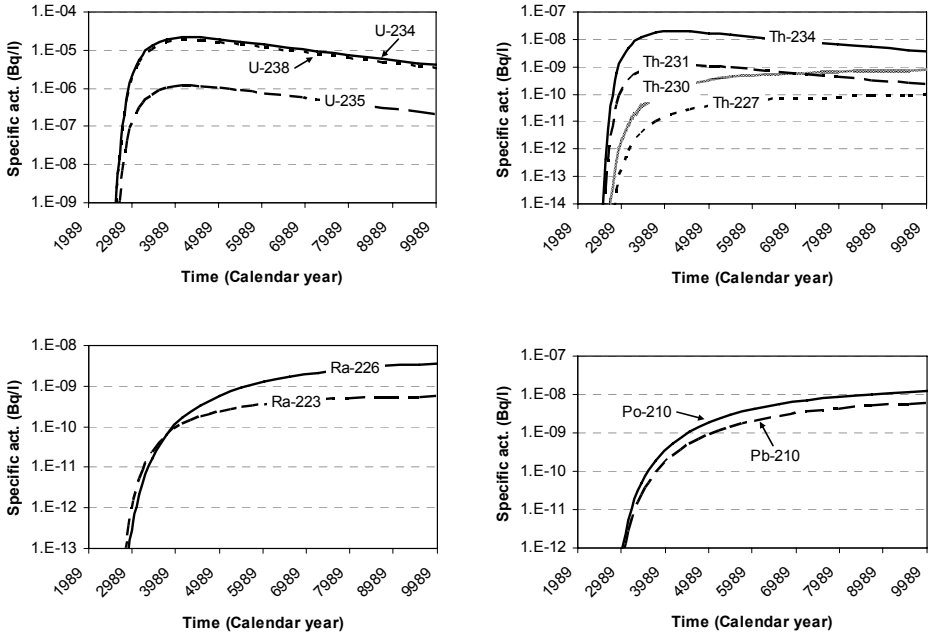

Fig.7. Specific activities to the Ebro river that would result from the discharge of the alluvial aquifer.

It is worth noting that simulation time has been extended until 10,000 years in order to be able to observe significant trends. In general the specific activities are very low, easily masked by background levels.

Conclusions

The main conclusion of the risk assessment is that, although some enhanced levels of radionuclides could occur in groundwaters inside the site, the doses can reach dose limits on drinking water only at long term and under very pessimistic assumptions. Furthermore, dilution in both the aquifer and the Ebro river leads to very low levels of radionuclides in this river, which would be masked by background levels.

Acknowledgments

The support of Maria Chantall Coll, from Ercros, is gracefully acknowledged.

References

ICRP (1996). ICRP Publication 72, Age dependent Doses to members of the Public from Intake of Radionuclides: Part 5. International Commission on Radiological Protection, Pergamon Press.

Enviros (2006). AMBER 5 Reference Guide. Enviros Consulting Limited, Culham, United Kingdom. www.enviros.com/amber

WHO (2006). Guidelines for drinking-water quality, third edition, incorporating first addendum. © World Health Organization 2006, ISBN 92 4 154696 4. http://www.who.int/water_sanitation_health/dwq/gdwq3rev/en/index.html


Uranium Mining
and Hydrogeology

Integrated Methodology for the Environmental Risk Assessment of an Abandoned Uranium Mining Site

Maria de Lurdes Dinis and António Fiúza

Geo-Environment and Resources Research Center (CIGAR), Mining Department, Engineering Faculty, University of Porto, Rua Dr. Roberto Frias, 4200-465, Porto, Portugal, mldinis@fe.up.pt; afiuza@fe.up.pt.

Abstract. We developed an integrated approach to evaluate quantitatively the fundamental data required to perform a risk assessment induced by the existence of uranium mine tailings disposals or any other form of low activity waste storage. From the characteristics of the radioactive sources the different types of possible releases are evaluated using phenomenological models. The concentrations in the main environmental compartments are deduced. To this data we apply models of environmental transport, dispersion and fate within each environmental compartment, as well as models of inter-compartment transfer. The activity is then predicted at predefined exposition locations, in each environment compartment. Models of transfer to the food chain were also developed allowing to estimate concentration of different radioisotopes in all the media. This data, complemented with an exposure scenario, allows a quantitative environmental risk assessment.

Introduction

The large volumes of ore manipulated in the extraction and processing operations of radioactive ores produced huge rates of useless solid wastes which were disposed, in the past, in open air areas. These waste storages generate liquids and/or gaseous releases. Wind, rainfall and biological processes tend to provoke the dispersion of the released compounds in the environment contributing to the transport, transfer and fate processes through the atmosphere, superficial aquatic systems or subsoil, leading to the contamination of new environmental sub-

compartments. Such dispersion is of particular concern for the radioactive wastes due to the long decay periods resulting in long-term exposures.

The exposure to these materials may follow from inhalation of contaminated air, or ingestion of contaminated water or, less directly, through ingestion of contaminated foodstuffs. Although less direct this pathway may be quite significant as a result of biological magnification into the foodstuffs. External exposure to gamma radiation is also possible.

When modeling contaminant release and transport mechanisms for each environmental compartment generally the major output chosen is the contaminant concentration in each exposition point selected (for instance, breathing air at a certain height, superficial soil and water from wells). This will allow the assessment of doses, if an additional exposure scenery is considered.

We intended to apply mathematical models with phenomenological basis to the release, the dispersion and the intercompartimental transfer of low level radioactive substances. Multicompartment models were developed and adapted with the purpose to predict the activity concentration in predefined exposure points located in each one of the compartments; our research works focused essentially in the development of models concerning the release mechanisms, the radionuclides transport, its intercompartimental transfer and fate, consolidating the scientific base for estimating exposure assessments of selected components from the local ecosystem.

The models developed in this study were, after calibration, validated using data from the surrounding areas of the former Urgeiriça uranium mine site.

Methods and Results

A systematic analysis was performed in order to consider the integrated approach of the following points: i) sources; ii) release mechanisms; iii) transport mechanisms or dispersive vectors (air and water); iv) transfer mechanisms between the environmental compartments; v) estimate of concentrations in each environmental compartment using dispersion models with spatial variation; vi) definition of the privileged exposure points and vii) identification of exposed receptors.

The important routes of contamination have been identified as a basis for developing the appropriate models. The radionuclides of major concern were also identified in each one of the compartments, based on their chemical, physical and radiological properties.

It was also incorporated a radionuclide transfer model through the food chain, including also, in a more complete version of this conceptual model, the radionuclides distribution within an organism for a relevant trophic level (pasture animals) adapted from the biokinetic models present in the specialized literature.

It was also necessary to use direct extensive measurements from a contaminated site in order to calibrate the models and for its subsequent validation. The mathematical models were coded into simulation programmes developed in Matlab.

The values for the parameters existing in the models were obtained from different sources: some parameters were taken from measurements at the Urgeiriça uranium tailings piles; others were obtained from published data referring to this site. The remaining unknown parameters were obtained from available measurements referring to other sites or from literature references, when on-site data was not available.

In the selected methodology the following main components were considered: a source term (radionuclide concentration distribution in the wastes); a multi-layer cover for the wastes (radon flux attenuation and concentrations at release available for dispersion); atmospheric pathway (radon release and dispersion by the wind); groundwater pathway (release and transport in underground waters); surface water transport (discharge and transport into superficial waters), incorporation into the flora and subsequent transfer into the food-chain. For each compartment a potential receptor or an exposition point were defined. The concentration within each compartment can then be easily transcribed to doses values based on a simplified exposure pathway and a pre-defined critical group.

Source

The usage of the models requires a previous knowledge of the main characteristics of the source: type of waste, geometry of the disposal and average chemical grades. The primary releases from the source may be alternatively provided by the user, estimated by a mathematical model or back-calculated from measured concentrations at the receptor location.

In a undisturbed uranium ore deposit secular equilibrium occurs between the ^{238}U and its decay products and between ^{235}U and its decay products. This means that as the parent nuclide has a very long half-life in relation to its radioactive daughters its concentration remains constant in time and that the activity of the daughters will be also time constant, proportional to that of the parent. This equilibrium may be disturbed by the hydrometallurgical treatment of uranium ore as a consequence of different radionuclides solubility.

Only certain nuclides are extracted by the leaching process which means that all other members of the uranium decay chain remain in the tailings at their original activities. For instance, in the ^{238}U chain, only ^{238}U and ^{234}U are easily soluble; after half a year, the activities of the nuclides ^{234}Th and ^{234}Pa have decayed to the level of the ^{238}U. The activities remain at this level for tens of thousands of years (due to the 80 000 year half-life of ^{230}Th) and for an average 1 kg/ton ore about 71% of the radioactivity originally present in the ore remains in the tailings due to ^{230}Th and its radioactive descendents.

The estimative of the radionuclides content in the tailings was done assuming initial equilibrium before leaching in the two uranium series ^{238}U and ^{235}U. The soluble isotopes were extracted with the average leaching recovery and the insoluble isotopes remained in the tailings. We admitted, based on the historical concentration ore from the region, that the major part of the tailings resulted from an ore with the average grade of 1 kg U_3O_8/ton being leached with a 90% recovery and a

small part resulted from an ore with an average grade of 0,2 kg/ton which was not submitted to leaching.

Using equations based in these assumptions that include as parameters the isotopes half-lives, and as input the uranium chemical grade, it is possible to quantify the activity that will be generated by the different members of the decay chain. As result one obtains the activity concentration for each radionuclide present in the solid wastes of the uranium tailings or waste piles (Table 1).

Multi-layer cover design

For the case study considered, the former Urgeiriça uranium tailing disposal, the area and the average thickness of the deposit were estimated as 12 hectares and 14 m, respectively. The tailings are characterized by an average radium content of 12 900 Bq/kg, although they also contain much higher values in some spots (50 kBq/kg). The natural radioactive background in this region is 30 Bq/kg.

The radioactive decay of ^{226}Ra produces gaseous ^{222}Rn which decays into a series of short half-life products that are hazardous if inhaled. Tailings also emit gamma radiation which can increase the incidence of cancer and genetic risks.

A cover design and placement will give long term stability and control to acceptable levels of radon emission and gamma radiation, preventing also erosion and water infiltration into the tailings; generally this consists in enclosing the tailings with compacted clay or native soil to prevent the radon release and then covering this layer with rocks and vegetation[1].

Radon migration to the surface is a complex process controlled mainly by porosity and moisture of the crossed media; coverers are efficient in attenuating the radon flux, as the duration of travelling for radon becomes longer and more radon

Table 1. Activity distribution by the radionuclides presents in the solid wastes considering the treatment of a uranium ore with the average grade of 1 kg/ton being leached at 90%.

Nuclide	λ (s^{-1})	Activity (Bq/kg)	Activity (Bq/kg) R=90 %	Mass at Equilibrium (g/t)	Activity (Bq)
^{238}U	4,87 x 10^{-18}	10375	1037,5	84,19	87,35
^{234}Th	3,33 x 10^{-7}	10375	1037,5	1,21 x 10^{-9}	1,26 x 10^{-9}
^{234}Pa	1,01 x 10^{-2}	10375	1037,5	3,98 x 10^{-14}	4,13 x 10^{-14}
^{234}U	8,17 x 10^{-14}	10375	1037,5	4,94 x 10^{-3}	5,12 x 10^{-3}
^{230}Th	2,65 x 10^{-13}	10375	10375	1,50 x 10^{-2}	1,55 x 10^{-1}
^{226}Ra	1,36 x 10^{-11}	10375	10375	2,87 x 10^{-4}	2,98 x 10^{-3}
^{222}Rn	2,10 x 10^{-6}	10375	10375	1,82 x 10^{-9}	1,89 x 10^{-8}
^{218}Po	3,79 x 10^{-3}	10375	10375	9,92 x 10^{-13}	1,03 x 10^{-11}
^{214}Pb	4,31 x 10^{-4}	10375	10375	8,55 x 10^{-12}	8,87 x 10^{-11}
^{214}Bi	5,86 x 10^{-4}	10375	10375	6,29 x 10^{-12}	6,52 x 10^{-11}
^{210}Tl	8,75 x 10^{-3}	10375	10375	4,13 x 10^{-13}	4,29 x 10^{-12}
^{214}Po	1,46 x 10^{-4}	10375	10375	2,52 x 10^{-11}	2,61 x 10^{-10}
^{210}Pb	9,98 x 10^{-10}	10375	10375	3,62 x 10^{-6}	3,76 x 10^{-5}
^{210}Bi	1,60 x 10^{-6}	10375	10375	2,25 x 10^{-8}	2,34 x 10^{-8}
^{210}Po	5,73 x 10^{-8}	10375	10375	6,31 x 10^{-8}	6,55 x 10^{-7}

will decay to non-gaseous nuclides, which are trapped by the cover system. Thereby, the efficiency depends on the capacity of the cover material for decreasing the diffusivity of radon in the media.

The basic equations of diffusion across a porous medium were used for estimating the theoretical values of the ^{222}Rn flux from the ^{226}Ra content in the waste material. The algorithm developed incorporates the radon attenuation originated by an arbitrary cover system placed over the radioactive waste disposal. As an alternative, it can be estimated the thickness of the cover that allows a radon flux inferior to the acceptable one.

An engineered cover design of 5,15 m average thickness composed by sand, clay and gravel was proposed on the basis of the rehabilitation plan for the site (Pereira et al. 2004). A simulation was done with this cover design to estimate the resulting radon flux attenuation and the corresponding concentration at 1 m above the soil, as the measured data refers to this height.

First, it was necessary to estimate the flux and the concentration considering a non-existing cover system. The values obtained in these conditions were 7,19 $Bq.m^{-2}.s^{-1}$ for the radon flux and 547,4 Bq/m^3 for the concentration (Dinis 2007). The average value measured in the Urgeiriça tailings pile for the radon concentration was 557 Bq/m^3. This corresponds to a dose of 5,2 mSv/year, resulting from the exposure to radon in outdoor air, assuming that the receptor spends 1760 h outdoor in a year (a 20 % outdoor residence time), with an equilibrium factor between ^{222}Rn and its decay products of 0,6 and for a dose conversion factor of 9 $nSv.h^{-1}$ per $Bq.m^{-3}$ (Grasty and LaMarre 2004).

The radon flux attenuation estimated by the model for the cover design proposed was about 187 $\mu Bq.m^{-2}.s^{-1}$ and the resulting concentration at the average breathing height was about 0,0142 Bq/m^3 (Dinis 2007).

The efficiency of these materials were also tested considering that the tailings will be covered with 0,5 m of clay plus a layer of overburden to achieve a surface flux inferior to the permissible one, which was considered to be 0,74 $Bq.m^{-2}.s^{-1}$. The radon flux attenuation through the clay component cover is 2,63 $Bq.m^{-2}.s^{-1}$ with a concentration of 200,23 Bq/m^3. The value obtained for the second layer is 1,52 m which gives a total cover thickness of 2,02 m. The resulting concentration at the breathing height is 56,34 Bq/m^3 which corresponds to a dose, in the same previous conditions, of 0,53 mSv/year. This dose is inferior to 1 mSv/year, the limit derived from the European guidelines concerning the exposure of the general public to artificial radionuclides (Dinis 2007).

Atmospheric pathway

The air-transport is one of the principal pathways whereby radionuclides released from wastes sites may reach living organisms. Radionuclides may be discharged to the atmosphere through particle suspension and specially by radon emanation. Once airborne, the radionuclides will disperse downwind and deposit on ground surfaces in a pattern dependent on local meteorology, the location of the point releases, the nature of terrain downwind of the release and the physical and chemical

characteristics of the emission. Radon will decay according to its own kinetic parameters.

The objective of this model is to predict the concentration of radionuclides at specific locations surrounding the source. The basic data needed in this model include the release rate of each radionuclide, physical characteristics of the source (release height, area, etc.) and meteorological data (stability class, wind speed, precipitation, etc.).

For the atmospheric pathway a two-dimensional model is used for calculating the radon flux diffusion from the tailings, followed by an estimation of the radon concentration at a defined mixing height from the soil which will be the starting point to the atmospheric dispersion, considered either simultaneously in each wind direction or only in the prevailing wind direction.

For the estimative of the radon concentrations it was used a box model concept which has implicit a mass balance formulation. The contamination source is defined by an emission area, or the sum of several areas, generating a constant emission rate, where the radon is diluted directly in the ambient air-breathing zone above the contaminated source zone. The box volume is defined by its length, width and the mixing height.

As a consequence of a steady state assumption, the concentration is constant in time and the mass flow rate entering into the box is equal to the flow rate leaving the box. Also the concentration is spatially homogeneous based on the assumption of complete mixing inside the compartmental box.

The atmospheric dispersion is modeled by a modified Gaussian plume equation, which estimates the average dispersion of contaminants released from the source; a plume dispersion model accounts for the contaminant transport from the source area at a specific wind-speed to a downwind receptor. The radon concentration dispersion is then simulated from the release point, at the mixing height, for defined distances in different wind directions, with different wind velocities, as well as in the dominant wind direction.

It was considered that the site is composed by four contaminated areas with different radium content. The global area was conceptually defined as a regular octagon as the national meteorological data corresponds to octants. Each octagon sector has a characteristic average wind speed according to its direction (N S E W NW NE SE SW).

The medium point for the global area was defined by the arithmetic average of the medium point for each singular area; the release point source is located in the centre the polygon area. The air breathing or mixing height was defined as 1,7 m.

The ^{222}Rn concentration was calculated in each sector at this height without cover system. The average value obtained was 5,96 $Bq.m^{-2}.s^{-1}$ (for a radium content in the tailings of 10375 Bq/kg) and the average concentration for the compartmental box was estimated in 73,2 Bq/m^3. The prevalent wind direction is to NE and the resulting concentration in this direction is 658 Bq/m^3 at the vicinity of the site (Fig. 1).

Dispersion in the dominant wind direction is the situation that better fits reality according to the comparison between the model results and the radon concentration measured in this direction.

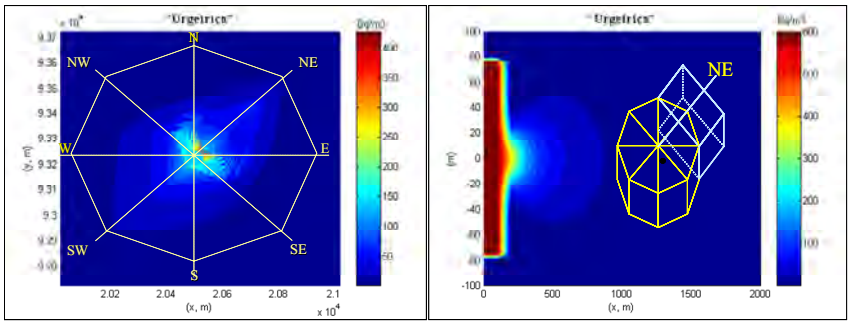

Fig.1. Radon dispersion in each wind direction and in the dominant wind direction (Bq/m^3).

Groundwater

Often groundwater is an important pathway for contaminations found in the subsoil. Contaminants leached from the waste move downwards through the unsaturated zone to the saturated where they are dispersed by advection, hydrodynamic dispersion and diffusion. The contaminants may ultimately discharge to a well or to a surface stream. Humans are exposed to radioactive contaminants by using the water from well or the surface stream and eventually by eating organisms living in the stream.

For the groundwater pathway a two-direction model is proposed for simulating the contaminants release from the tailings pile and its migration process through the soil to the groundwater. The final result is the radionuclide concentration in the groundwater as function of the elapsed time, at a defined distance from the waste pile, where a well is supposed to be located.

The model calculations are broken down into three linked sub-models: i) contaminant leaching from the tailings; ii) vertical movement of the dissolved contaminant downward to the water table through the unsaturated zone and iii) migration of the contaminant in saturated groundwater to the receptor point.

A leaching model based on a sorption-desorption process is used for describing the contaminant release from tailings. The leachate concentration is determined by a partition coefficient (K_d), which describes the relative extent of contaminant transfer to pore water, by soil properties, such as bulk density and moisture, and by the magnitude of the contamination described by the total amount at the source and by the thickness.

The vertical flow transporting the dissolved contaminants is considered to be one-dimensional. It is assumed that there is retardation during the vertical transport which is estimated assuming that the adsorption-desorption process can be represented by a linear isotherm.

Movement and fate of radionuclides in groundwater follow the transport components represented by the basic diffusion/dispersion–advection equation: an ana-

lytical solution was used for the one dimensional transport of a reactive substance with simultaneous retardation and radioactive decay.

The radionuclides initially considered in the simulation model were uranium, thorium, radium, polonium and lead. It was observed that ^{230}Th and ^{210}Pb are not transported to significant distances by the groundwater. This may be explained by the particle-reactive nature of thorium and lead. For polonium the results were in accordance with the expected, based on the assumption that due to the slow rate of contamination migration only the radionuclides with relatively long half-life are of importance in the transport process.

Analytical measures of the uranium and radium activity in groundwater and superficial waters from the Urgeiriça site were used for comparison with the model results. The analytical results show somehow similar values with those obtained in the model. The medium value for total uranium in the well water was about 1,6 Bq/L and for radium was about 0,4 Bq/L. These values are achieved in the model within the first 30 years after the aquifer contamination. These results correspond to an effective dose of 0,082 mSv/Bq for ^{226}Ra and of 0,053 mSv/Bq for ^{238}U, considering an annual ingestion rate of 730 L and an effective dose coefficient of 2,8 x 10^{-4} mSv/Bq and 4,5 x 10^{-5} mSv/Bq for ^{226}Ra and for ^{238}U, respectively.

Considering radionuclides dispersion through groundwater system, it was observed that there are two preferential plume contamination directions, whether uranium or radium is considered. These two directions suggest that SW-NE direction is preferential to radium dispersion and that NW-SE direction is preferential to uranium dispersion (Fig. 2). This allowed us to identify two preferential contamination targets: at south to radium and at north to uranium.

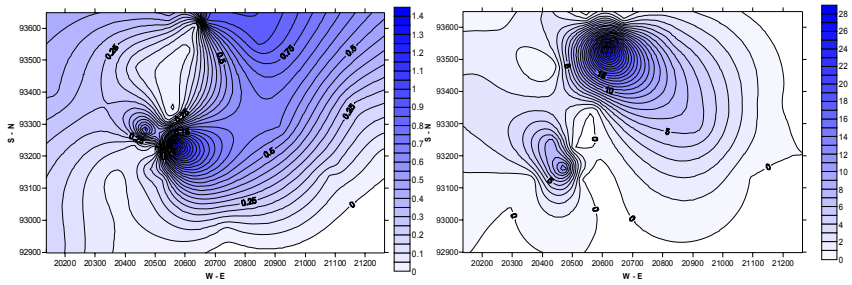

Fig.2. Radium and Uranium contamination dispersion in groundwater (Bq/L).

Surface water transport

Surface water can be an important pathway for contaminants transport from a waste disposal; the surface water bodies include lakes, streams, rivers and runoff processes. Contaminants present on the surface of a waste site may become suspended or dissolved in surface runoff and be transported to adjacent bodies of surface water. Exposure to humans may occur then through drinking and using con-

taminated surface water or by eating organisms living in these water bodies and by external irradiation from radionuclides sediments.

This model describes the radionuclides transport and transfer in superficial waters. The specific case of radionuclides discharge into stream waters was considered for applying this model to the study site.

The radionuclide transport and fate in surface waters are described by the advection-diffusion equation in a three dimension form (IAEA 2001). The generic governing equation was simplified to obtain appropriate solutions, according to the water body to consider, estimating the radionuclide concentration in steady state flow conditions at a defined distance from the discharge point, where is considered to be located the exposure point or the potential receptor.

The liquid effluents from the uranium chemical treatment at Urgeiriça site have been discharged for many years into a stream near the contaminated site, "Ribeira da Pantanha", which is also the main watercourse that drains the mining area. For this reason a simulation was done with the discharge into this watercourse of an effluent contaminated with a radium concentration of 271 Bq/m^3.

Several exposure points were considered along this watercourse strategically defined by the available experimental data. Radium concentration in superficial waters was estimated at these points to determine the relation between the diluted concentrations and the distance to the discharge local. The concentration in the river sediments was also estimated for the same exposure points.

The model results suggest a clear decrease in radium concentration downstream with the distance to the discharge point. Radium concentration in sediments follows the same variation pattern.

Comparing the model results with the measured data for radium concentration in the exposition points it was observed that the highest values both in water and sediments do not correspond to the discharge point considered but at a distance comprised between 1650 and 2750 m distant from the discharge point. The radium concentration continues to decrease with the distance afterwards. This suggested that probably there are other contamination sources besides the discharged effluent as the model considers the contaminated effluent as the only source of contamination.

Transfer to flora

Modeling the radionuclide transfer to vegetation has implicit several simpler processes which describe and quantify mathematically the radionuclides transfer mechanisms, such as uptake, transport, translocation and absorption by leaves. The main goal in this step was to develop a radionuclide transfer model through food chain by the ingestion of contaminated vegetation.

Vegetation may be contaminated through direct deposition, root uptake or irrigation with contaminated water. The material resuspension from superficial soil may occur due to the wind, rain or mechanical factors, with later deposition onto vegetation surface. A model was developed to describe each one of these conta-

mination pathways: root uptake, deposition and resuspension, either from deposition or from irrigation with contaminated water from a well.

The different contamination processes were combined in a global model to simulate the radionuclide transfer resulting from each one of the contamination processes. The final output is the total concentration in the vegetation combining the internal contamination with the external contamination.

The conceptual model is based on the assumption that each one of the transfer processes may have origin either in soil or in the air. In the first case, the processes involved are deposition (characterized by the deposition velocity), interception (described by the interception factor) and retention (described by the weathering half-life). In the second case, the radionuclide behavior in soil and its mobilization reflects the radionuclides physics and chemical properties, soil properties, the type of vegetation and local hydrology and geology characteristics.

The model was applied to ^{238}U, ^{234}Th, ^{234}U, ^{230}Th, ^{226}Ra, ^{222}Rn, ^{214}Pb, ^{210}Pb. It was observed that deposition is the most expressive pathway. The lowest values were obtained for ^{222}Rn which may be explained by its physical state; being an inert gas it can easily disperse into the atmosphere without suffering deposition. The ^{214}Pb is almost inexistent which may be explained by the fact that the weathering decay constant is almost equivalent to the radioactive decay constant; this means that when ^{214}Pb decays to its daughter isotope, it is simultaneously removed.

Some authors (Madruga et al. 2000) studied ^{226}Ra uptake from Urgeiriça uranium tailings. It was observed that plant uptake for total radium concentration in the tailings follows a non-linear function form ($\log C_p = \log a + b \log C_s$), tending however to a linear relationship at higher radium concentration in the tailings (Madruga et al. 2000). This function was used in this sub-model.

Sheppard and Sheppard (1985) proposed a dose-response curve for plant uptake of essential and non-essential elements to explain this radium absorption behavior. These authors reported that plants readily uptake elements essential for plant growth when substrate concentrations are low (deficient), whereas plant uptake of non-essential elements is generally constant at high substrate concentration. On the other hand, at high substrate concentrations, plant uptake of essential and non-essential elements can either be constant (no toxicity) or can decrease leading to toxicity or death (Martinez and Periánez 1998).

Considering this approach to ^{226}Ra absorption it appears that radium behave as an essential element at low substrate concentrations as plant uptake depends on radium concentration in the tailings.

Transfer into the Food-chain

Food chains are biosphere pathways through which humans are exposed to environmental contaminants. They represent the contaminants bioaccumulation in the edible portion of animals and plants that are affected by their release and dispersion from the contaminated site. Food chains consist of one or more trophic levels between the physical environment and human intake of contaminants.

Radionuclides deposition can be a significant pathway to human exposure starting by ingestion of contaminated pasture by animals and then by the ingestion of contaminated animal products (dairy or meat). Plants in general tend to accumulate radionuclides in a scale dependent on many factors and within animals and humans, certain tissues tend to accumulate selected radionuclides. The relevant incorporation of the radionuclides in the milk is usually due to the ingestion of contaminated pasture. This transfer process is often called the *pasture-cow-milk* exposure route.

A dynamic compartmental model was developed to describe the radionuclide behavior in the pasture-cow-milk exposure route and predict the activity concentration in each compartment following an initial radionuclide deposition.

The dynamic model is defined by a system of linear differential equations with constant coefficients based in a mass balance concept. For each compartment a transient mass balance equation defines the relations between the inner transformations and the input and output fluxes. The fluxes between the compartments are estimated with a transfer rate proportional to the amount of the radionuclides in the compartment. The concentration within each compartment is then transcribed to doses using a simplified exposure pathway and a pre-defined critical group.

The first model considered for the transfer through the food chain is relatively simple and classic and considers as initial state a contaminated pasture that is consumed by a cow producing a certain quantity of milk. A more sophisticated model is also described taking into account the spread of the radionuclide within the cow by including the sub-compartments involved: the gastrointestinal system (GIT), the plasma and the bones, in the case of radium simulation. The endpoints are radium concentrations in the soil, pasture, GIT, plasma, bone and milk.

For the exploration of the model several radionuclides were defined as relevant but only for radium and polonium was done a complete model simulation. For uranium, thorium and lead it was only applied the simple model due to either the irrelevance of the results or the lack of data to define the necessary parameters and validate the model. It wasn't possible to obtain data referring to the study site concerning this exposure route. Data from other similar contaminated sites were used.

For radium transfer through this pathway seven sub-compartments were defined: soil, pasture, GIT, plasma, bone surface, bone volume and milk. Concerning to radium absorption, model results (Fig. 3) are coherent with data published referring to radium absorption through this pathway (Leggett and Eckerman 2003; IAEA 2004; Beresford et al. 2004). After ingestion, radium is quickly spread to organs tissues until its maximum absorption, followed by an immediate decrease in blood.

However, the sub-compartment represented by bone tissue doesn't follow this pattern as some organs and tissues, notably bones, have the capacity to concentrate radium from blood and, although some of the radium is excreted over a long time, a portion will remain in the bones throughout the organism's lifetime. This is due to the radium chemical similarity with calcium.

For ^{210}Po it was necessary to define 14 sub-compartments to account all transfers rates and 36 kinetic transfer constants. This implied to define a 14 differential equations system (Dinis and Fiúza 2007). Concerning ^{210}Po transfer through the

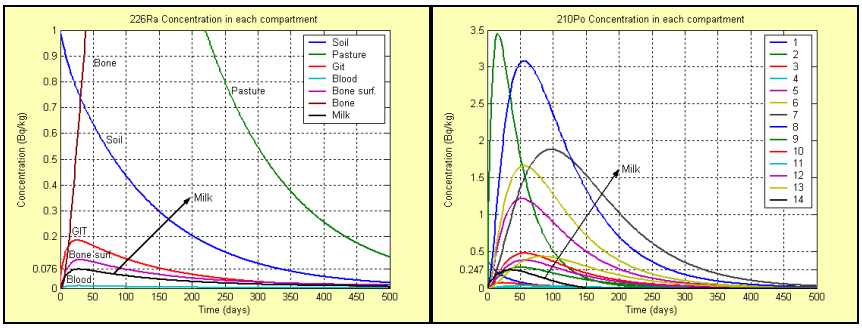

Fig.3. Radium and Polonium concentration in each compartment, complete model (Bq/kg).

food-chain there are no experimental studies documenting ^{210}Po transfer from feed to animal products. The only experimental works documented refer to the direct ^{210}Po introduction into animal body or to animal's products collection from contaminated areas. Nevertheless, simulation results for ^{210}Po (Fig. 3) fit within the range of values given in the literature although many assumptions had to be done due to the limited available data; conservative parameters had to be used in some cases (Leggett and Eckerman 2003; IAEA 2004; Beresford et al. 2004).

Discussion and Conclusions

An integrated global model has been developed for evaluating the external exposure resulting from radionuclide dispersion having as main logical structure a global conceptual model and as secondary tools some particular and restricted quantitative sub-models of transfer and fate. The assessment requires a clear definition of the environmental path and the final fate for each toxic element retained.

For each step involved in the global conceptual model, release and transport by dispersive vectors, phase transfer resulting in retardation and attenuation and environmental exposure of biota, flora, cattle and humans, data were collected and adapted from different sources. The final result is an integrated model for assessment of external exposure originated by low activity radioactive wastes.

The mathematical realization of the sub-models is not uniform: i) some are partially formulated as a set of first order differential equations and partly analytical equations are applied; ii) some sub-models are solved by a set of analytical equations and some of these are analytical solutions of the differential equations. The underlying equations are described in detail for each sub-model in Dinis (2007).

A sensitivity analysis was performed in order to identify the most critical site-specific parameters in each sub-model.

The radon release and transport through the tailings depends on radon diffusion coefficient which greatly varies with material moisture and porosity. These parameters will vary over the year due to the climatic changing. It also depends on radium content in the tailings, which is highly heterogeneous at Urgeiriça tailings,

and on the water retention, which is also a seasonal parameter, with spread values at the Urgeiriça site. The major complexity in radon flux estimative relies precisely on these on-site parameters variability, both in space and in time.

When modeling radon dispersion the obvious limitations are related to the reduction of the source to a point, being implicit a flat terrain (topography is not considered), wind velocity is constant with height and the dispersion is only two-directional. Nevertheless, the errors arising from these assumptions will have a negligible effect for the exposure assessment, because the distance to the exposed receptors is large compared to the stack height, area or facility size.

For the groundwater pathway it is assumed that vertical transport occurs through a partially saturated porous media. The mathematical model that quantifies this transport has implicit the estimative of the retardation factor and flow velocity. The simplified approach used is acceptable as any error introduced at this stage would only affect the radionuclide arrival time and has little effect on concentration in well water for long-lived radionuclides. The exception is for short-lived radionuclides; however these are not a major concern in this pathway as only radionuclides with relatively long half-life are of importance in the transport process due to the slow rate of contamination migration.

Many specific soil parameters can affect the time it takes for a radionuclide to travel to groundwater. In particular, the radionuclide distribution coefficient (K_d) plays an important role in determining the resulting potential exposure because it is a measure of how readily one species sorbs to a surface and sorption retards the overall movement of radionuclides. This is the most critical parameter due to its variability and due to the complexity for determining its value as it is influenced by many factors.

Transfer to flora sub-model is rather complex as it is necessary to understand and transcribe to the conceptual model the interactions between the contaminants and the soil components, vegetation, as well as the interactions between the contaminants themselves.

These processes will be described by the on-site specific parameters: interception factor, translocation factor, transfer soil-plant and K_d values, which will depend mostly on soil properties, plant specie, local hydrology and geology and radionuclides physical and chemical properties.

The parameters independent of the radionuclide characterize environmental and ecological characteristics that vary from site to site and also with the spatial scale considered. These parameters related to vegetation, soil and fauna characteristics, can be directly obtained from on-going site investigation or estimated with simple models. However, the experimental data will always and only represent a limited set of environmental conditions.

Some parameters are specific for each radionuclide and they are responsible for differences in distribution in the compartments, as well as for their retention and elimination from the system. For instance, the quantity absorbed by vegetation generally is estimated by a transfer factor (FT) which defines the ratio between the activity in the vegetation and the activity in the soil. This is one of the parameters presenting a vast lack of data and consequently unreliable intervals of confidence.

Studies documenting radionuclide transfer from crop to animal products are not abundant and most of them do not contain the necessary information as the radionuclide concentration in the animal's diet. The existing studies are the result of acute controlled feeding exposure, direct radionuclide introduction into animals or sample collection from animals feeding near contaminated areas.

References

Beresford N.A., Broadley M.R., Howard B.J., Barnett C.L., White P.J. (2004), Estimating Radionuclide Transfer to Wild Species-Data Requirements and Availability for Terrestrial Ecosystems, Journal of Radiological Protection (24): A89-A103, online: stacks.iop.org/JRP/24/A89.

Dinis M.L. (2007), Phenomenological Models for the Inter-Compartmental Distribution of Radioactive Substances, Doctoral Degree in Environmental Engineering, Porto, FEUP.

Dinis M.L., Fiúza A. (2007), Models for the Transfer of Radionuclides in the Food Chain, in: International Conference on Environmental Radioactivity from Measurements and Assessments to Regulation, Book of Extended Synopses, IAEA-CN-145, pp. 322-323.

Grasty R.L., LaMarre J.R. (2004), The Annual Effective Dose From Natural Sources of Ionising Radiation in Canada, Radiation Protection Dosimetry, Vol. 108, No. 3, pp. 215-226, DOI: 10.1093/rpd/nch022.

IAEA International Atomic Energy Agency (2001), Generic Models for Use in Assessing the Impact of Discharges of Radioactive Substances to the Environment, Safety Reports Series N.º 19, IAEA: Vienna, Austria.

IAEA International Atomic Energy Agency (2004), Biomass – 7, Testing of Environmental Transfer Models Using Data from the Remediation of a Radium Extraction Site, Report of the Remediation Assessment Working Group of Biomass, Theme 2.

Leggett R.W., Eckerman K. F. (2003), Dosimetric Significance of the ICRP's Updated Guidance an Models, 1989-2003, and Implications for U. S. Guidance, Oak Ridge National Laboratory, ORNL/TM-2003/207.

Madruga M.J., Brogueira A., Alberto G., Cardoso F. (2001), ^{226}Ra Bioavailability to Plants at the Urgeiriça Uranium Mill Tailings Site, Journal of Environmental Radioactivity, 54, pp. 175-188.

Martinez-Agguire A., Periánez R. (1998), Soil to Plant Transfer of ^{226}Ra in a Marsh Area: Modelling Application, Journal of Environmental Radioactivity, 39(2), 199-213.

Pereira A.J.S.C., Dias J.M.M., Neves L.J.P.F., Nero J.M.G. (2004), Modeling of the long term efficiency of a rehabilitation plan for a uranium mill tailing deposit (Urgeiriça – Central Portugal), XI International Congress of the International Radiation Protection Association.

Sheppard M., Sheppard S.C. (1985), The plant concentration ratio concept as applied to natural U. Health Phys., 48, 494500.

Modeling the water flow in unsaturated waste rock pile: an important step in the overall closure planning of the first uranium mining site in Brazil

Mariza Franklin[1], Horst Monken Fernandes[2] and Martinus Th. van Genuchten[3]

[1]Institute of Radiation Protection and Dosimetry, Av Salvador Allende S/N – Recreio, Rio de Janeiro, Brazil.
[2] International Atomic Energy Agency, Wagramer Strasse 5, A-1400 Vienna, Austria
[3] U.S. Salinity Laboratory, USDA-ARS, 450 W. Big Springs Road, Riverside, California, USA.

Abstract. Release of acid drainage from mining-waste disposal areas is a problem found in many mine sites all around the world. An understanding of waster flow and the geochemical processes within mining-waste is important to the long-term prediction of contaminant loading to the environment. This is the first of two papers and describes the water flow in one of the waste rock piles of the first uranium-mining site in Brazil by the use of the numerical model HYDRUS-2D. The obtained results indicated that a steady state condition is achieved after 500 days of simulation. The average flow inside the pile was about 0.4 cm/d. The outflow estimated by the model was in good agreement with the measured values. However, it must be emphasized that result only improved when the flux through the macropores was taken into account.

Introduction

The first uranium production center in Brazil began operation in 1982 at Poços de Caldas in the state of Minas Gerais. After 13 years of intermittent operation, the mining activities were suspended definitively in 1995. Uranium was extracted from large open pit mine. In the development of the mine 44.8 x 10^6 m^3 of rock were removed. From this amount, 10 million ton was used as building material (roads, ponds, etc). The rest was disposed into two major rock piles, waste rock pile 4 (WRP4) and 8 (WRP8). The milling process produced approximately

2.39×10^6 m^3 wastes that were disposed into the tailing dam. These areas require large efforts for reclamation of vegetation, soil, and ground and surface water system (Franklin et al. 2007).

The major environmental problem of this mining site is the generation of acid mine drainage (AMD). This phenomenon occurs when the sulphides, mainly pyrite, present in the tailings or waste rocks comes into contact with oxygen and water. It was estimated that acid drainage generation will last for 600 and 200 years from waste rock piles and tailings dam, respectively (Fernandes and Franklin 2001). The acid drainage from these sources has the potential to impact significantly on the quality of groundwater and surface bodies due to the acidic pH values (2-3) and the elevated concentrations of metals and radionuclides.

Numerical modeling techniques can lead to a better quantitative understanding of the physical and geochemical processes leading to the production of AMD in sulphidic wastes. In our study of water flow inside WRP-4, we focus on variably-saturated flow through of the pile as affected by the infiltration of rainfall. This pile was chosen because most of the infiltrating water is collected in a single holding pond. This allows for a better consistency of the calculations of the water flow modeling. Water flow through the pile is very much influenced by the grain size distribution of the waste material, the prevailing water content of the pile, the degree of compaction of the material, the rainfall conditions, and the depth of the water table inside the pile. Because of the very heterogeneous and structured (macroporous) nature of the waste site, the infiltrated water is expected to move predominantly through preferential flow paths. Preferential flow has been found to be more a rule rather than an exception in macroporous soils and fractured rock (Mohanty et al. 1997, Simunek et al. 2003). Most of the waste rock is under unsaturated conditions, with the waste being subjected to intermittent wetting and drying as a function of rainfall, evaporation and drainage. Understanding this complex internal flow system is critical in order to predict the potential for AMD.

The purpose of this paper is to investigate the generation of AMD in a real waste rock pile using comprehensive numerical model - HYDRUS-2D (Simunek et al. 2006) to simulate variably-saturated fluid flow through the highly macroporous or fractured waste pile. This paper is the first of a couple paper, the simulations were used to obtain the understanding of how the water flow (and consequently the generation and evolution of AMD) are affected by the internal structures of the pile. In the second paper will discuss the geochemical processes involved in this system.

Modeling Approach

In a numerical model studies, confidence on the final results will depend, in a first place, on the accuracy with which the model is able to simulate the hydro-physical processes within the pile. In general, these models require an extensive characterization program. A field program was conducted on the top and slope surfaces of the WRP-4. The program was composed by 12 sampling points. Six of them were

fixed in order to form a transect, with 50 meter intervals between each of the sampling points. Three of these points were positioned at the top of the pile (P1, P2 and P3) and the others were located at the slope of the pile (B1, B2 and B3). To increase the consistency of the measurements at the top of the pile, two other points were located 10 m to the right and 10 m to the left of each one of the three points (P1.1, P1.2; P2.1, P2.2; P3.1, P3.2).

Waste Characterization

The methods of construction of the waste rock piles can alter significantly the water flow inside the pile affecting the extent and severity of AMD. End- dumping was the method of construction of the WRP-4. This method induces the formation of stratified piles where the finer particles generally concentrate near the crest, while the coarser particles are found at the base of the pile (Morin et al. 1991, Fala et al. 2005). Construction reports of WRP-4 and field evidence confirm the grain size segregation provoked by the construction methods (IPT 1984, Franklin et al. 2007).

Field measurements using the Guelph permeameter were conducted on the top and slope of the pile aiming the characterization of different hydraulic domains. The saturated hydraulic conductivity (K_{sat}) values measured on the top of the pile varied by one order of magnitude (2.06×10^{-4} – 1.04×10^{-3} cm/s). Measurements of hydraulic conductivity in the toe (sampling point B3) and in the middle (sampling point B2) of the slope of the pile were not possible to be accomplished due to the coarse-grained characteristics of the material. However, saturated hydraulic conductivities greater than 10^{-2} cm/s are very likely at these locations since these are the highest values that can be measured with the Guelph permeameter. Measurements of K_{sat} in the slope of the pile were only possible to be accomplished in sampling point B1 located at a distance of 5 meters from the top (9.05×10^{-4} cm/s). Only a few studies could be found in the literature discussing the variability of the hydraulic conductivity in waste-rock piles. One study reported K_{sat} values ranging from 10^{-2} to 10^{-5} cm/s (Morin et al. 1991). Similar values were obtained for waste rock material from two other mining sites: the South Dump of the Doyon mining site in Canada and the Nordhalde dump of the Ronnenberg mining district in Germany (Lefebvre et al. 2001). Our values of K_{sat} are well within this range.

The saturated hydraulic conductivity was also measured in the laboratory by means of constant-head permeameters. It has been reported that K_{sat} values obtained in the laboratory are often higher than those measured in the field (Vieira and Fernandes 2004). The K_{sat} values measured in samples collected in the top of the pile also varied by one order of magnitude (8.23×10^{-4} – 1.95×10^{-3} cm/s). Samples collected in sampling point B1 presented a K_{sat} value of 3.43×10^{-3} cm/s. The difference between the average values obtained in the field and in the laboratory was approximately 30%, with the laboratory values mostly being higher than the field values.

The soil-water characteristic curves were determined for each sampling point using a large pressure plate apparatus. The results revealed that it was not possible

to clearly differentiate between the different groups of materials inside the pile (Fig. 1). However, the shape of the curves for hillslope points B1 and B2 were quite different from the other curves. The water content at a suction of 6.6kPa showed considerable variation among the various sampling points, thus reflecting the heterogeneous grain size distribution inside of the pile. Coarser materials generally show a more abrupt change in the water content with changes in the pressure head near the inflection point of the retention curve, while fine-textured materials require a larger range of suctions to similarly modify the water content. The data in figure 1 indicate that the average values of the water content at the top of the waste pile are generally about 40% higher than those at hillslope points B1 and B2. This reflects the increase in grain size from the top to bottom and side of the pile (and hence smaller air-entry suctions) due to grain size segregation conditioned by the construction method of the pile.

Conceptual model of the WRP-4

The conceptual model of WRP-4 is based on a 2D vertical Cartesian cross-section of the waste pile, 700 m wide and 20 m high. The selected section was through to best represent the preferential of water inside the pile since the section follows the topographical slope of the valley. The WRP-4 was considered as a heterogeneous unsaturated-saturated system containing waste rock layers showing significant variations in grain size. The probable segregation of material with depth suggests

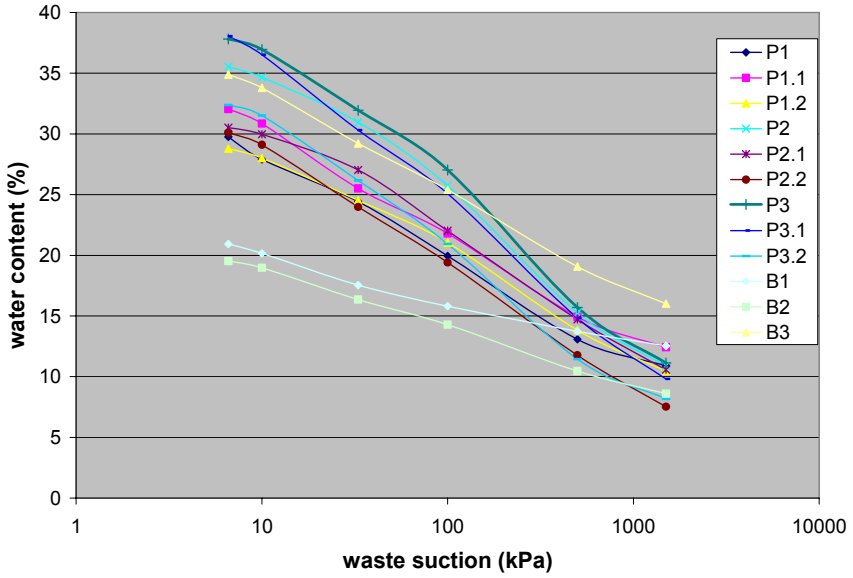

Fig.1. Measured soil water characteristic curves at sampling points.

that the saturated hydraulic conductivity will be higher close to the base of the pile, and that preferential flow is very likely within the system. Preferential flow in especially the high-conductivity bottom layers should provide rapid conduits for water, thereby minimizing rapid changes in the elevation of the water table during relatively wet periods. This conceptual model of WRP-4 was based on qualitative description and data obtained from the characterization and monitoring program conducted by the operator of the mine. The top and the hillslope surfaces of the pile were assumed exposed to precipitation and evaporation. The bottom of the pile was considered impermeable, due to compacted clay layer placed at the bed of the pile, and the water can drain freely from the specific point in the toe of the pile.

We assumed the flow system is at steady state in that a constant rainfall rate is maintained at the surface during the entire simulation. The imposed boundary flux represents the measured average value of the rainfall rate at the site minus the runoff and evaporation rates. The same strategy was used by Linklater et al. (2005), and the predicted concentrations were consistent with observed long term average data (> 3 years). It was also assumed that porosity and permeability are not affected by consolidation of the waste rock, nor by mineral precipitation or dissolution.

In order to observe the effect of internal structure of the pile on flow system, two compositional models for WRP-4 were tested in the simulations. Case 1 assumes that the pile consists of only one type of material, characterized by a representative value of the hydraulic conductivity, while Case 2 assumes that the pile consists of five layers with each layer having its unique grain size distribution and soil hydraulic properties. As well as two hydraulic models (van Genuchten-Mualen model and modified van Genuchten model) were tested to assess the influence of the macropores.

Numerical simulation approach

The discretization of the waste rock pile (WRP-4) domain was made via a triangular finite element mesh, including a total of 17,674 elements and 9,172 nodes.

We assumed that the initial distribution of the pressure head inside the WRP-4 waste pile was known. This condition was obtained by the linear interpolation of the pressure head between 7 m at the lower boundary to -2 m at the surface. This distribution was thought to be realistic for the site and found to also minimize numerical oscillations. Three different boundary conditions were imposed: (1) an impermeable bottom boundary; (2) a constant long-term flux F of 0.0032 m/d along the top and hillslope side of the pile as a result of rainfall, evaporation and runoff; and (3) a seepage face along a small boundary segment at the toe of the pile from which groundwater could exit the waste pile. The environmental data used in the model as representative of the properties of the waste-rock were those obtained by field measurements and by laboratory assays.

Four simulations scenarios were implemented to assess the influence of the macropores in the flow system: S1 for Case 1 (uniform profile) without considering

preferential flow; S2 for Case 1 considering the influence of macropores; S3 for Case 2 (layered profile) without preferential flow; and S4 for Case 2 with the influence of macropores.

The functions of van Genuchten (van Genuchten 1980) based on measured retention data and K_{sat} were used to describe the hydraulic properties for simulations S1 and S3 that do consider macropore flow. The modified model of van Genuchten as proposed by Vogel and Císlerová (1988), which uses composite hydraulic functions, was used to describe the hydraulic properties for scenarios S2 and S4 involving preferential flow.

Numerical simulations were performed for a period of 5 years to obtain a quantitative description of the system's evolution to steady-state, leading to certain spatial distributions of the pressure head, water content and flow velocity.

Results and Discussion

The estimated seepage flow rate from the pile for all simulations was in good agreement with the measured data, having a maximum difference of only 6%. These results demonstrate the ability of the code to accurately simulate the water budget.

A remarkable characteristic of the results (shown in the fig. 2), observed for all simulations, was that after about 500 days the flow process reached steady-state conditions.

The results did not show significant differences between the simulations for the uniform and layered profiles. The fig. 3 shows the comparison of the distribution of the pressure head (m) between scenario S1 (uniform profile) and S3 (layered profile) to illustrate that similarity. However, preferential flow was found to have

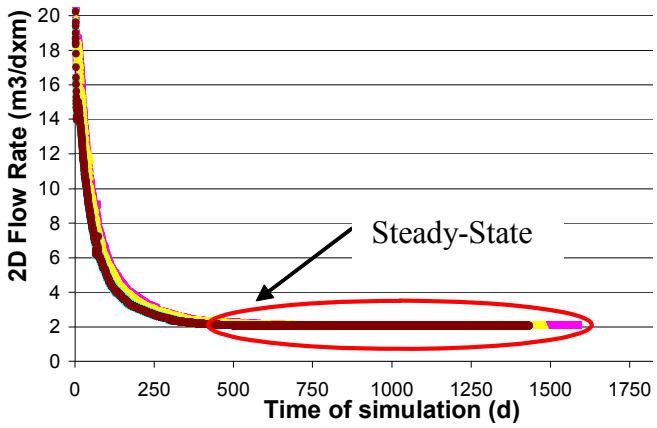

Fig.2. Variation of the 2D flow rate of the WRP-4 with the days of the simulation.

a major effect on the predictions. For this reason we discuss the results in a grouped way.

Simulation S1 and S3 for the homogeneous and layered profiles, but without macropore flow, showed that water infiltrating the pile formed a partially saturated wetting front that slowly travelled downward and then toward the seepage face. After approximately 500 days, the flow process reached a steady-state condition (see figure 2). Despite the fact that the discharge rate along the seepage face agreed well with measured values, the water table inside of the waste pile was far too high, most of the site became saturated (see figure 4a). This suggests that water flow within the pile was not simulated correctly, most likely because the standard van Genuchten hydraulic functions cannot account for preferential flow through the large macropores between the rock fragments.

When we used the modified functions accounting for macroporosity (simulations S2 and S4), the water table inside the pile dropped substantially, leading to an approximately 28-m thick saturated zone when steady-state was reached. This shows that the modified hydraulic functions are far more appropriate for the flow process at the site, even though the estimated water level was still almost three times higher than the measured level inside the pile. This difference may be explained by the fact that an impermeable bottom boundary condition was used in our simulations. Other factors that could have contributed to the difference are uncertainty about the measured water levels and the geometry of the domain (which we smoothed somewhat to improve computational speed). Fig. 4 shows calculated

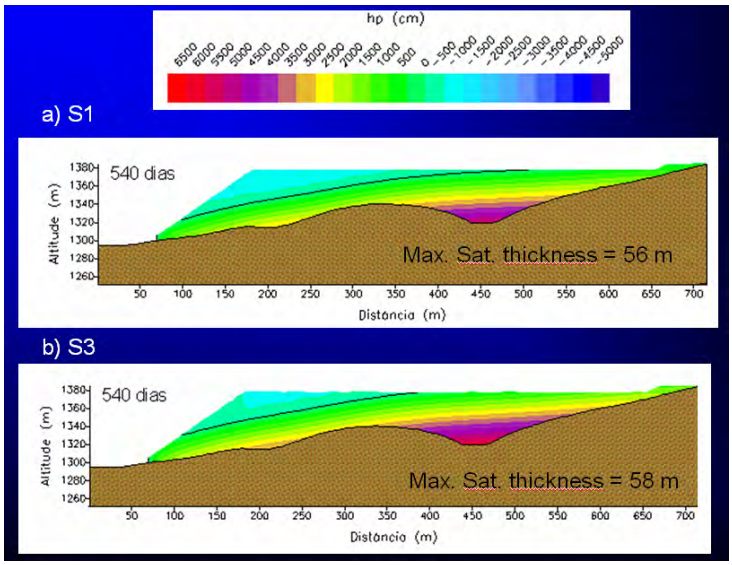

Fig.3. Distribution of the pressure head (m) to scenarios: S1 (uniform profile) without considering preferential flows (a) and S3 (layered profile) without considering the preferential flows (b).

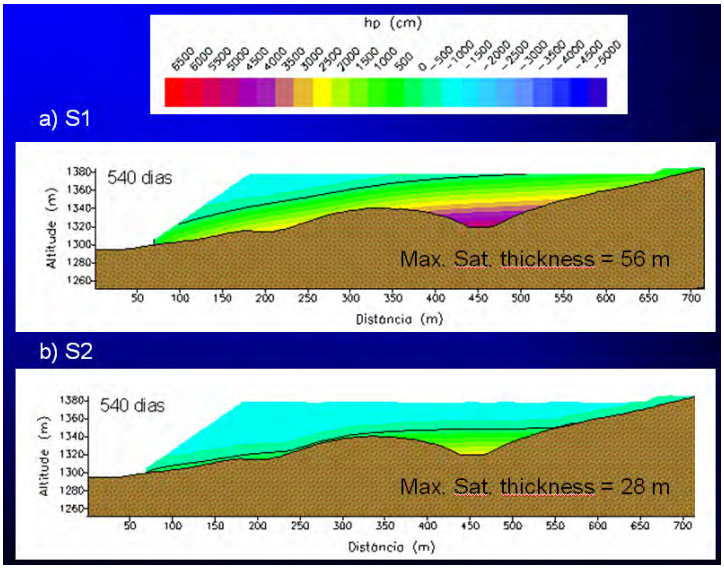

Fig.4. Distribution of the pressure head (m) to scenarios: S1 (uniform profile) without considering preferential flows (a) and S2 (uniform profile) considering the preferential flows (b).

pressure head distributions inside WRP-4 for the S1 and S2 simulations.

The modeled data indicate that the velocity field has huge variations, with values varying from 0.2 to 66 cm/d for the S1 and S3 simulations (no preferential flow) and from 0.3 cm/d to 234 cm/d, for the S2 and S4 simulations (considering preferential flow). However, most of the pile showed very low velocities of about

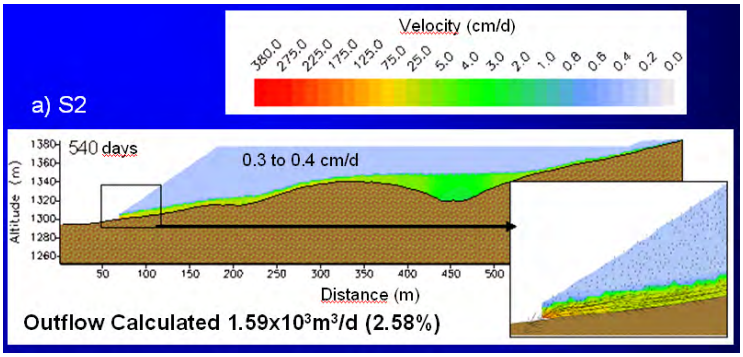

Fig.5. Distribution of the velocity field (cm/d) inside WRP-4 after 540 days of simulation (scenario S2 – Uniform profile - considering the preferential flows).

0.4 cm/d. As expected, the highest velocities were found in the outflow area along the seepage face near the bottom of the pile. A direct comparison between modeled and measured values was not possible because of a lack of field observations. A plot of the calculated velocity field inside WRP-4 for the S2 simulation is shown in fig. 5.

Conclusions

Our results show that the hydraulic regime of the waste site reached steady-state conditions after about 500 days of simulation. The conceptualization of the waste pile as being composed of several layers with different standard porous media hydraulic functions did not lead to realistic simulations of the flow process inside the flow domain. Water flow inside of the pile could be simulated well only after considering preferential flow.

Our strategy to simulate preferential flow using composite retention and hydraulic conductivity functions rather that more sophisticated but parameter-intensive dual-porosity or dual-permeability models (e.g., Simunek et al. 2003) seemed satisfactory for the WRP-4 site. This approach bring a different perspective in the simulation of the hydro-physical processes in heterogeneous waste rock piles.

The overestimation of the saturated zone at the base of the pile may be attributed to the invoked boundary conditions in the simulations. Those data reinforce the need of calibration of the accomplished modeling. The accurate simulation of the water table is important since unsaturated conditions favor the oxidation of pyrite by oxygen that will diffuse into the air-filled pore spaces of the rocks.

The calculations provided considerable insight into the behavior of unsaturated flow systems in WRP-4. All the consequences on AMD generation and evolution are here based on the flow system alone. The simulation of the geochemical processes involved in this system is being explored in another paper of this conference.

References

Instituto de Pesquisas Tecnológicas – IPT (1984) Considerações sobre a evolução do botafora 4. São Paulo: IPT, (Relatório No 50).

Fala, O., Molson, J.W., Aubertin, M., Bussière, B. (2005) Numerical modelling of flow and capillary barrier effects in unsaturated waste rock piles. Mine Water &The Environ., 24, 4, 172-185.

Franklin, M.R., Fernandes, H.M., van Genuchten, M.Th., Vargas Jr.,E.A. (2007) Application of water flow and geochemical models to support the remediation of acid rock drainage from the uranium mining site of Poços de Caldas, Brazil. Proceedings of the 11th International Conference on Environmental Remediation and Radioactive Waste Management - ICEM2007. Bruges, Belgium

Fernandes, H.M., Franklin, M.R. (2001) Assessment of acid rock drainage pollutants release in the uranium mining site of Poços de Caldas – Brazil. J. of Environmental radioactivity, 54, 5 – 25.

Lefebvre R., Hockley D., Smolensky J., Gélinas P. (2001) Multiphase transfer processes in waste rock piles producing acid mine drainage 1 : conceptual model and system characterization. J Contam. Hydrol. 52, 137-164.

Morin, K. A., Gerencher, E., Jones, C. E., Konasewich, D.E. (1991) Critical literature review of acid drainage from waste rock. Prepared for CANMET, Department of Energy, Mines and Research Canada under MEND (NEDEM) Project No. 1.11.1, 175p.

Mohanty, B. P.; Bowman, R. S.; Hendrickx, J. M. H., van Genuchten, M. Th. (1997) New piecewise-continuous hydraulic functions for modeling preferential flow in an intermittent-flood-irrigated field. Water Resources Res., 33, 9, 2049–2063

Simunek, J., Jarvis, N. J., van Genuchten, M. Th., Gärdenäs, A. (2003) Review and comparison of models for describing non-equilibrium and preferential flow and transport in the vadose zone. J. Hydrol. 272, 1-4, 14-35.

Simunek, J., van Genuchten, M. Th., Sejna, M. (2006) The HYDRUS Software Package for Simulating the Two- and Three-Dimensional Movement of Water, Heat, and Multiple Solutes in Variably-Saturated Media Version 1.0. Technical Manual PC Progress, Prague, Czech Republic

van Genuchten, M.T. (1980) A closed-form equation for predicting the hydraulic conductivity of unsaturated soils. Soil. Sci. Soc. J. 44, 892-898.

Vieira, B.C., Fernandes, N.F. (2004) Landslides in Rio de Janeiro: The role played by variations in soil hydraulic conductivity. Hydrological Processes, 18, 4 ,791-805.

Vogel, T., M. Císlerová (1988). On the reliability of unsaturated hydraulic conductivity calculated from the moisture retention curve, Transport in Porous Media, 3,

Developing a 3D data model for geohazard assessment in a former uraniferous mining site

Sorin Mihai[1] and Daniel Scradeanu[2]

[1]National Institute for Metals and Radioactive Resources, Bucharest, Romania
[2]University of Bucharest, Faculty of Geology and Geophysics

Abstract. The study provides new information about the most important risks inside and surroundings area of a former uraniferous mining site (northern part of Avram Iancu mine - Romania). A 3D model was developed for assessing slide, flood, erosion, subsidence, groundwater contamination hazard. This model is usable for geospatial analysis, being able to provide the necessary data about the relationship between various geological, geotechnical, hydrogeological, geophysical, parameters involved in radioactive contamination specific processes and synergy of natural and man-made induced phenomena (landslides, mining subsidence, etc.).

Introduction

This study focus on 3D modelling techniques that brings together geological data from 2D and 3D representations, underground and surface mining architecture, geospatially defined in situ sampling data, environmental and geomorphology data about the mining and surroundings areas.

The most important parts of this methodology that we've pointed by using 3D modeling techniques are: Observation, Integration, Infrastructure and Geospatial analysis. Observation task require measurements of geological, hydrogeological, geophysical, geochemical processes that are at the origin of geohazards. Integration focused on the processing required changing data, measurements especially, into information that can be used by the model.

Infrastructure means the database architecture and techniques used for the storage and dissemination of data while the geospatial techniques provide the visual representation of modelled phenomena in static and dynamic state. The main objective of this 3D model is its application for mitigation geohazard processes, but further on is a support for numerical modeling of various contaminant transports

in groundwater and surface water systems, surface stability due to mining subsidence and numerical analysis of contaminated dumps slope stability and prognosis of erosion processes.

This modelling was performed on easting side of the former Avram Iancu uraniferous mine. The tools used for data achievement, data processing and graphic representation are implemented on a 3D GIS platform.

In addition to the problem of creating a system capable of offering 3D modelling and functionality, there is a further problem concerning the type of 3D model chosen as the basis for 3D GIS. The model contains knowledge about reality, so we have to consider the types of real world objects it must represent. Two kinds of real world objects may be differentiated in terms of prior knowledge about their shapes and location. These objects from the two categories coexist. Traditional GIS models the objects of each category independently with the result that two separate kinds of systems or subsystems have been developed.

The first category, regarded as 'sampling limited', is for objects having discrete properties and readily determined boundaries, such as buildings, roads, bridges, mining works, fault blocks, rivers, aquifers. The second category, known as 'definition limited', is for objects having various properties that can be defined by means of classification, using property ranges. For example, soil strata may be classified by grain-size distribution; moisture content, colloid or pollutant in the water by percentage ranges; carbon monoxide in the air by concentration ranges, and so forth. These objects may be regarded as 'fuzzy spatial objects'.

Site description

The Avram Iancu uranium mine was considered as one of the most important production centers for uranium ore, exploited for a long period of time. The place is situated in the southern part of the Bihor mountains, in a region that is situated between the hydrographic basin of Ariesul Mic and Crisul Negru rivers.

The region is a high mountain area with altitudes between 720m and 1840m, where the geological structure is formed of crystalline slates belonging to the Unit of Biharia. The geological complex is formed of chlorite slates with albite porphyryblasts, quartzy-chlorite-albite slates, chlorite mica-schist, crystalline limestone and magma products metamorphosed with granodiorite intrusions. The hydrothermal activity led to the establishment of some economical areas in the region, some of these being based on the uranium extraction - one at the Avram Iancu mine and another one at the former Baita open pit. The uranium mine was exploited through the horizontal drifts. The risk assessments made in the area revealed as main sources of surface and underground pollution the waste water of the mines and the waste rock piles where the low-radioactive uranium waste rock was deposited. The production center Avram Iancu was closed due to the exhaust of the ore reserves and due to the reorganization of the mining activity at national scale. Starting with 1952, the year when the mine was opened, important quantities of uranium waste rock with low radioactivity were generated and deposited in

different dump-sites, positioned on the valleys of Ariesul Mic, Crisul Negru and Dedes rivers, on terrains with slopes of more than 20^0 (Fig.1). All this waste rock piles (Fig.2) must be ecologically rehabilitated in such a way that the limits of the maximum admissible concentration of the pollutants, established through the national and European legislation are not exceeded.

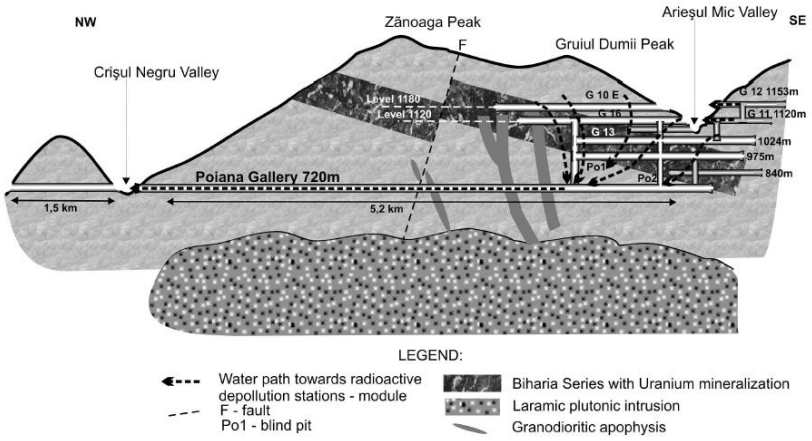

Fig.1. The characteristic cross-section through the mining ore body

Fig.2. Waste dumps along Ariesul Mic river with pregnant erosional phenomena. On the left bank it may be seen the concrete seal of Aries Shaft.

Methodology used for building the 3D model

Building the 3D Avram Iancu model, required succesive phases as specified below:

- Building the digital terrain model (DTM) using 1:2000 scale maps, high precisin GPS measurements especially on waste dumps perimeter (with Trimble GeoExplorer GPS), and satellite maps (Fig.3).
- Overlay on digital terrain model different objects: waste dumps, hydrographic network, adits' and shaft openings, gabion walls, culverts, etc.
- Building the underground mining works network (drafts, shafts) by digitising the horizont maps and georeferenced into the 3D model (Fig. 4).
- Constructing the ore pockets using the drilling data, mining works geological mapping, existing profiles from the realised exploitation. These data were analysed and used by special software for building the ore bodies (Fig.5).
- Building the schematic geological structure (for the preliminary phase) that will include the main tectonic elements (Fig.6).

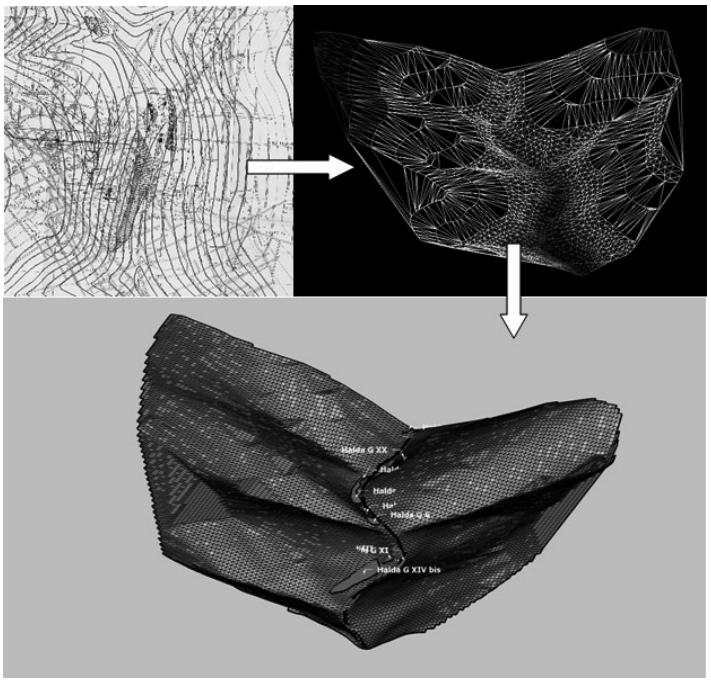

Fig.3. The steps need for building the digital terrain map (DTM).

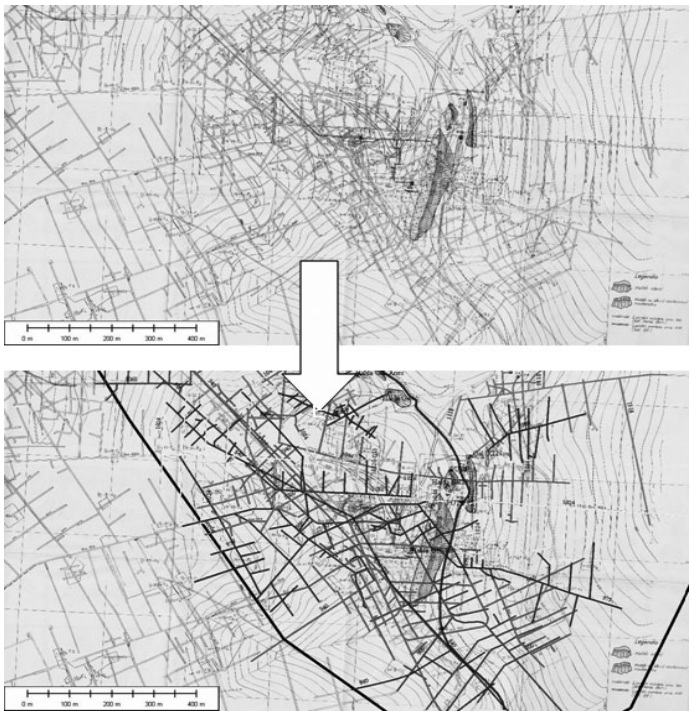

Fig.4. Underground mining works vectorization from ordinary maps.

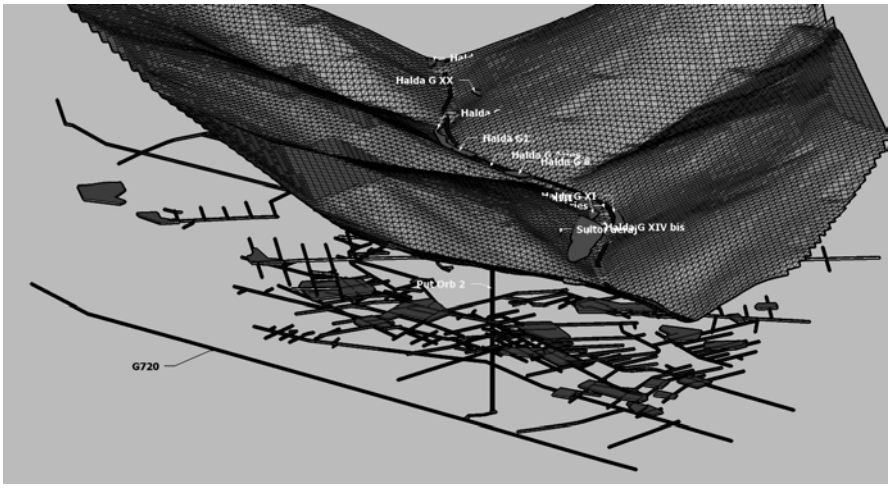

Fig.5. Building the mining works and ore pockets under the model surface.

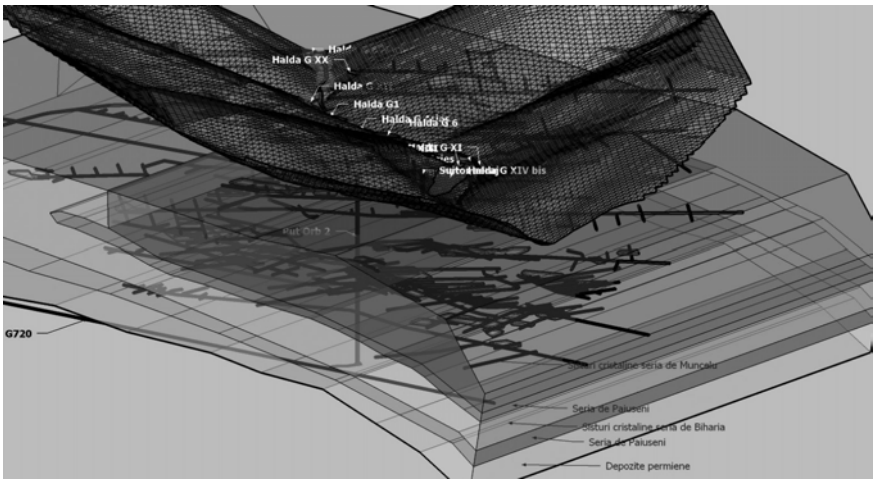

Fig.6. Integration of succesive steps into the final model.

Conclusion

Having designed the integrated data model, unified data structures and introduced methods of construction, demonstrating the 3D spatial model's applicability is the last objective. This will be achieved through various steps of spatial data processing, using both simulated and real data.

The main objective of this 3D model is application for mitigation geohazard processes, but further on is a support for numerical modeling of various contaminant transports in groundwater and surface water systems, surface stability due to mining subsidence and numerical analysis of contaminated dumps slope stability and prognosis of erosion processes.

References

Archibald, N. J., Holden, D., Mason, R. and Green, T., (2000) A 3D Geological Model of the Broken Hill 'Line of Lode' and Regional area: Unpublished report, Pasminco Exploration.

Jill McCoy, Kevin Johnston, (2002) Using ArcGis Spatial Analyst, published by ESRI, USA

Richard H. Groshong, Jr. (2006) 3D Structural Geology – A Practical Guide to Quantitative Surface and Map Interpretation, Springer

Alias Abdul Rahman, Marakot Piloak (2007) Spatial Data Modelling for 3D GIS, Springer

Uranium and heavy metals in Phosphate Fertilizers

Ashraf E. M. Khater[1&2]

[1]National Center for Nuclear Safety and Radiation Control, Atomic Energy Authority, Cairo, Egypt,
[2]Physics Department, College of Sciences, King Saud University, Riyadh, Kingdom of Saudi Arabia

Abstract. Agricultural applications of chemical fertilizers are a world wide practice. The specific activity of uranium-238 and heavy metals (As, Cd, Cu, Pb and Se) in phosphate fertilizers depends on the phosphate ore from which the fertilizer produced and on the chemical processing of the ore. Composite phosphate fertilizers samples where collected and the uranium-238 specific activity, in Bq/kg, and As, Cd, Cu, Pb and Se concentration in ppm were measured. The annual addition of these elements in soil due to soil fertilization were calculated and discussed.

Introduction

Since the 1950s, the application of plant nutrients, including phosphate fertilizers, has increased substantially. More than 30 million metric tons of phosphate fertilizers are annually consumed worldwide, which increase crop production and land reclamation (Lambert et al. 2007). The long-continued application of phosphate fertilizers can redistribute and elevate uranium and toxic heavy metals, such as As, Cd and Pb, in soil profiles and consequently their transfer to the food chain, mainly in acid soils. It can also raise these elements concentrations in irrigation runoff/drainage waters (da Conceicao and Bonotto 2006). This work aims at estimating the concentration of uranium and heavy metals (As,Cd, Cu, Pb and Se) in phosphate fertilizers used in Saudi Arabia and to investigate the possible environmental hazards.

Material and methods

Sampling and sample preparation

Thirteen phosphate fertilizer samples of ten different brands were collected from the local market of Riyadh City. Five of those brands were of granular form, while the other five were leafy (water soluble) phosphate fertilizers. Samples were pulverized and homogenized.

Analytical Techniques

Gamma spectrometric analysis; the dried samples were transferred to polyethylene containers of 100 cm^3 capacity Uranium-238 specific activity was measured using well calibrated gamma spectrometry based on hyper-pure germanium (HpGe) detectors. The HpGe detector had a relative efficiency of 40% and full width at half maximum (FWHM) of 1.95 keV for ^{60}Co gamma energy line at 1332 keV. The gamma line transition 1001 keV was used for ^{238}U specific activity calculation and the spectrometer was calibrated using reference uranium ore sample (IAEA-RG-U).

Inductively Coupled Plasma- Mass Spectrometer (ICP-MS); the concentration of As, Cd, Cu, Pb and Se were measured using ICP-MS after chemical dissolution and dilution. Standard solutions were used for calibration and quality control measures.

Results and discussion

Specific activity of ^{238}U in Bq/kg and concentration of As, Cd, Cu, Pb and Se in ppm in phosphate fertilizers in Saudi Arabia and their statistical summary are given in table 1 and 2 respectively. The granule fertilizers are applied directly to the soil and dissolved slowly in the irrigation water. The leafy fertilizers (powder form) are dissolved in water that is spraying onto plants' leaves. The average activities (range) of ^{238}U was 1017 (173.8-2234) Bq/kg and <20 Bq/kg in granule and leafy phosphate fertilizers, respectively. In the locally produced fertilizer samples, the ^{238}U, average (range) 1791 (1273 – 2234) Bq/kg, are much higher than that in imported fertilizer samples, 242 (174 – 368) Bq/kg, and vice versa for ^{226}Ra, 3.7 (2.7 – 4.9) and 145 (35.0 – 283) Bq/kg, respectively. Moreover, the specific activities of ^{238}U and ^{226}Ra in imported granule fertilizers are comparable with $^{226}Ra/^{238}U$ activity ratios in the range of 0.2-0.8 and in the range 0.6-0.8 after excluding one imported phosphate sample (PH8). Also, their activities are strongly correlated with correlation coefficient (R^2) value of 0.95 (Khater et al. 2008).

Generally, the specific activities of natural ^{238}U series radionuclides in phosphate fertilizers depend on their levels in the used raw phosphate ore material. Radioactivity levels in phosphate ores are varied according to their geological origin (sedimentary, volcanic or biological origin) where ^{238}U and its decay products tend to be elevated in phosphate deposits of sedimentary origin due to the accumulation of dissolved uranium, in the form of uranyl complex, in the sea water during geological formation of the phosphate rocks. A typical concentration of ^{238}U in sedimentary phosphate deposit is 1500 Bq/kg (UNCEAR 1993; Khalifa and El-Arabi 2005). During phosphate fertilizers manufacture the phosphate ore is firstly attacked by sulfuric acid to produce the phosphoric acid (green acid) where uranium will be mainly concentrated in the phosphoric acid while radium, polonium, thorium and other insoluble radionuclides will be precipitated as sulfate salts and concentrated in the phosphogypsum by product. That could explain the high concentration of ^{238}U in locally produced phosphate fertilizers. Mazzilli et al. ,2000, found that 90% of ^{226}Ra and 80 % of ^{232}Th fractionate into phosphogypsum, while ^{238}U is being predominantly incorporated in phosphoric acid. The ^{238}U in phosphoric acid occurs as $[(UO_2)SO_4]$ and $[U(SO_4)_2]$ that as water soluble (Rothbaum et al., 1979). ^{226}Ra is more enriched in phosphogypsum and has a chemical behavior similar to calcium and may occur substituted in $CaSO_4.nH_2O$ or (Ba, Sr) SO_4 (radiobarite). $^{226}Ra/^{238}U$ activity ratios in phosphate fertilizers, table 1, indicate the occurrence of chemical fractionation and their concentrations are deviated from the secular equilibrium conditions. The variations of these ratios depend on the origin of the phosphate ore and/or on the chemical processing of the ore during fertilizers manufacture. The relatively low ^{238}U concentration in imported granule

Table 1. Specific activity of ^{238}U in Bq/kg and concentration of As, Cd, Cu, Pb and Se in ppm in phosphate fertilizers in Saudi Arabia

Type	Sample	U-238±E[&]	As	Cd	Cu	Pb	Se	P_2O_5 %	Ra-226[#]/ U-238
Granule fertilizers	PH 1*	1774±3	7.6	7.6	20	<DL	29.15	46	0.002
	PH 2*	2234±5	-	-	-	-	-	46	0.002
	PH 3*	1884±2	7.5	7.51	22	<DL	28.04	46	0.003
	PH 4*	1273±1	-	-	-	-	-	23	0.002
	PH 5[+]	193±0.34	0.49	0.50	17	0.67	-0.82	17	0.66
	PH 6[+]	233±0.32	0.51	0.50	14	0.66		17	0.59
	PH 7[+]	368±0.42	1.0	1.0	11	1.6	23.92	18	0.77
	PH 8[+]	174±0.23	4	4.1	111	0.63	0.79	17	0.20
Leafy Fertilizers	PH 9	< 20	0.01	0.10	63	0.09	2.21	20	-
	PH 10	< 20	0.21	0.21	9.2	0.11	1.71	44	-
	PH 11	< 20	0.26		29	0.06	3.60	30	-
	PH 12	< 20		0.02	26	<DL	0.14	20	-
	PH 13	< 20	0.04	0.04	<DL	<DL	3.61	52	-

[&] Error * locally produced + imported # Khater et al., 2008

fertilizers could be explained due to the low content in the phosphate ore that used as row material. For the leafy fertilizer samples, the specific activity of U-238 was less than the lower limit of detection, 20 Bq/kg.

By comparing uranium concentration intervals in phosphate fertilizers from different countries, the highest uranium concentration were found, in ascending order, in phosphate fertilizers from USA (221 ppm), Germany (186 ppm), and Saudi Arabia (180 ppm) but the ranges of uranium concentration in these fertilizers are wide, 8.9-221 ppm (116-2470 Bq/kg ^{238}U), 3.2-186 ppm (45-2300 Bq/kg ^{238}U) and 14-180 ppm (174-2234 Bq/kg ^{238}U), respectively (Hamamo et al. 1995; Pfister et al. 1976; Al-Shawi and Dahl 1995; Lal et al. 1985; Barisic et al. 1992; Vucic and Ilic 1989; Yamazaki and Geraldo 2003). Uranium concentration is correlated with the phosphorus percentage (P_2O_5%) in phosphate rock and fertilizers. Since the natural uranium can substitute calcium in the phosphate rock structure due to the similarity in ionic size between U4+ and Ca2+ the correlation between ^{238}U and phosphorus percentages (P_2O_5%) in granule phosphate fertilizers is very strong with correlation coefficients (R^2) of 0.9 (Guzman 1992 from da Conceicao, Bonotto, 2006).

Most fertilizers contain trace amounts of trace elements. Several studies have shown that heavy metals in phosphoric fertilizers can accumulate in soil and become readily available to plants. In term of fertilizer use, As, Cd, Cr, F, Sr, Th, U and Zn are the elements that have a potential risk of accumulation in soil (Sauerbeck 1992 from Modaihsh et al. 2004) McLaughlin et a. (1996) assessed the potential for contamination by phosphate fertilizers and concluded that Cd and F

Table 2. Statistical summary of ^{238}U specific activity in Bq/kg and As, Cd, Cu, Pb and Se concentrations in phosphate fertilizers used in Saudi Arabia.

	Granule			Leafy	All
	Local	Import	All		
U-238	1791 ± 199, 397* (1273-2234), 4	242 ± 44, 88 (174-368),4	1017 ± 308, 870 (174-2234), 8	< 20	1017 ± 308, 870 (174-2234), 8
As	7.6 ± 0.03,0.05 (7.5-7.6), 2	1.5 ± 0.86, 1.71 (0.49-4.1), 4	3.5 ± 1.4, 3.4 (0.49-7.6),6	0.11 ± 0.05, 0.12 (< dl-0.26), 5	2 ± 0.9, 3 (< dl-7.6), 11
Cd	7.5 ± 0.03,0.04 (7.5-7.6), 2	1.5 ± 0.85, 1.7 (0.5-4.1), 4	3.5 ± 1.4, 3.4 (0.5-7.6), 6	0.09 ± 0.04, 0.08 (0.02-0.21), 4	2.2 ± 0.97, 3.1 (0.02-7.6), 10
Cu	20.8± 0.88,1.25 (22-42), 2	38 ± 24, 49 (11-111), 4	32 ± 16, 39 (10.5-111),6	32 ± 11, 23 (9-63), 4	32 ± 10, 32 (9.2-111), 10
Pb	< DL	0.89 ± 0.23, 0.46 (0.63-1.58),4	0.71 ± 0.25, 0.57 (< dl-1.58), 5	0.07 ± 0.02, 0.05 (< dl - 0.11), 4	0.42 ± 0.17, 0.52 (< dl - 1.6), 9
Se	28.6 ± 0.56, 0.79 (28-29),2	12.4 ± 11.6, 16.4 (0.79-24), 2	21 ± 6.7, 13 (0.79-29), 4	2.3 ± 0.65, 2.2 (0.14-3.6), 5	10.3 ± 4.2, 13 (0.14-29), 9
P_2O_5 %	40 (23 - 46)	17 (17-18)	29 (17 - 46)	33 (20 - 52)	30 (17 - 52)

* Mean± Standard error, standard deviation (range), number of samples

would accumulate at faster rates than As,Pb or Hg (Modaihsh et al. 2004). Table 2 shows the average concentrations, it is clear that there are variations in heavy metals concentrations in local produced and imported, and generally in granule and leafy fertilizers. For U, As, Cd and Se, their concentrations in local fertilizer are relatively higher than that in imported and Except for Cu, concentrations of U, As, Cd, Pb and Se in granule fertilizer are relatively much higher than that in leafy fertilizers.

The calculated annual addition of ^{238}U, As, Cd, Cu, Pb and Se due to the phosphate fertilizers application are given in table 3. Generally, if we consider the UK annual allowable limit for Cd and Pb, 0.166 and 33 Kg/ha, and assuming the complete accumulation of both element in soil tope surface, it will need at least 35 up to thousands of year to reach these limits (da Conceicao and Bonotto, 2006).

Conclusions

This study represents preliminary results of ^{238}U, As, Cd, Cu, Pb and Se concentrations in phosphate fertilizers in Saudi Arabia. Uranium concentration is fall in the lower range of uranium concentrations in phosphate fertilizers from different countries. The annual addition of ^{238}U, As, Cd, Cu, Pb and Se and their accumulation in top soil were calculated. To reach the annual allowable limit (for As, Cd, Cu, Pb and Se) it will take tens or thousands of years. These calculations are theoretically correct but practically the situation is different, if we consider the excess

Table 3. The annual addition[#] of ^{238}U, As, Cd, Cu, Pb and Se due to the phosphate fertilizers application.

Type	Sample	U-238		As	Cd	Cu	Pb	Se
		Bq/m^2	Bq/kg	g/ha				
Granule fertilizers	PH 1	106	1419	4.6	4.5	12	-	18
	PH 2	134	1787	-	-	-	-	-
	PH 3	113	1507	4.5	4.5	13	-	17
	PH 4	76	1018	-	-	-	-	-
	PH 5	12	154	0.29	0.30	10	0.40	-
	PH 6	14	186	0.31	0.30	9	0.40	-
	PH 7	22	294	0.60	0.62	6	0.95	14
	PH 8	10	139	2.4	2.4	66	0.38	0.47
Leafy Fertilizers	PH 9	-	-	0.01	0.06	38	0.05	1.3
	PH 10	-	-	0.12	0.12	6	0.07	1.0
	PH 11	-	-	0.16	-	18	0.04	2.2
	PH 12	-	-	-	0.01	15	-	0.08
	PH 13	-	-	0.03	0.02	-	-	2.2

Annual application rate is 600 kg/hectare (10000 m^2)
* locally produced + imported

application of fertilizers and the other environmental pathways of these elements such as water and food-chain.

Acknowledgement

The authors acknowledge the financial support of Saudi Arabian Basic Corporation (SABIC) 2006 fellowship and College of Science/Research Center- King Saud University. Author acknowledges the technical assistant of Mr. M.S. Al Hussin (SASO) during gamma-ray spectrometry and ICP-MS analyses.

References

Al-Shawi A.W., Dahl R. (1995) Determination of thorium and uranium in nitrophosphate fertilizer solution by ion chromatrography. J. Chromatogr. A 706: 175–181.

Barisic D., Lulic S., Miletic P. (1992) Radium and uranium in phosphate fertilizers and their impact on the radioactivityof waters. Water Res. 26 (5): 607–611.

Da Conceicao F. T. and Bonotto D. M. (2006) Radionuclides, heavy metals and fluorine incidence at Tapira phosphate rocks, Brazil, and their industrial (by) products. Environmental Pollution 139: 232-243

Hamamo, H., Landsberger, S. Harbotile G., Panno S. (1995) Studies of radioactivityand heavy metals in phosphate fertlizer. J. Radioanal. Nucl. Chem. 194:331–336.

Khalifa N. A., El-Arabi A.M. (2005) Natural radioactivity in farm soil and phosphate fertilizer and its environmental implications in Qena governorate, Upper Egypt J. Environ. Radioact. 84 (1): 51-64.

Khater A.E.M., AL-Sewaidan H.A. (2008) Radiation exposure due to agricultural uses of phosphate fertilizers. Accepted for publication in Radiation Measurement.

Lal N., Sharma P.K., Sharma Y.P., Nagpaul K.K. (1985) Determination of uranium in fertilizers using fission track method. Fert. Res. 6: 85–89.

Lambert R., Grant C., Sauve C. (2007) Cadmium and zinc in soil solution extracts following the application of phosphate fertilizers. Sci. Total Environ. 378: 293–305.

Modaihsh A.S., Al-Swailem M.S., Mahjoub M.O. (2004) Heavy metals content of commercial inorganic fertilizers used in the Kingdom of Saudi Arabia. Agricultural and Marine Sciences 9(1):21-25.

Pfister H., Philipp G., Pauly H. (1976) Population dose from natural radionuclides in phosphate fertilizers. Radiation and Environmental Biophysics 13 (3): 247-261.

Rothbaum H.P., McGaveston D.A., Wall T., Johnston A.E., Mattingly G.E.G. (1979) Uranium accumulation in soils from long-continued applications of superphosphate. Journal of Soil Science 30 (1):147-153.

UNSCEAR (1993). Ionizing radiation: Sources and biological effects. United Nations Scientific Committee on the Effects of Atomic Radiation Report.

Vucic N., Ilic Z. (1989) Extraction and spectrophotometric determination of uranium in phosphate fertilizers. J. Radioanal. Nucl. Chem. 129: 113–120.

Yamazakia I. M., Geraldo L. P. (2003) Uranium content in phosphate fertilizers commercially produced in Brazil Applied Radiation and Isotopes 59:133–136

Uranium accumulation in sandy soil in an arid region due to agricultural activities

Ashraf E.M. Khater[1&2], A.S. Al-Saif[2] and H.A. AL-Sewaidan[2]

[1]National Center for Nuclear Safety and Radiation Control, Atomic Energy Authority, Cairo, Egypt,
[2]Physics Department, College of Sciences, King Saud University, Riyadh, Kingdom of Saudi Arabia

Abstract. This work aims at studying the accumulation of uranium in sandy soil in an arid region due to the agricultural activities i.e. long time phosphate fertilizer application. Twenty eight soil samples and 14 well water samples were collected from 14 locations. Two soil samples were collected from each location; one from, 20 years ago, cultivated soil and the other from uncultivated soil. Leachable and total uranium concentrations in soil and uranium concentration in water were determined by ICP-MS. Physical (caly, silt and sand percentages) and chemical properties (pH, EC, major actions and major anions) of soil samples, and chemical properties of water samples were estimated. The mean (range) acid leachable and total uranium-238 specific activities in soil samples were 11.1 (7.9-19.7) and 23.9 (21.1-27.3) Bq/kg dry weight respectively. The mean (range) of uranium concentration in water samples were 24.8 (2.9-87.2) Bq/l. The effect of agricultural activities, i.e. long-time phosphate fertilization and changes of soil physical and chemical properties, on uranium concentrations in soil and underground well water were discussed.


Uranium Mining
and Hydrogeology

Uranium in anthropogenic Lakes of the New Central German Lake District

Wolfgang Czegka[1], Frank W Junge[1], Jörg Hausmann[2] and Rainer Wennrich[3]

[1]Sächsische Akademie der Wissenschaften zu Leipzig, Dept Pollutants Dynamics, Karl-Tauchnitz-Straße 1, 04107 Leipzig
[2]Geotechnisches Sachverständigenbüro Dr.-Ing. habil. Bernd Müller, Wiesenring 2, 04159 Leipzig [3]UFZ - Helmholtz Zentrum für Umweltforschung, Department Analytik, Permoserstraße 15, 04303 Leipzig

Abstract. In Central Germany the largest anthropogenic-technogenic lake landscape of Europe will be formed up to year 2050 by flushing of the widely extended former open-cast lignite mines. This new Central German Lake district (Neuseenland) consists of many small and big lakes, which corresponding to its typology should be serve in future for various utilizations (landscape lake, recreation lake, water supply service lake (see Czegka et al. 2008)). Hydrogeology and geochemistry of the drainage basin were characterized by collecting numerous data. This study is focussed on the geochemistry of uranium. The investigated lake waters have low to intermediate Uranium concentrations (from ≤ 2 to 12 µg/L, mean 3.68µg/L). Like in Lower Lusatia there is no definite correlation between pH and U concentration (Bozau & Stärk 2005). The study also contains data from Lake Zwenkau in a early stage of flooding – here the uranium content varies from 30 –87 µg/L. A comparison with local background data (Müller et al. 2002; Czegka et al. 2005) is given.

Intro

Central Germany, the region around Leipzig – Halle is divided on three states (Saxony, Saxony-Anhalt and Thuringia). This region was in the pre-mining structural state characterized on the one hand by medium-sized and small rivers in distinctive, partly wooded meadow landscapes, and on other hand by a relative lack of standing water bodies. Starting at about 1900 (more intensively since 1930) a

large-area lignite open-cast mining altered the landscape and water regime more intensively. With the loss of importance of the brown coal industry in the 1990ies the general framework changed basically.

With regard of the shut down of the open-cast mining in the early nineties of the last century the remaining open-pits holes are streamed within a clear manageable time period. The economic reorientation of the region is aimed among others at the development of tourism and leisure and recreation economics in the harmony with the arising lake landscape. In order to merchandize the upcoming lake landscape over the state frontiers the upcoming lake landscape was named Neuseenland or Mitteldeutsches Seenland (english "New Central German lake District" NCGLD). This artificial and commercial name was accepted and established in the geographical thesaurus and in daily use (newspapers, ads etc.).

Our area of interest (AOI), the New Central German Lake District covers the Central German lignite area in sensu strictu also all the mining area west of the Elbe river situated in Saxony, Saxony-Anhalt and Thuringia. In the north the line Osternienburg -- Dessau Gräfenhainichen - (Elblineament) forms the upper limit, in the south the Central German uplands between Zeitz and Altenburg. The investigation area (AOI) is limited in the west by the Mansfeld country and in the east by the push moraine of the Dahlen-Düben heath.

The main subdivision of the AOI is:

- the Weißelsterbecken (so called Südraum Leipzig) --
- so called Nordraum (mainly the Region Delitzsch – Bitterfeld - Gräfenhainichen
- and the Halle - Merseburger area.

The lake landscape was divided in different subregions. For details see Czegka et al. (2008). As there pointed out inside the lake landscape more than 595 larger lakes are stand waters of various genesis exists at the moment (2008). The maximum area of a lake is 21 km², only four seas expanse more than 10 km² , the medium lake size lies at 0.47 km² (47 hectares).

Regional geogenic Uranium background

The NCGLD is incorporated inside the catchment areas of the middle and lower Weisse Elster (mean anual waterflow 25 m^3/s) and the lower Saale (mean annual waterflow m^3/s).

Both Weisse Ester and Saale river are draining the saxo-thuringian industrial region was one of the most badly polluted tributaries in the Elbe river system (Fig. 1). In terms of its uranium content the focus has to be turned to the catchment area of the Weisse Elster, which can be divided into three sections: the mainly geogenic upper course; the upper middle course dominated by the aureole of granite in the western Erzgebirge and the anthropogenically contaminated tributaries coming from the east; and the lower middle course together with the lower course influenced by uranium mining in Ronneburg. The input of uranium in the lower

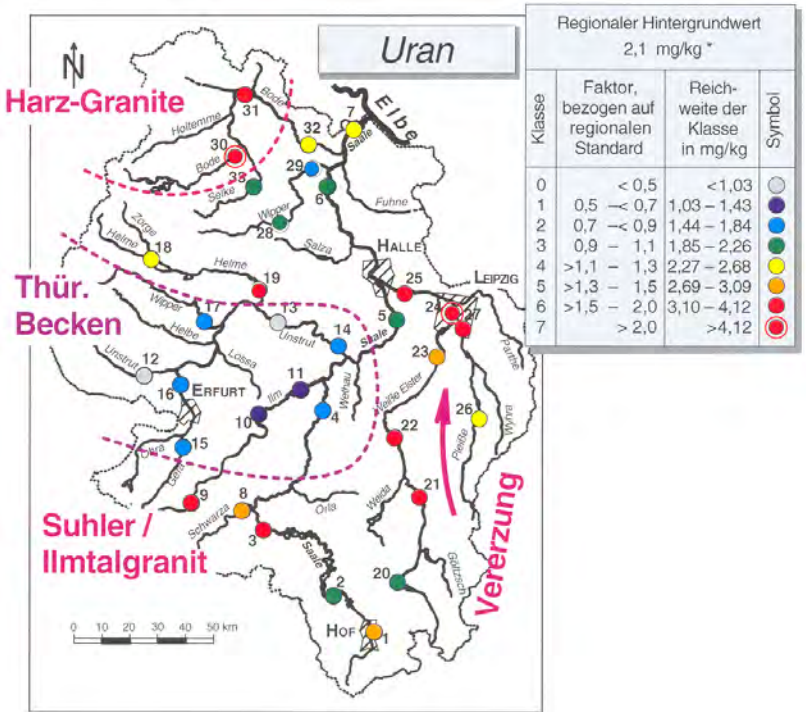

Fig.1. Lokal Uranium background (from Müller et al 2003).

Saale is mainly from her contributaries Weisse Elster, Bode and Wipper (Hercynian plutobic complexes).

According to Müller et al. (2003), the catchment area of the Weisse Elster and the Pleisse can be divided in terms of geogenic background values into eight subregional areas (Table 1). The background values listed in Figure 1 or Table 1 are means calculated from 12–20 samples containing background levels. Uranium's mean geogenic background in the Weisse Elster catchment is 3.3 mg/kg. This is below the generally accepted argillaceous rock standard according to Turekian & Wedepohl (1961) of 3.7 mg/kg, but which is based on the total extract. The background value for uranium in the upper course is far lower at just 2.0 mg/kg. However, it rises to 4.2 mg/kg in the area of Berga downstream of the inflow of tributaries (especially Göltzsch and Trieb) whose courses touch the west Erzgebirge granite complexes (Bergen and Kirchberg granites). In the Gera region the mean background value drops back to 3.6 mg/kg. All other sub-regions – with the exception of the Leipzig district – have values which are around or below the argillaceous rock standard.

The lower Saale region (lower Saale and Wipper-Bode) is affected on a apparent lower level (1.9 – 2.7 mg/kg U).

Table 1. The local geogenic background values of uranium (in mg/kg) in fine-grained river sediment of the Weisse Elster and lower Saale catchment area (after Müller et al. 2003).

River	Sampling area	Geogenic background for uranium	No. of samples	Landscape
Weisse Elster	Pirk-Geilsdorf	2	20	U-Mining
	Eula upstream of Berga	4.2	12	U-Mining
	Ahlendorf between Gera and Zeitz	3.6	16	NCGLD
	Großstorkwitz (near Pegau)	2.9	17	NCGLD
	Cospuden and Leipzig-Süd	4.6	18	NCGLD
	Rassnitz and Zöschen, SE of Halle	3.9	15	NCGLD
Pleisse	Münsa and Kraschwitz	2.5	12	NCGLD
	Markkleeberg-Ost	3.1	14	NCGLD
Mean for the area of the Weisse Elster		3.3	124	
lower Saale	Calbe-Bernburg	2.75	3	NCGLD
Wipper-Bode	Güsten-Stassfurt	1.84- 2.6	3	NCGLD

Materials and methods

The data collection according the hydrochemistry of the anthropogenic formed lakes in the investigation area was made by sampling campaigns which were carried out in the six-month-rhythm (summer, winter) since 2004. From the about 600 waterbodies 160 genotypic lakes came into the choice. The watersampling was carried out in accordance with Selent et al. (1998). The recording of the parameters temperature, conductivity and pH was carried out with mobile instruments (WTW PH 90/96, LF96) in situ.

At selected singulary lakes data like the oxygen saturation with WTW Oxi 96 furthermore as well as chlorophyll a with a BackScat I-Fluorometer Black-Scat 1101.6 LP/eexCHIa/2R / Fa. Haardt Optik/ Microelectronik were sampled.. Opacity was measured both with the Secci disk and with the opacity probe HT (Fa. Lange & Co). The token water samples at were tread in a cascading micro filtration (Whatman GF/C 47 mm / Satorius CA < 45 µm, 10 cm).

Lakes

From the more than 600 lakes of the NCGLD Description lake 14 were sampled for Uranium. Additional three special cases –a long-time observation on lake Kulkwitz, lake Zwenkau which is a lake in statu nascedni and the lake Muldenstausee which is circulated by a major river is given. In contradiction to the Lusatian lakes described in Bozau & Stärk (2005) these lakes are with different pH

Table 2. Uranium content of selected lake waters in NCGLD.

Lake	Major Elements	Cond. [µS/cm]	pH	SAK [1/m]	Th [µg/L]	U [µg/L]
Kahnsdorfer See	Ca-SO_4	2640	3	84	2.3	3.6
Stausee Rötha	Ca-Mg-SO_4-HCO_3	904	7.7			4.8
Markkleeberger See	Ca-SO4-HCO_3	1839	8	5.6		1.1
Störmthaler See	Ca-SO_4	1928	3.4	22.58	0.87	2.9
Cospudener See	Ca-Mg-SO_4	1908	7.4	24.2		0.82
Restl 397 Theisen	Ca-Mg-Na-SO_4	1875	7.8	15.74		1.5
Geiseltalsee	Ca-Na-Mg-SO_4-Cl	1588	8	10.18		1.7
Süßer See	Ca-Mg-Na-SO_4-Cl	1594	8.4	10.7		12
Salziger See	Ca-Mg-Na-SO_4-Cl	11120	7.7	26.8		12
Goitsche	Ca-SO_4-HCO_3	737	7.5	8.32	0.017	0.57
Merseburg-West	Na-Ca-Cl-SO_4	6570	6.7	7.8		0.41
Kulkwitzer See	Ca-SO_4	2050	7.6	1.7		2.8

value, different main element chemism and in a different stage of lake genesis and ripening. Uranium values are listed in table 2.

The average uranium content is 3.68 µg/L the median value 2.25 µg/L. The minimum is at 0.41µg/L the maximum value at 12.00 µg/L. The World Health Organisation (WHO) recommendations for drinking water give a provisional limit of 2.0 µg/L Uranium (Bozau & Stärk 2005).

Lowest Uranium values are found in lake Goitsche and Merseburg West. Both are flooded with river water. Lake Merseburg West are feed by river Saale a non uranium contamined river. Lake Goitsche were flooded during a single flood event from river Mulde on august 2002 within hours. Lake Cospuden was flooded between 1992 and 2000 in major with draining water from active mines- only in minor by groundwater.

On the other hand the maximum value (12µg/L) can be found in the lakes Salziger See and Süsser See, both subrosion lakes affected by the flushing of surface waters from agricultural used areas. Lakes mainly feeded by groundwater shows us values from 1.1 – 3.8 µg/L.

Lake Kulkwitz

Lake Kulkwitz is situated at the western outskirts of the city Leipzig and serves there as a recreation region (public beach). It derived from the two open pit Kulkwitz North and south (closed in 1963). From 1963 till 1983 the pits were filled slowly with ground and precipitation water and formed today lake Kulkwitz. Today lake Kulkwitz is in major feed by groundwater. Lake Kulkwitz is one of the a

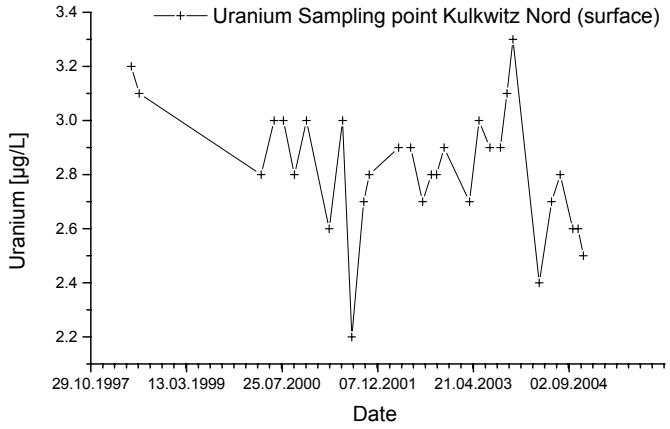

Fig. 2. Time series (1997-2004) of Uranium on surface water lake Kulkwitz North.

long term observation objects of the SAW working group (see e.g. Hausmann 2006). The surface area is about 150 ha the maximal deep at 30m (mean deep 17m) his volume about 27 million m^3. It is a water from the Ca-SO_4 type

In the context of the long term observation from 1997 till 2004 analyses of uranium are available. In figure 2 you can see the development of the U content at the surface at Kulkwitz North from1997 to 2004. It changes from 2.2. to 3.3 µg/L. The mean and median value is 2.8.

Figure 3 shows us a typical deep section at Kulkwitz North . It is accurate to see that the surface is light enriched and from –1 m till the stratum at 27 m the uranium content doesn't change.

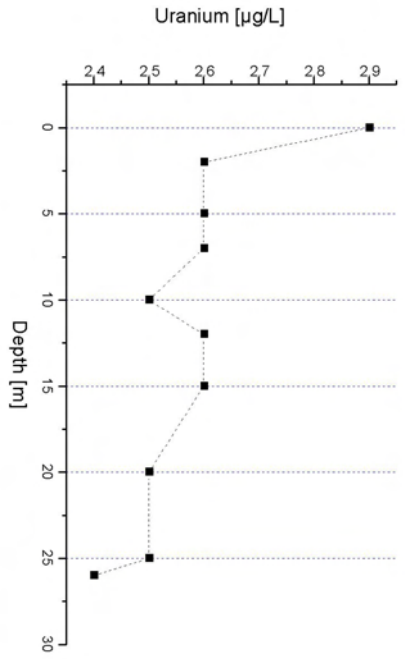

Fig 3. Uranium depth profile on lake Kulkwitz North.

Lake Muldestausee

Lake Muldestausee derived from the former lignite open pit "Tagebau Muldenstein "(1955 - 1975). In 1975 the redirected river Mulde flooded the former open pit which was closed at his lower side with a dam. This redirection allowed the rise of the Goitsche open pit which was before 1975 covered partly by the riverbed of the Mulde (for details see Zerling et al. 1999).

Since 1975 the river flows through lake Muldestausee and makes this lake unique in the NCGLD. The flow is a discrete path inside the lake water body. The surface of lake Muldestausee is 6.05 km^2 and the max deep of 30 m and the volume is about 18 Mio m3.

Samples were taken on three locations at the incoming river and left and right the main stream in the lake water body (fig. 4) . Also here the uranium content on surface of the water body is lightly enriched. According investigations in Junge & Jendryschik 2003 the enrichment factor is 1.12 in epilimnion (data basis time series Sept 1992 based on 60 samples from epilimnion and 33 from hypolimnion).

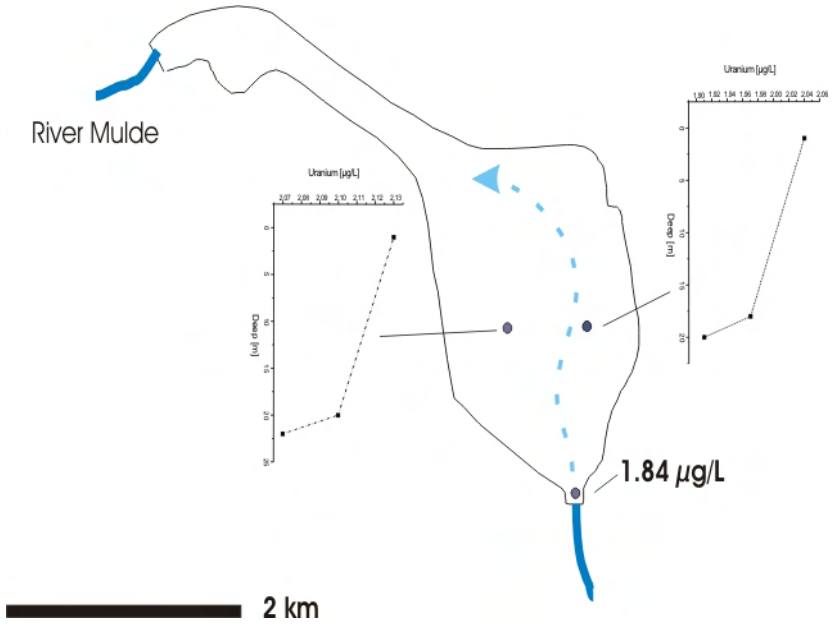

Fig.4. Sample points and depth profile on lake Muldestausee.

Flooding of Lake Zwenkau

The new „Lake Zwenkau“ in the southern outskirts of the city of Leipzig (“Südraum Leipzig”), arises in the hollow form of the former opencast lignite mine Zwenkau (till 1969 named opencast mine [Tagebau] Böhlen I+II) which was started in 1921 and shut down officially on 30-09-1999.

The initial flooding of the future lake started in autumn 2006 with mine draining water from active open cast mines and shall end in 2013 (supporting water will supplied till 2018). With about of 10 km^2 surface the „Lake Zwenkau“ will form the largest standing waters of the new Leipzig Neuseenland (New Leipzig Lake District) and will count under the 50 largest lakes in Germany (Regionalforum Mitteldeutschland 2007, Czegka et al. 2006). The water body of lake Zwenkau has an high potential of acidification caused by parts of the lignite tailings. On reason of the planned integration in the future regional drainage network, the hydrochemical development of Lake Zwenkau is in the special interest.

Geological Background

From regional geological view the open-cast mine Zwenkau lies in the "Weißelsterbecken" more exactly at the Knautnaundorf-plateau only the east end merely extends up to the Weisse Elster flood plain . Here the brown coal leading layers

(Borna layers) are large-arealy extensive bearings of coal leading seams, arose at the southern margin of the Weisselster-Basin. The Borna layers were build at the litoral during the Lower Oligocene (after older nomenclature Middle Oligocene) and topped by sediment overlays (Böhlen layers). Later in the Pleistocene pre- and early glacial river terraces (Eissmann 1994) were accumulated. The last were overlayed by and intercalated with glacial sediments (varved clays, till, glaciofluvial sands) from Elsterian and Saalian times. Weichselian sediments (loess, fluvial gravels) and Holocene river sediments (gravels, alluvial clay) complete the sequence.

During the Holocene the coverage of the recent floodplains started. During the lignite mining the excavated material of the overlying Böhlen and quaternary layers were mixed tilted. The tailings inside the Zwenkau open cast mine consist mainly of an mixture of marine fine grained sands (Grauer Sand and Muschelsand), coarse clay (Brauner Schluff, Bänderschluff, Glaukonitschluff and Muschelschluff), quaternary gravels, sands and silts. The marine sediments are burden with pyrite. Several areas with know strongly differentiated geochemical content on reason of mining methods can be defined (Wiegand 2002).

Hydrogeological and hydrological Situation

The essential ground water aquifers are in the Tertiary and Quaternary. Only 4 of the 5 general ground water aquifers in the southern Leipzig area were exposed in the open-cast mine Zwenkau. The general ground water flow direction went of the southeast to the northwest (Glässer 1995).

For the digging of the lignite in situ, it was necessary to lower the aquifer intensive in a larger area. Because of the result of the dehydration the ground waterlevel was lowered with irreversible results for the area water balance far beyond the limits of the real mining area, what led to a collapse of the hydrochemical and hydrodynamic balance. Currently the hydrochemical and hydrodynamic system is still in change.

Water

Since the end of 2004 from the laugh at the bottom water drainage station the Lake Zwenkau is developing continual. This growing Lake Zwenkau is fed by four potential water sources:

- Ground water
- Precipitation water
- Feeder water from the mining area
- Tailings residual water

As a fifth source – charging water from River Weisse Elster- is in discussion.

Ground water

The pH value of the groundwater are despite of the high chemical charge in the pH range of 5.8 to 6.5 (we can call it low to weak acid). The conductivity range is from 1700 to 2000 µS/cm (Wiegand 2002) . An overview about the chemical content is given in figure 5. We can it classify as a Ca-Mg-SO_4 defined – water.

Precipitation water

The Südraum Leipzig is distinguished by his low precipitation. The mean precipitation is 577 mm/a during the period 1996-2006. Specially in the time during march till September the evaporation is higher than the precipitation, in general we can denote the region as a region of water deficiency. The pH of the rain it self is between 5.6 and 6.8; conductivity lies between 130- 140 µS/cm (Wiegand 2002). As main cation elements Ca and NH4 are dominant in the precipitation water. As mayor anions sulphate and hydrogen carbonate can be named. In general the rain water can be described as sulphatic hydrogencarbonatic earthalkaline water.

Tailings residual water

We can differentiate the tailings area high and low kaolinite content nevertheless pyrite is ubiquitous. In the kaolinite rich regions inside the „V“ shaped tailings rain water is collected and caught. Since dewatering stopped groundwater enforces this process. In rainy month these laughs in the “V” shaped tailings never fell dry. The caught water leaches the sediment and became a high salinary leachate which flows slow but continuous in small streams towards the Lake Zwenkau. Figure. 5 shows the development of conductivity in the tailing lake in “W5” (waterbody 5 [W5]) (Czegka et al. 2007). Conductivity varies between 5800 –4900 µS/cm. The pH is almost stable at 2.5 - 2.8. We can classify this water as an Mg-Ca Fe-SO_4 defined water. Here the uranium content lies from 59 – 37 µg/L and from 2006 till 2007 a discrease can be seen.

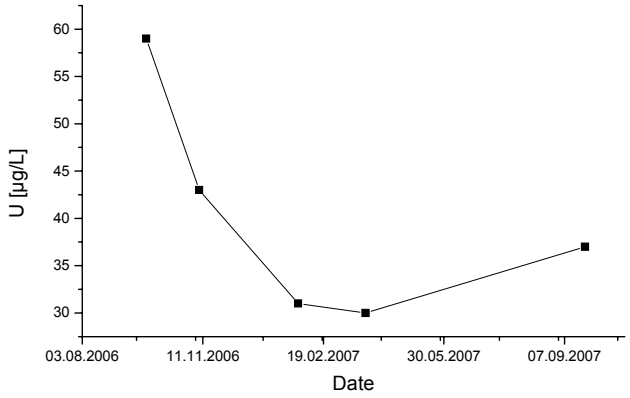

Fig.5. Uranium content in Waterbody 5 (W5) of lake Zwenkau 2006-2007.

Infiltration water

Since end of 2006 about 15–17 qm^3 water from the working lignite mine Profen discharged to lake Zwenkau. These water consists from a mixture of different groundwater. Mean pH is about 7, conductivity ~ 1000µS/cm. Chemistry is dominated by the Ca-Na -SO4-HCO3 water type.

Development of the waterbody Lake Zwenkau

Since middle of 2004 from the draining water laugh around the drainage station on the deepest point of the lignite mining area Zwenkau the development of Lake Zwenkau started. In October 2006 the discharge of infiltration water from the active open pit Profen commenced. Since this time the sea level rises about 1,5 cm a day.. During this 2006- 2008 the conductivity decreased from 9600µS/cm to ~2800 µS/cm. The solved evaporation residue reduced from 4900mg/L to 3500 mg/L . The pH of the salinity water varies between 2.4 and 3.0 – but no general tendency can be seen. It lies with in the Iron buffer system and is driven by the Fe content of the tailings. The chemistry of the lake water is a hard Ca –Mg-SO_4 defined water. As shown in figure 6 the uranium decreased simultanly from 90 µg/l to 30 µg/L. Uranium is highly coupled with the Fe content (regress coefficient 0.994). Other sources of U in the former lignite open pit is lignite which has uranium concentrations from 3-6 mg/kg (Bozau & Stärk 2005) with is slightly higher than the U contents of the upper crust (0.91 mg/kg), the arguillious standard (3.61 mg/kg) or the local regional background (2.69-3.10 mg/kg).

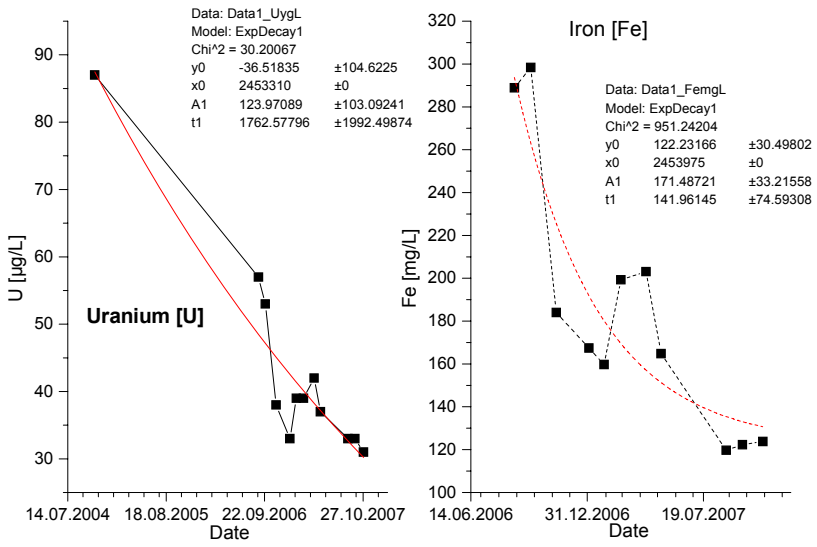

Fig.6. The development of the uranium (in µg/L) and iron (in mg/L) content in lake Zwenkau waterbody from 2004 to 2007.

Conclusions

In Central Germany the largest anthropogenic-technogenic lake landscape of Europe will be formed up to year 2050 by flushing of the widely extended former open-cast lignite mines.

The investigated lake waters have low to intermediate Uranium concentrations (from ≤ 2 to 12 µg/L, mean 3.68µg/L which is above the WHO recommendations for drinkwater). The Uranium content depends from main water supply. Like in Lower Lusatia there is no definite correlation between pH and U concentration (Bozau & Stärk 2005).

The example of the flooding of lake Zwenkau shows that in initially states of flooding the oxidation product of weathering - mainly the sulphate, the still available acid and the high iron concentrations are mobilizing Uranium.

References

Bozau E, Stärk H J (2005) Uranium contents in acidic lakes and groundwater of Lower Lusatia (Germany) in Uranium in the Environment. In: „Uranium in the environment. Mining impacts and consequences“, B.J. Merkel & A. Hasche-Berger (eds.), Springer, Berlin – Heidelberg – New York, 871-875

Czegka W, Hanisch C, Junge, F W, Zerling L, Baborowski M, (2005) Changes in Uranium concentration in the Weisse Elster river as a mirror . In: „Uranium in the environment. Mining impacts and consequences“, B.J. Merkel & A. Hasche-Berger (eds.), Springer, Berlin – Heidelberg – New York, 875-884

Czegka W, Junge F W (2007) Zwenkau: the genesis from a lignite open cast mine to a recreation lake. Hydro- and geochemical impacts. SDGG

Czegka W, Junge F W, Hausmann J, Wennrich R (2008) Hydrochemical und geochemical parameters of new developing lakes of the Neuseenland (New Central German lake district) – an overview – ZDGG: 159: 141-154.

Eissmann L (1994) Grundzüge der Quartärgeologie Mitteldeutschlands. In Eissmann, L. Litt, Th. (1994) Das Quartär Mitteldeutschlands – Altenburger Naturwiss. Forschungen, 7, 55-135.

Glässer W (1995): Das gestörte Grundwasserregime im Südraum Leipzig und deren Veränderungen durch den Braunkohlenbergbau. HTWK Sonderheft, Leipzig, 6-8.

Hausmann J (2006): Der Kulkwitzer See - Referenzobjekt für die Entwicklung anthropogener Standgewässer in der Bergbaufolgelandschaft Mitteldeutschlands.- unveröff. Diplomarbeit, Universität Leipzig: 72 p.

Junge F W, Jendryschik K (2003) Investigations into Distribution of Element Concentrations in a recent Damm and their seasonal and hydrographical Correlation (Bitterfelder Muldestausee, Saxony-Anhalt). Acta hydrochim.hydrobiol. 31 (4-5): 378-390.

Müller A, Zerling L, Hanisch C (2003) Geogene Schwermetallgehalte in Auensedimenten und –böden des Einzugsgebietes der Saale. Ein Beitrag zur ökologischen Bewertung von Schwermetallbelastungen in Gewässersystemen.- Abh. d. Sächs. Akad. d. Wiss. zu Leipzig, Math.-nat. Kl. 59 (6), Leipzig, Weimar, Halle 123p.

Regionalforum Mitteldeutschland [Ed.] (2007) Mitteldeutsche Seenlandschaft Seenkatalog. 1 Aufl. Regionaler Planungsverband Westsachsen.

Selent, K.D., Gruppe, A [Eds.] (1998) Die Probennahme von Wasser - ein Handbuch für die Praxis.- Oldenbourg, München

Turekian KK, Wedepohl K H (1961) Distribution of the elements in some major units of the earth´s crust . Bull Geol.Soc. Am 72: 171-192

Wiegand U (2002) Hydro- und geochemische Prozesse in oberflächennahen Kippensedimenten des Braunkohletagebaues Zwenkau. Diss. Univ. Leipzig, 111 p.

Wimmer, R. (2008): Das Hydrogeologische Idealprofil für den Nordraum von Leipzig. ZDGG 159/2 in print

Zerling, L., Müller, A.; Jendryschik, K.; Hanisch, C, Arnold, A. (2001) Der Bitterfelder Muldestausee als Schadstoffsenke. Abh. d. Sächs. Akad. d. Wiss. zu Leipzig, Math.-nat. Kl. 59 (4), Leipzig, Weimar, Halle 69p.


Uranium Mining
and Hydrogeology

Closure of Underground Mine of Lincang Uranium Mine

Lechang Xu, Xueli Zhang, Jie Gao, Guangzhi Wei and Xin Shang

Beijing Institute of Chemical Engineering and Metallurgy, CNNC. P. O. Box 234, Beiijng City, China, 101149

Abstract. Linchang Uranium Mine is a small mine/mill complex and left 17 adits inclined shaft (V 1850) and 4 open raises after closure. Among them, 5 adits and the inclined shaft overflowed water, containing radioactive and non-radioactive constituents, such as, U, 226Ra, Cd, Cr6+, As, Pb, Cu, Mn, SO42- and F-.

All adits and inclined shaft released radon with concentrations of 0.126—14.9Bq/L at the exits.

The adits and inclined shaft with overflowing were flooded by combination of water-proof dam and curtain grouting, and the other adits were sealed by placing rock walls and open raises without overflowing were closed by backfilling.

All adits, inclined shaft and open raises were permanently closed down after backfilled with clay soil or mixed soil outside the water-proof dams and rock walls.

All adits, open raises and the inclined shaft do not release radon and waste water after closing down.

Introduction

Lincang uranium mine is a small mine/mill complex. It began production in 1970 and was closed in 1994. The uranium mine extracted ores of No. Ⅱ, Ⅲ, Ⅴ, Ⅵ, Ⅷ mining area containing pyrite. The mill process adopted filtration leaching of non-crashed ore by H_2SO_4 and MnO_2, and extraction of settled leachate by organic phase. The final product was $(NH_4)_4UO_2(CO_3)_3$.

The uranium mine left 1 tailings pile, 18 mining waste piles, 2 open pits, 39 surface subsidence pits, 4 patios, 17 adits and 1 inclined shaft. The remediation began in 2001 and completed in the end of 2007.

The adits and inclined shaft released radon and water containing radioactive and non-radioactive constituents, resulting in adverse environmental impact. Therefore, it is important to close the all the adits and shaft so as to stop to release radon and water from the adits and shaft.

Study Area

In this region, annual average temperature is 16.8 °C~17.7 °C; average precipitation and evaporation is 1163.9 mm and 1580.9 mm, respectively.

The orebody is hosted by the lower formation containing coal of Neogene sediments of intermont nonmarine Mengtuo Fault Basin NE-SW orientated as base of Lincang granite. The strata are quaternary (Q) and clasolite bed containing coal (N^2), sandstone- conglomerate bed ($N^{1-(2+3)}$) and granite clasolite bed (N^{1-1}) of Neogene sediments from upper to lower.

The hydrogeological type of the mine is medium. Conglomerate containing uranium ores is the main aquifer. There is not any complete aquitard. under and above ore bed. Groundwaters are mainly porous phreatic water and interstrated unconfined water. There is local interstrated confined water and fissure confined water. There is hydraulic relation between surface water and groundwater. Hydraulic connection also exits between different aquifer. Groundwater type is fistly $SO_4^{2-}.HCO_3^{-}$-$(K^{+}+Na^{+})$, $HCO_3^{-}.SO_4^{2-}$ -$(K^{+}+Na^{+})$, secondly, $HCO_3^{-}.SO_4^{2-}$-$(K^{+}+Na^{+}).Ca^{2+}.Mg^{2+}$.

The uranium ores were mined by conventional open pit and underground methods by combination of adit and inclined shaft development (Fig.1).

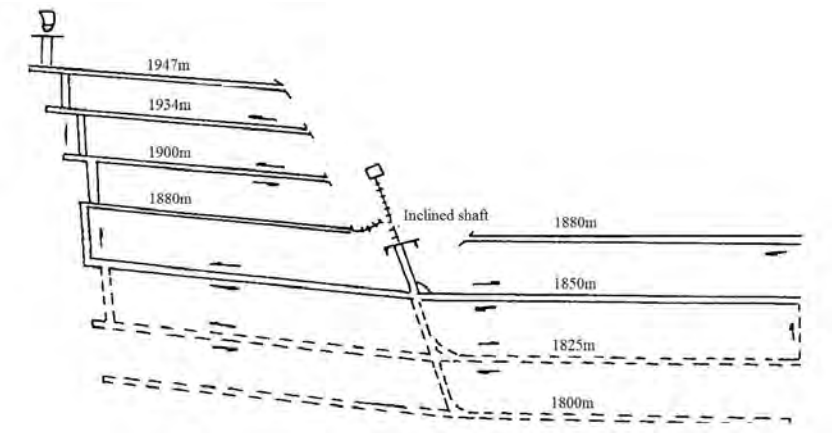

Fig.1. Development of □, □ mining area.

Table 1. Overflowing water chemistry, mg/L (except flow m^3/d, ^{226}Ra Bq/l, and pH)[a]

Location	flow	U	^{226}Ra	Cd	Cr^{+6}	As	Pb	Mn	SO_4^{-2}	F-	pH
II 1925	15.1	31.8	0.782	1.00	5.700	8.478	3.125	2.67	2455	2.90	2.47
V 1850	105	0.39	6.16	0.015	1.667	0.095	0.277	2.76	1381	2.02	4.95
III 1925	52.0	0.01	1.40	0.001	0.733	0.015	0.025	1.11	104	0.57	6.10
III 1942	9.68	0.005	0.035	0.016	0.333	0.094	0.025	0.42	20.2	0.24	5.95
limit		0.05		0.005	0.05	0.05	0.05	0.1	250	1.0	6.5-8.5

[a] U and ^{226}Ra: annual mean; non-radioactive constituents: single monitoring in dry season.

Table 2. ^{222}Rn concentrations of air at the exits of the adits and inclined shaft (Bq/L)

location	□1972	□1950	□1948	□1948	□1925	□1964	□1942	□1934	□1925
^{222}Rn	14.9	1.04	0.126	0.412	3.29	0.212	0.306	1.55	10.7
location	□1925-1	□1925-2	□1947	□1934	□1942	□1900	□1800	□1850	□1880
^{222}Rn	4.77	1.34	2.90	0.325	3.24	0.825	1.68	0.150.	—

Environmental Issues of the Adits and Inclined Shaft

Linchang mine left 17 adits and 1 inclined shaft (V 1850) after closure. Among them, 5 adits and the inclined shaft overflowed water, containing radioactive and non-radioactive constituents, such as, Cd, Cr6+, As, Pb, Cu, Mn and SO42-, exceeding relevant regulatory limits (Table 1). Additionally, the adits and the inclined shaft were releasing radon. Radon concentrations at the exits were 0.126~14.9Bq/L (Table 2).

Closure technologies of adits and inclined shaft

Flooding is the most environmentally friendly, technically safest option to limit contaminated water from the underground mine to overflow. VI 1880, V 1880, V 1990, III 1925, III 1942, II 1925 adits and inclined shaft with overflowing and potential overflowing were flooded by combination of water-proof dam and curtain grouting, and the other adits were sealed by placing rock walls and open raises without overflowing were closed by backfilling (Fig.2 ~Fig.7).

All adits, inclined shaft and open raises were permanently closed down after backfilled with clay soil and mixed soil respectively, outside the water-proof dams and rock walls. Effective radium of grout spreading is 0.4m. Grouting fluid ingredient is water: cement 1:1, accelerator of 0.5% sodium chloride and 0.05% Triethanol Amine and suspension agent of 7% kaoline and 10% PCC (a water-tight

patent material). The 0.2m gap between the two water-proof dams constructed in a flooding adit and some curtain grouting boreholes around the adits wall between the two water-proof dams are used to grout.

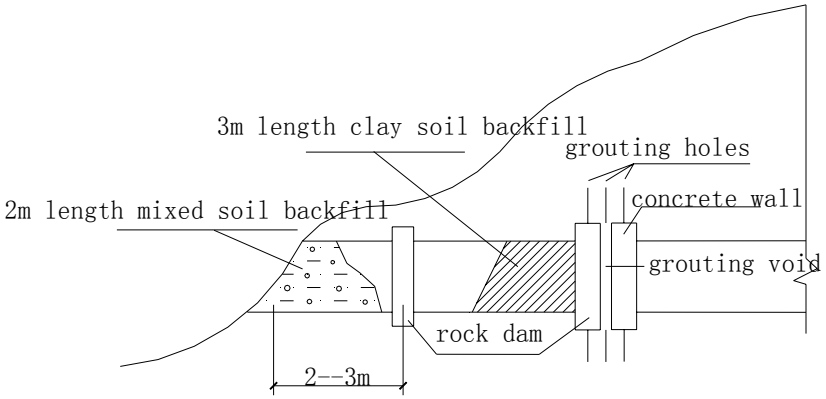

Fig.2. Cross-section of sealing adits and inclined shaft with drainage.

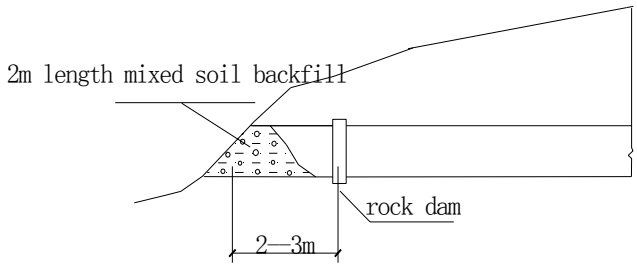

Fig.3. Sealing cross-section of adits and inclined shaft without drainage.

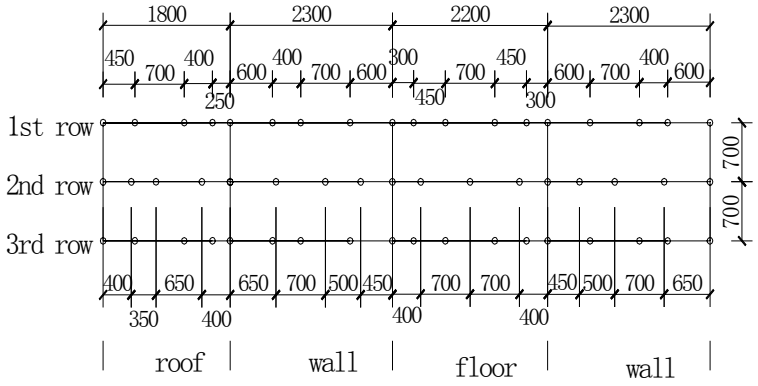

Fig.4. Diagrammatic cross-section of grouting holes for water blocking of inclined shaft.

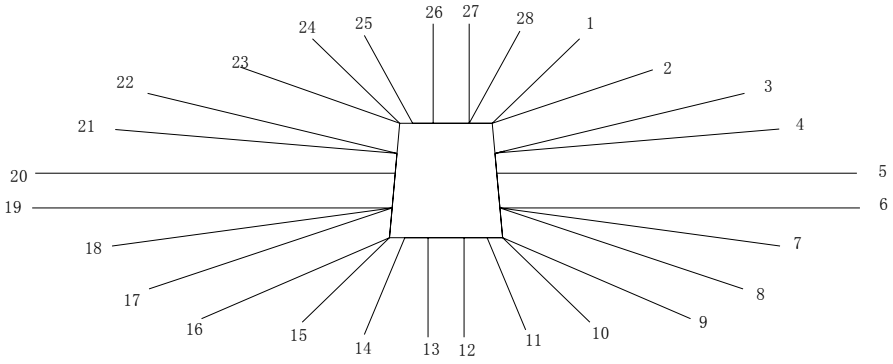

Fig.5. Grouting holes display of 1st and 3rd row for water blocking of inclined shaft.

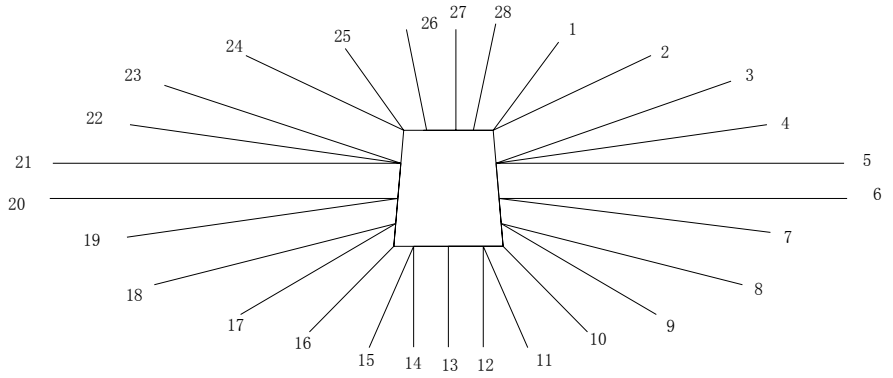

Fig.6. Grouting holes display of 2nd row for water blocking of inclined shaft.

Fig.7. The inclined shaft before and during closure

Conclusions

Linchang Uranium Mine is a small mine/mill complex and left 17 adits, 1 inclined shaft (V 1850) and 4 open raises after closure. Among them, 5 adits and the inclined shaft overflowed water, containing radioactive and non-radioactive constituents, such as, U, ^{226}Ra, Cd, Cr^{6+}, As, Pb, Cu, Mn, SO_4^{2-} and F^-. All adits and inclined shaft released radon with concentrations of 0.126—14.9Bq/L at the exits.

The mine developed shallowly and has mainly porous phreatic water and interstrated unconfined water with less water yield. Therefore, it is the most effective remediation method to plug and seal the underground mine by curtain grouting and /or backfilling. All adits, open raises and the inclined shaft do not release radon and waste water after remediation.

Small scale uranium mine remediation in northern Australia

Peter Waggitt [1] and Michael Fawcett [2]

[1]Am Modena Park 12/8, A-1030, Vienna, Austria
[2]PO Box 781, Howard Springs, NT 0835, Australia

Abstract. During the 1950s and 60s uranium was mined at 13 locations in the South Alligator Valley of Australia's Northern Territory. At the completion of mining sites were simply abandoned and there was no remediation as this was not then a legal requirement.

The paper describes the planning and consultation stages, experiences involving the cleaning up of remnant uranium mill tailings and the successful implementation of the initial remediation works at a number of sites. In conclusion, the paper describes the on-going planning and design processes for the final remediation works, which are due to be completed in 2009.

Introduction

Uranium mining has been more or less continuous in northern Australia's Pine Creek geosyncline since 1949. The location of the area is shown in Figure 1. The first mine was at Rum Jungle, shortly followed by the discovery and exploitation of the South Alligator Valley (SAV) uranium field (Annabel, 1977). An associated mine was at Sleisbeck, about 40km to the southeast of Guratba (Coronation Hill) in the headwaters of the Katherine River. More than 50 radiological anomalies were found in the SAV and between 1955 and 1964, 13 of these were mined for uranium. The mines were all relatively small and infrastructure that developed in parallel with the mines included roads, two major settlements, several smaller camps, a battery and an ore treatment site, and a small mill using solvent extraction technology. The total production from these mines was about 875t U_3O_8. At the end of mining the sites were all simply abandoned, there being no legal requirements for remediation (Waggitt, 2004).

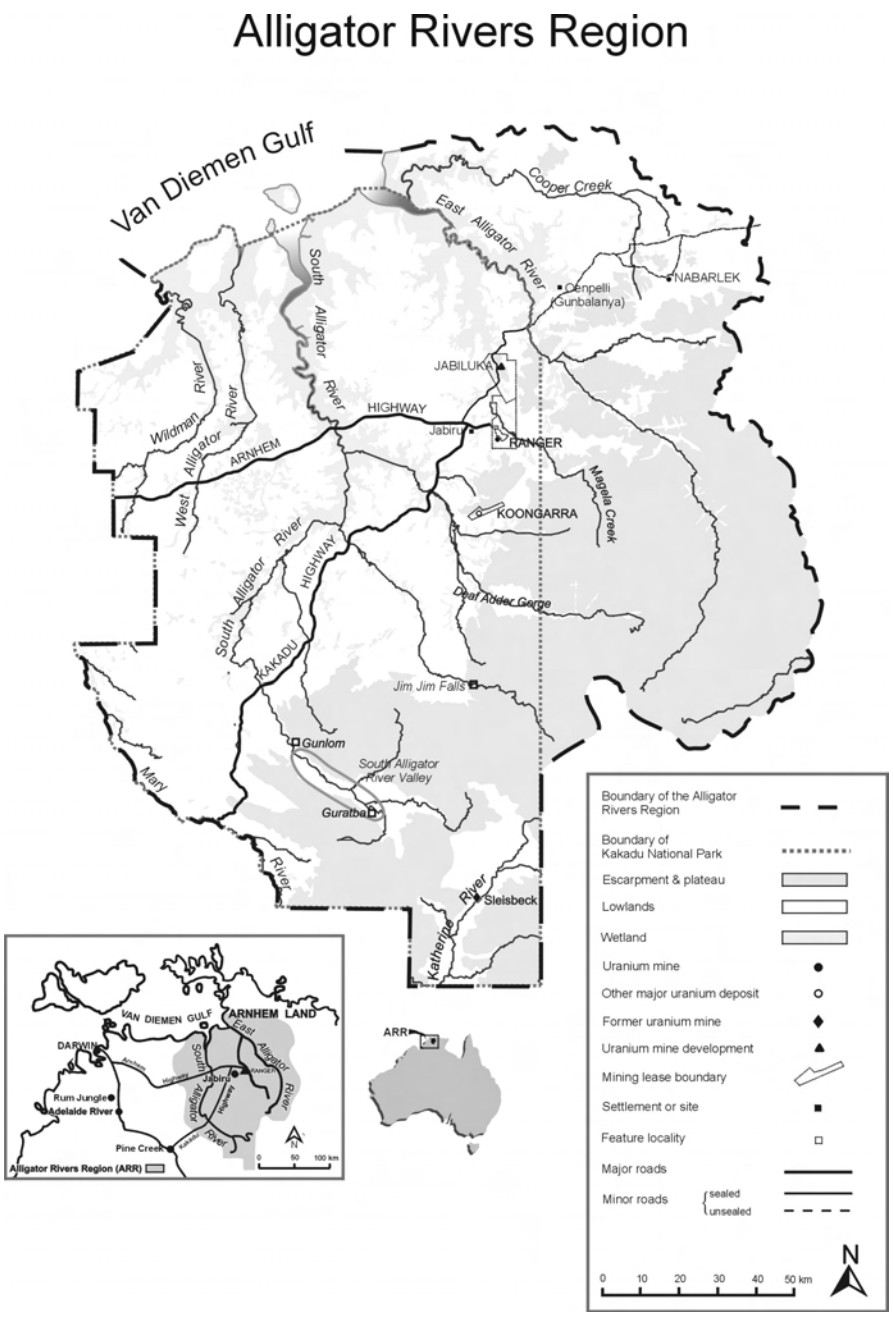

Fig.1. Location map

Stages 1 & 2 of the Kakadu National Park were created in areas to the north of the SAV in 1979. At the same time there was an expressed intention to include the SAV in a later extension as Stage 3 of the Park. Throughout the development of pastoral and mining activity there had been no effective consultation with the Aboriginal Traditional Owners of the land (TO's).

Planning the modern remediation

In the early 1990s a program to reduce radiological and physical hazards was implemented at the 13 mine sites. This involved the sealing of adits and shafts, the dismantling of the mill, cleaning of radioactive ore and tailings residues and burial of all of this material at a number of locations in the valley (Waggitt, 1998). It was planned to be a hazard reduction program and was not intended to be a full remediation program and no plans for full remediation of the sites were made at that time.

In 1996 the Gunlom Land Trust (GLT) was successful in its land claim over the former Gimbat pastoral lease. The GLT is the sub-group of the Aborginal Jawoyn Nation that represents the TO's who are the specific custodians for the lands within which the project is located. This group numbers less than 70 persons. Once the land claim was granted it was agreed that the GLT would lease the area back to Parks Australia for continuing use as part of Kakadu National Park. However, a clause in the lease required that the authorities *"develop and implement a plan of rehabilitation to limit and, where possible, reverse the impact on the environment of all former mining activities"* by the end of 2015.

Throughout the mining period there had been little or no consultation between those exploiting the area and the TOs. Early in this modern planning process consultation began with the establishment of a Consultative Committee. This committee was set up with a majority of TOs and the remainder being representatives of the various State and Federal Government Departments and other authorities involved in the remediation programme.

During the remediation project the members of this consultative committee developed a great deal of mutual trust and respect, with all parties contributing to a process that is transparent and relevant to everyone involved. The TOs consider they are responsible for the management and well being of the land and those people using it, with the association going back over 40,000 years (Press & Lawrence, 1995). Also the TOs have a system of community decision making that is built around consensus rather than the western notion of "democratic majority rule". Thus the time scale for decision making by TOs seems a lot longer than "westerners" might be accustomed to; hence patience and understanding are essential elements in such cross-cultural situations.

In 1997, during the early stages of the planning process it was made clear by the TO's that a number of cultural issues would have to be borne in mind when drawing up the rehabilitation plan. They emphasized that the special cultural significance of the whole area had to be acknowledged when decisions were being

made on how work was to proceed. In particular this meant limiting the use of explosives and heavy machinery to avoid excessive noise that might disturb malevolent spirits located in the area.

After an appraisal process was completed all the sites were divided into two groups: those sites with radiological issues and those without. This enabled the initial remediation planning to go ahead whist radiological standards for site clean-up were developed and negotiated with the relevant authorities. Also it was decided that the site at Sleisbeck would be amongst the earliest to be remediated. As the furthest location it offered the greatest logistical challenge and could also be used as a test and development site for methods of road construction and filling operations to be used elsewhere.

The remediation works

The planning process took several years to complete as each stage had to be approved by all the stakeholders before moving on. Also funding could not be sought until the plan was complete. The planning was held up by the need to undertake additional studies. These included looking at groundwater conditions to determine levels and the extent of hydrocarbon pollution around a former fuel storage area; in addition there were some new radiation surveys (Tims et.al, 2000). Also the discovery of asbestos in many of the buildings and around former camp sites required special studies and the engagement of specialist clearing contractors. Finally in 2005 the Commonwealth Government created a budget for the remediation works and the planning stage was completed. Following a conventional tendering process the first remediation field work began in the dry season of 2007. The sites included in the first season's earthworks plan were Guratba (Coronation Hill) and Sleisbeck.

Sleisbeck

Sleisbeck site is located approximately forty two kilometres east of Guratba (Coronation Hill). The site access road was an un-maintained 4WD track in generally poor condition. There is one crossing of the South Alligator River required between Guratba and Sleisbeck.

The main works undertaken at this site were in three phases:

- Upgrading of the access track between Guratba and Sleisbeck.
- Sleisbeck Pit - backfilling of pit with material from adjacent truck dumps followed by placement of a cover layer of material sourced from nearby costean spoil piles and disused formed roadways.
- Sleisbeck Pit area - backfilling of selected costeans that presented a potential safety hazard to humans and/or fauna.

Sleisbeck access track

Along the track the upgrading works were restricted to grading of the track surface where required, some minor realignments, decreasing approach and departure angles through drainage courses and construction of a new crossing point at a location on the South Alligator River. For cultural reasons track upgrading works were limited to the minimum amount required to achieve safe and efficient access.

Preparation of the access rack for mobilization of the contractor's camp and equipment was a straightforward operation. The minor upgrading of the track reduced the travel time between Guratba and Sleisbeck in a four wheel drive vehicle from approximately two hours to just under one hour.

Sleisbeck pit and surrounding area

The first task to be undertaken was to pump out the pit in preparation for backfilling. The water was no more than 5 metres deep at the deepest point. Previous analysis had shown the water to be non-hazardous and so it was simply pumped to a nearby seasonal swampy area. After pumping there was a layer of sediment/mud across the floor of the pit approximately one metre thick which was left in-situ.

The earthworks contract called for the reclaiming of five areas of waste rock (truck heaps), and the placement of that material in the open pit. Prior to commencing reclaiming the truck heaps it was necessary to clear the majority of the vegetation covering them. The rationale for removing the vegetation was mainly to minimise the amount of organic material likely to be incorporated in the reclaimed truck dump material and placed in the pit backfill; also it was decided to preserve the trees for spreading back over the stripped areas at the end of the job to provide fauna habitats and to assist in the establishment of new vegetation.

Reclaiming of the waste rock from the five truck dumps was completed over a period of approximately seven days, using all-terrain dump trucks (ADT). A Caterpillar D400 Water Truck operated dust suppression throughout the period when the ADT's were hauling. Water for dust suppression was sourced from the Katherine River, approximately three kilometres east of the pit.

Waste rock was placed in the pit in nominal one metre thick layers and was watered and track-rolled before the next layer was placed. Additionally the trucks' routes were varied through the pit to further assist compaction of these layers. No specific compaction specification was required, as the purpose of compaction was simply to maximise storage capacity in the pit.

After taking gamma readings across truck heap #3 the decision was made to leave one section of it undisturbed. This decision was based on the fact that all gamma readings across that area were at background level and additionally the area had a significant cover of mature vegetation. As well as the background gamma readings, this area could be visually distinguished by the colour of the waste material. The colouring of this material was consistent with the near surface clayey-gravels exposed in the pit wall and in surrounding costeans and had probably been mined as un-mineralized overburden.

Table 1. Radiological outcomes at the Sleisbeck site.

Site	Coordinates* - Zone 53L		γ before	γ after
	Easting	Northing	μSv/hr	μSv/hr
Site 1	0264959	8475606	10.0	0.10
Site 2	0265092	8475584	14.0	0.60
Site 3	0264994	8475688	7.0	0.25

* WGS 84 datum

A radiological hot spot had been identified on the northern wall of the pit during earlier field investigation programmes. The contract specified that "*Depending on the final fill level of the pit, it may be necessary to place additional quarry material against the pit high wall in order to cover a section of elevated radiological activity. The section of elevated radiological activity in the pit highwall is to have a cover of a minimum thickness of 1.0 metre vertically and horizontally*." It was not necessary to place additional fill to cover this section, as backfilling the pit raised the surface level of the fill to approximately the topography that would have been present prior to mining.

Previous studies and field undertaken by the Environmental Research Institute of the Supervising Scientist (***eriss)*** had defined three areas of increased radiological activity within the waste rock of the truck dumps. Prior to reclaiming the waste rock, these three sites were located and gamma readings taken with a hand held instrument; additionally their co-ordinates were recorded by GPS to facilitate their location after the waste rock had been reclaimed. Once work was completed the sites were re-visited and the second gamma survey showed that the clearing operation had been successful. The survey results are in Table 1 above.

The inert cover material for placement over the truck heap material was sourced from two locations. The first was spoil piles remaining from when costeans were excavated on the flood plains immediately to the east of Sleisbeck pit. This material was ideal to provide the majority of the cover layer and was spread across the backfilled pit surface in a single layer to a nominal depth of 700 mm, without compaction. The second source was a disused track to the north-east of the pit which provided material for the upper 300 mm layer. The track was built across the floodplain in the 1960s and had been constructed from fill to provide an elevated pavement. This fill had been sourced from a quarry in the next hill east of Sleisbeck pit. This material was selected for use as a rock armouring layer over the pit due to its higher content of more competent erosion-resistant material.

Once all the waste rock had been recovered from the truck heaps the footprint of each area was ripped to a depth of approximately 300 mm in order to break up compaction and provide a moisture retaining seedbed for subsequent revegetation. Once the shallow ripping had been completed, the stockpiled cleared vegetation was spread back across the ripped areas. Revegetation of the site was undertaken in December 2007 using local provenance seed to the greatest extent possible. An inspection undertaken early in 2008 has confirmed that the works have come through the first wet season successfully.

Guratba (Coronation Hill)

Guratba site (formerly known as Coronation Hill) is located approximately 16.5 kilometres east of the Gunlom Road "T" intersection and access to the site is a maintained (narrow) public road requiring one crossing of the South Alligator River between the "T" intersection and Guratba.

Guratba is of great significance to the Gunlom Land Trust traditional owners and as with Sleisbeck there are significant cultural restrictions that had to be taken into account and complied with when planning and undertaking these works..

Guratba site had been left in poor condition as a result of mining and exploration activities that have occurred at the site over the past 50 years, most recently in the late 1980s. These activities were, for the most part, abandoned with minimal or no attempt at rehabilitation. The exploration benches for drill rig access on the eastern side of the hill were visible from a great distance both from the ground and the air. Ongoing (active) erosion had been observed on the hillside due to water collection and concentration on the benches, and there were numerous open (uncapped) exploration drill-holes across the site. No significant radiological or geochemical issues had been identified at this site during the preliminary assessment works. In the early stages of planning for this work a number of possible working methods were explained to the TOs for their consideration and approval.

The overall objective of works at Guratba was to remove the visual impacts of all previous mining and exploration activities. The basic rehabilitation concept was for the site to be "landscaped" with minimal ground disturbance using the smallest sized equipment practicable. This was achieved by returning the material that had been cut to form the benches back to the approximate positions it been excavated from to "smooth" the hillside. In addition all the open drill holes were to be plugged.

As well as the "landscaping", senior TOs had requested that a small stockpile (~200 m^3) of black rock, located near the lower adit at the toe of the hill, be returned to the open cut. This carbonaceous rock (black rock) had been mined from underground workings in the hill and the TOs identified this material as "the essence of Bula" (a malevolent spirit being) and that it must returned to the hill for safety.

Once the work using the selected earth moving option was completed the whole site was re-vegetated to establish a tree and grass cover that would eventually blend in with the surrounding countryside. An inspection undertaken in 2008 at the end of the wet season showed that the earthworks had stood up well with very few erosion concerns and very little maintenance would be required in the dry season.

Future plans

In the dry season of 2008 work will be undertaken on the remaining sites, including the removal of asbestos from some camp site locations. It is hoped that by the

end of 2008 all the remaining sites will be ready for final remediation and the design for containment of radioactive wastes will be approved by the regulatory authorities so that project, including the building of the containment can be completed by the end of 2009. This containment will be used for the disposal of the radioactive materials arising from the hazard reduction programme. The various smaller repositories in the SAV will be excavated and their contents relocated to the new final containment structure. The final steps in the project will be the development and implementation of an agreed stewardship programme, including monitoring and surveillance activities.

Conclusions

The result that is being achieved at both Sleisbeck and Guratba is a combination of science, technology, social awareness and pragmatism. The chosen set of options provide a trade–off between radiological dose, risk, legal compliance and the long term stability of containments on the one hand; and respect for traditional beliefs and values, such as minimizing disturbance to country, protection of sacred sites and ceremonial places, meeting social concerns and observation of tradition on the other. The process by which these outcomes are being achieved has been developed over time and may be unique. However the process, although having many site specific features, does stand as an example of cross-cultural co-operation of which all parties can be justifiably proud.

References

Annabel R I. (1977). The uranium hunters. Rigby, Adelaide

Press, A.J., Lawrence, D., (1995). Kakadu National Park: reconciling competing interests. in Kakadu: natural and cultural heritage and management; eds Press AJ, Lea D, Webb A & Graham A. pub Australian National University, North Australia Research Unit, Darwin

Tims, S., Ryan, B., Waggitt, P., (2000). γ Radiation survey of exposed tailings in the area around Rockhole mine. Internal Report 332. Supervising Scientist for the Alligator Rivers Region, Darwin NT, Australia

Waggitt, P.W., (1998). Hazard reduction works at abandoned uranium mines in the upper South Alligator valley, Northern Territory. In Radiological aspects of the rehabilitation of contaminated sites, Editors, Akber RA & Martin P, Workshop Proceedings, Darwin & Jabiru 20-22 June 1996. pub. South Pacific Environmental Radioactivity Association (SPERA), Christchurch, New Zealand

Waggitt, Peter W. (2004) Uranium mine rehabilitation: The story of the South Alligator Valley Intervention. *Journal of Environmental Radioactivity, Volume 76, Issues 1-2, 2004, Pages 51-66*

The remediation of a uranium mining and milling site in Slovenia

Michael Paul[1], Boris Likar[2], Zmago Logar[2] and Thomas Metschies[1]

[1]Wismut GmbH, Jagdschänkenstr. 29, 09117 Chemnitz, Germany
[2]Rudnik Žirovski Vrh, Todraz 1, 4224 Gorenja Vas, Slovenia

Abstract. Uranium mining in Slovenia was conducted by the state owned company RŽV started relatively late compared to other East European countries. During the short time of the production activities in the Žirovski Vrh Mountains from 1982 to 1990 in total 452 t of U_3O_8 have been produced. Besides an underground mine the company has run a milling and processing plant which produced the yellow cake. Mining and milling resulted in various waste rock and tailings piles situated close to the mine site. After 1990 an extensive remediation program started in spite of the fact that the company had paid considerable attention to protect the environment during the production phase. The total remediation costs are estimated at about 86.3 Mio € with about one third to be spent between 2006 and 2010. The main remediation effort is connected with the closure of the underground mine workings and the stabilisation and covering of the mill tailings pile. The paper outlines the general remediation strategy which is followed for the closure of the mine as well as the stabilization the waste rock and mill tailings piles. Several site specific problems which occurred during remediation and specific remedial solutions implemented are discussed. To show general trends followed in the remediation of uranium mining legacies this still ongoing project is compared to closure projects conducted in other countries.

Introduction

The only uranium mine in former Yugoslavia was located at the Žirovski Vrh Uranium Mine (RUŽV) which is today on the territory of the Republic of Slove-

nia. Uranium mining and milling was conducted in close distance to the town of Skofja Loka about 45 km west from Ljubljana. Uranium mineralization in the ore bearing sandstone formations was discovered in 1960, while exploitation of the deposit started in 1982. A milling and processing facility was constructed in the vicinity of the mine where the production of yellow cake began in 1984. As in other Eastern European countries uranium production ceased without any preparation in 1990. At the Žirovski Vrh uranium mine this was right at the end of the ramp-up phase when the planned production capacity had been reached. As a result the mined uranium ore was just a small part of the prospected reserves of 16,000 t U_3O_8 of the deposit.

In total only 610,000 tons of sandstone ore with an average uranium content of 0.7 kg U/t were processed. About 452 t of yellow cake were produced. During the operation 3.307 Mio t of rock material was excavated: This included 630,000 t of high grade ore, 206,000 t of low grade ore and 2.468 Mio t of mine rock waste.

As at other uranium mining operations in the Eastern European countries no remediation strategy existed with the necessary funds allocated when production was stopped. The former mining company started to prepare remediation plans, technical documentation as well as budget plans for a controlled end of mining activities including the reduction of the environmental impacts in the short and long term. Insufficient funding resulted in a significant delay of the start of physical remediation works as late as 2001. Based on planning documents a governmental decree was stipulated in 2001 fixing the extent of the remediation works and setting a time and budget schedule. The remediation works were scheduled for the years 2001-2005. The total project costs for the remediation within this programme were estimated at about 36 Mio €.

During the time period between 1990 until the start of the works in 2002 the company had been assuring the safety of the mining and milling objects. Within this time (1991-2000) the dismantling of the milling and processing facilities was conducted including the safe removal of the process chemicals on the base of the operating license. In 1994 a landslide occurred at the mill tailings site Boršt. A paleoslide below the base of the pile had been activated resulting in an continuous displacement of up to 1.5 m within a 4 year period. The sliding occurred under the western part of the tailings pile with clearly visible movements on the top of the pile. To stabilise the landslide by reducing the water inflow from the hinterland a dewatering tunnel with drainage wells was constructed in the bedrock below the tailings impoundment between 1994-1996.

General Remediation Strategy

Closure of the underground mine

The underground mine extends 2,000 m in NW-SE and 150 m in NE-SW direction with a depth of up to 180 m. About 60 km of underground mine workings were built mostly with a profile to allow trackless mechanization for production and

transport. The uranium ore was mined by room-and-pillar work from 14 blocks with 200 m width on 4 horizons.

Backfilling of all mine openings was considered not feasible. Therefore mainly partial stabilisation and dewatering measures were conducted. The closure of the underground mine workings was finished in 2006. The closure plans considered

- Removal of contaminated materials from the mine as well as the dismantling of the technological equipment,
- Backfilling of mine workings connected to the soil surface,
- Backfilling of geotechnical unstable parts of the mine,
- Implementation of a mine dewatering system,
- Measures for reduction of long-term contaminant release and
- Demolition of surface mining objects.

The backfilling of open shafts and adits was conducted for geotechnical stabilisation and to avoid unauthorized access to the underground mine workings. In addition geotechnical instable blocks situated close to the soil surface were backfilled with concrete. This was supposed to avoid cracking of the roof leading to ground settlements which would have also influenced groundwater inflow into the mine openings from an upper aquifer.

The deepest mine access was by the adit P-10 at the bottom of the Brebovčica valley. Only a small volume of open mine workings were below this valley level. It was therefore possible to discharge all infiltrating mine waters using this adit. The remediation concept assumes that a flooding of mine workings will not occur. Therefore special attention was focussed on ensuring a long-term stable dewatering regime. Dewatering channels and drainage pipes were constructed to collect and discharge the mine waters to the central mine water outflow via the former adit P-10. The discharge system was constructed with redundant elements at central parts such as the mine water discharge through pipes in the backfilled adit P-10. Collection of sediments by dams are to ensure the long-term function of the system.

The volume of discharged mine water is in the range of 60-100 m^3/h and not expected to rise in the long-term. Uranium concentrations are less than 0.3 mg U_3O_8/L and, as other constituents, well below emission limits. An increase of the concentrations is not expected in the long-term since preferential flow paths were implemented in the mine workings and water flow was diverted from ore containing parts of the mine. Mine workings with higher ore concentrations were backfilled. Additional drainage boreholes were drilled from the mine workings to collect groundwater and thereby to avoid direct contact of the water with the ore body. Closure of mine workings furthermore led to a reduction of air ventilation limiting oxidation processes which might have resulted in an increased mobilisation of contaminants. The discharged mine water is continuously monitored but treatment is not necessary.

Relocation of mine waste rock to a central pile

Close to shafts and adits numerous, mainly temporary mine waste rock piles with small volumes were deposited during active mining. They resulted from the geological exploration, the mine construction and the ore exploitation periods. This mine waste rock with in total 470,000 tons of material was relocated to the central mine waste rock pile Jazbec. The footprint of the mine waste rock piles and the auxiliary mine structures at the surface were remediated and revegetated.

Remediation of the mine waste rock pile Jazbec

Between 1983 and 2003 about 1.716 Mio. t of mine waste rock was deposited at the central pile Jazbec which was built in a narrow valley. In addition about 0.197 Mio t of low grade ore and 48,000 t of red mud from water treatment were dumped on this pile. After remediation of local piles waste rock material was relocated onto the waste rock pile Jazbec. The total area of the waste pile is 6.7 ha.

Parts of the valley bottom the pile was built on are marshy. Therefore at the bottom of the pile a drainage system was constructed which was made up of drainage pipes connected to a culvert in the centre line of the former valley. Later surface water discharges from the hinterland were also diverted into the culvert which is now situated below the pile. The average annual water discharge from the culvert is about 30 m^3/h (see Figs. 1 and 2).

The results of environmental monitoring show that the original drainage system has deteriorated. As a result seepage water from the pile is flowing into the underlying carstic bedrock. The objectives of the remediation consist in a reasonable reduction of the inflow of precipitation water into the pile and a reduction of surface water directed into the culvert at the bottom of the pile.

Remediation of the mine waste rock pile consists of

- Contouring of the mine waste rock pile to a general slope of 1:2,75 (20°) with 3 m wide berms placed in a vertical distance of 12 m,
- Construction of a cover with a total thickness of 1.95 m using autochthonous material from a borrow pit in the vicinity of the pile owned by the mining company RUŽV in combination with provisions for a safe surface water discharge,
- Improvement of the drainage culvert by excluding surface water inflow and long-term stabilisation by backfilling with drainage material.

Construction works at Jazbec started in 2006 and will be finished by the end of 2008.

Fig.1. Mine waste rock pile Jazbec before remediation (October 2005).

Fig.2. Jazbec pile after contouring and cover construction of the eastern slope (2007), at the bottom the outlet of the culvert draining to the Brebovčica creek.

Remediation of the mill tailings pile Borst

During uranium processing 0.61 Mio t of mill tailings were generated and deposited at the tailings pile Boršt. The tailings were trucked to the pile site about 2 km from the mill and dumped on a hillside. The pile area was covered by a sealing layer of clayey material including a drainage system. Two springs at the site were collected and the water was discharge through a pipe at the bottom of the pile.

The tailings pile has an area of 4.2 ha. The tailings were partly dumped on a paleoslide which was activated during the beginning of the 1990ies. About 3/5 of the tailings body is dumped on instable ground. The landslide was stabilised by constructing a drainage tunnel between 1994 and 1996. An interim cover made of material from the tunnel construction was placed on the tailings pile to reduce radon emissions.

The original design of remediation measures for the mill tailings site prepared in 2000 had to be considerably changed in 2005 when it became clear that the tailings pile was geotechnical instable due to the infiltration of precipitation and seepage waters into the tailings body.

Therefore as a precondition for cover construction stabilization measures became necessary including the construction of

- a rock dam toe,
- a pore water drainage curtain executed by drilled piles backfilled with drainage material, and
- a drainage trench to capture hinterland water inflow.

A high quality cover should guarantee a significant reduction of infiltrating precipitation. The cover will contain a sealing layer made of clay material and a storage layer from autochthonous material.

Construction works started in 2007 and will be finished by 2009.

Comparison with other uranium mining remediation projects

Scope of work

Abrupt closure of uranium mining and milling activities occurred in most Eastern European countries. As in Eastern Germany, Slovenian and Bulgarian production immediately stopped when the political changes took place at the beginning of the 1990ies while countries such as the Czech Republic and Romania have been continuing active uranium mining and milling even though with reduced capacity. In the Czech Republic the operations at Europe's last underground uranium mine in Rožná were indefinitely extended in May 2007 with reserves expected to allow mining till 2012. In Hungary uranium mining stopped in 1997 after the government made the decision for mine closure already in 1994 ensuring a transition time from production to remediation.

Table 1. Uranium produced in Eastern European Countries till 2004 by mining and milling [OECD 2005]

Country	Total Uranium Production [t U]
GDR	219,316
Czech Republic	109,061
Bulgaria	16,735
Hungary	21,084
Romania[1]	18,079
Yugoslavia[1]	382

As in other countries in Slovenia no preconditions for a controlled transition from the production to the closure phase were existent when mining stopped. Remediation had to start from one day to another. The duration of the transitional period depended on various aspects. The problem of provision of a sufficient funding was of major importance as well as the planning and permitting procedures. While remediation of the uranium liabilities in Eastern Germany was financially founded basically on the WISMUT-Act in 1991 ensuring a total budget of 6.2 billion. € for the remediation, this process lasted in Slovenia till 2001 when the "Novelty I of the programme of closeout of uranium ore exploitation in RUŽV" passed the parliamentary process.

Considering the uranium produced the mining an milling operation in Slovenia was rather small compared to the other East European Countries since the mining activities were just at the beginning of the exploitation of the uranium deposit when mining ceased (Table 1).

Remediation activities include the closure of the underground mines and open pits, stabilisation and covering of mine waste rock and tailings piles and removal and cleaning of milling and processing sites. Depending on the extent of mining operations the size of the objects to be remediated differs. As already described the remediation project in Slovenia is very special due to the small amount of uranium produced while facilities were designed for a greater production volume.

Organisational Structure

Most remediation operations in the Eastern European Countries have in common that the former mining company is also in charge for the remediation of the mining and milling sites. However, the workforce was drastically reduced in all cases. The organisational structure of the remediation activities differs significantly in the various countries influencing the share of planning and construction works provided by own personnel.

In case of the remediation in Slovenia RUŽV mainly manages the project including maintenance and monitoring activities, while design, construction and supervision is contracted. This is comparable to the situation in Estonia where the

company Ökosil Ltd. acts as project co-ordinator and implementation manager for the remediation of a former tailings pond at Sillamäe.

In other countries the successor of the mining company not only manages the operation but also realises considerable quantities of design and physical work. In these cases the companies were also reorganised that either the company or it's spin offs take over responsibilities of other remediation projects. In Hungary the company Mecsek-Öko is not only responsible for the remediation of the mining and milling liabilities but also manages the remediation of a former copper mine in the northern part of the country. The same appears for the Czech company DIAMO which apart from continuation of uranium and base metal mining became responsible for the remediation of decommissioned coal mines and waste oil lagoons of the Ostrava region. This assures that the wide experience gained during mining and remediation activities is transferred and effectively applied.

Financing

The extent and intensity of remediation projects is influenced by the available funds. All uranium mining operations in Eastern Europe have in common that no provisions were made for the remediation of the mining and milling liabilities. Therefore remediation had to be financed in mainly from the state budget, which was in most cases the reason for insufficient or unsteady funding. The development of remediation strategies e.g. for tailings piles was supported by various pilot projects on systematic remediation planning and on the transfer and training of western technical tools in the frame of an EU Phare Multi-Country program for Environment. This program, implemented from 1996 until 2000 in nine eastern European countries, has been integrated well by the beneficiaries in their own conceptual and detailed remediation planning (Hähne et al. 2007). Some of the remediation projects received additional support from extensive EU programmes (as e.g. Bulgaria) or from other multi-country programmes (Estonia). Nevertheless, for most of the countries the main funding had to be secured from the state budget.

Remediation of the mining and milling legacies in Slovenia was mainly boosted by a loan agreement between the Republic of Slovenia and the European Investment Bank (EIB). This loan of 20 Mio. € contributed a significant share of the originally estimated remediation costs of 36 Mio. € for the 5 year term between 2001 and 2005. It was furthermore important for the commitment of the government to a successful realisation of the remediation when it appeared that the costs will significantly increase due to site specific conditions which were not fully considered in the original designs. The RUŽV remediation case also shows that a significant share of costs is attributed to delays of remediation work in the 1990ies due to missing funding. During that time the existing conditions had to be maintained without substantial progress in the remediation.

Table 2. Total expected remediation costs at RUŽV

Period	Funds (Million EUR)
2006 - 2010	28,6
1990 - 2005	57,7
1990 – 2010 Total	86,3

Long-term activities

The Slovenian Radioactive Waste Agency (ARAO) will be responsible for the long-term stewardship after a 5 year transition period beginning at the end of the remediation work. The remediated mining objects will remain without economic use. All other land owned by the mining company will be transferred to public ownership or returned to the former owner. At the former mill site an industrial zone has been successfully introduced by different small entrepreneurs. Similar concepts for revitalisation of the mine sites also exist in other countries.

Unlike other projects long-term water treatment which may require significant funds is not necessary at Žirovski Vrh due to the fact that the concentrations in the mine and seepage waters are within the authorized limits. In addition there are no groundwater contaminations existent or expected in the future. At other remediation sites water treatment activities will be necessary over years to decades to avoid e.g. adverse impacts on drinking water resources such as in Hungary, or to surface and groundwaters as in East Germany (Paul et al., 2008).

Outlook and Conclusions

Remediation at Žirovski Vrh will continue until 2010 followed by a 5 year transition period where the stable conditions of environmental impacts will be achieved and a final declaration of the effectiveness of remedial measures can be issued. As for other remediated uranium mining and milling projects long-term monitoring, maintenance and care will be required to ensure the function of the constructed elements.

Compared to other remediation projects the specific costs for remediation, related to the amount of uranium produced, are considerably higher. The main reasons are to be attributed to (1) the early termination of the production, (2) a significant delay of the start of physical work due to insufficient funding and (3) to site specific conditions requiring special effort for e.g. additional geotechnical stabilisation measures. The organisational structure of RUŽV is oriented to manage the remediation and to ensure appropriate environmental and operational monitoring.

References

Hähne R., S. Murphy, J. Vrijen, 2007. State and Prospects of Closure and Remediation of Tailings Deposits from Uranium Processing and Heap Leaching in Europe. Proceedings of the International Mining Symposium WISMUT 2007: Closure and Revitalisation of Mining Sites for a Sustainable Regional Development.

IAEA, 2004. The long term stabilization of uranium mill tailings, Final report of a co-ordinated research project 2000–2004. IAEA-TECDOC-1403.

OECD, 2005. Uranium 2005: Resources, Production and Demand. Joint Report of OECD and IAEA. OECD 2005

Paul M, Kreyßig E, Meyer J, Sporbert U (2008) Remediation effects of the WISMUT project to surface waters in the Elbe watershed: An overview.- In: Proceedings of the 5th Conference on Uranium Mining and Hydrogeology, (this volume)

Feasibility Study on Crust Formation as CO_2 Sink in Uranium and Lignite Post-Mining Sites

Petra Schneider[1], N. Gottschalk[1], D. Zänder[2], R. Löser[1], T. Günther[2], B. Tunger[1], L. Eckardt[2] and S. Hurst[3]

[1] C&E Consulting und Engineering Chemnitz, Jagdschänkenstr. 52, D-09117 Chemnitz, Germany.
[2] Eurofins AUA GmbH, Löbstedter Straße 78, D-07749 Jena
[3] Saxon State Agency of Environment and Geology, Zur Wetterwarte 11, D - 01109 Dresden.

Abstract. As a part of the project "Crust formation as CO_2 sink" (supported by the Saxon State Agency of Environment and Geology) the feasibility of catalysed crust formation in mining residues was investigated by means of lab and field experiments. The sites for field studies included a former lignite mining site as well as a dump and tailings from former uranium mining. Project purpose was to investigate the occurrence of metal binding crust formations induced by CO_2 infiltration, but also to investigate the possibility to use post-mining sites for CO_2 sequestration.

Introduction

The capture and storage of CO_2 (CO_2 sequestration) is increasingly an option as strategy in the context of a climate protection (Duckat et al., 2004). For the storage of CO_2 two options were currently discussed: storage in the ocean or in geological reservoirs. The geological storage is seen as a promising possibility of CO_2 storage in near future. The discussion on the oceanic CO_2 storage is dominated by considerable uncertainties in the scientific findings and the unclear legal framework (Duckat et al., 2004).

The scope of the project was the investigation of strategies for CO_2 sequestration by crust formation in former mining sites. Crust formation (formation of secondary minerals, hard pans and gels) is one of the recent subjects under investigation (Hurst, 2005; Graupner et al. 2007; Rammlmair, 1997; Rammlmair & Meyer, 2000; Rammlmair & Grissemann, 2000). The formation of crusts and hard pans has been observed in mining dumps, located in Central Europe. Generally, hard

pans are formed by precipitation of colloids, circulating in soil pore water. They eventually agglutinate the soil particles to crusts marked by reduced pore volume (Rammlmair & Grissemann, 2000). In former investigations was found that hard pan formation can cause metal binding by sorption in mine dump sites. The investigation of CO_2 sequestration strategies like calcination became a highly advanced scientific topic in the recent years. In connection with crust formation another form of CO_2 sequestration as calcination has not been documented in the literature yet.

Lab and Field Investigations

Scope of work

The project was divided into two stages. In a first stage - lab scale - column tests were performed considering representative profiles from dump and tailings material and using CO_2 as gas input. In an accompanying investigation stage a similar experimental arrangement was realised on field scale. Following types of mining waste were considered: lignite overburden site Nochten (Lusatia), uranium tailings pond Lengenfeld (Vogtland) and uranium waste rock dump Schneeberg (Ore Mountains), see figure 1 for location.

Fig.1. Location of the field testing sites in the Free State Saxony, Germany.

Lab and field studies included gas and water analysis, soil investigations, isotopic studies, and mineralogical analysis. The supporting investigation methodology included:

- hydrochemical characterisation of the processes studied, using lab analyses, but also geochemical models,
- water balance calculations and geohydraulic characterisation of the test fields using models for the gas and water phase,
- mineralogical characterisation of the supposed crust formation using mineralogical analyses and geochemical modelling,
- characterisation of CO_2 flow and transformation processes using isotope data and process analysis.

Within the frame of the research project the central question was not only if a crust formation with the help of CO_2 can be induced, but also the process mechanism of a potential CO_2 sequestration. Previous studies have shown crust formation as effective way to reduce or eliminate heavy metal and radionuclide output from mining dump sites and tailings and consequently a improvement of the quality of leachate. A lasting crust formation can also be used for geotechnical stabilisation of mining dumps and tailings.

Conception of Lab and Field Tests

The first step was the investigation on laboratory scale with the help of column experiments using representative profiles from the lignite overburden site sites, as well as waste rock dump sites and tailings of former uranium mining sites. Accompanying investigations were implemented in the field scale. The columns had a total height of 130 cm and a diameter of 30 cm (see Figure 2). To measure the carbon dioxide concentration at the column head, a drainage layer was installed. There was further realised a discontinuous irrigation with distilled water and a continuous fumigation using technical CO_2.

Following types of columns were operated accompanying each field test site:

- one column containing waste rock dump material without fumigation as reference column,
- two columns containing waste rock dump material with CO_2 fumigation,
- one column containing waste rock dump material fumigated with CO_2 and a cover of fly ash and soil mixture. Purpose of the fly ash was to stabilise the pH for catalysis of the crust formation.

Water supply of the columns was realised by a sprinkling system. The required quantity was 125 ml of water per column. Column and field test site leachate were analysed for pH, electrical conductivity, selected heavy metals including uranium, cations, anions, CO_2, O_2, and grain size distribution.

Figure 3 shows the setting of the field sites. The need for field tests resulted from the scale problem to reproduce the natural situation. It was not expected to reach comparable stable conditions during the period of operation of the columns. The technical implementation included the installation of drainage pipes for water extraction and gas input. Gas input was controlled by a gas dosage system. The installation of a barrier for leachate collection was necessary in Nochten and Schneeberg due to the high permeability of the dump material. The dump material should remain more or less undisturbed, so that changes in boundary conditions (density, stratification, particle size distribution, permeability) should be reduced. The duration of the operation of the test fields was at least one year using . The test sites were exposed to natural precipitation.

The analysis of the solid waste rock dump material showed suitable conditions for the discharge of carbon due to their physics and geochemistry for the field sites in Lengenfeld and Schneeberg. The leachate of both sites had a higher pH value (Schneeberg 9.4, Lengenfeld 8.7), avoiding a situation of acidification. In Lengenfeld was found an increased barium level (170 mg/kg), in Schneeberg increased arsenic (680 mg/kg), barium (1700 mg/kg) and manganese levels (1900 mg/kg). These elevated concentrations were not found in the leachate. The waste rock material of Nochten had a very low pH, caused by acid mine drainage. This situation led to acidification and mobilisation of heavy metals.

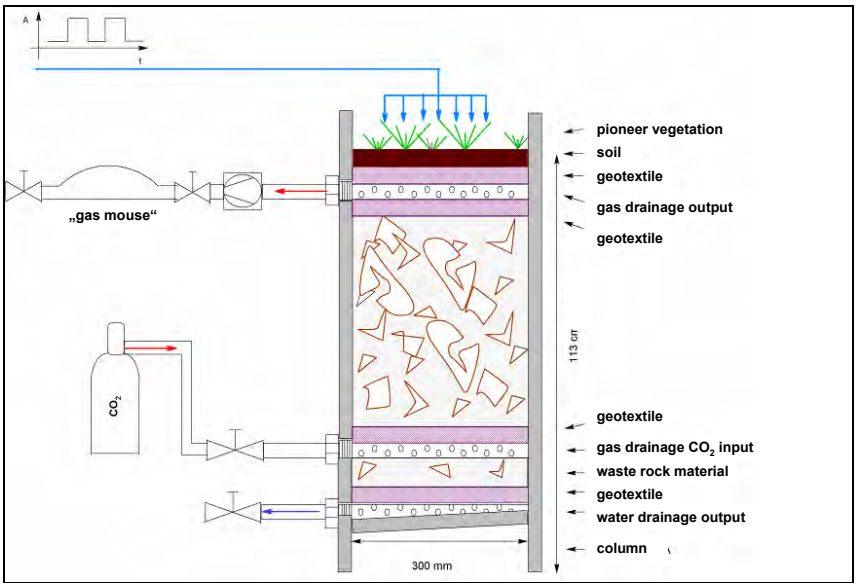

Fig.2. Setting of the lab columns.

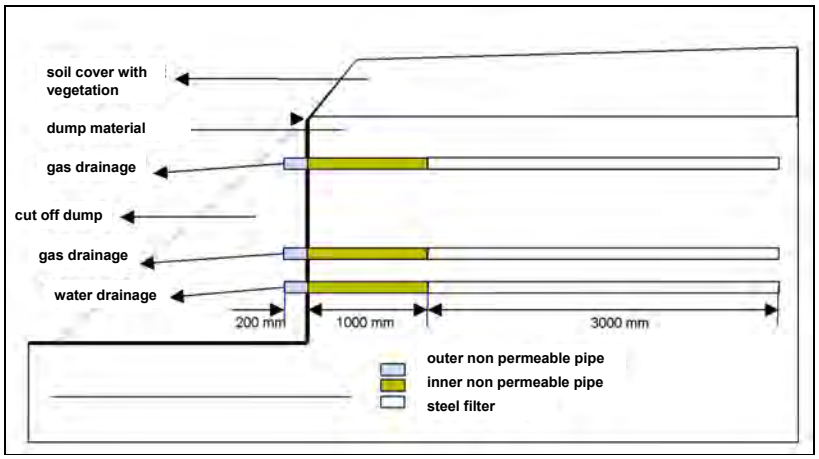

Fig.3. Setting of the field sites.

Geochemical Investigations, Isotope and Mineralogical Analysis

Following types of modelling workings were performed:

- Water balance using CoupModel and flow modelling using Hydrus-2D on the test fields,
- Geochemical modelling of the columns using PHREEQC,
- Gas balance modelling.

$^{12/13}$C-Isotope measurements were performed to ensure the origin of carbon and investigate changings in the carbon distribution of solids, leachate and gas. Following types of mineralogical analysis were carried out:

- Microscopic analysis of solid samples,
- Scanning electron microscopy (SEM),
- Element analysis using Energy X-ray micro-analysis (EDX).

Results

Lab and Field Tests: Concentrations of Metals

The results of the metals content of Lengenfeld site showed a decreasing content for As, Zn and Pb in the lab tests with CO_2. In the field tests with CO_2 was found a decreasing content for U and Ni, see table 1. This situation indicates that these metals were bound to the matrix during the tests.

Table 1. Behaviour of metals during the lab and field tests of Lengenfeld site.

Type of test	Content decreasing	Content after peak decreasing	Content increasing	Stable content stable
Lab tests with CO_2	As, Zn	Pb	Ni, Cu	U
Field tests with CO_2	Pb	Ni	As, Zn	Cu, U

The results of the metal contents of Schneeberg site showed a decreasing content for Pb, Zn and U in the lab tests with CO_2. In the field tests with CO_2 was found a decreasing content for U, Zn and As, see table 2.

Table 2. Behaviour of metals during the lab and field tests of Schneeberg site.

Type of test	Content decreasing	Content after peak decreasing	Content increasing	Stable content
Lab tests with CO_2	Pb	Zn, U	As, Ni, Cu	
Field tests with CO_2	U	Zn, As		Pb, Cu; Ni

The results of Nochten site showed a decreasing content for Ni and Zn in the lab tests with CO_2. In the field tests it was not possible to get enough leachate to establish time series of parameters, see table 3.

Table 3. Behaviour of metals during the lab and field tests of Nochten site.

Type of test	Content decreasing	Content after peak decreasing	Content increasing	Stable content
Lab tests with CO_2	Ni	Zn	As, U	Cu, Pb

In the tests was indicated a clearly positive influence of the fly ash identifiable by increased pH (Nochten) or stabilised pH (Lengenfeld and Schneeberg), so conditions for stabilisation of the test geochemistry could be provided.

Geochemical Investigations and Modeling

The leachate analysis served the characterisation of water components. It was found a changing in the geochemical system from a Ca-SO_4 water to a Ca-SO_4-HCO_3 water in Nochten and Schneeberg, so significant amounts of CO_2 were bound in the system. In Lengenfeld the same water type Ca-SO_4 was found all time, therefore may be concluded that the geochemical system Lengenfeld has the highest storage capacity for CO_2. With regard to the capacity of CO_2 storage in the geochemical system the study sites can be characterised as follows: Lengenfeld > Schneeeberg > Nochten. The geochemical modelling with PHREEQC resulted in mineral species dominated by oxides, hydroxides and silicates after fumigation.The highest absolute binding of CO_2 was observed in Schneeberg columns. There was observed a significant pH stabilising effect caused by the fly ash cover

in the Nochten (pH 4) and Lengenfeld (pH 8.7) columns. The mechanism of CO_2-binding can be described as fixing in the pores of the rock material, so mineral formation can occur in case of over-saturation of the pore water. But, generally has to be stated that the investigation period was to short to measure a formation of secondary minerals.

Isotope and Mineralogical Investigations

All measured values of exhausted gas were around -23 ‰ and thus in the field of δ^{13}-C reference values for C_3-plants. Since the gas from the bottom of the column has been abandoned, the CO_2 of the exhaust has to be produced by the column vegetation. The δ^{13}-C values of the leachate samples ranged from -20 to -29 ‰ and therefore differ significantly from the δ^{13}-C value of the irrigation water with 17 ‰. This is an indication for geochemical changes. The δ^{13}-C values of the reference columns were around -9 to -11 ‰. The δ^{13}-C values of the columns containing ash without fumigation were around -8 to -11 ‰. The measured δ^{13}-C values of the columns with fumigation with ash were between -8 and -12 ‰. With help of the carbon balance and the δ^{13}-C-isotope studies for all columns was found that the CO_2-amounts do not cause a carbonate precipitation yet, but an increasing concentration of HCO_3 in the pore water. The modelled increase of the saturation indices of the columns reflected also this situation, so CO_2 sequestration potential has to be evaluated taking into account the kinetics to form a new mineral. The results of the mineralogical investigations confirmed the PHREEQC modelling and showed mainly Fe/Mn-hydroxides as surface cover in the samples. A relevant calcium enrichment as note for a possible crust formation was found in the samples of Schneeberg and Lengenfeld enabled by the neutral pH.

Conclusion and Outlook

The results of the investigations have shown that a binding of CO_2 in post mining sites is feasible. The effectiveness of CO_2 sequestration depends on the composition of the mineral matrix and the pH of the soil system.

During the CO_2 input in columns and test fields, the saturation index for various minerals increased significantly. As the investigation results show, the binding of CO_2 happened in the pores of the soil matrix. There is a significant CO_2 binding potential in the waste rock dumps and tailings of former uranium mining sites. Due to the climatic situation (low temperature, high rainfall), the kinetics of the reactions, however, in comparison to crust formation processes in arid landscapes is much slower. No CO_2 binding was observed in the test materials of the lignite overburden site Nochten due to the very low pH in the mining waste. A positive influence of fly ash as soil cover was observed, especially in test columns with originally acidic to slightly alkaline pH range. Lab experiments and modelling have shown a binding of CO_2 in the system. These results were confirmed by the

field tests. Although the formation of crusts as secondary minerals and/or hard pan formation was not measured due to the short investigation period, the models showed that at a longer time scale this must be the binding mechanism.

A verification of these binding mechanisms during further investigations is necessary. Further tests should cover a longer period and the selection of the experimental conditions considering pH and composition of the mineral matrix of the soil to find optimum conditions for a sustainable crust formation. Additionaly to post-mining sites, areas containing clayey material with neutral soil pH should be included in the investigation programme. In case of testing agricultural land, the influence of the CO_2-content on plant growth should be included in the investigation programme in order to use potential synergies due to plant ecology and the soil potential as CO_2-sink. In this case potential soil salinisation has to be taken into account. Additionaly, further topics should include the detailed investigation of mass balances and strategies for technical applications. A potential application field can be seen in the injection of CO_2 during the process of precision farming.

References

Duckat, R.; Treber, M.; Bals, C.; Kier, G. (2004): CO_2-Abscheidung und Lagerung als Beitrag zum Klimaschutz ? Ergebnisse des „IPCC Workshops on Carbon dioxide capture and storage“ vom November 2002 und Bewertung durch Germanwatch.

Graupner, T; Kassahun, A.; Rammlmair, D.; Meima, J. A.; Kock, D.; Furche, M.; Fiege, A.; Schippers, A.; Melcher, F. (2007): Formation of sequences of cemented layers and hardpans within sulfide-bearing mine tailings (mine district Freiberg, Germany), Applied Geochemistry, 09.02.07

Grissemann, C.; Rammlmair, D.; Siegwart, C. ; Fouillet, N. (2000) : Spectral induced polarisation linked to image analysis : a new approach. In: Rammlmair, D., Mederer, J., Oberthür, T., Heimann, R.B.; Pentinghaus, H. (eds.): Applied Mineralogy in Research, Economy, Technology, Ecology and Culture, Vol. 2, Proceedings ICAM 2000, 561-564; Göttingen

Rammlmair, D. (1996): The role of gels in self organisation of slagheaps from the arsenic production site Muldenhütten at Freiberg, Saxony, FRG. In: Niedbalska, A; Szymanski, A.; Wiewiora, A. (Hrsg.) Proceedings ICAM 96, 378-382, Warschau.

Rammlmair, D.; Grissemann, C. (2000) : Natural attenuation in slag heaps versus remediation. In : Rammlmair, D. ; Mederer, J. ; Oberthür, T. ; Heimann, R.B. ; Pentinghaus, H. (Hrsg.): Applied Mineralogy in Research, Economy, Technology, Ecology and Culture. Proc. ICAM 2000, 645-648. Göttingen.

Rammlmair, D.; Meyer, L. (2000) : Crust formation : via column experiments to mathematical modelling. In: Rammlmair, D., Mederer, J., Oberthür, T., Heimann, R.B.; Pentinghaus, H. (eds.): Applied Mineralogy in Research, Economy, Technology, Ecology and Culture, Vol. 2, Proceedings ICAM 2000, 641-644; Göttingen.

Modelling and Assessment of Radionuclides Differential Transport in Groundwater

Maria de Lurdes Dinis and António Fiúza

Geo-Environment and Resources Research Center (CIGAR), Mining Department, Engineering Faculty, University of Porto, Rua Dr. Roberto Frias, 4200-465, Porto, Portugal, mldinis@fe.up.pt; afiuza@fe.up.pt.

Abstract. An overview of the essential features of groundwater transport of radioactive contaminants in a saturated porous media is presented and used in an integrated bi-dimensional phenomenological model of transport and fate. The conception and the assumptions implicit in the model are described. The output results are then compared with values estimated by different mathematical space interpolation techniques applied to experimental sample measurements obtained in the surroundings of a contaminated site. These interpolation methods allowed evaluating the spatial variability of the contamination, defining the contour of the plume. These values are then compared to those produced by the transport and fate model. This methodology was applied to uranium and radium, due to their special environmental concern.

Introduction

Groundwater is an important pathway for transport of radioactive contaminations in the subsoil. But this type of contamination is difficult to sample and monitor, requiring great dependence on models to predict the fate and transport as well as the variation of concentration along this pathway.

The contaminated groundwater may be considered a potentially significant exposure pathway if the radionuclide concentration in the groundwater exceeds the legal levels, or if the contamination at a particular site could eventually provoke the radionuclide concentrations in groundwater to exceed trigger values. If the concentrations of radionuclides in the groundwater downflow from the site, or in leachate at the site, exceed these values, and the groundwater in the vicinity of the site has the potential to be used as a source of drinking water, it is likely that

groundwater modelling will be useful, if not necessary; it is also an unavoidable support tool for the eventual decision of site remediation.

An important step in groundwater modelling is identifying the type and approximate quantities of the radionuclides present. This will not only determine the potential offsite impact, but it will also help to identify the magnitude of the risks to potential exposed receptors, the radionuclides mobility and the time period over which the radionuclides may be hazardous. The types of radionuclides will also determine whether radioactive decay and the ingrowth of radioactive daughters are important parameters that will need to be modelled. On the other hand, the ability to reliably predict the rate and direction of the groundwater flow and contamination transport has a critical role in planning and implementing groundwater remediation. This paper presents an overview of the essential components of groundwater water flow and contaminant transport modelling in saturated porous media. It is described the methodology used in groundwater modelling flow, the results of different mathematical interpolation techniques and software tools used to evaluate the spatial variability of radionuclides and define the underground contamination plume.

A contaminated site from a former uranium mine was taken as a case study. To evaluate the level of contamination in the site and in its vicinity, the radionuclides of the U-chain, in particular for uranium and radium concentration, were monitored in the groundwater of the site. Data from sampling points including holes and wells were used to assess the extension of radium and uranium contamination in groundwater.

Methods and Results

Radionuclides leach from the tailings, move downward through the unsaturated zone to the water table, and then migrate in the saturated ground water system. Usually, these calculations are broken down into three linked sub-pathways: (i) leaching of contaminants from the tailings, (ii) vertical movement of the dissolved contaminant downward to the water table through the unsaturated zone, and (iii) migration of the contaminant in saturated ground water to the receptor point.

We developed a previous model for simulating the radionuclides release from a uranium tailings pile and its migration process through the soil to the groundwater that is already published (Dinis and Fiúza 2005). We will present here the methodology developed to estimate the necessary parameters for modelling groundwater flow.

The release concentration of a radionuclide depends upon characteristics of both the waste and the site. In particular, for solid-waste disposal sites, a very important feature in radionuclides transport is the distribution of the nuclides between the aqueous and the solid phase. The distribution is characterized by the K_d parameter, which expresses the fraction of an element in solid form relatively to the fraction in soluble form. The following equation estimates the leachate concentration under equilibrium partitioning conditions (Dinis and Fiúza 2005).

$$C_L = M/(A \cdot \theta \cdot D + \rho \cdot K_d) \quad (1)$$

In the above equation, C_L (Bq/m^3) is the leachate concentration; M (Bq) is the amount of radionuclide in the source (Bq); A is the area of the source (m^2); θ (dimensionless) is the volumetric water content, which depends on saturation ratio (R_{sat}); ρ (g/cm^3) is the bulk density and K_d (cm^3/g) is the distribution coefficient.

Under saturation conditions the saturation ratio is equal to unity (R_{sat} = 1) and for unsaturated conditions it is a function of the infiltration rate I (m/yr), the saturated hydraulic conductivity, K_{sat} (m/yr), and also of the texture of the soil given by a soil-specific exponential parameter b (dimensionless). The saturation ratio can be estimated using the following equation (EPA 1996):

$$R_{sat} = (I / K_{sat})^{\left(\frac{1}{2 \cdot b + 1}\right)} \quad (2)$$

The Radionuclides Transport

Radionuclides may be transported through the unsaturated zone before reaching the saturated zone. Nevertheless, the contamination may also enter directly into the saturated zone.

In the unsaturated zone, the flux moves predominantly downward until it reaches the water table. A simple approach is used to estimate the flux transport time through the unsaturated zone. The water velocity for transport through the unsaturated zone, V_v (m/yr), may be estimated by the average infiltration rate, I (m/yr):

$$V_v = I / \theta \quad (3)$$

This parameter, I (m/yr), is given mathematically by a water balance equation based on the mass conservation law and is estimated as a function of the precipitation rate, P_r (m/yr), irrigation rate, I_r (m/yr), runoff (Cr) and evapotranspiration (C_e) coefficients:

$$I = (1 - C_e) \cdot [(1 - C_r) \cdot P_r + I_r] \quad (4)$$

Under saturated conditions, Darcy's law may be used to describe the volumetric flow of water through a porous medium. Radionuclide velocity transport estimative is based on water seepage velocity: for the contaminants that flow with water, contaminant velocity is the same as water velocity (vertical and horizontal). Groundwater seepage velocity may be calculated by the Darcy's velocity, V (m/yr), and by the soil effective porosity (ε_e):

$$V_{pw} = V / \varepsilon_e \quad (5)$$

Dissolved radionuclides may be transported at velocities lower or equal than the flow velocity of the aquifer due to sorption process. The retardation factor, R (dimensionless), is used to estimate the time that it takes to transport the radionuclides to a defined distance and can be estimated by the expression:

$$R = 1 + (\rho / \varepsilon_e) \cdot K_d \tag{6}$$

Transport and fate of radionuclides in groundwater follows the theoretical approach of the transport processes represented by the basic diffusion/dispersion-advection equation. For the case of unidirectional saturated advective transport of a single dissolved substance with three-dimensional dispersion in an isotropic homogeneous aquifer, the differential equation for solute transport can be approximated as follows (EPA 1996):

$$\frac{\partial C}{\partial t} + \frac{V_{pw}}{R} \cdot \frac{\partial C}{\partial x} = \frac{D_x}{R} \cdot \frac{\partial^2 C}{\partial x^2} + \frac{D_y}{R} \cdot \frac{\partial^2 C}{\partial y^2} + \frac{D_z}{R} \cdot \frac{\partial^2 C}{\partial z^2} - \lambda \cdot C \tag{7}$$

In this equation C (Bq/m^3) is the concentration in the liquid phase; D_x, D_y, D_z (m^2/yr) are the dispersivities in the x, y, z directions, respectively; λ (yr^{-1}) is the radioactive decay constant and V_{px} (m/yr) is the x component groundwater pore velocity. This expression may be solved by Green's functions to estimate the concentration in the aquifer at some point downgradient of the release where is located the exposition point or the water supply well (EPA 1996).

For a horizontal source of length L and width W centred at (0,0,0) in an aquifer of constant depth b, as shown in figure 1, the solution for the generic equation becomes (EPA 1996):

$$C = (M_0) / (\varepsilon_e \cdot R) \cdot [X(x,t) \cdot Y(x,t) \cdot Z(x,t)] \tag{8}$$

The release to the aquifer is given by M_0 (Bq) and X, Y, Z are the Green's functions in the x, y, z coordinate directions, respectively. The Green's functions for the boundary conditions defined may be expressed by the following equations (EPA 1996):

$$X = \frac{1}{2 \cdot L} \left(\operatorname{erf} \left(\frac{(W + L/2) - \frac{V_{pw}}{R}}{\sqrt{4 \cdot D_x \cdot t / R}} \right) + \operatorname{erf} \left(\frac{(W - L/2) - \frac{V_{pw}}{R}}{\sqrt{4 \cdot D_x \cdot t / R}} \right) \right) \cdot e^{(-\lambda \cdot t)} \tag{9}$$

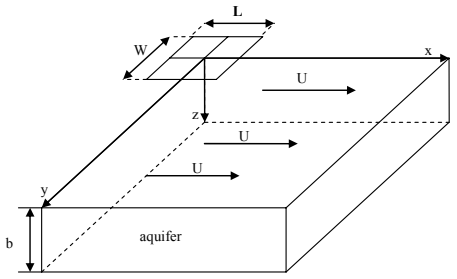

Fig.1. Groundwater dispersion model (EPA 1996).

$$Y = \frac{1}{2 \cdot W}\left(\operatorname{erf} \frac{(L/2 + y)}{\sqrt{4 \cdot D_y \cdot \frac{t}{R}}} + \operatorname{erf} \frac{(W/2 - y)}{\sqrt{4 \cdot D_y \cdot \frac{t}{R}}} \right) \quad (10)$$

$$Z = \frac{1}{b} \quad (11)$$

The elapsed time is represented by t (yr) and "erf" is the error function.

Case Study

A contaminated site from a former uranium mine was taken as a case study; the Urgeiriça site located in the central Portugal, near Nelas (Viseu). The mine is surrounded by small farms and country houses, with most of the local population living in the village Canas de Senhorim within about 2-km of the mine.

The mine's exploitation began in 1913 for radium extraction. The activity of the Urgeiriça mine was maintained until 1945, then exclusively dedicated to the production of radium. In 1951, a chemical treatment unit for the production of low-grade U_3O_8 concentrates was built and in 1967 it was transformed into a modern unit with the capacity to treat about 150 ton of ore per day (Bettencourt et al. 1990). Later, it was enlarged to a capacity of 300 ton/day and after to 600 t/day. In 1991 classical mining explorations ended, but the facilities were still used until 2000 for the treatment of liquors produced by heap leaching of marginal ores from small mines in the surroundings as well as groundwater from the Urgeiriça Mine, previously exploited by in-situ leaching. During almost a century, the total uranium concentrate (U_3O_8) production reached about 4730 ton, in addition to the radium salts, produced until 1945.

The extensive treatment of uranium ores at the Urgeiriça processing plant has led to the production of large amounts of solid wastes (tailings) which were deposited into dams in open-air areas. A prominent tailing pile is located near the mine (Fig. 2) occupying an area of 13,3 ha with an estimated volume of 1 390 000 ± 40 000 m^3 (Pereira et al. 2004).

The tailings are composed mainly of sand and silt particles that were transported as a pulp to the site from the solid-liquid separation by CCD[1], after being submitted to grinding and acid leaching. This waste material includes most of the radioisotopes of the uranium decay chains as well as other hazardous chemical elements resulting from the treatment process.

Rain water may infiltrate through the surface of the tailings, interacting with sludge materials and acid producing minerals, becoming strongly acid; eventually these acidic solutions may dissolve and transport radionuclides leading to the groundwater contamination.

[1] CCD – Counter Current Decantation

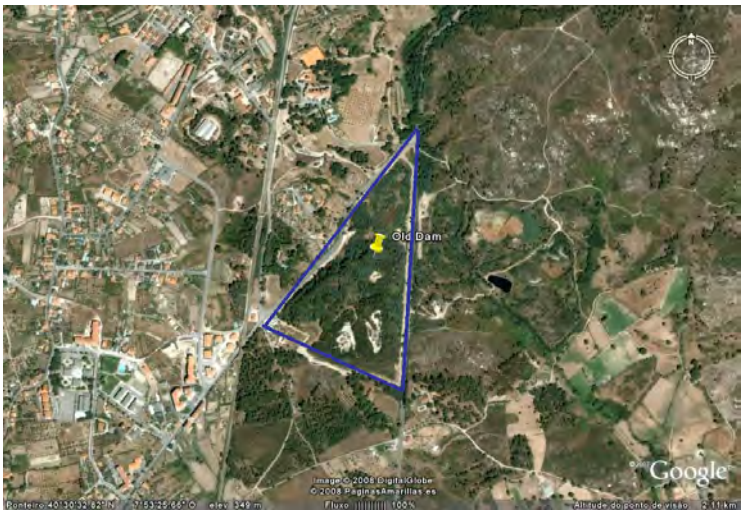

Fig.2. Aerial photo of Urgeiriça site. The village of Canas de Senhorim is located at the upper left corner of the tailings pile identified as BV – Barragem Velha (Old Dam) (Google Earth).

Using this model, a simulation was done for a release rate of radionuclides (M_0 in Bq) to an aquifer with a constant thickness of 3 m, originated by an horizontal contaminated source of length 425 m and width 625 m, centred at a point source with coordinates (212.5, 312.5, 0).

The necessary parameters were adopted from different sources: some resulted from data collected in the Urgeiriça tailings piles (Exmin 2003), others from data given previously by the National Uranium Company (ENU) and also from published data (Bettencourt et al. 1990; Pereira et al. 2004). The unknown parameters were estimated from available data.

Data concerning meteorological parameters, namely precipitation and evaporation were used for estimating the infiltrating water rate into the contaminated zone. The precipitation and evaporation data refers to the Caldas da Felgueira meteorological station (located at about 3 km to SE of the tailings pile).

A total area of approximately 133 000 m^2 was considered for the contaminated site. The radionuclide concentration was considered homogenous and equal in all the contaminated area: an average value for each radionuclide concentration was used. Specific hydrogeologic parameters were considered for each zone where the radionuclides transport occurs, namely for the contaminated tailings, for the unsaturated zone and for the saturated groundwater zone; this means that we used different densities, porosities, hydraulic conductivities, distribution coefficients and thicknesses. An hypothetical well water supply is considered to be located at the downgradient edge of the contaminated zone.

Sampled measurements on uranium and radium activity in groundwater from the Urgeiriça site were used for comparison with the model results.

The analytical values show somehow similar values with those produced by the model. The average value for total uranium in the water at the location of the hypothetical well was about 1,6 Bq/L and for radium was about 0,4 Bq/L. According to the output of the simulation these values are achieved within the first 30 years after the aquifer became contaminated. These results correspond to an effective dose of 0,053 mSv/yr for ^{238}U and of 0,082 mSv/yr for ^{226}Ra, considering an annual ingestion rate of 730 L and an effective dose coefficient of 4,5 x 10^{-5} mSv/Bq and 2,8 x 10^{-4} mSv/Bq for ^{238}U and for ^{226}Ra, respectively.

Two sampling campaigns were done at this site by Exmin (2003). The main goal was to evaluate potential seasonal variations in the chemical composition of the groundwater from the contaminated site and surroundings.

The water samples were collected in wells (66) and holes (26) in two different periods, June and November of 2001 (Exmin 2003). Only some of these sampling points were considered for this study, according to their higher probability of being contaminated. One of the criteria for the selection of the samples was the relation between its location and the source; samples collected upstream and to higher distances from the contaminated source have a lower probability of being contaminated by the past mine activities (Pereira et al. 2004b).

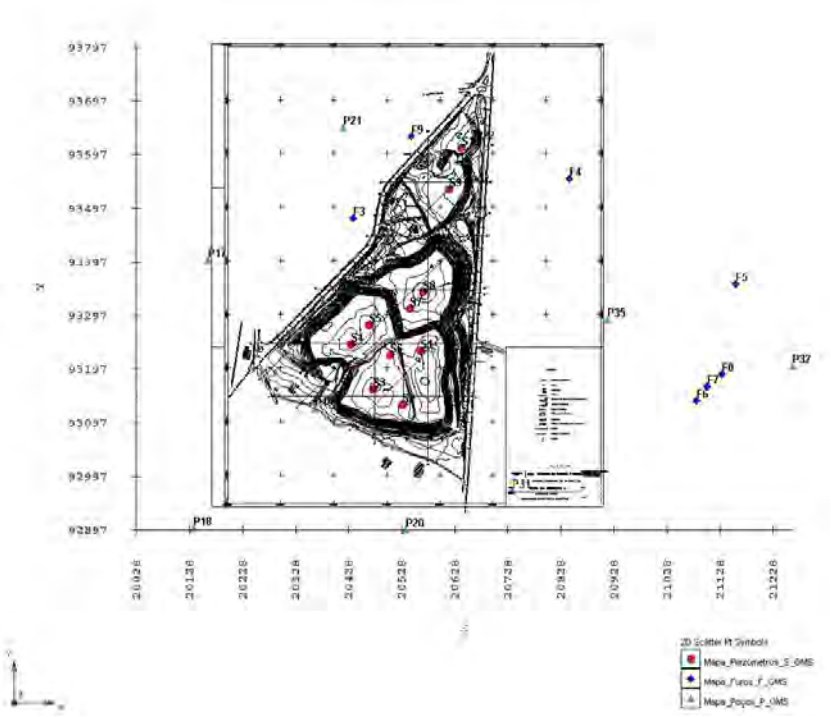

Fig.3. Location of the water samples collected at Urgeiriça uranium mining site.

Table 1. Summary statistic data analysis (wells, holes and piezometers water samples).

Parameters	U (Bq/L)	Ra (Bq/L)
N - number of water samples	26	26
μ - average	2,835	0,284
Median	0,204	0,137
Variance	36,310	0,120
σ/μ	2,126	1,238
Minimum	0	0
Maximum	28,73	1,47

In figure 3 are represented the sample points location for wells (P_{17}, P_{18}, P_{19}, P_{20}, P_{21}, P_{31}, P_{32} and P_{35}), holes (F_3, F_4, F_5, F_6, F_7, F_8 and F_9) and piezometers (S_1, S_2, S_3, S_4, S_5, S_6, S_7, S_8, S_9 and S_{10}). Data from 26 different points were analyzed for chemical and radiological parameters, namely for uranium and radium.

Table 1 shows a summary for the basic statistic parameters of uranium and radium concentration in groundwater for all the sampled points.

A simple observation of this table shows that the uranium concentration is significantly high, presenting as maximum 28,73 (Bq/L) and although the average value for radium is not severe (0,284 Bq/L), the maximum value is significantly high (1,47 Bq/L). However, and in particular for uranium, the analytical values showed a high variability for concentration (20 to 30 %) depending on the season in which the water samples were collected.

With the purpose to analyze the preferential direction of the contaminated samples, which have the presence of mining activities, a geostatistic study was performed for radium and uranium content in the selected water samples.

Different software were used: GMS (Groundwater Modelling System) and Surfer. Also different interpolation techniques were used in GMS software, including directional variogram analysis. This software has a powerful suite of interpolation tools in a two-dimensional geostatistic.

The following interpolation techniques were used from GMS software: linear interpolation (simple linear interpolation based on a triangulation of the scatter points); inverse distance weighted interpolation (includes constant, gradient, plane and quadratic nodal functions); clough-tocher interpolation (piece-wise cubic patch approach adapted from finite element method); natural neighbour interpolation (technique based on natural neighbours computed from Thiessen polygons) and kriging (ordinary and universal kriging routines with graphical variogram editing).

For the kriging interpolation technique the *Surfer* software was used as it has a better adjust and realist representation. A variogram analysis was also performed.

The following figures represent the results of these different interpolation methods. Only the most representative are presented here.

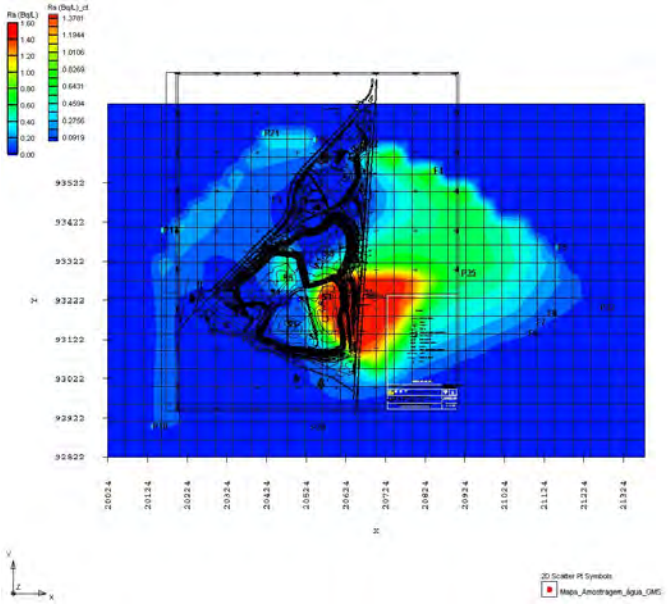

Fig.4. Clough-tocher interpolation (cubic triangular), Ra (Bq/L).

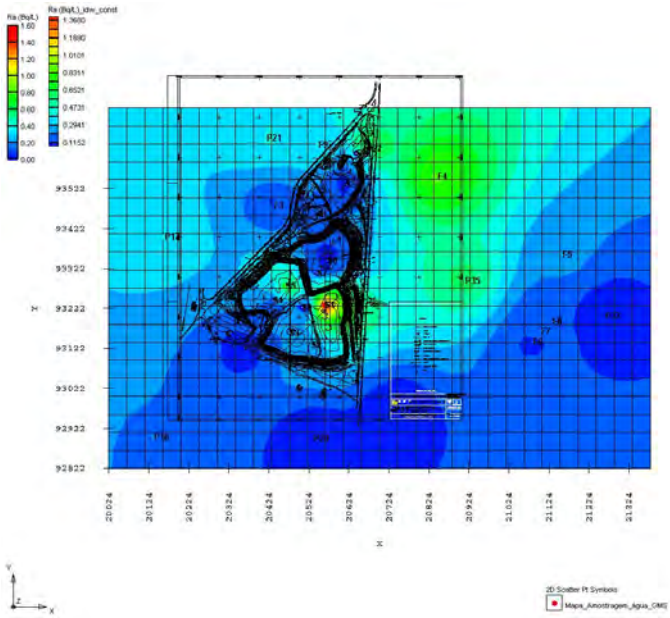

Fig.5. Inverse distance weighted interpolation (constant function), Ra (Bq/L).

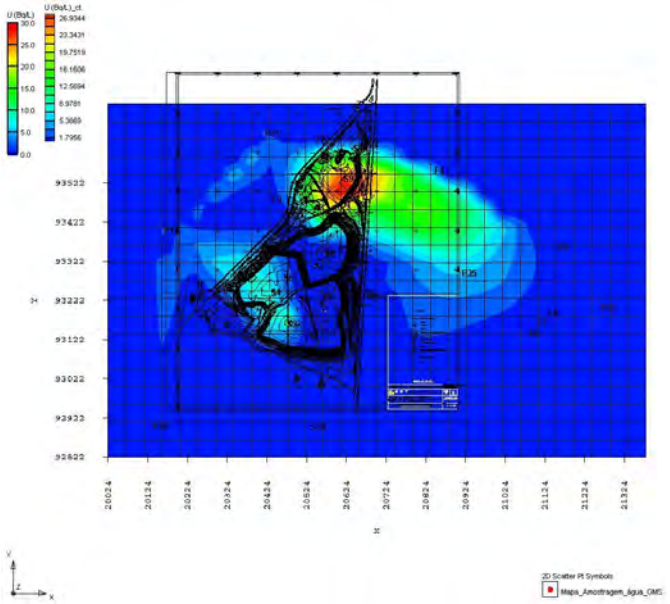

Fig.6. Clough-tocher interpolation (cubic triangular), U (Bq/L).

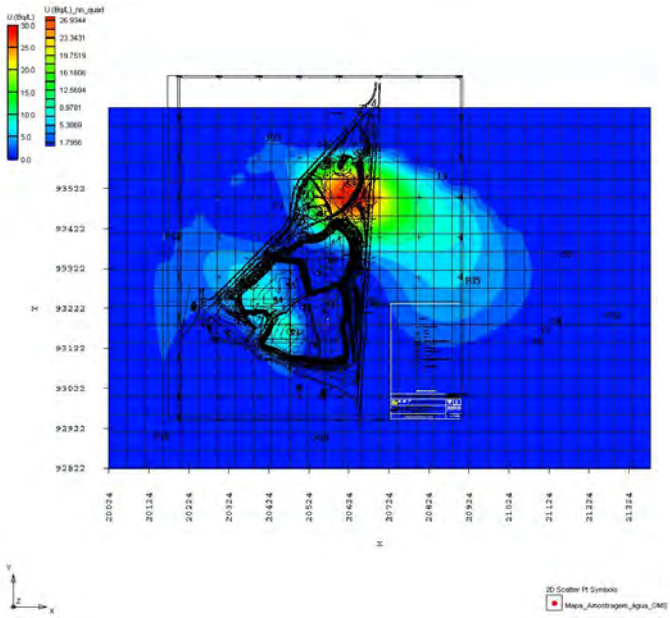

Fig.7. "Natural neighbor" interpolation (quadratic function), U (Bq/L).

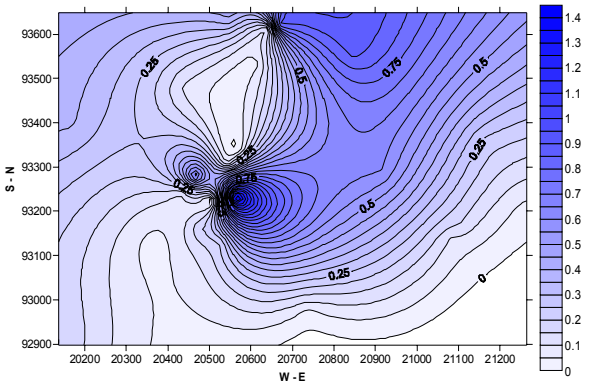

Fig.8. Dispersion of Ra contamination in groundwater (Bq/L) represented by kriging.

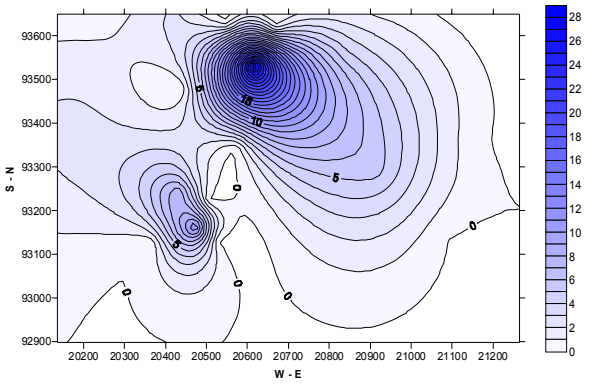

Fig.9. Dispersion of U contamination in groundwater (Bq/L) represented by kriging.

Conclusions

A previous model for radionuclides transport and fate in groundwater, based on a one-dimensional analytical solution, has been developed and already published (Dinis and Fiúza 2005). The results obtained in this study by applying Green's functions are in good accordance with those obtained with the previous model: the medium value for total uranium in the well water was about 1,6 Bq/L and for radium about 0,4 Bq/L. These values are achieved in the previous model within the first 30 years after the aquifer contamination and with the Green's functions method these values were also achieved within the same period of time.

Also it should be noted that the maximum values for both nuclides are higher than the standard values acceptable for radionuclides in groundwater at inactive uranium mill tailings site; the USEPA has established the Maximum Contaminant Level (MCL) for combined ^{226}Ra and ^{228}Ra of 0,185 Bq/L. The European Union

has also issued a Directive on the quality of drinking water, including regulations for radioactive substances. The EU Directive allows a Maximum Permissible Level (MPL) for ^{226}Ra of 0,122 Bq/L. This MPL was exceeded in 56% of the water samples analysed.

The estimative dose resulting from the two radionuclides considered was 0,135 mSv/yr. The recommended reference level of committed effective dose is 0,1 mSv from 1 year's consumption of drinking water.

The high radionuclides content registered for underground waters indicates that the site has been contaminated by the former mine works. Considering radionuclides dispersion through groundwater system, it was observed that there are two preferential plume contamination directions, whether uranium or radium is considered. These two directions suggest that SW-NE direction is preferential to radium dispersion and that NW-SE direction is preferential to uranium dispersion. This allowed us to identify two preferential contamination targets: at south for radium and at north for uranium.

The results obtained both by the groundwater pathway model and by the dispersion techniques assessment led to the forecast of unacceptable concentrations; this results should be taken into account in the management guidelines included in the design of the remediation process. These management guidelines should be based on factors such as efficiency of contamination reduction, legal requirements and physical constraints that are stressed in this study.

References

Bettencourt A.O., Teixeira M.M., Elias M.D., Madruga M.J. (1990), Environmental Monitoring in Uranium Areas. In: Environmental Behaviour of Radium, Vol. 2. Technical Reports Series N.º 310, pp. 281-294, IAEA, Vienna.

Dinis M.L., Fiúza A. (2005), Simulation of Liberation and Transport of Radium from Uranium Tailings, in: Uranium in the Environment - Mining Impact and Consequences, pp. 609-618. Broder J. Merkel; Andrea Hasche-Berger (Eds), 897 pp., Springer publishers - ISBN 10 3-540-28363-3; ISBN 13 978-3-540-28368-8.

EPA U. S. Environmental Protection Agency (1996), Documenting Ground-Water Modeling at Sites Contaminated with Radioactive Substances, U. S. Environmental Protection Agency, EPA 540-R-96-003, PB96-963302.

EXMIN (2003), Estudo Director de Áreas de Minérios Radioactivos – 2.ª fase, Companhia de Indústria e Serviços Mineiros e Ambientais, SA.

Pereira A.J.S.C., Dias J.M.M., Neves L.J.P.F., Nero J.M.G. (2004), Modelling Efficiency of a Rehabilitation Plan for a Uranium Mill Tailing Deposit (Urgeiriça, Central Portugal). XI International Congress of the Radiation Protection Association, Madrid, Spain, 23-28 May.

Pereira, A.J.S.C, Neves L.J.P.F., Dias J.M.M., Campos A.B.A., Barbosa, S.V.T. (2004b), Evaluation of the Radiological Hazards from Uranium Mining and Milling Wastes (Urgeiriça – Central Portugal), XI International Congress of the International Radiation Protection Association.

Infiltration and Contaminant-Transport Modeling for a Uranium Mill Tailings-Disposal Facility

Ryan T. Jakubowski[1], Douglas S. Oliver[2], and John J. Mahoney[1]

[1] MWH Americas, Inc., Steamboat Springs, Colorado
[2] MWH Americas, Inc., Salt Lake City, Utah

Abstract. Contaminant fate and transport modeling of uranium was performed for a uranium milling and tailings-disposal facility. Prior to final closure and site reclamation, and in support of the site's groundwater-discharge permit, the operator is required to prepare an infiltration and contaminant-transport model in order to demonstrate the long-term ability of the tailings-cover system to adequately contain and control tailings contaminants and protect nearby groundwater quality of the uppermost aquifer.

Infiltration through the tailings-cover system was predicted with the variably-saturated flow-and-transport code HYDRUS-1D. Predictive modeling was used to evaluate different reclamation scenarios, and the cover design was optimized to minimize infiltration rates through the cover and reduce construction costs. The infiltration model demonstrated that a vegetated, evapotranspiration (ET) cover would significantly reduce infiltration relative to that of a conventional cover. Average model-predicted long-term infiltration rates were reduced from approximately 1.0×10^{-2} cm/day for the original cover design to 1.0×10^{-4} cm/day for the ET cover design.

Modeling of potential uranium transport from the tailings through the tailings-cell liner and into the vadose zone was performed with HYDRUS-1D. Retardation rates for uranium (VI) were calculated based on equilibrium soil-water partition coefficients (K_d) using the mass of hydrous-ferric oxide (HFO) present in the bedrock and the equilibrated solution compositions predicted with the geochemical code PHREEQC. Surface-complexation coefficients for uranyl and uranyl-

carbonate were optimized to correlate with published sorption experiments. Neutralization of the infiltrating tailings-pore waters and sorption of solutes was determined with PHREEQC. The masses of HFO and calcite were determined for samples collected from the vadose zone. Through this method, a sorption value for the bedrock immediately beneath the tailings cells was estimated to be 8.47 kg/L. Assuming a volumetric moisture content of 7%, a retardation factor of 250 was calculated. Uranium, as a result of the solute's strong capacitance for sorption and resultant high-retardation coefficients, is predicted to migrate a limited distance (less than 1 m) below the liner system in 200 years; and is not predicted to be a threat to groundwater in the underlying perched aquifer.

Use of Na-Ferrate (VI) to prevent acid drainage from uranium mill tailings

Horst Monken Fernandes[1,2,*], Debra Reinhart [2] and Mariza Ramalho Franklin[1]

[1]Institute of Radiation Protection and Dosimetry. Av Salvador Allende s\n, Rio de Janeiro – RJ – Brazil. CEP 22780-160
[2] Debra Reinhart University of Central Florida, P.O. Box. 162450, Orlando, FL, 32816-2450, USA
[*] presently working at the Waste Technology Section of International Atomic Energy Agency

Abstract. Ferrate (VI) is a powerful oxidizing agent in aqueous media. Despite numerous beneficial properties in environmental applications, ferrate (VI) has remained commercially unavailable. Producing the dry, stabilized ferrate (VI) product required numerous process steps which led to excessive synthesis costs (over $20/lb) thereby preventing bulk industrial use. Recently a novel synthesis method for the production of a liquid ferrate (VI) based on hypochlorite oxidation of ferric ion in strongly alkaline solutions has been discovered (USPTO 6,790,428; September 14, 2004). This breakthrough means that for the first time ferrate (VI) can be an economical alternative to treating acid mining drainage generating materials. The objective of the present study was to investigate a methodology of preventing the generation of acid drainage by applying ferrate (VI) to acid generating materials prior to the disposal in impoundments or piles. Oxidizing the pyritic material in mining waste could diminish the potential for acid generation and its related environmental risks and long-term costs at disposal sites. Preliminary results presented in this paper show that the oxidation of pyrite by ferrate has half-life of about six hours. The stability of Fe(VI) in water solutions will not influence the reaction rate in a significant manner. New low-cost production methods for making liquid ferrate on-site makes this technology a very attractive option to mitigate one of the most pressing environmental problems in the mining industry.

Introduction

The operation of uranium mining and milling plants may give rise to huge amounts of wastes from both mining and milling operations. Terrestrial deposition is the predominant method of disposal for waste-rock and tailings. When pyrite is present in these materials, the generation of acid drainage may take place and result in the contamination of underground and superficial waters through the leaching of heavy metals and radionuclides (Fernandes et al., 1996). The acid generation process may continue long after the cessation of mining operations. Clean up costs can run into the millions of dollars per site.

Fernandes et al (1996) proposed that the mechanisms summarized in figure 1 may take place in the tailings pond environment: 1) wastes are introduced in the tailings dam along with an alkaline solution (pH ~ 10); 2) the solution moves downward to the base of the dam; 3) oxygen diffuses trough the tailings being the residual pyrite oxidized in this region. Pyrite oxidation generates acid solutions that will remove metals and radionuclides from the solid phase; 4) when the acid solution reaches the zone of the tailings in which the waters are alkaline (interface) the precipitation of the transported soluble species will take place. This region may be considered the neutralising zone.

Elberling et al (1994) reported that high oxidation rates are observed in the initial time after tailings deposition. During this initial period of high rates, an apparent shift occurs from kinetic to diffusional control over a period of time that depends on the composition and properties of the tailings. Based on simulation results the authors suggest that the overall rate of oxidation after a few years will be controlled dominantly by the diffusion of oxygen rather than by biological or non-biological kinetics in the tailings.

The thickness of the oxidation layer can be estimated by means of mathematical calculations if the Intrinsic Oxidation Rate (IOR) (Ritchie, 1995) is known. A net acid production in sulfidc tailings of 6.8 mol $H^{+}.m^{-3}$ has been reported (Snodgrass et al. 1982). This rate can be converted to IOR if pyrite oxidation reaction is taken into account as reported in equation 1.

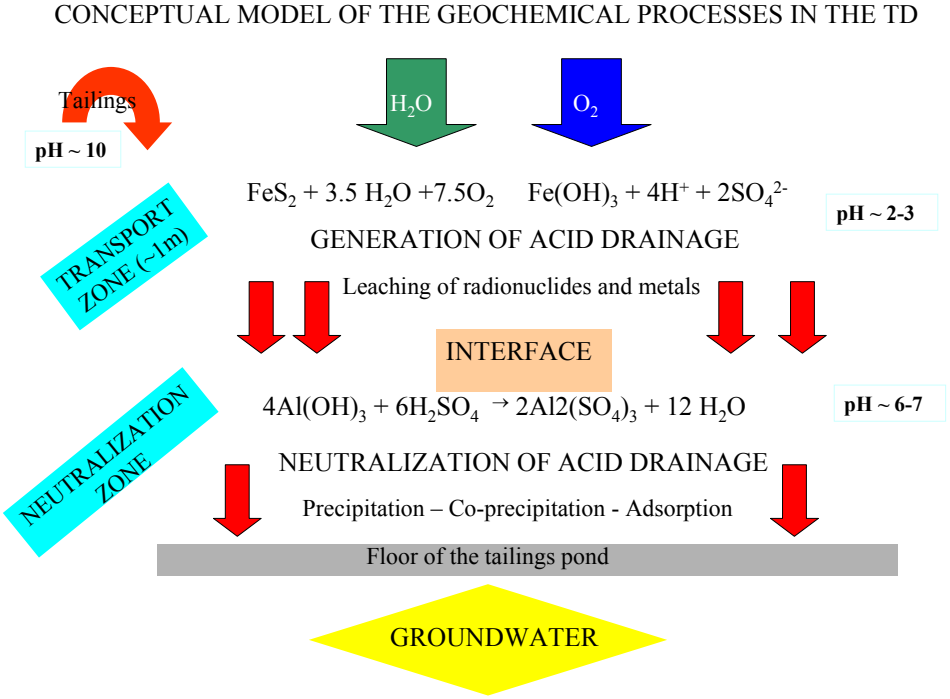

Fig.1. Basic geochemical processes occurring in the tailings environment

$$FeS_2 + 3.5\ H_2O + 3.25\ O_2 \rightarrow Fe(OH)_{3(am)} + 4\ H^+ + 2SO_4^{2-} \quad (1)$$

A value equal to 1.20 x 10^{-8} kg(O_2).m^{-3}.s^{-1} would be achieved. Elberling et al. (1994) reported a oxygen diffusion coefficient equal to 1 x 10^{-7} m^2.s^{-1} for well drained tailings. Under these assumptions, the thickness of the oxidising layer can be calculated by means of equation 2 as proposed by Ritchie (1995):

$$X = \sqrt{\frac{2DC_0}{IOR}} \quad (2)$$

Where, D = diffusion coefficient (m^2.s^{-1}); C_0 = air oxygen concentration (mg.m^{-3}); IOR = Intrinsic Oxidation Rate ($kg_{(O2)}$.m^{-3}.s^{-1})

A value of 2.0 m would be achieved for X. This value is very close to the oxidising layer thickness suggested by Fernandes et al (1996) for the tailings of the Poços de Caldas mining site This layer represents the acid generating portion of the tailings. The time T for all the pyrite present in the tailings be consumed would be achieved by means of equation 3 (Ritchie 1994):

$$T = N\varepsilon\rho_{rs}/IOR \quad (3)$$

Where, N = number of oxidizing layers; ε = mass of oxygen consumed per unit of sulphur oxidized mass; ρ_{rs} = sulfur density in the form of pyrite ($kg.m^{-3}$).

As in the case of the Poços de Caldas, N would be equal to 10 (10 layers of 2.0 m), and it would take about 200 years for all the pyrite present in the tailings be consumed if oxygen could diffuse throughout the tailings accumulated in the tailing pond.

Remedial Actions

So far, most of the strategies dealing with acid generation from mine wastes have focused on the inhibition of the catalytic oxidation of Fe^{2+} since, in the absence of such catalysis, the oxygenation rate of Fe^{2+} is too low to be of any consequence in the formation of acidity. Another possibility frequently considered is the exclusion of oxygen through sealing of the system, which is economically infeasible in most cases. A further method proposed by Belzile et al. (1997) is the use of passivating agents in order to create reversible interactions protecting and altering the surface of pyritic solids. They claim that the use of passivation (especially with pre-oxidation) proved to be effective.

The remediation scheme, considered to be able to reduce the acid drainage generation of the Poços de Caldas tailings dam to marginal environmental levels, was discussed by Leoni et al (2004). The application of a dry cover was selected as an operationally feasible strategy.. The total area to be covered would be 1.86×10^5 m^2 and accordingly to MEND (1995) costs associated with the selected remediation strategy would vary in the range of US$ 5 - 10 million

Use of Ferrate (VI) as an Oxidant

Ferrate(VI) is a powerful oxidizing agent in aqueous media. Under acidic conditions, the redox potential of Ferrate(VI) ion is the highest of any other oxidant used in wastewater treatment processes (Sharma, 2002) The standard half-cell reduction potential of ferrate(VI) has been determined as +2.20 V to + 0.72 V in acidic and basic solution, respectively. Ferrate (VI) exhibits a multitude of advantageous properties; as a disinfectant, flocculant, and coagulant based on its higher reactivity and selectivity than traditional oxidant alternatives (Sharma, 2002).

Murshed et al. (2003) used solid potassium ferrate (VI) to oxidize sulfide mine tailings but highlighted the necessity for ferrate manufacture to become economically feasible. In fact, although different methods for the production of ferrate (VI) have been developed in the past decades, generating products of high purity, the powdered product is extremely expensive. Manufacturing a stabilized ferrate (VI) product requires numerous process steps and leads to excessive synthesis costs that are too expensive for bulk industrial use. However, a novel synthesis method for the production of liquid ferrate (VI) based on hypochlorite oxidation of ferric ion in strongly alkaline solutions has been discovered recently (USPTO 6,790,428;

September 14, 2004). This process dramatically reduces the manufacturing cost of ferrate (VI). The patented ferrate (VI) synthesis processes use inexpensive chemicals to produce a ferrate (VI) product, thus providing an economical alternative approach to treating pyritic tailings.

The advantage of this approach, i.e., oxidation of the sulfid-rich tailings by ferrate(VI)) in comparison with other remediation schemes is that it can be seen as a permanent solution, i.e., when the pyrite material is oxidized to appropriate levels, no long-term acid generation and leaching of metals from these materials will take place. This approach offers great advantages in relation to other treatment techniques that involve long-term maintenance because they do not serve as a definitive solution.

The objective of the present project is to investigate the potential of a methodology to prevent the generation of acid drainage by applying ferrate (VI) to acid generating tailings prior to their disposal in impoundments or piles. Oxidizing the pyritic tailings and diminishing the potential for acid generation will reduce the long-term issues related to the disposal of this material and will reduce environmental risks at the disposal sites. The application of ferrate would take place in a slurry pipeline during the post-treatment of tailings prior their disposal into heaps or dams.

Methodology

Acid-generating mining spoils (like tailings and waste-rock residues) are rather a complex mixture of rock-occurring minerals and different chemicals that are added to the milling process. In addition to this, in tailings samples, ferrate may be reduced in oxidation reactions irrelevant to the oxidation of FeS_2. As a result, the mechanism of pure pyrite oxidation by Fe^{6+} is important to be evaluated in a first step. In a second step, a detailed understanding of the Fe (VI) reaction with tailings will be achieved. Therefore, the goal of this research was to delineate the kinetic oxidation of pyrite by Fe (VI). The following reaction protocol was used.

Na-Ferrate solution was prepared by the mixing of NaOH, $Ca(OCl)_2$ and $FeCl_3$. Twenty milliliters of de-ionized water were added to a beaker followed by 1.0g of pure pyrite to create slurry. The diameter of pyrite grains was 50 mesh. Consequently, the specific surface area of these grains were too low to be determined reliably by BET surface area analysis (Jerz and Rimstidt, 2004).

Run solutions were prepared by combining the appropriate volume of the ferrate solution with 20 mL of distilled water. The 1 gram of charge material (pyrite) was added to each of the run solutions. The solution pH was checked before and after each run by using a Metrohm Ion Analysis pH meter Model 719 S Titrino. The slurry was continuously stirred by a Teflon-coated magnetic bar in such away to create a vortex. Standard run length was about 30 minutes. Solutions were assayed at 5 minutes intervals during a run by extracting 0.1 mg aliquots. Prior to the Fe(VI) absorbance readings in a Ocean Optics ISS-UV-VIS spectrophotometer coupled with a OOICHEM Version 1.02.00 software the samples were filtered

through a 0.45 μm Fisherbrand nylon filter to remove suspended solids wit the aid of 13 mm Syringes (one syringe and one filter used for each analysis). The reduction of Fe (VI) was monitored by means of successive measures of its absorbance at 510 nm wavelength at different time intervals The Fe (VI) concentrations were determined by using a molar coefficient of 1150 M^{-1} cm^{-1}.

Sulfate determinations were made in one of the four experiments using an adaptation of the HACH Method 8051 in which a SulfaVer® powder pillow salt containing $BaCl_2$ was added to the samples prior to the absorbance readings in the spectral band of 450 nm. A calibration curve was constructed prior to the determination of sulfate concentration in the test solution. A regression coefficient, r^2 = 0.9889 was obtained for the sulfate calibration curve.

Finally, it must be remembered that Fe (VI) is not stable. For example, Na_2FeO_4 in 50% NaOH decomposes quite slowly at room temperature and may be kept with little decomposition for a month at 0°C (Murmann and Robinson 1974). If no oxidizable substances are present in the solution, the FeO_4^{2-} reacts with water over a period of an hour or less depending on the temperature and pH, and liberates molecular oxygen.

In order to examine the stability of the ferrate solution, a same amount of ferrate solution was added to a beaker containing only distilled water and the absorbance of Fe (VI) was monitored over time

Results and Discussion

Ferrate Stability

Fig. 2 shows the variation of Fe (VI) relative absorbance with time in the reference solution (distilled water + ferrate). The observed points in the graphic fit the linear equation y = -0.2813 x + 36.90 where y and x are the relative absorbance and time, respectively. The value of r^2 for this curve is 0.9684. The intercept represents the relative absorbance value at t = 0, i.e., 100%. After one hour, 50% of the initial content of Fe(VI) in solution was converted to Fe (III).

Fig. 3 shows the plots of ln $[Fe^{6+}]$ versus time for each of the runs. After 30 minutes the absorbance of Fe^{6+} could no be measured

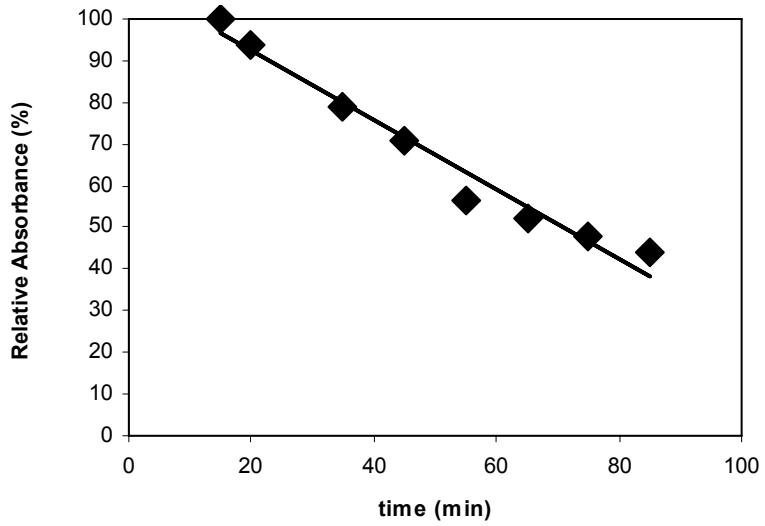

Fig.2. Variation of Fe (VI) absorbance with time.

The slopes of the of ln[Fe^{6+}] versus time plot for the three experiments were virtually the same and give a k' value of 1.0. This value for instance is practically five orders of magnitude higher than those reported for the oxidation of pyrite by Fe^{3+} (pH 2 and $mFe^{3+} = 10^{-3}$) (Wiersma. and Rimstidt1984) showing that the Fe^{6+} reduction of pyrite is far more efficient in the conditions of this work in comparison to the prevailing ones in their investigation (pH 13 and $mFe^{6+} = 10^{-2}$)

Amount of `Pyrite Consumed in the Reaction

The oxidation of pyrite can be evaluated by the production of sulfate. Sulfate concentration was measured in the test solution in one of the experiments. Care was taken to account for the initial sulfate concentration of the solution when pyrite was added to water. It was found that 72.81 mg (7.6×10^{-4} moles) of SO_4 were produced during the experiment. It corresponds to 0.024 g of sulfur. If it is taken into account that in this particular experiment the original concentration of sulfur was 0.67 g (present in pyrite) it can be inferred that 3.6% of pyrite was destroyed in about 30 minutes. On the other hand 1.0×10^{-3} moles of Fe^{6+} were consumed in the process of pyrite oxidation. It can be roughly estimated that 0.027 moles of Fe^{6+} would be necessary to destroy 100% of the pyrite in the system (0.0105 moles of FeS_2). This gives us a relation of 3 moles of Fe^{6+} for approximately 1 mol of pyrite. A relation of 1:5 has been previously proposed (Murshed, et al.2003). Just for comparison, the ratio of Fe^{3+} to FeS_2 is 14 to 1 in the oxidation reaction of pyrite by Fe^{3+} (Wiersma. and Rimstidt, 1984).

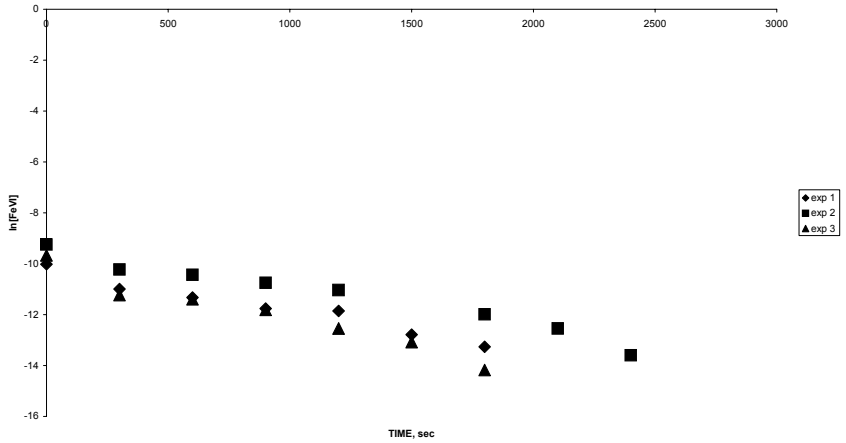

Fig.3. Plot of ln [Fe^{6+}] versus time (in seconds) for the three runs (25°C, pH 13.0). The first data point corresponds to concentration of the solution before the addition of pyrite at time = 0).

Application to the Pocos de Caldas Mining Site

Fernandes et al (1996) reported that the amount of tailings deposited in the tailings dam of the Poços de Caldas uranium mining site during 15 years of operation was about 1.89 x 10^6 tons of tailings. These authors also report that the average concentration of pyrite in these tailings is about 0.2%. As a result of the geochemical processes pictured in figure 1, the concentrations of radionuclides and heavy metals in seepage waters made it necessary the treatment of the liquid effluents leaving the tailings dam.

According to the preliminary results reported in this work, it can be estimated that about 4,840 metric tons of Fe(VI) (1.61 x 10^5 m^3 of ferrate solution) would have been necessary to oxidize the total amount of pyrite contained in the Poços de Caldas tailings prior to their deposition in the tailings dam, i.e., if the whole amount of tailings were to be treated.

However, it was demonstrated above that it would not have been necessary to treat the total amount of the deposited tailings. Only the layer with a thickness of 1 to 2 m does contribute to the acid generation.

Taking this picture into account as well as the costs associated with the application of other remediation strategies the oxidation of pyritic tailings with Fe(VI) shows a great potential to be used in the abatement of acid generation in sulfide rich tailings especially if well planned remediation schemes are put in place.

Conclusions

The preliminary results presented in this paper represent the first step in the description of the mechanism and rate law equation of the oxidation of pyrite by Fe (VI), which is a very important issue in the planning of sulfide rich tailings treatment. It could be demonstrated that the half-life of the reaction of pyrite oxidation by Fe(VI) is about 6 minutes, which is significantly less than the time needed to reduce 50% of the Fe (VI) by water. This issue is very important because it allows for different adjustments in the ratio of solid to liquid phases in the treatment slurry.

Future steps of this research involve the determination of the real reaction rate and examine the dependency of the reaction rate with pH and temperature. After the understanding of the overall mechanism of FeS_2 oxidation by Fe (VI) tailings samples will be assayed and the economic feasibility of the oxidation of pyritic tailings by ferrate will be assessed.

The stoichiometry of the oxidation reaction seems to be 1 mol of FeS_2 to 3 moles of Fe(VI). The production of ferrate by the technology used in this work represents an enormous contribution to this objective.

References

Belzile, N. Maki, S., Chen, Y.W. and Gldsack, D. (1997). Inhibition of pyrite oxidation by surface treatment. Science of the Total Environment 196: 177 -186.

Elberling, B.,Nicholson, R.V. and Sharer, J.M. (1994) A Combined Kinetic and Diffusion Model for Pyrite Oxidation in Tailings: A Change in Controls with Time. Journal of Hydrology 157: 47 - 60.

Fernandes, H.M., Franklin, M.R., Veiga, L.H., Freitas, P. & Gomiero, L.A., (1996) Management of uranium mill tailings: Geochemical processes and radiological risk assessment. Journal of Environmental Radioactivity. 30: 69-95.

Jerz, J.K and Rimstidt, J.D. (2004). Pyrite oxydation in moist air. Geochimca et Cosmochimica Acta. 68 (4) : 701 – 714.

Leoni, G.L.M., Soares, M.S. and Fernandes, H.M. (2004). Computational modeling of final covers for uranium mill tailings impoundments •Journal of Hazardous Materials, 110 (1-3):139-149

Murmann, R.K. and Robinson, P.R. (1974) : Experiments utilizing FeO_4^{2-} for purifying water. Water Research 8: 543 – 547.

Murshed, M., Rockstraw, D. A., Hanson, A.T. and Johnson, M. (2003) Rapid oxidation of sulfide mine tailings by reaction with potassium ferrate. Environmental Pollution 125: 245 – 253.

Ritchie, A.I.M (1994) Sulfide Oxidation Mechanisms: Controls and Rates of Oxygen Transport. In: Short Course Handbook on Environmental Geochemistry of Sulfide Mine-Wastes. eds J.L.Jambor & D.W.Blowes. Mineralogical

Ritchie, A.I.M, (1995) Application of Oxidation Rates in Rehabilitation Design. In: Second Australian Acid Mine Drainage Workshop. Eds. N.J. Grundon & L.C. Bell, Charles Town, 101 - 116

Sharma V.K. (2002) Potassium ferrate (VI): an environmentally friendly oxidant. Adv. Environ. Res. 6: 143-156,

Snodgrass, W.J, Lush, D.L. and Capobianco, J. (1982) Implications of Alternative Geochemical Controls on the Temporal Behaviour of Elliot Lake Tailings. In: Management of Wastes from Uranium Mining and Milling, IAEA-SM-262/43. International Atomic Energy Agency, Vienna, p. 285 - 308.

Wiersma, C.L. and Rimstidt, J.D. (1984). Rates of reaction of pyrite and marcasite with ferric iron at pH 2. Geochimica et Cosmochimica Acta, 48 (1) :85-92

Chemical Behaviour of Uranium in the Tailings Material of Schneckenstein (Germany)

Taoufik. Naamoun[1] and Broder Merkel[2]

[1]Faculty of Sciences B.P.1171 Sfax 3000 Tunisia
Former Institute of Applied Physics, T.U. Bergakademie, Freiberg, Germany
[2]Department of Geology, T.U. Bergakademie, Freiberg, Germany

Abstract. Any assessment of contaminant risks from waste material requires an understanding of ways of binding or of the specific chemical forms of trace metals in the material of study and consequently their mobility and participation in the water cycle. For that purpose, hydrochemical investigation was carried out. The distribution of uranium species and saturation indices were calculated by means of the hydrochemical model PHREEQC. Whereas, a seven steps sequential chemical extraction was the tool to define its different compound forms in the processed sediments. The data analysis shows the high uranium contents in most analysed water samples. Moreover, the mentioned above model indicates the change of the tailing sediments with depth from aerobic to post aerobic or anaerobic conditions. Also, it illustrates the presence of uranium mostly (90%) in its high soluble form $UO_2(CO_3)_3^{4-}$. This is in agreement with the results of the selective extraction procedure which proves the association of important amounts of its contents with the carbonate phase (until 24%). Moreover, as between 30 and 80 % of the non residual uranium is in association with the nodular hydrogenous fraction, the decrease of the E_h values in the study areas enhance its solubility.

Introduction

Uranium mill tailings are a high volume, low specific activity radioactive waste typically disposed in surface impoundments. Indeed, they are the crushed ore residues from the uranium extraction. Except where ores have high carbonate content, the commercial extraction of U from ores generally involves leaching with sul-

phuric acid (H_2SO_4). The effluent (termed ‘‘raffinate’’ or ‘‘barren solution’’) and tailings from the mill are discharged as a slurry to a waste-retention pond or to mined-out underground workings for disposal. As the ores typically are low grade, essentially all of the tonnage of ore processed at the mill is disposed of as tailings. Because solubilization of the uranium daughter nuclide ^{226}Ra from ore minerals in both sulphuric acid and sodium carbonate is low, the tailings remain a radiological hazard. Safe management of tailings has been the focus of regulatory and environmental research attention since the1950s (Landa, E. R., 2004). After the unification of East and West Germany in 1990, the federal government allocated approximately 13 milliards marks for the remediation and rehabilitation of former uranium mining and milling sites (Hurst and Glaser, 1998). The evaluation tailing area at the Schneckenstein site was carried out within the frame of a technical cooperation between the chair of hydrogeology of the TU Bergakademie Freiberg and the department of ecology and environmental protection of the TU Dresden (Germany).

In the present work, we focused our study on the distribution of uranium species in pore waters of the processed material by means of the hydrochemical model PhreeqC. Also, on the basis of the sequential extraction data we intend to describe the behaviour of uranium in the investigated tailings.

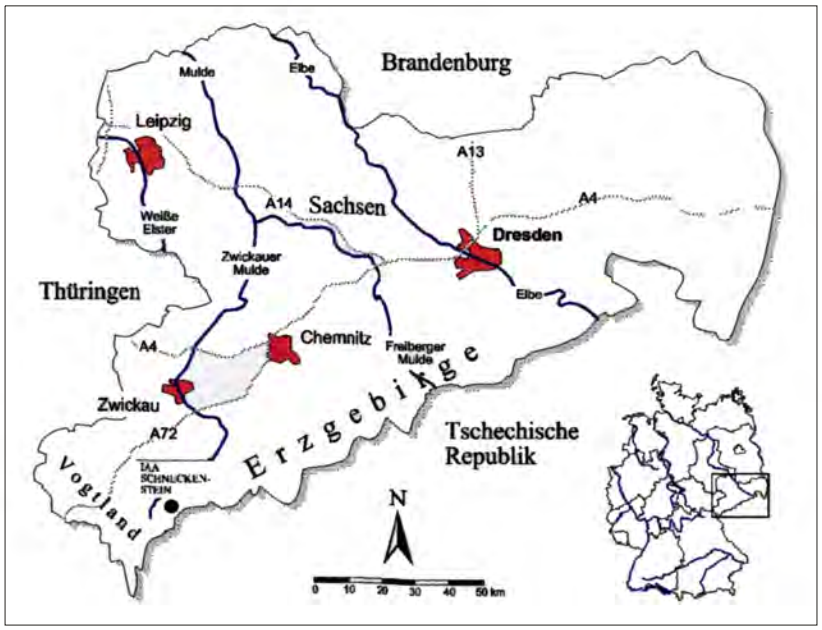

Fig.1. The area of investigation- Uranium tailings Schneckenstein

A short Description of the Site

The Schneckenstein site is located in the southwest of Saxony, in the Boda valley approximately 3 km from the village of Tannenbergsthal/county of Vogtland (Fig.1). The current surface of the site is situated at an altitude of 740 to 815 m above sea level.

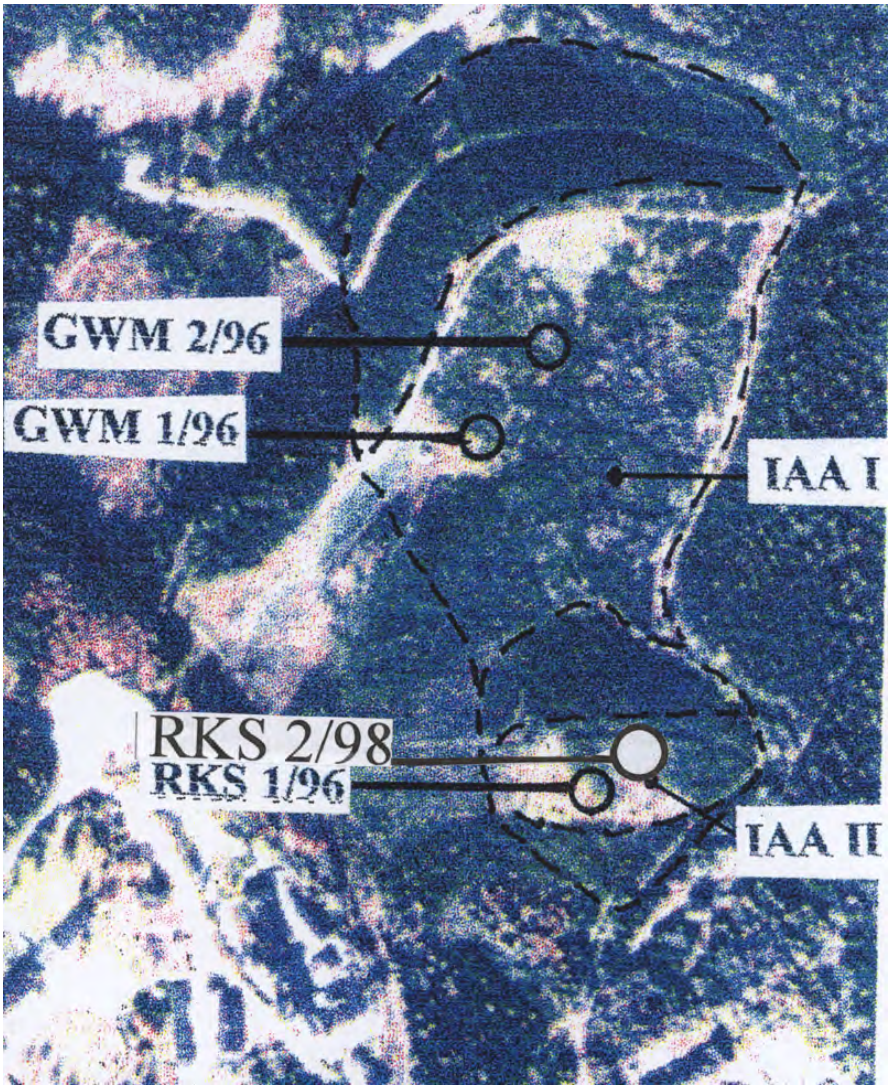

Fig.2. Location of the boreholes in the tailings sites IAA I & IAA II.

On the other hand, the uranium tailings Scheckenstein lie in the area of the watershed between the Zwickauer basin and the Eger. It belongs to the precipitation-richest of the entire Erzgebirge.

Depending on the altitude, 960 to 1160 mm precipitation fall annually (I.W. 1958) and the study area receives an average annual precipitation of 1053 mm. The mean annual temperature is 5.5 °C. The calculated evaporation is of 413 mm.

From the geological point of view, the area of investigation is located on the Southwest border of the Eibenstock granite. The Eibenstock granite could be considered a biotite-syenogranite and belongs to the group of the younger granites (JG1). It is medium to coarse-grained, serialporphyric and tourmaline bearing. Its intrusion is related to the upper Carboniferous series. The Eibenstock granite is covered with a weathered surface layer. Southwest of the investigation area follows the contact zone with quartz-schist.

Experimental Details

The investigations consist of two aspects, the field work and laboratory analyses.

Field activity and sampling

Four sediment cores were taken at the tailings sites by drilling four bore holes at different depths; two bore holes in each tailing respectively (Fig.2).

The first and the second bore hole (GWM 1/ 96; GWM 2 / 96) were drilled down to the granite foundation in Tailing 2 (IAA I). The third bore hole (RKS 1/ 96, Tailing 1(IAA II) was sunk to a depth of about eight meters, whereby the granite foundation was not reached due to technical problems. The fourth bore hole (RKS 2/ 98, Tailing1) is 12 m deep. The cores (diameter 50 mm) were cut into slices of 1 m length and transported in argon filled plastic cylinders to avoid contact with air. In the table 1, information about field activities are summarised.

Table 1. The location of boreholes in the tailings site

Location	Tailing I	Tailing I	Tailing II	Tailing II
Co-ordinate	45 3256	45 3258	45 3265	
	55 8723	558727	558703	
Depth under the deposit (m)	9.5	20.2	8	12
Filter-tube	1.00 m HDPE	1.00 m HDPE	1.00 m HDPE	1.00 m HDPE
Full-tube	9.00 m PVC	19.00 m PVC	8.00 m PVC	12.00 m PVC

Works in the laboratories

Pore water analysis

Two different procedures were used for the chemical water analysis.

Pore water extraction was conducted by mean of a high pressure device.

Due to the low permeability of the material on the one hand and the limited water content on the other, this procedure was not effective and only three samples were analysed. Directly after the extraction process the electric conductivity, the redox potential and the pH values were measured. For the trace elements determination including uranium, the water samples were filtered with 0, 2µm membrane filter then stabilised with diluted nitric acid (1ml acid/100 ml water) until a pH ~2 and finally filled in polyethylene bottles then stored in a refrigerator. For the measurement process, the ICP-MS equipment was used. The detection limit of uranium is 1µg/l.

Mixed pore water extraction

The procedure is similar to the first step of the Salomon and Forstner extraction procedure described in Salomon and Forstner, (1984) with the difference that in this time the analysed material was not crashed. The uranium concentration was determined using ICP AES equipment. Its detection limit is 81µg/l.

Sequential extraction procedure

Sediment samples characterised with their difference in mineral contents and metal concentrations were collected from the second borehole at different intervals (0,5-1,5m; 3,5-4,5m; 5,5-6,5m; 6,5-7,5m; 8,5-9,5m; 11,5-12,5m; 14,5-15,5m; 17,5-18,5m; 19,5-20,2). In order to avoid contamination, the soil sample was taken with a polyethylene spoon from the middle of each sample container. The samples were freeze-dried. They were subseque ntly ground in agate mortar until a grain-size≤63µm, homogenised and stored until needed.

The leaching procedure and reagents are shown schematically above in Fig.3. After the same DIN (DIN 38414/7) as in the last fraction presented in the diagram sited above, an aqua-regia unlocks for the entire samples from each depth interval was accomplished. Due to inaccurate uranium determination with X-ray fluorescence analysis, a fluoric acid unlock was accomplished for the entire samples. The procedure is as the following:

Into a well cleaned beaker, from each freeze dried sample, between 0.1 and 0.2g of well pulverised soil material was filled. 2.5 ml of HNO_3 with 5 ml HF were added to it. Without exhausting, the sample was two times heated for one hour at temperature of 50°C, then for half an hour at 100°C. Thereafter, it was evaporated to the dry with exhausting. After the cooling of the sample, the same volume of both acids was added to it and the same cited procedure was repeated. Then the sample was lifted by adding 2 ml of concentrated HNO_3 and shortly

heated. Finally, by adding an amount of approximately 10 ml of deionised water and heating, the concentrated precipitation was diluted. The resulting solution was filled in special bulb afterwards conserved.

To minimise losses of solid material, the selective extraction was conducted in centrifuge tubes polypropylene. Between each successive extraction, separation was effected by centrifuging at 4000 rpm. The supernatant was removed with a pipette and filled in polyethylene-bottles then analysed for trace metals, whereas the residue was washed with ~10 ml of deionised water. After centrifugation for 45 min, this second supernatant was discarded. The volume of rinse water used was kept to a minimum to avoid excessive solubilization of solid material, particularly organic matter. All reagents used in this work were of analytical grade. All glassware used for the analysis was previously soaked in weak nitric acid and rinsed with deionised water.

The uranium concentrations in the aqua-regia extracts were measured by means of ICP-AES, whereas ICP-MS was used for other fractions.

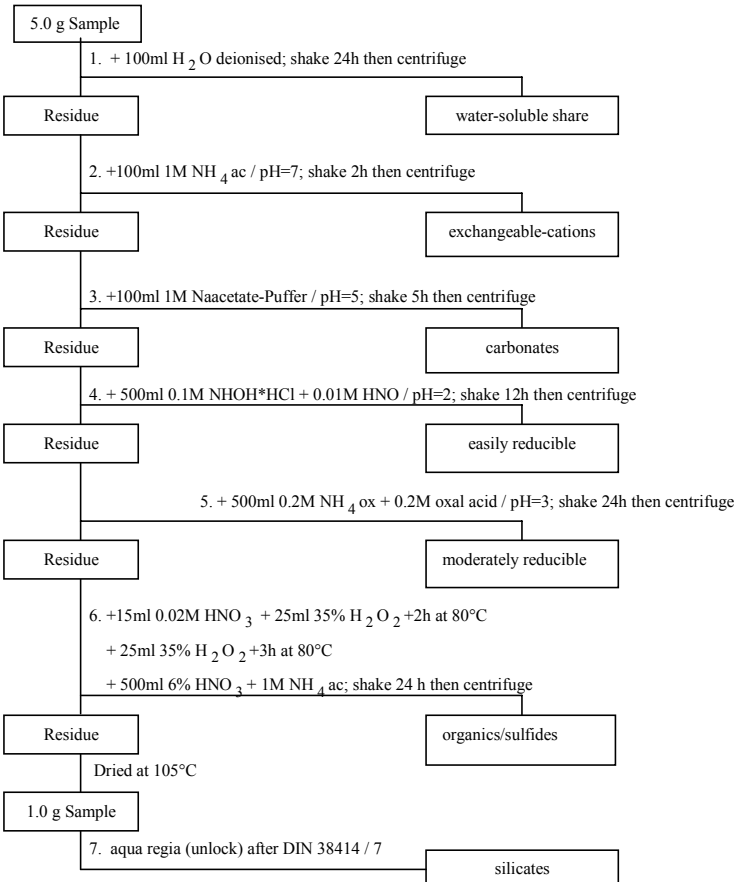

Fig.3. Sequential extraction –Scheme.

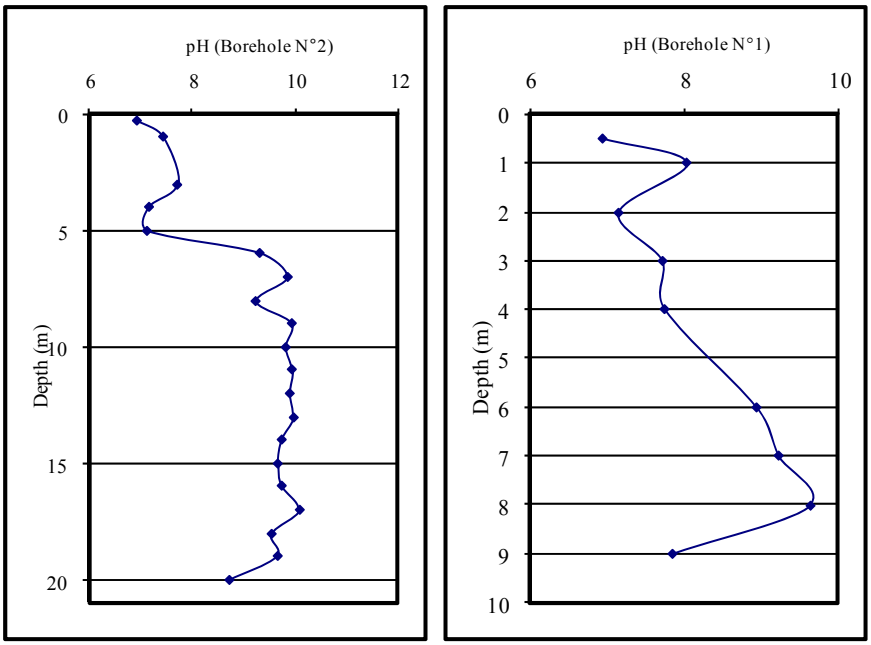

Fig.4. The change with depth of the pH value.

Results and discussion

Hydrochemical analysis and hydrochemical model

Chemistry of the porewater

Although the near neutral pH (pH~7), the uranium content is very high in all analysed samples. It increases with depth. It varies between 55 and 949 µg/l. The mean value is 423µg/l. The standard deviation is 467µg/l. Moreover, the measured E_h values are close to 400 mV. Thus, it can be concluded that for the first five meters of depth, the analysed water is in contact with well aerated untreated heap material.

Chemistry of the extracted porewater

In the first two cores, the extracted uranium content varies from 40 to 390µg/l and from 20 to 1650 µg/l with mean values of 190 and 1030 µg/l and standard devia-

tions of 150 and 520µg/l respectively. In the third and fourth ones, it differs from 340 to 1610 µg/l and from 0.5 to 4805 µg/l with mean values of 900 and 1208 µg/l respectively. The standard deviations are 600 and 1380 µg/l respectively.

The extracted uranium content is tremendously high in almost all analysed samples. This is due to the presence of uranium in its oxidised state, on one hand, and to the alkalinity of the prospected medium, on the other hand. As far as most of pH values exceed pH 8 in most tailing parts (Fig. 4), thus according to Langmuir, (1978) and Tripathi, (1979), the dissolved uranium is mostly in its mobile $UO_2(CO_3)_3^{4-}$ ionic form. In addition, with regard to the fact that most of the uranium amount is disposed to mobilisation by means of the leaching process, uranium is considered as most potential pollutant for the prospected areas.

Hydrogeochemical Model

In order to calculate the equilibrium speciation and saturation indices as well as to estimate the E_h of the chemical medium, the computer program PhreeqC (Parkhurst, 1995) windows version is used. The software is capable of simulating a wide range of geochemical reactions including mixing of water, dissolving and precipitating phases to achieve equilibrium with the aqueous phase and effects of changing temperature. It is also used to indicate mineral species and to provide estimates of element concentrations that had not been determined analytically as well as of molalities and activities of aqueous species, pH, pe, and saturation indices.

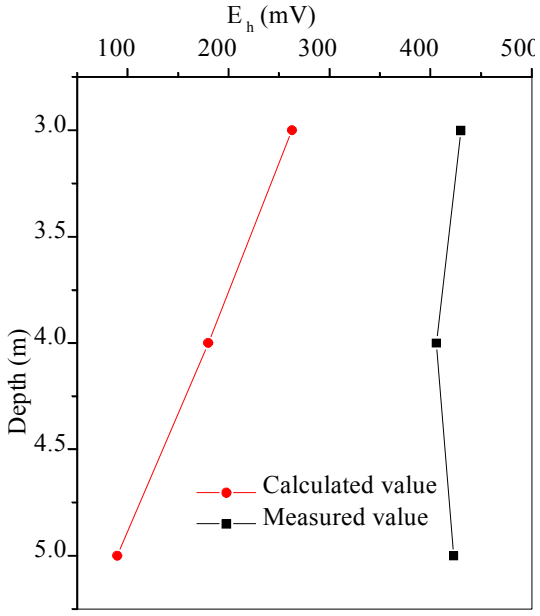

Fig.5. The change with depth of E_h; calculated and measured values.

As illustrated in the Fig. 5, for the three extracted pore water samples, the calculated Eh values are considerably lower than the measured ones. In addition, the tailings environment becomes under post aerobic or reducing conditions with depth mainly at the interval of depth that coincide with the beginning of the processed material. This is due probably to the presence of an appreciable amount of humic substances in the processed material as already mentioned above on one hand, and to the absence of any supplying of oxygen on the other. The considerable difference between the recorded and the calculated values is probably due mainly to the influence of the climatic factors onto such measurements.

Comparing the recorded values for the extracted pure and mixed pore water samples of the mentioned three sediments as demonstrated in the Fig. 6, the calculated E_h values by means of the arsenic species are considerably lower. This is due to the influence of the change of the used species for modelling on the one hand and of the added de-ionised water that affect the chemistry of the analysed sediments on the other hand. In addition, for all extracted mixed pore water samples, the recorded values illustrate the change of the chemical conditions between the heap materials and the tailing sediments characterised by the considerable decrease of the mentioned factor with depth that indicates the change of the medium to post aerobic or anaerobic conditions. Since large amounts of trace metals are bound to nodules, the anoxic conditions of the treated material favour the dissociation of such compounds i.e. the supplying of the pore water by such contaminants. The recorded results demonstrate the usefulness of the used procedure and the PHREEQC model for qualitative resolving geochemical problems.

In spite of the extreme high uranium contents in almost all analysed samples,

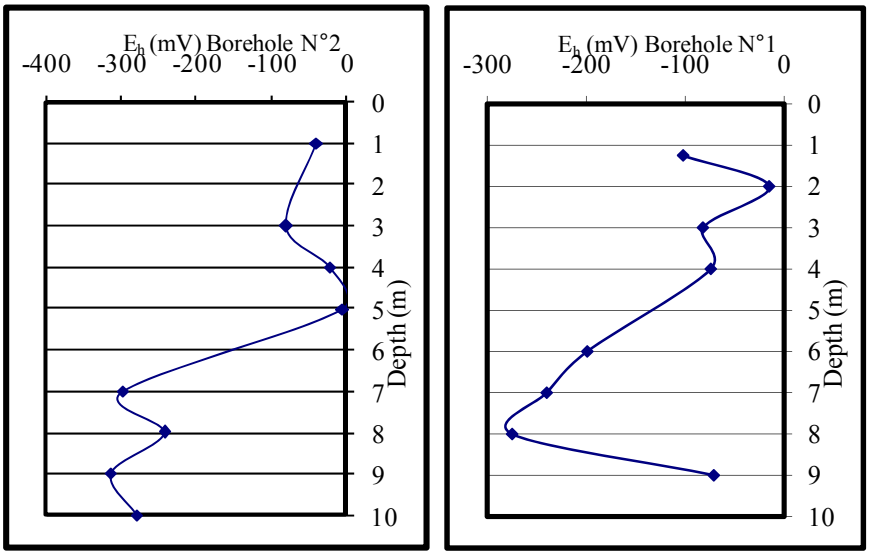

Fig.6. The change with depth of calculated E_h.

non of the mineral phase is oversaturated. In addition, all the tailing extracts show the soluble uranium only in aqueous mobile species. This is in agreement with the findings of Langmuir, (1978) and Tripathi, (1979). The $UO_2(CO_3)_3^{4-}$ specie is the dominant one, exceeding 90 % of the total aqueous uranium amount. About 10 % of the soluble uranium is shared between the $UO_2(OH)_3^-$ and $UO_2(CO_3)_2^{2-}$ species. According to Merkel and Sperling, (1998), organic substances highly absorb uranium. Therefore, although the recorded low DOC content in most samples, the mentioned substances certainly limit the mobility of uranium. In addition, the uranium carbonates are frequently negatively loaded. Consequently, the presence of clays such as chlorite and kaolinite in the tailings material causes the immobilisation of uranium through cation exchange.

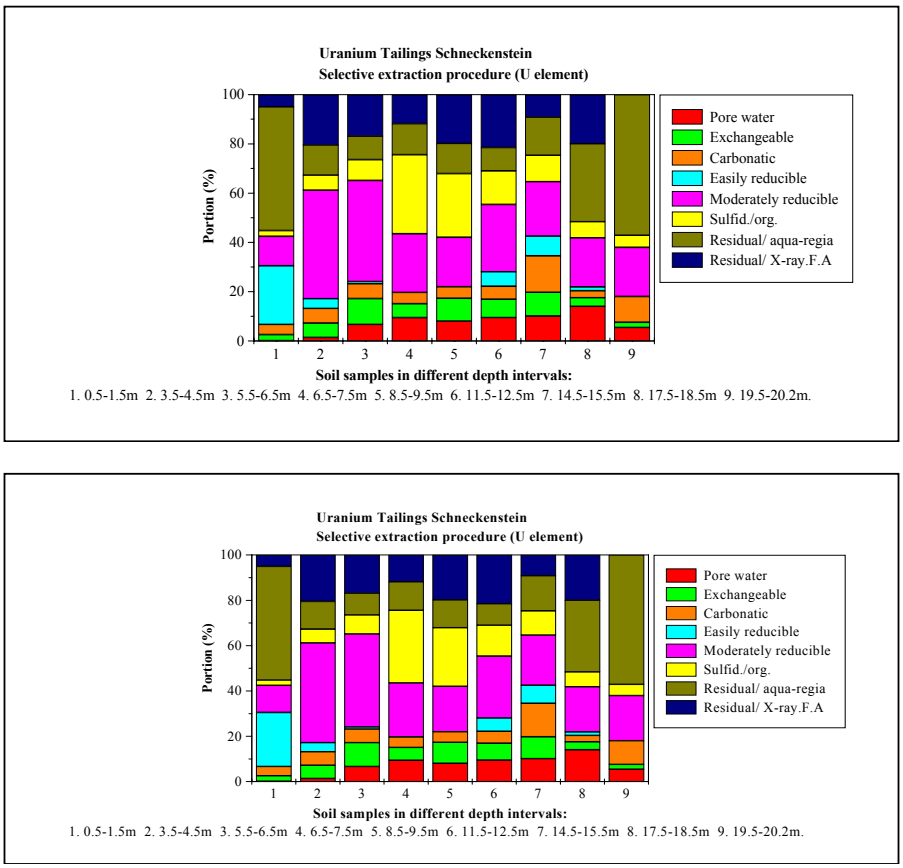

Uranium Tailings Schneckenstein
Selective extraction procedure (U element)
Portion (%)
0
20
40
60
80
100
1
2
3
4
5
6
7
8
9
Soil samples in different depth intervals:
1. 0.5-1.5m 2. 3.5-4.5m 3. 5.5-6.5m 4. 6.5-7.5m 5. 8.5-9.5m 6. 11.5-12.5m 7. 14.5-15.5m 8. 17.5-18.5m 9. 19.5-20.2m.
Pore water
Exchangeable
Carbonatic
Easily reducible
Moderately reducible
Sulfid./org.
Residual/ aqua-regia
Residual/ X-ray.F.A

Fig.7. The distribution of uranium in different fractions.

Sequential Extraction Procedure

The whole uranium content ranges from 11.8 to 225.6 ppm. Since U tends to replace Y due to some energetic similarities (ionic size, charge, electronegativities, etc.); association with some minerals such as feldspars chlorite, hornblende and biotite, by different mechanisms (isomorphous substitution in the lattice or the concentration in lattice defects; adsorption along crystal imperfections and grain borders). This is partly responsible for the association with lithogenous fraction in range 24-57 % (Fig. 7). In addition, the most of the U amount was dissolved by the aqua regia dissolution. Therefore, U is not largely attached to clays but primarily bound to resistate minerals and the greater ease of its mobilisation than that of Th. These findings are supported by the work of Pliler and Adams, (1962).

Besides, a significant amount of uranium from the non residual fraction is in association with the sulphide-organic phase. It varies between ~ 5 to 42 %. This is due to the intensive absorption of uranium from water essentially in reducing environments by humic substances (Szalay, 1958; Armands and Landergren, 1960; Boyle, 1982) and to the uranium precipitation by reduction from its hexavalent state in sulfide-rich sediment as well (Van Wambeke, 1971).

Further, because an appreciable amount of U is often in association with biotite (Boyle, 1982); the frequent association of uranium with hematite in reducing environments (Van Wambeke, 1971) and its tendency to be adsorbed and coprecipitate by hydrous ferric oxide and manganese dioxide fractions (Boyle, 1982), results in a considerable mass from the non residual uranium with the nodular hydrogenous fraction mostly in a moderately reducible phase ranging between 30 and 80 %. This is may be due to the widely spread iron oxides and hydroxides resulting from the abrasion and dissolution of iron minerals such as biotite and hematite during the mineral processing in the area of study.

Furthermore, since uranium forms very stable complexes with carbonate ion in forms of $UO_2(CO_3)_3^{4-}$ and $UO_2(CO_3)_2^{2-}$ complexes at pHs equal or above 8; then the degassing of CO_2 tends to coprecipitate $UO_2CO_3^0$ with other minerals (Gascoyne, M., 1992). Based on the alkalinity of the environment a considerable amount of its non residual fraction ranging from ~ 6 to 24 % is associated with the carbonate phase.

In addition, an important amount of the non residual U varying from ~ 5 to 14 % is associated with the exchangeable. This is attributed to the presence of most of the soluble uranium in its $UO_2(CO_3)_3^{4-}$, $UO_2(OH)_3^-$ and $UO_2(CO_3)_2^{2-}$ ionic forms (Langmuir, 1978 and Tripathi, 1979) which increases the exchangeability of uranium with clays such as chlorite and kaolinite, and the ability of U to substitute for calcium in some minerals.

The non residual uranium associated with the pore water phase ranges from ~ 0.5 to 29 %. Besides, the presence of chemical components such as: sulphate, chloride, nitrate, carbonate, phosphate, or humic matter in the interstitial waters together with the pH value of the medium control the uranium species in the water phase. Thus due to the low content of most of the mentioned components in the tailings material except carbonates and the alkalinity of the study environment, most of uranium associated with the pore water phase is expected to be in carbon-

ate ionic forms and mainly in the form of $UO_2(CO_3)_3^{4}$ ion (Langmuir, 1978 and Tripathi, 1979). In addition, the amount of the soluble uranium associated with the phase is found very low in the first two samples (heap material). This is attributed mostly to the near neutral pH values in the first interval.

Conclusion

The hydro geochemical model PhreeqC together with the sequential extraction provided valuable information showing the dominant uranium species in the tailing sediments as well as the chemical conditions affecting its behaviour. Of its share, the sequential extraction adds very significant information concerning the compound forms of uranium in the study area.

The considerable decrease of E_h with depth indicates the change of the study environment to post aerobic or anaerobic. 90 % of the total aqueous uranium amount is in the form of $UO_2(CO_3)_3^{4-}$ specie. The other 10 % of the soluble uranium is shared between the $UO_2(OH)_3^{-}$ and $UO_2(CO_3)_2^{2-}$ species.

High amount of the non residual uranium is in association with the soluble phases (carbonatic, exchangeable and pore water). The presence of carbonates in the tailings material together with the alkaline pHs, enhance the solubility of uranium. Also, the decrease of the E_h values in the study areas increases the dissolution of nodules; hence the solubility of uranium associated to these compounds.

Finally, the prediction of the chemical behaviour of uranium in the study environment depends on many factors such as pH -E_h conditions and the presence of iron, sulphur, carbonates and organic matter. However a decrease of E_h decreases its solubility as well its mobility.

References

Landa, E. R., (2004). Uranium mill tailings: nuclear waste and natural laboratory for geochemical and radioecological investigations. Journal of Environmental Radioactivity 77, 1–27

Langmuir, D., (1978): Uranium solution-mineral equilibria at low temperatures with applications to sedimentary ore deposits. Geochim Cosmochim Acta, 42, 547-570.

Tripathi, V. S., (1979): Comments on Uranium solution-mineral equilibria at low temperatures with applications to sedimentary ore deposits. Geochim. Cosmochim. Acta, 43, 1989-1990.

Parkhurst, D. L., (1995): PHREEQC, a computer program for speciation, reaction-path, advective-transport, and inverse geochemical calculations. Water-resources Investigations report 95-4227. Lakewood, Colorado.

Merkel, B. and Sperling, C., (1998): Hydrogeochemische Stoffsysteme II. DVWK-Schriften H. 117

Pliler, R. and Adams, J.A.S., (1962): The distribution of thorium and uranium in a Pennsylvanian weathering profile, Geochim. Cosmochim. Acta, **26**, 1137-46.

Szalay, A., (1958): The significance of humus in the geochemical enrichement of uranium. In: proceed. 2nd U. N. Inter. Conf. Peaceful Uses Atomic Energy, Vol. 2, Survey of raw material resources, Geneva, 182-186.

Armands, G. and Landergren, S., (1960): Geochemical prospecting for uranium in northern Sweden: The enrichment of uranium in peat; in: Noe-Nygaard, A. et al. (eds.). Genetic problems of uranium and thorium deposits, 21st Inter. Geol. Cong., Copenhagen, 51-66.

Boyle, R. W., (1982): Geochemical prospecting for thorium and uranium deposits, Develop. Econ. Geol., 16. Elsevier-Scientific Publ Co, Amsterdam-Oxford-New York, 498 pp.

Van Wambeke, L., (1971): The geology of uranium and thorium. In: Lesmo, R. (ed.). Report of the session Part II (1969), The geology of uranium and thorium.E.N.I. – Scuola Enrico Mattei (Italia).

Gascoyne, M., (1992): Geochemistry of the actinides and their daughters. In: Ivanovich, M & Harmon, R. S. (eds.). Uranium- series disequilibrium. Clarendon Press. Oxford. 910 pp.

DIN 38414, Part 7: Deutsche Einheitsverfahren zur Wasser-, Abwasser- und Schlammuntersuchung. Aufschluß mit Königswasser... Beuth- Verlag Berlin Köln. Germany.

Salomons, W. & Forstner, U., (1984): Metals in the hydrocycle, Springer Verlag, Berlin-Heidelberg, 349 pp.

Institut fur wasserwirtschaft, (1958): Abflußhöhen- u. Niederschlagskarte f. das 20jährige Mittel (1921-1940), Karl-Markx Stadt, M 1: 200 000 Institut f. Wasserwirtschaft Berlin. Hurst, S. and Glaser, K., (1998): Uranbergbausanierung-eine Herausforderung an die Fachgremien, Uranium Mining and Hydrogeology II, Proc. Of the Intern. Conference and Workshop, Freiberg, Germany, Verlag Sven von Loga, Köln.


Uranium Mining
and Hydrogeology

Impacts of Uranium Mining on Environment of Fergana Valley in Central Asia

Isakbek Torgoev, Yuriy Aleshin and Gennadiy Ashirov

Institute of Physics and Rock Mechanics, 98 Mederova Str. Bishkek, 720017,
E-mail: geopribor@mail.ru

Abstract. After collapse of the USSR and curbing of uranium extraction numerous pits, mines, waste dumps and tailings remained in the territory of Fergana valley in Central Asia. These objects pose a serious threat to the environment and population of the region. This paper considers the most problematic areas (hotspots) where various components of the environment are systematically polluted with radionuclides and toxicants.

Introduction

Fergana valley is an extraordinary region of Central Asia from political, social, economic and environmental perspective. It is one of the most densely populated regions in this part of the world. Today over 10 mln. people live in the valley. The highest density of the population is up to 500 people per 1 km^2 in specific areas. Mining and processing companies operating on the basis of mineral deposits such as uranium, mercury, antimony, gold, lead, zinc, coal, oil and etc. have been the leading industries in the valley for a long period of time (Fig. 1).

The territory of Fergana valley has been one of the main mineral resources bases of natural uranium for former Tzar Russia and USSR (Torgoev et al. 2002). During 1942-1998 over dozens of uranium pits extracting and processing ores of so called Fergana type had been operating in border areas of Kyrgyzstan, Tajikistan and Uzbekistan, within mountainous framing of the valley. These ores are formed through processes of hydrogenous epigenetic stratal oxidation of cavernous permeable limestones of Paleogenet age. Huge volume of radioactive wastes stored in waste dumps and tailings have been inherited from operation of uranium pits for many years. Under conditions of arms race and due to momentary interests of military and industrial complex of the USSR these waste tailings were placed on the surface of collecting areas, often directly in river-beds and flood-lands flowing into densely populated areas of Fergana. Due to these reasons tailings represent long-term threat to welfare of people living not only within the tailings

location, but also at some significant distance, in places of dissipation and accumulation of the river flow in densely populated flat areas of the valley (Torgoev and Aleshin. 2003).

The main body of this paper contains evaluation of impact of uranium tailings on the environment of the region under consideration.

Description of Natural Conditions of the Region

Fergana valley is intermontane trough located on the western extremity of Tyan-Shan mountain system. Flat area of Fergana trough of 22 thous km^2 is framed by mountainous ridges formed of secondary Neozoic and partially Paleozoic strata (limestones, shales). The valley is filled with heavy alluvial sediments from numerous rivers of mudflow risk flowing into the valley.

The major water-ways cutting the trough are rivers Syrdariya, Naryn and Karadarya related to closed basin of Aral sea. Resources of surface water of Fergana valley are formed of total influx of Naryn and Karadarya rivers and shallower right-bank and left-bank inflows. These resources on average amount to 25 km^3 per year; its larger part (21 km^3) is spent for irrigation of agricultural lands through numerous channels. It should be noted that water resources of Fergana valley, specifically its dissemination in terms of area and time, act as a dominating factor of policy, economy and ecology of the region.

The climate of the valley is moderately continental, typical for semi-arid zone with sharply hot summer and comparatively cold winter. Average temperature of July month is 25 – 28^{0}C; of January - from – 1 to – 3^{0}C. Precipitation in the flat area is from 100 to 400mm. per year. During the last 15-20 years substantial

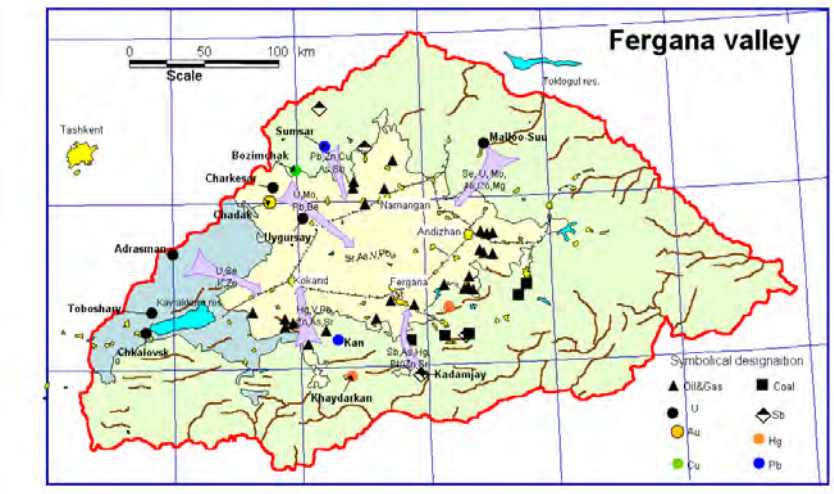

Fig. 1 Uranium and other mining processing location on the territory of Fergana Valley

change of climate both in flat and mountainous area of the trough, accompanied by aggravation of dangerous natural processes and phenomena, has been observed.

Geological, tectonic and climate features of the region pre-determine high risk of dangerous geological processes, especially in sub-montane and mountain areas of Fergana trough, where uranium pits are located. The most dangerous processes and phenomena include earthquakes, landslides and avalanches, mudflows and floods, glacial lake outburst floods. Due to specific mountainous framing (relief) of the valley destructive processes such as landslide or accident at tailings located in narrow valleys of mountainous rivers may lead to (Domino effect) ecological catastrophe of regional scale (Torgoev et al. 2005).

History of Uranium Prospecting and Extraction in Fergana Valley

The date of first findings of radioactive uranium minerals discovered in the mountain framing of Fergana valley is close to the date of discovery of radium by the Curies in the end of XIX century (Torgoev and Aleshin 2003). A source of these findings was Tuya-Muyun mining pit ($\varphi = 40^0\ 22`$ N, $\lambda = 72^0\ 35`$ E), where during 1907-1913 over 820 thous. tons of ore, called "tuyamunit" had been extracted. The composition of this ore is expressed in the following formula: $Ca(UO_2)_2(VO_4)$ n H_2O (n = 4 – 10).

Geological exploration works in Fergana valley started in 1922. By 1940 Soviet geologists discovered four new uranium deposits in Taboshar (1925), Mailuu-Suu (1934), Uigursai (1938) and Adrasman (1940). In the beginning of 1940-ies of XX century due to increased military use of atomic energy a boom of uranium mining is observed in this region. At the same time large-scale uranium exploration works were carried out, which led to discovery of dozens uranium deposits, mainly confined to outcrop of Paleogene limestones, framing northern and eastern side of Fergana valley (Adrasman, Kyzyljar, Charkesar, Shekaftar, and etc.).

In November 1942 in the very beginning of works under Atomic Project, the Government of the USSR made a decision to expand extraction and processing of ores of Taboshar deposit that had been started in 1926. During 1944-1945 commercial production of ores of Mailuu-Suu deposit was launched. In 1947 on the basis of Fergana deposits Leninabad Mining-Chemical Factory (LMCF) was built in Chkalovsk city in record-breaking time (Fig. 1). LMCF supplied the first Soviet uranium to the military industry of the country. Up to about mid-1950s enterprises of the LMCF, including hydrometallurgical factories (HMF) in Mailuu-Suu town, processed rich uranium ores and concentrates supplied from Eastern Germany, Chekoslovakia and Bulgaria.

Uranium ores were extracted and processed at LMCF in Fergana valley up to 1998. Collapse of the USSR and political, social and economic crises in newly independent states of the region resulted in chaotic dismantling of uranium extraction in the region and gave birth to a complex of serious environmental problems. The most serious of such problems was environment pollution in the areas of waste burial. This specifically related to the first post-war tailings that were exploited in Mailuu-Suu, Taboshar and Gafurov at the initial stage (1945-1955) of

atomic industry development. At this stage environmental danger caused by radioactivity of extracted and processed uranium raw and its wastes was seriously underestimated. Dozens of years later such myopia coupled with mistakes and errors in selecting a place for wastes burial, exploitation, conservation and recultivation of waste dumps and tailings resulted not only in worsening of environmental situation in the areas of wastes burial, but also in threat of breaking-out of radionuclides along the furcated hydrographic network of rivers and channels of the region. Analysis of the major ecological problems related to environment pollution in the "hotspots" of Fergana valley is provided below.

Hotspots of Fergana Valley

As a result of multi-year operation of mining ores in various areas of Fergana valley, 94 mln. tons of mine waste and low grade ores with up to 0.02% of uranium content have been accumulated in the dumps formed due to underground mining. Over 80 mln. tons of mine refuses piled in tailings were formed due to chemical processing of uranium ores at HMFs. There are 34 uranium tailings in the valley. These tailings are located in Mailuu-Suu, Adrasman, Gafurov, Taboshar and Chkalovsk (Degmai) towns and are the most problematic areas (hotspots) of Fergana valley. Ecological problems, in particular, sources of environment pollution and potentially possible devastation of tailings in the area near Mailuu-Suu town have been detailed in a number of publications (Aleshin et al. 2002, Aleshin and Torgoev 2005, Torgoev et al. 2002).

The most unfavorable ecological situation in the territory of Tajik part of Fergana valley is observed around Taboshar village ($\varphi = 40^0\ 34`$ N, $\lambda = 69^0\ 38`$ E), where uranium ore was first extracted in 1926 and the first HMF in the region was launched in 1942. Uranium ore was extracted by mining method (underground and open), whereas after 1975 – by underground leaching (mines # 5 and 7). Upon closing down of the mining pit and HMF mines, pits and dumps of total volume of 34 mln.m^3 and of 610 thous. m^3 area, as well as tailings of total volume of 7.7 mln. m^3. and of 576 thous. m^2 area remained near Tabosahr village where over 11 thous. people live. On top of all, due to accident at the tailing located in Sarysmahlysai tract radioactive wastes were re-laid on the area of about 100 thous. m^2. Non-recultivated dumps of Lean Ore Factory (LOF) of 2 mln. tons weight pose a serious threat due to their erosion and leaching by rainwater. Table 1 contains results of gamma and alpha-spectrometric analysis of wastes samples in Taboshar performed in June 2006 (Yunusov 2007). Table 1 demonstrates increased content of radionuclides comparing with established indicator of total alpha-activity for soil amounting to 600 Bq/kg is observed.

Drainage waters from tailing, tapering out as springs pose a special problem in Taboshar. IAEA experts found springs with high content of sulphates (9,2 – 9,6 g/l) hydrocarbonates (1,8 g/l), as well as dissolved uranium and other radionuclides of uranium-thorium series at the foot of the tailings # 1 and 2. Total alpha-activity of drainage waters is 1200 – 1500 Bq/l, whereas concentration of the sum of uranium nuclides U^{238} and U^{234} reach 1110 – 1450 Bq/l or 50 – 70 mg/l of

weight concentration which is close to concentration of industrial solutions of uranium. Under conditions of arid climate drainage waters form sulphate complexes of concentrated uranium with its content up to 12-15 thous. Bq/kg along the banks of streams (Yunusov 2007). Drainage waters of the tailings leaking through dams and beds of facilities pollute the surrounding territories and nearby streams. The situation is exacerbated by the fact that local citizens due to lack of water in the region organized livestock watering in this area and its pasture on the areas adjacent to springs and streams. In the territory of the tailings coated in 1980 by a layer of neutral soil, citizens set up vegetable gardens; near this territory, within the boundaries of sanitary protective zone citizens started building houses using materials of the dumps. Finally degradation and devastation of protective drainage facilities of the tailings and dumps led to breaking-out of radionuclides into the environment of the area and their dissemination toward Syrdarya river through the surface waters. Table 2 contains data about levels of radiation pollution in the area of industrial objects and residential zone in Taboshar village (Yunusov 2007).

As Table 2 demonstrates in general, large concentrations of radon in the air of industrial objects are not high, however exhalation of radon from the tailings' surface exceeds the established standard indicating to insufficiently reliable coating of this area with neutral soil (gas sealing). It is well known that the most dangerous radionuclide for the human health is gas exuded on all objects, i.e. radon (Table 2). This is especially relevant to the tailings, as radon discharge from the tailings exceeds 4-5 times the discharge of radon from underground workings of uranium mines due to high degree of tails decomposition.

Uranium tailings of Tajikistan located near Chkalovsk town (a capital of ura-

Table 1. Content of Natural Radionuclides ($Bq \cdot kg^{-1}$) in Samples Taken from Dumps and Tailings Located in Taboshar and Chkalovsk (Degmai) Towns

Sample collection area	U^{238}	Ra^{226}	Th^{230}	Pb^{210}	Po^{210}
LOF dumps (sample 1)	1405 ± 200	6570 ± 600	5600±1050	5885 ± 470	5350 ± 580
LOF dumps (sample 3, washing-out from the dump)	800 ± 70	1735 ± 130	1025 ± 300	1950 ± 145	1840 ± 190
Tailing 1 – 2 (sample of tails)	585 ± 60	3010 ± 240	2900 ± 530	3895 ± 290	3250 ± 370
Tailing 1 – 2 (sample of uranite salt)	12210±900	55,9 ± 27	Not found	Not found	Not found
Degmai tailing near Chkalovsk town	980 ± 100	7620±580	15600±1700	14600±1070	13200±1320

nium Fergana) pose a serious ecological threat. There are 9 tailings in this region accommodating 54.4mln. tons of wastes of uranium ore processing not only from Tajikistan, but also from other countries. The largest in Fergana valley Digmai tailing, which is referred to the currently operating tailings is located at Digmai hills, between Chkalosvk and Khodjent (Leninabad) cities. The tailing has been used since 1963: on the area of 692 thous. m^2 about 6 mln.tons of wastes of vanadium processing and almost 30 mln.tons of uranium processing are laid.

One of the major ecological problems within the area of this huge tailing is dissemination of radon and radioactive dust from its non-recultivated and dried surface. As Table 1 shows tails of this tailing are characterized by higher concentration of natural radionuclides of uranium-thorium series comparing with other tailings in the region. Table 3 present results of identification of degree of activity of radionuclides in aerosols of Tajik objects under consideration (Yunusov 2007), particularly increased content of radionuclides in the air. On top of all the Table shows that radionuclide composition of aerosols within Digmai tailing area is substantially shifted toward long-term sub-products of uranium.

Table 2. Characteristics of Radiation Pollution in Area of Dumps and Tailings of Taboshar Village

Measurement Area	Capacity of equivalent dosage of gamma rays μ.Sv h^{-1}	Volumetric activity of radon Bq m^{-3}	Radon EEVA Bq m^{-3}	Radon flux density (average) Bq $m^{-2}s^{-2}$	Thoron EVA Bq m^{-3}
Tailings # 1 and 2 on fault sections	0,4 – 0,5 to 0,8 – 0,9	45	2,57	3,8 ± 1,2 (9,9 ± 3,0)*	0,33
Tailing # 3 on fault sections	0,3 – 0,4 up to 0,6	35	8,78	-	-
Tailing # 4	0,3 – 0,5	25	3,0	4,8 ± 1,6	-
LOF dumps	0,76 – 2,8 surface 0,35 – 0,4 slopes	17	2,0	0,86 ± 0,25 1,06 ± 0,28	0,17
Pit	0,48 – 0,56	20	1,92	0,09 ± 0,03	0,23
Mountainous area located at 4-km. distance from Taboshar town	0,12 – 0,23	12	3,3	-	0,12

Table 3. Activity of Radionuclides in Aerosols of Tajik Uranium Pits

Air sample collection place	Volumetric activity of radionuclides in air, 10^{-5} Bq m^{-3}				
	U^{238}	Ra^{226}	Pb^{210}	Th^{228}	K^{40}
Taboshar	1,8 ± 1,8	1,9 ± 0,5	47,5 ± 3,4	0,5 ± 0,2	10,4 ± 0,9
Digmai tailing	3,4 ± 3,4	40,9 ± 1,7	125 ± 6,3	5,8 ± 2,3	20,2 ± 1,7
HMF – Chkalovsk town	15,6 ± 22	4,8 ± 0,6	12,9 ± 6,3	0,5 ± 0,2	12,7 ± 1,1

Input of uranium isotopes into total activity of aerosols does not exceed 2%; the remaining 86% fall to the basic elements of uranium series (Ra^{226}, Pb^{210}, Th^{228}). Characteristic feature of dust formed in the area of the tailing is prevalence of radium in its content comparing with uranium, which is caused by analogous correlation of these elements in the source of dust forming, i.e. the tails (Table 1).

Content of radon (Rn^{222}) in atmospheric air in windless weather reaches 1000 Bq/m^3, whereas exhalation of radon exceeds from 10 to 60 times the standard value (Yunusov 2007). According to the estimates annual flow of radon into surface layer of the atmosphere can reach up to 31 kKu per year. Such a strong flow of ra-

Fig.2. Unreclamated surface of Uranium Digmai tailing (Tajikistan)

don into the air should form high concentrations of its decomposition products, Po^{210} and Pb^{210} within the composition of aerosols and atmospheric precipitations which precipitate on lands, including agricultural lands adjacent to the tailing. This was confirmed by measurement of specified decomposition products within a radius of 1 km. from the tailing. Results of measurements, notably 44 Bq/kg for Po^{210} and 26 Bq/kg – for Pb^{210} evidence intensive pollution of these lands with radon decomposition products.

During examination of dry condition of dust formation processes on surfaces of the tailings located in the territory of Central-Asian region, it was identified that a gust of strong wind can blow up to 1 thous. m^3 of sand and dust from the surface of tailing of 100 thous. m^2 area. If the winds in the region under consideration are often and strong (V > 2 m/s) the dust can be blown away for a long distance (kilometers) from the tailing later forming a halo of pollution of soil and agricultural lands of the region populated by 100 thous. people.

Wastes of uranium-bearing ores extraction and associated ecological problems are observed in the territory of Uzbek part of Fergana valley in Charkesar village (Fig. 1). Charkesar deposit (Charkesar-1 and Charkesar-2) was worked by underground (mountain) method, then by underground leaching. Total volume of radioactive materials buried in Charkesar in 4 dumps amounts to 415 thous. m^3, whereas area occupied by these dumps is 130 thous. m^2. During recultivation works in 1989 all dumps were coated with a layer of neutral soil, however at present coating and edges of the dumps are destroyed by rain and flood waters. A village where over 1.5 thous. people live is located nearby the mines and dumps.

Ecological problems within the area of the village are typical problems of hotspots of the region (Torgoev et al. 2005). Yet there are ecological problems affecting health of the population, in particular, people living in stone-made houses, which were built of materials from the dumps and then plastered with sand brought from the area located nearby Uigursai uranium deposit. According to the survey one half of 250 houses and public buildings in Charkesar village contains high activity of gamma rays (0,6 – 1,2 μSv/h), whereas exhalation of radon reaches 3000 Bq/m^3 (the standard value is 100 Bq/m^3).

Mine waters, streaming from mine workings pose a serious threat to citizens of Charkesar and adjacent areas. The most dangerous are waters from mine # 2 with an average water flow 3-5 l/s. Uranium was first extracted by excavation method, then by leaching, therefore micro-component composition of the water streaming to the surface is similar to technological solution injected into the mine. On the other hand the water is enriched with uranium and other mineralization. It has been identified that mine waters contain anomaly high concentration of beryllium (200 MAC), manganese (75 MAC), lead (53 MAC) and selenium (2 MAC). Concentration of radionuclides in this water amounts to 23,4 Bq/l of uranium (compare with the standard of 9,6 Bq/l), 1433 Bq/l of radon (compare with the standard of 80 Bq/l), 15,9 Bq/l of radium (compare with the standard of 0,94 Bq/l). The same “Charkesar” set of toxicants has been found in bottom sediments of streams, whereas total alpha-activity of bottom sediments varies from 35 to 80 thous. Bq/kg. Similarly to other hotspots of Fergana local population uses stream water for watering their fruit and vegetable gardens and for watering livestock.

It is not an accident that according to physicians and a number of NGOs dealing with environmental issues in the region a number of onco-diseases among people living in the areas located in the territory of uranium mines increases every year. Increased level of radioactive radiation of the population, penetration of radionuclides into the food chain of people coupled with impact of heavy metals and other toxicants cause diseases of blood-forming organs, premature deliveries and congenital malformation among infants. For instance, a number of people suffering from cancer in Mailuu-Suu town is four times higher than the average indicator throughout the country, whereas average weight of congenital malformation within the structure of infant morbidity is 2.8 times higher the average indicator throughout Kyrgyzstan (Bykovchenko et al. 2005).

Conclutions

Evaluation and analysis of environmental situation in the areas of uranium extraction and processing in the territory of Fergana valley in Central Asia show that virtually in all these areas, and especially in the areas of wastes dumps systematic pollution of various components of the environment with radionuclides and other toxic pollutants is observed. The most dangerous for the environment and the population is pollution of vitally important for the region surface waters (of rivers and streams) within the basins of which wastes are located. Pollution identified in the areas of uranium mines, pits and dumps of HMFs and tailings in Fergana valley is caused by poor gas and hydraulic sealing and gradual degradation and devastation of their protective facilities and drainage systems. Due to unauthorized access of the local population to such objects, searching for metals, construction materials and growing food products on such areas, organizing livestock watering, unsealing of old and emergence of new sources of radio active radiation and pollution is taking place. As a result negative effect of these radio-active and toxic pollutants for health of the population is observed not only in the area of their location but also at a sufficient distance from them.

Given the above it is necessary to perform a set of engineering and technical projects aimed at organizing safe and long-term isolation of radioactive wastes, rehabilitation of polluted territories within the nearest future. Not less important is conduction of sanitary-hygienic, medical-biological measures and informational campaigns aimed at increase of awareness of the population about threats and risks associated with wastes' radioactivity.

References

Aleshin Yu. G., Torgoev I.A., Shmidt G. (2002). Environmental Risk Management at Uranium Tailings Ponds in Mailuu-Suu, Kyrgyzstan. Uranium in the Aquatic Environment. Proceedings of the International Conference Uranium Mining and Hydrogeology

III and the International Mine Water Association Symposium, Freiberg, Germany; Springer. Berlin. Heidelberg.

Aleshin Yuriy, Torgoev Isakbek (2005). Long-term aspects of waste rock piles and tailings in Kyrgyzstan. Uranium in the Environment. Mining Impact and Consequences, Springer Berlin. Heidelberg.

Bykovchenko Y.G., Bykova E.I., Belekov T. et al. (2005). Man-caused Pollution of Kyrgyzstan's Biosphere with Uranium, Bishkek (In Russian).

Torgoev I.A., Aleshin Yu. G., Havenith H.-B. (2002). Impact of Uranium Mining and Processing on the Environment of Mountainous areas of Kyrgyzstan. Uranium in the Aquatic Environment. Proceedings of the International Conference Uranium Mining and Hydrogeology III and the International Mine Water Association Symposium, Freiberg, Germany; Springer. Berlin. Heidelberg.

Torgoev I.A. and Aleshin Yu. G. (2003). Ecological risk in territory uranium tailing of Kyrgyzstan. Environmental Protection against Radioactive Pollution. Birsen and Kadyrzhanov (eds). Kluwer Academic Publishers.

Torgoev I., Aleshin Yu., Kovalenko D., Chervontsev P. (2005). Risk assessment of emergency situation initiation in the Uranium tailings of Kyrgyzstan. Uranium in the Environment. Mining Impact and Concequenses, Springer Berlin, Heidelberg.

Yunusov M.M. (2005) Radiation Objects of Northern Tajikistan and Degree of Their Impact on the Environment. International Conference for Scientists and Experts to Make scientific and technical Assessment of Minkush Area Radioactive Wasters Tailings Problem under the Auspices of OSCE Centre in Bishkek (In Russian).

The Rum Jungle U-Cu Project: A Critical Evaluation of Environmental Monitoring and Rehabilitation Success

Gavin M. Mudd[1,*] and James Patterson[2]

[1]Environmental Engineering, Dept of Civil Engineering, Monash University, Clayton, VIC 3800 Australia (*Gavin.Mudd@eng.monash.edu.au)
[2]Environmental Engineering Researcher, Sydney, NSW Australia

Abstract. The Rum Jungle uranium-copper project, located south of Darwin, Australia, operated from 1954 to 1971. The poor solid and liquid waste management practices during the project led to long-lasting environmental impacts. A large rehabilitation project was undertaken in the 1980's followed by nearly 15 years of monitoring. This paper reviews the environmental performance of the project during operation, its subsequent rehabilitation and the implications of ongoing problems at the site, especially acid mine drainage and impacts on water resources.

Introduction

In the Australian mining industry, the former Rum Jungle uranium-copper project holds a special place for many reasons. It was the first project to commercially mine and export uranium (for nuclear weapons) in the 1950's, it was a major part of the post-war Northern Territory economy, it caused ongoing environmental pollution which reached many kilometres downstream, it was among the first generation of polluting former mine sites to be rehabilitated in the 1980's and this was followed by a decade-long post-rehabilitation monitoring program. It is therefore possible to assess the pollution loads leaving the site prior to and following rehabilitation, providing a unique and important case study for such mines, especially the long-term effectiveness of rehabilitating former uranium mines. Although there are numerous papers on Rum Jungle, this paper seeks to synthesize the key data and analyse it from an independent environmental perspective. The paper briefly reviews the Rum Jungle project, followed by a detailed compilation and critical evaluation of the available environmental monitoring data, giving a unique case study of the environmental performance of uranium mine site rehabilitation.

The Rum Jungle U-Cu Project – A Brief History

The Rum Jungle uranium-copper project (U-Cu) has been an important mining project in Australia, for many reasons as noted previously. This section is a brief history to understand the project, rehabilitation and environmental monitoring.

The mineral potential of the 'Rum Jungle' region, just south of Darwin, had been noted since the 1870's, primarily for Cu and gold (but nothing of interest). The region is located in the tropical wet-dry climate of northern Australia; Fig. 1.

Following the advent of the nuclear weapons race in 1945, the Australian government vigorously promoted uranium prospecting. In 1949, local pastoral owner and amateur prospector Jack White realised that his green minerals from the bed of the Finniss River were most likely U. The significance was realised, with the Australian government taking over in the 'national interest' (Lichaz and Myers 1977). By late 1951 two modest U deposits were proven at White's (U-Cu) and Dyson's (U). During 1952 export agreements were finalised for nuclear weapons. The project was owned by the Australian government, operated under contract by Consolidated Zinc (CZ, later to become CRA Ltd, now Rio Tinto Ltd) and was financed by the US-UK Combined Development Agency (CDA).

First uranium oxide (U_3O_8) production was in 1954. White's and Dyson's were mined as open cuts and were completed by late 1958, with the mill processing stockpiled U and U-Cu ore as well as a small amount of purchased U ore. In 1959, exploration discovered the Rum Jungle Creek South (RJCS) U deposit, and proved larger than White's and Dyson's combined. The RJCS site was mined over 1961-63, and allowed processing to continue at Rum Jungle until 1971.

The Intermediate Cu deposit adjacent to White's was mined by CZ over 1964-65 separate to the CDA contract and toll processed through the mill, plus a Cu heap leach experiment. The Brown's Pb-Cu-Ni-Co-Ag prospect was studied but abandoned as uneconomic due to low grades and difficult processing (Brown's 'oxide' mine was developed in 2008, a major sulphide project is expected soon).

The project was operated on a 'production' basis – environmental impacts were clearly not considered important. During the early years of operation (1954-61), tailings were discharged to a flat low-lying area (later known as 'Old Tailings Creek) adjacent to the mill, though the tailings proved highly eroded.

About 1 ML/day of liquid effluent was discharged into the Finniss River, containing acids (pH 1.5), metals and radionuclides. At times liquid wastes would disappear into holes which opened up at the Cu cementation launders for several weeks, until the area was covered and later abandoned (see Davy 1975). About 640,000 t of tailings was also discharged and covered 35 ha, with some 10-25% of these tailings having been eroded by 1984. In 1961, tailings were directed to the former Dyson's open cut, and then to White's from 1965-71.

The site was a major source of environmental pollution for the Finniss River – due to tailings and liquid waste discharges but also due to the acid mine drainage (AMD) derived from the tailings but especially waste rock dumps. The scale of the problem was identifed by the late 1950's but was ignored due to the political nature and perceived importance of the Rum Jungle project.

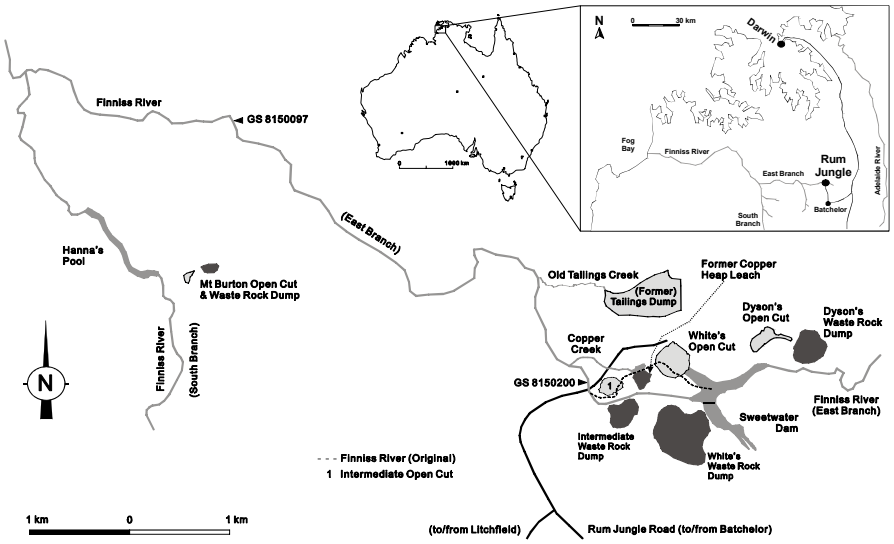

Fig.1. Location and site map of the Rum Jungle U-Cu project, Northern Territory.

After closure in 1971, no major works were undertaken to reduce pollution and by the mid-1970's Rum Jungle project was infamous for its extreme pollution, such as the absence of all biota for 15 km down the Finniss River and contamination of ~100 km^2 of floodplains (Davy 1975). The environmental legacy of Rum Jungle was also a major issue during the Ranger Inquiry (Fox et al. 1977).

The Australian government conducted major rehabilitation works over 1982-86 costing some $18.6 million. The project was amongst one of the earliest in Australia to remediate an AMD site, with the primary objectives being : (i) reduction in Finniss River pollution loads (70% each for Cu-Zn, 56% for Mn); (ii) reduction in public health hazards (including radiation); (iii) reduction in pollution loads in White's and Intermediate open cuts; (iv) aesthetic improvements and revegetation.

Although the RJCS site was ignored during the Rum Jungle program, as it was considered to have no major pollution problems, it was later found to present a public radiological exposure issue due to its popularity for recreational swimming. RJCS was then addressed with additional works in 1991 to cover the waste rock dump and achieve unrestricted public use of the site.

Given the importance of Rum Jungle as a test case for AMD remediation in mining, a major environmental monitoring program was initiated from 1986, running until 1998. The data and associated analysis of results are contained in Allen and Verhoeven (1986), Kraatz and Applegate (1992), Kraatz (1998) and Pidsley (2002), with pre-rehabilitation environmental studies given by Davy (1975).

Rum Jungle has been visited over 2004 to 2007, and still remains a major AMD pollution source to the Finniss River – despite the rehabilitation works. It is in this context that the available environmental monitoring is presented, analysed and discussed. The site remains a critical case study, providing numerous insights into mine rehabilitation, and of particular relevance for uranium mining.

Geology and Hydrogeology of the Rum Jungle Region

The geology and and hydrogeology of the Rum Jungle region is complex, with the most recent descriptions given by McKay and Miezitis (2001) and CR (2005).

Rum Jungle is on the western part of the Pine Creek Geosyncline, with regional geology comprising Palaeoproterozoic metasediments (low-grade greenschist facies) unconformably over-lying Archaean granitic basement (the Rum Jungle Complex). Surficial rocks are often intensely weathered. The Giant's Reef Fault has caused some 4-5km of displacement, leading to an embayment structure which is the location of most mineralised zones. Geologic cross-sections of White's, Dyson's, Intermediate and Rum Jungle Creek South are given by Fraser (1980).

The hydrogeology is comprised primarily of surficial weathered aquifers and underlying fractured rock aquifers of varying significance. Groundwater is found between 2-12 m from the surface, and varies with the wet-dry monsoonal climate (see Fig. 2), suggesting active recharge into unconfined aquifers and dynamic discharge processes such as transpiration or to surface water features (CR 2005). Karstic solution features in dolomite are often present. The extent of hydraulic connection between shallow and deep aquifers remains uninvestigated.

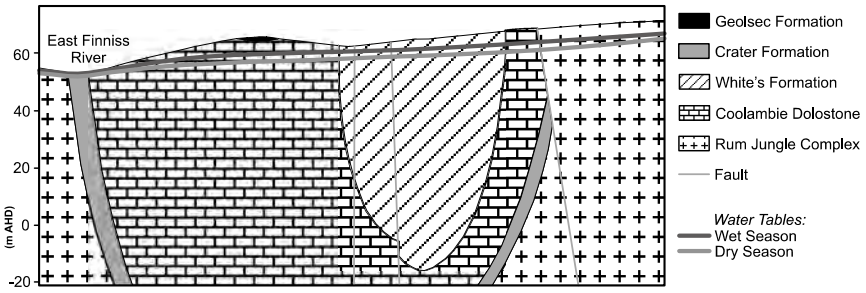

Fig.2. Hydrogeologic cross-section of Brown's area, Rum Jungle (adapted from CR 2005).

Rum Jungle Rehabilitation Project

Given the environmental significance of the ongoing pollution at Rum Jungle, the Australian government funded a major rehabilitation program from 1982 to 1986. As this was amongst the first generation of former mines with major acid mine drainage to be rehabilitated in Australia (as well as it being a former uranium mine), a decade-long environmental monitoring program was established.

Rehabilitation Measures (1982-86)

The Rum Jungle rehabilitation program was primarily aimed at reducing the metal loads reaching the Finniss River, as well as reducing public hazards. Specific components included : excavation of remnant tailings and the Cu heap leach pile for deposition into Dyson's open cut, re-contouring of waste rock dumps and construction of soil covers to limit infiltration and AMD generation, treatment of polluted waters in White's open cut, rehabilitation of the former mill and stockpile areas, and partial re-diversion of the East branch of the Finniss River and removal of the Acid and Sweetwater Dams.

Environmental Monitoring (1986-1998)

Environmental monitoring was undertaken during rehabilitation works and for some 12 years afterwards, including surface water hydrology and water quality, groundwater, biodiversity (eg. fish or macroinvertebrate surveys), waste rock dump hydrology, and sediment analyses. Sampling and analytical methodology are detailed in the four principal reports (see earlier). All results presented below are derived from these reports (unless otherwise noted). Some additional data has been included from research work (years 1998/99 to 2000/01).

No pre- and post-rehabilitation radon or gamma surveys are available, despite recent recommendations of the need for such assessments (see Pidsley 2002).

The primary point for determining the effectiveness of rehabilitation project in reducing metal loads in surface waters was set as GS8150097 (~5.6 km downstream, see Fig. 1). Monitoring has been reported as both concentration and load data, usually including metals, sulphate and pH. Analytical methods have evolved over time, such as early years being totals only, while latter years included total and dissolved metals. Despite U being a critical issue, it has commonly not been included in routine water quality analyses for all wet seasons. Similarly, radium (^{226}Ra) was only monitored for the first two wet seasons after rehabilitation.

Monitoring Results

Open Cuts

White's open cut (OC) remains a major source of pollutants, with Intermediate OC minor only. A water quality profile of White's OC is given in Table 1, and clearly shows the more polluted waters at depths below 30m. It is considered that White's OC is still contributing some 2-3 t Cu per wet season at GS8150097.

Table 1. Water quality profile of White's open cut, April 1998.

Depth	pH	DO	E.C.	Ca	Mg	SO_4	Cu	Mn	Zn	Ni	Fe	Al
m	-	mg/L	µS/cm					all mg/L				
0	6.8	6.6	157	4	13	61	0.1	0.31	0.04	0.06	0.46	0.09
5	6.5	5.9	172				0.1	0.34	0.05	0.06	0.44	0.13
10	6.1	5.3	110	3	8	41	0.1	0.32	0.03	0.06	0.35	0.18
15	5.7	5.2	115				0.1	0.46	0.04	0.06	0.19	0.13
20	5.4	5.5	151	6	11	64	0.2	0.74	0.04	0.09	0.06	0.13
25	5.4	5.4	171				0.2	0.78	0.05	0.08	0.07	0.14
30	4.4	4.6	274	12	20	137	0.8	2.45	0.11	0.23	0.13	1.88
31	4.1	3.6	458				1.3	4.42	0.18	0.37	0.21	5.2
32	3.7	0.1	993				3.1	17.65	0.42	1.01	0.87	14.8
33	3.8	0	7168				54	244	5.49	18.55	378	215
34	3.8	0	7478				60	269	7.4	16.7	404	226
35	3.8	0	7558	481	902	8270	62	254	7.75	19	420	236

Waste Rock Dumps

The infiltration target for soil covers over WRD's was set at 5% of incident rainfall (compared to ~50% previous). Although there have been technical issues with the lysimeters used to monitor infiltration, including failure of several lysimeters, the available monitoring data shows good performance initially (ie. <5%), followed by a gradual decline or increase in estimated infiltration, shown in Fig. 3.

Recent visits to the Rum Jungle site clearly show that significant infiltration rates must still be occurring, as seepage flows from White's WRD can be seen through-out the dry season (photo included in Fig. 3). Although direct sampling and analysis of this water is not available, it is known to contain U from 1 to 8 mg/L (pers. comm., Brown, 2002). It is abundantly clear that the WRD's continue to act as major pollutant sources for the Finniss River.

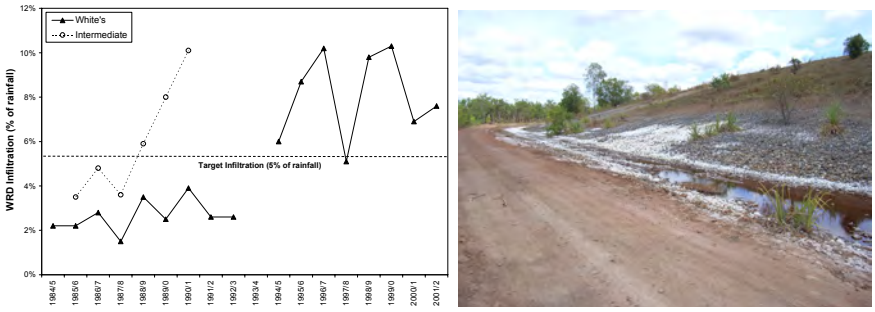

Fig.3. Waste rock dump infiltration : monitored infiltration rate (left), White's WRD in July 2007 (right) – note the active seepage flow and characteristics (photo G M Mudd).

Surface Water

Only a brief examination of hydrologic and surface water quality data is possible herein, and so only key data is presented. The results of a Finniss River water quality profile are shown in Fig. 4, with metal loads for Cu and Zn shown in Fig 5. A comparison of water quality at GS8150097 with guidelines is given in Table 2.

There is clearly seasonal behaviour in metal concentrations and loads (Table 2).

To further illustrate this, typical maximum concentrations in the first flush waters of the early wet season are compiled and shown in Fig. 6. Smaller wet season flows lead to higher concentrations, with a gradual decline over time. Additional photos of the former Sweetwater Dam are given in Fig. 7.

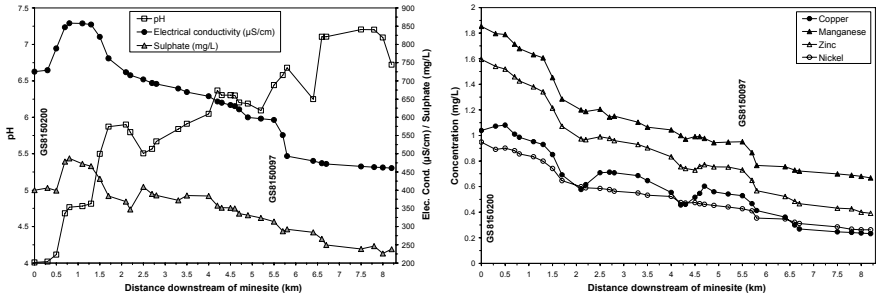

Fig.4. Profile of Finniss River water quality downstream from Rum Jungle (22 April 1994).

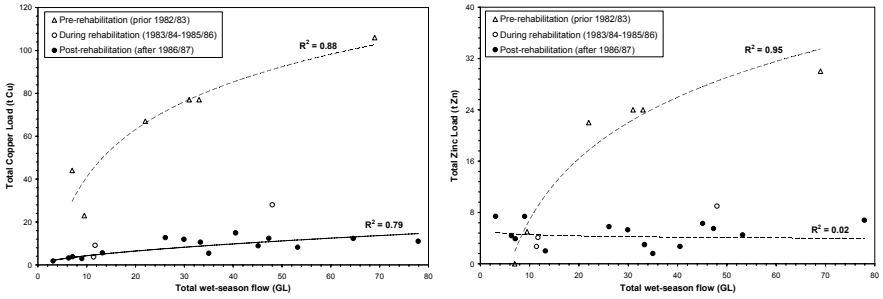

Fig.5. Cu-Zn loads in Finniss River at GS8150097 before, during and after rehabilitation.

Table 2. Summary of GS8150097 water quality during the 1992/93 wet season, compared to current water quality guidelines (ANZECC and ARMCANZ 2000).

	Al	Ca	Fe	As	Co	Cr	Cu	Mn	Ni	Pb	Th	U	Zn
		← all mg/L		all µg/L →									
Average	3.6	9.9	1.7	4.1	176	5	485	860	169	76	3.3	33	209
Minimum	0.21	4.2	0.096	0.6	53	0.7	180	430	53	2	0.02	6	49
Maximum	9	29	14	41	480	33	1100	2000	430	880	26	63	670
ANZECC[a]	ND	ND	ND	14	ND	1[b]	1.4	1900	11	3.4	ND	6[c]	8

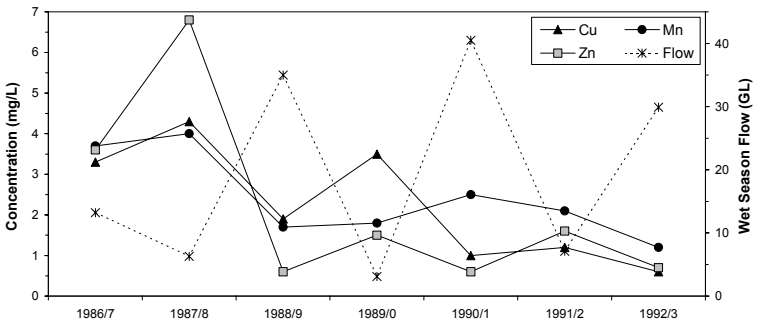

Fig.6. First flush metal concentrations, early wet season, versus total wet season flows.

Fig.7. Former Sweetwater Dam, July 2007; Note – the water and flow in the left photo is continuing seepage from White's waste rock dump (see Fig. 3) (photo's G M Mudd).

ND – not determined (no data). [a] Water quality values based on 95% species protection for fresh waters. [b] Value is for Cr^{6+} only. [c] Value is from the Ranger uranium project.

Groundwater

Groundwater remains the least monitored environmental component of the Rum Jungle site. Although some monitoring and assessment has been undertaken, the latter stages of the monitoring program did not include groundwater (see Pidsley 2002). It is important to note that there was no remediation of contaminated groundwater during the rehabilitation project, despite it being identified as heavily polluted and an ongoing source of pollutants.

The available groundwater monitoring data, shown in Fig. 8, suggests a linear relationship between pollutant concentrations and EC, with Cu and SO_4 generally extremely high. Given the nature of AMD, this relationship can be expected.

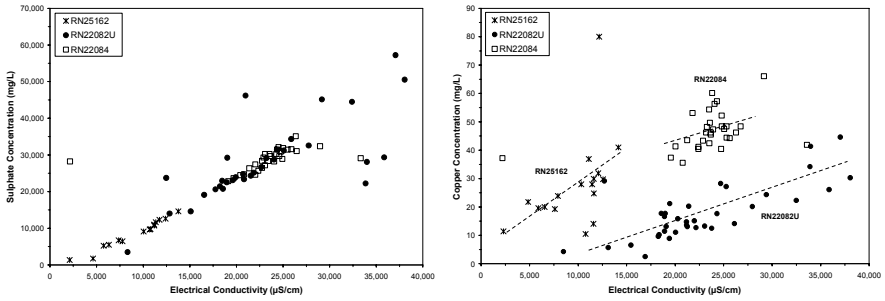

Fig.8. SO_4 (left) and Cu (right) concentrations versus electrical conductivity in 3 bores in the vicinity of White's waste rock dump (dashed lines indicative only).

Sediments

Concentrations of metals in streambed sediments have been examined, though only at specific times for a Finniss River profile. Some data has been obtained for sediment quality, while other data was obtained during ecological studies. The sediment data, Table 3, clearly shows the essentially background concentrations upstream compared to elevated levels downstream.

Biodiversity

The biodiversity in the Finniss River has been studied in the 1970's and again following rehabilitation works, mainly through fish diversity and abundance surveys and macroinvertebrate species and diversity studies (including benthic surveys and pollutant bioavailability and archival studies in mussels).

The original 1970's surveys established that the Finniss River immediately downstream of Rum Jungle was largely devoid of biota, with the first flush of wet

Table 3. Sediment quality profile along the Finniss River (East Branch), compared to current sediment quality guidelines (ANZECC and ARMCANZ 2000) (mg/kg dry weight).

	Distance From Rum Jungle (km)	Ba	Cd	Co	Cu	Fe	Mn	Ni	Pb	U	Zn
Up-Stream	-18	58	0.05	5	17	5454	101	5	16	4	<DL
	-0.2	65	0.04	11	30	9221	230	5	15	2	<DL
	-0.01[a]	77	0.3	7	33	4326	201	3	10	3	<DL
Down-Stream	4	76	0.3	269	**3643**	12284	582	**371**	127	129	**1896**
	8	84	0.35	193	**1061**	8426	209	**191**	138	45	**1748**
	11	58	0.22	202	**404**	10510	551	**98**	37	17	112
SQG low[b]		ND	1.5	ND	65	ND	ND	21	50	ND	200
SQG high[b]		ND	10	ND	270	ND	ND	52	220	ND	410

<DL – less than detection limit. ND – not determined. [a] On upstream junction of East Branch with the Rum Jungle site. [b] For the sediment quality guidelines, 'low / high' means low / high probability of biological effects (that is, 'high' values would give rise to effects).

season rains being particularly problematic (Davy 1975). Following rehabilitation works, various biodiversity surveys have established a return of biota to the East Branch, with apparently lower overall bioavailable metal loads. In addition, recent research on Cu ecotoxicity to black-banded rainbow fish (*Melanotaenia nigrans*) from the Finniss River has suggested an evolving Cu tolerance to the mine leachates still emanating from the site (Gale et al 2003). Thus, overall biodiversity surveys suggest some measure of success, though this has to be moderated with the significant physical and chemical evidence of ongoing pollutant generation and release (eg. Fig.'s 3 and 7).

Discussion and Conclusion

As noted previously, the Rum Jungle rehabilitation project has been a critical case study on AMD pollution and remediation, especially for U mining. There is a common belief that the legacy of the Rum Jungle project has been addressed and rehabilitated satisfactorily (perhaps people who have not visited the site in recent years). The above review of the rehabilitation project and associated monitoring data raises a significant number of issues.

Despite the extent of reported monitoring and studies, critical gaps remain in facilitating a more hollistic and accurate picture of the ongoing pollution cycle at Rum Jungle. For example, samples upstream of the site are extremely rare, with the only known data being that obtained for biodiversity surveys – despite being a very common design in environmental monitoring and impact assessment studies. Sampling and monitoring is often insufficient in spatial / temporal scale to allow an accurate whole-of-site mass balance to be determined, meaning pollutant load accounting from primary source terms is difficult or impossible. In addition, there is possible groundwater discharge ~0.5-1 km downstream of GS8150200 (Fig. 4), potentially explaining spikes in SO_4 and Cu. Groundwater remains heavily contaminated and is very likely to be contributing to major pollutant loads in surface waters along with loads derived from White's open cut and all waste rock dumps.

The radiological characterisation and assessment of the site remains poor, despite clear evidence of extreme U concentrations in seepage from White's WRD and accumulated U in Finniss River sediments (Table 3).

The Rum Jungle remains a polluting site – as evidenced by the range of available monitoring data and recent site inspections. Annual pollutant loads remain 4-12 t Cu, 3-7 t Zn and 1,250-4,800 t SO_4 – although they could be seen as meeting rehabilitation objectives, they are clearly ecologically significant metal loads. Given that groundwater remains contaminated and waste rock dump infiltration is increasing, pollutant loads into the Finniss River can be expected to intensify in the future. The Rum Jungle U-Cu site, despite significant effort, has not met the test of time and remains a recalcitrant and polluting mine.

References

Allen CG and Verhoeven TJ (Editors) (1986) The Rum Jungle rehabilitation project - final project report. Northern Territory Dept of Mines & Energy, Darwin, NT, June 1986

ANZECC and ARMCANZ (2000) Australian and New Zealand guidelines for fresh and marine water quality. Canberra, ACT, October 2000

Brown P (2002) personal communication, Freiberg, Germany, September 2002

CR (2005) Browns Oxide project - public environmental report. Prepared by Enesar Pty Ltd for Compass Resources Ltd (CR), November 2005

Davy DR (Editor) (1975) Rum Jungle environmental studies. Australian Atomic Energy Commission, AAEC/E365, Lucas Heights, NSW, September 1975, 322p

Fraser WJ (1980) Geology and exploration of the Rum Jungle uranium field. Proc. "Uranium in the Pine Creek Geosyncline", Sydney, NSW, June 1979, pp 287-297

Gale SA, Smith SV, Lim RP, Jeffree RA and Potocz P (2003) Insights into the mechanisms of copper tolerance of a population of black-banded rainbowfish (*Melanotaenia nigrans*) exposed to mine leachate, using $^{64/67}$Cu. Aquatic Toxicology, 62, pp 135-153

Kraatz M (Editor) (1998) Rum Jungle rehabilitation project - monitoring report 1988-1993. Dept Lands, Planning & Environment, Darwin, NT, March 1998, 180p

Kraatz M and Applegate RJ (Ed's) (1992) The Rum Jungle rehabilitation project, monitoring report 1986-88. Tech Rep 51, Conservation Commission NT, Darwin, NT

Lichaz W and Myers S (1977) Uranium mining in Australia. In "Ground for concern - Australia's uranium and human survival", Ed. M Elliott, Penguin, pp 25-63

McKay AD and Miezitis Y (2001) Australia's uranium resources, geology and development of deposits. AGSO-Geoscience Australia, Mineral Resource Report 1, 200p

Pidsley SM (Editor), 2002, Rum Jungle rehabilitation project – monitoring report 1993–2002. Dept. Infrastructure, Planning & Environment, Darwin, NT, July 2002, 244p


Uranium Mining
and Hydrogeology

Potential of *Brassica juncea* and *Helianthus annuus* in phytoremediation for uranium

Beate Huhle[1,2 *], Herman Heilmeier[1] and Broder Merkel[2]

[1] Institut für Biowissenschaft, TU Bergakademie Freiberg, Leipziger Str. 29, D-09599 Freiberg (Germany)
[2] Lehrstuhl für Hydrogeologie, TU Bergakademie Freiberg, Gustav-Zeuner-Str. 12, 09596 Freiberg (Germany)
[*] present address: Lehrstuhl für Bodenökologie, Universität Bayreuth, Dr.-Hans-Frisch-Straße 1-3, 95448 Bayreuth (Germany)

Abstract. To investigate the efficiency of the phytoremediation of uranium-contaminated soil by *Brassica juncea* and *Helianthus annuus*, greenhouse experiments with both plant species and soil from the "Fuhrberger Feld" (near Hanover, Germany) with defined enhancement of the uranium concentrations up to approximately 6 mg kg^{-1} have been carried out. Part of the test plants was treated with citric acid buffer (pH =4.8). Plants of both species were grown in soil from the "Fuhrberger Feld" without any treatment (control plants). The plants were harvested 13 weeks after settling and the uranium concentration in shoots and roots and the remaining soil was measured. The uptake of uranium into the shoot was clearly lower than into the roots. Uranium concentration in the shoots of the control plants was below the detection limit. The addition of the citric acid buffer caused an enhancement of the uranium concentration in the soil water by factors of up to approximately 80. A visible effect of this enhanced concentration on the uptake into the plant and on the distribution on shoot and root was only shown for *Brassica juncea,* where the concentration in the shoot doubled. The reverse effect was shown for *Helianthus annuus*, where the citric acid buffer treatment caused a lower concentration in roots and shoots compared to the untreated soil with the same uranium concentration.

Generally, the uranium uptake into the plants was very low (<1 µg per plant) for all experiments.

The results of these plant experiments point out that the effectiveness of uranium uptake into plants cannot be increased by citric acid buffer treatment in every case, even if the uranium concentration in soil solution is increased considerably. No decrease of uranium concentration in soil due to the uptake into plants could be shown. Thus a special suitability of *Brassica juncea* and *Helianthus annuus* for phytoremediation could not be proven.

Introduction

Mankind affects the cycles of many elements and compounds. These changes become important, if they cause an endangerment for humans or the basis of human existence. In the last decades the investigation of uranium in soils and in ground waters gained importance due to its potential hazard. Thereby especially the chemotoxical effect of uranium is relevant, since uranium compounds cause damages of liver and kidneys among others (Merkel and Dudel 1998).

Since uranium, like all metals, is not degradable, its entries in soils or ground waters should be reduced or prevented and already entered uranium must be removed from the environmental compartments.

An in situ method to remove metals from soils is phytoremediation. Thereby plants take up metals from the soil and accumulate them in their harvestable aboveground organs, mainly in their shoots. The aboveground plant biomass is then harvested and burned, in order to remove the contaminants permanently from the soil (Cherian and Oliveira 2005)

These practices are suitable for treatments of large areas with minor concentrations of impurities (Negri and Hinchman 2000). The success of phytoremediation depends on different factors such as a sufficient production of biomass by the plants in which they have to enrich high quantities of the metals. Indeed finding a suitable plant for removing metals is not that easy, because most of the known hyperaccumulator plants have small biomasses (Baker and Brooks. 1989). In addition these plants need to be plantable and harvestable with agricultural methods. Also they should mainly accumulate the hazardous metals in large quantities (Blaylock et al. 1997).

Uranium which is sorbed at clay minerals and humus particles, as well as uranium in connection with the Fe-Mn-oxides is immobile and therefore not available for plants. However, roots can mobilize metals by acidifying with citric acid or other organic acids, changes of redox conditions or formation of organic complexes (Alloway 1999). These so called chelates increase the fraction of dissolved metals in the soil solution. Chelates can make insoluble cations plant available,

they increase there transport to the plant roots and supply more of the allready absorbed cations (Shahandeh and Hossner 2002b).

The uptake of actinides from soils by terrestrial plants is considered as low. Thereby the enrichment of uranium in plants occurs particularly in their roots (Hossner et al. 1998).

Helianthus annus (Annual sunflower) and *Brassica juncea* (Indian mustard) show a high ability for the accumulation of uranium in comparison with other plants (Ebbs et al. 1998, Huang et al. 1998, Shahandeh and Hossner 2002, Chang et al. 2005). However, prior examinations were accomplished mostly with high soil uranium contents (>100 mg U kg^{-1} soil) or non soil typical substrates (Schönbuchner 2002). No publications were available about soils with lower uranium contents, wherefore Phytoremediation is mainly applicable in practice. Therefore, a controlled greenhouse experiment was set up to investigate how much uranium can be taken up by the plants with different soil uranium content and how the addition of citric acid buffer affects the uptake of uranium.

Methods

The goal of this work was to determine whether soils with uranium contents of slightly over 5 mg U kg^{-1} can be regenerated by phytoremediation. The amount of 5 mg U kg^{-1} is the tolerance value for a gardening-agricultural use from soils after Eikman and Kloke (1993).

Table 1. Overview over the most important treatment steps for investigation of the potential for Phytoremediation of *Brassica juncea* and *Helianthus annuus*

time [d]	
0	sowing of the seeds into a planting bowl
11	Sorting of the plants at the two leaves state into a planting pallet [1]
31	Repot into planting containers with a diameter of 11 cm - volume about 0.8 l [1]
51	Repot into planting containers with a diameter of 20 cm - volume about 5 l arrange plants over control treatments and prepared soils
53	Installation of the suction cups in the planting pots and beginning of the soil water sampling
70	1. citric acid buffer treatment
73	2. citric acid buffer treatment
77	Harvest

[1]soil was mixed with Basacote Plus 9M- fertilizer (fertilizer contents: 16% N, 8% P_2O_5, 12% K_2O, 2% MgO, 5% S, 0.02% B, 0.05% Cu, 0.4% Fe, 0.06% Mn, 0.015% Mo, 0.02% Zn) to avoid any kind of nutrient limitation

Therefore two plant species *Brassica juncea* and *Helianthus annuus* were planted in sandy farmland soil from northern Germany (Fuhrberger field), which has an uranium content of 0.96 mg kg^{-1} soil due to the application of uranium containing P fertilizers. A natural soil should be used, because artificial substrates have clearly different sorption characteristics.

The plants were grown in a greenhouse under natural light conditions (temperature range 7-39 °C). The most important vertices of the procedure are held in table 1

After 51 days 12 plants of each species were set in 5L pots, whereby 8 of 12 plants were set in soils to which 5 mg uranium per kg soil was added. Uranium was added as uranyl acetate dihydrate solution ($(CH_3COO)_2UO_2$ * 2 H_2O). Additionally 3.7 mg P per kg soil was added as dipotassium phosphate (K_2HPO_4) to simulate the input of uranium via fertilizing. In each case 4 plants were grown with the same treatment: soil with natural uranium content, soil with additional uranium, soil with additional uranium and citric acid treatment (Table 2). Plants were grown for 20 days in the different soils.

Citric acid buffer was chosen because it is environmentally harmless and completely naturally degradable as well as citric acid has shown a relatively constant effectiveness in removing metals (Francis and Dogde 1998). In previous studies the addition of citric acid to the soils has led to a strong increase of the uranium uptake into the plants (Huang et al. 1998, Chang et al. 2005).

After 70 days of growing 250 ml of citric acid buffer solution was added to 4 of the pots of *Brassica juncea* and *Helianthus annuus* respectively. The amount of solution added should not correspond to more than 5-10 Vol% of the soil in order to prevent a leakage of solution. Since citric acid has a pH value below 3 and such a pH value causes damages to plant roots a citric acid buffer solution with 4.8 mmol l^{-1} citric acid ($C_6H_8O_7$ * H_2O) and 5 mmol l^{-1} trisodium citrate ($C_6H_5Na_3O_7$*2 H_2O) with a pH value of 4.8 was used.

It is assumed that plant metabolism chances after the bloom time to a smaller transpiration. Therefore blooms of both plant species were cut, those of *Brassica juncea* twice, and those of *Helianthus annus* were only removed once.

Table 2. Different plant treatments after 50 days of growing in farmland soil for the investigation of the potential for phytoremediation

Brassica juncea (Indian mustard)	*Helianthus annus* (Annual sunflower)
● 4 x control (farmland soil with approx. 1 mg/kg)	● 4 x control (farmland soil with approx. 1 mg/kg)
● 4 x farmland soil + approx. 5 g U/ kg and 3.7 mg phosphate/ kg	● 4 x farmland soil + approx. 5 g U/ kg and 3.7 mg phosphate/ kg
● 4 x farmland soil + approx. 5 g U/ kg and 3.7 mg phosphate/ kg + two times citric acid buffer treatment	● 4 x farmland soil + approx. 5 g U/ kg and 3.7 mg phosphate/ kg + two times citric acid buffer treatment

Plants were harvested after 77 days, 4 days after the second citric acid treatment, since the highest uranium uptake should take place up to then, according to literature (Huang et al. 1998). Plants were cut off 1 cm above soil surface, weighed (leaves, stem and roots separately) and dried afterwards at 70°C to 80°C. Roots were washed carefully before drying.

Plants samples were milled with a ultra centrifugal mill (Retsch ZM 1000, Speed 10000 rpm) and sieved to <0.63 µm. To quantify the amount of uranium absorbed by the plants uranium contents per g plant (dry weight) were examined after digestion according to DIN EN 13805. To control the completeness of the digestion the reference material Virginia Tobacco Leaves (CTA-VTL-2) from Poland was used.

To investigate the mobility of uranium in the soil solution, soil water was sampled with suction cups (Al_2O_3-cups, Haldenwanger, Waldkraiburg, Germany), which were conditioned before with 8.44 µg l^{-1} uranyl nitrate solution. The soil solutions of the 4 pots with the same treatment were sampled in one bottle. When a sufficient amount of sample was present, uranium content and pH values of the soil solution were measured.

To control the distribution of uranium in the soils with added uranium 3 soil samples were examined for their uranium content after digestion. Also the used fertilizer was investigated for its uranium content. The samples were dried at 70 to 80°C, milled, sieved to <63 µm and digested by aqua regia dissolution according to DIN EN 13346 (2001-04).

The concentration of trace elements was measured in the soil solutions as well as in the solutions from digestion of plants, soil and fertilizer. Trace elements concentrations were determined with the ICP-MS (VG Elemental, Winsford, England). The detection limits for uranium were between 0.006 and 0.009 µg l^{-1}.

Results

Uranium concentrations and pH in soils

Uranium concentrations of three sub samples of the soils with added uranium differ strongly (4.7-18.6 mg kg^{-1}). The average value was 10.4 mg U kg^{-1} soil. The different uranium concentrations seem to have no influence on the uranium concentration in the soil solution (see Uranium contents in soil solution). The fertilizer used contained 4.0 mg U kg^{-1}.

The amount of the sampled soil solutions was prone to strong fluctuations. Therefore it was not possible to get constantly enough soil solution for pH measurement. Generally the pH values of the soil solutions in the pots without treatment with citric acid buffer were within the range of 5.2-7.1 for *Helianthus annuus*, 5.8-6.8 for *Brassica juncea*. There was no apparent pH difference between the solutions of the soils with different uranium concentrations.

A growth of algae was determined in some of the soil water sample bottles14 days after beginning of the sampling. Since the algae could affect the water characteristics due to metabolic procedures, they were rinsed out immediately and slight remaining remnants in the bottles were removed mechanically.

After the first treatment with citric acid buffer the pH value of the soil solutions of both plant species increased to 7.4 for *Helianthus annuus* and 7.3 for *Brassica juncea*. Three days after the second citric acid buffer addition, the pH values in the soil of both plant species amounted 6.6 and was higher than for the parallel treatment without citric acid buffer. In addition to the increasing pH value the citric acid buffer led to a staining of the soil water by dissolved humic acids.

Because of defects of the suction cups soil solutions could not be sampled regularly, three times there was not enough sample material for the measurement of the uranium concentrations. The soil solution of the *B. juncea* control treatment had uranium concentrations in the range of 0.2-1.5 µg l^{-1}, those of *H. annuus* in the range 0.2-2.9 µg l^{-1}. Soil solutions of soils treated with uranyl acetate dihydrate and dipotassium phosphate had uranium concentrations of 0.4-2.5 µg l^{-1} for both species. The uranium concentrations in these solutions were mostly higher than those of the control soils (Table 3).

After the citric acid buffer addition the uranium concentrations of the soil solutions increased. The uranium concentrations in soil solution of *B. juncea* reached a concentration of 19 µg l^{-1} three days after the first citric acid treatment, three days after the second citric acid buffer treatment 76 µg l^{-1}. This is an 8 and 32 time increase of the uranium concentration in the soil solution compared to soil without citric acid buffer treatment.

The uranium concentrations of the soil solutions of *H. annuus* were even higher. The maximum concentrations appeared after the first citric acid buffer treatment (241 µg l^{-1}), three days after the second treatment the concentration reaches 93 µg l^{-1}, which correspond to an 83- and 32-fold increase, respectively, compared to soil without citric acid buffer treatment.

Table 3. Ranges of the uranium concentrations in the soil solution of the different plant treatments and number of measured samples (U = uranyl acetate dihydrate and dipotasium phosphate, C= citric acid buffer)

Treatment	***Helianthus annuus***		***Brassica juncea***	
	number of measurements	U in soil solution [µg l^{-1}]	number of measurements	U in soil solution [µg l^{-1}]
control	3	0.2-2.9	4	0.2-1.5
with U	6	0.4 -2.4	4	0.4-2.5
with U and C	2	93.1-240.9	2	19.3-76.1

Uranium concentrations of the plants

For all plants an uptake of uranium in their roots could be proven. Also the uranium concentrations of the roots were substantially higher than in the shoots (Fig.1).

The uptake of uranium from soils of the control treatments (0.96 mg U kg^{-1} soil) in the roots accounted for both plant species 0.02 mg U kg_{DW}^{-1}on average. Since the average dry weight of the roots of both species was not different, the average uranium content in the roots was the same. An uptake of uranium into the shoots could not be detected for the control plants of both species (<7*10^{-4} mg U kg_{DW}^{-1}).

Plants which have been grown in soils with added uranium showed a higher uptake of uranium than control plants. Uranium concentrations in the roots of *H. annuus* were on average 0.07 mg kg_{DW}^{-1} and higher than those of *B. juncea* (0.05 mg kg_{DW}^{-1}).

For both plant species the addition of citric acid buffer to the soil did not yield any increase of the uranium concentration in the roots. *H. annuus* even had lower uranium concentrations in roots and shoots. However *B. juncea* showed an increased uranium concentration in the shoots.

Even if the uranium concentrations of *H. annuus* were lower than that of *B. juncea* after citric acid treatment, the total amount of uranium in the plants was higher for *H. annuus* (0.49 µg) than that of *B. juncea* (0.45 µg) due to its larger biomass (Table 4).

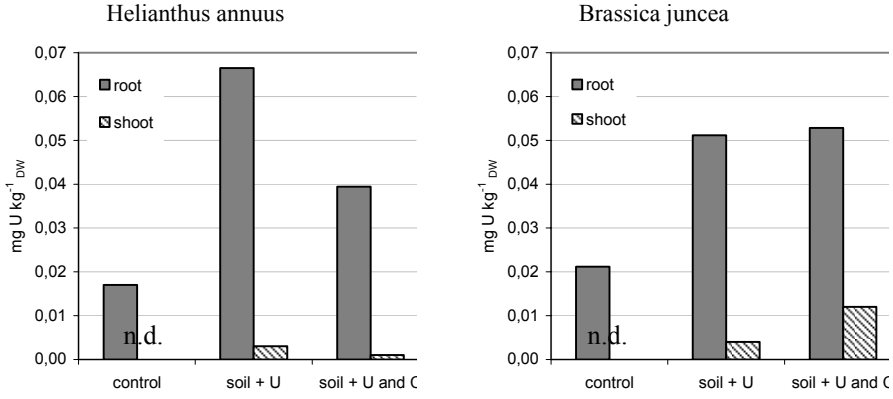

Fig 1. Uranium concentrations (mean value of 4 plants) of *Helianthus annuus* and *Brassica juncea* in the roots and in the shoots for the different treatments, U = uranyl acetate and dipotasium phosphate, C =citric acid buffer, DW = dry weight, n.d. = not detectable

For the calculation of the soil/plant transfer factor a soil uranium concentration of 6 mg kg^{-1} was assumed. This value was calculated as mean value for the soil uranium concentration after the treatment with uranyl acetate dihydrate.

Table 4. Uranium fraction transported from the roots into the shoots (amount (branch) [µg] /amount (plant) [µg]), total uranium uptake (mean value) and Transfer factor plant/soil for the different treatments of *Brassica juncea* and *Helianthus annuus,* C =citric acid buffer

	From roots into shoots shifted fraction [%]	Total uptake into the plant [µg]	Transfer factor plant/soil
Helianthus annuus			
control	-	0.17	$1.6*10^{-3}$
with U	0.14	0.76	$6.2*10^{-3}$
with U + C	0.11	0.49	$3.7*10^{-3}$
Brassica juncea			
control	-	0.16	$1.8*10^{-3}$
with U	0.10	0.42	$4.9*10^{-3}$
with U + C	0.18	0.45	$5.6*10^{-3}$

The soil/ pant transfer factor was in the order of 10^{-3} for all plant treatments (Table 4). The higher soil uranium concentration led to an increase of 2-4 times for *H. annuus* and 3 times for *B. juncea.* The reaction to the addition of citric acid buffer to the soil differs depending on the plant specie.

Discussion

Uranium concentration and pH in soils

The differences of the uranium concentrations in the prepared farmland soil are caused by inhomogeneous distribution of the uranyl acetate dihydrate in the soil. These differences of the soil uranium concentrations are assumed to be at a small scale compared to the pot and the root volume, and therefore did not affect the total uranium content in one pot and in the soil solutions.

The uranium concentration in the used fertilizer (4.0 mg U kg^{-1}) is small compared to literature data (6-39 mg U kg^{-1}, Kratz and Schnug 2005, Uyanik et al. 1999). Also only small amounts of this fertilizer were used for fertilization. Therefore they should not have any important effect on the measured uranium concentrations of the soils and plants of this investigation.

The determined effective soil pH of the farmland soil from the Fuhrberger Feld amounts 5.8. As far as it was recognizable from the measured pH values the addition of uranyl acetate dihydrate solution and dipotassium phosphate had no effect on the pH value of the soil solution.

The first citric acid buffer treatment of the soils led to two clearly visible responses: First the pH value of the soil solution increased 8-83 times. This increase

can possibly be explained by the dissolution of alkaline acting cations. The second reaction the yellow colouring of the solution is probably due to the protonation and simultaneous dissolving of humic substances.

The increase of the pH value of the soil solution to greater 6.5 after the citric acid buffer treatment could be one reason for the higher solubility of uranium and thus a higher concentration of uranium in the soil solution. However the chelate forming agency of the citrate is more likely the reason for the increased uranium concentration. Anyway the mobilization of uranium by citric acid as described in the literature (Huang et al. 1998) is confirmed by these results. The addition of the citric acid buffers to the soil and the following increased concentration of the uranium in the pore water should be a good precondition for the uptake of uranium into the plants.

Uranium uptake by *Helianthus annuus* and *Brassica juncea*

The uptake of uranium into the plants was with a maximum concentration of <1µg per plant and 0.07 mg kg_{DW}^{-1} in the roots very low, compared to the available uranium per pot (approx. 30 mg). In comparison to the literature values of Kabata Pendias (2001) who stated concentrations of plant ashes with 0.6 mg kg^{-1} no notably uptake has been shown for *H. annuus* and *B. juncea* in this investigation.

The analysis of a reference material (Virginia Tobacco Leaves) indicted that the digestion was not complete (systematic error up to 30.5%), however, this error has only small influence because of the low amount of uranium in the plants.

The plants have shown a higher accumulation of uranium in roots than in shoots, as expected. However a high uptake of uranium into the shoots is desirable, as the part of the plant which can be harvested easily.

Influences that could have affected the uranium uptake into the plants are the following:

Phosphate: Rufyikiri et al. (2006) determined that an increased P-content in the soil leads to a decreased U absorption into the plants. Hence, the phosphate which was added to the soil together with the uranium can increase the fixation of uranium in the soil and thus reduce the availability of uranium for plants.

Soil pH value: The soil pH of 5.8 is near the sorption maximum of clay minerals at pH 6.0 to 6.5 (Scheffer and Schachtschabel, 2002). Therefore due to adsorption processes less uranium can get into to the mobile phase than at lower pH values. Also this is the pH range in which stable uranium phosphate complexes are formed.

Nutrient conditions of the soil: The uptake of metals and probably also that of uranium into the roots is influenced by the nutrient conditions in the soil. Lower nutrient availability in the soil leads to higher metal accumulation in the roots (Schroetter et al. 2004).

In this study the plants were provided sufficiently with nutrients to exclude any limitation by lack of nutrition. Due to the addition of the Basacote plus 9M fertilizer (NPK fertilizer) it can be assumed that the soil contained sufficient amount of

plant-available potassium, whereby no KCl addition was necessary as compensation for the addition of dipotassium phosphate in the treated soils.

Uranium concentration of the soil and the soil solution: A higher uranium concentration in the soil and thereby soil solution led to an increased uranium uptake into the plants, for both plant species. However, the presence of larger quantities of uranium in the soil solution alone cannot be crucial for an improved uptake of uranium by plants, because the higher uranium concentration in the soil solution caused by the citric acid buffer only leads to an higher uptake of uranium for *Brassica juncea* (uranium concentration in the shoots doubled).

Citric acid buffer: The strongly increased availability of uranium in the soil solution of *H. annuus* (32-83 times higher than without treatment) did not yield a higher uranium content in the plant, whereas *B. juncea* showed a higher uptake. A reason for the different responses of the two plant species to the treatment with citric acid buffer could be a different absorption ability of uranium citrate complexes due to different metabolic characteristics of *H. annuus* and *B. juncea*.

Dushenkov et al. (1997) determined a high affinity for uranium for *Helianthus annuus* in a hydroponic. Probably *H. annuus* preferentially takes up water dissolved uranium species, but no citric complexes. Possibly the citric acid buffer has even led to a release of uranium which was adsorbed at the root surface of *H. annuus*.

A further reason for the small effect of the citric acid addition on the uranium uptake could be the late growth stage of the plants at that time. With a smaller growth rate the uptake of nutrients and metals into the plant decreases. Therefore the effect of the higher concentrations of uranium in the soil solution is weakened by a smaller uptake. The success of this method could possibly be increased by the addition of the citric acid buffers at an earlier time.

Two methodical facts have to be mentioned especially for further investigations in this field: the timing of the investigation and distribution of the artificially added uranium to the soil.

The time window of the investigations has to be smaller and seed should grow up already in the soil with higher uranium content, as it would be in a large scale application. Plants that are used for phytoremediation in the fields should not grow there for a long time, because after blooming the uptake of plants is lower than in the growing stage. Also it should be avoided that the contaminated plants are eaten by animals. This should be reflected in the experiments for phytoremediation.

Even if we act on the assumption that the irregular distribution of the artificially added uranium in the soils did not affect the uptake of uranium into the plants, a clear definition of the reference parameters (in this case soil uranium concentration) for the calculation of the uptake of uranium from the soil would be preferable. Thereby it must be noted that evenly addition of uranium to natural soil represents a certain challenge, since natural soils are less homogeneous than artificial substrates.

However, the determined soil/plant transfer factors at this investigation are in the same range as that of the control plants (approx. 10^{-3}) as well as determined transfer factors for field grown dump plants without any treatment 10^{-4} to 10^{-3} (Schönbuchner 2002, Whicker et al 1999).

In conclusion it can be said, that *Brassica juncea* and *Helianthus annuus* under the accomplished experimental condition and the determined soil removed only very small quantities of uranium from the soil. Thus for both plant species no suitability for phytoremediation could be proven.

References

Alloway JB (1999) Schwermetalle in Böden, Analytik, Konzentrationen, Wechselwirkungen. Springer Verlag Berlin Heidelberg

Baker AJM, Brooks RR (1989) Terrestrial higher plants which hyperaccumulate metallic elements: a review of their distribution, ecology and phytochemistry. Biorecovery 1: 81-126.

Blaylock MJ, Salt DE, Dushenkov S, Zakharova O, Gussman C, Kapulnik Y, Ensley BD, Raskin Y (1997) Enhanced Accumulation of Pb in Indian Mustard by Soil-Applied Chelating Agents. Environ.Sci.Technol,. 31, 860-865.

Chang P, Kim K-W, Yoshida S, Kim S-Y (2005) Uranium accumulation of crop plants enhanced by citric acid. Environmental Geochemistry and Health 27, 529-538.

Cherian S, Oliveira MM (2005) Transgenic Plants in Phytoremediation: Recent Advances and New Possibilities. Environ. Sci. Technol., 39, 9377 -9390.

Dushenkov S, Vasudev D, Kapulnik Y, Gleba D, Fleischer D, Ting KC, Ensley B. (1997) Removal of uranium from water using terrestial plants. Environ. Sci. Technol., 31, 3468-3474.

Ebbs SD, Brady DJ, Kochian LV (1998) Role of uranium speciation in the uptake and translocation of uranium by plants. J. Exp. Bot. 49, 1183-1190.

Eikmann T, Kloke A (1993) Nutzungs- und schutzgutbezogene Orientierungswerte für (Schad-) Stoffe in Böden. In Rosenkranz D; Einsele G, Harreß HM (Ed..) (1988 ff.): Bodenschutz: ergänzbares Handbuch der Maßnahmen und Empfehlungen für Schutz, Pflege und Sanierung von Böden, Landschaft und Grundwasser. Erich Schmidt Verlag, Berlin

Francis AJ, Dodge CJ (1998) Remediation of Soils and Wastes Contaminated with Uranium and Toxic Metals. Environ. Sci. Technol., 32, 3993 -3998.

Hossner LR, Loeppert RH, Newton RJ, Szaniszlo PJ (1998) Literature Review: Phytoaccumulation of Chromium, Uranium, and Plutonium in Plant Systems. Amarillo National Resource Center for Plutonium. Online: www.uraweb.org/reports/anrc9803.pdf (last view January 2007)

Huang JW, Blaylock MJ, Kapulnik YK, Ensley BD (1998) Phytoremediation of uran contaminated soils: role of organic acids in triggering uranium hyperaccumulation in plants. Environ. Sci. Technol., 32, 2004-2008.

Kabata-Pendias A (Ed.) (2001) Trace elements in soil and plants. 3. Edition, CRC Press LLC

Kratz S, Schnug E (2005) Rock phosphates and P fertilizer as sources of U contamination in agricultural soils. In: Merkel BJ, Hasche-Berger A (Ed) (2006): Uranium in the Environment: mining impact and concequences. Springer Berlin Heidelberg, 57-67.

Lambers H, Chapin FS III, Pons TL (1998) Plant physiological ecology. Springer-Verlag, Berlin

Merkel B, Dudel G (1998) Untersuchungen zur radiologischen Emission des Uran-Tailings Schneckenstein. AG: Sächsisches Staatsministerium für Umwelt und Landesentwicklung, Dresden.

Negri MC, Hinchman RR (2000) The use of plants for the. treatment of radionuclides. - In Raskin I, Ensley BD: Phytoremediation of toxic metals: Using plants to clean up the environment. John Wiley & Sons, Inc, New York, 107-132.

Rufyikiri G, Wannijn J, Wang L, Thiry Y (2006) Effects of phosphorus fertilization on the availability and uptake of uranium and nutrients by plants grown on soil derived from uranium mining debris. Environmental Pollution 141, 420-427.

Scheffer F, Schachtschabel P (2002) Lehrbuch der Bodenkunde. Spektrum Akademischer Verlag, Heidelberg

Schönbuchner H (2002) Untersuchungen zu Mobilität und Boden-Pflanze-Transfer von Schwermetallen auf/in uranhaltigen Haldenböden. Jena, Friedrich-Schiller-Universität, Chemisch-Geowissenschaftlichen Fakultät, Dissertation. Online: http://deposit.ddb.de/cgi-bin/dokserv?idn=966060989&dok_var=d1&dok_ext=pdf&filename=966060989.pdf (last view Januar 2007)

Schroetter S, Lamas M, Rivas M (2004) U-Transfer Boden Pflanze. - Statusseminar Uran-Umwelt-Unbehagen, Institut für Pflanzenernährung und Bodenkunde, Bundesforschungsanstalt für Landwirtschaft

Shahandeh H, Hossner LR (2002) Role of soil properties in phytoaccumulation of uranium. Department of Soil and Crop Sciences, Water, Air, and Soil Pollution 141, 165–180.

Shahandeh H, Hossner LR (2002b) Enhancement of uranium phytoaccumulation from contaminated soils. Soil Science, 167, 269-280.

Uyanik A, Tinkiliç N, Odabaşoğlu M, Karaca H (1999) Spectrophotometric Determination of Uranium in Waste Water of Phosphoric Acid and Fertilizer Manufacturing Process. Turk J Chem 23, 275 -284.

Whicker FW, Hinton TG, Orlandi KA, Clark SB (1999): Uptake of natural and anthropogenic actinides in vegetable crops grown on a contaminated lake bed. J. Environ. Radioactivity 45, 1-12

Uranium uptake and accumulation in *Phragmites australis* Trin. ex Steud. depending on phosphorus availability, litter contamination and ecotype

Carsten Brackhage and M. Wartchow

Institute of Ecology and Environmental Protection, TU Dresden, Germany

Abstract. Macrophytes in natural and constructed wetlands can influence radionuclide and heavy metal immobilisation either directly by uptake and accumulation and/or indirectly (biomass production – litterfall and root turnover – decomposition) providing for complexing substances. We investigated the influence of phosphorus availability in combination with uranium contaminated plant litter on uranium uptake and accumulation as well as productivity in two different ecotypes of *Phragmites australis* Trin. ex Steud. in a culture experiment.

It is shown that decreasing phosphorus fertilization without plant litter results in phosphorus deficiency in the plants (higher N/P-ratio) and hence decreasing biomass production as would be expected. However, decreasing phosphorus availability in the substrate is not correlated with increasing U-concentrations in any of the investigated plant parts but with the overall removal of uranium by plants. Adding a litter layer from *Phragmites australis* is resulting in additional P-availability and hence no observable P-deficiency in the plants. The litter layer is successfully absorbing uranium which was added as uranyl nitrate. This does not result in different uranium concentrations compared to the treatments without a litter layer. Adding a litter layer already contaminated with uranium has the same effect: plants are sufficiently provided with phosphorus but do not exhibit lower uranium concentrations. The same can be stated for treatments with contaminated litter and additional uranium application.

Finally no difference in uranium concentrations was observed für different ecotypes in any of the treatment. Due to different biomass production higher uranium content could be observed for one of the investigated ecotypes.

Applications of NH_4Cl and citrate: Keys to acceptable phytoextraction techniques?

Gerhard Gramss and Hans Bergmann

Friedrich-Schiller-University, Institute of Geological Sciences, Burgweg 11, D-07743 Jena, Germany

Abstract. Treatment of *Brassica* sp. with NH_4Cl raising DW to 150 % and the content in protein-N to 4 % increased uptake of the protein-associated transition metals (Cd) Co Cu Fe Mn Ni Zn to >500 % (calculated from increases in DW x N_{org}). Uptake of non-physiological metals such as U increased little more than with the DW. Citrate traces stimulated exclusively uptake of Co Mn. Leaching of (hazardous) metals dropped to 60 % by precipitations and plant uptake.

Introduction

Chelate-assisted phytoextraction of soil heavy metals by crop plants with treating periods of several decades increases primarily the leaching problem and is therefore met with scepticism (Evangelou et al. 2007). In a search for alternatives, Wang et al. (2006) demonstrated the existence of soil-specific pH optima for growth and Cd Zn uptake by the hyperaccumulator plant, *Thlaspi caerulescens*. Zaccheo et al. (2006) replaced nitrate supply by a combination of ammonium and nitrification inhibitor to increase uptake of Cd Cu Ni Pb Zn by sunflower soil-type dependent to means of 130 to 270 %. Daily applied doses of NH_4Cl or casein acidified a metalliferous soil and increased the DW of Chinese cabbage shoot to 165 % and the concentrations of Cd Cu Ni Zn to 250 to 350 %. The treatment reduced leaching of humic colloids and soil minerals to 76 % (Gramss et al. 2004). A subsequent trial showed that shoot DW production of Chinese cabbage and the content in N_{org} and free amino acids correlated with the availability of nitrate as the mineralization product of soil-applied NH_4^+, amino acids (AA), and amines. Contemporarily, NH_4^+ applied to soil or derived from organic-N sources liberated Ca^{2+} and Mg^{2+} from the soil matrix which, in turn, precipitated humic substances (HS) and minerals from the saturated soil solution to reduce the leaching problem (Gramss et al. 2006). Shock application of citrate (>5 to 50 m*M*) as high-affinity phytochelant of U caused leaching problems in spite of its short residence time in soil (Jones and Darrah 1994) but triggered an excessive plant acquisition of (haz-

Table 1. Concentrations of citric acid and mineral-acid ligands (mg kg^{-1} ± SD) in untreated Settendorf soil (ion chromatography) and rate and destiny of the daily ligand applications.

	Citric Acid	Cl^-	F^-	HCO_3^-	NO_3-N	$PO_4^{3-}HPO_4^{2-}$ $H_2PO_4^-$	SO_4^{2-}
Untreated soil	0	65±0.2	7.3±0.4	315±5	172±4	34±3	114±19
Daily supply	112[a]	35	0	0	14[b]	95	0

[a] Non-derivatized citric acid not retrievable at 24 h after application.[b] N added as NH_4^+.

ardous) elements due to root damage (Gramss et al. 2004; Huang et al. 1998). Applied at 3 m*M* over 26 d, citrate served as microbial C source and caused moderate increases in soil pH and in a selective metal uptake by vigorous Chinese cabbage plants (Gramss et al. 2004).

In the present study, cultivars of *Brassica chinensis*, *B. juncea*, and *Beta vulgaris rapaceae* potted on a metalliferous soil were daily treated with metabolizable doses of NH_4Cl, $(NH_4)H_2PO_4$, and/or citric acid in a concentration typical of field conditions over 47 d with the goal to determine the role of NH_4^+, of its mineral-acid anions, Cl^- and $H_2PO_4^-$, and of the citrate chelant on the development of soil pH, the solubility of minerals and HS, on DW production, protein content, metal uptake and shoot translocation of 20 elements by the plants as well as on leaching conditions from the planted soil to propose further steps on the path to acceptable phytoextraction strategies.

Materials and Methods

Overburden soil from uranium mining (Settendorf, Germany) of pH_{aqu}, 7.20; C_{org}, 2.50 % (w/w); and N_{org}, 2009 mg kg^{-1} had the following total metal content (in mg g^{-1}): Al, 15975; As, 27.3; Ba, 80; Ca, 4932; Cd, 9.3; Co, 36.9; Cr, 26.8; Cu, 323; Fe, 19401; K, 3103; Li, 26.7; Mg, 4400; Mn, 843; Mo, 1.2; Na, 225; Ni, 67.8; P, 605; Pb, 68.5; Sr, 57.8; Ti, 36.7; U, 80.8; V, 30.5; and Zn, 842. The potted soil (0.210 kg DW) was seeded to several cv. of Chinese cabbage (*Brassica chinensis)*, Indian mustard (*Brassica juncea)*, and beet (*Beta vulgaris rapaceae)*. Seedlings were daily irrigated with deionized water, with aqueous solutions of 42 mg citric-acid carbon (equivalent to 1.62 m*M* citrate in the soil water), with 14 mg N kg^{-1} soil (applied as NH_4Cl or $(NH_4)H_2PO_4$) and a combination of NH_4Cl/citric acid from day 7 to 54 in a phytotron. Unplanted soils were treated in the same way to demonstrate changes in ligand composition (Table 1) and metal solubility.

Metal concentrations were determined (by ICP-AES) for unplanted control and postharvest soils (*aqua regia* extraction; solubility in 1:10 soil:water suspensions), and for microwave-digested root and shoot tissues. Soil NH_4^+ (Aquamerck ammonium test); NO_3^- (spectrophotometrically; Schinner et al. 1993); N_{org} in soil and plant tissue (Kjeldahl); and free amino acids (Amino acid analyzer LC3000) in shoot tissues were also recorded. The portion of dissolved humic substance in 1:10

soil:water suspensions was quantified spectrophotometrically ($A_{340;\ 450;\ 650}$) and gravimetrically.

Results and Discussion

With the daily applications of citric acid and/or NH_4 salts over 47 d, soil pH, the concentrations of mineral and humic acid ligands, and thus the concentrations and plant-availability of elements in the soil solution changed considerably (Tables 1

Table 2. Water-solubility (mg kg^{-1} soil) of elements and humic substances (HS) in unplanted control soil and postharvest soil of Chinese cabbage after daily treatment with water, citric acid, and/or NH_4-salts for 47 d.

	Brassica chinensis									
	Unplanted soil					Postharvest soil				
Element	Water	Citrate	NH_4Cl	NH_4Cl Citrate	(NH_4) H_2PO_4	Water	Citrate	NH_4Cl	NH_4Cl Citrate	(NH_4) H_2PO_4
Macronutrients										
Ca	147	107[a]	**375**[a]	**441**[ab]	**187**[a]	48.6	**71.9**[c]	**264**[c]	**280**[c]	**248**[c]
K	270	335[a]	**239**[a]	**215**[ab]	**314**[a]	243	246	66.7[c]	63.9[c]	141[c]
Mg	116	124[a]	**161**[a]	**177**[ab]	**147**[a]	116	121[c]	**161**[c]	**158**[c]	**166**[c]
P	14.5	18.6[a]	**11.2**[a]	9.34[ab]	**451**[a]	9.65	11.2	4.33[c]	4.02[c]	**569**[c]
Trace elements										
Al	375	**661**[a]	113[a]	73.1[ab]	**379**	656	628[c]	192[c]	176[c]	376[c]
Ba	0.65	1.03[a]	**0.47**[a]	**0.46**[a]	**0.66**	1.04	1.00	0.46[c]	0.47[c]	0.73[c]
Cd	0.08	0.12[a]	**0.09**	**0.13**[a]	**0.14**[a]	0.11	0.13[c]	**0.12**	**0.11**	**0.20**[c]
Co	0.17	0.34[a]	0.03[a]	0.06[a]	0.18	0.33	0.39	0.12[c]	**0.22**[cd]	0.19
Cr	0.53	0.81	0.21[a]	0.17[a]	0.58	0.83	0.83	0.23[c]	0.25[c]	0.49[c]
Cu	3.05	3.96[a]	**1.82**[a]	**1.56**[a]	**4.05**[a]	4.37	4.79	**3.26**[c]	**2.72**[cd]	4.76
Fe	137	**251**[a]	42.0[a]	28.4[ab]	135	246	240	82.1[c]	79.6[c]	164[c]
Li	0.56	**0.98**[a]	0.20[a]	0.14[ab]	**0.59**	0.97	0.93	0.29[c]	0.28[c]	0.59[c]
Mn	2.53	**4.99**[a]	**2.68**	**9.53**[ab]	**5.91**[a]	4.01	4.49	**2.55**[c]	**5.90**[cd]	**5.20**[c]
Ni	1.14	1.85[a]	**0.76**[a]	**0.86**	**1.54**	1.25	1.46	**0.98**	**1.35**[d]	**2.42**[c]
Pb	0.57	**1.52**[a]	0.19[a]	0.14[a]	0.54	0.93	0.82	0.32[c]	0.36[c]	0.26[c]
Sr	1.08	0.91[a]	**2.35**[a]	**2.73**[a]	1.05	0.54	0.65[c]	**1.39**[c]	**1.50**[c]	**1.18**[c]
Ti	3.07	**6.53**[a]	1.02[a]	0.73[a]	2.97	5.00	4.55	1.91[c]	1.95[c]	3.73[c]
U	0.31	0.29	0.03	0.01	0.19	1.70	2.69	0.95[c]	0.68[c]	1.14
V	0.70	1.13[a]	0.08[a]	0.04[a]	0.75	1.29	1.19	0.43[c]	0.40[c]	0.80
Zn	12.7	22.2[a]	**7.52**[a]	**9.10**[ab]	**15.1**[a]	21.6	21.8	**11.0**[c]	**14.2**[c]	**24.5**[c]
HS	3054	4642[a]	1014[a]	832[a]	2488[a]	4548	4543	1520[c]	1543[c]	3344[c]
pH	7.20	7.56[a]	6.80[a]	6.67[ab]	6.44[a]	7.53	7.62[c]	7.07[c]	7.03[c]	6.18[c]

Solubilities and pH values significantly different ($p \leq 0.05$) from those in the water treatment of unplanted soil ([a]) or postharvest soil ([c]). Solubilities and pH values in the NH_4Cl/citrate treatments significantly different ($p \leq 0.05$) from those of NH_4Cl treatments in unplanted soil ([b]) or postharvest soil ([d]).

Concentration of the element grew dramatically more (boldface fount) or less (shaded) than the appertaining concentration of dissolved HS as its main ligand. This was shown by calculating the quotient from element:HS concentration in the soil solution.

and 2). Differences in the availability of N determined the plants' DW production and protein content and therefore their mode and rate of metal uptake and shoot translocation. In the citrate treatment, microbial degradation of the daily citric-acid supplements increased the alkalinity of unplanted soil by 0.4 pH units and thus the solubility of the dominating HS ligand with its associated trace elements to 150 % of the water control. Concentrations of Al Fe Li Pb Ti in the soil solution, as well as Mn as the only element with high affinity to chelation with citric anion, increased significantly more than the concentration of HS. Contemporarily, concentration increases of dissolved Ca K Mg P Cu Sr were lower than 150 % to indicate a less intimate association with humic substance. The presence of *B. chinensis* in water-treated soil adapted pH and solubility conditions exactly to the level of those in citrate-treated unplanted soil (Table 2), apart from losses in Ca K P by plant uptake. Treatment with citric acid had then no further visible effects on solubility conditions in planted soil.

Application of NH_4Cl acidified unplanted soil by 0.4 pH units upon the formation of NO_3^- (Tables 2 and 3). High concentrations of the exchange cations, NH_4^+ and H^+ liberated Ca Mg from the soil matrix which precipitated 67 % of the HS (Ong and Bisque 1968) and 12 % from the sum of solubilized Table-2 elements in comparison to the water treatment. Contemplated in detail, solubility of Al Co Cr Fe Li Pb Ti given in normal fount diminished at the same rate as their HS ligand, whereas Ba Cd Cu Mn Ni Sr Zn (boldface fount) did not and indicated thus net solubilization. The conditions in postharvest soils of *B. chinensis* were similar. Treatment with NH_4Cl reduced the solubility of HS by 67 %, and the sum of solubilized elements by 42 % in comparison to the water treatment (Table 2). Relations of the single elements to HS resembled those in unplanted soil.

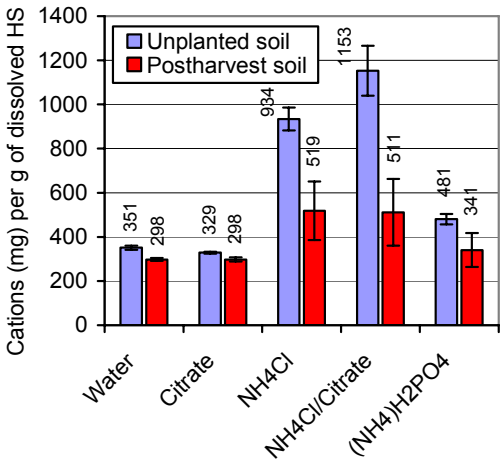

Fig.1. Sum of dissolved cations in mg g^{-1} of dissolved humic substance (HS) as their main ligand (according to Table 2) in the solution of unplanted control soils and postharvest soils of Chinese cabbage. Error bars, ± SD.

Table 3. Water-solubility of NH_4-N and NO_3-N (mg kg^{-1} soil) in unplanted control soil and postharvest soil of Chinese cabbage after daily treatment with water, citric acid, and/or NH_4-salts for 47 d, and the resulting effects on shoot N_{org} (mg kg^{-1} DW) and dry weight (g).

	Brassica chinensis				
	Water	Citrate	NH_4Cl	NH_4Cl/Citrate	$(NH_4)H_2PO_4$
NH_4-N, unplanted soil	52.9	39.2[a]	366[a]	252[a]	313[a]
NH_4-N, postharvest soil	20.3	17.8[a]	36.6[a]	36.6[a]	149[a]
NO_3-N, unplanted soil	172	77.0[a]	232[a]	255[a]	220[a]
NO_3-N, postharvest soil	6.94	2.92	5.72	0	51.5[a]
Total shoot N_{org}	7727	6549	28620[a]	24633[a]	47810[a]
N_{org} of free amino acids	1745	ND	10130[b]	ND	ND
Shoot dry wt	1.013	0.922	1.306[a]	1.504[a]	0.413[a]

[a] Values significantly different ($p \leq 0.05$) from those in the water treatment.

[b] Treatment with NH_4Cl increased the concentrations of free Ala G-Aba Arg Asp Gln Glu Gly Leu Pro Ser Thr , with the underlined compounds having been appeared above the detection limit of 10 pmol.

Combined application of NH_4Cl and citric acid conferred notable solubility gains to Mn Zn in unplanted, and to Co Mn Zn in planted soil. These metals show preference to chelation with citric anion (Gramss et al. 2006). Treatment with $(NH_4)H_2PO_4$ acidified unplanted and planted soils by 0.76/1.02 pH units but stabilized dissolved HS at 81/74 % of the level in water-treated soil. Owing to the enormous P concentration, Cu Ni Zn with the tendency to form phosphate complexes at neutral pH (Schachtschabel et al. 1998) showed relatively higher solubility (Table 2).

Quantitative proportions between the dominating HS ligand and the sum of dissolved cations in the solution of the treated soils are depicted in Fig. 1. Outstanding values of dissolved cations g^{-1} of HS denote the NH_4Cl and NH_4Cl/citrate, but not the other treatments. Low pH conditions (Sumner et al. 1991), shortage in HS ligands, and the excessive Cl^- supplements (Table 1) should give rise to the formation of the far more plant-available free cations and metal-chloride complexes (McLaughlin et al. 1998).

Table 4. Water-solubility of NH_4-N and NO_3-N (mg kg^{-1} soil) in postharvest soils of beet and Indian mustard after daily treatment with water, NH_4Cl, or NH_4Cl/citric acid for 47 d, and the resulting effects on shoot N_{org} (mg kg^{-1} DW) and dry weight (g).

	Beta vulgaris rapaceae			*Brassica juncea*		
	Water	NH4Cl	NH4Cl/Citrate	Water	NH4Cl	NH4Cl/Citrate
NH_4-N, postharv. soil	22.4	44.8[a]	48.8[a]	20.3	59.0[a]	57.0[a]
NO_3-N, postharv. soil	0.65	373[a]	112[a]	2.96	433[a]	162[a]
Total shoot N_{org}	13033	40133[a]	31665[a]	42778	42793	52313[a]
Shoot dry weight	0.473	0.409	0.691[a]	0.412	0.05-0.57[b]	0.498

[a] Values significantly different ($p \leq 0.05$) from those in the respective water treatment.

[b] Concentration of N species toxic to 80 % of plants.

Dry weight production and N_{org} content of the plants were nevertheless dominated by the nitrogen supply (Tables 3 and 4). Microbial consume of citric-acid supplements sequestered N resources in unplanted and postharvest soils and reduced DW and N_{org} content of *B. chinensis* shoots by 15 % (Table 3). The daily $NH_4(Cl)$ doses were continuously nitrified and then completely taken up by *B. chinensis* cv. Chico F1. Its shoot DW increased to 130 to 150 %, N_{org} to 370 %, and the content in free amino acids with candidates for the *in-planta* transport of elements (Haydon and Cobbett 2007) to 580 %. In Indian mustard and beet, shoot N_{org} reached the toxic threshold of 4 % and interfered with plant growth (Table 4). Similarly, supplements of $(NH_4)H_2PO_4$ inhibited growth of *B. chinensis* at 5 % N_{org} and 2.5 % P by DW in the shoot (Tables 3 and 5).

Table 5. Element concentrations (mg kg^{-1} DW) in Chinese cabbage shoots after daily treatment with water, citric acid, and/or NH_4-salts for 47 d. S/R, shoot-to-root concentration quotient given in italics.

		Brassica chinensis				
Element		Water	Citrate	NH_4Cl	NH_4Cl/Citrate	$(NH_4)H_2PO_4$
Macronutrients						
Ca	Shoot	17868	20225	34408[a]	26772[a]	29674[a]
	S/R	*1.83*	*2.34*	*3.47*[a]	*2.79*[a]	*1.72*
K	Shoot	16577	14477[a]	16706	14027	28514[a]
	S/R	*1.30*	*1.69*[a]	*1.55*	*1.85*	*1.63*[a]
Mg	Shoot	3631	3842	4635[a]	4676[a]	4782[a]
	S/R	*0.71*	*1.28*[a]	*1.13*[a]	*1.24*[a]	*0.95*[a]
P	Shoot	3210	3445	2495[a]	1877[a]	24445[a]
	S/R	*0.78*	*1.33*[a]	*0.87*	*0.62*	*1.18*[a]
Trace elements						
Al	Shoot	178	119[a]	178	240	306
	S/R	*0.02*	*0.03*	*0.02*	*0.05*	*0.06*
Cd	Shoot	5.88	5.59	29.1[a]	19.4[ab]	15.7[a]
	S/R	*0.53*	*0.71*	*0.62*	*0.47*	*0.35*[a]
Co	Shoot	0.71	2.39[a]	1.96[a]	4.98[ab]	1.39[a]
	S/R	*0.07*	*0.22*[a]	*0.17*[a]	*0.27*[ab]	*0.12*[a]
Cu	Shoot	18.0	13.2[a]	49.1[a]	33.7[a]	46.6[a]
	S/R	*0.09*	*0.13*[a]	*0.17*[a]	*0.11*[a]	*0.08*
Fe	Shoot	225	229	732[a]	139[b]	116
	S/R	*0.04*	*0.02*	*0.12*[a]	*0.06*[b]	*0.03*
Mn	Shoot	37.4	109[a]	190[a]	347[ab]	169[a]
	S/R	*0.16*	*0.78*[a]	*0.96*[a]	*1.69*[ab]	*0.63*[a]
Ni	Shoot	5.79	5.59	21.7[a]	22.6[a]	70.1[a]
	S/R	*0.06*	*0.11*[a]	*0.23*[a]	*0.28*[ab]	*0.41*[a]
U	Shoot	2.86	0	1.53	4.65	3.08
	S/R	*0.02*	*0*	*0.01*	*0.04*[ab]	*0.02*
Zn	Shoot	262	221[a]	1068[a]	733[a]	1158[a]
	S/R	*0.39*	*0.47*[a]	*0.62*[a]	*0.48*[a]	*0.29*[a]

Shoot concentrations or S/R quotients significantly different ($p \leq 0.05$) from those of the water treatment ([a]), and those of the NH_4Cl/citrate to the NH_4Cl treatment ([b]).
Shoot concentrations and S/R quotients of As Ba Cr Li Pb Sr Ti V were little influenced by the different treatments (data not shown).

The need in biocatalytic transition metals by proteins and proteids should be greatly responsible for the rate of their uptake, translocation to, and distribution in the shoot (Hill et al. 1979). In comparison to *B. chinensis* plants of the water treatment, shoots of citrate-treated plants contained elevated concentrations of Co Mn, the elements of highest affinity to citrate, whereas the need in Cu Zn declined together with the N_{org} content (Table 5). Plants treated with NH_4Cl combined N_{org} increases to 370 % in shoot tissue with a mean of 361 % in biocatalytic metals, but also 500 % in the content of Cd. The lower N_{org} content in NH_4Cl/citrate treated plants went along with a lower need in biocatalytic metals but once more in elevated Co Mn concentrations.

Table 6. Element concentrations (mg kg^{-1} DW) in beet and Indian mustard shoots after daily treatment with water, NH_4Cl, or NH_4Cl/citric acid for 47 d. S/R, shoot-to-root concentration quotient given in italics.

		Beta vulgaris rapaceae			*Brassica juncea*		
Element		Water	NH_4Cl	NH_4Cl/Citr	Water	NH_4Cl	NH_4Cl/Citr
Macronutrients							
Ca	Shoot	30284	49162^{a}	45012^{a}	19053	29147^{c}	31815^{c}
	S/R	*3.01*	*3.94*	*3.34*	*2.53*	*1.69*^{c}	*3.83*^{cd}
K	Shoot	28371	20024^{a}	16893^{a}	26600	31385	23786
	S/R	*1.47*	*0.72*^{a}	*1.06*^{b}	*1.88*	*1.66*	*1.59*
Mg	Shoot	4626	4474	4557	3902	3842	3723
	S/R	*0.49*	*0.60*^{a}	*0.65*^{ab}	*1.49*	*0.88*^{c}	*1.08*^{c}
P	Shoot	7467	3285^{a}	2578^{ab}	2990	3762^{c}	2283^{c}
	S/R	*1.63*	*0.98*^{a}	*0.86*^{a}	*1.01*	*1.17*	*1.04*
Trace elements							
Al	Shoot	164	181	161	251	362	204
	S/R	*0.03*	*0.03*	*0.03*	*0.07*	*0.05*	*0.03*^{c}
Cd	Shoot	37.2	65.2^{a}	73.8^{a}	7.65	23.1^{c}	20.4^{c}
	S/R	*0.74*	*0.87*	*1.00*	*0.75*	*0.72*	*1.05*^{c}
Co	Shoot	1.69	1.13	5.64^{ab}	0.95	0.85	3.25^{cd}
	S/R	*0.14*	*0.11*	*0.26*^{ab}	*0.15*	*0.12*	*0.25*^{cd}
Cu	Shoot	22.4	20.4	20.8	24.2	40.3^{c}	48.0^{cd}
	S/R	*0.20*	*0.07*^{a}	*0.07*^{a}	*0.11*	*0.15*^{c}	*0.17*^{c}
Fe	Shoot	75.9	78.4	77.3	95.0	128	133
	S/R	*0.03*	*0.02*	*0.03*	*0.06*	*0.05*	*0.05*
Mn	Shoot	320	319	766^{ab}	66.9	83.1^{c}	278^{cd}
	S/R	*0.90*	*0.94*	*1.64*^{ab}	*0.59*	*0.61*	*1.16*^{cd}
Ni	Shoot	17.7	66.9^{a}	62.7^{a}	6.56	14.9^{c}	32.2^{cd}
	S/R	*0.23*	*0.65*^{a}	*0.54*^{a}	*0.15*	*0.28*^{c}	*0.48*^{c}
U	Shoot	3.57	0.62	10.77	1.27	0	44.2^{cd}
	S/R	*0.03*	*0.01*	*0.08*^{ab}	*0.01*	*0*^{c}	*0.52*^{cd}
Zn	Shoot	1490	1325	1151	264	949^{c}	742^{cd}
	S/R	*1.11*	*0.87*	*0.97*	*0.63*	*0.93*^{c}	*0.92*^{c}

Shoot concentrations or S/R quotients significantly different ($p \leq 0.05$) from those of the water-treated beet (^{a}) or mustard shoots (^{c}), and those of the NH_4Cl/citrate to the NH_4Cl treatments in beet (^{b}) and mustard (^{d}). Shoot concentrations and S/R quotients of As Cr Li Pb Sr V in beet, and As Cr Li Pb Sr Ti V in mustard were little influenced by the different treatments (data not shown).

In the chlorotic *B. chinensis* plants of the $(NH_4)H_2PO_4$ treatment, the enormous N_{org} and P concentrations may have interfered with physiological equilibria and promoted the uptake of Cu Ni Zn because of their tendency to form phosphate complexes. Shoot tissues of *B. juncea* showed virtually the same preferences for biocatalytic transition metals in the NH_4Cl treatment (Table 6). Additional supply of citrate increased the content in Co Mn Ni U further. Unlike in *Brassica* sp., increases in shoot N_{org} up to the toxic threshold in beet were followed by higher Cd Ni concentrations in the NH_4Cl, and by further increases in Co Mn concentrations in the NH_4Cl/citrate treatment (Table 6).

The ratio between shoot N_{org} and the content in biocatalytic metals of water-treated plants was exactly retained by NH_4Cl treated *B. chinensis* (Figs. 2.1 and 2.2). The ratio changed due to over-proportional increases in Co Mn uptake by citrate-treated *B. chinensis*, and by the selective uptake mode of treated beet.

The elevated need of the protein-enriched plants in biocatalytic metals was frequently met by higher rates of root-to-shoot translocations (Tables 5 and 6). This set of elements was also preferentially solubilized by citric acid (U>Mn>Co>Ca Cu Ni Zn>Mg Sr) and in particular by AA (Cu>>Co Ni> Zn>Cd>Ca Fe Mg Mn) in Settendorf soil (Gramss et al. 2006). Their favoured uptake should be facilitated by affinities to AA residues of proteins in the ion exchange channels of root cell plasma membranes (Williams et al. 2000) but also by the contribution of citrate and AA in their xylem transport (Haydon and Cobbett 2007). A lack in these affinities may explain that uptake of As Ba Cr Li Pb Sr Ti V was not enhanced.

It is concluded that *Brassica* sp. treated with NH_4Cl promise to extract the 5-fold quantity of biocatalytic transition metals such as (Cd) Co Cu Fe Mn Ni Zn (calculated from the increases in DW x shoot N_{org}) from metalliferous soil, with a

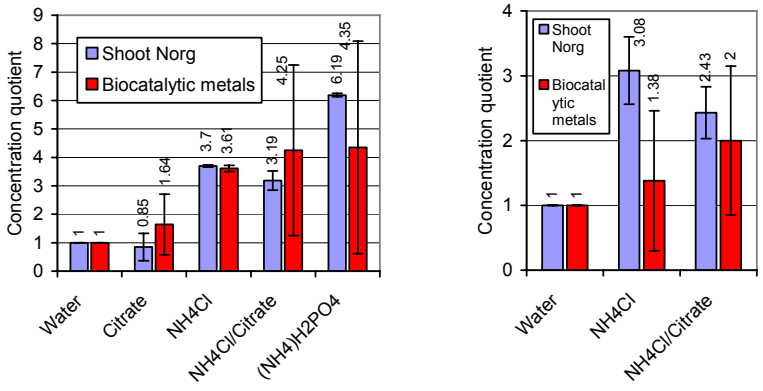

Figs. 2.1 and **2.2**: Relative changes in the shoot concentration of N_{org} and in the mean of its single associated biocatalytic metals, Co Cu Fe Mn Ni Zn, in Chinese cabbage (2.1; left) and beet (2.2). All single concentrations had been divided by those in water-treated plants which served as reference (= 1.0 ± 0).
Error bars, ± SD. Conspicuous deviations from means were due to over-proportional shoot concentration increases of Co Mn Ni in citrate treatments, and of Ni in the $(NH_4)H_2PO_4$ treatment.

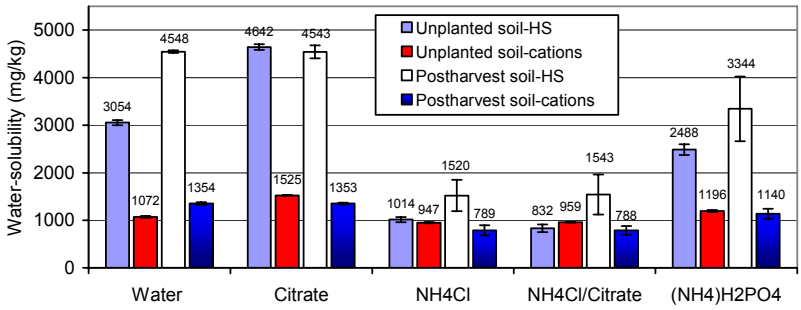

Fig. 3. Potential leaching (mg kg^{-1} soil) of water-soluble humic substance (HS) and of elements according to Table 2 from unplanted control soil and postharvest soil of Chinese cabbage. Elements are bound to HS or coordinated otherwise. Error bars, ± SD.

leaching rate reduced to 60 % that of untreated soil (Fig. 3). Application of citrate traces promoted uptake of Co Mn in all of the tested plants. Uptake of further non-physiological (hazardous) elements increased little more than with the shoot DW (data not shown). The treatment should avoid to drive shoot N_{org} concentrations above the toxic threshold of 4 % by DW. With the consideration of perennial plants in further trials it is intended to reduce the number of crop rotations across the remediation process.

Summary

Chelate-assisted phytoextraction of soil heavy metals extending for decades amplifies primarily the leaching problem. In a search for alternative technologies, *Beta vulgaris rapaceae, Brassica chinensis*, and *Brassica juncea* plants were potted on the metalliferous soil from uranium mining and daily treated with 14 mg N kg^{-1} soil (applied as NH_4Cl or $(NH_4)H_2PO_4$), and/or citric acid at a common field concentration of 1.62 m*M* over 47 d. In unplanted control soil, degradation of citric acid resulted in pH (+0.36 units) and thus in solubility and leaching rate increases (+52 %) of metal-humic complexes but also in microbial consume of soil NH_4^+ and NO_3^-. Citric acid applied to plant-soil systems reduced thus N_{org} content and DW of *B. chinensis* shoots but increased exclusively shoot concentrations of Co/Mn (3.4/2.9 times). These metals are preferentially chelated by citric anion. Supply of NH_4Cl to, and its nitrification in unplanted soil resulted in pH (-0.4 units) and solubility (leaching) decreases of humic substances (-67 %) and minerals (-12 %). This effect persisted in soil planted to *B. chinensis* (-67/-42 %). Daily N doses were completely taken up. Relative to water-treated plants, shoots of *B. chinensis* attained dry weights of 130 to 150 %, 370 % N_{org}, and 580 % N in free amino acids. N_{org} increases of 370 % attracted a 361-% increase in the concentration of the biocatalytic, protein-associated transition metals, (Cd) Co Cu Fe Mn Ni and Zn. Combined application of NH_4Cl and citric acid reduced pH (-0.53 units) and the solubility of humic substances (leaching; -73 %) of unplanted soil in com-

parison to the water treatment further. Concentrations of Co and Mn in the soil solution, chelated by citric anion, were higher than in the NH_4Cl treatment. The N_{org} content of *B. chinensis*, due to soil microbial competition for N, reached only 319 % and attracted 229 % the concentration of Cu Fe Ni and Zn but the 7.0/9.3-fold concentration of Co/Mn in comparison to water-treated plants. Soil treatment with $(NH_4)H_2PO_4$ failed to reduce leaching of soil minerals significantly. Treated *B. chinensis* plants with the elevated concentrations of 5 % N_{org} and 2.5 % P by DW in the shoot grew depressive. *Brassica juncea* reactions to the treatments resembled those of *B. chinensis*. In *B. vulgaris rapaceae*, however, NH_4Cl/(citric acid) treatments increased selectively the shoot concentrations of Ca Cd (Co) (Mn) and Ni. Evaluating the different treatments it is recommended to use *Brassica* sp./NH_4Cl combinations to retrieve the 5-fold quantity of transition metals (calculated from increases in DW x N_{org}) from metalliferous soil with a leaching rate reduced to 50 % in comparison to water-treated controls. Uptake of further elements including uranium increased little more than with the shoot DW of the N-sufficient plants. Trace supplements of citrate stimulated exclusively Co and Mn uptake by all plant species and should only be applied in remediations of soils with Co Mn toxicity problems. Treatments should avoid to increase shoot N_{org} concentrations above the toxic threshold of 4 % by DW.

References

Evangelou MWH, Ebel M, Schaeffer A (2007) Chelate assisted phytoextraction of heavy metals from soil. Effect, mechanism, toxicity, and fate of chelating agents. Chemosphere 68: 989-1003

Gramss G, Büchel G, Bergmann H (2006) Soil treatment with nitrogen facilitates continuous phytoextraction of heavy metals. In Uranium in the Environment. Eds. BJ Merkel and A Hasche-Berger. pp 483-493. Springer, Berlin

Gramss G, Voigt K-D, Bergmann H (2004) Plant availability and leaching of (heavy) metals from ammonium-, calcium-, carbohydrate-, and citric-acid-treated uranium-mine-dump soil. J Plant Nutr Soil Sci 167: 417-427

Haydon MJ, Cobbett CS (2007) Transporters of ligands for essential metal ions in plants. New Phytol 174: 499-506

Hill J, Robson AD, Loneragan JF (1979) The effects of copper supply and shading on re-translocation of copper from mature wheat leaves. Ann Bot 43: 449-457

Huang JW, Blaylock MJ, Kapulnik Y, Ensley BD (1998) Phytoremediation of uranium-contaminated soils: Role of organic acids in triggering uranium hyperaccumulation in plants. Environ Sci Technol 32: 2004-2008

Jones DL, Darrah PR (1994) Role of root derived organic-acids in the mobilization of nutrients from the rhizosphere. Plant Soil 166: 247-257

McLaughlin MJ, Andrew SJ, Smart MK, Smolders E (1998) Effects of sulfate on cadmium uptake by Swiss chard: I. Effects of complexation and calcium competition in nutrient solutions. Plant Soil 202: 211-216

Ong HL, Bisque RE (1968) Coagulation of humic colloids by metal ions. Soil Sci 106: 220-224

Schachtschabel P, Blume H-P, Brümmer G, Hartge KH, Schwertmann U (1998) Lehrbuch der Bodenkunde. 14th edn. Enke, Stuttgart

Schinner F, Öhlinger R, Kandeler E, Margesin R (1993) Bodenbiologische Arbeitsmethoden. 2nd edn. Springer, Berlin

Sumner M E, Fey MV, Noble AD (1991) Nutrient status and toxicity problems in acid soils. In Soil acidity. Eds. B Ulrich and ME Sumner. pp 149-182. Springer, Berlin

Wang AS, Angle JS, Chaney RL, Delorme TA (2006) Soil pH effects on uptake of Cd and Zn by *Thlaspi caerulescens*. Plant Soil 281: 325-337

Williams LE, Pittman JK, Hall JL (2000) Emerging mechanisms for heavy metal transport in plants. Biochim Biophys Acta 1465: 104-126

Zaccheo P, Crippa L, Di Muzio Pasta V (2006) Ammonium nutrition as a strategy for cadmium mobilisation in the rhizosphere of sunflower. Plant Soil 283: 43-56


Uranium Mining
and Hydrogeology

Ecological Solutions of Contaminated Environment Remediation from Uranium Mining Activities in Romania

Nicoleta Groza

R&D National Institute for Metals and Radioactive Resources, Bucharest, Romania

Abstract. The use of constructed wetland for bioremediation purpose in Romanian uranium mining industry could be an innovative solution that complies with the social, economic and environmental context.

In order to improve wastewater from uranium mining industry and at the same time the environmental conditions, this paper aims to demonstrate the constructed ecosystems efficiency and to examine its ecological and socio-economical aspects through an implementation plan based on analysis of governance, policy, costs and financing options.

The paper is directed at developing knowledge for the innovative use of this function and for the benefit of uranium mining wastewater management, moreover it will generate directly targeted knowledge to support practical and political governance.

The paper research it will be generate the elaboration of a new national technology for uranium waste water and contaminated soil remediation based on using of biophytodepuration processes.

It is an energy efficient pleasing method of sites remediation with low to moderate levels of contamination and it can be used in conjunction with other more traditional remedial methods as a finishing step to the remediation process.

This technology will allowed a removal rate of heavy and radioactive metals about 95% comparing with 60 – 70% for conventional treatment.


Uranium Mining
and Hydrogeology

Assessment of rehabilitated uranium mine sites, Australia

Bernd Lottermoser[1] and Paul Ashley[2]

[1]School of Earth & Environmental Sciences, James Cook University, Townsville, Queensland 4811, Australia
[2]Earth Sciences, University of New England, Armidale, New South Wales 2351, Australia

Abstract. Recent research on rehabilitated uranium mine sites located in wet climates has revealed the varied success of the applied rehabilitation efforts. In comparison, there is little knowledge of the status and environmental impacts of rehabilitated uranium mines in dry climates. Mary Kathleen and Radium Hill represent first generation Australian uranium mines, which are located in semi-arid regions. The aim of this communication is to report on the current environmental status and potential hazards of these former uranium mine sites.

Introduction

Australia has been a significant uranium producer since 1954, with first generation (1954-1971) uranium mines previously operating in the Northern Territory (South Alligator Valley, Rum Jungle), Queensland (Mary Kathleen) and South Australia (Radium Hill). These mines have undergone rehabilitation immediately upon or well after mine closure. Rehabilitation strategies and environmental impacts of individual mine sites thereby depend on the mineralogical and geochemical properties of the ore as well as local hydrological and climatic factors. For example, Australia's uranium deposits are located in widely different climates, ranging from monsoonal tropical to arid conditions. In the wet and seasonally wet climatic conditions, ARD development and the leaching of waste repositories are dominant pathways of contaminants into surrounding environments (e.g. Rum Jungle, Mary Kathleen). Recent research on rehabilitated uranium mine sites located in wet climates (Richards et al. 1996; Menzies and Mulligan 2000; Taylor et al. 2003) has revealed the varied success of the applied rehabilitation efforts. In comparison, there is little knowledge of the status and environmental impacts of rehabilitated uranium mines under more arid conditions. The Mary Kathleen and Radium Hill

mine sites represent such uranium mines that were rehabilitated in the 1980s (Fig.1).

The objective of this paper is to review some of the characteristics, environmental impacts and failed rehabilitation methods pertaining to uranium mine sites in semi-arid Australia.

Radium Hill

The Radium Hill mine, in northeastern South Australia, operated from 1954 to 1961. It is in semi-arid grazing land, drier and of lower relief than at Mary Kathleen. At Radium Hill, underground mining occurred with processing of ore on site, resulting in the generation of mill tailings dams and numerous dumps of waste rock material. Some of the latter was crushed and used for local construction purposes, including buildings, roads and railway ballast, despite it exhibiting low-level radioactivity. After mining ceased, most infrastructure was demolished and removed, but there was no remediation of the waste dumps and tailings repositories. About 1980, capping of the main tailings storage facility (TSF) was performed and this action lessened the effects of wind and water erosion. The region is currently used for low density grazing and has low human visitation.

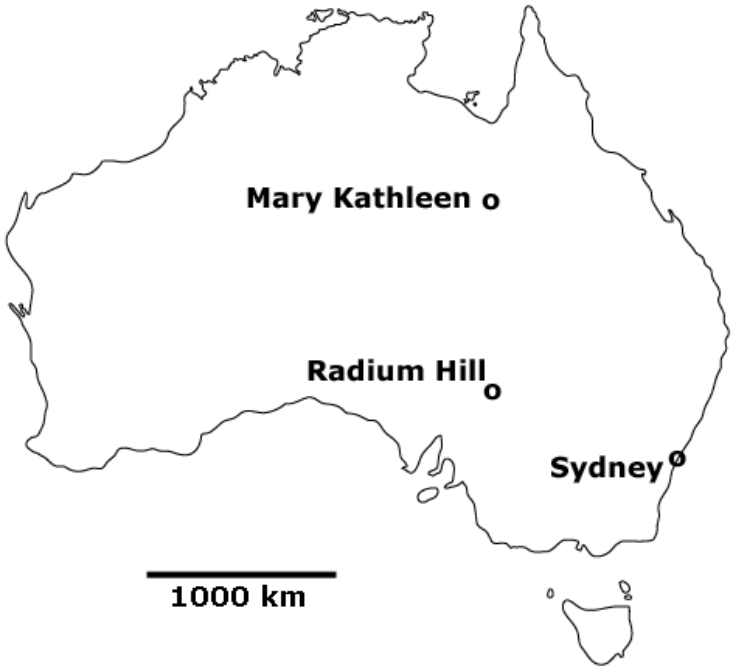

Fig.1. Location map of the Radium Hill and Mary Kathleen uranium mine sites, Australia.

Mineralised rock at Radium Hill comprises quartzofeldspathic gneiss, schist, amphibolite and pegmatite, with the ore minerals (davidite-brannerite-uraninite) being part of a refractory Fe-Ti-U-REE oxide assemblage. Sulfide minerals are very sparse and together with the dry climate, there is little evidence for chemical processes mobilising U and related elements from tailings and waste rock dumps. Physical dispersion processes have been significant at Radium Hill, with wind dispersion of tailings fines occurring in the district prior to capping of the main tailings repository, and water erosion of both the tailings material and waste rock dumps. Local soils have been impacted through physical dispersion by increased geochemical (U, Th, REE, V, Cr) and radiochemical loadings. Plants growing on impacted soils and waste rock dumps display biological uptake of U and other lithophile elements. Capped tailings repositories are unstable landforms and since 1980 have been subject to rill erosion, exposing significantly radioactive tailings (Fig. 2). However, radiation doses at Radium Hill are low, except in the immediate vicinity of exposed tailings. Visitors to the site will not be exposed to excessive radiation levels.

Mary Kathleen

Mary Kathleen, in northwest Queensland, operated from 1956 to 1963 and again from 1976 to 1982. It is situated in a region with a semi-arid climate, high evaporation rate and a summer rainfall maximum causing ephemeral flooding and sediment transport. The open scrub and woodland has been used for low density cattle grazing. Rehabilitation of the Mary Kathleen open pit mine, mill and tailings repo-

Fig.2. Rill erosion of the soil capped tailings storage facility, Radium Hill, South Australia (height of facility approximately 6 m). The soil capping is being removed, resulting in the exposure of radioactive tailings in rills.

sitory sites occurred between 1982 and 1985. This involved the dry capping of the tailings repository with rolled soil/loam/clay and overlying unmineralised waste rock, disposal of contaminated waste into the bottom of the pit and allowing its subsequent flooding, and the partial to complete capping of many of the waste rock dumps. The area was returned to cattle grazing and public access.

Mineralised rock at Mary Kathleen (ore and waste rock) is dominated by a metasomatic calc-silicate assemblage, with minor amounts of sulfide minerals, rare earth minerals and uraninite. Although calcite is commonly present, there is oxidation of sufficient sulfides to generate acid conditions in the pit lake, the upper part of the TSF and seepage from the latter. Pit walls are locally encrusted with transient soluble sulfates and there is evident mobility of Fe, Ca, Cu, U and REE. Pit water is slightly acid, Ca-SO_4-rich and exceeds recreational water quality guideline values for TDS, Fe, Mn, SO_4, Cu and Ni, and livestock water guidelines for Cu and U.

Seepage water from the TSF is slightly acid (pH 5.5), metal- and SO4-rich, and radioactive (Fig. 3). There is rapid precipitation of Fe oxyhydroxides, with absorbed U, REE, Y, As and radionuclides. Further downstream, surface and groundwaters become near-neutral, but increase in salinity such that there is widespread precipitation of sulfates. Although release of U and other metal/metalloid contaminants from the TSF is insignificant, concentrations of TDS, U and SO4 in surface waters exceeds livestock water guidelines.

Waste rock dumps at Mary Kathleen have steep sides and are not stable long-term landforms. They are subject to physical and chemical processes that can con-

Fig. 3. Seepage point at the base of the tailings dam wall, Mary Kathleen, Australia. Abundant sulfate efflorescences and Fe-oxyhydroxide precipitates form from the acid, saline, radioactive seepage water (pH: 5.5; salinity: 0.31 %). Bolders in the retaining wall are approximately 1 m in diameter.

tribute to stream and soil loadings of U and other metal/metalloid contaminants. Where covered by benign soil/rock, plant growth has occurred, but sulfide oxidation processes has restricted plant colonisation in uncovered or disturbed zones. Many plant species at Mary Kathleen growing in the mine void, on waste dumps and contaminated soil display uptake of U and other metal/metalloids at levels of 10-100 x those on background sites. Radiation levels in the open pit average 5.65 mSv/year and are less on the waste dumps. Consequently, casual visitation to the site is not considered a hazard.

Conclusions

At Radium Hill, rehabilitation efforts have been restricted to capping of tailings, but following a 20 year period of prior extensive wind dispersal of exposed tailings that has impacted local soils. Physical erosion of waste repositories is of ongoing concern (Lottermoser and Ashley 2006). It is evident that the capped tailings repositories will degrade in time, causing increased erosional dispersal unless further remediation measures are implemented. The erosion of capped waste repositories, particularly by infrequent rainstorm events, highlights the fact that dry capping of waste dumps in semi-arid terranes may not necessarily lead to the permanent containment of wastes.

At Mary Kathleen, it was predicted upon mine site rehabilitation (Flanagan et al. 1983; MINENCO 1986; MKU 1986; Ward et al. 1984): (a) that the tailings porewaters would not infiltrate into the local aquifer; (b) that there would be little chance of ARD and of metal and radionuclide mobility from the waste rock dumps and tailings repository; and (c) that seepage water quality would not pose a problem for human or stock health, despite sulfate contamination of the groundwater being the main long term environmental impact. Twenty years after rehabilitation, it is evident that some rehabilitation measures have been quite successful in reducing dispersion of U and related elements into the surrounding environment (e.g. the TSF cover). By contrast, the predictions made on the geochemical behaviour of waste rock dumps and the TSF proved to be incorrect. There is still significant physical and chemical mobility of contaminants from the TSF into ground and surface waters, contaminants are being transferred into plants, and there is a threat to stock health. Physical erosion and chemical leaching of waste rock repositories and the leaching of the tailings repository are the dominant pathways of contaminants into surrounding environments (Lottermoser and Ashley 2005; Lottermoser et al. 2005).

References

Flanagan JC, Morton WH, Ward, TA (1983) Groundwater management around uranium mine waste areas, Mary Kathleen, Australia. In: International Conference on Groundwater and Man, Australian Water Resources Council Conference Series no 8. Australian Water Resources Council, pp. 81-88

Lottermoser BG, Ashley PM (2005) Tailings dam seepage at the rehabilitated Mary Kathleen uranium mine, Australia. J Geochem Explor 85: 119-137

Lottermoser BG, Ashley PM (2006) Physical dispersion of radioactive mine waste at the Radium Hill uranium mine site, South Australia. Aust J Earth Sci 53: 485-499

Lottermoser BG, Ashley PM, Costelloe MT (2005) Contaminant dispersion at the rehabilitated Mary Kathleen uranium mine, Australia. Environ Geol 48: 748-761

Menzies NW, Mulligan DR (2000) Vegetation dieback on clay-capped pyritic mine wastes. J Environ Qual 29: 437-442

MINENCO (1986) Mary Kathleen uranium mine rehabilitation water quality prediction studies. Unpublished report, Australian Groundwater Consultants Pty Ltd

MKU (Mary Kathleen Uranium Ltd) (1986) Rehabilitation of the Mary Kathleen Mine. Unpublished report, Mary Kathleen Uranium Ltd.

Richards RJ, Applegate RJ, Ritchie AIM (1996) The Rum Jungle rehabilitation project. In: Mulligan D (ed.) Environmental Management in the Australian Minerals and Energy Industries 1996. University of New South Wales Press, pp. 530-553

Taylor G, Spain A, Timms G, Kuznetzov V, Bennett J (2003) The medium-term performance of waste rock covers - Rum Jungle as a case study. In: Farrell T, Taylor G (eds.) 6th International Conference on Acid Rock Drainage 2003. Australasian Institute of Mining & Metallurgy, pp. 383-397

Ward TA, Hart KP, Morton WH, Levins DM (1984) Factors affecting groundwater quality at the rehabilitated Mary Kathleen tailings dam, Australia. In: 6th Symposium on Uranium Mill Tailings Management. Colorado State University, Denver, pp. 319-328

Radiological Assessment of the rehabilitated Nabarlek Uranium Mine, Northern Territory, Australia

A. Bollhöfer[1], P. Martin[1,2], B. Ryan[1], Kirrilly Pfitzner[1], A. Frostick[1,3], K. Evans[1] & D. Jones[1]

[1] Environmental Research Institute of the Supervising Scientist (***eriss***), Darwin, NT 0801, Australia
[2] International Atomic Energy Agency (IAEA), A-1400 Vienna, Austria
[3] Charles Darwin University, Darwin, NT 0809, Australia

Abstract. The Nabarlek mine site is located in the remote Western Arnhem Land, in the wet-dry tropics of the Northern Territory of Australia. The Nabarlek ore body was a relatively compact, high-grade ore body that extended from the surface to a depth of 72 metres, and was mined out during the dry season of 1979. The ore was stockpiled, and subsequently milled and sold over an eight year period that ended in 1988. The mill tailings, together with scraped sludge from the bottom surfaces of runoff and evaporation ponds, were placed back in the mined out pit when operation ceased. These were covered by geotextile, followed by a 1-3 m thick graded rock and leached sand layer. With final decommissioning in 1995, remaining contaminated material and plant equipment were placed in the remaining pit void and covered with another layer of waste rock. Other areas rehabilitated were the plant area, the evaporation ponds, several runoff ponds, and the ore, waste rock and topsoil stockpile areas.

The Supervising Scientist Division of the Australian Government Department of the Environment, Water, Heritage and the Arts conducts regular visits to the Nabarlek site as part of an ongoing assessment of the status and radiological conditions of the land and water resources within the Nabarlek area. Extensive field surveys have been conducted to estimate the magnitude of exposure pathways, and the location, extent and seasonal variability of the sources. Work has also focussed

on the analysis of groundwater monitoring data, and groundwater modelling indicates a uranium plume moving to the north east from the pit where tailings have been stored, in agreement with general groundwater movement in the area. An erosion modelling study has shown that erosion of radionuclides off-site occurs. However, the impact is likely to have existed pre mining, as indicated by a study of stable lead isotopes in sediments in a nearby Creek. The ingestion pathway was modeled, using dietary information gathered from local Aboriginal people and measurements of radionuclide in bush food items, water and soils. Concentration factors from other studies in the Top End of Australia were applied. In this paper we will present the site specific radiological dose model and major conclusions concerning the present radiological footprint of the rehabilitated Nabarlek site.

Groundwater-climate relationships, Ranger uranium mine, Australia: 1. Time series statistical analyses

Mobashwera Kabir[1], Kais Hamza[2], Gavin M. Mudd[1,*] and Anthony R. Ladson[1,3]

[1]Institute for Sustainable Water Resources, Department of Civil Engineering, Monash University, VIC 3800 Australia (* Gavin.Mudd@eng.monash.edu.au)
[2]School of Mathematics, Monash University, VIC 3800 Australia
[3]Presently SKM Consulting Pty Ltd, Melbourne, VIC Australia

Abstract. This paper presents the results of applying specific time series statistical techniques to observed historical groundwater-climate data at the Ranger uranium project. By developing and applying existing statistical techniques, rarely used in mining studies, improved confidence about the understanding of the groundwater-climate relationship at the Ranger uranium project is obtained. This forms a sound basis upon which future climate scenarios can be used to predict the response of the groundwater after rehabilitation and into the long-term, especially with respect to potential climate change impacts.

Introduction

The relationship between groundwater and climate is critical to understand in the design of uranium mine rehabilitation, especially in tropical regions with intense monsoonal rains and extended dry seasons. The Ranger uranium mine is located in the wet-dry tropics of northern Australia and is surrounded by the world heritage-listed Kakadu National Park (Fig. 1) – making it imperative to understand the groundwater-climate relationship to ensure that appropriate rehabilitation designs are implemented upon mine closure.

There are a variety of techniques which can be used to model the relationship between groundwater and climatic conditions. The complex geology, topography and climatic variability of the Ranger project area makes a deterministic process-based model a challenging task. For a simpler approach, this paper presents the application of time series statistical techniques, an approach rarely used in mining projects (companion conference papers present physical modelling approach).

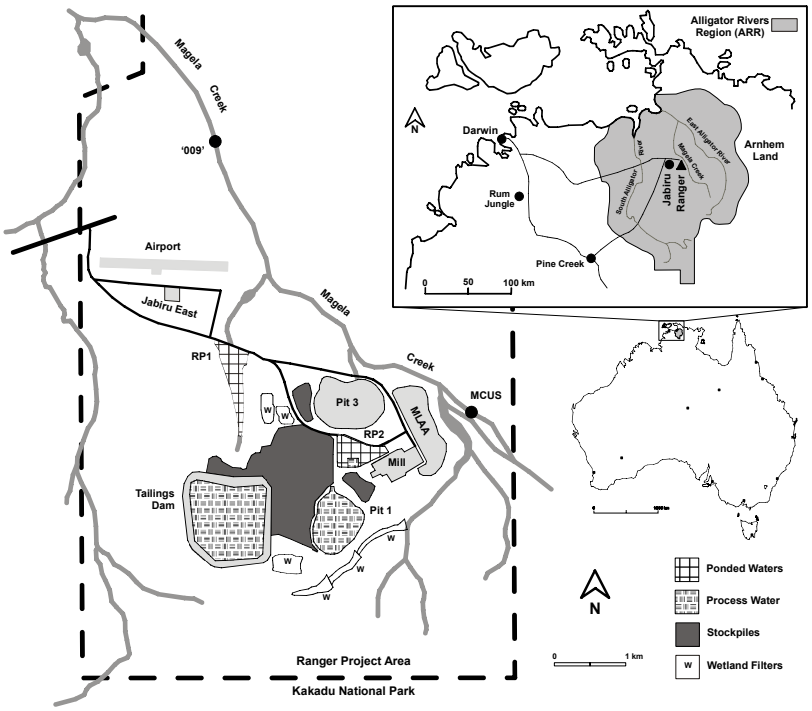

Fig.1. Location and outline of the Ranger uranium project, Northern Territory, Australia.

Ranger uranium project, Northern Territory, Australia

The Ranger uranium deposits were first discovered and 1969, and after extended controversy and debate, was approved for development in 1977. Production began in August 1981, and is currently at 5,000 t U_3O_8/year via open cut mining and a conventional mill. At present, mining is scheduled to be completed in 2012, with milling of ore stockpiles to be completed by 2020. The site is located on freehold indigenous land, controlled by the Mirarr traditional owners.

The Ranger project is located in the Alligator Rivers Region and is surrounded by the world-heritage listed Kakadu National Park (Fig. 1). The area has a wet-dry monsoonal climate, with average annual rainfall of ~1,450 mm and pan evaporation of ~2,500 mm. Virtually all rainfall occurs during the monsoonal months of December to March, leading to a strongly positive water balance over this time.

After completion of mining and milling, the Ranger site will be rehabilitated, and a key legal criterion for tailings is that they "will not result in any detrimental environmental impacts for at least 10,000 years" (Senate 2003). As groundwater is the key driver for long-term migration, it is therefore critical to understand groundwater-climate relationships (especially in light of potential climate change

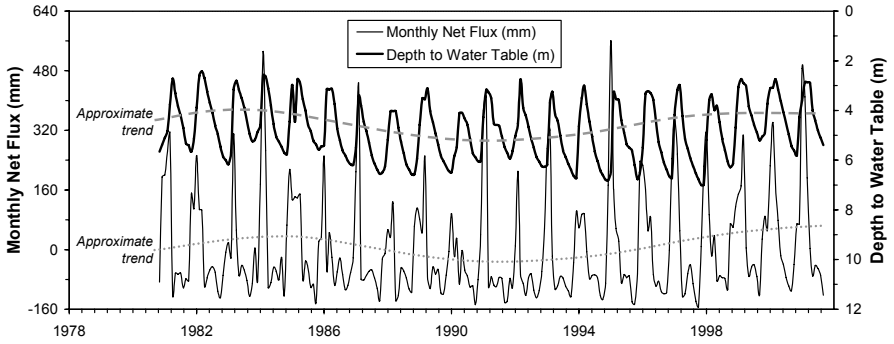

Fig.2. Monthly net flux (rainfall minus estimated evapotranspiration) versus groundwater response, Ranger site. Note both annual variation plus longer term decadal variation.

impacts). Given Ranger's location, there is a range of climate and groundwater monitoring data which can be analysed, with an example shown in Fig. 2.

Methodology and approach

Conceptual hydrologic model

The groundwater behaviour at the Ranger site is treated as a one-dimensional and effectively vertical flow system, based on the large head changes each wet season relative to minor lateral flow. In this manner, the recharge of groundwater during the wet season causes a rise in the water table, while the negative flux during the dry season (due to both soil evaporation and vegetative transpiration) leads to a subsequent decline in the water table. The monthly climatic flux is shown in Fig. 3. The extent of this annual cyclical movement of groundwater is dependent on soil types, underlying geology and relatively flat topography (see Kabir et al 2008). The groundwater bores chosen for analysis were screened based on long-term trends and no evidence of direct mining impacts on head levels (eg. seepage).

All data is obtained from monitoring of groundwater and climate (rainfall, pan evaporation) at the Ranger site, courtesy of Energy Resources of Australia Ltd (ERA, mine owner) or the Office of the Supervising Scientist (OSS, Federal agency) (further details are given in Kabir, 2008).

Time series statistical techniques – brief review

Although times series statistical techniques (TSST) methods are widely used in other disciplines (e.g. economics, hydrology), they have seen little application in groundwater studies(e.g. Fig. 2). Only a brief review is possible herein; for a more thorough treatment see Brockwell and Davis (2002).

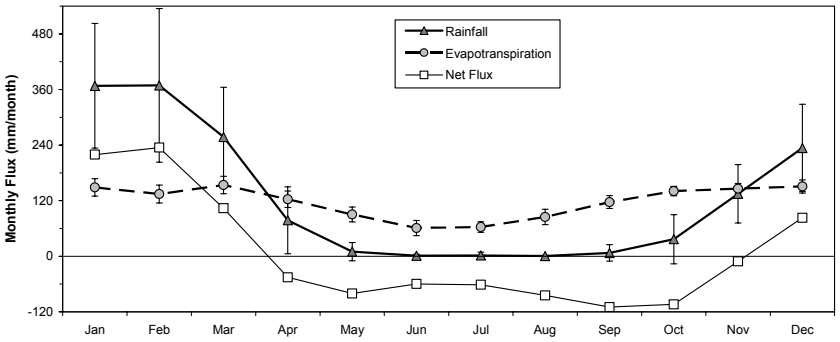

Fig.3. Monthly rainfall, estimated evapotranspiration and net flux.

At its simplest conceptual basis, time series techniques involve developing a statistical relationship between an independent variable (e.g. climate data as cause) and a dependent variable (e.g. groundwater response as effect).

In this study, exploratory data analysis was undertaken to examine seasonality, trends and random noise (e.g. Fig. 2). Classical decomposition techniques were used to address this, and represents a univariate time series model, given as (Brockwell and Davis 2002):

$$X_t = m_t + s_t + A_t \qquad \text{(Eq.1)}$$

$$\text{and} \qquad EA_t = 0,\ s_{t+d} + A_t \qquad \text{and} \sum_{j=1}^{d} s_j = 0 \qquad \text{(Eq.2)}$$

where X_t is the dependent variable at time t (ie. groundwater), m_t is the long-term trend component, s_t is the seasonal component, A_t is the random noise component (a zero-mean stationary process), EA_t is the expected value of A_t, and d is the period of seasonal components.

The seasonal component is calculated such that the period length (d) ensures the values are the same. For example, a period of 12 is used for monthly data. The algebraic sum of the 12 months seasonal components should equal zero (*Eq. 2*). The seasonal components of the net flux and groundwater level are given in Fig. 3.

A univariate autoregressive moving average (ARMA) model could explain the time series of climate and groundwater data of four selected bores, however, the causal relationship between climate and groundwater levels requires multivariate analyses. Therefore two specific TSST methods, namely the transfer function noise (TFN) model and the multivariate autoregressive (MA) model, were used for modelling the groundwater-climate data.

The first TSST model applied in this paper is the TFN model, and involves transforming data to generate zero-mean stationary data sets. The TFN model can then be represented as (Brockwell and Davis 2002):

$$Y(t) = T(B).X(t) + N(t) \qquad \text{(Eq.3)}$$

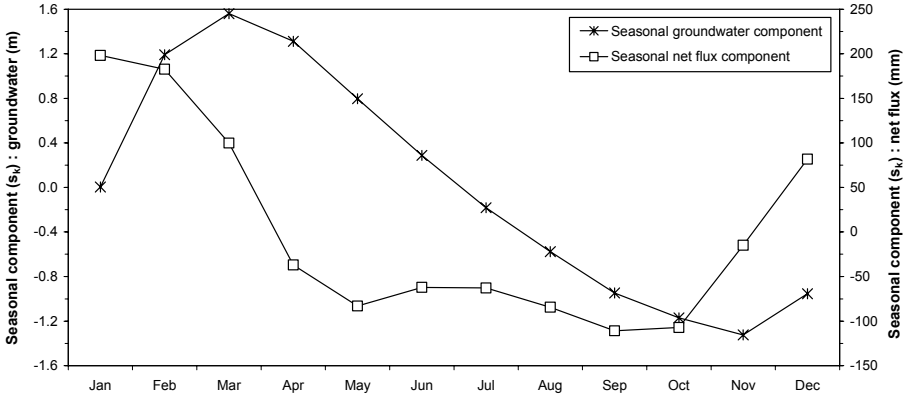

Fig.4. Seasonal components of climatic net flux and groundwater level data.

where *Y(t)* is the dependent variable (ie. groundwater), *X(t)* is the independent variable (climate), *T(B)* is a causal time-invariant linear filter, B is back shift operator and *N(t)* is a zero-mean stationary process (uncorrelated with *X(t)*).

The second TSST model developed is a Yule-Walker multivariate autoregressive (MA) model using monthly data.

Further theoretical discussion, development and references for both TSST models can be found in Brockwell and Davis (2002).

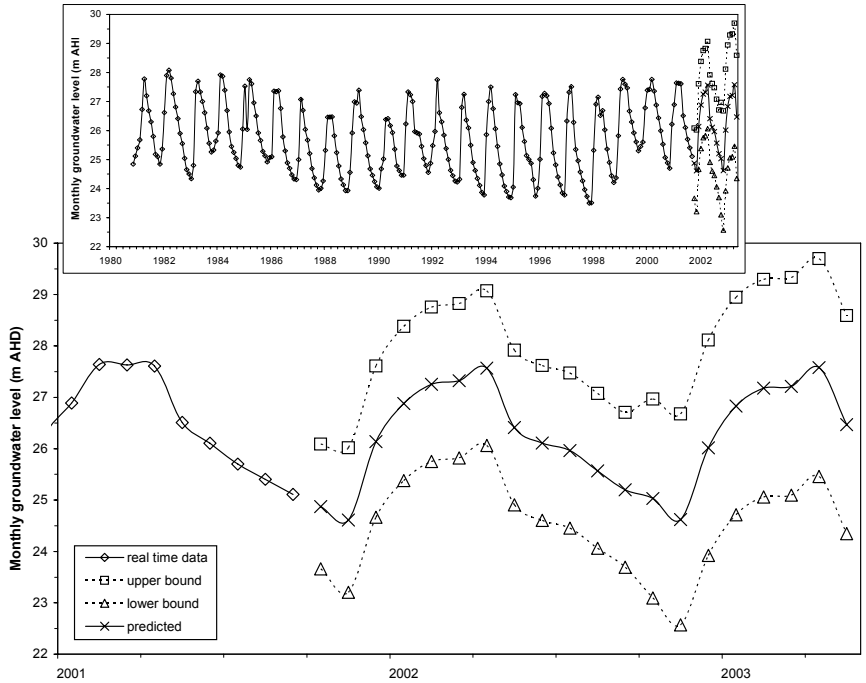

Fig.5. Predictions of groundwater level by the transfer function noise (TFN) model.

Results

Monthly groundwater levels have been predicted for twenty months by analysing twenty two years monthly data (Fig. 5) by TFN model. The monthly net flux and monthly groundwater levels have been predicted for twenty years by analysing twenty-two years monthly data, shown in (Fig. 6) by MA model.

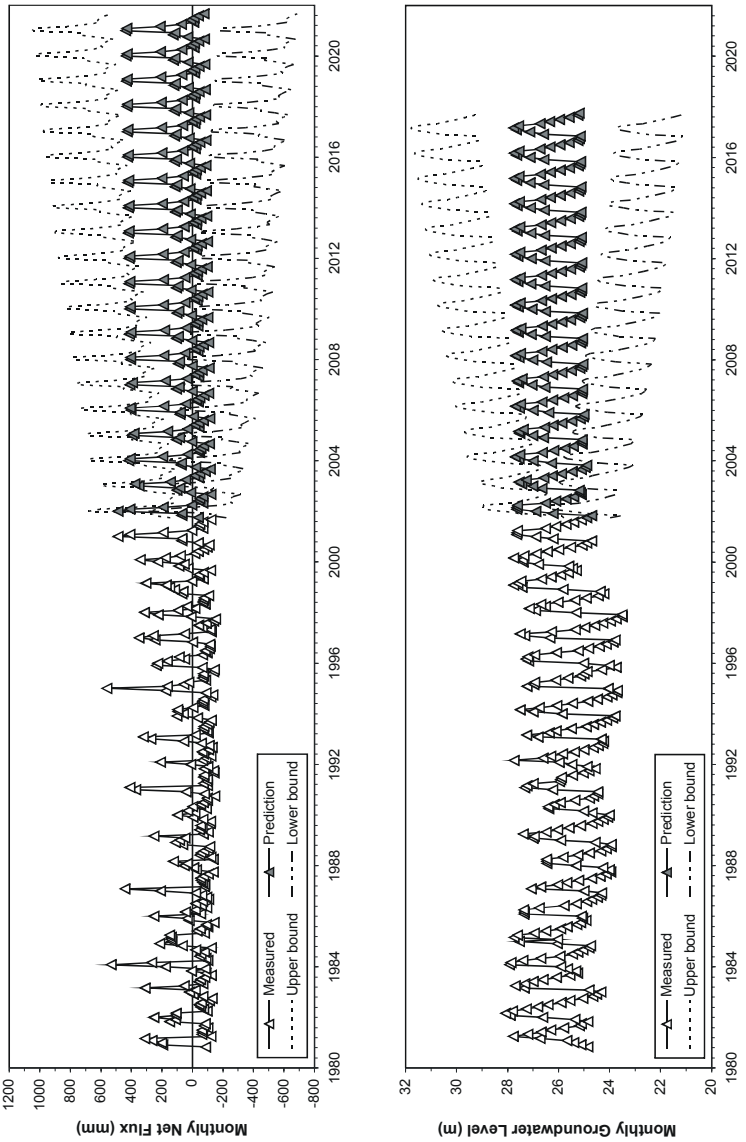

Fig.6. Predictions of monthly net flux (left) and groundwater levels (right) by multivariate autoregressive (MA) model.

The TFN model is represented by:

$$\text{Input} \quad X(t) = -0.012\,X(t-1) + 0.121\,X(t-2) + 0.266\,X(t-3) - 0.201\,X(t-4) - 0.551\,X(t-5) + Z(t) + 0.190\,Z(t-1) - 0.367\,Z(t-2) - 0.438\,Z(t-3) + 0.276\,Z(t-4) + 0.935\,Z(t-5) \quad \text{(Eq.4)}$$

$$\text{Transfer} \quad T(B) = 1.7\,B / (1 - 0.283\,B) \quad \text{(Eq.5)}$$

$$\text{Noise} \quad N(t) = W(t) + 0.5135W(t-1) + 0.336W(t-2) + 0.2365W(t-3) \quad \text{(Eq. 6)}$$

Model performance was evaluated in the light of existing statistical criteria, such as model simplicity, model fitness and the Akaike Information Criterion with Correction AICC (Akaike 1969), combined with the appropriateness of the physical basis of the two methods. In Table 2, to compare the statistical performance of the monthly-based models, a number of criteria have been considered. These are the AICC statistic, root mean square error (RMSE), and square of correlation coefficient (R^2) for the models. It is found that the TFN model performs better than the AR model with respect to RMSE and R^2, while the reverse is true for the AICC statistic. The AICC statistic is a standard selection criterion when the competing models are of the same type, where a minimum value indicates the best model, but it does not make sense when comparing two different types of models. In this case, the TFN model is structurally different from the MA model. From this basis, the TFN model can be said to be better than the AR model.

The groundwater levels are predicted by the monthly TFN and MA models for the period November 2001 to October 2002 and compared to measured values (ie. a model validation test). The results are shown in Fig. 7 and confidence intervals are compared in Table 2. In the validation test the two models are similar.

Table 1. Statistical evaluation and comparison of TFN and MA models.

Model	AICC	RMSE	R^2
Transfer function noise (TFN)	6698	0.166	0.761
Multivariate autoregressive (MA)	6585	0.173	0.760

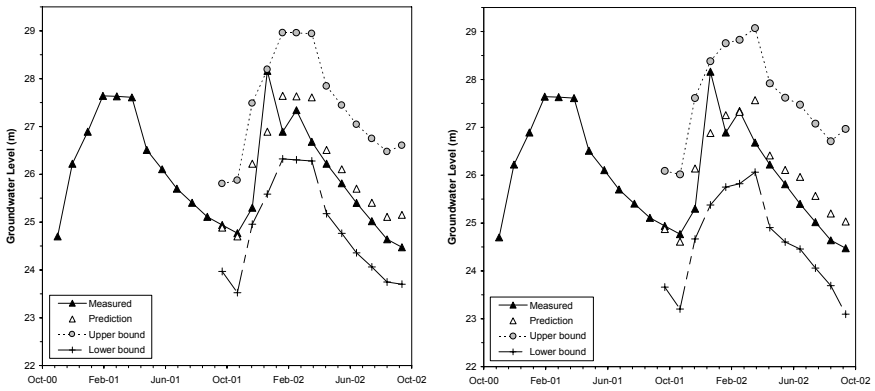

Fig.7. Validation of TFN model (left) and MA model (right) for Nov. 2001 to Oct. 2002.

Table 2. Average confidence interval range for TFN and MA models, Nov. 2001 to Oct. 2002 validation.

Model	Average range of confidence interval (m)
Transfer function noise (TFN)	2.94
Multivariate autoregressive (MA)	2.56

Technically, TFN models are superior to MA models in explaining the groundwater-climate relationship. The theory of MA model considers the mutual dependence of all the series of the process. For instance, the net flux at time t+1 is represented as function of net flux at t, t-1, t-2 … together with groundwater level at t, t-1, t-2 … as well and a noise component. However, in the TFN model, the previous values of the groundwater level series are not considered explicitly. From the scientific point of view, there does exist a strong causal relationship between net flux and groundwater level, but the relationship is not two way. That means net flux influences groundwater level but groundwater level does not influence net flux to any significant extent (ie. the influence is effectively one way). Although the evaporative flux depends on soil moisture content, which in turn is influenced by the nearness of groundwater level to the surface, the importance of this variable is much less than other factors such as intensity and duration of radiative energy, relative humidity, temperature gradient, soil thermal conductivity, vegetation type, wind speed, etc., which influence the evaporation and transpiration process. The statistical fits and confidence intervals of both models, however, are comparable. Therefore, the TFN model is more acceptable than the MA model in representing the system and predicting future groundwater levels.

Discussion

To select the appropriate method of analysis of the groundwater-climate relationship, reviews of the various classes of models were performed. The three basic features, useful for distinguishing approaches to modelling are (CRCCH 2005):

- the nature of the basic algorithms (empirical, conceptual or process-based);
- whether a statistical or deterministic approach is taken to input or parameter specification;
- whether the spatial and temporal representation is lumped or distributed.

The review of key climate feedbacks which are related to groundwater recharge and hydrologic processes suggests that to manage the complex interaction between climate and groundwater recharge, the development of a balanced modelling framework is necessary. Data-based statistical techniques are more preferable than deterministic models when the latter requires too much simplification of the complex system. Comprehensive modelling of groundwater-climate relationships could go to the ultimate extent of including a variety of processes, such as heat flow, groundwater flow and pumping, vapour fluxes, cloud cover, vegetative transpiration, soil evaporation, variable geology and soils, and so on. However, such complexity is clearly unrealistic given the large spatial and temporal uncertainties involved in all of these aspects and processes.

Climatic conditions and variability undoubtedly govern or contribute to shallow groundwater levels (e.g. Fig. 2) (see also Alley 2001; Glassley 2003; Loáiciga 2003; Michaud et al 2004), yet a complete process representation is computationally and physically unrealistic given the complex variability of processes and inter-dependence of many factors. This is not to ignore the value of sound physical or process-based models, but it highlights that different approaches such as time series statistics can be used to compliment such models and analyses, often providing efficient numerical techniques which effectively combine the complexity of natural processes into functional statistical relationships.

Conclusions

Groundwater levels will be the major driver for the potential transport of solutes from a rehabilitated Ranger uranium mine, especially levels relative to non-mine areas. To ensure that the rehabilitation achieves its legal obligations to protect the surrounding water resources and ecosystems for 10,000 years from tailings, it is vital to understand and be able to model the groundwater-climate relationship. This is a fundamental objective to ensure a sustainable post-mining land use and protection of the recognised world-heritage values of the region.

To bridge the gap between the observation scale (~monthly data) and modelling scale (long-term prediction) (Bloschl and Sivapalan 1995), we have used common time series statistical techniques. These methods identify the underlying patterns and the qualitative description of the groundwater-climate relationship, such as seasonal variability or long-term trends.

The application of a classical decomposition model to the groundwater-climate data for Ranger was used first to gain an understanding of the relationship. The timing of the peak and trough between the two seasonal data sets indicates that the lag between them is less (2 months) during high groundwater levels (wet season) and much more (4 to 5 months) during low groundwater levels (dry season). Hence the process has a variable lag throughout the year.

Thus, for improved understanding of the physics with the help of statistics, a classical decomposition model has been used with historical net flux and groundwater level data for the Ranger uranium mine site. A transfer function noise (TFN) model and multivariate autoregressive (MA) model were then developed by using the net flux and groundwater level data to predict the future groundwater level. Some of them have been found to be numerically efficient and others have the quality of best fit.

Finally the statistical performance is almost equal for both the TFN model and MA model but the physical representation is better in TFN than MA. Therefore a monthly-based TFN should be the recommended model for the prediction purpose in future research.

References

Akaike H (1969) Fitting autoregressive models for prediction. Annals of the Institute of Statistical Mathematics, 21, pp 243-247

Alley WM (2001) Ground Water and Climate. Ground Water, 39(2), pp 161

Bloschl G and Sivapalan M (1995) Scale issues in hydrological modelling: a review. Hydrological Processes 9, pp 251-290

Brockwell PJ and Davis RA (2002) Introduction to time series and forecasting. Springer-Verlag, New York, USA

CRCCH (2005) General approaches to modelling and practical issues of model choice. Cooperative Research Centre for Catchment Hydrology, Series on Model Choice, see http://www.toolkit.net.au/modelchoice/

Glassley WE (2003) The impact of climate change on vadose zone pore waters and its implication for long-term monitoring. Computers and Geosciences 29(3), pp 399-411

Kabir M (2008) Modelling groundwater-climate relationships at the Ranger uranium mine, Australia. PhD Thesis (In Preparation), Dept. of Civil Eng., Monash University

Kabir M, Mudd GM and Ladson AR (2008) Groundwater-climate relationships, Ranger uranium mine, Australia : 2 validation of unsaturated flow modelling. Proc. “Uranium mining and hydrogeology V”, Freiberg, Germany, September 2008

Loáiciga HA (2003) Climate change and groundwater. Annals of the Association of American Geographers 93(1), pp 30-41

Michaud YC, Rivard et al. (2004) Groundwater resources and climate change: Trends from eastern Canada. American Geophysical Union, Spring Meeting 2004.

Senate (2003) Regulating the Ranger, Jabiluka, Beverley and Honeymoon uranium mines. Environment, Communications, Information Technology and the Arts References Committee, Australian Senate, Canberra, Australia, 355p

Groundwater-climate relationships, Ranger uranium mine, Australia: 2. Validation of unsaturated flow modelling

Mobashwera Kabir[1], Gavin M. Mudd[1,*] and Anthony R. Ladson[1,2]

[1]Institute for Sustainable Water Resources, Department of Civil Engineering, Monash University, VIC 3800 Australia (*Gavin.Mudd@eng.monash.edu.au)
[2]Presently SKM Consulting Pty Ltd, Melbourne, VIC Australia

Abstract. This paper presents the results of applying an unsaturated flow model to observed historical groundwater-climate data at the Ranger uranium project, Northern Territory, Australia. Based on observed data, a one-dimensional model was developed to fit historical data for several bores. Statistical evaluation of varying porosity and hydraulic conductivity was undertaken, thereby giving a reasonable model configuration. The model is thus confirmed as suitable for predicting the impacts of future climate change scenarios on water table fluctuations.

Introduction

The relationship between groundwater and climate is critical in the design of uranium mine rehabilitation, especially in tropical regions with intense monsoonal rains and extended dry seasons. The Ranger uranium mine is located in the wet-dry tropics of northern Australia and is surrounded by the world heritage-listed Kakadu National Park (Fig. 1). It is imperative to understand the groundwater-climate relationship to ensure that appropriate rehabilitation designs are implemented upon mine closure (see also companion paper Kabir et al 2008).

A variety of techniques can be used to model groundwater fluctuations as a function of climatic conditions. The complex geology and climatic variability of the Ranger region makes a deterministic, detailed process-based model a difficult task. For an alternative viable approach, this paper uses the unsaturated flow model Seep/W (Krahn 2004) based on a one-dimensional conceptual model of the groundwater-climate system. Given the relatively flat topography and large annual fluctuations in the water table versus minor lateral flows, the flow system can be simplified as effectively vertical, thereby allowing direct implementation in Seep/W. The refined model can then be used for a variety of purposes.

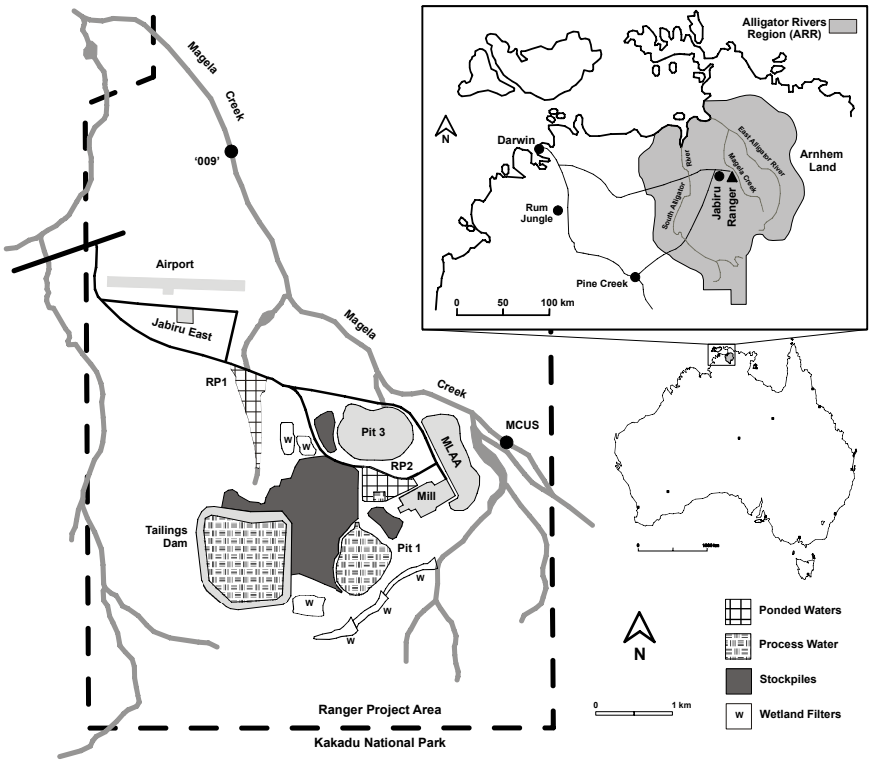

Fig.1. Location and outline of the Ranger uranium project, Northern Territory, Australia.

Hydrogeology of the Ranger site

The Ranger uranium project was briefly described in the companion paper Kabir et al (2008). Although there have been numerous studies on the hydrogeology and water balance at Ranger, only a few have directly examined the relationship between groundwater and climate, especially rainfall-evaporation and recharge (e.g. Vardavas, 1993; Woods 1994). A brief review of the hydrogeology is presented, followed by a justification of the modelling approach used for this work.

In the past, hydrogeology studies at Ranger have commonly focussed on water or tailings management issues. The hydrogeology is considered to comprise three principal aquifer types – alluvial sands and gravels (Type A), lateritic layers, clayey sands to weathered rocks (Type B), and fractured rocks (e.g. schists, dolomite) (Type C), shown in Fig. 2 (Ahmad and Green 1986; Woods 1994; Brown et al 1998). The most important shallow aquifers are found as weathered and lateritic soils (by area), with annual variations in the water table being between 1 to 5 m.

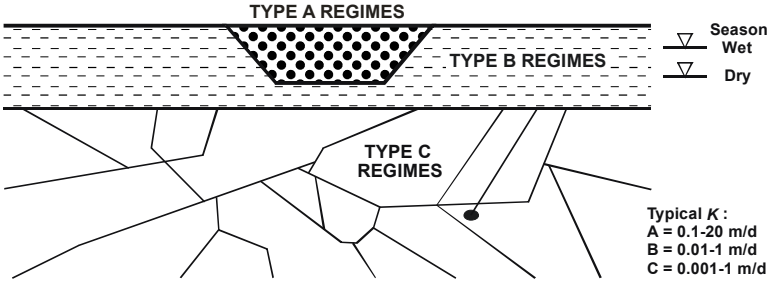

Fig.2. Conceptual hydrogeology of Ranger, including approximate wet and dry season position of the water table (adapted from Ahmad and Green 1986; Woods 1994).

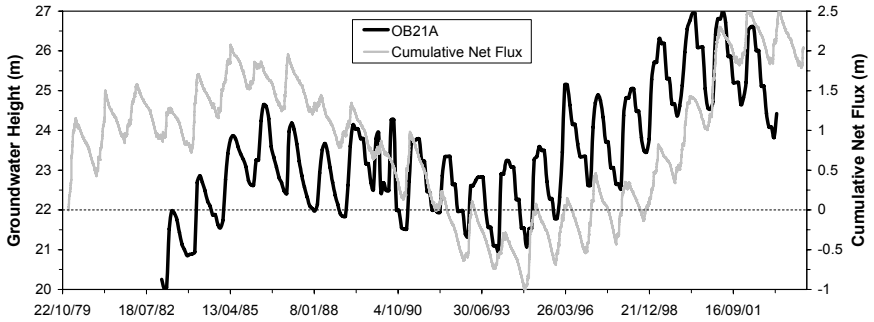

Fig.3. Variation of groundwater (bore OB21A) and cumulative climatic net flux.

One example of the seasonal groundwater movement compared to cumulative net flux (rainfall – evapotranspiration) is given in Fig. 3, showing annual variation along with long term climatic variability (ie. wetter versus dryer periods).

Seep/W model structure and development

A one-dimensional conceptual model of groundwater-climate interaction was adopted (e.g. Type B). A homogenous vertical column was defined with no-flow boundaries on all sides except the surface where net climate flux was applied (rainfall – evapotranspiration) at monthly time steps. Soil properties were based on previous work, such as porosity, saturated hydraulic conductivity and unsaturated moisture retention (characteristic) curve (e.g. Willett et al 1993; Akber 1991), while the unsaturated hydraulic conductivity function was defined from the characteristic curve (e.g. van Genuchten or Fredlund-Xing models, see Krahn 2004).

As noted above, the hydrogeology of the Ranger area is highly heterogeneous, leading to differing average responses of the water table to the annual wet season (e.g. annual fluctuation, or Δh, of 1-5 m). Obtaining reliable spatial data on all of the above properties is difficult and still includes residual uncertainty. As such a range of Seep/W models were developed with varying soil parameters to assess this uncertainty. This allowed a choice of optimum properties for each bore to be

used for assessing climate change impacts (see Kabir et al 2008b). In this work, saturated hydraulic conductivity (*K*, 0.3 to 30 m/30 days) and effective porosity (*n*, 2.5% to 20%) were varied. All model results were statistically evaluated using the measures in Table 1, to ascertain the 'goodness of fit' for each model.

Table 1. Statistical objective functions[a] used to assess model fit.

Measure[b]	Expression[b]	Range	Decision Rule
E (Nash-Sutcliffe criterion)	$E = 1 - \frac{\sum_{t=1}^{T}(h_o^t - h_m^t)^2}{\sum_{t=1}^{T}(h_o^t - \overline{h_o})^2}$	-∝ to +1	+1 is desirable
r (linear correlation coefficient)	$r = \frac{\sum_{t=1}^{T}(h_m^t - \overline{h_m})(h_o^t - \overline{h_o})}{\sqrt{\sum_{t=1}^{T}(h_m^t - \overline{h_m})^2}\sqrt{\sum_{t=1}^{T}(h_o^t - \overline{h_o})^2}}$	-1 to 1	+1 is desirable, -1 is undesirable
Ratio	$Ratio = \overline{h_m} \,/\, \overline{h_o}$	0 to ∝	+1 is desirable
RMSE (root mean square error)	$RMSE = \sqrt{\sum_{t=1}^{T}(h_m^t - h_o^t)^2} \Big/ T$	0 to ∝	0 is desirable
$\overline{d}$ (mean error)	$\overline{d} = \overline{h_m} - \overline{h_o}$ where $\overline{h_m} = \sum_{t=1}^{T} h_m^t \Big/ T$	-∝ to +∝	0 is desirable
S_e (standard error)	$S_e = \sqrt{\frac{S^2}{T-1}}$ & $S^2 = \frac{\sum_{t=1}^{T}(d^t)^2}{T} - \overline{d}^2$	0 to ∝	0 is desirable
β	$\beta = \overline{d} \Big/ \sqrt{S^2/(T-1)} = \overline{d} \Big/ S_e$	0 to ∝	0 is desirable

[a] From Zheng and Bennett (1995), Middlemis et al (2001), Nash and Sutcliffe (1970).
[b] Primary variables are *h* head; *t* time step number (T total time steps); *d* model – measured difference; Subscript 'm' / 'o' – model / observed values; ¯ (overscore) average (e.g. $\overline{h_m}$ = average modelled head).

Results

Nine model were developed with the combinations of K=0.3, 3 and 30 m/30days and n=2.5, 5 and 10%. Statistical evaluations of model runs are given in Tables 2 and 3, with an example in Fig. 4. An example of measured versus modelled groundwater heads (bore OB21A) is graphed in Fig. 5.

From Tables 2 and 3, optimum (desirable) values of criteria $\overline{h_m}$, *E*, *Ratio, RMSE,* β, $\overline{d}$, and S_e are found to in one model combination, while criterion *r* is found to be in a different model run. The difference, however, between *r* values in these models is mostly marginal. To achieve better consistency between the criteria, runs are extended to additional set of combinations for n=20%. The direction

of changes of the criteria are again found to be mostly inconsistent. The best bore with consistent model parameter comes out to be OB27 with K 30 n 20.

Table 2. Statistical assessments[a] of Seep/W model runs versus soil parameters (K, n).

	$\overline{h_m}$	*E*	*r*	*Ratio*	*RMSE*	β	$\overline{d}$	S_e
Desired value	–	1	1	1	0	0	0	0
OB1A[b], $\overline{h_o}$ = 25.83 m, Δh = 3.17 m (*K* m/30 days, *n* %)								
K 0.3, n 2.5	25.43	-0.56	0.23	0.98	0.09	4.37	0.4	0.09
K 3, n 2.5	21.57	-30.2	***0.42***	0.84	0.42	12.94	4.26	0.33
K 30, n 2.5	1.83	-3781	0.3	0.07	4.62	5.47	24	4.39
K 0.3, n 5	25.69	-0.37	0.09	0.99	0.09	1.54	0.14	0.09
K 3, n 5	23.3	-11.07	0.33	0.9	0.26	11.99	2.53	0.21
K 30, n 5	22.01	-18.69	**0.35**	0.85	0.33	16.09	3.82	0.24
K 0.3, n 10	**25.82**	**-0.11**	0.16	**1**	**0.08**	**0.11**	**0.01**	**0.08**
K 3, n 10	23.94	-4.16	0.26	0.93	0.17	14.98	1.89	0.13
K 30, n 10	23.81	-0.12	0.33	0.92	0.17	16.75	2.02	0.12
K 0.3, n 20	***25.83***	***0.03***	0.21	***1***	***0.07***	***0.06***	***<0.01***	***0.07***
K 30, n 20	24.71	-0.99	0.3	0.96	0.11	13.9	1.12	0.08
OB20[b], $\overline{h_o}$ = 18.09 m, Δh = 1.67 m (*K* m/30 days, *n* %)								
K 0.3, n 2.5	16.82	-1.5	0.59	**0.93**	0.1	21.86	1.27	0.06
K 3, n 2.5	13.14	-42.81	***0.72***	0.73	0.41	18.18	4.94	0.27
K 30, n 2.5	9.76	-123.84	**0.63**	0.54	0.7	18.12	8.33	0.46
K 0.3, n 5	17.1	-0.67	0.59	***0.95***	0.08	19.12	0.99	***0.05***
K 3, n 5	14.39	-19.95	**0.63**	0.8	0.29	22.36	3.7	0.17
K 30, n 5	14.08	-23.53	0.61	0.78	0.31	22.49	4.01	0.18
K 0.3, n 10	***17.2***	***-0.42***	0.62	***0.95***	***0.07***	**17.79**	***0.88***	***0.05***
K 3, n 10	15.56	-7.28	0.54	0.86	0.18	30.49	2.53	0.08
K 30, n 10	15.14	-9.78	0.56	0.84	0.2	33.93	2.95	0.09
K 0.3, n 20	**17.17**	**-0.59**	0.6	***0.95***	**0.08**	***17.23***	**0.92**	0.05
K 30, n 20	16.09	-3.86	0.53	0.89	0.14	35.98	2	**0.06**
OB21A[b], $\overline{h_o}$ = 23.42 m, Δh = 2.14 m (*K* m/30 days, *n* %)								
K 0.3, n 2.5	24.98	-0.59	***0.75***	1.07	0.12	-22.7	-1.56	***0.07***
K 3, n 2.5	20.75	-8.13	0.66	0.89	0.29	11.34	2.67	0.24
K 30, n 2.5	17.14	-31.94	0.35	0.73	0.55	16.6	6.28	0.38
K 0.3, n 5	**24.62**	**-0.34**	0.7	**1.05**	**0.11**	**-14.97**	**-1.2**	**0.08**
K 3, n 5	20.24	-5.75	0.55	0.86	0.25	21.87	3.17	0.15
K 30, n 5	18.96	-11.53	0.34	0.81	0.34	24.09	4.45	0.18
K 0.3, n 10	***23.33***	***0.37***	**0.72**	***1***	***0.08***	***1.18***	***0.09***	**0.08**
K 3, n 10	19.86	-5.83	0.37	0.85	0.25	33.79	3.55	0.11
K 30, n 10	19.58	-7.05	0.24	0.84	0.27	32.97	3.84	0.12
K 0.3, n 20	21.77	-0.71	0.71	0.93	0.13	24.27	1.65	***0.07***
K 30, n 20	20.03	-5.05	0.34	0.86	0.24	36.91	3.39	0.09

[a] Best fits are highlighted in grey shaded bold-italic text; next closest fits are bold only.
[b] Model runs with K 3 not available.

Table 3. Statistical assessments[a] of Seep/W model runs versus soil parameters (K, n).

	$\overline{h_m}$	*E*	*r*	*Ratio*	*RMSE*	β	$\overline{d}$	S_e
Desired value	–	1	1	1	0	0	0	0
OB27[b], $\overline{h_o}$ = 8.87 m, Δh = 2.00 m (*K* m/30 days, *n* %)								
K 0.3, n 2.5	10.15	-1.54	0.62	1.14	0.13	-20.57	-1.28	**0.06**
K 3, n 2.5	10.92	-5.37	0.77	1.23	0.2	-21.73	-2.05	0.09
K 30, n 2.5	11.09	-6.16	0.77	1.25	0.21	-23.58	-2.21	0.09
K 0.3, n 5	10.18	-2.1	0.42	1.15	0.14	-15.78	-1.31	0.08
K 3, n 5	10.69	-3.55	0.78	1.2	0.17	-27.86	-1.81	0.07
K 30, n 5	10.46	-2.82	**0.79**	1.18	0.15	-21.31	-1.58	0.07
K 0.3, n 10	9.92	-1.84	0.42	1.12	0.13	-10.71	-1.05	0.1
K 3, n 10	9.52	-0.04	0.72	1.07	0.08	-11.2	-0.65	**0.06**
K 30, n 10	9.42	0.23	0.77	1.06	0.07	-10.54	-0.54	***0.05***
K 3, n 20	***8.61***	**0.28**	0.62	**0.97**	0.07	***4.26***	***0.27***	**0.06**
K 30, n 20	**8.56**	***0.37***	***0.81***	**0.96**	***0.06***	**5.51**	**0.31**	**0.06**
OB41[b], $\overline{h_o}$ = 14.89 m, Δh = 1.69 m (*K* m/30 days, *n* %)								
K 0.3, n 2.5	12.24	-18.29	***0.55***	0.82	0.19	25.11	2.84	0.11
K 3, n 2.5	8.77	-168.18	**0.53**	0.59	0.57	15.74	9.43	0.6
K 30, n 2.5	-20.62	-26838	0.35	-1.38	7.21	***5.22***	65.38	12.54
K 0.3, n 5	12.59	-13.31	0.36	0.85	**0.17**	23.99	**2.44**	**0.1**
K 3, n 5	10.57	-69.46	0.42	0.71	0.37	21.34	6.39	0.3
K 30, n 5	9.97	-90.09	0.38	0.67	0.42	21.26	7.15	0.34
K 0.3, n 10	**12.92**	**-9.64**	0.21	**0.87**	***0.14***	21.71	2.05	***0.09***
K 3, n 10	12.08	-26.33	0.35	0.81	0.23	23.99	3.89	0.16
K 30, n 10	12.4	-21.75	0.39	0.83	0.21	23.92	3.57	0.15
K 0.3, n 20	***12.93***	***-5.53***	-0.24	**0.89**	0.18	19.29	***1.67***	***0.09***
K 30, n 20	12	-13.5	-0.01	0.82	0.27	24.29	2.6	0.11

[a] Best fits are highlighted in grey shaded bold-italic text; next closest fits are bold only.
[b] Model runs with K 0.3-n 20 (OB27) and K 3-n 20 (OB41) not available.

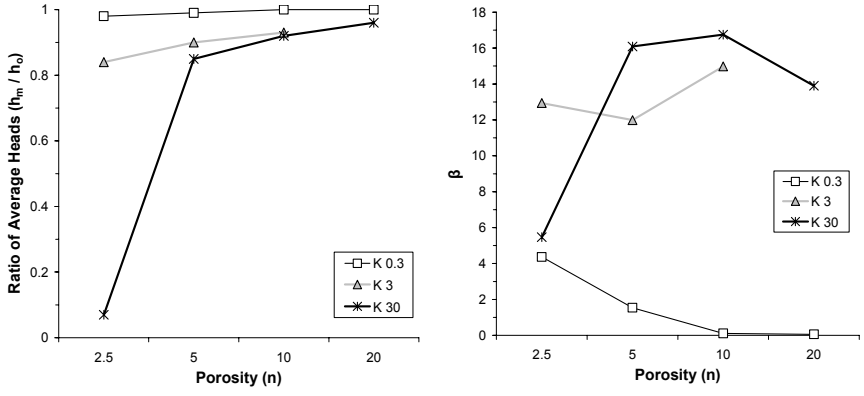

Fig.4. Example of the variation of selected statistical evaluations for bore OB1A.

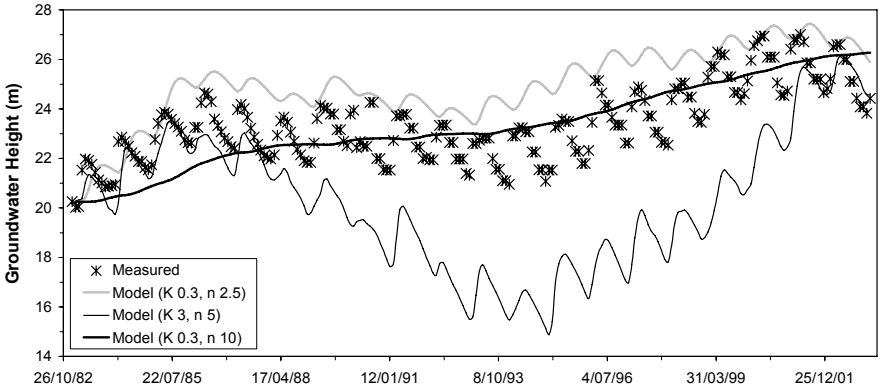

Fig.5. Observed versus modelled groundwater levels in bore OB21A.

Discussion

Based on all results above, the performance of the models for OB27 achieves the best result since this bore successfully includes the best E and r values in one combination of hydraulic conductivity and porosity. Another important aspect of the results is that the best model may not necessarily be unique, rather it corresponds to a range of parameter values for most of the bores. For example, with respect to the statistical evaluation of parameter combinations, OB41 shows a lot of scatter while OB27 shows a consistent parameter combination.

If we analyse the importance of all criteria in context to the primary objective of the modelling, the most important criterion is considered to be the r value as this deals with both the magnitude and direction of deviation whereas other criteria deal with magnitude only (see Middlemis et al. 2001).

The relative influence of porosity (n) on the annual average groundwater fluctuation (Δh) can be explored by comparing OB20 and OB21A, since they are close to each other. The model results show the importance of n in the amplitude of Δh. OB20 performs well with n of 10% to 20% and a measured average annual groundwater variation (Δh) of 1.67m, whereas OB21A performs well with n of 5% to 10% with Δh of 2.14m. This shows that annual fluctuations are higher for lower porosity (all other factors remaining the same).

The results also show that hydraulic conductivity is important in modelling the annual and longer term response of groundwater (as should be expected). Based on field work at Ranger (e.g. Willett et al 1993; Akber 1991), it is clear that the weathered near surface geology and aquifers at Ranger are highly variable and heterogeneous. The approach adopted in this paper is clearly a simplification which allows for efficient modelling at the expense of more thorough discretisation of model parameters (K, n, others). As such, the approach adopted herein of using a simplified one-dimensional homogenous model appears reasonable.

Conclusions

This paper presented the results of applying an unsaturated flow model (Seep/W) to observed historical groundwater-climate data at the Ranger uranium project. The approach adopted a one-dimensional groundwater-climate model to fit historical data for several bores, with varying values for hydraulic conductivity and porosity to assess uncertainty due to the heterogeneous geology of the area. All model runs were evaluated with a range of statistical measures for goodness of fit. In summary, the research approach utilised herein demonstrates that a simplified conceptual model implemented via an unsaturated flow model can achieve a robust model configuration with reasonable statistical confidence.

References

Ahmad M and Green DC (1986) Groundwater regimes and isotopic studies, Ranger mine area, Northern Territory. Australian Journal of Earth Sciences, 33, pp 391-399

Akber RA and Harris F (1991) Proc. of the workshop on land applications of effluent water from uranium mines in the Alligator Rivers Region. Office of the Supervising Scientist, Jabiru, Australia, September 1991, 360p

Brown PL, Guerin M, Hankin SI and Lowson RT (1998) Uranium and other contaminant migration in groundwater at a tropical Australian uranium mine. Journal of Contaminant Hydrology, 35, pp 295-303

Kabir M, Hamza K, Mudd GM and Ladson AR (2008a) Groundwater-climate relationships, Ranger uranium mine, Australia : 1 time series statistical analyses. Proc. "Uranium mining and hydrogeology V", Freiberg, Germany, September 2008.

Kabir M, Mudd GM and Ladson AR (2008b) Groundwater-climate relationships, Ranger uranium mine, Australia : 3 predicting climate change impacts. Proc. "Uranium mining and hydrogeology V", Freiberg, Germany, September 2008.

Krahn, J (2004) Seepage modelling with SEEP/W. Geo-Slope International Ltd, Canada

Middlemis H, Merrick N and Ross J (2001) Groundwater flow modelling guideline. Prepared by Aquaterra Consulting Pty Ltd for the Murray-Darling Basin Commission, Canberra, Australia, January 2001, 133p

Nash JE and Sutcliffe J (1970) River flow forecasting through conceptual models, Part 1, A discussion of principles. Journal of Hydrology, 10, pp 282-290

Vardavas IM (1993) A simple groundwater recharge-depletion model for the tropical Magela Creek catchment. Ecological Modelling, 68, pp 147-159

Willett IR, Bond WJ, Akber RA, Lynch DJ and Campbell GD (1993) The fate of water and solutes following irrigation with retention pond water at Ranger uranium mine. Office of the Supervising Scientist, Sydney, Australia, Research Report 10, 132p

Woods PH (1994) Likely recharge to permanent groundwater beneath future rehabilitated landforms at Ranger uranium mine, Northern Australia. Australian Journal of Earth Science 41, pp 505-508

Zheng C and Bennett GD (1995) Applied contaminant transport modeling: theory and practice. Van Nostrand Reinhold, New York

Groundwater-climate relationships, Ranger uranium mine, Australia: 3. Predicting climate change impacts

Mobashwera Kabir[1], Gavin M. Mudd[1,*], Anthony R. Ladson[1,2] and Edoardo Daly[1]

[1]Institute for Sustainable Water Resources, Department of Civil Engineering, Monash University, VIC 3800 Australia (*Gavin.Mudd@eng.monash.edu.au)
[2]Presently SKM Consulting Pty Ltd, Melbourne, VIC Australia

Abstract. This paper presents the results from using a validated unsaturated flow model to predict groundwater response to climate variability and climate change at the Ranger uranium project, Northern Territory, Australia. A Monte Carlo-style approach was adopted, with 30 statistically generated replicates for each of the 5 models and 7 scenarios from the IPCC climate change projections, giving 1050 model runs in total. The results are presented in terms of predicted groundwater levels to 2100. The paper demonstrates the usefulness of this modelling approach in understanding the future impacts from climate change on groundwater levels.

Introduction

The relationship between groundwater and climate is critical in the design of uranium mine rehabilitation, especially in tropical regions with intense monsoonal rains and extended dry seasons. The Ranger uranium mine is located in the wet-dry tropics of northern Australia and is surrounded by the world heritage-listed Kakadu National Park (see companion paper, Kabir et al 2008, for location map).

Given that climate change is predicted to lead to significant hydrologic changes across northern Australia (e.g. Hennessy et al. 2007), such as changing rainfall and evapotranspiration, it is critical to use the available data to best understand what this means for groundwater recharge, levels and therefore minesite rehabilitation.

This paper develops an approach to model the potential impacts of climate change and climate variability on groundwater levels through a Monte Carlo technique. The unsaturated flow model used is taken from Kabir et al (2008), and compliments other methods to model groundwater-climate relationships such as time series statistical techniques.

Climate variability and climate change

For this research work, the processes of climate variability and climate change need to be carefully defined, followed by a brief review of northern Australia.

According to the UN Framework Convention on Climate Change (UNFCCC), climate change refers to long-term processes occurring over several decades or centuries which leads to changes in average climatic conditions, and includes both anthropogenic and natural causes (Houghton et al 2001). Climate variability is considered to range from inter-annual to inter-decadal and is related to natural phenomena. However, the Intergovernmental Panel of Climate Change (IPCC) definition of climate change means any change in climate over time, whether due to natural variability or as a result of human activity – different to the UNFCCC.

There is an abundance of literature on the processes and controls on climatic conditions across northern Australia. The most common indices used in this area include sea surface temperature (SST) differences between certain regions, such as the Southern Oscillation Index (SOI) to predict El Nino (dry, leading to 'ENSO') or La Nina (wet) climatic periods, Indian Ocean Dipole (IOD) (Ashok et al. 2003; Chang et al 2006), Pacific Decadal Oscillation (PDO) (Mantua et al 1997; Zhang et al 1997; Mantua and Hare 2002; Verdon and Frank 2006a,b) and Interdecadal Pacific Oscillation (IPO) (Power et al 1999). In general, they describe whether climatic conditions are more likely to be warm/ cool, or wet/dry, based on differential SST's between particular regions. They are commonly correlated to major continental regions, such as eastern Australia or western Americas, occur on different cycles (e.g. annual to decadal or longer) and widely used to predict likely climatic conditions. Northern Australia is influenced by the variable combination of all of these indices (with PDO perhaps being the least important).

The models used by the IPCC to predict climate change are not consistent in tropical northern Australia (Alley et al 2007), meaning for the Ranger mine site there is uncertainty regarding the nature and magnitude of change. Less than 66% of models agree on the sign of the change (increase/decrease of precipitation in Dec-Jan-Feb), and is probably related to complex interaction of multiple factors.

There is an increasing recognition that rising temperature is exacerbating the impact of any rainfall reduction (Cai 2007). As a result of reduced precipitation and increased evaporation, dryer periods are projected to intensify in southern and eastern Australia (Hennessy and Fitzharris 2007; Hennessy et al. 2007). But there has been an increasing trend in rainfall over much of north and northwest Australia over recent decades, which has contrasted with decreases over the rest of the continent. Also, Smith and Suppiah (2007) argue that the trends in rainfall totals and average intensities in northern Australia are largely unrelated to trends in ENSO and most likely reflect the influence of other factors.

The degree to which climate change will impact on the frequency or magnitude of all of the above indices and processes remains uncertain and difficult to predict. For example, ENSO events will still occur without any climate change or they may alter due to climate change, with different climate models predicting variable changes such as intensity, duration, wet/dry, warm/cool and so on (see Knutson et al 1997; Timmermann et al 1999; Collins 2000a,b; among others).

Although periods of flood and drought risk in eastern Australia have been correlated to the PDO and IPO, they appear to have minimal influence in northern tropical Australia. However, due to their importance in overall climatic conditions across Australia, they are retained in algorithms to generate net flux data sets.

A number of fundamental issues need to be considered. The non-linearity in the strength of ENSO for Australia, the occurrence of IOD in relation to ENSO for Australia, the relationship between IOD and ENSO in Australia, the uncertainty of future influence of IOD on ENSO of Australia, and the interaction of ENSO events with local climate of the Kakadu region.

There exists non-linearity in the strength of ENSO events in Australia. The differences in the strength of relationship between El Nino (La Nina) with wet (dry) condition can be described as follows.

As a typical tropical phenomenon, the evolution of the IOD is strongly linked to the annual seasonal cycle – the phenomenon develops during May/June, peaks in September/October, and diminishes in December/January (Chang et al 2006). Therefore the IOD influences the Australian winter climate (Ashok et al. 2003). The El Nino events in Australia usually emerge in the March to June period and strongest influence occurs in the six months of June to November (BoM 2007a). The cooling of La Nina is relatively strongest during October to March period (BoM 2007a). Therefore the overlapping of IOD with ENSO is more prevalent with El Nino than La Nina. However, the link between IOD and ENSO has been reported to be have been broken or weakened by climate change (Kumar et al 1999), giving rise to further uncertainty in winter climate conditions in Australia.

The increased dry conditions caused by El Nino occur during the dry season, compared to the increased wet conditions caused by La Nina which occur during the wet season. Therefore if we do not consider the influence of IOD with ENSO, the impact will be greater for both El Nino and La Nina. If we do consider the IOD influence with ENSO, the rainfall in the site being summer rainfall, it is not counteracted by IOD, thus the wet season will still be unimpacted by IOD. Similar results have been recognised by others (Bayliss, pers. comm., 2007). A tabular representation of the links between IOD and ENSO is shown in Table 1.

The predictability of interdecadal climate events remains an area of uncertainty. By reviewing the existing understanding of the ENSO, IPO, PDO, and IOD events, some conditional aspects of these natural processes have been identified. We translate this understanding, observations and possibilities into our algorithm for generating the spells of ENSO events for the Ranger site and combine this with IPCC predicted climate data to generate net flux data sets for modelling.

Table 1. Annual links between ENSO and IOD events.

J	F	M	A	M	J	J	A	S	O	N	D	J	F	M	A	M
				IOD start				IOD peak			IOD end					
			El Nino months													
								La Nina months								
Wet season				Dry season						Wet season						Dry

Modelling methodology

A Monte Carlo-style approach is adopted to generate multiple replicates of input data for numerous model runs. A multi-step algorithm is developed to generate a series of net flux data, incorporating average climate data, predicted climate change trends from IPCC global climate models (GCMs), ENSO and IOD events.

Climate change models and predicted data

The IPCC make the output data from GCMs available, and in Australia this is from the CSIRO through the OzClim software (CSIRO 2006). The OzClim data used for this report is from the Third Assessment report series, as the 2007 reports and data were not yet available.

The GCMs hydro-climate data available from OzClim were rainfall and point potential evapotranspiration (PPET). For application in flow models, however, PPET needs to be converted to areal actual evapotranspiration (AAET). All PPET data was converted to AAET based on standard methods (e.g. Morton 1983).

In 2004, Hennesy et al (2004) undertook a detailed performance evaluation of 12 GCMs for the Northern Territory, Australia, in simulating the current regional climate. Based on this study, other IPCC reports and related literature, five GCMs were selected for extracting future climate change data for the Ranger mine site, namely the CSIRO: Mk2, HadCM2, HadCM3, ECHAM4/OPY and CSIRO: DARLAM 125km GCMs. Further to the physical models, IPCC use six future emission scenarios as inputs to the various GCMs, called A1B, A1FI, A1T, A2, B1 and B2, and they have remain unchanged from the Third to Fourth Assessment reports. An additional scenario, IS92cc, was also available from OzClim, giving a total of seven scenarios for each of the five GCMs. Further details regarding all GCMs and emissions scenarios is available in the varous IPCC literature. Annual net flux data for all 7 IPCC scenarios from the HadCM3 model is shown in Fig. 1.

Climate variability algorithm

We summarise the findings of the literature review and translate these into decision rules and address ambiguity in generating the conditional random process.

Decision for PDO: Random selection of PDO positive (El Nino enhanced), and

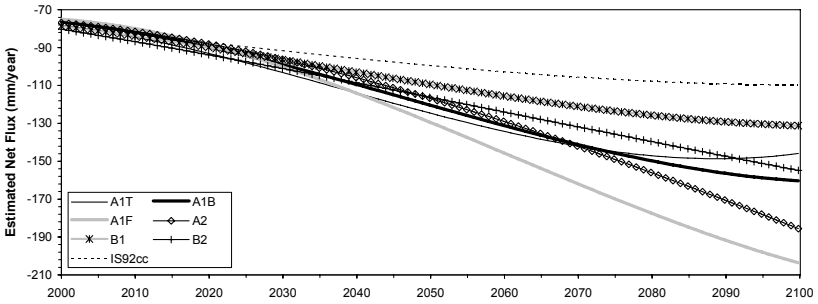

Fig.1. Estimated net flux for all scenarios (HadCM3 GCM)

PDO negative (La Nina enhanced) and PDO zero (both non enhanced)

Decision for IOD-ENSO relationship for Australia: La Nina is stronger than El Nino for Australia while IOD ENSO inverse relationship exists.

Decision for IOD-ENSO relationship for site:

- Irrespective of the existence of the link between IOD and ENSO, the site wet season is supposed to be consistently and strongly influenced by La Nina.
- With the dry season, if the link (inverse relation between ENSO and IOD) remains broken then the El Nino will be stronger for the site.
- And if the relationship is again established then the El Nino might become weakly related to dry condition for the site.

There could be concern for the IOD-El Nino relationship in future predictions but nothing for the IOD-La Nina relationship.

Ambiguity 1: PDO duration is to be randomly selected from 20 to 40 years. This broad guideline comes from the studies based on the IPO during past hundred years (e.g. Verdon and Wyatt 2004).

Ambiguity 2: The randomly selected PDO duration is covered by selecting random ENSO duration of 0 to 8 years. The guidelines for selection of frequency limit of ENSO events have been obtained by analysing the past 100 year's events in Australia (BoM 2005; BoM 2007a,b). For positive or negative PDO the cycle is selected to be 0 to 5 years and for transitional PDO the cycle is selected to be 6 to 8 years.

Ambiguity 3: The IOD-El Nino inverse relationship can exist or not.

The amplitude of ENSO events in the context of present research relate to the rainfall and AAET in ENSO months. We assume during El Nino years that when rainfall is less, AAET is also less. During La Nina years, when rainfall is more, then AAET is also more. But practically, however, this relationship is not linearly correlated, meaning rainfall is unbounded while AAET is bounded as suggested by Morton's equation (Morton 1983). We use the historical percentile records of AAET to cut off the point of wet conditions' AAET.

For the ENSO events, the ranking from ENSO1, ENSO2 … to ENSO5 goes with the 99.99, 90, 10, 5, 1 percentile values of rainfall and AAET. If PDO is for La Nina, it will be always enhanced (because it is independent of IOD), if PDO is for El Nino, it may be enhanced or not (because it depends on IOD). For enhanced La Nina we use the 99.99 percentile value, and for non-enhanced La Nina we use 90 percentile values. For El Nino we use 10, 5 and 1 percentile values. The ranges of percentile values are extracted from reviewing the indices of Expert Team on Climate Change Detection and Indices (ETCCDI) (Alexander et al. 2006, 2007).

Combining climate change and variability

We combine the net flux for ENSO and non-ENSO years and months to generate stochastically generated data. The combined data of the stochastically generated net flux is indicated by NFi,jSTO, meaning the net flux for ith month of jth year of any randomly generated century. We obtain 35 sets of net flux data from OzClim for 100 years from 2000 to 2100 and 35 sets of multiplying factors are computed as NFi,2000+jOZ(k) / NFi,2000OZ(k), where NFi,2000+jOZ(k) is used to indicate

the net flux for ith month (i = 1 to 12) of jth year (j = 0 to 100) predicted by Oz-Clim for the kth set (k = 1 to 35). Therefore, the predicted data NFi,jPRED(k) is as follows:

$$NF_{i,j}^{PRED(k)} = NF_{i,j}^{STO} \times NF_{i,2000+j}^{OZ(k)} / NF_{i,2000}^{OZ(k)} \quad \text{(Eq.1)}$$

The number of replicates is selected as 30, based on the guideline of Janssen et al (1993), where it is stated that for random sampling the number of samples to be taken should be larger than ten times the number of parameters included in the Monte Carlo analysis. We use three numbers of ambiguities, leading to 30 replicates. The overall algorithm for conditional random generation of ENSO events is shown in Fig. 2. The total number of sets of $NF_{i,j}^{PRED(k)}$ is therefore 1050 (35 GCM-scenario combinations and 30 replicates).

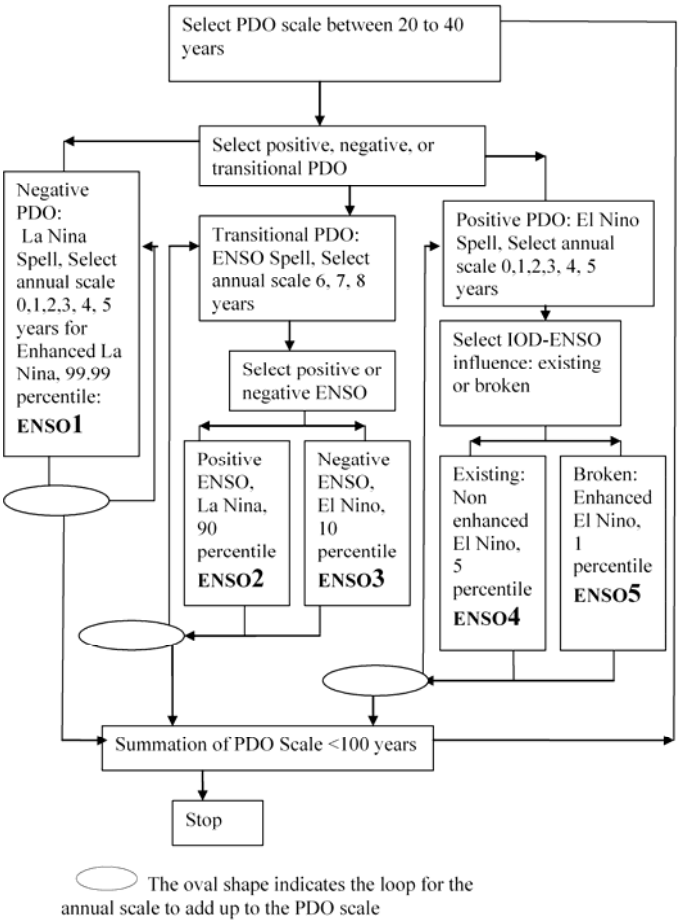

Fig.2. Algorithm flow chart for the generation of ENSO rain and AAET data (climate change and natural climatic variability) for the Ranger site

A major issue not addressed by the above approach and algorithm is extreme events such as tropical cyclones. In reality, such severe events would cause intense flooding rather than an extreme rise of the groundwater level (Kabir 2008). Therefore, in the monthly-based time series data, we neglect tropical cyclone events whose duration is normally 3 to 5 days only.

Results

One sample set of net flux data is shown in Fig. 3. The cumulative net flux was also computed to assess the influence of wet and dry periods on net flux, which can not be seen from the monthly net flux data. The SeepW model result of the computed groundwater level for that net flux is also shown in Fig. 3.

The aggregrate results from all 30 replicates and 7 scenarios of the HadCM3 GCM are shown in Fig. 4, giving mean (μ) groundwater level for each scenario and the maximum/minimum mean plus/minus standard deviation (±σ). Yohe et al (2007) used HadCM3 in IPCC's Fourth Assessment report in the assessment of global water resource availability. Complete results are given in Kabir (2008).

The results of groundwater levels in Fig's 3 and 4 establishes two key findings. Firstly, that longer term trends in climatic conditions are indeed critical in shaping overall groundwater levels (e.g. Fig. 3). Secondly, despite all 7 IPCC scenarios predicting a long-term decline in net flux and dryer overall hydrologic conditions, climate variability, giving rise to extended wetter or dryer periods, can achieve major rises or declines in groundwater levels which appear to outweigh the trends predicted under climate change scenarios.

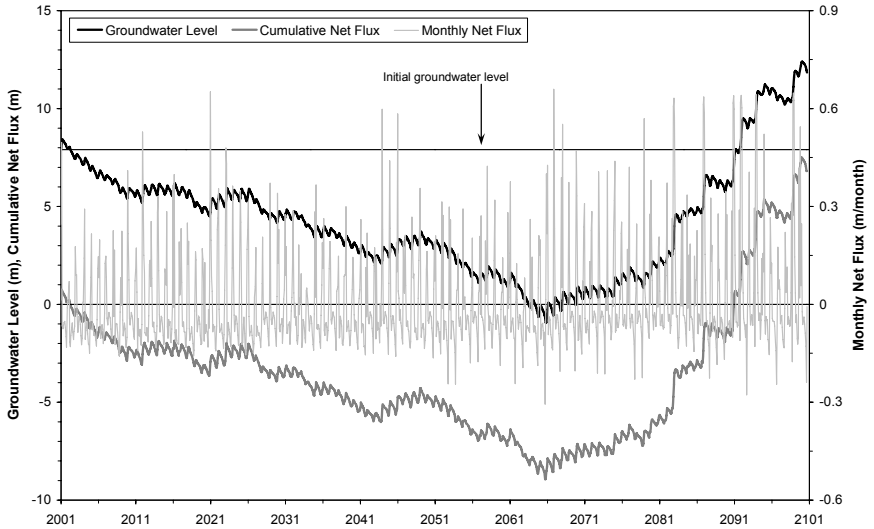

Fig.3. Generated monthly net flux, cumulative net flux and modelled level response (bore OB27, CSIRO MK2, Scenario A2).

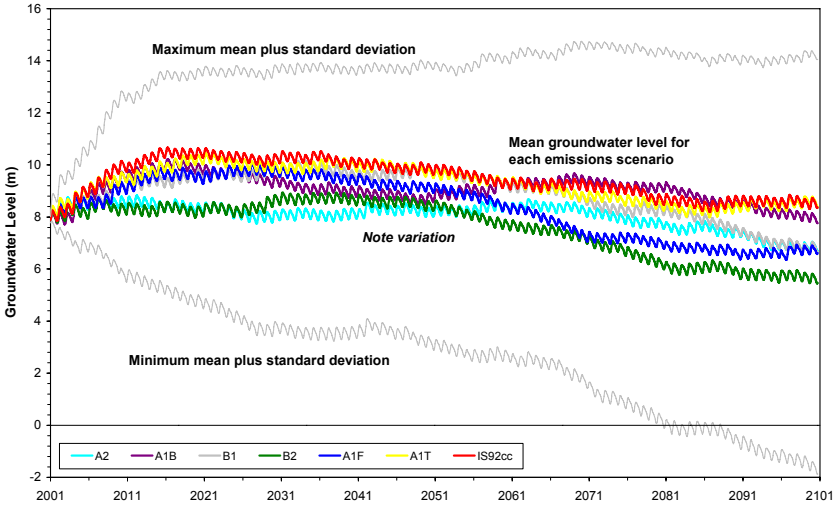

Fig.4. Modelled mean groundwater levels (bore OB27), HadCM3 GCM and A2, A1B, B1, B2, A1F, A1T and IS92cc emission scenarios; max/min mean ± standard deviation

Conclusions

This paper sought to build on previous modelling work by developing a methodology to assess the impacts on groundwater levels from potential climate change scenarios and climate variability.

Climate variability was predicted by combining the current understanding of important climate indices such as El Nino/La Nina, IPO, PDO and IOD into a stochastic algorithm for generating climate data. Data for climate change predictions were obtained from IPCC global climate models and future emissions scenarios. These two components were then combined to produce an input data set of net flux for use in the previously validated unsaturated flow model for the Ranger site. Summary results were then presented in terms of mean groundwater level over time under each scenario for the HadCM3 GCM, including maximum/minimum ± standard deviation groundwater level at each time step from all model runs. The algorithms incorporate current climate knowledge, and can be updated as new knowledge or udnerstanding comes to light.

Overall, the results show the critical importance of climate variability as well as climate change. Under extended wet periods, groundwater levels are predicted to rise significantly, while the major declines are expected under lengthy dry climatic periods. The modelling shows that although the impact of climate change could be significant, it must also be considered in the face of climate variability. The paper, combined with the two concurrent papers, therefore provides a sound basis and methodology upon which to understand the potential impacts of climate change and climate variability on groundwater levels. This, in turn, is critical with respect

to different uranium mine rehabilitation approaches in a wet-dry tropical climate surrounded by a region of very high conservation and cultural values.

References

Alexander LV, Hope P et al (2007) Trends in Australia's climate means and extremes: a global context. Australian Meteorological Magazine, 56, pp 1-18

Alexander LV, Zhang X et al (2006) Global observed changes in daily climate extremes of temperature and precipitation. Journal of Geophysical Research, 111(D05109), pp 1-22

Alley R, Berntsen T et al. (2007) Climate change 2007: The physical science basis. Intergovernmental Panel of Climate Change, Cambridge University Press, UK

Ashok K, Guan Z et al (2003) Influence of the Indian Ocean Dipole on the Australian winter rainfall. Geophysical Research Letters, 30(15), doi:10.1029/2003GL017926

Bayliss P (2007) Personal communication. Office of the Supervising Scientist, May 2007

BoM (2005) El Nino, La Nina and Australia's climate. Bureau of Meteorology, Commonwealth of Australia, Accessed 31 July 2007, http://www.bom.gov.au/lam/epage.shtml

BoM (2007a) ENSO wrap-up. Bureau of Meteorology, Commonwealth of Australia, Accessed 31 July 2007, http://www.bom.gov.au/climate/enso/index.shtml#impacts

BoM (2007b) El Nino – Detailed Australian analysis. Bureau of Meteorology, Commonwealth of Australia, Accessed 31 July 2007, http://www.bom.gov.au/climate/enso/australia_detail.shtml

Cai W (2007) What will happen to future Australian rainfall? Proc. "Greenhouse 2007: The latest science and technology", Sydney, Australia, October 2007

Chang P, Yamagata T et al (2006) Climate fluctuations of tropical coupled systems - the role of ocean dynamics. Journal of Climate – Special Section, 19, pp 5122-5174

Collins M (2000a) The El-Nino Southern Oscillation in the second Hadley Centre coupled model and its response to greenhouse warming. Journal of Climate, 13, pp 1299-1312

Collins M (2000b) Understanding uncertainities in the response of ENSO to greenhouse warming. Geophysical Research Letters, 27, pp 3509-3512

CSIRO (2006) Ozclim – Climate change data (Version 2.0.1), CSIRO Australia (website: http://www.csiro.au/ozclim/home.do)

Hennessy K and Fitzharris B (2007) Australian climate change impacts, adaptation and vulnerability. Proc. "Greenhouse 2007: The latest science and technology", Sydney, Australia, October 2007

Hennesy K, Page C et al (2004) Climate change in the Northern Territory. CSIRO Consultancy report for the NT Department of Infrastructure, Planning and Environment.

Hennessy K, Fitzharris B et al (2007) Australia and New Zealand. In "Climate change 2007: Impacts, adaptation and vulnerability", Working Group II, Intergovernmental Panel on Climate Change, Cambridge University Press, UK, pp 507-540

Houghton JT, Ding Y et al (Eds.) (2001) Climate change 2001: The scientific basis. Working group I, Intergovernmental Panel on Climate Change, Cambridge University Press, UK

Janssen PHM, Heuberger PSC et al (1993) UNSCAM 1.1: A software package for sensitivity and uncertainty analysis. RIVM Report 959101004, Bilthoven, The Netherlands

Kabir M (2008) Modelling groundwater-climate relationships at the Ranger uranium mine, Australia. PhD Thesis (In Preparation), Dept. of Civil Eng., Monash University

Kabir M, Mudd GM and Ladson AR (2008) Groundwater-climate relationships, Ranger uranium mine, Australia : 2. Validation of unsaturated flow modelling. Proc. "Uranium mining and hydrogeology V", Freiberg, Germany, September 2008

Knutson TR, Manabe S et al (1997) Simulated ENSO in a global coupled ocean-atmosphere model: multidecadal amplitude modulation and CO2-sensitivity. Journal of Climate, 10, pp 138-161

Kumar KK, Rajagopalan B et al (1999) On the weakening relationship between the Indian monsoon and ENSO. Science, 284, pp 2156-2159

Mantua NJ and Hare SR (2002) The Pacific Decadal Oscillation. Journal of Oceanography, 58, pp 35-44

Mantua NJ, Hare SR et al (1997) A Pacific interdecadal climate oscillation with impacts on salmon production. Bulletin of the American Meteorological Society, 78(6), pp 1069-1079

Morton FI (1983) Operational estimates of areal evapotranspiration and their significance to the science and practice of hydrology. Journal of Hydrology, 66, pp 1-76

Power S, Casey T et al (1999) Interdecadal modulation of the impact of ENSO on Australia. Climate Dynamics, 15, pp 319-324

Smith I and Suppiah R (2007) Characteristics of the northern Australian rainy season. Proc. "Greenhouse 2007: The latest science and technology", Sydney, Australia, October 2007

Timmermann AJ, Oberhuber J et al (1999) Increased El Nino frequency in a climate model forced by future greenhouse warming. Nature, 398, pp 694-696

Verdon DC and Frank SW (2006a) Long-term behaviour of ENSO: Interactions with the PDO over the past 400 years inferred from paleoclimate records. Geophysical Research Letters, 33(L06712), pp 1-5

Verdon DC and Frank SW (2006b) Long term drought risk assessment in the Lachlan catchment – A paleoclimate perspective. Proc. "30th Hydrology and Water Resources Symposium", Engineers Australia, Launceston, Australia, December 2006

Verdon DC and Wyatt AM (2004) Multidecadal variability of rainfall and streamflow: eastern Australia. Water Resources Research 40(W10201), pp 1-8

Yohe GW, Lasco RD et al (2007). Perspectives on climate change and sustainability. In "Climate change 2007: Impacts, adaptation and vulnerability", Working Group II, Intergovernmental Panel on Climate Change, Cambridge University Press, UK, pp 811-841

Zhang Y, Wallace JM et al (1997) ENSO-like interdecadal variability. Journal of Climate, 10, pp 1004-1020

Environmental Impacts from the North Cave Hills Abandoned Uranium Mines, South Dakota

James Stone[1] and Larry Stetler[2]

[1]Department of Civil and Environmental Engineering, South Dakota School of Mines and Technology, Rapid City, South Dakota, 57701, USA, James.Stone@sdsmt.edu
[2]Department of Geology and Geological Engineering, South Dakota School of Mines and Technology, Rapid City, South Dakota, 57701, USA, Larry.Stetler@sdsmt.edu

Abstract. This study evaluated environmental impacts from historical uranium mining to soil, water, and air resources occurring on private lands surrounding the North Cave Hills complex within Custer National Forest, northwest South Dakota. Surface water concentrations of As, Cu, Mo, U, and V exceeded established background concentrations within approximately 27 km of stream length flowing below abandoned mines. Uranium concentrations in soils were mostly below the background value of 22 mg/kg and had a generally decreasing trend with increasing distance from the source areas, with higher values were associated with washover deposits and channeling of sediments.

Introduction

Uranium exploration in northwestern South Dakota began in 1954 when the Atomic Energy Commission planned to fly airborne surveys over the Slim Buttes. Weather conditions precluded flying the Slim Buttes and instead, the survey was flown over the North Cave Hills (NCH) (Curtiss, 1955). As a result, the first claims were staked in the NCH on August 15, 1954 and mining ensued that year. Mine sites were located primarily within an approximately two mile wide northwest trending strip crossing the central NCH, referred to as the hot zone. Mining was permitted under the General Mining Laws and Public Law 357, which required no form of restoration. Most mines and mining prospects were located on United States Forest Service (USFS) administered land, but at least two actively mined sites and several prospects and exploration cuts and digs were located on

private land surrounding the NCH. Most of the uranium mines were abandoned coal strip mines located on relatively flat areas along the top of the numerous buttes that characterize the area. Mining consisted of the removing overburden (up to 80 feet) to reach the ore zone which consisted of uranium-bearing lignite beds. Mining activity increased through the next decade but ceased altogether in 1964.

During mining, most of the overburden and mine spoils were pushed over the edges of the buttes where subsequent erosion has spread materials over almost 1,000 acres in the NCH alone. Since mining ceased, additional deposition has occurred down-slope onto private land by water and wind transport. The bluffs and slopes immediately below mine sites often were covered by spoils forming highly over-steepened talus slopes, several of which have failed or are deeply incised. Currently, spoils are mostly devoid of vegetation and their composition has promoted water channeling, gullying, and tunneling. In addition to mined sites, numerous prospecting pits or contour benches were excavated on both USFS and private land and have been mapped and documented (Pioneer, 2005). Characterization of the abandoned mine sites on USFS land has occurred (Pioneer, 2005; Portage, 2005) but no work had characterized off-site impacts on surrounding private land. A Joint Venture agreement between the United States Department of Agriculture-Forest Service and the South Dakota School of Mines and Technology (including a subcontract with Oglala Lakota College) was established in 2006 to address potential off-site impacts. Funding for this on-going study has been provided through US-EPA CERCLA. Objectives of the NCH project were to determine whether heavy metal and radionuclide environmental contaminants have been transported from historical mine sites located on USFS land onto surrounding private land. Mechanisms of environmental transport most likely include the following:

- erosion of spoil sediments through surface runoff into adjacent drainages;
- erosion of spoil sediments through slope failures below mined bluffs
- dissolution of hazardous metals within runoff water that form tributaries to streams;
- erosion/deposition of small particle contaminants by wind transport;
- infiltration of hazardous metals and radionuclides into local and regional ground water aquifers.

Methods

Target analytes for metals and radionuclides and analytical methods and procedures for determination of analyte concentration were similar to those used in previous investigations (Pioneer, 2005; Portage, 2005). Metals of interest included: U, As, Se, Cu, Mo, Pb, Th, and V. Water samples were further analyzed for gross alpha radiation, Ra^{226}, and U^{235}.

A watershed approach was developed to discern potentially impacted surface waters. It was assumed that all runoff water and eroded sediments (except for wind erosion) would ultimately end up in adjacent drainages and subsequently

migrate downstream through established drainage networks. Surface-water sampling events were divided into two separate phases. Initial Phase I sampling evaluated target analyte concentrations of all potentially impacted drainages at the USFS/private land boundary. Phase I data also were used to establish background concentrations based on sampling locations assumed to be unaffected by mining activities. These data were used subsequently to evaluate which drainages were most heavily impacted. After evaluation of the Phase I results, drainages with the highest environmental concern were selected for Phase II sampling which continued downstream to a point where target analyte concentrations were comparable to established background levels. Phase I and II sampling located are shown in Figure 1.

Ground-water quality was evaluated by selecting 34 wells that were evenly distributed around the NCH within eight km of the USFS boundary. Approximately half of the wells were domestic supply wells and the others were stock wells. Well depths ranged between 10 and 240 m and represented shallow unconfined alluvial aquifers and deep confined aquifers. Samples were collected after pumping a volume of water equal to or exceeding two times the casing volume.

Airborne dust particulates were collected from 30 locations in two sampling phases. Phase I sampling occurred within the set 8 km radius from the USFS boundary. These data were used to establish background concentrations in regions where impacts from wind were assumed to be negligible. Phase I results were utilized to identify directions and regions to obtain additional samples in Phase II until a reduction in concentrations were observed. Airborne dust particulates were collected using a portable wind tunnel (Stetler, 1999) following these criteria:

- sites were high elevations above stream courses to ensure dust was either deposited directly by air or was derived by soil-forming processes;
- sampling sites were designed in a 'gridded' network around the NCH and were sufficiently distributed in accordance with the prevailing wind directions;
- sites were at locations that had physical indications of the presence of fine-grained surface materials derived from mechanisms excluding fluvial processes;
- locations had surfaces where dry and loose fine-grained materials were readily available to wind processes and could be collected either from the existing surface or generated through preparation of a standard loose surface (Saxton et al., 1998).

Additional dust samples were collected using a stainless steel soil scoop to skim the extreme upper layer of soil from the surface in areas inaccessible to the wind tunnel.

Samples collected to represent potential environmental transport by the above listed mechanisms were compared to established background values calculated using:

$$mean + 3x \,\text{standard deviation} \tag{1}$$

These values were determined using samples collected from non-impacted drainages and represent natural metals concentrations. For airborne dust particulates, a background value of mean + 2 × standard deviation was used.

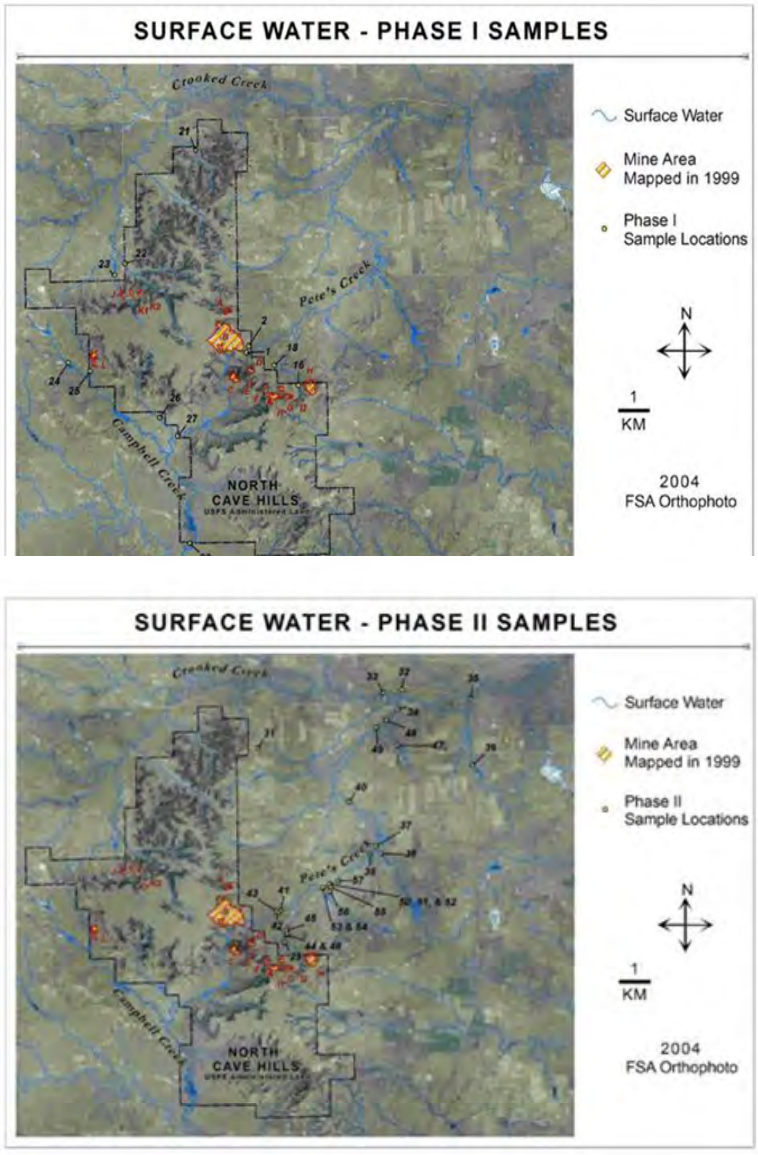

Fig.1. North Cave Hills Phase I and II surface water sampling locations.

Results

The key metals of interest in this study were U and As, although concentrations for the full suite of analytes listed above were determined from each sample. A complete listing of all metals and detailed discussion of trends and occurrences were given by Stone et al. (2007) or can be downloaded at http://uranium.sdsmt.edu. In the following text, only U and As results will be presented.

Soils

Soil samples were collected from cores (0.3—8 m deep) drilled in numerous watersheds surrounding the mined and non-mined areas. Two or more composite samples were prepared from most of the deeper cores. Shallow cores yielded a single sample. Background concentrations were determined using sites representing pristine environments not affected by mining.

Uranium concentrations in soils were mostly below the background value of 22 mg/kg and had a generally decreasing trend with increasing distance from the source areas (Stone et al., 2007). Higher values were associated with washover deposits and channeling of sediments. Values exceeding 3× background were located immediately below Bluff B (Figure 2).

Arsenic concentrations followed a trend similar to U concentrations. Background concentration was 32 mg/kg and was exceeded at several locations at values up to 64 mg/kg. The highest As value (96 mg/kg) was at the site with the highest U concentration.

Results showed that 14 watersheds were potentially impacted by sediment transport from previous mining activity. The most impacted area was in the Upper Pete's Creek drainage below Bluff B where two U samples were 3× and 4× of background. All other U concentrations were below 2× background.

Surface Water

Fourteen watersheds were identified within the study that were potentially impacted by uranium mining. Four pristine watersheds were used to determine background concentrations for all analytes. Sampling of surface water was completed in two phases; Phase I was a large-scale attempt to define contamination regionally, and Phase II sampling isolated impacted areas and delineated contaminant extent. Results indicated there were two impacted areas: the Upper Pete's Creek watershed below and east of Bluff B where surface waters were derived from direct runoff of the spoils piles, and the Schleichart Draw which received runoff down the western slopes of the North Cave Hills.

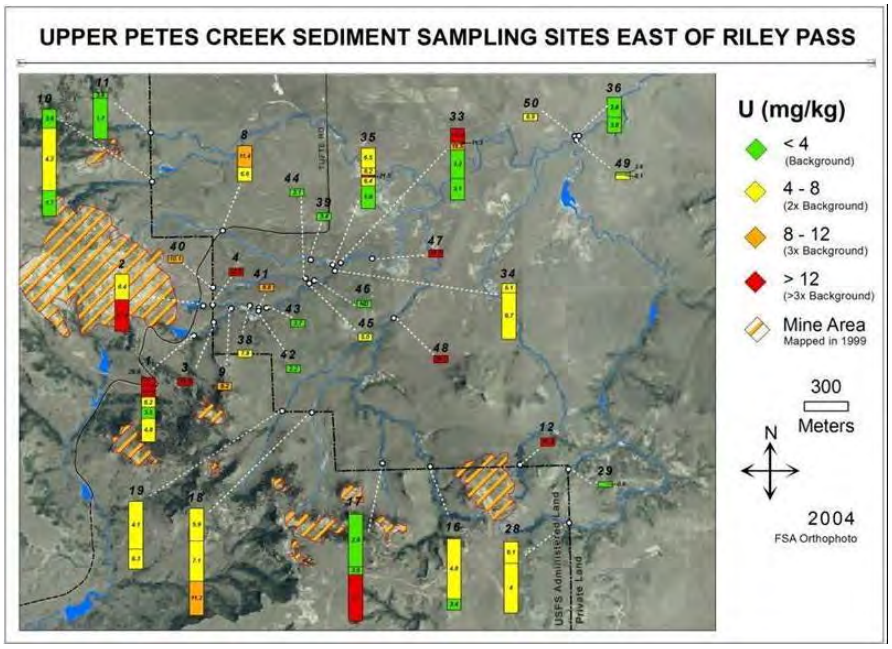

Fig 2. Uranium concentrations of core samples in the upper Pete's Creek.

Phase I sampling indicated elevated U and As concentrations in both watersheds. Elevated U concentrations in the Upper Pete's Creek drainage ranged from 2.9× to 5× above the background value of 0.027 mg/L. Elevated As concentrations ranged from 28× to 33× above the background value of 0.020 mg/L. In Schleichart Draw, elevated U concentrations were 3.6× background. These results were used to define Phase II sampling to isolate the contamination and identify locations with the greatest contamination.

Phase II sampling indicated severe contamination in the Upper Pete's Creek watershed below and to the east of Bluff B where the highest U and As concentrations were 23× and 89× background, respectively (Figure 3). Sampling in the downstream direction showed that natural attenuation of contaminant concentrations has occurred within a distance of ~5 km below Bluff B. Below-background values were observed for all analytes at the confluence of Pete's Creek and Crooked Creek, ~ 15 km northeast of Bluff B.

Ground Water

Contaminant occurrence was ubiquitous in ground-water samples at all depths of wells tested and was distributed within the study area both up and down gradient. The exceptions were thorium, arsenic, and vanadium, which were not detected in any samples. Trends of occurrences suggest that metals detected were regional, naturally occurring contaminants and not directly attributable to uranium mining.

Water quality was compared against maximum contaminant levels (MCLs) established by the US EPA (US EPA, 2006). Uranium was detected in seven wells and ranged from 0.001 to 0.064 mg/L. One well was 0.064 mg/L and exceeded the MCL of 0.03 mg/L by a factor of two. This well was 18 m deep and was fed by shallow alluvial gravels with hydraulic connectivity to uraniferous lignites updip from the well. A second well contained a U concentration of 0.027 mg/L and was also a shallow well in alluvium.

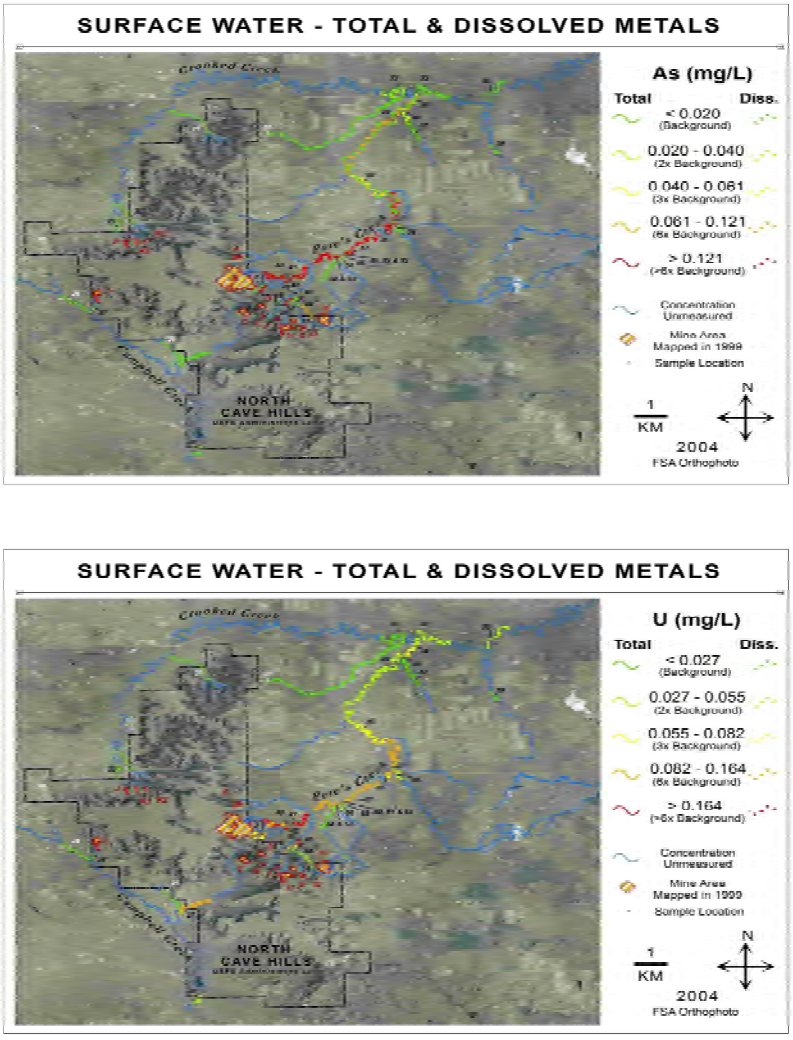

Fig 3. North Cave Hills surface water results for total and dissolved arsenic and uraniu

Many elements in the U decay series can contribute radionuclide counts in a sample. Analysis to determine which element contributed what amount of radioactivity is expensive and time-consuming. Thus, gross alpha counts were used to assess the radioactivity of the sample. The EPA has established a MCL of 15 pCi/L for gross alpha. Twenty-six of the 34 wells contained gross alpha radiation ranging from 1.8 to 44.4 pCi/L. Distribution of these wells were up and down gradient and at depth from 18 to over 240 m. Three wells exceeded the MCL for uranium. The two highest concentrations were the shallow wells discussed above and the third highest concentration was a 122-m-deep well completed into the Fox Hills sandstone located northeast of Bluff B.

In addition to U concentrations and gross alpha contents, three wells contained Ra^{226} in concentrations ranging from 0.5 to 0.7 pCi/L and were all well below the MCL of 5 pCi/L. Two of the wells had concentrations of 0.7 pCi/L and were the same wells as those with the highest gross alpha contents discussed above. U^{235} was detected in five wells at concentrations between 0.3 and 1 pCi/L, up and down gradient of the mine sites. There is no MCL for U^{235}

Data collected and analyzed during the ground-water study indicate that metals and radionuclides were natural components of the ground-water systems. Further, the distribution of the contaminants shows metals were dissolved between the recharge areas to the west and the North Cave Hills. It is not clear if the abandoned uranium mines in the North Cave Hills contribute directly to the metals content of the ground water. Most likely the chemistry of surface water and local springs were affected by the mines but the deep aquifers should not be affected directly. Shale confining layers above the deep sources theoretically protect infiltrating waters from reaching these aquifers. The exception would be the presence of deep fracture systems allowing local infiltration to reach the water table, i.e., a leaky confining layer. These conditions will be evaluated in future studies.

Aerosols

Results of the surface dusts indicate the general ubiquity of target analytes in the soils around the North Cave Hills. Uranium was present in all but two samples and arsenic was present in all samples. Vanadium, copper, and thorium also were present in all samples and lead occurred in all but one sample. Molybdenum and selenium had the least occurrences.

Thirteen samples contained uranium concentrations in excess of the calculated background value of 0.74 mg/kg. Distribution of these sites extended across the entire sampling area and were classified into three distinct domains:

1. Eight locations, including the three with the highest uranium concentrations (1.96, 1.66, and 1.6 mg/kg), occurred in a northwest to southeast trend cutting across the center of the North Cave Hills and containing the largest abandoned uranium mine areas. The long axis of this high-concentration area also correlated to the predominant wind direction, indicating a probable wind influence on the observed distribution. The greatest uranium concentration (1.96 mg/kg)

occurred on the western side of the North Cave Hills below and upwind of Bluffs J-K and upwind of all of the abandoned mine sites;
2. Two locations north of the North Cave Hills had uranium concentrations greater than 1.0 mg/kg and both were in a direction of minimal above-threshold wind occurrences;
3. Two locations in a topographic low between the North and South Cave Hills (Bull Creek drainage) had uranium exceedences.

Uranium concentrations were below background levels in all areas away from these three identified areas of high concentrations.

Arsenic was detected in all samples and five contained concentrations above the calculated background value of 11.93 mg/kg. All exceedence concentrations were east and south of the North Cave Hills. However, concentrations below the background level that were between 9.8 and 11.6 mg/kg were located near the exceedence locations and appeared to form a similar northwest to southeast pattern across the center of the North Cave Hills as was noted for uranium domain 1. Two locations in the north were close in value to the As background level that corresponded to uranium domain 2. Thus, there is some evidence for wind distribution of fine particles that contained these metals

Discussion

Significant environmental degradation has occurred from transport of heavy metals and radionuclides downstream of abandoned uranium mines in the North Cave Hills. The most impacted regions occurred down gradient of Bluff B and in Schleichart Draw in the SW of the study area. Surface water contained U and As up to 90× background values and sediment had concentrations 4× background levels. Metals in sediments and surface water were naturally attenuated within ~15 km below the mine sites, although large deposits of contaminated soils occurred on private lands

Ground water contained many metals and radionuclides in both the up and down gradient directions and at shallow to deep aquifer depths. This indicated that metals contamination was regional in extent and most likely were not affected by U mining

Aerosol dust had significant metals concentrations in nearly all locations sampled. Uranium was ubiquitous and contained at least one plume of high concentrations that correlated to the predominant wind direction. All metals concentrations in aerosols were decreasing or below background levels within about 15 km from the mine sites. Although U, As, and other metals were detected in aerosols, their concentrations were on average seven times less than metals concentrations in soils, indicating aerosol transport of metals remains low

References

Curtiss, R. E. (1955) A Preliminary Report on the Uranium in South Dakota. South Dakota Geological Survey, Report of Investigations No. 79, 102 pages. http://jurassic2.sdgs.usd.edu/pubs/pdf/RI-079.pdf

Pioneer Technical Services. (2005) Draft Final Engineering/Cost Analysis (EE/CA) for the Riley Pass Uranium Mines, Harding County, South Dakota. http://www.fs.fed.us/r1/custer/projects/Planning/nepa/Riley_Pass/index.shtml

Portage (2005) Final Human Health and Ecological Risk Assessment for the Riley Pass Uranium Mines in Harding County, South Dakota. http://www.fs.fed.us/r1/custer/projects/Planning/nepa/Riley_Pass/EECA/Appendix%20D.pdf

Saxton, K.E., D. Chandler, L.D. Stetler, C. Claiborn, B. Lamb, and B. Lee. (1998) Predicting PM10 and PM2.5 dust emissions from agricultural wind erosion. Proc. Specialty Conf., Emission Inventory: Living in a Global Environment, Dec. 8-10, New Orleans, LA., VIP-88:1119-11129.

Stetler, L.D. (1999) Design and construction of a portable wind tunnel for soil erosion research. in Higgins, K.E. (ed), Proc. SD Acad of Sci., 78:23-33.

Stone, J.J., L.D. Stetler, and A. Schwalm. (2007) Final report: North Cave Hills abandoned uranium mines impact investigation, SDSM&T (http://uranium.sdsmt.edu), 202 pg., App A-F.

US EPA (2006) Drinking water contaminants, http://www.epa.gov/safewater/contaminants/index.html#listmcl

Radioactivity in soils and horticulture products near uranium mining sites

Fernando P. Carvalho and João M. Oliveira

Nuclear and Technological Institute, Department of Radiological Protection and Nuclear Safety, E.N. 10, 2686-953 Sacavém, Portugal (E-mail: carvalho@itn.pt)

Abstract. Uranium mining in Portugal was performed mainly in small mines spread over a wide and populated region in the Centre-North of the country. In villages near old uranium mines, soils are used for horticulture production and to provide pasture for livestock grazing. Soil samples as well as agriculture products including cabbage, potatoes, oranges, and other fruits were analyzed for alpha emitting radionuclides. Samples from areas far from uranium mining sites were also included in the survey. Results of uranium series radionuclides showed that soils of regions with different geology may contain very different radionuclide concentrations. Concentrations of radionuclides in soils and vegetables of reference areas may display values similar to those near uranium mining sites in the same geological province, indicating that enhancement of radionuclides in the terrestrial food chain, with the exception of ^{226}Ra, generally is not high. Concentrations in soils and horticulture products of these uranium counties generally were two orders of magnitude higher than concentrations measured in soils and vegetables in a sedimentary region in the South of Portugal.

Introduction

During the XXth century in Portugal were exploited 60 uranium ore deposits for radium and uranium production. The last uranium mine and the facilities for uranium ore processing and production of uranium oxide concentrates, in Urgeriça, Canas de Senhorim, were closed in 2001 (Carvalho, in press). So far, most of the former mining and milling sites were not rehabilitated and mining waste has been stockpiled at the surface, in general near the old mines (Nero et al., 2004; Carval-

ho, in press). Most of these radium-uranium mines were located in the centre-North of the country, already a densely populated area, and villages and towns developed near the mines over the years. With discontinuation of the uranium mining activity and the close out of the mining company, there have been concerns about the impact of uranium waste on the environment and on human health. Despite of engineering works meanwhile started in the Canas de Senhorim county to cover the waste piles from Urgeiriça mine and milling facilities, it was of high relevance to the region to know whether the long lasted uranium mining activity had contaminated with radioactive materials the soils of those regions and whether radionuclides could be transferred through the consumption of agriculture products.

In the framework of a research project to assess the current impact of the legacy of uranium mining industry on public health, we undertook the comparative analysis of soils and kitchen garden products in the counties with uranium mines and in counties without uranium mines. Preliminary results of this study are presented here.

Materials and Methods

The counties to be investigated were selected in the region of uranium mining in the Centre North of Portugal, districts of Viseu, Guarda and Coimbra. As the natural radiation background and natural radioactivity in uranium production regions usually are not homogenous and are higher than the average Earth crust, the selection of counties was thoroughly considered. In order to encompass the range of concentrations likely to be found in soils, for this study were selected counties with old uranium mines and waste piles of uranium mining and milling waste, counties with old uranium mines but where there has been no chemical treatment of radioactive ore and thus no milling tailings, and counties with no mines and even no uranium deposits identified. These were the counties of Seia and Celorico da Beira in the district of Guarda, and Campo and Queirã in the district of Viseu. In the Viseu district also the counties of Moreira de Rei (this one with past mining activities and mining waste piles not covered), and Canas de Senhorim (with past mining activity and with waste and milling tailings). The county of Sátão was selected as a comparison term in this region, but this county is mostly on schist and only partly on granite. Another reference area selected were the counties of Serpa and Ourique, in the Alentejo, South of Portugal, with no record of uranium deposits and with clay and schist instead of granites (Figure 1).

Soil samples were collected in agriculture areas, in all these counties, 2 to 6 sites in each. The 20 cm top soil layer was sampled with a spade in 4 sites within a circle of 3 m radius per sampling location, and the soil portions combined in one sample. In the laboratory the soils were dried in the oven at 60ºC, and than sieved through a metallic mesh in order to retain the 63 μm grain size fraction for analysis,

Samples of cabbage leaves, potatoes and fruits, such as oranges, apples and quinces, were collected in each county according to availability. These samples

were carefully washed and only cabbage leaves, peeled potatoes, and pulp of fruits were retained for deep freezing, homogenization and analysis.

The analyses were performed by radiochemical methods followed by radioactivity measurements with Ortec Eg&G OctetePlus alpha spectrometers according to techniques described in detail elsewhere (Oliveira and Carvalho, 2006; Carvalho and Oliveira, 2007). Analytical quality control was performed with analysis of certified reference materials and participation in intercomparison exercises organized by the IAEA (Pham et al., 2006; Povinec et al., 2007). Results are expressed in dry weight for soils and in fresh weight for horticulture products.

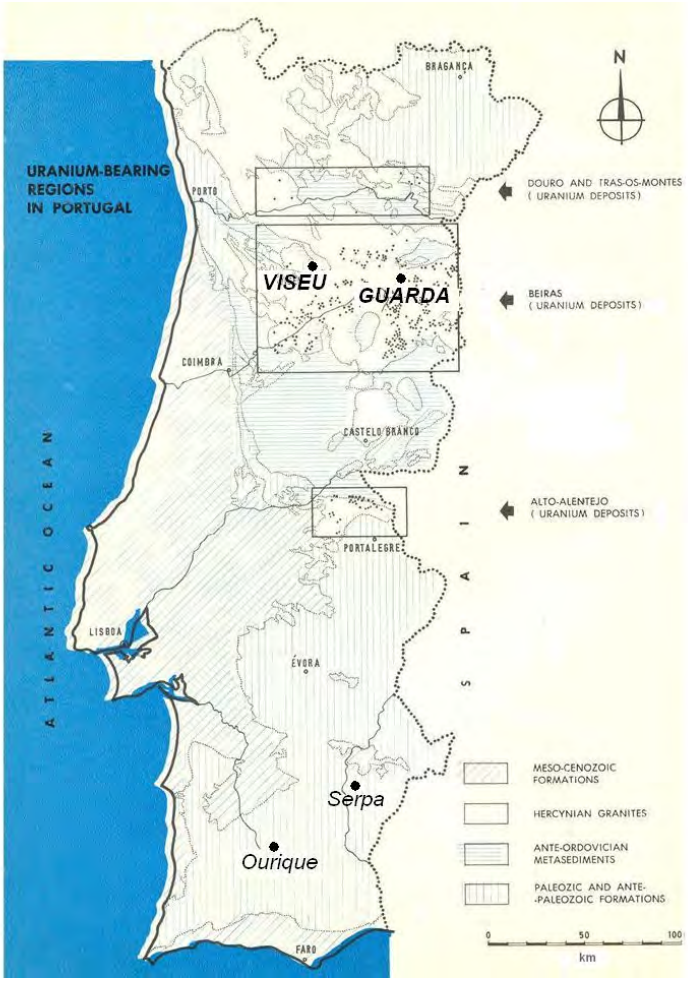

Fig.1. Old uranium mines of Portugal and sampling regions.

Results and discussion

Average radionuclide concentrations in soil samples of several counties are shown in Table 1. In all soils, activity concentrations of uranium (^{238}U) were higher than those of thorium (^{232}Th). In counties with no identified uranium deposits and no uranium mines, radionuclides of the uranium series are in near radioactive equilibrium with the parent radionuclide ^{238}U. In contrast to this, in soils of Canas de Senhorim in average there is higher activity concentration of ^{226}Ra than ^{238}U, and this disruption of secular radioactive equilibrium in soils was introduced by the uranium extraction activity.

Comparing the average levels of radioactivity, the uranium producing counties, especially Moreira de Rei and Canas de Senhorim displayed variable uranium and uranium daughter's concentrations in soils but higher than in the reference counties (Table 1). However, the counties with no uranium mining history display lower but variable background concentrations. For example, Seia and Celorico da Beira, in the granite region also, contain higher uranium concentrations than Sátão which is a county already in the transition to the schist region. Concentrations even lower than in Sátão were measured in soils of Serpa and Ourique, in a region of sedimentary origin of the Alentejo province, south of Portugal, (Figure 1).

Leafy vegetables, such as cabbage, typically displayed ^{238}U concentrations ranging from about 0.1 to 0.6 Bq kg-1 (wet weight) and ^{226}Ra concentrations from 0.5 to 5 Bq kg-1 (wet weight). Cabbage leaves from the county of Canas de Senhorim displayed in average higher concentrations of uranium isotopes and radium than the other counties (Table 2). It must be stressed that cabbage leaves may contain an important contribution of radionuclides from atmospheric depositions, variable from region to region. Although likely to be transferred through food chain as well, their concentration in cabbage leaves, therefore, may not be entirely due to root uptake from the soil. Radioactivity in peeled potatoes is likely to reflect better the plant uptake and accumulation in the tuber with plant growth than cabbage leaves. Potatoes from the county of Canas de Senhorim showed uranium, ^{230}Th and ^{226}Ra concentrations about two orders of magnitude higher than reference counties (Table 3).

Orange pulp, protected from atmospheric depositions, likely reflects also true root uptake of radionuclides. Indeed, oranges grown in the Canas de Senhorim county displayed average concentrations of uranium higher than oranges from reference counties (Table 4). It may be noted, however, that oranges from Sátão contain more ^{226}Ra and ^{210}Po than those from Canas and the same was observed with cabbage (Table 3). This allows hypothesizing that mineralogical and chemical composition of soils and irrigation water, may also contribute to high concentrations of uranium daughters in horticulture products even in the absence of uranium mining waste. Although oranges are prone to concentrate radium, this does not seem the case for apples and quince from the same region (Table 5).

Table 1. Radionuclide concentrations (Bq kg^{-1} dry weight) in soils (fraction <63 μm).

County		^{238}U	^{235}U	^{234}U	^{230}Th	^{226}Ra	^{210}Po=^{210}Pb	^{232}Th
Seia and Celorico (N)	Mean	220	11	228	223	253	241	217
	SD	31	2	22	61	69	44	93
Campo and Queirã (N)	Mean	199	10	219	172	571	300	67
	SD	53	2	58	54	424	92	17
Rio de Mel (M)	Mean	257	12	258	282	370	266	167
	SD	6	0.2	2	3	5	12	3
Moreira de Rei (M)	Mean	602	27	676	652	575	456	187
	SD	119	7	193	92	88	8	41
Sátão (N)	Mean	68	2.8	72	72	118	71	50
	SD	2	0.0	2	2	16	9	2
Canas de Senho-rim (MW)	Mean	348	16	352	552	560	525	256
	SD	61	3	71	353	406	412	72
Serpa and Ouri-que (N)	Mean	26	1.1	26	51	59	29	45
	SD	7	0.4	8	16	15	6	15

(N) No uranium deposits and no mines in the county.
(M) Old uranium mines in the county.
(MW) Old uranium mines and milling waste.

Table 2. Radioactivity in cabbage (mBq kg^{-1} fresh weight).

County		^{238}U	^{235}U	^{234}U	^{230}Th	^{226}Ra	^{210}Pb	^{210}Po	^{232}Th
Seia and Celorico	Mean	58	3	60	70	919	980	-	24
	SD	11	1	12	25	484	533		4
Sátão	Mean	94	4	97	60	1538	-	407	9
	SD	6	1	5	20	629	-	133	3
Canas de Senhorim	Mean	234	11	234	48	2014	-	357	17
	SD	170	9	172	2	1455		134	4
Serpa and Ourique	Mean	10	1.2	16	3.1	92	146	298	4.1

Table 3. Radioactivity in potatoes (mBq kg-1 fresh weight).

County		^{238}U	^{235}U	^{234}U	^{230}Th	^{226}Ra	^{210}Pb	^{210}Po	^{232}Th
Sátão	Mean	38	1.2	37	9	64	-	622	5.3
	SD	2	0.3	2	2	4	-	20	1.6
Canas	Mean	350	17	361	267	108	-	162	17
	SD	430	22	443	225	74	-	42	8
Serpa and Ourique	Mean	1.8	0.2	2.0	2.3	7.8	16	4.1	2.8
	SD	0.2	0.1	0.4	0.5	3.3	6	2.3	0.4

Table 4. Radionuclide concentrations (mBq kg^{-1} fresh weight) in oranges.

County		^{238}U	^{235}U	^{234}U	^{230}Th	^{226}Ra	^{210}Pb	^{210}Po	^{232}Th
Sátão	Mean	27	1.4	30	12	748	-	446	4.1
	SD	1	0.3	1	1	46	-	25	0.5
Canas	Mean	20	0.9	19	-	346	-	430	-
	SD	0.3	0.2	1	-	82	-	18	-
Serpa and Ourique	Mean	2.2	0.6	2.8	3.0	15	19	8	2.3
	SD	1.3	0.1	1.8	2.0	6	5	7	1.5

Table 5. Radionuclide concentrations (mBq kg^{-1} fresh weight) in other fruits (apple and quince).

County		^{238}U	^{235}U	^{234}U	^{230}Th	^{226}Ra	^{210}Pb	^{210}Po	^{232}Th
Sátão	Mean	19	1.0	20	-	52	-	238	-
	SD	3	0.2	3	-	27	-	64	-
Canas de Senhorim	Mean	23	1	21	17	92	-	354	5
	SD	11	0.5	10	9.6	44	-	46	2

The overall results show a slight enhancement of uranium series radionuclides in horticulture products grown in kitchen gardens and farms of Canas de Senhorim and Moreira de Rei in comparison with similar products from other counties in the region and in regions of south of Portugal.

Conclusions

Average concentrations of uranium series radionuclides in the soils of uranium mining counties, in particular those of Canas de Senhorim and Moreira de Rei, are slightly elevated above the levels measured in reference counties with no mining activities. Concentrations measured in horticulture products were also in average slightly higher in uranium producing counties. Nevertheless, these enhanced levels are one or two orders of magnitude above concentrations measured in reference counties and, although deserving attention and radiological surveillance, do not seem high enough to cause a noticeable irradiation of the consumers.

References

Carvalho F. P. (2007). Environmental Health Risk from Past Uranium Mining and Milling Activities. *In*: Environmental Health Risk IV, C.A. Brebbia (Ed.), pp 107-114. Wessex Institute of Technology Press, UK.

Carvalho F.P. *(In press)*. Past uranium mining in Portugal: legacy, environmental remediation and radioactivity monitoring. UMREG. International Atomic Energy Agency; Vienna.

Carvalho, F.P., Oliveira, J.M., Madruga, M.J., Lopes, I., Libanio, A., Machado L. (2006). Contamination of hydrographical basins in uranium mining areas of Portugal. In: *Uranium in the Environment: Mining Impacts and Consequences*. B.J. Merkel and A. Hasche-Berger Editors, pp 691-702. Springer-Verlag Berlin Heidelberg Publ.

Carvalho, F.P., Oliveira, J.M. (2007). Alpha emitters from uranium mining in the environment. *Journal of Radioanalytical and Nuclear Chemistry* 274: 167-174.

Carvalho, F.P., Oliveira, J. M. Lopes, I. Batista A. (2007). Radionuclides from past uranium mining in rivers of Portugal *Journal of Environmental Radioactivity 98:298-314.*

Nero, J.M. Dias, J.M. Torrinha, A.J., Neves, L.J., Torrinha, J.A. (2005). Environmental evaluation and remediation methodologies of abandoned radioactive mines in Portugal. In: Proceed. of an *International Workshop on Environmental Contamination from Uranium Production Facilities and Remediation Measures*, held in Lisbon 11-13 Feb 2004, pp.145-158. International Atomic Energy Agency, Vienna.

Oliveira, J.M., Carvalho, F.P. (2006). A Sequential Extraction Procedure for Determination of Uranium, Thorium, Radium, Lead and Polonium Radionuclides by Alpha Spectrometry in Environmental Samples. (Proceedings of the 15th Radiochemical Conference). *Czechoslovak Journal of Physics* 56 (Suppl. D): 545-555.

Pham M.K., Sanchez-Cabeza J.A., Povinec P.P., Arnold D., Benmansour M., Bojanowski R., Carvalho F.P., Kim C.K., Esposito M., Gastaud J., Gascó C.L., Ham G.J., Hedge A.G., Holm E., Jaskierowicz D., Kanisch G., Llaurado M., La Rosa, J., Lee S.-H., Liong Wee Kwong L., Le Petit G., Maruo Y., Nielsen S.P., Oh J.S., Oregioni B., Palomares J., Petterson H.B.L., Rulik P., Ryan T.P., Sato K., Schikowski J., Skwarzec B., Smedley P.A., Tajaán S., Vajda N., Wyse E. (2006). Certified reference material for radionuclides in fish flesh sample IAEA-414 (mixed fish from the Irish Sea and North Sea*). Applied Radiation and Isotopes* 64: 1253-1259.

Povinec, P.P., Pham, M., G, Barci-Funel, R. Bojanowski, T. Boshkova, W. Burnett, F.P. Carvalho, et al. (2007). Reference material for radionuclides in sediment, IAEA-384 (Fangataufa Lagoon sediment). *Journal of Radioanalytical and Nuclear Chemistry 273:383-393.*


Uranium Mining
and Hydrogeology

Monitoring and remediation of the legacy sites of uranium mining in Central Asia

Alex Jakubick[1], Mykola Kurylchyk[2], Oleg Voitsekhovich[3]and Peter Waggitt[2]

[1]UMREG, 78269 Volkertshausen, Germany, alexjakubick@gmail.com
[2]IAEA, Vienna, Austria
[3]Ukrainian Hydrometeorological Institute Kiev, Ukraine

Abstract. The results are presented of an IAEA Regional Project dealing with the present state and challenges of remediation of the uranium mining and processing legacy sites in Tajikistan, Uzbekistan, Kyrgyzstan and Kazakhstan. Specific recommendations are made for each of these countries pointing out the most urgent measures required.

We are no other than a moving row
Of magic shadow-shapes that come and go
Round with the Sun-illumined Lantern held
In Midnight by the Master of the Show

The Rubaiyat of Omar Khayyam

Introduction

During the 1970s and 80s, more than 30% of the uranium production of the former Soviet Union (USSR) came from the Central Asian republics. The extensive uranium production left behind a huge legacy of mining and processing wastes. The mining and milling technologies applied in USSR and allied countries originated from the same engineering unit of the USSR Ministry for Medium Scale Machine Industry and for this reason the uranium production legacies in Central Asia, Russian Federation, Ukraine and Eastern Europe exhibit very similar characteristics and remediation of the legacies encounters similar problems.

Along with the independence of the Central Asian countries also the national responsibility for management of natural resources was declared at a conference in Almaty, December 21, 1991 and the former institutions responsible for common

economic policies and transfer among the Central Asian republics in this sector were eliminated. Thus, the uranium industry in the newly independent countries had to face the world market individually at a time of stagnant uranium markets - the uranium spot market price at that time was US$ 20-25 per kg of U. At the same time the global growth in environmental awareness made the application of increasingly more stringent regulations to uranium mining and processing necessary. By 1995 most of the conventional uranium mines in Central Asia had to shut down and only mines survived that could be concerted to In Situ Leach (ISL) mining. The decommissioning and closure of the conventional uranium mines happened with very little technical or regulatory experience and without any funding for closure and remediation.

In summer 2003, the global uranium market started recovering and approximately a year later the Central Asian Republics of Uzbekistan, Tajikistan, Kyrgyzstan and Kazakhstan approached IAEA with the request to receive technical assistance and expert advice to deal with the legacy sites of the uranium industry. Following this requests, the presented regional project TC RER9086 has been established at IAEA.

State of the legacy sites

Tajikistan

The past mining and processing of uranium in Tajikistan created more than 170 million tons of waste rock and tailings piles containing approximately 240-285 x 10^{12} Bq of radionuclides. The State Enterprise, SE "Vostokredmet" estimates that the tailings and waste rock piles of Tajikistan contain approximately 55 million tons of uranium. The volume of tailings is disproportionately larger than the volume of the waste rock because a considerable proportion of uranium ore processed in the country was imported from the neighboring states but also from Eastern European countries. The processing was at the former Leninabad Mine-Chemical Combine (predecessor of SE "Vostokredmet") and at the hydrometallurgical plants operating directly at the mining sites, such as Adrasman, Taboshar, Isphara. The critical issue concerning these sites is that they are often in the immediate neighborhood of residential areas (Chkalovsk) or in the watershed of the internationally important Syr-Daria River flowing through the Fergana Valley, which is the most populated area in the region providing most of the agricultural produce.

Already a brief inspection of the legacy wastes at the Taboshar, Adrasman and Degmay sites revealed that the present state of the waste containment is inadequate.

The Degmay tailings pond is without any soil or vegetative cover and the surface of the tailings is a source of persistent dusting. Under the climatic conditions

Fig.1 Desiccation cracks in uncovered tailings at Degmay.

of the region the tailings surface is permanently dry and shows deep desiccation cracks (Fig. 1).

The Rn-222 exhalation from the tailings (measured during the summer period) was 36-65 Bq/ m^2 s; the ambient Rn-222 concentration varied between 200 and 1000 Bq m^{-3}. An interim covering of the tailings surface could be easily accomplished using the earth material of the sandy hills just behind the tailings pond. Immediate remedial measures, however, cannot be presently implemented because the remediation of the site is to be resolved within an overall remediation master plan, which would include the remediation/re-utilization of the uranium processing waste in Chkalovsk.

The monitoring of the water pathway at Degmay shows an increased sulfate and radionuclides content in the ground water, thus indicating an impact of the tailings on the local ground water. The measurements, however, were done on integral ground water samples taken by bailing from monitoring wells intersecting and feeding from all aquifers underlying the site. To predict the movement of the radioactive plume and assess the potential risk to the Syr Daria River or to the shallow ground water system communicating with the river, measurements of the ground water contamination in the individual aquifers are needed. New observation boreholes are currently planned for this purpose. To ensure that the new monitoring wells provide satisfactory results it is recommended that the selection of the bore hole locations, the design, construction and instrumentation of the observation wells be done (and peer reviewed) under auspices of IAEA.

The most prominent feature at the Taboshar legacy site is a pile of several million tons of ground low grade uranium ore, the “Taboshar Hill” (Fig.2) placed in a morphologically exposed position. The pile was never stabilized and/or covered and is fully exposed to wind and water erosion.

Fig. 2. "The Taboshar Hill", a pile of ground low grade uranium ore.

The tailings deposits I and II are morphologically less exposed and placed topographically lower than the Taboshar Hill. Although the tailings have been preemptively covered, the cover thickness is by to days standards insufficient and considerably damaged by burrowing animals; the tailings material is exposed at a number of places.

Feasible remedial options for the site include (a) repair of the existing covers, (b) construction of new covers, (c) relocation of the waste into the former open pit mine located close to the "Taboshar Hill" or, (d) a combination of in situ remediation and relocation decided individually for each pile on the basis of remedial investigations and a feasibility study.

Irrespective which site remedial option is adopted, the remediation of the, flooded open pit mine would be required because the elevated position and open surface of the pit makes the pit function as a recharge area for the local groundwater and as a continuous source of ground water contamination. Just above the city of Taboshar the mine water is freely discharging from two abandoned adits used by the local population mainly for irrigation purposes.

The impact of the radon exhalation and dusting from the waste piles, including from the "Taboshar Hill", is less of an immediate health concern due to the convenient exposure of the site to winds. Nevertheless, the inadequate state of the piles and the stubborn insistence of the herdsmen to use the site for pasture provide sufficiently justification for remediation of the piles.

In conjunction with the site remediation of more immediate concern are the contaminated seepages from the tailings piles I and II which carry high concentrations of sulfate (SO_4 9200-9600 mg/l), carbonates (HCO_3 1780 – 1800 mg/l), uranium (U 53-74 mg/l) and also low concentrations of radium. The rate of the discharge varies with the season and during the hot season the seepage water can evaporate entirely leaving behind precipitates of carbonate, sodium and sulfate complexes of uranium (Fig.3).

Fig.3. Uranium salt precipitates on the shore of the "Taboshar Creek"

The precipitated white salt often contains yellow Uranile crystals reaching U concentrations of 10-20 Bq/g. The tailings pile seepages discharge into a creek originating under the "Taboshar Hill" running through the site collecting the (mostly contaminated) surface runoff from the site. The local population uses the creek for watering of domestic animals, irrigation of rice paddies, gardens and orchards situated along the creek.

Radiation exposure and uncontrolled spreading of contaminated material due to unauthorized digging and collection of non-ferrous metals from the old piles and mines is a common problem in all Central Asian countries and presents a real radiological concern in Taboshar as well.

Uzbekistan

Between 1964 and 1995, the uranium mining in Uzbekistan was solely by conventional mining. The ore mined in the mountainous Eastern part of the country at sites, such as Yanghiabad (Tashkent district) and Charkesar in the Fergana Valley (Namangan district) used to be sent for processing to the Leninabad Mining Chemical Industrial Combine in Tajikistan (now SE Vostokredmet). The ore from the sandstone type uranium deposits in Central Kyzylkum (Navoi and Samarkand regions) were processed in Uzbekistan at the Navoi Mining Chemical Combine (NMCC) in Uzbekistan. Consequently, the only uranium tailings legacy in the country is at the NMCC site. After introduction of the In Situ Leach (ISL) mining in 1995, all conventional uranium mines were closed down.

The most important legacy sites of the pre-1995 mining era are the former the open pit mine at Uchquduq, where the low-grade uranium ore was left piled up on the site without any safety measures and the mines at Yanghiabad and Charkesar.

At the Yanghiabad site, which extends over 50 km^2, approximately 500,000 m^3 of waste rock have been left on the site (Fig. 4).

Fig. 4. Open mine adit and extensive uncovered waste rock piles at the Yanghiabad site.

Measurements around the mine adit show a gamma dose rate of 1.4-2.5 μS/h and 0.60-2.0 μSv/h at the site. The gamma dose rate in the city of Yanghiabad (background) is 0.2-0.4 μSv/h.

The mine adit has been left open thus allowing unhindered access for humans and animals and uncontrolled escape of radon exhalation and mine water drainage from the mine. The mine water contains up to 30 Bq/l uranium and traces of toxic metals. The mine discharges flows directly into the close by river used by the local population for drinking and irrigation purposes.

To assess the environmental and health impact of the mine water drainage, a systematic monitoring of the river water in Yanghiabad and above the city of Angren is proposed. Based on the results of the monitoring it should be possible to decide whether water treatment is required for the mine drainage and what type of water treatment would be suitable (a small water treatment plant, an engineered wetland etc.).

The Charkesar legacy site is in the foothills of the Kuraminskiy Mountain Range in the northwestern part of the Fergana Valley, approximately 20 km from the regional town of Pap. The mine site is on the right bank of a small mountain river separating the site from the village of Charkesar (population of 2 500 people). There are 2 abandoned mines at the site, Charkesar-1 and Charkesar-2. The mining was by conventional methods and later by underground leaching down to a depth of 280 m. After mine closure in 1995, most of the miners and professionals left because of lack of work opportunities in the area.

The total volume of the mine wastes amounts to 482,000 m^3 and is spread over an area of 20.6 ha. The piles of low grade ore and waste rock have been partly covered by a soil layer but the cover has deteriorated due to erosion by rain. The gamma dose rate at the site is 3.0 to 4.5 μSv / h. The shaft of the underground mine is open and presents a safety hazard because the site is frequented by the local population disregarding the posted warning signs.

There is a mine water overflow (approximately 3-5 L/s) through the ventilation shaft located on a small elevation on the site. The overflowing mine water is contaminated and shows the visual characteristics of acid mine drainage. However, the observed iron stains could be due to the residual acid from the former underground mine leaching. The ^{238}U activity of the mine water is in the range of 26 - 36 Bq/l. The mine water also contains 5.2 Bq/kg of Pb^{214}, 4.0 Bq/kg of Bi^{214}, and

Fig. 5. The Charkesar-2 legacy site behind the wall, Charkesar village on the left bank of the river and mine water overflow from a ventilation shaft.

2.7 Bq/kg of Ra^{226}. The soil in contact with the mine water contains 2.7 Bq/g of U and 62.8 Bq/g of Ra^{226}. After a short run, the overflowing mine water discharges into the river bordering the site.

The drinking water used in the village (from a spring) does not show elevated uranium concentrations but -unrelated to the legacy site- contains substantially elevated concentrations of heavy metals, exceeding the WHO standards.

The mine site is enclosed by a stone wall on which warning signs are posted indicating presence of radioactivity (Fig. 5). Disregarding the signs, the local population, along with their cattle, continues accessing the site through the numerous places where the wall has been destroyed.

Although the risk of living next to a not remediated site should not be underestimated, of more immediate concern in Charkesar are the indoor Rn levels. Systematic measurements carried out within a NATO project in public buildings where mine waste rock was used for construction showed indoor radon concentration between 670 and 1410 Bq/m^3. It would be advisable to carry out a similar indoor radon survey also in private homes where waste rock material has been used for construction.

Concerning remediation, the first measures to be taken at Charkesar are (a) the preparation of a reliable mine waste inventory, (b) implementation of a systematic monitoring program and, (c) based on the indoor radon measurements in the village, preparation of recommendations for remediation of selected houses, as well as (d) education/information of the inhabitants of Charkesar on "what precautions must be observed when living in the neighborhood of a uranium mining legacy site".

The uranium tailings at the Navoi site, present the most significant accumulation of legacy wastes in Uzbekistan. Approximately 57 M t (solid mass) of uranium tailings having a specific activity of 10 - 110 kBq/kg were produced at the Hydrometallurgical Plant No. 1 (HMP-1) between 1964 and 1995. The tailings were discharged into a "flat" tailings impoundment structure 5 km from the processing plant. The impoundment is 5 to 15 m high and subdivided into 8 compartments. The impoundment extends over an area of 637.1 ha. The dose rate measured 10 cm above the uranium tailings surface is 0.5-1.7 μSv/h (500-1700 μR/h), the average radon exhalation from the tailings is 4.1 Bq/m^2sec.

After closure of the conventional uranium mines, HMP-1 was refurbished for processing of gold ore (from the Muruntau Open Pit Mine). For disposal of the gold processing residues the "old" discharge pipeline and tailings impoundments continued being used. Regarding the remediation of the uranium tailings in the impoundment advantage was taken of the fact that the "gold" tailings are not radioactive and highly impermeable. The discharge regime of the "gold" tailings was adjusted to serve the covering of the radioactive uranium tailings as well. By systematically spreading the "gold" tailings over the uranium tailings the required attenuation of the gamma radiation (< 1 μSv/h [100μR/h]) and radon exhalation (to an effective dose of less than 1mSv/a) has been achieved. Due to the impermeable nature of the very fine "gold" tailings the percolation of the rain water into the uranium tailings could be prevented as well.

The attenuation layer is built gradually by hydraulically spreading thin (15 to 20 cm thick) layers over the dried out tailings surface. A drying and consolidation time of 15 to 20 days is usually required for each thin layer to acquire the necessary shear strength. The desiccation cracks which develop during the drying phase are filled during placement of the next layer. While the "gold" tailings cover layer is drying in one compartment the discharge continuous into the next compartment. The overall thickness of the attenuation layer required to meet the specified criteria is usually achieved by building a 0.7 to 1.5 m thick gold tailings layer. The final surface - after sufficient shear strength has been gained to carry machines - is then capped by a 30 cm thick top soil layer, which is vegetated to prevent wind erosion and dusting.

So far, more than 7 million tons of "gold" tailings have been placed as a uranium tailings cover: Compartment No. 5 (100 ha) received a 1.5 m thick cover; Compartment No. 6 (80 ha) has a 3.5 m thick cover; Compartment No. 3 (110 ha) has a 0.5 m cover. Currently (2008) the covering of the compartments No. 4, 7 and 8 is ongoing. It will take approximately 13 to 15 M t of gold tailings to complete the construction of all attenuation layers and approximately 2 M t of top soil to cap all compartments.

Kyrgyzstan

The development of the uranium industry in Kyrgyzstan was very similar to the other Central Asian republics. There are 25 waste rock and 35 tailing piles in Kyrgyzstan, from which 30 tailings piles contain old uranium tailings and five piles contain NORM wastes from production of non-ferrous metals; the main legacy sites are at Mailuu-Suu, Shekaftar, Minkush, Kaidji-Say, Ak-Tuz and Kara Balta.

The Mailuu-Suu uranium deposit was exploited between 1946 and 1967 during which the Western Mining Chemical Combine in Mailuu-Suu (Figure 6) produced 10,000 t U_3O_8 and left behind 1.4 to 2.0 millions m^3 mining and milling waste deposited in 23 tailings and 13 mine waste piles on the territory of the former enterprise, some of which are within the town boundaries.

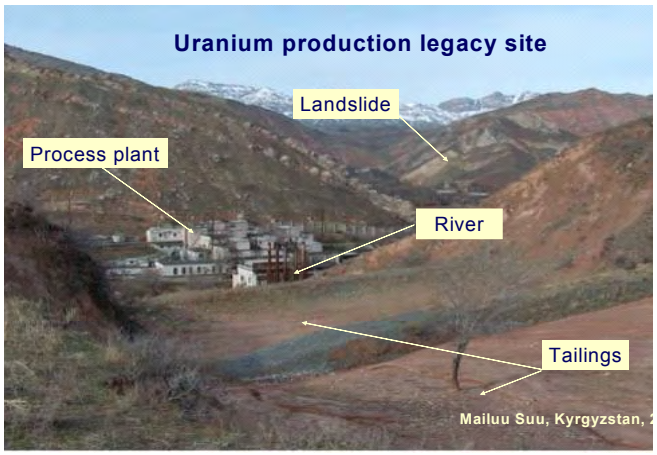

Fig.6. Mailuu-Suu located in the upper watershed of the Naryn River, 50 km from the Fergana valley.

The majority of the tailings dumps are located along the Mailuu Suu River. After closure of production 1966/67 the waste piles were abandoned without remediation. The staff of the industrial complex continued supervision and maintenance of the tailings piles until 1991. After 1991, the monitoring activities became sporadic.

The remediation priority of the Mailuu Suu site is justified by the large volume of tailings on the site and the possibility of extensive landslides, possible flooding and ultimate structural failure, loss of containment and uncontrolled release of tailings from some of the impoundments. The overall hazard is heightened by the possibility of seismic events.

The average gamma-radiation exposure dose rates over the surface of the covered tailing piles are up to 1 μSv/h (from 60-100 μR/h). Typically, the background levels are 0.25 μSv/h (25-30 μR/h). At places where the cover is breached, the gamma-radiation exposure dose rate can reach 15 μSv/h (1500 μR/h) and high radon exhalation must be expected. The average annual gamma exposure dose rate was estimated to be 0.17-0.36 mSv/a. The annual dose rate "hot spots" can be up to 2-14 mSv/a. For a number of tailings piles it can be expected that the exposure may exceed 1 mSv/a. In spite of the sporadic data on the contamination of the river and lack of a proper radiological risk assessment it is safe to state that the radiological (however, not the socio-political) impact of the tailings landslide into the river (the worst case scenario) is probably overestimated.

Presently, several internationally funded remediation projects are ongoing at Mailuu-Suu from which the World Bank project is the most prominent. One of the most significant achievements of the recent years is the mitigation of the potential landslide "Tektonic" and of several other landslide prone spots close to the tailing piles of Mailuu Suu.

Another significant uranium tailings legacy site is located in the mountainous terrain of the Min-Kush area. The tailings are deposited in four impoundments at 4 sites: Tuyuk-Suu, Taldy-Bulak, "K" and "D". The mill operated from 1955 till

1960 and generated approximately 1.9 million m^3 tailings. The tailings impoundments, Tuyuk-Suu (approximately 2 km from Min Kush), Taldy-Bulak (approximately 9 km from Min Kush) are near the river Tuyuk Suu; the tailings impoundments "D" and "K" are located in a high mountain bowl (approximately 11 km from Min Kush). The regular supervision and maintenance of the impoundments ceased 1991. Presently, the monitoring and maintenance of the impoundments is sporadic.

Although the Tuyuk Suu and Taldy-Buluk impoundments present only a moderate risk for the Tuyuk Suu River, the river is a tributary to the Syr Daria River and thus any contamination would have a cross border relevance, which would politically suffice to justify remediation. What is, however, more urgently needed at the site is the implementation of a monitoring and maintenance regime, particularly the regular cleaning of the by-pass canals at both tailings impoundments and the maintenance of the cover at Taldy-Buluk.

In a socially and ecologically sensitive situation on southern shore of the Isyk-Kul Lake is the relatively small Kaji-Say mine and mill site. The facility was in operation from 1952 till 1966, using acid extraction procedures to obtain uranium from the ash residues of the brown coal mined locally. The coal was burnt in a heat and power generation plant providing the ash for uranium extraction. The tailings were deposited near the power plant and industrial complex on the mountain terraces approximately 2.5 km from the Lake Isyk-Kul, which is the receptor of primary concern. Approximately 150,000 m^3 of uranium tailings and other industrial wastes are placed on an area of approximately 1.1 ha.

After 1966, till 1991 the supervision and maintenance of the tailings was conducted by the staff of the industrial complex. Presently, there are no regular inspections of the site, the access is not controlled and the site fencing is not maintained. The system of water diversion canals on the slopes above the pile has been destroyed.

Approximately 2 km downstream of the tailings, observation boreholes have been placed to follow the contamination release from the pile into the ground water; so far no ground water contamination has been reported.

In conjunction with the association of the uranium tailings with coal ashes the concern has been raised in 1995 that acid generation might occur in the pile. This could neither be confirmed nor disproved as there are no measurements of pH in the (rarely occurring) direct seepage from the pile. Neither were any signs (staining) observed during the IAEA mission to the site in 2007.

Severe erosion and tailings displacement can be observed on the pile. Because the tailings at Kadji-Say originate from coal ash processing and the grain sizes are very fine, the tailings are prone to be transported by erosion in larger amounts and over longer distances than regular mill tailings. To prevent contamination of the Lake Isyk-Kul the Ministry of Emergency ordered in 1992 the construction of a protective dam below the main tailings pile. Prior to this, large quantities of tailings have already been already displaced.

In 2006, financed by ISTC, the waste pile was covered with a mixture of ash-clay, which later proved to be an unsuitable material for the purpose. The cover was not completed and the face of the pile at the lower end remained exposed. The

Fig.7. Tailings pile dam and cover built at Kadji-Say 2006 and state of the pile 2007

cover was designed as a multi-layer cover with the objective to reduce radon exhalation and gamma radiation as well as protect against erosion (Fig. 7).

Although gamma radiation exposure is a minor hazard at the site – measurements on the tailings indicated 1.8-1.9 μSV/h (180 and 190 μR/h) (the background levels are ~0.2 μSv/h (20-30 μR/h)) - covering of the pile would help contain the waste. Due to the remoteness of the location the Kadji-Say tailings pile does not present an immediate hazard for the local population. The persistent erosion of the tailings and the risk of potential contamination of the Lake Isyk-Kul remain, however, the primary concerns at the site. The most important remedial actions would be the cleaning and repair of the existing run-off diversion channels above the pile, covering and re-vegetation of the pile surface and slopes and regular monitoring and maintenance of the site.

An independent assessment by IAEA experts of the conditions at the legacy sites at Ak-Tuz and Kara-Balta would be desirable.

Kazakhstan

Among the Central Asian countries, Kazakhstan has the strongest economy and the fastest growing uranium production. Regarding the potential for further growth it is important to note that approximately 20% of the world uranium resonably assured resources are in Kazakhstan. The responsibility for the active uranium mining is with the National joint stock company KAZATOMPROM.

A compilation made in 1993 identified 127 uranium mining/milling legacy sites located in three areas:

- Northern Kazakhstan
  The legacy sites related to 12 uranium deposits: In the Kokshetau area (sites No.: 8, 9, 1, 3, 12); in the group of mines Kosatchinnoe, Shatskoe, Glubinnoe, Agashskoe, Koksorskoe; Manybaiskoe mine; in the Stepnogorsk HM-Processing plant tailings disposal site. The total amount of waste is 81.2 Mt;
- Southern/Central Kazakhstan

The legacy sites relate to 4 deposits: Kurday, Vostochniy, Zapadniy in the Zhanbyl region (in Southern Kazakhstan) and Karasaiskiy, Ulken-Akzhal in Central Kazakhstan. The total amount of waste is 117.8 Mt;

- Western Kazakhstan

  The legacy sites relate to 2 deposits and the Koshkar Ata tailing site near Aktau. The total amount of waste is 58.9 Mt

The production in the listed mines was suspended in 1995. The inventory of the legacies totaled (approximately): 368 M m^3 mine waste piles; 13 M m^3 low grade ore piles, 869 K m^3 ore stockpiles, 4.9 M t of metal scrap and building debris and 865 ha of contaminated areas.

To deal with the legacy sites, the Government of Kazakhstan adopted a suitable legislative framework for the task and established the State Program for "Remediation of (the sites left behind by) Uranium Mining Enterprises and Mitigation of the Consequences of Mining of the Uranium Deposits defined for the period 2001-2010". The responsibility for the implementation of the program was given to the SE Uranlikvidrudnik established in 2000.

The first remedial action included 6 sites in Northern and 2 sites in Southern Kazakhstan. The work done in accordance with the standards defined in the governmental decree "Sanitary Rules for Mitigation, Remediation and Interdepartmental Transfer of Installations for Mining and Processing of Radioactive Ores (SP LKP-98). Beyond radiation protection, the goals of remediation were to prevent contamination of the rivers; unauthorized access to the legacy sites; use of mining waste as building material and dusting from the contaminated surfaces.

Because of the great climatic differences in Kazakhstan, the specific conditions of the legacy site(s) played an important role in selection of the remedial solutions. The legacy sites in Northern Kazakhstan are located in a prairie-type environment in a moderately humid zone. The legacy sites in Central and Southern Kazakhstan are either in semi-deserts having an arid climate or in a humid mountainous area, such as the sites in Southern Kazakhstan (Kurday mine, Panfilov deposit).

By 2007, the remediation was completed at the mine sites No. 12, 3, 1, Kossachinoye, 8, 9, and 14 in Northern Kazakhstan and Kurday as well as in parts of the Vostochnyj mine (where mining continues in other parts of the mine). The remediation included (a) sealing and cementation of the shafts and raises, (b) removal of the contaminated soil, (c) collection of the scrap metal, disposal of the contaminated and recycling of the not contaminated scrap metal, (d) decommissioning, dismantling, demolition and/or decontamination of related buildings and structures, (e) disposal of the contaminated debris into waste piles, (f) grading of the surface and concentration of the waste into rock and mixed waste rock/debris piles, (g) covering of the piles with a soil cover up to 1 m thick, (h) fencing of the area if located within 5 km of a settlement (Fig. 8).

Fig.8. Covering of a stabilized waste rock pile at the mine site No. 9 in N Kazakhstan.

The completed work included the decommissioning and sealing of 43 shafts and 22 ventilation shafts and raises, remediation of approximately 75 M m^3 of waste piles, 30 M m^3 of mixed waste piles, 6.7 M m^3 of low grade ore piles and approximately 400 ha of contaminated land. This means that by end of 2007 approximately 20 % of the legacy sites have been remediated.

The safe flooding of the mines and handling of the contaminated mine water proved to be a challenge and the issue of water treatment will have to be addressed in the next phase of the remedial program. Figure 9 shows an example of a mine wall collapse in an open pit mine in Northern Kazakhstan after ground water rebound.

Fig.9. Collapse of the mine No. 3 after ground water rebound in N Kazakhstan.

Part of the future challenges is the remediation of the tailings impoundments of the former Stepnogorsk Hydrometallurgical Plant. There are 46.8 Mt of the tailings deposited in three compartments of a tailings impoundment, which extends over 734 ha. The present state of the compartments is as follows: compartment No. 1 is filled, compartment No. 2 is operational and receives tailings from the plant and compartment No. 3 is left to evaporate. Presently, approximately 1.5 M t of tailings are being discharged into the impoundment annually. In all 3 compartments the tailings surface is dry but unconsolidated below the surface crust. The monitoring of the tailings impoundment shows that there is no contamination beyond the boundary of the sanitary zone.

The only recommendation regarding this site is to take up the monitoring of the tailings dust for alpha activity.

The present (2008) remedial work is focusing on the stabilization of the tailings at Stepnogorsk in Northern Kazakhstan and on the first remedial steps at the Koshkar-Ata site on the Caspian Sea, near Aktau in Western Kazakhstan. The completion of the works is expected by 2010.

At the Koshkar-Ata site, the operations of the former Caspian Hydrometallurgical Plant left behind approximately 52 M t of mine waste spread over an area of 66 km^2 and a uranium tailings pond extending over an area of 77 km^2. Although the tailings at Koshkar-Ata are very close to the Caspian Sea, the contamination of the sea is not of prime concern because the tailings are deposited in a natural depression where the ground water level is consistently lower than the level of the Caspian Sea. Approximately half of the tailings pond area is covered by water -the extent of the water cover varies with the seasons- while the other half of the tailings pond is dry and a source of radon exhalation and dusting. The gamma-dose rates over the tailings vary from several Sv/h to approximately 10μSv/h. Measurements by Uranliquidrudnik show that in the southern parts of the tailings pond the gamma dose rates exceed even 10 μSv h^{-1} (1 mR h^{-1}). The explanation for the high dose rate is that in the southern part of the tailings pond an area of more than 15.8 km^2 was used for dumping of radioactive sources; Approximately 140 Kt of radioactive waste unrelated to uranium processing were disposed here. Unfortunately, the same part of the tailings pond is also a popular scavenging ground for scrap metals. Thus the remediation goals for the site are the prevention of dusting and of unauthorized collection of scrap metals from the tailings.

The present remedial plans for the southern part of the “Koshkar Ata” tailings deposit foresee the placement of a concrete cover over the tailings and a subsequent covering with waste rock from the adjacent pile. The planed remedial solution deviates considerably from the practice of tailings remediation and it is proposed to initiate an international review of these plans. It is considered even more important to propose an international review of the overall remediation plans for the Koshkar Ata site.

In the close vicinity of the tailings pond is the location of the scrap metal yard where the decommissioned equipment of the former Caspian Hydrometallurgical Plant was collected. Although the storage yard is surrounded by a concrete wall a timely resolution of the fate of the collected scrap metal is strongly advised.

Project conclusions and challenges of remediation

The IAEA project team studied all and inspected almost all significant uranium mining and milling legacy sites in Central Asia. Giving allowance to the differences in climatic and geographic conditions, the legacy problems in Central Asia are similar to the issues encountered in other countries:

The mine waste piles, tailings impoundments/ponds and closed out mines were built many years ago and incorporate outdated engineering solutions. Impound-

ments and covers, if present at all, are susceptible to structural instability due to slope movement, landslides, erosion and damage by burrowing animals.

The most important constraints to remediation are:

- Costs of remediation and limited availability of national funding.

In none of the Central Asian countries have been funds set aside for mine closure and remediation. In none of the Central Asian countries, except for Kazakhstan, is adequate funding available from the national budget to pursue the remediation of the legacy sites in a systematic manner. A simple comparison of the GNPs of the Central Asian Republics shows clearly why it is more difficult to launch effective national remediation programs in Uzbekistan, and even more so Kyrgyzstan and Tajikistan than in Kazakhstan. The case of Mailuu Suu, however, demonstrates that international projects/funding can be a very effective incentive for the national government to allocate funds or match funding to the remediation of the legacy sites. In spite of the presently buoyant uranium market the remediation of the legacy sites is a public responsibility, similar to the governmental responsibility for the national infrastructure and the national governments should view remediation as an investment into revitalization of the post-mining regions.

- Inadequate institutional framework for mine closure and environmental remediation.

Following the declaration of the national responsibility for management of resources by the Central Asian Republics in Almaty, December 1991 inspection, monitoring and maintenance programs at the legacy sites have been discontinued. This is of significant concern, given that the structural and environmental integrity at the sites is highly dependent on maintenance of the containment and functionality of various installations, such as the surface water diversion canals etc. The requirement to assess, monitor and, if justified, remediate the legacy sites must come from a consistent set of legal, health and environmental protection requirements and from the mining law. It is essential that the national regulations conform to the international standards of IAEA and other relevant institutions (ICRP etc.) and operators, regulators and stakeholders are aware of the international practice in this area.

- Inadequate knowledge of the inventory of the legacy components and the risks associated with them.

Except for a few cases, there are presently not sufficiently reliable data for assessment of the "realistic" risks presented by the legacy sites. Specific remedial plans and monitoring and maintenance programs must be based on remedial investigations and feasibility studies, which follow from the overall environmental impact assessment to be technically sound and cost effective.


Uranium Mining
and Hydrogeology

Valorification of the natural capital from the former uraniferous mining area situated in the Romanian Carpathians. Study Case: The Natural Park of Gradistea de Munte – Cioclovina

Dan Bujor Nica, Dragos Curelea, Liliana Ciobanu and Alexandru Petrescu

Research and Development National Institute for Metals and Radioactive Resources.70, Bd.Carol I, Sector 2, 020917, Bucuresti, Romania, E-mail:icpmrr@icpmrr.ro

Abstract. The objective of the present study case is to demonstrate that the geographical landscape affected by the uraniferous mining activities can be recovered in the benefit of the touristic activity, of the biodiversity conservation, as well as historical and cultural patrimony preservation. In order to re-organize the post-mining geographical space by enhancing the balance between economic activities and environmental protection a solution with positive long-term effects is suggested and discussed in the paper.

Introduction

The investigation is focused on the mining area of Gradistea de Munte situated in the Sureanu Mountain which belongs to the central part of the Southern Carpathian Mountains. This area includes Gradistea de Munte and Costesti villages both placed in the district of Hunedoara. Nowadays, this territory represents an important part of Gradistea de Munte – Cioclovina National Park (G.M.C.N.P) established in 2003.

Despite the archaeological, anthropological, ethnographical, geological, speological, flora and fauna complexities, all attractions which are harmoniously divided into exceptional landscape, the consequences of mining activities that were developed in two stages between 1958 and 1988, can be felt. These mining activities investigated a rare earth mineralization with noticeable thorium content ±uranium.

The map of the region illustrates the existence of 14 galleries and 4 waste rock dumps derived from mining processes. The mining wastes are disposed into a perimeter of 8 -9 km^2 and they have a total approximate volume of 120,000 m^3.

The environmental problems are visible in the proximity of the mine galleries where the natural landscape and runoff water are affected; the sterile rocks contain different types of low radioactive rare earth minerals with thorium and uranium. Because of their radioactive potential, the local population and potential investors in tourism are afraid and distrustful of the future development of the area. The further recovery of natural capital depends on the environment quality and for this reason an assessment of the environmental impact in this abandoned mine site and its surrounding areas is required. The purpose of this study is to initiate a suitable environment restoration program to allow for the returning of the land use to the same status which existed prior to mining.

Study area location

The mine perimeter is situated in a mountainous area that is crossed over from South to North by the Gradistea River which drains the affluents of the Northern slopes that form the Sureanu Mountain. The altitude reaches over 2,000 m in the mountain peaks and it gradually descends while approaching the Mures River valley, the slope heights in the studied area ranging between 700m and 1,279m.

The surface runoff waters are gathered by Gradistea River, which is an affluent of the Mures River; the rivers meet near Orastie town.

The mountain slopes are covered with deciduous forests and, rarely, coniferous trees. The main road starts from Orastie and goes across Ludesti, Orastioara, Costesti and Gradistea de Munte villages, along the Valley of Gradistea River. The local inhabitants get their income from forest exploitation and animal farming.

Geologic setting and mineralization

The Sureanu Mountain Massif belongs to a metamorphic unit known as the Getic Nappe, Upper Proterozoic Sebes–Lotru Series which comprises of mesometamorphic rocks, such as: mica-schists, gneisses, quartzite-schists, amphyblites, paragneisses affected by migmatized processes.

The metamorphic rocks are divided into four petrographical assamblages according to the dominant rock types,forming a large synclinorim structure. The tectonic evolution generated a major system of NE-SW regional faults, which are also affected by a number of cross local faults striking from NW to SE and from NE to SW. The regional faults have enhanced the penetration of magmatic rocks and the development of hydro-metasomatic processes.

The main mineralization is associated with quarzo-feldspar migmatized gneiss lenses and it consists in yttrium and cerium rare earth associated with thorium and

uranium oxides and silicates. The radioactive minerals have a high content of Th ± U and they disseminate into host rock without forming important accumulations. The following useful minerals were identified to be: monazite, orthite,uranothorianite, thorite, xenotime, zircon, apatite, rutile, sphene, rare earth with niobium, yttrium and tantalum as well as thorium ± U,Ca,Fe,Ti.; small quantities of cassiterite, magnetite, hematite, pyrite,chalcopyrite, galene and ilmenite were also identified.

Site assessment procedures

In order to observe the impact of mining sources on pollution and to assess the ecological risk and the danger for human health, two procedures were adopted:

- observe and document physical factors (contamination, erosion, instability etc)
- discuss with the community the quality of life, as influenced by radioactivity.

The identified mine galleries and waste rock dumps derived from mining processes are located on the abrupt slopes of the left affluents of Gradistea River named, from East to West, as follows: Larga, Jerosu and Pustiosu brooks (Fig.1); the very old mine galleries are now collapsing and are difficult to identify. The waste rock dumps and mining water represent the main potential pollution sources and they have not only a physical impact on the environment, but a psychological one on the natives, which associate the incidence of cancer diseases in their communities with the presence of low radioactive waste rocks. In this context it is important to point out that a lot of gneissic lenses outcrop have a natural radioactivity that exceeds the external gamma irradiation level of waste rock dumps.

To describe the mining waste rocks, water, soils and sediments in the northern part of G.M.C.N.P., old mine reports and bibliographical information were reviewed and two field-work campaigns were carried out in order to gather laboratory samples and to run external gamma irradiation measurements.

Results

Characteristics of waste rock dumps

The waste rock dumps impact consists of a lot of disturbance types, but the present study is focused on the radioactive and heavy metals content which could generate surface water contamination due to waste rock dumps drainage and human irradiation. The results of laboratory analysis are presented in Table 1.

The external gamma irradiation measurements were done in a grind that covers the horizontal surface of the dump. The sections exceeding the acceptance level (0.30μSv/h) were outlined as it can be seen in Fig.2

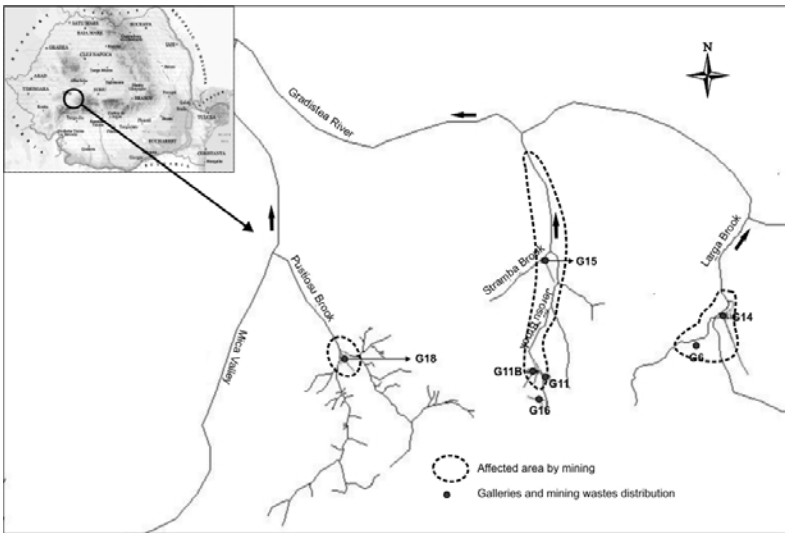

Fig.1. Study – area location and hydrographical basin investigated.

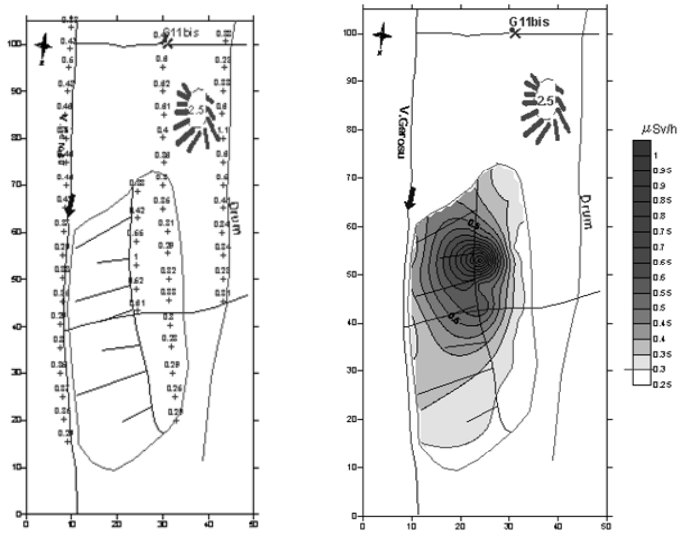

Fig.2. The external gamma irradiation measurements on the surface of a waste rocks dump (Jerosu Brook- G11B)

Table 1. Chemical composition of mining waste (maximum values).

Petrografical/ mineralogical content	Element %by weight	Larga Brook	Jerosu Brook	Pustiosu Brook
Micaschists, amphybolites, quartzite-schists, migmatized rock , gneisses containing rare earth with Th ± U, magnetite, galene, pyrite, chalcopyrite	U_{nat}	0,0133	0.0197	0.015
	Th	0.043	0.047	0.035
	Ra^{226}*	2.12	2.76	1.98
	Zn	0.0189	0.016	0.014
	Ni	0.0019	0.0015	0.0018
	Cr	0.004	0.0063	0.0065
	V	0.0093	0.0038	0.0031
	Co	0.0006	0.0019	0.0015
	Pb	0.150	0.006	0.0026
	Cu	0.007	0.005	0.005
	Cd	0.0001	0.075	0.0001

* Specific activity (Bq/g)

Table 2. The level of external gamma irradiation and the aproximative size of affected surfaces.

Waste rock dump	Total surface of the dump (m^2)	The contaminated surface,m^2		
		Total surface (m^2)	External gamma irradiation level (µSv/h)	
			0.30 – 0 .45	> 0.45
Gal 14 Larga	11,038	3,409	3,159	250
Gal.16 Jerosu	3,342	3,204	1,604	1,600
Gal.11 B. Jerosu	1,465	1,234	684	550
Gal.15 Jerosu	1,596	713	483	230
Gal.18 Pustiosu	2,424	1,405	945	460

Characteristics of mining and surface water

The discharges of out-flowing mining water are not important, oscillating between 1 and 3 l/s. The chemical analysis results are presented in Table 3; in the same table one can be see the chemical composition of runoff water which collects the out-flowing mining and the waste rock dumps drainage water.

Table 3. Chemical composition of mining and runoff water (maximum values)

Element	Outflowing mining water			Runoff water		
mg/l	Larga Brook	Jerosu Brook	Pustiosu Brook	Larga Valley	Jerosu Valley	Pustiosu Valley
U_{nat}	0.016	0.008	0.009	bdl	0.04	bdl
Th	bdl	bdl	bdl	bdl	bdl	bdl
Cu	0.01	0.04	0.01	0.001	bdl	0.002
Zn	0.03	0.03	0.02	0.01	0.03	0.03
Ni	bdl	0.40	bdl	bdl	bdl	bdl
Sn	bdl	bdl	bdl	bdl	bdl	bdl
Cr	0.02	0.03	0.03	0.03	0.02	0.02
Fe	0.09	4.45	0.06	0.01	0.13	bdl
Co	0.01	0.01	bdl	bdl	0.01	bdl
Pb	bdl	bdl	bdl	bdl	0.018	bdl
pH	6.51	6.87	6.91	6.0/7.0	6.0/7.5	5.5/7.0

* bdl-bellow detection limit

Characteristics of soils and sediment samples

The chemical analysis results of the soil and sediments samples collected in the areas near pollution sources are included in Table 4; they can be compared to the chemical composition of a blank essay which comes out of the influence area of mining wastes, tested for its content in radioactive elements only.

Table 4. Chemical composition of soils and sediments

Element	Larga Valley			Jerosu Valley			Pustiosu Valley		
p.p.m.	max.	min.	blank essay	max.	min.	blank essay	max.	min.	blank essay
$U_{nat.}$	8	4	8	16	3	3	42	7	6
Th	8	-	-	170	7	7	94	5	5
Ra^{226}*	0.1	0.05	0.1	1.063	0.025	0.025	0.525	0.088	0.072
Cu	10	9	-	16	8	-	19	11	-
Pb	7	4	-	22	5	-	14	6	-
Zn	70	56	-	136	70	-	61	52	-
Ni	14	10	-	14	7	-	28	8	-
V	90	75	-	91	65	-	76	63	-
Cr	50	43	-	39	34	-	48	40	-
Cd	1	sld	-	1	0	-	1	sld	-
Co	18	15	-	19	12	-	22	12	-

* Specific activity (Bq/g)

Discussion

Environmental impacts on surface water

The results of chemical analysis demonstrate that the impact of out-flowing mining water and the waste dumps drainage on surface water could be neglected. A single sample from Jerosu Brook, collected at the bottom of a waste rock dump, has an uranium content of 0.04 mg/l. Regarding the heavy metals, their total concentration ranges between 0.06 and 0.20 mg/l; these values are situated bellow acceptable limits indicated for surface water category by Regulation of Ministry of Environment (NTPA 001/2002). All the brooks crossing over the mining areas are flowing down to Gradistea River; the characteristics of the river water flowing down stream the mining area is similar in composition with the water in the spring beside, which is used for consumption in Gradistea de Munte village (Table 5).

According to the obtained data, the surface water cannot represent an environmental hazard due to the following reasons :

- the high chemical stability of the rare earth forming minerals;
- high and permanent water discharge of the waterflow of brooks and rivers.

Table 5. Comparative chemical data between Gradistea River water and spring potable water

Location	Elements(mg/l)										
	U_{nat}	Th	Cu	Pb	Zn	Ni	Sn	Cr	Fe	Co	pH
Gradistea River	bdl	bdl	bdl	bdl	bdl	bdl	bdl	0.03	0.07	0.02	6..32
Gradistea spring	bdl	bdl	bdl	bdl	bdl	bdl	bdl	0.02	bdl	bdl	6..38

* bdl – below the detection limit

Impacts on soil and sediments

In soil and sediments samples radioactive element concentrations ranges between 4 and 42 ppm for U_{nat} and between 5 and 170 ppm for Th; the soil specific activity ranges between 0.10 and 1,063 Bq/g (Table 3). The Romanian National Commission for Nuclear Activities Inspection recommends the use in forestry of soils having the specific activity between 0.20 and 1.00Bq/g (NMR-03/2003).

Heavy metal concentrations do not exceed the reference level to forestry soils indicated by the Ministry of Environment and Forestry (ord. 756/1997).

According to the obtained data, the lands surrounding the derelict mine site can be considered weakly polluted.

External Gamma irradiation impact

The external gamma irradiation level exceeds The Romanian National Commission for Nuclear Activities Inspection and European guideline value of 0,3 μSv/h (NMR-03/2003), but the influence of gamma irradiation do not spread over waste rock dump sites. In order to clarify the influence of gamma irradiation on human health, the exposure risk was calculated using a program offered by World Information Service on Energy-Uranium Project, named Radiation Dose to Risk Converter. The guideline for gamma irradiation dose is 1 mSv/year and it is considered to correspond with an excess risk for cancerous diseases of 0.35% (1 in 286 cases), during a life span of 70 years. Five scenarios were taken into account depending on exposure time and maximum value of external gamma irradiation on dump surface. Only in one case the acceptable risk of 0.35% is exceeded: if a person constantly lives or works above the anomalous area; in fact, this is a hypothesis that is not very likely to be fulfilled due to the remoteness of the perimeter, which is located far away from residential centers. A moderate risk, between 0.35% and 0.80 % could be for workers and shepherds if they spend yearly 2,000 hours for 40 years. There is no way for the tourists and the occasional visitors to face any risk and much less the people living in the villages situated downstream of the confluence of Pustiosu Brook and Gradistea River (Fig.1). Therefore, the residents fear regarding the cancerous diseases is not justified.

Recommendations

The environmental assessment of the mining perimeter Gradistea de Munte proves that human mining intervention has not radically affected the ecologic balance. Therefore, the restoration recommendations will be adapted to the desired end land use in conjunction with the inherent nature and toxicity of the mine site. As known, the designated area will maintain its current use as natural park. In order to increase the natural capital value some remediation measures are required.

The mine subsidence will be avoided by refilling the abandoned galleries with waste rocks derived from the dumps, followed by closuring with dams.

Waste rock dumps require to be stabilized for stopping material slide and for keeping the natural direction of runoff waters which have been modified by mining activities. Subsequently, they will be covered with local soil and vegetation. Covering the piles is expected to mitigate the external gamma irradiation by 20% which is in the benefit of human health improvement.

Neither mining water nor runoff water need any depollution treatment on the account of their low concentration in radioelements and heavy metals; the natural attenuation processes are expected to bring the water quality to background values.

A special attention should be paid to the instruction of the local population concerning the real situation of the radioactivity levels in the area and the prevention measures that should be taken against accidental contaminations.The local inhabi-

tants and the visitors have to be convinced that the site restoration measures will keep safe their health and will allow the unrestricted use of the land surrounding the radioactive sources derived from mining activities.

Conclusions

The natural and cultural patrimony value of G.M.C.N.P. is reduced by the presence of a derelict mining site which was not yet restored. Though the mining activity does not severely modify the ecosystem, the waste rock dumps are in contrast with the landscape, affect the normal flow direction of surface waters and have a low content of radioactive minerals. This last aspect especially worries the local inhabitants and minimizes the interest of the local community to use tourism as an engine for economic sustainable development.

Risk assessment has demonstrated that specific restoration measurements, which do not require a lot of effort, are needed in order to allow the geographical space reorganization and the development of economic ecologic activities.

Nature conservation, tourism and forestry represent the most appropriate options of land use, capable to utilize and in the same time to protect the natural park ecosystem.

Considering the wealth and variety of touristic attractions inside G.M.C.N.P., it is expected that serious problems in finding interested investors for the land, will not be faced.

Aknowlegements

This study was supported by Ministry of Research and Education under the contract CEEX 723/2006.

References

Balteanu,D.,Dunitrascu Monica,Ciupitu D.(2003) Ariile naturale protejate, sc. 1 :1 ,000,000, Editura Academiei Romane,Bucuresti

Barnthouse,L.W.,O'Neill,R.V.,Bartell,S.M.,Suter, GW,II.(1986)Population and ecosystem theory in ecological risk assessment,American Society for Testing and Materials,pp.82-96

Cohrssen,J.,Covello,VT.(1989) Risk analysis:a duide to principles and methods for analyzking health and ecological risks.Washinton,DC:Council on Environmental Quality

Comisia Nationala pentru Controlul Activitatilor Nucleare (2003) MNR-03,Romania

EPA (1993) – U.S. EPA:Federal Guidance Report No.12:External Exposures to Radionuclides in Air;Water and Soil,EPA 402-R-93-081,September 1993

ICRP60 (1991),1990 Recommendations of the International Commission on Radiological Protection,ICRP Publication 60,Oxford

International Atomic Energy Agency,(1997) Environmental Impact Assessment for Uranium Mine,Mill and In Situ Leach Projects,IAEA-TECDOC-979,Vienna

Lazarescu,I.(1983),Protectia mediului inconjurator si industria miniera,Editura Scrisul Romanesc,Craiova,91-165

Mining Sector Environmental Management, Management Procedures Guide (2002), Harworth Mining Consutancy Limited,URS Corporation,Agraro Consult SRL

Niculescu ,GH. (1996) Les principaux caracteres geographiques des Carpates Meridionales et les activites economiques specifiques.In :Niculescu,GH.,Muica,Cristina (ed.) Carpates Meridionales et Stara Planina(Balkan).Etudes Geographiques .C.R.Coll.Roumain-Bulgare,102-109,Bucuresti

WISE (2007)-World Information Service on Energy-Uranium Project- Radiation Dose to Risk Converter,vizat Ianuarie-Februarie 2007,htpp://www.wise-uranium.org/rdcri.html

From remediation to long-term monitoring - The concept of key monitoring points at WISMUT

Elke Kreyßig, Uwe Sporbert and Sven Eulenberger

Wismut GmbH, Jagdschänkenstr. 29, D-09117 Chemnitz, Germany

Abstract. This paper details the approach chosen by Wismut GmbH (remediation of uranium ore mining legacies) to turn the existing remediation related groundwater monitoring network into what might be described as a network of key monitoring points to prepare for long-term monitoring tasks. Concepts and methods as well as procedures are exemplified for a specific site.

Remediation tasks of Wismut GmbH

Wismut GmbH is a federal government owned corporation. Its mission is to remediate the legacies left behind by more than 40 years of intense mining and processing of uranium ores. The area of operation comprises the Free States of Saxony and Thuringia where a total of 1.400 kilometres of open mine workings, 311M m^3 of waste rock material and 160 M m^3 of radioactive sludges had either to be decommissioned, stabilised or put to recultivation. The legacies left behind by uranium ore mining have caused impacts to the environment, that need to be either eliminated by appropriate remediation measures or reduced to acceptable limits. The Wismut environmental remediation project is unique, even by international standards, in the fields of mine reclamation and environmental protection. Following the abrupt cessation of mining operations in 1990,gradual analysis of environmental damages and conception of remediation options were getting under way to meet the remediation challenge. From this time on, a continuously extending monitoring network was established to identify and assess pollutant dispersion into the environment. Major contaminant sources and proposed remedial actions include:

- mines being flooded;
- in situ rehabilitation of mine dumps involving contouring, capping, and vegetating, in some cases relocation;
- in situ stabilisation of tailings ponds (tailings management areas, TMA) by the removal of supernatant water, dewatering, covering, and vegetating;
- clean-up of plant areas.

Successful implementation of these remediation measures required the construction of powerful water treatment plants to collect and treat contaminated water, resulting by the remediation process. It contains the removal of heavy metals and radionuclides and the discharge of effluents to receiving streams. Water treatment residues are immobilised and put into safe disposal.

Hence, rehabilitation turns out to be a very dynamic process calling for permanent change also with regard to the measuring networks required to monitor environmental impacts. The basis requirement of this effort is to record impacts on the subjects of protection, e.g. soil, air, and water, both from individual objects and from remedial measures before, during, and after remediation. As remediation progresses to completion, the focus is gradually shifting to the post-remedial phase.

Chronological Evolution of monitoring networks

Starting in 1990, measuring network was put in place to identify remediation needs. This network evolved into long-term monitoring, using fixed monitoring locations and involving those measurements which are independent of remedial actions and which are performed according to defined methods (basic monitoring). A remediation related monitoring intensifies the basic monitoring temporarily. It results in a more dense object and process related monitoring with the goal to survey the impacts of the remedial process for the environment. Measurement and sampling methods are identical to those used in the basic monitoring scheme. Altogether Wismut established and ran a water monitoring network comprising up to 2,000 measuring stations for groundwater and nearly the same number for surface waters. Their specificity varies a lot among the 7 sites of Wismut GmbH. According to the terminology used in the Water Framework Directive, these are operator's monitoring networks to survey point-shaped contaminant sources.

As remediation advances to completion, there is a need to define a philosophy of post-remedial or long-term monitoring, respectively. Its focus should be on demonstrating that or how, respectively, the initial remediation objectives were met. With regard to the complexity and uniqueness of the remediation effort, development and transfer of the know how for similar rehabilitation projects has been borne in mind. That’s why, for Wismut long-term monitoring is an indispensable tool to collect data and experience to this end.

Therefore, the concept calls strongly for a streamlining of the monitoring locations network with the objective of identifying those monitoring locations, parameters, and frequencies among the current monitoring scheme and the recorded hydrogeological findings, which describe essential contaminant flows at the site with regard to their dispersal dynamics and trend behaviour beyond the termination of the remedial action. The selected monitoring locations are to form what is termed the key monitoring network, onto which all further activities are to be based (e.g. site model, long-term monitoring).

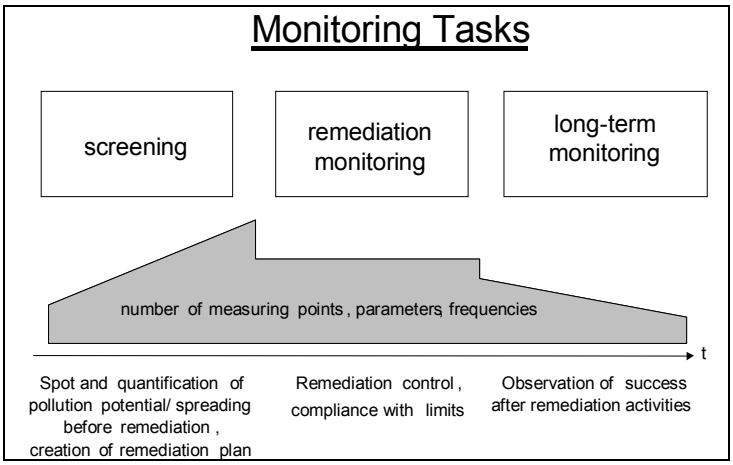

Fig. 1. Configuration of monitoring networks and their tasks over time

Basic concept for the configuration of key monitoring networks

As a rule, German requirements for the configuration of monitoring networks, enshrined in bodies of rules and regulations as well as in guidelines, are restricted to large-scale monitoring networks (of national dimension) and have only limited application to the more region-related issues concerning WISMUT sites (point-shaped contaminant sources). The subsequent boundary conditions were postulated for the design of key monitoring networks at Wismut sites:

1. Key monitoring networks have to ensure the long-term post-remedial surveillance of *basic and spatially significant* impacts on groundwater by objects of Wismut GmbH with regard to continued assessability of dispersal dynamics and trend behaviour. For large-scale objects, direct object relations are recommended, while smaller-scale objects having smaller, sometimes superimposing impacts should be considered as forming a complex.
2. As a rule, key monitoring networks should provide data on upgradient characteristics (local background data), the remaining contaminant source properties (characterisation of contaminant inventory) as well as on downstream characterisation (quantification of contaminant release).
3. As a rule, spatial cut-off criteria should be selected in a way to allow the source relation to the object/complex to be unequivocally established (object-related measuring points). Measuring locations with a population relation (e.g. drinking water supplies) should be integrated wherever impacts on water use are to be considered or have to be precluded in the sense of negative evidence (person related measuring points).

Table 1. Classification according to post remediation contaminant sources with regard to the design of a long-term monitoring system

Post remediation contaminant sources		
Left in place		Removed
Contaminant release is reduced as planned	Contaminant release for a limited period activated	Contaminant release is finished
e.g. mine dumps capped, TMA stabilised in situ	e.g. flooding of mines	mine dump relocation, replacement of contaminated ground at plant sites
Long-term monitoring tasks		
Monitoring of contaminant reduction, assessment of contribution to large-scale environmental impacts	Monitoring of admissible groundwater impact, monitoring of contaminant fade away	Monitoring of contaminant plume of fade away

4. Temporal cut-off criteria primarily result from the sources relaxation behaviour and from their hydrological neighbourhood (table 1).

As a result, the remaining contaminant sources to be monitored have to be bipartited into:

- on-going emissions before and after remediation with planned reduction of contaminant release (e.g. impacts on groundwater by seepage from mine dumps or pore water and seepage downgradient of a TMA stabilised in situ).
- emission sources activated for a limited period of time (e.g. impacts on groundwater by rising flooding water or new erected emission points during remediation intended to merge formerly diffuse releases for controlled discharge).

Minimum monitoring periods are derived from the impact duration of contaminant sources remaining after remediation is completed. Simultaneously, a decision on a limit related or trend related procedure has to be made. As, for the time being, the era of long-term monitoring has dawned only for a limited number of remediation objects of Wismut GmbH there is need for concepts and coordination with all parties concerned with regard to cut-off criteria for the termination of monitoring.

1. Parameters identified as major contaminant parameters during the remediation process (signature of the deposit or of the mining method, respectively) should be selected in the design for the key monitoring network (key or trend parameters). They – along with in situ parameters – are to be designed for each sampling. In addition to this and at a lower frequency, data required for general water quality characterisation should be collected (basic parameters).
2. The frequency of measurements/sampling at key measuring locations is to be adapted with regard to the intensity and dynamics of concentration changes and taking aquifer flow rates into account.

3. Specific measuring tasks shall be identified for the selected locations of the key monitoring network.

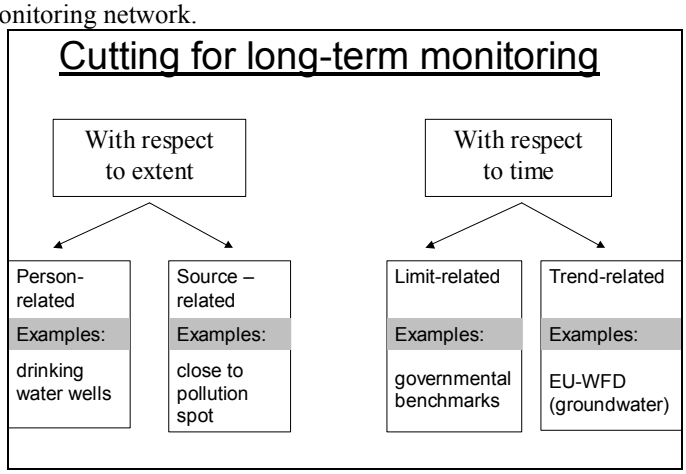

Fig.2. Temporal and spatial cut-off criteria for the operation of a key monitoring network

Procedure for the selection of monitoring locations

Considering the above boundary postulates for the design of key monitoring networks, optimisation of groundwater monitoring networks may be based on the subsequent design planning:

- hydrogeological assessment;
- extended geostatistical methods;
- modelling.

At Wismut the hydrogeological assessment constitutes the basis of all further design specifications. It comprises the interpretation and technical evaluation of any information on the geological characteristics of the area of investigation, of available data on water quality, the structural suitability of monitoring stations, the analysis of critical emission pathways, the determining of redundancies, the application of basic statistical methods as well as the final reduction to key monitoring locations.

Application of these design planning approaches also implies the maintenance of objects or complexes of objects, respectively into which small-scale objects are to be consolidated.

If available, results of contaminant transport modelling will also be consulted to support the configuration of key monitoring networks. The professional evaluation of the geological/hydrogeological and hydrochemical conditions will be performed by in-house site geologists.

Measuring points selection criteria, depicted in figure 3, are also to be taken into consideration with a view to obtaining long-term measurement series providing comparable data with regard to trends.

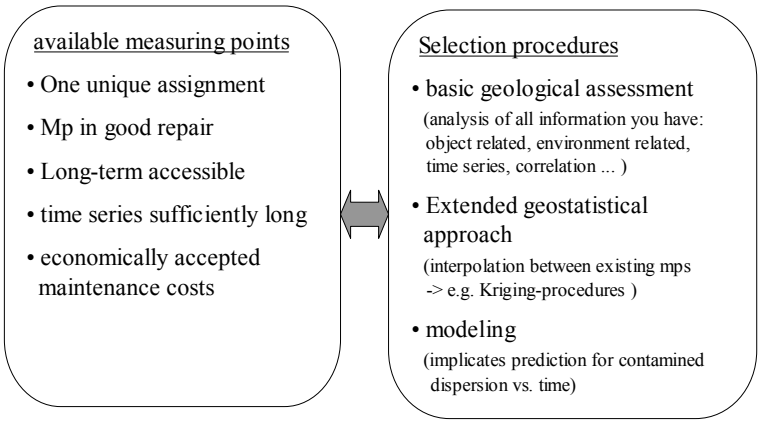

Fig. 3. Selection criteria for measuring points

Design processing involves the following:

a. Interpretation of information on geological and hydrogeological conditions, including data on groundwater quality, characterisation of upgradient groundwater flow and location of relevant groundwater discharges.
b. Analysis of the state of repair of measurement locations identified according to specifications under a).
c. Review of measurement locations selected as suitable according to specifications under b) for potential redundancies. Analysis of redundancies normally involves conventional statistical procedures (evaluation of time series, identification of correlations). In addition to conventional approaches, extended geostatistical methods are also suited to analyse redundancies. This concerns in particular interpolation applications whereby statistically firm estimates are generated for addition to available measurement data.

Combining the requirements specified above, figure 4 illustrates the definition of key measurement points.

A convenient electronic system (ALWIS) available at Wismut allows integration of all relevant data and provides full access to data banks holding chemical and groundwater level data along with mapping functionality as well as geological and design data. Also implemented into the software application are tools for spatial data interpolation.

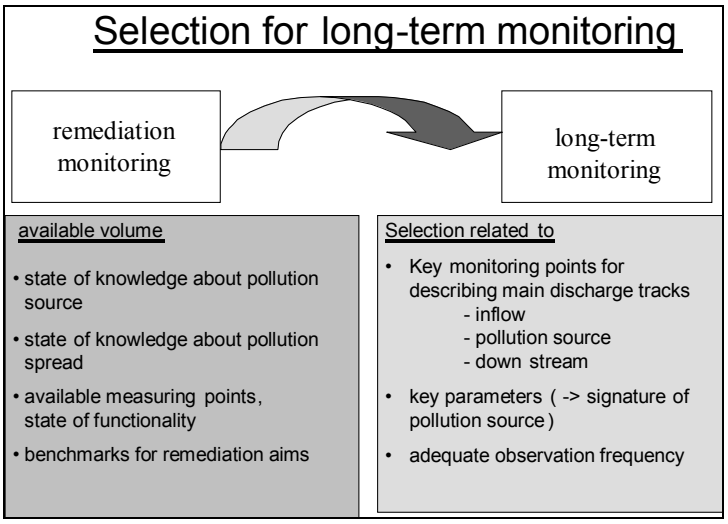

Fig. 4. Selection for long-term monitoring

Configuration of a key monitoring network demonstrated for the Helmsdorf TMA

Configuration of a key monitoring network is exemplified below for the Helmsdorf TMA rehabilitation object at the Crossen site. The Crossen site is located in the outskirts to the north of the township of Zwickau in the Free State of Saxony. Uranium ore processing installations at the site were active until 1989. Apart from the Dänkritz I tailings pond, the Crossen plant area, the Crossen mine waste dump as well as the areas operated by DFA-Logistics and Saxonian ore reserve supply, the Helmsdorf TMA is the most significant remediation object at the site. The TMA was operated from 1958 through 1989. It holds about 50 Mm^3 of tailings and covers a surface of circa 200 ha. Rehabilitation of the Helmsdorf TMA is implemented as dry in situ stabilisation involving removal of supernatant water, contouring of dam areas, and capping of the tailings surface. The main receiving stream of the investigation area is the Zwickauer Mulde river. At the western edge of the rehabilitation area, the main watershed is located by a North-South direction, which divides discharges from TMA roughly to the Eastern part only. Contained by dam structures in the East, North, and West, the tailings body of the Helmsdorf TMA constitutes the source of contaminated seepage discharges. Groundwater discharge from the Helmsdorf TMA is confined to the Eastern edge toward the receiving stream Zwickauer Mulde river. These discharges are in the first place via local fault zones along valley structures running east-north-east to west-south-west (especially Oberrothenbach fault, Wüster Grund fault and Niederhohndorf fault).

During the initial phase of the rehabilitation project the groundwater surveillance network at the Helmsdorf TMA rehabilitation object embraced more than 400 groundwater measuring and monitoring wells. By 2007 the number of monitoring locations attached to the Helmsdorf TMA has shrunk to 222. The remediation progress and the subsequent transition to post-remedial care make further optimisation of the number of monitoring locations imperative. As a consequence, relevant key monitoring locations have to be selected from the existing stock. Selection of key monitoring locations was based on the hydrogeological assessment as described above. Focus area for the key monitoring network at the rehabilitation object Helmsdorf TMA is the surveillance of tectonic faults having relevance as aquifer upstream and downstream of the site as well as of the contaminant source and its immediate geogenic subsoil.

In the future, the upgradient groundwater flow will be monitored by a total of 13 key measuring points located in the area of fault zones to the South, Southwest, and to a lesser degree to the West of the TMA. Surveillance of the contaminant source property embraces monitoring of dam structures, tailings, and the immediate geogenic subsoil at the Helmsdorf TMA site. 46 key measuring locations are attached to this task. This currently relatively elevated number of measuring locations is due to the inclusion of dam stability measuring points and will undergo significant down-scaling in the future.

Downstream flow monitoring focuses on fault zones of relevance to contaminant release located at the Eastern edge of the Helmsdorf TMA. Measuring points have been assigned to major discharge patterns with due regard to their distance to the Helmsdorf TMA. This ensures surveillance of the close-up, transition, and far-away ranges. Some key measuring stations in the downstream groundwater flow field are arrayed as groups of measuring points embracing individual locations

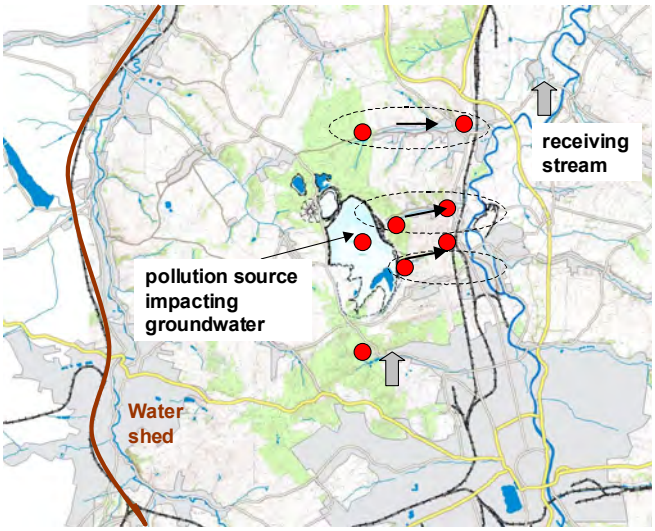

Fig. 5. Example of long-term monitoring for a tailing pond with interactions to groundwater

with varying filter depth intervals. 34 key measuring points were selected for downstream groundwater monitoring. So the key monitoring network at the Helmsdorf TMA embraces a total of 93 groundwater monitoring wells which allow to sufficiently characterise post-remedial impacts to groundwater in the area of the Helmsdorf TMA. Compared to 2007 their number was scaled down by 129 units with further reductions to be expected with regard to dam stability monitoring locations. The number of 93 key monitoring locations is to be achieved by the gradual dismantling of still existing but potentially no longer needed groundwater monitoring wells by the time of transition to the after-care phase. Measuring points and groups of measuring points are assigned to specific monitoring tasks.


Uranium Mining
and Hydrogeology

Official supervision measurements for remediation and monitoring of Wismut GmbH in Saxony

Thomas Heinrich, Antje Abraham and Werner Preuße

Staatliche Umweltbetriebsgesellschaft, Geschäftsbereich Umweltradioaktivität, Altwahnsdorf 12, 01445 Radebeul, Germany

Abstract. Official measurements are carried out in Saxony in order to supervise independently the actions for remediation of former uranium mining sites and the corresponding monitoring programs of Wismut GmbH. The state laboratories for environmental radioactivity (part of the *Staatliche Umweltbetriebsgesellschaft UBG*) are in charge for that supervision in the Free State of Saxony performing official measuring programs and comparisons in order to fulfill the legal demands. This paper gives a short overview of the history and exemplary findings of the official supervision measurements.

Development of the official measuring programs

Following World War II uranium mining resulted in environmental pollution and elevated radiation exposure in the densely populated and industrialized regions of the today's free state of Saxony. According to the German unification treaty the GDR state ordinance on guarantee of nuclear safety and radiation protection (VOAS 1984) remained in force after 1990 and is since then the basis of the monitoring of the former uranium mining and processing sites.

Starting in 1991, by order of the Saxon state ministry for environment and agriculture, the Saxon state laboratories for environmental radioactivity which became part of the *Staatliche Umweltbetriebsgesellschaft* (UBG) in 1993 is in charge for official surveillance of selected points of the monitoring networks which are located in surroundings of the sites of the former uranium mining company Wismut GmbH.

In September 1996 the Saxon state authority for environment and geology (LfUG) obliged the Wismut GmbH by official order to continue the so-called basic monitoring as a long-term monitoring. As independent state laboratory the

UBG is performing the official supervision of the Wismut basic monitoring program by sampling and measuring environmental samples in parallel to those of the Wismut GmbH and a separate monitoring of points where emissions can affect the environment (immission monitoring). The basic monitoring of the Wismut GmbH is supplemented with a monitoring of remedial actions which is defined by permissions of the regulatory authority LfUG and limited in time depending on the remedial action.

With implementation of the directive on emission and immission monitoring regarding mining (REI-Bergbau 1999), the monitoring programs of the Wismut GmbH and of the state authorities were modified in 1999 regarding methodical equivalence and comparability.

The example "exposure pathway water"

In order to supervise the emission monitoring at discharge points of the Wismut GmbH, UBG is performing control measurements of samples of Wismut GmbH as well as independent sampling and measurement comparisons.

Measurement comparisons

Starting in 1997 so-called Stichtagsbeprobungen have been established as an annual intercomparison-like exercise for the specific sample type of mining related water where partly high saline concentration can make high demands to the laboratory. Here, after jointly sampling of Wismut GmbH and UBG, the sample material is homogenized, shared and distributed between the participating laboratories who are routinely measuring natural radionuclides.

A number of analytical methods as gamma-ray spectrometry, alpha-particle spectrometry, liquid scintillation emanation counting, emanation counting in Lucas cells, gross alpha counting of Ba(Ra)SO_4-precipitate, ICP-MS, ICP-OES and kinetic phosphorescence analysis are applied by the participants in order to determine the main parameters uranium and radium-226. A total of up to 12 laboratories of Wismut GmbH, of authorities (also other German federal states and Federal office for radiation protection - BfS), of companies (contractors of Wismut GmbH) and of further institutions are participating in these annual exercises.

Using the findings of the 10 ??? comparisons so far since 1997, the participants can analyze their deviations and improve their analytical methods if necessary. In particular, specific reproducibility standard deviations for the analysis of the main parameters radium-226 and uranium can be derived from these exercises. The resulting reproducibility variation coefficients are used to classify the differences, which show up in parallel measurements between a company under supervision and the supervising laboratory, as being acceptable or not. Fig.1 and Fig.2 show the reproducibility variation coefficients obtained in the comparison exercises since 1997 and those from further intercomparisons.

An important outcome of the continuously repeated comparison exercises and the conclusions drawn by the participating laboratories is the improvement of the quantitative agreement which is reflected by a significant decrease of the reproducibility variation coefficients during the last 10 years showing the success of this kind of external quality assurance.

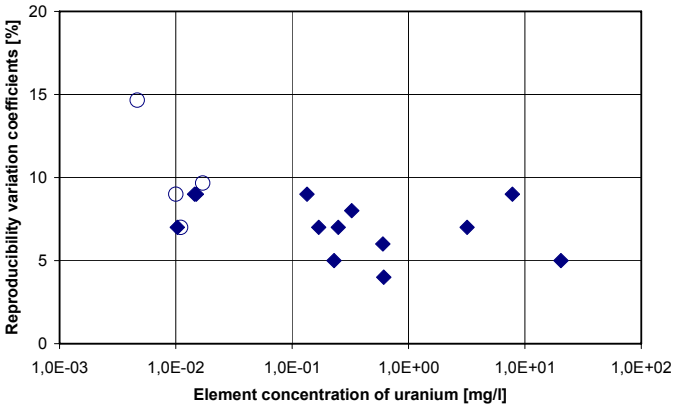

Fig.1. Reproducibility variation coefficient for uranium analysis in water determined from 10 ??? interlaboratory exercises organized by UBG. The additionally included empty symbols stand for data from internal Wismut GmbH comparisons.

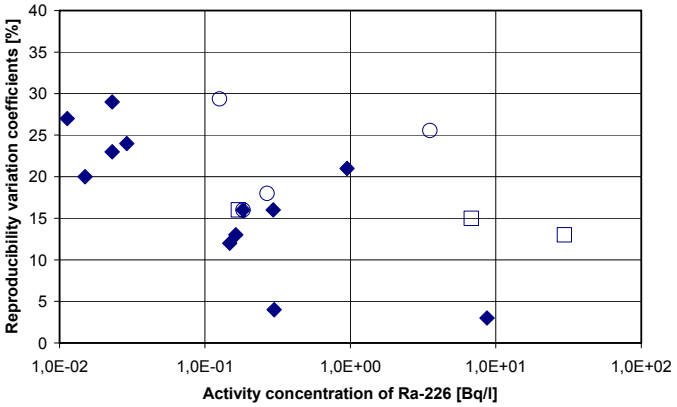

Fig.2. Reproducibility variation coefficients for radium-226 analysis in water determined from 10 ??? interlaboratory exercises organized by UBG. The additionally included empty symbols stand for data from official intercomparisons held by the German Federal office for radiation protection (BfS, see circles) and internal Wismut GmbH comparisons (squares) respectively.

The years until 2003 were characterized by reproducibility variation coefficients in the range of up to 30%. This could be attributed to the use of methods of different applicability for the specific kind of mining water samples which were to be analyzed by the participating laboratories.

Mainly the widely used gross alpha counting of $Ba(Ra)SO_4$-precipitate (DIN38404/18 1994) does not always have sufficient ruggedness against the demands from mining water. The method has originally been described as a standard procedure for the determination of Ra-226 in water where the effect from other alpha particle emitting nuclides is negligible. Water from former uranium mining sites does not always fulfill this condition. The presence of other radium isotopes (Ra-223, Ra-224), which cannot be identified from a gross alpha measurement, result in an overestimation of Ra-226. Co-precipitated long-lived alpha particle emitters are another possible interference if being present in high excess compared to radium in the original sample. Here decontamination factors in the order of 10^3–10^4 for uranium and thorium have to be considered (Goldin 1961).

The other methods for Ra-226 determination focus on the radiation of progenies of Rn-222 in radioactive equilibrium. A high selectivity because of specific mono-energetic gamma-rays or the noble gas properties of radon avoids interferences due to similar chemical or physical properties of other isotopes. In this sense gamma-ray spectrometry is based on the main gamma-ray emitters Bi-214 and Pb-214 while alpha-particle emanation counting uses the alpha-particle emitters Rn-222, Po-218 and Po-214 after appropriate separation of Rn-222.

Using almost exclusively gamma-ray spectrometry or emanation counting for the determination of Ra-226 reproducibility variation coefficients around 10% could be achieved from 2004 on.

Control measurements

Within the scope of the supervising measurement programs of the state laboratory, measurements of aliquots of about 100 water samples per year are performed by UBG in parallel to those of Wismut GmbH in order to evaluate the correctness of the analytical results of the Wismut GmbH.

The reproducibility variation coefficients (uranium: 10%, radium-226: 20% as mean from comparisons over 10 years) from the interlaboratory exercises (see above) are used to assess quantitatively the agreement of the results. Fig.3 (radium-226) and Fig.4 (uranium) show the comparison between the results obtained by UBG and by Wismut GmbH respectively. Except of a few values a high degree of agreement can be concluded from the figures. Outliers are discussed in detail in order to find the cause for such large deviation. In case of frequent and systematic occurrence this reveals systematic errors in the laboratory which were not detected by the internal quality assurance.

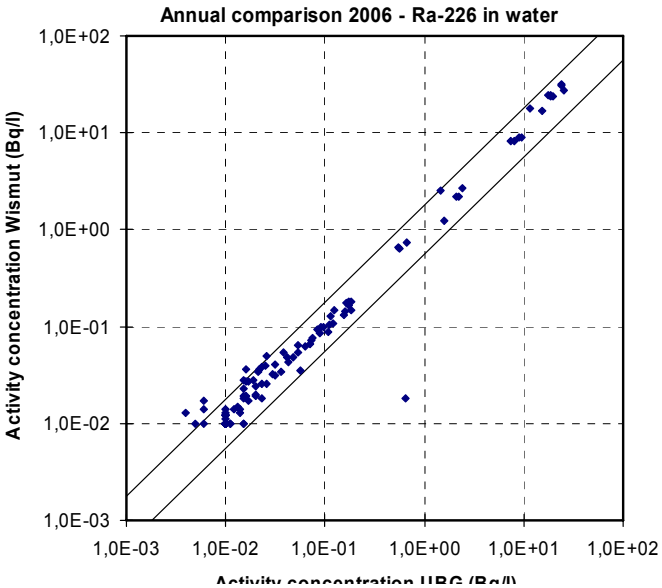

Fig.3. Comparison of aliquot results for radium-226 in water. The straight lines stand for the range of acceptable agreement which results from the reproducibility variation coefficient obtained from interlaboratory exercises. Values outside that range are considered to be not corresponding with a probability of 95%.

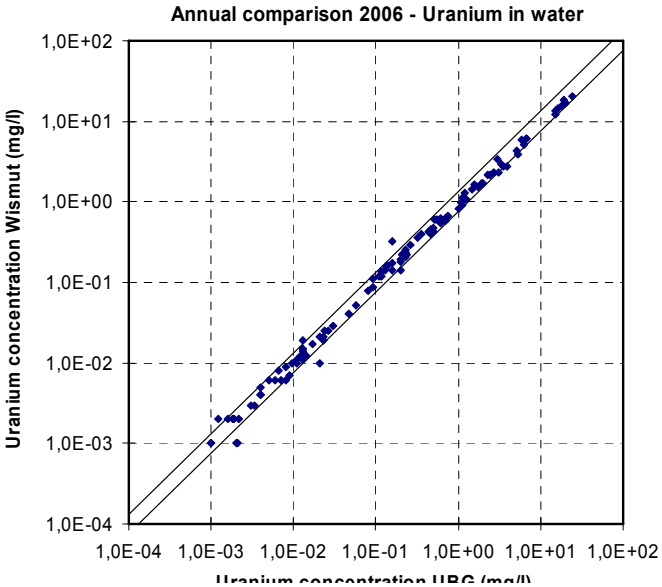

Fig.4. Comparison of aliquot results for uranium in water. The straight lines stand for the range of acceptable agreement which results from the reproducibility variation coefficient obtained from interlaboratory exercises. Values outside that range are considered to be not corresponding with a probability of 95%.

References

VOAS (1984) Verordnung über die Gewährleistung von Atomsicherheit und Strahlenschutz vom 11.10.1984 DDR GBl I Nr. 30, Seiten 348 ff. 21.11.1984

REI-Bergbau (1999) Richtlinie zur Emissions- und Immissionsüberwachung bergbaulicher Tätigkeiten, unveröffentlichte Richtlinie des Bundesministeriums für Umwelt, Naturschutz und Reaktorsicherheit; 1999

DIN 38404/18 (1994) Bestimmung der Radium-226-Aktivitätskonzentration in Trink-, Grund-, Oberflächen- und Abwasser (C18).

Goldin A.S. (1961) Determination of dissolved radium. Anal. Chem. 81, 406–409.

Underground in-situ mine water treatment in a flooded uranium mine at the WISMUT Königstein site - motivation, activities and outlook

Ulf Jenk[1], Kerstin Nindel[1] and Udo Zimmermann[2]

[1]Wismut GmbH, Jagdschaenkenstraße 29, 09117 Chemnitz, Germany, Tel: +49 (0)3718120141, e-mail: u.jenk@wismut.de, k.nindel@wismut.de,
[2]Wismut GmbH, Niederlassung Königstein, Tel: +49(0) 33502152402, e-mail: u.zimmermann@wismut.de

Abstract. At the WISMUT Königstein site, uranium was mined also by acid in-situ leaching in the underground. Since 2001, the mine is flooded. The flooding water (low ph value and relative high Eh values) must be collected and pumped to the surface were it undergoes an expensive water treatment. It is expected that water treatment is needed in a long-term scale. To shorten the period for conventional water treatment alternatives are investigated by WISMUT. The present paper is a continuation of a UMH IV contribution and describes recent results and activities.

Site Characteristics

Within the WISMUT rehabilitation project in Germany the remediation of the Königstein mine near Dresden is a very special case. The mine is situated in an ecologically sensitive and densely populated area (Fig.1). From the early sixties through 1990, approximately 19,000 t of uranium were produced.

Fig.1. View of the Königstein mine site.

The ore body is located in the 4th sandstone aquifer, the deepest of four hydraulically isolated aquifers in a Cretaceous basin. The 3rd aquifer is an important water reservoir for the Dresden region and is environmentally and economically very sensitive.

The uranium was extracted from the 4th sandstone aquifer initially using conventional mining methods, but later an underground block leaching method using sulphuric acid (2 to 3 g/l H_2SO_4) was implemented. Especially due to the reactions of the oxidizing sulphuric acid, the geochemical nature of the deposit was substantially changed, with a high level of pollution remaining within the deposit, mainly sulphate, heavy metals and naturally occurring radionuclides. Remaining pore water in the sandstone water is characterized by pH 2.0, EC 700 mV, 10 g/l SO_4^{2-}, 2 - 3 mg/l Fe, 200 mg/l Zn, 200 mg/l U and 300 mg/l Al.

Considering the existing pollution potential and the importance of the overlying aquifer a concept of controlled flooding was developed. The major element of this approach is a control drift system which allows collection of draining flooding water down-gradient of the deepest part of the mine. The flooding water collected in this control drift system is treated and discharged to the Elbe river (Fig. 2).

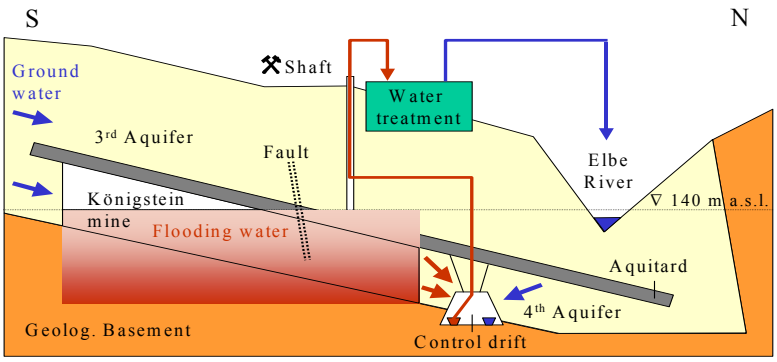

Fig.2. Schematic cross section of the Königstein uranium mine and principle of the current flooding status.

The concentrations of hazardous substances in the water due to natural attenuation by dilution and wash-out are only slowly declining. The flooding water must therefore be drained, collected and pumped to the surface were it undergoes sophisticated and expensive water treatment. WISMUT expects that water treatment will be needed over a long-term period.

Efforts to Support the Flooding Process

To shorten the period for conventional water treatment and to comply with obligations of flooding permissions alternatives are investigated by WISMUT. In the focus are measures to minimize the release of contaminants into the water in-situ, i.e. to immobilize radionuclides and heavy metals locally at the site were they are currently released from their source.

Measures inside the mine workings

Considering the specific geotechnical and technological conditions of the mine, a new technology to reduce contaminant potential in the source (leaching blocks) was developed. The application based on the injection of supersaturated BaSO4-solutions to precipitate dissolved contaminants and to cover reactive mineral surfaces. This immobilization technology (direct source immobilization) has been applied in the southern part of the mine as part of the closure plan. From 2002 to 2005 about 1.6 million m3 of sandstone have been treated successfully in the southern part of the mine with about 325,000 m3 solution (Jenk et al. 2006).

Current activities

At the present time the mine is partially flooded and flooding up to 140 m above see level is permitted and in preparation. Access to the mine is strongly restricted and only possible in the control drift system in the northern part. Finally, the mine will be flooded completely.

Regarding current predictions and concepts water treatment is planned to continue for a period of at least 10 years (pump by special boreholes connected to the control drift system). Due to pumping and natural water inflow into the flooded mine (4^{th} aquifer) a convection will develop in the flooding water body from south to north. During this time period it is possible to influence the flooding water body from the surface by injection using boreholes.

Basically, an influence of the hydrochemical conditions must have a lasting effect to restore 'close-to-pre-mining' conditions to the extent feasible. This requires that in the flooding water the redox potential must be lowered, and the pH value must be raised. As a consequence, it is expected that dissolved radionuclides and heavy metals will be fixed inside the mine and reduced in the flooding water.

In the light of results obtained from laboratory work done so far, two promising approaches are being developed further:

A) Chemical approach: Injection of substances with the capacity to reduce redox potential and raise pH

The goal of the approach consists in immobilising contaminants at their source. R&D done (at laboratory level) during the flooding preparation phase have demonstrated that contaminant precipitation may be induced by the addition of sodium sulphite to the flooding water.

Transfer of these findings to potential application in the flooded mine requires, as a next step, the validation of the observed effects in a scaled-up pilot test. Based on laboratory test data, a pertinent test concept was developed and a pilot plant was conceived in cooperation with WISUTEC.

At the end of 2006, the pilot plant housed in a container with a reactor volume of 1.3 m^3 was put in place at the Königstein site. About 10 m in length, the reactor is filled with rock species that are typical of the site and with flooding water to imitate the mine at a reduced scale (Fig. 3).

A first pilot test on the effect of sodium sulphite was run from March 2007 to February 2008. The Brandenburg University of Technology (BTU Cottbus) contributes to the scientific analysis of the results.

Fig.3. Investigation container with reactor on site at the Königstein mine site.

Assessments performed so far, largely confirm laboratory test results. Added doses of sodium sulphite react primarily by reducing the redox potential. In agreement with the computation results, pH was raised to ca. 4. Such pH rise is sufficient to precipitate iron and aluminium hydroxides. Mobilised heavy metals and trace elements deceleratedly migrate through the filter and are partly fixed.

Following an initial assessment of the first test stage, an increase of the possible buffer potential by the addition of sodium hydroxide is being investigated. Starting in April 2008, a second test to this end is run with a combined injection solution (sodium sulphite – sodium hydroxide).

B) Chemico-microbiological approach: Stimulation of autochthonous sulphate-reducing micro-organisms

Funded by the Federal Ministry of Education and Research, the 3-year joint project was initiated in July 2006 and is implemented in conjunction with our research partner Groundwater Research Institute Dresden (GFI Dresden). The project is supervised by a project advisory board of representatives of the scientific community and authorities of Saxony.

The approach also aims at immobilising contaminants at their source. The addition of propagable elementary iron is intended to generate a reduction zone within the flooded mine and to stimulate the metabolism of autochthonous sulphate-reducing bacteria. This is to be used to get mineralisation processes going and cause the immobilisation of contaminants onto the mineral phases generated.

Studies on forms of contaminant binding in rock and iron hydroxide sludges in the mine revealed that besides oxidised contaminant species occurring incorporated into iron (hydr)oxides and in spite of oxidation there is a considerable portion of contaminants occurring in reduced form. Analysis of the microbial inventory of the mine has uncovered an elevated microbial diversity in the solid samples and the presence of sulphate-reducing bacteria. In batch tests, the metabolism of autochthonous sulphate-reducer was stimulated by the addition of iron powder and H_2/CO_2. This led to the formation of sulphides and the removal of dissolved contaminants from the aqueous phase. Mobilisation of contaminants by the reductive solution of iron hydroxide sludges was not observed (Kassahun et al. 2007).

Feasibility of target processes was demonstrated. Vital to these processes, sulphate-reducing micro-organisms were documented also in repeated sampling of mine rock and sludge (various substances from underground). Pelletised, iron-containing foam glasses were developed to serve as reactive materials. They also have a pH buffering effect. These materials are presently being optimised and tested for their suitability for being placed in the flooded mine.

Larger-scale pilot plant tests on process development and field test preparation are scheduled for 2008. To this end, a second investigation container will be put in place at the Königstein site.

Under most favourable conditions a reduction zone will be established in the mine. The changed water milieu will then ensure permanently that mobilization of contaminants becomes minimized.

As a next step it is planned to test the feasibility of the approaches under field conditions, i.e. in a very local part of the mine the milieu conditions will be biased towards pre-mining conditions. Final target of the investigations is the development of a large-scale technology for the in situ treatment of the flooding water in the Königstein mine.

References

Jenk U, Zimmermann, U, Ziegenbalg G, (2006) The use of $BaSO_4$ supersaturated solutions for in-situ immobilization of heavy metals in the abandoned Wismut GmbH uranium mine at Königstein, Uranium in the Environment, Springer, 2006

Kassahun A, Hoffmann M, Jenk, U (2007) Voruntersuchungen zur Etablierung einer Reduktionszone in der gefluteten Urangrube Königstein, Proceedings des Internationalen Bergbausymposiums WISMUT 2007, Wismut GmbH 2007

Acknowledgement

Parts of this research have been carried out in co-operation with BTU Cottbus, Germany and GFI Dresden, Germany and are encouraged by the Federal Ministry of Education and Research (FKZ 02WN0755).

Remediation effects of the WISMUT project to surface waters in the Elbe watershed: An overview

Michael Paul, Elke Kreyßig, Jürgen Meyer and Uwe Sporbert

WISMUT GmbH, Development Engineering & Monitoring Division,
Jagdschänkenstr. 29, 09117 Chemnitz

Abstract. The closure of the former East German uranium industry performed under the WISMUT project since 1990 caused, besides other remediation effects, a significant amendment of the water quality of the surface waters downstream the remediation sites, exclusively located in the Elbe watershed. The paper presents the development from the emission point of view and discusses the evolution of the water quality in selected receiving streams, focusing on the Weiße Elster and Zwickauer Mulde catchments.

Introduction

Since 1991 WISMUT GmbH is carrying out the closure of the former East German uranium mining industry. The WISMUT project comprises the full scope of environmental remediation, including the closure of five underground mines at Ronneburg, Schlema, Königstein, Pöhla, and Dresden-Gittersee, the stabiliation of tailings ponds at Seelingstädt and Crossen, the remediation of numerous waste rock piles, the demolition of contaminated facilities, and finally area clean-up. By the end of 2007 about 85 % of the remediation works have been realized, active remediation is expected to be completed by 2015. A recent review of the results of the WISMUT project has been presented elsewhere (Leupold and Paul, 2007).

In order to handle mine waters as well as contaminated seepage and surface waters, at each of the seven individual WISMUT sites a water treatment plant is being operated. As a major outcome of the remediation activities conducted over an 18 years period the impact of the mining legacies to ground and surface waters has been substantially minimized. Until now this aspect of the WISMUT project has not yet been reviewed in a comprehensive manner. Therefore, this paper presents an overview on the remediation effects of the WISMUT project to water resources, describing the recent status, but also comparing it with the initial condi-

tions at the end of production in 1990. The discussion will be focused on the impact on surface water resources, as larger scale impacts are possible for surface waters only. Groundwater contamination, on the other hand, is typically restricted to the very local scale at the former production sites, due to hydrogeological controls which prevent contaminant transport in groundwater on a larger scale, but also due to remaining groundwater depression cones still existing at most of the former mine sites where mine flooding has not completed yet.

Hydrological setting

All former WISMUT production sites are located in the Elbe watershed (Fig. 1). Water-borne emissions are influencing the Elbe river either directly (Königstein) or indirectly via the Weiße Elster catchment (Seelingstädt, Ronneburg) or the Zwickauer Mulde watershed (Pöhla, Schlema, Crossen). The former Gittersee mine is currently dewatered to a small tributary of the Elbe river (Kaitzbach). After completion of a dewatering tunnel which is recently under construction, the Gittersee mine waters will be finally discharged to the Elbe directly.

All sites are humid, revealing a positive water balance. The mean annual precipitation ranges from about 625 mm at Ronneburg to 1027 mm at Pöhla (uncorrected values, time series 1971-2000).

Monitoring approach

As an integral part of the remedial action the environmental impact to ground and surface waters is monitored in order to provide evidence of compliance with the

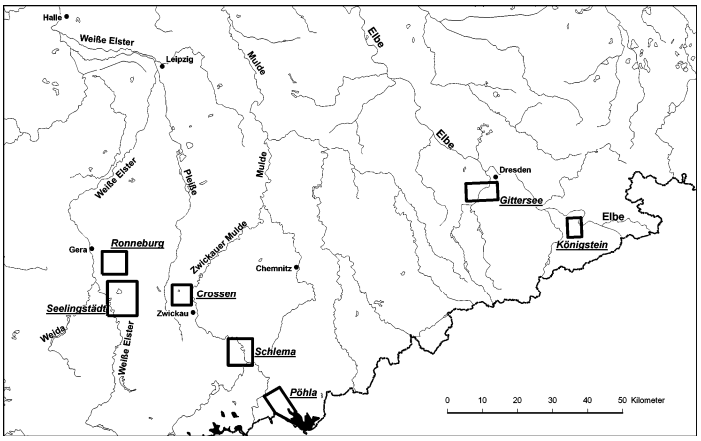

Fig. 1. Location of the WISMUT sites in the Elbe watershed.

existing permits, but also to gain information about the effects of the remediation works to the pollution situation in ground and surface waters downstream. In order to achieve this goal WISMUT is operating specific networks of monitoring stations in all relevant surface water courses, as well as several hundreds of groundwater wells to monitor ground water flow and contaminant transport. As an example, in the Weiße Elster catchment area recently some 50 surface water measuring points are operated for immission monitoring, thereof eight automatic stations, detecting Q, T, pH, EC and O_2 continuously.

The results of these monitoring programs are reported to the regulating authorities on a regular basis. Although the environmental impact of the legacy of uranium mining and milling is by far not restricted to radiation, special attention is dedicated to the supervision of the radioactive emissions into the environment; the results of the surveillance of such radioactive emissions are reported annually. Accordingly, the paper will concentrate on the water-borne radioactive emissions, especially on uranium. However, emissions of heavy metals, arsenic and salinity which are also typical contaminants of concern at several sites, will be additionally discussed where relevant.

Surface water sampling frequency is quite variable at the various monitoring points, according to flow rate, total contaminant concentration and the variability of the relevant parameters. While the most important emission points are monitored on a daily or, monitoring stations with a lower importance are being operated with a monthly sampling frequency. Flow rate detection, however, is continuously at the emission points used for load calculation, flow data for the 1st order receiving waters (Elbe, Zwickauer Mulde, Weiße Elster) are obtained from official measuring gauges run by the Federal states of Thuringia and Saxony.

Radionuclides and heavy metals were measured in surface waters from unstrained acidified sample aliquots (called 'original') unless otherwise noted. For the Thuringian sites (Ronneburg and Seelingstädt) in 2007 the analysis of heavy metals was changed to the dissolved phase according to a request of the authorities. Analyses were executed in WISMUT's accredited in-house lab with varying detection limits. For the key parameter uranium the detection limit is 1 µg/L using kinetic phosphorescence analysis.

Monitoring of the transport of radionuclides and heavy metals bound to suspended matter (SPM) was initiated in the course of the commissioning of new water treatment facilities, using sediment traps at 18 stations located upstream and downstream of the emission sources (6 in the Zwickauer Mulde catchment, 12 in the Weiße Elster watershed), based on a monthly sampling frequency. SPM heavy metal concentrations reported below refer to the <63 µm fraction of the sediment samples which were separated by wet sieving and digested in aqua regia.

Emissions into surface watersheds

In terms of a classification of the water-borne emissions a clear distinction has to be made between (a) Controlled discharge from hydraulic structures or water

treatment plants, which are collected and monitored for volume and quality, and (b) Diffuse leakage of seepage waters, generated from waste rock dumps, tailings ponds and contaminated areas, which remains uncollected and must be evaluated by immission monitoring and modeling (Schmidt and Lindner, 2005). In 2007 WISMUT was operating 39 discharge points for water-borne emissions (controlled discharges), thereof 11 based on a radiation protection permit. The most important discharge points are those of the seven water treatment plants (Table 1).

The amount of mine, seepage and surface waters discharged into the surface water catchments downstream the former mining and milling areas and their inherent contaminant loads is a very meaningful tool to judge the impact situation at the different sites, but also within entire catchment areas, or for WISMUT as a whole. In 1989, the last year of regular production, WISMUT's total annual discharges amounted to 32.5 Mm^3 of water, containing 27.5 t of U. By 2007 these controlled emissions decreased to 16.5 Mm^3 of water, carrying 2.4 t U. Accordingly, closure and remediation activities led to a decrease in uranium loads by more than 90 %. Over the same time period the Radium-226 discharge decreased even more dramatically, from 23.4 GBq in 1989 to 0.3 GBq in 2007. A graph documenting this development for WISMUT's total radioactive discharges has been presented by Schmidt and Lindner (2005) for the time series 1989/2004; the further development until 2007 did not exhibit any significant change compared to 2004.

This load reduction for uranium and radium is a result of a multitude of remediation activities, which are, however, dominated by the following:

- **Cessation of uranium production** at the end of 1990, which resulted in the stop of the discharge of process waters, especially at the two large uranium mills at Seelingstädt and Crossen.
- **Reduction of mine water discharge from the underground mines** as a result of mine flooding. Fully fledged flooding was initiated as follows: 1991 at Schlema-Alberoda, 1992 at Pöhla, 1995 at Dresden-Gittersee, and 1997/2000 at Ronneburg (southern and northern mine fields). During the flood water rise, which happened at these four mines initially in an uncontrolled manner, the discharge of mine water was stopped completely, dramatically improving the surface water quality downstream. Flooding of the Königstein mine, which was started in 2001, was realized in a controlled way from the beginning, as a consequence of the special site conditions at this huge underground leach mine (cf. Jenk et al. 2008).
- **Construction and operation of state-of-the-art water treatment plants.** To sustainably manage and treat contaminated mine and seepage waters the construction of modern water treatment plants was a crucial element of the remediation program (see Table 1). The first water treatment plant constructed after 1990 was the facility at Helmsdorf which was commissioned in 1995. Mine water treatment plants went in operation, according to the status of flood water rise, from 1995 (Pöhla) to 2006 (Ronneburg). Most facilities are currently being operated as lime precipitation plants, with capacities ranging from 100 m^3/h at Gittersee to 1150 m^3/h at Schlema-Alberoda. The passive treatment facility at Pöhla, a constructed wetland with a maximum throughput of 20 m^3/h, replaced

a conventional treatment plant laid out for 80 m^3/h since 2005. Annual water treatment at WISMUT's mine sites amounts to more than 10 million m^3 (2004) with costs on the order of Euro 15 million.

- **Area clean-up, waste rock pile and tailings pond remediation.** Especially at Ronneburg, Aue, Seelingstädt, and Crossen contaminated seepage and tailings pore waters were diffusely impacting the receiving streams. The removal of supernatant water from the tailings management facilities, waste rock relocation, cover construction on waste rock dumps and tailings dams to minimize infiltration in combination with re-vegetation, and the expansion of water collection facilities were measures to diminish adverse effects to ground and surface waters located downstream.

Fig. 2 illustrates the 1989 to 2007 time series for the discharged water volumes and uranium loads, respectively, for each of the seven WISMUT sites individually. It becomes obvious that the development of discharges is clearly dependent on the progress of the remediation activities, but also from the hydrological conditions, directly affecting the water volumes discharged (e.g. dry periods in the early and late 1990s, wet periods 1995/1996, in 2002 and 2007). At Ronneburg the discharged volumes decreased sharply in 1998 as a result of the start of mine flooding. At the Schlema-Alberoda site uranium loads also decreased significantly in the course of mine flooding since 1991, interrupted by a peak in 1996/1997 as a result of mine water discharge necessary to prevent acute risks for the ongoing closure works in the underground mine. The graphs for Seelingstädt and Crossen are more steady, related to the ongoing progress according to the 'dry remediation approach'. The Königstein uranium discharge dropped dramatically since 2001 due to the commissioning of a modern HDS lime precipitation plant.

Table 1. WISMUT's water treatment plants, status 2007.

Site	Type of feed water	Max. capacity [m^3/h]	Commissioning	Uranium in feed water (2007)	Uranium discharge limit	Uranium discharge 2007 annual average	Uranium load, permitted	Uranium load 2007 discharge
				[mg/L]	[mg/L]	[mg/L]	[kg/a]	[kg/a]
Schlema	M	1150	1999/ 2001[b]	2.6	0.5[c]	0.14	5300	831
Königstein	M	650	2001	13	0.5[c]/0.3[d]	0.019	1708	78
Gittersee [a]	M	100	1997	0.08	-	0.08	-	-
Ronneburg	M,U	500	2006	0.2	0.3[c]/0.1[d]	0.052	547	239
Helmsdorf	S	250	1995	6.0	0.5[c]	0.14	950	164
Seelingstädt	S	300	2001	1.3	0.5[c]/0.3[d]	0.082	788	174
Pöhla [e]	M	20	2005	0.02	0.2[c]	0.02	35	2

M=Mine water, U=Surface water, S=Supernatant and seepage water, a Treatment of the Gittersee mine water does not account for uranium, b Water treatment plant units 1 and 2, respectively, c maximum concentration, d annual average concentration, e constructed wetland, which replaced a conventional treatment plant operated from 1995-2004, facility is operated for the removal of As, Fe, and Ra-226

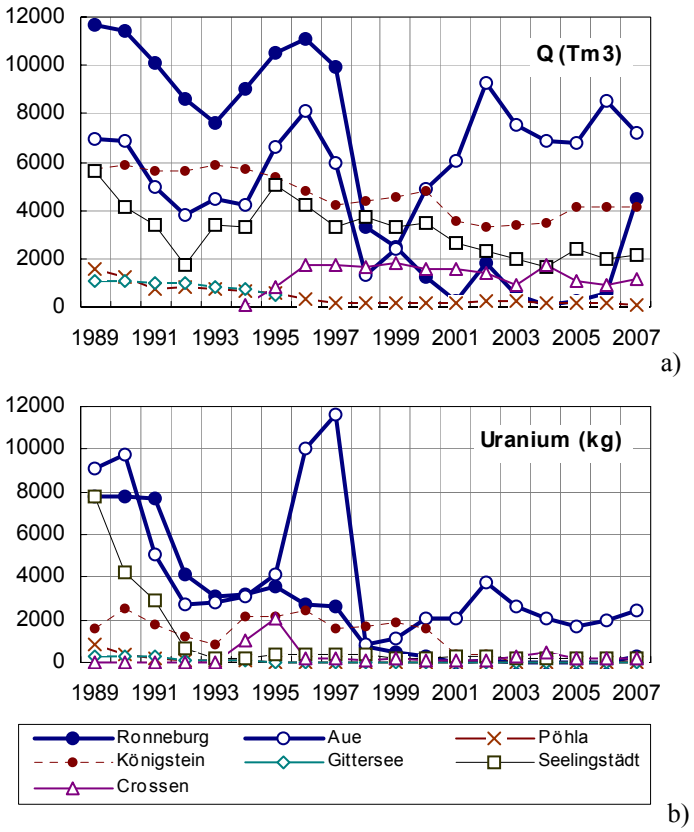

Fig. 2.. Annual water-borne discharges per remediation site, 1989-2007. a) Water volume, b) uranium loads

Table 2. Uranium discharges by watershed, selected years from the 1989-2007 time series

	Weiße Elster with Pleiße [kg/a]	Zwickauer Mulde [kg/a]	Elbe [kg/a]
1989	15,620	10,030	1,840
1990	12,008	10,130	2,730
1993	3,296	2,847	960
1997	2,929	11,820	1,586
2000	403	2,175	1,553
2003	221	2,873	33
2006	217	2,142	46
2007	413	2,637	78

Table 2 summarizes the uranium loads discharged by watershed for selected years of the 1989/2007 time series. The biggest remediation effect can be demonstrated for the Weiße Elster/ Pleiße system, where the uranium loads decreased from 15.6 t in 1989 down to 0.4 t in 2007. Compared to that the emissions into the Zwickauer Mulde watershed remained on a higher level, with annual loads between 2 and 3 t dominated by the Schlema site.

Impact on receiving streams

Water-borne impacts from the WISMUT mining and milling sites were most severe for smaller tributaries, but also detectable at the 1st order receiving waters of Elbe, Zwickauer Mulde and Weiße Elster, although to a different degree. Recently, the direct impact to the Elbe river due to emissions from Königstein/Gittersee is on a very low level, mainly due to the river's high flow rates ($MQ_{1976\text{-}2000}$ at Schöna 312 m^3/s), but also caused by the efficiency of water treatment at Königstein and the relative insignificance of the emissions from Dresden-Gittersee. So, even downstream Königstein no significant WISMUT-impact is detectable with recent uranium concentrations of <1 µg/L.

In contrast to that, WISMUT-borne emissions are still persistent both in the Zwickauer Mulde with a focus on uranium and arsenic (Schneider and Reincke, 2005), and in the Weiße Elster, here mostly concerning uranium, sulfate and hardness.

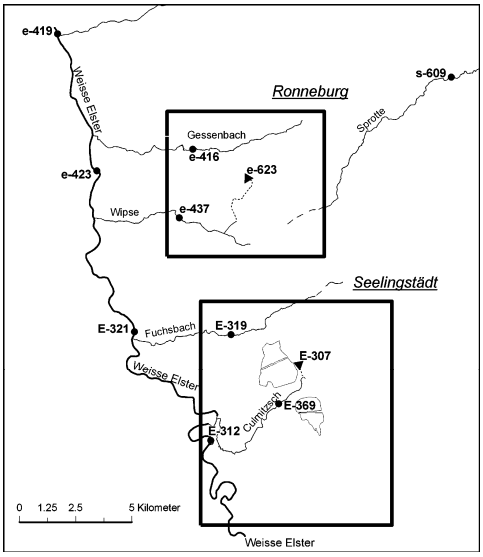

Fig. 3. Important emission points and monitoring stations at the Ronneburg and Seelingstädt sites in the Weiße Elster watershed. E-307 Discharge point of the Seelingstädt Water Treatment Plant, e-623 Discharge point of the Seelingstädt Water Treatment Plant

Weiße Elster watershed

The impact to the Weiße Elster river caused by WISMUT is primarily related to the river's middle reaches, between the towns of Berga and Gera (see Fig. 3). The rivers average flow rate in the area of concern can be characterized by the station at Gera-Langenberg located close to monitoring station e-419 (see Fig.3), which is 15.4 m^3/s ($MQ_{1956-2000}$).

Emissions from the former production sites at Seelingstädt and Ronneburg are drained by four small creeks tributary to the Weiße Elster river: Culmitzsch, Fuchsbach, Wipse and Gessenbach (see Fig. 3). At the Ronneburg site a smaller part of the mine waters was formerly discharged to the Sprotte system, which is tributary to the Pleiße river, reaching the Weiße Elster far downstream in the urban area of Leipzig (Fig. 1). The water-borne mass transport from the Ronneburg mine field which will be discussed below in more detail is entirely captured by three monitoring stations: e-437 with a catchment area A_E of 12.3 km^2, e-416 (A_E = 18.9 km^2), s-609 (A_E = 118.3 km^2).

Table 3 summarizes water quality data for four main monitoring stations along the Weiße Elster river: E-312 (upstream Seelingstädt), E-321 (downstream Seelingstädt), e-423 (downstream Wipse confluence), and e-419 (downstream the entire WISMUT area). The data demonstrate, that the water quality of the river has improved significantly since 1990 at any of the stations impacted by WISMUT. Uranium concentrations dropped considerably, the concentration increase for uranium between E-312 and e-419 has shrunk to 3 µg/L. Sulfate and hardness, which

Table 3. Indicative surface water quality data for monitoring stations at the Weiße Elster River, time series 1990-2007, Median values. SO_4 in mg/L, hardness (H) in °dH, U and heavy metals in µg/L.

	E-312 (upstream Seelingstädt site)							E-321 (downstream Seelingstädt site)						
Year	SO_4	H	U	Ni	Cu	Zn	As	SO_4	H	U	Ni	Cu	Zn	As
1991	125	8.9	nd	nd	nd	nd	<8	385	13.2	nd	nd	nd	nd	nd
1993	115	9.2	<50	91	68	117	<8	316	14.6	<50	20	76	94	<8
1997	100	9.5	3	nd	nd	nd	1	174	12.2	16	nd	nd	nd	2
2000	91	8.9	2	5.5	<5	53	2	190	12.4	8	<5	<5	68	3
2003	140	9.6	3	<5	<5	15	1.4	170	12.2	8	<5	<5	16	<1
2006	104	8.0	2	<5	<5	17	<1	151	10.3	7	<5	<5	<10	<1
2007	81	7.3	1	<5	<5	<10	<1	116	9.4	5	<5	<5	<10	1.4

	e-423 (downstream Wipse creek)							e-419 (downstream Ronneburg site)						
Year	SO_4	H	U	Ni	Cu	Zn	As	SO_4	H	U	Ni	Cu	Zn	As
1990	333	17.2	320[b]	nd	nd	nd	nd	365	18.5	320[a,b]	nd	nd	nd	nd
1993	243	15.6	10	26	15	318	nd	252	18.8	300[b]	39	15	457	nd
1997	210	15.2	13	20	nd	110	nd	250	17.1	15	23	nd	68	nd
2000	164	11.7	4	24	<5	53	nd	112	11.9	5	11	<5	57	nd
2003	169	12.9	6.5	<5	<5	30	nd	239	16.3	8	<5	<5	30	nd
2006	157	11.0	2.5	6	<5	17	1.1	179	11.8	4	<5	<5	23	1
2007	134	10.6	4	<5	<5	12	1.6	137	11.5	4	<20	<20	14	1

[a] value for 1992; [b] U determined with ICP-OES

are limited at e-423 (450 mg/L, 19°dH), have dropped by 2007 to about 40-60 % of the 1990 values.

Compared to that, the results of the SPM investigations documented in Table 4 do not reveal a very clear overall trend for all monitoring stations since the start of the investigations in 2001/02. In the Weiße Elster river the values at the upstream station E-312 are more or less constant, with a certain variation for uranium. This is in general agreement with the findings of Czegka et al (2005). Concentrations for Cu, Ni, Zn, and Cd at the downstream station e-419 show a clear decline, whereas U and As contents do not. Quality standards according to the ThürWRRLVO (2004) for As (40 mg/kg), Cu (160 mg/kg) and Zn (800 mg/kg) which have been defined as a measure for the 'Good ecological status' according to the EC Water Framework Directive (EC-WFD), are recently met in the Weiße Elster river. Recent sediment data for s-609 (Sprotte) confirm a very low contamination level for all elements measured, uranium concentrations in the sediment are close to geogenic background, which is between 3-4 µg/L in the Weiße Elster and Pleiße watersheds (Czegka et al. 2005).

Although the comparison of the uranium concentrations between E-312 and e-419 does not provide evidence of a significant enrichment trend within the WISMUT area, the SPM data for e-437 (Wipse) and e-416 (Gessenbach) demonstrate that both creeks are still significant uranium and heavy metal carriers. However, both creeks are recently revealing a clear uranium decline, the Gessenbach as a result of the waste rock relocation and area clean-up in its catchment, the Wipse mainly due to the continuous discharge of treated mine water from the Ronneburg water treatment plant since late 2006.

To further demonstrate the tremendous improvement of the water quality of the receiving waters of the Ronneburg mine field since 1990, the uranium concentrations in the surface waters of Gessenbach, Wipse and Sprotte are summarized in

Table 4. Uranium and heavy metal concentration bound to suspended matter (SPM) in the Weiße Elster River and its tributaries dewatering the Ronneburg mine site. Time series 2002-2007, Annual mean values based on monthly sampling, fraction < 63 µm, in mg/kg.

	E-312 (upstream Seelingstädt)						e-419 (downstream Ronneburg)					
Year	U	As	Cu	Ni	Zn	Cd	U	As	Cu	Ni	Zn	Cd
2002 [a]	11	27	85	94	782	3.1	15	22	101	92	1277	4.6
2003	25	29	99	89	788	3.6	31	24	104	90	1276	4.5
2004	13	22	107	90	791	3.0	15	29	117	94	1250	4.4
2005	11	22	100	89	887	nd	8.4	21	95	85	1059	nd
2006	18	18	74	74	551	nd	10	19	76	68	802	nd
2007	27	20	79	70	688	2.4	65	27	68	59	463	1.3

	e-437 (Wipse)						e-416 (Gessenbach)				s-609 (Sprotte)							
Year	U	As	Cu	Ni	Zn	Cd	U	As	Cu	Ni	Zn	Cd	U	As	Cu	Ni	Zn	Cd
2002[a]	120	92	985	211	406	2.6	68	19	582	364	1329	7.4	4.5	15	29	49	176	0.5
2003	99	239	621	246	467	2.8	72	28	434	347	1135	5.9	4.0	17	35	42	194	0.5
2004	214	600	1401	216	595	2.9	163	40	1036	411	1376	8.6	3.3	19	40	44	230	0.9
2005	173	420	1133	278	673	nd	70	47	620	321	801	nd	2.8	19	32	41	186	nd
2006	81	224	589	213	425	nd	55	41	302	202	487	nd	3.6	17	31	39	178	nd
2007	85	51	337	136	285	1.8	42	24	161	84	279	1.7	5.6	17	34	38	278	1.0

[a] September 2001-August 2002

Fig. 4 for the time period between 1990 and 2007. At the end of production in 1990 Wipse and Sprotte were mainly impacted by the discharge of mine waters from the Ronneburg underground mine, which were only treated by simple aeration and sedimentation, mainly to remove dissolved iron. Total mine water discharge averaged to >1000 m^3/h for the whole mining district. For the time period between 1992 and 1997, mine water discharge to the Wipse creek amounted to about 800 m^3/h, carrying 2.4 g/L of SO_4, 1.25 mg/L of Ni, 0.6 mg/L of Zn, and 0.3 mg/L of U (average values, cf. Paul et al. 2005). After initiation of the flooding process at Ronneburg's southern mine fields in 1998 surface water quality improved abruptly, accompanied by a drop of the uranium concentrations by one order of magnitude. Since 2006 treated mine water is being discharged to the Wipse creek with a volume of up to 500 m^3/h, which, however, is not traceable in the uranium concentration graph due to the effectiveness of water treatment (Table 1).

The former impact affecting the Sprotte also decreased dramatically, most significantly after complete cessation of the mine water discharge from the Beerwalde and Drosen mine fields in 2000. Meanwhile, uranium concentrations in the Sprotte creek at monitoring station s-609 reached 4 µg/L, also benefiting from the much higher natural flow rates compared to Wipse and Gessenbach (catchment area 118.3 km^2, 2007 average flow: 0.26 m^3/s).

In contrast to Wipse and Sprotte, the contamination of the Gessenbach was originally caused by diffuse influx of seepage waters from different waste rock dumps and a seepage water reservoir. After waste rock relocation between 1991 and 2002 and the ongoing remediation activities in the Gessenbach catchment uranium concentrations dropped significantly, roughly by one order of magnitude.

Zwickauer Mulde catchment

Since remaining emissions from Pöhla are marginal, the WISMUT-related impact to the Zwickauer Mulde is dominated by the Schlema and Crossen sites. The mean flow rate of the Zwickauer Mulde's middle reaches can be assessed using the data from Zwickau-Pölbitz (located upstream Crossen) with 13.6 m^3/s ($MQ_{1976-2000}$).

Table 5 summarizes water quality data for four monitoring stations along the Mulde river referring to upstream Schlema (m-131), downstream Schlema (m-111), upstream Crossen (M-201), and downstream Crossen (M-205). As for the Weiße Elster a decreasing trend of the impact related to the WISMUT sites can be clearly demonstrated over time. Recent uranium and arsenic contents downstream the two sites are 8 µg/L and 6 µg/L, respectively (2007, median values), which corresponds to a decrease by 80 % for uranium and 60% for arsenic since 1993. The comparison with the corresponding stations upstream is nevertheless documenting a persistent impact, for uranium at both sites, for arsenic at Schlema only.

Table 5. Indicative water quality data for Monitoring stations at the Zwickauer Mulde, time series 1990-2007, Median values. SO_4 in mg/L, hardness (H) in °dH, U and heavy metals in µg/L.

	m-131 (upstream Schlema)							m-111 (downstream Schlema)						
Year	SO_4	H	U	Ni	Cu	Zn	As	SO_4	H	U	Ni	Cu	Zn	As
1993	48	5.0	4	63	16	93	8	65	6.3	19	53	12	84	15
1997	50	3.6	2	24	5	60	7	75	5.6	63	20	7	63	21
2000	60	3.7	2	13	5	54	8	94	6.0	10	10	6	38	16
2003	64	3.8	3	14	13	74	11	102	6.8	15	11	11	58	18
2006	42	4.0	2	22	<5	52	7	81	6.4	10	16	<5	38	13
2007	38	3.4	2	14	<5	52	6	54	4.7	8	6	<5	35	9

	M-201 (upstream Crossen)							M-205 (downstream Crossen)						
Year	SO_4	H	U	Ni	Cu	Zn	As	SO_4	H	U	Ni	Cu	Zn	As
1993	83	6.8	28	124	152	160	18	82	7.3	43	89	196	163	15
1997	83	7.4	37	8	5	70	16	112	7.9	40	6	<5	80	16
2000	73	6.4	6	10	6	79	13	96	6.7	10	12	9	94	11
2003	116	nd	15	7	<5	56	11	124	nd	18	6	<5	66	10
2006	82	nd	8	9	<5	36	9	92	nd	10	9	<5	37	8
2007	52	5.0	6	7	<5	36	6	61	5.6	8	6	<5	36	6

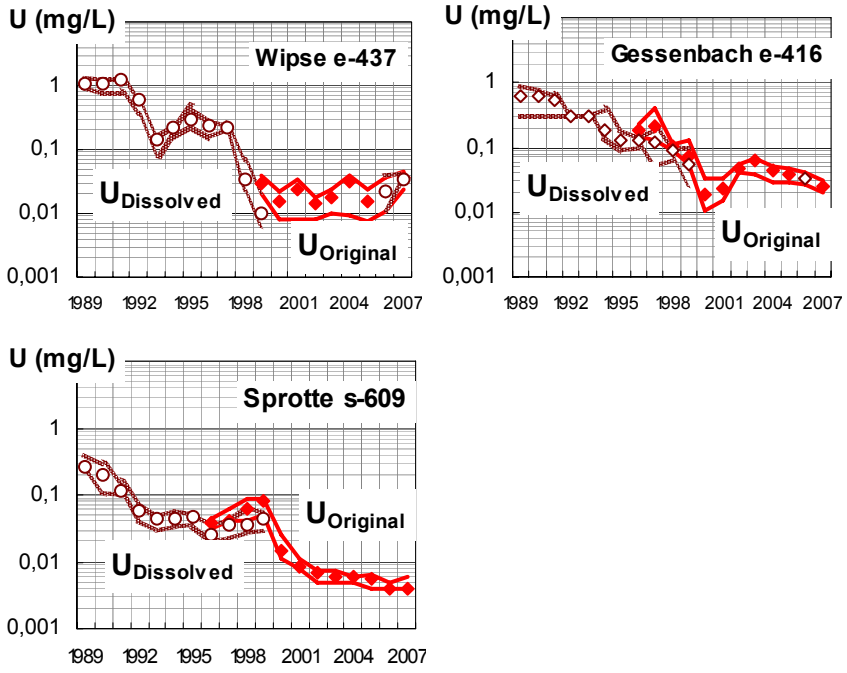

Fig.4. Uranium concentrations in the second order receiving streams dewatering the Ronneburg mining area (Wipse, Gessenbach, Sprotte). Time series 1989-2007. Annual median value, 25 and 75 percentile. U was analyzed as U-dissolved (until 1999, according to demands from REI Bergbau 1993) and U-original (since 1996/1999), respectively.

The uranium and arsenic contents of the suspended matter documented in Table 6 confirm a significant arsenic enrichment at Schlema, which is, however, mostly attributed to the emissions from the abandoned Schneeberg mine, the most important arsenic emitter within the entire Zwickauer Mulde watershed, but being not in responsibility of WISMUT (cf. Meyer et al. 2008). The Crossen reach, in contrast, acts as an arsenic sink, which is also the case for the entire longitudinal profile from m-131 to M-205. The relevant quality standard for As (40 mg/kg) is, however, considerably overrun already upstream the WISMUT area, due to significant emissions from abandoned mine sites and historical smelters in the upper Erzgebirge mountains. Since a general downward trend is lacking, the attainability of the 'Good ecological status' for the Zwickauer Mulde is more than questionable for the foreseeable future due to the arsenic fluxes from the entire catchment area regardless of the development of any other component.

Uranium shows a significant increase from upstream to downstream stations, whereas the distance between m-111 and M-201 acts as a sink. The total increase is dominated by the Schlema site, since 90 % of WISMUT's uranium discharge to the Zwickauer Mulde river is originated from here according to the discharge statistics of the last ten years. Significant influxes from upstream are, however, also present for uranium, documented by the values at m-131.

The impact situation at smaller tributaries in the Mulde catchment has improved considerably. In 2007 the lower reaches of Schlemabach, Silberbach and Alberodabach at the Schlema site as well as of Luchsbach and Pöhlwasser at Pöhla did not reveal any significant contamination due to WISMUT objects. At Crossen, a residual impact to the Zinnbach and the Oberrothenbach creek is still existing due to diffuse seepage from the Helmsdorf and Dänkritz tailings management areas, which is expected to decline further as a result of the ongoing remediation activities.

Table 6. Uranium and arsenic concentration bound to suspended matter (SPM) in the Zwickauer Mulde. Time series 2002-2007, annual mean values based on monthly sampling, < 63 μm fraction. SF 1a, 4, 20, 21 = sediment traps located close to the monitoring stations.

	SF 1a/ m-131		SF 4/ m-111		SF 20/ M-201		SF 21/M-205	
Year	U [mg/kg]	As [mg/kg]	U [mg/kg]	As [mg/kg]	U [mg/kg]	As [mg/kg]	U [mg/kg]	As [mg/kg]
2002	40	189	122	203	67	178	80	138
2003	32	375	90	322	65	178	88	178
2004	33	213	80	256	51	151	66	150
2005	33	237	83	258	43	160	52	155
2006	35	258	82	277	52	147	55	121
2007	32	200	98	206	63	168	73	144

Conclusions

The remediation activities under the WISMUT project caused substantial improvements in the water quality of the Weiße Elster and Zwickauer Mulde rivers downstream the WISMUT areas including the corresponding tributaries are, based on declining emissions since 1990. Although water management regimes were constant over a couple of years, certain changes are to be expected in the course of the finalization of mine flooding in Ronneburg, Dresden-Gittersee, and Königstein. However, water treatment will be necessary at all sites for decades to assure the quality status reached.

The commissioning of an additional water treatment facility for the seepage waters of waste rock dump 371 at Schlema, which is planned for 2009, will further decrease the uranium emissions to the Zwickauer Mulde.

Environmental quality standards for the aquatic phase of the surface water as published in 2006 (proposal for a Directive of the European Parliament and of the Council on environmental quality standards in the field of water policy and amending Directive 2000/60/EC) contain in case of heavy metals goal concentrations, e.g. for Ni (20 µg/L). Comparing these with current water quality data for the Weiße Elster and Zwickauer Mulde rivers it can be concluded that the residual impact from the WISMUT legacies will not prevent target achievement. However, potential standards for other relevant parameters especially for uranium are still under discussion.

Critical parameter concentrations in the suspended matter, which are of relevance to reach the 'Good ecological status' according to the EC-WFD (e.g. Zn, Ni, As) are recently met in the Weiße Elster river downstream the WISMUT area. For the Zwickauer Mulde the same is not likely to happen in the foreseeable future, due to the constantly high arsenic influxes from the entire catchment area. Therefore, the management of arsenic fluxes in the Mulde watershed must further be addressed with high priority.

Acknowledgement

The authors like to thank Mrs. Arndt who kindly helped in preparing the figures.

References

Czegka W, Hanisch C, Junge F, Zerling L, Baborowski M (2005) Changes in Uranium concentration in the Weisse Elster River as a mirror of the remediation in the former WISMUT mining area.- In: Uranium in the environment. Mining impact and consequences, pp. 875-884

Jenk U, Nindel K, Zimmermann U (2008) Underground in-situ mine water treatment in a flooded uranium mine at the WISMUT Königstein site – motivation, activities and out-

look.- In: Proceedings of the 5th Conference on Uranium Mining and Hydrogeology, (this volume)

Leupold D, Paul M (2007) Das Großprojekt WISMUT – Nachhaltige Sanierung und Revitalisierung von Uranerzbergbaustandorten in Sachsen und Thüringen. Bergbau 10: 438-444

Meyer J, Paul M, Jenk U (2008) Mine water hydrology of the Schneeberg mine (Saxony) fifty years after flooding.- Proceedings of the 10th IMWA Meeting, Karlovy Vary (in press.)

Paul M, Gengnagel M, Baacke D (2005) Integrated water protection approaches under the WISMUT project: The Ronneburg case. In: Uranium in the environment. Mining impact and consequences, pp. 369-379

Schmidt P, Lindner T (2005) Development of water-borne radioactive discharges at WISMUT and resulting radiation exposures.- In: Uranium in the environment. Mining impact and consequences, pp. 640-645

Schneider P, Reincke H (2005) Contaminated Sediments in the Elbe Basin and its Tributary Mulde.- In: Uranium in the environment. Mining impact and consequences, pp. 655-662

Radiological hazards from uranium mining

Bruno Chareyron

CRIIRAD (Commission de Recherche et d'Information Indépendantes sur la Radioactivité), Immeuble CIME, 471 av Victor Hugo, 26 000 Valence, FRANCE, E-mail : bruno.chareyron@criirad.org

Abstract. At all the French uranium mines where it made radiological surveys, the CRIIRAD laboratory discovered situations of environmental contamination and a lack of proper protection of the inhabitants against health risks due to ionizing radiation. Radiological problems are not only to be addressed during mining or milling operations but also on the longer term after mine closure.

Uranium and its by-products

All natural uranium isotopes (238U, 234U, 235U) are radioactive. The most common isotope, 238U, decays naturally into a succession of 13 other radioactive nuclides. All are metals (thorium 230, radium 226, lead 210, polonium 210, etc) except one, radon 222, which is a radioactive gas.

Uranium and its decay products emit various ionizing radiation such as alpha and beta particles and gamma radiation.

The Earth's crust has a typical 238U activity of about 40 Becquerels per kilogram (Bq/kg). Since the creation of the Earth, this level of radiation has decreased by two-fold because 238U half-life is very long and equal to the age of the planet earth (4.5 billion years).

This presence of natural uranium in the Earth crust, and therefore in numerous building materials made out of natural minerals, is the main source of exposure of mankind to ionizing radiation.

This is especially due to the diffusion of radon gas from the soil and materials containing uranium- and its accumulation in the air inside buildings and dwellings. This radiological hazard is now well documented and International (The International Commission on Radiological Protection, ICRP) and European (Euratom) regulations determine recommendations and action levels in order to lower radon concentration inside buildings and reduce cancer risks.

The health impacts of ionizing radiation even at low doses include the increase of various types of cancers, genomic instability, life-shortening and negative impacts on all the body functions.

Radiological situation before extraction

The activities of uranium ores have an important variability. Typical ore with a uranium content of 0.2 % has a 238U activity of about 25,000 Bq/kg. The total activity, including all the 238U by-products and the 235U decay chain will therefore exceed 360,000 Bq/kg. Such material should be managed with a great deal of caution due to the risks of exposure to ionizing radiation.

As long as the ore remains buried underground - the depth being a few tens and even a few hundreds of meters - the radiation levels at the surface of the earth remain low and usually have the same order of magnitude as of typical natural radiation levels. Except in places where the ore reaches the ground surface (typically a few square meters), the protection offered by the soil is usually sufficient to reduce the risks for the people living in the area.

Indeed, alpha and low energy beta particles are stopped by a thin layer of soil (much less than 1 cm.). Even penetrating gamma radiation does not cross a layer of soil of a few meters.

Regarding the radiological characteristics of air and water, the situation is more complex. Nevertheless before mining activities most of the radon gas remains trapped inside the soil. Because of its short half-life (3.8 days) a lot of the gas atoms will disintegrate inside the soil during their migration before reaching the biosphere.

The amount of nuclides in underground water may remain low if the minerals containing uranium are trapped in unpermeable layers.

Radiological situation during uranium extraction

The radiological situation is reversed as soon as the uranium extraction begins. There are many reasons for this.

Radioactive dust is transferred to the atmosphere by mining operations, extraction and crushing of ore, uranium milling, management of waste rocks and tailings. This has to be emphasized because some of the nuclides contained in the uranium decay chains (such has thorium 230) are very radiotoxic when inhaled. For example, when inhaled, a given activity of actinium 227 (part of the 235U decay chain) gives a radiation dose 5 times higher than the same activity of plutonium 238 (Euratom 1996).

Radon gas is transferred to the atmosphere by the vents of the mines and by diffusion from radioactive rocks and tailings (Chareyron and Castanier 1994).

Surface and / or underground water is contaminated by uranium and its by products. Some of them are very radiotoxic when ingested (Chareyron and Castanier 1994). Lead 210 and polonium 210 for example are among the most radiotoxic elements. When ingested, a given activity of polonium 210 gives a radiation dose 4.8 times higher than the same activity of plutonium 239 (Euratom 1996).

Huge amounts of waste rocks, with activities exceeding the normal activity of the earth crust by one to two orders of magnitude are dispersed into the environment and may be used for landfill, road construction or even building (Chareyron 2002b).

Huge amounts of radioactive tailings (with typical total activities exceeding 100,000 and even 500,000 Bq/kg) are generated and stored without proper confinement (Chareyron and Castanier 1994).

Long term contamination after mines closure

Even decades after the shut down of uranium mines and mills, the radioactive contamination of the environment will remain. This is due to the fact that 238U half life is very long (4.5 billion years).

But even the tailings from the mills - whose uranium content is lower than the initial uranium concentration in the ore - will remain radioactive on the long term. They contain all the radioactive metals included in the uranium decay chain which have not been extracted in the mill, especially thorium 230 and radium 226 whose half lives are 75,000 years and 1,600 years respectively.

This long term impact will occur in many ways. Some examples are given below, based on studies performed by the CRIIRAD laboratory since 1992 in France (and Niger).

Transfer of radionuclides to the aquatic environment

Accumulation of radioactive metals in sediments and plants of rivers, ponds, and lakes by contaminated waters from former mines (and also tailing deposits, unco-

Table 1. Radioactivity of sediments upstream and downstream Saint-Pierre [a] mine (year 2003, 2004, 2006).

Sample type	Sample Location	Year	Uranium 238 (Bq/kg dry)	Radium 226 (Bq/kg dry)	Lead 210 (Bq/kg dry)
Sediment	Brook, upstream	2006	76	77	123
Sediment	Ditch. near Lake, downstream	2003	49,900	1,191	1,387
Sediment	Ditch. near Lake	2006	144,000	430	2,150
Sediment	Lake, downstream	2004	126,000	735	3,533

[a] Saint Pierre mine is located in Cantal (France). Uranium extraction took place from 1956 to 1985. The mining companies were SCUMRA, then Total Compagnie Minière. The site is now under COGEMA-AREVA's responsibility (Chareyron 2004, 2005a; Chareyron and Constantin Blanc 2007).

vered waste rock deposits, etc.) is a problem that is not yet properly addressed by the companies.

The CRIIRAD laboratory discovered that sediments, aquatic plants and soil from river banks downstream former uranium mines have such a contamination that they deserve in many cases the terminology: “radioactive waste” (238U activity or the activity of some of its by-products were exceeding 10,000 Bq/kg).

Some results are summarized in tables above (Table 1) and below (Tables 2 to 4).

As shown in the table above (Table 2) the accumulation of uranium and or radium downstream uranium mines is usually more intense for surface soil sampled from the river shore than for river sediments (one order of magnitude in this example).

Bioaccumulation of radioactive metals can be extremely high in the biota. In some cases, the contamination of aquatic plants by radium 226 downstream uranium mines can exceed 100,000 Bq/kg dry (Table 3). This shows that the mine water treatment system is not operating properly.

The problem of bioaccumulation is usually not taken into consideration by the companies nor the administrations in charge of environmental monitoring and regulatory control.

It should be noted as well that radioactive metals are transported far away from the mines. At Les Bois Noirs mine, uranium accumulation in sediments is still 54 times above background value 12 km downstream the mine (Table 2). Uranium

Table 2. Radioactivity of sediments and soil upstream and downstream Les Bois Noirs [b] uranium mine (year 1996, 2001 and 2006).

Sample type	Sample Location	Year	Uranium 238 (Bq/kg dry)	Radium 226 (Bq/kg dry)	Lead 210 (Bq/kg dry)
Sediments	River, upstream	1996	87	85	109
Marshy soil	downstream tailings pond	2001	7,900	18,400	7,500
Sediments	River, 25 m downstream water discharge	2001	510	770	390
Soil	River shore 25 m downstream discharge	2001	5,900	10,600	4,100
Deep sediment (20/30 cm)	Dam, 12 km downstream	1996	4,048	1,928	1,613
Sediment	Dam, 12 km downstream	2006	4,700	1,630	1,680

[b] Les Bois Noirs mine is located in the Loire department (France). Uranium has been extracted there from 1955 to 1980 by the CEA and then COGEMA-AREVA. (Chareyron 2002b, Chareyron 2008b).

and radium accumulation in aquatic plants are 4 to 6 times above background value 30 km downstream the discharge pipe from the mine (Table 3).

Table 3. Radioactivity of aquatic plants upstream and downstream Les Bois Noirs [b] uranium mine (Year 2001 and 2006)

Sample type	Sample Location	Year	Uranium 238 (Bq/kg dry)	Radium 226 (Bq/kg dry)	Lead 210 (Bq/kg dry)
Fontinales	River, upstream	2001	109	144	323
Fontinales	Drain downstream tailings pond	2001	32,400	113	1,250
Fontinales	River, 25 m downstream the discharge pipe	2001	9,000	93,600	1,430
Fontinales	River 1.5 km downstream	2001	3,500	37,800	600
Fontinales	River, 9 km downstream	2001	1,900	5,500	480
Fontinales	River, 30 km downstream	2001	450	990	210
Fontinales	Inside discharge pipe	2006	3,400	143,000	6,000
Fontinales	River < 1 km downstream	2006	10,200	147,000	2,400

Table 4. Radioactivity of sediments and soil upstream and downstream (PDL) Puy de l'Age[c] and (BZN) Bellezane[d] uranium mines (year 1993, 2004).

Sample / Mine	Sample Location	Year	Uranium 238 (Bq/kg dry)	Radium 226 (Bq/kg dry)	Lead 210 (Bq/kg dry)
Sediment	River, upstream	1993	73	60	68
Sediment / PDL	River, downstream	1993	13,470	28,740	7,282
Sediment / BZN	River, downstream	1993	36,167	1,971	1,928
Sediment / BZN	River, 1.5 m downstream	2004	63,000	13,400	2,770

[c]Puy de l'Age mine is located in the department of Haute-Vienne (Limousin, France). The mine has been reclaimed by COGEMA-AREVA in 1993 (Chareyron and Castanier, 1994).
[d]Bellezane mine is located in the department of Haute-Vienne (Limousin, France). Uranium has been extracted from 1975 to 1992 by COGEMA-AREVA (Chareyron and Castanier, 1994, Chareyron 2006).

Dispersal of radioactive minerals

At many places, radioactive minerals from the mines are kept by local people or former workers unaware of the radiological hazards which are, in some cases, very significant.

For example, the CRIIRAD laboratory discovered in France that an inhabitant living near Les Bois Noir former uranium mine was keeping a sample of waste rock with a dose rate of 1 milliSievert per hour at the surface of the stone (Chareyron, 2002a). This figure is about 5,000 times above local background level.

The gamma doserate was 18.3 microSievert per hour at a distance of one meter. Staying at a distance of 1 meter during only 10 minutes per day will lead to exceeding the annual maximum permissible dose for members of the public i.e. 1 milliSievert per year (Euratom, 1996).

Dispersal of radioactive waste rocks and radon gas accumulation

Re-use of radioactive waste rocks for landfill has been in some areas a common practice. CRIIRAD demonstrated that several places near a French uranium mine were contaminated including the car park of a restaurant, the yard of a farm, several sawmill buildings, kilometres of path and roads, etc. (Chareyron 2002b).

In one case, a sawmill building had been built several decades ago directly on the radioactive waste rocks taken at the mine. Due to gamma radiation and radon gas accumulation, the radiation dose inside the building could exceed the annual maximum permissible dose for members of the public by a factor exceeding 20. The mining company had therefore to pay during year 2003, for the evacuation of 8,000 m^3 of radioactive waste rock from the sawmill back to the former open pit (Chareyron 2002b).

Dispersal of contaminated scrap metal

Dispersal and re-use of contaminated scrap metal from the mines or mills has also been a common practice.

During 2003, the CRIIRAD laboratory discovered in Niger that radioactive scrap metal was sold in Arlit city. One piece was a pipe from the uranium mill. It was sold without previous decontamination and the 226Ra activity of the crust inside the pipe exceeded 200,000 Bq/kg. Such a practice cannot be justified.

The mining company COGEMA (now known as AREVA) stated that before 1999, no radiation limit was used for scrap metal recycling. Later, a dose limit of 1 microGray per hour at a distance of 50 cm had been applied. Such a limit is much too high. If someone uses such metallic pieces inside his house – which is common in African countries –staying 3 hours per day at a distance of 50 cm will lead to exceed the annual maximum permissible dose for members of the public. (Chareyron 2003, 2005b).

At present, discussions are still going on with the mining company, local NGO's and the administration, in order to decide whether radioactive rocks used at other places will or will not be evacuated (ski resort house, garage of a citizen, etc.).

Radioactive material have been detected again in 2007 inside private houses or at scrap merchants (Chareyron 2008a).

Problems posed by the disposal of tailings

The disposal of radioactive tailings and their control on the long term, has not received yet satisfying solutions, taking into consideration their activity, radiotoxicity and long half-lives. Some examples from France (where about 50 million tons of tailings are stored) and Niger are given below.

In France 1.5 million tons of tailings have been dumped in a former open pit (Bellezane mine) but the CRIIRAD laboratory discovered that the finest fraction of the radioactive material could reach the underground galleries underneath the pit. Furthermore, the mine water treatment plant was not efficient enough to prevent the contamination of the river and meadows downstream (Chareyron and Castanier 1994, Chareyron 2006).

In Niger, more than 20 million tons of radioactive tailings are stored in the open air, near SOMAÏR and COMINAK mills, a few kilometers away from the cities of ARLIT and AKOKAN (about 70,000 inhabitants). Radon gas and radioactive dust can be scattered away by the powerfull winds of the desert (Chareyron 2003, 2005b, 2008a).

Conclusion

At all the French uranium mines where it made radiological surveys, the CRIIRAD laboratory discovered situations of environmental contamination and a lack of proper protection of the inhabitants against health risks due to ionizing radiation.

This is due to the lack of proper regulations, a poor awareness of the radiological hazards associated with uranium and its by products, insufficient monitoring practices, the lack of controls by the local and national administration, etc.

When the mines are shut down, the radioactive waste remains, and it seems that the costs for managing this radioactive legacy will have to be largely supported by the society, not the companies.

If such a situation occurs in a so-called "developed country" one should fear what could actually happen in other parts of the world. The preliminary mission made by CRIIRAD to Niger confirmed this fear. In Gabon, the improvement of the conditions in which tailings are disposed is being paid for by the European Community and not by the mining company. The former workers and local popu-

lation do not benefit any more from medical care and they receive no compensation when they become sick, years and decades after the mine shut down.

References

Chareyron B, Castanier C (1994) CRIIRAD, Etudes radioécologiques sur la division minière de la Crouzille, Février 1994

Chareyron B (2002a) Compte rendu de mesures effectuées par le laboratoire de la CRIIRAD sur un bloc de minerai d'uranium présent chez un particulier de la commune de Saint-Priest-La-Prugne (Loire)

Chareyron B (2002b) Rapport CRIIRAD N°03-38, Bilan radioécologique du Site Bois Noirs, octobre 2002

Chareyron B (2003) Note CRIIRAD N°03-40. Compte rendu de mission à Arlit (Niger) du 3 au 11 décembre 2003. Décembre 2003

Chareyron B (2004) Rapport CRIIRAD N°04-05. Contrôles radiologiques préliminaires dans l'environnement de la mine d'uranium de Saint-Pierre (Cantal). Mars 2004

Chareyron B (2005a) Note CRIIRAD N°05-02. Analyse de sédiments lors de la vidange du lac de Saint-Pierre (Cantal). Mars-avril 2005

Chareyron B (2005b) Note CRIIRAD N°05-17. Impact de l'exploitation de l'uranium par les filiales de COGEMA-AREVA au Niger. Avril 2005

Chareyron B (2006) Note CRIIRAD N°06-41. Remarques sur le projet COGEMA-AREVA de stockage de boues et sédiments contaminés sur le site de Bellezane (Haute-Vienne). Juin 2006

Chareyron B, Constantin-Blanc T (2007) Rapport CRIIRAD N°07-68 Expertise 2006 Phase 2 Tome 1 Milieu aquatique. Situation radiologique de la mine d'uranium de Saint-Pierre (Cantal) et de son environnement. Octobre 2007

Chareyron B (2008a) Note CRIIRAD N°08-02 AREVA : du discours à la réalité – L'exemple des mines d'uranium du Niger. Janvier 2008

Chareyron B (2008b) Note de synthèse CRIIRAD N°08-50 Ancien site d'extraction d'uranium AREVA des Bois Noirs / Suivi CRIIRAD-Collectif des Bois Noirs 2006-2007. Avril 2008

EURATOM (1996) Directive 96/29/Euratom du Conseil, du 13 mai 1996, fixant les normes de base relatives à la protection sanitaire de la population et des travailleurs contre les dangers résultant des rayonnements ionisants. L 159

Radiological evaluation of elevated uranium concentration in ground and surface waters encountered at uranium ore mining and processing sites

Peter Schmidt and Thomas Lindner

Wismut GmbH, Jagdschänkenstraße 29, D-09117 Chemnitz

Abstract. With a view to licensing procedures and stakeholder consultations and in particular to discussions with locals living near former uranium mining sites, it is absolutely essential to apply/follow a science-based and generally accepted course of action when it comes to evaluate uranium (levels) in water. This paper depicts the evaluation process as performed in Germany and how it was applied to the environmental remediation of legacies left behind by former uranium ore mining of Wismut.

Introduction

Specialist literature as well as guidelines and recommendations issued by national and international agencies rate chemo-toxic risks to human health emanating from uranium in water higher than the corresponding radiological risks. Public perception, however, is in the first place dominated by the possible radiation hazard due to uranium in water. It is therefore imperative to assess incorporation via the aquatic pathway of uranium on the basis of scientifically substantiated risks to human health. Such assessment also implies harmonised and generally accepted exposure pathway analyses. These analyses, in turn, provide a valuable tool when it comes to justify and optimise remediation decisions based on measured or predicted uranium concentrations in ground or surface waters.

Radiological assessment basis

Basically, there are two approaches to assess radionuclides in the environment:
a) a limit or reference value related approach, and
b) a dose-related approach.

In the limit or reference value related approach, measured or predicted concentrations are being compared to corresponding limits or reference level values as prescribed in federal acts, recommendations or regulatory notices of approval. Limits for nuclide discharge to receiving streams (e.g. maximum concentration limits in discharge water or approved maximum loads for discharge via the aquatic pathway) also provide feasible assessment bases. The value related approach is easy to handle and efficiently applicable to discussions with concerned people (stakeholders). This approach draws its justification from the proper definition of limit and reference values based on generic exposure assessments.

The dose-related assessment approach is based on an exposure pathway analysis. It finds application in complex exposure situations, whenever there is a probable exceeding of reference or limit values calling for decisions on justification and optimisation of intervention measures. Figure 1 exemplifies the exposure pathways to be analysed on principle for contamination of a surface water body:

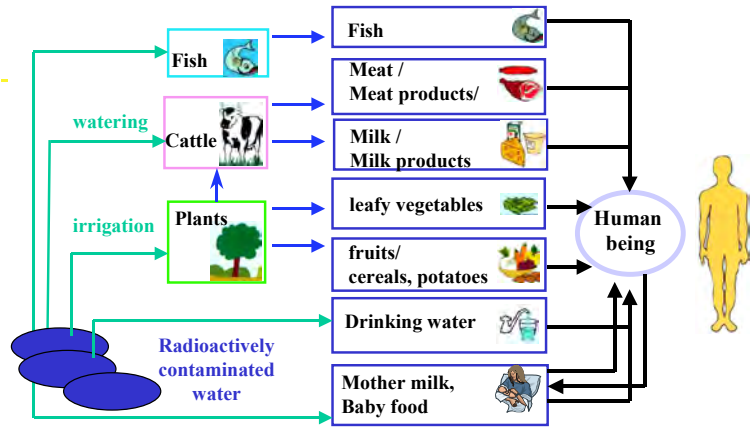

Fig.1. Schematic of an exposure pathway analysis for radionuclides in surface waters.

Limits and reference values for uranium in water

At present, there is no legislative provision in Germany to legally stipulate, from a radiological point of view, maximum allowable concentrations of uranium nuclides in water, except if one defines the Groundwater Ordinance (BMU 1997) as a regulation on "zero values" for anthropogenically induced uranium concentrations, because this ordinance prohibits the discharge into groundwater of carcinogenic

Table 1. Limit and reference values as defined by VOAS and the SSK recommendation.

VOAS 1984		SSK 92	
Nuclide / element	**Maximum concentration limit for discharge to receiving streams**	**Nuclide / element**	**Reference value of permissible concentration in drinking water at mining sites**
U_{nat}	0.16 mg/l	U_{nat}	7 Bq/l (0.3 mg/l)[b]
U-238[a]	5 Bq/l		**Effective dose reference level for drinking water**
U-234	4 Bq/l		
U-235	5 Bq/l		0.5 mSv p. a.

[a] Provided that there are nuclide mixtures, the summation formula is to be used.
[b] Assuming the existence of a radioactive equilibrium between U-238 and U-234 as well as of a natural isotopic ratio (U-235 : U-238 = 0.7 % by weight).

substances, thereby also of radioactivity. Unlike in some countries in Europe and overseas, there are also no limit values for uranium nuclides in drinking water. The German Drinking Water Ordinance evaluates radionuclides in drinking water by applying the reference level for the effective dose of 0.1 mSv/a (BMU 2001). From that, secondary reference values may be derived on the basis of an exposure pathway analysis (cf. section 2.2)

Technically, uranium levels in waters at sites remediated by WISMUT might be assessed by using a recommendation on the maximum allowable concentration of uranium in drinking water issued by the German Commission on Radiological Protection in 1992 (SSK 1992) and the Nuclear Safety and Radiological Protection Ordinance VOAS of the former GDR (SAAS 1984) which is still in effect. The appropriate limit and reference value data are compiled in Table 1. While the recommendation of the Commission on Radiological Protection has found rare application in licensing procedures, VOAS, in contrast, is still being applied to the licensing of discharge limits.

Dose related assessment approach for uranium in water

Adopted in 1999 by the German Federal Ministry for the Environment, Nature Conservation and Nuclear Safety, the "Calculation Bases for the Determination of Radiation Exposure due to Mining-caused Environmental Radioactivity" (Calculation Bases Mining CBM-99) provide a recognised assessment basis for elevated uranium concentrations in waters at mining site locations (BMU 1999). The assessment is not limited to uranium but also extends to / includes all other naturally occurring radionuclides of the U and Th decay series having dose relevance. In essence, the Calculation Bases Mining provide guidance on how to implement an exposure pathway analysis, whereby the following parameters are being provided:

- definition of exposure pathways to be considered;
- consumption rates (age-dependent): the subsequent age-groups are being considered: "< 1a", "1-2a", "2-7a", "7-12a", "12-17a" and "adults";
- dose coefficients for the incorporation of radionuclides (also age-dependent);

- transfer factors for radionuclides, e.g. for the subsequent transitions: water → plant when irrigated; water → livestock watering; plant/livestock → human organism when consuming food [age-dependent), etc. (cf. Fig. 1); as well as
- generic background values for naturally occurring radionuclides in waters.

The Calculation Bases Mining CBM-99 are intended to determine the effective dose to a reference person at the most adverse point of impact. Basically, this implies a conservative assessment approach. However, taking site-specific conditions (whenever possible, use of measured nuclide concentrations versus modelling results, consideration of local consumption habits, elimination of low-realistic exposure pathways, consideration of site-specific background levels) into account will allow to calculate sufficiently realistic values for doses to the population at mining locations. As a result of the exposure pathway analysis, the established effective doses are compared to the reference level of 1 mSv/a, and then serve as a benchmark for the assessment of liabilities left behind by uranium ore mining. Under the WISMUT environmental rehabilitation project this reference level serves as a criterion in the decision-making on remediation actions.

Assessment results

Generic considerations

In an initial step, all potential effective doses to a standard reference person caused by uranium via the aquatic pathway are being calculated pursuant to CBM-99 (cf. Table 2). The consideration starts from the assumption that the person in case consumes 100 percent drinking water contaminated by former mining activities as well as 25 percent of local foodstuff contaminated via the aquatic pathway. The

Table 2. Annual effective dose to a reference person via the aquatic pathway according to CBM-99 from an uranium concentration in water of 1 mg/l.

Exposure pathway	Age-group-specific effective dose [mSv/a]					
	< 1a	**1-2 a**	**2-7 a**	**7 -12 a**	**12 -17a**	**Adult**
Drinking water consumption (DW)	0.487	0.312	0.210	0.266	0.352	0.410
Fish consumption (Fi)	0.002	0.005	0.003	0.004	0.004	0.004
Meat consumption (Me)	0.002	0.002	0.005	0.005	0.006	0.005
Dairy products consumption (Di)	0.022	0.028	0.019	0.017	0.017	0.009
Leafy vegetable consumption (L)	0.025	0.018	0.014	0.015	0.018	0.014
Fruit/vegetable consumption (F)	0.166	0.121	0.124	0.109	0.104	0.055
Potatoes consumption (P)	0.166	0.078	0.059	0.061	0.060	0.040
Cereal products consumption (C)	0.066	0.058	0.105	0.105	0.121	0.080
Consumption of mother milk or milk powder related products prepared with the water (MM_MP)	1.027[a]	-	-	-	-	-
Total	**1.963**	**0.622**	**0.539**	**0.582**	**0.682**	**0.617**

[a] here: dose from the consumption of "milk powder (related) products MP"

data in Table 2 are in addition based on the assumption that uranium concentration in water equals 1 mg/l. Background levels were not considered. Equilibrium between U-234 and U-238 as well as a natural ratio of uranium isotopes were assumed (i.e., 12.2 mBq/l U-234 and U-238, respectively; 0.55 mBq/l U-235).

As a matter of principle, it has to be noted that uranium nuclides U-234 and U-238 dissolved in waters tend not to be in radioactive equilibrium (sometimes, increases of U-234 versus U-238 by a few percent up to a factor of 2 have been observed). Therefore, the radiological assessment of U_{nat} with the assumption of a radiological equilibrium between U-234 and U-238 is an approximation. The third uranium nuclide to be considered is U-235, for which an activity ratio of 0.045 is assumed to U-238 (corresponds to a natural isotopic ratio of 0.7 percent by weight). One has also to consider that in addition to uranium nuclides other nuclides of the uranium decay series may just as well contribute to the effective dose via the aquatic pathway at uranium mining sites. Such nuclides are primarily Th-230, Ra-226, Pb-210 and Po-210 of the U-238 series and Pa-231 as well as Ac-227 of the U-235 series. Given the lower solubility of the elements, these nuclides are normally present in water in significant lower concentrations. However, given their dose coefficients (denotes the effective dose build-up for each incorporated radionuclide; unit = Sv/Bq) which are partly in orders of magnitude greater than for U-238, these nuclides must not be left unconsidered in an exposure pathway analysis. The outcome of this is that the entire nuclide vector must be well-understood to perform the radiological assessment of the aquatic pathway at uranium mining sites. By way of example, Table 3 lists nuclide vectors for contaminated waters in the neighbourhood of uranium mining legacies left behind by WISMUT. Effective doses based on these nuclide vectors are listed in Table 4.

With regard to the data contained in Table 4 it should be noted that the effective doses were for the most part calculated very conservatively, i.e. more elevated than occurring in reality. The reason for this is that all exposure scenarios as well as standard consumption rates for a reference person were considered according to CBM-99. Such an approach is totally unrealistic in terms of an effluent from a water treatment plant which is directly discharged to a major receiving stream where it is immediately diluted and hence no longer available for use in accordance with standard scenarios defined by CBM-99.

Exposure evaluation with a view to using locally contaminated groundwater in the neighbourhood of a flooded uranium mine is also a bit out of touch with reality as such waters are not being used for the time being and will have to be subject to use restrictions in the future. It might be argued however, that the “concept of usable aquifer” being currently under discussion in Germany is to be integrated into a revision of the Calculation Bases Mining. Under this concept, groundwater is to be evaluated by the assumption of a fictitious well from which water is used for all standard scenarios according to CBM-99. Such an approach makes sense to demonstrate the degree of groundwater contamination. Though, in the mind of the authors of this paper, such approach is not suited to serve as a remediation objective and even less to perform optimisation analyses for a "pre-existing situation". This should only be done on the basis of realistic water use scenarios.

Table 3. Exemplary nuclide vectors V in waters contaminated by WISMUT uranium mining operations.

Activity concentration in water [Bq/l]								
U-238	**U-234**	**Th-230**	**Ra-226**	**Po-210**	**Pb-210**	**U-235**	**Pa-231**	**Ac-227**
Groundwater in the surroundings of a flooded uranium mine in Schlema [V_{MINE}]								
19,1	19,0	0,06	< 0,073	0,045	0,02	0,886	<0,05	0,042
Seepage from a mine dump in Schlema [V_{DUMP}]								
2,4	2,46	0,006	0,006	0,002	0,008	0,11	0,007	0,006
Effluent from the water treatment plant in Seelingstädt [V_{WTP}]								
1,55	2,0	< 0,15	<0,008	0,003	<0,025	0,071	n.d.[b]	<0,01
Contaminated surface water near the tailings management area Dänkritz [V_{TMA}]								
15,6	15,0	< 0,22	0,12	n.d.[a]	<0,025	0,72	n.d.[b]	<0,01

[a] not determined, Po-210 concentration set to be equal to that of Pb-210
[b] not determined, Pa-231 concentration set to be equal to that of Ac-227

Table 4. Conservatively calculated doses to locals via the aquatic pathway at WISMUT mining sites (all aquatic exposure pathways, consideration of generic background values acc. to CBM-99).

Nuclide vector	**Age-related effective annual dose [mSv/a]***					
	< 1a	**1 -2 a**	**2 -7 a**	**7 -12 a**	**12 -17a**	**Adult**
V_{MINE}	3,94	1,20	1,0	1,1	1,21	1,09
V_{DUMP}	0,45	0,13	0,11	0,12	0,14	0,13
V_{WTP}	0,56	0,13	0,11	0,12	0,14	0,13
V_{TMA}	3,05	0,93	0,78	0,84	1,0	0,87

Finally, it should be noted with regard to data in Table 4 that generic background levels of naturally occurring radionuclides generically assumed for Germany (acc. to the Calculation Bases Mining CBM-99) were being taken into consideration for their calculation. In uranium mining regions natural background levels are more elevated which reduces the mining-related dose contribution.

Consideration closer to reality

More realistic dose values may be obtained on the basis of a site-specific consideration with due regard to actual exposure scenarios. The case study below starts from a fully determined (i.e. measured) nuclide vector for contaminated surface waters (Lerchenbach creek) in the neighbourhood of the Trünzig TMA. The appli-

Table 5. Nuclide vector $V_{TRÜNZIG}$ and associated site-specific background nuclide vector V_{BGRD}, as well as generic background vector $V_{BGRDgen}$ acc. to CBM-99

Activity concentration in water [Bq/l]									
Nuclide vector	**U-238**	**U-234**	**Th-230**	**Ra-226**	**Po-210**	**Pb-210**	**U-235**	**Pa-231**	**Ac-227**
$V_{TRÜNZIG}$	5,2	6,1	0,17	0,02	0,025	0,024	0,24	0,015	0,015
V_{BGRD}	0,17	0,17	<0,01	<0,01	<0,005	<0,005	0,01	<0,001	<0,001
$V_{BGRDgen}$	0,02	0,02	0,002	0,02	0,002	0,005	0,001	0,001	0,001

cation of a typical background nuclide vector measured on site (cf. Table 5) gets the assessment one step further toward "close to reality".

The subsequent non-precludable scenarios were considered:

- consumption of creek water as drinking water and use of the water for preparation of milk powder-related baby food (up to 100 % use made of contaminated water);
- fish from the creek, crop irrigation / livestock watering with creel water; locally produced food represents 25 percent of foodstuff consumption.

The figures below represent corresponding dose values for the population. In addition to the effective dose to all age-groups (cf. Fig. 2), focus for the critical exposure group infant "< 1a" and the age group "12-17a" is on contributions from individual exposure pathways (cf. Fig. 3). Figure 4 shows the nuclide specific contribution to the exposure for the age group "12-17 a" for the exposure pathway "drinking water consumption" and "consumption of field and garden products".

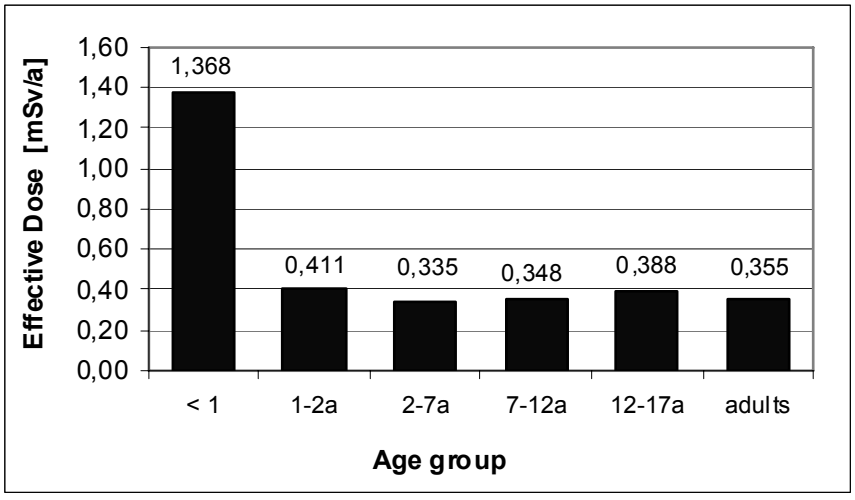

Fig.2. Non-precludable effective dose via the aquatic pathway to locals in the surroundings of the tailings management area Trünzig.

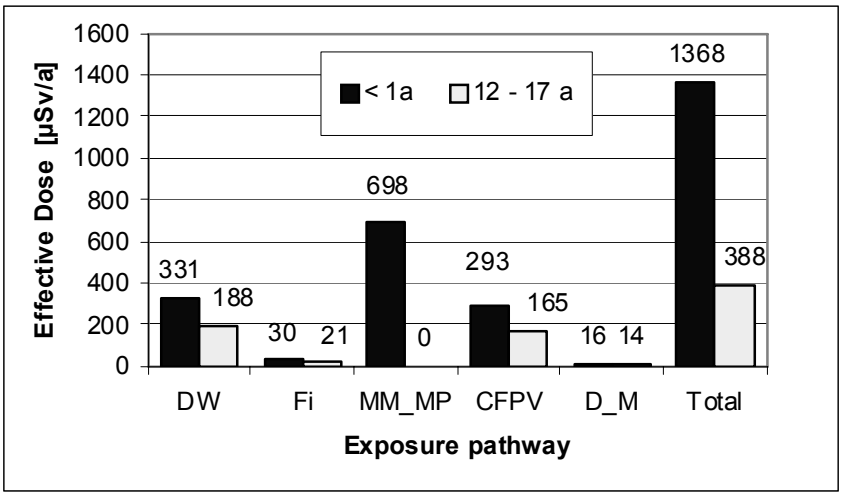

Fig.3. Contributions of individual exposure pathways for the age groups "< 1a" and "12-17a", exposure via the aquatic pathway in the surroundings of a tailings management area (DW – drinking water; Fi – fish consumption; MM_MP – mother milk or consumption of milk powder-related products prepared with the water, CFPV – consumption of cereals/fruits/potatoes/vegetable; D_M - consumption of dairy and meat products.

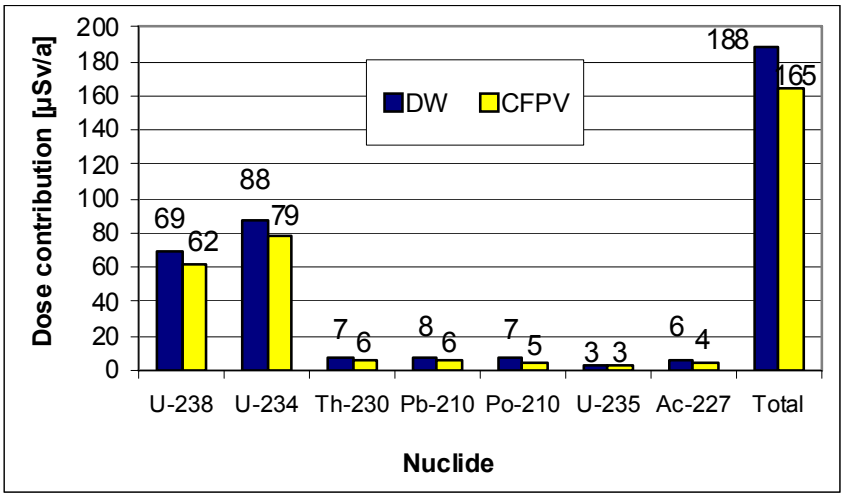

Fig.4. Nuclide specific contributions to effective dose to age groups "12 -17a" (DW - drinking water, CFPV – consumption of cereals/fruits/potatoes/vegetable).

Conclusions

The conclusions below may be derived both from the illustrated results and from a host of exposure pathway analyses that have been performed so far under the WISMUT rehabilitation project with regard to the aquatic pathway:

1. An exposure pathway analysis is essential to a comprehensive radiological assessment of uranium in ground and surface waters. This implies the application of appropriate calculation bases to yield consistent and close to reality analysis findings.
2. Adopted by the Federal Ministry of the Environment in 1999, the Calculation Bases Mining CBM-99 have proven their worth as a mature tool for a consistent, scientifically substantiated and accepted assessment of radionuclides in waters at mining sites.
3. At WISMUT sites in East Germany, exceedance of the 1 mSv criterion by exposure via the aquatic pathway is ascertained almost exclusively for the age group "< 1a", whereas the lesser realistic, but not entirely precludable exposure pathway "use of contaminated drinking water for baby food preparation" constitutes the critical factor for that exceedance.
4. Due to different solubility of chemical elements in water nuclides as a rule are in a radioactive disequilibrium. The outcome of this is that the entire nuclide vector must be well-understood to perform the radiological assessment of the aquatic pathway at uranium mining sites.
5. In the neighbourhood of tailings management areas and of chemical uranium processing sites, exposure via the aquatic pathway is chiefly dominated by the nuclides U-234 and U-238 due to the solubility of uranium in water. Nuclide vectors in seepage or mine waters with elevated concentrations of Ra-226 and/or Ra-228 as well as of their daughter nuclides may result in exposures where other radionuclides in addition to those of uranium are significant dose contributors.

References

BMU (1997) Bundesministerium für Umwelt, Naturschutz und Reaktorsicherheit (German Federal Ministry for Environment, Nature Conservation and Nuclear Safety BMU): Verordnung über den Schutz des Grundwassers gegen Verschmutzung durch bestimmte gefährliche Stoffe, Grundwasserverordnung – GwVO vom 18. März1997 (German Groundwater Act).

BMU (1999) Bundesministerium für Umwelt, Naturschutz und Reaktorsicherheit (German Federal Ministry for Environment, Nature Conservation and Nuclear Safety BMU): Calculation Bases for the Determination of Radiation Exposure due to Mining-caused Environmental Radioactivity (Calculation Bases Mining CBM-99).

BMU (2001) Bundesministerium für Umwelt, Naturschutz und Reaktorsicherheit (German Federal Ministry for Environment, Nature Conservation and Nuclear Safety BMU):

Verordnung über die Qualität von Wasser für den menschlichen Gebrauch - TwVO vom 21. Mai 2001 (German Drinking Water Ordinance).

SAAS (1984) Staatliches Amt für Atomsicherheit und Strahlenschutz der DDR (GDR State Board for Atomic Safety and Radiation Protection SAAS): Verordnung über die Gewährleistung von Atomsicherheit und Strahlenschutz (VOAS), GBl., Teil I, Nr. 30, vom 21. November 1984. (Nuclear Safety and Radiological Protection Ordinance of the former GDR).

SSK (1992) Strahlenschutzkommission (German Commission on Radiological Protection SSK): Radiation Protection Principles Concerning the Safeguard, Use or Release of Contaminated Materials, Buildings, Areas or Dumps from Uranium Mining, Publication of the SSK, Vol. 23, Gustav Fischer Verlag, Stuttgart, 1992.

Radiologically Relevant Radionuclide Depositions in the Agriculturally Used Parts of the Mulde River Floodplains

Johannes Richter[1], Stefan Ritzel[1], Rainer Gellermann[2], Kristin Nickstadt[2] and Rolf Michel[3]

[1]Sächsisches Landesamt für Umwelt und Geologie, Zur Wetterwarte 11, 01109 Dresden.
[2]HGN Hydrogeologie GmbH, Grimmelallee 4, 99734 Nordhausen.
[3]Universität Hannover, Zentrum für Strahlenschutz und Radioökologie, Herrenhäuser Straße 2, 30419 Hannover.

Abstract. Since the early investigations after the German reunification it is well known, that the floodplains of the Rivers Zwickauer Mulde and Vereinigte Mulde are highly contaminated with natural radionuclides as a consequence of the former uranium mining and milling activities in Saxony. In 2007 a project was launched in order to investigate the radionuclide contents in farmed land of the Mulde River floodplains. Based on results of former investigations as well as GIS-dissection of maps with agricultural areas and flooding areas with flooding frequency, 22 sites have been selected for this study. On these areas systematic sampling of soil will be carried out. The received data of contamination should be radioecologically analysed and the resulting radiation exposure to members of the public due to ingestion of the field crops cultivated in these areas should be estimated. In this contribution first results of the study will be presented.

Introduction

Since the early investigations after the German reunification associated with the „radiological brown fields land register“ (Altlastenkataster) it is well known, that the floodplains of the Mulde River system are highly contaminated with natural radionuclides as a consequence of the former uranium mining and milling activities in Saxony (Ettenhuber and Gehrcke 2001). In spite of extensive research

projects, particularly after the August-2002 inundation event, still are missing publications of representative data for natural radionuclides in the agriculturally used areas affected by the Mulde Rivers (Geller et al. 2004). Therefore, the Free State of Saxony launched a project in 2007 to investigate the radionuclide contents in farmed land of the Mulde Rivers' floodplains.

A main goal of this investigation is to determine representative values for the contamination of agriculturally used floodplains of the Zwickauer Mulde and the Vereinigte Mulde Rivers with natural radionuclides. Later, the received data for the specific activities of these nuclides will be radioecologically analyzed, and there will be estimated the resulting radiation exposure to members of the public due to ingestion of the field crops from these areas.

In a first step was performed a literature review and a GIS-dissection of maps with agricultural areas and flooding areas taking into account flooding frequency, and former investigations. As a result of this analysis had been selected 22 agriculturally used sites for this study. On these areas will be carried out this summer systematic sampling of soil. Additionally, at two sites soil profiles will be investigated. As far as the radioactive disequilibria allow, the results of this study will be used to assess the radionuclide balances in the soil profiles, too.

In the following sections, the first results of this study as well as the methodology of the planned field-investigations will be discussed.

Literature review

As a first step of the investigation a literature review was carried out in order to summarize the previous knowledge of radionuclide concentrations in farmed land of the Mulde Rivers floodplains. The focus of this review was to describe the geogenic and anthropogenic influences to the soils of the investigation areas, especially from the use of phosphate-fertilizers.

The most important study regarding the geogenic background was the side-project "radionuclides in sediments and alluvial soils" of the radiological brown fields land register carried out from 1994 to 1995 (GRS 1996). In this study was carried out a statistic evaluation of the river floodplains influenced and non-influenced by the former uranium-mining. The median values for the specific activities in no-influenced alluvial soils can be quoted as 70 Bq kg^{-1} U-238, 75 Bq kg^{-1} Ra-226, 51 Bq kg^{-1} Pb-210 and 55 Bq kg^{-1} Po-210. Agriculturally uses parts of river-floodplains had not been taken into account, and not discriminated respectively in that study.

In the last years the topic "uranium in agriculturally used soils" was very present in the public discussion, so that the German radiation protection agency (BfS) together with the federal institute for risk assessment (BfR) in 2007 published a study concerning the risk assessment for consumers (BfR and BfS 2007). Conclusion of this study was that there is no evidence today in Germany for harmful influences of uranium towards public health from the use of phosphate-fertilizers. On the other hand, the uranium discharged to agriculturally used soils

was very high in the past in some regions of Germany, reaching 9–18 g ha^{-1} per year, but today it is still decreasing (BfR and BfS 2007). A consequence of this discharge could be the increase of the uranium background-value in soils of 0,08 % to 0,16 % per year, relating to a mean geogenic background value of 3,3 mg kg^{-1} (40 Bq kg^{-1}). The uranium concentrations in mineral phosphate-fertilizers, which are used in Saxony today, can reach mean values from 104 to 177 mg kg^{-1} dry weight, depending on their origin (Dittrich and Klose 2008). In the period 1945–1990 during the former German Democratic Republic, were used only phosphate-fertilizers with very low Uranium concentrations (10–28 mg kg^{-1} dry weight, origin from the Soviet Union.) Therefore, the influence to the background-values of uranium in agriculturally used soils in Saxony is expected to be negligible; anyway it has to be considered in the evaluation of this study.

Investigation area

The river Mulde is a left-hand tributary of the Elbe in Saxony/ Germany. It's two headwaters Freiberger Mulde and Zwickauer Mulde confluence near the town Colditz and creates the Vereinigte Mulde. It is well known from several studies (e.g. GRS 1996) that the sediments of the Zwickauer Mulde and of Vereinigte Mulde are affected by the former uranium mining and milling in Saxony. In order to assess the radioecogical relevance of these contaminations, a study has been launched to investigate the sediments of agriculturally used areas of the floodplains of the Zwickauer Mulde and the Vereinigte Mulde).

The knowledge of the radionuclide distribution in the river Mulde allows some conclusions regarding possible phenomena of radionuclide input into the arable land are:

- In the dissolved form uranium occurred in high concentrations during the active mining and uranium ores processing in the catchment area of the Zwickauer Mulde (Friedrich 1991). Therefore, it was transferred to the arable land via the infiltration of water during inundation events. Due to this input it may be relatively mobile and easily transferred into the groundwater but also into the plants. Consequently, the transfer factor soil – plant of uranium may be higher than in "common" soils.
- In the particulate matter and river sediments the uranium is also enriched, vs. Ra-226 and Pb-210. In this form, the radionuclides are deposited during flood events and accumulate at the surface of unploughed grassland areas. On ploughed fields these nuclides are mixed and consequently diluted by ploughing.

Additional effects, like fertilizer use, capillary rising of groundwater and the temporal changes of river water quality make the system rather complex and require more data for assessments. The study described in this paper is focussed on one aspect only and intends to collect data on radionuclide distribution pattern in soils.

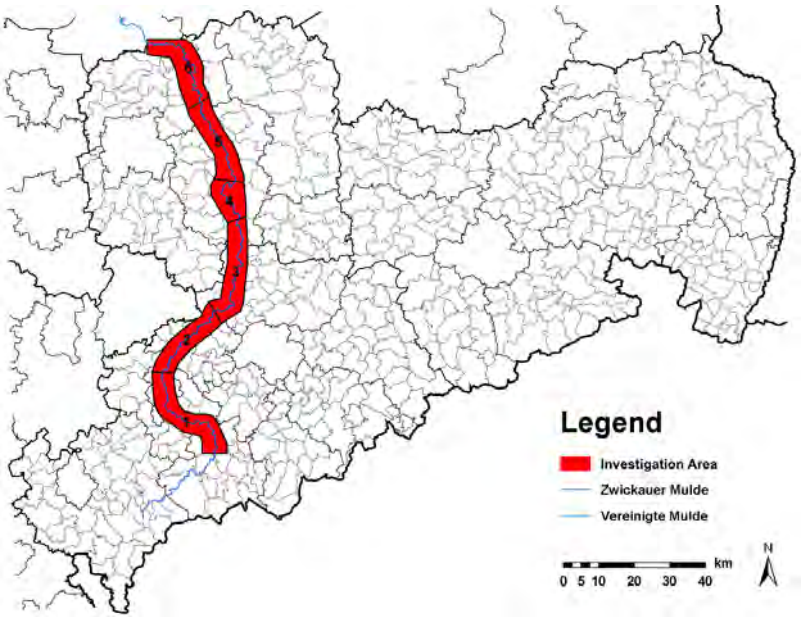

Fig.1. Investigation area at the Zwickauer Mulde and Vereinigte Mulde with its division into 6 sections (Saxony)

Against the background of the phenomena described above, the investigation area (see Fig. 1) is divided into sections with similar properties (downstream):

1	Aue to Mosel	Zwickauer Mulde
2	Mosel to Penig	Zwickauer Mulde
3	Penig to river mouth of Freiberger Mulde	Zwickauer Mulde
4	River mouth of Freiberger Mulde to Nerchau	Vereinigte Mulde
5	Nerchau to Eilenburg	Vereinigte Mulde
6	Eilenburg to boundary of Saxony	Vereinigte Mulde

As a first step the available information was used to identify those areas, which are expected to be contaminated on an enhanced level.

GIS supported pre assessment of sampling areas

In order to identify suitable sampling areas for a systematic investigation of contamination patterns, a GIS supported analysis of the available data was conducted.

As data base for agriculturally used areas was used the land register of the Saxon Regional Office for Agriculture (Sächsische Landesanstalt für Landwirtschaft).

The intensity of influences by the river is assumed directly related to the flood recurrence period. The corresponding data were gained from Saxon State Office

for Environment and Geology (Sächsisches Landesamt für Umwelt und Geologie). The data on frequency, water depth at flood event, retention duration and flow velocity has been evaluated. For further considerations only such areas were selected, which have a flooding depth between 0.5–2 m in a flood event by a flood recurrence period of 5–20 years.

With the GIS data model layers of agriculture area and altitudes of flooding depth between 0.5–2 m were intersected. The received areas are utilized as grasslands (83 %), cropland (15 %) and other culture (2 %), which could be assessed as potentially contaminated.

Areas less than 1 hectare have been excluded from further examination. Could be identified a total number of 280 potentially contaminated areas above 1 hectare. These areas cover 1900 hectare, about 75 % of them are grassland (cf. pic.2).

Further selections were carried out in compliance with choice of preferential sedimentation areas (slip-off slop, meander, and bayou) and equal distribution in the 6 sections of the investigation area.

Preliminarily were selected 50 potentially suitable sampling areas. Picture 3 shows the sampling areas and the potentially contaminated areas.

The results of this GIS supported pre-assessment will be used not only for the selection of sampling areas but also for the transfer of the later results to a more general view.

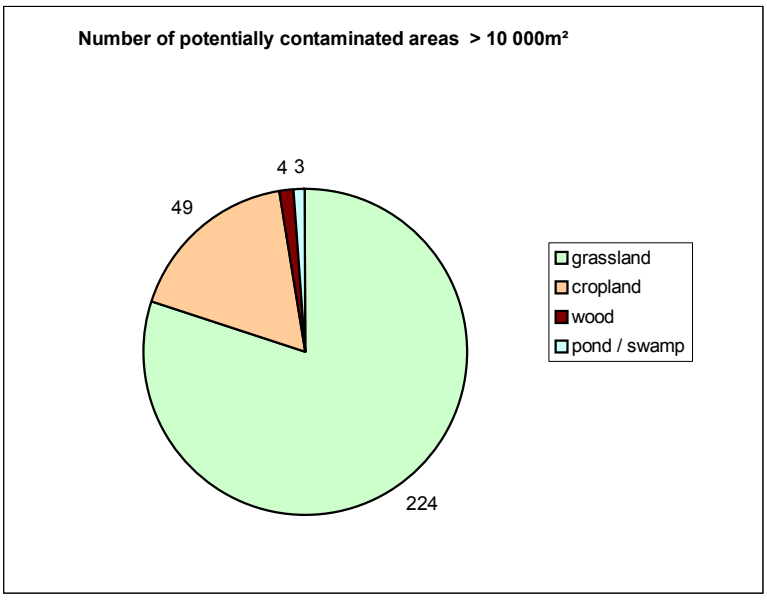

Fig.2. Number of potentially contaminated areas (> 1 hectare) in the investigation area

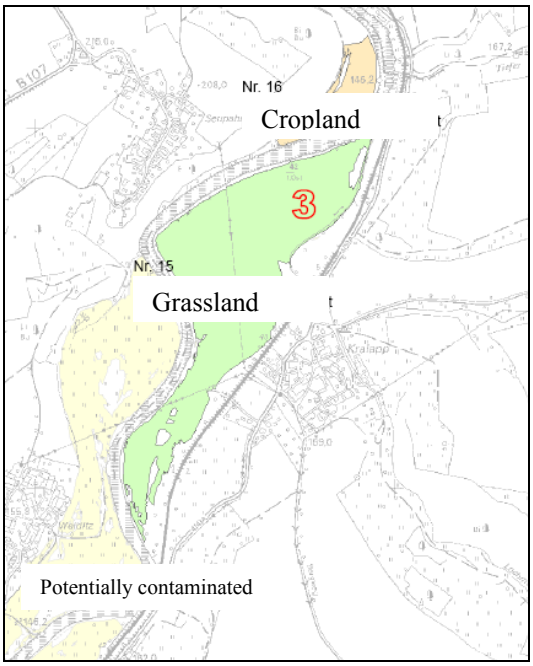

Fig.3. Sampling areas and potentially contaminated areas

Specification of sampling areas

Sampling areas were chosen using data on radionuclide contents from published results of former investigations.

The following data sources have been used:

1. Results of airborne radiation measurements (aero-gamma-spektrometry)
   Specific activities above 16 mg kg–1 uranium were found in section 5 of the investigation area.
2. Investigation of alluvial soils (GRS 1996)
   Alluvial soils were investigated in 1996. Specific activities up to 1400 Bq kg–1 U-238 and 1100 Bq kg–1 Ra-226 were found in section 2 of the investigation area.
3. Atlas of Soils of Saxony (LfUG 2007)
   It is useful to get a general idea of uranium and thorium content of subsoil and topsoil in Saxony.
4. Investigation of river sediments (Michel et al. 2005), (Beuge et al. 1999)
   River sediments in the investigation area have specific activities up to 1000 Bq kg–1 U-238 and 250 Bq kg–1 Ra-226.

Table 1. Sampling areas and land use

crop	Number of sampling areas	Number of soil samples
Wheat	7	14
Barley	5	10
Maize	3	6
Rape	2	4
Grassland	5	10

The final selection of sampling areas had to take into account the legal constraints of accessibility of the land and was carried out by personal inspections of the pre-selected areas.

Field Enquiry, Sampling and Analytics

The final investigation program includes 22 sampling areas close to the rivers of Zwickauer Mulde and Vereinigte Mulde.

Predominantly, agricultural croplands are chosen because of the direct human food intake potentially resulting from these areas. Among these, the areas cultivated with wheat, barley, corn and rape are preferred due to their particular radiological relevance. Extended areas cultivated with further relevant crops like root vegetable have not been found in the floodplains.

From the radioecological point of view the grasslands are related to the human exposure via the pathways grass-cow-milk-human or grass-cow-meat-human. Ploughing does not disturb sedimentation and soil development.

Average samples of surface soil are collected from the 22 sampling areas. In accordance with the actual "German guidelines for the calculation of radiation exposure due to radioactivity from mining activities" (Berechnungsgrundlage Bergbau, BMU 1999), samplings of grassland soils are carried out in depths of 0–10 cm, and sampling of agricultural croplands in depths of 0–30 cm. One average sample of surface soil consists of at least 20 incremental samples. The measurements of dose rate are documented on every sampling point.

2 sampling areas are specified for detailed investigations based on results of average samples of soil (1 wheat field and 1 grassland). Surveying and mapping of dose rate will be carried out. The conditions of sedimentation will be checked by manual drilling (1 m). Small pits will be excavated (1 m) for sampling of soils in diverse depths. Further characteristics of pedology (soil texture, soil type, colour...) will be surveyed using the "German Soil science mapping instruction" (Bodenkundliche Kartieranleitung). The density of soils will be determinated.

Sampling takes part in June of 2008 (grassland and maize) and in August of 2008 (corn and rape). All soil samples will be measured by gamma-spectroscopy. Activity concentrations of the relevant radionuclides will be investigated. Additionally, Cs-137 and Th-230 will be measured.

Conclusion and outlook

At the conference are presented interim results. Exposure calculations will be carried out with the measurements of dose rate and activity concentration. Additional possible paths of exposure are included, which will be checked during the sampling (garden plots, play ground).

References

Beuge, P., Greif, A. , Hoppe, T. et. al. (1999) Die Schwermetallsituation im Muldesystem - Abschlussbericht an das BMBF. Bände I-III, ISBN 3-924330-28-X

Bundesministerium für Umwelt, Naturschutz und Reaktorsicherheit (1999) Berechungsgrundlage zur Ermittlung der Strahlenexposition infolge bergbaubedingter Umweltradioaktivität (Berechungsgrundlagen Bergbau), überarbeitete Fassung vom 07.12.2005.

Bundesinstitut für Risikobewertung (BfR) and Bundesamt für Strahlenschutz (2007) BfR empfiehlt die Ableitung eines europäischen Höchstwertes für Uran in Trink- und Mineralwasser. Gemeinsame Stellungnahme Nr. 020/2007 des BfS und des BfR vom 5. April 2007, download : http://www.bfr.bund.de/cm/208/bfr_empfiehlt_die_ableitung_eines_europaeischen_hoechstwertes_fuer_uran_in_trink_und_mineralwasser.pdf.

Dittrich, B., Klose, R. (2008) Schwermetalle in Düngemitteln - Bestimmung und Bewertung von Schwermetallen in Düngemitteln, Bodenhilfsstoffen und Kultursubstraten, Schriftenreihe der Sächsischen Landesanstalt für Landwirtschaft, Heft 03/2008, download : http://jaguar.smul.sachsen.de/lfl/publikationen/download/3358_1.pdf.

Ettenhuber, E., Gehrcke, K. (2001) Radiologische Erfassung, Untersuchung und Bewertung bergbaulicher Altlasten – Abschlussbericht. Bundesamt für Strahlenschutz, BfS-SCHR-22/01, Berlin.

Friedrich, J. (1991) Uranium und seine Isotope in Flusssedimenten aus von Bergbau beeinflussten Gebieten. Diplomarbeit, Bergakademie Freiberg.

Geller, W., Ockenfeld, K., Böhme, M., Knöchel, A. (2004) Schadstoffbelastung nach dem Elbe-Hochwasser 2002. Endbericht des BMBF Ad-hoc-Projekts „Schadstoffuntersuchungen nach dem Hochwasser vom August 2002 - Ermittlung der Gefährdungspotentiale an Elbe und Mulde“, ISBN 3-00-013615-0, download: http://www.ufz.de/data/HWEnd1333.pdf.

Gesellschaft für Anlagen und Reaktorsicherheit mbH (GRS) and Beak Consultants GmbH (1996) Radionuklidbelastung von Sedimenten und Auenböden - Datenerfassung, Erstauswertung, Ergebnisdarstellung, Freiberg.

Michel, R., Feuerborn, J., Knöchel, A., Miller, F., Ritzel, S., Treutler, H.-C., Tümpling, W. v. , Wanke, C. (2005) Radionuclides in the Mulde River System after the August-2002 Flood. Special Issue: Displacement of Pollutants during the River Elbe Flood in August 2002. Acta hydrochim. hydrobiol. 33/5 (2005) 492-506.

Sächsisches Landesamt für Umwelt und Geologie (LfUG) (2007) Bodenatlas des Freistaates Sachsen, Teil 4 Auswertungskarten zum Bodenschutz.

Radiological Investigation and Ecological Risk of South Coastal Section of Issyk-Kul Lake

Azamat Tynybekov[1], Zheenbek Kulenbekov[2] and Meder Aliev[3]

[1]Intemational Science Center, Department of Ecology, Bishkek, Kyrgyz Republic, azamattynybekov@mail.ru
[2]Kyrgyz Russian Slavic University, Bishkek, Kyrgyz Republic, ji-mi_kulen@yahoo.co.uk
[3]Kyrgyz Russian Slavic University, Bishkek, Kyrgyz Republic, medera@inbox.ru

Abstract. The radiation environment is caused (Tien-Shan mountains) by natural factors and industries activity on extraction and processing of uranium raw material on the territory of republic. After closing and conservation of uranium mines and mine factories there was a plenty of radioactive wastes and tailing dumps on the territory of the Kyrgyz Republic. They are exposed to destruction under the impacts of anthropogenic and natural factors. There is a distribution of radioactive substances on an environment which represents danger to health of the population and to a gene pool as a whole. The given area is located in ecologically adverse zone as inhabitants of this region are exposed both to daily and to potential ecological risk.

Introduction

Investigation and operation of uranium deposits was made from the middle of 40th years, and to the end of 70th years, the extraction of nuclear fuel has been already stopped on the territory of Kyrgyz Republic (fig.1.). For this time the part of uranium deposits has been utilized, and other part has been inhibited. The mountain dumps of radioactive wastes had been formed during prospecting, searching and developing industrial and mountain works on uranium sites (mines (shaft), cuts of career). Owing to operation of uranium deposits, enrichments of uranium raw material have arisen sediment bowls and tailing dams with the big contents of uranium, thorium and other radioactive elements with a lump more than 34 million tons (fig.2.; Hamby & Tynybekov., 1999).

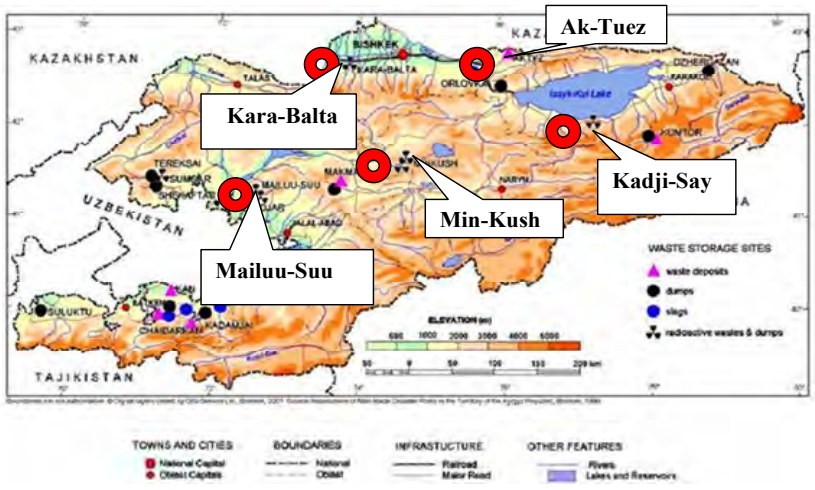

Fig.1. Uranium tailings in the Kyrgyz Republic.

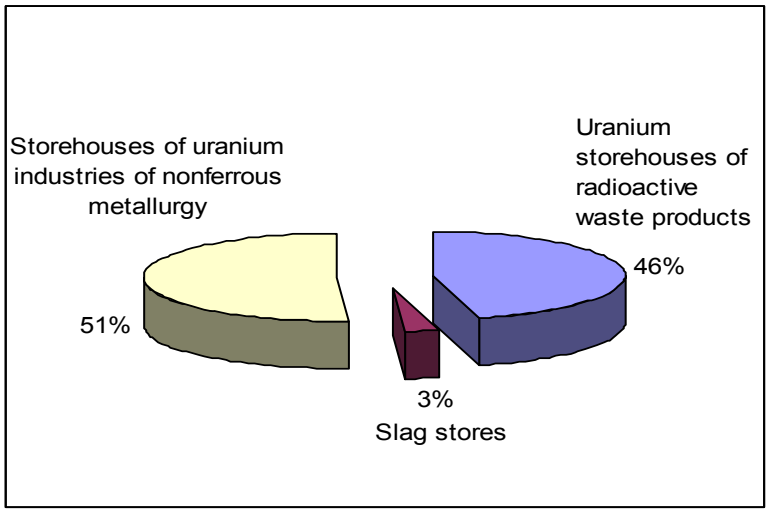

Fig.2. Total amount of uranium tailings in Kyrgyzstan

Our work purpose was to carry out researching the radiation background of southern coastal areas of Lake Issyk-Kul.

The research sites were a coastal zone of Lake Issyk-Kul and settlements. For the achievement of the purpose the following problems had been put:

- To carry out the measurements of a radiation background of researching areas with definition of coordinate characteristics and revealing the ecological condition degree of the territory;

- To investigate the soil structure of researching region on the contents of radioactive elements along the rivers and settlements.
- To present the received results as radioecological maps.

The sites of conducted investigation located in southern coastal area of Lake Issyk-Kul including 7 settlements and 5 rivers (fig.3). in Djety-Oguz and Ton districts. It was studded natural radiation background of locality, as well as defined content of radioactive elements: Thorium (Th), Radium (Ra). 2000 measurements were maid and 400 probes were selected.

Soil probe selection and preparation of them for analyzing according to common accepted method: the probes were selected with envelope method to expect every work which represents a part of soil, which typical for layer of this soil type. In case of controlling the soil pollution of Kadji-Sai tailing dump; the probe areas were outlined along the vectors "wind rose". It was withdrawing 5 probe points of each probe area. Common probe mass of one area was consisting of no more 1 kg. All taken probe were transported in glass container (the weight is 200 grams) until process of analyzing. After probes delivery at laboratory we separated big clods of soil with pistil, cleaning up from the roots, insects, stones, glasses ect. and sifted through sieve with 1 millimeter of hole diameter.

Analysis of soil probe was conducted in radiometric laboratory of Physics Institute, National Academy of Science, Kyrgyz Republic using maintenance of scintillation gamma spectrometer.

This device is aim at measurements activity and concentrations of radioactive isotopes, which are decaying with accompany gamma radiation and allow defining

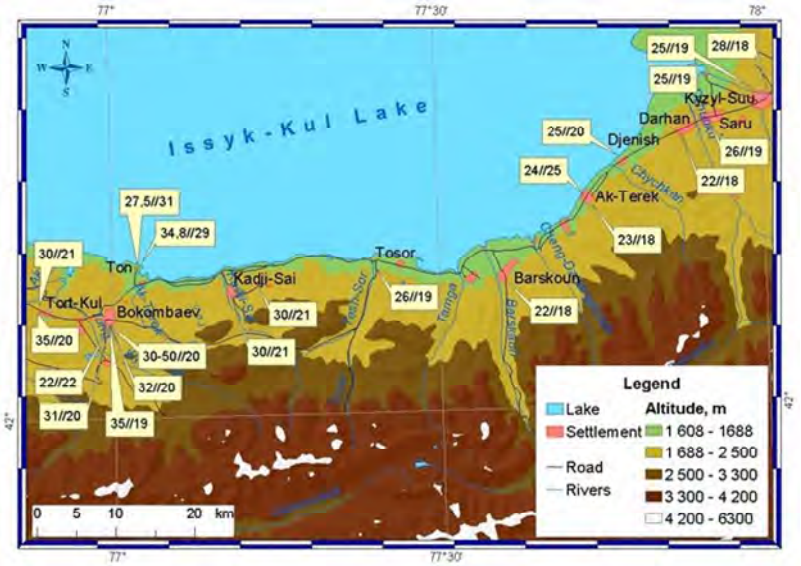

35//19 – *index of internal and external radiation (mcR/hour)*

Fig.3. The targets of conducted investigation in southern coastal area of Issyk-Kul lake.

content of gamma active radionuclides. It was defining the quantity radioactive elements. The common picture of radioactive element (thorium, radium) which content inside of soil in this region was defined under the analyzing results and other data were worked out.

Distribution and processing of obtained data were conducted using personal computer and special softwares.

Also selective measurements of radiation level inside of dwellings in different settlements of Issyk-Kul province were conducted. The selection of investigating houses was casual character, though trying to cover both relatively new and old buildings. (Table1) shows radiation level indices of inside and sort of dwellings including the measurements conducting daytime in fall-summer period. Minimum content of radon was marked due to often ventilation in air of the dwelling. There-

Table 1. Radiation background indices of inside dwellings in different places of Issyk-Kul region.

Coordinates		Locality	Sort of building	Radiation background	
Latitude	**Longitude**			**Inside**	**Outside**
42.73903	77,9764	Ton, northern part of Kuturgu village (v)., reserve	Brick building without roof	18.3E-05	
42.15849	77,14992	State farm «Ton»	New breeze block house	2.75E-05	3.15E-05
42.15849	77,14992	State farm «Ton»	New pise building	3.48E-05	2.89E-05
42.206078	77,685500	Nearby Kuturga v.	Brick building	2.14E-05	1.83E-05
42.206816	77,683890	Ak-Terek v.	New house	2.40E-05	2.49E-05
42.152013	77,037504	Nearby Ak-Terek v.	Fisherman house	2.30E-05	1.806-05
		Bokombaev .	House (yard)	2.20E-05	2,25E-05
		Tort-Kul v.	New house	3.00E-05	2.10E-05
42.115	76,997	«	New pise building	3.50E-05	1.906-05
42.115	76,997	«	Pise building	3.10E-05	2.00E-05
		«	Brick building	3.20E-05	2.00E-05
		«	Two floor house	3.00E-05	
42.148	77,175	Kadji-Sai v.	Old school	1.60E-05	1.90E-05
42.4573	76,1859	Bokombaev v.	Old school		2.00E-05
42.5772	76,6386	“Shahter” summer resort	Building	1.50E-05	
42.681	77,219	Balykchy town	Brick building	2.50E-05	1.80E-05
42.487	78,336	Kosh-Kel v	Pise building with cement base	2.10E-05	1.50E-05
42.488	78,3364	Nearby Karakol town	Pise building	2.10E-05	1.30E-05
42.487	78,336	Karakol town	University building	2.80E-05	1.80E-05
42.468	78,3364	«	Wooden house	6.00E-05	1.80E-05

fore radiological survey of radiation background was conducted inside of dwelling including coordinate characteristics for longitude and latitude, date and time measuring as well as sort of buildings in coastal area of Lake Issyk-Kul.

Methods

The technique of measurement represented simultaneous removal of coordinate values of a site from the help of satellite device GPSR and measurement of a radiating background by exponometer-detector Eberline. During expeditions the parameters of a radiating background were saved in the memory of exponometer-detector. The satellite device automatically fixed with regular frequency a longitude and latitude of a deposit, and also kept these data in the memory.

The places with the increased indications of a radioactivity were determined which were located at the beach near Dzhenish and Tosor villages, a territory of shop №7 near Ton village and tailing near Kadji-Sai village as well.

The increasing of γ-background up to130 mcR/h was revealed on southern coast of Lake Issyk-Kul, on separate sites of the beach in the area of Dzhenish village as well as near Tosor village in same gulf Ak-Chii makes index-103 mcR/h. These anomalies are due to output of poorly radioactive engender which contains thorium and radium elements that are the products of uranium disintegration.

One of such representing danger tailing is located on southern part of Issyk-Kul hollow, on the coast of Lake Issyk-Kul in a lower reaches of the river Kadji-Sai (fig.4.). From the north it is limited to the coast of Lake Issyk-Kul, and from the south - the second lakeside ridge of Terskei Ala-Too. It is in Ton area of Issyk-Kul region. The area of a deposit concerns to high-mountainous, an absolute elevation mark of Lake Issyk-Kul is 1608,8м, actually marks of deposits and working settlements are within the limits of 1700-1850 m, in 1,5 km to the east from Kadji-Sai village in a dry valley.

Kadji-Sai area is the former uranium mine which is settling down near to the of lake Issyk-Kul, had been worked since 1949-1967, it was buried nearby to Kadji-Sai settlement, 2,5 km from the lake Issyk-Kul. About 400 thousand m^3 tailing waste products are stored in Kadji-Sai area and tailing area[2] is 10 thousand m^2, and on other data the volume of tailing weight makes[3] 150 thousand m^3.

Tailing dams contain uranium waste products. Capacity of an exposition doze of radiation scale varies from 30-1500 mcR/h. Tailing dams consist of two parts; one half is built up by economic constructions of an electrotechnical factory, and on other part is located gold dump, creating additional loading tailing dam.

Ashes in dam were small. There was only the ash in waste products.

Any work were not carried out after collapse of the USSR on maintenance of safety and recultivation of tailing practically, that has considerably strengthened the threat on an ecological condition. The constructions have been destroyed and

[2] data given by Torgoev I.A. in 1994

[3] Momunaliev S.M. 1996

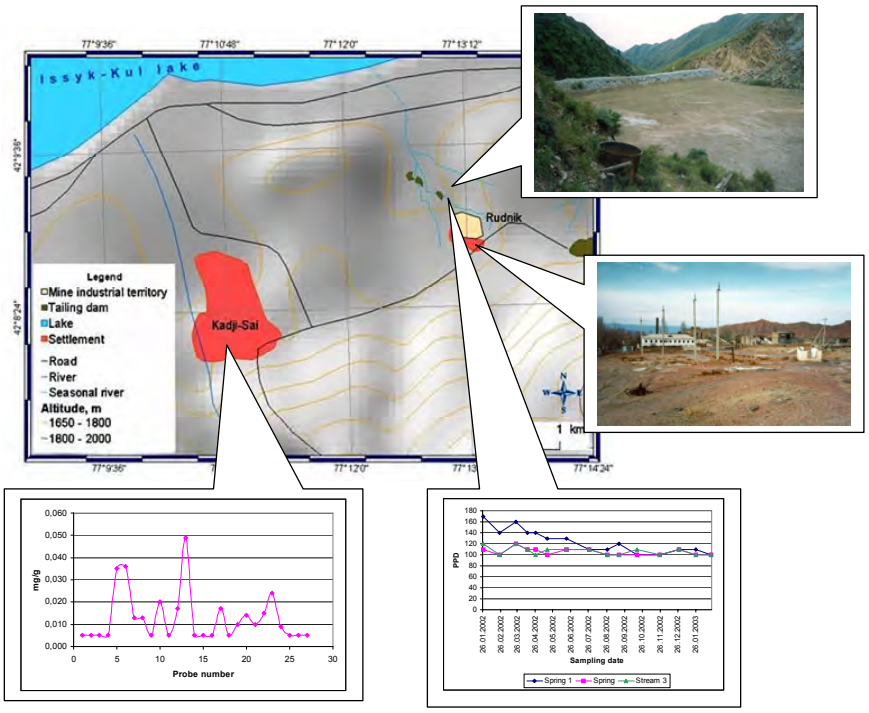

Fig.4. Kadji-Sai uranium tailing dam

drainage channels were covered with slime in connection with the absence of means for repair and regenerative works as well.

The impact of natural and anthropogenic factors on condition of tailing dams

The mine is close to the Lake Issyk-Kul; there is a possibility of danger for lake infection with radioactive waste products.

Now Kadji-Sai tailing and a protective dam are under the natural and anthropogenic impacts, and there is a process of tailing destruction. Mine in Kadji-Sai area is exposed to washout, high waters and landslides which result in carrying out of radioactive materials on the surface that is one of potential polluters of the southern coast of Lake Issyk-Kul.

In 1997 the sites were found out 2-3 meters wide and of 200-300 meters length with a radio-activity up to 300 mcR/h. Storm rains in 1998 also considerably damaged an isolated layer and the tailing dam in Kadji-Sai area is 1,5 km from the coast of the lake, therefore the radiating background on its separate sites has also appreciably increased that had caused the alarm of country public and the nature protection organizations (Tynybekov 2001).

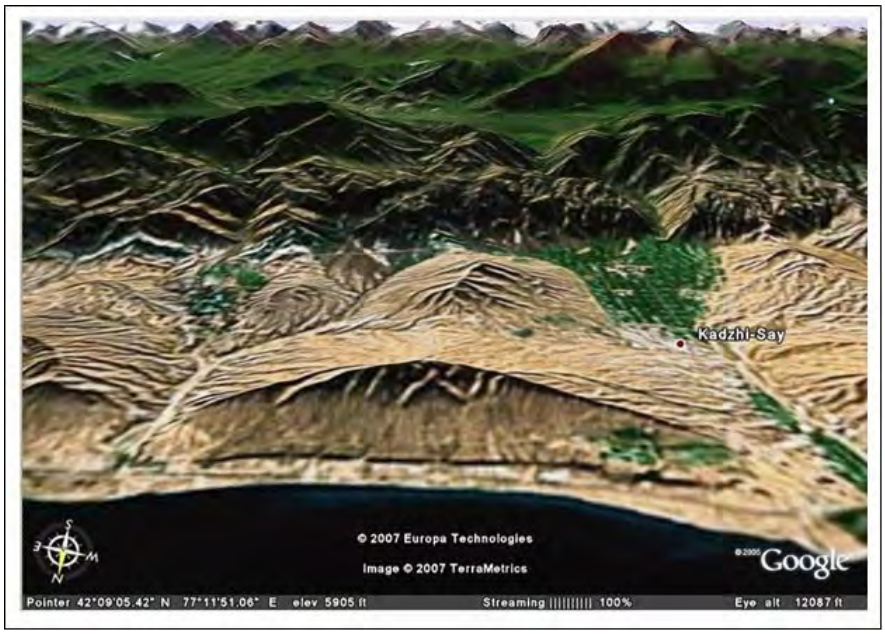

Fig. 5. Satellite images of the Kadji-Sai village and Djilu-Bulak mining territory (Google source)

The unique constraining structure on a site is the dam below. The main thing is tailing dump as the protective dam possesses low stability. The washout of tailing dam will lead to radioactive, chemical pollution of the big water areas of Lake Issyk-Kul. Strengthening of protective dams and construction of new water-currents can be solving a problem only insignificantly.

Ecological risks

Analytical research for susceptibility of radioactive tailings to natural risk was carried out. In our case, we considered the Ton area, where tailing dam in Kadji-Sai area is located. The given area is located in ecologically adverse zone as inhabitants of this region are exposed both to daily and to potential risk (Tynybekov 2001). Satellite images of the Kadji-Sai village and Djilu-Bulak mining territory (it is Google source; fig.5).

Concerning natural process; a valley of the river Tone differs by freshet and mud stream danger. there are 3 lakes (Tuiyk-Tor, Keltor, Korumdy) in it upper altitude which are glacial lakes of outburst-danger. The probability of their outburst is increased with global warming of climate; it was received as a result of research that on Tien-Shan had maximum warming by 0.6^0degree. Per one year it is marked in average to a mountain zone of internal Tien-Shan, minimal is on

0.2^0degree to a high-mountainous zone. The greatest warming is during winter-spring months (1.1^0-0.8^0) and least in July in a high-mountainous zone - 0.1^0degree. For a congelation, Tien-Shan the negative greatest effect in a similar situation renders use in temperature in autumn-spring months on 0.5^0degree, i.e. cause of increase within the period of thawing for 30-40 days that conducts to essential acceleration of thawing of glaciers.

Outburst of lakes may cause high waters along a way of the river the charge is up to 2335 m^2/sec. It is dangerous to the population living near the channel and near the rivers. In a zone of destruction alter the outburst of these lakes we find area near the shore - a part of the Kadji-Sai village. The general area of mudstream danger sites in Ton region makes 0.16 km , with the population more than 200 people. As a result of calculation of a seismic danger degree of Djeti-Ogyz and Ton areas, more seismically dangerous is Ton region. There are 7 settlements (Kadji-Sai, Bokonbaevo and etc.) and 3170 buildings where 22 thousand people live in a zone of 8-ball seismicity in the Ton area.

Local residents search for nonferrous metals do carry out excavation in a radioactive burial ground. Artificial destruction of shielding layer of tailings may result of increasing a radiation background. It is possible, that in non-shielded layer of tailing the polluted water and underlying rocks or coastal sites filtered. There is a threat of radiating infection due to a small outflow of uranium waste products from collapsing radioactive tailings. In our case the dangers of the impact of uranium tailings on an environment in a zone is great at occurrence of ecological failure or an accident as the protective dam has low stability. Washout of tailings will become a result of radioactive and chemical pollution of large territories which may include rivers, arable land, settlements and a coastal zone of the Lake Issyk-Kul. The storm rains in 1998 had strongly damaged isolation layer and a dam of the tailing in 1.5 km from the coast of the lake. The radiation background on separate sites has noticeably elevated (Tynybekov 2004).

According to the medical statistics of the Kyrgyz Republic, the death rate for malignant tumors in the Kyrgyz Republic amounts to 61.7% of deaths for the entire population. However, in the Issyk-Kul region the rate is 81.6 out of 100 patients, a rate of more than 1.5 times higher than for the general population in the Republic. Among the malignant diseases recorded in the Issyk-Kul region the most recorded cause of death is stomach cancer (10%), second is lung cancer (8.6%), third is malignant tumors of lymphatic system (3.9%).

For people living on the southern coast of Issyk-Kul in the Dzhety-Oguz district (78.5 %) and in Karakol town (86.2 %) the death rate among the population exceeds the data for the general Issyk-Kul region (62.9 %), and exceeds the rate for all of the Kyrgyz Republic (61.7 %).

In the Issyk-Kul basin drilling into natural water resources taps into warm water containing normal levels of radon. Large settlements along the shores of the lake and popular recreational resorts have been established. For decades local villagers and guests at Issyk-Kul many health resorts have bathed in this warm water believing it to be healthful for them (Tynybekov et al. 2007).

Results of radiological researches

For finding-out a real radiological situation of the region and studying the section with increased radiation, in 1997-2000 the researches were carried out in Issyk-Kul region under the grant of INTAS (the European Union) and CRDF (USA).

As a result of research it has been found out, that the average data of levels γ-radiation are within the limits of natural radiating background (**NRB)** in most part of the investigated territory, the γ-background does not exceed 20-25 mcR/h, only the increased levels of radiation have been fixed in some local sites.

During scientific-researching works was conducting several expedition on southern coastal section of Issyk-Kul lake while were measuring radiation background and selected water and soil probs. Obtained measurement results of locality were analyzed including coordinate characteristics and map was drawn up for these data, which visually demonstrated common radio-ecological situation in researching areas and locality nearby rivers mouth inflowing lake (fig. 6-7).

The selected measurements of gamma background was made inside of dwelling in different settlements of Issyk-Kul province while implementing the investigation were conducted. The analyzing result showed a significant difference of exposure dose of inside of studding settlements. On fig.3 represents average indices of inside and outside radiation and difference in their levels. The analyzing result showed significant difference of radioactivity level inside of dwelling.

It was defined locality with high radioactivity volumes, which is in the territory of former producing lot No.7 nearby Ton village. The high radioactivity level in different places was interpreted with higher content of radioactive element of thorium.

The results of fulfilled work showed that on investigated territory common outside radiation is in standard limit, but inside radiation level exceed the natural standard in several times.

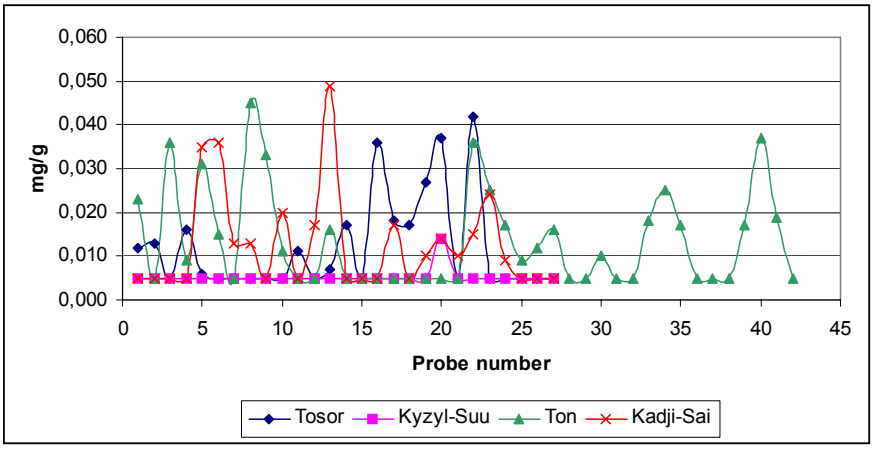

Fig.6. Thorium content in water of south coast of Issyk-Kul Lake (mg/g).

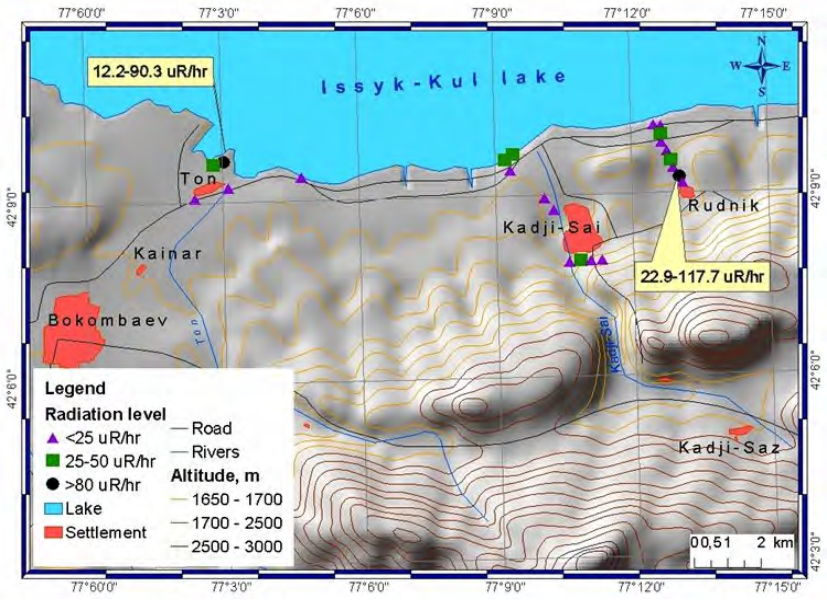

Fig.7. Indication of radiation level near the shop No.7 and tailing dumps

There is the necessity to conduct detailed further investigation to find out reasons high contents of radon in air of dwellings, an ecological risk investigation as well.

References

D.Hamby, A.K. Tynybekov. (1999) "Radiological monitoring of Southern coast of Lake Issyk-Kul". Physics Health. USA. Vol.77, №4: 427 – 430.

Tynybekov A.K. (2001) Radiological researches in a southeast part of Lake Issyk-Kul. International Conference Human Health and Environment. Strategies and Programs in New Millenium, INTAS. Advanced Monitoring Conference Grants, Bishkek, Kyrgyz Republic.: 70-75

Tynybekov A.K. (2001) Problems of influence of radioactive storages on ecology. International conference ECO-INFORMA. Environmental risk the Global Community Argonne National Laboratory., USA. Network Poster N-P7.

Tynybekov A.K. (2004) Research of ecological risk modeling: influence of uranium storage on environment ARW NATO, Baku. Kluwer Academic Publishers, Radiation Safety Problems in the Caspian Region.: 79-84

Tynybekov A.K., Lelevkin V.M., Kulenbekov J.E. (2007) Environmental Problems of the Kyrgyz Republic and Central Asia. ARW NATO. Environmental Change and Human Security. Recognizing and Acting on Hazard Impacts.. The PELL CENTER, Newport, R.I.02840.

Natural occurring uranium nanoparticles and the implication in bioremediation of surface mine waters

Martin Mkandawire[1] and E. Gert Dudel[2]

Dresden University of Technology, D-01069 Dresden
[1] Institute of Materials Science
[2] Institute of General Ecology & Environmental Protection, Tharandt

Abstract. We investigated the fractionation of mobile uranium in surface water from an abandoned uranium-mining site in eastern Germany. The water samples were sequentially ultra-filtrated to fractionate uranium into different sizes and delineate the colloidal and nanoparticle from dissolve U phases. The results revealed that only 20% of total dissolved uranium filtrates were lower than five kDa (i.e. ca. 1-3 nm). Between 30-40% of the total mobile U were either associated with colloids or exist as nanoparticles. Among others, biotic activities contribute significantly to the formation of colloidal or nanoparticle U. Thus, we discuss the implication of natural occurring colloidal and nanoparticle U on bioremediation technology.

Introduction

The immobilization of uranium from the water pathway benefits from reduction from U (VI) to U (IV). The latter is less soluble than the former as a result and reduction result into formation of uranium precipitates that are presumed immobile. The reduction of U (VI) to U (IV) is one of the major processes in aquatic bioremediation of uranium by microorganisms, such as metal-reducing bacteria (Suzuki *et al.*, 2005). The bacteria from the families *Geobacteraceae* and *Desulfovibrionaceae* induced redox-transformations from U (VI) to insoluble U (IV) phase and precipitate iron sulphides (Suzuki *et al.*, 2002). However, the U (IV) precipitates predominately exist as nanoparticles uraninite (UO_2) (Fredrickson *et al.*, 2000; Wielinga *et al.*, 2000). Further, UO_2 species also form abiotically when U (VI) is reduced by Fe (II)-oxides (Dodge *et al.*, 2002). Furthermore, bio-immobilised

U (VI) species are associates with organic colloids especially in form of particulate and dissolve organic mater, iron, and silicon containing colloids. Colloids are defined to be between 1 and 1000 nm, while nanoparticles are between 1 and 100 nm in size (Nowack and Bucheli, 2007). Usually, all filtrates through 0,45µm are soluble fraction per definitionem. A new definition is of truly soluble fraction is imerging as all between 2 nm.

A few studies have shown that colloids are quite mobile in the aquatic system (Guo *et al.*, 2001; Kottelat *et al.*, 2008; Nowack and Bucheli, 2007). This revelation bring a number of question on use of redox-transform from U(VI) to an insoluble U(IV) phase as a mean of immobilising uranium from the water pathway. The questions that rise include does transformation to U (IV) species also adsorption of U on particulate organic matter real mean reduced uranium mobility and reduced ecotoxicity risk? Further, what is the effectiveness of bioremediation of uranium in aquatic system as well as what are limits of using bio-transformation of U (VI) to U (IV) as a main bioremediation process? Disregarding re-oxidation of the solid-phase products for the moment, one issue of great concern for the stability of the product is how unreduced aqueous U (VI) interacts with the precipitating nanoparticles. There are also indications that solid-phase of U (IV) precipitate and organic matter contained large fraction of unreduced U (VI). Hence, the colloids may have transport-facilitating effects on immobile U (IV) and transport-impeding effects on mobile U (VI) (Zänker *et al.*, 2007).

The partitioning of U between dissolved and colloidal phases affects its geochemical behaviour. The variability in the partitioning of U to the colloidal fraction depends on specific water chemistry parameters, U concentrations and composition or concentration of organic matter. Generally, the aquatic colloids, including organic biopolymers and inorganic nanoparticles, are abundant in natural waters, and play a crucial role in regulating the speciation, bioavailability, and mobility in aquatic environments (Guo *et al.*, 2007). In view of this, we investigated the behaviour of dissolved uranium in a tailing pond of a former uranium mine site in Vogtland, eastern Germany where enhanced natural attenuation is facilitated through the association of microorganisms with aquatic macrophyte. The objective of this study was to quantify the colloidal U and consequently assess their mobility in surface mine water.

Material and methods

Mine water sampling

The water used for fractionation of uranium was sampled from two sampling points at wetland ponds of the Shaft 362 of abandoned uranium mine at Mechelgrün close to Neuensalz, Revier Zobes (Vogtland) in south-west of federal state of Saxony in eastern Germany. Immediately after collection, samples were

filtered through a pre-cleaned 1.2 µm pore glass-fibre filter into pre-washed containers. Then, the filtered water samples were transportation to laboratory for uranium fractionation to different sizes using ultrafiltration. The samples were handled according to DIN standards for handling heavy metal contaminated water.

Sequential ultrafiltration

Figure 1 summarises the steps in the ultrafiltration procedure used in the study. At least 5 L of pre-filtered mine water samples were ultrafiltered on a 0.2 µm membrane within 24 h of collection. The ultrafiltration was conducted at high pressure with ultrafiltration membranes with size or molecular weight cut-off of 450 nm, 200 nm, 100 kDa (25 nm), 30 kDa (10 nm) and 5 kDa (1–3 nm).

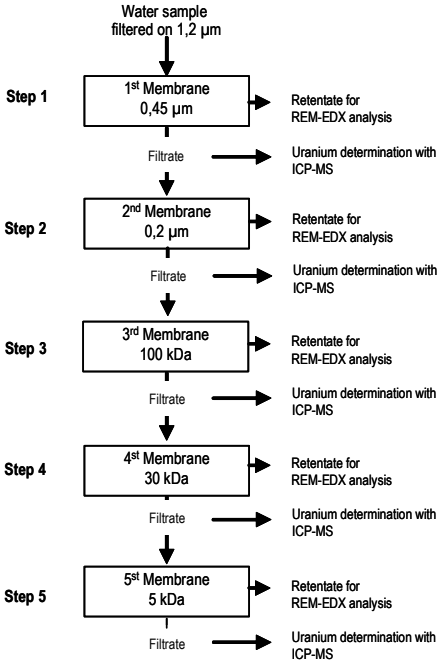

Fig. 2. The sequential ultrafiltration procedure used in the study as per modification from Guo *et al.* (2001)

The permeate flow rates were about 55.6 ml s^{-1} for the 200 nm, 100 and 20 kDa membranes and 7.0 ml s^{-1} for the 5 kDa membrane. Before use, each ultrafilter membrane was soaked in nanopure water overnight and precleaned by ultrafiltering of nanopure water before sample processing. From the onset of the experiment to its conclusion, 20 ml of the permeate were sampled for analysis of uranium, other metals and organic carbon after each ultrafiltration step. The ultrafiltration

procedure used in the current study was modified from Eyrolle and Charmasson (2001) and Guo *et al.* (2007)

Analysis

Filtered water samples on 1.2 µm, 0.45 µm and 0.2 µm, permeates from each ultrafiltration step were analysed for organic carbon, heavy metals and uranium. The samples were then analysed for multi-element using Inductive Coupled Plasma-Mass Spectrography (ICP-MS ELEMENTAL PQ2 VG +, London. England). Total and dissolved organic carbon (TOC and DOC) in the water sampled were determined with FORMACS HT TOC/TN Analyser (Scalar, Breda, the Netherlands). The measurements were conducted according to DIN EN 1484 (1997) Further, Scanning Electron Microscope coupled with EDX (SEM Carl Zeiss, Jena) function was used to characterise the colloid population on the retentants on filter membranes. All reagents in the study were of analytical grade (Suprapur, Merck GmbH Darmstadt, Germany).

Results and discussion

Physicochemical properties of the mine water

To ensure representative samples, selected physicochemical parameters of the mine waters were measured during each field sampling. The Eh, pH, conductivity, temperature, iron and dissolved oxygen concentrations recorded at the two sampling points in the tailing ponds are presented in table 1. The quantity of mobile nanoparticles in surface depended strongly on solution chemistry, including pH, ionic strength, and anions. The maximum particle release occurred at the lowest ionic strength condition, while alkaline pH favours particle release. In general, the colloidal U concentrations decreased with increasing conductivity. Therefore, the pH and conductivity measured in the surface mine water favoured slightly the release of colloids and formation of nanoparticles in the water.

Table 1. Selected physicochemical properties of the mine water during the sampling in the tailing pond at the abandoned uranium mine Neuensalz/Mechelgrün (Vogtland). SP1 was a spring on the tailing dam while SP2 was right in the swamp below.

Parameter	Sampling point	
	SP 1	SP 2
pH	6.8 ± 0.2	7.7 ± 0.5
Conductivity	326 µS cm^{-1}	763.4 ± 185.3 µS cm^{-1}
Eh	326.7 ± 32.5 mV	230.75 ± 24.8 mV

Partitions of the uranium

The concentrations of U in the permeate solutions sampled after every step of ultrafiltration, shows that there is considerable and significant reduction in the concentration as the sequential filtration narrows down low molecular weight, also presumed in size (Fig. 2). This can be attributed to retention of the bigger particles on the filtration membrane. The result shows that highest retention of uranium were on the 30 kDa, which represented the retention of uranium particles size bigger than 10 nm. This suggests that the uranium must be associated with colloidal particles. The second highest retention was followed by 5 kDa, which represents particle fraction size between 1 and 3 nm. However, this the actual retained particle had sizes between 1 and 10 nm. The amounts of organic carbon, heavy metals and uranium measured in permeate of below 2 nm (i.e. 5 kDa) ultrafiltration are the truly dissolved fractions. Those measured between 2–100 nm are nanoparticles, while some of measure within this range extending to 450 nm is colloidal.

The mean colloidal U percentage calculated from concentration differences between initial solution and the permeate solution, reveals that nanoparticle and colloidal U accounted for ca. 30-40% of the total dissolved U in the mine waters with increasing trends in the lower parts of the pond. Apparently, only 23.6±6% is the truly dissolved fractions in the mine waters. It is likely that the complexation of U with DOM rather than with carbonate, which gives the complex a higher ratio of charge to radius, could cause the lower retention and thus the higher permeation of

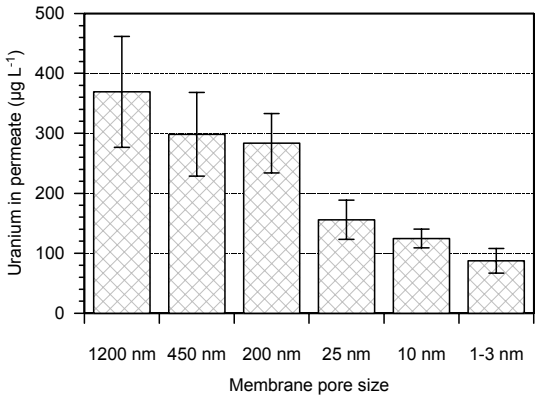

Fig. 3. Uranium fractionation in permeates through membranes of different sizes obtained in sequential ultrafiltration of the mine water. The values of permeate through 1200 nm-pore membrane represents uranium associated with sizes between 450 and 1200 nm; permeate through 450 nm-pore membrane, sizes between 200 and 450 nm; permeate through 200 nm-pore membrane, sizes between 25 and 200 nm; permeates through 10 sizes between, are 10 to 25 nm big; and through 1-3 nm-pore, between 1 and 10 nm big. The values from 1-3 to 25 nm are calibration of relative size to corresponding weights in kDa. All values are mean of four repeated measurements and the bars are standard deviations.

colloidal U (Eyrolle and Charmasson, 2001). Association of dissolved U with colloidal macromolecules (e.g. DOM) and nanoparticles is relatively high. Probably, some fraction of dissolved U may have been classified mistakenly as colloidal due to anionic retention by the ultrafiltration membranes (see discussion below). Nevertheless, the formation of uraninite as well as adsorption of dissolved U on organic macromolecules (e.g., humic acids) or inorganic nanoparticles (e.g., iron oxides) occurs largely in surface mine water environments.

Association of U with other chemical partitions

The relationship of permeate concentration of uranium with other chemical fractions shows that uranium associated highest with the organic carbon particles, followed by iron and silicon containing colloids, then aluminium and calcium containing colloids containing (data not shown). The higher colloidal U fractions in the waters seem to result from complexation of U with natural organic matter. The micrographs of the colloids associated with uranium and separated by a 0.2 µm-pore membrane are shown in Fig. 3. The EDX analysis of colloidal particles and crystal showed high iron containing followed by calcium and silicon. The EDX procedure could not show the organic colloids properly because of carbon coating used as a procedure on SEM.

Thus, the observed association indicates circumstantially that majority of the uranium nanoparticles and colloids had biogenic origin really?, inorganic c is also possible?. Generally, when the DOC concentration generally decreases and the speciation of U is affected significantly by lower DOC concentrations (Guo *et al.*, 2001; Guo *et al.*, 2007; Yoshioka *et al.*, 2007). Decreased DOC concentration and changes in U speciation result in a progressively lower colloidal U fraction.

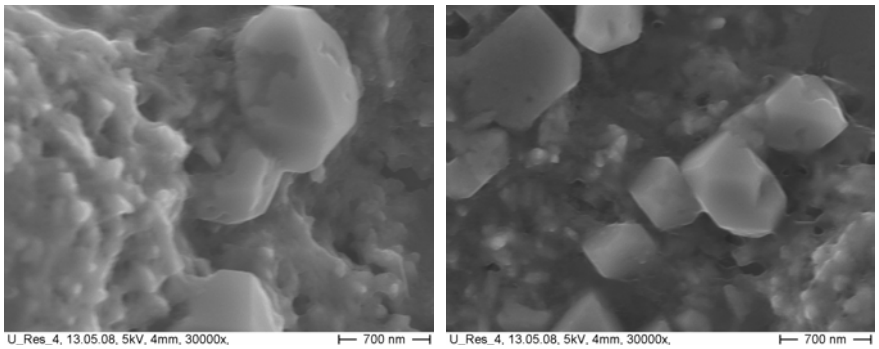

Fig. 4. SEM graphics of crystals and colloidal particles of the retentant on the 0.2 µm-pore filter membrane during the sequential ultrafiltration. The EDX results (not shown) reveal high association of the crystal with uranium

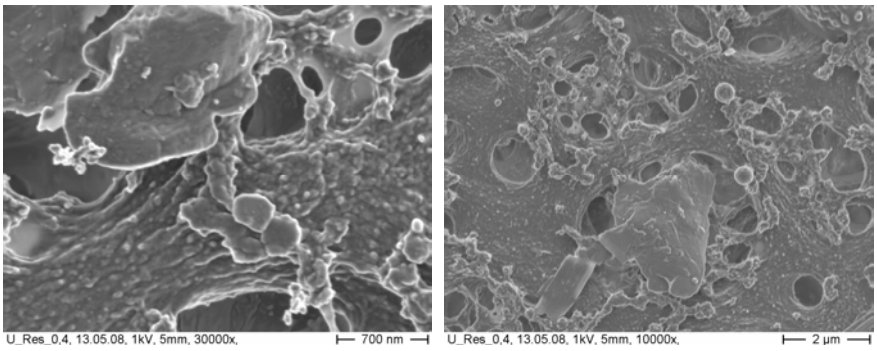

Fig. 5. SEM micrographs of 0.2 µm-pore membrane illustrating that the membrane retained even smaller particles than the pore size.

Limits and reality of the partitioning using ultrafiltration

The results show that the retention of uranium during ultrafiltration is relatively high. On one hand, the higher values suggest that uranium was either mostly adsorbed to colloids or present as nanoparticles. On the other hand, modelling with PhreeqC predicted that major inorganic and organic complexed U species include uranyl carbonato species, such as $(UO_2)(CO_3)_2^{2-}$, $(UO_2)(CO_3)_3^{4-}$, uranyl phosphate, and uranyl fulvates and humates in the surface mine waters. Further, dissolved U species in pure inorganic solutions largely exist as anionic complexes (Guo *et al.*, 2007).These speciation predictions imply that there is a high probability of over estimated the colloidal U fractions, when ultrafiltration issued because of the retention of negatively charged ionic complexes and species.

A few studies have confirmed that presence of negatively charged uranium species in water during ultrafiltration, which results in a higher rejection rate or larger retention of dissolved U by ultrafiltration membranes (Guo *et al.*, 2001; Guo *et al.*, 2007). Thus, there is necessity to confirm the current results using other methods like estimation of the colloidal fractions that are retained regardless of being smaller then the pores with constant permeability models (Guo *et al.*, 2007). Therefore, much as this study show high retention of colloidal and nanoparticle uranium, there should be caution when interpreting colloidal U results from conventional sequential ultrafiltration approach.

Implication of colloidal and nanoparticle uranium on bioremediation

A few dissimilatory metal-reducing microorganisms reduce uranium from soluble U (VI) to insoluble U (IV) concurrently with NO_3^-, Fe^{3+}, and SO_4^{2-} especially in shallow water sediment in surface mine water (Behrends and Van Cappellen, 2005; Fredrickson *et al.*, 2000; Lovley *et al.*, 1993). The U (IV) species mostly ex-

ists as UO_2 nanoparticles (Kumar *et al.*, 2003), which can flow easily with water stream. The soluble U (VI) persists in subsurface environments because of insufficient electron donors to consume dissolved oxygen and stimulate the activity anaerobic respiration of dissimilatory metal-reducing microorganisms (Hofmann *et al.*, 2003; Zänker *et al.*, 2007). Thus, U (VI) is reduced concurrently with Fe^{3+} and prior to reduction of SO_4^{2-}. The other source of uranium nanoparticles in surface mine water is the reduction of aqueous U (VI) by Fe (II). The reaction occurs rapidly in the presence of surfaces, possibly because of changes in the redox potential due to surface complexation. The connection between redox centres is through the crystal lattice (Basnakova *et al.*, 1998; Kelly *et al.*, 2003). The control on the U (VI)-Fe (II) redox reaction is the ability of a two-electron transfer to occur during a single U (VI) complexation reaction (Kohler *et al.*, 1996). Thus, the presence of both inorganic and organic colloids in the water facilitates these processes. Therefore, the uranium nanoparticles and uranium associated with colloids formed in during bio-reduction has important implications for uranium reactivity, fate and effects (Riotte *et al.*, 2003). On the other hand, these tiny particles can be transported with water in environment. Hence, bio-precipitation of uranium through bio-reduction of U (VI) to U (IV) informs of insoluble uraninite cannot be presumed immobile. Likewise, bio-colloidal uranium is still mobile and can be transported from contaminated to uncontaminated sites with the flowing water.

Conclusion

While U dominant and soluble in neutral and alkaline water in form of U carbonatre complexes …The significant retention of uranium on the membranes suggests the existence of natural uranium nanoparticles and colloids in surface waters in abandoned uranium mines. While uranium in natural waters is very soluble and highly mobile as U(VI), the current results suggests that colloidal and nanoparticles uranium do also contribute significantly to uranium mobility in the mine surface water. The results have implication on remediation. The bioremediation of uranium by metal-reducing bacteria involves microbial-induced redox-transformations from U (VI) to an insoluble U (IV) phase, which exists predominately as nanoparticles of UO_2. Further, solid-phase U (IV) precipitate actually contained a large fraction of unreduced U (VI). Furthermore, uranium is adsorbed on bio-colloids. The uranium nanoparticles are likely to be mobile and they can be easily transported as flocculation in the aquatic environment. Therefore, this is new realisation a challenge to bioremediation of uranium because insoluble uraninite likewise uranium adsorbed on bio-colloids can be immobile.

Acknowledgement

The authors pay tribute to Mr. Jörg Schaller and Mr. Lothar Keydel for water sampling.

References

Basnakova, G., Stephens, E.R., Thaller, M.C., Rossolini, G.M. and Macaskie, L.E., (1998) The use of Escherichia coli bearing a phoN gene for the removal of uranium and nickel from aqueous flows. Applied Microbiology & Biotechnology, 50(2), 266-272.

Behrends, T. and Van Cappellen, P., (2005) Competition between enzymatic and abiotic reduction of uranium(VI) under iron reducing conditions. Chemical Geology, 220(3-4), 315-327.

Dodge, C.J., Francis, A.J., Gillow, J.B., Halada, G.P., Eng, C. and Clayton, C.R., (2002) Association of Uranium with Iron Oxides Typically Formed on Corroding Steel Surfaces. Environ. Sci. Technol., 36(16), 3504-3511.

Eyrolle, F. and Charmasson, S., (2001) Distribution of organic carbon, selected stable elements and artificial radionuclides among dissolved, colloidal and particulate phases in the Rhône River (France): Preliminary results. Journal of Environmental Radioactivity, 55(2), 145-155.

Fredrickson, J.K., Zachara, J.M., Kennedy, D.W., Duff, M.C., Gorby, Y.A., Li, S.-m.W. and Krupka, K.M., (2000) Reduction of U(VI) in goethite ([alpha]-FeOOH) suspensions by a dissimilatory metal-reducing bacterium. Geochimica et Cosmochimica Acta, 64(18), 3085-3098.

Guo, L., Hunt, B.J. and Santschi, P.H., (2001) Ultrafiltration behavior of major ions (Na, Ca, Mg, F, Cl, and SO4) in natural waters. Water Research, 35(6), 1500-1508.

Guo, L., Warnken, K.W. and Santschi, P.H., (2007) Retention behavior of dissolved uranium during ultrafiltration: Implications for colloidal U in surface waters. Marine Chemistry, 107(2), 156-166.

Hofmann, T., Baumann, T., Bundschuh, T., Kammer, F., Leis, A., Schmitt, D., Schäfer, T., Thieme, J., Totsche, K.-U. and Zänker, H., (2003) Aquatische Kolloide I: Eine Übersichtsarbeit zur Definition, zu Systemen und zur Relevanz. Grundwasser, 8(4), 203-212.

Kelly, S.D., Newville, M.G., Cheng, L., Kemner, K.M., Sutton, S.R., Fenter, P., Sturchio, N.C. and Spotl, C., (2003) Uranyl incorporation in natural calcite. Environmental Science & Technology, 37(7), 1284-1287.

Kohler, M., Curtis, G.P., Kent, D.B. and Davis, J.A., (1996) Experimental invesitgation and modelling of uranium (VI) transport under variable chemical conditions. Water Resources Research, 32(12), 3539-3551.

Kottelat, R., Vignati, D.A.L., Chanudet, V. and Dominik, J., (2008) Comparison of Small- and Large-scale Ultrafiltration Systems for Organic Carbon and Metals in Freshwater at Low Concentration Factor. Water, Air, & Soil Pollution, 187(1), 343-351.

Kumar, D., Bera, S., Tripathi, A.K., Dey, G.K. and Gupta, N.M., (2003) Uranium oxide nanoparticles dispersed inside the mesopores of MCM-48: synthesis and characterization. Microporous and Mesoporous Materials, 66(2-3), 157-167.

Lovley, D.R., Widman, P.K., Woodward, J.C. and Phillips, E.J.P., (1993) Reduction of Uranium by Cytochrome C3 of *Desulfovibrio vulgaris*. Applied and Environmental Microbiology, 59(11), 3572-3576.

Nowack, B. and Bucheli, T.D., (2007) Occurrence, behavior and effects of nanoparticles in the environment. Marine Chemistry, 107, 156-166.

Riotte, J., Chabaux, F., Benedetti, M., Dia, A., Gerard, M., Boulegue, J. and Etame, J., (2003) Uranium colloidal transport and origin of the 234U-238U fractionation in surface waters: new insights from Mount Cameroon. Chemical Geology, 202(3-4), 365-381.

Suzuki, Y., Kelly, S.D., Kemner, K.M. and Banfield, J.F., (2002) Radionuclide contamination: Nanometre-size products of uranium bioreduction. Nature, 419(6903), 134-134.

Suzuki, Y., Kelly, S.D., Kemner, K.M. and Banfield, J.F., (2005) Direct Microbial Reduction and Subsequent Preservation of Uranium in Natural Near-Surface Sediment. Applied and Environmental Microbiology, 71(4), 1790-1797.

Wielinga, B., Bostick, B., Hansel, C.M., Rosenzweig, R.F. and Fendorf, S., (2000) Inhibition of bacterial promoted Uranium reduction: Ferric (Hydr)oxide as competitive electron accepter. Environ. Sci. Technol., 34, 2190-2195.

Yoshioka, T., Mostofa, K., Konohira, E., Tanoue, E., Hayakawa, K., Takahashi, M., Ueda, S., Katsuyama, M., Khodzher, T., Bashenkhaeva, N., Korovyakova, I., Sorokovikova, L. and Gorbunova, L., (2007) Distribution and characteristics of molecular size fractions of freshwater-dissolved organic matter in watershed environments: its implication to degradation. Limnology, 8(1), 29-44.

Zänker, H., Ulrich, K.-U., Opel, K. and Brendler, V., (2007) The role of colloids in uranium transport: a comparison of nuclear waste repositories and abandoned uranium mines. In: Cidu, R. and Frau, F. (Editors), IMWA Symposium 2007: Water in Mining Environments, Cagliari, Italy.

Treatment of historical uranium contaminated radioactive waste at necsa for disposal

J.J. Badenhorst and W Meyer

Nuclear Waste Research, South African Nuclear Energy Corporation (NECSA), PO Box 582, Pretoria, South Africa, JacobaBadenhorst@necsa.co.za

Abstract. Uranium containing effluents generated in research laboratories at the South Africa Nuclear Energy Corporation (NECSA) was deemed as low level waste and due to the quantities was stored in containers. These waste typically included solvents from analytical laboratories, from fuel reprocessing research and enrichment operations.

In 2005, the policy on the management of radioactive waste in South Africa (DME, 2005) forced the treatment of these effluents as a long term solution. Options that were considered included: development of long-term storage containers, reprocessing/purification of the effluent or the encapsulation for disposal in a geological repository.

The purpose of the research is to evaluate the possibility of recovering uranium from the different historical uranium contaminated effluent (acidic, alkaline, organic, surfactants, detergents etc.) with newly developed ion exchange materials for final disposal. Research results will be presented regarding the recovering of uranium from these “troublesome” waste streams.


Uranium Mining
and Hydrogeology

Peat deposits as natural uranium filters? - First results from a case study in a dolomitic gold mining area of South Africa

Frank Winde

North West University, School of Environmental Sciences and Development, Private Bag X6001, Potchefstroom, 2520, Republic of South Africa

Abstract. Associated with a karst spring which drains a large system of interconnected dolomitic aquifers the studied peatland is the single most important water source for a downstream municipality. Owing to the reported ability of peat to remove U and other heavy metals from polluted waters it is anticipated that the GMB peatland may potentially serve as a natural buffer between polluting mines upstream and downstream users. Based on long-term water quality trends, real-time observations and geochemical data indications for U-pollution at the peatland are presented and associated sources, pathways and transport mechanisms discussed.

Introduction

Peat consists of partially decomposed wetland plants accumulating in waterlogged environments where complete mineralization cannot be achieved. With 99% of all known peat deposits being located in humid regions of the northern hemisphere peat in southern Africa is a generally scarce resource. This is particular true for the semiarid interior plateau of South Africa where the studied peatland is located. The peatland owes its existence mainly to a strong perennial discharge of groundwater from the Gerhard Minnebron (GMB) Eye (spring) and can thus be classified as a karst fen. The water is mainly used by local farmers and feeds into the water supply system of Potchefstroom with some 300.000 people.

The GMB eye is one of the lowest lying outflow points of an extensive system of interlinked dolomitic karst aquifers (called ‘compartments’) a number of which is severely impacted on by deep level gold mining operations. Apart from large-scale dewatering of three of the compartments which lowered the groundwater table by up to 1000m in places this also includes pollution of dolomitic groundwater

through filling caves and sinkholes connected to the aquifer with uraniferous tailings, discharging polluted effluents into the Wonderfonteinspruit (WFS) as main drainage of the dolomites as well as through significant volumes of seepage flowing from tailings deposits directly into the underlying karst aquifer. While the possibility of mining-related water pollution of the GMB spring has been discussed in previous studies, the actual extent, exact sources as well as pathways and mechanisms are still largely unknown (Wolmarans 1978, Grundling 2002, Bredenkamp 2007).

Using C^{14}-based age determination fairly consistent accumulation rates of around 0,3mm/a were found with the oldest sample at 4,5m depth dating back almost 11.800 years. Since 1993 an estimated 60% of the peat has been extracted from the wetland mainly for mushroom production (casing substrate) and as enhancer for horticultural soil. In view of the rapid destruction of a potentially beneficial resource the Department of Water Affairs and Forestry (DWAF) commissioned a study to assess associated environmental impacts (Winde 2007).

Of particular interests in this regard is a potential function of peat to buffer possible mining-borne pollution through its widely reported ability to remove U and other contaminants from the water phase (Owen and Otton 1995; Brown *et al.* 2000, Ringquist and Oeborn 2001, Ringquist *et al.* 2001, Coggins *et al*. 2005, Van Roy et al. 2006). Such buffer function could be vital in a possible (worst case) post-mining scenario where the GMB eye is expected to be one of only three karst springs through which large volumes of highly contaminated mine water may surface from a vast system of flooded underground mine voids (Winde *et al.* 2006).

In this paper first results of the study are presented including a brief characterisation of the hydrogeological setting of the GMB peatland and potential U-loads affecting the associated karst aquifer. Based on this indications for U-pollutions as found in previous studies are presented and compared to own findings. The latter include a preliminary quantification of the total contribution of the peatland system to the downstream water supply system, geochemical data and *in-situ* observations of hydrodynamic processes including responses to events such as heavy rainfall.

Hydrological and hydrogeological conditions

The GBM eye together with the upper and lower Turffontein eyes is one of three major outflow points of dolomitic groundwater from a large karst aquifer called ‘Boskop-Turffontein Compartment’ (BTC). This compartment is the largest and lowest lying one in a succession of several others located further up in the Wonderfonteinspruit (WFS) catchment. Separated from each other by near impervious, north-south trending syenite and dolorite dykes these compartments used to feed large volumes of dolomitic groundwater via so-called eyes (karst springs) into the WFS as reflected in its Afrikaans name (‘Miraculous Fountain Stream’). Originating south of the sub-continental divide near Krugersdorp the 90km-long WFS runs over approx. 80km across several dolomitic compartments to finally join the upper

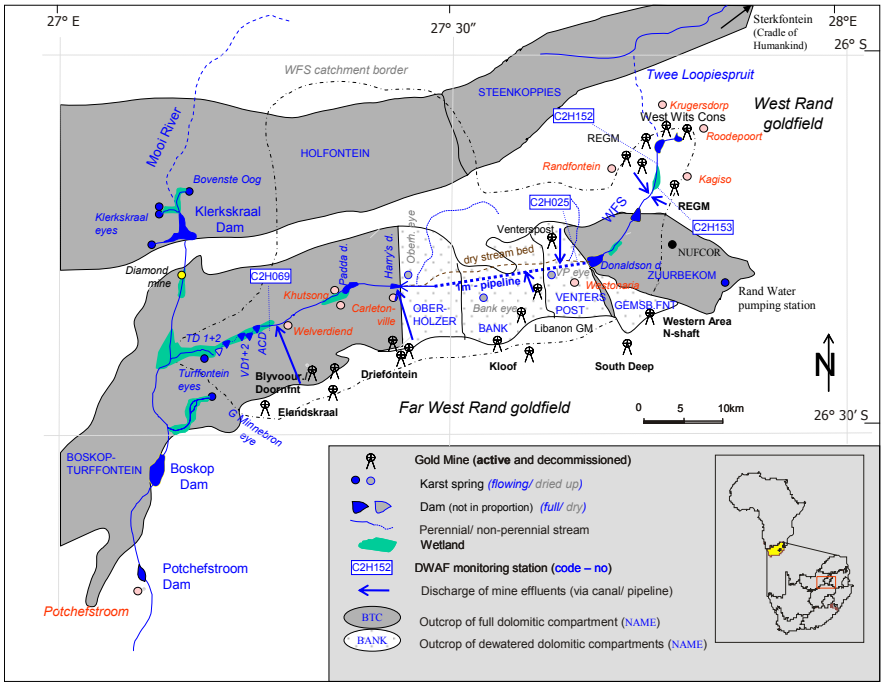

Fig. 1: The Study area

Mooi River. The GMB peatland however falls outside the (surface) catchment of the WFS and feeds via an unnamed stream (here called GMB-stream) also in to the upper Mooi river, some 4km upstream of Boskop Dam as main reservoir for the water supply of some 300.000 people of the Potchefstroom municipality (Fig. 1).

Most of the groundwater is stored in the upper 40-100 m of the outcropping Malmani dolomite in what is termed the ‘cavernous zone’. This zone consists of a network of caves and cavities interconnected by solutions slots, underground channels and fractures totalling a storage capacity which exceeds that of the full Vaal Dam (as second largest dam in SA) by several times. The 2,6 bn years old dolomite has been subject to exceptionally extensive karstification resulting in the five longest caves in southern Africa being in the WFS catchment and a number of eyes (karst springs) which are amongst the strongest in the southern hemisphere (Swart *et al.* 2003a and b).

Owing to large volumes of dolomitic groundwater pushing into underlying mine workings deep level gold mines soon embarked on the ‘dewatering’ of dolomitic compartments in order to reduce the excessive costs for pumping the water from depths of up to 3km back to surface. Dewatering was effected by pumping out more water from the receiving mine void than the karst aquifer could naturally be recharged lowering the groundwater table by up to 1000m in places. Consequences of the large-scale dewatering included the drying up of four springs with a total discharge of approximately 135 Ml/d as well as irrigation boreholes as

predicted but also some unforeseen effects such as the wide-spread occurrence of sinkholes and dolines often with disastrous effects on people's live and infrastructure (Swart *et al.* 2003 b). During an above average wet period in the mid 1970s many sinkholes had formed right in the stream channel of the WFS diverting large volumes of stream water directly into the underlying mine void partly defeating the original purpose of dewatering. In order to counteract the increased recharge in 1977 the stream was diverted into a 32 km-long pipeline carrying the water across the three dewatered compartments (Venterspost, Bank and Oberholzer) to the non-dewatered BTC. From here on the WFS runs for the last 35km or so in its original stream bed (Fig. 1).

Currently gold mines pump approximately 113 Ml/d back into the WFS while using some of the abstracted groundwater for internal purposes such as tailings disposal.

Apart from severe impacts on the surface water system through the drying up of springs, diversion of stream flow and changing natural runoff characteristic, deep level gold mining also irreversibly changed the hydrogeological system by mining through the dykes.

With more than 43km of tunnels, through fares etc. running through dykes mining hydraulically linked previously separate compartments (derived from Swart *et al.* 2003a). This also applies to the full (non-watered) BTC which is now connected to three dewatered compartments upstream forming one single Mega-compartment'. In a future rewatering scenario this results in the final water level being controlled by the elevation of the lowest lying springs i.e. the two Turffontein eyes, the GMB eye and possibly some smaller eyes near Boskop dam. With the GMB spring being the largest low lying spring it will form a major decant point for polluted mine water, which after the cessation of mining and subsequent rewatering, will emanate from the vast network of flooded mine voids. While the three springs together currently yield a total of approx. 80 Ml/d (of which close to 80% come from the GMB eye) this could well rise to over 200 Ml/d. Judged by the extreme poor water quality of water decanting from the flooded mine void in the head water region of the WFS where pH values <2 and U-concentrations of 16 mg/l have been measured, such concentrated outflow could have catastrophic consequences for downstream water users and the environment (Winde *et al.* 2006).

Analyses of recent satellite imagery have revealed that the WFS over past few years did not reach the Mooi River but dried up some 12-16 km upstream of the confluence. Entering the BTC with an average flow rate in the region of >100 Ml/d it is suspected that most of the stream water is lost to the underground karst aquifer in from of so-called 'bed loss' recharging the BTC (losses through evaporation are assumed to be counterbalanced by sewage effluent discharge from several municipalities such as Carletonville, Khutsong and Welverdiend).

It was further established that the GMB spring is not the only source of water for the downstream peatland but that artesian groundwater discharge in the upper part of the wetland through sub-aquatic springs and diffuse seeps also contributes significantly. With approximately 100 Ml/d this contribution is of same order of magnitude as the actual spring flow rendering the GMB peatland system the single most important water source for Potchefstroom (Winde 2007).

In view of the relatively high levels of U-pollution detected in the WFS catchment (IWQS 1999, Wade *et al.* 2002, Coetzee *et al.* 2002, Du Toit 2006, Barthel 2007, Coetzee *et al*. 2006) such filter function may be of importance under current conditions. Under the extreme conditions of the above-mentioned worst case rewatering scenario, however, it is questionable whether the remaining peat deposits at GMB could retain any significant amount of the large contaminant load, which in the case of U alone could initially amount to approximately 1000 kg/d (100 Ml/d at 10 mg U/ l). Given the very limited hydraulic conductivity of peat it is also questionable whether volumes totalling >200 Ml/d could effectively filter through peat in the first place.

Uranium pollution: extent, sources and pathways

The Wonderfonteinspruit

U in the WFS area mainly originates from mined gold reefs (ore bodies) where it is associated with Au. Owing to above average U-grades compared to other (also low grade) ore bodies in SA many gold mines in the West Rand and Far West Rand also produced U as a by-product. Recently local gold mines receives competing offers from various national and international interest groups participating in the current U-renaissance to rework their tailings dams and extracting U. While uraniferous slimes dams (as tailings deposits are called in SA) were generally seen as an environmental liability in the past with not much reference to the actual U-levels being made, they are now perceived as assets highlighting their above-average U-grades (Hill 2007, 2008 a and b).

This coincides with mining related U-pollution in the WFS catchment receiving extraordinary media attention often sensationalizing alleged health effects on residents, downstream water users, animals and crops. While effects of U-pollution on health are still largely un-quantified and mainly based on anecdotal and circumstantial evidence sound scientific evidence exists for the significantly elevated levels of U especially in aquatic environment of the WFS catchment (Faanhof *et al.* 1995, Kempster *et al.*, 1996, IWQS 1999, Wade *et al.* 2002, Coetzee *et al*. 2006, Du Toit 2006, Barthel 2007).

An overview of U concentrations as found in a screening survey is shown in Fig. 2.

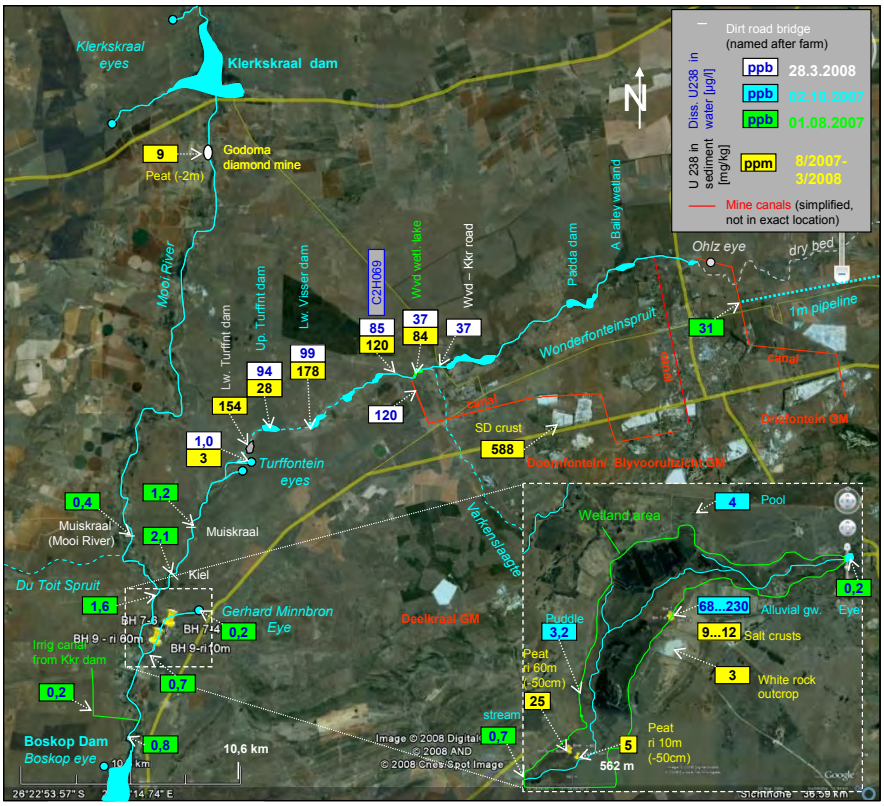

Fig. 2: Uranium concentrations in water and sediment samples taken during screening surveys conducted between August 2007 and March 2008 (map base: Google Earth, 14.6.2008)

In case of bed loss from the WFS constituting a major water source for the BTC the possibility of associated U-pollution of the receiving aquifer is a major concern. In the most comprehensive study to date in terms of water analyses, weekly water samples (later monthly) were taken over a period of a full year at several point along the WFS. Maximum U-concentration detected in stream water of the WFS ranged from >400µg/l in the head water region (C2H152) to >200 µg/l in the lower WFS (C2H157) (Fig. 1). U-concentrations in mine effluents, as a major U-source reached up to 2600 µg/l (IWQS 1999). A survey conducted as part of the project between August 2007 and March 2008 confirmed that little has changed regarding the overall patterns of water contamination along the WFS (Fig. 2).

Owing to the diversion of approx. 30 Ml/d of highly polluted decant water from the flooded mine void of the West Rand goldfield (also known as 'Western Basin') into the WFS (after treatment) U-levels in the head water region recently rose again resulting in an estimated 1400 kg U/a (60µg/l at 65Ml/d) being exported via the 1m-pipeline directly onto the BTC (based on data from Dorling 2008). Com-

pared to a load of approx. 500 kg/a in 1997 (31,4 µg/l at 45Ml/d) this is an increase of some 900 kg U/a (IWQS 1999). The contribution from decant water is in addition to U originating from mining residues that cover a large proportion of the head water catchment.

Right where the WFS starts flowing on the BTC its receives a second major U-input in form of mines effluents from the Driefontein gold mine adding another 1200 kg U/ a (estimated based on average U-concentration of 126 µg/l in 1997 as per IWQS 1999 and an exceptionally low discharge of only 26 Ml/d in this year). Based on the normal discharge of some 50Ml/d the associated U load is well over 2300 kg/d.

The last direct U-input into the WFS is received via two canals from the Blyvooruitzicht and Doornfontein GM area discharging mine effluents as well as stormwater run off. The latter frequently also carries considerable amounts of eroded tailings material. Based on 2008 data this area adds some 400 kg/a to the total load of the stream (120 µg/l at 10Ml/d). Counting only the U-input associated with the direct discharge from the three major mining areas mentioned the WFS receives over 4t of dissolved U per annum.

In view of the recent discovery that most of the time the stream flow does not reach the Mooi River it can be concluded that all of the received U must either be stored in the fluvial systems (i.e. immobilized in aquatic sediments and floodplain soils etc.) or be diverted into the karst aquifer underlying the stream bed or both. Several sampling programmes recently conducted in the lower WFS indicated that significant amounts of U indeed accumulated in fluvial sediments especially in dams downstream of Welverdiend (Fig. 1). With close to 1000ppm U such sediments by now display higher U-levels than the mined ore and the tailings as original sources of the U-pollution. Winde (2006 b) discusses a number of site-specific mechanisms enabling shallow farm dams to remove dissolved U from stream water more effectively than other parts of the stream resulting in above average sediment contamination. Sediments in the Coetzee dam downstream of Welverdiend contain an estimated 6t of U (based on data in Coetzee *et al.* 2002). Compared to the estimated load it received over the past 40 years of its existence (some 64t, 100 µg/l at 44 Ml/d) this constitute approx. 9% of the total U-influx. Owing to site specific peculiarities it is likely that this rate of U-immobilisation is exceptionally high compared to other parts of the fluvial system. With most of the >100Ml/d of the WFS stream flow gradually disappearing into the cavernous dolomite it can thus be estimated that some 90% of the U-load also enter the BTC aquifer (i.e. 10% are retained in sediments). This would result in close to 2200 kg of dissolved U polluting the dolomitic groundwater of the BCT.

Boskop-Turffontein Compartment – Gerhard Minnebron peatland

With an est. 400km² of surface catchment area the three mentioned eyes in the BTC have an appreciable potential to dilute U-inputs from the WFS (Winde 2007).

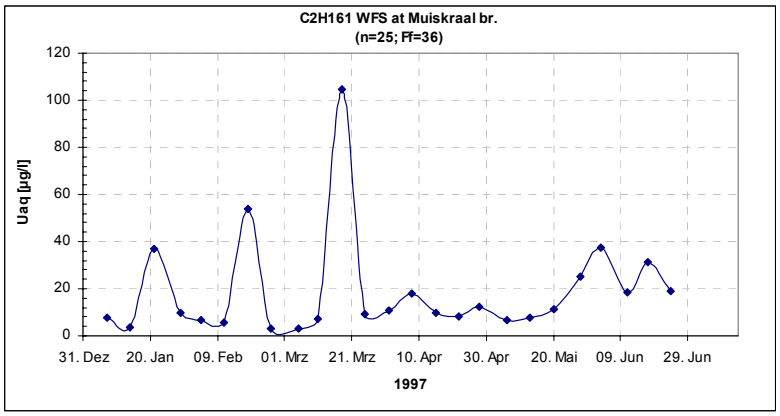

Fig. 3: Dynamic of U-concentration of exfiltrating groundwater in the lower WFS (Muiskraal bridge, DWAF measuring point C2H161; Data source: IWQS 1999)

However, data for the Turffontein eyes, which are the closest to the WFS channel system and thus most likely to be affected first, suggest that U-levels are temporarily elevated to 10-20 times the natural background level reaching maxima of up to 7 µg/l (average 0,9µg/l; n=31; IWQS 1999). Moreover, in our screening survey it was found that the U-concentrations steadily increase downstream of the eye from 1µg/l to 2,1µg/l possibly through contributions of groundwater diffusely exfiltrating in the lower lying parts of the stream channel near the confluence with the Mooi River. U-concentration measured in a weekly monitoring program of the Blyvooruitzicht GM for the period February 2003 to March 2006 displays significantly higher U-levels fluctuating from 1 to 172 µg/l. On average the groundwater-fed stream in this part of the BTC contained 13 µg/l (n=105) (Blyvooruitzicht GM 2008). With 18,7 µg/l an even higher U-level was measured in 1997 at the nearby station C2H161 (at Muiskraal bridge, Fig. 2) in 1997 (IWQS 1999). This constitutes an estimated U-load of >200 kg U/ a (est. flow rate of 30 Ml/d) , equaling some 5% of the estimated load the BTC receives further upstream through seepage from the WFS. The wide range of U-levels at this point fluctuating between 2,9 and 104 µg/l could be indicative of an event-driven pollution regime. This is supported by most U-peaks occurring during the rainfall season (Fig. 3)

In the absence of flow data U-concentration in the different stream components can used to assess mixing ratios. With 1,6 µg/ l U in stream water after the confluence with the Mooi River the contribution of water from the WFS catchment is close to 75% of the total flow in the combined stream (at the time of sampling) and this despite the fact the WFS dried up well above the Turffontein springs. It is therefore likely that in the confluence area additional groundwater discharge from the BCT occurs which increases stream flow in the lower Mooi River. Such discharge of groundwater is also suggested by satellite imagery showing significantly darker wetlands commonly associated with inundated areas (Winde 2007).

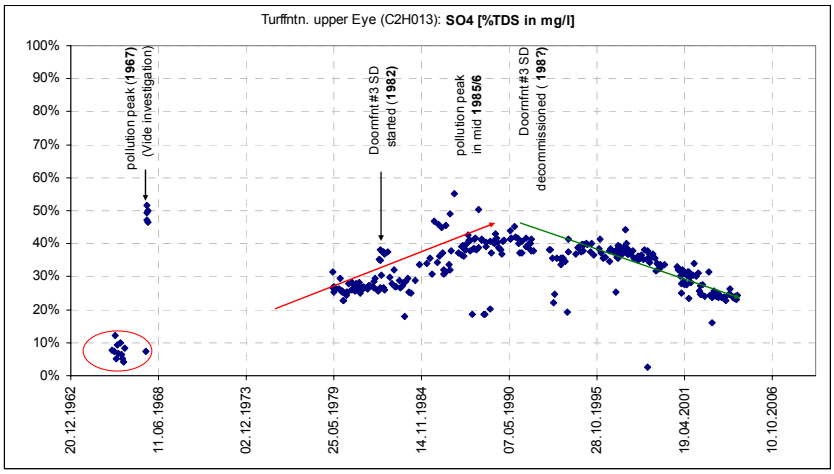

Fig. 4: Changes in the proportion of sulfate at the Turffontein upper eye as indication of mining-related impacts on groundwater quality in the BTC

Originating from the oxidation of sulphides in mined reefs sulfate is commonly used as an indicator for mining-related impacts. With sulfate being dominant in many mining-impacted waters close relations exist between sulfate concentrations and EC. However, relying only on the EC might be misleading in instances where decreasing sulfate levels are compensated by other salts from alternative sources. Using therefore the proportion of sulfates on the total concentration of dissolved solids (TDS) Fig. 4 indicates continued deterioration of water quality at the upper Turffontein eye at least since 1979 (when the monitoring started) with a first peak in 1967. From the mid 1980s, however, water quality started to improve.

Higher levels of mining-borne pollution in the past may have been associated with higher levels of U-pollution as well. A possible means of indirectly detecting such historic pollution peaks is the analyses of sediments which act as geochemical memory of the river. More importantly though it needs to be analysed what the actual reason for the improvement is as this could help to identify exact sources and pathways of U-pollution. It has also been suggested that the commissioning and decommissioning of a nearby slimes dam at the Doornfontein GM coincides with the deterioration and improvement respectively of the spring water (Stoch L 2007 pers. communication). Should this be correct it could provide an opportunity to not only identify sources of U-pollution other than the WFS (i.e. individual slimes dams in this case) but also alternative underground pathways within the karst system.

In this context it is important to note that slimes dams in the area are frequently covered with a greenish-yellowish crust which in case of a SD at Blyvooruitzicht contained 588 ppm U. Readily dissolvable on contact with water these crusts are a major U-source for polluting surface run off from slimes dams. In view of the fact that drainage lines downstream of the Doornfontein slimes dams are dotted with

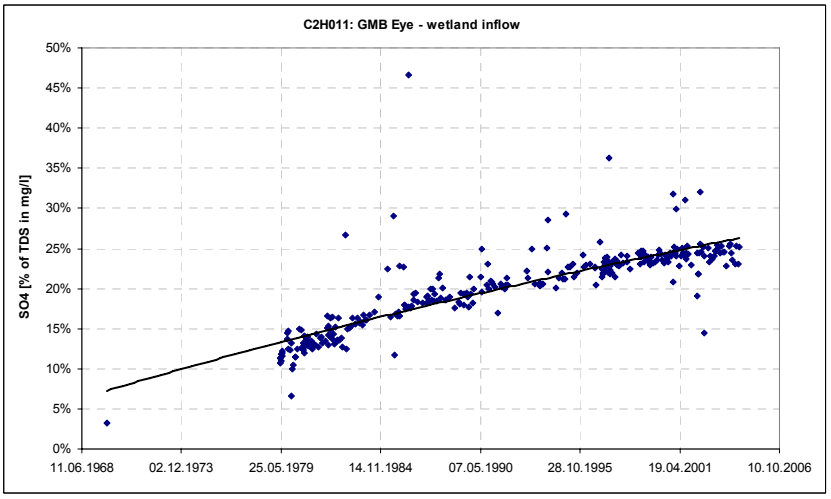

Fig. 4: Proportion of sulfate at the GMB eye as indication of mining-related impacts on groundwater quality in the BTC (with logarithmic trend line added) (data source: DWAF)

open sinkholes a rapid transport of highly polluted stormwater via sinkholes directly into the underlying karst aquifer is possible.

At the GMB eye a similar tendency of the water quality is discernable albeit at a generally lower level. Weekly monitoring data from DWAF covering some 40 years suggest that the sulfate proportion at the GMB eye steadily increased indicating increasing impacts of pollution from upstream mining (Fig. 4).

Wolmarans (1984) suggested in this context that seepage from the polluted WFS forms a pollution plume below the stream bed which gradually mixes with underlying groundwater on its way towards the lower lying GMB eye (even though this falls outside the surface catchment of the stream). Owing to the associated dilution, advection and dispersion pollution levels at the GMB eye are considerably lower than in the stream. Since the Turffontein eyes are located directly in the stream channel of the WFS such plume would naturally effect them first which is consistent with the fact that EC levels at GMB in 1969, i.e. 2 years after first pollution peaks occurred at Turffontein, still indicate pristine conditions. Owing to a gap in monitoring data it is not possible to determine when exactly water quality at GMB started to deteriorate. In 1979 when monitoring was re-started SO_4-levels had already risen considerably from 3% of the TDS to well over 10% and continue to do so ever since. With current levels of 25% of the TDS SO_4-levels at GMB are still below the maximum of >40% reached at Turffontein eyes some 20 years ago (Fig. 4). At EC maxima of 75-80 mS/m (750-800 µS/cm) water quality is now approaching levels at the Turffontein springs. However, in contrast to Turffontein no clear tendency of improvement is yet discernable even though the increase seem to follow a logarithmic function starting to flatten out (Fig. 4). This could be indicative of a slow moving plume which already passed Turffonte-

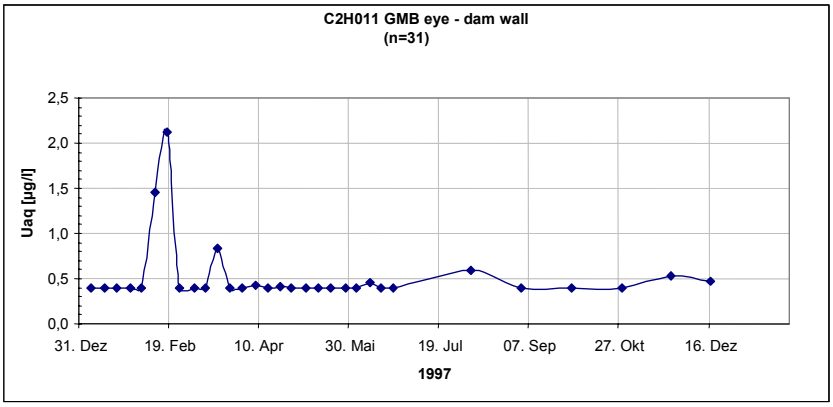

Fig. 5: U concentration at the GMB eye (data: IWQS 1997)

in and whose centre (i.e. the most polluted part) is now approaching GMB. Should the trend of flattening continue it seems possible that GMB may reach the turning point below the maximum pollution level of Turffontein, i.e. with SO_4 levels well below 40% of the TDS. This, in turn, would be consistent with the higher dilution through unpolluted groundwater at GMB which has a significant larger flow rate than the Turffontein eyes.

Data from IWQS (1999) suggest that U-levels at GMB in 1997 were still mostly around 0,4µg/l and thus in the region of global U-background values for (discharge-unweighted) freshwater (DWAF 1996). However, on at least two occasions U-levels in the weekly samples increased significantly reaching a maximum of 2µg/l (i.e. 500% of normal U-concentration) (Fig. 5).

While such isolated peaks could possibly be ascribed to analytical errors and treated as irrelevant outliers real time *in-situ* observations of water quality in the spring suggest that such peaks may indeed occur as a result of storm events in the area. Changes in pH and EC at the GMB eye in response to a storm event observed through *in-situ* datalogger clearly indicate a drop in pH and a corresponding rise in EC some 6d after the rain storm. Given that acid mine drainage causes exactly the observed changes (dropping pH due to high acidity and rising EC due to high salt load esp. sulphates) this could well indicate a rainfall-triggered impact by upstream mines. Acid rainfall which also lead to dropping pH values even in well-buffered dolomitic water (Winde *et al.* 2004) can be eliminated as cause of the observed response since this is accompanied by dropping EC values (quasi 'distilled' rain water with low mineral content). Such rather isolated events may also explain the six exceptionally high EC values at GMB found in the monthly monitoring program (Fig. 4).

These relative low U-concentrations at GMB are confirmed by Grundling (2002) reporting U-levels in grab samples of water from the GMB wetland ranging from 0µg/l to 1,5µg/l (n=5) corresponding with in/ near-stream sediments (not peat) displaying between 4 and 40ppm U (n=3). Derived from semi-quantitative

ICPMS scans the sediment concentrations are likely to contain a significant analytical error. A similar range of U-levels was found by Smuts (1997) in peat from the GMB wetlands ranging from 5ppm (325cm below surface) to 15ppm in 4m depth and the maximum of 35ppm in 2,8m depth. With no clear depth gradient it remains unclear in how far this relates to the rather recent mine pollution given that peat at 4m depth formed some 11,000 years ago. In order to determine the extent to which surface and/or groundwater may move through undisturbed peat *in-situ* porewater dynamics in peat are currently observed using quasi-continuous datalogger controlled measurements in two different transects comprising a total of nine boreholes.

Longitudinal profiles of water quality parameters in the wetland revealed that generally the quality of water deteriorates as it flows through the wetland displaying considerably higher EC values at the outflow than at the eye. The total salt load increases by some 6t/d, while the U-concentration more than triples rising from 0,2 to 0,7µg/l. Owing to the drastic increase of flow associated with the discovered sub-aquatic groundwater discharge in the upper reaches of the wetland the U-load increases by a factor of 35 (2g/d to 70g/d). With a total export of approximately 26 kg U per year the peatland would contribute some 10% of the total U-load reaching Boskop Dam (>200kg come from the Turffontein eyes area) as main drinking water reservoir for Potchefstroom. While this is still a relatively small pollution load compared to several tons of U per year found in the WFS it may indicate a future problem.

In view of the frequently reported ability of wetlands and peatlands in particular to aid the natural purification of polluted water this finding is somewhat unexpected. It was further found that at a number of sites poor quality groundwater enters the wetland from its fringes (Fig. 2). In an un-mined area with no peat deposits present located between two peat mining operations shallow groundwater was found displaying EC values of 3000 to 6000µS/cm which even exceed EC-levels in tailings seepage of the upstream mining area. This water also contains between 50 and 70µg/l U which rose to 230ppm after the first spring rain (Fig.2). Why the influx of (clean) rainwater resulted in an increase of U in the near surface part of the groundwater is not entirely clear. One possibility is the dissolution of salt crusts (mainly consisting of $MgSO_4$ and some 5% of NaCl) which formed during the dry winter period over large areas on dry vegetation and sediment. Containing 9 to 12ppm U the redissolution of these crusts may well have resulted in higher U-levels in near surface groundwater.

Similar salt crusts with an increased proportion of NaCl (>30%) were found in the unmined part of the peatland near a groundwater puddle containing 3,2 µgU/l (Fig. 2). Elevated U-levels (4µg/l) were also detected in water of a pool near the northern bank of the upper peatland (‘willow seep pool’, Fig. 2). This fits in a trend of steadily increasing U-concentration in groundwater surfacing along or near the drainage line downstream of the Turffontein springs: 1,0 ppb (Turffontein upper eye) --> 1,2 ppb at Musikraal --> 2,1 ppb at Kiel --> 4 ppb at GMB willow seep and 3,2 ppb at GMB lower part of the wetland port 9. This again appears to be quite different from groundwater at the GMB eye which has on average a U-

level which is about ten times lower. However, with a 5-6 day delay after rain events similar high U-concentration sporadically occur.

Summary and conclusion: Hydrogeological model

Despite the sketchy data and large uncertainties a first approximation of an hydrogeological model is attempted in order to synoptically combine available information. The following, preliminary model therefore is more tool for further research than for making predictions of any kind.

Running some 25km or so over cavernous dolomite of the BTC the WFS loses more than 100Ml/d on average to the underlying aquifer. Owing to U-pollution that originates from several gold mining areas this is associated with a U-load of some 4t/a affecting groundwater in the BTC as single largest resources supplying Potchefstroom municipality. Apart from three distinct outflow points in form of karst springs (Turffontein and GMB eyes) large areas of diffuse groundwater discharge exist in lower lying areas around the confluence of the Mooi River and the WFS as well as the GMB peatland. Groundwater discharged in these low lying areas (i.e. deeper groundwater) displays higher U-levels than (more shallow) groundwater discharged at higher levels e.g. at the GMB eye. However, with a lag of 5-6 days intense rain events in the upstream catchment also seem to cause pollution of the more shallow groundwater. With easily dissolvable and highly uraniferous salt crusts covering many slimes dams stormwater runoff from tailings entering nearby sinkholes is a possible explanation for such event-related pollution. This even more since these sinkholes are located well above the stream channel of the WFS possibly linking to a karst system on a higher level that feeds GMB eye. With a distance of some 18 km and a time lag of 6 days this would require an average flow speed of some 3 km/d (3,3cm/s) which does not seem unreasonable for flow in an open channel karst system.

In this context it needs to be stressed that karstification of dolomite is confined to the outcrop of chert-rich formations. According to Erasmus E (2008, personal communication) interlayered sequences of chert-rich and chert-free formations in a gently south dipping column possibly resulted in three to four hydraulically largely disconnected karst systems running more or less parallel to the WFS separated from each other by unweathered dolomite. In such system it is conceivable that different sources affect different parts of the aquifers in the same compartment without necessarily interacting with each other.

Unclear however remains the origin of the highly polluted groundwater found at the left bank between the two peat mining operations. Owing to the extremely elevated EC it is unlikely that a distant mining source is responsible. Currently investigations are underway to explore in how a far on outcrop of weathered carbonate could be a potential natural U-source.

U-levels in the peat at GMB indicate above natural background levels of U in certain areas without displaying clear spatial patterns. So far it seems that higher than global average U-levels in peat (5-10ppm) are mainly of naturally origin

since such level were also found in peat from the upper Mooi River (Fig. 2) not impacted on by gold mining.

In exceptionally wet years it was observed that the WFS reaches the confluence with the Mooi River. Together with water from the non-perennial du Toit Spruit (Fig. 2) entering the system neat the confluence this may even result in an overland inflow of flood water into the GMB peatland. Such inflow however is unlikely to be a major source of U-pollution owing to the large dilution by unpolluted runoff from non-mining areas.

Acknowledgement

The study is funded by the Department of Water Affairs and Forestry of South Africa (project no. 213-2006) which is gratefully acknowledged.

References

Barthel R (2007): Assessment of the radiological impact of the mine water discharges to members of the public living around Wonderfonteinspruit catchment area. BSA-project-no. 0607-03, BS Associates, Consulting Engineers and Scientists, Report to the National Nuclear Regulator (NNR), contact no RRD/RP01/2006, Bedfordview, pp. 225, unpublished

Blyvooruitzicht Gold Mine (2008) Uranium concentration in water dowsntream and upstream of the discharge canal. Weekly sampling, Feb. 2003 to Jan. 2008, unpublished.

Bredenkamp DB (2007): Use of natural isotopes and groundwater quality for improved recharge and flow estimates in dolomitic aquifers. Water SA, 33, 1; 87-92

Brown PA, Gill SA, Allen SJ (2000): Metal Removal from wastewater using peat. Water Research, Vol. 34, No. 16, pp. 3907-3916

Coetzee H, Winde F, Wade P (2006): An assessment of sources, pathways, mechanisms and risks of current and potential future pollution of water and sediments in gold mining areas of the Wonderfonteinspruit catchment (Gauteng/ North West Province, South Africa). WRC report no. 1214/1/06, ISBN 1-77005-419-7, Pretoria

Coggins AM, Jennings SG, Ebinghaus R (2005): Accumulation rates of the heavy metals lead, mercury and cadmium in ombrotrophic peatlands in the west of Ireland. Atmospheric Environment 40 (2006), p. 260-278

Coetzee H, Wade P, Ntsume G, Jordaan W (2002) : Radioactivity study on sediments in a dam in the Wonderfontein Spruit catchment. DWAF-Report 2002, Pretoria

Dorling D (2008): Uranium concentration in the upper Wonderfonteinspruit. Monitoring results for th eperiod February 2006 to Januray 2008, 23 samples, unpublished

Du Toit S (2006): Practical applications – effects of mine water drainage on the Krugersdorp Game Reserve. Paper presented at the 2-day conference of the Water Institute of South Africa, Mine water division on mine water decant, Randfontein, October 2006m unpublished, pp 8

DWAF (Department for Water Affairs and Forestry) (1996): South African Water Guidelines. Volume 1: Domestic Water Use. Pretoria

DWAF (Department for Water Affairs and Forestry) (2004): Water quality data for station C2H011 G Minnebron Eye, unpublished

Faanhof A, van Veelen M, Pulles W (1995): Radioactivity in water sources: a preliminary survey. DWAF report no. N/0000/00/REQ/0695, Pretoria.

Grundling PL (2002): EIA for Stander expansion to portions 4,8 & 9. Envrionmental Impact Assessment report, unpublished

Hill M (2007): First Uranium studies second Ezulwini shaft. Mining Weekly online, www.miningweekly.com, published 27.7. 2007.1p

Hill M (2008 a): Harmony could start uranium production in 2010. Mining Weekly online, www.miningweekly.com, published 22.5. 2008. pp 2

Hill M (2008 b): Gold Fields looking to develop West Wits surface assets. Mining Weekly online, www.miningweekly.com, published 9.5. 2008.pp 2

IWQS (Institute for Water Quality Studies) (1999): Report on the radioactivity monitoring programme in the Mooi River (Wonderfonteinspruit) catchment. Report No: N/C200/00/RPQ/2399.

Kempster PL, van Vliet HR, Looser U, Parker I, Silberbauer MJ, du Toit P (1996): Overview of radioactivity in water sources: uranium, radium and thorium. Final report. IWQS-No: N/0000/00/RPQ/0196. Pretoria.

Owen DE, Otton JK (1995): Mountain wetlands: efficient uranium filters - potential impacts. Ecological Engineering 5, 77 – 93

Ringquist L, Holmgren A, Oeborn I (2001): Poorly humified peat as an adsorbent for metals in wastewater. Water Research 36 (2003), p. 2394-2404

Ringquist L, Oeborn I (2001): Copper and zinc adsorption onto poorly humified Sphagnum and Carex peat. Water Research 36 (2002), p. 2233-2242

Smuts WJ (1997): Characteristics of South African peats and their potential exploitation. PhD, Faculty of Science, UP, unpublished, pp. 222

Swart CJU, James AR, Kleywegt RJ, Stoch EJ (2003 a): The future of the dolomitic springs after mine closure on the Far West Rand, Gauteng, RSA. Environmental Geology (2003), 44, 751-770.

Swart CJU, Stoch EJ, van Jaarsveld CF, Brink ABA (2003 b): The Lower Wonderfontein Spruit: an expose'. Environmental Geology, 43, 635-653.

Van Roy S, Vanbroekhoven K, Dejonghe W, Diels L (2006): Immobilization of heavy metals in the saturated zone by sorption and in situ bioprecipitation processes. Hydrometallurgy 83 (2006), p. 195-203

Wade PW, Woodbourne S, Morris WM, Vos P and Jarvis NV (2002) Tier 1 risk assessment of radionuclids in selected sediments of the Mooi River. WRC-Project No K5/1095

Winde F (2006 a): Challenges for sustainable water use in dolomitic mining regions of South Africa – a case study of uranium pollution, Part I: sources and pathways. Physical Geography, ISSN 0272-3646, 27, 2, 335-346

Winde F (2006 b): Challenges for sustainable water use in dolomitic mining regions of South Africa – a case study of uranium pollution, Part II: Spatial patterns, mechanisms and dynamics. Physical Geography, ISSN 0272-3646, 27, 2, 379-395

Winde F (2007): A hydrological study on the Gerhard Minnebron wetland to determine how the wetland system functions and fits into the Wonderfonteinspruit catchment due to licence applications to harvest peat and existing peat harvesting operations (DWAF project no 2006-231). Report on reconnaissance phase (1 November 2006 – 30 April 2007), DWAF, Pretoria, unpublished, 52pp.

Winde F, Stoch EJ, Erasmus E (2006): Identification and quantification of water ingress into mine voids of the West Rand and Far West Rand goldfields (Witwatersrand basin) with a view to long-term sustainable reduction thereof. Final report to Council for Geocience, proj. no 5512, pp. 261, Pretoria, unpublished

Winde F, Wade P, van der Walt IJ (2004): Gold tailings as a source of waterborne uranium contamination of streams – the Koekemoerspruit (Klerksdorp goldfield, South Africa) as a case study. Part III: Fluctuations of stream chemistry and their impacts on uranium mobility. Water SA, 30 (2), 233-240

Wolmarans JF (1984): Ontwatering van die dolomietgebied aan die verre Wes-Rand: gebeure in perspektief. DSc Thesis, University of Pretoria, 205 pp., unpublished.

Uranium sorption and desorption behavior on bentonite

Samer Bachmaf, Britta Planer-Friedrich and Broder J. Merkel

Department of Hydrogeology, Technische Universität Bergakademie Freiberg, Gustav-Zeuner Str.12, 09599 Freiberg, Germany.

Abstract. Columns packed either with bentonite and quartz or only with quartz were used to investigate the sorption and desorption of U(VI) in the presence or absence of sulfate, carbonate, and phosphate at pH 6.5. A considerable difference in the breakthrough and desorption curves was revealed for columns with and without bentonite. With bentonite in the system considerable differences were obtained with respect to the presence of the ligands sulfate, phosphate, and carbonate. With sulfate a slight decline of uranium sorption was found, while phosphate enhanced sorption slightly. On contrary, carbonate suppresses uranium sorption to a high extent. Distinct differences were obtained for the desorption, however, in all experiments it could be shown that more uranium was desorbed than previously sorbed, indicating that the natural bentonite contained substantial amounts of uranium.

Introduction

Retardation and transport of U(VI) are initially affected by their sorption/desorption reactions at solid/solution interfaces. Among the more common candidates in this regard bentonite (2:1 clay mineral) is an important material for technical purposes. Conventional batch sorption experiments were widely performed to investigate the U(VI) sorption onto clay minerals (Tsunashima 1983; McKinley et al. 1995; Pabalan et al. 1996; Chisholm-Brause et al. 2001; Hyun 2001). Because batch techniques have some limitations such as breakdown of soil aggregates, solubilization of soil components due to soil sample agitation, and relatively low solid to solution ratios, continuous column experiments were considered as an appropriate technique to study the transport of U(VI) in porous media. Sulfate together with carbonate and phosphate ions are important inorganic li-

gands that may influence the U(VI) sorption and transport in the subsurface. Sulfate is often present in groundwater, particularly in the vicinity of in-situ leaching mines and uranium milling production sites, where sulfuric acid was utilized in the leaching process. Carbonate is a strong ligand at alkaline conditions controlling the mobility of U(VI) in groundwater significantly by the formation of uranyl-carbonate complexes, which are weakly sorbed on many mineral surfaces (Hsi and Langmuir 1985; Waite et al. 1994). Phosphate is a common component in subsurface systems and plays an important role in governing the mobility of U(VI) (Payne 1996; Cheng et al. 2004, 2007). The effect of these complexing ligands on U(VI) sorption by bentonite during batch experiments was reported elsewhere (Bachmaf et al. 2008).

In this work, we investigated the transport of U(VI) in bentonite-sand packed columns in the presence or absence of the above mentioned inorganic ligands. Our major aim was to verify if the effects of sulfate, carbonate, and phosphate reported in our previous batch systems are also true with flow through conditions.

Materials and methods

Materials

The clay mineral used as the adsorbent in the column experiments was a Morocco bentonite IBECO, acquired from the Federal Institute for Geosciences and Natural Resources (BGR) in Hannover. The mineralogy of the < 2-μM clay fraction according to powder X-ray diffraction (XRD) verified that the bentonite is mainly composed of montmorillonite (80.3 %) and small amounts of impurity phases such as plagioclase, orthoclase, cristobalite, and quartz (12.1 %, 5.5 %, 1.3 %, and 0.9 %, respectively). Table 1 lists the chemical composition according to X-ray fluorescence (XRF) analysis. No pre-treatment was conducted for the bentonite before the experiments to preserve its natural conditions. The quartz sand used in this work termed F32 was supplied from (Quarzwerke Frenchen, Germany). The sand has an average grain size of 0.24 mm and a specific theoretical surface area of 102 cm^2/g. XRD characterizations found 98.6±0.26% quartz and 1.4±0.26% calcite. The chemical analysis indicates that quartz sand contained 99.7% SiO_2, 0.2% Al_2O_3, and 0.03% Fe_2O_3. Calcite and a small amount of iron oxides was removed from the sand by washing with diluted (1:10) 65% nitric acid for 24 hours, rinsing with deionised water, and air-drying in the laboratory.

U(VI) stock solutions of $5 \cdot 10^{-6}$ mol/L were prepared by dissolving uranyl nitrate hexahydrated $UO_2 (NO_3)_2.6H_2O$ (Chemapol, Germany) in Milli-Q ultra pure water (18 MΩ/cm). The solutions of 0.005 molar sodium sulfate, 0.003 molar sodium hydrogen carbonate, and 0.003 molar sodium hydrogen phosphate were prepared by dissolving Na_2SO_4, $NaHCO_3$, and $Na_2HPO_4 \cdot 12H_2O$, respectively (all of Merck, Germany) in the appropriate volume of distilled water. A 0.005 molar

EDTA solution was prepared using Etheylenediaminetetraacetic acid Diaammonium salt (Fluka, Germany). The pH of input solutions was adjusted to a pH of 6.5 with diluted NaOH or HCl and controlled by a pH glass electrode and a hand meter (WTW GmbH, Germany).

For constant ionic strength a 0.01 molar sodium chloride (Merck, Darmstadt-Germany) solution was added to all input solutions. U(VI) concentrations were photometrically determined by the arsenazo III method, 0.15 % (m/v) Arsenazo (1,8-dihydroxynaphthalene-3,6-disulphonic acid-2,7-bis[(azo2)-phenylarsonic acid)] (Riedel-de-Häen, Germany), 200 mg of high-purity Zn granules (Fluka, Germany), 37 % HCl (Baker, Germany), and 1g / 100 mL ascorbic acid and oxalic acid (both Chemapol, Germany) were used (Meinrath et al. 1999; Savvin 1961).

Experimental setup

Column experiments were conducted at room temperature using a total of eight glass columns of 2.4 cm inner diameter, 40 cm height, glass wool filter within the top cap and about 0.5 cm layer of granular silica beads at the bottom, covered with aluminum foil. Four columns were packed with a mixture of 10% bentonite (34 g) and 90% treated quartz sand (300 g) resulting in an average effective porosity of 0.2. The last four columns, used as blank columns, were filled with washed quartz sand only. The solutions were pumped from bottom to top at an average of about 80 µl/min over sorption and desorption period using a high precision peristaltic pump with planetary drive ISMATEC IPC 24 canals (Ismatec SA, Switzerland), however some changes of the flow occurred during the experiments. All columns were pre-conditioned using respective solutions but without uranium for about 12 h. The experiments were run for 160 days respectively the exchange of 480 pore volumes. After achieving breakthrough in all columns or after 72 days, uranium

Table 1. Chemical composition of Morocco bentonite, IBECO.

Compound/element	[wt.%]
SiO_2	53.2
TiO_2	0.2
Al_2O_3	21.2
Fe_2O_3	2.0
MgO	2.1
MnO	0.007
CaO	1.3
Na_2O	1.95
K_2O	0.952
P_2O_5	0.041
SO_3	0.14
Cl	0.002
LOI	16.63

LOI: loss of ignition

concentrations in all solutions were set to zero in order to investigate desorption. After 113 days, all input solutions were switched to a 0.005 molar EDTA solution. During the first week of both sorption and desorption experiments daily samples from the outlet solutions were collected. After that, three samples per week and column were taken. The effluents collected were immediately filtered with 0.2 µm cellulose acetate filters (Membrex, Germany) and analyzed for U(VI) and pH. The experimental setup is presented in Fig. 1.

Since sorption onto clay minerals can be controlled by surface complexation at pH >6 (McKinely et al. 1995; Catalona et al. 2005) and the investigation of surface complexation reactions on clay minerals was the focus of this research, the pH of the input solution for all columns was adjusted at pH 6.5. A higher pH was not recommended since then for the uranium concentrations chosen (0.005 µmol/L) oversaturation of certain uranium minerals (such as Schoepite, $UO_2(OH)_2$(beta), and $(UO_2)_3(PO_4)_2$) was calculated by means of PHREEQC and the LLNL data base.

By comparing the flow rate of the effluents in columns packed with bentonite and those in their blank columns, it is noteworthy that after approximately two weeks from starting the pumping the flow rate in the first four columns seems to be slower than those in the columns packed with only sand. This phenomenon

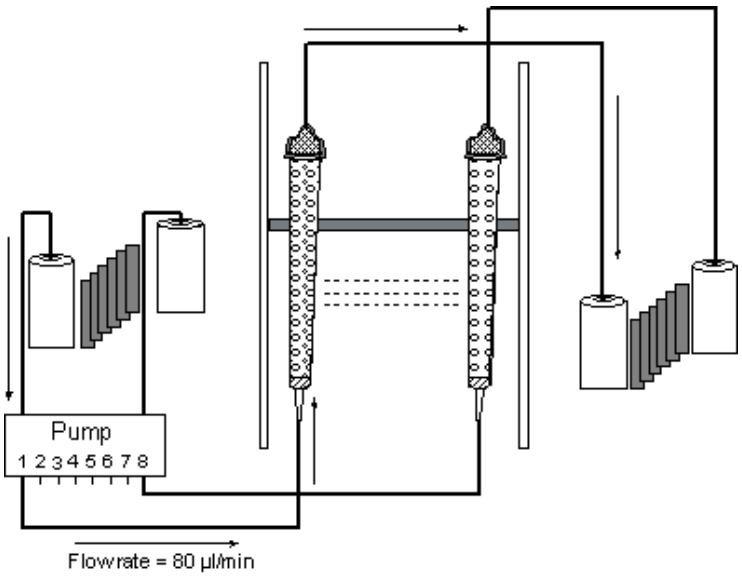

Fig.1. Experimental setup of column experiments, columns 1 to 4 were packed with 10% bentonite and 90% quartz sand, columns 5 to 8 were packed solely with quartz sand. Input solutions 1 and 5 (0.01M NaCl), input solutions 2 and 6 (0.01M NaCl+0.005M Na_2SO_4), input solutions 3 and 7 (0.01M NaCl+0.003M $NaHCO_3$), input solutions 4 and 8 (0.01M NaCl+0.003M Na_2HPO_4), [U]=5×10^{-6}M during the first 72 days, pH=6.5

could be explained by the intercalation of water molecules and U(VI) species between clay mineral layers that induces swelling in clay structure, which leads to a slight decrease in the permeability in the columns containing bentonite.

Results and discussion

A slight variation between effluent and influent pH of all the columns was observed (variation < 0.5 units). It is assumed that this minor pH variation have no significant impact on the results. The uranium breakthrough curves for the columns 1 to 4 (mixture of bentonite and quartz sand) are shown in Fig 2. Less than 10% of Uranium makes it through the column for the first 40 days in column 1 (uranium nitrate solution without complexing ligand) due to effective sorption. However, after 55 days breakthrough was complete. With sulfate as complexing ligand a slight decline of uranium sorption was found, while phosphate on contrary slightly enhanced sorption and extended the breakthrough point to 65 days. On contrary, carbonate suppresses uranium sorption to a high extent.

Uranium was hardly sorbed onto bentonite in the presence of carbonate due to the dominance of negatively charged uranyl carbonate species $UO_2(CO_3)_2^{2-}$ at pH

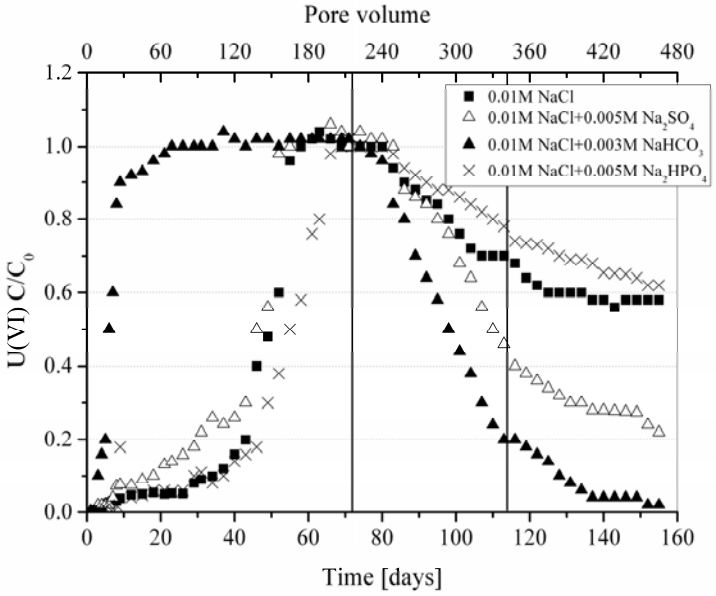

Fig.2. Experimental breakthrough curves of U(VI) in 0.01M NaCl (filled square) , in 0.01M NaCl+0.005M Na_2SO_4 (open triangles), in 0.01M NaCl+0.003M $NaHCO_3$ (filled triangles), and in 0.01M NaCl+0.003M Na_2HPO_4 (crosshairs), flushed into the bentonite and washed sand packed columns, [U]=5×10^{-6}M, pH=6.5.

6.5 according to calculated species distribution (Table 2). The $UO_2(CO_3)_2^{2-}$ complex is thus assumed to be more stable than any UO_2-surface complex that might form. To explain the minor but still significant differences in the three other variations of the experiment is more difficult. This is due to the dissent of the thermodynamic data assembled in different databases resulting in partly contradictory results (table 2). Thermodynamic modeling gives little hints why we see less sorption for the column with sulfate since the calculated uranium speciation shows no difference to the pure UO_2 solution (table 1). The same is true for the experiment with phosphate as ligand since phosphate enhanced sorption. It can be speculated that a uranyl-phosphate surface complex on montmorillonite is stronger than a comparable uranyl surface complex.

This adsorption can be explained by the fact that U(VI) sorbs preferentially to the reactive octahedral iron surface sites $Fe[(O,OH)_6]$ over $Al[(O,OH)_6]$ surface sites (Catalano and Brown 2005). Our modeled and experimental observations suggest no precipitation of U(VI) minerals. The saturation indices of U(VI) minerals calculated by PHREEQC and LLNL database showed negative values and thus under saturation. Our previous works elucidated that U(VI) slightly tends to adsorb to the surfaces of reaction vessels under alkaline conditions. Therefore, it can be assumed that 5% loss of U(VI) was attributed to adsorption to the surfaces of our experimental system and not due to its adsorption on bentonite surfaces.

Mass balance was calculated for the columns either packed with bentonite and sand or only sand by calculating the amount of U(VI) adsorbed and desorbed from

Table 2. Calculated species distribution in % for the four input solutions using PHREEQC and the data bases LNNL, WATEQ4F, and NEA_2007. Significant differences occur for 4 setups making it difficult to develop models to explain the sorption and desorption behavior

Data bases	only UO_2	%	SO_4	%	PO_4	%	CO_3	%
LNNL	$UO_2(OH)_2$	71.2	$UO_2(OH)_2$	70.1	$UO_2PO_4^-$	61.0	$UO_2(CO_3)_2^{2-}$	72.4
	$(UO_2)_2CO_3(OH)_3^-$	21.2	$(UO_2)_2CO_3(OH)_3^-$	21.6	UO_2HPO_4	38.9	UO_2CO_3	10.5
	UO_2OH+	3.2	UO_2OH+	3.3	$UO_2(OH)_2$	0.2	$(UO_2)_2CO_3(OH)_3^-$	9.4
WATEQ4F	$(UO_2)_3(OH)_5^+$	72.3	$(UO_2)_3(OH)_5^+$	70.6	$UO_2(HPO_4)_2^{2-}$	100	$UO_2(CO_3)_2^{2-}$	86.6
	UO_2OH^+	10.2	UO_2OH^+	10.4			UO_2CO_3	9.6
	UO_2CO_3	4.4	UO_2CO_3	4.3			$UO_2(CO_3)_3^{4-}$	3.6
NEA_2007	$(UO_2)_2CO_3(OH)_3^-$	73.2	$(UO_2)_2CO_3(OH)_3^-$	72.7	$UO_2PO_4^-$	61.0	$UO_2(CO_3)_2^{2-}$	47.4
	UO_2OH^+	5.1	UO_2OH^+	5.2	UO_2HPO_4	38.7	UO_2CO_3	26.2
	UO_2CO_3	5.0	UO_2CO_3	4.9			$(UO_2)_2CO_3(OH)_3^-$	18.4
	$(UO_2)_3(OH)_5^+$	13.0	$(UO_2)_3(OH)_5^+$	12.6			$UO_2(CO_3)_3^{4-}$	7.8
	$UO_2(OH)_2$	1.8	$UO_2(OH)_2$	1.8				
	UO_2^{2+}	0.4	UO_2SO_4	1.0				
	$(UO_2)_4(OH)_7^+$	1.0	UO_2^{2+}	0.5				

the columns over sorption and desorption period (table 3). It is noticeable that the amount of uranium desorbed from all columns was significantly higher than sorbed before. This is a clear indication for a significant amount of uranium sorbed naturally at the bentonite used. Additionally, the comparison between the cation exchange capacity (CEC) of bentonite (112 meq/100g) with the sorption capacity in the columns exhibited an apparent difference indicating that surface complexation of U(VI) on bentonite is three orders of magnitude below the total exchange capacity of bentonite.

The breakthrough curves of U(VI) for solutions free of or containing sulfate, carbonate, and phosphate for the blank columns packed with washed quartz sand are plotted in Fig 3. In contrast to the experimental data displayed in Fig 2, insignificant retardation of uranium was exhibited for all 4 columns. After two weeks from starting the sorption experiment, breakthrough was achieved. However, even in this case carbonate is minimizing sorption to a certain extent.

When the U(VI) concentration was set to zero in the input solution (desorption period), almost all U(VI) sorbed was recovered from all blank columns after approximately 3 weeks. Similar to the columns with bentonite two ligands used showed a significant impact on the desorption behavior: carbonate column recovered less uranium than the columns solely treated with UO_2 and those with sulfate as ligand. On contrary from the columns containing the phosphate containing more uranium was recovered. EDTA as final input solution had no significant impact since most of the uranium had been desorbed before. Our experimental results concur with those by Cheng et al. (2007), who found a small reversible U(VI) sorption in column packed with pure quartz sand.

Table 3. Mass balance for sorption and sorption capacity in the columns for the four setups.

Columns Packed with	Inlet solutions	Total U adsorbed in µmol	Total U desorbed in µmol	sorption capacity in meq/100g
Bentonite and sand	solely U	24.3	33.2	0.14
Bentonite and sand	Sulphate as ligand	21.5	25.2	0.12
Bentonite and sand	Carbonate as ligand	3.1	16.4	0.01
Bentonite and sand	Phosphate as ligand	27.6	36.5	0.16
Sand	solely U	3.2	11.2	-
Sand	Sulphate as ligand	2	10	-
Sand	Carbonate as ligand	0.4	7.4	-
Sand	Phosphate as ligand	2.3	13.4	-

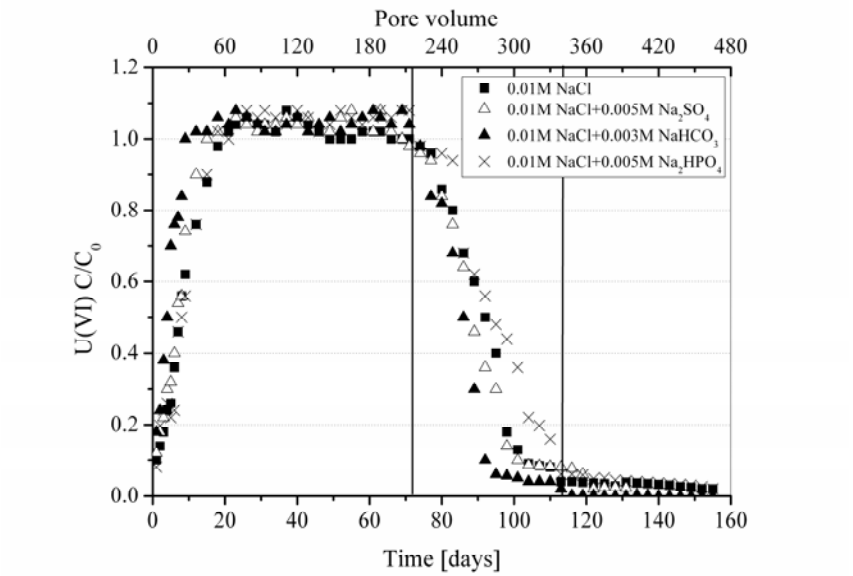

Fig.3. Experimental breakthrough curves of U(VI) in 0.01M NaCl, in 0.01M NaCl+0.005M Na_2SO_4, in 0.01M NaCl+0.003M $NaHCO_3$, and in 0.01M NaCl+0.003M Na_2HPO_4 flushed into the washed sand packed columns, [U]=5×10^{-6}M, pH=6.5.

Summary

This work exhibited a clear difference in uranium breakthrough and desorption curves in columns packed with bentonite and their respective blank columns indicating an effective U(VI) retardation due to surface complexation on bentonite. The substantial amount of uranium sorbed already on the natural bentonite induces an inequality in the mass balance calculated for the amount of U(VI) sorbed and desorbed over sorption and desorption period. The effect of ligands used on the U(VI) sorption/desorption revealed a similar behavior for columns free of and those containing bentonite. With sulfate a slight decline of uranium sorption was observed, while phosphate slightly enhanced sorption and delayed the breakthrough peak. On contrary, carbonate suppressed U(VI) sorption significantly.

References

Bachmaf S, Planer-Friedrich B, Merkel J M (2008) Effect of sulphate, carbonate, and phosphate on the uranium(VI) sorption onto bentonite. Radiochimica Acta 96: 359-366.

Catalano JG, Brown GE (2005) Uranyl adsorption onto montmorillonite: Evaluation of binding sites and carbonate complexation. Geochimica Et Cosmochimica Acta 69: 2995-3005

Cheng T, Barnett MO, Roden EE, Zhuang JL (2004) Effects of phosphate on uranium(VI) adsorption to goethite-coated sand. Environmental Science & Technology 38: 6059-6065

Cheng T, Barnett MO, Roden EE, Zhunag JL (2007) Reactive transport of uranium(VI) and phosphate in a goethite-coated sand column: An experimental study. Chemosphere 68: 1218-1223

Hsi CKD, Langmuir D (1985) Adsorption of Uranyl onto Ferric Oxyhydroxides - Application of the Surface Complexation Site-Binding Model. Geochimica Et Cosmochimica Acta 49: 1931-1941

Hyun SP, Cho YH, Hahn PS, Kim SJ (2001) Sorption mechanism of U(VI) on a reference montmorillonite: Binding to the internal and external surfaces. Journal of Radioanalytical and Nuclear Chemistry 250: 55-62

McKinley JP, Zachara JM, Smith SC, Turner GD (1995) The influence of uranyl hydrolysis and multiple site-binding reactions on adsorption of U(VI) to montmorillonite. Clays and Clay Minerals 43: 586-598

Meinrath G, Volke P, Helling C, Dudel E G, Merkel B.J (1999) Determination and interpretation of environmental water samples contaminated by uranium activities. Fresenius J. Anal. Chem. 364, 191

Pabalan RT, Bertetti FP, Prikryl JD, Turner DR (1996) Uranium(VI) sorption onto selected mineral surfaces: Key geochemical parameters. Abstracts of Papers of the American Chemical Society or in book Adsorption of metals by Geomedia 211: 55-Geoc

Payne TE, Davis JA, Waite TD (1996) Uranium adsorption on ferrihydrite - Effects of phosphate and humic acid. Radiochimica Acta 74: 239-243

Savvin SB (1961) Analytical use of arsenazo III: determination of thorium, zirconium, uranium and rare earth elements. Talanta 8, 673.

Tsunashima A, Brindley GW, Bastovanov M (1981) Adsorption of Uranium from Solutions by Montmorillonite - Compositions and Properties of Uranyl Montmorillonites. Clays and Clay Minerals 29: 10-16

Waite T D , Davis J A, Payne T E , Waychunas G A Xu N (1994) Uranium(VI) adsorption to ferrihydrite: Application of a surface complexation model. Geochimica et Cosmochimica Acta 58, 5465


Uranium Mining
and Hydrogeology

Uranium(VI) sorption on montmorillonite and bentonite: Prediction and experiments

Cordula Nebelung and V. Brendler

Forschungszentrum Dresden-Rossendorf, Institute of Radiochemistry, P.O. Box 510 119, 01314 Dresden, Germany

Abstract. The sorption characteristics of U(VI) on bentonite and montmorillonite were investigated in batch experiments for understanding the near-field behaviour in geological nuclear repositories. Sorption parameters were determined in batch tests. The sorption on bentonite (KWK) was studied at different dry bulk densities of the clay (1.3, 1.6, 1.9 g/cm^3) at pH 8 for the U(VI) concentration dependence (10^{-4} to 10^{-9} m). The sorption on the pure mineral montmorillonite (SWy-1) in 0.1 M $NaClO_4$ was determined for the concentration dependence at pH 5.5, and pH dependence between pH 3 and 11). A scientifically founded description of sorption processes at the mineral-liquid surface is possible with the surface complexation models (SCM), the ion adsorption on surface sites as complexation reaction. We use the diffuse double layer model (DDL) to predict the sorption with the code MINTEQA2 (Version 4.03, US EPA May 2006), thermodynamic data of aqueous and solid species from the NEA-TDB (Guillaumont et al. 2003), the mineral characterization and the respective protolysis data (Pabalan et al. 1997) and surface complex constants from (Pabalan et al. 1998).

The prediction of U(VI) sorption on montmorillonite at the pH dependence was very good. The modelling of the sorption on montmorillonite and bentonite versus U(VI) concentration shows a good agreement of measured and predicted values.

References

Guillaumont, R. et al. (2003) "Update on the chemical thermodynamics of U, Np, Pu, Am, Tc. Chemical Thermodynamics", Vol. 5 (OECD Nuclear Energy Agency, ed.), Elsevier, Amsterdam.

Pabalan, R.T. et al. (1997) Aquat. Geochem. 2, 203-226.

Pabalan, R.T. et al. (1998) in: Adsorption of metals by geomedia. Variables, mechanisms, and model applications; Jenne EA (Ed.), Academic Press; San Diego.

Acknowledgment

Funding by the European Commission (NF-PRO C2-ST-C-01) is gratefully acknowledged.

Which factors influence the immobilization of uranium in soils and sediments?

Angelika Schöner [(1)] and Chicgoua Noubactep [(2)]

[(1)] Institut für Geowissenschaften, Martin-Luther-Universität Halle-Wittenberg, Von-Seckendorff-Platz 3; D-06120 Halle, Germany.
[(2)] Geowissenschaftliches Zentrum der Universität Göttingen, Goldschmidtstr. 3; D-37077 Göttingen, Germany.
Corresponding author: angelika.schoener@geologin.de , Tel: +49 (0) 345 5526138 / Fax: +49 (0) 345 5527220

Abstract. Natural enrichment of uranium in soils and sediments is feasible to study the migration and immobilisation processes of radioactive elements in the geological environment. The investigations covered geological, geochemical, hydrogeological, hydrologic and radiometric aspects. The identification of the available uranium phases and its association with sediment phases was one of the main interests. Main controls in soil-aquifer systems include flow rate and water quality, mineralogical composition and physico-mechanical soil properties, vegetation and microbiological activity. A hydrologic regime with slow flow rates and vertical flow paths facilitates essential contact time between water and solid surfaces. Sufficient contact time (water/solid) allows for chemical retention mechanisms in aquifer material, in soils additionally plant associated and microbiological processes, e. g. bioreduction, biosorption or bioaccumulation. The latter are capable of retaining high U concentrations on the dry mass basis as frequently shown by laboratory investigations.

Secondary enrichment of uranium as frequently observed in organic-rich soils and sediments may suggest, that biological processes are fundamental in pre-concentration by means of uranium entrapment. Thereby pore-water depletion of uranium occurs, resulting in retention through plant detritus or microorganisms. At least when the biomass degrades or dies back, the biosorbed or bioaccumulated

uranium will be integrated in the soils. Hence, as remobilisation or resuspension are a matter of concern, mainly from laboratory studies it is concluded that uranium reduction and (bio-)mineralisation of U(IV) species are crucial for conservation. However in field scale, with the help of spectroscopic, wetchemical and mineralogical investigations the presence of a hexavalent immobile uranium phase could be proved. In applying advanced imaging methods (TEM) and microbiological complementary studies (DNA isolation) more detailed conclusions on uranium retention mechanisms can be drawn.

Determination of Uranium source term in a Polluted Site: a multitechnique study

Vannapha Phrommavanh[1)], Michaël Descostes[1,2)], Catherine Beaucaire[1)], Michel L. Schlegel[3)], Olivier Marie[4)], François Bonniec[5)] and J.P. Gaudet[6)]

[1)]Laboratory for measurement and modelling of the migration of radionuclides, CEA Saclay DEN-DANS/DPC/SECR, F-91191 Gif-sur-Yvette cedex (France)
[2)]UMR 8587 CEA – Université d'Evry – CNRS (France)
[3)]Laboratory for the Reactivity of Surfaces and Interfaces, CEA Saclay DEN-DANS/DPC/SCP, F-91191 Gif-sur-Yvette (France)
[4)]Service Radioanalyse Chimie et Environnement, CEA DAM/DIF/DASE, F-91680 Bruyères-le-Châtel (France)
[5)] Laboratoire de Radioanalyse et de Chimie de l'Environnement, CEA Saclay DSM/SAC/UPSE/SPR, F-91191 Gif-sur-Yvette (France)
[6)]CNRS-INPG-IRD-UJF-LTHE, BP 53, F-38041 Grenoble Cedex 09

Abstract. This study aims at understanding a potential migration of uranium in a polluted calcareous peat-land. Aqueous uranium monitoring indicates a seasonal variation of uranium content. During winter, aqueous uranium was found to be mostly under the +VI oxidation state, which is potentially mobile, while it was reduced into less soluble U(IV) species in summer. These observations were correlated with changes of the redox potential due to the activity of sulphate-reducing bacteria. A companion study (Phrommavanh et al., 2008 in this congress) focuses on the determination of the uranium aqueous speciation. Concurrently, one has to know the origin of the source term which is a part of the understanding of the uranium mobility. Several techniques were used in order to discriminate the chemical form of uranium: gamma spectrometry and aqua regia extractions on soil samples, porous PTFE quartz cells in order to sample the aqueous fraction, SEM observations with automatic U particles detection and XANES to assess the U redox state. The association of these different techniques gave consistent results with an increasing U content at a depth of 0.8 m. Such a localisation is explained by a redox front where anoxic and reducing conditions prevail.


Uranium Mining
and Hydrogeology

Peculiarities of radionuclide distribution within rock destruction zones (by the example of the objects at the Semipalatinsk Test Site)

Ella Gorbunova

Institute for Dynamics of Geospheres, Russian Academy of Sciences, 38-1 Leninsky prosp., Moscow, Russia, e-mail: emgorbunova@bk.ru

Abstract. Underground nuclear explosions (UNE) at the Semipalatinsk Test Site (STS) produced irreversible deformations in geological environment. Field study of these effects allow us to ascertain the basic mechanisms of man-induced destabilization of rocks, i.e. changes in physic-mechanical characteristics and filtering structure, hydrogeodynamical and radiation situations.

Introduction

During 1970 – 1980 field studies of filtering structure of UNEs at STS (Nuclear tests 1997) included:

- Drilling of vertical and horizontal boreholes;
- Geophysical borehole measurements (in particular, gamma-ray method);
- Interval hydrogeological testing;
- Water and rock sampling for determination of radionuclide content.
- The following characteristics have been determined:
- Mechanical effects of explosions;
- Permeability of various zones within irreversible massif deformations;
- Distribution of radionuclides in underground water and rock massif.

The monitoring of STS radiating situation is continuing now. The data of experimental investigations are evidence of radioactive contamination of geological environment within the formed man-induced zones.

Investigations

Structure of a central part of underground nuclear explosion (CP UNE) has been investigated at some STS objects, where nuclear weapon improvement tests took place. Sizes of man-induced fracture zones depend not only on charge parameters, but also on physical-mechanical properties of involved tectonic structure (fractures, stratigraphic and geological boundaries, lihtological structure of enclosing rocks).

The zones of interest include a cavity, rock crush and fracture zones, induced fractures, split-off, and chimney. Figure 1 shows a diagram of UNE central zone studied in more details. Consequences of post-explosion deformations presented in the massif connected with the epicentral zone of UNE are partially retraced on the day surface.

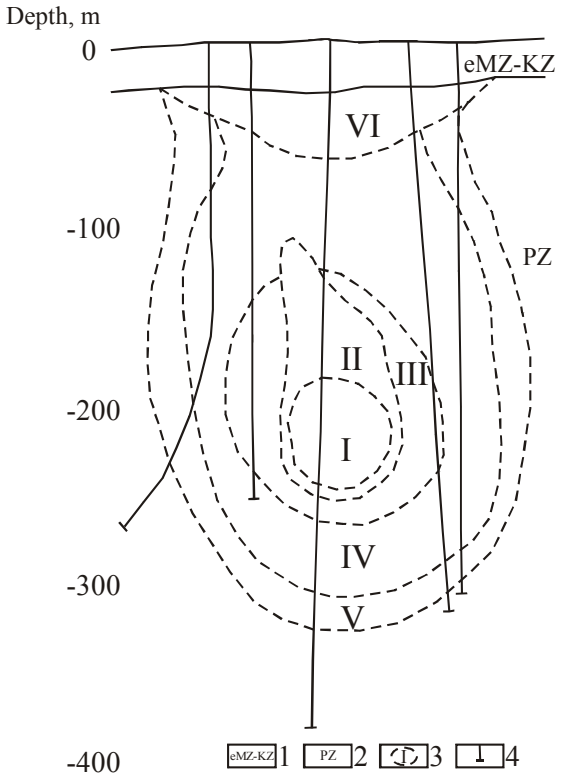

Fig 1. Diagram of UNE central zone (1 – Neogene-quaternary sediments; 2 – Paleozoic rocks; 3 – zones of the irreversible deformations in geological environment: I – cavity, II – chimney, III - rock crush, IV – fracture zone, V – induced fractures, VI – split-off; 4 – experimental borehole)

According to the diagram the major part of post-explosion radioactive material remains melted in the containment cavity. Within the crush zone rocks are transformed into loose dust. Within the fracture zone rocks are destroyed to landwaste and rock debris. The induced fractures is characterized by renewal of natural joints and generation of new ones – radial split-offs intersecting in the explosion ground zero and concentric fractures. This zone is asymmetric with the maximum thickness up the strike and the minimum one found below the cavity. The split-off zone is formed at the interface of materials with different acoustic impedance.

Each zone of induced fractures is specified by individual range of alteration of filtration characteristics. Data of hydrogeological investigations of CP UNE allow us to estimate the permeability of each zone. According to implemented analysis of the filtration characteristics within CP UNE zones of high-permeable, permeable and low-permeable rocks are defined. The filtration coefficient higher than 1m/day is mainly typical for the explosion cavity, the climney and rock shifting zones. The low-permeable rocks with filtration coefficient less than 1 m/day are confined within outlying regions of destruction massif. As a whole, the value of the filtration coefficient depends on the zone position relative to the central part of the explosion.

The selected zones have asymmetrical forms due to geological structure of considered massif. The profile of permeability and fracture porosity within the defined zones of irrevesible deformation massif is specified with filtration heterogeneity, controlling the level of the radioactive contamination of the bearing rocks and underground water.

The experimental data of the radionuclide content testify radioactive pollution of rocks within the limits of fractured zones and, separately, in the zones of renovated tectonic fractures. As a whole, the duration of existence of sealed cavity impacts on dynamics of radioactive conversions and influences the representativeness of radionuclides in the destruction zones after cavity depressurization. The moment of a rock caving and formation of a chimney is a major factor, which determines the nature of the radioactive contamination in all zones of induced and natural fractures.

A number of radionuclides (volatile, having gas predecessors and tritium) which were not totally fixed in melt released out of cavity and dispersed within zone of man-made fracturing (Izrael and Stukin 2000).

Laboratory investigations of samples, taken from different zones of irreversible deformation massif, show that the refractory radionuclides are mainly fixed within rock melt. Melt lens is formed in the lower part of the cavity, accounts for less than 5 percent of cavity volume and contains nearly 95 - 98 percent of all radionuclides. The radioactivity of the explosion partition products decreases nearly three times during one year. The specific concentration of the refractory radionuclides in the unaltered rock not far from cavity contact is six orders lower. The radionuclide compounds possessing volatiles are located nearby the explosion epicentre zone (^{125}Sb, ^{103}Ru, ^{106}Ru). Tritium, radioactive isotopes of iodine, radioactive inert gases and products of radioactive disintegration (^{90}Sr, ^{137}Cs, ^{140}Ba) are presented in the distant zone.

Geological environment including UNE hypocenters is a natural barrier on the path of radionuclide migration. Field data of UNE central part demonstrate evidences of geological environment contamination within man-made zones and, in some cases, within zones of renewal fracturing. Enrichment of destruction zones and microcracks in some minerals is observed, which are characterized by high contain of radioactive inert gases. The gaseous precursors of radionuclides with larger half-life period are characterized by deeper penetration into crystal structure of minerals (Ananiyeva et al. 2000). For example, ^{137}Cs concentration in rock-formed minerals decreases in the following sequence: biotite > magnetite > feldspar > quartz.

During CP UNE progressive floodings radionuclides are desorbed from the fractured surfaces. Radionuclides with intrinsic volatilites (^{103}Ru, ^{106}Ru, ^{125}Sb) and tritium as well as radionuclides with volatile (gaseous) precursors on the chains of radioactive conversions (^{89}Sr, ^{90}Sr, ^{91}Y, ^{137}Cs, ^{140}Ba) can migrate with underground water.

Water filled up UNE Central Zone is usually weak-active (rarely – middling-active) and contains products of long-living fission fragments and tritium (Logachev 2002). The formation of halo of radioactive contamination of underground water is related to progressive dilution of an isolated area containing the long-lived radionuclides. It is necessary to analyse the ratio of radionuclides in the rock-water system.

The local zones with man-made damages in the underground water circulation were determined for the areas of UNE tests (Gorbunova 2005). Formation of depression cones within the 0.3 - 0.5 km radius from the epicenter testifies to establishment of hydraulical connection between the UNE cavity and water-bearing horizon. This connection is indirectly confirmed by higher tritium and other radionuclides concentrations.

Accordingly, allocation of sites with damaged water circulation on the basis of archival and current data allow to determine the existence of potential sources of concealed radionuclide migration. Contour tracing of post explosive deformations on the day surface by different methods (reconnaissance observation of UNE epicenters, remote probing) serves as indirect corroboration of deep irreversible deformations in rock massif.

Discussion and perspectives

To obtain reliable information of the consequences of man-induced destabilization of STS resources it is necessary to arrange and conduct complex investigations of damaged geological environments including UNE epicenters. Data of CP UNE field study may be of special scientific interest and reliability as UNE radionuclides are located in limited scope of geological settings.

For these purposes we plan the following scientific, methodical and experimental studies of rock massif under UNE:

- classification and integration of data on permeability of destruction zones and radionuclide distribution within the central part of the underground nuclear explosion;
- working out the technique for field and laboratory investigations of alterations of filtration characteristics of geological environment and radionuclide distribution in the zones of irreversible deformation of rock massif as a consequence of UNE;
- realization of the expeditionary works to estimate destruction zone permeability and radioactive contamination of the geological environment at the selected objects;
- processing of the experimental data for determination of radionuclide closing-down safety in the destruction zones and
- determination of the principal mechanism of the radionuclide distribution in rock massif and underground water after UNE to estimate probable after-effects of the radioactive contamination of geological environment.

The results of the reconnaissance survey at STS revealed that a few sampling boreholes are still accessible for measurements (Fig.2). Higher gamma dose rates were recorded within wellhead areas of a few boreholes. As a whole, the density of the radioactive contamination is close to a background level.

Fig.2 Photograph of the examined object at STS, Autumn 2003.

Retrospective analysis of archival data on environmental contamination during UNE allow to choose the STS sites which may be interesting from the viewpoint of radionuclide contamination in the zones of irreversible rocks deformations.

To determine changes in radioactive situation within CP UNE we plan to work out the technique of field and laboratory sampling integration with subsequent analysis of representative samples of rocks and water. Radiation safety assurance is extremely important part of UNE field study. The field survey at defined STS

sites will allow to describe in details conditions of radionuclide distribution, determined by man-made dislocation of geological environment under UNE. The main pathways of radionuclide migration will be studied in the zones of rock destruction in the boreholes. The field survey will be conducted under permanent dosimetric monitoring of radiation situation on technical sites.

The comparison of produced experimental data on geological environment with available archival data will be of the practical value. The repeated survey at the selected sites allows determining the stability of the intervals of radioactive contamination of the geological environment. The defined principal mechanism of radionuclide distribution within the destruction zones will be used to appraise the possible after-effects of radionuclide contamination of geological environment.

Basing on comparative analysis of the radionuclide content in core samples, taken in specified intervals, the conversion of the radionuclides in studied destruction zones will be monitored. Pursuant to data of determination of the radioactive contamination of the underground water the rate of dilution of the radioactive contamination halo will be determined.

The produced data allow classifying the defined zones of irreversible mass deformation on the permeability level for different radionuclides. The results of the field investigations expand the available approaches to appraisal of radioecological situation in UNE locations. Creation of databank on radionuclide distribution in UNE central part is the base for development of effective decisions related to rehabilitation of geological environment, contaminated due to UNEs conducted on the territory of STS.

Conclusions

UNE hypocenters and zones of irreversible rock mass deformation are related to potential radionuclide source. During decades the long-lived radionuclides migrated in man-caused disturbed environment. Lack of methods for long-term prediction on state assessment of formed zones of irreversible deformation define experimental sites as unsteady objects. The areas where UNEs have been conducted can be considered as test sites for long-term underground storage of special hazardous radwastes.

The data of field works of conditions of radionuclide distribution within CP UNE are of the particular interest for development of radioecological safety aspects of territory exploration, adjacent to STS. The experimental data on radionuclide content allow working out the recommendations on test site territory rehabilitation.

Organization and realization of complex investigations of radioactive contamination of the geological environmental will promote the development of monitoring of radiation-ecological situation on the objects of higher risk in case of the occurrence of supernumerary situations and the terrorist threat.

References

Ananiyeva L.A., Dubasov Yu.V., Savonenkov V.G., Smirnova E.A. (2000) Radionuclide Leaching from Underground Nuclear Explosion Products in Granite. 1. Tests with rock samples from precavernous area. J Radiochemistry, v.42, #5: 462-465

Gorbunova E (2005) Typification of radioactive contamination conditions in ground water at the Semipalatinsk Test Site. Uranium in the environment. Mining impact and consequences. Springer: 823-829

Izrael YuA, Stukin ED (2000) Phenomenology of ground waters contamination after underground nuclear explosion – Radioactivity during nuclear explosions and accidents. Proceeding of the International Conference. Moscow April, 24-26 2000. St. Petersburg: Hydrometeoizdat, volume 1: 616-623

Logachev VA (2002) Nuclear tests in USSR: Current radioecological condition of the sites. Moscow: IzdAt: 652

Nuclear tests in USSR (1997). Begell-Atom, LLC-publishing, volume 2: 302


Uranium Mining
and Hydrogeology

Complexation of Uranium by Sulfur and Nitrogen Containing Model Ligands in Aqueous Solution

Claudia Joseph, B. Raditzky, Katja Schmeide, Gerhard Geipel, Gert Bernhard

Forschungszentrum Dresden-Rossendorf, Institute of Radiochemistry, P.O. Box 510 119, 01314 Dresden, Germany

Abstract. The interaction of U(VI) with organic model ligands is examined using time-resolved laser-induced fluorescence spectroscopy (TRLFS) and TRLFS with ultrafast pulses (fs-TRLFS). As example for sulfur containing ligands benzenesulfonic and 4-hydroxybenzenesulfonic acid are studied. For nitrogen containing model ligands nicotinic and anthranilic acid are examined as a function of pH. For evaluating the strength of interaction complexation constants are determined.

Introduction

The long-term safety assessment of nuclear waste disposals requires detailed knowledge of the transport and interaction behavior of actinides within the technical, geotechnical and geological barriers. Humic substances (HS), ubiquitous in natural environments, are able to influence the migration of actinides due to their ability for complex and colloid formation and their redox properties. It is known, that especially carboxylic (e.g., Shanbhag and Choppin 1981) and phenolic hydroxyl groups (e.g., Pompe et al. 2000) are able to complex metal ions. In addition to these oxygen containing functional groups, HS also offer sulfur and nitrogen containing functionalities.

In HS sulfur is available in amounts of 0 – 2% (Stevenson 1982). Regarding to their oxidation states, reduced sulfur (e.g. sulfides, thiols) or oxidized sulfur groups (e.g. sulfonates, sulfates) could be found (Solomon et al. 2003). It is known, that in complexation studies of HS with zinc (Xia et al. 1997) and mercury (Skyllberg et al. 2006) reduced sulfur groups (probable thiols) are favored to coordinate the metal ions.

It is established that HS contain 2 – 6% nitrogen (Stevenson 1982), consisting of proteinaceous materials (e.g. peptides, amino acids), heterocyclic compounds (e.g. pyrimidines) and amino sugars (Schulten and Schnitzer 1998). Xia et al. discovered that copper, nickel and cobalt form complexes with HS involving also amine functional groups (Xia et al. 1997). There are also various complexes of

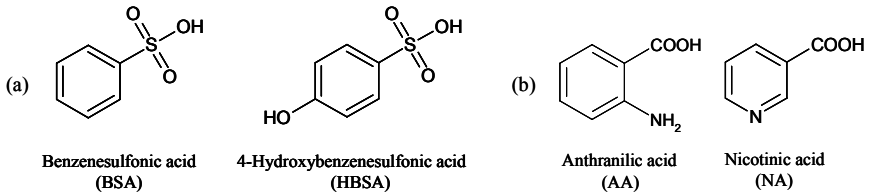

Fig.1. Structure of investigated sulfur (a) and nitrogen (b) containing model ligands.

uranium with multidentate N-donor ligands reported, where uranium is coordinated via oxygen and nitrogen functional groups at the same time (Sessler et al. 2006). The interaction of uranium(VI) with oxygen functionalities of HS is preferred against sulfur or nitrogen groups in literature.

The aim of this work is to determine the influence of various sulfur and nitrogen containing functional groups on the U(VI) complexation and to evaluate their contribution in comparison to oxygen containing functional groups. For this, simple organic model ligands that can occur as building blocks for HS are used in the first instance with the objective to transfer the results to HS. As model ligands we used benzenesulfonic acid (BSA), 4-hydroxybenzenesulfonic acid (HBSA) as well as anthranilic acid (AA) and nicotinic acid (NA). Their structures are given in Fig.1. Depending on the prevailing physical and chemical properties of the considered ligands two different TRLFS systems were used. For example, AA shows typical emission spectra with a short lifetime after excitation. Thus, for the measurement a fs-TRLFS system was applied. On the other hand, the complex formation studies of U(VI) with NA were performed at pH 2.5. At this pH, NA does not show significant luminescence emission, thus the U(VI) fluorescence was monitored using TRLFS.

Experimental

Solutions and reagents

Stock solutions of U(VI) perchlorate (0.1 M (UV-vis); 4.92·10-3 M (TRLFS)) were used. Ligand stock solutions of benzenesulfonic acid (Fluka), 4-hydroxybenzenesulfonic acid (Acros Organics), nicotinic (Sigma-Aldrich) and anthranilic acid (Merck) were prepared freshly for each experiment. The pH values were adjusted with HClO4 and NaOH. The ionic strength was kept constant at 0.1 M by adding a 0.2 M NaClO4 stock solution (NaClO4·H2O, Merck, p.A.). All solutions were prepared with Milli-Q-water. The experimental conditions are given in Table 1.

TRLFS measurements

TRLFS experiments were performed at a fixed U(VI) concentration as a function of model ligand concentration. Laser pulses at 266 nm with an average pulse energy of 300 µJ (Nd:YAG laser system, Continuum, Minilite) were used for the excitation of the U(VI) luminescence. The emitted luminescence light from the initial and complex solutions was detected by a Jobin-Yvon iHR spectrograph. The resulting spectra were measured in time-resolved mode using an ICCD camera (1024 pixel, Jobin-Yvon). The TRLF spectra were recorded from 371 to 674 nm were recorded by averaging 100 laser pulses using a gate time of 2 µs. Delay times varied from 65 to 10065 ns after application of the laser pulse in 100 ns increments.

fs-TRLFS measurements

Using a pulsed Nd:YVO4 laser (Spectra Physics) with an excitation wavelength of 266 nm and pulse energies of about 150 µJ, the emitted fluorescence of the organic ligands was collected by an intensified CCD camera system with 1376 useable pixels (Picostar HR, La Vision Inc.). The delay generator allows time delays between 0 and 100 ns in various steps from ps up to ns. The detailed description of the laser system is given in (Geipel et al. 2004). The spectra were measured at a gate width of 2 ns with delay times ranging from 0 to 20 ns for the experiments with HBSA and from 0 to 40 ns for AA. The detected wavelength ranged from 278 to 481 nm for the studies with HBSA and from 347 to 550 nm for AA. The fs-TRLFS experiments were carried out at constant ligand concentration as a function of U(VI) concentration at various pH values (cf. Table 1).

Table 1. Experimental conditions.

Model Ligand	Method	c(Model Ligand) [M]	$c(UO_2^{2+})$ [M]	pH
BSA	TRLFS	$0 – 8\cdot10^{-4}$	$5\cdot10^{-5}$	2
	UV-vis	$0 – 2\cdot10^{-2}$	$1\cdot10^{-3}$	2
HBSA	fs-TRLFS	$1\cdot10^{-4}$	$0 – 3\cdot10^{-3}$	2.5
NA	TRLFS	$0 – 8\cdot10^{-4}$	$5\cdot10^{-5}$	2.5
AA	fs-TRLFS	$1\cdot10^{-5}$	$0 – 3\cdot10^{-4}$	1.5 – 6.5

Results and Discussion

Benzenesulfonic acid

Because the complexation experiments were performed as function of pH value, it is important to know at which pH value the protonated or deprotonated species exist. Literature values for the acidity constant (pKa) of BSA varied in a wide range from -6.56 ± 0.06 (Cerfontain et al. 1975) to 2.55 (Dean 1985). Therefore, several methods were applied to determine the acidity constant for BSA.

i. Potentiometric titration experiments proved that the acidity of BSA is beyond the definition and working range of the pH-electrode. That means, the pKa must be significantly smaller than 0.
ii. Fluorescence studies with ultrafast pulses (fs-TRLFS) showed a self-quenching effect of BSA, therefore the measured spectra could not be analyzed.
iii. UV-vis spectra recorded as a function of proton concentration exhibit no isosbestic point, which is required for pKa-calculations.

Thus, with the accomplished experiments no pKa for BSA could be determined. Because of this result, we based our complexation experiments upon the literature value given in (Cerfontain et al. 1975), which was determined by ^{13}C-NMR. We postulated that at the investigated pH of 2 the sulfonic acid group is completely deprotonated.

We studied the complexation behavior of BSA with U(VI) using UV-vis absorption spectroscopy. The spectrum of the free U(VI) shows no difference to the spectra of U(VI) in the presence of BSA. A probable reason is that there is no interaction between the uranyl ion and the model ligand. This thesis was proved by TRLFS experiments. The spectra of the uranyl ion as a function of BSA concentration at pH 2 showed a decrease of the luminescence intensity with increasing BSA concentration. This behavior is characteristic of static luminescence quenching due to the complex formation. The luminescence decay was monoexponential in all samples. But the lifetime of the free uranyl ion decreased with increasing BSA concentration. This indicates an additional dynamic luminescence quenching. With the Stern-Volmer equation the determined lifetimes could be used to calculate the luminescence intensities if no dynamic quenching occured. In case of BSA revised intensities obtained by lifetime relation did not show any decrease. Within the experimental uncertainties, they are constant. Therefore, no complexation constant could be calculated with the measured TRLFS spectra. In conclusion, using UV-vis absorption spectroscopy and TRLFS it could be demonstrated that no interaction of U(VI) with the sulfonic acid group takes place.

4-Hydroxybenzenesulfonic acid

In this work, we used a HBSA sodium salt. Thus, the sulfonic acid group can be regarded as completely dissociated. With pKa2 = 8.56 ± 0.05, determined by potentiometric titration and comparable to those in the literature (Bates et al. 1943, Zollinger et al. 1953), the hydroxyl group should not be deprotonated at the inves-

tigated pH 2.5. Because HBSA shows a typical fluorescence spectrum with a short lifetime of about 2 ns after excitation, the complexation behavior of the ligand with U(VI) was studied with fs-TRLFS. The obtained fluorescence spectra show peak maxima at about 300 nm. HBSA also exhibits a photochemical process during excitation, observable by the appearance of a second peak between 360 and 480 nm. This probably indicates an excited state energy transfer in the HBSA, which leads to the appearance of a second fluorescent species. During the measurement the second peak does not show any change of its intensity in all samples. Therefore, only the first part of the spectra was analyzed. Fig.2a shows the fluorescence spectra of the main peak as a function of the U(VI) concentration. The spectra exhibit a decrease of the fluorescence intensity of HBSA with increasing U(VI) concentration, which is due to complex formation. Using a modified logarithmic form of the mass action law (Eq. 1) the stoichiometry of the complex and the stability constant were determined graphically via slope analysis.

$$\log ([FQ_x]/[F]) = x \log [Q] + \log K \quad (1)$$

with $[FQ_x]$ concentration of the formed complex
$[F]$ concentration of the fluorophore
$[Q]$ concentration of the quencher

Fig.2b shows the validation plot for the complexation of U(VI) with HBSA. The intersection conforms to the formation constant log K. In all experiments a slope near 1 was calculated, suggesting a predominant 1:1 complex. The complex formation of UO_2^{2+} with HBSA can be written as:

$$x\ UO_2^{2+} + y\ HOC_6H_4SO_3^- + z\ H^+ \rightleftarrows [(UO_2)_x(HOC_6H_4SO_3)_yH_z]^{(2x-y+z)} \quad (2)$$

The complexation constants determined as average for several independent measurements is log K_{110} = 2.76 ± 0.15. That means, that in contrast to BSA, HBSA is able to coordinate the uranyl ion. The complex seems to be formed via the sulfonic acid group. We assume that the hydroxyl group has a stabilizing effect on the complexation. Computational modelling studies are planned to clarify the effect of the hydroxyl group.

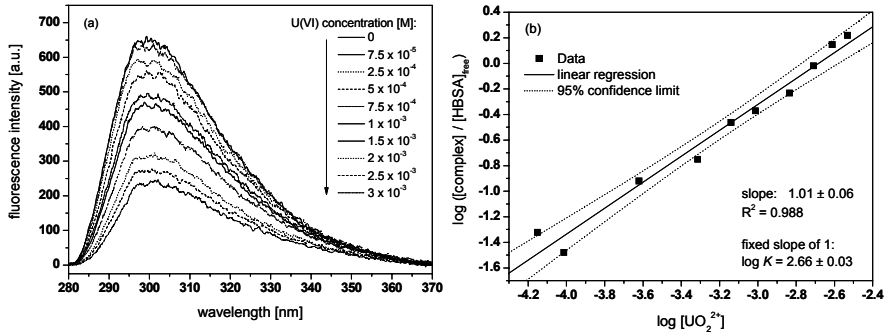

Fig.2. (a) Fluorescence spectra of 1 x 10^{-4} M HBSA at pH 2.5 as a function of U(VI) concentration, (b) Validation plot (slope analysis) of complexation of HBSA with U(VI).

Anthranilic acid

The U(VI) complexation with anthranilic acid (AA) was studied as a function of pH. There are several pKa values known in the literature, for AA we used pKa1 = 2.01 and pKa2 = 4.78 from the NIST database (Martell et al. 1998). Like other amino acids AA is an amphoteric compound (Wiklund and Bergman 2006). Therefore, the carboxylic group can occur dissociated even at low pH values. The spectra were recorded in a pH range from 1.5 to 6.5 to ascertain the influence of the amino and the carboxylic acid group on the complex formation depending on their grade of dissociation.

The fluorescence emission spectrum of AA ranges from 360 to 520 nm and shows a peak maximum at about 405 nm. Fig.3a shows examples of the obtained fluorescence spectra at pH 6.5. The spectra exhibit a decrease of the fluorescence intensity of AA with increasing U(VI) concentration at all measured pH values. The fluorescence decay was monoexponential in all samples. Only at pH 4.6 a bi-exponential decay occurred. Three different lifetimes were detected, each relatable to an AA species. The averaged lifetimes are $\tau_1 = 1.17 \pm 0.03$ ns (AA with $-NH_3^+$ and -COOH), $\tau_2 = 2.61 \pm 0.10$ ns (AA with $-NH_2$, -COOH) and $\tau_3 = 8.61 \pm 0.16$ ns (AA with $-NH_2$, $-COO^-$). At pH 4.6 the two lifetimes τ_2 and τ_3 could be identified simultaneously.

Fig.3b shows the validation plot for the complexation of U(VI) with AA. In all experiments log *K* at a slope near 1 was calculated, suggesting a predominant 1:1 complex. The complexation constants, determined as average of several independent measurements, are presented in Table 2. Because of the similarity of the determined stability constants we assume that carboxylic groups are mainly responsible for complex formation between AA and U(VI). Therefore, the complex formation can be written as:

$$x\ UO_2^{2+} + y\ H_2NC_6H_4COO^- + z\ H^+ \rightleftarrows [(UO_2)_x(H_2NC_6H_4COO)_yH_z]^{(2x-y+z)} \quad (3)$$

Due to the high amount of deprotonated carboxylic groups at pH 6.5 (97 %) we assume that the complex stability constants would not increase further with in-

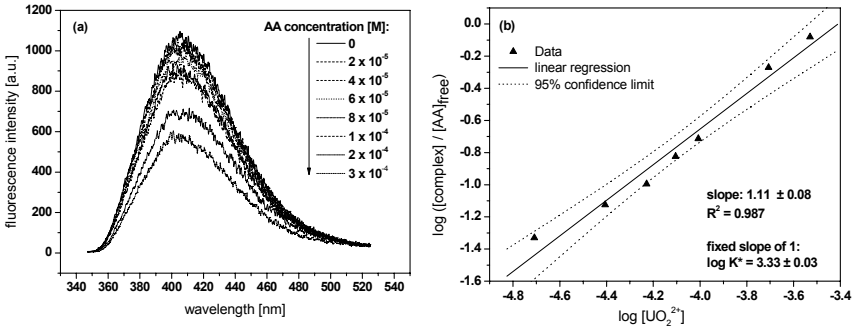

Fig.3. (a) Fluorescence spectra of 1 x 10^{-5} M AA at pH 6.5 as a function of U(VI) concentration, (b) Validation plot (slope analysis) of complexation of AA with U(VI) at pH 6.5.

creasing pH. The calculated log K = 3.34 ± 0.09 is in good agreement with the constant log K = 2.95 determined potentiometrically in a mixture of ethanol and water (Mahmoud et al. 1996).

In the literature it can be found, that the nitrogen of the amino group does not seem to coordinate to U(VI) (Alcock et al. 1996). But in comparison to benzoic acid with log K = 2.68 ± 0.04 (Vulpius et al. 2006), which offers only a carboxylic group, the complexation constant of AA with U(VI) is higher, suggesting an involvement of the nitrogen containing functional group in the coordination process. The amino group has probably a stabilizing effect on the binding of U(VI) to the carboxylic group, for example via non-covalent interactions between the oxygen atoms of the uranyl ion and the hydrogen atoms of the amino group. To find out whether or not the amino group itself is able to bind U(VI), complexation studies of U(VI) with aniline are in progress.

Table 2. Summary of the averaged complex stability constants log β of the U(VI) complexes identified in this study.

ligand	pH	*x y z*	complex species $M_xL_yH_z$	log β
		1 0 0	UO_2^{2+}	
HBSA	2.5	1 1 0	$(UO_2HOC_6H_4SO_3)^+$	2.76 ± 0.15
AA	1.5		-	-
	2.5	1 1 0	$(UO_2H_2NC_6H_4COO)^+$	2.88 ± 0.38
	3.5	1 1 0	$(UO_2H_2NC_6H_4COO)^+$	2.91 ± 0.11
	4.6	1 1 0	$(UO_2H_2NC_6H_4COO)^+$	3.16 ± 0.09
	5.6	1 1 0	$(UO_2H_2NC_6H_4COO)^+$	3.23 ± 0.12
	6.5	1 1 0	$(UO_2H_2NC_6H_4COO)^+$	3.34 ± 0.09
NA	2.5	1 1 0	$(UO_2C_5H_4NCOO)^+$	3.83 ± 0.06
	2.5	1 2 0	$UO_2(C_5H_4NCOO)_2$	7.71 ± 0.02

Nicotinic acid

Fig.4a shows the luminescence spectra of U(VI) as a function of the NA concentration at pH 2.5. The luminescence decay was monoexponential in all samples. No shifts of the main emission bands were detected. We therefore conclude that only the free uranyl ion is present as fluorescent species in the solutions and the formed complex does not show any luminescence in the considered wavelength range. With increasing NA concentration a strong decrease of the U(VI) luminescence intensity was observed.

In analogy to HBSA and AA we performed a slope analysis using the modified logarithmic form of the mass action law (Eq. 1). Unlike to AA a slope of 1.32 ± 0.10 was calculated. In Fig.4b the validation plot for the complexation of U(VI) with NA is shown. The data points were separated into two sections (Section 1: [NA] = 3 x 10^{-5} to 1 x 10^{-4} M, Section 2: [NA] = 2 x 10^{-4} to 5 x 10^{-4} M) and the slope of each section was calculated separately. The results indicate the formation of 1:2 complexes at concentrations above 1 x 10^{-4} M NA. We used the factor analysis program SPECFIT (Binstead et al. 2007) for analysis of the mixed spectra

and determination of the complex stability constants. For calculation we used NA dissociation constants of $pKa_1 = 2.04$ and $pKa_2 = 4.74$ reported in (Donge et al. 1998). The complex formation of UO_2^{2+} with NA can be written as:

$$x\ UO_2^{2+} + y\ C_5H_4NCOO^- + z\ H^+ \quad \rightleftarrows \quad [(UO_2)_x(C_5H_4NCOO)_yH_z]^{(2x-y+z)} \qquad (4)$$

The averaged complex stability constants calculated with SPECFIT of $\log \beta_{110} = 3.83 \pm 0.06$ and $\log \beta_{120} = 7.71 \pm 0.02$ are in good agreement with constants determined for the complex formation of U(VI) with picolinic acid, which is isomer to nicotinic acid. The formation constants for $[UO_2(Pic)_i]^{2-i}$ were found to be $\log \beta_1 = 3.75$, $\log \beta_2 = 7.48$ (Brandau 1970). We suggest that the uranyl ion is bound to the carboxylic group, like detected for U(IV) using IR spectroscopy (Singh and Singh 1979). In comparison to the complexation of U(VI) with AA or benzoic acid (Vulpius et al. 2006), the complex stability constant determined for the 1:1 complex of NA with U(VI) is considerably higher. Therefore, it is also possible that nitrogen exerts a stabilizing effect or that nitrogen could be coordinated to U(VI), as already described for the complexation of U(VI) with 8-hydroxychinoline (Ünak et al. 1993). In order to answer this question further studies will be performed.

Conclusion

With our spectroscopic studies we demonstrated, that U(VI) interacts with sulfur containing functional groups. Interestingly, we did not see any interaction of U(VI) with benzenesulfonic acid. In contrast, 4-hydroxybenzenesulfonic acid forms a complex with U(VI) at pH 2.5. Apparently, the hydroxyl group has a stabilizing effect on the complexation. Anthranilic acid forms 1:1 complexes with the uranyl ion at pH values from 2.5 to 6.5. Unlike anthranilic acid, nicotinic acid

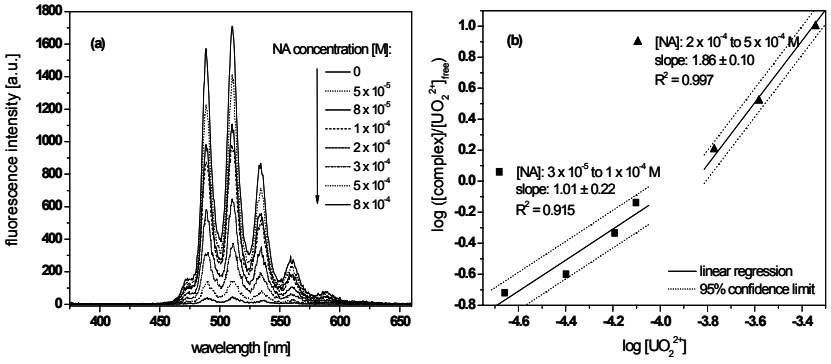

Fig. 4. (a) TRLF spectra of U(VI) (5×10^{-5} M) as a function of NA concentration at pH 2.5, (b) Separated slopes of the complex formation of NA with U(VI) at pH 2.5.

forms a 1:1 complex as well as a 1:2 complex at ligand excess of 1:20 (U:NA). In both complex formations we assume a predominant binding of the uranyl ion via the carboxylic group of the ligand. In spite of this, the nitrogen containing functional groups seem to have an influence on the stability of the formed complexes. The specification of the stabilizing effect of the nitrogen containing groups requires further studies.

Concerning HS, it can be concluded, that uranium(VI) prefers complexation via carboxylic and phenolic hydroxyl groups. Uranium complex formation with the studied sulfur or nitrogen containing functionalities plays only an inferior role.

Acknowledgement

The Federal Ministry of Economics and Technology funded this work (02E10156).

References

Alcock N W, Kemp T J, Roe S M, Leciejewicz J (1996) The roles of N- and O-coordination in the crystal and molecular structures of uranyl complexes with anthranilic and pyrazinic acids. Inorg Chim Acta 248: 241-246

Bates R G, Siegel G L, Acree S F (1943) The second dissociation constant of p-Phenolsulfonic acid and pH values of phenolsulfonate-chloride buffers from 0°C to 60°C. J Res Bur Stand 31: 205-223

Binstead R A, Zuberbühler A D, Jung B (2007) SPECFIT global analysis system version 3.0.39, Spectrum Software Systems

Brandau E (1970) Komplexbildung von fünf- und sechswertigen Actiniden mit Heterocyclischen Karbonsäuren. KFK-1068, Forschungszentrum Karlsruhe, Germany, p. 27

Cerfontain H, Koeberg-Telder A, Kruk C (1975) Solutes in sulfuric acid. Part VII. Ionization of benzenesulfonic acid; determination of pKBH by 13C NMR. Tetrahedron Lett 42: 3639-3642

Dean J A, ed. (1985) Lange's handbook of chemistry. McGraw-Hill, New York

Dongre V G, Janrao D M, Kamble V W (1998) Potentiometric Studies on Some Ternary Complexes of Uranyl Ion with Pyridine Carboxylic Acids and Some Amino Acids. Asian J Chem 10: 730-734

Geipel G, Acker M, Vulpius D, Bernhard G, Nitsche H, Fanghänel Th (2004) An ultrafast time-resolved fluorescence spectroscopy system for metal ion complexation studies with organic ligands. Spectrochim Acta A 60: 417-424

Hallé J-C, Lelievre J, Terrier F (1996) Solvent effect on preferred protonation sites in nicotinic and isonicotinic anions. Can J Chem 74: 613-620

Mahmoud M, Ibrahim S, Hassan A (1996) Ternary Complexes of N-(2-acetamino)iminodiacetic acid and some aromatic acids. Isolation and stability constants in solution. Transit Metal Chem 21: 1-4

Martell A E, Smith R M, Motekaitis R J (1998) NIST Critically Selected Stability Constants of Metal Complexes Database, Version 5.0, U.S. Department of Commerce, Gaithersburg, MD, USA

Pompe S, Schmeide K, Bubner M, Geipel G, Heise K H, Bernhard G, Nitsche H (2000) Investigation of humic acid complexation behavior with uranyl ions using modified synthetic and natural humic acids. Radiochim Acta 88: 553-558

Schulten H-R, Schnitzer M (1998) The chemistry of soil organic nitrogen: a review. Biol Fertil Soils 26: 1-15

Sessler J L, Melfi P J, Pantos G D (2006) Uranium complexes of multidentate N-donor ligands. Coordin Chem Rev 250: 816-843

Shanbhag P M, Choppin G R (1981) Binding of Uranyl by Humic Acid. J Inorg Nucl Chem 43: 3369-3372

Singh M, Singh R (1979) Complexes of Uranium(IV) and Thorium(IV) with α-Picolinic Acid, Nicotinic Acid, Anthranilic Acid and N-Phenylanthranilic Acid. J Indian Chem Soc 56: 136-137

Skyllberg U, Bloom P R, Qian J, Lin C-M, Bleam W F (2006) Complexation of mercury(II) in soil organic matter: EXAFS evidence for linear two-coordination with reduced sulfur groups. Environ Sci Technol 40: 4174-4180

Solomon D, Lehmann J, Martinez C E (2003) Sulfur K-edge XANES spectroscopy as a tool for understanding sulfur dynamics in soil organic matter. Soil Sci Soc Am J 67: 1721-1731

Stevenson F J (1982) Humus Chemistry. John Wiley&Sons, New York

Takata S, Kyuno E, Tsuchiya R (1968) Formation Constants of Chromium(III) Complexes with (N N)- (O,O)- and (N,O)-Type Ligands and Their Relationship to Structure. B Chem Soc Jpn 41: 2416

Ünak P, Özdemir D, Ünak T (1993) Determination of the stability constants of uranyl complex with 8-Hydroxyquinolinium sulfate. J Radioanal Nucl Chem Le 176: 55-64

Vulpius D, Geipel G, Baraniak L, Rossberg A, Bernhard G (2006) Complex formation of U(VI) with 4-hydroxy-3-methoxybenzoic acid and related compounds. J Radioanal Nucl Ch 270: 661-667

Wiklund P, Bergman J (2006) The Chemistry of Anthranilic Acid. Curr Org Synth 3: 379-402

Xia K, Bleam W, Helmke P A (1997) Studies of the nature of binding sites of first row transition elements bound to aquatic and soil humic substances using X-ray absorption spectroscopy. Geochim Cosmochim Acta 61: 2223-2235

Zollinger H, Büchler W, Wittwer C (1953) Wirkung der Sulfosäuregruppe auf aromatische Systeme: Hammett's σ-Werte des SO3--Substituenten. Helv Chim Acta 36: 1711-1722

Characterizing As, Cu, Fe and U Solubilization by Natural Waters

Chicgoua Noubactep[1], Angelika Schöner[2] and M. Schubert[3]

[1] Angewandte Geologie, Universität Göttingen, Goldschmidtstraße 3, D - 37077 Göttingen, Germany.
[2] Institut für Geowissenschaften, Ingenieurgeologie, Martin-Luther-Universität Halle; Von-Seckendorff-Platz 3, D - 06120 Halle, Germany.
[3]Department of Analytical Chemistry; Helmholtz Centre for Environmental Research -UFZ, Permoserstrasse 15, D-04318 Leipzig, Germany.

Abstract. The effects of carbonate concentration and the presence of in-situ generated iron oxide and hydroxide phases (iron oxyhydroxides) on arsenic (As), copper (Cu), and uranium (U) release from natural rocks were investigated under oxic conditions and in the pH range from 6 to 9. For this purpose non-disturbed batch experiments were conducted with a constant amount of each contaminant bearing rock/mineral and different types of water (deionised, mineral, spring, and tap water). For comparison parallel experiments were conducted with 0.1 M Na_2CO_3 and 0.1 M H_2SO_4. The favourable role of carbonate bearing minerals for U and Cu transport could not be confirmed by using dolomite. The presence of elemental iron and pyrite retards As, Cu and U solubilization. This study shows that using natural materials in laboratory investigations is a practical tool to investigate natural processes.

Introduction

Leaching tests are used by environmental scientists to help assess the ability of a pollutant to partition from a solid waste into surrounding aqueous phases (Meima and Comans 1998, Townsend et al. 2003). A laboratory test usually determines the leaching potential from waste materials following a pre-determined experimental protocol (AFNOR 1988, DIN 38414 S4, MSTM 2001, US EPA 1999). Typically, a leaching test involves the preparation of waste samples (e.g., particle size reduction) and leaching solution, the mixing of the samples with the solution, the filtra-

tion of the mixture, and the analysis of the extracts. Different batch leaching tests have been commonly used in various countries for regulatory purposes (Cappuyns and Swennen 2008, van der Sloot et al. 1997). All these tests use synthetic solutions (including dionised water) as illustrated below for three European countries. Alternative leaching methods are: (i) tank tests, (ii) column tests, (iii) field tests (Cappuyns and Swennen 2008, Townsend et al. 2003).

The German DIN 38414 S4 batch test is standardized for water, wastewater, sediment, and sludge testing. This test uses a 100-g size-reduced sample with unbuffered dionised water using a liquid-to-solid (L/S) ratio of 10:1; the test is run for 24 hours while agitating.

The French AFNOR X 31-210 batch test is standardized for granular solid mineral waste (AFNOR, 1988). The test is similar to the German batch test (DIN 38414 S4) but uses a smaller particle size (less than 4 mm).

The Dutch NEN 7349 test (NEN 1995) is a batch leaching test for granular wastes. This test is a serial batch test consisting of five successive extractions of waste material with dionised water. The test is first run at pH 4 using nitric acid at an L/S ratio of 20:1 for 23 hours, followed by four successive extractions with fresh leaching solution.

A survey of the above-enumerated batch leaching tests shows major differences in the pH value, particle size, and L/S ratio. Other important factors influencing chemical leaching from waste material may include leaching time, complexation with organic (CH_3COOH) or inorganic (CO_3^{2-}/HCO_3^-) chemicals, redox conditions, and chemical speciation of pollutants of interest. Therefore, a number of potential shortcomings of the leaching tests have been enumerated: for example (i) the arbitrary L/S ratio may not be representative of the actual field conditions; (ii) the role of kinetics is minimized as the test is performed for a standard duration; (iii) the pH of leaching fluid does not necessarily represent the pH of the leaching environment. The pH of the leachate during the test is highly dependent on the buffering capacity of the waste materials, which may lead to inaccurate determination of waste behavior in the environment (Cappuyns and Swennen 2008, Townsend et al. 2003).

In the present study, no attempt has been made to control more parameters than in previous works. The detailed field conditions at a contaminated site will certainly vary over the time. However, available contaminants are likely leached by natural waters which mostly differ in their acidity (pH value and carbonate content). Furthermore, it must be expected that the CO_2 partial pressure (and thus HCO_3^- content) below the surface may be higher than the atmospheric partial pressure (Baas-Becking et al. 1960). Therefore, in the present work the attention is focused on characterizing the leaching capacity of natural waters for four inorganics from natural materials (minerals or rocks): arsenic (As), copper (Cu), iron (Fe) and uranium (U). The experiments were performed with 10 g/L solid material in 22 mL leaching solution and under non-disturbed conditions (no agitation/stirring) for a duration of 14 days. The results indicate that the use of natural waters and natural materials may be a powerful extension of available leaching tests.

Materials and Methods

Non-disturbed batch experiments were conducted. The batches consisted in adding 22 mL of a leaching solution to 0.22 g of a contaminant-bearing rock (resulted mass loading 10 g/L). The leaching time was 14 days (336 hours). Further experiments were conducted in tap water with contaminant-bearing rock (10 g/L) and three different additives (5 g/L): (i) dolomite ($CaMg(CO_3)_2$), (ii) elemental iron (Fe^0) or (iii) pyrite (FeS_2). Thus, the extent of As, Cu and U solubilization by tap water as influenced by carbonate minerals and iron oxyhydroxides (iron oxide and hydroxide) was characterized. To mimic natural conditions dionised water (DW) and various waters were used. Table 1 summarizes the carbonate content and simulated effects. The used mineral water ($[HCO_3^-]$ = 1854 mg/L or 30.4 mM) contains for instance more than 20 times more HCO_3^- than the used tape water ($[HCO_3^-]$ = 89 mg/L or 1.4 mM). Two known technical leaching solutions (0.1 M Na_2CO_3 and 0.1 M H_2SO_4) were used for comparison.

The used As-bearing mineral (As-rock) originates from Otto-Stollen in Breitenbrunn/Erzgebirge (Saxony, Germany). The material was selected on the basis of its high arsenic content. A qualitative SEM analysis shows the presence of As, Ca, F, Fe, O, S and Si. The average arsenic content has been determined as 80%. The mineral is primary an hydrothermal vein material and arsenic occurred as native arsenic and Loellingite.

Two iron bearing minerals were used: (i) a Chalcopyrite ($CuFeS_2$) from Ashio (Japan) was crushed and sieved to several fractions. This mineral was not further characterized. (ii) a pyrite mineral (FeS_2) from the Harz mountains (Germany) having an elemental composition of: Fe: 40%, S: 31.4%, Si: 6.7%, Cl: 0.5%, C:0.15% and Ca <0.01% was used as a pH shifting reagent as well as an iron oxide producer in experiments aiming at characterizing the effects of iron oxides on contaminant release.

The used copper ore (Kupferschiefer) originates from Mansfeld (Germany). The material was crushed and sieved to several fractions. Typically, the Kupferschiefer from Mansfeld content up to 2 % Cu (Mäller et al. 2008, Schreck et al. 2005, Schubert et al. 2003, Schubert et al. 2008).

The used uranium bearing rock was crushed and sieved. The fraction 0.250 to 0.315 mm was used without any further pre-treatment. The rock contains around 0.6 % U and is further composed of: 74.16 % SiO_2, 0.19% TiO_2; 7.42 % Al_2O_3, 1.64 % Fe_2O_3, 0.03% MnO; 0.86 % MgO, 12.68 % CaO, 1.53 % Na_2O, 1.45 % K_2O, 0.04 % P_2O_5 and 0.18% SO_3.

The used dolomite mineral was crushed, sieved and the fraction 0.63 to 1.0 mm was used. The mineralogical composition is: SiO_2: 1.2%, TiO_2: 0.03%; Al_2O_3: 0.4%, Fe_2O_3 0.6%, MgO: 20.24%, CaO: 30.94%, Na_2O: 0.04%. Dolomite is a carbonate mineral; it is assumed that its dissolution will increase the kinetics of Cu and U which are known to form stable complex with carbonates.

The used metallic iron (Fe^0 carrier) is a scrap iron from MAZ (Metallaufbereitung Zwickau, Co.). Its elemental conditions are determined as 3.52% C, 2.12% Si, 0.93% Mn, 0.66% Cr, and 92.77% Fe. The materials were fractionated by siev-

Table 1. pH value, HCO_3-content and simulated conditions of the used waters.

Water	Code	pH	$[HCO_3^-]$ (mg/L)	mimicked conditions
Deionized	DW	5.8	0	HCO_3-poor Water
Tap	TW1	8.3	89	Current groundwater
Spring	SW	7.6	95	Current groundwater
Mineral	MW	6.4	1854	HCO_3-rich G-water

ing. The fraction 1.0-2.0 mm was used without any further pre-treatment. The material was used as contaminant-removing agent.

Two different sources of tap water were used: (i) TW1 from the city of Göttingen (Lower Saxonia, Germany) has a composition (in mg/L) of Cl^-: 7.7; NO_3^-: 10.0; SO_4^{2-}: 37.5; HCO_3^-:88.5; Na^+: 7.0; K^+: 1.2; Mg^{2+}: 7.5; Ca^{2+}: 36; and an initial pH 8.3. (ii) TW2 from the village of Krbeck (Lower Saxonia, Germany) has a composition (in mg/L) of Cl^-: 9.6; NO_3^-: 9.45; SO_4^{2-}: 32.9; HCO_3^-:92.5; Na^+: 8.4; K^+: 1.0; Mg^{2+}: 7.2; Ca^{2+}: 35; and an initial pH 7.8.

The used spring water (SW) from the Lausebrunnen in Krebeck (administrative district of Göttingen) was used as proxy for natural groundwater. Its composition was: Cl^-: 9.4; NO_3^-: 9.5; SO_4^{2-}: 70.9; HCO_3^-: 95.1; Na^+: 8.4; K^+: 1.0; Mg^{2+}: 5.7; Ca^{2+}: 110.1; and an initial pH 7.8.

A commercially available mineral water (MW) was used as proxy for HCO_3-rich groundwater. Its composition was: Cl^-: 129; NO_3^-: 0.0; SO_4^{2-}: 37.0; HCO_3^-: 1854; Na^+: 574; K^+: 14.5; Mg^{2+}: 60.5; Ca^{2+}: 99.0; and an initial pH 6.4.

Analysis for As, Cu and U was performed by inductively coupled plasma mass spectrometry (ICP-MS) at the Department of Geochemistry. Analysis for Fe was performed by UV-VIS spectrophotometry (using a Cary 50 from Varian). All chemicals used for experiments and analysis were of analytical grade.

The pH value was measured by combination glass electrodes (WTW Co., Germany). The electrodes were calibrated with five standards following a multi-point calibration protocol (Meinrath & Spitzer 2000) and in agreement with the new IUPAC recommendation (Buck et al. 2002).

All experiments were performed in triplicates. Error bars given in the figures represent the standard deviation from the triplicate runs.

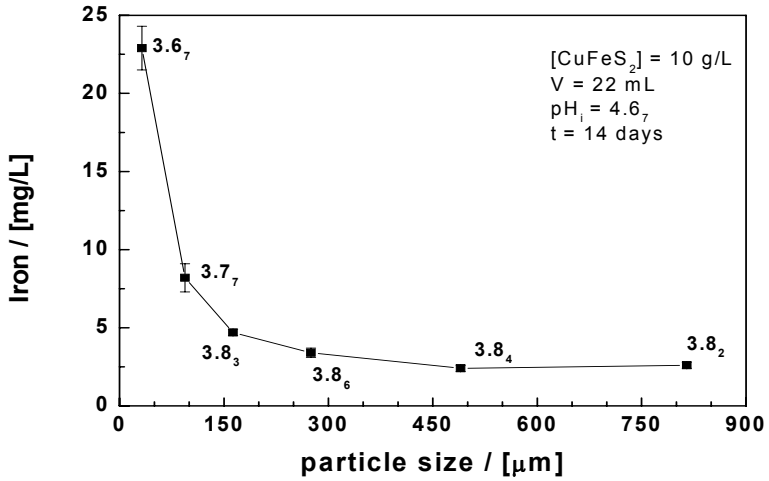

Fig.1. Dependence of the dissolved iron concentration on the particle size of $CuFeS_2$. The values on the curve are the final pH values of the triplicates. The represented lines is not fitting functions, its just joint the points to facilitate visualization.

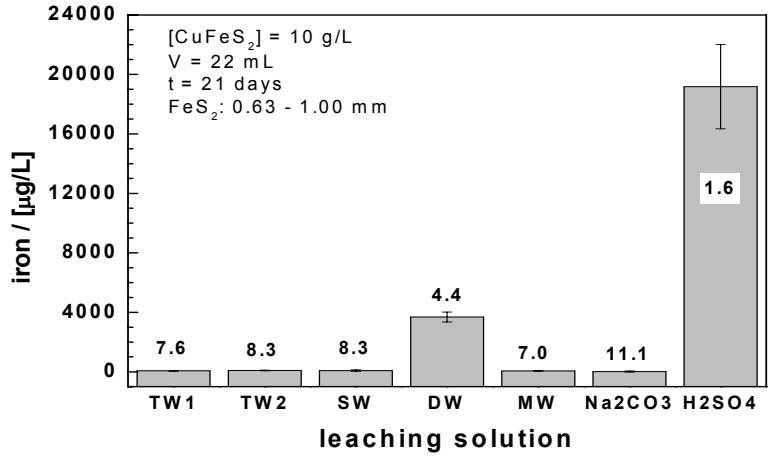

Fig.2. Total Fe concentration as a function of the leaching solution for $CuFeS_2$. The experiments were conducted in triplicates. Error bars give standard deviations.

Rationale for Choice of leaching time

A major characteristic of batch tests is the homogenization of experimental vessels to accelerate mass transport and shorten the time to reach a pseudo-equilibrium. In the present study no effort was done to accelerate mass transfer. Furthermore, the objective was not to achieve any steady state (pseudo-equilibrium) but rather to compare contaminant solubilization under different conditions. Previous studies (e.g., Noubactep et al. 2006) showed that while using essay tubes of about 20 mL capacity and tap water a leaching time of 14 days (336 hours) was sufficient to achieve reproducible leaching results in non-disturbed experiments. The suitability of this leaching time was verified in preliminary works by investigating the effect of material particle size on the extent of contaminant release from each material (including $CuFeS_2$ – next section). The results (not shown) confirmed the well-known trend that the smaller the particle size, the larger the extend of contaminant leaching from the material into the solution. This observation validates the suitability of the used leaching time (14 days) for this study.

Results and Discussion

The solubilization extent of each contaminant after 14 days was characterised by its aqueous concentration. To characterize contaminant (As, Cu, U) solubilization from the natural materials while taking individual properties of CO_3-bearing and Fe-bearing minerals into account, Four different experiments have been performed for each contaminant bearing rock: I) rock alone, II) rock + Dolomite, III) rock + pyrite, and IV) rock + elemental iron (system I, II, III and IV). The solubilization of iron from calcopyrite ($CuFeS_2$) will be first presented.

Iron release from calcopyrite ($CuFeS_2$) in different waters

The following particle size fractions (d in mm) of chalcopyrite: $d \leq 0.063$, $0.063 \leq d \leq 0.125$, $0.125 \leq d \leq 0.200$, $0.200 \leq d \leq 0.355$, $0.355 \leq d \leq 0.630$, and $0.63 \leq d \leq 1.00$ were used to investigate the extent of iron release into dionised water (DW) as function of the particle size. The results depicted in figure 1 show clearly that the extend of iron release is a decreasing function of the particle size. The evolution of the final pH value (values on the experimental points – Fig.1) confirms the role of pyrite as pH shifting agent. Accordingly, the more reactive the fraction the lower the pH value and the higher the iron concentration.

Figure 2 depicts the results of iron solubilization from chalcopyrite in different leaching solutions. It can be seen that for all solutions with initial pH > 7 the extend of Fe release was low and very similar. Only dionised water (DW) and 0.1 M H_2SO_4 depicted higher Fe release. This result is consistent with the pH dependence of iron solubility (Rickard 2006). It is well-known that the dissolution of iron sulfides induces acidification (McKibben and Barnes 1986). Induced acidity

Table 2. Total contaminant concentrations as influenced by the nature of the additive for 14 days. In-situ generated iron oxyhydroxides (systems with Fe^0 and FeS_2) retarded contaminant release from all used rocks. Dolomite (HCO_3^- producer) has no significant effect on Cu and U release under the experimental conditions of this work.

Additive	**[As]** (mg/L)	**[Cu]** (µg/L)	**[U]** (µg/L)
No	136 ± 2	66 ± 7	923 ± 60
Dolomit	131 ± 1	75 ± 11	963 ± 41
Pyrit (FeS_2)	107 ± 3	58 ± 11	743 ± 24
Iron (Fe^0)	76 ± 6	48 ± 13	114 ± 32

accelerates further mineral dissolution. The more acidic the initial pH value, the more intensive the mineral dissolution (DW vs. 0.1 M H_2SO_4).

As, Cu and U release from natural rocks in different waters

Figure 3 depicts the results of As, Cu and U solubilization from the corresponding bearing rocks in different leaching solution. Generally, the carbonate content and the pH value of the used solution are responsible for observed differences (Appelo and Postma 2005).

Arsenic release is solely increased in 0.1 M H_2SO_4 (Fig 3a). This result is not surprising since arsenic (As^{III} or As^{V}) is available as anions. No complex formation between carbonate and As is possible. Therefore, the repeatedly reported carbonate enhanced solubilization of As (e.g., Anawar et al. 2004) can only occurs through an indirect mechanism, e.g. concurrence for adsorption sites.

Fig. 3 b and c show that the maximal leaching extent for Cu and U was achieved in H_2SO_4. The fact that the leaching extent was minimal in dionised water (DW) suggests that at near neutral and basic pH values the carbonate concentrations is the major factor determining metal solubilization. In this regard, it is interesting to note that the used mineral water ($[HCO_3^-]$ = 1854 mg/L = 30.4 mM) was more efficient at leaching both Cu and U than the 0.1 M Na_2CO_3 solutiuon ($[HCO_3^-]$ = 100 mM). The 0.1 M Na_2CO_3 solution contents three times more carbonate than MW. Working with $NaHCO_3$ rather than Na_2CO_3 could have help to discuss these results in more details. Nevertheless, considering the pH values of both leaching solution (6.4 for MW vs. 11.2 for Na_2CO_3) it is evident, that MW is more suitable for experiments targeted at investigating natural systems. Consequently, instead of using technical solution largely and satisfactorily employed in the hydrometallurgy for instance, environmental scientists should focus their attention on available natural (or natural-near) leaching solutions.

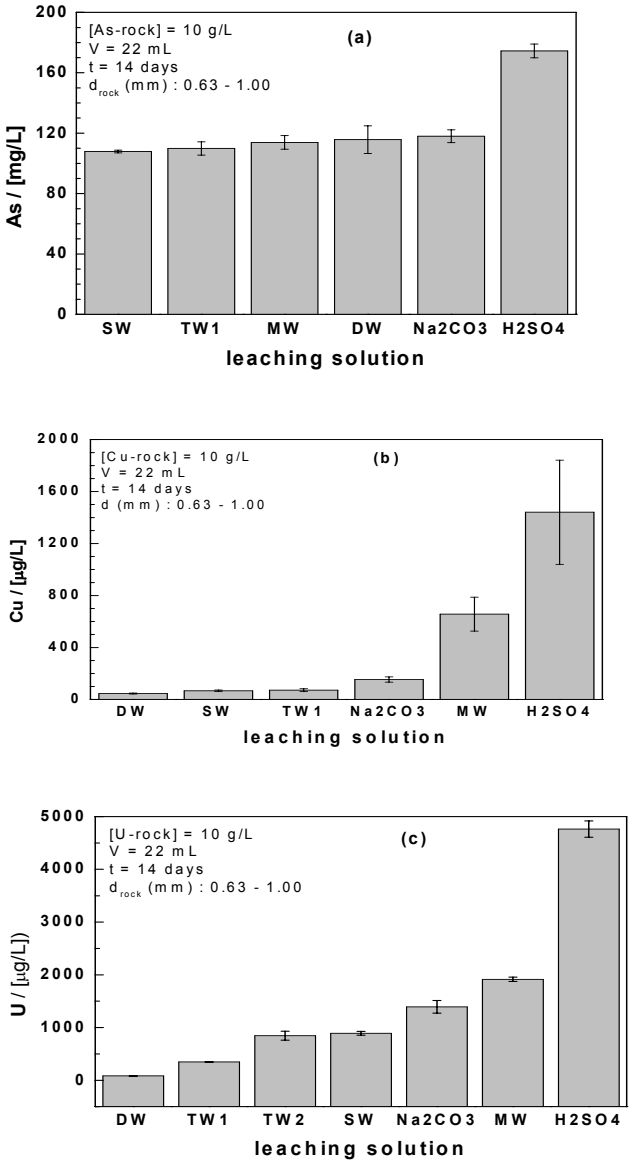

Fig.3. Total contaminant concentration as a function of the leaching solution for a rock particle size of 0.630–1.00 mm.

Effects of carbonate and iron oxyhydroxides on contaminant release

Table 2 summarizes the contaminant concentrations after 14 days in the investigated systems (I through IV). Taking system I (rock alone) as reference, the results can be summarized as follows:

i. elemental iron (Fe^0) and pyrite (FeS_2) significantly inhibit As, Cu and U release from natural materials. The major mechanism of release inhibition is co-precipitation with in-situ generated iron corrosion products (Noubactep 2007).
ii. elemental iron (Fe^0) was more efficient in inhibiting contaminant release than pyrite (FeS_2). The higher efficiency was exhibited for U (only 12 % of the amount release in the reference system). The relative difference of the extent of contaminant release by both materials varies in the same order: U > As > Cu attesting that the same process is responsible for contaminant removal in both systems, namely the co-precipitation with in-situ generated iron oxyhydroxides.
iii. dolomite (HCO_3^-) has no significant effect on Cu and U as the relative difference of the extent of contaminant release is very comparable to the percent standard deviation from the triplicates.
iv. dolomite (HCO_3^-) significantly inhibits As solubilization and this is likely due to the adsorption of solubilised As onto the surface of dolomite.

Concluding Remarks

The evaluation of potential risk to groundwater for a given contaminant is performed via two different procedures: (i) a leaching test is performed and the contaminant concentration in the leachate is compared directly to applicable water quality standards; (ii) the theoretical concentration of a contaminant in a waste (mg/kg) is compared to a risk-based leaching level. The risk-based leaching level represents the theoretical concentration of a contaminant in a waste (mg/kg) that results in a leachate concentration that exceeds the applicable groundwater standard for that contaminant (Cappuyns and Swennen 2008, Townsend et al. 2003). As discussed above a major problem of the procedure is the use of synthetic leaching solution.

The possibility of using natural / natural-near waters has been satisfactorily explored in the present study. The results presented above suggest that column tests involving a continuous flow of natural waters (as leaching solution) through site specific waste material may be a powerful tool to investigate leaching behavior under representative conditions than batch tests. Although the problems inherent to column tests may subsist (flow channeling, clogging, biological activity) this approach may allow a more realistic estimation of the evaluation of potential risk to groundwater. It can be anticipated that data gain from such experiments will be more useful for modelling purposes.

Acknowledgments

Dr. T. Heinrichs (Angewandte Geologie - Georg-August-Universität Göttingen) is kindly acknowledged for the SEM analysis. R. Pfaar is kindly acknowledged for technical support. The used As-bearing mineral, pyrite and chalcopyrite were purchased by the Department of Geology of the Technical University Bergakademie Freiberg. The used scrap iron was kindly purchased by the branch of the Metallaufbereitung Zwickau, (MAZ) in Freiberg. The work was partly supported by the Deutsche Forschungsgemeinschaft (DFG-No 626).

References

AFNOR, Assoication Francaise de Normalisation (1988): Dechéts: Essai de lixivation X31-210, AFNOR T95J, Paris, France.

Anawar HM, Akai J, Sakugawa H (2004) Mobilization of arsenic from subsurface sediments by effect of bicarbonate ions in groundwater. Chemosphere 54: 753-762.

Appelo CAJ, Postma D (2005) Geochemistry, Groundwater and Pollution. second ed. A.A. Balkema, Rotterdam.

ASTM, American Society for Testing and Materials (2001) Annual Book of ASTM standards, Vol. 11.04, D 3987-85.

Baas-Becking LGM, Kaplan IR, Moore D (1960) Limits of the natural environments in terms of ph and oxidation-reduction potenzials. J.Geol. 68: 243-284.

Buck RP, Rondinini S, Covington AK, Baucke FGK, Brett CMA, Camoes MF, Milton MJT, Mussini T, Naumann R, Pratt KW, Spitzer P, Wilson GS (2002) Measurement of pH. Definition, standards, and procedures (IUPAC Recommendations 2002), Pure Appl. Chem. 74: 2169-2200.

Cappuyns V, Swennen R (2008) The Use of Leaching Tests to Study the Potential Mobilization of Heavy Metals from Soils and Sediments: A Comparison. Water Air Soil Pollut. 191: 95-111.

DIN 38414-4: 10.84 Deutsche Einheitsverfahren zur Wasser-, Abwasser- und Schlammuntersuchung; Schlamm und Sedimente (Gruppe S); Bestimmung der Eluierbarkeit mit Wasser (S 4).

McKibben MA, Barnes HL (1986) Oxidation of pyrite in low temperature acidic solution: rate laws and surface textures. Geochim Cosmochim Acta 50:1509-1520.

Meima JA, Comans RNJ (1998) Application of surface complexation/precipitation modeling to contaminant leaching from weathered municipal solid waste incinerator bottom ash. Environ. Sci. Technol. 32: 688-693.

Meinrath G, Spitzer P (2000) Uncertainties in determination of pH. Mikrochem. Acta, 135: 155-168.

Müller N., Franke K., Schreck P., Hirsch D., Kupsch H. (2008): Georadiochemical evidence to weathering of mining residues of the Mansfeld mining district, Germany. Environ. Geol. 54: 869-877.

NEN 7349 (1995) Leaching characteristics of solid earthy and stony building and waste materials. Leaching tests. Determination of the leaching of inorganic components from granular materials with the cascade test. 1st ed, February 1995, Delft, 10pp.

Noubactep C (2007) Processes of contaminant removal in "Fe^0–H_2O" systems revisited. The importance of co-precipitation. Open Environ. J. 1: 9-13.

Noubactep C, Sonnefeld J, Sauter M (2006) Uranium release from a natural rock under near-natural oxidizing conditions. J. Radioanal. Nucl. Chem. 267: 591-602.

Rickard D. (2006) The solubility of FeS. Geochim. Cosmochim. Acta 70: 5779-5789.

Schreck P, Schubert M, Freyer K, Treutler HC, Weiß H (2005) Multi-metal contaminated stream sediment in the Mansfeld mining district: metal provenance and source detection. Geochem. Explor. Environ. Anal. 5: 51-57.

Schubert M, Morgenstern P, Wennrich R, Freyer K, Paschke A, Weiß H (2003) The weathering behavior of complexly contaminated ore processing residues in the region of Mansfeld/Germany. Mine Water Environ. 22: 2-6.

Schubert M, Osenbrück K, Knöller K (2008) Using stable and radioactive isotopes for the investigation of contaminant metal mobilization in a metal mining district. Appl. Geochem. In Press. (Available online 16 April 2008)

Townsend T, Jang Y-C, Tolaymat T (2003) A guide to the use of leaching tests in solid waste management decision making. Department of Environmental Engineering Sciences University of Florida. Report #03-01(A).

US EPA, US Environmental Protection Agency (1999) Waste Leachability: The Need for Review of Current Agency Procedures, EPA-SAB-EECCOM-99-002, Science Advisory Board, Washington D.C.

van der Sloot H, Heasman L, Quevauiller P (1997) Harmonization of leaching /extraction tests. Elsevier, Amsterdam, The Netherlands.


Uranium Mining
and Hydrogeology

Flow in a brine-affected aquifer at a uranium mill tailings site near Moab, Utah, USA

David Peterson[1], John Ford[2] and Jim Moran[2]

[1]S.M. Stoller Corporation, 2597 B ¾ Road, Grand Junction, Colorado, 81502, USA
[2]S.M. Stoller Corporation, 105 Technology Drive, Suite 190, Broomfield, Colorado 80021, USA

Abstract. Uranium and ammonia contamination occurs in moderately saline to briny groundwater down-gradient of a 16-million-ton tailings pile on the west side of the Colorado River near Moab, Utah. Some of the water salinity was caused by historical leaching of the tailings, but the brine is mostly attributed to natural dissolution of deep evaporite sediments. It has been suggested that tailings-derived contaminants flow below the river and impact a wetlands preserve east of the river, but hydraulic data and density-dependent flow and transport modeling indicate that sub-river flow is unlikely. Moreover, water chemistry data suggest that uranium and ammonia in groundwater beneath the wetlands are naturally caused and not derived from tailings leachate.

Introduction

A former uranium milling facility known as the Moab site is located on the west side of the Colorado River at the northwest end of Moab Valley (Fig.1) in east-central Utah, USA. Seepage of fluids from a 16-million-ton tailings pile on the property has produced groundwater contaminant plumes of both uranium and ammonia that migrate from the pile to the river. The U.S. Department Energy (DOE) currently manages the site and is responsible for its cleanup. The S.M. Stoller Corporation (Stoller) was the DOE contractor for the site from 2002 to 2007 and conducted the work discussed in this paper.

The Colorado River flows from north to south across Moab Valley and separates the Moab site from the Matheson Wetlands Preserve (wetlands preserve), which is a riparian area located between the river's east bank and the City of Moab (Fig.1). Several hydrologic investigations have shown that the river acts as a

discharge site for groundwater in the region, including contaminated groundwater flowing eastward from the tailings pile and westward-flowing water from beneath the wetlands preserve. In 2003, a separate study of local groundwater chemistry conducted by University of Utah researchers confirmed the discharge of shallow groundwater to the river but also concluded that deeper, contaminated groundwater flows beneath the river from the Moab site to the wetlands preserve where it detrimentally affects the environment.

This paper examines groundwater flow and transport processes in the vicinity of the Colorado River in Moab Valley, providing multiple lines of evidence that the sub-river flow suggested in the University of Utah study is unlikely. Much of the discussion focuses on the unique presence of very saline groundwater, including brine, particularly near and underneath the river. Using both hydraulic data and a numerical model of density-dependent flow and transport, we hypothesize that observed salinity distributions result from saltwater upconing, which in turn infers that both shallow and deep subsurface water discharges to the river. We subsequently use chemical signature analyses to argue that the chemistry of groundwater beneath the wetlands preserve is solely the result of natural processes occurring east of the river, and that the presence of uranium and ammonia in wetlands groundwater is unrelated to the Moab site.

Study Area Hydrology

Groundwater in the Moab Valley occurs primarily in a northwest-trending alluvial aquifer that is bounded to the northeast and southwest by low-permeability, sedimentary bedrock formations. The uppermost 4 to 5 meters (m) of alluvium on both sides of the river are dominated by fine-grained deposits, but sediments below this depth are generally coarse, consisting mostly of sands and gravels deposited by the river during the Pleistocene Epoch. The Paradox Formation, a Pennsylvanian-age evaporite formation containing gypsum and halite, defines the base of the alluvium in the vicinity of the river. Although the exact thickness of the alluvial aquifer beneath the river is unknown, well drilling in the area indicates that it is greater than 120 m (Doelling et al. 2002).

Regional hydrogeologic investigations by the State of Utah and the U.S. Geological Survey (Blanchard 1990; Freethey and Cordy 1991) indicate that groundwater in both the valley alluvium and surrounding bedrock migrates toward and discharges to the Colorado River from both the east and west. Convergence of flow on the river is supported locally by measured groundwater levels in shallow portions of the alluvial aquifer at both the Moab site and the wetlands preserve (U.S. Department of Energy 2003; Gardner and Solomon 2003). Fig.1 illustrates observed flow directions in shallow groundwater. Depths to the top of the saturated zone (water table) just west of the river at the Moab site are generally about 3 to 4 m below ground surface (bgs), and comparable depths at the wetlands preserve tend to range from 0 to 3 m bgs.

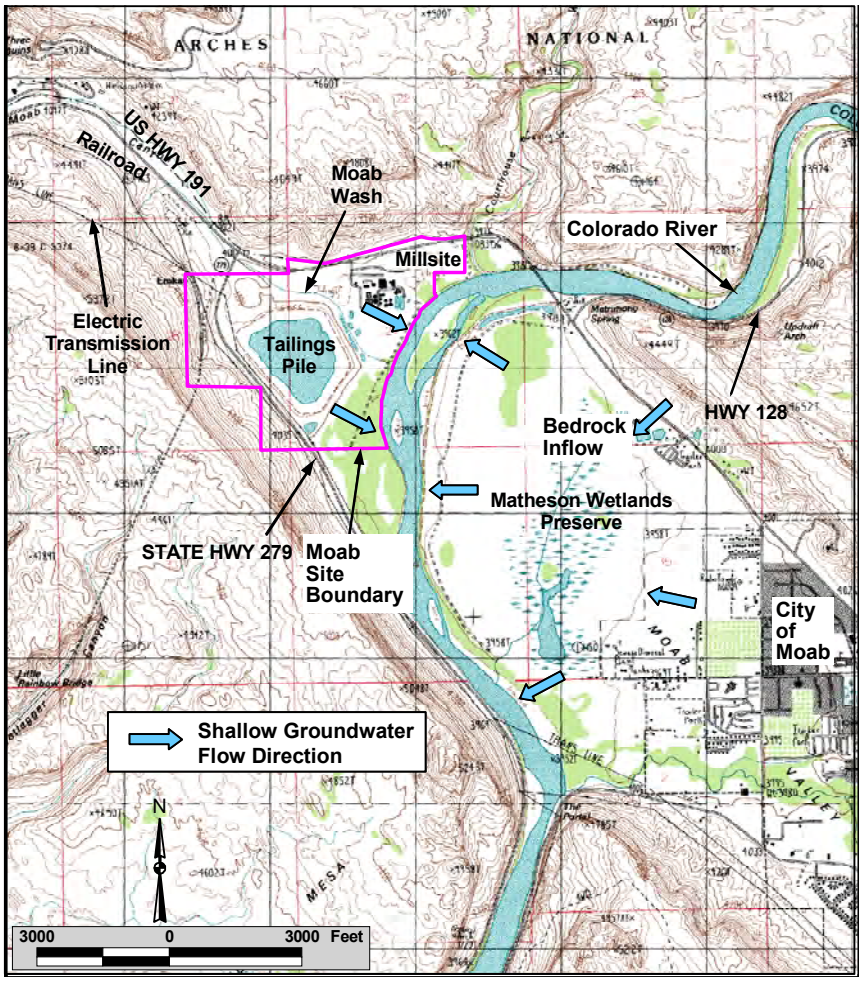

Fig.1. Map of the study area and shallow groundwater flow directions.

The chemistry of groundwater in the alluvial aquifer is noteworthy for the wide range of salinities exhibited on both sides of the Colorado River, with total dissolved solids (TDS) concentrations varying from those for freshwater (TDS < 1,000 milligrams per liter [mg/L]) to those for brine (TDS > 35,000 mg/L). Consistent patterns are observed in the spatial distribution of salinity. In shallow portions of the alluvial aquifer, TDS generally increases with proximity to the river. At any given location on either side of the river, TDS typically increases with depth. At distances of about 300 to 1,000 m from the river, it is common for well nests in the alluvium to reveal TDS concentrations ranging from those for slightly saline water (TDS = 1,000 to 3,000 mg/L) (McCutcheon et al. 1993) in shallow groundwater to as much as 100,000 mg/L at depths of about 40 m bgs. At well nests located along the river's east and west banks, it is not unusual for the TDS

concentration to be as large as 30,000 to 60,000 mg/L in the shallowest portion of the saturated zone and to increase with greater depth.

Although the spatial distributions of TDS in groundwater are generally similar on respective sides of the river, salinity levels down-gradient of the tailings pile at the Moab site are distinguishable from those in other areas in that they show signs of being historically influenced by tailings leachate. In particular, moderately saline (TDS = 3,000 to 10,000 mg/L) and very saline (TDS = 10,000 to 35,000 mg/L) (McCutcheon et al. 1993) waters tend to dominate the shallow flow system between the east toe of the pile and the river. Such large salinities are generally not observed beneath the wetlands at equivalent distances and depths east of the river.

Much of the hydrogeologic characterization work in the study area (U.S. Department of Energy 2003, 2007) has focused on the delineation of a brine surface, which is defined as a surface along which TDS concentration equals 35,000 mg/L. From the TDS distribution patterns mentioned above, it can be deduced that the brine surface becomes shallower with proximity to the river and intercepts the riverbed.

The ammonia plume currently observed down-gradient of the tailings pile resulted from the use of ammonia-bearing compounds in the milling processes. Concentrations of this contaminant in alluvial groundwater between the pile and the river typically range between 100 to 1,000 mg/L ammonia as nitrogen (NH_3-N) (U.S. Department of Energy 2003). Discharge of the ammonia to surface water near the west bank of the river poses a potential threat to the well being of endangered fish species in the river. Uranium concentrations in shallow groundwater between the tailings and the river tend to vary between 0.5 to 5 mg/L.

Concentrations of ammonia and uranium in groundwater at the wetlands preserve are significantly lower than those observed in contaminated groundwater at the Moab site. Although some groundwater just east of the east bank of the river exhibits ammonia concentrations as large as 3.5 mg/L as nitrogen, NH_3-N levels below the central part of the wetlands are typically less than 0.5 mg/L. Uranium concentrations in wetlands groundwater generally range from 0.0001 to 0.1 mg/L.

The Matheson Wetlands Preserve contains a variety of vegetation types, including willows, cottonwoods, and tamarisk. The Colorado River floods the riparian area on average about once every 8 to 9 years. Periodic flooding of the preserve and the potential for biogeochemical processes to occur within it suggest that the chemistry of shallow groundwater in the area is subject to considerable spatial and temporal variability.

Modeling

Under the direction of DOE, Stoller developed a conceptual hydrogeologic model of the study area (U.S. Department of Energy 2003) to help explain groundwater flow processes and observed water chemistry on both sides of the river. The model assumes that flow in the alluvial aquifer flow is affected by water density, which

varies with changes in TDS concentration, and that this density-dependent flow is governed by the dissolution of sediments comprising the upper part of the Paradox Formation. In keeping with observed convergent flow on the Colorado River in shallow parts of the aquifer (Fig.1), the model further assumes that flows in deeper portions of the aquifer, at the alluvium/Paradox Formation contact, are also generally toward the river. This means that deeper aquifer flow beneath the Moab site is to the east and southeast, and that comparable flow beneath the wetlands preserve is to the west and northwest.

The DOE conceptual model further assumes that saltwater upconing occurs in the vicinity of the river, in which saline waters resulting from dissolution of Paradox Formation sediments migrate upward as they approach the river and eventually discharge to surface water. Such a conceptualization is analogous to the saltwater upconing that occurs when a pumping well screened above saline groundwater pulls the saltwater upward to elevations that it would not otherwise reach. Under this analogy, the river represents a well that is capable of removing the saline water from the local environment. Fig.2 schematically shows this concept as it applies to the Moab Valley.

The density-dependent processes in this flow system are similar to those presented by Konikow et al. (1997) as part of a study of deep-circulating groundwater passing over a buried salt dome and followed by upward water migration and discharge to the ground surface. Such a system is characterized by a brine surface that has a curvilinear shape between the deep saline water source and the point of discharge (Fig.2), and groundwater velocities that decrease with depth, eventually becoming unmeasurable at some depth below the brine surface. Accordingly, groundwater velocities within the brine at some depth directly below the river are expected to be so small as to reflect no vertical or horizontal flow.

It is noteworthy to point out that saltwater upconing to the extent that the brine surface intercepts the Colorado River is unique. Although this phenomenon has been documented in a river/aquifer system in Kansas (McElwee 1985), other studies of saline water upwelling below rivers in the southwest USA rarely show brine in shallow groundwater. The significant upconing in Moab Valley is not surprising given that the alluvial aquifer is bounded on both sides and underneath by low-permeability bedrock, and that the only subsurface outlet for the alluvial

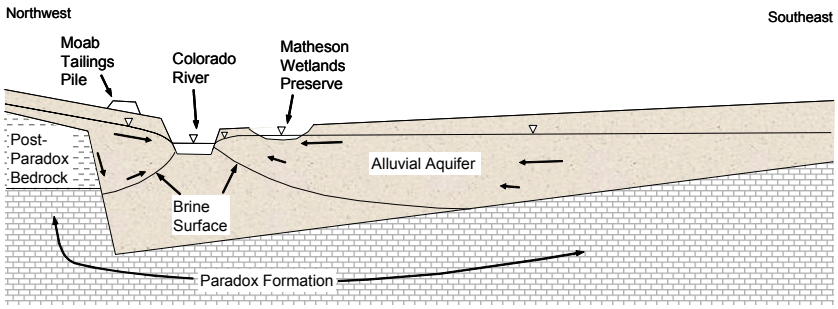

Fig.2. Conceptual model of density-dependent groundwater flow in the study area.

groundwater is a small area adjacent to where the river leaves the valley on its south side (Fig.1).

A numerical model of density-dependent flow and transport was developed (U.S. Department of Energy 2003) to evaluate the applicability of the DOE conceptual model to groundwater processes occurring on the west side of the river in general and the Moab site in particular. The modeling was performed using the numerical simulator SEAWAT (Guo and Langevin 2002), which computes flow potential in terms of equivalent freshwater head and water density. SEAWAT treats TDS as the primary transport constituent and can handle multiple secondary constituents to ascertain the effects of salinity on their migration.

The numerical modeling accounted for flow in a cross section that coincided with a flow stream-tube identified during characterization of the Moab site (U.S. Department of Energy 2003). The cross-sectional trace began at the northwest end of the site at Moab Wash (Fig.1), passed through the tailings pile in a southeastward direction, and terminated at the center of the Colorado River channel. Processes incorporated in model simulations (Fig.3) included inflow as subsurface discharge from bedrock sediments upgradient of a major fault (Moab Fault) that bisects the site, subsurface inflow from the Moab Wash, seepage from sand zones on the margins of the tailings pile, and evapotranspiration from tamarisk vegetation between the pile and the river. The river was assumed to constitute a prescribed head boundary, and a no-flow boundary condition was used along the southeast end of the simulation domain (Fig.3) to reflect flow convergence on the river from both the east and the west. Influx of salinity resulting from the dissolution of Paradox Formation sediments was simulated using a diffusion boundary condition that was applied by Konikow et al. (1997) in their representation of flow over salt domes. Because depth to the Paradox Formation is unknown, this diffusion mechanism was invoked at a series of depths that varied with location within the cross-section. Beneath the up-gradient end of the tailings pile, salt diffusion was assumed to occur along a steep rock face (Fig.3) that first exposes the Paradox Formation at a depth of about 50 m bgs. From the toe of the rock face to the model's southeast end, diffusion was assumed to occur from deep groundwater located at a depth of 95 m bgs. A prescribed TDS concentration of 300,000 mg/L was applied to each of the boundary cells used to simulate salt diffusion from the Paradox Formation.

Steady-state model runs conducted with the numerical model to account for pre-mining conditions proved successful for simulating the shallow groundwater potentiometric surface at the site and in matching the curvilinear brine surface currently seen underneath and down-gradient of the tailings pile (U.S. Department of Energy 2003; Peterson et al. 2004). These results indicated that most of the current salinity distribution in groundwater west of the river is attributable to natural processes. However, transient runs designed to account for historical use of the pile improved the model's ability to match the current preponderance of moderately saline to very saline groundwater in the shallow subsurface between the pile and the river. Simulations of recent conditions at the site indicated that evapotranspiration from tamarisk plants comprises a large portion of groundwater outflow at the site, signifying that evapotranspiration at the wetlands preserve is also

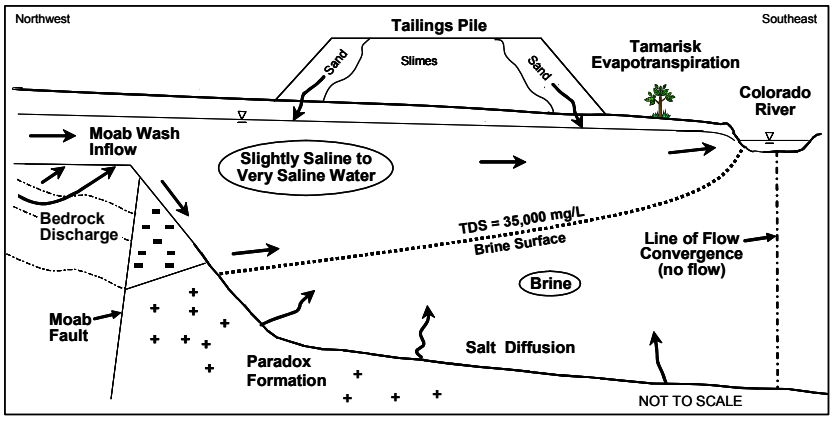

Fig.3. Processes incorporated in the numerical cross-section model.

significant. The other major outflow component, discharge to the river, was confined to a few model cells located just east of the river's west bank. Although this latter result was expected given that most groundwater discharge to rivers occurs within limited zones near their banks (Haitjema et al. 2001), the upwelling brine provided an additional impediment to discharge farther east of the riverbank (Peterson et al. 2004).

Alternative Conceptual Model

Simultaneous to DOE's conceptualization of groundwater flow in the northwest end of Moab Valley as being density-dependent due to saltwater upconing near the Colorado River, two University of Utah researchers (Gardner and Solomon 2003) developed a different perception of the local hydrogeology. In particular, they concluded that contaminants associated with historical operation of the Moab site migrated under the Colorado River to the Matheson Wetlands Preserve during past years, and probably continue to do so under current conditions. The inferred repercussions of such phenomena included detrimental impacts on the wetlands environment.

The alternative model was based primarily on the interpretation of trans-river subsurface hydraulic gradients, measured uranium concentrations in shallow groundwater, and isotope data. The hydraulic gradients were derived using values of equivalent freshwater head at a common elevation of about 14 m below the bed of the Colorado River, as estimated from water level and salinity data at nine wells on both sides of the river and screened in brine. Gardner and Solomon (2003) used this information to infer that groundwater within the brine migrated under the river in a south-southeastward direction from the Moab site. Uranium concentrations on the order of 0.02 to 0.06 mg/L in the northern half of the wetlands preserve were interpreted as being potentially related to Moab site contamination. The research-

ers used two cross sections depicting measured oxygen isotope ratios ($\delta^{18}O$) in groundwater on both sides of the river to assert that the ratios did not comport with the river acting as a discharge site for all water in the alluvial aquifer.

2006 Assessment of the Wetlands Preserve

In 2006, Stoller conducted a new investigation of the wetlands preserve (U.S. Department of Energy 2007), partly for the purpose of evaluating Gardner and Solomon's (2003) conclusions regarding sub-river flow. Using measured water levels from three different occasions at several wells and piezometers, this study confirmed that shallow groundwater beneath the wetlands generally flows in a westward direction toward the Colorado River, as illustrated in Fig.1. In addition, a persistent shallow groundwater mound was identified in the northeastern part of the preserve, adjacent to the bedrock formation that bounds the alluvial aquifer on its northeast side. This area of elevated groundwater, which was identical to mounding reported earlier by Gardner and Solomon (2003), caused local groundwater movement toward the southwest and was attributed to subsurface inflow from the bounding bedrock (denoted as bedrock inflow in Fig.1).

Water chemistry data collected during the 2006 study were examined with the intent of identifying the origin of dissolved uranium and ammonia in the wetlands groundwater (U.S. Department of Energy 2007). The ratio of measured activity concentrations of uranium-234 (U-234) and uranium-238 (U-238) in samples collected at the preserve were compared with equivalent ratios in samples from Moab-site wells down-gradient of the tailings pile. This analysis revealed two rad-

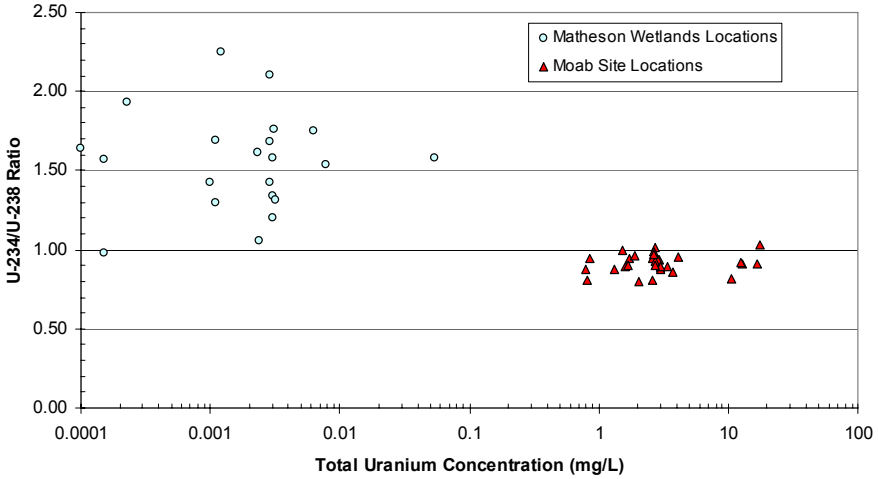

Fig.4. Uranium isotope ratios in groundwater at the Moab-site and the wetlands preserve.

ically different data clusters (Fig.4), with the wetlands samples typically exhibiting isotope ratios ranging from 1 to more than 2, and the Moab site wells mostly showing ratios on the order of 1 or less. These results indicated that the Moab-site water was relatively young, originating as leachate from the tailings pile, whereas uranium in the wetlands groundwater could be attributed to the inflow of much older water from bedrock on the north side of the Moab Valley (U.S. Department of Energy 2007). Apparent decreases in uranium concentration between the inflow area and the river were ascribed to biogeochemical processes.

The ammonia chemistry observed at wetlands wells during the 2006 study showed that NH_3-N concentrations on the east side of the river range from 0.1 to about 4 mg/L, and that ammonia levels generally increase with increasing TDS concentration (U.S. Department of Energy 2007). The correlation between ammonia and salinity suggested that the larger ammonia concentrations on the east side of river are the result of Paradox Formation dissolution at large depths, subsequent upward flow of groundwater via saltwater upconing, and dilution due to mixing with less saline water.

Conclusions

Groundwater flow in the vicinity of the Colorado River in Moab Valley is heavily influenced by the presence of highly saline water, including brine that exhibits TDS concentrations of 100,000 mg/L or more. Most of the brine observed in shallow groundwater near both the east and west banks of the river is caused by the dissolution of deep evaporite sediments by groundwater that subsequently intercepts the river via saltwater upconing. Numerical modeling of salinity-driven, density-dependent groundwater flow in the study area and examination of groundwater chemistry on both sides of the river indicates that sub-river migration of water from the Moab site to the Matheson Wetlands Preserve is unlikely. Accordingly, dissolved uranium and ammonia in groundwater on the east side of the river and beneath the wetlands preserve can be attributed to natural processes and is unrelated to contamination at the Moab site.

References

Blanchard P (1990) Ground-water conditions in the Grand County area, Utah, with emphasis on the Mill Creek-Spanish Valley area. State of Utah Dept of Natural Resources.

Doelling H, Ross M, Mulvey W (2002) Geologic map of the Moab 7.5' quadrangle, Grand County, Utah. Utah Geological Survey.

Freethey G, Cordy G (1991) Geohydrology of Mesozoic rocks in the Upper Colorado River Basin in Arizona, Colorado, New Mexico, Utah, and Wyoming, excluding the San Juan Basin. U.S. Geol Survey Prof Paper 1411-C.

Gardner P, Solomon D (2003) Investigation of the hydrologic connection between the Moab mill tailings and the Matheson Wetlands Preserve. Univ of Utah, Dept of Geol Geophysics.

Guo W, Langevin D (2003) User's guide to SEAWAT: a computer program for simulation of three-dimensional variable-density ground-water flow, U.S. Geol Survey OFR 01-434.

Haitjema H, Kelson V, de Lange W (2001) Selecting MODFLOW cell sizes for accurate flow fields. Ground Water 39(6): 931-938.

Konikow L, Sanford W, Campbell P (1997) Constant-concentration boundary condition: lessons from the HYDROCOIN variable-density ground water benchmark problem. Water Resources Research 33(10): 2253-2261.

McCutcheon S, Martin J, Barnwell Jr T (1993) Water quality. Handbook of Hydrology: 11.1-11.73, McGraw-Hill.

McElwee C (1985) A model of salt-water intrusion to a river using the sharp interface approximation. Ground Water 23(4): 465-475.

Peterson D, Kautsky M, Karp K, Wright T, Metzler D (2004) Modeling of density-dependent groundwater flow and transport at the uranium mill tailings site near Moab, Utah. Tailings and Mine Waste '04, A.A. Balkema.

U.S. Department of Energy (2003) Site observational work plan for the Moab, Utah, site. DOE Report GJO-2003-424-TAC.

U.S. Department of Energy (2007) Fall 2006 assessment of Matheson Wetlands hydrogeology and ground water chemistry. Report DOE-EM/GJ1441-2007.

Problems of the hydrogeological monitoring of objects of the Prydneprovsk Chemical Plant (Dneprodzerzhynsk, Ukraine)

Oleksandr Skalskyy[1] and Victor Ryazantsev [2]

[1] Institute of geological sciences, National Academy of Sciences of Ukraine, Gonchara Str. 55-b, 01054, Kiev, Ukraine
[2] Committee of the nuclear regulation and radiation safety, chief of management of safety of radiation technologies, 9/1 Arsenalna Str., 01011, Kiev, Ukraine

Abstract. The Pridneprovsk Chemical Plant (PChP) was one of the first uranium plant in the former Soviet Union. Nowadays the area of PChP is highly radioactive and chemically contaminated. The area contains some contaminated buildings and wastes of uranium production, which are placed in nine tailings. The radiactive elements of the uranium range migrate from the tailings into the graundwater and move toward discharge areas. During the years 2005-2007 some envestigations were carried out to assess the groundwater contamination, develope the Geology-hydrogeological Informative System and create the mathematical models of groundwater flows and migration of contaminating matters. The mathematical models where built by means of Visual ModFlow 3 PRO software package, MapInfo and Surfer computer programs. For the simplified simulation of radionuclide transport with groundwater the EcoLego computer code was used.

Location of Prydneprovsk Chemical Plant (PCh.P) and general characteristic of its tailings

Location

PCh.P is located in Dneprodzerzhynsk town, near Dnepropetrovsk sity. The Dneprodzerzhynsk town and PCh.P are located at the right bank of the River Dnepr

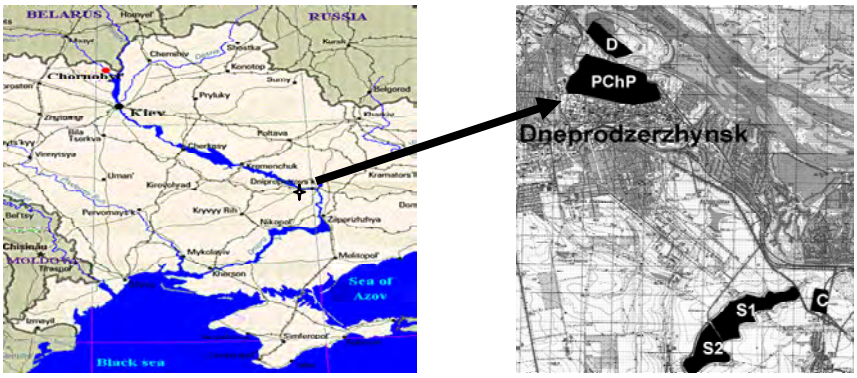

Fig.1. Location of Prydneprovsk Chemical Plant and its external tailings: D - tailing "Dneprovskoe"; C – "Base C"; S1 – 1st section of tailing "Sukhachevskoe"; S2 – 2nd section of tailing "Sukhachevskoe".

(see Fig.1). Territory of PCh.P is located on the terrace of the river Dnepr (middle and lower parts) and on the slope of Quaternary Plato (upper part). There are 3 tailings in the territory of PCh.P: "Western", "Central Iar" and "Souse-Eastern". They occupy the lower parts of the former ravines, which interfaced with Dnepr River terrace. The external tailing "Dneprovskoe" is located not far from PCh.P, at the flood plain of Dnepr River. Other external tailings are located on the Quaternary Plato (see Fig.1).

General characteristics of tailings

General characteristics of tailings are shown in the Table 1.

Table 1. General characteristics of the PCh.P tailings

Tailing names	Period of operation	Area, hectares	Amount of the waste, $x10^6$ t	Volum, $x10^6 m^3$	Gross activity, TBk
„Western"	1949-54	6.0	0.77	0.35	180
„Central Iar"	1951-54	2.4	0.22	0.10	104
„South-Eastern"	1956-80	3.6	0.33	0.15	67
"Sukhachevskoe" 1st section	1968-83	90	19.0	8.6	710
"Sukhachevskoe" 2nd section	1983-92	70	9.6	4.4	270
„Base C"	1960-91	25	0.3	0.15	440
„Dneprovskoe"	1954-68	73	12.0	5.9	1400
„Lantan fraction"	1965-88	0.06	0.0066	0.0033	130
„Blast furnace N6"	1982	0.2	0.04	0.02	330

Tailing of „Lantan fraction" is buried on the right side of 2nd section of tailing "Sukhachevskoe". And the „Blast furnace N6" is buried on the northern part of tailing "Base C", which was used for storage of uranium ore from Ukrainian and foreign suppliers.

Hydrogeological conditions and monitoring system

Hygrogeological conditions

Territory, where the PCh.P and its tailings are located, is built by means of Archeozoic and Proterozoic age rocks with weathering crust, above which spread consequently the rocks of Neogene and Quaternary ages. The Archeozoic and Proterozoic crystalline rocks are widespread and consist of granites. In the upper part the granites are fractured and together with of the weathering crust, contain lower confine-unconfined aquifer (Voicekchovich O. et al.,2005).

Neogene layer is widespread on a Quaternary plateau and represented by sandy deposits. Deposits contain unconfined aquifer, which builds the hydraulically joined complex along with the lower aquifer forms. From roof the Neogene deposits are covered by red and variegate clays of quaternary age. Over the layers of red and variegate clays, loess layers are bedded.

In loess layer unconfined aquifer sporadically exists. On the slope of plateau towards Dnepr River aquifers in Neogene and loess rocks pass to unconfined aquifer in alluvial deposits, which is usual for terrace and flood plain of Dnepr river. Alluvial aquifer together with aquifer in crystalline rocks is combined into aquifer complex.

Except aquifers of natural origin, tailings “Dneprovskoe” and “Western” content the saturated layers in the wastes of uranium production. Saturation of uranium production wastes increases migration of radionuclides toward the lower aquifer and to the recharge regions. General characteristics of saturated deposits are shown in the Table 2.

Dnepr River is the main discharge region For Neogene and Alluvial aquifers. In addition the groundwater from internal PHc.P tailings partly discharges into small river Konoplianka, which flows between PHc.P and tailing “Dneprovskoe”. The aquifer in loess deposits discharges into streams, which run along gullies system.

The layout of groundwater head isolines for PHc.P and tailing “Dneprovskoe” location are shown on the Fig.2. The illustration is created by means of filtration modeling (Bugai D. et al., 20070. The Visual ModFlow 3 PRO mathematical

Table 2. General characteristics of saturated deposits

Rock	Permeability, m/day	Water yield, part per unit	Porosity, cm^3/cm^3	Average thickness, m
Wastes	0,04-2,7	0,15	0,36-0,42	8,0
Loess	0,02-0,1	0,15	0,58-0,88	10
Alluvial sands	3-10	0,15	0.3-0.35	8
Neogen sands	4-10	0,15	0,3-0.35	10
Weathered crust and fractured zone	3-7	0,02	0,1	

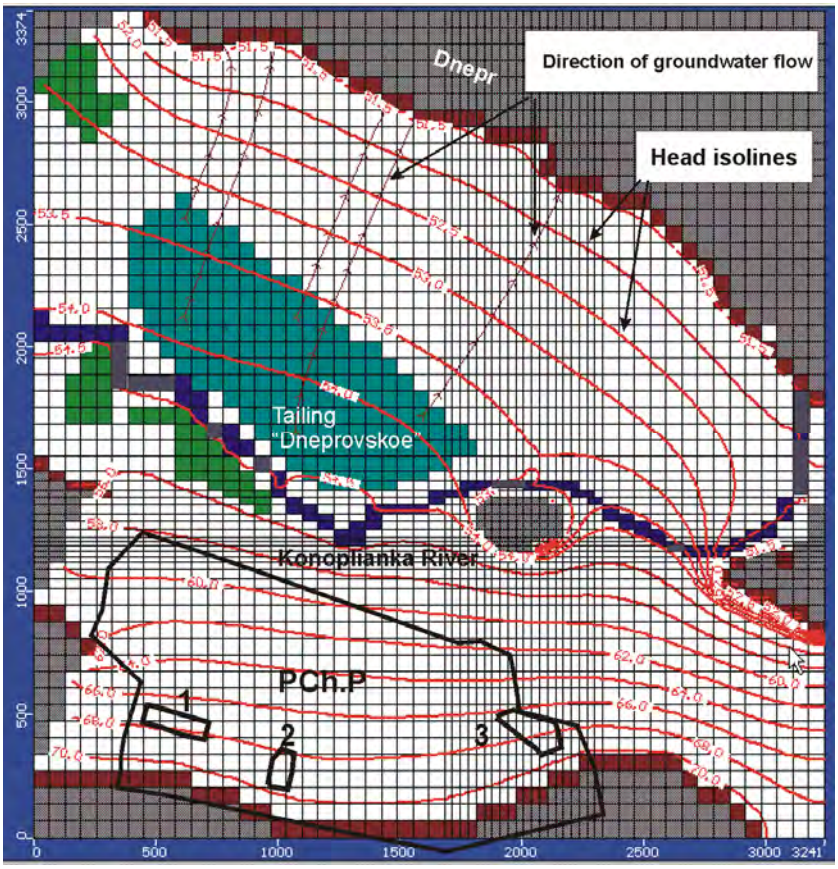

Fig. 2. The layout of groundwater head isolines for PHc.P and tailing "Dneprovskoe" location (1 – tailing "Western", 2 – tailing "Central Iar", 3 – tailing "Souse-Eastern").

modeling software, MapInfo and Surfer computer programs where used for such modeling. The filtration model includes aquifers in crystalline rocks and in the alluvial deposits. The geological layers were put into the calculation module of filtration model taking into account relief of their bedding. Geology-hydrogeological Informative System, which includes cartographic information, geological layers layout, wells, and contamination of groundwater, was used for mathematical model creation. Spatial steps of calculation net of the mathematical model are 62 - 15 m.

From the tailing "Dneprovskoe" groundwater flows to the Dnepr River with the gradients of head ≈ 0,003-0,004. The unabsorbed particle associated with groundwater flow needs approximately 40 - 50 years to get to the Dnepr River. Groundwater gradients of head of the PCh.P region are much higher. The unabsorbed particle, associated with groundwater flow from internal tailings of PCh.P

("Western", "Central Iar" and "Souse-Eastern"), needs approximately 3 - 5 years to get to Konoplianka River.

Monitoring system

In the year 2000, the Ministry of Fuel and Energy of Ukraine created the enterprise «Barrier» to execute control and monitoring of radioactive contaminated materials (including groundwater), radiation level of environment. Starting the year 2000, the management of the enterprise «Barrier» tried to organize monitoring, using other appropriate organizations. Unfortunately, these efforts had no sufficient effect. The reasons: absence of the grounded observation network and regulation of observations, insufficient funds reserves, provided by the Ministry, absence of required monitoring and sampling equipment, lack of trained personnel.

The system of the hydrogeological monitoring, controlled by the enterprise «Barrier», consists of 57 wells. 49 wells situated on the tailing "Dneprovskoe". Tailing "Western" is equipped by 4 wells, the tailing "Central Iar" is equipped by 3 wells. There are no monitoring wells on the tailing "South-East". Also, there is no network of monitoring wells on the tailing "Base C". The current state of monitoring wells, situated on both sections of tailing «Sukhochevskoe», have not been investigated yet. The P.Ch.P monitoring wells are shown on the Fig.3.

In spite of big number of existing monitoring wells, it is impossible to carry out the sampling of groundwater, using most of them. The well filters are muddy and wells are not pumped out systematically. In addition, some wells are not under control of the enterprise «Barrier».

The process of systematical monitoring system development began in 2004. This process was initiated by the professionals of the «Center of monitoring researches and nature protection technologies», «Institute of hygiene and medical ecology», National Academy of Sciences of Ukraine and "The permanent inspection of the Committee of the nuclear regulation and radiation safety". The "Conception and suggestions to the program of environment radiation control and monitoring in the region near former Prydneprovsk chemical plant" was developed in 2007.

In 2005-2007 the basic researches of the monitoring system of environment and preliminary regulation of observations were carried out. Some results of groundwater monitoring are represented in Table 3.

The biggest radionuclides contamination of underground environment was registered in the regions where the tailings are located and in technogenic aquifers, which appear in the wastes of uranium production. Uranium isotopes migrate to aquifer in the sandy alluvial deposits.

Macroionic composition of groundwater is variegated, and their salinity in the areas of depositories is very large - ten times exceeds standards, existing for drinking water. Very large salinity is observed in water of technogenic aquifer of tailing "Western" – about 100 g/L. In chemical composition of groundwater the chlorine anion and the sodium cation are prevailing. Anions of sulfate and hydrogen carbo-

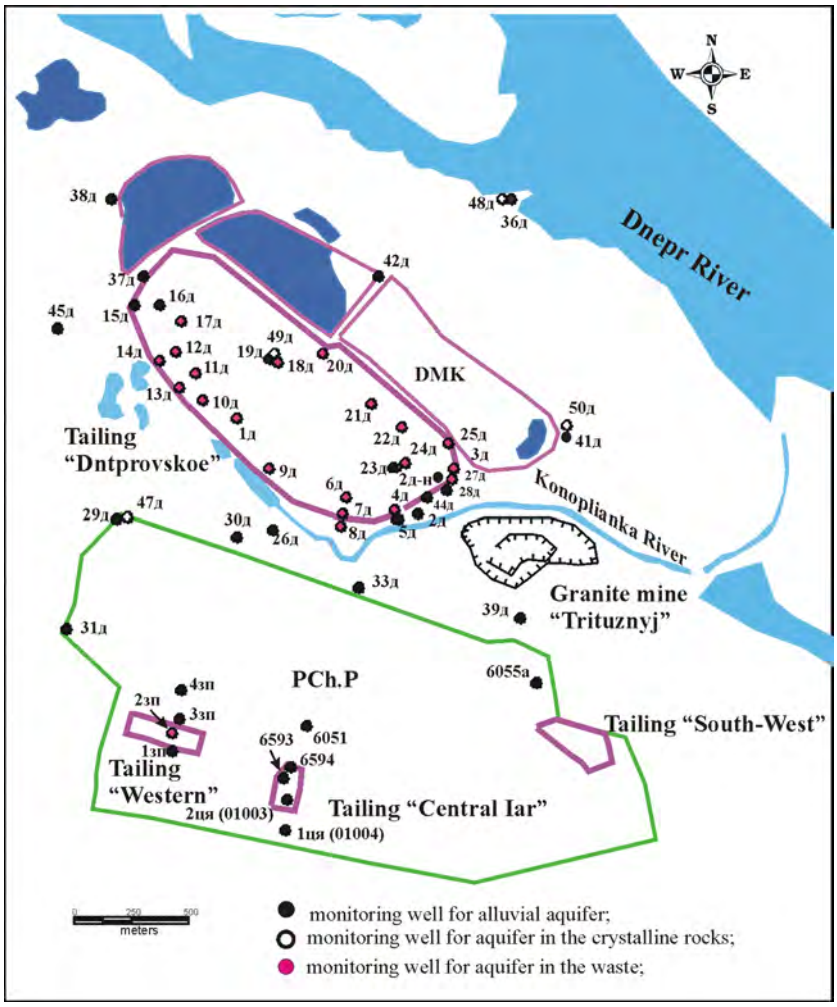

Fig. 3. The P.Ch.P monitoring wells network.

nate are prevailing in technogenic aquifer of tailing "Dneprovskoe". Cations are represented by ammonium, magnesium, potassium, sodium and calcium.

Efforts of the Ukrainian side in development of monitoring system for objects of former PCh.P are supported IAEA within the framework of regional project RER/9/094: "*Upgrading National Capabilities in Controlling Public Exposure*". Currently, the enterprise has minimum quantity of equipment, required for observations and sampling of groundwater.

Table 3. Content of uranium isotopes in groundwater of PCh.P tailing location in comparison 2005/2006 (Voicerhovich O. et al., 2006).

Well #	Salinity, g/L	U-234, Bk/L	U-238, Bk/L	Σα, Bk/L	Σβ, Bk/L	$^{234}U/^{238}U$
6593a	2,0	1,19±0,25	1,58±0,26	3,0±0,9	1,0±0,3	0,75
	1,8	1,8±0,4	2,3±0,4	6,7±1,2		
6594	3,6	28,4±4,3	31,6±4,3	56±11	25±5	0,9
	4,4	64,2±12,8	45,9±9,3	115±22		1,4
1-3П	2,3	0,56±0,11	0,35±0,07	0,81±0,24	0,93±0,	1,6
	1,8	0,32±0,08	0,23±0,05	0,55±0,11	28	1,4
2-3П	91	506±76	562±77	1180±177	151±30	0,90
	86	481±82	419±82	900±180		1,15
3-3П	11,4	376±56	384±56	1160±174	276±55	0,98
	10,3	314±62	286± 56	600±120		1,1
2-Д	7,3	0,73±0,16	0,90±0,18	2,62±0,78	4,6±1,4	0,81
	7,2	<0,03	0,20±0,02	0,23±0,04		0,42
4-Д	6,4	0,26±0,05	0,22±0,05	0,84±0,24	10±3	1,18
	11,1	2,5±0,5	2,4±0,5	5,0±1,0		1,04
19-Д	19,3	7,3±1,3	6,8±1,3	15,1±3,0	7,9±2,3	1,07
	18,4	9,38±2,40	5,69±0,31	16,0±3,2		1,6
16-Д	2,3	2,36±0,35	2,41±0,35	5,8±1,4	-	0,98
			5,4±1,2	5,8±1,2		
48-Д	5,8	0,09±0,03	0,09±0,03	< 0,2	2,0±0,6	
		0,40±0,06	0,43±0,06	0,8±0,04		1,00
MPC		0,5	0,5	0,1		

Assessment of radionuclide migration

Computer program for simulation

To create the mathematical model of radionuclide migration a software package the Ecolego was used. In this software package the conceptual model of the studied system is set by the matrix of co-operation (Fig. 4).

The diagonal elements of such matrix correspond the components (compartments) of the designed system. External diagonal elements describe connections between compartments and processes of radionuclide transfer. For simulation of radionuclide migration by groundwater, the software package Ecolego was completed by special computer code (Dugai D. et al., 2007).

Radionuclide migration from tailing “Dneprovskoe” was simulated. The model describes migration of ridionuclides along the ribbon (tubes) of groundwater in the

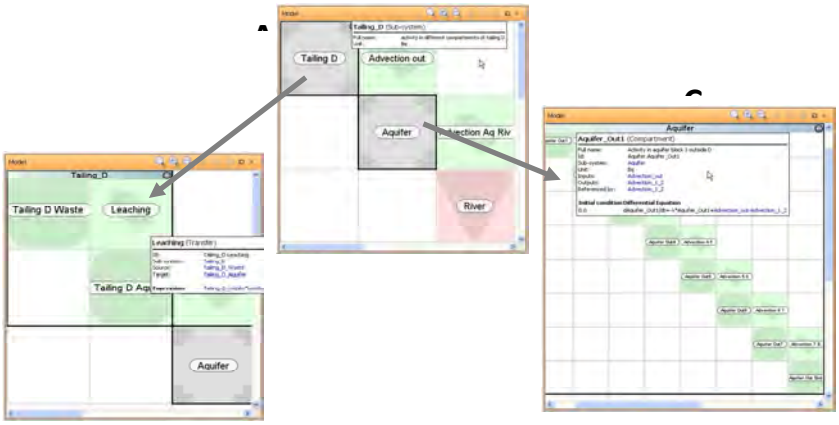

Fig.4. Matrix of co-operation of the Ecolego program for the model of radionuclide migration from tailing: (A) general matrix; (B) matrix for under-system "tailing"; (C) matrix for under-system "aquifer".

system: "Tailing - alluvial aquifer – Dnepr River". A model takes into account vertical infiltration of muddy porous solutions from the body of tailing to alluvial aquifer, and farther lateral convective-dispersion transport of radionuclides in aquifer towards the Dnepr River (the delay correction, as a result of adsorption).

All basic radionuclides of uranium row exist in the migration model: uranium-238, uranium-234, thorium-230, radium-226, lead-210 and polonium-210. A model estimates radinuclides supply from the source of migration, concentration changes in the source caused by lixiviation of radionuclides by groundwater and radioactive disintegration. Groundwater flow from tailing "Dneprovskoe" in direction of Dnepr was designed as a tube of flow with geometrical sizes, with parameters, corresponding the filtration model.

Migration parameters of model

The simulation of radionuclides migration from tailing "Dneprovskoe" is executed for two scenarios: "base" (that is most credible) and "conservative" (that is most pessimistic). On the basis of the review of literary sources and calculations of Kd in-situ the set of distribution coefficients was formed. Received coefficients where used for simulation of radionuclides migration from tailing "Dneprovskoe". This set Kd is shown in the Table 4. The table contains the Kd estimations for tails and the alluvial aquifer.

As the "base" for alluvial aquifer we used the Kd set offered in the report of J.Serne (Pacific Northwest Laboratory, 2007). The PNNL set does not have the Kd estimation for to thorium, therefore absorbsion coefficient for thorium was used basing on the reports of Sheppard and Thibault (1990). The beginning of simulation is the year 2000.

The term of prediction constitutes 5000 years. A model fixed, that initial radioactive contamination is concentrated in two compartments: in the tails of processing of uranium ores and in alluvial aquifer directly under the bowl of tail. Concentration of radionuclides in alluvial aquifer outside the bowl of tailing is equal to zero, because there is no reliable and standard information about radioactive contamination of alluvial aquifer outside tailing. Before the simulation of radionuclides migration from tailing "Dneprovskoe" by the Ecolego package, the simplified estimations of radionuclides convective transport speed in aquifer toward the Dnepr River where executed. This simplified simulation considered the delay caused by absorbsion. The results of estimation are shown in the Table 5.

Table 5. Prognostic speed of convective transport of radionuclides in aquifer (considering the delay, caused by adsorbtion) (V_{RN}) and proper time of migration from tailing "Dneprovskoe" to Dnepr River (T_{RN})

Migrant	Base scenario		Conservative scenario	
	V_{RN}, m/year	T_{RN}, years	V_{RN}, m/year	T_{RN}, years
Water	24	41	49	21
Radionuclide				
U	2,8	354	12,4	81
Th-230	0,005	205232	0,024	41056
Ra-226	0,07	13694	0,36	2749
Po-210	0,04	27375	0,18	5485
Pb-210	0,02	41056	0,12	8563

Table 4. The Kd set for the simulation of radionuclides migration from tailing "Dneprovskoe"

Radionuclide	Kd, ml/g		
	Tailings	Alluvial aquifer	
	Base kit	Base kit	Conservative kit
U	30	5	1
Th-230	10000	3000	600
Ra-226	700	200	40
Po-210	2000	400	80
Pb-210	1300	600	125

The prognosis of groundwater transport of uranium from tailing "Dneprovskoe" into the Dnepr River under different scenarios of rehabilitation

Prediction based on migration model, created by the Ecolego program, demonstrates characteristics of radionuclides transport with groundwater from tailing "Dneprovskoe" in Dnepr River under different scenarios. The results of calculations are shown in the Table 6. For conservative scenario the noticeable entry of uranium into the Dnepr River begins through ≈50 years, and gains it's maximum within ≈ 300 years. Maximum entry of uranium in the Dnepr River for conservative scenario is in twice more than for a base scenario. Simulated rehabilitation measures (coverage of tailing by a soil screen, removing of tails) demonstrate diminishment of current and cumulative entry of uranium to the Dnepr River. According to the simulation data, the entry of uranium into the Dnepr River is jdiminished approximately twice in comparison with the base scenario. Creation of soil screen and removing of tails have similar effect in the period within 500 years.

Table 6. Descriptions of prognosis entry of uranium in the Dnepr River under different scenarios

Scenario	Maximum entry of U in Dnepr River, $\times 10^{12}$ Bk/year	The term of maximum entry, year	*Cumulative entry of U in Dnepr River, $\times 10^{16}$ Bk*	
			for 1000 year	for 5000 year
Base	8,7	2000	0,06	2,7
Conservative	21	300	1,6	3,7
Soil screen	4,7	1800	0,058	1,2
Removing of tails	3,9	1400	0,058	0,6

Conclusions

- The development of the system of the hydrogeological monitoring for the areas of uranium waste tailings is required.
- It is necessary to extend the existing network of monitoring wells and train the personnel of the enterprise "Barrier", to provide of systematic observation and sampling groundwater.
- It is necessary to conduct researches of physical and chemical forms of existence of radionuclides in tails.
- It is necessary to study the spatial distribution of radionuclides in the area of the PCh.P objects.
- It is necessary to estimate actual coefficients of distributing radionuclides in the saturated rocks.
- Mathematical simulation and "cost benefit analyse" of rehabilitation measures for each tailing is required.

References

Voicekchovich O. et al. Scientifically methodical accompaniment and regulations grounding of the complex monitoring of influence of uranium objects of former PCh.P on the environment and population. Center of Monitoring Researches and Nature Protection Technologies Kiev, 2005

Voicekchovich O. et al. Implementation of works according to the programs and regulations of the radiation monitoring. Center of Monitoring Researches and Nature Protection Technologies Kiev, 2006

Ecolego 3 user guide. Facilia AB, Stockholm, 2007

Bugai D. et al. Simulation of processes of radionuclide migration at uranium objects (tailing "Dneprovskoe"). Geo-Eko-Consulting, Kiev, 2007


Uranium Mining
and Hydrogeology

Characterization of U(VI) behaviour in the Ruprechtov site (CZ)

Dušan Vopálka[1], Václava Havlová[2] and Michal Andrlík[1]

[1]Department of Nuclear Chemistry, Faculty of Nuclear Sciences and Physical Engineering, Czech Technical University in Prague, Břehová 7, CZ-115 19 Prague 1, Czech Republic
[2]Nuclear Research Institute Řež plc., CZ-250 68 Řež near Prague, Czech Republic

Abstract. Natural analogue study at the Ruprechtov site (Czech Republic) was aimed to investigate and understand the behaviour of natural radioelements in sedimentary formation. The isotopic exchange tests with ^{233}U were used to compare the results of exchangeable uranium (U_{ex}) determination with the results of the first steps of sequential leaching tests. Measured interaction isotherms showed a significant dependence of uranium uptake on the phase ratio (V/m) values. The reason can be assigned to changes in liquid phase composition caused by dissolution of mineral phases.

Introduction

Detailed study of natural processes in the real scale and under real conditions should help for better understanding of retardation processes in the vicinity of deep geological repository. Underground laboratories, field tests and natural analogues can be the possible ways to approach the real conditions. The Ruprechtov natural analogue site was chosen for research because its geological and geochemical conditions resemble sedimentary sequences which can cover potential host rocks for underground waste repositories (Noseck and Brasser, 2006).

The Ruprechtov site is situated in the NW part of the Czech Republic in Hroznětín part of Sokolov Basin, which is filled with Oligocene Miocene sediments with thickness up to 100 m. Uranium accumulation is distributed heterogeneously within volcanodetritic layers in the depth of 10-40 m. The uranium deposits in this region are described in literature (e.g. Komínek et al. 1994) as of sedimentary origin, the granitoids of the Karlovy Vary and Smrčiny plutons being the primary source of the uranium.

Comprehensive investigations of U-argillitized clay-organic matter – granite system – groundwater of the site has been performed since 1995, including drilling, field tests, groundwater monitoring, sediment and groundwater sampling and characterization, laboratory experiments and geochemical and hydrogeological modelling (e.g.Noseck et al. 2002; Havlová et al. 2006). Uranium was found predominantly in U(IV) form (max. 700 ppm), being a clear proof of reducing conditions within the rock layers. Only a small part of U_{tot} is formed by U(VI). Predominantly U(VI) was present in groundwater, however in very small concentration (4.2 mg/l). We assume U(VI) to be the most stable form of uranium under oxidizing conditions and can be mobilized by surface and underground water. Study of the element behaviour under real conditions can help to quantify processes of retention/mobilization within potential sedimentary cover of the host rock. For the application of migration model, which should describe the migration of contaminants in the environment, it is necessary to know the formal description of interaction of studied contaminant with the solid phase. The obvious laboratory methodology that includes batch and column experiments, changing the initial concentration of studied species, should respect the initial amount of studied species accessible from the solid phase. This demand was fulfilled in our experimental work with the use of ^{233}U as the tracer. In the first step we planned to determine the amount of U(VI) accessible in contact with real underground water from rock samples using the modified methodology, in which concentration changes of both natural uranium and ^{233}U are checked. In the second step the obtained knowledge should be used to the building of an interaction model based on the results of determination of equilibrium isotherms of U(VI) on different types of rock.

Experiments and results

Sequential extraction and isotope exchange using ^{233}U

Rock samples from six bore cores from Ruprechtov site were crushed, powdered and sieved, and fraction < 0.063 mm was used in all types of batch experiments performed.

The sequential extraction method, which is a classical approach that enables to determine trace metal forms in sedimentary rocks, was used in a slightly modified and reduced scheme with the aim to obtain the information about the uranium amount that is attainable from the rock in contact with the underground water composition which is characteristic for the site (Havlová et al. 2006).

The first two steps of leaching of the standard method were used: (i) 1M $MgCl_2$, contact time 1 hour, pH 7 – determines uranium bound on exchange position and (ii) 1M $NaCH_2COOH + CH_3COOH$, contact time 5 hours, pH 4.8 – determines uranium bound in carbonates (Henderson et al. 1998).

Determination of uranium accessible to leaching with natural water and exchangeable with ions in real groundwater was performed by isotope exchange with ^{233}U in simulated seepage water. This approach that determines so called exchangeable or "labile" (Davis and Curtis, 2003) uranium U_{ex} was with a success used for the determination of exchangeable uranium on the material from the waste rock pile at Schlema-Alberoda, Saxony (Vopalka et al., 2006). The quantity U_{ex} (mg/kg) was calculated from measured values of uranium concentrations and distribution coefficient K_d by equation (1). The distribution of ^{233}U between rock and liquid phase that enabled determination of K_d was measured with liquid scintillation counting; evaluation of concentration change of natural uranium was based on determination by means of ICP-MS.

$$U_{ex} = \frac{C(V + K_d.m) - C_0.V}{m} \tag{1}$$

Here C_0 and C represent respectively initial and equilibrium concentrations in the liquid phase (mg/L), m – weight of the rock phase (kg) and V – volume of the liquid phase (L). As only small differences were observed between K_d values corresponding to contact times 15 and 30 days, the contact time of 30 days was chosen as representative for the determination of equilibrium values. The U_{ex} values were determined for at least 3 values of phase ratio V/m between 20 – 100 L/kg, no significant effect of V/m values U_{ex} was observed, also due to the great variability of U_{ex} values for some rock samples.

Comparison of results of accessible uranium determination obtained by both methods is summarized in Table 1. As selected samples were taken from different layers of the site (NA10 – kaolinized granite, NA11 and NA12 – argillized clay, NA13 – argillized clay, NA14 – argillized clay with high content of organic matter and uranium, NA15 – kaolinized granite), three types of modelled seepage water were used in equilibrium batch experiments. According to the geological characterization of the horizon of their origin they are called "granitic, upper tertiary, and lower tertiary" waters. Total uranium content was determined after total dissolution of samples using ICP-MS.

Table 1. Comparison of exchangeable uranium U_{ex}-values with results of first two steps of sequential leaching (step 1: 1M $MgCl_2$, 1 hour, pH 7; step 2: 1M $NaCH_2COOH$ + CH_3COOH, 5 hours, pH 4.8). Water types: granitic (pH 6.6), upper tertiary (pH 7.25) and lower tertiary (pH 6.55).

Borehole	Depth m	Water type	U-total mg/kg	Sequential leaching steps 1 and 2, mg/kg	U_{ex} mg/kg	equil. pH
NA10	15.43	granitic	23	17.5	18 ± 4	7.9
NA11	16.27	upper teriary	94	39	29 ± 3	8.5
NA11	38.17	lower tertiary	39	7.15	10 ± 2	8.2
NA12	40.31	granitic	42	5.7	n.d.	7.9
NA13	46.4	lower tertiary	212	74	134 ± 12	2.6
NA14	51.73	lower tertiary	724	70.5	325 ± 50	2.6
NA15	12.7	upper tertiary	55	22.4	13.3 ± 4	8.5
NA15	31	granitic	62	33.6	7.4 ± 3	8.2

The comparison of both methods for determination of exchangeable uranium was successful for majority of samples studied. According to this fact it can be concluded that U(VI) accessible for the exchange and transport processes is the uranium bound on the surface of the mineral grains and/or is locked in minerals, dissolution of which is consistent with dissolution of carbonates. The anomalous behaviour of two samples, which contact with modelled seepage water caused great decrease of pH value, is presumably caused by self-leaching by sulphuric acid originated from oxidation of pyrite present in samples.

Batch kinetic and equilibrium experiments

A broad set of equilibrium interaction experiments was performed with four selected samples that were obtained from crushed borehole cores from different places of the site (Andrlík 2006). The differentiation of the samples properties is demonstrated in Table 2.

The homogenized and sieved fractions (< 0.063) of all four samples was contacted with modelled water GWO4 (Na^+ $2.1\cdot10^{-3}$ M, Mg^{2+} $1.1\cdot10^{-3}$ M, Ca^{2+} $1.75\cdot10^{-3}$ M, SO_4^{2-} $8.12\cdot10^{-4}$ M, HCO_3^- $2.21\cdot10^{-3}$ M, Cl^- $3.95\cdot10^{-3}$ M; pH 8.2), in which uranyl nitrate was dissolved in the concentration range from $1\cdot10^{-7}$ mol/L to $2\cdot10^{-4}$ mol/L. The water phase was spiked with ^{233}U in concentration about $1\cdot10^{-7}$ mol/L. The water-to-solid ratio in batch experiments was changed in the range 5 - 400 mL/g. The change of the ^{233}U activity during experiments was measured by liquid scintillation counting. To assess time necessary to obtain equilibrium conditions the sets of experiments with contact time 7, 14 and 30 days were performed.

The results of experiments, in which the influence of parameter variation on the K_d values was studied by this method, showed a great differences in release/uptake qualities of studied samples. The selected results are collected in Tables 3-6, for which the presented uranium concentrations at the end of experiment C were

Table 2. Rock sample characterization: silicate analyses, TOC, TIC and S content (%)

Borehole		NA10	NA11	NA12	NA14
Depth	m	15.43	16.27	40.31	51.73
TOC	%	0.06	1.39	1.34	13.34
TIC	%	4	10	11	20
Fe_2O_3	%	0.67	9.72	9.8	4.36
TiO_2	%	0.02	4.49	3.33	2.3
CaO	%	0.1	0.83	1.64	1.66
K_2O	%	2.42	0.81	0.76	0.71
SiO_2	%	80.27	52.26	51.28	43.26
Al_2O_3	%	12.4	19.1	19.1	10.4
MgO	%	0.05	0.8	1.03	0.98
S	%	0	0.204	0.97	2.95

Table 3. Measured K_d values for the sample from borehole NA10 as dependence on phase ratio V/m, initial concentration C_0 and contact time t.

V/m mL/g	C_0 mol/L	t days	K_d mL/g	V/m mL/g	C_0 mol/L	t days	K_d mL/g
40	$3{\cdot}10^{-6}$	7	17.1	7	$3{\cdot}10^{-6}$	7	14.1
40	$6{\cdot}10^{-6}$	7	16.8	7	$6{\cdot}10^{-6}$	7	10.3
40	$3{\cdot}10^{-6}$	14	21.3	7	$3{\cdot}10^{-6}$	14	16.3
40	$6{\cdot}10^{-6}$	14	19.2	7	$6{\cdot}10^{-6}$	14	12.9
10	$6{\cdot}10^{-6}$	14	12.2	10	$6{\cdot}10^{-6}$	28	13.4

computed using K_d values determined from the change of activity of the spike and U_{ex} values determined in a precedent set of experiments.

Results of the study of uranium release/uptake from the sample NA10 (Table 3) showed a noticeable desorption of uranium from the solid phase. In supplementary experiments with no uranium added into the initial solution reached uranium concentration in the liquid phase (for V/m = 10 mL/g) the value about $1.3{\cdot}10^{-6}$ mol/L. Furthermore, in all experiments presented in Table 3, the computed concentration on the solid phase (capacity) was lower than determined initial capacity, which was equal to exchangeable amount U_{ex}. The increase of K_d with time gives the hint that contact time of 14 days is not sufficient for this sample to the reach the equilibrium and from the decrease of K_d with the increase of initial concentration C_0 results the non-linear shape of interaction isotherm.

In all experiments performed with the material from borehole NA11 (Table 4) sorption dominated. Very high K_d values measured for high V/m and low C_0 values indicated extremely non-linear shape of sorption isotherm with significant dependence on the phase ratio V/m.

For systems, in which the solid phase contains known amount of the exchangeable species (here U_{ex}), it is possible to convert set of measured K_d data into the

Table 4. Measured K_d values for the sample from borehole NA11 as dependence on phase ratio V/m and initial concentration C_0; contact time t = 30 days.

V/m mL/g	C_0 mol/L	C mol/L	K_d mL/g	V/m mL/g	C_0 mol/L	C mol/L	K_d mL/g
400	$1{\cdot}10^{-6}$	$2.8{\cdot}10^{-8}$	26726	400	$6{\cdot}10^{-6}$	$4.3{\cdot}10^{-7}$	6092
100	$1{\cdot}10^{-6}$	$6.8{\cdot}10^{-8}$	7853	100	$6{\cdot}10^{-6}$	$3.0{\cdot}10^{-7}$	3033
20	$1{\cdot}10^{-6}$	$3.2{\cdot}10^{-7}$	1048	20	$6{\cdot}10^{-6}$	$5.2{\cdot}10^{-7}$	825
10	$1{\cdot}10^{-6}$	$6.1{\cdot}10^{-7}$	546	10	$6{\cdot}10^{-6}$	$1.3{\cdot}10^{-7}$	283
400	$3{\cdot}10^{-6}$	$2.8{\cdot}10^{-8}$	13307	400	$2{\cdot}10^{-5}$	$2.5{\cdot}10^{-6}$	2955
100	$3{\cdot}10^{-6}$	$6.8{\cdot}10^{-8}$	4684	100	$2{\cdot}10^{-5}$	$2.1{\cdot}10^{-6}$	1036
20	$3{\cdot}10^{-6}$	$3.2{\cdot}10^{-7}$	1142	20	$2{\cdot}10^{-5}$	$1.1{\cdot}10^{-6}$	665
10	$3{\cdot}10^{-6}$	$6.1{\cdot}10^{-7}$	493	10	$2{\cdot}10^{-5}$	$1.9{\cdot}10^{-6}$	267
400	$4{\cdot}10^{-5}$	$6.7{\cdot}10^{-6}$	2048	20	$4{\cdot}10^{-5}$	$2.3{\cdot}10^{-6}$	463
100	$4{\cdot}10^{-5}$	$5.8{\cdot}10^{-6}$	647	10	$4{\cdot}10^{-5}$	$3.4{\cdot}10^{-6}$	199

Table 5. Measured K_d values for the sample from borehole NA12 as dependence on phase ratio V/m and initial concentration C_0; contact time t = 30 days.

V/m mL/g	C_0 mol/L	C mol/L	K_d mL/g	V/m mL/g	C_0 mol/L	C mol/L	K_d mL/g
400	$1{\cdot}10^{-5}$	$1.1{\cdot}10^{-6}$	3104	400	$1{\cdot}10^{-4}$	$1.2{\cdot}10^{-5}$	3031
100	$1{\cdot}10^{-5}$	$4.3{\cdot}10^{-7}$	2228	100	$1{\cdot}10^{-4}$	$9.0{\cdot}10^{-6}$	1028
20	$1{\cdot}10^{-5}$	$2.9{\cdot}10^{-7}$	664	20	$1{\cdot}10^{-4}$	$4.5{\cdot}10^{-6}$	425
10	$1{\cdot}10^{-5}$	$4.0{\cdot}10^{-7}$	374	10	$1{\cdot}10^{-4}$	$6.9{\cdot}10^{-6}$	131
400	$4{\cdot}10^{-5}$	$4.3{\cdot}10^{-6}$	3371	400	$2{\cdot}10^{-4}$	$6.5{\cdot}10^{-5}$	841
100	$4{\cdot}10^{-5}$	$3.6{\cdot}10^{-6}$	1030	100	$2{\cdot}10^{-4}$	$5.9{\cdot}10^{-5}$	238
20	$4{\cdot}10^{-5}$	$2.1{\cdot}10^{-6}$	354	20	$2{\cdot}10^{-4}$	$2.7{\cdot}10^{-5}$	130
10	$4{\cdot}10^{-5}$	$1.0{\cdot}10^{-6}$	366	10	$2{\cdot}10^{-4}$	$2.3{\cdot}10^{-5}$	103

functional dependence of solid phase concentration q on the liquid phase concentration C by means of simple balance relations. In the equilibrium state this dependence represents the equilibrium (sorption) isotherm.

In the case of experiments with sample NA11 this transformation conduced to isotherms of Langmuir type for which the capacity on the relevant range of concentration in the liquid phase dramatically increases with phase ratio V/m. Such relation was observed in systems in which the sorption was controlled by cation exchange (Klika et al. 2007). Here this effect is relatively higher and no ion-exchange can be supposed as in the measured pH range about 8 neutral and/or negatively charged uranyl carbonate complexes should dominate.

Also experiments with the sample from borehole NA12 (Table 5) are characterized by sorption, which is in range of initial concentration in the liquid phase $> 1{\cdot}10^{-5}$ mol/L higher than that in the case of the sample from NA11. The great extent of sorption disabled for this sample the determination of U_{ex} using isotope exchange of natural uranium and ^{233}U.

On the contrary to samples NA11 and NA12 desorption dominated the experiments with the sample from borehole NA14 (Table 6). In all experiments with this

Table 6. Measured K_d values for the sample from borehole NA14 as dependence on phase ratio V/m and initial concentration C_0; contact time t = 30 days.

V/m mL/g	C_0 mol/L	C mol/L	K_d mL/g	V/m mL/g	C_0 mol/L	C mol/L	K_d mL/g
50	$3{\cdot}10^{-7}$	$2.6{\cdot}10^{-5}$	12	50	$3{\cdot}10^{-6}$	$3.1{\cdot}10^{-5}$	7
20	$3{\cdot}10^{-7}$	$5.6{\cdot}10^{-5}$	8.7	20	$3{\cdot}10^{-6}$	$4.5{\cdot}10^{-5}$	7
10	$3{\cdot}10^{-7}$	$1.4{\cdot}10^{-4}$	1.9	10	$3{\cdot}10^{-6}$	$1.4{\cdot}10^{-4}$	1.9
5	$3{\cdot}10^{-7}$	$3.1{\cdot}10^{-4}$	0.2	5	$3{\cdot}10^{-6}$	$3.1{\cdot}10^{-4}$	0.2
50	$1{\cdot}10^{-6}$	$3.1{\cdot}10^{-5}$	5	50	$6{\cdot}10^{-6}$	$3.2{\cdot}10^{-5}$	8.5
20	$1{\cdot}10^{-6}$	$5.3{\cdot}10^{-5}$	11	20	$6{\cdot}10^{-6}$	$6.4{\cdot}10^{-5}$	6.9
10	$1{\cdot}10^{-6}$	$1.4{\cdot}10^{-4}$	1.4	10	$6{\cdot}10^{-6}$	$1.5{\cdot}10^{-4}$	1.5
5	$1{\cdot}10^{-6}$	$3.2{\cdot}10^{-4}$	0	5	$6{\cdot}10^{-6}$	$3.2{\cdot}10^{-4}$	0.1

Table 7. Measured K_d values for the sample from borehole NA14 as dependence on phase ratio V/m and initial concentration C_0; contact time t = 30 days.

V/m mL/g	C_0 mol/L	C mol/L	K_d mL/g	V/m mL/g	C_0 mol/L	C mol/L	K_d mL/g
50	$3\cdot10^{-7}$	$2.6\cdot10^{-5}$	12	50	$3\cdot10^{-6}$	$3.1\cdot10^{-5}$	7
20	$3\cdot10^{-7}$	$5.6\cdot10^{-5}$	8.7	20	$3\cdot10^{-6}$	$4.5\cdot10^{-5}$	7
10	$3\cdot10^{-7}$	$1.4\cdot10^{-4}$	1.9	10	$3\cdot10^{-6}$	$1.4\cdot10^{-4}$	1.9
5	$3\cdot10^{-7}$	$3.1\cdot10^{-4}$	0.2	5	$3\cdot10^{-6}$	$3.1\cdot10^{-4}$	0.2
50	$1\cdot10^{-6}$	$3.1\cdot10^{-5}$	5	50	$6\cdot10^{-6}$	$3.2\cdot10^{-5}$	8.5
20	$1\cdot10^{-6}$	$5.3\cdot10^{-5}$	11	20	$6\cdot10^{-6}$	$6.4\cdot10^{-5}$	6.9
10	$1\cdot10^{-6}$	$1.4\cdot10^{-4}$	1.4	10	$6\cdot10^{-6}$	$1.5\cdot10^{-4}$	1.5
5	$1\cdot10^{-6}$	$3.2\cdot10^{-4}$	0	5	$6\cdot10^{-6}$	$3.2\cdot10^{-4}$	0.2

sample uranium concentration increased significantly in the liquid phase. These results corresponded with determination of U_{ex} (Table 1), where for this sample is presented the highest U_{ex} value from all the group of samples examined. This sample differs from others also by the pH decrease during the experiment. The highest decrease of pH was observed for smaller values of phase ratio. This fact is in an agreement with assumption about release of sulphates from the sample, supported by known high content of sulphur in the rock material NA14 (Table 2).

In the study of uranium interaction with samples from NA11, NA12 and NA14 was observed only small difference for contact times 15 days and 30 days, so experiments with contact time of 30 days could be treated as description of equilibrium.

Conclusions

The great differences of qualities concerning U(VI) release/uptake was observed in eight samples originated from the Ruprechtov site. The differences that are related to both amount of exchangeable uranium in samples studied and sorption/desorption behaviour of them arise from the differences of the chemical and mineralogical composition of rock materials, from which the samples were prepared. The isotope exchange of uranium present in samples with ^{233}U proved that first two steps of standard sequential leaching procedure give a good information about the amount of U(VI) in rock samples that is attainable to transport in zone saturated by underground water. Great differences observed in release/uptake characteristics among the four selected samples, interaction with uranium of which was elaborated, indicated the necessity of the further research on the site that could help to better formulate the basic features of a site specific transport model.

Acknowledgement

The research was supported by the Ministry of Education of the Czech Republic under contract MSM 6840770020, RAWRA, Czech Republic and EC IP FUNMIG.

References

Andrlík M (2006) Uranium interaction with rock materials (in Czech), diploma thesis, CTU in Prague, 73 pp.

Davis JA, Curtis GP (2003) Application of surface complexation modeling to describe uranium (VI) adsorption and retardation at the uranium mill tailings site at Naturita, Colorado. Report NUREG/CR-6820, U.S. Geological Survey, Menlo Park, CA, p. 29

Havlová V, Laciok A, Vopálka D, Andrlík M. (2006) Geochemical study of uranium mobility in tertiary argillaceous system at Ruprechtov site, Czech Republic. Czechoslovak Journal of Physics 56, Suppl. D: D81-D86

Henderson PJ, McMartin I, Hall GE, Percival JB, Walker DA (1998) The chemical and physical characteristics of heavy metals in humus and till in the vicinity of the base metal smelter at Flin Flon, Manitoba, Canada. J Envir Geol 34: 39-58

Klika Z, Kraus L, Vopálka D (2007) Cesium uptake from aqueous solution by bentonite: Multicomponent sorption with ion-exchange models. Langmuir 23: 1227-1233

Komínek J, Chrt J, Landa O (1994) Uranium mineralization in the western Krušné hory Mts. (Erzgebirge) and the Slavkovský les region, Czech Republic. In: Mineral deposits of the Erzgebirge / Krušné hory - Germany / Czech Republic (v Gehlen K, Klemm DD, eds.), Monograph Series on Mineral Deposits 31, Gebrüder Bornträger, Berlin – Stuttgart, 209-230

Noseck U, Brasser T (2006) Radionuclide transport and retention in natural rock formations. Ruprechtov site. Report GRS-218, Gessellschaft für Anlagen- und Reaktorsicherheit (GRS) mbH, Braunschweig, 157 pp.

Noseck U, Brasser T, Laciok A, Hercik M, Woller F (2002) Uranium migration in argillaceous sediments as analogue for transport processes in the far field of repositories (Ruprechtov Site, Czech Republic). In: Uranium in the Aquatic Chemistry (Merkel BJ et al., eds.), Springer, 207-215

Vopalka D, Benes P, Doubravova K (2006) Modelling of uranium release from waste rock pile. In: Uraniun in the Environment (Merkel BJ, Hasche-Berger A, eds), Springer, 253-262.

Spectroscopic study of the uranium(IV) complexation by organic model ligands in aqueous solution

Katja Schmeide and Gert Bernhard

Forschungszentrum Dresden-Rossendorf, Institute of Radiochemistry, P.O. Box 510119, 01314 Dresden, Germany

Abstract. The complexation of uranium(IV) with the organic model ligands citric acid, succinic acid and mandelic acid has been investigated in dependence on acidity (0.1 M to 1.0 M) and ionic strength (0.11 M to 1.0 M) by UV-Vis spectroscopy. In the citrate media, the formation of 1:1 and 1:2 complexes was detected. The stability constants for 1:1 and 1:2 uranium(IV) citrate complexes of the type $M_pH_qL_r$ were determined with $\log \beta_{101} = 13.5 \pm 0.2$ and $\log \beta_{102} = 25.1 \pm 0.2$. The stability constants determined for the complexation of uranium(IV) with succinic acid and mandelic acid are lower.

Introduction

Risk assessments predicting the transport of actinides under environmentally relevant conditions require basic knowledge of their interaction with complexing ligands, their sorption and redox behavior, their solubility, as well as their ability to form colloids. Both the speciation and the mobility of actinides in aquatic systems strongly depend on their oxidation state due to the different precipitation, complexation, sorption and colloid formation behavior of the various oxidation states (e.g., Silva and Nitsche 1995; Choppin 2006; Kim 2006). Under reducing conditions as prevalent in deep underground nuclear waste repositories as well as in the depth of flooded uranium mines, actinide species occur in lower oxidation states. For instance, in contrast to U(VI) which is mobile, U(IV) is much less mobile due to the low solubility of U(IV) hydrous oxide ($UO_2 \cdot xH_2O$(am)) (Neck and Kim 2001; Geipel 2005; Opel et al. 2007). However, in the presence of inorganic or organic ligands U(IV) may become mobile due to formation of soluble complexes. Thus, the speciation of U(IV) in aqueous solution has to be studied to predict its migration behavior in natural environments.

The seepage and mine waters of former mining areas in East Germany contain several inorganic and organic complex forming agents (Bernhard et al. 1996; Geipel et al. 2000). However, data for the complexation of U(IV) with inorganic and organic ligands are scarce. Moreover, for instance complexation constants determined for the U(IV) complexation with citric acid (Adams and Smith 1960; Nebel and Urban 1966; Shalimov et al. 1974) vary strongly. Thus, according to the NEA Thermodynamic Database (Hummel et al. 2005) the stoichiometry of the U(IV) citrate species formed and thus, the stability constants are still uncertain. Recently, new data on U(IV) citrate complex formation were published (Bonin et al. 2008).

In this work, citric acid, succinic acid as well as mandelic acid were chosen as model ligands to study the U(IV) complexation. These ligands stand for a variety of organic ligands in aqueous systems. The complex formation constants for the U(IV) complexation are determined applying UV-Vis absorption spectroscopy. Thereby, the hydrogen ion concentration and the ionic strength were varied between 0.1 M and 1.0 M and 0.11 M and 1.0 M, respectively.

Experimental

Sample preparation

U(IV) stock solutions were prepared by electrochemical reduction of U(VI) perchlorate stock solutions (0.02 M UO22+ in 2 M or in 1 M HClO4). The oxidation state purity of the U(IV) stock solution was verified by UV-Vis spectroscopy and fluorescence spectroscopy. Sample solutions were prepared in an inert gas glovebox (N2 atmosphere, < 20 ppm O2) using CO2-free Milli-Q-water (Milli-RO/Milli-Q-System, Millipore, Molsheim, France). Ligand stock solutions were prepared freshly for each experiment (citric acid: reagent grade (Aldrich), succinic acid: analytical grade (Merck), mandelic acid: for synthesis (Merck)). The sample solutions ([U(IV)] = 1×10-3 M, [ligand] = 0 to 0.2 M) were prepared by volume mixture of the U(IV) stock solution with various volumes of the ligand solutions. The hydrogen ion concentration ([H+]: 0.1, 0.5, and 1.0 M) was adjusted by adding aliquots of 5 M HClO4 (previously degassed by bubbling N2 through the solution) simultaneously taking into account the [H+] stemming from the U(IV) stock solution. The total concentration of U in the solutions was determined by inductively coupled plasma mass spectrometry, ICP-MS (Elan 9000, Perkin Elmer).

Spectroscopic measurements

The UV-Vis absorption spectra were recorded with a high-resolution dual beam UV/Vis/NIR spectrophotometer (CARY-5G, Varian). The measurements were performed using a 1-cm quartz glass cuvette (Hellma) in the spectral range from

800 to 300 nm with a speed of 60 nm/min at room temperature (22±1 °C). The cuvette was always filled and sealed in the inert gas box. Each spectrum was analyzed in two regions of wavelength: 446 to 524 nm and 570 to 727 nm.

In addition, after recording the UV-Vis spectra, the fluorescence spectra of all solutions were measured to quantify the amount of reoxidized U (excitation wavelength 266 nm). The amount of U(VI) in the sample solutions was ≤1.2% of the total U content. For calculations, the U(IV) concentration was corrected by the U(VI) concentration.

Calculations

Stability constants were determined using the factor analysis program SPECFIT (Binstead et al. 2005). For this, the acidity constants of citric acid (pK_{a1} = 5.31, pK_{a2} = 4.17, pK_{a3} = 2.84 at I = 0.5 M $NaClO_4$) (Hummel et al. 2005), succinic acid (pK_{a1} = 5.12, pK_{a2} = 3.93 at I = 0.5 M) (Martell et al. 1998) and mandelic acid (pK_a = 3.18 at I = 1.0 M) (Martell et al. 1998) as well as the formation constants of U(IV) hydrolysis species (Guillaumont et al. 2003) were applied. Ionic strength corrections were conducted applying the Specific Ion Interaction Theory (SIT) (Ciavatta 1980, Guillaumont et al. 2003).

Results and discussion

U(IV) complexation with citric acid

The complexation of U(IV) with citric acid has been investigated in dependence on hydrogen ion concentration (0.1, 0.5, and 1.0 M). From the pK_a values reported for citric acid (cf. paragraph Calculations) follows, that the citric acid is completely protonated in the pH range applied in this work. That means, citric acid does not contribute to the ionic strength under these pH conditions. Thus, the ionic strength of the sample solutions is mainly determined by $[H^+]$.

Exemplary, Fig. 1 shows the evolution of the U(IV) spectrum in the two wavelength ranges analyzed for increasing citric acid concentrations (0 to 0.2 M) at an acidity of $[H^+]$ = 0.5 M. In the wavelength range 570 to 727 nm, the solvated U^{4+} shows absorption maxima at 649.1 nm and 671.7 nm in the absence of citric acid. With increasing citric acid concentration the intensity of the peak at 649 nm decreases and simultaneously, the peak is shifted to longer wavelengths. At U(IV):citric acid ratios higher than 1:20 the intensity of this peak increases again. In the wavelength range 446 to 524 nm, the intensity of the peak at 495 nm decreases with increasing citric acid concentration. The intensity of the shoulder at 486 nm increases when the U(IV):citric acid ratio is higher than 1:20. These

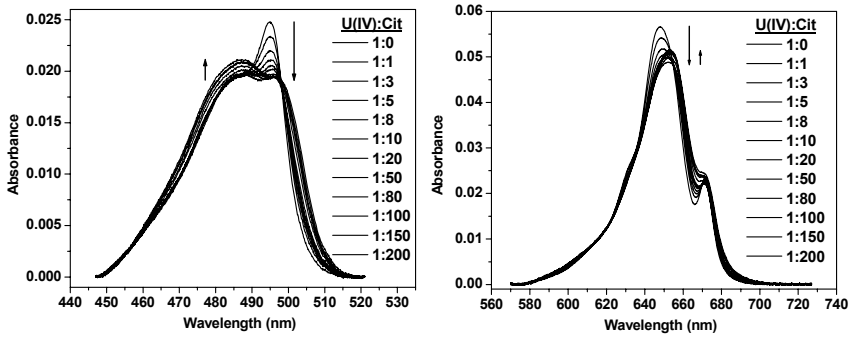

Fig.1. Two wavelength ranges of the UV-Vis spectra for 1×10^{-3} M U(IV) as a function of the citric acid (Cit) concentration at $[H^+] = 0.5$ M and I = 0.5 M.

changes of the U(IV) spectrum can be attributed to the complexation of U(IV) by citric acid.

The experimental data were analyzed considering the most basic form of the citrate anion Cit^{3-}. The U(IV) citrate complexation reaction can be expressed as:

$$p\ U^{4+} + q\ H^+ + r\ Cit^{3-} \rightleftarrows U_pH_qCit_r^{(4p+q-3r)}$$

For the calculation of the stability constants, 8 datasets were analyzed (4 series of experiments ($[H^+]$ = 1 M, 0.5 M, 0.1 M (2x)) with 2 wavelength ranges each). Thereby, the formation of 1:1 and 1:2 complexes was detected in the citrate media. Within the experimental uncertainty, no significant effect of the acidity and ionic strength of the sample solutions on the stability constants has been observed. The mean values of the stability constants were determined with $\log \beta_{101} = 13.5 \pm 0.2$ und $\log \beta_{102} = 25.1 \pm 0.2$. Due to the strong complexation of U(IV) by citric acid, the U(IV) hydrolysis is prevented. The stability of An(IV) citrate complexes against hydrolysis is already described in the literature (e.g., Durbin et al. 1998; Suzuki et al. 2006). Furthermore, U(IV) is stabilized against oxidation due to complexation. The stability of U(IV) against oxidation can further be explained by the reducing properties of citric acid (Bonin et al. 2007; Sevostyanova 1982).

Table 1. Stability constants for the system An(IV) citrate.

	Th(IV)	U(IV)	Np(IV)	Pu(IV)
$\log \beta_{101}$	11.6 (I = 0.1 M) [a]	11.5 (I = 0.5 M) [b]	13.6 (I = 0.6 M) [d]	15.3 (I = 0.5 M) [e]
	13.0 (I = 0.5 M) [b]	12.8 (I = 0.8 M) [c]		17.6 (I = 0.15 M) [f]
	12.5 (I = 0.3 M) [c]	13.5 ± 0.2 [g]		13.8 (I = 1.0 M) [c]
$\log \beta_{102}$	21.1 (I = 0.1 M) [a]	19.5 (I = 0.5 M) [b]	25.3 (I = 0.4 M) [d]	30.2 (I = 0.5 M) [e]
	21.0 (I = 0.5 M) [b]	24.1 (I = 0.8 M) [c]		25.0 (I = 0.15 M) [f]
	22.9 (I = 0.3 M) [c]	25.1 ± 0.2 [g]		26.6 (I = 1.0 M) [c]

[a] (Raymond et al. 1987), [b] (Nebel and Urban 1966), [c] (Bonin et al. 2008), [d] (Bonin et al. 2007), [e] (Nebel 1966), [f] (Yule 1991), [g] (this work: I = 0.11 to 1.0 M).

The log β values determined for 1:1 and 1:2 complexes in this work are higher than the values reported by (Nebel and Urban 1966) with 11.5 and 19.5 and also slightly higher than the values reported by (Bonin et al. 2008) with 12.8 and 24.1.

From Table 1 follows that the log β values obtained for U(IV) complexation by citric acid fit well in the series of log β values determined for the complexation of further tetravalent actinides (Th(IV), Np(IV), Pu(IV)) by citric acid.

In the literature, most of the studies assume that An(IV) is complexed by the most basic form of the citrate anion (Cit^{3-}) (Nebel 1966; Nebel and Urban 1966; Raymond et al. 1987; Bonin et al. 2007; Bonin et al. 2008). However, recent structural studies on uranyl complexes with citric and citramalic acids (Felmy et al. 2006; Thuéry 2007; Thuéry 2008) suggest that citrate is bound to the cation both by its carboxylate site to the central carbon atom and by its hydroxyl group in alpha position (chelate formation), i.e. with the acid-base form H_2Cit^-. This option also has to be taken into account.

U(IV) complexation with succinic acid and mandelic acid

The complexation of U(IV) with succinic and mandelic acid has been investigated at an acidity of $[H^+] = 0.5$ M and an ionic strength of 0.5 M and 1.0 M, respectively. From the pK_a values reported for these ligands (cf. paragraph Calculations) follows, that the ligands are completely protonated under the experimental conditions applied in this work.

Fig. 2 and Fig. 3 show the evolution of the U(IV) spectrum in the two wavelength ranges analyzed for increasing succinic and mandelic acid concentrations (0 to 0.2 M) at an acidity of $[H^+] = 0.5$ M.

Especially, the spectra obtained for the U(IV) succinate system (cf. Fig. 2) show that the changes of the peak intensity and position are much weaker pronounced than in case of the U(IV) citrate system.

For the U(IV) complexation by succinic acid, the formation of 1:1 complexes of the type $M_pH_qL_r$ was detected with log $\beta_{101} = 9.0 \pm 0.2$ (I = 0.5 M). This value

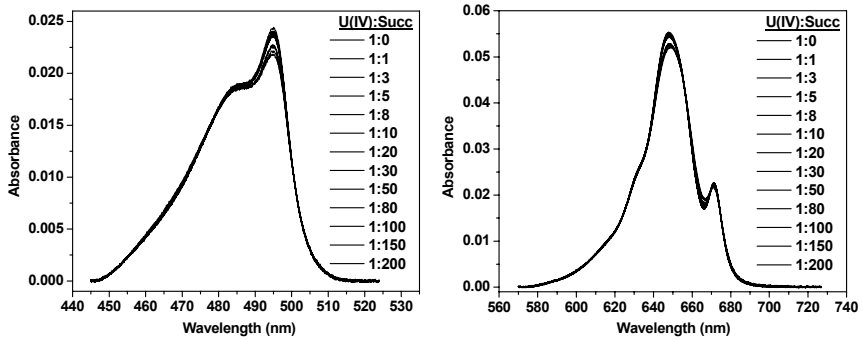

Fig.2. Two wavelength ranges of the UV-Vis spectra for 1×10^{-3} M U(IV) as a function of the succinic acid (Succ) concentration at $[H^+] = 0.5$ M and I = 0.5 M.

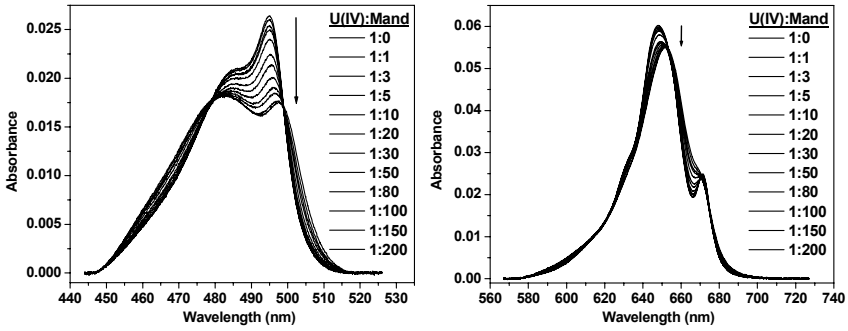

Fig.3. Two wavelength ranges of the UV-Vis spectra for 1×10^{-3} M U(IV) as a function of the mandelic acid (Mand) concentration at $[H^+] = 0.5$ M and I = 1.0 M.

is lower than the stability constant determined with log K = 9.78 (I = 0.5 M) by means of solubility experiments by (Merkusheva et al. 1970).

In contrast to succinic acid, the formation of 1:1 and 1:2 complexes in solution was observed for the U(IV) complexation by mandelic acid. The stability constants for 1:1 and 1:2 U(IV) mandelate complexes of the type $M_pH_qL_r$ were determined with log $\beta_{101} = 4.6 \pm 0.2$ and log $\beta_{102} = 8.3 \pm 0.2$. In the literature, there are no data available that we are aware of on the U(IV) complexation by mandelic acid.

Conclusion

The stability constants for 1:1 and 1:2 U(IV) citrate complexes were determined with log $\beta_{101} = 13.5 \pm 0.2$ and log $\beta_{102} = 25.1 \pm 0.2$. This shows a strong interaction between U(IV) and citric acid. That means, the uranium speciation in citrate containing waters is strongly influenced by the U(IV) citrate complex.

The comparison of the stability constants determined for the U(IV) complexation with various ligands shows that the interaction of U(IV) with succinate and mandelate is much weaker than the interaction of U(IV) with citrate.

Due to complexation with organic ligands the solubility and the mobility of U(IV) in aquatic systems is increased.

Acknowledgments

We would like to thank the Federal Ministry of Economics and Technology (BMWi) for financial support under the contract number 02E10156, A. Ritter for her help in performing the experiments and U. Schaefer for ICP-MS analyses.

References

Adams A, Smith TD (1960) The formation and photochemical oxidation of uranium(IV) citrate complexes. J Chem Soc: 4846-4850

Bernhard G, Geipel G, Brendler V, Nitsche H (1996) Speciation of uranium in seepage waters of a mine tailing pile studied by time-resolved laser-induced fluorescence spectroscopy (TRLFS). Radiochim Acta 74: 87-91

Binstead RA, Zuberbühler AD, Jung B (2005) SPECFIT - Global analysis system, Version 3.0.37, Spectrum Software Associates

Bonin L, Den Auwer Ch, Ansoborlo E, Cote G, Moisy P (2007) Study of Np speciation in citrate medium. Radiochim Acta 95: 371-379

Bonin L, Cote G, Moisy Ph (2008) Speciation of An(IV) (Pu, Np, U and Th) in citrate media. Radiochim Acta 96: 145-152

Choppin GR (2006) Actinide speciation in aquatic systems. Marine Chem 99: 83-92

Ciavatta L (1980) The specific ion interaction theory in evaluating ionic equilibria. Ann Chim (Rome) 70: 551-567

Durbin PW, Kullgren B, Xu J, Raymond KN (1998) Development of decorporation agents for the actinides. Rad Protec Dos 79: 433-443

Felmy AR, Cho H, Dixon DA, Xia Y, Hess NJ, Wang Z (2006) The aqueous complexation of thorium with citrate under neutral to basic conditions. Radiochim Acta 94: 205-212

Geipel G, Bernhard G, Rutsch M, Brendler V, Nitsche H (2000) Speciation in water released from mining and milling facilities. In: The environmental challenges of nuclear disarmament (Baca TE and Flokowski T, eds.), Kluwer Academic Publishers, Netherlands, p. 323-332

Geipel G (2005) Speciation of actinides. In: Handbook of elemental speciation II (Cornelis R, ed.). Wiley & Sons Ltd., London, p. 522

Guillaumont R, Fanghänel Th, Fuger J, Grenthe I, Neck V, Palmer DA, Rand MH (2003) Update on the chemical thermodynamics of uranium, neptunium, plutonium, americium and technetium. Chemical Thermodynamics Vol. 5. (OECD Nuclear Energy Agency, ed.) Elsevier, Amsterdam

Hummel W, Anderegg G, Rao L, Puigdomènech I, Tochiyama O (2005) Chemical thermodynamics of compounds and complexes of U, Np, Pu, Am, Tc, Se, Ni and Zr with selected organic ligands. Chemical Thermodynamics Vol. 9. (OECD Nuclear Energy Agency, ed.) Elsevier, Amsterdam

Kantar C, Honeyman BD (2005) Plutonium (IV) complexation with citric and alginic acids at low Pu_T concentrations. Radiochim Acta 93: 757-766

Kim JI (2006) Significance of actinide chemistry for the long-term safety of waste disposal. Nuclear Engineering and Technology 38: 459-482

Martell AE, Smith RM, Motekaitis RJ (1998) NIST critically selected stability constants of metal complexes database, Version 5.0, U.S. Department of Commerce, Gaithersburg, MD, USA

Merkusheva SA, Kumok VN, Skorik NA (1970) Radiokhim 12: 175-178

Nebel D, Urban G (1966) Potentiometrische Untersuchungen zur Komplexbildung von Ce^{III}, Ce^{IV}, Th^{IV}, U^{IV} und Citrat in wässriger Lösung. Z Phys Chem 233: 73-84

Nebel D (1966) Spektralphotometrische Untersuchung des Gleichgewichtes Pu^{IV}-Citrat in wässriger Lösung. Z Phys Chem 232: 161-175

Neck V, Kim JI (2001) Solubility and hydrolysis of tetravalent actinides. Radiochim Acta 89: 1-16

Opel K, Weiß S, Hübener S, Zänker H, Bernhard G (2007) Study of the solubility of amorphous and crystalline uranium dioxide by combined spectroscopic methods. Radiochim Acta 95: 143-149

Raymond DP, Duffield JR, Williams DR (1987) Complexation of plutonium and thorium in aqueous environments. Inorg Chim Acta 140: 309-313

Sevostyanova EP (1983) Stability of Np(IV), Np(V), and Np(VI) in citric acid solutions. Soviet Radiochemistry 25: 321-326

Shalimov VV, Kiiko NI, Zaitsev BN, Tebelev LG, Mikolaev VM (1974) Uranium(IV) citrate complexes. Complexing and extraction of actinides and lanthanides. (Vdovenko VM, ed.), Akademiya Nauk SSSR, Moscow, p. 3-7

Silva RJ, Nitsche H (1995) Actinide environmental chemistry. Radiochim Acta 70/71: 377-396

Suzuki Y, Nankawa T, Yoshida T, Ozaki T, Ohnuki T, Francis AJ, Tsushima S, Enokida Y, Yamamoto I (2006) Reduction behavior of uranium in the presence of citric acid. Radiochim Acta 94: 579-583

Thuéry P (2007) Uranyl ion complexation by citric and citramalic acids in the presence of diamines. Inorg Chem 46: 2307-2315

Thuéry P (2008) Novel two-dimensional uranyl-organic assemblages in the citrate and D(-)-citramalate families. CrystEngComm: 10, 79-85

Yule L (1991) A comparison of the binding of plutonium and iron to transferrin and citrate. Thesis, University of Wales

Uranium Speciation - from mineral phases to mineral waters

Gerhard Geipel and Gert Bernhard

Research Center Dresden Rossendorf, Institute of Radiochemistry, P.O.Box 510119, D-01314 Dresden, Germany, g.geipel@fzd.de

Abstract. Uranium ammunition can generate locally high concentrations of uranium in the environment.

Weathering processes of the uranium metal lead in a first step to the formation of uranium minerals[1]. Depending on the composition of the soil the formation of several types of minerals can be estimated. Especially the content of phosphate from fertilizers and the aluminium from soil components are involved in the mineral formation.

By use of time-resolved laser-induced fluorescence spectroscopy (TRLFS) the mineral type can be determined without any destruction. A large database of luminescence spectra, obtained from uranium minerals of the collection of the Technical University Mining Academy Freiberg, enables us to identify the formed uranium mineral[2]. It was found that mainly the mineral sabugalite was formed during weathering processes[1]. Other experiments with pure calcium and phosphate containing solution lead to the formation of the mineral meta-autunite[3].

In a second step the formed minerals than undergo further weathering processes, forming dissolved uranium species.

In the former uranium mining areas of eastern Germany we could discover a new dissolved uranium carbonate species[4,5]. However, the uranium concentration of about 2 mg/L in these mining related waters is relatively high. Nevertheless the carbonate and calcium concentration are high enough to form a very stable dical-

cium-uranyl-tricarbonate species. This species is of great importance, as its existence explains the uranium migration at the Hanford site[6].

In addition to the calcium species it can be stated that also the other alkaline earth elements form this type of alkaline earth uranyl carbonate species[7,8,9,10].

Following the uranium migration in the soil we could detect in the experiments that mainly carbonate species are formed. The pure carbonate species do not show any luminescence properties at room temperature. Therefore the samples have to be frozen to temperatures below 220 K[11], in order to minimize the dynamic quench effect of the carbonate anion. This increases also the luminescence intensity and the luminescence lifetime of all carbonate containing species.

Nevertheless, in one case of the soil experiment also hydroxo species were found. This may be connected to a non-equilibrium with atmospheric CO_2 in this column.

Following the possible transport of uranium under environmental conditions we may start with the weathering of uranium compounds in the soil or in a mining waste rock pile. The seepage water contains about 2 mg/L uranium and the speciation is mainly influenced be the formation of the dicalcium-uranyl-tricarbonate species. The input of these seepage water leads to a dilution of the uranium by about three orders of magnitude. Using the cryogenic technique in TRLFS[12] we could also determine the uranium speciation in the river water nearby the former uranium mining area. The uranium concentration was about 2 µg/L uranium and in the river water mainly uranyl-tricarbonate species are formed.

Despite this uranium can migrate down to the groundwater. In this case uranium may come back to the food chain by the production of mineral waters. We have studied the uranium speciation in several German mineral waters with uranium concentrations between 50 ng/L and 5 µg/L. In agreement with speciation calculations the sparkling and the calcium poor waters contain uranium as uranyl-tricarbonate species, whereas the non-sparkling waters if they are rich in calcium show clearly the formation of the dicalcium-uranyl-tricarbonate species. Using cryogenic TRLFS the detection limit for uranium species was estimated to be

about 50 ng/L. Additionally a Hungarian medicinical water shows a uranium concentration of 150 µg/L. Due to the high mineralisation of this water also the dicalcium-uranyl-tricarbonate species was determined.

Summarizing it can be concluded that the most natural waters contain uranium as tri-carbonate species. According to investigations of Carriere[13] these uranium species are less hazardous than phosphate and citrate species.


Uranium Mining
and Hydrogeology

Coordination of U(IV) and U(VI) sulfate hydrate in aqueous solution

Christoph Hennig, Satoru Tsushima, Vinzenz Brendler, Atsushi Ikeda, Andreas C. Scheinost and Gert Bernhard

Forschungszentrum Dresden-Rossendorf, Institute of Radiochemistry, P.O. Box 510119, D-01314 Dresden, Germany, E-mail: hennig@esrf.fr

Abstract. Sulfuric acid has been used for *in situ* leaching of uranium ores at several places, among them Königstein/Germany. The fate of the remaining leaching solvents may pose a substantial problem when released into aquifers used for drinking water. The current available thermodynamic data on uranium sulfate species in aqueous solution are not sufficient because typical leaching solutions commonly exceed the limit of ionic strengths of conventional models. The application of spectroscopic techniques may help to provide the missing data. We review here coordination data of U(IV) and U(VI) sulfate in aqueous solutions with high ionic strengths investigated by several spectroscopic techniques (mainly EXAFS) combined with XRD studies and DFT calculations. The observed results expand the current knowledge of uranium sulfates substantially beyond the available information based mainly on thermodynamic data.

Introduction

In situ leaching of uranium ore, so-called solution mining, recently became popular because it saves maintaining costs for mine operation and reduces large uranium mill tailing deposits. The technique is based on injecting the leaching liquid into the ore deposit, followed by pumping back the uranium-bearing liquid to the surface where further processing occurs. *In situ* leaching allows the recovery of uranium without conventional surface or underground mining. Two different techniques are currently in use: the well established acidic leaching with sulfuric acid and the newer alkaline leaching with carbonate solutions. Both techniques are based on the high solubility of uranium in oxidation states IV and VI. The carbonates belong generally to the strongest uranium complexes. Even U(V) can be sta-

bilized in carbonate solvents which otherwise disproportionates easily (Ikeda et al. 2007).

The *in situ* leaching with sulfuric acid has been applied to the Königstein uranium mine near Dresden/Germany (Lange et al. 1991). The site is a historical placer deposit where uraninite from weathering residues has been enriched in porous sandstone (average of 500g U/t). Uranium mining took place between 1967 and 1990, first partly, later exclusively by *in situ* leaching with sulfuric acid. In total a volume of $2 \cdot 10^6$ m^3 of sulfuric acid with a concentration of 2-3 g/L has been used. The leaching solution was injected into prepared sandstone blocks directly from the ground tunnel floor with a leaching duration of 3-5 years. A uranium concentration of 10-80 mg/L was obtained in the extracted solvents. About 18 000 t of uranium was extracted mainly with this method during the mining activity. The leaching liquid was oxic, and therefore most of the uranium was oxidized to U(VI). But even U(IV) is well soluble in sulfuric acid. As a positive effect, the leaching liquid did not contain appreciable amounts of Ra-226, the decay product of U-238, which is a main problem for the waste treatment. The reason is that radium precipitates together with barium and remains in the ore body (Baraniak et al. 1997) because it is, similar to other alkaline earth metals, insoluble in sulfate solutions.

The risk of *in situ* leaching technology is the migration of the uranium loaded leaching liquid out of the mining zone into aquifers and the unpredictable problems and costs of restoring the drinking water reservoirs. The uranium mine Königstein undergoes therefore, since it has been abandoned in 1990, an intense remediation until today (2008).

Uranium can occur in aqueous solution with the oxidation states III, IV, V and VI. The oxidation state III is not stable against reoxidation under environmental conditions. Uranium(V) undergoes easily a disproportionation reaction where UO_2^+ is decomposed to U^{4+} and UO_2^{2+}. U(III) and U(V) have therefore not to be considered in the subsequent discussion. The solubility of uranium differs by several orders of magnitude depending on its oxidation state, pH and the type of ligands available in the solution. The solubility of U(IV) is very low except for low pH values. Furthermore, if only weak ligands are present in the solution, the formation of U(IV) colloids is likely. In contrast, U(VI) is well soluble and therefore it is rather mobile in the environment. Sulfate enhances the solubility by forming strong complexes.

Despite the enhanced technical use of sulfuric acid in leaching process of uranium ore and extended remediation activities, the aquatic chemistry of uranium sulfate is not fully understood. The actual knowledge on the coordination of uranium sulfate hydrate will be summarized here briefly.

U(IV) sulfate

Uranium (IV) forms strong complexes with sulfate. Binary sulfate complexes coordinated by SO42- and H2O molecules dominate at low pH. With increasing

pH hydrolysis occurs, and OH- compete with the sulfate coordination forming ternary sulfate complexes (also known as basic sulfates). The current NEA thermodynamic database (Guillaumont et al. 2003) reports only two binary sulfate species: USO42+ and U(SO4)2(aq):

$$U^{4+} + SO_4^{2-} \rightleftharpoons USO_4^{2+} \qquad \log K^0 = 6.58 \pm 0.19$$

$$U^{4+} + 2SO_4^{2-} \rightleftharpoons U(SO_4)_2(aq) \qquad \log K^0 = 10.51 \pm 0.20$$

In contrast, it has been shown recently with X-ray absorption fine structure (EXAFS) spectroscopy (Fig. 1) that U(IV) species can be coordinated by up to 5 SO_4^{2-} ions in aqueous solution.

EXAFS allows a comparison of the coordination in solution (Fig. 1, top) with that in solid state (Fig. 1, bottom) where structural parameters can be extracted by single crystal diffraction (Fig. 3, right). The first rather broad peak in the Fourier transform (FT) of EXAFS results from the backscattering signal of 9 oxygen atoms in the first coordination sphere. These oxygen atoms belong to sulfate in monodentate (mon) and bidentate (bid) coordination, as well as oxygen to water molecules. The distances between oxygen and uranium vary as follows: U-O_{H2O}~2.41 Å, U-O_{Smon}~2.32 Å, U-O_{Sbid}~2.47 Å. The peaks at higher distances are backscattering signals from sulfur atoms in bidentate (U-S_{bid}=3.08 Å) and monodentate (U-S_{mon}=3.67 Å) sulfate coordination. The solution species occur e.g. as $[U(SO_{4,bid})_2(SO_{4,mon})_2 \cdot nH_2O]^{4-}$ and $[U(SO_{4,bid})_3\ (SO_{4,mon})_2 \cdot mH_2O]^{6-}$. Fig. 2 shows the coordination number N_{Sbid} and N_{Smon} as a function of the sulfate concentration. The coordination number N_{Sbid} increases, whereas N_{Smon} decreases with increasing $[SO_4^{2-}]$. Hence, with increasing sulfate concentration the bidentate coordination becomes more dominant.

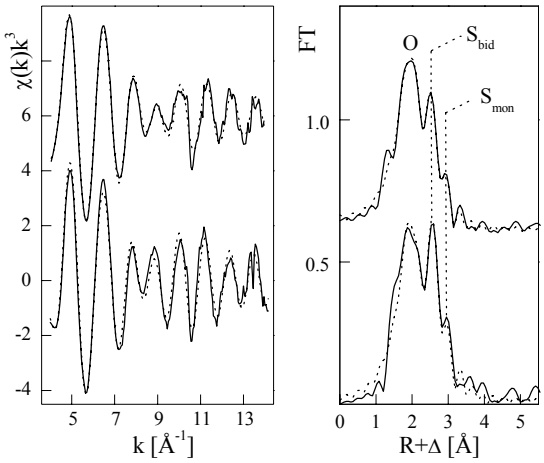

Fig.1. Left: U L_3-edge k^3-weighted EXAFS data (left), and right: the corresponding Fourier transforms (FT) of U(IV) sulfate in solution at pH 1.5, 50 mM U(IV) and 1.95 M SO_4^{2-} (top) and the crystalline precipitate obtained at pH 1.5 (bottom). (Hennig et al. 2008a).

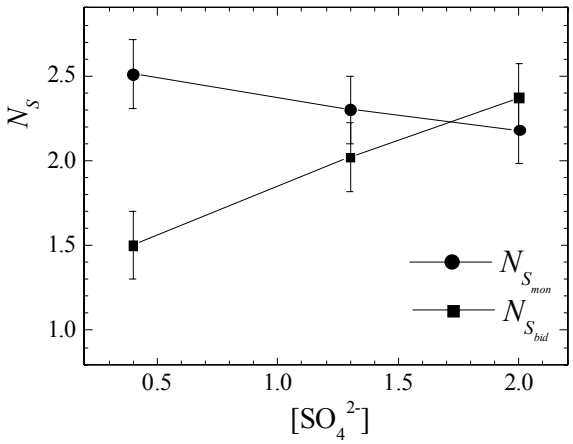

Fig.2. U(IV) sulfate coordination at pH 1, 50 mM U(IV). Number of sulfur neighbors N_{Sbid} and N_{Smon} as function of $[SO_4^{2-}]$ taken from Ref. (Hennig et al. 2008a).

Crystal structures of uranium(IV) sulfates reveal either eight- or nine-fold coordination by oxygen atoms from sulfate or water molecules. The resulting coordination polyhedra are distorted squared antiprism with N=8 (Fig. 3, left) or a tricapped trigonal prism with N=9 (Fig. 3, right).

The driving force to generate a N-fold coordination polyhedron is the coordination mode of sulfate. An exclusive monodentate coordination is related with a lower coordination number (usually N=8), whereas higher coordination (N=9) can be observed if a part of the sulfate groups occur in bidentate coordination. Bidentate coordinated sulfate groups show rater long U^{4+}-O distances (2.42-2.49 Å) and are therefore less space consuming than monodentate sulfate groups with compa-

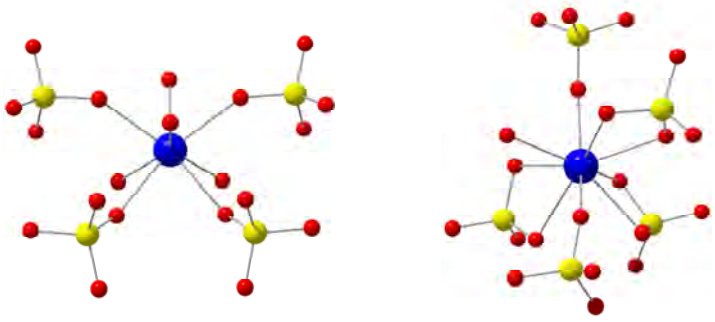

Fig.3. U(IV) coordination obtained from crystal structure data. Left: $U^{4+}(SO_4)_4(H_2O)_4^{4-}$ (Kierkegaard 1956) and right: $U^{4+}(SO_4)_5H_2O^{6-}$ (Hennig et al. 2008b). The coordination of the solution species in Fig. 1 is similar to the polyhedron of $U^{4+}(SO_4)_5H_2O^{6-}$.

rable short U^{4+}-O distances (2.29-2.32 Å). Even a coordination number *N*=10 has been observed for Np(IV) where the sulfate in the $Np^{4+}(SO_4)_5^{6-}$ polyhedron is exclusively bidentate coordinated (Charushikova et al. 1999).

However, this coordination behavior changes completely, if the pH increases a value of ~1.5 where hydrolysis becomes dominant for U(IV). Under these conditions SO_4^{2-} is partly replaced by OH^-. The hydrolysis species have the strong tendency to form polynuclear and polymeric species related with lower solubility. The EXAFS of such a complex in a sample whose pH has been increased to 1.8 is shown in Fig. 4. At this pH value the complex precipitates immediately from the solution. The spectrum of the precipitate indicates a rearrangement of the SO_4^{2-} groups from mixed bidentate/monodentate in solution to exclusively monodentate coordination in the precipitate. The rearrangement of the sulfate groups during crystallization is a typical behavior of sulfate, frequently forming monodentate bridging sequences in solid structures. The FT of the precipitate shows a U-U distance of 3.87 Å. This short distance is typical for uranium hydroxides, where the OH^- group acts as bridging ligand (Tsushima 2008).

U(VI) sulfate

Uranium(VI) forms easily trans-dioxo bonds. This process can be understood in the context of hydrolysis. If the acidity of the protons on an associated water molecule is high, then an adjacent free water molecule becomes a Bronsted base and removes a proton by forming H3O+ and leaving the metal as hydroxide. If cation charge is very high, as in case of U6+, the remaining OH– protons can be acidic enough to be released by forming a trans-dioxo group:

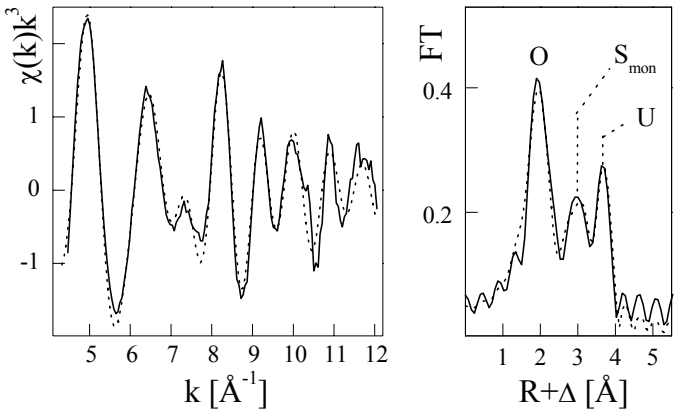

Fig.4. U L_3-edge k^3-weighted EXAFS data and their Fourier transform of U(IV) precipitate (Hennig et al. 2007).

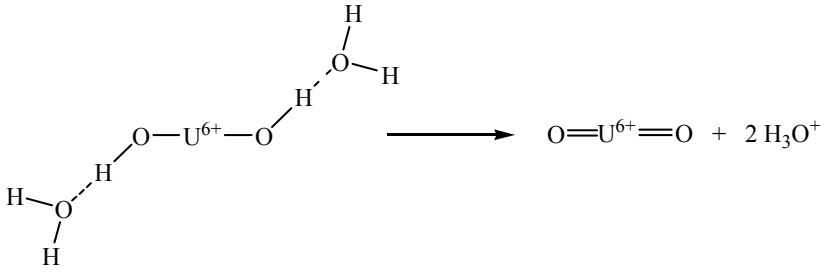

Thus the formal charge in the uranyl ion is reduced to UO_2^{2+}. This ion is very stable over the whole pH-range. Due to the double bond of the oxo groups (also axial oxygens O_{ax}) the U-O_{ax} bond length is short (typically between 1.76 and 1.82 Å). The oxo group restricts the coordination to the equatorial plane. The uranyl ion forms binary sulfato complexes in acidic solution. At pH values > 3, hydrolysis of uranyl causes formation of various ternary species comprising bridging hydroxide/oxide and sulfate ligands. The major ternary complexes found so far are $(UO_2)_2(OH)_2(SO_4)_2^{2-}$, $(UO_2)_3(OH)_4(SO_4)_3^{4-}$, and $(UO_2)_5(OH)_8(SO_4)_n^{2-2n}$, with n = 5 or 6 (Moll et al. 2000). Thermodynamic data are available for three binary sulfate species, UO_2SO_4(aq), $UO_2(SO_4)_2^{2-}$ and $UO_2(SO_4)_3^{4-}$ (Guillaumont et al. 2003).

$$UO_2^{2+} + SO_4^{2-} \rightleftharpoons UO_2SO_4(aq) \qquad \log K^0 = 3.15\pm0.12$$

$$UO_2^{2+} + 2SO_4^{2-} \rightleftharpoons UO_2(SO_4)_2^{2-} \qquad \log K^0 = 4.14\pm0.07$$

$$UO_2^{2+} + 3SO_4^{2-} \rightleftharpoons UO_2(SO_4)_3^{4-} \qquad \log K^0 = 3.02\pm0.38$$

There occurs a substantial change in the sulfate coordination mode with increasing $[SO_4^{2-}]/[UO_2^{2+}]$ ratio. These changes can be analyzed besides X-ray absorption and diffraction also by IR, UV-vis and luminiscence spectroscopy, because the uranyl unit shows unique vibration modes and electron excitations, respectively.

Fig. 5 shows EXAFS spectra of U(VI) in solutions with low and high sulfate concentration. The FT´s are dominated by the peak of the 2 axial oxygen atoms of UO_2^{2+} in a U-O_{ax} distance of 1.77±0.02 Å. Due to the presence of several ligands, the equatorial oxygen (O_{eq}) shell is split into different superimposed peaks. The coordination of uranium with sulfate can be derived from the sulfur backscattering signals. At 0.05 M SO_4^{2-}, where UO_2SO_4(aq) is the dominant species, monodentate sulfate coordination prevails and bidentate coordinated sulfate exists only to a minor extent. In the sample with 3.0 M SO_4^{2-}, where $UO_2(SO_4)_2^{2-}$ is the dominant species, a strong peak appears at R+Δ = 2.6 Å. Considering the effect of the phase shift Δ, a true U-S distance of 3.12 Å has been observed, indicating a bidentate sulfate coordination.

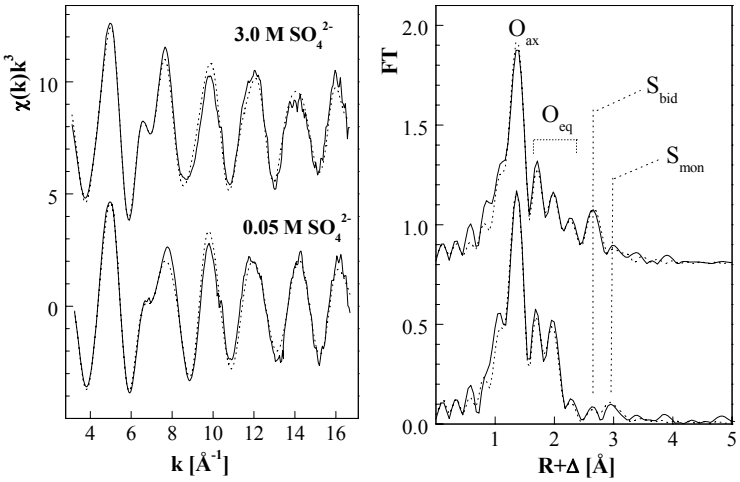

Fig.5. U L_3-edge EXAFS (left) and the corresponding Fourier Transforms (right) of U(VI) aquo sulfato species with 0.05 M U(VI), taken from Ref. (Hennig et al. 2007).

The Figures 6-8 show potential U(VI) sulfate coordination isomers of $UO_2SO_4(aq)$, $UO_2(SO_4)_2^{2-}$ and $UO_2(SO_4)_3^{4-}$ optimized by density functional theory calculation (DFT). $UO_2SO_4(aq)$ is the dominant species in solutions with low $[SO_4^{2-}]/[UO_2^{2+}]$ ratios of 1-5 (Fig. 6). IR spectroscopy (Gál et al. 1992), High-energy X-ray scattering (Neuefeind et al. 2004) and EXAFS (Hennig 2007) revealed that the sulfate in $UO_2SO_4(aq)$ is predominantly monodentate coordinated, although there is also evidence for a second isomer with bidentate coordination (Hennig et al. 2007) as shown in Fig. 6, right.

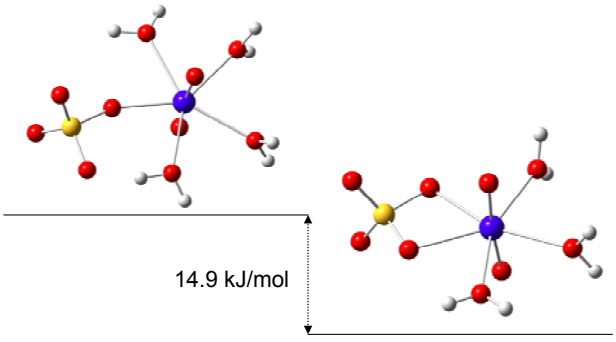

Fig.6. The structures of $UO_2SO_4(aq)$ complexes in solution obtained from DFT calculation taken from Ref. (Hennig et al. 2007).

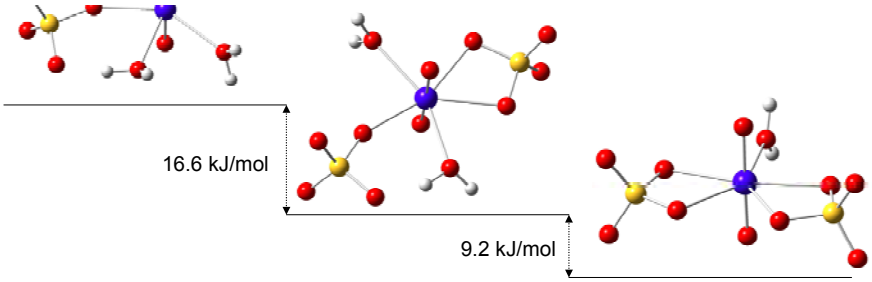

Fig.7. The structures of $UO_2(SO_4)_2^{2-}$ complexes in solution obtained from DFT calculation taken from Ref. (Hennig et al. 2007).

The existence of these two isomers can be explained by the small difference in the Gibbs free energy ΔG of only 14.9 kJ/mol (Vallet and Grenthe 2007, Hennig et al. 2007). At higher $[SO_4^{2-}]/[UO_2^{2+}]$ ratios of 40-60 the species $UO_2(SO_4)_2^{2-}$ (shown in Fig. 7) has its stability range, although it always exist in equilibrium mainly with $UO_2SO_4(aq)$. The stability range of $UO_2SO_4(aq)$ and $UO_2(SO_4)_2^{2-}$ has been extracted from UV-vis spectra by statistical techniques (Hennig et al. 2008c). It is interesting to note that among the possible species shown in Fig. 7, the one with two bidentate coordinated sulfate groups dominate in solutions (Nguyen-Trung et al. 1992, Moll 2000, Hennig 2007). Recently, this has been confirmed by HEXS measurements (Hennig et al. 2008c).

The increase of the $[SO_4^{2-}]/[UO_2^{2+}]$ ratio is limited by the solubility of sulfate in aqueous solution. The only way to increase the ratio is therefore to lower the

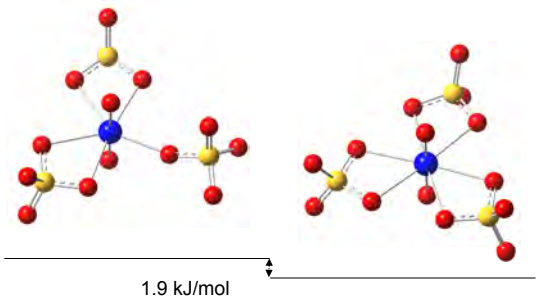

Fig.8. The structures of $UO_2(SO_4)_3^{4-}$ complexes in solution obtained from DFT calculation taken from Ref. (Hennig et al. 2007).

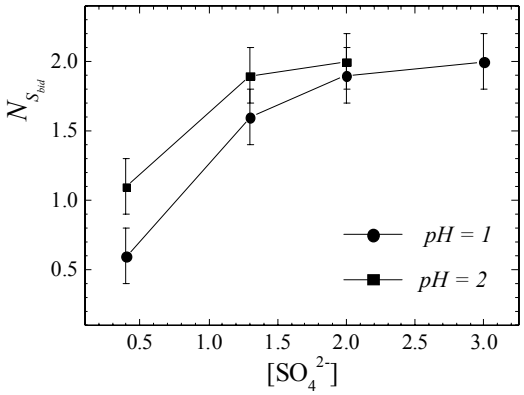

Fig.9. U(VI) sulfate coordination. Number of sulfur neighbors N_{Sbid} as function of [SO_4^{2-}] at pH 1 and pH 2, taken from Ref. (Hennig et al. 2007).

U(VI) concentration. The required concentration is too low to obtain structure information from X-ray absorption spectroscopy and X-ray diffraction. Emission spectroscopy provides signals even in solutions with only 10^{-5} M U(VI).

In such solutions a [SO_4^{2-}]/[UO_2^{2+}] ratio > 10^4 can be reached where the species $UO_2(SO_4)_3^{4-}$ occurs to be stable (Geipel et al. 1997, Vercouter et al. 2007). Because fluorescence spectroscopy does not provide structural information, there is a lack of information concerning the coordination. The estimation of ΔG from DFT calculation indicates a very small energy difference of only 1.9 kJ/mol between the two potential species depicted in Fig. 8. The only hint that a species with three bidentate sulfate ligands may exist in aqueous solution is given by the crystal structure of $[N_2C_5H_{14}]_2$ $[UO_2(SO_4)_3]$ (Doran et al. 2003). As the synthesis of this structure has been performed under elevated p/T conditions of hydrothermal synthesis conditions it is not clear whether this structure is representative for the solution species existing under ambient conditions in aqueous solutions. The small difference of ΔG is a strong hint that the two isomers of $UO_2(SO_4)_3^{4-}$ shown in Fig. 8 may exist together in equilibrium.

There is a general trend that at low [SO_4^{2-}]/[UO_2^{2+}] ratios the monodentate sulfate coordination prevails whereas the bidentate coordination becomes dominant at higher ratios. This tendency has been observed in a series of U(VI) samples studied with EXAFS with increasing sulfate concentration as shown in Fig. 9. If one compare the known crystal structures of U(VI) sulfate with the solution species, an obvious difference can be noticed: there are several structures coordinated by up to 5 SO_4^{2-} groups, in this case mainly in monodentate coordination mode. However, crystal structures are sometimes not representative for the coordination in solutions because coordination may change during the crystallization process (Hennig et al. 2008b). This is especially the case for U(VI) sulfates which easily undergoes polymerization by forming 2D networks. In such networks, the sulfate group acts as bridging ligand among the UO_2^{2+} ions. Such polymers show a low solubility and do not form stable solution species.

Acknowledgements

This work was supported by the DFG under contract HE 2297/2-1.

References

Baraniak L, Thieme M, Kunke H, Bernhard G, Nitsche H (1997) Verhalten des Radiums im Flutungsprozeß des Uranbergwerks Königstein. Wiss Zeitschr TU Dresden 46:90-94

Charushnikova IA, Krot NN, Starikova ZA (1999) Crystal structure and spectroscopic properties of double potassium neptunium(IV) sulfate. Radiochem 41:104-108

Doran MB, Norquist AJ, O´Hare D (2003) Exploration of composition space in templated uranium sulfates. Inorg Chem 42:6989-6885

Gál M, Goggin PL, Mink J (1992) Vibrational spectroscopic studies of uranyl complexes in aqueous and non-aqueous solutions. Spectrochim Acta A 48:121-132

Geipel G, Brachmann A, Brendler V, Bernhard G, Nitsche H (1996) Uranium(VI) sulfate complexation studied by time-resolved laser-induced fluorescence spectroscopy (TRLFS). Radiochim Acta 75:199-204

Guillaumont R, Fanghänel T, Fuger J, Grenthe I, Neck V, Palmer DA, Rand MH (2003) Update on the chemical thermodynamics of uranium, neptunium, plutonium, americium and technetium. Elsevier Science Publishers, Amsterdam

Hennig C, Schmeide K, Brendler V, Moll H, Tsushima S, Scheinost AC (2007) EXAFS investigation of U(VI), U(IV), and Th(IV) sulfato complexes in aqueous solution. Inorg Chem 46: 5882-5892

Hennig C, Kraus W, Emmerling F, Ikeda A, Scheinost AC (2008a) Coordination of a uranium(IV) monomer in aqueous solution and in solid state. Inorg Chem 47:1634-1638

Hennig C, Servaes K, Nockemann P, Van Hecke K, Van Meervelt L, Wouters J, Fluyt L, Görrler-Walrand C, Van Deun R (2008b) Species distribution and coordination of uranyl chloro complexes in acetonitrile. Inorg Chem 47:2987-2993

Hennig C, Ikeda A, Schmeide K, Brendler V, Moll H, Tsushima S, Scheinost AC, Skanthakumar S, Wilson R, Soderholm L, Servaes K, Görrler-Walrand C, Van Deun R (2008c) The relationship of monodentate and bidentate coordinated uranium(VI) sulfate in aqueous solution. Radiochim Acta (in press)

Ikeda A, Hennig, C, Tsushima S, Takao K, Ikeda Y, Scheinost AC, Bernhard G (2007) Comparative study of uranyl(VI) and –(V) carbonato complexes in an aqueous solution. Inorg Chem 46:4212-4219

Kierkegaard P (1956) The crystal structure of $U(SO_4)_2 4H_2O$. Acta Chem Scand 10:599-616

Lange G, Mühlstedt P, Freyhoff G, Schröder B (1991) Der Uranerzbergbau in Thüringen und Sachsen – ein geologisch-bergmännischer Überblick. Erzmetall 44:162-171

Moll H, Reich T, Hennig C, Rossberg A, Szabó Z, Grenthe I (2000) Solution coordination chemistry of uranium in the binary UO_2^{2+}-SO_4^{2-} and the ternary UO_2^{2+}-SO_4^{2-}-OH^- system 88:559-566

Neuefeind J, Skanthakumar S, Soderholm L (2004) Structure of the UO_2^{2+}-SO_4^{2-} ion pair in aqueous solution. Inorg Chem 43:2422-2426

Nguyen-Trung C, Begun, GM, Palmer DA (1992) Aqueous uranium complexes. 2. Raman spectroscopic study of the complex formation of the dioxouranium(VI) ion with a variety of inorganic and organic ligands. Inorg Chem 31:5280-5287

Vallet V, Grenthe I (2007) On the structure and relative stability of uranyl(VI) sulfate complexes in solution. C R Chimie 10:905-915

Vercouter T, Vitorge P, Amekranz B, Moulin C (2008) Stoichiometries and thermodynamic stabilities for aqueous sulfate complexes of U(VI). Inorg Chem 47: 2180-2189


Uranium Mining
and Hydrogeology

Uranium partitioning during water treatment processes

Ashraf E.M. Khater[1&2]

[1]National Center for Nuclear Safety and Radiation Control, Atomic Energy Authority, Cairo, Egypt,
[2]Physics Department, College of Sciences, King Saud University, Riyadh, Kingdom of Saudi Arabia.

Abstract. Water samples were collected from underground water purification plant to study the variation in uranium concentration through the treatment processes and its relation to physical and chemical properties of water. Samples represent the different treatment processes (input, output, after filtration, sludge tank, reverse osmosis permit and reject, and waste water ponds). Uranium concentration in the collected samples were measured using ICP-MS. Uranium concentrations in water samples show a wide range of variation from 0.06 to 35 $\mu g.L^{-1}$. The chemical properties of water samples Water physical and chemical properties, i.e. pH, EC, major cations (Ca, Mg and K) and major anions (CO_3, HCO_3, Cl and SO_4) were determined. The effect of water treatment processes on uranium concentration; dose assessment due to water drinking (before and after treatment) and the radio-ecological assessment were discussed.

Introduction:

Generally, the occurrence of radionuclides in the underground water is meanly due to the leaching of the salts from the bed-rocks. The concentration of uranium in water depends on several factors. These include the uranium concentration in the aquifer rock, the partial pressure of carbon dioxide, and the presence of oxygen and complexing agents in the aquifer. The characteristics of water that mainly determine its capacity to dissolve, carry or deposit elements are its pH, temperature, redox potential, concentration and properties of dissolved salts, flow rate and residence time (Pontius 2000; Shabana and Al-Hobiab 1999).

The health effects and risk of uranium can be divided radiological risk of uranium isotopes and the chemical risk as a toxic heavy metal. US Environmental Protection Agency (EPA) has classified uranium as a confirmed human carcinogen (group A). EPA has suggested that only zero tolerance is a safe acceptable limit for the carcinogenic risk from uranium and finalized a realistic regulation levels as maximum contaminant level (MCL) of 30 $\mu g.L^{-1}$, Canada proposed interim maximum acceptable level (IMAC) of 20 $\mu g.L^{-1}$, and World Health Organization (WHO) strictly recommended a reference level of 2 $\mu g.L^{-1}$(Kim et al. 2004). Many publication studied the concentration of uranium and natural radionuclides in drinking water (Singh et al. 2008; Godoy and Godoy 2006; Shabana and Al-Hobaib 1999; Babu et al. 2008; WHO 2004; IAEA 2003; Pontius 2002; Ahmed 2004; Katsoyiannis et al 2007), uranium removal from drinking water (Gafvert et al 2002; Jimenez and Rufo 2002; Huikuri et al. 1998) and radiological dose and risk assessment (erranz et al 1997; Kurttio et al. 2006; Orloff et al. 2004; Kim et al. 2004; Jia and Torri 2007).

This work aims at shading more light on the variation of uranium concentrations through the water purification and treatment processes and its relation to the physical and chemical properties of water samples.

Materials and methods

Eight water samples were collected from underground water treatment plant in Hail region- Saudi Arabia that derives water from 18 drilled wells, 500-600 m depth, in a circle of 10 km^2 area and produces 10^5 m^3/d. The main treatment processes include aeration, coagulation-flocculation and filtration, reverse osmosis and chlorination. Water samples represent the different water treatment steps (input after aeration, after filtration (sand filter), sludge tank, reverse osmosis permit, reverse osmosis reject, output water and two samples from the evaporation ponds. Water samples were collected in 5 L capacity polyethylene containers and transferred and kept in darkness for preservation. Uranium concentrations, $\mu g.L^{-1}$, were measured using PerkinElmer model ELAN-9000 ICP-MS at ALS Chemex- Canada. Water physical and chemical properties such as pH, EC (electric conductivity, $dS.cm^{-1}$), major cations (Ca, Mg and K) and major anions (CO_3, HCO_3, Cl and SO_4) were determine using standard methods (Al-Omran 1987).

The variation percentage of uranium concentration in water samples relative to input water were calculated using the following equation:

$$\Delta = (C - C') \times 100/C$$

where: C; uranium concentration in input water
C'; uranium concentration in the sample

Positive and negative percentage mean that uranium decontamination is achieved in the treatment process and the treatment process increases uranium concentration, respectively (Jimenez 2002)

Results and discussions

Uranium concentration in ppb, its calculated activity concentration in $mBq.L^{-1}$ (1 $\mu g.L^{-1}$ = 12.4 $mBq.L^{-1}$) and variation percentage (Δ) are given in table 1. Uranium concentration was not changed before the reverse osmosis process, only variation percentage of -2 % after filtration. Uranium concentration in the treated water (output) was below the 2 $\mu g.L^{-1}$ WHO standard, which is the strictest (Kim et al 2004).

Uranium removal percentage from water by reverse osmosis process was 99 % while the increasing of uranium in reverse osmosis reject water was very close to 300 %. Huikuri et al, 1998, studied the effectiveness of small commercial POE (point of entry) reverse osmosis equipment for removing simultaneously water radioactivity and salinity from a bedrock water. Reverse osmosis is one of the few water treatment methods which can be applied for simultaneous removal of U, Ra, Pb, Po and water salinity, i.e. water is almost completely demineralized (Huikuri et al 1998).

Uranium variation percentage (removal) was 96% for the final treated water. The decrease in uranium removal percentage from that of reverse osmosis step (99%) could be due the presence of uranium in the reagents used and to the dissolution of uranium associated with colloids and other substances, during water treatment processes (Jimenez 2002).

Wash water are sequentially collected in 6 evaporation ponds. Uranium concentrations in evaporation ponds enhanced due to evaporation process where the variation percentages were – 108 % and - 778 % and it will increase more by evaporation. It is expected that uranium and other radionuclides, and heavy element will be accumulated to reach very high concentrations in evaporation ponds. This situation should be considered very carefully to prevent the contamination of the surrounding environment.

Table 1. Uranium concentrations ($\mu g.L^{-1}$) and activity concentrations ($mBq.L^{-1}$) in water samples.

Ser. No.	Samples	Uranium		Δ*
		µg/L	mBq/L**	
1	Input (after airation)	4	49	-
2	After sand filter	4	51	-2
3	From sludge tank	4	52	-5
4	Reverse Osmosis permit	0.06	0.74	99
5	Reverse Osmosis reject	16	195	-293
6	Output	0.17	2	96
7	Evaporation bond-1	8	103	-108
8	Evaporation bond-2	35	435	-778

*varaition precentage in uranium concentration relative to input water

**(1 µg/L = 12.4 mBq U-238/L)The reverse osmosis reject and sand filter back-

Table 2. Physical and chemical properties of water samples.

Ser. No	Samples	pH	EC	Major cations (meq/L)				Major anions (meq/L)		
			dS/cm	Ca	Mg	Na	K	CO_3	HCO_3	Cl
1	Input (after airation)	8.3	1.2	6	4	4	0.15	1.3	1.5	7
2	After sand filter	8.3	1.1	5	3	4	0.15	1.3	1.0	8
3	From sludge tank	8.2	1.1	6	4	4	0.15	1.3	2	7
4	Reverse Osmosis permit	8.4	0.22	1	0.59	0.84	0.1	6	0.5	
5	Revers Osmosis reject	8.5	1.7	10	6	13	0.27	1.3	3	18
6	Output	7.9	0.32	1.5	0.89	1.9	0.13	3	1.2	4
7	Evaporation bond-1	8.3	5	26	16	26	0.63	1.3	3	36
8	Evaporation bond-2	7.6	17	66	39	106	1.9	1.3	1.5	138

Physical and chemical properties [pH, EC, major cations (Ca^{2+}, Mg^{2+}, Na^{+} and K^{+}) and major anions (Co_3^{2-}, HCO_3^{-}, Cl^{-} and SO_4^{2-}) of water samples are given in table 2.

pH values ranged from 7.6 to 8.5 where U and most heavy elements are increasingly sorbed on oxides, clays and other silicates. The absord fraction may be very close to 100 % above pH 7. It was reported that uranium concentrations enhanced in all water that has been purified within the acidic pH (<7) (Jimeneze 2002). It obvious that the reverse osmosis process remove not only U but also other anions and cations with variation concentration percentages more than 400% for Ca, Mg and Na, about 200 % for HCO_3^{-}, and about 50 % for K^{+}.

Correlation coefficients between uranium concentration and physical and chemical properties of water samples are given in Table 3. There are strong correlation (correlation coefficient) between uranium concentrations and EC (0.93), Ca (0.93), Mg (0.93), Na (0.94), Cl (0.94) and SO_4 (0.92). The correlation is good (-0.56) with pH values and weak with CO_3 (-0.39) and HCO_3 (0.32). The strong correlation could be explained due to the demineralization of water during treatment processes specially during reverse osmosis process or due to the chemical beha-

Table 3. Correlations between uranium concentration and physical and chemical properties of water samples

	U	Δ	pH	EC	Ca	Mg	Na	K	CO_3	HCO_3	Cl	SO_4
U	1											
Δ	-1	1										
pH	-0.56	0.55	1									
EC	0.93	-0.92	-0.72	1								
Ca	0.93	-0.93	-0.68	1.0	1							
Mg	0.93	-0.93	-0.68	1.0	1	1						
Na	0.94	-0.94	-0.73	1.0	0.99	1	1					
K	0.93	-0.93	-0.73	1.0	0.99	1	1.0	1				
CO_3	-0.39	0.43	0.14	-0.3	-0.33	-0.3	-0.27	-0.27	1			
HCO_3	0.32	-0.31	0.25	0.1	0.18	0.2	0.09	0.11	-0.63	1		
Cl	0.94	-0.94	-0.71	1.0	0.99	1	1.0	1.00	-0.25	-0.03	1	
SO_4	0.92	-0.92	-0.66	1.0	1.0	1	0.98	0.99	-0.31	0.20	0.98	1

vior of uranium. For example, uranium can form soluble complexes in most ground waters with chloride, sulphate and under oxidizing conditions with carbonate which keep uranium in solution (Shabana and Al-Hobiab 1999).

The calculation of committed effective dose for adult due to uranium-238, in raw and purified water, intake. These calculations based on annual consumption rate of 730 $L.y^{-1}$ and dose coefficient for ingestion of ^{238}U by adult member of public of $4.5x10^{-8}$ $Sv.Bq^{-1}$. The committed effective doses due to drinking water before and after purification were 1.6 and 0.66 $\mu Sv.y^{-1}$, respectively, which are below 100 $\mu Sv.y^{-1}$ the reference level of the committed effective dose recommended by the WHO (Jia and Torri 2007).

Acknowledgment

Author acknowledges the technical support of Dr. H.Al-Swaidan and Mr. A. Slsaif during water sampling and soil department –King Saud University for water chemical analysis.

References

Ahmed N (2004) Natural radioactivity of ground and drinking water in some areas of Upper Egypt. Turkish J. Eng. Env. Sci. 28: 345-354

Al-Omran M A (1987) Evaluation of some irrigation water in central region in Saudi Arabia. J. Coll. Agric. King Saudi University. 9: 363-369

Babu M, Somashekar R, Kumar S, shivanna K, Krishnamurthy V (2008) Cocentration of uranium levels in groundwater. Environmental Science and Technology 5(2): 263-266

Gafvet T, Ellmark C, Holm E (2002) Removal of radionuclides at a waterwork. Environmental Radioactivity 63: 105-115

Godoy J, Godoy M (2006) Natural radioactivity in Brazilian groundwater. Environmental Radioactivity 85: 71-83

Herranz M, Abelairas A, Legarda F (1997) Uranium content and associated effective doses in drinking water from Biscay (Spain). Appli. Radiat. Isot. 48 (6): 857-861

Huikuri P, Salonen L, Raff O (1998) Removal of natural radionuclides from drinking water by point of entry reverse osmosis. Desalination 119: 235-239

International Atomic Energy agency (IAEA) (2003) Extent of environmental contamination by naturally occurring radioactive material (NORM) and technological options for mitigation. Technical Reports series No. 419: 33-49

Jia G, Torri G (2007) Estimation of radiation dose to member of the public in Italy from intake of some important naturally occurring radionuclides (238U, 234U, 235U, 226Ra, 228Ra, 224Ra and 210Po) in drinking water. Appli. Radiat. Isot. 65:849-857

Jimenez a, Rufo D (2002) Effect of water purificiation on its radioactive content. Water Research 36: 1715-1724

Katsoyiannis I , Hug S , Ammann A, Zikoudi A, Hatziliontos (2007) Arsenic speciation and uranium concentrations in drinking water supply wells in Northern Greec: correlation

with redox indicative parameters and implications for groundwater. Science of the Total Environment 383:128-140
Kim Y, Park H, Kim J, Park S, Cho B, sung I, Shin D (2004) Health risk assessment for uranium in Korean groundwater. Environmental Radioactivity 77: 77-85
Kurttio P, Salonen L, Ilus T, Pekkanen J, Pukala E, Auvinen A (2006) Well water radioactivity and risk of cancers of the urinary organs. Environmental research 102: 333-338
Orloff K, Mistry K, Charp P, Metcalf S, Marino R, Shelly T, Melaro E, Donohoe a, Jones R (2004) Human exposure to uranium in groundwater. Environmental Radioactivity 94: 319-326
Potius F W (2000) Defining a guidline for uranium. American Water Association Journal 92:18-24
Shabana E, Al-Hobaib A (1999) activity concentrations of natural radium, thorium and uranium isotopes in ground water of two different regions. Radiochim. Acta 87: 41-54
Singh J, Singh H, Singh S, Bajwa B (2008) Estimation of uranium and radon concentration in some drinking water samples. Radiat. Meas. Doi: 10.1016/j.radmeas.2008.04.004
World Health Orgnization (WHO) (2004) Uranium in drinking water. WHO/SDE/WSH/03.04/118

Speciation of Uranium in a Polluted Site: a TRLFS study

Vannapha Phrommavanh[1], Thomas Vercouter[2], Michaël Descostes[1,3], Catherine Beaucaire[1] and J.P. Gaudet[4]

[1]Laboratory for measurement and modelling of the migration of radionuclides,
[2]Laboratory of speciation of radionuclides and molecules, CEA Saclay DEN-DANS/DPC/SECR/, F-91191 Gif-sur-Yvette cedex
3 *UMR 8587 CEA – Université d'Evry – CNRS (France)*
[4]CNRS-INPG-IRD-UJF-LTHE, BP 53, F-38041 Grenoble Cedex 09

Abstract. The uranium speciation in a polluted soil was investigated to assess the possible impact on geo- and biosphere. During winter, uranium was found to be mostly under the +VI oxidation state, which is potentially mobile, while it was reduced into less soluble U(IV) species in summer. These observations were correlated with changes of the redox potential due to the activity of sulphate-reducing bacteria. The potential migration of uranium is also highly dependent on its aqueous speciation, particularly concerning U(VI). In this work, the speciation of U(VI) was investigated in real samples by using time-resolved laser-induced fluorescence spectroscopy (TRLFS) and speciation calculations. We show that U(VI) speciation can be determined in carbonate-rich solutions and at ambient temperature by using TRLFS on chemically-treated samples, to remove U(VI)-fluorescence-quenching molecules such as organics.

No U(VI) was detected by TRLFS in the samples collected during the summer period, while the uranyl ion would mainly form calcium carbonate complexes in the winter-collected samples. The relative concentrations of $Ca_2UO_2(CO_3)_3$, $CaUO_2(CO_3)_3^{2-}$, and $UO_2(CO_3)_3^{4-}$ will be discussed according to TRLFS results on synthetic carbonate solutions. These complexes have similar fluorescence features. They are usually hardly detected at ambient temperature by TRLFS equipped with a nanosecond-pulse excitation laser because of their fluorescence in the nanose-

cond time scale. However, we show in the present work that, despite their very short fluorescence lifetimes, U(VI) carbonate species can be quantitatively measured at low concentration by applying a proper signal treatment.

Uranium(VI) Sulfate Complexation as a Function of Temperature and Ionic Strength Studied by TRLFS

Aleš Vetešník[1], Miroslava Semelová[1], Karel Štamberg [2] and Dušan Vopálka [2]

[1]Centre for Radiochemistry and Radiation Chemistry, Faculty of Nuclear Science and Physical Engineering, CTU, Břehová 7, 11519 Prague 1, Czech Republic
[2]Department of Nuclear Chemistry, Faculty of Nuclear Science and Physical Engineering, CTU, Břehová 7, 11519 Prague 1, Czech Republic

Abstract. Time-resolved laser-induced fluorescence spectroscopy (TRLFS) was used to direct study of uranium(VI)-sulfate complexation. By varying sulfate concentration ($4x10^{-4}$ – $7.5x10^{-1}$ M) at fixed pH (= 2), uranium concentration (=$1x10^{-5}$ M) and ionic strength (= 1), we were able to identify, as well as to quantify all relevant uranium-sulfate complexes, at two temperatures (293.15 and 298.15 K). The corresponding stability constants were estimated from the measured species distribution. The estimated stability constants are in relatively good agreement with the values derived from the literature.

Introduction

Time-resolved laser-induced fluorescence spectroscopy (TRLFS) has become widely used to direct studies of uranium (VI) complexation. To optimize the resolving capabilities of our TRLFS setup, a speciation study was performed on the system H_2O - UO_2^{2+} – SO_4^{2-} - $NaClO_4$.

The fluorescence spectra of the sulfate complexes appear to depend on the ionic strength. Although in 0.1 M Na^+ ionic medium the maximum intensity peaks of $UO_2(SO_4)_2^{2-}$ are red-shifted by about 3 nm with respect to UO_2SO_4, in 3 M Na^+ ionic medium the individual spectra of UO_2SO_4, $UO_2(SO_4)_2^{2-}$, $UO_2(SO_4)_3^{4-}$ could not be determined unambiguously (Vercouter et al. 2008). Consequently, in high ionic media, the identification of the uranium-sulfate complexes relies only upon the nonlinear least-squares analysis of the intensity decays. In the range of applied sulfate concentrations, the number of fluorescing complexes extends from three up to six, and each fluorescing complex is characterized by two parameters. For such

number of parameters, the regression problem is highly illconditioned (Petersson and Holmstrom 1997). Even a small systematic error in measured data can lead to unrealistic parameter estimates. It is thus important – in order that the interpretation of measured data be credible - to know which species are present in a solution under given conditions, especially under given temperature.

It is well known from literature that temperature dependence of stability constants, or equilibrium constants generally, is described by the integrated Van´t Hoff expression (equation 1):

$$\log_{10}\beta^0(T) = \log_{10}\beta^0(T_0) + \frac{\Delta_r H_m^0(T_0)}{R\ln 10}\left(\frac{1}{T_0} - \frac{1}{T}\right) \quad (1)$$

where R is the gas constant, $\beta^0(T)$ is the stability constant at temperature T, $\beta^0(T_0)$ is the stability constant at reference temperature T_0 (298.15 K) and $\Delta_r H^0_m(T_0)$ is the molar reaction enthalpy of given complexation reaction (it is assumed that this quantity does not vary with temperature in the range $(T\text{-}T_0)$). The complexation reactions taking place in our system can be generally formulated as follows: $UO_2^{2+} + nSO_4^{2-} \leftrightarrow UO_2(SO_4)_n^{(2-2n)+}$ (n=1,2,3). The values of molar reaction enthalpy for the creation of the first two species, i.e., if n=1 and n=2, can be found in literature (Grenthe et al. 2004), but it does not hold for the third species (n=3). In such a case, the tabulated data of standard molar formation enthalpy, $\Delta_f H^0_m$, characterizing the bonding (formation) of individual reactants, can be used for the calculation of reaction enthalpy. If the values of both types of enthalpies are not available, it is necessary to seek an appropriate system having analogical chemical properties and reaction mechanism and to estimate the missing enthalpy quantity, with the greater or minor accuracy, by the analogy. (The estimation of the value of molar reaction enthalpy for the creation of the third species (n=3) is described in chapter Results.)

Preparation of solutions

Three stock solutions, namely 0.1 M uranyl sulfate, 1 M Na_2SO_4 and 2 M $NaClO_4$ were prepared; in addition, the solutions of approx. 17 M H_2SO_4 and 5 M NaOH were used for adjustment of pH value. All the solutions were prepared by dissolving analytical grade reagents in ultra-pure water (Milli-Q Plus). pH was measured using a glass electrode (Radiometer, combined, GK2401C) and pH-meter (ORION, Model 52A). The electrode was calibrated by means of standard buffers and the pH measurement, with a precision of 0.05 pH, were made: (i) at laboratory temperature, and (ii) at temperature used in the course of fluorescence measurements.

The following sets of working solutions were prepared by mixing of the stock solutions:

a) $1\text{x}10^{-5}$ M U(VI) at pH 2 and ionic strength equal to 1 at different sulfate concentrations ($5\text{x}10^{-4}$ M – $4\text{x}10^{-1}$ M SO_4^{2-});

b) $1x10^{-5}$ M U(VI) at pH 2 and ionic strength equal to 2 at different sulfate concentrations ($5x10^{-4}$ M – $7.5x10^{-1}$ M SO_4^{2-}).

TRLFS measurements

The measurements were carried out in 3.5 ml quartz cell. The sample temperature was maintained constant with a precision of ±0.05 ºC using FLASH 200™ cuvette holder and was monitored independently of cuvette holder thermometer using a ThermoLogR high accuracy thermometer (±0.01 ºC). With the repetition rate of 10 Hz, the sample was excited by 4 ns laser pulses of the wavelength 266 nm and of the energy 12.5 mJ (VIBRANT™ Tunable Laser System). The laser output energy was monitored by a laser energy meter (FieldMaxII-P™). The fluorescence emission perpendicular to the laser beam, was focused by two lenses on the entrance slit of a monochromator (MS257™). The emission spectra were recorded in the 438- 609 nm (600 lines mm^{-1} grating) range using an ICCD camera (Andor iStar), whose logic circuits were synchronized with the laser pulses. This allows the intensifier to be switched on with determined time delay. For each sample, the time delay was varied in the time interval 0.18-124.68 μs in 0.5 μs steps; the intensifier was switched on for 2 μs. The whole system was controlled by a PC.

Data processing

To compensate for the fluctuation of the output energy of the laser system, the intensities of recorded fluorescence spectra were normalized to the respective values of the laser pulse energy as detected by the laser energy meter.

For each sulfate concentration S, the decay of the fluorescence intensity $I_\lambda^S(t)$ was fitted to the multi-exponential model:

$$\tilde{I}_\lambda^S(t_j) = \sum_{i=1}^{N} \alpha_{\lambda,i}^S \exp(-t_j / \tau_i), \tag{2}$$

where the integer N denotes the number of fluorescing species, τ_i is the fluorescence lifetime of the i-th species, and the pre-exponential factor $\alpha^S_{\lambda,i}$ was considered to be proportional to the fractional concentration of the i-th species c^S_i, i.e.

$$\alpha_{\lambda,i}^S = K_{\lambda,i} c_i^S, \quad \sum_{i=1}^{N} c_i^S = 1 \tag{3}$$

Note, that the proportionality constant $K_{\lambda,i}$ was assumed independent of the total sulfate concentration.

A least-squares analysis was applied to test the consistency of the model (equation 2) with the measured data, as well as to optimize the parameter values for the model. In the range of measured fluorescence intensities, the standard deviation of each datapoint can be approximately assumed to be proportional to the square root of the fluorescence intensity. Thus, for each wavelength, the least squares criterion was considered as

$$\chi_\lambda^2 = \sum_{j=1}^{n} \frac{\left[I_\lambda^S(t_j) - \tilde{I}_\lambda^S(t_j)\right]^2}{I_\lambda^S(t_j)} \equiv \sum_{j=1}^{n} [\hat{D}_\lambda^S(t_j)]^2 \tag{4}$$

The goodness-of-fit was judged visually by the examination of the reduced deviation

$$D_{\lambda}^{S}(t_j) = \hat{D}_{\lambda}^{S}(t_j)/(n-p) \tag{5}$$

where n is the number of datapoints and p is the number of parameters. If the model fits the data, then $|D^S_\lambda|$ is randomly distributed around unity. On the other hand, if $|D^S_\lambda|$ exceeds significantly unity, the model is very likely not adequate and it is desirable to increase the number of exponential terms. However, attention should be paid to avoiding the problem of overfitting, i.e. incorporating into the model a systematic error, even of a small amount.

At least five intensity decays at different emission wavelengths were analyzed simultaneously to recover the τ_i values and the $\alpha^S_{\lambda,I}$ values. The uncertainties in the estimated parameters were determined using a support plane analysis (Lakowicz 2006).

With the aim to obtain the values of stability constants, namely, $\beta_1 = [UO_2SO_4]/([UO_2^{2+}].[SO_4^{2-}])$, $\beta_2 = [UO_2(SO_4)_2^{2-}]/([UO_2^{2+}].[SO_4^{2-}]^2)$ and $\beta_3 = [UO_2(SO_4)_3^{4-}]/([UO_2^{2+}].[SO_4^{2-}]^3)$, the Newton-Raphson multidimensional non-linear regression procedure was used for fitting the experimentally determined concentrations of i-th species, c^S_i, as a function of sulfate concentration, S. The goodness-of-fit was evaluated by χ^2 – test and the criterion *WSOS/DF* (weighted sum of squares divided by degrees of freedom) (Herbelin and Westall 1996) was calculated. If $WSOS/DF \leq 20$, then there is a good agreement between experimental and calculated data. In addition, two methods based on Davies equation or Specific Ion Interaction Theory (SIT) were used to the calculation of stability constants for I = 0 and their results were compared. The estimated stability constants are in relatively good agreement with the values derived from the literature.

Results

Calculation of stability constants at different temperatures

The resulting values of stability constants for temperature interval from 10 to 80 ^{0}C and for ionic strength equal to 0 or 1, calculated by means of equation 1 and using the SIT method, can be found in Table 1. It is evident that the influence of temperature on complexation of uranyl with sulfate cannot be neglected: the values of stability constants significantly decrease with decreasing temperature. As for the influence of ionic strength, it is interesting that the values of stability constants of the first two species (UO_2SO_4 and $UO_2(SO_4)_2^{2-}$) are lower for $I = 1$ than those for $I = 0$ (what is expectable), whereas in the case of the third species ($UO_2(SO_4)_3^{4-}$) the opposite is true. Of course, the data are calculated and should be experimentally validated. We hope that such a validation will be obtained in the course of our further study.

Table 1. Molar enthalpies, $\Delta_r H^0_m(T_0)$, and the logarithmic values of stability constants, β_1, β_2 and β_3, calculated at different temperatures, T, and at ionic strength equal to zero and one.

Stability constants:	Log $\beta_1^0(T)$ $I = 0$	Log $\beta_2^0(T)$ $I = 0$	Log $\beta_3^0(T)$ $I = 0$	Log $\beta_1^0(T)$ $I = 1$[e]	Log $\beta_2^0(T)$ $I = 1$[e]	Log $\beta_3^0(T)$ $I = 1$[e]
$\Delta_r H^0_m(T_0)$ [kJ.mol^{-1}]:	19.5 ± 1.6[c]	35.10 ± 1[c]	53.32 [a]	19.5 ± 1.6[c]	35.10± 1[c]	53.32 [a]
T [^{0}C]						
10	2.959	3.814	2.525	1.707	2.562	2.865
20	3.082	4.035	2.861	1.806	2.759	3.201
25[b]	3.140[c]	4.140[c]	3.020[d]	1.851	2.851	3.360
30	3.196	4.241	3.174	1.893	2.938	3.514
40	3.304	4.435	3.467	1.970	3.101	3.807
50	3.404	4.616	3.743	2.037	3.248	4.083
60	3.499	4.786	4.001	2.095	3.382	4.341
80	3.672	5.098	4.475	2.201	3.626	4.815

[a] The value guessed from the analogy with uranylcarbonate complexes (see the text).
[b] The reference temperature. [c] Grente et al. 2004. [d] TDB NEA 2005
[e] The SIT method was used.

When estimating the molar reaction enthalpy for creation of $UO_2(SO_4)_3^{4-}$ (see Table 1, footnote "a"), the analogy between binding (formation enthalpy) of uranyl ($n = 0$), uranylcarbonate ($n = 1,2,3$) and uranylsulfate ($n = 1,2$) species was assumed, namely in such a way, that the guess of molar formation enthalpy of uranyltrisulfate complex was based on this analogy; and because the molar formation enthalpies for uranyl and sulfate were found in literature (Grenthe et al. 2005), the calculation of needed reaction enthalpy, using the well known procedure, was relatively simple.

TRLFS data

We were able to identify, together with the free uranyl UO_2^{2+}, all relevant uranium-sulfate complexes, namely, UO_2SO_4, $UO_2(SO_4)_2^{2-}$, $UO_2(SO_4)_3^{4-}$. The main emission wavelengths of these uranium-sulfate complexes are very similar, except for the emission at about 477 nm, which originates from a different excited state of U(VI) (Fig.1, Table 2). Thus, it was only possible to identify fluorescing species by their lifetimes. The measured lifetimes of UO_2^{2+} and $UO_2(SO_4)_2^{2-}$ fall into the confidence intervals of the respective lifetimes published in (Geipel et al. 1996). On the other hand, the lifetime confidence intervals of $UO_2(SO_4)_2^{2-}$, $UO_2(SO_4)_3^{4-}$ do not overlap with published data (Geipel et al. 1996), they are shifted down by about 0.5 μs (Table 2). This can be attributed to a possible lifetimes sensitivity to experimental conditions used, rather then to any measurement error. The uncertainties in the measured flurescence intensities of the species are

Table 2. Spectroscopic data: Fluorescence lifetimes and main emission wavelengths of free uranyl (UO_2^{2+}) and uranium-sulfate complexes (UO_2SO_4, $UO_2(SO_4)_2^{2-}$, $UO_2(SO_4)_3^{4-}$ at 20ºC.

Species	UO_2^{2+}	UO_2SO_4	$UO_2(SO_4)_2^{2-}$	$UO_2(SO_4)_3^{4-}$
Lifetime (μs)[a]	2.7±0.2	4.2±0.3	8.5±1.0	15±1.5
Lifetime (μs)[b]	2.7±0.3	4.3±0.5	11.0±1.0	18.3±1.0
Main emission wavelength [a]	472-488-510-534-560	477-493-515-539-563	478-493-515-539-563	478-493-515-539-563
Main emission wavelength [c]	471-488-510-534-560[d]	477-493-515-538-565[d]	481-496-518-542-569[d]	477-494-516-539-565

[a] This work. [b] Geipel et al. 1996. [c] Vercouter et al. 2008. [d] 0.1 M Na^+ ionic medium

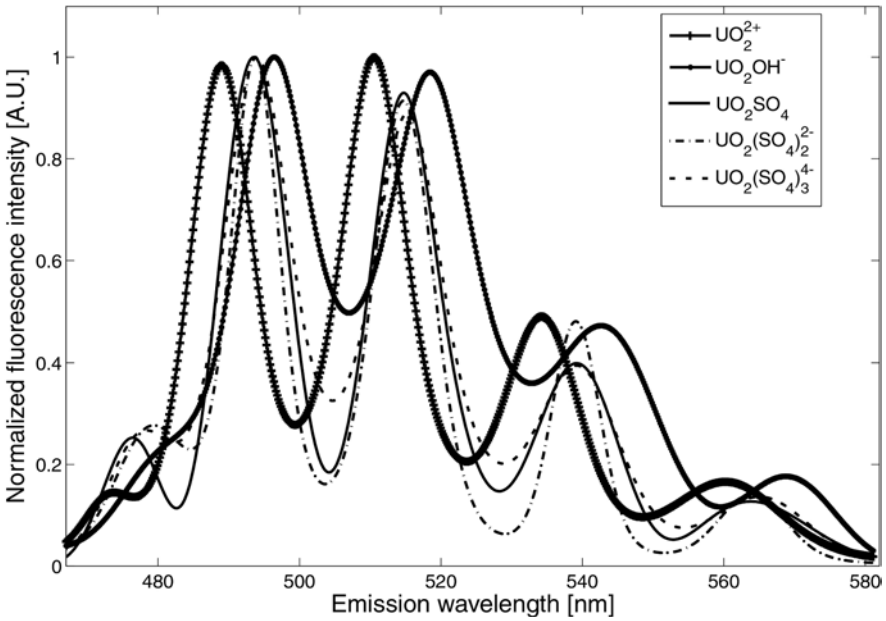

Fig.1. Fluorescence spectrum of free uranyl UO_2^{2+}, uranium-hydroxo complex UO_2OH^+ together with uranium-sulfate complexes (Spectra was not corrected to the wavelength-dependent efficiency of our detection system).

relatively high, up to 20% in the sulfate concentration range of 10^{-2}-10^{-1} M SO_4^{2-} (Fig. 2A).

The calculation of stability constants

The experimental results, illustrated in Fig. 2 B,C for T = 20 ^{0}C, were fitted in the way described above and the values of stability constants and of the criterion *WSOS/DF* were obtained (see Table 3). As for the *WSOS/DF*, the higher values than 20, especially for T = 20 ^{0}C, obtained in our case reflected the relatively high

experimental error (approx. ± 20 %) of determination of the species concentrations.

From Table 3 we see that the experimentally obtained values of stability constants, i.e. at $I = 1$, well correspond with the calculated data in Table 1, namely in that these values increase in the sequence: $\beta_1 - \beta_2 - \beta_3$. As for the conversion to zero ionic strength, the SIT and Davies methods lead to similar values of constants

Table 3. Logarithmic values of stability constants, β_1, β_2 and β_3, experimentally determined at different temperatures, T, and at ionic strength equal to one. The values for $I = 0$ were obtained by conversion of experimental data ($I = 1$) using SIT method and Davies equation

Stability constants	Log $\beta_1^0(T)$	Log $\beta_2^0(T)$	Log $\beta_3^0(T)$	Log $\beta_1^0(T)$	Log $\beta_2^0(T)$	Log $\beta_3^0(T)$
T [^{0}C]		20			25	
$I = 1$ (exper. data)	1.90	3.33	4.47	2.32	3.75	4.11
$I = 0$ SIT	3.18	4.61	4.13	3.61	5.04	3.77
$I = 0$ Davies eq.	3.07	4.40	4.47	3.49	4.82	4.11
WSOS/DF		30.50			23.60	

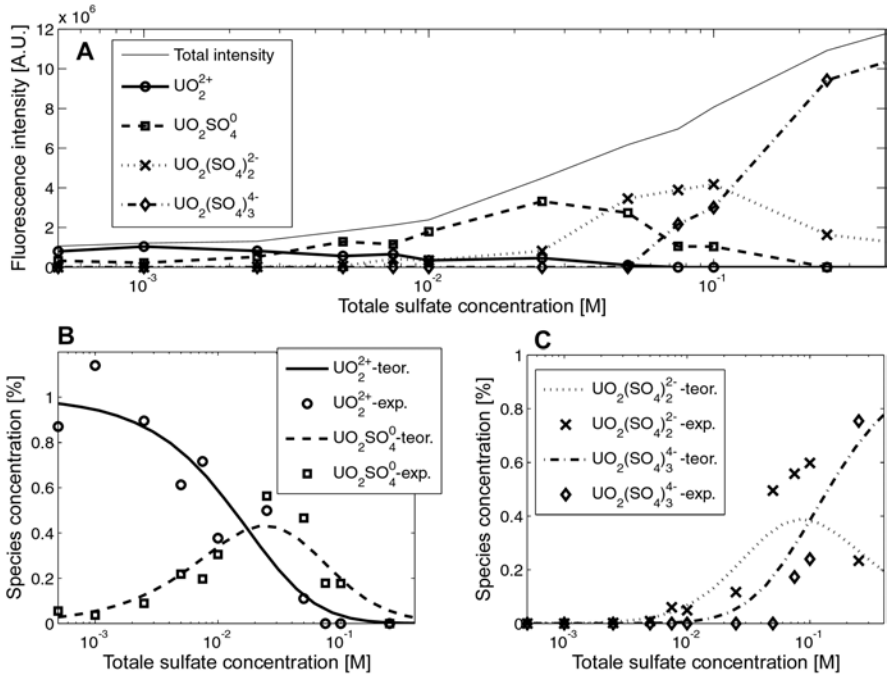

Fig.2. Distribution of uranium-sulfate complexes as a function of the total sulfate concentration. **A**: measured fluorescence intensities; **B** and **C**: calculated species concentration.

for uranylsulfate and uranyldisulfate; in the case of uranyltrisulfate, the values of β_3 obtained by these methods are significantly different.

Conclusion

TRLFS has been applied with some problems to the speciation study of the system H_2O - UO_2^{2+} – SO_4^{2-} - $NaClO_4$ at two temperatures and for I = 1. Studies for temperature range approx. from 30 to 70 ^{0}C and for ionic strength equal to 2 are under progress.

References

Geipel G et al. (1996) Uranium (VI) sulfate complexation studied by time-resolved laser-induced fluorescence spectroscopy (TRLFS). Radiochimica Acta 75: 199-204

Grenthe I et al. (2004) Chemical thermodynamics of uranium. NEA OECD, Paris France

Herbelin A L, Westall J C (1996) FITEQL-A computer programm for determination of chemical equilibrium constants from experimental data, Version 3.2. Report 96-01. Corvallis, Oregon : Department of Chemistry, Oregon State University

Lakowicz J R (2006) Principles of Fluorescence Spectroscopy. Third Edition. Springer, Singapore

Petersson J and Holmstrom K (1997) A review of the parameter estimation problem of fitting positive exponential sums to empirical data. Technical Report IMa-TOM-1997-08, Malardalen University, Sweden

TDB NEA (2005) Thermochemical Database (TDB) Project. http://www.nea.fr/html/dbtdb/

Vercouter T et al. (2008) Stoichiometries and thermodynamic stabilities for aqueous sulfate complexes of U(VI). Inorg Chem. 47 : 2180-2189

Preliminary study of interaction between tailing and the hydrologic cycle at a uranium mine near Tatanagar, India

S.K. Sharma

24 National Road, Dehradun 248001, India E-mail: SKS105@rediffmail.com

Abstract. The tailing piles at the mine near Tatanagar were leached by water from the nearby geothermal springs present in Hazaribagh area in Jharkhand where few radioactive hot springs are reported. Water percolating through the tailing was found to be seriously contaminated by high levels of radium of the order of 7 to 9 ppm. A study has been undertaken in order to investigate the interaction of the tailing with the hydrological cycle. The results show that groundwater is present within the tailing pile and that this water has a high electrical conductivity compared with the groundwater of the adjacent natural area. When the groundwater from the tailings reached the external environment or mixes with the natural groundwater, serous environmental impacts occurred.

Introduction

In India, progress and pollution come as a package deal. Though, nuclear energy is the cleanest source of power, no soot, smoke or green house gases. And, if the safety norms are strictly adhered to, there will be insignificant fractional increase of back-ground radiation either in the operating area or outside the power plants. Located near Tatanagar in the Sighbhum district of Jharkhand State, the uranium for the country's nuclear program is mined here from three underground mines up to a depth of 700m below the earth's surface. The nuclear waste which is called "tailings" or "uranium tailing" comes from the mines and mills as a waste after the uranium ore is mined and processed for purification and it is then dumped in the tailing ponds. The poisonous nuclear waste has the potential to cause unimaginable damage to the surroundings specially where the water table is low in the area and surface water flows through it. The devastating effects caused to local people due to uranium mining and the interaction of tailings with groundwater at uranium

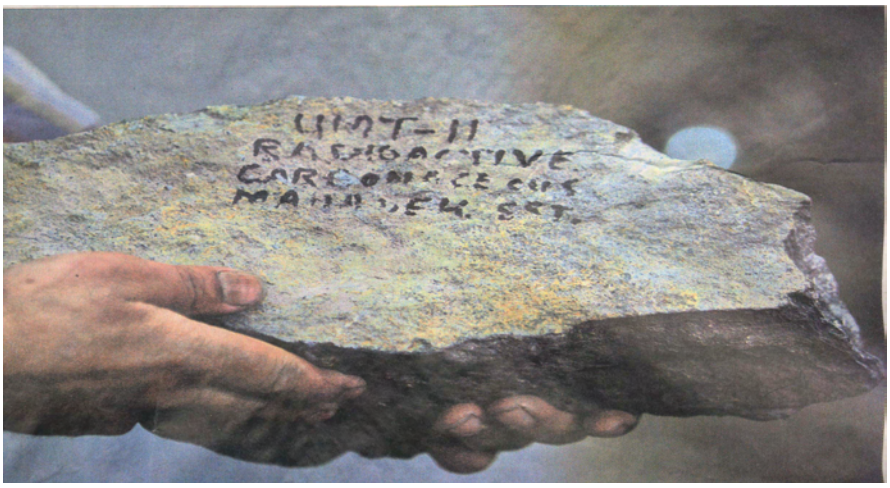

Fig.1. Mined Uranium ore (Uraninite) for retrieving the rare uranium

mine near Tatanager in Jharkhand State has been investigated where local people are fighting this invisible enemy. The following Fig 1 shows the mined Uranium ore (Uraninite) near Tatanagar for retrieving the rare uranium.

Brief geology and geothermal history of the area

The exposed rocks in southern Bihar show two facie, an un-metamorphosed one in the south and a metamorphosed one in the north, separated by a major thrust zone of 2 to 5 km wide and is bordered on its north and south by well marked shearing. The rocks within the thrust zone are metamorphosed shales and sandy shales with subordinate metavolcanics such as chlorite schist, amphibole schists etc. Near the northern border of the zone are bands of quartz – mica – schist with tourmaline and kyanite. It is postulated that the mineralization took place in three stages. The earliest was the formation of apatite – magnetite lenses, followed by the bands of chlorite and amphibole -schist. Uranium mineralization is noticed in the form of disseminated uraninite, torbernite and autunite along the chlorite schist. Workable grade of uranium bearing ore, mounting to a few million tons are present and mined from the uranium mines near Tatanagar in Jharkhand. There are many thermal springs near Tatanager area, in southern Bihar indicated by “triangles” at Jharia and Surajkund. in the following Fig 2 (Ravishankar, et al. 1991).

The following Fig. 3 shows that these springs are flowing over the crystalline and metamorphic (Archaean and Proterozoic age) rocks represented by "d" and the thermal springs are shown by +79 etc (Prasad, 1996).

Data collection at tailing pond

The chemical composition and radium concentration of thermal water has been collected from one of the tailing ponds, Figure 4, near Tatanagar and has been summarized in Table 1.

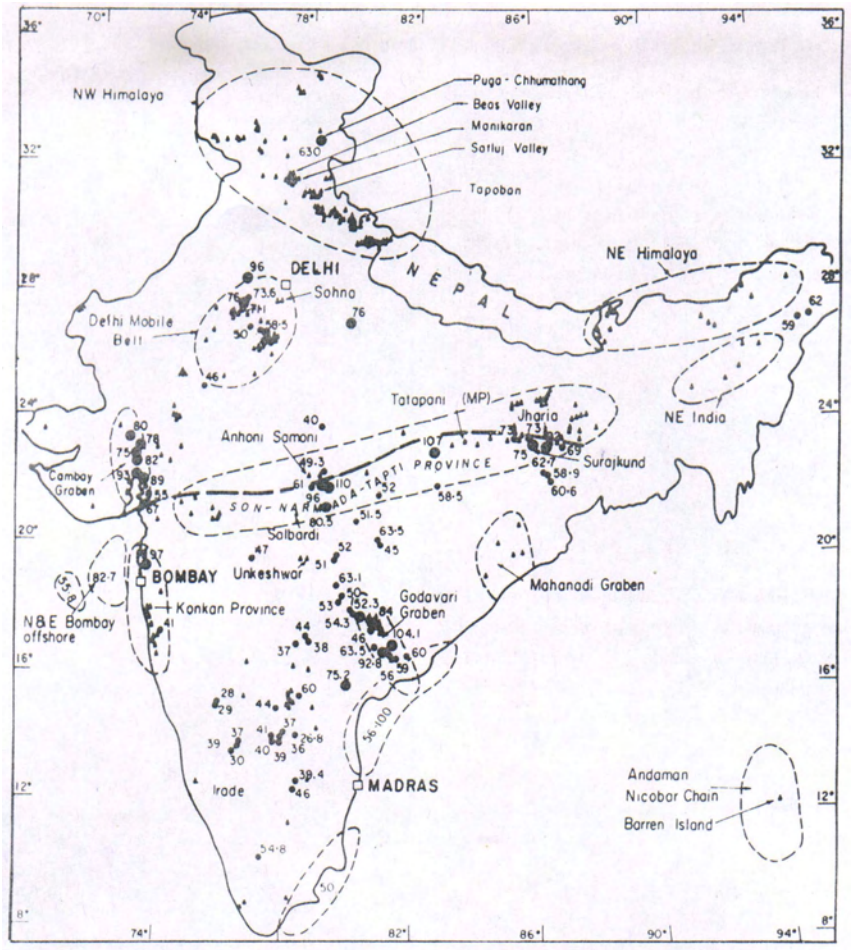

Fig.2. Geothermal provinces of India (after GSI, 1991).

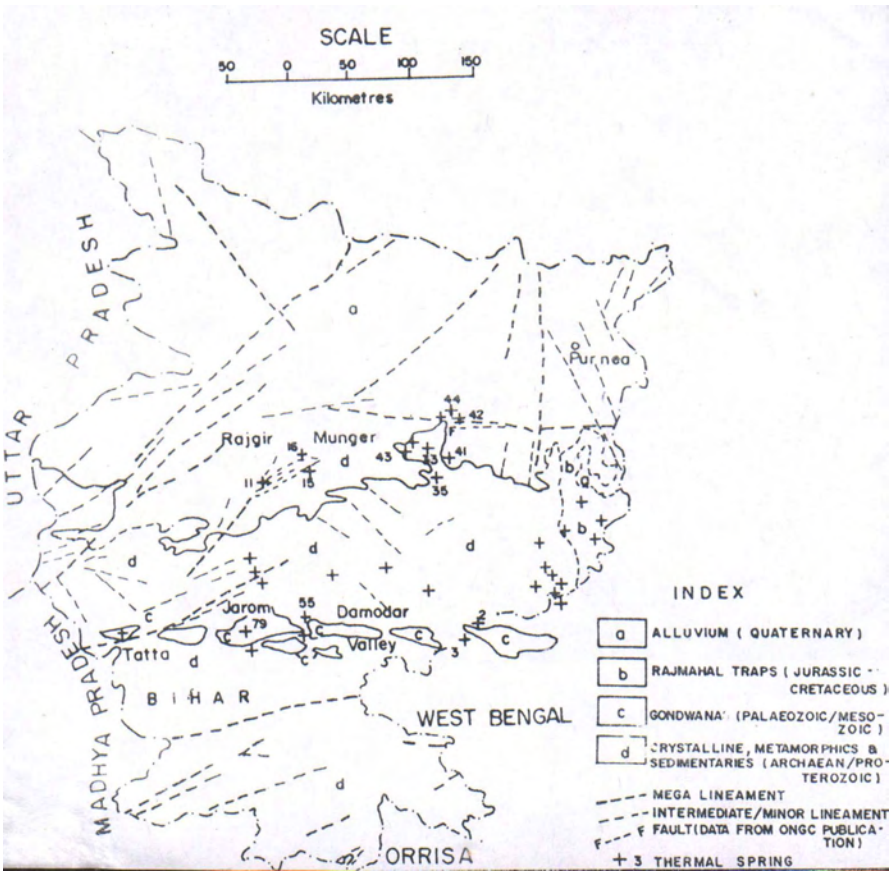

Fig.3. Thermal springs around Tatanagar (after GSI, 1996).

Table 1. Chemical composition and radium concentration of thermal water.

1	pH	>9
2	TDS	520 ppm
3	F	21 ppm
4	Ca	2.8 ppm
5	Mg	0.3 ppm
6	Na	150 ppm
7	K	6.5 ppm
8	Cl	90 ppm
9	SiO_2	110 ppm
10	Radium	7 to 9 ppm

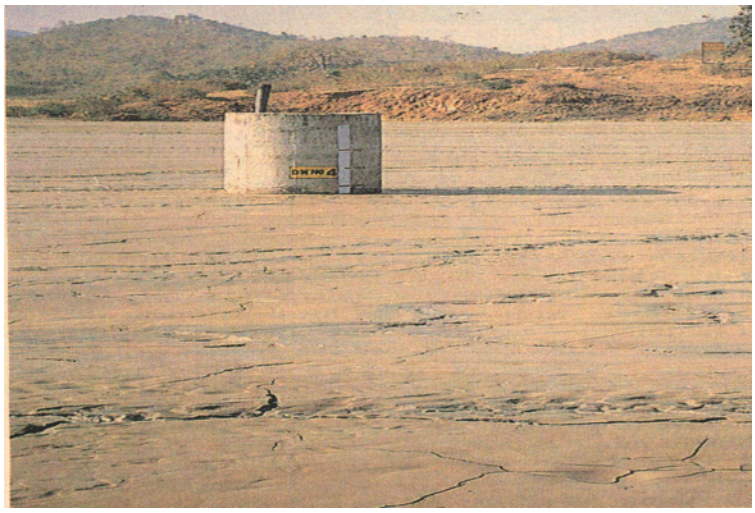

Fig.4. One of the tailing ponds to store nuclear waste (after SOE, 2001).

The following Fig 5 shows the surface water is being contaminated with the radio-active waste sediments /dust. The data collected from the local residents reveals that the water in wells and small tributaries (locally called 'nallas') has become black, and sometimes the water tastes salty, soap does not produce enough foam and the cloths remain unclean.

According to the Uranium Corporation of India Limited (UCIL) policy which is the Government agency responsible for ensuring the safety of uranium mining sites, the local habitants and the environment in India, all villages within five kilometers of the mine and tailing ponds should be evacuated but the settlement is found well within 100 to 200m thus putting the residents at a great health risk.

Interpretation

It is observed that the contents of the tailing ponds are highly radio-active, even though uranium has been extracted but the ponds / tailings remains radio-active for a very long time. Radio-active tailings have permeated the groundwater and contaminated surface water sources. The thermal spring water coming in contact with these tailing also becomes radio-active and the concentration of radium of the order of 7 to 9 ppm in these waters becomes an invisible enemy. Local habitants suffer from fatigue, lack of appetite, respiratory ailment, infant mortality, skeletal deformities such as fused fingers, skin disease, leukemia, thalassemia and even Parkinson's disease have been reported (Bhatia, 2001).

The radium values in thermal waters varying from 7 to 9 ppm from the tailing pond can be compared with that of Karia of Portugal.

Fig.5. Rain water washing away the sediments at uranium mine.

Conclusions

When the contaminated was seen to be reaching the external natural environment, the mining authorities decided to collect and pump the water for neutralization. The study described here aimed to investigate possibility that infiltrated rainwater and natural runoff are reaching the tailing pond material where they form new groundwater in contact with the tailing materials. Radium salts have clearly been dissolved and, in the future this contaminated groundwater will reach the natural hydrological cycle. The purpose of this study was to evaluate the interaction between the tailing materials and the hydrological cycle. The tailings were leached by the groundwater, thermal springs or the rainwater and the outflows of water was found to be seriously contaminated by high levels of radium, of the order of 7 to 9 ppm. The local people are poor in the region and are entirely dependant on this radio-active contaminated water available to them for agriculture and their day to day domestic activities. They have less awareness of radiation and its ill-effects and thus, are subjected to variety of diseases.

Recommendations

The high potential for pollution by dissolution of toxic salts inside the tailing ponds suggests that planning for environmental control should include the best possible dealing of substratum before tailing are deposited. Moreover, no settlement be permitted within five kilometers of the uranium mine to safeguard the health of local habitants.

Acknowledgements

The author thanks to the team of the Geological Survey of India for fruitful discussions and valuable suggestions to complete this write up.

References

Bhatia, B (2001) Fighting and invisible enemy. The Hindu Survey of the Environment:129-135 ppPrasad, J.M (1996) Geothermal energy resources of Bihar, Geothermal Energy in India,GSI. Spl. Pub. No 45 : 99-117pp.

Ravishankar, Guha S.K., Seth, N.N, Muthuraman,K., Pitale, U.L., and Sinha, R.K (1991) Geothermal Atlas of India. Special Publication No. 19, Geol.Sur. Ind : 144 pp.


Uranium Mining
and Hydrogeology

The distribution of uranium in groundwater in the Bushmanland and Namaqualand areas, Northern Cape Province, South Africa

Nicolene van Wyk and Henk Coetzee

Council for Geoscience, Private Bag X112, Pretoria, 0001, nvanwyk@geoscience.org.za

Abstract. Several research projects looking at naturally occurring uranium have been undertaken in the Bushmanland and Namaqualand areas since a water sampling program undertaken in the 1980s highlighted a uranium anomaly in groundwater. In some areas within the region, the host rocks have elevated levels of uranium; however near sampled boreholes with elevated uranium concentrations in groundwater, the concentrations in the rocks are relatively low. Predictive models have shown no correlation between uranium levels in rocks and in groundwater in this region. Elevated levels of uranium in drinking water and its health effects formed the basis of this study.

Introduction

The Bushmanland and Namaqualand areas are semi-arid, water-stressed and receive low rainfall of 80 – 100 mm per annum. High temperatures and high evaporation rates (approximately 3200mm per annum) are also experienced. Fig.1 indicates the location of the study area. The farmers and local communities are solely dependant on groundwater for drinking, domestic use and livestock watering. In the event of rainfall water is stored in tanks for drinking purposes. Due to the harsh climate no food crops are grown in the sampled area and only livestock, mainly sheep, are reared.

Previous studies undertaken by various South African researchers have highlighted the occurrence of naturally occurring uranium in the groundwater at Bushmanland and Namaqualand areas.

Previous research

Anomalous uranium concentrations in groundwater were identified during a routine regional water-sampling program performed by the Atomic Energy Corporation (AEC) in the 1980's in the Bushmanland and Namaqualand areas (Toens, 1999). Other researchers have studied this anomaly for various reasons. The Council for Geoscience (CGS) and Swedish Geological AB undertook a project in 2005 to "calibrate and verify a predictive model for the incidence of naturally occurring hazardous trace constituents in groundwater". This predictive model indicates that there is no clear correlation between the elevated levels of uranium in the rocks and the groundwater.

During 2007 the CGS undertook a project focusing on naturally occurring elements in groundwater and their potential effects on human health. The anomalous uranium occurrence was chosen as one of the two elements of interest for the study. This study focused on the exposure pathways and exposure rates of uranium to humans and animals. The study also highlighted the distribution of uranium in different geological formations with no uranium mineralization. This paper presents the uranium concentrations collected during 1981, 2005 and 2007 and the distribution thereof.

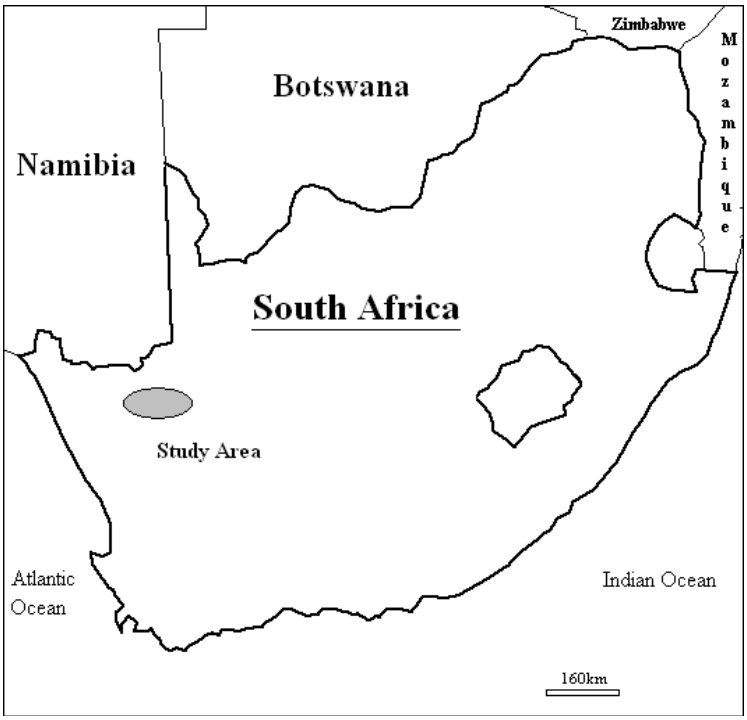

Fig.1. The location of the study area.

Sampling

The sampling sites for the 2007 sampling campaign were selected using the AEC 1981 and the CGS 2005 databases. Boreholes with the elevated uranium concentrations were resampled in 2007. The sampling sites are farms to the south, southeast and southwest of the town Pofadder. Pofadder is a small town which acts as a regional business centre for the farms surrounding it. The town itself is supplied with drinking water from the Orange River.

The sampled boreholes are constantly in use and supply the individual farms with drinking water, water for other domestic uses and livestock watering. The boreholes are equipped with windpumps and samples were collected at the windpumps. Sampling water which had run through longer lengths of pipe was avoided where possible. pH, electrical conductivity and temperature were measured and recorded in the field at the time of sampling.

Twenty samples were collected according to CGS sampling procedures (van Wyk, 2006). Three 100ml samples were collected at each site, one of which was filtered through a 0.45µm filter and acidified with nitric acid for metal analysis, another was filtered for anion analysis and the remaining sample was not filtered to be used for total alkalinity analysis.

The samples were submitted to and analysed by the Council for Geoscience Laboratory by ion chromatography for anions, ICP-MS for metals and spectrophotometry for alkalinity. Radionuclide analyses were not performed on any of the samples in this or the previous studies.

Results and discussion

The concentration of uranium in the groundwater at all of the sampled boreholes exceeds the World Health Organization (2005) drinking water guideline of 0.015mg/l for all samples collected in the current study and most in the previous studies. It is important to note that this guideline is based on the chemical toxicity of uranium and is therefore not affected by disequilibrium between uranium and its radioactive progeny. This guideline was used to compile a risk assessment in terms of the exposure of uranium to human and animals and the health effects thereof. The fact that measured concentrations exceed the WHO guideline indicates a definite hazard and suggests that follow-up and/or remedial action is required. The ingestion of uranium through drinking water is potentially harmful to the bones and kidneys in humans (Selinus *et al*, 2005). Toens *et al.* (1999) report a positive correlation between the elevated levels of uranium in groundwater and atypical lymphocyte counts, as well as noting a reported high rate of heamatological anomalies related to leukemia in the study area.

Table 1 presents the uranium concentrations from 1981, 2005 and 2007.

Table 1. The uranium concentrations 1981, 2005 and 2007 (all concentrations presented in mg/l).

No.	Farm Name	Uranium (1981 study)	Uranium (2005 study)	Uranium (2007 study)
1	De Neus	0.175	*	0.114
2	Grappies	0.229	*	0.266
3	Hartebeesvlei	0.235	*	0.071
4	HouMoed I	0.056	0.05	*
5	HouMoed	*	*	0.053
6	Onder Houmoed	*	0.06	*
7	Kalkvlei	0.17	*	0.063
8	Kouberg I	0.052	*	*
9	Kouberg II	0.034	0.01	*
10	Lucas Vlakte I	0.182	*	*
11	Lucas Vlakte II	*	*	0.013
12	Lucasvlei Vlakte	0.112	*	*
13	Middelputs I	0.048	*	*
14	Middelputs II	*	0.05	*
15	Middelputs III	*	*	0.064
16	Millerton	0.097	*	*
17	Naroegas I	0.075	*	*
18	Naroegas II	*	0.13	*
19	Neelsvlei I	0.034	*	0.137
20	Neelsvlei II	*	0.05	0.050
21	Neelsvlei III	*	*	0.056
22	Nousees	0.036	*	0.055
23	Nuwedam	0.062	*	0.060
24	Pof Dorp	0.0178	*	0.062
25	Rooiduin	0.05	0.06	*
26	Spieël Pan	0.484	*	0.478
27	Spitsberg	0.116	0.10	*
28	Suurwater	0.024	0.01	*
29	Uitkyk	0.034	0.05	*
30	Valsvlei	0.361	*	0.375
31	van Tittens Vlei	0.169	*	0.167
32	Van Tiddensville II	*	*	0.160
33	Velskoen	0.0178	0.01	*
34	Volmoed I	0.393	*	0.110
35	Volmoed II	*	*	0.117
36	Willem se opdam	0.132	*	0.129

* No data available for that particular year

The distribution of uranium

The highest concentrations of uranium in the groundwater occur in the Quaternary sediments to the east/southeast of Pofadder. The predictive model by Tarras-

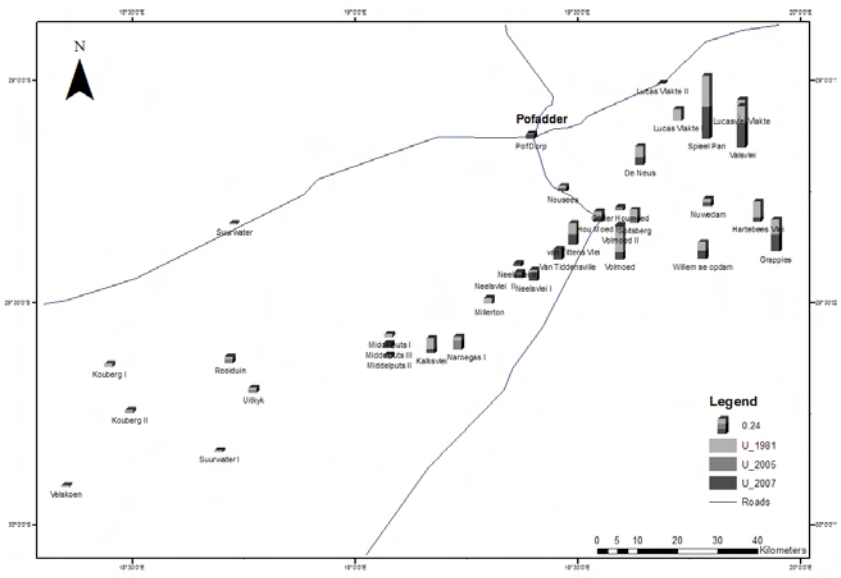

Fig.2. The sampling locations, the height of the stack indicates the uranium concentration.

Wahlberg et al. (in press) however indicates that no clear correlation exist between uranium levels in rocks and the elevated concentrations in the groundwater.

Fig. 2 illustrates the spatial distribution pattern of uranium in the groundwater of the area in all three studies. The height of the stacks indicates the uranium concentrations. In Fig.2 a trend or pattern can be observed. The pattern is an axis that lies east to southwest and the concentrations gradually decrease from east to southwest.

Conclusions

Groundwater is the main source for drinking, domestic use and livestock watering on the farms in the study area. Since the uranium concentration exceeds the WHO 2005 guideline at all the boreholes sampled excepting one, the exposure of humans and animals to the potentially harmful water containing uranium is therefore certain by ingestion.

The anomalous uranium concentrations exist on a northeast-southwest trend, decreasing towards the southwest. Other models have shown that there is no clear correlation between the elevated levels of uranium in the rock and in the groundwater, making it impossible to reliably predict uranium concentrations in the groundwater using geological information. A comprehensive programme of borehole sampling is therefore required to quantify the risk to the public with confidence and to develop and implement a management plan to address this problem.

Recommendations

Alternative water sources should be explored such as pipelines from the Orange River towards the north of Pofadder, the collection of rain water and the use of water purification methods for drinking water on remote farms. The radiological risk due to the use of this water was not assessed and this should be addressed, as well as possible risks due to bioaccumulation, particularly where groundwater is used for stock watering.

Acknowledgements

We would like to acknowledge:

The friendly farmers in the Bushmanland and Namaqualand area for the access to the boreholes

J.S. Venter for the assistance with the fieldwork and the generation of maps

The AEC/NECSA for the 1981 water quality data

The CGS and Swedish geological for the 2005 data

The CGS laboratory for the analysis

The Environmental Geoscience Unit, CGS for the funding for the project

References

Tarras-Wahlberg, H., Wade, P., Coetzee, H., Chaplin, S., Holmström, P., Lundgren, T., van Wyk, N., Ntsume, G., Venter, J and Sami, K. (in prep) Project to calibrate and verify a predictive model for the incidence of naturally occurring hazardous trace constituents in groundwater: FIELD SAMPLING, LEACHING TESTS, GEOCHEMICAL MODELLING AND GROUNDWATER POLICY IMPLICATIONS. Water Research Commission. 196pp

Sami, K, and A L Druzinski (2003) Predicted Spatial Distribution of Naturally occurring Arsenic, Selenium and Uranium in Groundwater in South Africa - Reconnaissance survey, Water Research Commission, Pretoria, WRC Report No. 1236/1/03, 84pp.

Selinus O, A.B., Centeno JA, Finkelman R, Fuge R, Lindh U, Smedley P Essentials of Medical Geology. Impacts of the natural environment on public health, ed. O. Selenus. 2005: Elsevier

Toens, P.D., W Stadler, and N.J. Wullschleger. (1999) The association of groundwater chemistry and geology with atypical lymphocytes (as a biological indicator) in the Pofadder area, North Western Cape, South Africa. Pretoria: Water Research Commission.

van Wyk, N.(2006) Surface water sampling procedure. Report 2006-0199, Council for Geoscience: Pretoria. 12pp.

World Health Organisation (2005) Uranium in Drinking Water - Background document for development of WHO Guidelines for Drinking-water Quality, World Health Organisation, WHO/SDE/WSH/03.04/118, 26pporld Health

Uranium minerals of Bukulja mountain controls on storage reservoir water

Zoran Nikić[1], Jovan Kovačević[2] and Petar Papić[3]

[1]Faculty of Foresty, University of Belgrade, 11030 Belgrade, Kneza Višeslava 1, Serbia. E-mail: znikic@yubc.net
[2]Geological Institute of Serbia, 11000 Belgrade, Rovinjska 12, Serbia
[3]Faculty of Mining and Geology, University of Belgrade, 11000 Belgrade, Djušina 7, Serbia

Abstract. Headwaters of the Bukulja stream on southern slope of Bukulja Mountain were confined in 1976 by the Garaši Dam for water supply to Aranđelovac and nearby communities. Geological explorations from 1949 detected several uranium occurrences on Bukulja Mt. and later identified uranium mineral deposits. This work considers the trend of total beta-particles radioactivity in the Garaši storage reservoir for the period 1991-2004. Samples for radioactivity analyses were collected from three depth levels near the dam: directly below the lake surface, at the lake mid-depth and above the lake bottom. A highly plausible assumption is that the rising trend of total beta radioactivity in Garaši lake water is genetically associated with the geological nature of the terrain.

Introduction

The Garaši Dam is located some sixty kilometers south of Belgrade in Šumadija, central Serbia. Constructed in 1976 on the Bukulja stream, the dam confined water for water supply to Aranđelovac and nearby communities. The Bukulja stream is a left tributary of the Ljig River that flows into the Kolubara, a river of the Black Sea drainage system. The artificial storage lake has a catchment area of 21.6 km^2 on southern slopes of Bukulja Mountain.

There are no industrial, tourist or military structures in the catchment. Intermittent geological investigations from 1949 revealed several occurrences and deposits of uranium minerals on Bukulja. This suggests that natural geological factors in the catchment over a sufficiently long period may affect water in the artificial lake.

An analysis of total radioactivity of beta particles in water of the Garaši storage in the observation period from 1991 to 2004 was correlated with the uranium occurrences and deposits in the dam catchment. The resulting data were the grounds on which we based the recommendations in the Conclusion.

Study

The only use intended for the Garaši Dam was the drinking water supply. Pumped from the lake water is conducted to a purification plant and there from distributed to consumers. The dam is located at Garaši, directly after the confluence of the Velika Bukulja and the Mala Bukulja streams. The dam is a rockfill embankment with reinforced-concrete face and a vertical central clay-core. Its length at crest is 390 m, height 35 m, and storage volume of the lake at max water level 296.5 m above datum is 6,270,000 m^3.

Subject

Southern slopes of Bukulja are drained into the storage lake. Elevation of the highest Bukulja point is 696 m. Average mean amounts of precipitation in Bukulja perimeter for the period 1980-2003 ranged from 750 mm to 890 mm. Around 55% of the storage perimeter is under forest.

Nuclear mineral deposits identified on Bukulja are of economic interest. The mineralized area of Bukulja is complex in structure and geology. It belongs to the Šumadian metallogenic region, the Serbian-Macedonian metallogenic province. Uranium minerals of Bukulja are classified (Jelenković 1991) into two groups:

Group I: Endogenic uranium minerals are spatially and genetically associated with granitic rocks of Bukulja. These are low-temperature hydrothermal lithogene (lateral secretion) deposits and uranium minerals in pegmatites.

Group II: Exogenic uranium infiltration minerals in the Neogene Belanovica Basin. These minerals formed and deposited in clastic sediments (sandstones and conglomerates with infrequent coaly interbeds).

Mineralogical examinations in 1950s of sediments carried by the Velika Bukulja indicated almost all minerals, petrographic constituents of Bukulja Mountain (Višić 1961). Nevertheless, a rockfill dam was constructed in 1976 immediately downstream of the Mala Bukulja and the Velika Bukulja confluence to impound water for municipal water supply.

Dams for water supply are generally built in high mountains, in the source areas of rivers, foremostly to avoid pollution by human activities. Running stream or river water is not always of the drinking water quality after it has been stored behind a dam (Nikić 1997). A dam constructed to form an artificial lake drastically changes the natural flow of the retained stream. Incapable of carrying stream load over the dam it deposits sediments in the lake. Composition of fine sediment in the lake depends on the composition of rocks in the catchment. Additionally to

reducing physically the useful storage of the lake, sediments develop chemical reactions and biological processes that affect the quality of lake water. The problem is even more complicated if there are metallic, or energy-producing or nuclear mineral deposits in the catchment.

Methods

Hydrometeorological Institute of Serbia is the agency that monitors water quality in the Garaši storage from 1991 under provisions of the Water Law and the Systematic Water Quality Control Act of the Serbian Government. Water monitoring results are published in the Hydrological Yearbook, which was a source of information for the present analysis of total beta-particle radioactivity in the Garaši storage water.

Monitoring for the Garaši storage consisted of water sampling for physical and chemical analyses. Samples were collected from three lake depths: directly below the surface, mid-depth and immediately above the bottom. Lake depth at the dam was between 20 m and 22 m. Within the study period 1991-2004, one series of analyses was performed, mostly in the summer (June-October) every year, excluding 1999 (war hostilities), and 1994 and 2000. For the same period of study, different analytical methods were employed to determine total radioactivity of beta particles in the lake water. The methods used and the obtained information allow certain inferences.

We checked the Hydrological Yearbooks information on each analyzed element, interpreted and graphically presented, and discussed the total beta radioactivity trend for the period 1991-2004.

Available sources of information were used to analyze geological setting of the catchment before new geological and hydrogeological reconnaissance of the terrain.

Results and discussion

Uranium occurrences and deposits

This presentation of uranium minerals on Bukulja Mountain is based on both published and unpublished documentation funds and on field reconnaissance data. Lithologic units that build up the topographical catchment of the Garaši lake (Fig. 1) are: alluvium (al) around 6 %, diluvium-proluvium (dpr) around 5 %, sands, clays, gravels, sandstones and coarse conglomerates (M_3^1) some 15 %, slate clay, metasandstone (F) around 27 %, and granite monzonite (γδ) about 47 % of the catchment area.

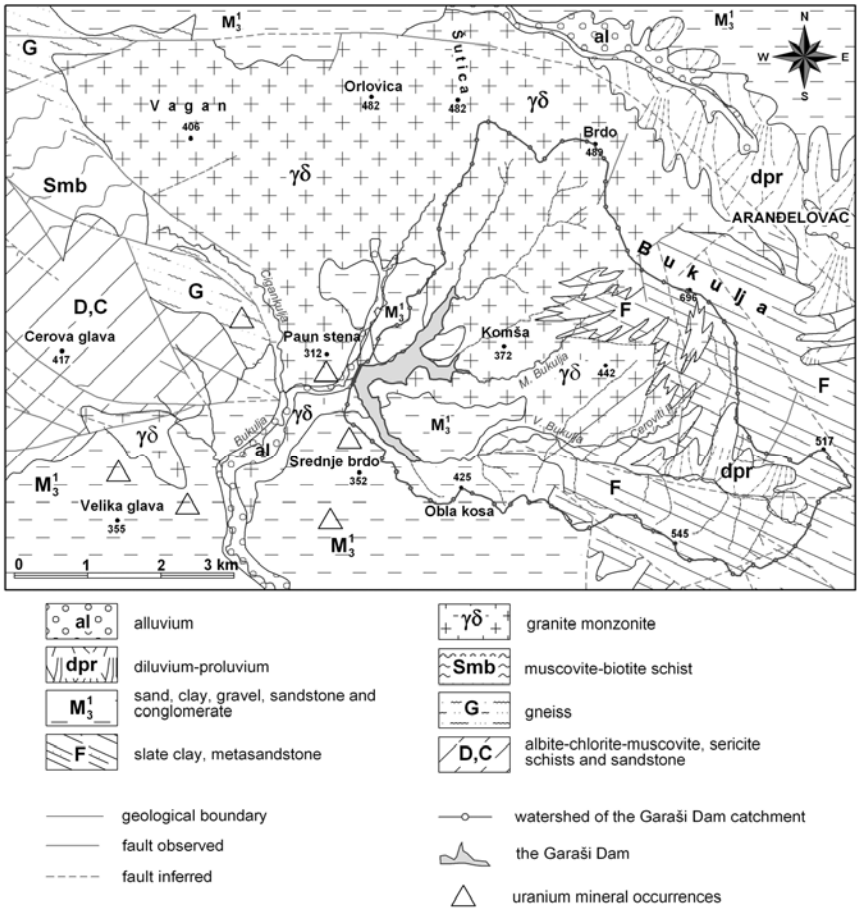

Fig. 1. Geological Map of the Garaši Dam catchment perimeter (Filipović et al. 1978; Brković et al. 1980; revised).

Uranium in granitic rocks of Bukulja

Almost half (47%) of the Garaši topographical catchment is composed of granitoid rocks of Bukulja (Fig. 1). The granitoid massif of Bukulja irrupted during the Miocene into a series of Upper Cretaceous sedimentary rocks and metamorphosed them to a high grade at the contact (Brković et al. 1980). The massif extends in the east-west direction. Its extreme southern outcrops in the Paun Stena area are located some 750 m downstream of the Garaši Dam (Fig. 1).

The granitoid massif of Bukulja is largely composed of granitic biotite and biotite-muscovite monzonite, except in the southwest where it includes granite porphyry. Essential mineral constituents of the massif are quartz, andesine, potassium feldspar, biotite and muscovite, and accessory minerals are tourmaline, zircon,

apatite and magnetite. Vein-rock constituents are pegmatite, aplite and aplopegmatite found either in the granitoid massif itself or in contact rocks of its envelope. The vein rocks consist of muscovite, plagioclase, tourmaline and biotite (Brković et al. 1980; Filipović et al. 1978).

Occurrences of uranium were detected in the late 1950s in several locations of Bukulja (Paun Stena, Milan Stream, Cigankulja, Podgroblje and some others). The mineral occurs in uraniferous bodies along fault zones, in intervals of varied thickness from tens of centimetres to over one metre. The identified uranium minerals are pitchblende, sooty pitchblende, autunite and coffinite (Jelenković 1991). Uranium minerals occur in dispersed concentrations, incrustations or coatings along mylonitised and cataclastic zones within the hydrothermally altered granitic rocks. The amount of uranium in granitic rocks of Bukulja is 4.31 ppm (Omaljev, 1983), and uranium concentration at ground surface in Paun Stena ore zone is 566 g/t (Rončević et al. 1990).

Uranium found in pegmatite surrounding the granitoid massif is uneven dispersions in the host rocks of quartz-tourmaline association. It forms irregular grains. The crystals vary in size from tens of microns to 2 mm (Višić 1961; Radusinović 1963). Uranium concentrations in 59 samples of groundwater from granitoid rocks (measured in 1976) varied from 0.1 to 151.7 μg/L; radioactivity (Ra) varied from 0.06 to 2.625 Bq/L and Rn from 1.48 to 440 Bq/L (Pokrajac 1977).

The 1991 hydrogeological investigations in Bukulja granitoid massif registered several anomalous sites. Water-contained uranium amounted to 85 μg/L in Orlovica-Šutica area, northern part of the massif (Protić 1993). In the western, Vagan area of the massif, radon concentration was less than 400 Bq/L in dominantly hydrocarbonate water of 210-979 mg/L mineral content. Radon concentrations were anomalous in a spring of the Ceroviti stream in the Garaši Dam catchment, then in the Hajdučica spring north of Vagan peak and in test well BC 3/89 in the Cigankulja Brook. Radon concentrations are variable with the time, but generally approximate 1000 Bq/L for the Ceroviti stream, less than 1445 Bq/L for Hajdučica spring and less than 1237 Bq/L for BC 3/89. The uranium concentration measure was the highest (1300 μg/L) in water from an adit in Paun Stena, the water type was SO_4-Ca,Mg, different from any surrounding groundwater (Protić 1993).

Granitic rocks of Bukulja have deeply altered. Groundwater in these rocks reacts chemically with rocks and with organic material in the soil. Except where bonded in crystal lattice and in resistant minerals, uranium is known to leach from rock during weathering processes. Chemical decomposition of minerals is far more intensive in the presence of free CO_2, from soil, in water besides principal anions and kations (Perlman 1979). Waters rich in this gas are providing greatly for uranium solution on its way through systems of fractures in granitic rocks.

Uranium in Neogene rocks of Belanovica basin

About 15% of the Garaši topographic catchment is part of the large Belanovica Neogene basin (Fig. 1) with its northern border at the foot of Bukulja massif. Uranium was discovered in Miocene rocks of the Belanovica Basin in the late 1950s. Its distribution is limited to a coastal facies of conglomerate and sandstone (Višić

1961). Uranium deposits in these rocks are Srednje Brdo and Kamenac, and occurrences are Gaj, Šljivica and Kovačevac (Rončević et al. 1990).

The Belanovica Basin is a trough in east-west direction filled with Neogene sediments more than 400 metres deep (Protić 1991). Freshwater lake deposits in the basin are of the Upper Miocene age (M_3^1) and distinct lithofacial heterogeneity. The lithotypes grade from breccias to clays. There are two facies of sediments differentiated by granulometric composition and by environment of derivation. These are the facies of sandy clay and sandstone and the facies of conglomerate and sandstone (Višić 1961) with a blurred boundary between them.

Fluvial-terrigeneous deposits are suitable geochemical and lithological environments for uranium mineralization, which is a complex process controlled among other factors also by continuous groundwater supply of uranium (Perlman 1989). The sources of uranium mineralization of terrigeneous deposits in the Belanovica Neogene Basin were granitic rocks of Bukulja or disintegrated uranium mineral in these and in metamorphic rocks (Radusinović 1963).

The principal uranium deposit of the Belanovica Neogene basin is Srednje Brdo, the village area of Jelovik. A rectilinear distance from Srednje Brdo to Garaši Dam is about thousand metres. The terrain between the uranium deposit and the southern end of the Garaši storage reservoir is composed of Miocene sedimentary rocks (Fig. 1).

Ore bodies in the Srednje Brdo uranium deposit vary in size from 0.4 m to 5 m, or have an average size of 1.1 m. Mineral concentrations are localized in different lithological units at different levels of the deposit. There are eight ore levels at the altitudes between 280 m and 180 m. Ore bodies are horizontal or subhorizontal with mineralized surfaces of a few hundreds of square metres to 90,000 m^2 (Rončević et al. 1990). Most of uranium mineral precipitated in reducing environment and adsorbed on organic (carbonaceous), rarely clay, material. The principal uranium mineral is pitchblende, to a lesser extent coffinite, or a mixture of the two minerals, with low amounts of phosphorus and calcium. The minerals are fine dispersions in the carbonaceous material. There are also some minerals formed in the oxidizing environment; these are secondary uranium minerals – autunite and metaautunite (Rončević 2005).

The Srednje Brdo deposit is a small, relatively poor uranium deposit. Within coarse-clastic detritus, uranium may leach and subsequently redistribute. Under favourable hydrogeological conditions, uranium continuously precipitates in some sediment levels, leaches from them and concentrates in other places.

Total beta-radioactivity in water trend for 1991-2004

Figure 2 shows a changing trend of the total beta radioactivity in the Garaši Dam for the period 1991-2004. The three figures show the trend for three water depths: directly under the lake surface, at the lake mid-depth and above the lake bottom.

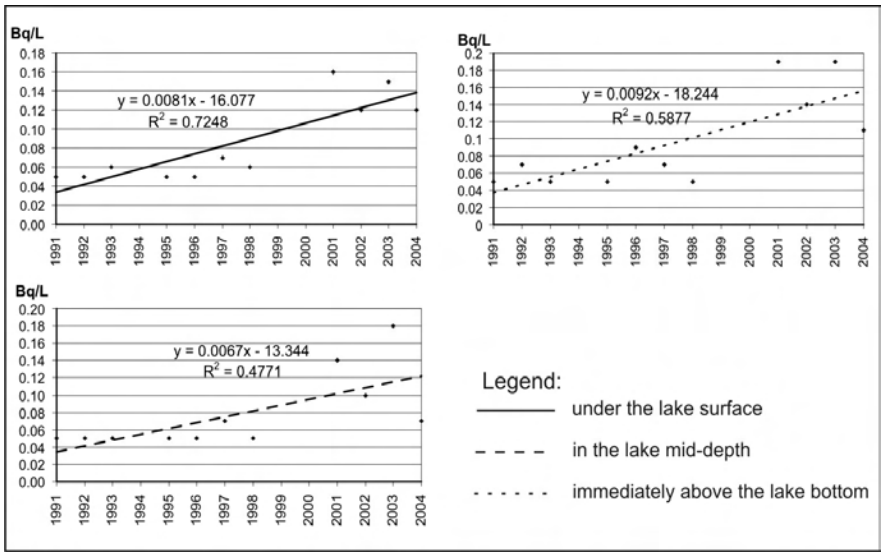

Fig. 2. Trend of total beta radioactivity in Garaši storage at the Dam

Radioactivity measurements of beta particles in the Garaši Dam water between 1991 and 2004 show a rising trend for each sampling depth. The rise is particularly notable for 2001-2004. Total radioactivity is still below the maximum allowed concentration, but prediction of its future tend is a matter of concern.

Conclusions

The Garaši Dam constructed in 1967, impounded water for supply to Aranđelovac and nearby communities. A specific feature of the storage reservoir is the occurrence of uranium minerals within its catchment perimeter.

Analyses of total beta-particle radioactivity in the Garaši water from 1991 to 2004 show a rising trend. The source of the radioactivity is the natural occurrence of uranium. Any prediction of further radioactivity change, based on the trend to present would be delicate.

While measured radioactivity in the Garaši storage is below the contamination level for drinking water, the present trend may lead to a health hazard to consumers of such water. To prevent the contamination hazard and to protect human health it is necessary to analyse water and mud in the reservoir, to organize efficient monitoring, and to explore geologically, hydrogeologically and otherwise in detail the dam catchment. The results will lead to valid conclusions for decision on the necessary measures.

References

Brković T, Radovanović Z, Pavlović Z (1980) Base geological map at scale 1:100,000 sheet Kragujevac and textual explanation (in Serbian). Federal Geological Institute, Belgrade

Filipović I, Marković B, Pavlović Z, Rodin V, Marković O (1978) Base geological map at scale 1:100,000 sheet Gornji Milanovac and textual explanation (in Serbian). Federal Geological Institute, Belgrade

Jelenković R (1991) Uranium minerals of Shumadia: Genetic and morphological types (in Serbian). Belgrade University, Faculty of mining and geology. Special editions 2, Belgrade

Collective authorship (1992-2005) Hydrogeological yearbook, 3 water quality (in Serbian). Hydrometeorological Institute of Serbia, Belgrade

Nikić Z (1997) Contribution to the methodology of hydrogeological investigations for prediction and control of water quality in surface storages (in Serbian). Proceedings of Scientific Symposium '100 Years of Hydrogeology in Yugoslavia', Beograd, 227-233.

Omaljev V (1983) Uranium distribution in the south of Bukulja massif (in Serbian) Radovi Geoinstituta, 16, Belgrade, 145-169

Perlman A.I (1979) Geochemistry (in Russian). High School, Moskva

Pokrajac S (1977) Study, implementation, development and introduction of some methods in the nuclear mineral research (Geochemical tests) (in Serbian). Geoinstitute Documentation Fund, Belgrade

Protić D (1991) Contribution to the study of hydrochemical interaction in the Srednje Brdo uraniferous area, Belanovica basin, Shumadia (in Serbian). Serbian Geological Society Records for 1987, 1988 and 1989. Belgrade, 437-440

Protić D (1993) Overview of Bukulja granitic rocks hydrogeochemical examinations on uranium. (in Serbian). Radovi Geoinstituta 28, Belgrade, 213-219

Radusinović D (1963) Uranite discovery on Bukulja mountain (in Serbian). Radovi 3. Institute of Niclear Minerals, Belgrade, 43-51

Rončević G, Kovačević D (1960) Srednje Brdo uranium deposit in neogene rocks of the Belanovica basin (in Serbian). Proceedings: XII Congress of Yugoslavian geologists, book III, Ohrid, 612-621

Rončević G (2005) Uranium mineral deposits in neogene rocks of the Belanovica basin (in Serbian). Radovi Geoinstituta 40, Belgrade, 141-154

Višić S (1961) Uranium occurrences and deposits on Bukulja mountain (in Serbian). Radovi 1, Institute of Nuclear Minerals, Belgrade, 45-66

Migration of uranium in groundwater in three naturally occurring anomalous areas in South Africa

Henk Coetzee[1], Nicolene van Wyk[1], Peter Wade[1], Patrich Holmstrom[2], HåkanTarras-Wahlberg[2] and Shane Chaplin[2]

[1]Council for Geoscience, Private Bag X112, Pretoria, 0001, henkc@geoscience.org.za
[2]Swedish Geological (Hifab AB) PO Box 19090 SE-104 32 Stockholm Sweden

Abstract. Desktop-level predictive modelling has identified a number of areas in South Africa where naturally elevated uranium concentrations may be expected in groundwater. Three areas were selected for the verification of an existing geological risk model based on known anomalous uranium concentrations in the rocks. Water sampling, laboratory simulations and geochemical modelling showed no clear correlation between uranium levels in groundwater and neighbouring rock material. These conclusions were used to inform the development of policy recommendations regarding groundwater development where elevated uranium concentrations are predicted.

Introduction

Background

As surface water resources are being depleted, governments in many developing countries have increasingly turned to promoting and developing groundwater resources. With the increased utilisation of groundwater, a number of health problems, mainly related to arsenic contamination have emerged during the last decade. For example, arsenic is now recognized as the most widespread and serious inorganic contaminant of drinking water extracted from groundwater sources, and

has taken the proportions of a major disaster affecting more than 35 million people in Bangladesh (Adeel 2001).

South Africa is a water-stressed country, and increasing attention is therefore being given to groundwater as a nationally important resource. As a result of exhausted surface water resources, groundwater is increasingly being utilised for rural supply and irrigation in South Africa. Approximately two thirds of the rural communities are now dependent on groundwater.

The Constitution of the Republic of South Africa enacted in 1996 contains both the Bill of Rights and the framework for government in South Africa. Included in the Bill of Rights are two provisions which have direct relevance to water management and usage. These are sections 27 and 24, which state that:

- "Everyone has the right to have access to, among other rights, sufficient food and water, and the State must take reasonable legislative and other measures, within its available resources, to achieve the progressive realisation of these rights"; and
- "Everyone has the right to an environment that is not harmful to their health or wellbeing, and to have the environment protected, for the benefit of present and future generations, through reasonable legislative and other measures that prevent pollution and ecological degradation, promote conservation, and secure sustainable development and use of natural resources while promoting justifiable economic and social development".

Currently the South African government is promoting the drilling of new boreholes and increased use of underground water resources for the development of rural areas. The promotion of groundwater resources is being carried out with little or no knowledge of potential toxic trace constituents and the processes leading to the accumulation of these trace constituents in the aquifers.

The project to calibrate and verify a predictive model for the incidence of naturally occurring hazardous trace constituents in groundwater

The work presented in this paper formed part of the Project to calibrate and verify a predictive model for the incidence of naturally occurring hazardous trace constituents in groundwater, undertaken by the Council for Geoscience (South Africa) and Swedish Geological AB (Sweden). This project looked at the results of a previous geological risk mapping project (Sami and Druzinski 2003) which provided a simple predictive model of the possible natural occurrence of high levels of hazardous trace elements in South African groundwater. The project focused on a number of elements (arsenic, chromium and uranium) at a number of sites in South Africa. This paper presents the findings of the studies on uranium in the Bushmanland-Namaqualand Region and the Karoo Uranium Province.

Geological risk mapping and sampling studies carried out in recent years have indicated that there are relatively large risk zones for a number of hazardous elements in South Africa (Sami and Druzinski 2003). Uranium, arsenic, selenium and chromium were identified as potentially problematic, as they can occur natu-

rally at high concentrations in groundwater. Groundwater abstraction practises also play an important role in facilitating mobilisation of these elements from the bedrock into the water.

Aims of the project

The aim of this project was twofold, firstly looking at the verification of the relatively simplistic models used for geological risk mapping and secondly to translate the results of the verification exercise into policy recommendations for the development of groundwater. This was achieved via:

1. Field sampling of groundwater and surrounding rock units at a number of test sites, where elevated uranium was predicted to occur in groundwater.
2. Leach testing of rock samples in an attempt to replicate aquifer conditions under a variety of pumping regimes to investigate the mobility of uranium.
3. Constructing and verifying geochemical models to predict water quality based on regional mineralogy.
4. Development of policy recommendations with respect to groundwater abstraction in areas suspected of presenting a high risk with respect to trace metals, including uranium.

Field sampling and results

Field site selection

Field sites were selected on the basis of known uranium mineralisation and known elevation of uranium concentrations in groundwater. Two sites were selected in the Karoo Uranium Province (Cole 1998) on orebodies close to the towns of Beaufort West and Sutherland, where exploration boreholes intersecting uranium orebodies were known to exist and where the local farming community was largely dependent on groundwater for domestic use. A further study area was identified traversing the Bushmanland and Namaqualand Regions, where a regional geochemical anomaly with known radioelement enrichment is found (Andreoli et al. 2006) and previous studies have identified elevated concentrations of uranium and arsenic in groundwater and linked these to regional health anomalies (Toens et al. 1999). The sampling areas are shown on Fig 1.

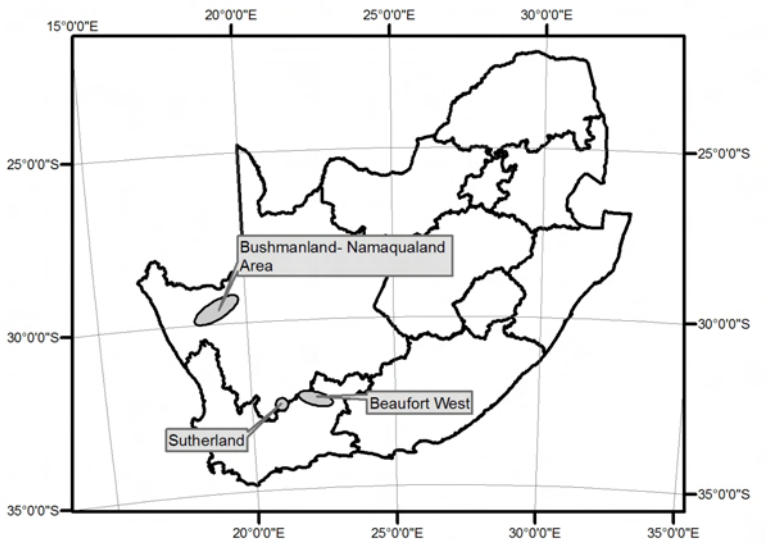

Fig.1. Location of the three sampling areas in the western portion of South Africa.

Sampling

Water samples were collected from boreholes largely used for domestic and stock-watering purposes in the case of the Bushmanland-Namaqualand area and the "background" samples collected in the Karoo Uranium Province. A number of exploration boreholes, dating back to uranium exploration activities in the 1970s and 1980s were also sampled in the Karoo Uranium Province. All the domestic and stock-watering supply boreholes were fitted with wind pumps or "National Pumps" (motorised pumps using the same mechanism as a wind pump) while a small 12V sampling pump was used for purging and sampling the exploration boreholes. In all cases, water was pumped from the boreholes, closely monitoring the pH, Eh and electrical conductivity and samples were only collected when these parameters were all stable. Samples were filtered in the field and the fractions selected for metal analysis acidified with nitric acid. Non-acidified splits were also collected for anion analysis. A total of 23 water samples were collected, 13 from the Bushmanland-Namaqualand area and 10 from the Karoo Uranium Province. In the latter area, 3 samples were collected from farm boreholes equipped with wind pumps, 6 from exploration boreholes and 1 from a groundwater monitoring borehole.

Samples were submitted to the Council for Geoscience Laboratory (Pretoria, South Africa), with check samples submitted to the Analytica Laboratory (Sweden) for quality control analysis. Metal analyses were performed by ICP-MS and anion analyses by ion chromatography.

At each site, rock samples were collected with the aim of representing the aquifer material. Additional rock samples, for example oxidised uranium ore collected from an open pit trial mine on the farm Rietkuil near Beaufort West, were collected where possible, to best represent the source of the suspected uranium in the groundwater. These were submitted to the Council for Geoscience's Environmental Laboratory for leach testing and to the Council for Geoscience's Laboratory for chemical analysis by x-ray fluorescence.

Analytical results

Uranium was measured at potentially harmful levels in 7 farm boreholes in the Bushmanland –Namaqualand Region and 1 domestic borehole and 2 exploration boreholes in the Karoo Uranium Province (See Fig 2). It is interesting to note that the arsenic anomaly previously associated with the Bushmanland Namaqualand region and positively correlated with health impacts (Toens et al. 1999) could not be confirmed, even though some of the same boreholes were sampled in this study. Later discussion with Dr Phillip Kempster at the Department of Water Affairs and Forestry's Resource Quality Services in Pretoria confirmed that these results may have been the product of an analytical error which was not identified at the time of the analyses.

Rock sample analyses showed high levels of uranium associated with the ore deposits in the Karoo Uranium Province, with a mean of 5200mg/kg U (n=5) on the orebody samples, but no highly anomalous uranium concentrations in rock samples could be associated with the regional groundwater anomaly identified in the Bushmanland-Namaqualand region, with a mean of 5.7mg/kg U (n=16).

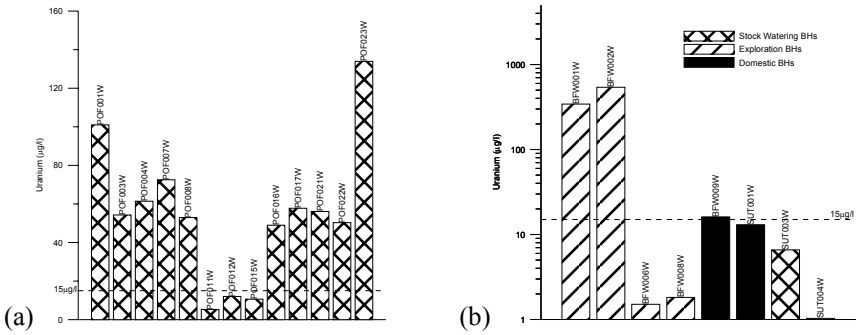

Fig 2. Uranium analysis results for borehole water from (a) the Bushmanland-Namaqualand area and (b) The Karoo Uranium Province. The dashed line at 15µg/l shows the World Health Organisation's guideline level for drinking water (World Health Organisation 2005)

Leach testing

As part of the project, a leach testing facility was established and samples submitted for analysis. Four sets of leach tests were undertaken:

1. Batch tests: which were used for the characterisation of samples and their interactions with water (Nordtest 1998).
2. Availability tests: which estimate the total available fraction of the contaminant of interest in a sample via a 2-stage leach-test at pH values of 7 and 4 in the two stages (Nordtest 1995a).
3. Column tests: which provided the closest analogue to the percolation of water through an aquifer (Nordtest 1995b).
4. Humidity-cell tests (ASTM 1998), which simulate alternating periods of oxidising and water-saturated conditions and were used to simulate an extreme end-member of a borehole being pumped periodically.

The aim of the leach tests was to represent the various pumping regimes likely in rural water supply boreholes and to determine how these could affect the chemical conditions, in particular redox within a borehole. The humidity cell tests were chosen to represent a low-yielding borehole which is periodically pumped, lowering the water table sufficiently to draw oxygen into the aquifer, followed by a period of recovery before pumping again takes place.

In general the various leach tests on non-ore-body samples yielded relatively minor quantities of uranium. Some higher levels of uranium were leached from some samples collected in mineralised zones; however water in these areas would not normally be used for drinking purposes. Batch leach test results showed insignificant correlations with groundwater collected at corresponding sites, while availability and column tests performed on one mineralised sample from the Karoo Uranium Province showed significant mobility of uranium in the aquifer material sampled (Only one sample representative of the aquifer itself could be sampled at these sites).

In all the leach tests performed, relatively small amounts of the elements of interest were extracted, with the exception of ore samples. Most of the boreholes sampled were either far from the lithologies of interest or likely to have been contaminated by mining activities.

These results agree with the results of the chemical modelling described in the following section, *i.e.* that the naturally elevated levels of hazardous trace elements in groundwater observed in field sampling is unlikely to be the results of simple interactions between groundwater and the surrounding aquifer material, but are likely to result from interactions within a localised mineralised zone within the aquifer or recharge area or localised zones of anomalous chemical conditions within the aquifer

Geochemical modelling

The main aim of undertaking the modelling work was to assess the usefulness and efficiency of geochemical models in predicting the concentrations of potentially harmful trace elements in groundwater. Groundwater managers are ultimately interested in whether or not risk areas for groundwater contamination can be identified in this way, using the geological data held by various institutions.

Water and rock chemistry data collected in the field investigation was used as input into the models. The first task involved element speciation modelling, whilst the second involved definition of mineral phases in equilibrium with borehole water. The element speciation modelling is important for determining both the toxicity and mobility of uranium, and this information was used to determine which elements are controlling redox chemistry in each borehole (e.g. As V/As III, Fe III/Fe II etc).

The speciation modelling suggested that uranium existed mainly in the highly mobile U(VI) form. The modelling of controlling redox couples found that boreholes in the Karoo Uranium Province and the Bushmanland-Namaqualand Region had redox chemistry dominated by uranium and iron pairs, while Arsenic dominated one borehole from Bushmanland.

Uranium saturation indices were variable between and within the regions. This means that borehole specific conditions are driving trace metal release from the bedrock and that few broad regional generalisations can be made. An important exception is that uranium appears to leach from the bedrock in Bushmanland to a greater extent than in other regions with the result that relatively high uranium concentrations in groundwater are found, despite relatively low concentrations in the bedrock. The reasons for this are yet to be clarified. Further equilibration modelling was conducted which showed that the solutions were not in equilibrium with the dominant uranium bearing minerals known to exist.

The conclusion for the modelling work is that the conceptual model of bulk solution in geochemical equilibrium with the host rock matrix in the aquifer is an oversimplification of a more complex process. The fundamental difficulty with the conceptual model is the definition of the flow regime in fractured rock terranes with fractures of varying size. There are both kinetic and thermodynamic effects to be considered.

In the kinetic realm, the larger fractures will exhibit faster flow rates of solution through them, affording the host rock less time to react with the bulk solution, although this is likely to be further complicated by the long residence times for groundwater in the semi-arid to arid areas sampled. These chemical reactions will thus contribute less of the elements of concern into the bulk solution than those occurring in smaller fractures, in which solution will flow more slowly, affording the reactions more time to progress. In the thermodynamic realm, larger fractures present less surface area than smaller fractures, which guarantees a lower bulk concentration of the elements of concern in the larger fractures. Waters exhibiting different residence times in contact with the host rock, and experiencing different ratios of bulk water to rock surface area thus combine in a borehole to form a

composite solution. The high degree of variability in conditions at different locations adds a further layer of complication to predicting the occurrence of metal/metalloid contamination.

Conclusions and implications for groundwater policy in South Africa

Conclusions

Measured groundwater chemistry, in particular the uranium concentrations, were found to correlate with neither a simple risk model based on local geology nor the analytical results for local rocks, even when the highest risk scenario of a borehole sunk into a uranium ore deposit is considered. Furthermore, simple laboratory and numerical models of the aquifer-groundwater interactions did not explain the field results. These results point to more complex processes driving groundwater chemistry, which are unlikely to be identified via modelling exercises.

Variability in the chemistry between boreholes further suggests that conditions may be extremely site specific, requiring sampling of individual boreholes in areas where naturally high levels of trace elements such as uranium are likely to occur in groundwater. Furthermore, lessons can be learned from other regions of the world, where pumping regimes have been found to affect water chemistry.

One of the sampling areas for the study was selected on the basis of the reported co-occurrence of uranium and arsenic in the groundwater. Sampling in the area failed to locate any arsenic anomalies. This highlighted the fact that historical data cannot be taken at face value and sampling and analysis for verification purposes may also be required where elevated trace element concentrations are suspected in groundwater.

All of these factors need to be taken into account in new groundwater developments and a precautionary approach, based on sampling and analysis as well as follow-up sampling will generally be required.

Groundwater policy implications

The review of policy implications has highlighted the following:

- That regional mineralogy based geochemical models and leaching tests did not prove to be accurate enough for water quality risk assessment purposes. By contrast, groundwater field sampling showed that large variations in water quality exist over relatively small spatial scales.
- The importance of recognising regional problems where they exist (and having regional management plans to cope with these).

- Current policy does not explicitly state or recognise the problem of natural contamination by trace elements, or the groundwater usage habits which can lead to such problems. Specifically, repeated drawdown and recharge of aquifers leading to changes in redox chemistry can result in contaminant release into the water.
- Other stakeholder institutions are important, specifically the Catchment Management Groups and Water User Associations, in addition to the Departments of Health, Agriculture, Minerals and Energy, and Environment and Tourism. As custodian of the study findings the Water Research Commission has some duty to ensure dissemination of the relevant findings to these stakeholders.
- South African policy statements around water quality monitoring are mostly directed towards monitoring site based contamination, i.e. from industry, mines etc. The current study shows more regional based problems can exist and monitoring policy needs to take account of these. Trace element monitoring should be standard practise in most monitoring work, and pH and redox potential need to be measured in the higher risk areas to help determine likely speciation.

References

Adeel, Z. (2001) Policy Dimensions of the Arsenic Pollution Problem in Bangladesh. In *BUET-UNU International Workshop on Technologies for Arsenic Removal from Drinking Water* Dhaka, Bangladesh

Andreoli, M.A.G., R.J. Hart, L.D. Ashwal, and H Coetzee (2006) Correlations between U, Th Content and Metamorphic Grade in the Western Namaqualand Belt, South Africa, with Implications for Radioactive Heating of the Crust *Journal of Petrology* 47 (6):1095-1118.

ASTM. (1998) D 5744-96, Standard test method for accelerated weathering of solid materials using a modified humidity cell. In *Annual Book of ASTM Standards* 259-271.

Cole, D.I. (1998) Uranium. In *The mineral resources of South Africa*, edited by M. G. C. Wilson and C. R. Anhausser, Council for Geoscience, Pretoria 642-652.

Nordtest (1995a) Solid waste, granular inorganic material: Availability Test, Nordtest, Espoo, NT ENVIR 003, 6pp.

——— (1995b) Solid waste, granular inorganic material: Column test, Nordtest, Espoo, NT ENVIR 002, 6pp.

——— (1998) Solid waste, granular inorganic material: Compliance batch leaching test, Nordtest, Espoo, NT ENVIR 005, 12pp.

Sami, K, and A L Druzinski (2003) Predicted Spatial Distribution of Naturally occurring Arsenic, Selenium and Uranium in Groundwater in South Africa - Reconnaissance survey, Water Research Commission, Pretoria, WRC Report No. 1236/1/03, 84pp.

Toens, P.D., W Stadler, and N.J. Wullschleger (1999) The association of groundwater chemistry and geology with atypical lymphocytes (as a biological indicator) in the Pofadder area, North Western Cape, South Africa, Water Research Commission, Pretoria, Report Number: 839/1/98, 141pp.

World Health Organisation (2005) Uranium in Drinking Water - Background document for development of WHO Guidelines for Drinking-water Quality, World Health Organisation, WHO/SDE/WSH/03.04/118, 26pp.

Acknowledgements

The assistance of the following people and organizations are gratefully acknowledged:

Funding for the project was provided by the Water Research Commission (South Africa) and the Swedish International Development Agency (SIDA). Additional work on the project was supported by the Council for Geoscience.

NECSA, in particular, Dr Marco Andreoli and Mr Piers Pirow, for the provision of historical groundwater data from the Bushmanland-Namaqualand Region.

Alf Lewin and Frans Minnaar for assistance with the sampling in the field.

Dr Doug Cole of the Council for Geoscience for assistance in selecting and locating the field sites in the Karoo and assistance with the sampling.

Dr Tom Lundgren for his assistance in establishing the leaching facility at the Council for Geoscience.

The farmers in the Bushmanland-Namaqualand, Beaufort West and Sutherland regions for providing access and assistance in sampling.

Uranium transfer around volcanic-associated uranium deposit

Vladislav A. Petrov, Antje Wittenberg, Ulrich Schwarz-Schampera and Jörg Hammer

Bundesanstalt für Geowissenschaften und Rohstoffe, Stilleweg 2, 30655 Hannover

Abstract. Only about 60% of the annual consumption in the nuclear fuel cycle is provided by primary uranium production at present. Hence, a strong demand for additional exploration of additional uranium resources is identified in many countries. Hence, a large potential exists for unconventional uranium deposits such as mobilization areas in the surroundings of known deposits. Besides environmental aspects a deep understanding concerning the migration and accumulation behaviour of uranium isotopes and related elements is necessary. As an example we will present data of the Tulukuevskoe deposit, SE Transbaikalia, Russia. Here, primary UO_2 mineralization is mined from the Tulukuevsky open pit (TOP). The pitchblende is subject of secondary remobilization and transformations within the vadose zone of the deposit. Seven years of field and laboratory studies indicated that a uranium speciation dominated by carbonate complexes and gradually shifted from the $UO_2(CO_3)_3^{4-}$ to the $UO_2(CO_3)_2^{2-}$ species field with enhanced formation of uranylcarbonates (Petrov 2005). Three remobilization areas varying in their mineral-chemical composition, transport parameters and the oxidizing degree of the welded tuffs are conceptualized. Sensitivity to the sequential variations in hydrochemistry and isotopic composition of fractured and meteoric waters is considered in the context of spatial-temporal development of the redox front. Identification and exploration of the redox front and of primary and secondary uranium enrichments is facilitated by the µ-energy dispersive x-ray fluorescence (EDXRF) technique that allows the high resolution *in-situ* determination of a number of elements simultaneously at the microscopic scale of typically 100 µm (Rammlmair et al.

2006). This method is fast and useful in order to localise primary uranium minerals as well as mobilised and secondary uranium-bearing phases. The results of the study are interesting also as an analogue of destruction of deep repository of nuclear waste.

References

Petrov V.A. et al. IAEA, **CN-128**: 260-264. (2005)

Rammlmair, D. et al. in *Handbook of Practical X-Ray Fluorescence Analysis* (eds. Beckhoff, B., Kanngießer, B., Langhoff, N., Wedell, R. & Wolff, H.) 640-687 (Springer, Heidelberg, 2006).

Selective Retention of U(VI) and U(IV) Chemical Species on Eichrom Resins: DGA, TEVA and UTEVA

Alexandru Cecal[1], Marian Raileanu, Doina Humelnicu, Karin Popa and Florica Ionica[2]

[1] "Al.I. Cuza" University, Faculty of Chemistry, 11-Carol I, 700506, Iasi, Romania
[2] "Petru Rares" National College, Piatra Neamt, Romania

Abstract. The paper deals with the retention of U(VI) and U(IV) species out of aqueous solutions, on Eichrom resins: as : DGA, TEVA and UTEVA. Some solutions of UO_2^{2+} and U^{4+} in HCl and HNO_3 were first prepared, having different concentrations. The retention of uranium species separately or out of mixture solutions on DGA, TEVA and UTEVA resins under various experimental conditions, in static contact between the solution and the solid masses, was followed spectrophotometically. The retention degree on resins of the U(IV) was higher than that of the U(VI) , for all three resins which were investigated, whereas the adsorption of U^{4+} and UO_2^{2+} ions on these solid masses decreased in the order below:

DGA > UTEVA > TEVA

FTIR spectres pointed out differences in the retention of U(VI) and U(IV) species on the three resins.

Introduction

The separation of uranium species on ion exchangers has been investigated by several authors (Korkisch 1969; Duff et al. 1996; Cotton et al. 1999). Thus Bock and other (Bock and Bock 1950) used the Dowex 1 anionite for the isolation of U(IV), U(VI), Th(IV) and Pa(V) species using as eluent various HCl solutions, namely: 3 M, 0.1 M, 10 M, as well as a 9 M + 1 M HF mixture. On the other hand, Tonosaki and Otoma (Tonosaki and Otomo 1959) separated the U(IV) species

from other metalic ions on Amberlite 1R-120 using a 4 M solution of H_2SO_4 as eluent.

Kraus and others (Kraus Moore and Nilson, 1956) later succeeded to separate U(IV) from U(VI) out of acid solutions, after the retention of these two species on Dowex 1, in the Cl^- form. In this situation elution war performed by means of 2 different HCl solutions : 3M for U^{4+} and 0.1 M for UO_2^{2+}.

Other methods for uranium species separations have also been reported.

Thus, Volkovich and others (Volkovich et al. 2005), by using EXAFS measurements, identified U(VI), U(IV) and U(III) species in the form of chlorine compounds, in eutectic melt of LiCl – $BeCl_2$, for example: $UOCl_2$, UCl_4, UCl_3, UCl_6^{2-}, UCl_6^{3-}, $UO_2Cl_4^{2-}$, etc., in a Cl_2, HCl and Ar atmosphere. Then they succeeded to isolate these species through cromatography.

Other authors (Abdelanos at al. 1998; Ortiz-Bernod at al. 2004) investigated the appearance of U(VI) and U(IV) species in the presence of some bacteriae (*Pseudomonos aeruginosa*, *Shewanella putrefacieus,* or others in the *Geobacteriaceae* family), following some redox processes developped both in ores and in the background waters near the uranium minerals. U(VI) and U(IV) species were then identified and separated by means of cromatographic methods.

Eichrom resins of the DGA, TEVA and UTEVA type were used by Horowitz and others (Horvitz et al. 1992; Horvitz et al. 1995; www.eichrom.com) to separate certain ions of the 4f and 5f elements, including a lot of isotopes of the actinides.

This paper is the follow-up of some of previous research (Raileanu and Cecal 2008) concerning the separation of U(VI) and U(IV) species under various working conditions, on the Eichrom resins.

Materials and methods

Reagents

The two uranium species were to be found in the innitial substances used, in solid state. $UO_2(NO_3)_2$ was purchased from the Fluka company and UCl_4 was prepared in our laboratory.

Uranium chloride (IV) resulted from the following chemical reactions:

$$UO_2^{2+} + 2H_2N\text{-}OH \xrightarrow{H^+} UO_2 + N_2 + 2H_2O + 2H^+$$

$$UO_2 + CCl_4 \rightarrow UCl_4 + CO_2$$

The first reaction was performed under low heating (35-40°C) during 24 hours, while the second was performed in a closed pressurized ICITPR-85 vial, in the presence of CCl_4 (90 % of the total volume), at a temperature of 250°C during 4 days (Raileanu 2006; Meyer and Pietsch 1936).

Then, by dissolving $UO_2(NO_3)_2$ and UCl_4 in distilled water with a pH < 5.5, the starting solutions were prepared, having a uranium (VI or IV) concentration of 0.01g/mL. The acid medium hindered the hydrolysis of the U(IV) species, as well as the formation of the $U_2O_7^{2-}$ or UO_4^{2-} precipitates.

After this stage, the three Eichrom resins:DGA – (N,N,N,'N' – tetrakis – 2 ethylhexyl – diglycolamide),TEVA – (Trialkyl – methylammonium nitrate or chloride),UTEVA – (Dipentyl – pentylphosphonate) were prepared for experiments weighing 0.1g out of each and putting them separately into 50ml Erlenmeyer glasses with stoppers.

Three distinct series of 72 samples of weighed resins were then achieved. In 24 glasses of first serie of solutions made of 5mL U(VI) and 5mL water were poured, in the next 24 glasses other solutions contained of 5mL U(IV) and 5mL water were added and in the last 24 glasses mixture solutions of 5mL U(VI) and 5mL U(IV) were put inside.

Then to three of the samples in each series 2mL HNO_3 or HCl solution were poured. These acid solutions had various concentrations: 0.01; 0.05; 0.1 and 1 M.

The samples prepared as described above were stirred intermittently at room temperature.

Working Procedures

After being stirred , out of each sample which was prepared as above an amount of 0.1 mL solution was extracted from the area above the solid mass, in order to determine spectrophotometrically the concentration of U(VI) and U(IV) in the solution. The absorbance measurements were performed with a UV – VIS Centra – V3157 spectrophotometer at the following wave lengths (Meyer and Pietsch 1936):

$$\lambda = 665 \text{ nm for U(IV)}$$

$$\lambda = 415 \text{ nm for U(VI)}$$

The uranium(IV and VI) species concentrations were determined out of two Lambert-Beer standardization straight lines drawn previously.

The retention degree of the U(IV) and U(VI) species on the DGA, TEVA and UTEVA resins was calculated using the relation:

$$G(\%) = \frac{[U]_i - [U]}{[U]_i} x100$$

in which $[U]_i$ and [U] stand for the concentrations of the uranium species in the initial solution and the final one respectively..

Then the the DGA, TEVA and UTEVA resins which retained the uranium species were dried at a temperature of 110°C in a drying closet, after which there fol-

lowed the preparation of samples necessary for the tracing of FTIR spectres, using a IR – 600 JASCO spectrometer.

Results and Discussion

Practical results are presented in Table 1 and in Figures 1-3.

Table 1 shows that out of the solutions containing just one compound U(IV) is better retained than U(VI). In the case of two compounds solutions also, U(IV) was adsorbed stronger than U(VI) one.

As compared to the retention of the U(IV) species out of the singular systems , in the case of mixtures solutions the retention degree of this species increases. the retention of U(VI) decreases regarding the results obtained of singular solutions.

It is probable that in the process of adsorbtion on the solid mass a synergic effect happens which is favorable for U(IV) and less favorable for the more voluminous uranyl ions.

Therefore it is obvious that the retention degree on resins is reversely proportional to the size of the uranium ion, namely: higher in the case of U^{4+}, where $r_{U^{4+}} = 0.96$ Å and lower in the case of UO_2^{2+}, where $r_{UO_2^{2+}} = 1.82$ Å.

Tabel 1 also points out that there are differences regarding the retention of uranium species out of solutions in which the concentration of the added acids varies.

Thus, in the case of solutions with added HCl the degree of retention of U(IV) and U(VI) species on resins is higher as compared to those with HNO_3, for equal concentrations.

It is possible that in the presence of Cl^- ions some anionic species of the type UCl_5^-, UCl_6^{2-} or even $UO_2Cl_3^-$ may appear which are more stable than the similar NO_3^- compounds.

Table 1. Retention degree of U(VI) and U(VI) species on the Eichrom resins

Resins	Uranium species	Retention (%) HCl medium [M]				HNO_3 medium [M]			
		0.01	0.05	0.1	1.0	0.01	0.05	0.1	1.0
DGA	$U(VI)_{single}$	13.5	22.8	31.1	43.0	12.9	18.9	22.7	30.3
	$U(IV)_{single}$	15.6	39.0	53.1	71.8	19.2	30.0	44.5	56.7
	$U(VI)_{mixture}$	11.1	15.4	20.8	32.6	9.1	13.7	18.1	25.3
	$U(IV)_{mixture}$	30.9	47.3	61.7	82.4	28.2	36.6	49.2	69.5
UTEVA	$U(VI)_{single}$	9.2	15.8	27.2	38.9	5.2	10.5	14.4	21.5
	$U(IV)_{single}$	21.5	35.1	42.7	59.5	8.4	20.3	33.2	39.6
	$U(VI)_{mixture}$	4.2	9.7	16.1	22.3	3.1	6.9	11.4	16.8
	$U(IV)_{mixture}$	29.4	40.7	55.5	78.1	18.1	31.6	48.2	62.4
TEVA	$U(VI)_{single}$	2.4	3.8	6.0	10.3	1.5	2.3	3.8	4.9
	$U(IV)_{single}$	9.4	12.3	18.4	23.6	7.0	8.2	14.3	18.8
	$U(VI)_{mixture}$	0.9	1.7	2.2	3.5	0.3	0.8	1.5	2.3
	$U(IV)_{mixture}$	13.5	19.2	23.8	29.1	9.7	13.7	19.0	22.2

Nevertheless such as chloride compounds but also other complex compounds with inorganic ions: $[U(CO_3)]^{2+}$, $[U(CO_3)_5]^{6-}$, $[U(OH)_2]^{2+}$, $[U(OH)_3]^{+}$, $[UO_2(CO_3)_2]^{2-}$, $[UO_2OH]^{+}$, $[UO_2(SO_4)_2]^{2-}$ etc were been described in some papers [Meinrath et al. 1999; Neck and Kim 2001], which confirm the above mentioned assumption.

From experimental data presented in Table 1 it can remark that the retention degree of uranium species on Eichrom resins varies as:

DGA > UTEVA > TEVA

which is connected with the chemical and surface structure of these adsorbents solid masses.

Taking into account the FTIR spectra. it may conclude that the U(VI) and U(IV) species were adsorbed on the DGA, TEVA and UTEVA resins, because the the position of vibrational bands were changed ,as can be observed in Fig.1-3.

Fig.1-3.

Under 1000 cm^{-1} appear characteristic vibrational bands for metal-ligand bonds.

For U(IV) adsorbed specie on resins, vibrational bands were found by: 240, 270, 410 and 1100 cm^{-1}(Fig.2), whereas for UO_2^{2+} specie an asymmetric stretch frequence at 930 cm^{-1} appeared together other distinguished vibrational bands , as: 750, 850 and 1000 cm^{-1} (Fig.3) .

These found in FTIR spectra vibrational bands correspond to those pointed out in similar studies [Nyguist and Kagel, 1971,or Nakamoto 1986 ,or Morss et al ,2006], which confirm the above presented results, on the selective retention of uranium species on DGA,TEVA and UTEVA resins.

Conclusions

It was investigated the adsorption of some uranium species, separately or in mixture solutions on DGA, TEVA and UTEVA Eichrom resins. The U(IV) species was retained better as U(VI) one in each experimental conditions.

The retention degree of each uranium species on the solid resin decreased as:

DGA > UTEVA > TEVA

By means of FTIR spectra the selective retention of each uranium specie on resins was proved.

References

Abdelonas A, Lu Y, Lutze W, Nuttall HE (1998) Reduction of U(VI) to U(IV) by ingenious bacteria in contaminated groundwater. J Contam Hydrology 35: 217-233

Bock R, Bock E (1950) Trenumgeiniger Metalle mit Dowex 1 Harges. Z Anorg Allg Chem 263: 146-168

Cotton F.A., Wilkinson G, Murillo CA, Bochmann M (1999) Advanced in inorganic chemistry, sixth edition, John Wiley & Sons, Inc.

Duff MC, Amrhein (1996) Uranium VI adsorption on goethite and soil in carbonate solutions. Soil Sci Soc Amer J 743:1393-1400

Horwitz EP, Dietz ML, Chiarizia R, Diamond H, Maxwell III SL, Nelson M (1995) Separation and pre4concentration of actinides by extraction chromatography using a supported liquid anion exchanger. Anal Chim Acta 310: 69-78

Horwitz EP, Dietz ML, Chiarigia R, Diamond H (1992) Separation and preconcentration of uranium from acidic media by extraction chromatography. Anal Chim Acta 266: 25-37

Korkisch JN (1969) Methods for separation of rare metal ions. Pergamon Press, Oxford,

Kraus KA, Moore GE, Nelson F (1956) Separation of U(IV) and U(VI) on Dowex 1. J Amer Chem Soc 78: 2692

Meinrath G, Volke P, Helling C, Dudel EG, Merkel BJ (1999) Determination and interpretation of environmental with samples contamined by uranium mining activities. Fresenius J Anal Chem 364: 191-202

Meyer RJ, Gmelins Pietsch E (eds) (1936) Handbuch der Anorganischen Chemie 8 Auflage Uran und Isotope System Nummer 55 Verlag Chemie Weinheim, pp. 138

Morss LR, Edelstein NM, Fuger J (2006) The Chemistry of Actinide and Transactinide Elements. IIIrd Ed. Springer Dordrecht

Nakamoto K (1986) Infrared and Raman spectra of inorganic and coordination compounds. J Wiley, New York

Neck V, Kim JI (2001) Stability and hydrolysis of tetravalent actinides. Radiochim Acta 89: 1-16

Nyguist R, Kagel R (1971) Infrared spectra of inorganic compounds. Acad Press, New York, pp. 195

Ortiz-Bernad J, Anderson RT, Vrionis HA (2004) Resistance of solid-Phase U(VI) to microbial reduction by bioremediation of uranium-contaminated groundwater. App Environ Microbiol 70: 7558-7560

Raileanu M, Cecal A (2008) Separation of U(VI) and U(IV) by means of ion exchange resin of DGA TEVA and UTEVA type. J Radioanal Nucl Chem 277:587-590

Raileanu M (2006) A desegregation method for uranium ores. Rev Chim Bucharest 57: 1210-1212

Tonosaki K, Otomo M (1959) Separation of U(IV) from Ti(IV) using Amberlite IR-120. J Chem Soc Japan Pure Chem Sect 80:1290

Volkovich VA, May I, Griffiths TR, Charmock JM, Bhatt AI, Lewin B (2005) Structure of chloro-uranium species in molten LiCl-BeCl2 eutectic. J Nucl Mat 344: 100-103

www.eichrom.com

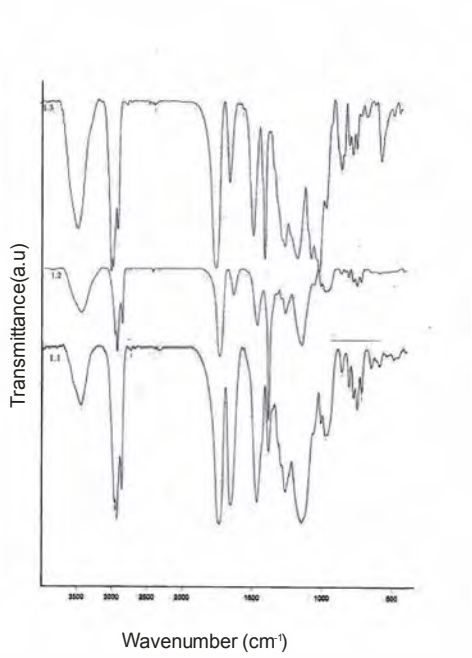

Fig.1. FTIR spectra of Eichrom resins: (1-1) DGA, (1-2) TEVA and (1-3) UTEVA.

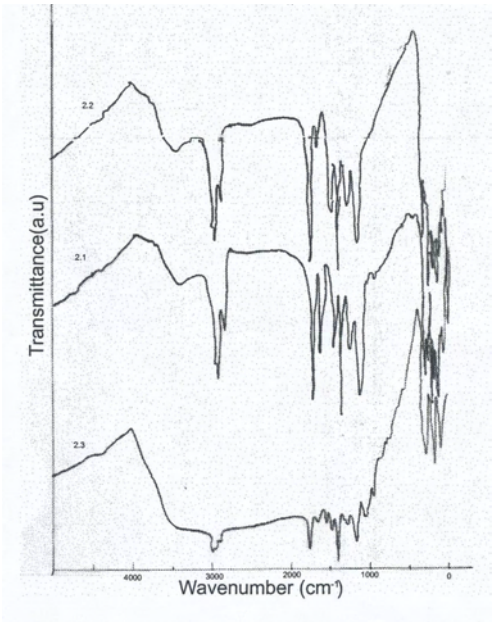

Fig.2. FTIR spectra of resins-U(IV): (2-1) DGA-U(IV), (2-2) TEVA-U(IV) and (2-3) UTEVA-U(IV).

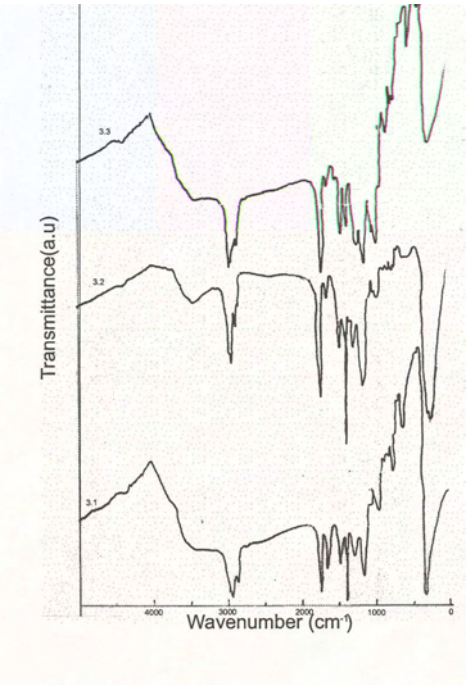

Fig.3. FTIR spectra of resins-U(VI): (3-1) DGA-U(VI), (2-2) TEVA-U(VI) and (3-3) UTEVA-U(VI).

The biogeochemistry of uranium in natural-technogenic provinces of the Issik-Kul

Bekmamat M. Djenbaev, A. B. Shamshiev, B. T. Jolboldiev, B. K. Kaldybaev and A. A. Jalilova

Institute of Biology & Pedology of NAS of the KR, Kyrgyz Republic, Bishkek, 720071, Phone 996 (312) 655687, Fax. 996 312 657943, e-mail: bekmamat2002@mail.ru

Abstract. In territory of Kyrgyzstan there is a large number of radioactive sources. They are concentrated man-caused solids of fine-dyspersated waste of reprocessing and concentration, which in depend on reprocessed ore kinds and concentrate have radioactive nuclides, unhealthy heavy metals compounds, and also toxic substances, used as reagents in extraction from valued components of mineral. Tailing dumps of radioactive waste in the cities of Mailuu-Suu, Kadji-Sai, Min-Kush and Kara-Balta occupied in all nearly 3600 m^2.

Introduction

In territory of Kyrgyzstan there are a large number of radioactive sources (about 1200). The used sources are stored in a long-term storage facility, which was built in 1965 under a typical RADON design replicating similar facilities in other republics of the former Soviet Union. Because of natural cataclysm such as: earthquake, landslip, mud flows and erosion processes the threat of the further pollution of territory by radioactive substances is increased. As a result of these natural processes, a line of uranium tail deposits was is damaged. The majority of tail deposits and the warehouse premises are in the started condition and are poorly supervised. Kyrgyz Republic collides by serious problems of radioecological character connected with production of uranium and his processing activity in the country. In connection with disintegration USSR in territory of Kyrgyzstan in an ownerless condition have appeared - 36 tail deposits, 25 mountain dumps, from them 31 tail deposits and 28 dumps (Fig. 1). The condition these dumps and storehouses (tail deposits) is a pitiable condition. Radioactive withdrawals, heavy metals and the toxic substances pollute an environment: superficial and underground waters, atmospheres, ground, plant etc.

Many tail deposits were formed within the limits of the occupied items (Kadji-Sai, Min - Kush, Mailuu-Suu etc.).

As priorities for Kyrgyzstan on radiating safety for the intermediate term period the following areas were designated at an advice of the experts from technical co-operation of IAEA: 1) Rehabilitation of consequences of production of uranium and its processing activity. 2) Health: improved nuclear diagnostics and services of radiotherapy. 3) Management of knowledge and rational use of nuclear technologies. By radiometric shooting is established, that the level of an exposition doze in the hollow (natural-technogenic provinces) of the Issik-Kul both settlement of Kadji-Sai and territory (technogenic), contiguous to it, rather low (Fig. 2).

Pearls of a nature of lake Issik-Kul involved, involves, and will involve the scientists and researchers, and to draw steadfast attention in preservation and rational use of greatest resources of a nature of edge. However, under influence natural-technogenic pressure and climatic factors should serve the base to development of strategy of development of biospheric territory of one of which overall objectives, is the preservation of natural environment of plants, animals and man.

In this connection by us spent complex radioecological and radiobiogeochemical research in the given uranium natural-technogenic province of Issik-Kul (biosphere territory) in which will allow a province to receive the objective information on a condition of natural environment.

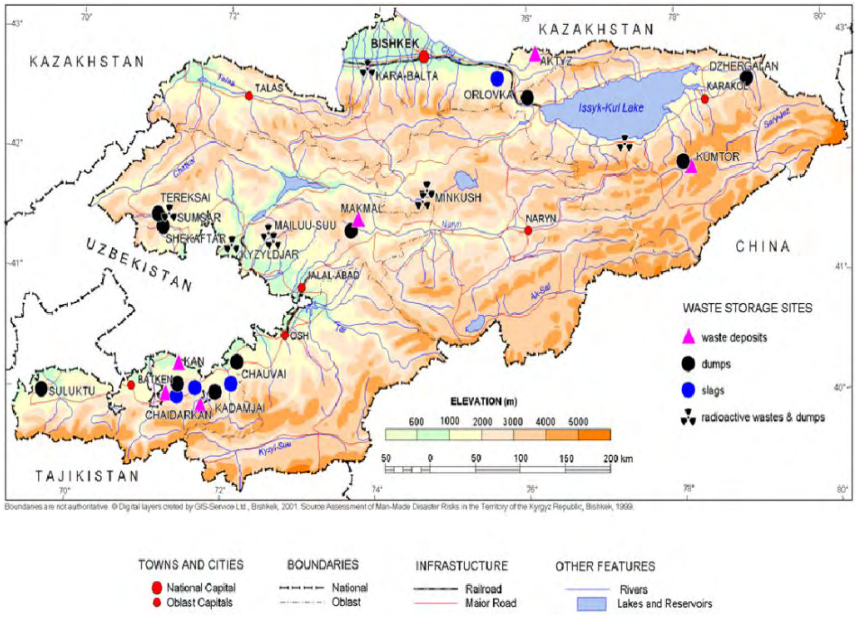

Fig.1. Waste storage sites.

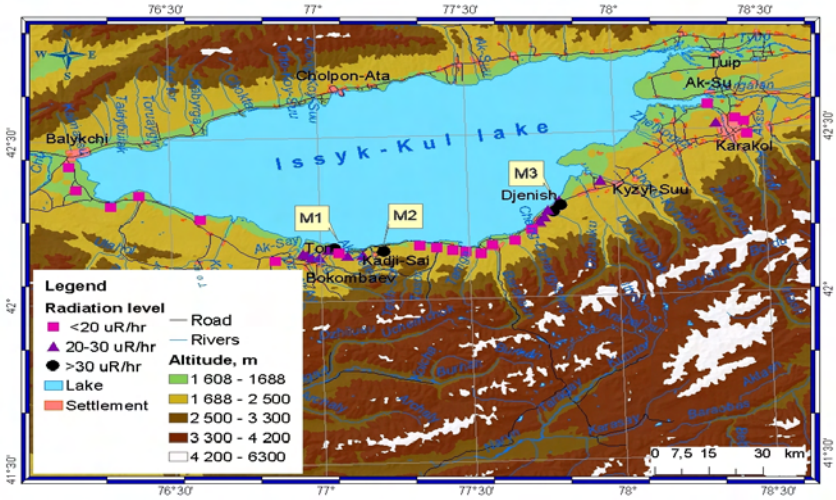

Fig.2. Natural-technogenic provinces of the Issik-Kul

Methods of researches

The gathering of the samples of soils, natural waters, plants and animals we are spent by view of geochemical landscape and meteorological conditions. Processing of samples carried out in laboratory of biogeochemistry of Biology and Soil Institute of National Academic Science of Kyrgyz Republic with use of soil and geological maps by consultation of geologists. The equipments used during researches were Radon radiometer RRA--01m-03, Dosimeter-radiometer DKS-96, Sampling system POU-04, Photo-electro-colorimeter (SPECOL), Gamma spectrometer etc. Distribution and processing of the received information were made on special software of PC.

During process of researches were selective measurements of a level of radiation and uranium in the given subregion and tails. Gathered the samples of soils, water and plants in different places for the further research in laboratory conditions.

Results of researches

Volume of the saved tails of the technogeic province of Kadji-Sai (industrial withdrawals) makes about 150 thousand m^3. For 40 years has taken place intensive destruction of a coastal part in area of the industrial withdrawals (Fig.3). The part of radioactive ashes reached to Issik-Kul, but it was so unsignificant, that for Issik-

Fig.3. Kadji-Sai (industrial withdrawals).

Kul makes a drop in the sea, according to the different researchers in the lake contains about 100 thousand tons of uranium.

By radiometric shooting is established, that the level of an exposition doze in the hollow of Issik-Kul and both settlement of Kadji-Sai and territory contiguous to it, rather low and changes from 150 up to 470 nzv\hour.

According to the scientist biogeochemists and geochemists the hollow of Issik-Kul is a natural uranium biogeochemical province. Here function mountainous-ores combine on processing uranium ore from 1948 on 1969 yy. Now tail-deposit with uranium withdrawals is in 2,5 kms to east from an inhabited settlement, but because of the natural factors (rains, earth waters, landslips and селей) represents ecological threat to lake Issik-Kul and nearest settlements. But after closing mountainous-ores combine of Kadji-Sai weight not inhibited radioactive-industrial withdrawals, meeting in the coast of Djil-Bulak (Fig.4), underwent intensive destruction, the carry of its part in a mouth of coast and further lakes is possible. This was promoted here by often storm rains. The part of radioactive ashes reached to Issik-Kul, but it was so unsignificant.

The different parts of Issik-Kul have the different contents of uranium in water (table 1, fig.5). It is caused by non-uniformity of processes of evaporation and distil coastal zones occurring in different parts of Issik-Kul. On the average waters of Issik-Kul contain 3.0 x 10-6% of uranium.

The general level of uranium from streams №1 and №2 of the Kadji-Sai (from tails) in comparison with water of lake Issik-Kul is more from 2-5 times, and in

comparison with the river Kichi-Ak-Suu and river Bulan-Segeti from 40 - 100 times.

However it is necessary to note, that streams from tails not the lake always reaches, only in the spring and autumn periods he gets in lake. By us the analyses were spent before and after a rain, but the results have shown, that on a level and isotope structure of the special distinctions it is not revealed.

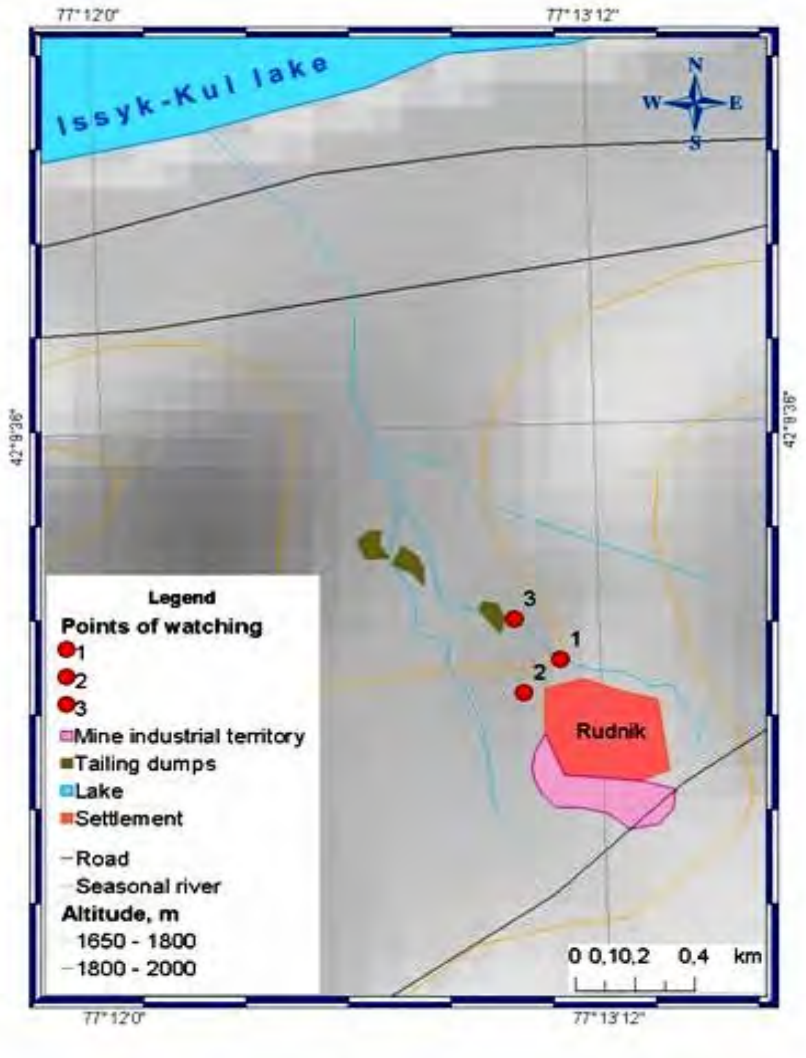

Fig.4. Scheme map of operating observations of outlet in the Djil-Bulak valley.

Table 1. The contents of uranium in water of the lake Issik-Kul

No	Place of selection of tests of water	U in water %
1	Northern coastal zone (Cholpon-Ata)	3.331*10-6
2	East (a gulf of Tup)	3,1*10-6
3	a) Southern (Tamga) b) Southern (Bay Kolsovka) c) Southern (a gulf of Ton)	1.7*10-6 3.68*10-6 2.3*10-6
4	Western (a gulf of Rybachi)	4,32*10-6

Table 2. Comparison uranium-isotope data given by results of approbation 1966-1970 yy and 2003-2004 yy(Matychenkov, Tuzova, 2005)

Place of approbation	$\gamma = {}^{234}U/{}^{238}U$		The content of U 10^{-6} g/l (9)
	1966-1990(1-6)	2003-2004 (12)	
river Toruaigyr	-	1,49±0,01	11,0-19,0
river Chon-Ak-Suu	1,39±0,01	1,42±0,01	6,7-10,7
river Tup	1,43±0,01	1,34±0,08	2,6-8,7
river Djergalan	1,23±0,01	1,20±0,02	4,7-13,0
river Chon-Kyzyl-Suu	1,23±0,01	1,20±0,02	4,3-11,2
river Barskaun	1,14±0,01	1,08±0,07	7,2-2,7
river Ak-Terek	1,23±0,01	1,24±0,02	0,42-47,0
river Tamga	1,22±0,01	1,22±0,06	15,1-21,6
river Urukty	1,51±0,02	1,62±0,02	2,6
Chink 3 Djergalanskaia	1,20±0,02	1,32±0,06	0,6-15,6

Table 3. Background meanings of the contents of alfa-active isotopes in the soils around of Issik-Kul.

Place of selection	Layer cm	Activity of the soils on isotopes, Bq/kg									
		U-238		Ra-226		Pb-210		Th-228		Ra-228	
			+/		+/		+/		+/		+/-
Kara-Oi	0-5	71,8	12,7	35,1	3,9	147,4	13,0	39,5	2,2	35,2	8,8
	5-10	50,8	7,3	37,7	3,4	64,6	11,4	49,0	1,9	60,1	7,5
	10-15	44,0	1,7	35,1	3,2	50,1	7,2	45,6	1,8	52,3	3,5
	15-20	51,7	7,4	46,1	3,5	50,2	7,7	49,9	1,9	53,6	7,7
Kichi-Aksu	0-6	71,5	14,3	51,0	3,4	88,5	18,4	69,1	3,6	72,4	7,2
	6-11	52,1	6,5	43,2	3,1	71,7	10,2	43,2	3,3	59,2	19,7
	11-20	54,9	7,3	45,4	3,5	68,6	7,6	64,3	3,8	64,1	7,5
Ak-Terek (sand)	0-3	260,0	30,0	103,0	8,0	169,0	30,0	915,0	57,0	846,0	70,0

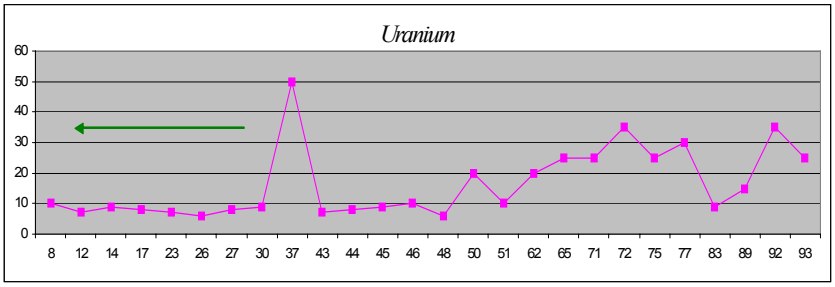

Fig.5. Uranium, thorium and potassium (%) consistent in south coast of Issyk-Kul Lake.

In the table 2 is shown for comparison of a parity 234U/238U in the various periods and average contents of uranium, where there are small deviations.

The analysis of samples soil and dirt has shown, that on tail deposits in the top horizon of a bulk ground (0-20 cm) the contents of uranium changes from 1,1 up to 2,6·10-6 g/g, with depth he grows - up to 3,0·10-6 g/g. The large concentration of uranium there is an average zone of tail deposits, where the contents of uranium in the top horizon of a ground is equal 4,2·10-6 g/g, and in the bottom horizon, on depth 40-60 cm - 35,0·10-6 g/g or in 8,3 times is higher.

The level of a radiating background on a surface of industrial zone and tails rather not high. More detailed researches of isotope structure of a soil cover of subregion have shown also, that in the top layers he is rather higher in comparison with the bottom layers, and in sand of Ak-Terek in comparison with soil covers others investigated soils much above and changes from 3 up to 20 times (table. 3).

Conclusion

1. In researched territory the general level of an external radiating background of subregion is within the limits of norm.
2. The raised radioactive anomaly of three types is marked on technogenic sites:
   a) the natural anomalies of a radio-activity are connected to layers, seldom acting from under friable adjournment, radioactive brown coal Jurassic age.
   b) technogenic anomaly, in hundreds time exceeding a background, are dated to fenced by a concrete wall dumps grey thin-granular substance.
   c) technogenic anomaly in the cascade from four settlings, the activity in tens time is higher than a background, with an equal flat surface lowered downwards on a valley from a mine field.

References

Aitmatov I.T., Torgoev I.A., Alyoshin U.G Geo environmental problem of mining complex of Kyrgyzstan //The Science and new technologies. - 1997. N1. 34-42 p.

Djenbaev B.M. Geochemical ecology of erth-water organisms. - Bishkek, 1999. p.178.

Djenbaev B.M., Myrsaliev A.M. The role of biogeochemical environment in the studies of microevol. Processes //1-st Speciation Conf., c/o Ms Ulla Schroedel, GSF- Forschungszentrum, - Mjunxen, 1998. - p. 213.

Karpachev B.M., Meng S.V. Research of radiation in Kyrgyzstan. - Bishkek, 2000. p 56.

Kovalskij V.V., Vorotnitskaia I.E., Lekarev V.S. Uranium biochemical food circuits in conditions of hollow of Issyk-Kul. The works of Biochemical laboratory. Science , 1968, X11. p. 2-36.

Sultanbaev A.S. Agricultural aspects of biogeochemistry and radioecology of uranium in mountain landscapes of Kirghiz SSR. The dissertation of doctor's degree 1982. p. 45.

Tynybekov A. K., Hamby D. M.. A screening assessment of external radiation levels on the shore of lake Issyk-Kul in the Kyrgyz Republic. //Health Physics, volum 77, number 4. October 1999. p. 427-430.

Radioactivity in soils and horticulture products near uranium mining sites

Fernando P. Carvalho and João M. Oliveira

Nuclear and Technological Institute, Department of Radiological Protection and Nuclear Safety, E.N. 10, 2686-953 Sacavém, Portugal (E-mail: carvalho@itn.pt)

Abstract. Uranium mining in Portugal was performed mainly in small mines spread over a wide and populated region in the Centre-North of the country. In villages near old uranium mines, soils are used for horticulture production and to provide pasture for livestock grazing. Soil samples as well as agriculture products including cabbage, potatoes, oranges, and other fruits were analyzed for alpha emitting radionuclides. Samples from areas far from uranium mining sites were also included in the survey. Results of uranium series radionuclides showed that soils of regions with different geology may contain very different radionuclide concentrations. Concentrations of radionuclides in soils and vegetables of reference areas may display values similar to those near uranium mining sites in the same geological province, indicating that enhancement of radionuclides in the terrestrial food chain, with the exception of ^{226}Ra, generally is not high. Concentrations in soils and horticulture products of these uranium counties generally were two orders of magnitude higher than concentrations measured in soils and vegetables in a sedimentary region in the South of Portugal.

Introduction

During the XXth century in Portugal were exploited 60 uranium ore deposits for radium and uranium production. The last uranium mine and the facilities for uranium ore processing and production of uranium oxide concentrates, in Urgeriça, Canas de Senhorim, were closed in 2001 (Carvalho, in press). So far, most of the former mining and milling sites were not rehabilitated and mining waste has been stockpiled at the surface, in general near the old mines (Nero et al., 2004; Carval-

ho, in press). Most of these radium-uranium mines were located in the centre-North of the country, already a densely populated area, and villages and towns developed near the mines over the years. With discontinuation of the uranium mining activity and the close out of the mining company, there have been concerns about the impact of uranium waste on the environment and on human health. Despite of engineering works meanwhile started in the Canas de Senhorim county to cover the waste piles from Urgeiriça mine and milling facilities, it was of high relevance to the region to know whether the long lasted uranium mining activity had contaminated with radioactive materials the soils of those regions and whether radionuclides could be transferred through the consumption of agriculture products.

In the framework of a research project to assess the current impact of the legacy of uranium mining industry on public health, we undertook the comparative analysis of soils and kitchen garden products in the counties with uranium mines and in counties without uranium mines. Preliminary results of this study are presented here.

Materials and Methods

The counties to be investigated were selected in the region of uranium mining in the Centre North of Portugal, districts of Viseu, Guarda and Coimbra. As the natural radiation background and natural radioactivity in uranium production regions usually are not homogenous and are higher than the average Earth crust, the selection of counties was thoroughly considered. In order to encompass the range of concentrations likely to be found in soils, for this study were selected counties with old uranium mines and waste piles of uranium mining and milling waste, counties with old uranium mines but where there has been no chemical treatment of radioactive ore and thus no milling tailings, and counties with no mines and even no uranium deposits identified. These were the counties of Seia and Celorico da Beira in the district of Guarda, and Campo and Queirã in the district of Viseu. In the Viseu district also the counties of Moreira de Rei (this one with past mining activities and mining waste piles not covered), and Canas de Senhorim (with past mining activity and with waste and milling tailings). The county of Sátão was selected as a comparison term in this region, but this county is mostly on schist and only partly on granite. Another reference area selected were the counties of Serpa and Ourique, in the Alentejo, South of Portugal, with no record of uranium deposits and with clay and schist instead of granites (Figure 1).

Soil samples were collected in agriculture areas, in all these counties, 2 to 6 sites in each. The 20 cm top soil layer was sampled with a spade in 4 sites within a circle of 3 m radius per sampling location, and the soil portions combined in one sample. In the laboratory the soils were dried in the oven at 60ºC, and than sieved through a metallic mesh in order to retain the 63 μm grain size fraction for analysis.

Samples of cabbage leaves, potatoes and fruits, such as oranges, apples and quinces, were collected in each county according to availability. These samples

were carefully washed and only cabbage leaves, peeled potatoes, and pulp of fruits were retained for deep freezing, homogenization and analysis.

The analyses were performed by radiochemical methods followed by radioactivity measurements with Ortec Eg&G OctetePlus alpha spectrometers according to techniques described in detail elsewhere (Oliveira and Carvalho, 2006; Carvalho and Oliveira, 2007). Analytical quality control was performed with analysis of certified reference materials and participation in intercomparison exercises organized by the IAEA (Pham et al., 2006; Povinec et al., 2007). Results are expressed in dry weight for soils and in fresh weight for horticulture products.

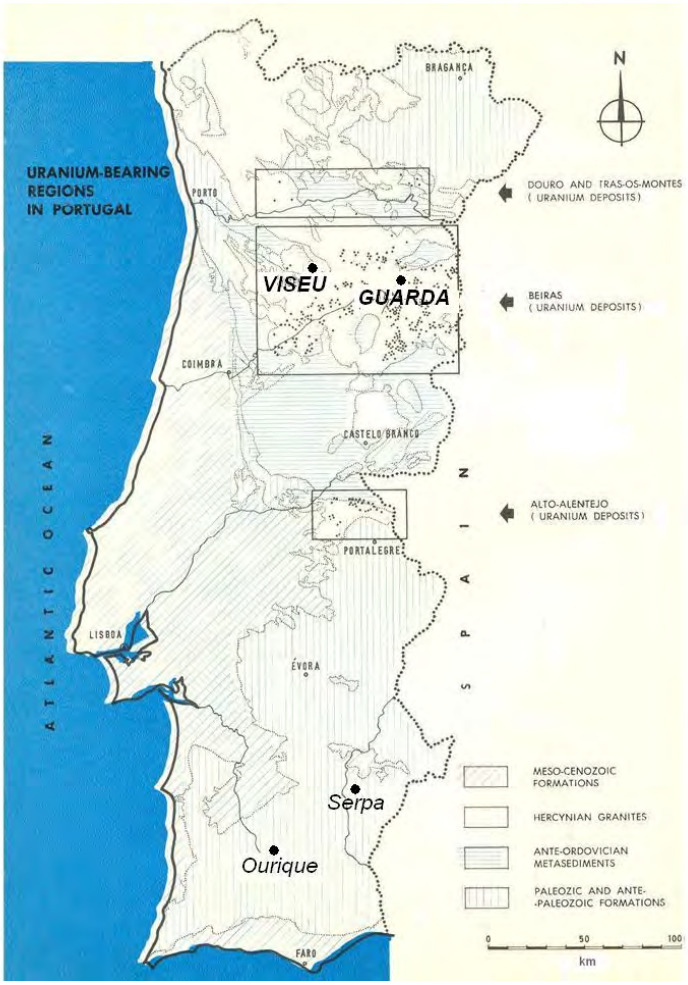

Fig.1. Old uranium mines of Portugal and sampling regions.

Results and discussion

Average radionuclide concentrations in soil samples of several counties are shown in Table 1. In all soils, activity concentrations of uranium (^{238}U) were higher than those of thorium (^{232}Th). In counties with no identified uranium deposits and no uranium mines, radionuclides of the uranium series are in near radioactive equilibrium with the parent radionuclide ^{238}U. In contrast to this, in soils of Canas de Senhorim in average there is higher activity concentration of ^{226}Ra than ^{238}U, and this disruption of secular radioactive equilibrium in soils was introduced by the uranium extraction activity.

Comparing the average levels of radioactivity, the uranium producing counties, especially Moreira de Rei and Canas de Senhorim displayed variable uranium and uranium daughter's concentrations in soils but higher than in the reference counties (Table 1). However, the counties with no uranium mining history display lower but variable background concentrations. For example, Seia and Celorico da Beira, in the granite region also, contain higher uranium concentrations than Sátão which is a county already in the transition to the schist region. Concentrations even lower than in Sátão were measured in soils of Serpa and Ourique, in a region of sedimentary origin of the Alentejo province, south of Portugal, (Figure 1).

Leafy vegetables, such as cabbage, typically displayed ^{238}U concentrations ranging from about 0.1 to 0.6 Bq kg-1 (wet weight) and ^{226}Ra concentrations from 0.5 to 5 Bq kg-1 (wet weight). Cabbage leaves from the county of Canas de Senhorim displayed in average higher concentrations of uranium isotopes and radium than the other counties (Table 2). It must be stressed that cabbage leaves may contain an important contribution of radionuclides from atmospheric depositions, variable from region to region. Although likely to be transferred through food chain as well, their concentration in cabbage leaves, therefore, may not be entirely due to root uptake from the soil. Radioactivity in peeled potatoes is likely to reflect better the plant uptake and accumulation in the tuber with plant growth than cabbage leaves. Potatoes from the county of Canas de Senhorim showed uranium, ^{230}Th and ^{226}Ra concentrations about two orders of magnitude higher than reference counties (Table 3).

Orange pulp, protected from atmospheric depositions, likely reflects also true root uptake of radionuclides. Indeed, oranges grown in the Canas de Senhorim county displayed average concentrations of uranium higher than oranges from reference counties (Table 4). It may be noted, however, that oranges from Sátão contain more ^{226}Ra and ^{210}Po than those from Canas and the same was observed with cabbage (Table 3). This allows hypothesizing that mineralogical and chemical composition of soils and irrigation water, may also contribute to high concentrations of uranium daughters in horticulture products even in the absence of uranium mining waste. Although oranges are prone to concentrate radium, this does not seem the case for apples and quince from the same region (Table 5).

Table 1. Radionuclide concentrations (Bq kg^{-1} dry weight) in soils (fraction <63 μm).

County		^{238}U	^{235}U	^{234}U	^{230}Th	^{226}Ra	^{210}Po=^{210}Pb	^{232}Th
Seia and Celorico (N)	Mean	220	11	228	223	253	241	217
	SD	31	2	22	61	69	44	93
Campo and Queirã (N)	Mean	199	10	219	172	571	300	67
	SD	53	2	58	54	424	92	17
Rio de Mel (M)	Mean	257	12	258	282	370	266	167
	SD	6	0.2	2	3	5	12	3
Moreira de Rei (M)	Mean	602	27	676	652	575	456	187
	SD	119	7	193	92	88	8	41
Sátão (N)	Mean	68	2.8	72	72	118	71	50
	SD	2	0.0	2	2	16	9	2
Canas de Senhorim (MW)	Mean	348	16	352	552	560	525	256
	SD	61	3	71	353	406	412	72
Serpa and Ourique (N)	Mean	26	1.1	26	51	59	29	45
	SD	7	0.4	8	16	15	6	15

(N) No uranium deposits and no mines in the county.
(M) Old uranium mines in the county.
(MW) Old uranium mines and milling waste.

Table 2. Radioactivity in cabbage (mBq kg^{-1} fresh weight).

County		^{238}U	^{235}U	^{234}U	^{230}Th	^{226}Ra	^{210}Pb	^{210}Po	^{232}Th
Seia and Celorico	Mean	58	3	60	70	919	980	-	24
	SD	11	1	12	25	484	533		4
Sátão	Mean	94	4	97	60	1538	-	407	9
	SD	6	1	5	20	629	-	133	3
Canas de Senhorim	Mean	234	11	234	48	2014	-	357	17
	SD	170	9	172	2	1455		134	4
Serpa and Ourique	Mean	10	1.2	16	3.1	92	146	298	4.1
	SD	6	0.0	4	1.3	43	38	182	0.9

Table 3. Radioactivity in potatoes (mBq kg-1 fresh weight).

County		^{238}U	^{235}U	^{234}U	^{230}Th	^{226}Ra	^{210}Pb	^{210}Po	^{232}Th
Sátão	Mean	38	1.2	37	9	64	-	622	5.3
	SD	2	0.3	2	2	4	-	20	1.6
Canas	Mean	350	17	361	267	108	-	162	17
	SD	430	22	443	225	74	-	42	8
Serpa and Ourique	Mean	1.8	0.2	2.0	2.3	7.8	16	4.1	2.8
	SD	0.2	0.1	0.4	0.5	3.3	6	2.3	0.4

Table 4. Radionuclide concentrations (mBq kg^{-1} fresh weight) in oranges.

County		^{238}U	^{235}U	^{234}U	^{230}Th	^{226}Ra	^{210}Pb	^{210}Po	^{232}Th
Sátão	Mean	27	1.4	30	12	748	-	446	4.1
	SD	1	0.3	1	1	46	-	25	0.5
Canas	Mean	20	0.9	19	-	346	-	430	-
	SD	0.3	0.2	1	-	82	-	18	-
Serpa and Ourique	Mean	2.2	0.6	2.8	3.0	15	19	8	2.3
	SD	1.3	0.1	1.8	2.0	6	5	7	1.5

Table 5. Radionuclide concentrations (mBq kg^{-1} fresh weight) in other fruits (apple and quince).

County		^{238}U	^{235}U	^{234}U	^{230}Th	^{226}Ra	^{210}Pb	^{210}Po	^{232}Th
Sátão	Mean	19	1.0	20	-	52	-	238	-
	SD	3	0.2	3	-	27	-	64	-
Canas de Senhorim	Mean	23	1	21	17	92	-	354	5
	SD	11	0.5	10	9.6	44	-	46	2

The overall results show a slight enhancement of uranium series radionuclides in horticulture products grown in kitchen gardens and farms of Canas de Senhorim and Moreira de Rei in comparison with similar products from other counties in the region and in regions of south of Portugal.

Conclusions

Average concentrations of uranium series radionuclides in the soils of uranium mining counties, in particular those of Canas de Senhorim and Moreira de Rei, are slightly elevated above the levels measured in reference counties with no mining activities. Concentrations measured in horticulture products were also in average slightly higher in uranium producing counties. Nevertheless, these enhanced levels are one or two orders of magnitude above concentrations measured in reference counties and, although deserving attention and radiological surveillance, do not seem high enough to cause a noticeable irradiation of the consumers.

References

Carvalho F. P. (2007). Environmental Health Risk from Past Uranium Mining and Milling Activities. *In*: Environmental Health Risk IV, C.A. Brebbia (Ed.), pp 107-114. Wessex Institute of Technology Press, UK.

Carvalho F.P. *(In press).* Past uranium mining in Portugal: legacy, environmental remediation and radioactivity monitoring. UMREG. International Atomic Energy Agency; Vienna.

Carvalho, F.P., Oliveira, J.M., Madruga, M.J., Lopes, I., Libanio, A., Machado L. (2006). Contamination of hydrographical basins in uranium mining areas of Portugal. In: *Uranium in the Environment: Mining Impacts and Consequences*. B.J. Merkel and A. Hasche-Berger Editors, pp 691-702. Springer-Verlag Berlin Heidelberg Publ.

Carvalho, F.P., Oliveira, J.M. (2007). Alpha emitters from uranium mining in the environment. *Journal of Radioanalytical and Nuclear Chemistry* 274: 167-174.

Carvalho, F.P., Oliveira, J. M. Lopes, I. Batista A. (2007). Radionuclides from past uranium mining in rivers of Portugal *Journal of Environmental Radioactivity 98:298-314.*

Nero, J.M. Dias, J.M. Torrinha, A.J., Neves, L.J., Torrinha, J.A. (2005). Environmental evaluation and remediation methodologies of abandoned radioactive mines in Portugal. In: Proceed. of an *International Workshop on Environmental Contamination from Uranium Production Facilities and Remediation Measures*, held in Lisbon 11-13 Feb 2004, pp.145-158. International Atomic Energy Agency, Vienna.

Oliveira, J.M., Carvalho, F.P. (2006). A Sequential Extraction Procedure for Determination of Uranium, Thorium, Radium, Lead and Polonium Radionuclides by Alpha Spectrometry in Environmental Samples. (Proceedings of the 15th Radiochemical Conference). *Czechoslovak Journal of Physics* 56 (Suppl. D): 545-555.

Pham M.K., Sanchez-Cabeza J.A., Povinec P.P., Arnold D., Benmansour M., Bojanowski R., Carvalho F.P., Kim C.K., Esposito M., Gastaud J., Gascó C.L., Ham G.J., Hedge A.G., Holm E., Jaskierowicz D., Kanisch G., Llaurado M., La Rosa, J., Lee S.-H., Liong Wee Kwong L., Le Petit G., Maruo Y., Nielsen S.P., Oh J.S., Oregioni B., Palomares J., Petterson H.B.L., Rulik P., Ryan T.P., Sato K., Schikowski J., Skwarzec B., Smedley P.A., Tajaán S., Vajda N., Wyse E. (2006). Certified reference material for radionuclides in fish flesh sample IAEA-414 (mixed fish from the Irish Sea and North Sea*). Applied Radiation and Isotopes* 64: 1253-1259.

Povinec, P.P., Pham, M., G, Barci-Funel, R. Bojanowski, T. Boshkova, W. Burnett, F.P. Carvalho, et al. (2007). Reference material for radionuclides in sediment, IAEA-384 (Fangataufa Lagoon sediment). *Journal of Radioanalytical and Nuclear Chemistry 273:383-393.*


Uranium Mining
and Hydrogeology

Mechanisms and capacity of sun driven uranium removal in natural and nature-like constructed wetlands

E. Gert Dudel, Kerstin Aretz, Carsten Brackhage, Holger Dienemann, Claudia Dienemann, Martin Mkandawire and Arndt Weiske

TU Dresden, Institut für Allgemeine Ökologie und Umweltschutz, Pienner Strasse 7, 01737 Tharandt, Germany

Abstract. Prerequisites for energetically independent - sustainable- passive water treatment systems are net primary production and a relatively slow to intermediate and turbulence, homogenous, and continuous through flow. Nutrients can be recycled and -if necessary- subsequently artificially applied. However, the situation is different when only the limited sorption capacity of litter, formerly bio-processed or fossil organic carbon (e.g. peat) is used. High regenerative and productive floating and emerse species (like duckweed and common reeds) are only partially in contact with the water and are adapted evolutionary to stagnant or very slow flowing waters. However, they are able to up-concentrate the U in orders of magnitude in the roots through transpiration driven rhizofiltration, and even initiate bio-mineralisation processes. They produce very different degradable litter qualities depending on species and nutritional status. Hence, the U accumulated in duckweed is recycled fast due to microbial decay. Few other species of emerse helophytes produces decay resistant leaf litter. Macrophytic submerse vascular plant and algae are light limited under water and grow relatively slow. A few species remain in vegetative state during winter period. However, some of the species like macrophytic algae *Chara* sp. posses a small ecological adaptation only to and very slow flowing waters, but more have a high U sorption capacity, like microalgae. However the latter grow very fast and are associated in biofilm (periphyton on above named macrophytes and litter) in flowing water, which have a U removal capacity of up-to some hundred mg m^{-2} d^{-1}. Furthermore, most submerse photo-

synthetic active organisms influence changes in milieu conditions (e.g. decrease of PO_4^{3-} concentration, exudation of bioligands, $CaCO_3$ precipitation by CO_2 uptake and pH change) leading to U complexation and co-precipitation. Under suitable sedimentation conditions in slow flowing water, U can be removed by bio-colloids and particulate organic matter (CPOM, FPOM) from detached biofilms and decayed litter. Furthermore, microbial redox-process concentrate up U in sediment but depending on conditions (organic matter quality and quantity in relation to e-acceptors hierarchy and supply, respectively). Based on own measured data and a meta-analysis for slight acid to alkaline and hard, it is estimated that the elimination capacity of the whole system can reach as high as some hundred g U m^{-2} annum^{-1} in temperate climate conditions. Hence, U elimination in sun driven constructed wetlands is possible, however, under a limited set of conditions and needs a patched community approach (ecological engineering in strict sense).

Extracellular defence reactions of rape cells caused by uranium exposure

Katrin Viehweger and Gerhard Geipel

TU Dresden, Institut für Allgemeine Ökologie und Umweltschutz, Pienner Strasse 7, 01737 Tharandt, Germany

Abstract. Uranium is a widespread radioactive toxic heavy metal, released into the biosphere mostly by military purposes and nuclear industry. It is taken up by plant root systems and its chemical toxicity is much more dangerous than the radiological. Thus cell suspensions of rape (*Brassica napus*) revealed specific extracellular defence reactions after uranium exposure. These include characteristic pH-shifts of the culture medium caused by contact with the heavy metal. At the same time a transient release of fluorescent compounds from the cells occurred. These phytoalexins probably belong to the widespread group of flavonoids detected by HPLC and thin layer chromatography (TLC). They are able to interact with uranium and hence can protect the cell against heavy metal poisoning. To gain an insight in these interactions time-resolved laser-induced fluorescence spectroscopy (TRLFS) was performed. Further investigations are under way to identify intracellular defence mechanisms, e.g. spatial patterns of a possible cytoplasmic pH-shift, the formation of proteins possessing thiol groups (phytochelatins), respectively.


Uranium Mining
and Hydrogeology

Microscopic and spectroscopic investigation of U(VI) interaction with monocellular green algae

Manja Vogel, Alix Günther, Johannes Raff and Gert Bernhard

Forschungszentrum Dresden-Rossendorf, Institute of Radiochemistry, P.O. Box 510119, D-01314 Dresden, Germany

Abstract. The green alga *Chlorella vulgaris* has the ability to bind high amounts of uranium(VI) in the pH range from 3 to 6 and to a lesser extend at higher pH values. The uranium removal is almost complete at pH 4.4 and 6 by metabolic active and inactive cells under the given experimental conditions. Laser-induced fluorescence spectroscopy was used for the characterization of uranyl species formed in solutions and biomass. Fluorescence spectroscopic investigations indicate differences of the formed algal uranyl complexes in dependence of the metabolic activity of cells and the uranyl speciation. Scanning electron microscopy demonstrates that the algal cell wall is involved in the binding of U(VI).

Introduction

The green algae (Chlorophyta) belong to the group of aquatic "low" plants, mostly living in fresh water, in salt and/or brackish water, in soils and in tree trunks. Due to the ubiquitous occurrence of algae in nature their influence on the migration processes of uranium and other actinides in biological and geological environments is of fundamental interest. Algae stand at the beginning of the natural food chain and play an economically relevant role as food as well as in food additives so that actinides taken up by algae can make their way into the food chain of humans and pose a health threat.

The monocellular *Chlorella* species are known to possess high binding capacities for heavy metals like copper, cadmium, zinc and lead. Some studies about the sorption behavior of *Chlorella* species regarding uranium were already published. Aim of this study was to characterize the molecular structure of the U(VI) complexes formed on/in metabolic active *C. vulgaris* cells compared to metabolic inactive cells (Günther et al. 2008) using time-resolved laser-induced fluorescence spectroscopy (TRLFS) and the quantitative analysis of the sorption process under

the given experimental conditions. The uranium speciation of algal cells after the sorption process as well as in initial and final media/solutions will be compared at different pH values. Additionally, scanning electron microscopy was used for the visualization of the uranium distribution on the cell surface.

Materials and Methods

Cultivation of algal cells and sorption experiments

C. vulgaris was grown in liquid algal full medium modified from Esser 2000 by replacing yeast extract and sodium acetate with 5 g/l glucose and glycine. The algae were incubated under air supply and light until the culture reaches the end of the exponential growth phase. Culture purity was verified by light microscopy. Living algal cells were harvested by centrifugation and washed with the solution used for the sorption experiments, namely 0.9 % sodium perchlorate, tap water or mineral medium. For the first sorption experiments with metabolic inactive cells, frozen algal biomass was resuspended in 0.9 % sodium perchlorate and incubated with $1 \cdot 10^{-4}$ M uranium. To keep algal cells metabolic active the sorption experiments were performed in bioreactors with tap water or mineral medium. Tap water was used because of its environmental relevance and mineral medium supplies all nutrients necessary for survival and growth of the algae. Mineral medium (Kuhl and Lorenzen 1964) was used without EDTA and with reduced phosphate (Na_2HPO_4 $0.5 \cdot 10^{-6}$ M, NaH_2PO_4 $4.5 \cdot 10^{-6}$ M). The sorption experiments with metabolic active cells started with a biomass concentration of 0.76 g algae dry weight / l and an initial uranium concentration of $1 \cdot 10^{-4}$ M. Immediately after addition of uranium, after 72 h and 120 h samples for fluorescence spectroscopy were taken, biomass was harvested by centrifugation and washed once with 0.9 % sodium perchlorate solution. The uranium concentration in initial and final solutions was quantified by ICP-MS analyses (ELAN 9000, Perkin Elmer). The concentrations of ions in the two growth media relevant for the uranium speciation are compared in Table 1. Dilution series of the algal culture were streaked on agar plates with solid algal full medium (Esser 2000) to determine the number of colony forming units in the day of sampling during the sorption experiments.

Table 1. Overview of relevant ions for uranium speciation in the initial solutions.

	Cl^- [M]	NO_3^- [M]	PO_4^{3-} [M]	SO_4^{2-} [M]	CO_3^{2-} [M]	Na^+ [M]	K^+ [M]	Ca^{2+} [M]	Mg^{2+} [M]
Medium	$2 \cdot 10^{-4}$	$1 \cdot 10^{-2}$	$5 \cdot 10^{-6}$	$1 \cdot 10^{-3}$	$< 1 \cdot 10^{-5}$	$5.5 \cdot 10^{-3}$	$1 \cdot 10^{-2}$	$1 \cdot 10^{-4}$	$1 \cdot 10^{-3}$
Tap water	$8 \cdot 10^{-4}$	$3 \cdot 10^{-4}$	$< 2 \cdot 10^{-6}$	$9 \cdot 10^{-4}$	$1 \cdot 10^{-3}$	$1 \cdot 10^{-3}$	$1 \cdot 10^{-4}$	$1 \cdot 10^{-3}$	$3 \cdot 10^{-4}$

SEM and EDX microanalysis

Scanning electron microscopy (SEM) was carried out with a high-resolution Hitachi S-4800 microscope. Secondary and backscattered electrons were used for the detection applying acceleration voltages of 1 kV (SE) and 10 kV (BSE). The chemical composition of single points (minimum size 1-2 µm) or areas of the uranium-containing depositions on the resuspended algal cells were determined with an energy dispersive X-ray (EDX) microanalysis system INCA (Oxford Instruments). This system employed an integrated Si-detector and S-UTW-window. Depth information up to several µm can be obtained. Details of the method are described in Schmidt et al. 1994.

The uranium containing algal samples were washed with 0.9 % (w/v) sodium chloride solution (pH 7.5) and were fixed in 4 % (w/v) glutaraldehyde (pH 7.5) for 24 h at 4°C. The cells were then washed again with 0.9 % (w/v) sodium chloride and were dehydrated by washing with rising ethanol concentrations. For the SEM- and EDX measurements the dehydrated samples were fixed with sticky conductive carbon tapes on the sample holder. The samples were coated with carbon for a better conductivity.

Time-resolved laser-induced fluorescence spectroscopy (TRLFS)

A Nd-YAG laser (Minilite, Continuum) with laser pulses at 266 nm and a beam energy of about 250 µJ was used for laser-induced fluorescence measurements of sorption experiments with metabolic active cells. The emitted fluorescence light of the initial and final solutions and the algal biomass were detected using a spectrograph (iHR 550, HORIBA Jobin Yvon) and a ICCD camera (HORIBA Jobin Yvon). The TRLFS spectra were recorded from 371.4 nm to 664.3 nm by accumulating 200 laser pulses using a gate time of 2 µs. Computer control over the whole system was ensured by the software Labspec 5. Samples from washed algae, initial and final solutions taken immediately after uranium addition, after 72 h and 120 h of the sorption experiments were used for the detection of uranium(VI) species by fluorescence spectroscopic measurements. A second laser system (described by Günther et al. 2008) with the same settings as written above was used for the laser-induced fluorescence measurements of the sorption experiments with inactive *C. vulgaris* cells after a contact time of 144 h.

Results and Discussion

The uranium speciation in the initial media was calculated with the computer program EQ3/6 (Wolery 1992) using the NEA data base (Guillaumont 2003). The uranium speciation depends on the uranium concentration, the pH values and the ionic strength in the initial media.

Sorption experiments with inactive algal cells were carried out with uranyl perchlorate solution, in which at pH 3 the free uranyl ion is the dominating species at an initial uranium concentration of $1 \cdot 10^{-4}$ M. At pH 6, the uranyl species $(UO_2)_3(OH)_5^+$ (65.4 %), $(UO_2)_4(OH)_7^+$ (18.5 %), UO_2OH^+ (2.7 %) and $(UO_2)_2CO_3(OH)_3^-$ (10.6 %) are the main species. Sorption experiments using metabolic active cells were done in mineral medium and tap water. In the mineral medium at pH 4.4 also the free uranyl ion (57.2 %) dominates the U(VI) speciation. Additionally, UO_2SO_4 (26.83 %) and the hydroxides UO_2OH^+ (6.2 %) and $(UO_2)_2(OH)_2^{2+}$ (5.9 %) are formed in a remarkable amount. In tap water with a pH of 7.1 uranyl carbonates are the main species with $Ca_2UO_2(CO_3)_3(aq)$ (85.12 %), $(UO_2)_2CO_3(OH)_3^-$ (9.89 %) and $UO_2(CO_3)_2^{2-}$ (2.84 %).

The amount of uranium removal from the perchlorate solutions by inactive algal cells depends on different parameters. At higher pH values and longer contact time an increase of binding capacity was detected. With a biomass concentration of 0.75 g algae dry weight / l at pH 3 algal cells could only remove 40 % of the initial uranium, whereas 96 % of the uranium was bound on algal biomass at pH 6. The different sorption behavior of algal cells in perchlorate solution with respect to the investigated pH values could be explained by an increasing deprotonation of functional groups on the surface of algal cells with increasing pH values.

From the tap water with pH 7.1 only low uranium amounts were removed by metabolic active algal cells within 72 h and 120 h (Fig.1). In the end only 30.4 % of the initial uranium amount was bound by the biomass. In contrast to that, algal

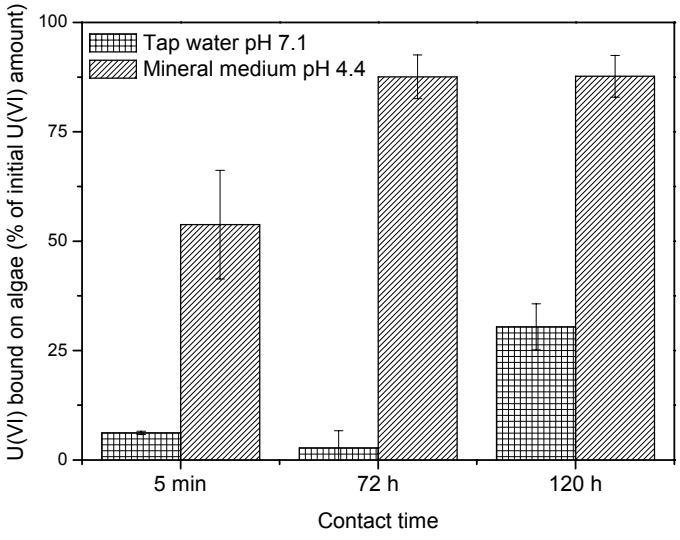

Fig.1. Amount of uranium(VI) immobilized on algal cells in tap water and mineral medium in percent of uranium concentration in initial solutions ($[U(VI)]_{initial}$: 23.8 mg/l ($1 \cdot 10^{-4}$ M)).

cells could remove 87.7 % of the uranium from the mineral medium with pH 4.4. An increase in contact time from 72 h to 120 h did not change the amount of total bound uranium on the biomass. In the mineral medium more than the half of the total uranium (53.8 %) is immobilized by the algal cells within the first few minutes of contact time (Fig.1). Differences in the sorption behavior of the metabolic active *C. vulgaris* cells can be explained by the formation of different uranyl species in tap water and mineral medium due to differences in the chemical composition (Table 1) and pH values of the two media. The uranyl species formed in tap water were poorly accumulated by algal cells. The fact, that in mineral medium nearly no cells survived (0.03 %) because of the high amount of accumulated uranium whereas in tap water 26 % of the cells survived (data not shown), indicates also that several uranium species in tap water are not bio-available for the algae. The results of the sorption experiments show that algal cells bind uranium on their cell surface. Furthermore metabolic active cells are able to take up uranium and/or to immobilize it by active metabolism. In the case of algal cells incubated in mineral medium, uranium directly affect the viability of the cells.

The localization and characterization of the uranyl-algal-complexes on the surface of metabolic inactive algal cells was investigated by Günther et al. (2008) using scanning electron microscopy (SEM) and energy-dispersive X-ray (EDX) microanalysis. The SEM-picture clearly shows the spherical cell shape of *C. vulgaris* (Fig.2a). Uranium is regularly distributed on the cell surface. The EDX analysis of selected areas of the cell surface in Fig.2b showed, additionally to carbon, oxygen and sodium uranium, phosphorus and sulphur as main elements.

The speciation of uranium in tap water, mineral medium, sodium perchlorate solution and bound by the alga *C. vulgaris* was investigated by TRLFS verifying the calculated U(VI) species by determined spectral lines (Fig.3 and Table 2).

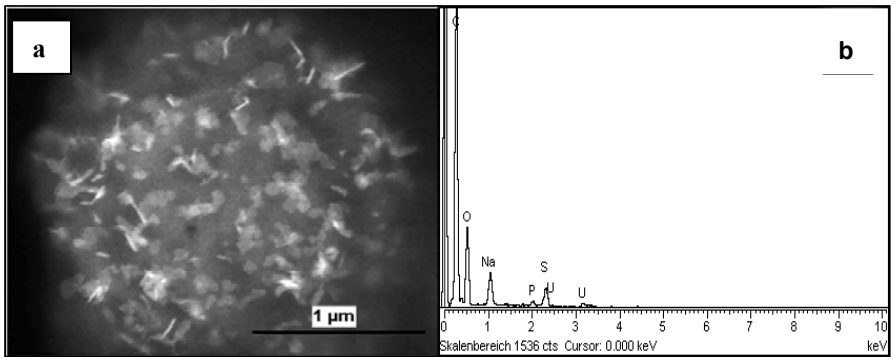

Fig.2. SEM-picture of *Chlorella vulgaris* cell contaminated with uranium at pH 5, coated with carbon (a) and the corresponding EDX-spectrum of cell surface (b).

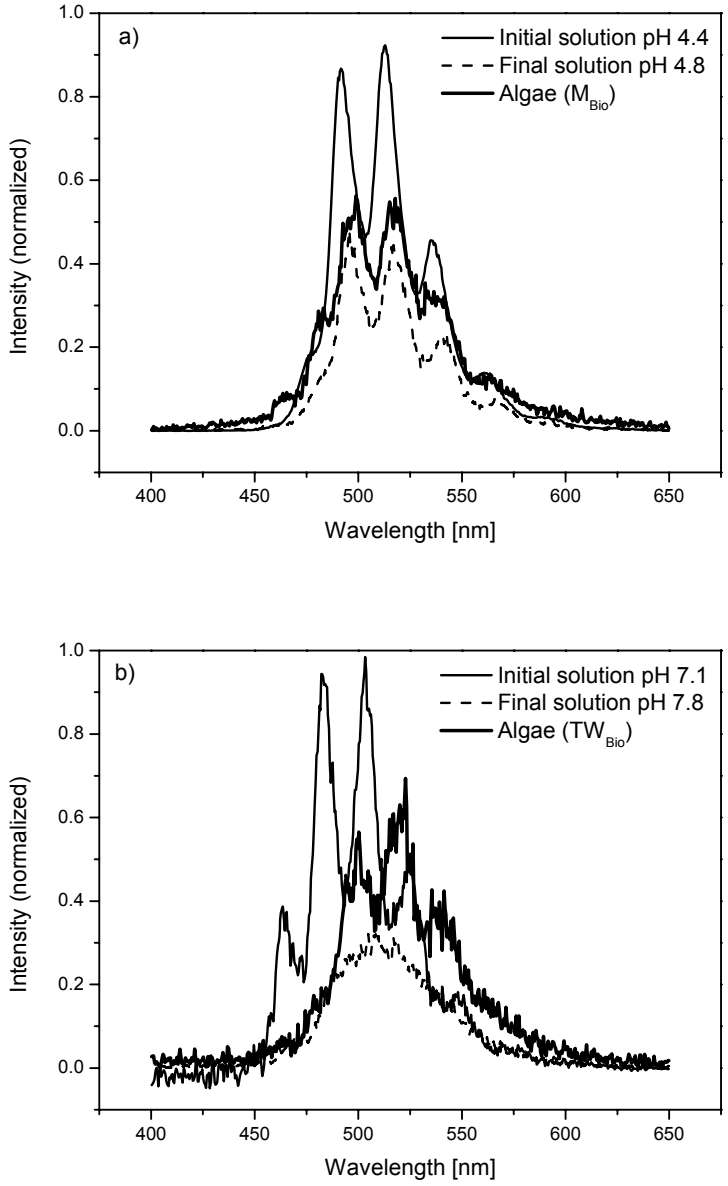

Fig.3. Luminescence spectra of U(VI)-algal complexes formed in mineral medium (a) and tap water (b), the initial solution with $1 \cdot 10^{-4}$ M U(VI) and the final solution after 120 h contact time.

In addition, the luminescence spectra of the different uranyl species were compared to those cited in literature (Table 3). The luminescence spectra show that uranyl species could be detected on/in the algal biomass grown in sodium perchlorate solution with pH 3 (A_{Bio}) and pH 6 (C_{Bio}), in mineral medium (M_{Bio}) and tap water (TW_{Bio}). So uranium remained in the oxidation state (VI) after the immobilization on algal cells. The emission maxima of the uranyl-algae-complexes of the samples A_{Bio} and C_{Bio} are shifted towards higher wavelengths compared to the maxima of the free uranyl ion in initial solution A and of the hydroxides in the initial solution C (Table 2). The uranyl-algae-complexes of the samples M_{Bio} and TW_{Bio} shows also a shift of the emission maxima towards higher wavelengths compared to the maxima of the free uranyl ion mixed with uranyl sulfates in the initial mineral medium and the maxima of the uranyl-carbonates in the initial tap water (Fig.3 and Table 2). This leads to the conclusion that the speciation in the initial solutions and on and/or inside the algal cells differs. The spectra of metabolic inactive algal cells at pH 3 (A_{Bio}) are comparable to those of model uranyl complexes with carboxylic ligands and also with the emission maxima of TW_{Bio}. The positions of the uranyl emission bands in the spectra of inactive algae at pH 6 indicate that uranium is coordinated by phosphate groups (Table 2 and 3). Obviously the uranyl-algae-complexes formed in the sorption experiment with metabolic inactive algal cells at pH 6 (C_{Bio}) (see Table 2) are other ones than those detected in/on metabolic active cells. Between the algal luminescence spectra of the systems M_{Bio} and TW_{Bio} minimal differences in wavelength occurred. However the differences are not high enough to be sure of having two different uranyl-algae-complexes.

Table 2. Luminescence emission bands of uranyl species in algal cells of *C. vulgaris* in comparison to the bands of the sum of uranyl species in uranyl perchlorate (initial solution A and C), mineral medium and tap water.

Sample	Emission bands						
Initial solution A (pH 3)[a]		472.3	489.1	510.2	533.3	558.3	586.9
Solution after contact time (pH 3)[a]		471.1	491.5	512.9	535.7	562.2	590.4
Algae (A_{Bio})[a]		481.6	497.9	518.5	539.3	565.3	595.7
Initial solution C (pH 6)[a]		483.4	497.4	513.2	533.2	555.8	585.7
Algae (C_{Bio})[a]		488.1	504.0	524.9	547.5	571.7	597.4
Initial solution mineral medium (pH 4.4)		475.3	492.5	513.3	536.0	560.8	590.7
Solution after contact time (pH 4.8)		481.0	496.7	517.3	540.4	565.6	594.1
Algae (M_{Bio})	462.2	481.7	497.7	516.8	538.3	564.8	590.0
Initial solution tap water (pH 7.1)	464.8	483.6	503.2	523.6	546.3	575.0	
Solution after contact time (pH 7.8)	Emission bands not definable.						
Algae (TW_{Bio})	465.0	481.8	498.6	519.0	540.2	561.6	590.0

[a] See reference Günther et al. 2008.

Table 3. Luminescence emission bands of different uranyl model compounds and uranium(VI) in other biosystems.

Species	Emission bands (nm)						Reference
UO_2^{2+}	471.3	488.9	510.5	533.9	559.4	585.5	Geipel (1996)
UO_2OH^+	480.7	497.3	518.4	541.3	566.4		Eliet (1995)
$(UO_2)_2(OH)_2^{2+}$	481.3	498.3	519.7	543.4	566.7	602.8	Eliet (1995)
$(UO_2)_3(OH)_5^+$	484	498	514	534	557	583	Sachs (2007)
$UO_2(malonate)_2^{2-}$	479	496	517	542	566		Brachmann (2002)
$UO_2(glycine)_2^{2+}$	478.7	495.3	516.7	540.6	565.0		Günther (2007)
UO_2SO_4		493	514	538	565		Bernhard (1996)
$Ca(UO_2)_2(PO_4)_2 \cdot 8 H_2O$	491.3	501.8	522.9	546.9	572.2	591.7	Geipel (2000)
U(VI) / *Lupine*, shoot		502.4	522.8	549.1	568.7		Günther (2003)
U(VI) / *B. sphaericus*		501.9	523.9	545.8	571.1		Panak (2000)

Interestingly the emission maxima of the spectra of the algae M_{Bio} and TW_{Bio} at the beginning of the sorption experiment (data not shown) lay closer to those of inactive algal cells at pH 6 (C_{Bio}) and shift over time to lower wavelengths. This suggests that the interaction of the uranium alters from the beginning of the experiment to the end. The reason for this may be due to the initial binding of the uranium on the cell surface followed by an uptake of the uranium into the cell by the metabolic active cells. Under the given sorption conditions the TRLFS spectral lines of the metabolic active algal biomass showed that after 120 h the uranium did not interact with phosphate groups on algal cells as it was detected for the metabolic inactive algal cells at pH 6, for higher plants and different strains of bacteria. The results for the uranyl-algae-complex are comparable to those emission maxima obtained for model uranyl complexes with carboxylic ligands (Table 3).

The current study displays that metabolic inactive and active algal cells bind uranium. The characterization of the uranyl complexes formed with the biomass by TRLFS showed that phosphate and carboxylic groups are important functional groups for the binding of uranium by algae depending on the pH values and metabolic activity of the investigated system. Scanning electron microscopy of inactive algal cells supports the results of TRLFS measurements that uranium at pH 6 binds on phosphate groups on the cell surface, because SEM investigations localize uranium in the immediate vicinity to phosphorus (Fig.2). Although the sorption experiments for metabolic active algal cells M_{Bio} and TW_{Bio} also took place in the middle pH range the results are not comparable to those of inactive algal cells

at pH 6 (C_{Bio}). An explanation therefore could be an uptake of uranium into the cells by metabolism leading to TRLFS results for the uranyl algae complex comparable to model uranyl complexes with carboxcylic ligands.

Acknowledgements

The Authors thank U. Schaefer for the ICP-MS measurements and C. Eckardt for the ion exchange chromatography.

References

Bernhard G, Geipel G, Brendler V, Nitsche H (1996) Speciation of uranium in seepage waters of a mine tailing pile studied by time-resolved laser-induced fluorescence spectroscopy (TRLFS). Radiochim Acta 74: 87-91

Brachmann A, Geipel G, Bernhard G, Nitsche H (2002) Study of uranyl(VI) malonate complexation by time-resolved laser-induced fluorescence spectroscopy (TRLFS). Radiochim Acta 90: 147-153

Eliet V, Bidoglio G, Omenetto N, Parma L, Grenthe I (1995) Characterisation of hydroxide complexes of uranium(VI) by time-resolved laser-induced fluorescence spectroscopy. J Chem Soc Faraday Trans 91: 2275-2285

Esser K (2000) Kryptogamen. Springer: Berlin, Heidelberg, New York

Geipel G, Berhard G, Rutsch M, Brendler V, Nitsche H (2000) Spectroscopic properties of uranium(VI) minerals studied by time-resolved laser-induced fluorescence spectroscopy (TRLFS). Radiochim Acta 88: 757-762

Geipel G, Brachmann A, Brendler V, Bernhard G, Nitsche H (1996) Uranium(VI) sulfate complexation studies by time-resolved laser-induced fluorescence spectroscopy. Radiochim Acta 75: 199-204

Guillaumont R, Fanghänel T, Fuger J, Grenthe I, Neck V, Palmer DA, Rand MH (2003) Update on the chemical thermodynamics of uranium, neptunium, plutonium, americium and technetium. Chemical Thermodynamics 5 (OECD Nuclear Energy Agency, ed.) Elsevier, Amsterdam

Günther A, Bernhard G, Geipel G, Reich T, Roßberg A, Nitsche H (2003) Uranium speciation in plants. Radiochim Acta 91: 319-328

Günther A, Geipel G, Bernhard G (2007) Complex formation of uranium(VI) with amino acids L-glycine and L-cysteine: A fluorescence emission and UV-Vis absorption study. Polyhedron 26: 59-65

Günther A, Raff J, Geipel G, Bernhard G (2008) Spectroscopic investigations of U(VI) species sorbed by the green algae Chlorella vulgaris. Biometals 21 (3): 333-341

Kuhl A, Lorenzen H (1964) Handling and culturing of Chlorella. In: Methods in cell physiology, vol. I: 159–187, Academic Press: New York

Panak PJ, Raff J, Selenska-Pobell S, Geipel G, Bernhard G, Nitsche H (2000) Complex formation of (UVI) with Bacillus-isolates from a uranium mining waste pile. Radiochim Acta 88: 71-76

Sachs S, Brendler V, Geipel G (2007) Uranium(VI) complexation by humic acid under neutral pH conditions studied by laser-induced fluorescence spectroscopy. Radiochim Acta 95: 103-110

Schmidt PF, Balk LJ, Blaschke R, Bröcker W, Demm E, Engel L, Göcke R, Hantsche H, Hauert R, Krefting ER, Müller T, Raith H, roth M, Woodtli J (1994) Praxis der Rasterelektronenmikroskopie und Mikrobereichsanalyse. Kontakt & Studium Band 444, Expert Verlag

Wolery TJ (1992) EQ 3/6 a software package for the geochemical modeling of aqueous systems, Report UCRL-MA-110662 part1, Lawrence Livermore National Laboratory, California, USA

Interactions of *Paenibacillus* sp. and *Sulfolobus acidocaldarius* strains with U(VI)

Thomas Reitz, Mohamed L. Merroun and Sonja Selenska-Pobell

Forschungszentrum Dresden-Rossendorf, Institute of Radiochemistry, P.O. Box 510119, 01314 Dresden, Germany

Abstract. The interactions of U(VI) with one representative each of the domains *Bacteria* and *Archaea* are compared. Our results demonstrate that U(VI) is bound by the cells of both microbial strains predominantly through phosphate groups. However, the comparison of the binding capacities and the structural parameters of the formed U(VI) complexes reveals significant differences. In the case of the bacterial strain *Paenibacillus* sp. JG-TB8, U(VI) is precipitated as a uranyl phosphate mineral phase. In contrast, organic phosphate groups are responsible for the U(VI) complexation by the archaeal strain *Sulfolobus acidocaldarius* DSM 639.

Introduction

The cessation of the intensive uranium mining and milling activities in the southeast part of Germany (Saxony and Thuringia) in 1990 left million tons of radioactive contaminated sludges and a large number of waste piles (Hagen and Jakubick 2005). The release of uranium from such sites into the environment is a subject of great public concern due to the chemical and radiological toxicity of this radionuclide. For the development of effective remediation strategies and reliable risk assessment, consolidated knowledge about the uranium behavior in contaminated sites is necessary. Beside the interactions with inorganic soil components, an important role in the migration behavior of uranium play the naturally occurring microorganisms. They can interact in multiple ways with radionuclides and other heavy metals in the environment via biosorption, bioaccumulation, biomineralization, and biotransformation processes (Lloyd and Macaskie 2002; Selenska-Pobell 2002; Merroun et al. 2005; Pedersen 2005). Microbial strains isolated from uranium contaminated sites were used as model systems for the investigation of these interaction mechanisms. A high number of studies were dedicated to elucidate the bacterial processes responsible for the binding of uranium. However, little is

known about the processes implicated in the complexation of this radionuclide by representatives of the second microbial life domain, the "*Archaea*".

The objective of the present work was to investigate whether the structural differences between the cell surfaces from representatives of archaea and bacteria influence the local coordination of U bound to the cells, at molecular scale using X-ray absorption spectroscopy (XAS).

XAS is among the few analytical methods that can provide information on the chemical environment of actinides in microbial samples at dilute metal concentrations. XAS is a nondestructive method, and no sample reduction or digestion is required which would alter the chemistry of the element of interest. The two microbial strains used are: *Paenibacillus* sp. JG-TB8, a bacterial uranium waste pile isolate, and *S. acidocaldarius* DSM 639, an archaeal strain, which was found in comparable soil samples.

Materials and Methods

Microbial strains and growth conditions

Paenibacillus sp. JG-TB8 was isolated from an anaerobic microbial consortium enriched from a soil sample of the uranium mining waste pile Haberland in Saxony. The strain was cultured in Luria Broth medium at 30°C. *Sulfolobus acidocaldarius* DSM 639 was obtained from the "German Collection of Microorganisms and Cell Cultures" and cultured at pH 2.5 and 70°C in a mineral salt medium (Brock et al. 1972) supplemented with 0.1% tryptone and 0.005% yeast extract.

U biosorption kinetics

The microbial cells grown to the late exponential phase were harvested by centrifugation and washed twice with 0.1M $NaClO_4$ (pH 4.5). The cells were resuspended and shaken in triplicate for 5, 10, 20, 30, 60, 120 min, at 30°C in 10 ml uranium solution (0.5mM $UO_2(NO_3)_2 \cdot 6\ H_2O$, pH 4.5). We used 0.1M $NaClO_4$ as a background electrolyte. Cells were then harvested and the metal content of the supernatants were analyzed by ICP-MS. To determine the amount of the bound uranium per gram of dry cell mass, parallel samples were weighed after drying for 48h at 70°C.

X-ray absorption spectroscopy (XAS) measurements

For the XAS studies, a similar procedure as described above was used for the sample preparation (0.5mM U, pH 4.5, 48 h). After contact with the uranium solu-

tion, cells were harvested and washed with 0.1M $NaClO_4$. The pelleted samples were dried in a vacuum incubator at 30°C for 24 h and powdered.

Uranium L_{III}-edge X-ray absorption spectra were collected at the Rossendorf Beamline at the European Synchrotron Radiation Facility (ESRF), Grenoble (France) (Matz et al. 1999) using a Si(111) double-crystal monochromator, and Si-coated mirrors for focusing and rejection of higher harmonics. The data were collected in fluorescence mode using a 13-element Ge detector. The energy was calibrated by measuring the yttrium (Y) K-edge transmission spectrum of an Y foil and defining the first inflection point as 17038 eV. The Extended X-ray Absorption Fine Structure (EXAFS) oscillations were isolated from the raw, averaged data by removal of the pre-edge background, approximated by a first-order polynomial, followed by μ_0-removal via spline fitting techniques and normalisation using a Victoreen function. Dead-time correction was applied. The ionisation energy for U L_{III}-electron, E_0, was arbitrarily defined as 17185 eV for all averaged spectra. The EXAFS spectra were analysed according to standard procedures using the program EXAFSPAK (George and Pickering 1995). The theoretical scattering phase and amplitude functions used in data analysis were calculated using FEFF8 (Ankudinov et al. 1998) using the crystal structure of meta-autunite, $Ca(UO_2PO_4)_2 \cdot 6\,H_2O$ (Makarov and Ivanov 1960). All fits included the four-legged multiple scattering (MS) path of the uranyl group, U-O_{ax}-U-O_{ax}. The coordination number (N) of this MS path was linked to N of the single-scattering (SS) path U-O_{ax}. The radial distance (R) and Debye-Waller (σ^2) factor of the MS path were linked at twice the R and σ^2 of the SS path U-O_{ax}, respectively (Hudson et al. 1996). During the fitting procedure, N of the U-O_{ax} SS path was held constant at two. The amplitude reduction factor was held constant at 1.0 for FEFF8 calculation and EXAFS fits. The shift in threshold energy, ΔE_0 was varied as a global parameter in the fits.

Results and Discussions

Biosorption of uranium

Biosorption describes a metabolism-independent sorption of radionuclides and other heavy metals to biomass from even very dilute aqueous solutions. Negatively charged cell surface groups including phosphate, carboxylic, or hydroxylic residues are the main ligands responsible for the complexation of metals (Ferris and Beveridge 1986).

The uranium binding capacities of the cells of *Paenibacillus* sp. JG-TB8 and *S. acidocaldarius* as function of time are presented in Fig. 1. The results demonstrated that the saturation of the binding sites was reached for both strains after an incubation time of about 30 minutes. The binding capacity of the bacterial cells

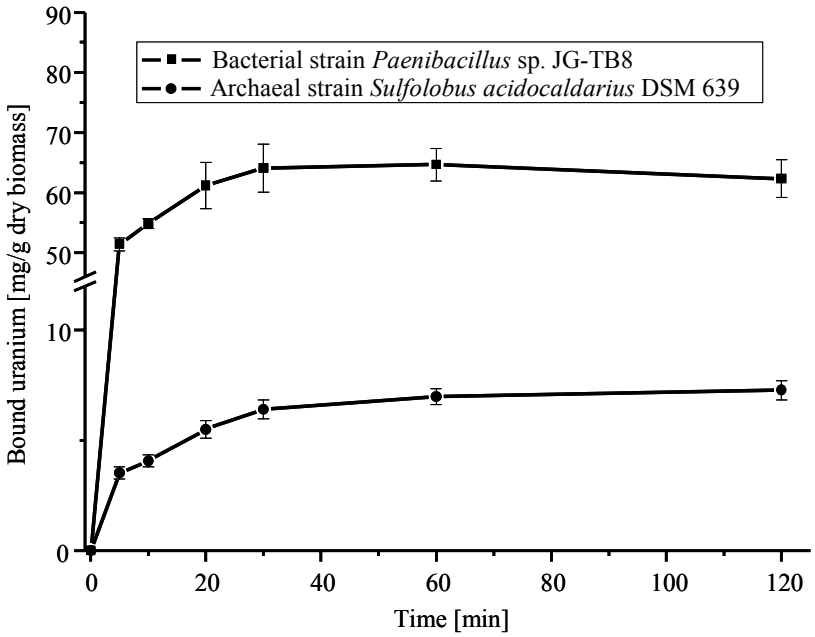

Fig.1. Sorption kinetics of uranium by the cells of *Paenibacillus* sp. JG-TB8 and *S. acidocaldarius* DSM 639 from a 0.5mM uranyl nitrate solution in 0.1M $NaClO_4$ (pH 4.5).

(65 ± 4 $mg/g_{dry\ mass}$) was determined to be about ten times higher than those of the archaeal cells (7 ± 0.4 $mg/g_{dry\ mass}$).

This difference on the U binding abilities of both microbial strains could be due to the structural differences between their cell surfaces. The cells of *S. acidocaldarius* are covered with a cytoplasma membrane surrounded by a membrane-anchored proteinaceous surface layer (S layer). The latter represents the only cell wall component of this archaeal species. Because of the low content of negatively charged amino acids and the absence of phosphorylated sites, this S-layer seems to be ineffective in the complexation of uranium. In this case a small amount of uranium might pass through the pores of the S-layer and is complexed by the reactive groups of the cytoplasma membrane. The cells of *Paenibacillus* sp. JG-TB8 possess a more complex cell wall structure, which includes a thick layer of peptidoglycan that is rich on phosphate and carboxylic groups and represents the major metal binding component of this bacterium.

X-ray absorption spectroscopy

X-ray Absorption Near-Edge Structure (XANES) analyses of the uranium complexes formed by the cells of both microbial strains indicated that U is present in these samples as U(VI) (data not shown).

The local coordination of U(VI) associated to the microbial cells at molecular scale was studied using EXAFS spectroscopy. The uranium L_{III}-edge k^3-weighted EXAFS spectra of the U species bound to the cells of *Paenibacillus* sp. JG-TB8 and *S. acidocaldarius* DSM 639, the reference compounds (meta-autunite and U-fructose 6-phosphate) as well as their corresponding Fourier Transforms (FT) are presented in Fig. 2. The peaks of the FT's are not corrected for EXAFS phase shift and therefore located at lower R-values (R+Δ) than the true near-neighbor distances (R).

In both U/microbial samples, quantitative fit results (data not shown) indicated that the adsorbed U(VI) has the common linear trans-dioxo structure: two axial

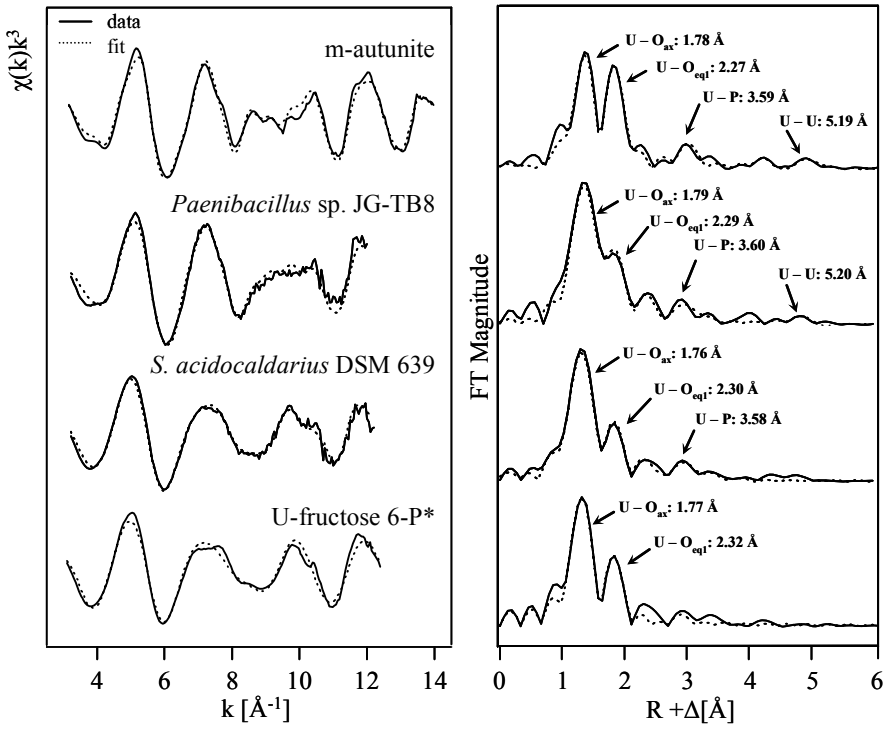

Fig.2. Uranium L_{III}-edge k^3-weighted EXAFS spectra (left) and corresponding Fourier transforms (right) of the uranium complexes formed by the cells of *Paenibacillus* sp. JG TB8 and *S. acidocaldarius* DSM 639 and those of the reference compounds, meta-autunite and U-fructose 6-P (*Koban et al. 2004).

oxygens at about 1.76 - 1.79 Å, and an equatorial shell of 4 to 6 oxygens at 2.29 - 2.30 Å. The U-O_{eq1} bond distance is within the range of previously reported values for phosphate bound to uranyl (Hennig et al. 2001; Merroun et al. 2002, 2003, 2005). The FT spectra of the U-treated microbial samples contain an FT peak at about R+Δ ~ 2.3 Å, interpreted as a contribution from oxygen neighbors (O_{eq2}). The fourth FT peak, which appears at R+Δ ~ 3 Å (radial distance R = 3.58 - 3.62 Å) is a result of the back-scattering from phosphorus atoms. This distance is typical for a monodentate coordination of U(VI) by phosphate (Hennig et al. 2001; Merroun et al. 2002, 2003, 2005).

In the case of the acidophilic and thermophilic archaeon *S. acidocaldarius* DSM 639, the high Debye-Waller factor of the U-O_{eq1} (second coordination shell in the FT) shell suggests the existence of more than one oxygen bond in the equatorial plane. The shell may be split into a shorter U-O_{eq1} distance, from the back-scattering contribution of phosphate oxygen(s) in a monodentate binding mode, and a longer bond distance from oxygen(s) of hydroxyl or carboxyl groups. The phosphate groups implicated in the coordination of U could have organic origin since the EXAFS spectrum shows high similarity to those resulting from the uranium complexes with organic phosphate groups, e.g. fructose phosphates (Koban et al. 2004).

Interestingly, the EXAFS spectrum of the U/*Paenibacillus* sp. sample is similar to that of meta-autunite (Hennig et al. 2001) with regard to the U-O_{eq}, U-P and U-U distances, suggesting that a similar inorganic uranyl phosphate phase was precipitated by the bacterial cells at pH 4.5, probably caused by the release of inorganic phosphates by the cells resulting from microbial activity.

In accordance to this an acidic phosphatase activity was demonstrated in the studied bacterial strain. This enzyme liberates inorganic phosphate groups, which were shown to be responsible for the uranium complexation and biomineralization (Martinez at al. 2007). Transmission electron microscopic studies coupled with energy dispersive X-ray analysis demonstrated that the formed precipitates are located at the cell surface and also intracellularly, as needle like fibrils and in polyphosphatic bodies (not shown).

The results presented in this work indicated that the cells of the investigated strains, *Paenibacillus* sp. JG-TB8 and *S. acidocaldarius* DSM 639, interact with uranium through different mechanisms, including biosorption at the cell surface and biomineralization processes. These microbial processes may influence the fate and migration of uranium in contaminated sites.

Acknowledgements

We thank A. Scheinost, A. Rossberg, C. Hennig, and H. Funke for their help in the EXAFS measurements and U. Schaefer for ICP-MS measurements.

References

Ankudinov A L, Ravel B, Rehr J J, Conradson S D (1998) Real-space multiple-scattering calculation and interpretation of X-ray absorption near-edge spectra. Phys Rev B 58: 7565-7575

Brock T D, Brock K M, Belly R T, Weiss R L (1972) Sulfolobus: A new genus of sulfur-oxidizing bacteria living at low pH and high temperature. Arch Microbiol 84: 54-68

Ferris F G, Beveridge T J (1986) Site specificity of metallic ion binding in *Escherichia coli* K-12 lipopolysaccharide. Can J Microbiol 32: 52-55

George G N, Pickering I J (1995) EXAFSPAK: A suite of computer programs for analysis of X-ray absorption spectra. Stanford Synchrotron Radiation Laboratory, Stanford, CA, USA

Hagen M, Jakubick A T (2005) Returning the Wismut legacy to productive use. *In*: Uranium in the environment, Springer Verlag, Berlin, Germany: 11-26

Hennig C, Panak P, Reich T, Roßberg A, Raff J, Selenska-Pobell S, Matz W, Bucher J J, Bernhard G, Nitsche H (2001) EXAFS investigation of uranium(VI) complexes formed at *Bacillus cereus* and *Bacillus sphaericus* surfaces. Radiochim Acta 89: 625-631

Hudson E A, Allen P G, Terminello L J (1996) Polarized X-ray absorption spectroscopy of the uranyl ion: comparison of experiment and theory. Phys Rev B 54: 156-165

Koban A, Geipel G, Roßberg A, Bernhard G (2004) Uranium(VI) complexes with sugar phosphates in aqueous solution. Radiochim Acta 92: 903-908

Lloyd J R, Macaskie L E (2002) Biochemical basis of microbe-radionuclide interactions. *In*: Interactions of bacteria with radionuclides. Elsevier Science, Oxford, UK: 313-342

Makarov E S, Ivanov V I (1960) The crystal structure of meta-autunite, $Ca(UO_2)_2(PO_4)_2 \cdot 6H_2O$. Doklady Akademi Nauk SSSR 132: 573-577

Martinez R J, Beazley M J, Taillefert M, Arakaki A K, Skolnick J, Sobecky P A (2007) Aerobic uranium (VI) bioprecipitation by metal-resistant bacteria isolated from radionuclide- and metal-contaminated subsurface soils. Environ Microbiol 9: 3122-3133

Matz W, Schell N, Bernhard G, Prokert F, Reich T, Claußner J, Oehme W, Schlenk R, Dienel S, Funke H, Eichhorn F, Betzel M, Pröhl D, Strauch U, Hüttig G, Krug H, Neumann W, Brendler V, Reichel P, Denecke M A, Nitsche H (1999). ROBL- a CRG beamline for radiochemistry and material research at the ESRF. J Synchrotron Rad 6: 1076-1085

Merroun, M L, Hennig C, Rossberg A, Geipel G, Reich T, Selenska-Pobell S (2002) Molecular and atomic analysis of the uranium complexes formed by three eco-types of *Acidithiobacillus ferrooxidans*. Biochem Sc Trans 30: 669-672

Merroun, M L, Hennig C, Rossberg A, Reich T, Selenska-Pobell S (2003) Characterization of U(VI)-*Acidithiobacillus ferrooxidans* complexes by using EXAFS, transmission electron microscopy and energy-dispersive X-ray analysis. Radiochim Acta 91: 583-591

Merroun, M L, Raff J, Rossberg A, Hennig C, Reich T, Selenska-Pobell S (2004) Interaction of U(VI) with bacterial strains isolated form uranium mining piles: spectroscopic and microscopic studies. Geochim Cosmochim Acta 68: A499

Merroun, M L, Raff J, Rossberg A, Hennig C, Reich T, Selenska-Pobell S (2005) Complexation of uranium by cells and S-layer sheets of *Bacillus sphaericus* JG-A12. Appl Environ Microbiol 71: 5542-5553

Pedersen K (2005) Microorganisms and their influence on radionuclide migration in igneous rock environments. J Nucl Radiochim Sci 6: 11-15

Selenska-Pobell S (2002) Diversity and activity of bacteria in uranium waste piles. *In*: Interactions of microorganisms with radionuclides. Elsevier, Oxford, UK: 225-254

Comparison of elimination capacity of uranium from the water pathway between periphytic algae, submerse macrophytes and helophytes (emerse vascular plants)

Kerstin Aretz and E. Gert Dudel

TU Dresden, Fakultät Forst-, Geo-, Hydrowissenschaften, Fachrichtung Forstwissenschaften, Institut für Allgemeine Ökologie und Umweltschutz, Pienner Str. 19, 01737 Tharandt, aretzkerstin@gmx.de

Abstract. One of the uranium-mining legacies is contamination of ground and surface waters with high toxic substances, including radioactive isotopes. Due to limited applicability of chemical cleaning procedures for such waters, the need for alternative technology has grown considerably. It was earlier observed that helophytes, emerse and submerse macrophytes and algae act as excellent sinks of uranium in wetlands (Brackhage & Dudel 2005, Mkandawire & Dudel 2005, Vogel & Dudel 2004, Vogel & Dudel). Thus, the proportion percentages range of uranium in organic matter (decayed litter) can be high too. However, the species specific elimination capacity of uranium on a specific area remains unknown, for example, under aerobic neutral to alkaline conditions with slightly soluble and mobile uranium. Consequently, we investigated and compared the uranium bioaccumulation capacity between higher aquatic plants, submerse macrophytes and their associated algae ("biofilm") in synthetic mine water (but without sediments) in the flowing-water simulation research facility of Federal Environmental Agency (UBA). The synthetic mine water was based on water quality and conditions in the "tailings" down stream of former uranium mine at Neuensalz-Mechelgrün, Vogtland (Saxony), which has P-Limitation, pH 7.2 ± 0.6, conductivity 600 to 700 µS cm^{-1}, and uranium concentration of about 200 µg L^{-1}. Under these conditions, helophytes (i.e. *Phragmites australis* TRIN. ex STEUD., *Typha latifolia* L. *Sparganium erectum* L.) accumulated up to 130 mg kg^{-1} uranium in dry matter during

summer, between 50 and 70% of the uranium accumulated in the roots, especially in *P. australis*. Submerse macrophytes take up even uranium more than helophytes that some could even accumulate ten-fold more. For instance, *Elodea canadensis* MICHX. accumulated up to 150 mg kg^{-1} DW; mill foil (*Myriophyllum spicatum* L.) had maximum accumulation of 1600 mg U kg^{-1} DW. Mill foil has feathered leaf structures, which probably provided comparatively large surface with high number of uranium sorption sites. Further the older leaves are carries for associated microalgae in biofilms, which have high biomass turn over and accumulation capacity too due to high surface volume ratio. Therefore, the autotrophic microphytes or periphyton ("biofilms") play a key role in the elimination of uranium from the water pathway.

References

Brackhage C, Dudel EG (2005). Immobilisation of Uranium from Mining Leachates using Wetlands: The Role of Macrophytes. International Symposium on Wetland Pollutant Dynamics and Control, September 4-8, 2005, Ghent, Belgium. Book of Abstracts, pp. 18-19.

Mkandawire M, Dudel EG (2005). Accumulation of arsenic in Lemna gibba L. (duckweed) in tailing waters of two abandoned uranium mining sites in Saxony, Germany. Science of the Total Environment, 336(1-3): 81-89.

Vogel K, Dudel, EG (2004). Deutschen Gesellschaft für Limnologie, Tagungsbericht 2004 (Potsdam), Weißensee Verlag, Berlin: 486-490.

Vogel K, Dudel, EG (2005). Deutschen Gesellschaft für Limnologie, Tagungsbericht 2005 (Karlsruhe), Weißensee Verlag, Berlin: 465-470.

Microbial transformations of uranium in wastes and implication on its mobility

Arokiasamy J. Francis

Environmental Sciences Department, Brookhaven National Laboratory, Upton, New York 11973 USA

Abstract. Uranium exists in several chemical forms in mining and mill tailings and in nuclear and weapons production wastes. Under appropriate conditions, microorganisms can affect the stability and mobility of U in wastes by altering the chemical speciation, solubility and sorption properties and thus could increase or decrease the concentrations of U in solution and the bioavailability. Dissolution or immobilization of U is brought about by direct enzymatic action or indirect non-enzymatic action of microorganisms. Although the physical, chemical, and geochemical processes affecting dissolution, precipitation, and mobilization of U have been extensively investigated, we have only limited information on the mechanisms of microbial transformations of various chemical forms of U in the presence of electron donors and acceptors.

Uranium in wastes

Uranium in wastes is present in various chemical forms and may eventually exist in the environment as elemental, oxide, coprecipitates, ionic, inorganic-, and organic-complexes, and naturally occurring minerals depending on the process and waste stream. Uranium in ores is present as uraninite and pitchblende and in secondary mineral phases associated with silicates, phosphates, carbonates, and vanadates (Katz et al., 1986). The concentration of uranium can vary between 0.5 and 20%, with the highest amount occurring in Canadian ores. Mill tailings, a by-product of the mineral extraction process, contain up to 2% uranium. The treatment process residues contain sulfates, ammonia, tertiary amines, and organic solvents (Metzler 2004). Carbonate leaching has been used for *in situ* extraction of uranium. The residual uranium that has not been extracted may be present as a result of newly formed insoluble mineral phases (e.g. $CaSO_4$, $MgCO_3$, $Fe(OH)_3$)

which provide surface sites for uranium adsorption (Bostick et al., 2002). However, there is lack of information on the chemical characterization of uranium in various waste forms. Uranium in the environment exists predominantly as U(VI) and U(IV) oxidation states while the former is more soluble and the latter quite insoluble and mobile.

Biotransformation of Uranium

Microbial activity could affect the chemical nature of U by altering the speciation, solubility and sorption properties and thus could increase or decrease the concentration in solution and their bioavailability. Under appropriate conditions, dissolution or immobilization of U is brought about by direct enzymatic or indirect non-enzymatic actions of microorganisms. These include (i) oxidation-reduction reactions, (ii) changes in pH and Eh, (iii) chelation or production of specific sequestering agents, (iv) bioaccumulation by biomass, (v) biocolloid formation, (vi) bioprecipitation, and (vi) biotransformation of radionuclide-organic and -inorganic complexes (Francis, 1990). Both aerobic and anaerobic microorganisms are involved in the mobilization and immobilization of various chemical forms of U.

Dissolution of Uranium

Dissolution of uranium in ores by autotrophic sulfur- and iron-oxidizing bacteria is due to production of sulfuric acid and by heterotorphic bacteria and by fungi due to production of organic acids and chelating agents has been well documented in the literature (Francis 1990).

Autotrophic microbial activity. The chemical and biochemical mechanisms involved in microbial leaching or biomining of metals have been extensively studied and are used commercially for extracting copper and uranium from ores. The iron and sulfur oxidizing bacteria play a significant role in the solubilization of uranium from ores and in mill tailings. The role of autotrophic bacteria *Thiobacillus ferrooxidans* in the extraction of uranium from ore is due to indirect and direct actions. The indirect mechanism is confined to its generating the oxidizing agent, ferric sulfate, and the solvent sulfuric acid and to the involvement of Fe^{2+}/Fe^{3+} in cyclically mediating the oxidation of insoluble uranium oxide to soluble uranyl ion $UO_2 + Fe^{3+} \rightarrow UO^{2+}{}_2 + Fe^{2+}$, whereas the direct action involves the oxidation of $UO_2 \rightarrow UO^{2+}{}_2$ without using the Fe^{2+}/Fe^{3+} complex as the chemical electron carrier.

Heterotrophic microbial activity. Dissolution of metals by heterotrophic microorganisms is due to production of organic acid metabolites, as well as lowering of the pH of the medium from the metabolism of organic compounds. In many cases, a combined effect is important. For example, when organisms secrete organic acids which may have a dual effect in increasing U dissolution by lowering

pH, and by complexation. Microbially produced dicarboxylic acids, ketogluconic acid, polyhydroxy acids, and phenolic compounds, such as protocatechuic acid, and salicylic acid are effective chelating agents and are known to accelerate their movement in soils. A wide variety of heterotrophic microorganisms, such as *Bacillus sp., B. luteus, B. subtilis, B. cereus, B. pumilis, Pseudomonas striata, P. viscosa, P. perolens, P. choloroaphis, Achromobacter xerosis, A. stoloniferum, and A. healii* may be involved in solubilizing uranium from granitic rock where uranium is generally present as an oxide (Bhurat et al., 1973). Such solubilization is due to the production of organic-acid metabolites, such as oxalic, isocitric, citric, succinic, hydrobenzoic, and coumaric acids via their carboxylic and phenolic groups (Berthelin and Munier-Lamy, 1983; Bloomfield and Kelso, 1973; Bloomfield and Pruden, 1975; Bloomfield et al., 1971). When microorganisms are grown in an iron-deficient medium, they elaborate specific iron chelators, such as siderophores. Iron-sequestering agents could play an important role in the complexation of radionuclides and so increase their solubility. *Pseudomonas aeruginosa* CSU, grown in the presence of uranium or thorium, elaborated several metabolic products which complexed both elements (Premuzic et al., 1985).

Immobilization of Uranium

The immobilization of uranium is brought about by bioaccumulation, bioreduction and bioprecipitation reactions. Uranium is reduced by a wide variety of facultative and strict anaerobic bacteria under anaerobic conditions in the presence of suitable electron donor. Microbially mediated U reductions play an important role in the biogeochemical cycles of U. Consequently, the potential exists for the use of anaerobic bacteria to concentrate, contain and stabilize uranium in contaminated groundwaters and in waste with concurrent reduction in waste volume. However, the long-term stability of bacterially reduced uranium in the natural environment is not known.

Biosorption and bioaccumulation of uranium. Biosorption and bioaccumulation of uranium has been observed in a wide range of microorganism (Sakaguchi, 1996; Strandberg et al 1981). It is still one of the intensely investigated areas of research because of the potential use of biomass to remove uranium from waste streams. Uranium forms complexes with the carboxylate, phosphate, amino, and hydroxyl functional groups present on the cell surface; and intracellularly, by binding to anionic sites or precipitating as dense deposits. Nuclear magnetic resonance spectroscopy (NMR), time resolved laser fluorescence spectroscopy (TRLFS), and extended X-ray fluorescence spectroscopy (EXAFS) have been used to determine the functional groups involved in the complexation of U with bacteria.

Extracellular and intracellular association of U with bacteria was observed but the extent of its accumulation differs greatly with the species of bacteria. Extracellular association of uranium with bacterial cell surfaces is primarily due to physical- and chemical- interactions involving adsorption, ion exchange, and complexa-

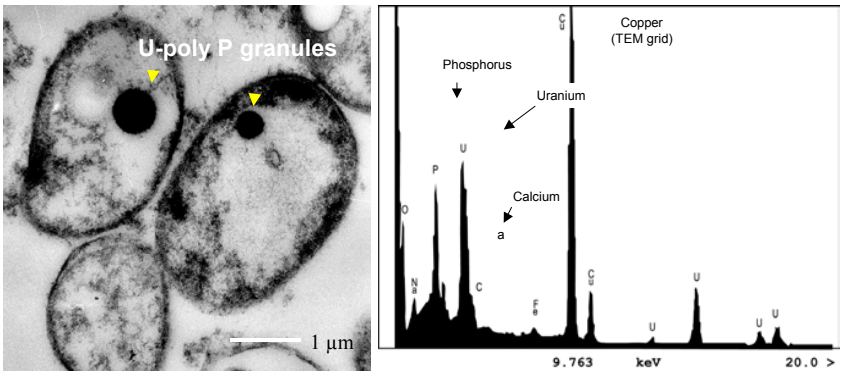

Fig.1. Intra- and extra- cellular accumulation of Uranium by *Halomonas* sp. After exposure to U, EDS shows U and P as the major constituents of the intracellular granules (Francis et al., 2004).

tion and does not depend on metabolism. Bacterial cell walls, exopolymers, proteins, and lipids contain functional groups, which are able to bind uranium. In *Halomonas* sp. U accumulated as electron-dense intracellular granules and was also bound to the cell surface (Figure 1). EXAFS analysis of the association of U with halophilic and non-halophilic bacterial cells showed that it was associated predominantly with phosphate as uranyl hydrogen phosphate and additional forms of phosphate such as hydroxophosphato or polyphosphate complexes as well as other ligands such as carboxyl species (Francis et al., 2004). These results demonstrate that phosphate, including the polyphosphates, bind significant amounts of uranium in bacteria.

Intracellular accumulation involves transporting the metal across the cell membrane, which depends on the cell's metabolism. The intracellular transport of the U into the cell involves an as-yet unidentified transport system. Uranium transport across bacterial cell membranes may be mediated by the mechanism used to convey metabolically essential ions; however, additional studies are needed to clarify the exact mechanism involved.

Polyphosphates are widely distributed throughout the bacterial cell. Numerous and varied biological functions are performed by polyphosphate including phosphate storage in the cell, a reservoir of energy for cellular functions, a chelator of metals (e.g., Mn^{2+} and Ca^{2+}), a pH buffer, a capsule for bacteria, and in physiological adjustments to growth, development, stress, and deprivation. In particular, the polyphosphates play a vital role in the dynamics of metabolic adjustments of cells to stationary phase and their survival in response to a variety of nutritional limitations and environmental stresses. The amount of polyphosphate that is stored by cells varies between bacterial species, and is determined in part by the rate at which it can be degraded for example, in response to the presence of metals, and the amount of inorganic phosphate secreted into the medium. In as much as all of

uranium exposure studies reported were conducted with cells in the stationary phase, the cells are responding to heavy metal stress by releasing phosphate from the mineralization of cellular polyphosphate.

Bioreduction of uranium. A wide variety of facultative and strict anaerobic bacteria reduced U(VI) added as uranyl-nitrate or uranyl carbonate to U(IV) under anaerobic conditions (Wall and Krumholz, 2006). These include axenic cultures of iron-reducing, fermentative, and sulfate-reducing bacteria. Mixed cultures of bacteria in uranium contaminated ground waters and in wastes also reduced uranium. However, the stability of bioreduced uranium is a major concern because they can be readily reoxidized to the soluble U(VI)from. Metals associated with or coprecipitated with iron and manganese oxides and hydroxides can be remobilized due to reduction of host metal Fe^{3+} and Mn^{4+} (hydro)oxides either chemically or enzymatically (Stone and Morgan, 1987; Francis and Dodge, 1990) under anaerobic conditions.

Biotransformation of uranium complexed with organic ligands

Naturally occurring soluble organic complexing agents present at the uranium-contaminated sites may not only affect the mobility of uranium but also affect the microbial transformation and reductive precipitation of uranium. Biotransformation of the complexed uranium should result in its precipitation and retard migration. There is a paucity of information on the mechanisms of microbial transformations of uranium complexed with naturally occurring low molecular weight soluble organic ligands.

We investigated the mechanisms of complexation and biotransformation of uranium with organic ligands ketogluconic, oxalic, malic, citric, protocatechuic, salicylic, phthalic, and fulvic acids and catechol. Potentiometric titration of uranium with the organic ligands confirmed complex formation and extended X-ray absorption fine structure (EXAFS) analysis and electrospray ionization-mass spectrometry (ESI-MS) showed that ketogluconic acid formed a mononuclear complex with uranium involving the carboxylate group, while malic acid, citric acid, and catechol formed binuclear complexes. Phthalic acid formed a bidentate complex involving the two carboxylate groups, while catechol bonded to uranium through the two hydroxyl groups. The hydroxycarboxylic acids were bound in a tridentate fashion to uranium through two carboxylates and the hydroxyl group.

Studies with anaerobic bacteria *Clostridium* sp. (ATCC 53464) and *C. sphenoides* (ATCC 53464) showed U(VI) complexed with organic ligands was reduced to U(IV) under anaerobic conditions with little precipitation of uranium. The reduction of U(VI)-citrate to U(IV)-citrate occurred only when supplied with an electron donor glucose or citrate. The bacteria did not metabolize the citrate complexed to the uranium. XANES analysis showed that the reduced form of uranium was present in solution while EXAFS analysis showed that the U(IV) was bonded to citric acid as a mononuclear biligand complex [U(IV)-cit_2] (Francis and

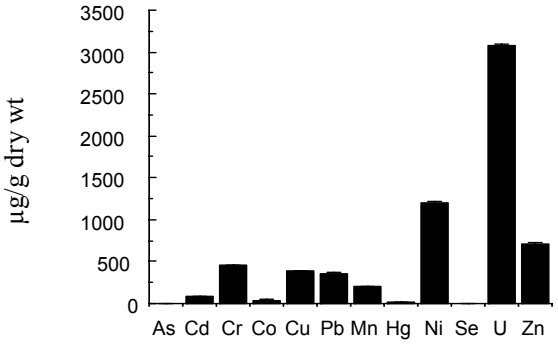

Fig.2. Analyses of metals in sludge (Francis et al., 1991).

Dodge, manuscript submitted). Also the sulfate-reducing bacteria *Desulfovibrio desulfuricans* and the facultative iron-reducing bacteria *Shewanella halotolerans* reduced U(VI) complexed with oxalate or citrate to U(IV) under anaerobic conditions with little precipitation of uranium (Ganesh et al., 1997). These results show that the complexed uranyl ion is readily accessible as an electron acceptor despite the inability of the bacterium to metabolize the organic ligand. These results also suggest that reduced uranium, when complexed with an organic ligand, can remain in solution; this finding is contrary to the conventional belief that reduced uranium will precipitate from solution. The persistence of reduced uranium complexed with chelating agents in subsurface environments is a major concern because of the potential for increasing the transport of the radionuclide.

Biotransformation of uranium in wastes and in sediment

We investigated uranium-contaminated sediment and sludge samples from the West End Treatment Facility, at the U.S. Department of Energy, Oak Ridge Y-12 Plant, Oak Ridge, TN (Francis et al., 1991). The sludge was generated from a ura-

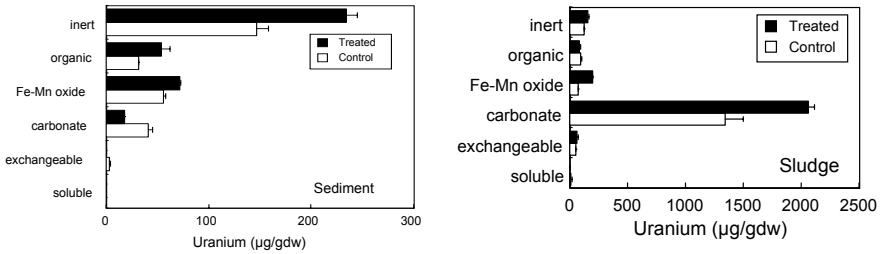

Fig.3. Mineralogical association of U in sludge and sediment before and after microbial action (Francis et al., 1991).

nium-process waste stream after biodenitrification of nitric-acid uranium waste water, and the sediment was from a contaminated pond (New Hope Pond) which received uranium-process waste water. Several million gallons of the sludge is in storage awaiting disposal. Both sediment and sludge samples contained varying levels of major elements, Al, Ca, Fe, Mg, K, and Na, and toxic metals As, Cd, Cr, Co, Cu, Pb, Mn, Hg, Ni, U, and Zn (Figure 2). The concentrations of uranium in sediment and sludge samples were 920 and 3100 ppm, respectively. In addition to those elements reported above, analysis of the sediment sample by X-ray fluorescence showed the presence of titanium, gallium, bromine, strontium, rubidium, yttrium, and zirconium. The sludge was low in organic carbon and nitrogen but high in ash and sulfate; the latter resulted from adding sulfuric acid and ferric sulfate during the waste treatment process. Chemical analysis of the sludge supernate showed that the pH was alkaline, it was high in dissolved inorganic carbon (DIC) and sulfate, and low in nitrate; the pH of the sediment supernate was near neutral and contained high dissolved organic carbon (DOC), and low levels of the other constituents tested.

The mineralogical association of cadmium, chromium, copper, manganese, nickel, lead, uranium, and zinc in the sludge and sediment was determined by a selective extraction procedure. Figure 3 shows these associations of uranium in the sludge and sediment before and after microbial action. A comparison of the total uranium obtained by digestion of the entire sample with the sum of the selective extractions showed good agreement within ±10% (±1 SEM).

The sediment and sludge samples amended with glucose showed an increase in total gas, CO_2, H_2, CH_4, and organic acids; pH was lowered by about 2.5 units.

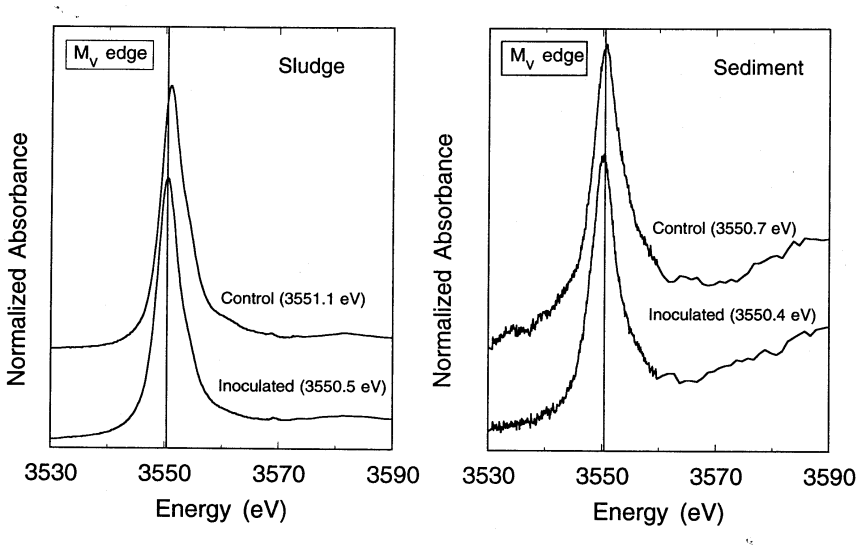

Fig.4. Comparison of XANES spectra of sludge and sediment before and after microbial treatment show reduction of U(VI) to U(IV) (Francis et al., 1991).

This change was due to the production of organic acid metabolites from glucose fermentation. The organic acids were acetic, butyric, propionic, formic, pyruvic, lactic, isobutyric, valeric, and isocaproic acids. A significant amount of gas was produced due to glucose fermentation by anaerobic bacteria, as well as from the dissolution of $CaCO_3$ in the sludge by the organic acids. A decrease in sulfate concentration was observed only in amended samples.

This treatment process removed a large fraction of soluble non-toxic metals such as Ca, K, Mg, Mn^{2+}, Na, and Fe^{2+}, and enriched and stabilized Cd, Cr, Cu, Ni, Pb, U, and Zn with the remaining solid phase due to direct and indirect actions of the bacteria (Francis, et al. 1991). Analysis of the mineralogical association of the metals in the wastes after microbiological action showed that many of the metals were redistributed with stable mineral phases, such as organic and silicate fractions (Figures 3). Metals associated with the exchangeable, carbonate, and iron oxide fractions were solubilized by indirect action due to the production of organic acid metabolites, whereas dissolution of iron oxides and metals coprecipitated with iron oxides was due to direct enzymatic reduction of iron. Uranyl ion associated with the exchangeable, carbonate, and iron-oxide fractions was released into solution by direct and indirect actions of the bacteria, and subsequently, was reduced enzymatically to insoluble U(IV). X-ray absorption near edge spectroscopic (XANES) analysis of uranium in the untreated (control) and treated sludge and sediment samples showed partial reduction of U(VI) $\rightarrow$ U(IV) in the sludge and complete reduction in the sediment (Figure 4). Figure 5 illustrates the mechanisms of anaerobic microbial transformations of uranium in mixed wastes. Uranium was predominantly associated with the carbonate fraction and to a lesser extent with the oxide, organic, and inert fractions; after microbial activity its concentration increased for all three fractions.

Substantial amounts of calcium, iron, potassium, magnesium, manganese, and sodium were solubilized from the waste, reducing the mass ~15-20% in these batch studies. Further reductions in waste volume can be achieved by optimizing the process using a continuous treatment system to solubilize and remove the bulk of non-toxic waste components, particularly calcium, potassium, iron, magnesium, and manganese. This biotreatment can be applied to mixed wastes containing ra-

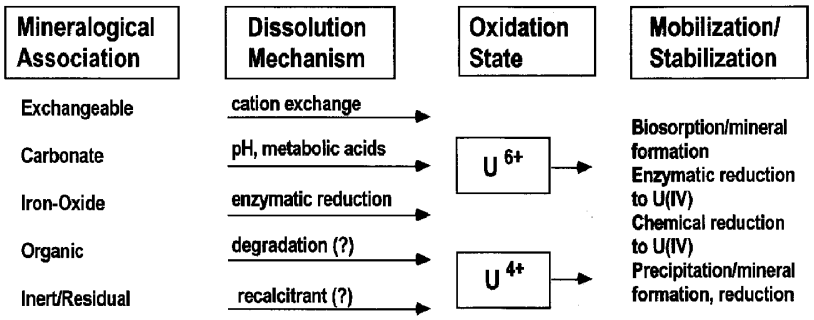

Fig.5. Proposed mechanisms of microbial ransformation of uranium in mixed waste.

dioactive elements and toxic metals generated from defense, energy, and industrial operations wastes to chemically convert the radionuclides and metals to more stable forms. Reducing the mass of the wastes means that more material can be stored or disposed of, can be handled easier, and can be transported. Converting the radionuclides and toxic metals to more stable forms allows the material to be processed chemically, for disposal in shallow or deep geological formations.

Fundamental information on the characterization of the uranium wastes and clear understanding of the mechanisms of interactions of microorganisms with uranium associated with naturally occurring minerals, uranium mining and mill tailing wastes, organic and inorganic ligands and colloids at the molecular level under various microbial process conditions will aid in the development of appropriate remediation strategies and long-term stewardship of contaminated sites.

Acknowledgement

This research was supported by the Environmental Remediation Sciences Program, Office of Biological and Environmental Research (OBER), Office of Science, U. S. Department of Energy, under contract No. DE-AC02-98CH10886.

References

Berthelin, J. and C. Munier-Lamy. 1983. Microbial mobilization and preconcentration of uranium from various rock materials by fungi. In R. Hallberg, (ed.) Environmental Biogeochemistry. Ecol. Bull., Stockholm. 35:395-401.

Bhurat, M. C., K. K. Dwivedy, K. M. V. Jayaram, and K. K. Dar. 1973. Some results of microbial leaching of uranium ore samples from Narwepahar, Bhatin and Kerudungri, Singhbhum District, Bihar. NML Technical J. 15:47-51.

Bloomfield, C. and G. Pruden. 1975. The effects of aerobic and anaerobic incubation on the extractabilities of heavy metals in digested sewage sludge. Environ. Pollut. 8: 217-232.

Bloomfield, C. and W. I. Kelso. 1973. The mobilization and fixation of molybdenum, vanadium, and uranium by decomposing plant matter. J. Soil Sci. 24:368-379.

Bostick, B. C.; M. O. Barnett; P. Jardine; S. Fendorf; S. Brooks. 2002. Speciation of uranium in packed soil columns. Soil Sci. Soc. Am. J. 66:99-108.

Francis A.J, J.B Gillow, C.J Dodge, R Harris, T.J Beveridge, and H.W Papenguth. 2004. Association of uranium with halophilic and nonhalophilic bacteria and archaea. Radiochim. Acta 92: 481-488.

Francis, A. J. and C. J. Dodge. 1990. Anaerobic microbial remobilization of toxic metals coprecipitated with iron oxide. Environ. Sci. Technol. 24: 373-378.

Francis, A.J. 1990. Microbial dissolution and stabilization of toxic metals and radionuclides in mixed wastes. Experientia 46: 840-851.

Francis, A.J., Dodge, C.J., and Gillow, J.B. 1991. Microbial stabilization and mass reduction of wastes containing radionuclides and toxic metals. Patent No. 5,047,152.

Francis, A.J. 1994. Microbial transformations of radioactive wastes and environmental restoration through bioremediation. J. Alloys and Compounds 213/214: 226-231.

Francis, A.J., C.J. Dodge, F. Lu, G. Halada, and C.R. Clayton. 1994. XPS and XANES studies of uranium reduction by Clostridium sp. Environ. Sci. Technol. 28: 636-639.

Ganesh R., K.G. Robinson, G.R. Reed, and G. S. Saylor. 1997. Reduction of hexavlaent uranium from organic complexes by sulfate- and iron-reducing bacteria. Appl. Environ. Microbiol. 63: 4385-4391.

Katz, J.J.; G.T. Seaborg; L.R. Morss. The Chemistry of the Actinide Elements, 2nd Ed., Vol. 1, Chapman and Hall, NY, 1986.

Metzler, D.R. 2004. Uranium mining: Environmental impact. Encyclopedia of Energy, 6:299-315.

Munier-Lamy, C. and J. Berthelin. 1987. Formation of polyelectrolyte complexes with the major elements Fe, Al, and trace elements U, and Cu during heterotrophic microbial leaching of rocks. Geomicrobiol J. 5:119-147.

Premuzic, E.T., A.J. Francis, M. Lin, and J. Schubert. 1985. Induced formation of chelating agents by Pseudomonas aeruginosa grown in presence of thorium and uranium. Arch. Environ. Contam. Toxicol. 14:759-768.

Sakaguchi, T. 1996. Bioaccumulation of Uranium. Kyushu University Press, Hukuoka, Japan.

Stone, A.T. and J.J. Morgan. 1987. Reductive dissolution of metal oxides, in: Aquatic surface Chemistry: Chemical Processes at the Particle Water Interface, pp 221-254. Ed. W. Stumm. John Wiley and Sons, Inc., New York.

Strandberg, G.W., S.E. Shumate II, and J. R. Parrot Jr. 1981. Microbial cells as biosorbents for heavy metals: accumulation of uranium by Saccharomyces cerevisiae and Pseudomonas aeruginosa. Appl. Environ. Microbiol.41: 237-245.

Wall, J. D. and L. R. Krumholz. 2006. Uranium reduction. Ann. Rev. Microbiol. 60: 149-166.

Uranium biomineralization by uranium mining waste isolates: a multidisciplinary approach study

Mohamed L. Merroun, Christoph Hennig and Sonja Selenska-Pobell

Department of Biogeochemistry, Institute of Radiochemistry, Forschungszentrum Dresden-Rossendorf 01314 Dresden, Germany

Abstract. Direct molecular techniques demonstrated that uranium mining waste piles are a reservoir of different bacterial groups with diverse metabolic activities. These bacteria developed different mechanisms to overcome the toxicity of this radionuclide including precipitation, sorption, intracellular accumulation, biomineralization etc. The present work overview the different mechanisms of biomineralization of uranium at acidic conditions by bacterial strains isolated from extreme environments including uranium mining waste piles using a multidisciplinary approach combining potentiometric titration, microbiological, spectroscopic (EXAFS/XANES) and microscopic (TEM/EDX) techniques. EXAFS studies indicated that the main mineral phase precipitated by the studied bacterial cells has similar structural parameters to that of m-autunite phase. Transmission electron microscope analysis showed strain-specific cell surface and/or intracellular uranium precipitation. The precipitation of uranium was mainly associated with the activity of acidic phosphatase by liberation of inorganic phosphates which precipitate uranium. The results found in this study will be helpful to fully understand actinide cycling and dispersal in the environment, particularly in the uranium mining wastes.


Uranium Mining
and Hydrogeology

Uranyl reduction by *Geobacter sulfurreducens* in the presence or absence of iron

Jonathan O. Sharp[1], Eleanor J. Schofield[2], Harish Veeramani[1], Elena I. Suvorova[1], Pilar Junier[1], John R. Bargar[2] and Rizlan Bernier-Latmani[1]

[1] École Polytechnique Fédérale de Lausanne, Switzerland
[2] Stanford Synchrotron Radiation Laboratory, Menlo Park, CA

Abstract. While the product of microbial U^{6+} reduction is often reported as the mineral uraninite, UO_2, there is increasing evidence that, in some cases, other compounds may be produced. In this study, we evaluate the product of U^{6+} reduction by the metal-reducing bacteria *Geobacter sulfurreducens* in the presence or absence of a reduced-phase iron phosphate precipitate produced during growth on Fe^{3+}. Our results demonstrate that uraninite is precipitated by resting cells in the absence of this mineral. In contrast, a complexed, non-crystalline U^{4+} product forms in the presence of biogenically reduced iron. We hypothesize that this different mineralogical outcome reflects enzymatic vs. sorption driven reductive processes.

Introduction

Reductive immobilization has been proposed as a strategy to attenuate depleted uranium in subsurface waters contaminated by mining or U enrichment activities. (Lovley et al. 1991; Meinrath et al. 2003). Bioremediation of uranium contaminated groundwater is based on the microbial *in-situ* reduction of soluble, and hence mobile, oxidized uranium, U^{6+}, to a comparatively insoluble reduced species, U^{4+} (Lovley et al. 1991; Lovley et al. 1993). However, the structure of the reduced uranium, inherent stability in the subsurface environment, and susceptibility to reoxidation are not well understood (Anderson et al. 2003).

A number of microorganisms have been identified as capable of reducing uranium, including metal-reducing bacteria (MRB) and sulfate-reducing bacteria (SRB). While the product of microbial U^{6+} reduction is often reported as the mineral uraninite, UO_2, there is increasing evidence that, in some cases, other compounds may be produced. In this study, we evaluated the product of U^{6+} reduction

by a MRB, *Geobacter sulfurreducens,* after growth in the presence or absence of iron and identified differences in the reduced uranium products formed using XAS (X-ray Absorption Structure) and electron microscopy.

Materials and Methods

Bacterial strain *Geobacter sulfurreducens* (DSMZ no. 12127) was grown using standard anaerobic techniques. Geobacter media at pH 6.8 (DSMZ media no. 826 and 579) was used to support what is referred to hereafter as fumarate- or iron-grown cells (Lovley and Phillips 1988). The distinction between each growth condition being the electron acceptor, either 8g/L Na_2-fumarate coupled to 0.82 g/L Na-acetate or 13.7g/L Fe^{3+}-citrate coupled to 2.5g/L Na-acetate. After growth, cells and iron precipitates (representing *ca.* 60% of total iron in the system as determined by soluble Fe in the supernatant) were harvested by centrifugation (10,000*g for 5 min), washed in anaerobic buffer, and added to a closed bottle (20% CO_2, balance N_2, pH = 7.0) containing 30mM HCO_3^-, 10mM PIPES, 20 mM acetate, and 1000 μM uranyl-citrate. Heat pasteurized controls were used to assess the biological component of the reduction. After one day, the cells and resulting precipitate were collected and processed by centrifugation under anaerobic conditions, washed in 100 mM bicarbonate, followed by final resuspension in MilliQ prior to structural analysis.

Composition, structure and morphology of iron precipitate particles were examined by transmission electron microscopy (TEM) and scanning transmission electron microscopy (STEM) imaging and X-ray energy dispersive spectrometry (EDS) chemical microanalysis (INCA, Oxford) in a FEI CM300UT FEG transmission electron microscope (300 kV field emission gun, 0.65 mm spherical aberration, and 0.17-nm resolution at Scherzer defocus). The images were recorded on a Gatan 797 slow scan CCD camera with a 1024x1024 pixels/14 bit detector and processed with the Gatan Digital Micrograph 3.11.0 software including Fourier filtering. Low dose illumination conditions were used to record the images in order to prevent sintering of particles under the electron beam. The specimens of particles for TEM examination were prepared on carbon films supported by Cu grids after drying residual water.

The phase identity was determined by analyzing selected area electron diffraction (SAED) patterns and the interpretation of images, SAED patterns and diffractograms were performed with the JEMS software package [JEMS, Stadelmann, http://cimewww.epfl.ch] using the known electron-optical parameters and crystallographic data for several phases contained uranium [Inorganic Crystal Structure Database, ICSD 2003].

Structural synchrotron and spectroscopic characterizations of biogenic minerals employed Uranium Extended X-Ray Absorption Fine Structure (U-EXAFS). All sample manipulation at SSRL was carried out under an anaerobic atmosphere (5% hydrogen, balance nitrogen). Centrifuged wet samples were loaded in Al sample holders with Kapton windows. Samples were stored wet and anaerobic until anal-

ysis. U L_{III}-edge transmission spectra were collected at SSRL beamlines 11-2 and 10-2, using Si (220) double-crystal monochromators. Samples were analyzed at 77K. EXAFS spectra were background subtracted, splined and analyzed using SIXPack (Webb 2005). Backscattering phase and amplitude functions required for fitting of spectra were obtained from FEFF 8 (Rehr et al. 1992).

Results and Discussion

Reduction of soluble uranium by cells of G. sulfurreducens grown with an electron acceptor / donor coupling of fumarate / acetate were contrasted with those grown on Fe3+ / acetate. After growth, cells grown on fumarate were harvested and washed without a visible precipitate other than cellular matter. In contrast, growth on iron was accompanied by the formation of a reduced precipitate which is characterized below. Resting cell assays for each growth condition were capable of removing soluble uranium (Fig. 1). Fumarate-grown cells (85 mg protein L-1) were most effective at removing soluble uranium. While pasteurization completely inhibited uranium precipitation in fumarate-grown cells, it had little effect on the removal of uranium in a suspension of cells and iron precipitate (ca. 3mmol iron in 50mL). A contrast of the iron-grown pasteurized and active incubations suggests that the biogenic precipitate was involved in abiotically removing uranium from solution through reduction or sorption. Cells and precipitates from these experiments were harvested after approximately 24 hours for further analysis. At the time of harvest, both pasteurized and active incubations from the iron-grown system had removed ca. 50% of the soluble uranium (data not shown).

Bacterial reduction of Fe^{3+} can result in the production of soluble Fe^{2+} complexes, precipitation of Fe^{2+} bearing minerals such as magnetite, siderite, vivianite or green rust, incorporation into clays, or sorption onto organic or inorganic phases (Bell et al. 1987; Dong et al. 2000; Fredrickson et al. 2000; Kostka and Nealson 1995; Kostka et al. 1996; O'Loughlin et al. 2003). In turn, reduced iron precipitates such as ferrous sulfides (Wersin et al. 1994) , green rust (O'Loughlin et al. 2003), and Fe^{2+} sorbed onto goethite (Fredrickson et al. 2000) have been reported to be involved in the removal of soluble U^{6+} from solution through sorption or reductive phenomenon.

In our batch incubations, we observed that *ca.* 60% of the soluble Fe^{3+} in solution was transformed to a white precipitate during growth. This precipitate turned green when exposed to oxygen. The anaerobic precipitate was analyzed by electron microscopy and demonstrated to have a mean crystal size of approximately 500 nm that was often found in association with the outer surface of bacteria. EDS spectra taken from representative particles showed the following elements: C, O, Na, P, Fe, Cl, K, Si, as well as Cu from the Cu grid. The Fe/P ratio was determined to be 1.5 ± 0.1 (Fig. 2) and the following possible composition can be determined: $NaHCO_3$, KCl, and $Fe_3(PO_4)_2$. Experimental electron diffraction patterns were compared to calculated ones for all possible Fe oxides and phosphates and further confirmed that the bulk of the iron precipitate was $Fe_3(PO_4)_2$ or vivia-

nite. A related species, *G. metallireducens*, produces vivianite when grown in ferric citrate media (Lovley and Phillips 1988) and siderite or magnetite after manipulation of soluble phosphate and carbonate concentrations (Vali et al. 2004).

When grown on fumarate, *G. sulfurreducens*, produced a reduced mineral structurally homologous to stoichiometric UO_2 (Schofield et al. 2008). However, in the presence of vivianite and cells, the primary product was a reduced uranium species lacking the U second-shell structure that is typical of UO_2 (Fig. 3). This product was determined to be sorbed species of reduced uranium that formed in association with the precipitate. Iron sulfides have been reported to partially reduce soluble uranyl to U_3O_8 through an analogous sorption driven phenomenon (Wersin et al. 1994). Thus, we hypothesize that the chemical reduction of U^{6+} by biogenic $Fe_3(PO_4)_2$ leads to the formation of sorbed U^{4+} whereas direct enzymatic reduction of U(VI) by active *Geobacter* cells produces UO_2.

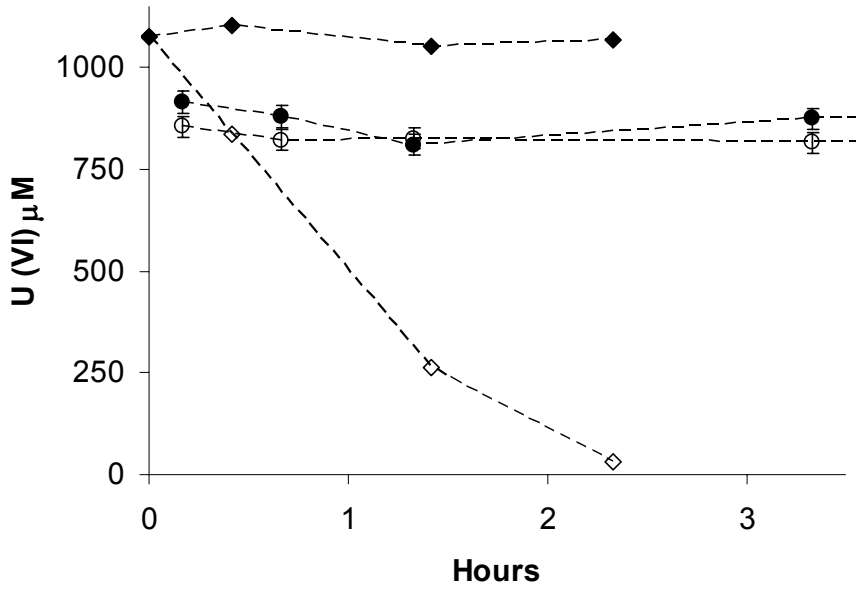

Fig.1. Removal of uranium by resting cells of *G. sulfurreducens* grown in the presence of fumarate/acetate (♦ pasteurized; ◊ active) versus Fe(III)/acetate-grown cells (● = pasteurized; ○ active).

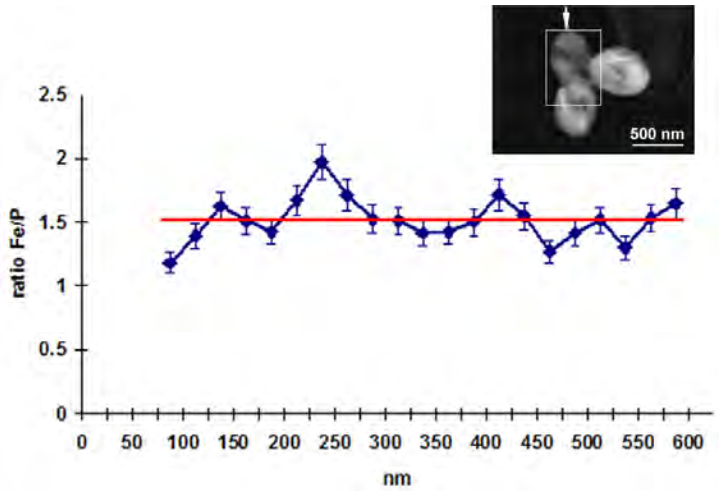

Fig.2. EDS analysis of the iron precipitate produced by *G. sulfurreducens* grown on Fe(III)/acetate to determine the Fe/P ratio throughout the particle. The TEM image in the upper right shows the representative particle used for EDS spectrum analysis.

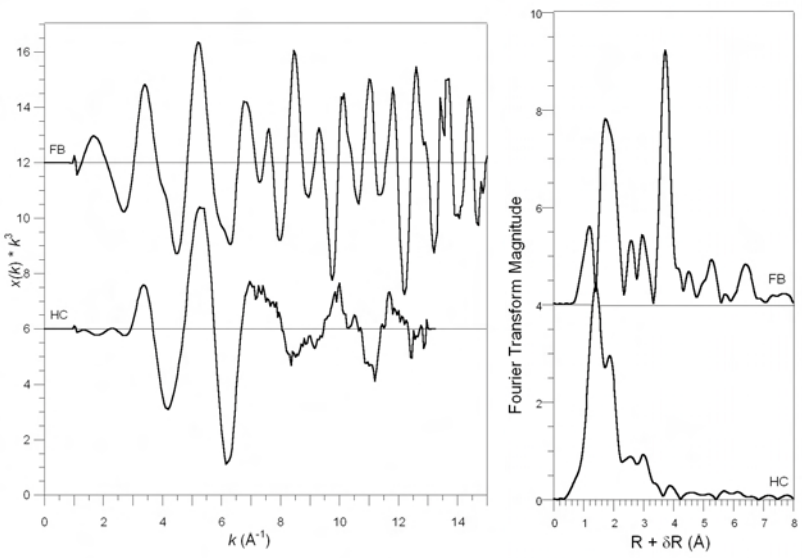

Fig.3. Uranium EXAFS and Fourier Transform spectra contrasting the reduced uranium produced by G. sulfurreducens harvested after growth on two different electron acceptors where FB = fumarate-grown and HC = iron-grown. The prominent peak at 3.8 Å on the Fourier Transform of fumarate-grown incubation provides evidence for a U-U bond characteristic of crystalline uraninite. This peak is absent in the iron-grown system.

Summary and Implications

This work demonstrates that biogenic U4+ can exist as either a nanoparticulate, crystalline uraninite (UO2) or a complexed reduced form depending upon bulk geochemical conditions. Specifically, we have observed that in the presence of an iron-phosphate precipitate (Fig. 2), the reduced product is primarily complexed U4+ presumably due to sorption driven processes. However, in the case of direct enzymatic reduction in the absence of a sorption-driven process, a bulk crystalline product, UO2, is obtained (Fig. 3).

The form and species of U^{4+} obtained by a bioremediation strategy has implications for the research direction most relevant to improving uranium bioimmobilization strategies. If indeed the complexed or adsorbed U^{4+} species is an important environmental product, its stability needs to be further explored. Presumably, an adsorbed phase is less stable than crystalline uraninite, suggesting that emphasis may need to be placed on promoting optimal conditions for the preferential production of the crystalline phase and by extension, a crystalline phase that is resistant to oxidation (Schofield et al. 2008; Ulrich et al. 2008).

Direct analysis of the state of immobilized uranium found in contaminated sites undergoing bioreduction is subject to interference and is precluded by the relatively high concentration required for reliable *in-situ* U EXAFS (Kelly et al. 2008; Suzuki et al. 2002). In the environment, particularly under the reducing conditions necessary for uranium reduction, prevalent reduced iron mineral phases could dominate the reduction of soluble U^{6+} resulting in a molecular U^{4+} product. While such reactions are considered favorable for overall uranium sequestration (Fredrickson et al. 2000), it is likely that their presence would alter the potential for reoxidation and dissolution. Hence their stability and association needs to be further studied.

MRB have demonstrated the capability to reduce uranium in laboratory soil columns (Moon et al. 2007) along with the concurrent reduction of solid phase iron. Stimulation of MRB has also been shown to both reduce and immobilize uranium in pilot field studies (Anderson et al. 2003; Wu et al. 2007). We are in the process of adapting soil column experiments to reveal speciation via U-EXAFS of immobilized uranium under similar MRB conditions. This approach will enable further exploration of the speciation of uranium and association with Fe^{2+} in more environmentally relevant conditions.

Acknowledgements

Work carried out at EPFL was funded by Swiss NSF grant # 20021-113784 and DOE OBER grant # DE-FG02-06ER64227. Portions of this research were carried out at the Stanford Synchrotron Radiation Laboratory, a national user facility operated by Stanford University on behalf of the U.S. Department of Energy (DOE), Office of Basic Energy Sciences and supported by the SSRL Environmental Remediation Science Program and BER-ERSD project number SCW0041. The

SSRL Structural Molecular Biology Program is supported by the Department of Energy, Office of Biological and Environmental Research, and by the National Institutes of Health, National Center for Research Resources, Biomedical Technology Program.

References

Anderson RT, Vrionis HA, Ortiz-Bernad I, Resch CT, Long PE, Dayvault R, Karp K, Marutzky S, Metzler DR, Peacock A and others. 2003. Stimulating the *in situ* activity of *Geobacter* species to remove uranium from the groundwater of a uranium-contaminated aquifer. Appl. Environ. Microbiol. 69(10):5884-5891.

Bell PE, Mills AL, Herman JS. 1987. Biogeochemical Conditions Favoring Magnetite Formation during Anaerobic Iron Reduction. Appl Environ Microbiol 53(11):2610-2616.

Dong HL, Fredrickson JK, Kennedy DW, Zachara JM, Kukkadapu RK, Onstott TC. 2000. Mineral transformation associated with the microbial reduction of magnetite. Chem. Geol. 169(3-4):299-318.

Fredrickson JK, Zachara JM, Kennedy DW, Duff MC, Gorby YA, Li SMW, Krupka KM. 2000. Reduction of U(VI) in goethite (alpha-FeOOH) suspensions by a dissimilatory metal-reducing bacterium. Geochim. Cosmochim. Acta 64(18):3085-3098.

Kelly SD, Kemner KM, Carley J, Criddle C, Jardine PM, Marsh TL, Phillips D, Watson D, Wu W-M. 2008. Speciation of Uranium in Sediments before and after In situ Biostimulation. Environ. Sci. Technol. 42(5):1558-1564.

Kostka JE, Nealson KH. 1995. Dissolution and Reduction of Magnetite by Bacteria. Environ. Sci. Technol. 29(10):2535-2540.

Kostka JE, Stucki JW, Nealson KH, Wu J. 1996. Reduction of structural Fe(III) in smectite by a pure culture of Shewanella putrefaciens strain MR-1. Clays Clay Miner. 44(4):522-529.

Lovley DR, Phillips EJP. 1988. Novel mode of microbial energy-metabolism: organic-carbon oxidation coupled to dissimilatory reduction of iron or manganese. Appl. Environ. Microbiol. 54(6):1472-1480.

Lovley DR, Phillips EJP, Gorby YA, Landa ER. 1991. Microbial reduction of uranium. Nature 350:413-416.

Lovley DR, Widman PK, Woodward JC, Phillips EJP. 1993. Reduction of uranium by cytochrome c3 of *Desulfovibrio vulgaris*. Appl. Environ. Microbiol. 59(11):3572-3576.

Meinrath A, Schneider P, Meinrath G. 2003. Uranium ores and depleted uranium in the environment, with a reference to uranium in the biosphere from Erzgebirge/Sachsen, Germany. J. Environ. Radioactivity 64:175-193.

Moon HS, Komlos J, Jaffe PR. 2007. Uranium reoxidation in previously bioreduced sediment by dissolved oxygen and nitrate. Environ. Sci. Technol. 41(13):4587-92.

O'Loughlin EJ, Kelly SD, Cook RE, Csencsits R, Kemner KM. 2003. Reduction of uranium(VI) by mixed iron(II)/iron(III) hydroxide (green rust): formation of UO2 nanoparticles. Environ. Sci. Technol. 37(4):721-7.

Rehr JJ, Albers RC, Zabinsky SI. 1992. High-order multiple-scattering calculations of x-ray absorption fine structure. Phys. Rev. Lett. 69(23):3397-3400.

Schofield EJ, Veeramani H, Sharp JO, Suvorova E, Bernier-Latmani R, Mehta A, Stahlman J, Webb SM, Clark DL, Conradson SD and others. 2008. Structure of biogenic UO2 produced by Shewanella oneidensis MR-1. *submitted*.

Suzuki Y, Kelly SD, Kemner KM, Banfield JF. 2002. Nanometre-size products of uranium bioreduction. Nature 419(6903):134-135.

Ulrich KU, Singh A, Schofield EJ, Bargar JR, Veeramani H, Sharp JO, Bernier-Latmani R, Giammar DE. 2008. Dissolution of biogenic and synthetic UO2 under varied reducing conditions. *submitted*.

Vali H, Weiss B, Li YL, Sears SK, Kim SS, Kirschvink JL, Zhang L. 2004. Formation of tabular single-domain magnetite induced by Geobacter metallireducens GS-15. Proc. Nat. Acad. Sci. USA 101(46):16121-16126.

Webb SM. 2005. SIXPack: a graphical user interface for XAS analysis using IFEFFIT. Phys. Scri. T115:1011-1014.

Wersin P, Hochella MF, Persson P, Redden G, Leckie JO, Harris DW. 1994. Interaction between Aqueous Uranium(Vi) and Sulfide Minerals - Spectroscopic Evidence for Sorption and Reduction. Geochim. Cosmochim. Acta 58(13):2829-2843.

Wu WM, Carley J, Luo J, Ginder-Vogel MA, Cardenas E, Leigh MB, Hwang CC, Kelly SD, Ruan CM, Wu LY and others. 2007. In situ bioreduction of uranium (VI) to sub-micromolar levels and reoxidation by dissolved oxygen. Environ. Sci. Technol. 41(16):5716-5723.

Characterization of the microbial diversity in the abandoned uranium mine Königstein

Jana Seifert[1], Beate Erler[1], Kathrin Seibt[1], Nina Rohrbach[1], Janine Arnold[1], Michael Schlömann[1], Andrea Kassahun[2] and Ulf Jenk[3]

[1]Technische Universität Bergakademie Freiberg, Interdisciplinary Research Centre, Department of Biosciences, Leipziger Strasse 29, 09599 Freiberg, Germany
[2]Groundwater Research Institute Dresden, Meraner Strasse 10, 01217 Dresden, Germany
[3]Wismut GmbH, Jagdschaenkenstrasse 29, 09117 Chemnitz, Germany

Abstract. The geochemical condition in the abandoned uranium mine Königstein is characterized by a high acidity combined with an increased level of pollution mainly with sulfate, heavy metals and radionuclides. The autochthonous microbial community was analyzed in respect to their bioremediation potential of those inorganic pollutants. Cultivation-independent methods, like fluorescence *in situ* hybridization (FISH) and terminal restriction fragment length polymorphism (T-RFLP) were used to screen various water and sludge samples for a first overview. 16S rDNA clone libraries were constructed to obtain detailed information about the bacterial communities of a sludge water, an anoxic sludge and a sandstone sample.

Introduction

Since the mining activities had stopped in 1990, the uranium mine Königstein has been partially flooded. This resulted in an encroaching release of heavy metals and radionuclides as contaminants in acidic, sulfate-rich waters. Thus, a protection of the adjacent groundwater aquifers and the nearby river Elbe is of great importance.

In this study the bioremediation potential of the mine environment to reduce the mobilization of the contaminants and thus, to reduce the treatment efforts to clean the mine water should be investigated. Therefore, several groundwater, mine drainage water, sludge and rock samples were investigated with cultivation-

Table 1. Overview of the samples investigated in detail and their geochemical properties (n.d.: not determined)

	Sludge water FL-4-01	Anoxic sludge FL-4-01(2)	Sandstone FE-4-02
pH	2.62	6.45	n.d.
Eh [mV]	858	236	n.d.
SO_4^{2-} [mg/L]	787	2220	n.d.

independent methods in respect of their microbial community compositions. Three characteristic samples were analyzed in detail (see Table 1).

The microbiology of acid mine waters was described by various authors (e.g. Johnson 2007). Aerobic environments are characterized by mineral oxidizing microorganisms (iron and sulfur oxidizers), which form acids and mobilize metals by their metabolic activities. Whereas iron and sulfur reducing microorganisms use the oxidized compounds as electron acceptors in anaerobic environments and enable an immobilization of metals by the chemical precipitation of sulfides.

Materials and Methods

Sampling

Groundwater, mine drainage water, sludge and sandstone samples were collected and handled in the lab under sterile conditions. Biomass for DNA extraction was collected by filtration through a 0.22 µm cellulose filter (Osmonics Inc., USA) from at least 1 L of groundwater and mine drainage water samples, respectively. From the sludge water sample FL-4-01 0.5 L were filtered. The filters were stored at –80°C until further analyses. Sludge and sandstone samples were homogenized under sterile conditions and stored at –80°C in aliquot parts until further analyses.

Water and sludge samples were concentrated and fixed with a 4% paraformaldehyde solution as described in Amann et al. (1990a) and were stored at -20°C until FISH analyses were performed.

DNA extraction, PCR amplification and cloning

DNA was extracted as described in Wilson (1994). PCR amplification of the bacterial 16S rRNA genes was performed with primers 27f (5'-AGAGTTTGATCCTGGCTCAG-3') and modified 1387r (5'-GGGCGGNGTGTACAAGGC-3') (Lane 1991; Marchesi et al. 1998). Each primer was added in a final concentration of 0.25 µM with a PCR premix from Ab-

gene (Epsom, UK). The thermocycler was run with the following temperature program: (120 s, 94°C; 30 x (30 s, 94°C; 30 s, 55°C; 90 s, 72°C); 300 s, 72°C). PCR products were purified by Montage PCR Centrifugal Filter Devices (Millipore, USA) and further cloned into vector pSC-A using a Strataclone PCR cloning kit (Stratagene, USA) following the manufacturer's instructions. At least 200 clones of every gene library were picked for amplified ribosomal DNA restriction analysis (ARDRA). The plasmid inserts were amplified and 3 µL of the PCR product were digested with RsaI and AluI, respectively. Digestion patterns obtained via gel electrophoresis were grouped and plasmid DNA of 1 to 3 representative clones per group was purified using a FlexiPrep kit (Amersham Bioscience, USA).

Sequence analysis

Plasmid inserts were sequenced on a Beckman Coulter CEQ 8000 sequencer using Genome Lab DTCS Quick Start kit (Beckman Coulter, USA). Sequences were assembled by using Staden Package v. 1.6.0. Comparisons to database entries were performed by using BLASTN (Altschul et al. 1990). All phylogenetic trees were calculated with two steps using ARB (Ludwig et al. 2004): reference sequences of the corresponding taxonomic group were calculated with the maximum-likelihood algorithm by applying an adequate taxonomic filter; the clone sequences were added using the parsimony algorithm without changing the tree topology and the filter.

Terminal restriction fragment length polymorphism

T-RFLP was done with sequenced clones showing similarities to sulfate reducing bacteria, and other clones from dominant sequence groups in the libraries, respectively, in order to construct a fragment library. This fragment library can be used to analyze the bacterial composition of various environmental samples, and batch experiments investigating microbial sulfate reduction.

Genomic DNA or plasmid DNA was amplified using the primers, reagents and PCR run as described in the penultimate preceding paragraph except that the forward primer 27f was labeled with a Cy5 fluorescence dye. PCR products were purified and the DNA concentration was fluorometrically measured (PicoGreen®; Mini Fluorometer TBS-380, Turner Biosystems). 50 ng DNA was digested for 3 h at 37°C with 0.1 U of the restriction enzyme and 1 x of the corresponding buffer in a 10 µl reaction mixture. The restriction enzymes were chosen due to restriction pattern analysis with the sequenced clones using the online program webcutter (http://rna.lundberg.gu.se/cutter2/). Digested DNA (1 - 2 µl) was prepared for the separation using Beckman Coulter CEQ 8000.

Table 2. Used probes and their respective optimized hybridization conditions

	EUB 338	SRB 385	SRB385Db	DSS 658	DSV698
Reference	Amann et al. 1990b	Rabus et al. 1996	Rabus et al. 1996	Manz et al. 1998	Manz et al. 1998
Sequence (5' -> 3')	GCTGCCTCC CGTAGGAGT	CGGCGTCGC TGCGTCAGG	CGGCGTTGC TGCGTCAGG	TCCACTTCCC TCTCCCAT	GTTCCTCCA GATATCTAC GG
Target group	Bacteria	delta-Proteo-bacteria and other bacteria	delta-Proteo-bacteria and other bacteria	*Desulfobacter-aceae* and other bacteria	*Desulfovibrio* sp., *Bilophila* sp., *Lawsonia* sp.
Formamide	35 %	30%	30%	40%	35%
Condition	90 min, 46°C	180 min, 37°C	180 min, 37°C	180 min, 46°C	180 min, 46°C

Fluorescence *in situ* hybridization

The fixed environmental samples were spotted on a Teflon-coated glass slide and were dehydrated using an ethanol treatment. The samples were stained with 4',6-diamidino-2-phenylindol (DAPI) for a first overview of the whole cell density. The specific detection of active bacterial genera, with the focus to sulfate reducing bacteria, was performed using published probes (see Table 2).

Results and Discussion

Water samples

FISH analysis

All samples were screened in respect to total cell numbers with the DAPI staining method. Samples of the groundwater and the water from the flooded mine area showed low cell densities. Hybridization experiments performed similar fluorescence signals using probe EUB 338. Almost no fluorescence signal was obtained using probes SRB 385 and SRB 385Db, which are specific for members of the *Deltaproteobacteria*. Members of this class are reported to be sulfate-reducing bacteria. Sample FL-4-01 showed single and irregular fluorescence signals using probes SRB 385Db.

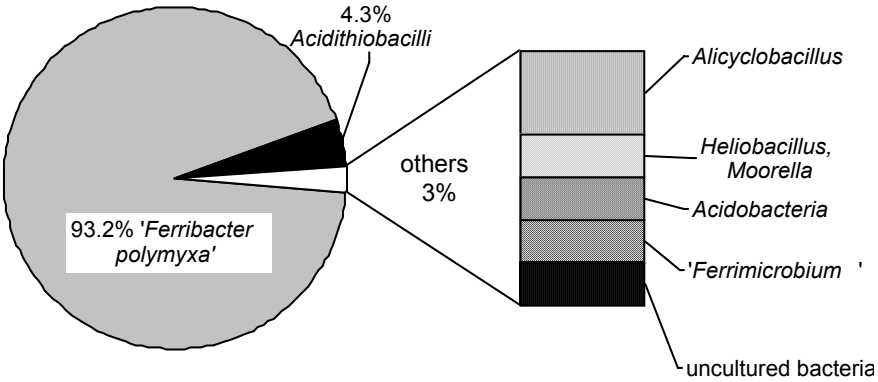

Fig.1. Results of the clone sequences and their respective frequencies in the clone library of the sludge water sample FL-4-01.

Sequence analysis

DNA extraction of the various water samples was, in correlation to the low cell density, of minor success. The DNA prepared from sludge water sample FL-4-01 was chosen for a detailed analysis creating a 16S rDNA clone library.

The analysis of 235 clones revealed a dominant abundance of sequences related to "*Ferribacter polymyxa"* PSTR (see Fig.1.). This bacterium affiliating with the class of *Betaproteobacteria* and is described as an autotrophic and acidophilic iron oxidizer (D. B. Johnson and K. B. Hallberg, sequence accession number EF133508, unpublished data). The filamentous cell clusters of these bacteria were described in the literature as 'macroscopic streamer' and they were clearly visible in the drainage water of the mine as well (Hallberg et al. 2006).

The second major sequence group showed similarities to *Acidithiobacillus ferroxidans*, an acidophilic iron and sulfur oxidizing bacterium (Brenner et al. 2005). This chemolithotrophic bacterium is the most common and best-investigated microorganism in respect to microbial leaching of sulfidic ores.

The sequence groups of minor frequencies showed similarities to various members of acidophilic heterotrophs.

Sludge and sandstone samples

FISH analysis

The sludge samples were primarily investigated with FISH using the probe EUB 338. The detection of a fluorescence signal was possible in all samples. The high background fluorescence of the sludge particles hampered the interpretation of the

fluorescence signals resulting from the correct hybridization with the RNA or the adsorption properties of the inorganic particles, respectively. Nevertheless, the *in situ* hybridization using probes SRB 385 and SRB 385Db showed fluorescence signals in sludge sample FL-4-01(2). Probes DSS 658 and DSV 698 were used to specify the detection of the *Deltaproteobacteria* members, both probes showed positive results. Thus, members of the sulfate-reducing bacteria *Desulfobacteraceae* and *Desulfovibrio* were present in the sludge sample FL-4-01(2).

Sequence analysis

A clone library of the sludge sample FL-4-01(2) was constructed to get detailed information's about the bacterial diversity and the expected sulfate-reducing bacteria. The same was done for the sandstone sample FE-4-02.

The sludge sample revealed a low diversity, compared to the sandstone sample, with a dominance of sequences affiliating to the class of the *Deltaproteobacteria*. The frequencies of various bacterial classes were in a range between 7% to 20% in the sandstone sample (see Fig. 2).

The phylogenetic tree (Fig. 3) shows the distribution of sequenced clones belonging to the classes of *Firmicutes* and *Deltaproteobacteria* from the two clone libraries. Both harbors genera described as sulfate, sulfite, thiosulfate, and sulfur reducing bacteria.

Sequences in the clone library of the sandstone (e.g. clone N35) showed similarties to *Desulfitobacterium* and *Desulfosporosinus*, which belong to the *Firmicutes*. *Desulfitobacterium* are often described to reductively dechlorinate chlorinated compounds, to reduce sulfur compounds except sulfate, as well as reducing

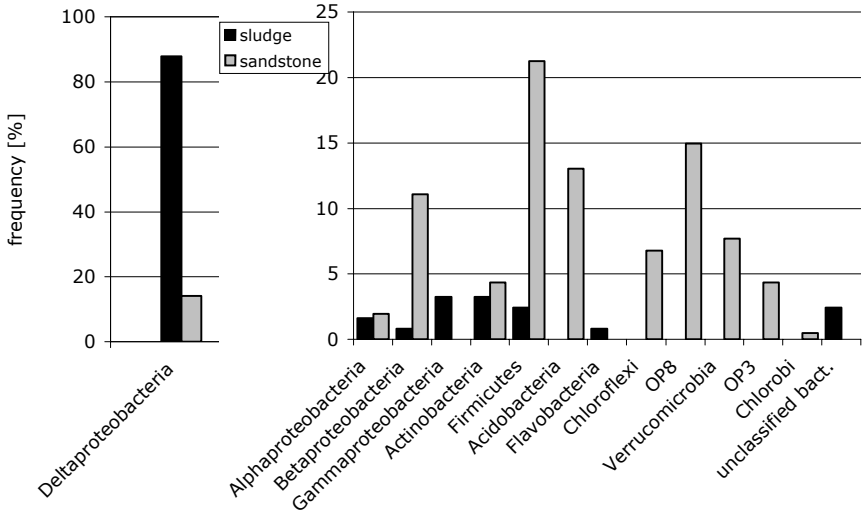

Fig.2. Frequency of the bacterial classes obtained by sequence analyses of clone libraries constructed with DNA of the sludge (FL-4-01(2)) and the sandstone (FE-4-02) sample.

nitrate (Utkin et al. 1994). *Desulfosporosinus* are spore-forming, sulfate-reducing bacteria that have been found in profundal sediments of oligotrophic lakes (Küsel et al. 2001) and in acid mine water (Church et al. 2007).

Sequences affiliating to the *Deltaproteobacteria* that could only be found in the sandstone sample were similar to *Synthrophobacter*, *Desulfomonile* and *Desulfobacca*. All genera are chemoorganotroph, mesophil and reduce sulfur compounds to H_SS. They were isolated from various anaerobic environments like sludge from waste treatment facilities, forested wetlands, fen soils or sulfidic biofilms (Kuever et al. 2005a).

A number of clones from the sludge sample showed similarities to uncultured bacteria obtained by the investigation of subseafloor sediments and to *Hippea ma-*

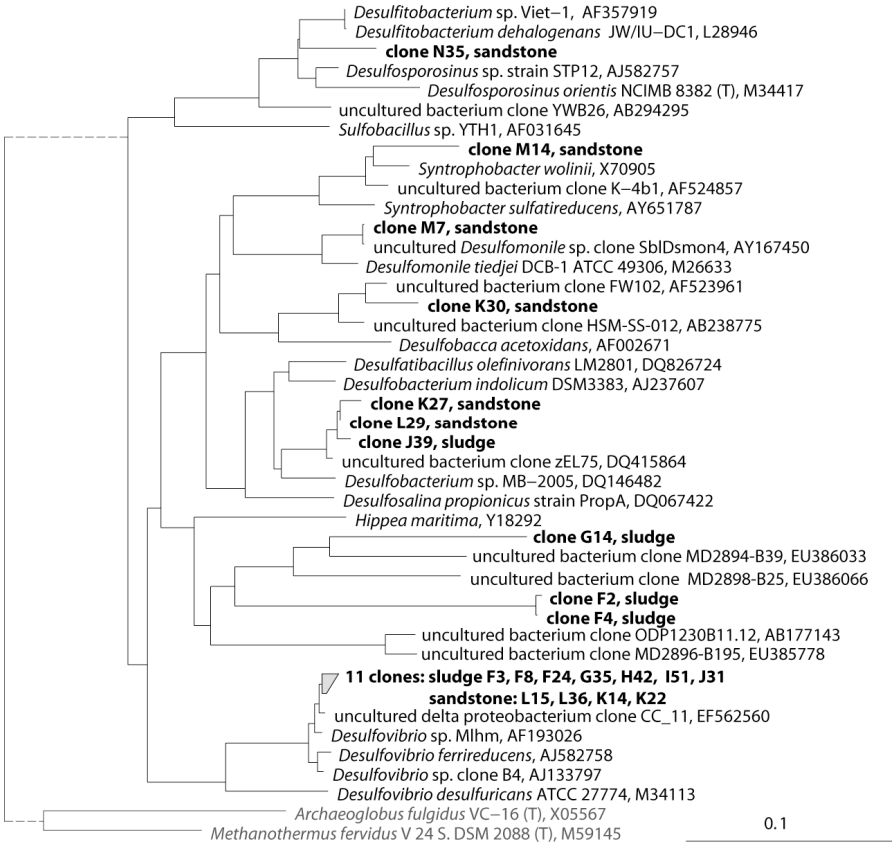

Fig. 3. Phylogenetic tree of 16S rDNA sequences of *Deltaproteobacteria* and *Firmicutes* from the sludge (FL-4-01(2)) and the sandstone (FE-4-02) sample. The sequence group within the *Desulfovibrionales* branch consists of 11 sequences from both samples. 16S rDNA sequences of *Archaeoglobus fulgidus* and *Methanothermus fervidus* were used as outgroup.

ritima, an anaerobic, thermophilic, sulfur reducing *Deltaproteobacteria*. The organism was isolated from marine sands near to hot vents and is able to use acetate, hydrogen gas, pyruvate and saturated fatty acids (Kuever et al. 2005b).

The majority of the clones from the sludge sample and a minor number of clones from the sandstone sample can be related to *Desulfovibrio*. This anaerobic Deltaproteobacterium is able to reduce sulfate, sulfite, thiosulfate and nitrate by the incomplete oxidation of alcohols, formate, lactate and pyruvate to acetate (Kuever et al. 2005c). *Desulfovibrio* seem to be oxygen-tolerant because of their occurrence in oxic/anoxic interfaces of biomats or even in oxic zones of marine and freshwater sediments (Dolla et al. 2007).

Conclusion

The investigation of the sludge water sample showed a dominance of acidophilic iron oxidizing *Betaproteobacteria*, and heterotrophic acidophiles in minor parts.

The anoxic sludge sample showed a dominance of the sulfate-reducing bacteria *Desulfovibrio* (ca. 70%) in association with other members of the *Deltaproteobacteria*, members of the *Alpha-*, *Beta-* and *Gammaproteobacteria*, *Actinobacteria,* and *Firmicutes*.

The sandstone sample revealed a high bacterial diversity. About 20% of the analyzed clones can be classified to sulfate-reducing bacteria, others are similar to aerobic and anaerobic bacteria with various physiological properties.

The obtained clones were used to create a fragment library for T-RFLP. This database was used to investigate various samples from the mine site, in which sulfate-reducing bacteria, like *Desulfovibrio* and *Desulfosporosinus* were detected.

This study showed the presence of sulfate-reducing bacteria in the mine. A stimulation of the growth of these organisms can be helpful to maintain a bioremediation process and inhibit the discharge of the pollutants by the flooding of the mine.

Acknowledgment

Financial support was given by Federal Ministry of Education and Research, Project Management Agency for Water Technology and Waste Management & WISMUT GmbH. We greatly thank G.E.O.S. Ingenieurgesellschaft mbH for the kind collaboration.

References

Altschul S F, Gish W, Miller W, Myers, E W, Lipman D J. (1990) Basic local alignment search tool. J Mol Biol 215: 403-410

Amann R, Krumholz L, Stahl DA (1990a) Fluorescent oligonucleotide probing of whole cells for determinative, phylogenetic, and environmental studies in microbiology. J Bacteriol 172: 762-770

Amann R, Binder B, Olson R (1990b) Combination of 16S rRNA-targeted oligonucleotide probes with flow cytometry for analyzing mixed microbial populations. Appl Environ Microbiol 56: 1919-1925

Brenner D J, Krieg N R, Staley J T (2005) The Proteobacteria Part B: The Gammaproteobacteria. 2 edn. Springer. New York

Church C D, Wilkin R T, Alpers C N, Rye R O, McCleskey R B (2007) Microbial sulfate reduction and metal attenuation in pH 4 acid mine water. Geochem Trans 8:10

Dolla A, Kurtz J, Teixeira M C, Voordouw G (2007) Biochemical, proteomic and genetic characterization of oxygen survival mechanism in sulphate-reducing bacteria of the genus Desulfovibrio. In Sulphate-reducing Bacteria. Edited by Barton L L & Hamilton W A. Cambridge University Press

Hallberg K B, Coupland K, Kimura S, Johnson D B (2006) Macroscopic streamer growths in acidic, metal-rich mine waters in north wales consist of novel and remarkably simple bacterial communities. Appl Environ Microbiol 72: 2022-2030

Johnson D B (2007) Physiology and ecology of acidophilic microorganisms. In Physiology and biochemistry of extremophiles. pp 257-270. Edited by Gerday C & Glansdorf N. ASM Press Washington D C.

Küsel K, Roth U, Trinkwalter T, Peiffer S (2001) Effect of pH on the anaerobic microbial cycling of sulfur in mining-impacted freshwater lake sediments. Environ Exp Bot 46:213-223

Kuever J, Rainey F A, Widdel F (2005a) Order VI. Synthrophobacterales ord. nov.. In Bergey's manual of systematic bacteriology. Vol two. The Proteobacteria Part C Alpha-, Beta-, Delta- and Epsilonproteobacteria. Edited by Brenner D J, Krieg N R, Staley J T. Springer

Kuever J, Rainey F A, Widdel F (2005b) Order I. Desulfurellales ord. nov.. In Bergey's manual of systematic bacteriology. Vol two. The Proteobacteria Part C Alpha-, Beta-, Delta- and Epsilonproteobacteria. Edited by Brenner D J, Krieg N R, Staley J T. Springer

Kuever J, Rainey F A, Widdel F (2005c) Order II. Desulfovibrionales ord. nov.. In Bergey's manual of systematic bacteriology. Vol two. The Proteobacteria Part C Alpha-, Beta-, Delta- and Epsilonproteobacteria. Edited by Brenner D J, Krieg N R, Staley J T. Springer

Lane D J (1991) 16S/23S rRNA sequencing, p.115-175 In Stackebrandt E & Goodfellow M. Nucleic acid techniques in bacterial systematics. John Wiley & Sons Inc.

Ludwig W, Strunk O, Westram R, Richter L, Meier H, Yadhukumar, Buchner a, Lai T, Steppi S, Jobb G, Förster W, Brettske I, Gerber S, Ginhart A W, Gross O, Grunmann S, Hermann S, Jost R, König A, Liss T, Lüßmann R, May M, Nonhoff B, Reichel B, Strehlow R, Stamatakis A, Stuckmann N, Vilbig A, Lenke M, Ludwig T, Bode A, Schleifer K H (2004) ARB: a software environment for sequencing data. Nucleic Acids Res 32: 1363-1371

Manz W, Eisenbrecher M, Neu T R, Szewzyk U (1998) Abundance and spatial organization of Gram-negative sulphate-reducing bacteria in activated sludge investigated by in situ probing with specific 16S rRNA targeted oligonucleotides FEMS Microbiol Ecol 25: 43-61

Marchesi J R, Sato T, Weightman A J, Martin T A, Fry J C, Hiom S J, Dymock D, Wade W G (1998) Design and evaluation of useful bacterium-specific PCR primers that amplify genes coding for bacterial 16S rRNA. Appl Environ Microbiol 64: 795-799

Rabus R, Fukui M, Wilkes H, Widdel F (1996) Degradative capacities and 16S rRNA-targeted whole-cell hybridization of sulphate-reducing bacteria in an anaerobic enrichment culture utilizing alkylbenzenes from crude oil. Appl Environ Microbiol 62: 3605-3613

Utkin I, Woese C, Wiegel J (1994) Isolation and characterization of Desulfitobacterium dehalogenans gen. nov., sp. nov., an anerobic bacterium which reductively dechlorinates chlorophenolic compounds. Int J Syst Bacteriol 44: 612-619

Wilson, K (1994) Preparation of genomic DNA from bacteria. In Current protocols in molecular biology, pp 2.4.1-2.4.2. Edited by Ausubel F M, Brendt R, Kingston R E, Moore D D, Seidmann J G, Smith J A, Struhl K. New York. John Wiley and Sons Inc.

Biogeochemical changes induced by uranyl nitrate in a uranium waste pile

Sonja Selenska-Pobell[1], Andrea Geissler[1], Mohamed Merroun[1], Katrin Flemming[1], Gerhard Geipel[1] and Helfried Reuther[2]

[1]Institute of Radiochemistry, [2]Institute of Ion-Beam Physics and Materials Research, Forschungszentrum Dresden Rossendorf, D-01314 Dresden, Germany

Abstract. Treatments with uranyl nitrate induced strong changes in a subsurface bacterial community of a uranium mining waste pile. Most of the bacterial populations, stimulated at the initial stages of the treatment, were affiliated with species able to use the added nitrate for respiration. Mössbauer spectroscopic analysis showed that at the later incubation stages, when nitrate was reduced, reduction of Fe(III) to Fe(II) occurred. Time-resolved laser-induced fluorescence spectroscopic (TRLFS) analysis revealed that most of the added U(VI) was bound in organic and inorganic phosphate phases both of biotic origin.

Introduction

The *in situ* bioremediation of uranium by stimulation of native U(VI)-reducing bacteria was under intensive investigations during the last decade (Holmes et al. 2002, Istok et al. 2004, Nevin et al. 2003, North et al. 2004, Nyman et al. 2006, Suzuki et al. 2003). In these studies different organic electron donors such as acetate, lactate, glucose, and ethanol were added to uranium mining waste waters or sediments. However, in the natural oligotrophic conditions of the uranium mining wastes the concentrations of the intrinsic inorganic ingredients are changed, in particular, those of uranium, nitrate, and sulfate (Finneran et al. 2002). Because the reduction of nitrate is thermodynamically more favorable than the reduction of Fe(III), U(VI), or sulfate, it is preferably used by microorganisms in the subsurface of the uranium wastes for anaerobic respiration (Finneran et al. 2002, Istok et al. 2004, Suzuki et al. 2003).

The process of natural attenuation of uranium in presence of nitrate under oligotrophic *aerobic* conditions was studied in our laboratory (Geissler and Selenska-Pobell 2005, Geissler et al. 2005). It was demonstrated, that treatments with uranyl nitrate of soil samples collected from the uranium mining waste pile Haberland,

situated near the town of Johanngeorgenstadt, Germany, strongly influenced the natural bacterial community structure and resulted in U(VI) immobilization via sorption and biomineralization. In the present work uranyl nitrate treatments of the same samples, but under *anaerobic* conditions, which correspond to those of the natural habitat, were performed. The behavior of the added U(VI) as well as the responses of the natural bacterial community to these treatments were monitored for different periods of time. The role of Fe(III), found in high concentrations in the untreated samples, as an electron acceptor capable to support the anaerobic metabolism of the nitrate-stimulated bacterial populations was studied as well.

Materials and methods

Samples studied

The original sample JG35-2 was collected in July 1997 from a depth of 2 m from the uranium mining waste pile Haberland, near the town of Johanngeorgenstadt. The sub-samples JG35+U4 and JG35+U3 were treated for 4 and 14 weeks, respectively, with 1mM uranyl nitrate solution as described earlier (Geissler and Selenska-Pobell 2005) but under anaerobic conditions. In parallel, control samples JG35-K4 and JG35-K2 were treated with sodium nitrate for 4 and 14 weeks, correspondingly, under anaerobic conditions as well (Table 1).

Time-resolved laser-induced fluorescence spectroscopy (TRLFS)

TRLFS measurements on uranium were carried out by a home-built spectroscopic system. As excitation source the output of a flash lamp pumped Nd:YAG laser with fourth harmonic generation (Inlite Continuum Inc., Santa Clara, USA) was used. The laser pulse (20 Hz repetition rate, 5 mJ per pulse) was directed to the sample. In a right angle set up the emitted luminescence was focused into a fiber,

Table 1. Samples analyzed.

Samples	Treatment	Incubation time	Uranium content [mg kg^{-1}]	Added nitrate [mg kg^{-1}]
JG35-2	Untreated	-	26	-
JG35+U4	Uranyl nitrate	4 weeks	~100	30
JG35-K4	Sodium nitrate	4 weeks	26	30
JG35+U3	Uranyl nitrate	14 weeks	~300	150
JG35-K2	Sodium nitrate	14 weeks	26	150

propagating the light to a 270 nm spectrograph (Acton Research, Inc., MA, USA). The wavelength dependent intensity was measured with an intensified CCD camera (Roper Scientific, 1024 pixel per line). The investigated samples were frozen and then put into a low temperature cuvette holder. The low temperature was provided by a cold gas system using liquid nitrogen as cooling agent. The sample temperature during the measurement was set to be 153 ± 2 K.

Mössbauer spectroscopy

0.5 g of the untreated sample JG35-2, as well as of the uranyl nitrate treated samples JG35+U4 and JG35+U3 were dried at 60 °C for 2 h in a vacuum concentrator (Eppendorf AG, Hamburg, Germany) and then pulverized. Mössbauer spectra were measured at room temperature with a conventional constant acceleration spectrometer in transmission geometry with a ^{57}Co(Rh) source with an activity of nominally 3.7 GBq and a krypton filled proportional counter. The evaluation of the spectra was performed by using the NORMOS least square fitting program of Brand (Brand 1987).

Molecular analysis of bacterial communities

DNA extractions from the studied samples, PCR amplifications of the 16S rRNA-gene fragments by using the primers 16Sdeg43F (5'-HRKGCBTWABRCATGCAA-GTC-3') and 16S1404R (5'-GGGCGGWGTGTACAAGGC-3'), and the DNA sequence analyses were performed according to (Geissler and Selenska-Pobell 2005).

Results and discussion

Fate of the added U(VI) in the uranyl nitrate treated samples as estimated by TRLFS

The uranium species formed in the uranyl nitrate treated samples JG35+U4 and JG35+U3 were studied by time-resolved laser-induced fluorescence spectroscopy (TRLFS). No analyzable uranium fluorescence spectra were obtained for the sample JG35+U4 due to the low concentration of the added uranium and the strong background emission which was assigned to the fluorescence of bacteria and of other organic compounds in the sample. The uranium fluorescence spectrum of the sample JG35+U3, which was supplemented with three times higher amount of uranium than the sample JG35+U4, were of very good quality and demonstrated three strong emission bands above the mentioned background which were located

at 496.8, 518.8 and 542.8 nm (Table 2). The red shift of about 8 nm in the emission bands of uranium compared to those of the free uranyl ion indicates that the U(VI) in the sample JG35+U3 was bound by phosphate groups (Bounhoure 2007, Koban and Bernhard 2007).

The fluorescence spectrum of the sample JG35+U3 was compared to the most similar spectra of organic and mineral uranyl phosphate species described in the literature. As evident from the data presented in Table 2, the fluorescence spectrum of the uranyl complexes found in the sample JG35+U3 is very similar to those of uranyl-adenosine mono phosphate (Merroun et al. 2003), uranyl glycerol- phosphate (DMPG) (Koban and Bernhard 2007), and also to the TRLFS uranyl spectrum of *Bacillus sphaericus* JG-A12, which was recovered from the studied uranium waste (Merroun et al. 2003). Less similar but with significant matches of particular emission bands were also the fluorescence spectra of another uranium mining waste isolate, *Acidithiobacillus ferrooxidans* D2 recovered from Denison Mines, Canada (Merroun et al. 2003), and of the purified S-layer protein of the strain *B. sphaericus* JG-A12 (Panak et al. 2000). Remarkable is also the similarity with the emission bands of inorganic phosphate compounds, such as phuralumite (Geipel et al. 2000), and uranyl hydro phosphate (Bounhoure 2007).

Table 2. Uranium fluorescence data of the JG35+U3 uranyl complexes compared to reference uranyl compounds with the most similar emission wavelengths

Compound/Species	Fluorescence emission maxima (nm)		
JG35+U3	**496.8**	**518.8**	**542.8**
UO_2^{2+}	488.9	510.5	533.9
UO_2-AMP (adenosine mono phosphate)	497.0	519.0	542.0
UO_2-DMGP (1,2-dimyristoyl-sn-glycero-3-phosphate)	497.0	519.3	542.4
Acidithiobacillus ferrooxidans D2	496.3	517.5	541.6
Vegetative cells of *Bacillus sphaericus* JG-A12	498.0	519.0	542.0
S-layer protein of *Bacillus sphaericus* JG-A12	498.2	517.7	541.0
UO_2HPO_4	497.0	517.0	541.0
Phuralumite ($Al_2(UO_2)_3(PO_4)_6 \cdot 10(H_2O)$	496.9	520.3	542.9

Determination of the Fe(III)/Fe(II) ratio in the uranyl nitrate treated samples

The high iron content of about 56.4 g Fe kg^{-1} in the original samples (Geissler and Selenska-Pobell 2005) arose our interest in the fate of this element, the oxidation state of which can be changed by different bacterial groups resulting in biotransformations of the natural iron containing minerals (Petrie et al. 2003). The latter can strongly influence the environmental behavior of uranium (Finneran et al. 2002).

The relative amount of Fe(III)- and Fe(II)-compounds in our samples, and in particular its change by the uranyl nitrate treatments, was determined via Mössbauer spectroscopy. The Mössbauer resonance absorption of the 14.4 keV γ-line of ^{57}Fe consists of a doublet both for Fe(III) as well as for Fe(II). However, the nuclear electric quadruple splitting Δ (about 0.8 mm s^{-1} for Fe(III) and about 2.4 mm s^{-1} for Fe(II)) as well as their isomer shift δ (about 0.2 mm s^{-1} for Fe(III) and about 1.2 mm s^{-1} for Fe(II)) are quite different for Fe in the two oxidation states. This allows a separation of the two doublets when they are superimposed in the Mössbauer absorption of a sample containing both Fe-species.

The Mössbauer absorption spectra of the 14.4 keV γ-line, emitted from an α-Fe source, were measured for the untreated sample JG35-2 as well as for the samples JG35+U4 and JG35+U3 treated with uranyl nitrate for 4 and 14 weeks, correspondingly. They represented an unresolved superposition of the two absorption doublets of the Fe(III)- and Fe(II)-compounds of our samples. We have fitted two doublets to these spectra with the quadruple splitting Δ_i and the isomer shifts δ_i (relative to the α- Fe γ-source) as well as the ratio $A_{Fe(II)}/A_{Fe(III)}$ of the areas of the two doublets as fitting parameters. The area ratio $A_{Fe(II)}/A_{Fe(III)}$ is proportional to the relative amount of Fe(II)- to Fe(III)-compounds in our samples. The results for these five parameters $\Delta_{Fe(II)}$, $\Delta_{Fe(III)}$, $\delta_{Fe(II)}$, $\delta_{Fe(III)}$, $\Delta_{Fe(II)}/\Delta_{Fe(III)}$ from the fits are given in Table 3. The most important result is the increase of the area $A_{Fe(II)}$ and the corresponding decrease of the area $A_{Fe(III)}$ with increasing the time of the uranyl nitrate treatment. This clearly demonstrates that the treatments with uranyl nitrate lead to an increase of the Fe(II)-compounds and corresponding decrease of the Fe(III)-compounds in the samples. In addition, the results show that $\Delta_{Fe(III)}$ and $\delta_{Fe(III)}$ are not changed by the uranyl nitrate treatment.

Interestingly, with the increase of the Fe(II) amount from 56.1% in the untreated sample JG35-2 to 62% (sample JG35+U4) and to 70.3% (sample JG35+U3), there are small but significant changes in the $\Delta_{Fe(II)}$ and in the $\delta_{Fe(II)}$ as well. This result indicates that the biotically produced Fe(II) compounds differ from those originally present in the samples before the treatments (Table 3).

Bacterial community changes induced by treatments with uranyl or sodium nitrate

Molecular analyses of the bacterial community structure established after the treatments with uranyl or sodium nitrate under anaerobic conditions revealed strong changes and propagation of populations not identified in the original sample JG35-2. These populations were originally present in very low numbers, below the limit of detection of the used 16S rRNA-gene retrieval, in the untreated samples. This result is similar to our previous observations made after the treatments with the same solutions of another portion of the sample JG35-2 under aerobic conditions (Geissler et al. 2005). However, due to the different aeration conditions, different novel groups of bacteria were established in each of the cases. The latter demonstrates the high capability of the natural bacterial community to "handle" U(VI) and nitrate in rather high and toxic concentrations at both aerobic and anaerobic conditions.

Characteristic for the anaerobically treated samples was the strong proliferation of *Firmicutes* populations, in contrast to the aerobically treated samples, where mainly actinobacterial and *Cytophagales* populations were induced (Geissler and Selenska-Pobell 2005).

In the sample JG35-K4 a high number of facultative anaerobic nitrate-reducing *Bacillales* such as *Bacillus bataviensis* LMG 21832 and *Bacillus drentensis* LMG 21831 was identified (Fig. 1). In the 4 weeks uranyl nitrate treated sample JG35+U4 a *Bacillus* population was identified, which affiliated with *B. sphaericus* JG-A12, recovered from the same uranium mining waste pile (Selenska-Pobell et al. 1999), while in the 14 weeks treated sample another, closely related to *B. niacini*, population was found (Fig. 1).

Table 3. Hyperfine parameters (δ_i, Δ_i) and spectrum areas of the studied samples

Samples	Fe(II)			Fe(III)		
	$\delta_{Fe(II)}$ mm s^{-1}	$\Delta_{Fe(II)}$ mm s^{-1}	A %	$\delta_{Fe(III)}$ mm s^{-1}	$\Delta_{Fe(III)}$ mm s^{-1}	A %
JG35-2	1.211(6)	2.421(11)	56.1(1.5)	0.230(7)	0.867(14)	43.9(1.1)
JG35+U4	1.193(5)	2.473(9)	62.0(1.3)	0.236(8)	0.849(15)	38.0(9)
JG35+U3	1.145(3)	2.381(6)	70.3(1.2)	0.235(6)	0.850(12)	29.7(7)

δ isomer shift in reference to α-Fe, Δ quadruple splitting, A spectrum area, value in brackets is the error of the last digit(s)

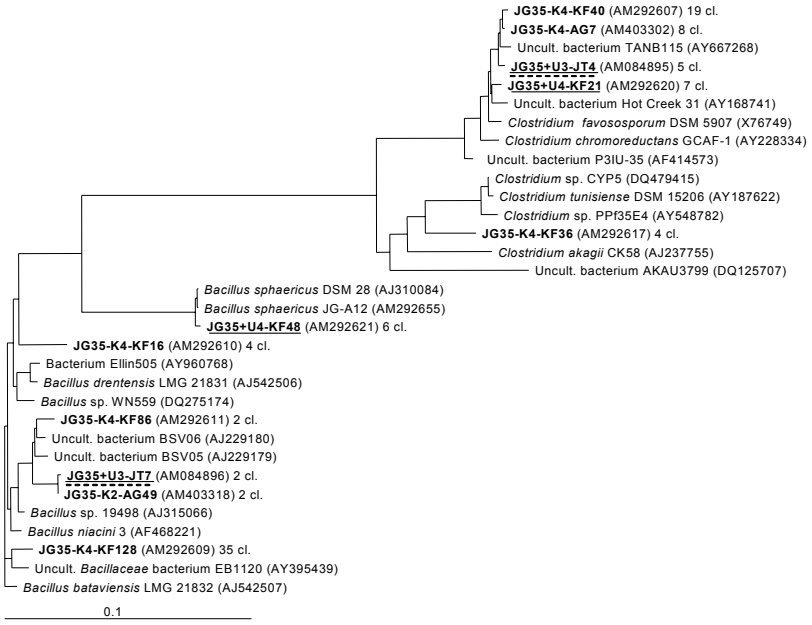

Fig.1. Phylogenetic tree of the 16S rRNA gene sequences affiliated with Firmicutes retrieved from the samples treated with uranyl nitrate JG35+U4 (4 weeks) and JG35+U3 (14 weeks) or with sodium nitrate JG35-K4 (4 weeks) and JG35-K2 (14 weeks). The number of clones (cl.) is written after the accession numbers.

As evident from the results presented in the Fig.1 an extremely high number of various clostridial groups able to fermentatively reduce nitrate to ammonia was found in the sample JG35-K4. In the sample JG35+U4 one relatively dense and obviously uranium tolerant population represented by the sequence JG35+U4-KF21 was identified. Interestingly, related to this population was the only *Clostridium* group identified at the later stages of the incubation in the sample JG35+U3 (sequence JG35+U3-JT4), but not in the sample JG35-K2 (Fig.1). One can speculate that the mentioned clostridial group was established under the selective pressure of the uranium added to the sample JG35+U3. In addition to nitrate, some *Clostridium* spp. are able to reduce U(VI) and Fe(III) (Francis et al. 1994, Dobbin et al. 1999). Because no measurable U(VI) reduction was found in the studied samples we suggest that the mentioned *Clostridium* population together with the small *Bacillus* population might be involved in the observed strong Fe(III) reduction in the sample JG35+U3.

The lower numbers of *Firmicutes* found in the sample JG35+U3 and especially in JG35-K2 can be explained also by the much higher concentration of nitrate (Table 1) added to these samples. The latter seems to be more favorable for other members of the bacterial community of the studied microcosm, such as *Betapro-*

teobacteria (see below). Recently, it was published that some *Clostridium*-like organisms cultivated from uranium wastes possess an ability to reduce uranium in presence of high nitrate concentrations by using methanol or glycerol as carbon sources (Madden et al 2007). We suggest, however, that no *Clostridium*-dependent U(VI) reduction could take place in our experiments due to the deficiency of appropriate electron donors at the studied oligotrophic conditions.

Very interesting is the response of the *Betaproteobacteria* to the treatments. The strong proliferation of diverse populations of this phylum observed in the sample JG35-K4 and especially in JG35-K2, which was incubated with five times higher amount of nitrate for 14 weeks, is in agreement with the common opinion that the oligotrophic and/or autotrophic *Betaproteobacteria* are the main denitrifiers found under anaerobic conditions (Akob et al. 2007, Tiedje 1988).

Because only one small betaproteobacterial population was found at the earlier stages of incubations in the uranyl nitrate treated JG35+U4, we suggest that the mentioned betaproteobacterial denitrifiers do not tolerate U(VI). However, most of the stimulated in the absence of U(VI) betaproteobacterial populations in the sample JG35-K2 were also predominant in the sample JG35+U3, which was incubated with uranyl nitrate for 14 weeks. In our earlier work (Geissler and Selenska-Pobell 2005) we demonstrated that after such long incubations with uranyl nitrate under aerobic conditions the added U(VI) was no longer bio-available to the members of the bacterial community. The immobilization and the decrease of the bioavailability of U(VI) seems to be the most probable reason for the proliferation of the uranium sensitive betaproteobacterial populations in the sample JG35+U3 as well.

In accordance to the observed strong reduction of Fe(III) in the sample JG35+U3, we suggest that some of the identified betaproteobacterial populations are possibly able to reduce Fe(III) analogically to the members of the species *Ferribacterium limneticum* (Cummings et al. 1999) or *Rhodoferax ferrireducens* (Finneran et al. 2003).

Interestingly, no members of *Deltaproteobacteria*, which represented one of the predominant groups in the untreated sample JG35-2 (Geissler and Selenska-Pobell 2005), were identified in the uranyl or sodium nitrate treated samples incubated under anaerobic conditions. This was surprising because representatives of *Deltaproteobacteria* are known for their ability to reduce Fe(III) and to immobilize uranium by reduction of soluble U(VI) to insoluble U(IV) (Lovley et al. 1991). One possible reason for our observations can be the oligotrophic conditions of our microcosms and also the high nitrate concentration during the initial stages of the incubations which are unfavorable for most *Deltaproteobacteria* (Anderson et al. 2003) and for the reduction of U(VI) (Finneran et al. 2002).

Because Mössbauer spectroscopic analysis revealed an increased Fe(III) reduction by increasing the incubation time from 4 to 14 weeks, we suggest that after the reduction of the added nitrate, Fe(III) was the main electron acceptor used by the bacterial populations established in the microbial community at the later stages of the treatments.

Within the time frames of our experiments most of the added U(VI) remained complexed by bacteria-borne phosphate groups in mixed organic and mineral

phases. Our results allow to conclude that the further uranium behavior will strongly depend on the structure of the newly established natural bacterial community in accordance to the geochemical changes in the studied environment. It is not excluded that immobilized U(VI) in the sample JG35+U3 will be reduced after some time by some of the Fe(III) reducers or by some deltaproteobacterial populations, which might start to propagate in the samples, due to accumulation of electron donors for U(VI) reduction in the biomass of the dead bacteria resulting from the treatments.

References

Akob DM, Mills HJ, Kostka JE (2007) Metabolically active microbial communities in uranium-contaminated subsurface sediments. FEMS Microbiol Ecol 59:95–107

Anderson RT, Vrionis HA, Ortiz-Bernad I, Resch CT, Long P E, Dayvault R, Karp K, Marutzky S, Metzler DR, Peacock A, White DC, Lowe M, Lovley DR (2003) Stimulating the *in situ* activity of *Geobacter* species to remove uranium from the groundwater of a uranium-contaminated aquifer. Appl Environ Microbiol 69:5884-5891

Bounhoure I, Meca S, Marti V, De Pablo J, Cortina JL (2007) A new time-resolved laser-induced fluorescence spectroscopy (TRLFS) data acquisition procedure applied to the uranyl-phosphate system. Radiochim Acta 95:165-172

Brand RA (1987) Improving the validity of hyperfine field distributions from magnetic alloys .1. unpolarized source. Nuclear Instruments & Methods in Physics Research Section B-Beam Interactions with Materials and Atoms 28:398-416.

Cummings DE, Caccavo Jr F, Spring S, Rosenzweig RF (1999) *Ferribacterium limneticum*, gen. nov., sp. nov., an Fe(III)-reducing microorganism isolated from mining-impacted freshwater lake sediments. Arch Microbiol 171:183-188

Dobbin PS, Carter JP, San Juan CGS, von Hobe M, Powell AK, Richardson DJ (1999) Dissimilatory Fe(III) reduction by *Clostridium beijerinckii* isolated from freshwater sediment using Fe(III) maltol enrichment. FEMS Microbiol Lett 176:131-138

Finneran KT, Housewright ME, Lovley DR (2002) Multiple influences of nitrate on uranium solubility during bioremediation of uranium-contaminated subsurface sediments. Environ Microbiol 4:510-516

Finneran KT, Johnsen CV, Lovley DR (2003) *Rhodoferax ferrireducens* sp. nov., a psychrotolerant, facultatively anaerobic bacterium that oxidizes acetate with the reduction of Fe(III). Int J Syst Evol Microbiol 53:669-673

Francis AJ, Dodge CJ, Lu F, Halada GP, Clayton CR (1994) XPS and XANES studies of uranium reduction by *Clostridium* sp. Environ Sci Technol 28:636-639

Geipel G, Bernhard G, Rutsch M, Brendler V, Nitsche H (2000) Spectroscopic properties of uranium(VI) minerals studied by time-resolved laser-induced fluorescence spectroscopy (TRLFS). Radiochim Acta 88:757-762

Geissler A, Selenska-Pobell S (2005) Addition of U(VI) to a uranium mining waste sample and resulting changes in the indigenous bacterial community. Geobiology 3:275-285

Geissler A, Scheinost AC, Selenska-Pobell S (2005) Changes of Bacterial Community Structure of a Uranium Mining Waste Pile Sample Induced by Addition of U(VI). *In:* Uranium in the Environment (eds. Merkel B. and Hasche-Berger A.), pp. 199-205

Holmes DE, Finneran KT, O'Neil RA, Lovley DR (2002) Enrichment of members of the family *Geobacteraceae* associated with stimulation of dissimilatory metal reduction in uranium-contaminated aquifer sediments. Appl Environ Microbiol 68:2300-2306

Istok JD, Senko JM, Krumholz LR, Watson D, Bogle MA, Peacock A, Chang YJ, White DC (2004) In situ bioreduction of technetium and uranium in a nitrate-contaminated aquifer. Environ Sci Technol 38:468-475

Koban A, Bernhard G (2007) Uranium(VI) complexes with phospholipid model compounds - A laser spectroscopic study. J Inor Biochem 101:750-757

Lovley DR, Phillips EJP, Gorby YA, Landa ER (1991) Microbial reduction of uranium. Nature 350:413-416.

Madden AS, Smith AC, Balkwill DL, Fagan LA, Phelps TJ (2007) Microbial uranium immobilization independent of nitrate reduction. Environ Microbiol 9:2321-2330.

Merroun ML, Geipel G, Nicolai R, Heise KH, Selenska-Pobell S (2003) Complexation of uranium(VI) by three eco-types of *Acidithiobacillus ferrooxidans* studied using time-resolved laser-induced fluorescence spectroscopy and infrared spectroscopy. Biometals 16:331-339

Nevin KP, Finneran KT, Lovley DR (2003) Microorganisms associated with urnium bioremediation in a high-salinity subsurface sediment. Appl Environ Microbiol 69: 3672-3675

North NN, Dollhopf SL, Petrie L, Istok JD, Balkwill DL, Kostka JE (2004) Change in bacterial community structure during in situ biostimulation of subsurface sediment cocontaminated with uranium and nitrate. Appl Environ Microbiol 70:4911-4920

Nyman JL, Marsh TL, Ginder-Vogel MA, Gentile M, Fendorf S, Criddle C (2006) Heterogeneous response to biostimulation for U(VI) reduction in replicated sediment microcosms. Biodegradation 17:303-316

Panak PJ, Raff J, Selenska-Pobell S, Geipel G, Bernhard G, Nitsche H (2000) Complex formation of U(VI) with *Bacillus*-isolates from a uranium mining waste pile. Radiochim Acta, 88:71-76

Petrie L, North NN, Dollhopf SL, Balkwill DL, Kostka JE (2003) Enumeration and characterization of iron(III)-reducing microbial communities from acidic subsurface sediments contaminated with uranium(VI). Appl Environ Microbiol 69:7467-7479.

Selenska-Pobell S, Panak P, Miteva V, Boudakov I, Bernhard G, Nitsche H (1999) Selective accumulation of heavy metals by three indigenous *Bacillus* strains, *B. cereus, B. megaterium* and *B. sphaericus* from drain waters of a uranium waste pile. FEMS Microbiol Ecol 29:59-67

Suzuki Y, Kelly SD, Kemner KA, Banfield JF (2003) Microbial populations stimulated for hexavalent uranium reduction in uranium mine sediment. Appl Environ Microbiol 69:1337-1346

Tiedje J M (1988) *In* A. J. B. Zehnder (ed.), Biology of Anaerobic Microorganisms, Wiley, New York, USA, pp. 179-244.

Comparative investigation of the interaction of uranium with lipopolysaccharide and peptidoglycan

Astrid Barkleit, Henry Moll and Gert Bernhard

Forschungszentrum Dresden-Rossendorf, Institute of Radiochemistry, P.O. Box 510119, 01314 Dresden, Germany

Abstract. Microorganisms are very important for the bioremediation of the environment because they are able to adsorb radionuclides and other heavy metals. They significantly influence mobilization and immobilization of metal ions in soils.

We investigated representative the complexation of the uranyl ion with main parts of bacterial cell walls. Lipopolysaccharide (LPS) is the principal component of the cell wall of gram-negative bacteria, whereas peptidoglycan (PGN) represents the basis of the cell wall of gram-positve bacteria. Both biomolecules contain a high density of metal-binding functionalities like carboxyl, amino, and hydroxyl groups. LPS offers additionally a high amount on phosphoryl groups, which are missing in PGN.

We investigated the interaction of the uranyl cation (UO_2^{2+}) with the biopolymers LPS and PGN by using potentiometric titration and time-resolved laser-induced fluorescence spectroscopy (TRLFS) over a wide pH range (2.4 – 9) and at environmentally relevant low uranium concentrations (10^{-4} – 10^{-5} M).

Using potentiometric titration, the dissociation constants of the respective functional groups were determined. Furthermore essential uranyl complexes and their stability constants were identified.

With the aid of time-resolved laser-induced fluorescence spectroscopy (TRLFS) the luminescence properties of uranyl complexes with the biopolymers and the as-

sociated stability constants were investigated. At low pH values both biomolecules effect an increase of the luminescence intensity and a red-shift of about 8-10 nm, compared to the free UO_2^{2+} ion. With LPS the luminescence intensity increases up to pH 8. In contrast to LPS, the PGN polymer causes a decrease of the luminescence intensity over pH 4.5, indicating, that a non-luminescent complex has built.

As a result from both methods, we found that the uranyl ion prefers with LPS phosphoryl coordination, whereas PGN, with a lack of phosphoryl groups, forms stable carboxylate complexes.

Environmental implications of Mn(II)-reacted biogenic UO_2

Harish Veeramani[1], Eleanor J. Schofield[2], Elena Suvorova[1], Jonathan O. Sharp[1], John R. Bargar[2] and Rizlan Bernier-Latmani[1]

[1]École Polytechnique Fédérale de Lausanne, Switzerland
[2]Stanford Synchrotron Radiation Laboratory, Menlo Park, CA, US

Abstract. The stimulation of microbial populations in U(VI) contaminated sites to promote U(VI) reduction and produce biogenic mineral uraninite (UO_2) is proposed as a promising strategy for remediation. The long-term success of such a strategy is contingent upon the enduring stability of UO_2 in the subsurface environment, not only under anoxic conditions but also during oxidation events. Sedimentary UO_2 often contain structural cation impurities that are shown to increase their stability to oxidation. By analogy, this study, considers the effect incorporation of Mn(II), a common groundwater cation, on the structure and reactivity of biogenic UO_2.

Introduction

Uranium (U) contamination of ground and surface water as a result of mining activities, use of nuclear weapons and nuclear fuel production threatens human and environmental health at numerous sites in the US and former East Germany (DOE-EM 1997; Meinrath et al. 2003). Uranium exists mainly in the hexavalent and tetravalent oxidation states, the former being mobile and soluble while the latter usually found to be an insoluble solid phase mineral – uraninite. In situ bioremediation of U(VI) contaminated sites by stimulating the indigenous U(VI)-reducing bacterial populations such as *Geobacter spp*, *Shewanella spp*, etc has been proposed as a means to immobilize uranium (Judy and Lee 2006). However, the re-oxidation of bacteriogenic uraninite (the expected product of bioremediation) is a concern because it is susceptible to re-oxidation by a diversity of environmental oxidants (Senko et al. 2002, 2005, 2007; Finneran et al. 2002). Identification of factors affecting the resistance of UO_2 to oxidative dissolution is fundamental to devising appropriate remediation strategies.

Naturally occurring sedimentary uraninites found in the environment serve as useful analogs to biogenic uraninite. They contain many structural impurities such as Ca^{2+} and Pb^{2+}, which are believed to stabilize the UO_2 structure and promote resistance to oxidation. Ground waters usually have large concentrations of divalent cations like Ca^{2+}, Mg^{2+}, Mn^{2+}, Fe^{2+} (USDOE). Uraninite is formed by a cascade of reactions starting with the reduction of hexavalent uranium to the tetravalent form followed by polymerization of U(IV) and nucleation which then leads to crystal growth under anoxic conditions. By analogy to sedimentary uraninites, we hypothesize that biogenic uraninites can acquire such cations during U(IV) polymerization and crystal growth and incorporate them within the crystalline structure, thereby potentially increasing the stability of the material under oxidizing conditions.

In this study, we assess the potential for the incorporation of Mn(II), a common ground water cation, into the structure of biogenic UO_2 and investigate its effect on reactivity of the mineral using a combination of aqueous chemical measurements, trans-mission electron microscopy (TEM) and a suite of synchrotron based techniques.

Materials and Methods

Cells of *Shewanella oneidensis* MR-1 were grown aerobically, harvested and U(VI) reduction performed according to the procedure reported elsewhere (Schofield et al. 2008). A small amendment of Mn(II) was made from a sterile 1M anaerobic stock of $MnCl_2$ prior to the amendment of an anaerobic stock of 10 mM uranyl acetate for the production of Mn-reacted UO_2. XRD was carried out on the experimental matrix to check for precipitation of undesirable exogenous mineral phases. Geo-chemical speciation of Uranium under our experimental conditions was simulated using MINEQL+. Biogenic UO_2 obtained was subjected to an alkaline treatment involving 1M NaOH followed by an organic solvent treatment (hexane) to remove the biomass as described previously (Schofield et al. 2008). The treated clean biomass free UO_2 was stored at pH 7 in MilliQ water until use.

The ratio of Mn(II) associated with biogenic UO_2 was determined by digesting an aliquot of the biogenic UO_2 using 0.1% HNO_3 and analyzing the digest for U(VI) and Mn(II) content. Analyses of U and Mn were carried out by kinetic phosphorescence analysis (KPA) & inductively coupled plasma optical emission spectrometry (ICP-OES) or high-resolution ICP-mass spectrometry (HR-ICP-MS) respectively. To differentiate between adsorption and incorporation (the goal of the study was to investigate incorporation) of Mn(II) on or within UO_2 respectively, the characteristic sorption behavior of Mn(II) onto biogenic, NaOH-treated undoped UO_2 was assessed. 0.1 mg UO_2/L was added to polypropylene tubes containing an anaerobic solution (10 mL) of 0.01 M NaCl pre-adjusted to pH values ranging from 3 to 10, followed by addition of 1mM Mn(II). pH was adjusted using 0.5 M HCl or 0.5 M NaOH when necessary. Appropriate controls (no Mn(II) or no UO_2) were maintained to account for the adsorption of Mn(II) on the experimental materials, precipitation of Mn or the dissolution of UO_2. These tubes were equili-

brated overnight inside the anaerobic chamber, after which the pH was re-measured. Samples were withdrawn, filtered (0.2 μm polyethersulfone filter) and analyzed for total Mn & U as above. The first few drops of the filtrate were discarded to minimize errors due adsorption of analyte on the filter material.

High resolution transmission electron microscopy was carried out as described previously (Schofield et al. 2008). Surface area analysis was carried out to determine the surface area of clean biogenic UO_2 using a BET analyzer employing N_2 gas as the probe molecule. The cleaned biogenic Mn(II) reacted UO_2 was also analyzed using a suite of various synchrotron based techniques including 1) U L_{III} edge Extended X-ray Absorption Fine Structure (EXAFS) spectroscopy, 2) Mn K-edge EXAFS and 3) In-situ synchrotron based powder diffraction (SR-PD), all of which were carried out at SSRL. U L_{III} edge Extended X-ray Absorption Fine Structure (EXAFS) spectroscopy was carried out as described previously (Schofield et al. 2008). For Mn K-edge EXAFS sample preparation was similar to U-EXAFS. In situ synchrotron based powder diffraction (SR-PD) was also carried out on the samples to determine the crystallite size of biogenic UO_2.

Batch oxidative dissolution experiments were carried out in a simple chemical matrix composed of 30 mM $NaHCO_3$ and 20 mM of HEPES buffer at pH 8. NaOH-treated UO_2 was added to the dissolution matrix and 50 mL aliquots were dispensed into duplicate 200 ml capacity serum bottles inside the anaerobic chamber. The bottles were subsequently sealed and 50 mL of air was injected into each bottle. They were placed on a rotary shaker (180 rpm) at 25 ºC. At time intervals, 1 mL of sample was withdrawn, filtered using a 0.2 μm PES filter and analyzed for U(VI) using the KPA. One mL of air was injected each time a sample was withdrawn to maintain the equilibrium pressure.

Results and Discussion

Mn-reacted biogenic UO2 was produced through the reduction of U(VI) by Shewanella oneidensis MR-1 at different aqueous Mn(II) concentrations at pH 6.3 and 8 (Fig. 1). Uranium reduction was faster at pH 6.3 as compared to pH 8 but was comparable in the presence and absence of Mn(II) at a given pH. This suggests that Mn(II) did not affect biological U(VI) reduction. Geochemical speciation calculations using MINEQL+ indicate the dominance of two different uranium-carbonate species at pH 6.3 and 8 respectively (Fig. 2). Faster U(VI) reduction rates (pH 6.3) correspond to the dominance of a 1:2 aqueous uranium complex [UO2(CO3)22-] and slower rates (pH 8) to a 1:3 species [XRD analysis reveals the precipitation of rhodochrosite (MnCO3) at pH 8 but not at pH 6.3 (Fig. 3). Hence, the characterization of biogenic UO2 was carried out with samples synthesized at pH 6.3. The surface area of cleaned undoped biogenic UO2 was found to be about 50 m2/gram. Analysis of complete acid digests (KPA for total U; ICP-OES for total Mn) of the clean NaOH treated, Mn(II) reacted biogenic UO2 reveals association of Mn(II) with UO2. To determine whether the association of Mn(II) with UO2 was adsorption onto or incorporation within UO2, the Mn(II) reacted biogenic UO2 was subjected to multiple washings (5 times until no Mn

was detected in wash supernatant) at pH 5. Adsorption studies involving clean NaOH treated undoped UO2 indicate minimal Mn(II) adsorption and UO2 dissolution at pH 5 in an aqueous medium devoid of carbonate. Hence desorption of most surface adsorbed Mn(II) is expected upon repeated washing at pH 5. An aliquot of the pH 5 washed Mn(II) reacted biogenic uraninite was digested with 0.1% HNO3 and subsequently analyzed as before. A comparison of U:Mn ratios in the total acid digest of Mn(II) reacted UO2 indicates a considerable fraction (50 to 90%) of initial Mn(II) adsorbed on UO2. The remaining small fraction of Mn(II) that was not removed by pH 5 treatment, suggests that a fraction of Mn is localized and incorporated into the crystal lattice of biogenic UO2 and is unaffected by repeated washing. Thus, we conclude that a small but measurable fraction of Mn(II) is structurally bound to UO2. Furthermore, higher initial Mn(II) concentration during U(VI) reduction led to greater amount of Mn associated with biogenic UO2 which remained associated even after extensive washing at pH 5 (Table 1). Thus, the Mn(II) content in the UO2 crystal increases with increasing total Mn reacted with UO2 during its biogenic formation, consistent with incorporation of Mn(II) into UO2.

Detailed characterization of the size distribution of UO_2 nanoparticles obtained by analysis of Fourier-filtered HRTEM images of the different biogenic UO_2 indicate a decrease in the average particle size with increasing Mn concentration (Fig. 4; Table 2). This suggests a systematic and progressive decrease in average nanoparticle size with increasing incorporation of Mn(II) into UO_2. Rietveld refinements of the SR-PD data for varying Mn concentrations also demonstrate this trend of decreasing crystallite sizes with increasing Mn(II) concentration (Table 2). A possible explanation for this observation is the inhibition of particle growth and stabilization of small particles caused either by Mn(II) binding to the UO_2 surfaces and the subsequent poisoning of the surfaces to further growth or by the structural strain induced due to the incorporation of Mn(II).

Batch oxidative dissolution experiments were carried out at pH 8.0 in the presence of air, 30mM HCO_3^- and 20 mM HEPES buffer in closed systems. There is a significant and reproducible difference in the rate of oxidative dissolution of the two uraninites (Fig. 5): unreacted UO_2 re-oxidizes faster than 1 mM Mn-reacted UO_2. The results suggest that Mn-reacted UO_2 is more resistant to oxidation than unreacted UO_2. Interestingly at pH 8.0, the Mn-reacted UO_2 displays slower oxidation as compared to unreacted UO_2 despite its smaller particle size and greater surface area. Furthermore at pH 8, the potential for chemical oxidation of Mn(II) by O_2 at pH 8 could potentially lead to accelerated oxidative dissolution of UO_2 due to the formation of Mn(IV)oxides which are potent oxidants. Quite to the contrary, we observe slower re-oxidation of the Mn(II) reacted UO_2. The most likely explanation for this observation could be the tendency for the solid to be stabilized by the substitution of Mn in UO_2. The apparent dominance of this latter factor is consistent with the reported increase in stability conferred by Ca^{2+} and Pb^{2+} structural impurities.

The extent to which the incorporation of Mn(II) into the UO_2 lattice decreases its reactivity with respect to re-oxidation (as observed in the batch system) is being studied in our ongoing work involving continuous flow-through dissolution

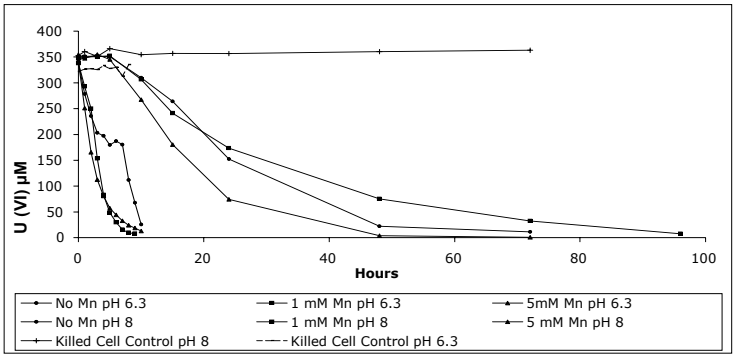

Fig.1. U(VI) reduction by *Shewanella oneidensis* MR1 at pH 6.3 and 8 in the presence of varying Mn(II) concentrations.

and soil column experiments in order to circumvent potential artifacts associated with batch systems.

Implications for U(VI) bioremediation

In this study, we demonstrated the incorporation of Mn(II) into the lattice of UO2 and evaluated the structure and reactivity of biogenic UO2 produced in the presence of Mn(II). The bioremediation of U(VI)-contaminated groundwater to produce UO2 will invariably occur in the presence of divalent cations, including Mn(II). Under the conditions considered in the present work, results suggests that Mn(II) incorporation into the lattice confers improved stability to biogenic UO2. If this observation is confirmed in more environmentally-relevant systems, it would strongly support the notion that the reactivity of uraninite is influenced its intrinsic composition and the geochemical conditions prevalent in the surrounding environment.

Acknowledgements

Work carried out at EPFL was funded by Swiss NSF grant # 20021-113784 and DOE OBER grant # DE-FG02-06ER64227. Portions of this research were carried out at the Stanford Synchrotron Radiation Laboratory, a national user facility operated by Stanford University on behalf of the U.S. Department of Energy (DOE), Office of Basic Energy Sciences and supported by the SSRL Environmental Remediation Science Program and BER-ERSD project number SCW0041. The SSRL Structural Molecular Biology Program is supported by the Department of Energy, Office of Biological and Environmental Research, and by the National Institutes of Health, National Center for Research Resources, Biomedical Technology Program.

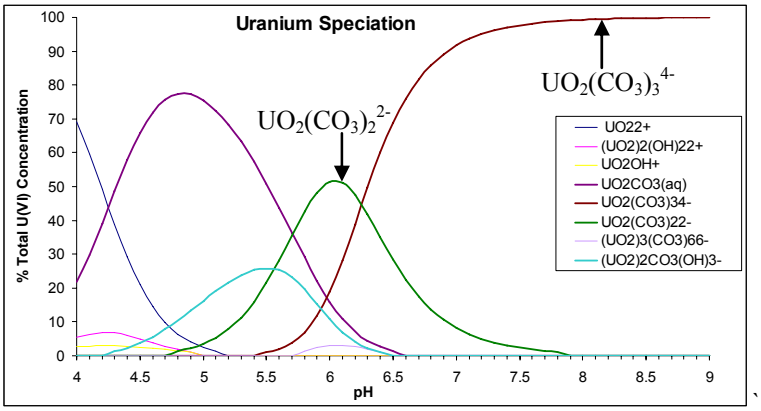

Fig.2. Initial U(VI) speciation in 30 mM HCO_3^- at various pH values.

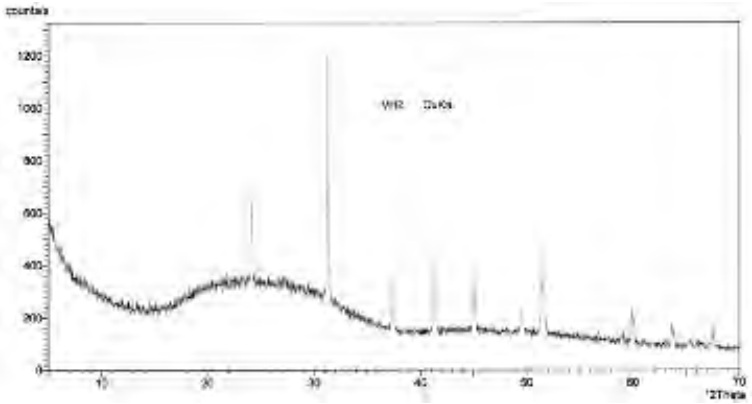

Fig.3. XRD indicating the presence of rhodochrosite at pH 8.

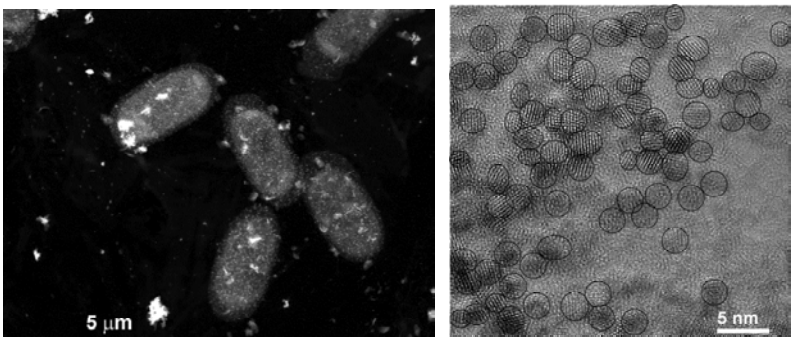

Fig.4. A) Scanning TEM showing the accumulation of UO_2 around *Shewanella oneidensis* MR1. **B)** Fourier-filtered HRTEM image of bacteriogenic UO_2.

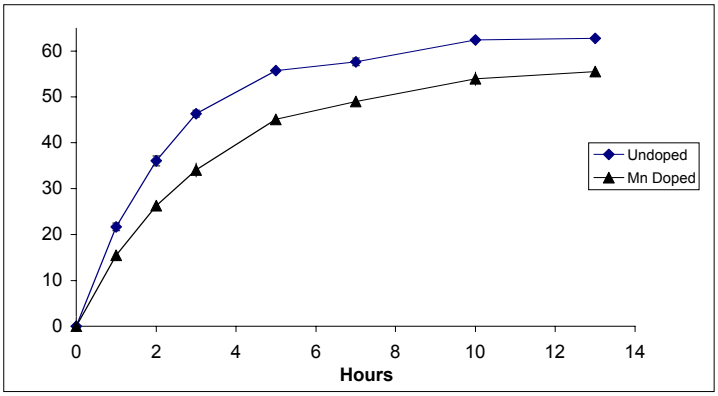

Fig.5. Comparison of initial U(VI) released by oxidative dissolution of biogenic UO_2 in air in a closed system at pH 8 in 30 mM $NaHCO_3$ and 20 mM HEPES. Data are indicated by symbols: unreacted UO_2 (♦) and 1 mM Mn-reacted UO_2 (▲).

Table 1. Ratios of U:Mn in various UO_2 synthesized under different concentrations of Mn – before and after pH 5 wash.

Mn(II) conc. (mM)	# Washes	U: Mn ratio	
		Before wash	After wash
0.1	5	150 : 1	340 : 1
1	5	4.91 : 1	32 : 1
5	5	0.33:1	1.2 :1

Table 2. Summary of particle and crystallite size obtained by HRTEM and in-situ synchrotron powder-diffraction data for Mn-reacted biogenic uraninite. Decreasing particle size with increasing Mn(II) conc.

Mn(II) Conc.	Average particle/Crystallite size (nm)	
	HRTEM	SR-PD
No Mn	2.5	3.52
0.1 mM Mn	2.2	2.36
1 mM Mn	2.2	2.35
5 mM Mn	1.9	1.45
8 mM Mn	1.6	-

References

DOE-EM. 1997. Linking Legacies: Connecting the Cold War Nuclear Weapons Production Processes to their Environmental Consequences. DOE/EM-0319. US Department of Energy, Washington, DC.:222 p.

Finneran KT, Housewright ME, Lovley DR. 2002. Multiple influences of nitrate on uranium solubility during bioremediation of uranium-contaminated subsurface sediments. Environmental Microbiology 4(9):510-516.

Judy DW, Lee RK. 2006. Uranium reduction. Annu Rev Microbiol 60:149-66.

Meinrath A, Schneider P, Meinrath G. 2003. Uranium ores and depleted uranium in the environment, with a reference to uranium in the biosphere from Erzgebirge/Sachsen, Germany. Journal of Environmental Radioactivity 64:175-193.

Schofield EJ, Veeramani H, Sharp JO, Suvorova E, Bernier-Latmani R, Mehta A, Stahlman J, Webb SM, Clark DL, Conradson SD and others. 2008. Structure of biogenic UO_2 produced by Shewanella oneidensis MR-1. Environ. Sci. Technol. submitted.

Senko JM, Istok JD, Suflita JM, Krumholtz LR. 2002. *In-situ* evidence for uranium immobilization and remobilization. Environ. Sci. Technol. 36(7):1491-1496.

Senko JM, Kelly SD, Dohnalkova A, McDonough JT, Kemner KM, Burgos WD. 2007. The effect of U(VI) bioreduction kinetics on subsequent reoxidation of biogenic U(IV). Journal: Geochimica et Cosmochimica Acta, 71(19):4644-4654; Journal Volume: 71; Journal Issue: 19.

Senko JM, Mohamed Y, Dewers TA, Krumholz LR. 2005. Role for Fe(III) Minerals in Nitrate-Dependent Microbial U(IV) Oxidation. Environ. Sci. Technol. 39(8):2529-2536.

USDOE. Old Rifle site Groundwater composition data. . http://www.lm.doe.gov/land/sites/co/rifle/rifleoldp/rifle_old.htm

The effect of temperature on the speciation of U(VI) in sulfate solutions

Linfeng Rao and Guoxin Tian

Lawrence Berkeley National Laboratory, Berkeley, California 94720, U.S.A.

Abstract. Sulfate, one of the inorganic constituents that could be present in the nuclear waste repository, forms complexes with U(VI) and affects its migration in the environment. Results show that the complexation of U(VI) with sulfate is enhanced by the increase in temperature. The effect of temperature on the complexation and speciation of U(VI) in sulfate solutions is discussed.

Introduction

Uranium is the most abundant radioactive element in the nuclear wastes generated by the nuclear industry including uranium mining and spent nuclear fuel reprocessing. Safe management of the nuclear wastes, the high-level nuclear wastes (HLW) in particular, calls for proper treatment and long-term disposal in geological repositories. Engineered barrier systems (e.g., waste packaging and drip shields) are implemented to prevent the waste forms from being eroded and/or breached. Though the engineered barrier systems are expected to last a very long time after the repository is closed, they may gradually deteriorate and eventually lose integrity. If this disastrous scenario occurs, water could contact the waste form, dissolve it, and carry radionuclides out of the repository. The migration of radionuclides, including uranium, in the post-closure environment of the repository is a great concern to the long-term performance assessment of the nuclear waste repository.

Complexation of U(VI) with inorganic ligands that exist in the groundwater of the repository (e.g., OH^-, F^-, SO_4^{2-}, PO_4^{3-} and CO_3^{2}) could affect the speciation of U(VI) and its migration in the environment. Moreover, the temperature of the HLW repository could remain significantly higher than the ambient even thousands of years after the closure of the repository. As Fig. 1 shows, the projected temperature in the vicinity of the waste form in the Yucca Mountain Repository of the United States is around 80-100^{o}C, even a thousand years after the closure of the repository (OCRWM 2002). As a result, predictions of the migration behavior of U(VI) in the repository cannot be made without taking into consideration the

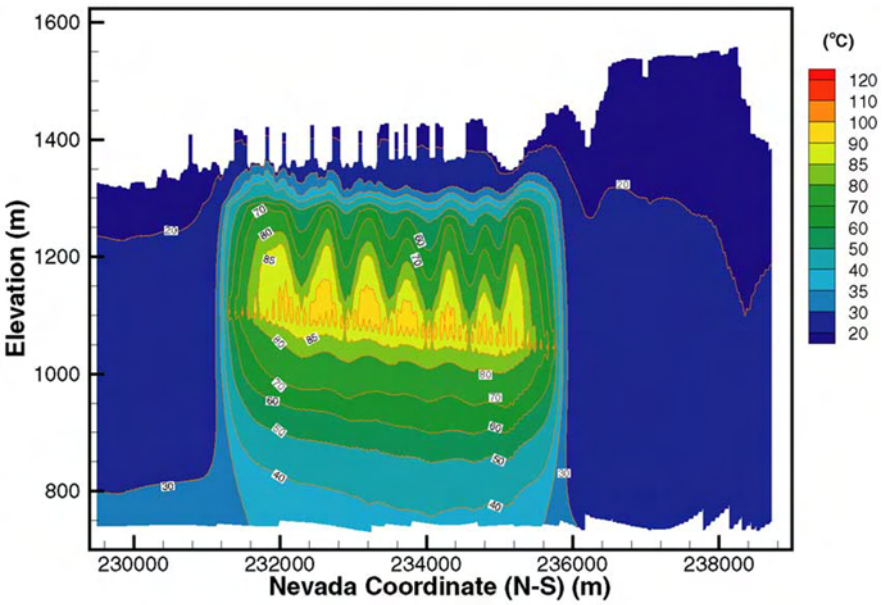

Fig.1. Temperature distribution at 1,000 years along NS#2 cross section of Yucca Mountain Repository (with ventilation) from the Mountain-Scale Thermal-Hydrologic Model (OCRWM 2002). The color band indicates that the temperature of the waste forms (200 - 300 meters below the ground surface) is around 80 – 100°C.

effect of temperature on the complexation of U(VI) with the ligands that may exist in the groundwater of the repository. Unfortunately, data on the complexation of U(VI) with many inorganic as well as organic ligands at elevated temperatures are not available at present (Grenthe et al. 1992, Guillaumont et al. 2003). To help with the performance assessment of the HLW repository and fill the gap in thermodynamic data on actinide complexation at elevated temperatures, we have studied the complexation of actinides with selected organic and inorganic ligands at elevated temperatures. This paper briefly summarizes the results on the complexation of U(VI) with sulfate at elevated temperatures and discusses the effect of temperature on the speciation of U(VI) in sulfate solutions.

Experimental

Chemicals

All chemicals were reagent grade or higher. Milli-Q water was used in preparations of all solutions. Preparation and standardization of the stock solution of uranyl perchlorate have been described elsewhere (Zanonato et al. 2004). A stock solution of sodium sulfate was prepared by dissolving appropriate amounts of sodium sulfate solid in water. The ionic strength of all solutions used in spectrophotometric titrations was adjusted to 1.0 M Na(ClO4/SO4) at 25oC. All the molar concentrations in this paper are referred to 25oC.

Variable-temperature spectrophotometry

UV/Vis absorption spectra of U(VI) (380 - 480 nm, 0.2 nm interval) were collected on a Varian Cary-5G spectrophotometer equipped with sample holders that were maintained at constant temperatures by a 1×1 Peltier controller. 10 mm quartz cells were used. Before being inserted into the sample holders, the sealed cells were immerged in an external constant-temperature water bath to be pre-equilibrated at the required temperature. This procedure successfully prevented condensation of water on the top of the cells during the titrations at high temperatures. Multiple titrations with different concentrations of U(VI) were performed. In each titration, appropriate aliquots of the Na2SO4 solution were added into the cell and mixed thoroughly before the absorption spectrum was collected. Usually 10 - 15 spectra were collected in each titration. Stability constants of the U(VI)/sulfate complexes (on the molarity scale) were calculated by non-linear least-square regression using the Hyperquad program (Gans et al. 1996).

Results and discussion

Stability constants of U(VI)/sulfate complexes at variable temperatures (25 – 70°C)

Spectrophotometric titrations were conducted at 25, 40, 55 and 70oC. The absorption spectra of a representative titration at 55oC are shown in Fig. 2. The first spectrum (the bottom one) shows the characteristic vibronic bands of free UO22+ in the UV/Visible region (□max ≈ 414 nm). Two distinct changes were observed as the concentration of sulfate was increased: (1) the positions of the absorption bands of U(VI) were shifted to longer wavelengths; (2) the absorbance of U(VI)

solutions increased significantly. Both changes suggest that U(VI)/sulfate complex(es) formed. Factor analysis of the absorption spectra by the Hyperquad program indicate that there are three absorbing species of U(VI), i.e., free UO22+ and two U(VI)/sulfate complexes. Therefore, the spectra were best-fit with the formation of successive 1:1 and 1:2 complexes, UO2SO4(aq) and UO2(SO4)22-, represented by equations 1 and 2.

$$UO_2^{2+} + SO_4^{2-} = UO_2SO_4(aq) \quad (1)$$

$$UO_2^{2+} + 2SO_4^{2-} = UO_2(SO_4)_2^{2-} \quad (2)$$

The stability constants of $UO_2SO_4(aq)$ and $UO_2(SO_4)_2^{2-}$ at 25, 40, 55 and 70°C were calculated and summarized in Table 1. In the calculation, the protonation constants of sulfate at different temperatures from the literature were used (Rao et al. 2006). Data in Table 1 indicate that U(VI) forms moderate complexes with sulfate and the complexes become stronger at higher temperatures – 2-fold and 10-fold increases in the values of β for $UO_2SO_4(aq)$ and $UO_2(SO_4)_2^{2-}$, respectively, as the temperature is increased from 25 to 70°C.

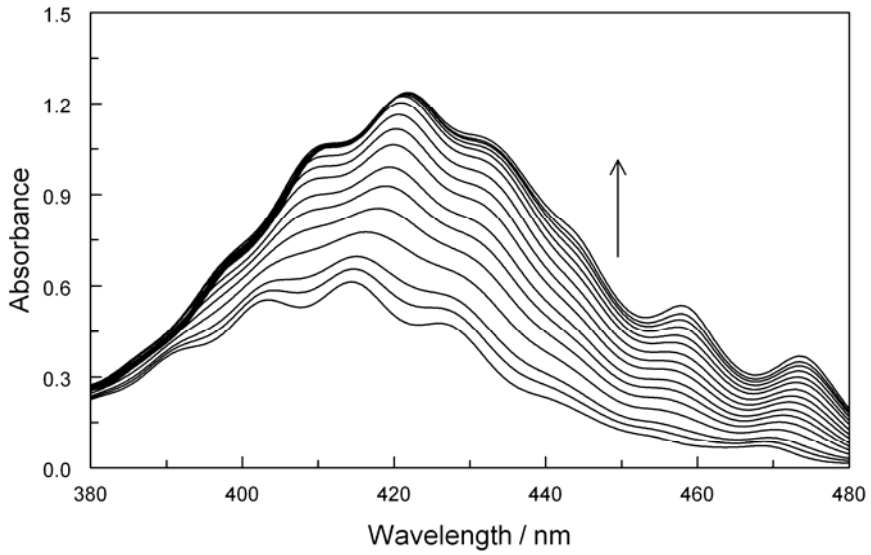

Fig.2. A representative spectrophotometric titration of U(VI)/sulfate complexation at 55°C. I = 1.0 M Na(ClO_4/SO_4). Initial solution: 2.50 mL, 0.071 M $UO_2(ClO_4)_2$/0.085 M $HClO_4$; titrant: 0.5 M Na_2SO_4. Final solution: 6.08 mL. The arrow indicates the increase of the sulfate concentration. The spectra are normalized for the concentration of U(VI).

Table 1. Equilibrium constants of the protonation and complexation of sulfate with U(VI).

Reaction	T /°C	Method[a]	log β (I = 1.0 M)	Ref.[b]
$H^+ + SO_4^{2-} = HSO_4^-$	25	cal	1.07 ± 0.09	(Rao et al. 2006)
	40	cal	1.14 ± 0.12	
	55	cal	1.28 ± 0.09	
	70	cal	1.38 ± 0.09	
$UO_2^{2+} + SO_4^{2-} = UO_2SO_4(aq)$	25	sp	1.96 ± 0.06	p.w.
	40	sp	2.04 ± 0.06	
	55	sp	2.20 ± 0.06	
	70	sp	2.32 ± 0.03	
$UO_2^{2+} + 2SO_4^{2-} = UO_2(SO_4)_2^{2-}$	25	sp	2.97 ± 0.03	p.w.
	40	sp	3.34 ± 0.03	
	55	sp	3.71 ± 0.06	
	70	sp	3.94 ± 0.15	

[a] Method: cal – calorimetry; sp - spectrophotometry.
[b] p.w. – present work.

Speciation of U(VI) in sulfate solutions at variable temperatures

The stability constants of U(VI)/sulfate complexes in Table 1, in conjunction with the equilibrium constants of U(VI) hydrolysis at elevated temperatures in the literature (Zanonato et al. 2004), allow us to calculate the speciation of U(VI) in sulfate solutions at variable temperatures as a function of acidity. The calculated speciation diagrams at 25 and 70oC are shown in Fig. 3.

At 25°C, in the absence of sulfate (Diagram A), the hydrolysis of U(VI) starts at about pC_H (i.e., -log[H^+]) 3.5 and the trimeric $(UO_2)_3(OH)_5^+$ species becomes dominant when pC_H > 5. The presence of 1 mM sulfate (Diagram B) only slightly changes the speciation. However, the presence of 100 mM sulfate (Diagram C) effectively suppresses the formation of the monomeric and dimeric hydrolysis species (UO_2OH^+ and $(UO_2)_2(OH)_2^{2+}$), significantly altering the speciation of U(VI) in the low pC_H region (from 3.5 to 5). When the pC_H is above 5, formation of the trimeric $(UO_2)_3(OH)_5^+$ species starts and becomes dominant at higher pC_H, where the strength of U(VI)/sulfate complexes is not sufficiently high to compete with hydrolysis.

At 70°C, the trends in speciation as the sulfate concentration is increased from 0 (Diagram D), 1.00 mM (Diagram E) to 100 mM (Diagram F) are similar to those observed at 25°C. However, because both the hydrolysis of U(VI) and the complexation of U(VI) with sulfate are enhanced at higher temperatures, the speciation at 70°C differs from that at 25°C. In particular, the U(VI) sulfate complexes, $UO_2SO_4(aq)$ and $UO_2(SO_4)_2^{2-}$, dominate in the low pC_H region when the sulfate concentration is 100 mM, with $UO_2(SO_4)_2^{2-}$ accounting for 80% up to pC_H 5.

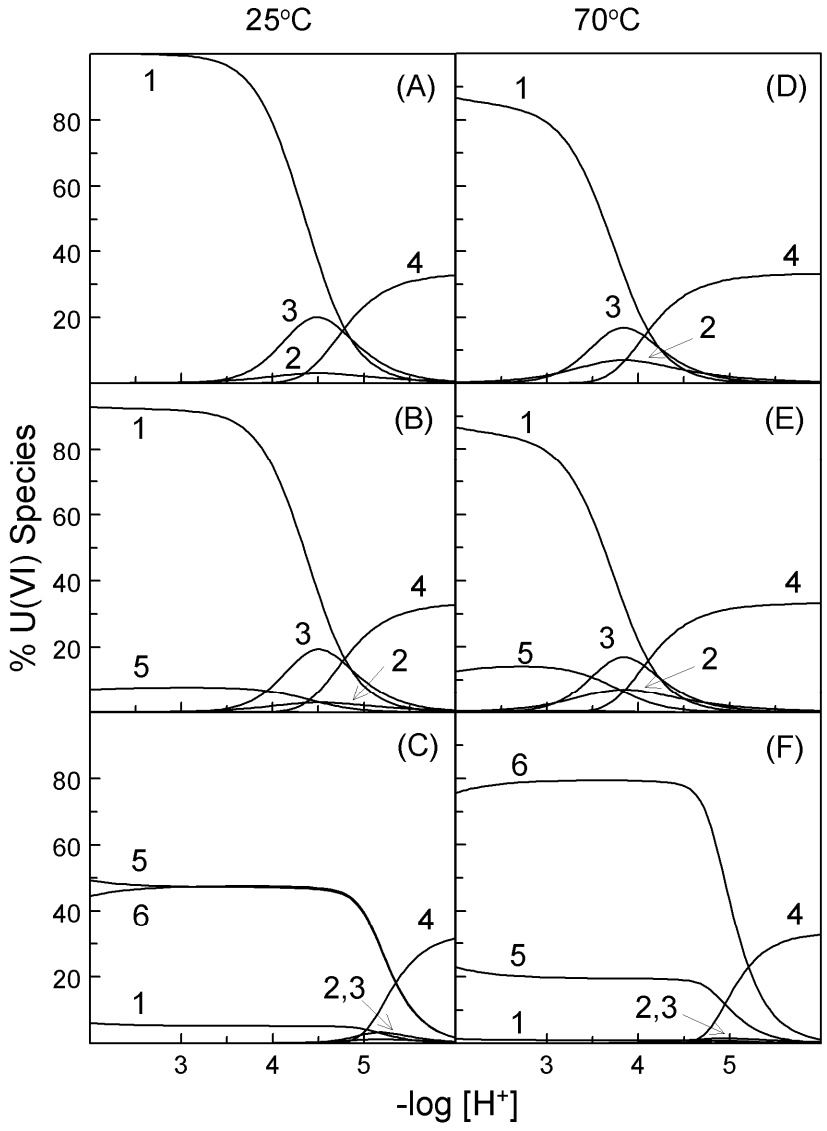

Fig.3. Speciation of U(VI) as a function of acidity in sulfate solutions at 25 and 70°C (I = 1.0 M). $C_{U(VI)}$ = 1.00 mM. $C_{sulfate}$ = 0 mM (A, D), 1.00 mM (B, E), 100 mM (C, F). Temperature: 25°C (A, B, C), 70°C (D, E, F). Species: 1 - free UO_2^{2+}, 2 - UO_2OH^+, 3 - $(UO_2)_2(OH)_2^{2+}$, 4 - $(UO_2)_3(OH)_5^+$, 5 - $UO_2SO_4(aq)$, 6 - $UO_2(SO_4)_2^{2-}$.

In summary, the presence of sulfate in high concentrations significantly affects the speciation of U(VI) in the low pC_H region (< 5), but has a negligible effect when pC_H > 5 where the higher hydrolysis species (e.g., $(UO_2)_3(OH)_5^+$) forms. The importance of U(VI)/sulfate complexation and its effect on U(VI) speciation in the low pC_H region is more significant as the temperature increases.

Acknowledgements

This work was supported by the Director, OST&I Program, Office of Civilian Radioactive Waste Management, U. S. Department of Energy, under Contract No. DE-AC02-05CH11231 at Lawrence Berkeley National Laboratory.

References

Gans P, Sabatini A, Vacca A (1996) Talanta 43: 1739 – 1753

Grenthe I, Fuger J, Konings R J M, Lemire R J, Muller A B, Nguyen-Trung C, Wanner H (1992) Chemical thermodynamics of uranium (Wanner H, Forest I, eds.) Elsevier, Amsterdam

Guillaumont R, Fanghanel T, Fuger J, Grenthe I, Neck V. Palmer D A, Rand M H (2003) Update on the chemical thermodynamics of uranium, neptunium, plutonium, americium and technetium (Mompean F J, Illemassene M, Domenech-Orti C, Ben Said K eds.) Elsevier, Amsterdam

OCRWM Report (2002) Yucca Mountain Science and Engineering Report Rev.1, DOE/RW-0539-1, Office of Civilian Radioactive Waste Management: North Las Vegas, NV

Rao L, Tian G, Xia Y, Friese J I (2006) Thermodynamics of neptunium(V) fluoride and sulfate at elevated temperatures, in Proceedings of the 11th International High-Level Radioactive Waste Management Conference (IHLRWM), April 30 – May 4, 2006, Las Vegas, Nevada, 374 - 378

Zanonato P, Di Bernardo P, Bismondo A, Liu G, Chen X, Rao L (2004) J Am Chem Soc 126: 5515 - 5522


Uranium Mining
and Hydrogeology

Safety functions derived from geochemistry for safety analysis of final disposal of high-level radioactive waste

Guido Bracke, Thomas Beuth, Klaus Fischer-Appelt, Jürgen Larue and Martin Navarro

Gesellschaft für Anlagen- und Reaktorsicherheit (GRS) mbH, Schwertnergasse 1, 50667 Cologne, Germany

Abstract. The most important barrier of the multi-barrier system is the confining host rock of a repository for high-level radioactive waste. The repository system, subsystems and components provide safety functions to prevent or delay the release of radionuclides from the waste to the biosphere. Geochemical processes within the waste, waste matrix and the near field provide some of these safety functions for isolation and retardation and can be characterized as effective, latent, supplementary or reserve safety functions. This paper focuses on safety functions related to geochemical processes.

Introduction

All chemical processes in a final repository can be called geochemical, including those in the waste and waste canister, since they take place in geological environment. Geochemical processes vary with the material, its location within the repository and with time. The most important geochemical processes are dissolution, precipitation and sorption. A detailed geochemical approach considers the interactions of the waste composition, the container materials, the different features of surfaces and transportation pathways in space and time. This results in complex interdependencies and cannot be modeled straightforward.

The implementation of geochemical processes in safety analyses using thermodynamic modeling has gained importance within the last years (Köster and Rudolph 1991; Kienzler et al. 2007). There are still open questions with regard to reaction rates of geochemical processes (Brown and Lowson 1997), the requirements of quasi-closed systems for geochemical modeling (Kienzler et al. 2007) and the quality of the thermodynamic data bases (Altmaier et al. 2008).

Currently, national and international work focuses on the generation of a consistent thermodynamic database for the geochemical modeling of radionuclides and solutions. The geochemical behavior of radionuclides on transportation and their reaction rates is less well known. The formation of colloids can not be modeled using thermodynamic data.

For the definition of source terms in numerical long-term safety analyses, time-dependent radionuclide concentrations are required. Therefore, research and development focused on geochemically based radionuclide concentrations. For practical reasons, solubility limits for radionuclides have been used that were obtained by geochemical modeling of equilibrated systems.

The following paper names geochemical safety functions and assigns them to technical components of the repository system. The geochemical processes that have been considered in the definition of geochemical safety functions are presented in the following.

Geochemical processes

Dissolution

Dissolution is the most important process controlling the release of radionuclides since dissolution in a fluid is the most important prerequisite for the transportation of radionuclides to the biosphere.

The dissolution process of spent fuel elements and vitrified radioactive waste was investigated in some detail e.g. by Bruno et al. (1998) and Grambow et al. (1996), respectively. Dissolution rates strongly depend e.g. on pH, Eh, speciation of radionuclides and radiolysis.

An integration of dissolution rates into safety analysis was not done so far because it is currently not possible to predict dissolution rates in a reliable way due to the high complexity of the mechanisms involved. In safety analyses, dissolution is often considered to be instantaneous for a certain period of time.

Precipitation

Precipitation takes place, when the solubility limit of a compound is reached. Precipitation is the reverse process of dissolution. Coprecipitation and the formation of solid solutions are similar processes. A reliable prediction in time is not considered to be possible in a number of cases since precipitation may be kinetically hindered e.g. by metastable phases. The geochemical equilibrium of dissolution and precipitation (which actually is rate dependent) is modeled using thermodynamic data.

Since precipitation and dissolution rates can not be predicted reliably in a number of cases, the geochemical equilibrium of a quasi-closed system with selected mineral phases is modeled to obtain the solubility limits of radionuclides.

Sorption

Sorption is a reversible (or irreversible) physical or chemical interaction of a dissolved species with surfaces which removes the species from the transporting medium. Sorption depends on surface characteristics, the sorbet, the sorbens, composition of the solvent, competition of ions, temperature and other physical conditions.

Reversible sorption delays the transport of radionuclides and can decrease their concentration in the fluid. If experimental data is available, sorption is considered in the transport calculation of the safety analysis.

Radiolysis

The radioactivity of high-level waste affects geochemical processes in the near field. Radiolysis will generate highly reactive products from water, an oxidizing environment and will enhance the dissolution and corrosion of constituents of the waste and the waste containers.

Gas generation

Gas generation is correlated with other geochemical processes such as corrosion, microbial degradation and radiolysis and can contribute to the transportation of (gaseous) radionuclides to the biosphere. Microbial degradation is not of relevance for high-level radioactive waste because of the low or missing amounts of organic compounds. Gas generation has not been considered in modeling of geochemical equilibriums due to a lack of suitable databases.

The relevance of gas generation can be illustrated using an example. Hydrogen gas formed by corrosion of steel or radiolysis embrittles the zircaloy cladding and may provide a reducing environment.

Colloids

Mobile and sorbing Colloids are considered to enhance the mobility of radionuclides. However, mobile colloids may be rare in the fluid phase of the near-field because of the high salinity of the fluids in most cases.

Other processes

Other geochemical processes might gain relevance in a repository system such as the volume increase due to the corrosion of metals, passivity of metal with increasing pH, dissolution of gas, swelling of minerals, saturation of fluids and sealing of pore space by mineral growth, mineral alteration, dilution effects and so on.

Repository system

The repository system comprises the **repository** and its geological environment, which includes all rock areas that have to be considered for the compliance proof of the safety principles and protection objectives for final disposal.

The repository is part of the repository system in which the radioactive wastes will be placed. It comprises the repository mine, the host rock and the **isolating rock zone**.

The isolating rock zone is part of the geological barrier which has to ensure the confinement of the waste for the isolation period in conjunction with the technical and geotechnical barriers assuming the "normal" or "expected" evolution of the repository.

The repository system and its subsystems with components of a high-level waste repository are depicted in Fig. 1 as proposed by GRS.

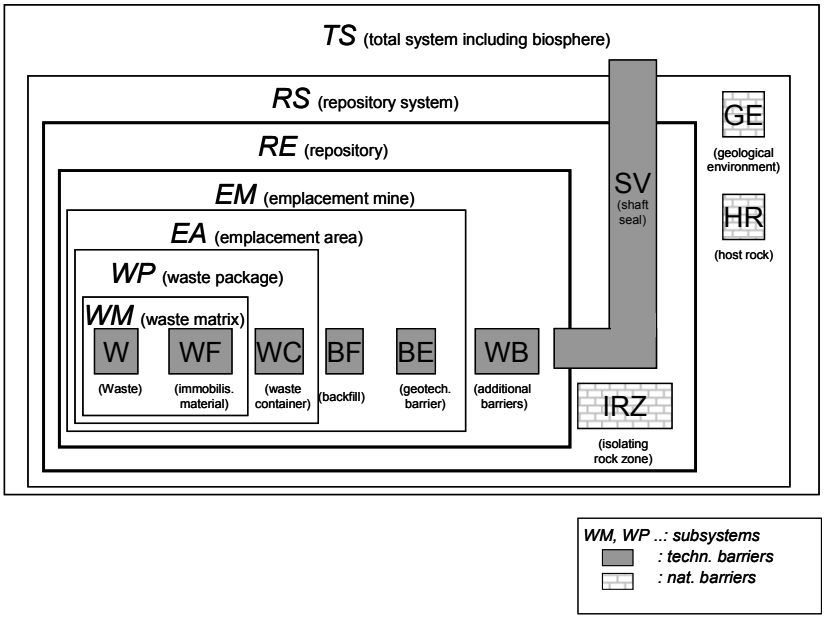

Fig.1. Schematic sketch of a final repository system with subsystems and components (barriers).

Safety functions

The concept of safety functions has recently been introduced into the safety evaluation of radioactive waste disposal systems (NEA 2004; IAEA 2006). It has been attempted to use safety functions to describe the defense-in-depth architecture of a repository system and to derive scenarios for safety analysis by analyzing relevant factors that may affect safety functions.

Top-level requirements for primary safety functions are "isolation or containment" or "limited or delayed release / retardation". In the context of geological disposal the difference between isolation and delayed release is a gradual one. The isolating rock zone may allow some minor release of radionuclides as long as protection objectives are met. The isolation function of a component may also be restricted to a limited period of time leading to a delayed release on the long-term.

The current definition for safety functions (Baltes et al. 2007) and related terminology is given below:

A safety function is a function, which fulfills safety relevant requirements in a safety related system, subsystem or single component. Through interaction of such functions the containment (isolation) as the primary safety function of the ***repository system*** *shall be guaranteed as well as the compliance with safety principles and protection objectives both in the operational phase and post closure phase of the repository.*

The characteristic of a safety function depends on its time of effectiveness, its relation to components, subsystems and other safety functions, its potential for a quantitative assessment and evaluation criteria.

Safety functions have been characterized as "effective", "latent", "supplementary", and "reserve" in a first attempt which has to be elaborated further.

"effective" safety function

Effective safety functions are those safety functions which in connection guarantee that the protection objectives are met for likely evolutions of the repository system. They are applied in a safety analysis and can be limited to certain time frames. An example would be the solubility of radionuclides which is limited by the geochemical environment or the isolation of the canister for a given time span.

"latent" safety function

This safety function takes action in a safety analysis if effective safety functions fail. Thus, they come into play in less likely evolutions of the repository systems.

This characterization is important for a number of geochemical safety functions. For example, the sorption of radionuclides on corrosion products and the volume increase of corrosion products depend on the evolution of the corrosion process and may not be active from the beginning. In the course of time, the safety

function “isolation” of the canister will be lost and the safety function “sorption on corrosion products” will be added.

“supplementary” or “reserve” safety function

This safety function is available but not applied in the safety analyses due to large uncertainties. Reserve safety function might for instance not be properly assessable, vary in their performance, or depend on certain circumstances et cetera. An example is the case of low dissolution or high precipitation rates which increase retardation but are usually neglected.

Geochemical safety functions

Geochemical safety functions of a general nature have been assigned to the technical components of the repository system in the following tables 1 – 5. The isolating rock zone (part of the host rock), the host rock and the geological environment provide additional safety functions related to geochemistry which are not covered here.

A further breakdown of the listed safety functions is possible. Detailed processes connected to the given general geochemical safety functions have to be specified with respect to the repository system and concept under consideration.

Table 1. Component: Waste.

Waste type	Waste	Primary safety function	Geochemical safety function
Vitrified	Vitrified HAW[1]	Retardation	Low dissolution rate
CSD-C[1]	Compressed pellets, HAW	Retardation	Low dissolution rate, low oxidation rate
spent BWR[1] and PWR[1] fuel elements	Spent fuel	Retardation	Low dissolution rate
spent THTR / AVR[1] fuel elements	Spent fuel	Retardation	Low dissolution rate

[1] HAW: High Active Waste, CSD-C: Colis Standard de Déchets Compactés, BWR: Boiling Water Reactor, PWR: Pressurized Water Reactor, THTR: Thorium-Hoch-Temperatur-Reaktor, AVR: Arbeitsgemeinschaft Versuchreaktor

Table 2. Component: Waste Matrix.

Waste type	Waste matrix	Primary safety function	Geochemical safety function
Vitrified	Glas	Isolation, retardation	Low dissolution rate of glas, formation of gel layer
CSD-C	Metal	Isolation, retardation	Low dissolution rate of metal, volume increase of corroded metal, sorption on corrosion products
Spent BWR and PWR fuel elements	Oxide, zircalloy	Isolation, retardation	Low dissolution rate, volume increase of corroded metal, sorption on corrosion products
Spent THTR / AVR fuel elements	Oxide, silicide, carbon, zircalloy	Isolation	Low dissolution rate, volume increase of corroded metal, sorption on corrosion products

Table 3. Component: Waste container.

Waste container	Primary safety function	Geochemical safety function
Concrete container	Isolation	Sorption of radionuclides, favourable geochemical conditions for precipitation of radionuclides, passivation of metal, delayed fluid access
Steel container	Isolation, retardation	Sorption on corrosion products, delayed fluid access, volume increase of corroded metals

Table 4. Component: Backfill.

backfill	Primary safety function	Geochemical safety function
Concrete	Retardation	Sorption and precipitation of radionuclides, passivation of metals
Crushed salt	Retardation	Sorption and precipitation of radionuclides
bentonite	Retardation	Sorption and precipitation of radionuclides, swelling of bentonite

Table 5. Component: Geotechnical barriers, additional barriers.

barriers	Primary safety function	Geochemical safety function
Concrete, bentonite, steel	Retardation	Sorption, precipitation, passivation

Conclusion and outlook

Geochemical safety functions were defined and assigned to technical components of the repository system, leading to the conclusion that there are many possibilities to implement geochemical safety functions in the design of a repository.

The distinction between effective, latent, and reserve safety functions clarifies the role of a specific safety function within the argumentation of the safety case. Due to data uncertainty and to the complexity connected to geochemical processes, presently many geochemical safety functions have to be characterized as "reserve". Therefore, attempts ought to be made to improve the characterization and quantification of geochemical safety functions in order to take advantage of them as effective or latent safety functions in the safety case.

References

Altmaier M, Brendler V, Hagemann S, Herbert HJ, Kienzler B, Marquardt CM, Moog HC, Neck V, Richter A, Voigt W, Wilhelm S (2008) "THEREDA - Ein Beitrag zur Langzeitsicherheit von Endlagern nuklearer und nichtnuklearer Abfälle". atw 53: 249-253

Baltes B, Röhlig KJ, Kindt A (2007) Sicherheitsanforderungen an die Endlagerung hochradioaktiver Abfälle in tiefen geologischen Formationen" Entwurf der GRS, GRS-A-3358 (only available in German language)

Brown PL, Lowson RT (1997) The use of kinetic modeling as a tool in the assessment of contaminant release during rehabilitation of a uranium mine. J. contam. Hydrol. 26: 27-34

Bruno J, Cera E, Duro L, Pon J (1998) Development of a kinetic model for the dissolution of the UO2 spent nuclear fuel. SKB Technical Report TR-98-22

Grambow B, Lutze W, Kahl L, Geckeis H, Bohnert E, Loida A, Dressler P (1996) Long-Term Safety of Radioactive Waste Disposal. Retention of Pu, Am, Np and Tc in the Corrosion of COGEMA Glass R7T7 in Salt Solutions. Final Report FZKA 5767

IAEA (2006) Geological Disposal of Radioactive Waste: Safety Requirements. IAEA Vienna: Report No. WS-R-4

Kienzler B, Metz V, Lützenkirchen J, Korthaus E, Fanghänel (2007) Geochemically Based Safety Assessment. Journal of Nuclear Science and Technology 44(3): 470-476

Köster R, Rudolph G (1991) The equilibrium concept – An extended approach to assess long-term radionuclide release from repositories. Nucl. Technol. 96: 192-200

NEA (2004) Post-closure Safety Case for Geological Repositories: Nature and purpose. NEA/OECD, Paris

Fault-related barriers for uranium transport

Vladislav Petrov[1], Valery Poluektov[1], Jörg Hammer[2] and Sergey Schukin[3]

[1]IGEM RAS, Moscow, Russia
[2]BGR, Hannover, Germany
[3]PPGKhO, Krasnokamensk, Russia

Abstract. This contribution presents data on the long-term retentive ability of diverse mineral infill of hydraulically active faults in respect to radionuclides migrating within the vadose zone of crystalline massifs by the example of the vein-type Tulukuevskoe uranium deposit in SE Transbaikalia, Russia.

Introduction

Conceptual approach to the spent nuclear fuel (SNF) isolation within the vadose zone of crystalline massifs is based on the assumption that oxidized meteoric water will inevitably destroy fuel rods and assemblages (Vadose Zone 2000). As a result the vast majority of the actinides and fission products will be leached from the uranium dioxide crystal lattice and may be transferred to the environment in unacceptable concentrations. The main pathways for transferring are hydraulically active fault zones. However, this probabilistic scenario does not mainly take into account the fact that different types of reactive barriers where retention of U(VI) and its reduction again to insoluble U(IV) form could be originated and preserved inside the fault zones over a long period of time.

These processes were indicated and studied in the vadose zone of the Tulukuevskoe deposit mined by an open pit in welded tuff strata up to the depth of 200 m. The vein-type primary pitchblende mineralization is located within the hydraulically active Fault 1A zone and exposed to oxidation and destructive transformation. As the result of ancient hypergene alteration and current oxidation the uranium undergoes to redistribution around the ore body, partial leaching and displacement downstream of redox front along the fault. A number of uranium concentrators were indicated inside the fault zone as follows: a) oxyhydroxides of Fe, Mn and Ti (hematite, goethite, leucoxene-like aggregates, etc.); b) solid and stable to oxidation carbonic matter in concentration up to 0.4 mass%; c) hypogene tucholite with uranium content up to 10 mass% formed as a result of interaction between bituminous matter and uranium-bearing hydrothermal solutions; d) aggregates of protoferrihydrite and ferrihydrite as a result of current microbial activity.

These materials form fault-related reductive and sorptive geochemical barriers for uranium transport in oxidizing unsaturated conditions.

Thus, the example of the Tulukuevskoe deposit's vadose zone shows that reactive barriers of high reductive-sorptive ability regarding to actinides can be formed along and inside the fluid conductive fault zones. This phenomenon has to be studied in detail and to be considered during conceptual and numerical filtration-transport modeling as well as in the context of the total system performance assessment of SNF underground facilities.

Results

The Mesozoic (135 Ma) welded tuffs, which have hosted the Tulukuevskoe uranium deposit, provide an outstanding example of processes governing uranium migration and accumulation in oxidizing fractured porous environment (Petrov et al. 2005). The vein-type deposit contains primary uraninite mineralization occurring as pitchblende subjected to secondary transformations within the upper part of the deposit, mined by the Tulukuevsky open pit (TOP) since 1972 till 1998.

Reconnaissance investigations at the TOP during 2000 have shown that the pit NW wall is the most convenient block to investigate the pathways preferential for meteoric water infiltration and redox front propagation in connection with uranium redistribution. The block consists of fresh and altered welded tuff varieties, the steeply-dipping Fault 1A zone at the flank and accompanying fracture network, ore body inside the fault zone at the depth of 60 m from the modern surface, and primary and secondary uranium mineralization of the ore body.

At seven levels of the block, the Sample Lines (from SL-A at 710 m asl to SL-G at 520 m asl) up to 200 m length are provided with Sample Points (SP) located every other 5 m. Besides, the gallery 250 m length located at SL-G along the Fault 1A footwall was investigated (Fig.1). Reasoning from the requirements of meteoric water filtration and uranium migration studies the following fieldwork activities in every basic SP have been performed: a) geological-structural surveying; b) investigation of lithological composition, nature and degree of hydrothermal-metasomatic alteration and oxidation of the rocks; c) sampling for subsequent petrographic, mineral-chemical, isotopic-geochemical, and petrophysical tests. Eight fracture water sources at the bottom and three sources inside the gallery of the TOP as well as atmospheric precipitates (water and snow) were sampled for hydrochemical and isotopic-geochemical analysis during 2001-2007. Fieldworks and laboratory tests consist of the following procedures:

- statistical data analysis of fractures, including strikes, dips, morphology, spacing and aperture, and mineral filling in order to quantify the hydraulic properties of the fracture network;
- radiometric profiling to obtain information on radioactivity of wall rocks and to identify ore accumulations;
- mineral-chemical analysis of differently altered rock varieties including optical microscopy, "wet" chemistry, XRF, INAA, X-ray diffraction diagnostics of

clay minerals, electronography, transmission electron microscopy for studying of Fe-oxyhydroxides, fission-track radiography analysis, coulometer titration for carbonic matter content determination;

- optical microscopy, ultraviolet lighting, scanning electron microscopy and energy-dispersion spectrometry studies of primary and secondary uranium minerals;
- isotopic-geochemical analysis of rocks using isotopic dilution method (isotope composition of U and Sr), ion-exchange chromatography (total concentrations of U, Rb, and Sr), mass-spectrometry ($\delta^{18}O$) analysis;
- hydrochemical tests consist of evaluation of the major constituents (Na+K, Ca, Mg, Fe_{sum}, HCO_3, Cl, SO_4, NO_2, NO_3, NH_4), U and total mineralization of water samples, ionometric measurements of the redox potential (Eh) and acidity (pH), mass-spectrometry ($^{234}U/^{238}U$ relations, δD and $\delta^{18}O$) measurements.

The analysis and synthesis of the data allow compiling a whole series of factors affecting ancient and recent redox front development and peculiar properties of uranium transport inside the Fault 1A zone.

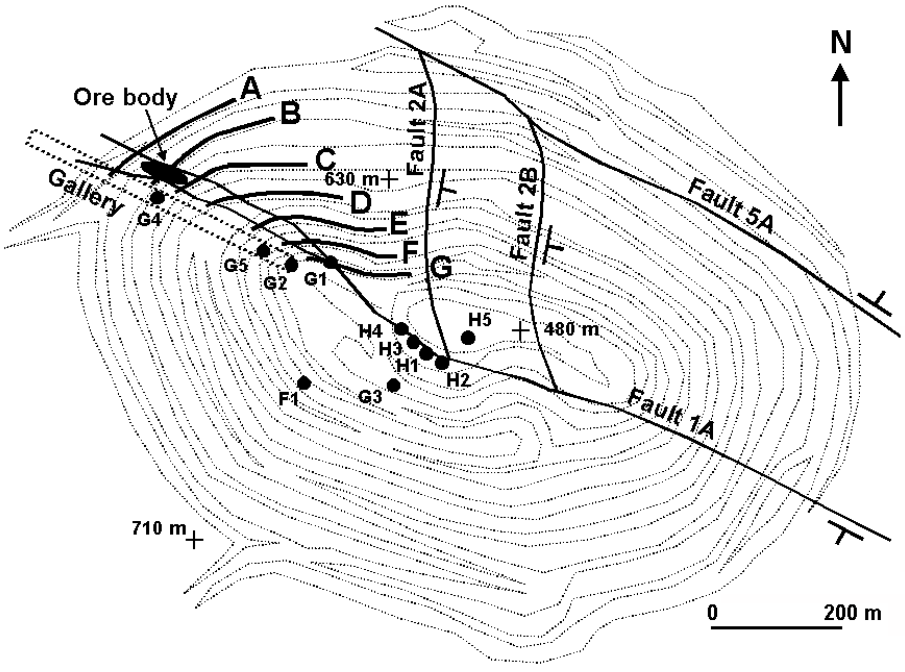

Fig.1. Surveying plan of the Tulukuevsky open pit (TOP) showing location of the Sample Lines (from A to G), gallery, Fault 1 zone, exposed ore body, and fracture water sources (black circles)

Mineral and weathering zoning

The Late Mesozoic hydrothermal processes in the strata are appeared as pre-ore, ore-related and post-ore mineral paragenesis (Andreeva and Golovin 1998). They organize external, intermediate and internal zones of mineral associations controlled by the Fault 1A zone. Relatively fresh rocks of gray-violet color determined by the fine-grained hematite form external zone where biotite is well preserved or partially replaced by ankerite. Intermediate zone consists of preserved fine-grained hematite and replaced feldspar by carbonates (ankerite, calcite and sideroplesite), mixed-layered illite-smectite, illite and quartz. Internal zone deeps along the Fault 1A with most intensive expansion of light-colour micas, carbonates and quartz as well as cataclasis and substantial fracturing. Post-ore argillization (smectite, kaolinite) is superposed predominantly on this zone.

Initial and hydrothermally altered rocks have undergone ancient and recent oxidation. Ancient processes form three horizontal subzones of hypergenesis (from top to bottom of the TOP): leaching (ancient vadose zone, SL-A+B+C at 710-630 m asl), complete oxidation (SL-D+E at 630-570 m asl) and incomplete oxidation (SL-F+G at 570-520 m asl). A horizon of the secondary uranium enrichment (ancient transition zone) is located at depth of 640 m asl. The ancient oxidation zone belongs to a hydroxide-silicate type with gradual transition of primary ores to uranium hydroxides and silicates and unchanged morphology of primary segregations (Belova 2000). This process can be described schematically by the chain: $U^{IV}O_2 + O_2 + H_2O$ (pitchblende) → $U^{VI}O_3$ x nH_2O + Me (hydropitchblende) → $MeU^{VI}{}_2O_7$ x nH_2O + Si (hydroxides such as velsendorphite) → $Me(UO_2)_2[SiO_4]_2$ x nH_2O (silicates such as uranophane), where Me = Ca, Pb, Ba, Sr, K, Na.

The development of modern oxidation is revealed by the formation of Fe and Mn oxyhydroxides such as goethite (FeOOH), Fe-vernadite (MnO_2 x nH_2O), hematite (Fe_2O_3), and (proto)ferrihydrite ($2.5Fe_2O_3$ x $4.5H_2O$). Goethite and Fe-vernadite have predominantly areal distribution along SL-A and B, whereas hematite is characterized by areal occurrence in the upper part of the section and linear distribution in its lower part in connection with steeply-dipping fractures.

There are prominent changes in $\delta^{18}O$ and Fe(III)/Fe(II) values of rock due to their degree of oxidation and position relatively the fluid-conductive Fault 1A zone. The $\delta^{18}O$ values into the Fault 1A core have no variations at different hypsometric levels. With the growth of distance from the fault core to the zone of dynamic effect a dramatic increase of ^{18}O concentration in rock takes place, and then it gradually declines in protolith. Evident growth in $\delta^{18}O$ values is observed in case of hydraulically active fracture occurrences in protolith. The profile of this type reflects long-term fluid-rock interaction, and most probably more than one stage of this interaction. The degree of Fe oxidation in the upper part is by far higher than in the lower part of the TOP. At the upper part the process of Fe(II) oxidation is approaching the completion, in rocks of the medium part this process is more developed while in rocks of lower part the process is at the initial stage. In addition, the behavior of the Fe(III)/Fe(II) value correlates with the behavior of the isotopic composition of oxygen.

One of the striking indicators of hypergene transformation of the rock is presented by clustered aggregates of ferrihydrite and protoferrihydrite, which occur inside the Fault 1A zone at the lower part of the TOP. Ferrihydrite is a broadly met unstable hypergene mineral belonging to the group of Fe(III) oxides. It might be viewed as a typical product of Fe(II) oxidation. Its formation is usually a result of vital function of Fe-bacteria, which are active at pH 6-7 and at a temperature ranging from 4 to 27°C (Chukhrov et al. 1975). As it follows from experimental data, ferrihydrite is an unstable mineral. Therefore its natural occurrence is possible only in geologically young formations. With time it spontaneously turns into hematite or, in the absence of substantial oxygen, it changes into goethite.

Distribution of carbonic material

Following to Melkov and Sergeeva (1990) definition we understand under the term "carbonic material" the carbon-hydrogen complexes containing variable amounts of O, N and S in solid, viscous and liquid state.

Within the TOP a solid carbonic material (SCM) is founded. Obtained data show that SCM occurs along the Fault 1A and diagonal fracturing zone with concentration ranges from 0.05 to 0.4 mass%. Inside the fault core there are not trails of SCM due probably to intensive oxidizing transformation of the matter. Because of ultra-fine size (<<0.001 mm) of SCM we did not perform its diagnostics for a while. Contrary to this the variety of SCM such as hypogene tucholite was founded into the Fault 1A core 10 m below the ore body. Tucholite is black amorphous material with chemical compositions (mass%): C 49.47, O 29.08, Mg 0.28, Ca 1.58, Al 0.81, Si 0.43, S 0.59, U 10.72 (in sum 92.96). Tucholite forms thin (0.5-1 mm) veinlets in calcite surroundings. In this case, tucholite aggregates have massive structures, and they form globular accumulations differing in size (0.2-2.5 mm) cemented with carbonate. The latter fact presumably reflects interaction (probably, immiscibility) of liquid bitumen and hydrothermal mineral-forming solution in fractured porous space of the Fault 1A. Time relations of tucholite and primary pitchblende are still vague, whereas neoformed fibrous uranophane is developed at the surface of tucholite aggregates.

Hydrochemistry and isotopy

Hydrochemical tests show that fractured waters percolating through the welded tuff block are characterized by carbonate-sulphate-chloride-sodium composition when carbonate and sulphate can change their position due to time. For the analysis of the change of such major constituents as HCO_3, SO_4, Na+K and Ca we used the concentrations of the Cl^- ion in the waters as a conservative tracer. There is positive correlation between values of the constituents and Cl^- with more and more scattered character of the fields with time. The total mineralization of the water is practically stable or shows the tendency to slightly increase whereas uranium concentrations decrease during observation period.

Seven-year investigations of change in Eh-pH conditions (Fig.2) show, that meteoric water is characterized by high oxidizing potential and mean acidity. However, there is a trend for atmospheric precipitates to become more acid. At the same time, fracture waters show tendency to shift from neutral-alkaline to neutral field and to become more oxidized from 2001 to 2003 and to revert to status of 2001 similarly to cyclic regime. In addition, the fracture water and atmospheric precipitates become closer in terms of oxidability.

The residence time of water in fracture-pore system of welded tuffs has been evaluated on the behavior of δD values in different sources (Dubinina et al. 2007).

In general, in sources controlled by the Fault 1A zone of discharge the residence time varies from 24 to 26 months while sources located at some distance from the fault show period from 30 to 42 months. The ^{18}O system behavior proves current interaction of water with a large oxygen reservoir of the rock silicate matrix. During the isotopic exchange with silicates at an ambient temperature the isotopic composition of water might tend towards ^{18}O enrichment. The $^{234}U/^{238}U$ relations in fracture water show a substantial 1.5-2.5-fold growth of ^{234}U content as compared to the equilibrium value. The variations of $^{234}U/^{238}U$ between different sources reach 90%. It is connected with different content of uranium in rocks, duration of water-rock interaction and climatic factor.

It is evident, that uranium in the context of denoted Eh-pH conditions of the vadose zone of the TOP should be in the +6 oxidation state and presents in solution in $UO_2(CO_3)_3^{4-}$ and/or $UO_2(CO_3)_2^{2-}$ complexes.

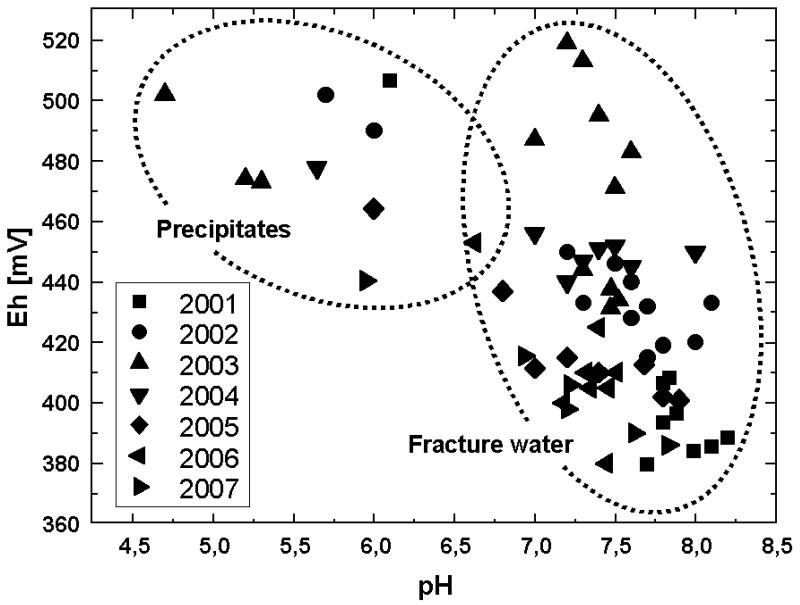

Fig.2. Dynamics of Eh-pH changes for fracture water and atmospheric precipitates of the TOP during 2001-2007.

Uranium repartition

Repartition of uranium in variously altered (external, intermediate and internal zones of mineral associations) welded tuffs and at different distances from the Fault 1A core was studied using fission-track radiography, ion-exchange chromatography and isotope dilution method.

Uranium of the external zone is mainly concentrated in the matrix (up to 10 ppm), and to a lesser extent in fiamme. The maximum density of tracks (up to 30 ppm) is observed near biotite and its opacitized leaflets as well as in rock debris. Quartz, plagioclase and K-feldspar fragments are disengaged from uranium. With the transition to the intermediate zone partial dilution of hematite, which serves one of the principal uranium sorbents, and the development of fine-grained carbonate-hydromica aggregates in the main mass take place. Uranium concentrations in minerals replaced by hydromica and carbonates remain low. Some portion of uranium is connected with impurities of leucoxinized accessory minerals (up to 150 ppm) and veinlets of Fe-Mn oxyhydroxides (up to 250 ppm). These processes of uranium redistribution are most clearly observed in upper part of the TOP outside the Fault 1A and uranium ore body.

As compared with the upper part of the section more contrast and intensive redistribution of uranium occurred at the bottom of the TOP. In the intermediate zone the ore-related Fe-chlorite (berthierine) intensively gathers uranium (up to 300 ppm). In the areas, where berthierine is absent, such minerals as carbonate, illite-smectite and a thin fringe of hematite, which sorbs uranium, develops on biotite. On the whole, higher concentrations of uranium are met in matrix near the grain boundaries of minerals and rock fragments as well as in mineralized microcracks (up to 500 ppm). High density of tracks in pseudomorphoses of hematite and leucoxene-like aggregate on titanomagnetite and biotite while decrease of track density in matrix and complete exportation of uranium from fiamme is observed.

The processes of uranium redistribution and accumulation are clearly connected with internal zone of mineral transformations and Fault 1A zone. Higher concentrations of uranium (up to 2500 ppm) in the areas of cataclasis and microbrecciation are associated with the contacts of fragments of rock and feldspar aggregates, as well as with mineralized fractures containing Fe, Mn and Ti oxides and hydroxides (up to 10000 ppm). Uranium could have been perfectly accumulated in hematite-leucoxene material due to redistribution and exportation from adjacent areas of matrix and fiamme. Thus, assessing the uranium distribution in various parts of internal zone of mineral transformations one can note that the highest concentrations of uranium are associated with minerals characterized by high sorption capacity such as Fe, Mn and Ti oxides and hydroxides, leucoxene-like aggregate, and berthierine.

Particularly remarkable is the behavior of uranium in connection with fluid-conductive Fault 1A zone at the ten-meters scale. Comparative analysis shows that uranium content in the fault core increases towards the lower hypsometric levels of the TOP from 15 ppm to 150 ppm. However, of SL-B and C the concentration of uranium demonstrates a trend to decrease towards zone of dynamic effect and

protolith. Contrary to that, at the SL-F decrease of uranium content at the distance no more than 3 m (zone of dynamic effect of the fault) and once again increase directly to protolith is recorded. The $^{234}U/^{238}U$ relation in rock components (extract and restite) differs from the equilibrium (5.5×10^{-5}). It indicates the development of younger than 1 Ma processes of uranium migration. Different nature and shift of $^{234}U/^{238}U$ deviation from the equilibrium value show that intensity of uranium migration processes at various hypsometric levels of the TOP vary substantially.

At the one-meter scale of fluid conductive fracture the change in uranium content is more complicated. Inside the fracture core (0 – 50 cm) high concentrations of uranium in Fe-Mn oxyhydroxide infill decreases at first, but than increases again at the distance of 1 m into the zone of dynamic effect which accompanied mainly by the pre-ore mineral associations. After that at the distance from 1 to 5 m uranium content decreases gradually to background values towards slightly altered and fresh protolith.

Discussion and conclusion

Natural analogue investigations aim to understand key phenomena and processes in natural systems related to those expected to occur in radioactive waste repositories and have become an integral part of the safety assessment of SNF facilities at the vadose zone of crystalline massifs (Smellie et al. 1997). Radionuclide transport processes (advection, matrix diffusion, dispersion, sorption, colloid-facilitated transfer, radioactive decay, chemical/biological transformation, etc.) at the vadose zones directly depend upon water flow behavior into the hydraulically active pathways due to liquid water is considered to be the principal medium in which solutes are transported through the rock sequences.

Summing up obtained field and lab test data on the vadose zone of the Tulukuevskoe deposit we could say that the overriding characteristic of the interactions results from coupled processes. The dominant processes can be grouped into two categories: those contributing to uranium release versus those contributing to uranium retardation. The significance and magnitude of the coupling varies both spatially and temporally. To identify priorities, the dominant processes were considered. This idea can be shown conceptually by using an interaction matrix (Fig.3) of the type offered by Wilder (1997). Here the key components are shown along the diagonal, and the interaction of processes is shown off diagonal. Rather than showing all components and all coupling, which can be very complex, it is the objective of this matrix to focus on the key parameters or components and on the key processes. In addition, the matrix should be considered as a basis of future investigations. Mainly, it is relevant to impact of colloids and microbiotic conditions on uranium migration and accumulation.

Within the vadose zone of the Tulukuevskoe uranium deposit there is fault related hydrothermal vein-type ore body subjected to ancient hypergene transformation and current oxidation. Ancient transformation forms three horizontal subzones: leaching (ancient vadose zone), complete and incomplete oxidation. A

horizon of secondary uranium enrichment indicates ancient transition zone. The ancient zone of oxidation belongs to a hydroxide-silicate type, of which the gradual transition of primary ores to uranium hydroxides and silicates is typical, with preservation of initial hydrothermal mineral morphology. The deposit opening by the open pit caused the recession of the groundwater table, and the ancient transformation zone turned out to be exposed to the effect of current oxidation processes. The current oxidation zone is characterized as immature, the one in the process of formation including neoformed minerals, such as uranophane, heyviite, carbonates and soluble uranyl sulphates, etc.

The current oxidation processes are controlled by steeply-dipping Fault 1A zone and large fracture families which form V-shape structure that appears for the preferential flow of liquid and gaseous phases of descending meteoric water. As the result of redox front propagation the uranium undergoes to redistribution around the ore body, partial leaching and displacement downward the fault. However the zonal interference of hydrothermal ore formation, ancient hypergene transformation and current oxidation makes complexity for deciphering of uranium transport processes. The mechanisms of uranium redistribution reflect the cumulative effect of hypogene (rock and ore) uranium behavior in hydrothermal conditions, which was later involved to redistribution in the course of the formation of the ancient and modern oxidation zones in U(VI) form.

The main difference in the behavior of hypogene and hypergene uranium is chiefly determined by the opposite trends of uranium migration processes: during ore forming stage uranium migrated from the central part of the Fault 1A to the adjacent rocks. In hypergene conditions, just on the contrary, uranium was redistributed and "moved" towards the central part of the Fault 1A, which was a channel for meteoric water flow.

Nevertheless within the fluid conductive Fault 1A zone a number of mineral phases with high sorption capacity regarding to actinides was originated and preserved over a long time. These mineral phases can be organized to the following row (in descending order): amorphous Fe oxides → ferrihydrite → goethite → hematite → leucoxene-like mineral → solid carbonic material → siderite, ankerite → oxidized berthierine and pyrite → calcite, smectite, mixed-layered minerals → illite → kaolinite → feldspars → quartz. Note that the sorption capacity of organic compounds (ferrihydrite) and solid carbonic materials needs to be further investigated.

Thus, the example of the Tulukuevskoe deposit's vadose zone shows that mineral and geochemical barriers controlled by structural elements are involved in the processes of retaining and accumulation of uranium. Particular importance of sorption and reducing barriers confined to hydraulically active faults and fractures must be taken into account for the development of conceptual and numerical models of actinide migration in oxidizing conditions. It is fundamentally important for evaluating of the long-term safety of SNF underground facilities located within the vadose (aeration) zones of crystalline rock formations.

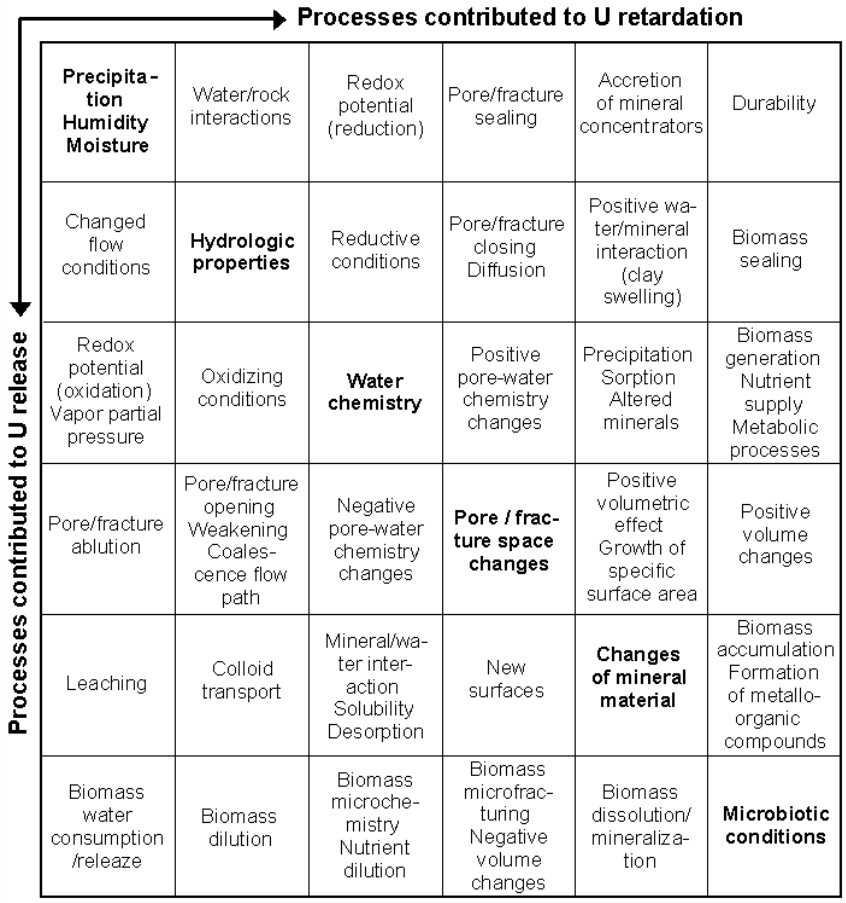

Fig.3. Simplified matrix showing interrelation of uranium transport processes in the vadose zone of the TOP.

Acknowledgements

We almighty appreciate colleagues from IGEM RAS Andreeva O.V., Dubinina E.O., Golubev V.N., Schulik L.S., Kartashov P.M. for the lab test assistance. This study was financially supported by the Presidium of RAS program No. 16, project NSh-6894.2006.5 and GAP CRDF RUG2-20202-MO06 project, and was carried out in the framework of the scientific and technical cooperation agreement between IGEM RAS and BGR.

References

Andreeva OV, Golovin VA (1998) Metasomatic processes at uranium deposits of Tulukuevskaya caldera, Eastern Transbaikalia, Russia. Geol Ore Dep 3: 205-220 (*in Russian*)

Belova LN (2000) Formation conditions of oxidation zones of uranium deposits and accumulation of uranium minerals in hypergenic zone. Geol Ore Dep 2: 113-121 (*in Russian*)

Chukhrov FV, Ermilova LP, Gorshkov AI (1975) Hypergene ferric oxides in geological processes. Moscow, Nauka Publ. (*in Russian*)

Dubinina EO, Golubev VN, Petrov VA (2007) Evaluation of meteoric water filtration time into the fractured porous environment of the Tulukuevskoe deposit. Proc Vinogradov´s Symp: 90-91 (in Russian)

Melkov VG, Sergeeva AM (1990) Importance of solid carbonaceous material for the formation of endogenous uranium mineralization. Moscow, Nauka Publ. (*in Russian*)

Petrov VA, Poluektov VV, Golubev VN et al. (2005) Uranium mineralization in oxidized fractured environment of the giant volcanic related uranium field from the Krasnokamensk Area. Proc Int Symp Uranium Prod. IAEA, Vienna, Austria: 260-264.

Smellie JAT, Karlsson F, Alexander WR (1997) Natural analogue studies: present status and performance assessment implications. Contam Hydrol 26: 3-17.

Vadose Zone: Science and Technology Solutions (2000) B.B. Looney and R.W. Falta (eds.). Battelle Press, Columbus, U.S.A.

Wilder DG (1997) Near-field and altered-zone environment report. Volume I: Technical bases for EBS design. LLNL Rep *UCRL-LR-124998*.


Uranium Mining
and Hydrogeology

Uranium glasses: the experimental leaching compared to the long-term natural corrosion

Radek Procházka, Vojtěch Ettler, Viktor Goliáš and Jakub Plášil

Institute of Geochemistry Mineralogy and Mineral Resources, Faculty of Science, Charles University, Prague, Czech Republic

Abstract. Corroded surface layers were formed naturally on the historical uranium-coloured glasses. Comparative batch leaching test was performed in laboratory and the glass dissolution rates with respect to main components including uranium were established. The residual alkali-leached surface corrosion layers even of experimental or natural origin showed the stable concentration of uranium.

Introduction

Historical uranium-coloured glasses deposited in the soil for 150 years have been invoked as natural analogues of nuclear waste to help to bring more light on long-term glass corrosion mechanisms, as they are valid real-time examples of degradation in natural environment. The glasses show massive corrosion layers developed on their surface during the burial period.

Laboratory leaching tests can predict the basic trends of glass leaching and selective dissolution of the glass components that leads to the surface corrosion layers formation. The validation of the natural dissolution rates by laboratory experiments gives more confidential results.

The glasses

The samples of historical glasses were collected in Czech Republic at the extinct dumps of the former glassworks in Podlesí near Kašperské Hory in Šumava region and in Kristiánov nad Kamenicí in Jizerské hory region. The glasses stemmed from the period from 1835 to 1865. The historical glasses contained typically 0.3 to 0.4 wt% of uranium in bulk.

The comparative laboratory leaching experiment was performed using the commercial uranium coloured glass pearls made recently by Jablonex a. s. manufacturer from Czech Republic.

Experimental and analytical methods

The bulk composition and SEM-BSE (scanning electron microscopy - backscattered electrons) micrographs of the glasses and surface crusts were performed on resin-impregnated polished sections using Cameca SX 100 electron probe microanalyzer (EPMA) at an accelerating voltage of 15 KV and beam current of 10 nA. A counting time of 10 s and SPI Supplies 53 Minerals Standard set #02753-AB were used for the major elements. An acquisition time of 40 s and the U-REE glass standard (certified by MAC) were employed for uranium analysis.

Infra red spectra were recorded from powdered samples in mixture with KBr using micro diffuse reflectance method (DRIFTS) on a Nicolet Magna 760 FTIR spectrometer (range 4000-600 cm^{-1}, resolution 4 cm^{-1}, 128 scans, Happ-Genzel apodization) equipped with Spectra Tech InspectIR micro FTIR accessory.

Thermo-gravimetric analysis was carried out using Stanton Redcroft Thermobalance TG 750 device at heating rate 10 °C min^{-1} in dynamic air atmosphere at flow rate 10 ml min^{-1}.

The leaching experiment protocol

Laboratory kinetic batch leaching experiment was performed on uranium glass pearls at a glass-surface-to-solution-volume (S/V) ratio of 40.05 m^{-1} in deionized water as a leaching medium (MilliQ+, Millipore® water purifying system). Before the experiment, the glass pearls were treated in an ethyl alcohol bath in ultrasonic cleaner. The leaching was conducted at 22 ± 3 °C in 250-ml HDPE bottles for 1, 2, 3, 6, 12, 24, 48 hours, 4, 7, 15, 30 days, 2, 6, 10 and 14 months.

Major cations (K, Na, Ca, Mg, Si) in leachates were analyzed by flame absorption atomic spectrometry under standard analytical conditions (AAS; Varian SpectrAA 280 FS). Uranium and aluminum were determined by inductively coupled plasma mass spectrometry (ICP-MS; VG Elemental PlasmaQuad 3).

Dissolution rate for each glass component was calculated from the experimental laboratory leaching data at each leaching time using the normalised glass mass lost value (NL) given by the following equation (Gin et al. 1994):

$$NL(i) = \frac{C(i)V}{wt\%(i) * SA} \quad (1)$$

where NL(i) is the normalized weight lost in g m^{-2}, C(i) is the concentration of element (i) in the leachate in mg l^{-1}, V is the leachate volume in ml, wt%(i) is the elemental fraction of the element in the original solid phase in wt %, and SA is the specimen geometric surface area in cm^2.

Natural leaching of the historical glass samples

As evidenced by SEM-BSE the glasses were naturally leached up to depth of 0.6 mm. The leached phase appears darker in BSE (because lower average atomic number) cracked by many fissures, which can be attributed to volume changes associated with the glass corrosion (Fig.1).

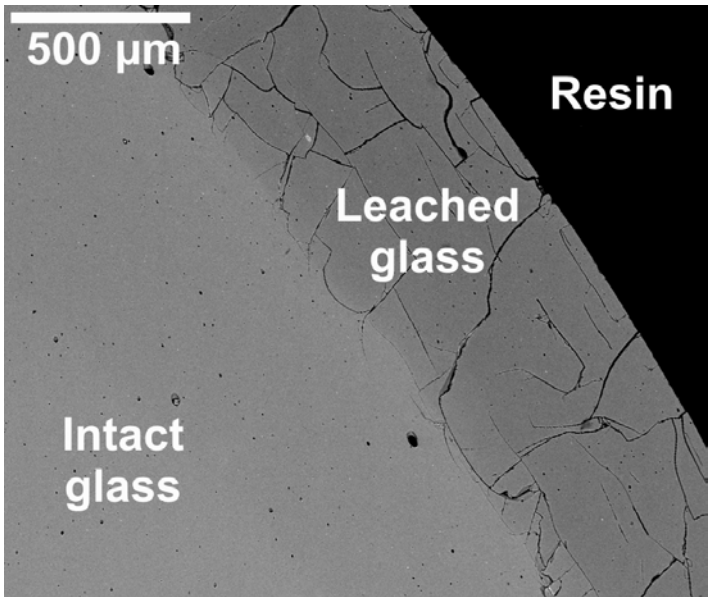

Fig.1. The SEM-BSE micrograph of the naturally leached historical uranium glass with the corroded surface layer cross-section.

Table 1. The composition of the historical glass coloured by uranium and its natural corrosion layer analysed by means of the EPMA (electron micro-probe analysis). The affected layer is poorer in alkalis whilst uranium concentration is stable.

wt %	Intact glass	SD	Leached glass[a]	SD
Na_2O	**1.42**	0.16	**0.19**	0.07
MgO	0.79	0.08	1.05	0.09
Al_2O_3	0.19	0.04	0.19	0.04
SiO	74.85	0.45	81.77	0.47
P_2O_5	1.91	0.11	2.71	0.13
SO_3	0.52	0.06	0.28	0.05
K_2O	**14.26**	0.27	**3.30**	0.13
CaO	2.78	0.07	3.01	0.08
UO_3	**0.35**	0.11	**0.39**	0.11
Total	97.07		92.89	

[a] Natural leaching

According to compositional changes evidenced by EPMA analyses of glasses and residual layers the preference release of alkalis occurred. This is explained by the selective ion-exchange of K^+ and Na^+ from the glass for H^+ ions from the natural leaching solution (Ojovan et al. 2006). The concentration of K_2O decreased from 14.26 wt % (bulk glass) basically to one quarter (3.30 wt %) in the ion-exchanged layer (Table 1). According to this a relative arise of SiO_2 concentration took place. Despite of massive changes involved by natural leaching uranium concentration remained stable or even higher in the residual glass (Table 1).

The hydration of glasses was investigated using the methods of infrared spectroscopy and thermogravimetry. The infrared spectra of original and leached glass showed several differences (Fig.2). Presence of the molecular H_2O was confirmed in the leached glass by features attributed to bending H-O-H and stretching OH vibrations (Table 2). The presence of silanol (≡Si-OH) groups is expected as well. Uranium in the glass is present in the form of uranyl ion $(UO_2)^{2+}$ (Maeda et al. 2001). Antisymmetric stretching vibration of uranyl group at the region of 1000 to 850 cm^{-1} did not came out probably because low concentration of $(=UO_2)$ groups moreover due to overlaping with principal Si-O vibration.

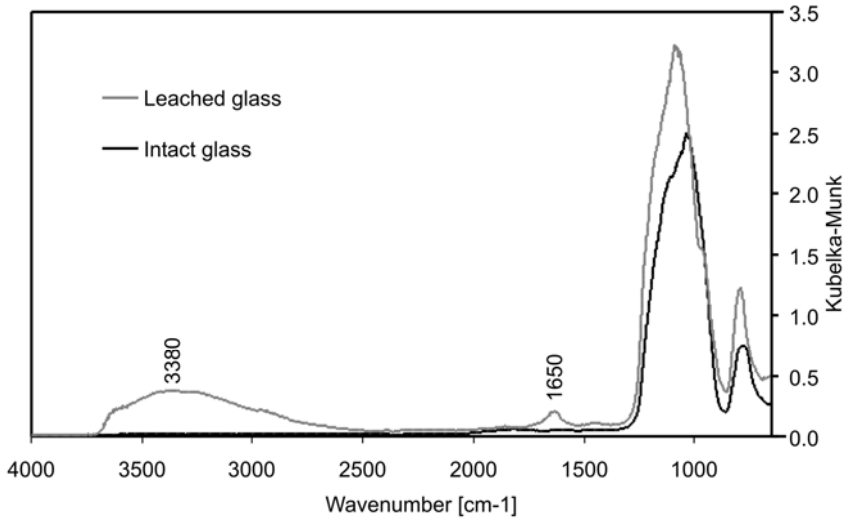

Fig.2. The IR spectra of the original and naturally corroded historical uranium glasses.

Table 2. Identification of the IR spectra features (intact and naturally corroded glass).

Intact glass	Leached glass	Tentative assignment
798 cm^{-1} ms	801 cm^{-1} s	symmetric stretching SiO vibration
1026 cm^{-1} vs	1093 cm^{-1} vs, 982 cm^{-1} sh	antisymmetric stretching SiO vibration
	1650 cm^{-1} w	bending H-O-H vibration
	3380 cm^{-1} mw	symmetric stretching OH vibration

ms: medium strong; s: strong; vs: very strong, mw: medium weak; w: weak; sh: shoulder

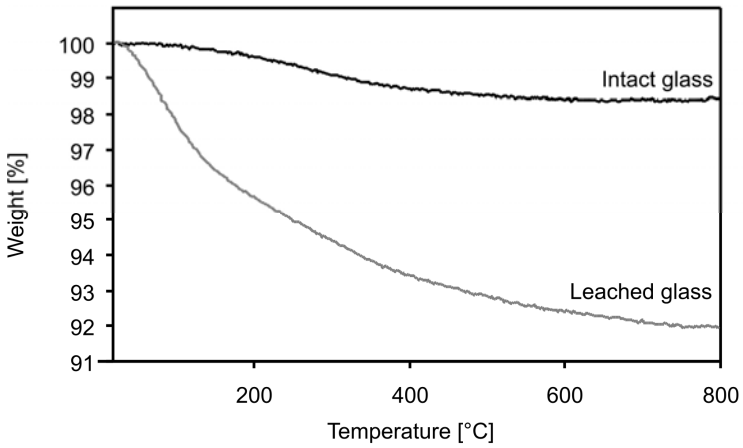

Fig.3. The thermogravimetric curves of original historical glass and naturally corroded surface layer.

The weight ignition loss of historical samples was measured in the unaffected glass core as well in naturally hydrated surface layer by thermo-gravimetry. At 800°C the decrease was 1.6 wt % for the original intact glass and 8.1 % for the leached glass (details in Fig.3). This indicates a large surface hydration, which occurred in the natural burial environment.

Leaching experiment with recently made glass

Leached surface layer of the thickness up to 3.4 μm (Fig.4) developed during the 14-month laboratory leaching experiment. According to the SEM-BSE observations the layer appears darker with the obvious micro-porosity.

As evidenced by WDS electron micro-probe analysis of the leached glass zone, uranium concentration remains stable although there is the significant release of Na and K. Sodium content decreased from 14.22 wt % (original glass) basically to one third (4.57 wt %). Potassium concentration in the leached layer was found decreased to 84% of the former glass. This is in agreement with the dissolution rates (given as NL(i)) established from the analyses of extracts after 14 months of leaching. These were highest for sodium (3.56 g/m^2) followed by potassium (2.34 g/m^2). Uranium final lost NL(U) was 1.98 g/m^2 and silicon NL(Si) was 1.96 g/m^2. The evolutions of NL values for all principal glass elements are illustrated in the Fig.5.

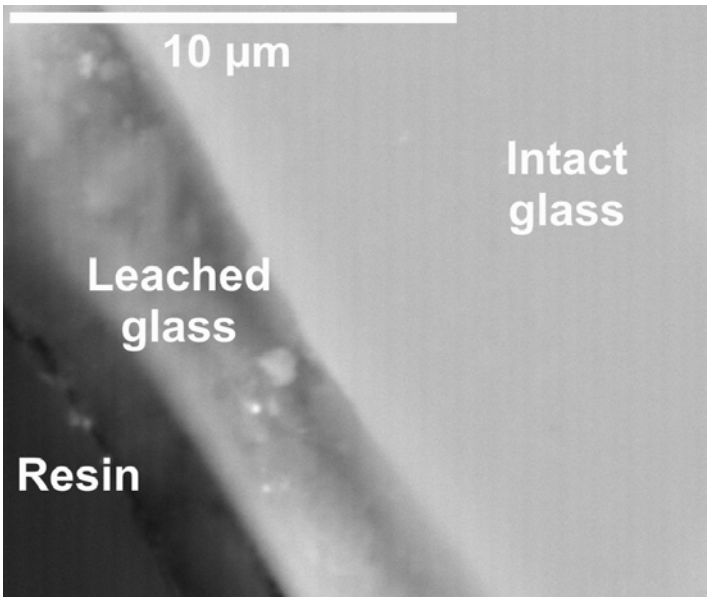

Fig.4. The SEM-BSE micrograph of the glass surface zone (cross section) after leached experimentally for 14 months period.

Table 3. The composition of recent-made uranium glass and the leached surface layer developed throughout laboratory leaching.

wt %	Intact glass	SD	Leached glass[a]	SD
Na_2O	**14.22**	0.46	**4.57**	0.32
MgO	2.35	0.27	2.11	0.26
Al_2O_3	0.09	0.08	0.22	0.08
SiO	70.93	0.90	76.70	0.99
K_2O	**5.25**	0.33	**4.41**	0.31
CaO	4.11	0.18	4.14	0.19
UO_3	**0.45**	0.14	**0.50**	0.14
Total	97.40		92.65	

[a] Experimental leaching

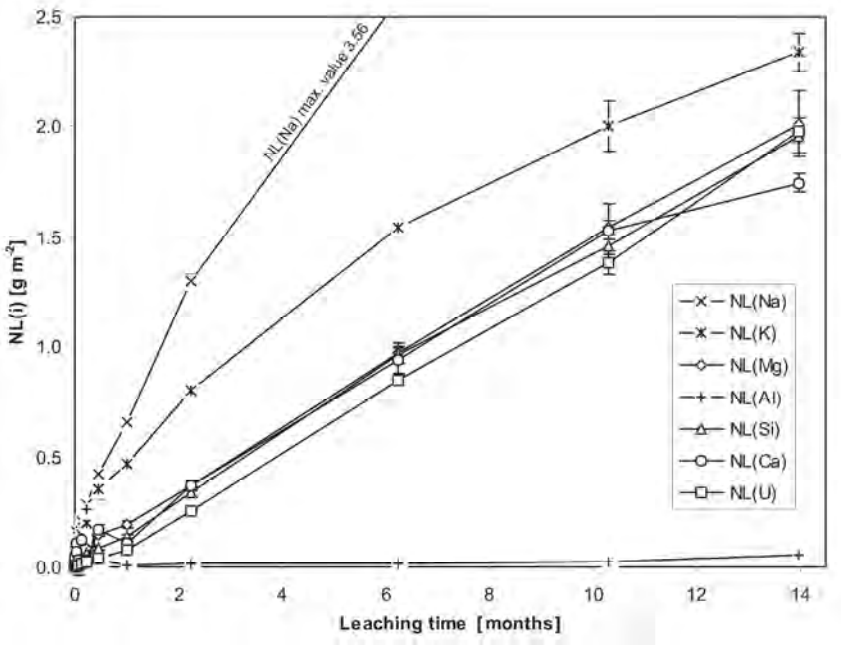

Fig.5. Experimental normalized glass mass losts (NL - given in grams of dissolved glass per square meter of the glass surface) calculated with respect to the main glass components.

Discussion

Maximal natural corrosion velocity values reach up to 4 μm/year (up to 0.6 mm/150 years). The leached layer developed during 14 months experimentally exhibits a thickness of up to 3.4 μm (Fig.4). Slightly lower values can be obtained by calculation of glass dissolution through the NL values. Considering the normalized glass mass lost calculated from the amount of Si as a major component released and the glass density of 2.76 g/cm^3, the hypothetical depth of congruent dissolution after 14 months would correspond to a 0.7 μm thick layer of completely dissolved glass. For uranium the leaching test showed the equivalent theoretical alteration depth as in the case of silicon. It is possible uranium can be fixed effectively in the leached layer by sorption on residual the glass (Procházka 2007). The glass mass lost calculated with respect to Na released corresponds to a theoretical depth of 1.3 μm of completely Na-removed glass. The only element decreased with time in the extract was Al, probably due to precipitation of newly formed solids.

Conclusion

The comparison of natural and experimental long-term corrosion of uranium-coloured glass characterizes the glass hydrolysis and preferential dissolution of particular glass components. The corrosion crusts observed during the laboratory experiments exhibit the same characteristics as these found on naturally altered glasses. The leached glass layer is depleted in alkalis relatively enriched in Si but exhibits no significant change in uranium concentration. The depth observed for experimental alteration (up to ~ 2.9 μm/year) corresponds with the average glass alteration rate calculated from the natural corrosion layer thickness (up to ~ 4 μm/year).

Acknowledgements

This study was supported by Charles University in Prague (GAUK 254/2006). The institutional funding was provided by the Ministry of Education, Youth and Sports of the Czech Republic (MSM 0021620855).

References

Čejka, J. (1999) Infrared spectroscopy and thermal analysis of the uranyl minerals. In Uranium: Mineralogy, Geochemistry and the Environment (P.C. Burns & R. Finch, eds.). Rev. Mineral. 38, 521-622.

Gin S, Godon N, Mestre J P, Vernaz E Y (1994) Experimental investigation of aqueous corrosion of R7T7 nuclear glass at 90°C in the presence of organic species. Appl Geochem 9: 255-269

Maeda T, Banba T, Sonoda K, Inagaki I, Furuya H (2001) Release and retention of uranium during the glass corrosion. J Nucl Mat 298: 163-167

Ojovan M I, Pankov A, Lee W E (2006) The ion exchange phase in corrosion of nuclear waste glasses. J Nucl Mat 358: 57-68

Procházka R (2007) Natural corrosion of the uranium-colored histiorical glasses. J Non-Cryst Solids 353: 2052-2056

Radiochemical methods analysis of U and Th: metrological and geochemical applications

Catherine Galindo[1], Said Fakhi[2], Abdelmjid Nourreddine[1] and Hassan Hannache[2]

[1]Institut Pluridisciplinaire Hubert Curien UMR 7178 CNRS/in2p3 and Université Louis Pasteur BP28, 67037 Strasbourg Cedex 2, France
[2]Laboratoire de Radiochimie, Faculté des Sciences Ben M'Sik, Département de Physique, BP 7955, Sidi Othmane, Casablanca, Maroc, s.fakhi@univh2m.ac.ma

Abstract. A present conference describes the methods for determination of U and thorium isotopes in natural samples and the study of their adsorption by the new activated adsorbents. The first part was carried out by using alpha spectrometry. The thin alpha sources were prepared by chemical electroplating of U and Th. Both elements were separated by using the ion-exchanges chromatography before their deposition. The dissolution of major solid sample was made by using alkaline fusion by LiB4O7 and LiBO2. The proposed methods have been applied for U, Th isotopes determination in the sedimentary rock: phosphate and its derivatives products and in the extracted solution from the black shale. The second part of the work was focused on the study of U, Th isotopes adsorption by new oil shale activated adsorbents.

Introduction

The present work is developed in the nuclear metrology field and its applications. It concerns essentially, the radionuclides analysis of three natural radioactive decay series: ^{238}U, ^{235}U and ^{232}Th. The radionclides concentration is in general, estimated from the radioactive equilibrium between the parent and decay product. However, this condition is frequently disturbed considering the different physical, chemical and geochemical properties of these elements in the nature. In such case, the determination of the radionuclide concentration requires the acquaintance of the sample nature and chemical and geochemical properties of each element. So, it is necessary to develop for each natural sample, the specific radioelement methods analysis (Galindo, 2006; Azouazi, 2000). It is this context that the present study

has been undertaken aimed both in the development of measuring techniques and the determination of the specific radioactivities of naturally occurring radionuclides in various natural samples: phosphates ores, phosphogypsum, phosphoric acid and black oil shale.

The second part of the work was focused on the study of U, Th isotopes adsorption by new activated oil shale adsorbents. Their preparation was carried out through different chemical and thermal procedures. The texture and composition of the raw rock as well as the adsorbents were studied before their use in the tests for elimination of the radionuclides from standard solutions prepared from uranyl and thorium nitrate (Khouya, 2005; Khouya 2005). Before that, the partitioning of U and Th in Moroccan black shale was studied by sequential extraction by means of the appropriate reagents (Galindo, 2007).

The measures are, generally, carried out by alpha spectrometry|. The thin alpha sources of U and Th isotopes are prepared by electroplating deposition. Both elements (U and Th) being firstly separate by ionic exchange chromatography. The influence of the sample dissolution step was studied by using alkaline fusion by LiB4O7 and LiBO2 (Galindo, 2007).To dose the total quantities of the uranium and thorium simultaneous determination of uranium (VI) and thorium (IV) ions by UV-Visible Spectrophotometry in Conjunction with Solvent Extraction was developed (Azouazi, 2003).

Experimental

Radiochemical separation

Generally 0.5 to 1g of the sample were ground, ashed at 850°C for 2 h and completely dissolved by peroxide fusion. The subsequent radiochemical procedure included enrichment of the radionuclides by coprecipitation with $Fe(OH)_3$. U and Th were subsequently isolated by conventional anionic exchange and extraction chromatography, followed by an electroplating step (Galindo, 2006).

Uranium and Thorium deposition

The sources for alpha counting were prepared by electroplating according to the protocol developed by Talvitie (Talvitie, 1972). For this propose uranium and thorium fractions were heated with 1 mL of concentrated H_2SO_4 and evaporated to about 1mL. After cooling to room temperature, the solutions were brought to 10 mL with doubly distilled water and the pH of each solution was adjusted to 2.3 with concentrated NH_4OH. The final solutions of uranium and thorium were transferred to the electroplating cell with a platinum disc anode (d = 15 mm and e = 1 mm) and a stainless steel cathode (d = 15 mm and e = 1 mm). The electrodeposi-

tion of uranium and thorium were conducted at 1.2 A and 2 V during 60 and 120 min respectively.

Alpha Spectrometry

The alpha counting was carried a using the CANBERRA Alpha Analyst spectrometer. The ion-implanted silicon detectors have sensitive areas of 450 mm^2 and 20-30 keV resolution through in the region interest, the detection efficiency was about 25%. Thin samples of thorium were counted on the day to minimize interference from ^{224}Ra daughter ingrowths, which has an alpha emission near that of ^{228}Th. Spectra were analyzed with the VisuAlpha software (Automatismes et Measures, Doudan, France).

Search of materials of nuclear interest

Preparation of adsorbents

New activated adsorbents have been produced from Moroccan oil shale. Their preparation was carried out through different chemical and thermal procedures:

Preparation of a powder from the raw rock.

The adsorbents were prepared from the powder **R** using two processes; the first is purely chemical and the second is based on a thermal treatment (Khouya, 2005). The materials obtained by both sequences are then activated by potassium permanganate, by H2SO4 or by H3PO4 acids (Khouya, 2006).

Adsorption Tests

A mass of 0.5g of each adsorbent is added to 200 ml of the uranyl nitrate or uranyl thorium solutions. The mixture was agitated in a batch reactor at atmospheric pressure and room temperature. The pH was maintained around 7 by addition of NaOH 0.1M or HCl 0.1M.

After a 2h shaking time to reach equilibrium, the solids were separated by filtration. The quantity of radionuclide adsorbed on the solid was determined by measuring the radioactivity in aliquots of the separated solution and comparing it with that of the initial solution by γ-ray spectrometry and UV Visible spectrophotometry method (Azouazi, 2003)

Distribution of natural-occurring U and Th in Black shale

Considering the interest of the use of Moroccan black oil shale as the raw material for production of a new type of adsorbent and its application to U and Th removal from contaminated solutions, the purpose of this part of work was to determine, by sequential extraction, its proper and natural content in U and Th.

Sequential Extraction

The sequential extractions (Galindo, 2007), described in Table 1 were performed under oxic conditions in constantly agitated centrifuge tubes with a sample size of 3 g. After each extraction stage, supernatant was separated from the residue by centrifugation at 3000 x gravity for 15 min and then passed through a 0.45 μm membrane filter into polypropylene bottles for analysis. The residue was rinsed twice with deionized water, hand shaken and separated by centrifugation and filtration. Inclusion of the filtration step proved necessary for adequate phase separation and reproducibility. The quantity of leached radionuclide was determined by alpha-ray spectrometry as described below.

Table 1. Sequential extraction procedure *(RT: room temperature)*.

Fraction	Extracting agent	Extraction conditions	
		Shaking time	Temperature
Method 1			
F1. Water soluble	30 mL deionized water	2 h	RT
F2. Exchangeable	25 mL 1M $MgCl_2$	24 h	RT
F3. Carbonates	35 mL 1M CH_3COONa + 1M CH_3COOH pH = 4.75	24 h	RT
F4. Manganese / iror hydroxides and oxides	35 mL 0.04M $NH_2OH{\cdot}HCl$ + 25% v/v CH_3COOH pH=2 (adjusted with HNO_3)	24 h	RT
F5. Organic matter + pyrite	25 mL 30% H_2O_2 + 15 mL 0.02M HNO_3 (pH = 2)	2 h	85°C
	15 mL 30% H_2O_2 + 9 mL 0.02M HNO_3 (pH = 2)	3 h	85°C
	35 mL 3.2M CH_3COONa in 20%HNO_3	0.5 h	RT
F6. Residual	/	/	/

Results and discussion

The results obtained by radiochemical analysis and measure the uranium and thorium isotopes by alpha spectrometry in the sediment phosphate and its derivatives products are summarised in the table 2.

The analysis of the results of the table 2 shows that:

- the sediments phosphates are not altered, because **^{238}U**; **^{234}U, ^{230}Th** are in radioactive equilibrium.
- the specific activity associated with ^{238}U is around 1156 Bq.Kg^{-1}, that is equivalent to 108, 8 ppm.
- the lower ^{232}Th/^{238}U reveals that the sediments phosphates are a marine origin
- the most salient observation is that the uranium was concentrated in the phosphogypsum at the level of 70 % and at the level of 1.9 % for the phosphoric acid.
- The phosphogypsum and phosphoric acid obtained from calcinated phosphates samples, concentrate uranium at the level of 22. 84 % and 70.24 % respectively.
- the radionuclide specific activities (Bq/Kg) in the fertilizer (F1 :DAPC) are relatively higher than those of the phosphates. These values must be corrected in considering the yield of the mass of the fertilizer product and the engaged mass of the phosphate.

Table 2. Specific activities of the radionuclides (in Bq.Kg^{-1}) found in the sedimentary phosphates rock and its derivatives products.

Sample	^{238}U (Bq /Kg)	^{235}U (Bq /Kg)	^{234}U (Bq /Kg)	^{232}Th (Bq /Kg)	^{230}Th (Bq /Kg)
Phosphate	1156 ± 46	72 ± 5	1168 ± 46	8 ± 1	1182 ± 71
F_1 Fertilizer	1528 ± 115	67 ± 15	1548 ± 116	26 ± 7	1958 ± 432
Phosphogypsum (PGc)	264 ± 9	23 ± 1	252 ± 9		
Phosphogypsum PGnc	811 ± 43	38 ± 3	830 ± 45		
phosphorique acid PHc	812 ± 31	50 ± 3	807 ± 36		
phosphorique acid PHnc	22 ± 1	1 ± 0.05	24 ± 1		

with: PH: phosphate sample from the Youssoufia mining center,
F_1: Fertilizers sample; (DAPC) The treated grains phosphates without organic matter
PG nc: phosphogypsum from not calcinated phosphate
PGc: phosphogypsum from calcinated phosphate
PHnc: phosphoric acid from not calcinated phosphate
PHc: phosphoric acid from not calcinated phosphate

Leaching results for U and Th

The activities of the natural radionuclides ^{238}U, ^{235}U, ^{234}U, ^{232}Th, ^{230}Th and ^{228}Th in the bulk shale sample are given in Table 3. The $^{234}U/^{238}U$ and $^{228}Th/^{232}Th$ activity ratios are near unity.

The raw black shale characterised by the lower $^{232}Th/^{238}U$ reveals that the sediments are a marine origin. It constitutes a closed system; because **^{238}U** and its decay product **^{234}U, ^{230}Th** are in radioactive equilibrium (the isotopic ratio is equal to the unity).

The sequential leaching results according the different stages (F1 to F6) as illustrated in the table3 show that:

- the water leaching phase (F1) contain less than 2% of U and Th,
- for the easily exchangeable fraction (F2), only 4% of the total ^{238}U was extracted and less than 1% of ^{232}Th,
- for the carbonate- bound fraction (F3), 10% of initially present ^{238}U was removed due to the dissolution of carbonates,
- for the destroyed reducible phase, 8% of ^{238}U is detected in the extracted fraction
- the amount in percent of uranium and thorium extracted during the step F5 from organic phase are 75 and 51 respectively,
- The silicates minerals contain only 3% and 49% of total U and total Th respectively.

Table 3. Leaching results for U and Th isotopes.

Element Fraction	^{238}U ($Bq.kg^{-1}$)	^{235}U ($Bq.kg^{-1}$)	^{234}U ($Bq.kg^{-1}$)	^{232}Th ($Bq.kg^{-1}$)	^{230Th} ($Bq.kg^{-1}$)	$^{234}U/^{238}U$	$^{230}Th/^{238}U$
Bulk sample	522 ± 41	26 ± 2	521 ± 41	21.9 ± 2.1	519 ± 48	1.0 ± 0.1	1.0 ± 0.1
F1	4.0 ± 0.4	< 0.2	7.4 ± 0.6	< 0.2	26 ± 2	1.8 ± 0.2	6.5 ± 0.9
F2	17 ± 1	1.1 ± 0.2	32 ± 2	< 0.2	2.9 ± 0.9	1.9 ± 0.2	0.17± 0.06
F3	53 ± 3	2.9 ± 0.5	100 ± 5	< 0.2	3.9 ± 0.9	1.9 ± 0.1	0.07 ± 0.02
F4	44 ± 3	2.1 ± 0.4	60 ± 3	< 0.2	4 ± 2	1.4 ± 0.1	0.09 ± 0.05
F5	394 ± 22	23 ± 2	308 ± 18	11.9 ± 1.3	371 ± 66	0.78 ± 0.06	0.94 ± 0.05
F6	19 ± 1	0.8 ± 0.2	19 ± 1	11.4 ± 1.3	92 ± 9	1.01 ± 0.09	5.4 ± 0.7
HCl + HF leaching	16 ± 1	0.8 ± 0.1	23 ± 2	13 ± 1	118 ± 10	1.5 ± 0.2	7.4 ± 0.8

Adsorption tests of radionuclides by the Black shale activated adsorbent

The yield of trapping of the radionuclides by the activated adsorbents is represented in the Fig.1 and Fig. 2.

Among the activated adsorbents which were the object of this part of study, the one prepared by thermal process, followed by activation by $KMnO_4$ ($\mathbf{RT_a}$) is very effective for the elimination of the ^{235}U, ^{234}Th and ^{226}Ra radionuclides (Fig.1 and Fig 2). It traps respectively 98 % of uranium, 99 % of thorium and 95 % of radium (Fig.1). The study of the kinetics of adsorption of uranium, thorium and radium by $\mathbf{RT_a}$ product (Fig.1), shows that the thermodynamic equilibrium, at ambient temperature and pH = 6.8, between the aqueous phase and the adsorbent is reached after 2 hours for ^{235}U and ^{234}Th, and 8 hours for radium. During these times, the rate of adsorption of the three elements increases rapidly versus time before reaching maximal values, to which correspond an adsorption yield of about of 100 % for uranium and thorium, and 85 % for radium.

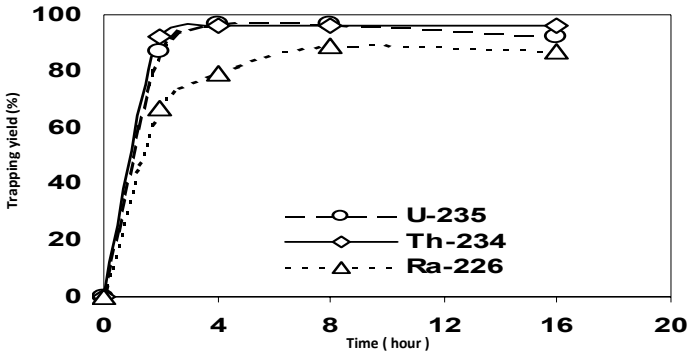

Fig.1: Kinetics of adsorption of ^{235}U, ^{234}Th and ^{226}Ra by ($\mathbf{RT_a}$).

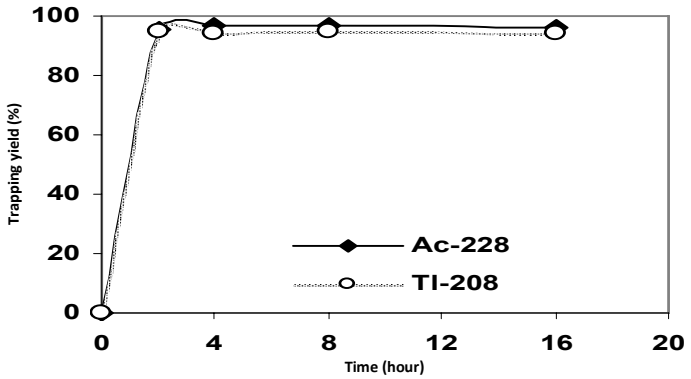

Fig. 2: Kinetics of adsorption of ^{228}Ac and ^{208}Tl by ($\mathbf{RT_a}$).

Conclusion

The achieved works by the Moroccan group in collaborations with Laboratoire RAMSES de l'Institut Pluridisciplinaire Hubert-Curien- IPHC de Strasbourg-France is subdivised into three basic groups:

- the development of the nuclear metrology of measure and applications;
- the development of the analytical and radiochemical methods;
- the study of the physicochemical procedures of selective adsorption and separation of elements.

The present conference constitutes a part of the accomplished works in those three categories. It concerns important applications of the sciences of the nuclear metrology and radiochemical analysis and the geochemical studies of the environmental samples.

References

Galindo C., Mougin L., Nourreddine A. (2007) An improved radiochemical separation of uranium and thorium in environmental samples involving peroxide fusion, Applied Radiation and Isotopes, 65, 9-16.

Azouazi M., Ouahidi Y., Fakhi S., Andres Y, .Abbé J.C., Benmansour M. (2000) Natural radioactivity in phosphates, phosphogypse and natural waters in Morocco. Journal of Environmental Radioactivity, Vol. 54. N°.2 231-242.

Khouya1 E., Fakhi S., Hannache H., Ichcho S., Pailler R., Naslain R.,AbbeJ.C. (2005) Production of a new adsorbent from Moroccan oil shale by chemical activation and its adsorption characteristics for U and Th bearing species. Phys. IV France 123 87-93.

Khouya E., Hannache H., Fakhi S., Ezzine M., Ichcho S., Pailler R., Naslain R., AbbeJ.C. (2005) ″Elaboration de nouveaux adsorbants activés à partir des schistes bitumineux marocains de Tarfaya par activation chimique en milieu sulfurique″. J. Phys. Chem. News 24 69-75

Azouazi M., Fakhi S., Hannache H., Grambow B., Abbe J.C., Andres Y. (2003) Spectrophotometric determination of U (VI) and Th (IV) with arsenazo III in conjunction with solvent extraction. Colloque International: Uranium Geochemistry, 13-16, Nancy-France, p.63.

Talvitie N.A. (1972) Electrodeposition of Actinides for Alpha Spectrometric Determination; Anal. Chem., 44 280 – 283.

Khouya E., Ichcho S., Legrouri K., Hannache H., Fakhi S., Nourredine A., Ezzine M., Pailler R., Naslain R. (2006) Activation des nouveaux précurseurs à base des schistes bitumineux par l'acide phosphorique : Influence des conditions expérimentales sur les propriétés des adsorbants préparés. Ann. Chim. Sci. Mat.; 31 (5), pp. 583-596.

Galindo C., Mougin L., Fakhi S., Nourreddine A., Lamghari A., Hannache H. (2007) Distribution of naturally occurring radionuclides (U, Th) in Timahdit black shale (Morocco), Journal of environmental Radioactivity, 92, , 41-54.

Characterization of the interactions between uranium and colloids in soil by on-line fractionation multi-detection methods

Céline Claveranne-Lamolère[12], Gaëtane Lespes[1], Jean Aupiais[2], Eric Pili[2], Fabien Pointurier[2] and Martine Potin-Gautier[1]

[1]LCABIE, UMR 5254-IPREM, Hélioparc, 2 av. P. Angot, 64053 Pau cedex 9, France
[2]Commissariat à l'énergie atomique, DIF/DASE/SRCE, centre CEA-DAM Ile de France, Bruyères-le-Châtel, 91297 Arpajon cedex, France

Abstract. It is acknowledged that colloids can be important for determining contaminant availability and mobility. We have used size exclusion chromatography (SEC) and asymmetrical flow field-flow fractionation (As-FFFF) coupled with refractometry (RI), multi angle laser light scattering (MALLS), ultraviolet (UV) and inductively coupled plasma mass spectrometry (ICP-MS) detectors to study colloidal binding of uranium in leachates. The nature, the molecular and size distribution and the quantitative uranium distribution over the colloidal phase are obtained.

Introduction

The IUPAC definition of colloids refers to compounds (organic or inorganic) with size ranged from 1 nm to 1 µm in one dimension. Natural colloids are extremely diversified in the environment, covering a large variety of different entities in environmental media such as clays, iron hydroxide, humic compounds, micro organisms, their associations, aggregates and many others (Buffle and Leppard 1995). Environmental colloids are of high interest because of their role especially in trace element mobility, bioavailability and transfer (Buffle and van Leeuwen 1992; Citeau et al. 2003).

In the past decades, the single radionuclide transport facilitated by colloids has attracted lots of researcher's attention (Kersting et al. 1999, Dai et al. 2001, 2002, Chunli et al. 2001, Matsunaga et al. 2004). In some cases, colloids are assumed to be responsible for this transport thanks to a strong chelating capacity and an im-

portant specific surface (Ticknor et al. 1996, Moulin and Moulin, 1995, Kersting et al. 1999). Despite a great deal of scientific interest, much information remains unknown. Classical studies use sequential fractionation (ultrafiltration) and off-line analysis (inductively coupled plasma mass spectrometry (ICP-MS) or thermo-ionisation mass spectrometry (TIMS) (Kersting et al. 1999, Dai et al. 2001, 2002). Although their high sensitive, such methods suffer from poor resolution and repeatability, and provide no information about the nature of the colloids.

The aim of this study is to characterize the interactions between uranium and colloids by using powerful on-line fractionation multi-detection techniques, allowing complementary information to be obtained (Jackson et al. 2005). The analytical techniques are size exclusion chromatography (SEC) coupled with refractometry (RI) and multi angle laser light scattering (MALLS) and asymmetrical flow-field flow fractionation (As-FFFF) coupled with UV, MALLS and ICP-MS. Thus it is possible to determine the nature (organics, inorganics or auto-colloids), the molecular mass and the size distribution (hydrodynamic and gyration diameter) and the quantitative uranium distribution over the colloidal phase.

Materials and methods

Soil sample

The present study concentrates on the influence of colloids on the migration behaviour of uranium in soil from a French nuclear site. The site is located at 25 km of Reims (Champagne). In situ experiments led to the dispersion of U-metal.
Samples were collected from the same location and at different depths: 0-30 cm (samples 1-A) and 30-60 cm (samples 1-B). Samples 1-A are supposed to be rich in humic substances and clays and 1-B is composed of chalk (mainly $CaCO_3$). Samples were collected in plastic bags and stored at 4°C.

Leaching experiments

Batch experiments were performed with two solutions. The first one represents artificial rain solution. The following inorganic salts were added per 1 liters of deionized water to prepare artificial rainwater (Davies et al. 2004): $NaNO_3$, 4.07 g; NaCl, 3.24 g; KCl, 0.35 g; $CaCl_2$ 2 H_2O, 1.65 g; $MgSO_4$ 7 H_2O, 2.98 g and $(NH_4)_2SO_4$, 3.41 g. The resulting solution has an ionic strength of 0.3 mM and a pH of 5.2. The composition of the artificial rainwater used is typical of many reported in the literature for studies carried out in both the Northern and Southern hemispheres. The second solution is water equilibrated with the samples 1-B. It represents in-depth conditions in the soil. 500 g of soil were placed in 1L polypropylene vials with 1 liter of deionized water. Then the conductivity was measured

regularly. When the value was stable, the equilibrium was assumed to be obtained (Collon et al. 2001).

The liquid/solid ratio (L/S) varied between 1 and 100 L/kg. The samples were shaken for 24 hours and subsequently centrifuged at 3500 rpm for 30 minutes. Then each sample was filtered using 0.45 µm filters before analysis.

Size exclusion chromatography

Size exclusion chromatography was carried out using two Shodex OH-pack-SB columns. These columns separate compounds within the approximate MW range 10^2 – 10^6 Da. The eluant for all SEC experiments was 2×10^2 M $NaNO_3$ and the sample injection was 100 µL. The detectors used were multi-angle laser light scattering (MALLS)-(DAWN HELEOS II, Wyatt technologies) and refractive index (RI)-(Waters 2410). Calibration of the detectors was performed using POE 20 kDa.

Asymmetrical flow field flow fractionation

The asymmetrical flow field-flow fractionation used was an Eclipse 2 (Wyatt technology). The spacer had 250 µm thickness for humic substances analysis and 350 µm for nanoparticles experiments. The channel dimensions were 26.5 cm in length and from 2.1 to 0.6 cm in width. The membranes used were 1 kDa for humic substances experiments and 10 kDa for nanoparticles analysis. Flows were controlled were controlled with an Agilent 1100 series isocratic pump equipped with a micro vacuum degasser. Detection chain consists in variable wavelength ultraviolet/visible spectrometer (UV)-(Agilent technologies 1100 series) and a multi angle laser light scattering (MALLS)-(DAWN DSP-F from Wyatt technologies). All injections (200 µL) were performed with an autosampler (Agilent technologies 1100 series). Data from UV and MALLS detectors were collected and treated with Astra 5.3 software (Wyatt technologies).

Results and discussion

Size exclusion chromatography

According to fig 1, there are two populations of particles for the water equilibrated with the sample 1-B and 4 populations for artificial rain water.

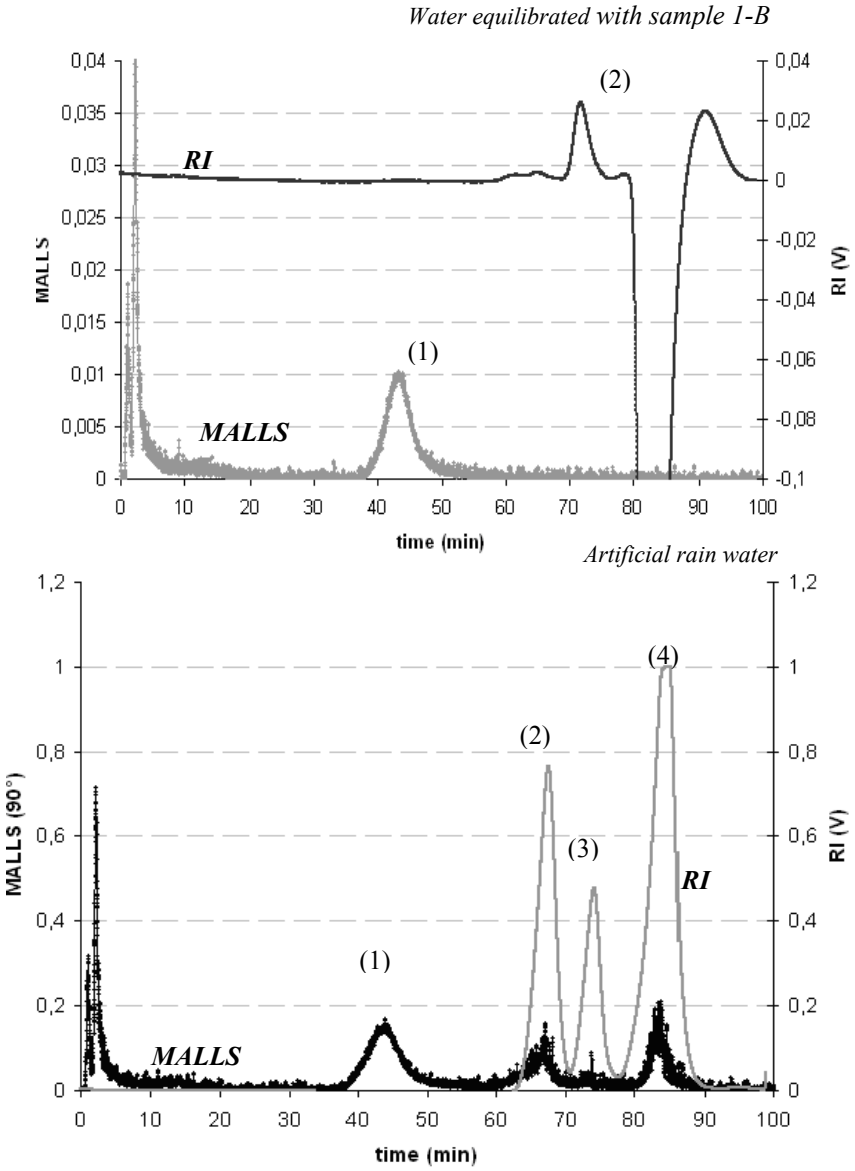

Fig.1. Chromatograms obtained with samples 1A (up) and 1B (down) and with refractometry (right axes) and MALLS (left axes) detection.

All these different populations could be humic substances as the protocol used (Hongve et al. 1996) is dedicated to extract them. So, the nature of the leaching agent seems to have a strong influence on the number and molecular masses of the

leached particles. In addition, transport of uranium could be support by rain water in the soil surface. However, more data are necessary to confirm this assumption.

Thereafter, the different ratios L/S were compared.

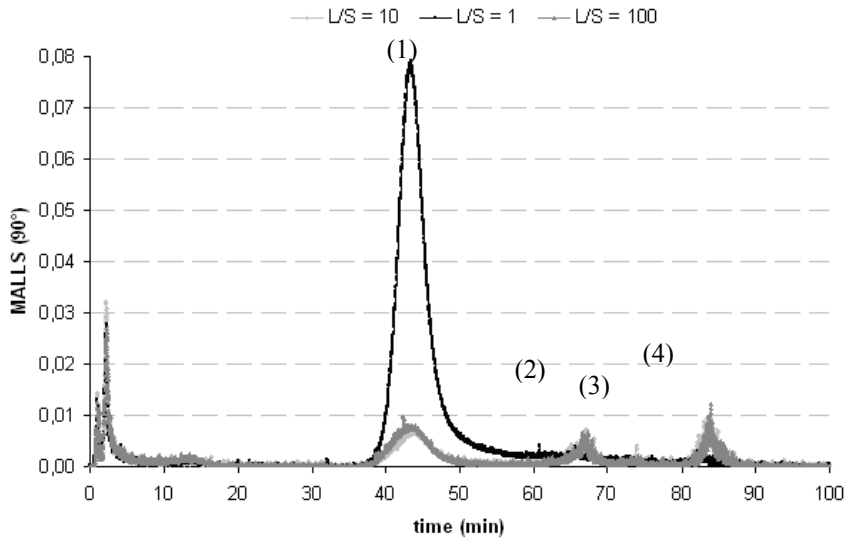

Fig.2. Comparison of the SEC/MALLS chromatograms obtained for various L/S ratios.

The chromatogram corresponding to L/S=1 shows a higher peak-1 than the chromatograms obtained with L/S= 10 and L/S=100, with similar retention times. Thus, it could be assumed that more colloids are extracted from the sample with a L/S ratio of 1 than with ratios of 10 and 100, partly due to dilution effect.

Asymmetrical Flow Field Flow Fractionation

The run sequences contained first, two short and consecutive steps of elution and focusing without injection to equilibrate the system and follow the signal baseline. Then, the injection started during a focus step. After the sample injection, the focus step was then kept to reduce the lateral extension of the sample due to the injection. Finally, the elution started with crossflow, leading to colloidal fractionation. When the fractionation step was over, a rinse step without crossflow was applied.

Two sets of operating conditions were used in order to make possible the fractionation of 2 types colloids: humic substances and nanoparticles. These conditions are presented in table 1 (Dubascoux et al, 2007, 2008).

The fractograms obtained for each condition are presented in fig 2.

Table 1. Analytical conditions for the fractionation of humic substances and nanoparticles.

	Humic substances	Nanoparticles
spacer (µm)	350	250
membrane	10 kDa	1 kDA
carrier liquid	NH_4NO_3 10 mM	NH_4NO_3 1 mM
flow (ml min)	1	1
crossflow (ml min)	3	0.8
time of analyze (min)	40	50

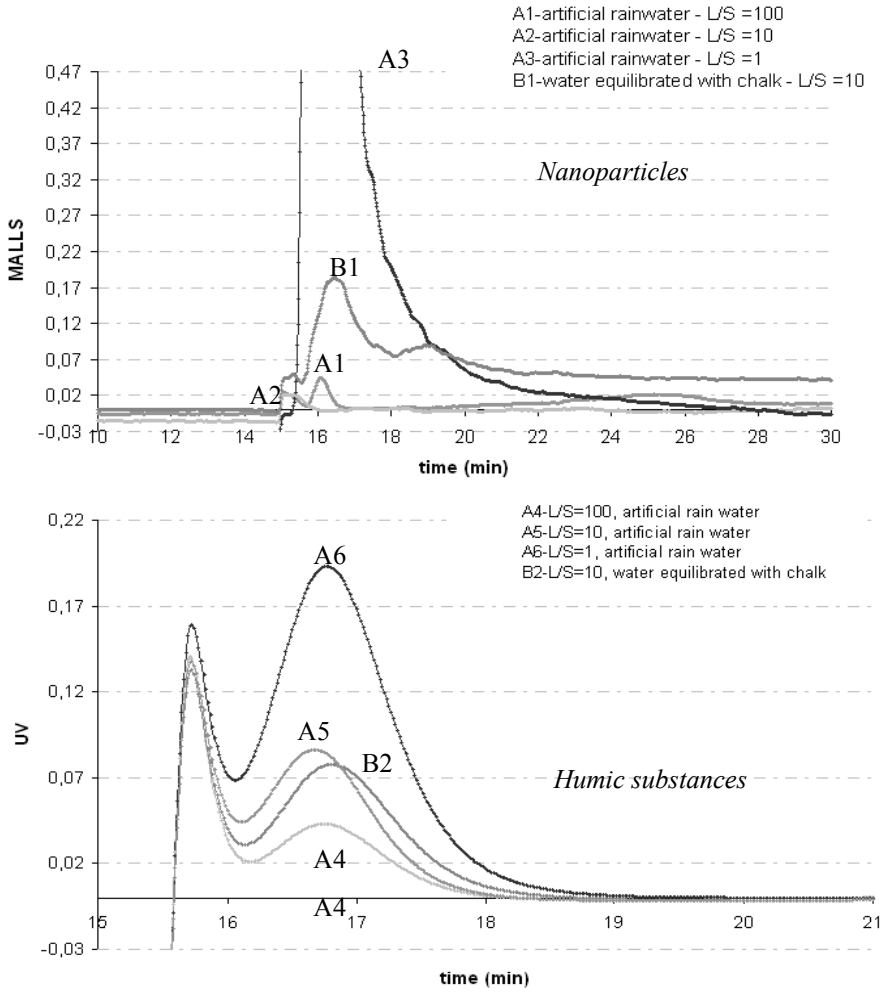

Fig.3. As-FFFF fractograms obtained for various L/S ratios and leaching reagents.

Table 2. Molecular masses calculated for humic substances and nanoparticles.

conditions of leaching	humic substances Mw (Da)	nanoparticles Mw (Da)
L/S = 10, water equilibrated with chalk	1773	4780
L/S = 1, artificial rain water	2139	76544
L/S = 10, artificial rain water	2286	6147
L/S = 100, artificial rain water	2020	4162

Only one population is observed for humic substances whereas 1 to 2 populations are present for nanoparticles. In the case of humic substances, L/S ratio seems to have a strong influence on the intensity of the signal and consequently on the concentration, whereas both L/S ratio and leaching reagent could strongly influence the nanoparticles signal. So, the influence of the L/S ratio on the concentration of colloids extracted is confirmed.

Molecular masses have been calculated with calibration curves using polystyrene sulfonate standards from 910 to 145 000 Da. The results are presented in table 2.

For L/S ratio equal 10, humic substances and nanoparticles leached with water equilibrated with chalk are smaller than when leached with artificial rain water. Moreover, for artificial rainwater, L/S could influence nanoparticles molecular masses. This phenomenon will must be confirmed by further study.

Conclusion

In this first work, information about influence of L/S ratio and leaching reagent on molecular masses has been obtained. At the same time, As-FFF and SEC fractionation have been optimised.

Another result wills be presented in the poster especially concerning uranium long-term behaviour and its mobility.

Acknowledgements

We gratefully acknowledge Bruno Grassl (team of physico-chemistry of polymers, EPCP, IPREM) and Julien Rigolini (EPCP, IPREM) for SEC measurements.

References

Buffle J and Van Leeuwen H P (1992) Environmental Particles 1: Chelsea USA, Lewis Publishers

Citeau L, Lamy I, Oort F V, Elsass F (2001) Earth and Planetary Sciences 332: 657-663

Chunli L, Y Y., Zhiming W, Shushen L, Zede G, Bing L, Ling J, Hong J, Ling W, Dan L and Zhongde D (2001) Radiochimica Acta 89: 387-391

Dai M H, Buesseler K O, Kelley J M, Andrews J E, Pike S, Wacker J F (2001) Journal of Environmental Radioactivity 53: 9-25

Dai M, Kelley J M, Buesseler K O (2002) Environmental Science and Technology 36: 3690-3699

Dubascoux S, Nia y, Slaveykova V.I, Lespes G, Fractionnement par couplage Flux- Force (FFF) des substances humiques : Optimisation et applications, Congrès international GRUTTEE, 29-31 Octobre 2007- Pau (France)

Dubascoux S, Le Hecho I, Potin-Gautier M and Lespes G (2008) Talanta, accepté pour publication

Kersting AB, Efurd D W, Finnegan D L, Rokop D J, Smith D K, Thompson J L (1999) Nature 39717: 56-59

Jackson B R P, Ranville J F, Ertsch P M B, Sowder A G (2005) Environmental Science and Technology 39: 2478-2485

Matsunaga T, Nagao S, Ueno T, Takeda S, Amano H, Tkachenko Y (2004) Applied Geochemistry 19: 1581-1599

Ticknor KV, Vilks P, Vandergraaf T T (1996) Applied Geochemistry 11: 555-565

Moulin V, Moulin C (1995) Applied Geochemistry 10: 573-580

Towards a more safe environment: Disposability of uranium by some clay sediments in Egypt

Samy Mohamed Abd-Allah[1], O.M. El Hussaini[2] and R.M. Mahdy[2]

[1]Soils Dept., Fac. Agric., Ain Shams Univ. Cairo, Egypt. P.o.Box 68 hadayek shoubra 11241, Cairo, Egypt. E-mail samyabdallah@hotmail.com
[2]Nuclear Materials Authority, Cairo, Egypt.
Present address: King Khalid University, Prince Sultan Bin AbdulAziz Centre for Research and environmental Studies. Abha 61421, P.O.Box 960 building 162 Saudi Arabia

Abstract. Due to the increase concerns about the environmental pollution problems, it is so important in waste disposal management to perform an accurate exploration of geological barriers, which must be suitable for waste materials disposal. Clay sediments play an important role as natural adsorbents to immobilize heavy and nuclear metals contaminants.

For the present study, the clay samples were collected from either clay exploitation localities or from nearby radioactive mineralization in Egypt. Obtained results indicated that uranium adsorption and desorption differ importantly in accordance with the source of clay sediment used. In addition, its adsorption increases by increasing uranium initial concentration. The obtained data were found to fit of Langmuir equation isotherms.

Adsorption maxima (B) for uranium were high for Abu Tartur bentonite followed by El Hafafit vermiculite and was the least for Kalabsha kaolinite. However, the binding energy (b) that affects the adsorption process can be arranged in the opposite direction. Desorption of uranium by HCl, NaOH and tap water show clear ability of the different sediments to release uranium. This was a function of leaching solution and binding energy. Finally, the changes in the clay sediments through adsorption and desorption processes were investigated in detailed by I.R spectroscopy.


Uranium Mining
and Hydrogeology

The Importance of Organic Colloids for the Transport of Uranium and other Decay Chain Elements in a Boreal Stream Network

Fredrik Lidman, L. Björkvald, B. Stolpe, S. Köhler, M. Mörth and H. Laudon

Umeå University, EMG, 90187 Umeå, Sweden

Abstract. Krycklan is a 68 km^2 catchment in northern Sweden, where hydrological, hydrochemical and biogeochemical research has been carried out for more than 30 years. Hence, the area has a well developed sampling infrastructure and long time-series, which has lead to a good understanding of the hydrological processes. During two years uranium activities in streams from 10 sub-catchments in the area were followed, which has resulted in more than 400 measurements. The material was then analyzed from a geostatistical perspective, and it could be shown the forest and wetland percentage was the single most important factor for explaining the spatial and temporal variability in uranium transport within the catchment.

The objective of the research has been to relate the large-scale landscape fate of uranium and other decay chain elements to specific biogeochemical processes, and therefore the connection between groundwater and surface water has been emphasized. Streams in the boreal region are typically characterized by a high content of dissolved organic carbon (DOC), and it has been found that uranium almost entirely is bound to DOC both in surface water and ground water in the Krycklan catchment. Therefore, Field-Flow Fractionation coupled to ICP-MS was used to investigate the size distribution of these organic carries and its variation throughout the spring flood, which is the main hydrological event in this area. A certain kind of 0.5-5 nm big organic colloids were found to play a very important role in the migration of uranium in from both mineral soils and wetlands to the streams.

The material is now being completed with measurements of uranium, thorium and radium isotopes. In many cases considerable disequilibria have been observed throughout the decay chains, which has provided additional information on the dynamics of the processes governing the migration of uranium, thorium and radium in the boreal region.

Assessments and decreasing of risks and damages from outbursts of Tien-Shan high mountains lakes

Alexander N. Valyaev[1], S.V. Kazakov [1], S.A. Erochin[2] and T.V. Tusova[2]

[1] Nuclear Safety Institute, RAS, Moscow, Russia
[2] Institute of Water Problems and Hydro Energy, NAS, Bishkek, Kyrgyz Republic

Abstract. Great ecological risk in Central Asia results from natural and man-made catastrophes and cataclysms (earthquakes, slips and others) Kyrgyzstan numerous U, Sb, Au and Hg tailing storages are often located near main rivers with power hydro electric stations (HES) with huge reservoirs and Tien-Shan high mountain outburst lakes. Their dams destroys from disasters or directed terrorist acts may cause huge over damming break water wave with great irreversible negative responses on environment and populations and hazard pollution of vast territories. Geophysical and engineer –geologic studying of some huge lakes, including the uranium isotope indicator for water dynamic, show their outburst growing in result of water volume increasing and underground thermo caster processes. Possible outburst scenarios parameters, risk and damages assessments are under consideration. Results will be applied for lakes classification on dangerous levels, risk management and development of counter measures for prediction/prevention of lakes catastrophes and reducing of negative damages. This approach may be used for many dangerous objects, such as HES, oil pipelines and others.

Motivation

All water objects (WO), such as rivers, lakes, seas and oceans, the artificial water constructions and the different water resources have the essential and important political, economic and ecological significance for any country. The constantly growing intensive industrial and agricultural activity made worse the WO situation. Non satisfactory or non sufficient systems of hydrological control of river's

flows and lakes, radiological and geo chemical monitoring created new negative problems both at regional state and global international levels. Especially complex and stress situation has been formed in the countries of Central Asia and Caucasus. It is connected with the following main moments (Valyaev et al. 2008a, 2008b):

1. The most part of WO is located in the mountain seismic active and dangerous regions with high probability of the natural catastrophes and cataclysms such as earthquakes, landslips, mudflows and others, which simulate the negative structural changes in the earth surface crust. In result some water sources may be disappeared and amounts of ground and underground water storages will be greatly depleted with the large additional pollution of water in WO.
2. Under the existence deficit of the natural and artificial water sources here the hot and drought climate causes the increasing water consumption on different industrial, agricultural and social needs.
3. It is necessary to provide the WO right management and its safety exploitation in conditions of its specifically complex construction and the large cumulative mechanical and corrosive wear of their elements: high dams with huge water mass in artificial reservoirs; significant drifts in rivers and water arteries. the huge water masses in artificial reservoirs press on the earth crust surface and stimulate frequent and intensive earthquakes, observed now in the regions of Kazakhstan and Kyrgyzstan Republics (Valyaev et al. 2008a, 2008b).
4. At the mountain territories of some Central Asia and Caucasus countries the high power operated and non operated industrial objects (nuclear power plants and nuclear reactors with their water heat sinks, nuclear fuel and weapon production plants with the numerous huge uranium tailing storages, tanks for saving of high radioactivity materials, rocket fuel and others) are often located near natural and industrial WO (Valyaev et al. 2008a, 2008b; Kazakov et al. 2006). These objects are very attractive especially for “terrorists of new generation”, who have wish to realize global ecological catastrophes with using of nuclear or radioactive weapon, to create “dirt nuclear bombs.” (Vandeenhove et al. 2003). Opportunity to perform deliberate attacks of terrorists near current centers of international terrorism, located in Chechnya, Afghanistan and some others so called zones of “frozen conflicts” with the using of explosives may cause such catastrophes and stimulate natural calamities. Consequences will be followed extremely negative irreversible environmental global effects such as pollution of World Ocean. at Kyrgyzstan territory there are about 100 mountain lakes with separated surface square value more than 1 km^2 and about 70 the large and dangerous lake outbursts have been happened during last 50 years. The prediction of WO behavior and decreasing of their risks are very important today.

Physical processes under outbursts of mountain WO and their risk assessments

Mountain WO is the high complex dynamic non equilibrium critical systems, that functioned in conditions of response of many and often non controlled natural and man-made factors. The direct physical experiments on such open systems and their natural modeling are impossible. It is effective to use the special space techniques and methods for these WO monitoring (Valyaev et al. 2003; Valyaev et al. 2005). Any mountain lake is represented as the space-temporal dynamic object with its transformations at the following stages: (1) slow evolution lake processes without collapse;(2) slow accumulation of lake defects till their collapse values; (3) instant catastrophic collapse of the lake. Two last collapse stages with lake outburst or its dam destroy in result earthquake, blast or rock slips, will create a huge break-through water wave (BWW) and its propagation over vast territories with huge economic and ecologic damages. BWW parameters and flooding size may be estimated for the separate lake and its high mountain location with using of special model or data on Regional Water Register.

Today we have very insufficient information on these thematic problems. And our consideration is only our first step in this direction. The lake outburst can be realized by the three following mechanisms: (1) Its dam destroy; (2) Subterranean outburst along intra-glacial and intra-moraine tunnels; (3) Coincidence of dam destroy and subterranean outburst.

We used the uranium-isotopic method to determine sources of moraine-glacial lakes feeding and assess of its outburst danger. Mountain moraine-glacial lakes are formed from atmospheric precipitates in melted snow water form, “young” ice of glacier beetling over lake (meteoric waters) and water from melted “aged” buried ice, lying in adjoining rocks of lake edges and bottom (waters, leached from rocks; Tuzova et al. 1994; Tuzova 2006; Erohin 2006). Waters from first source are characterized by extremely low U content and balanced ratio of its even isotopes (C = (0.39± 0.02) ppm; γ =1.02±0.02) (Valyaev et al. 2008b). Waters from melted buried ice are noted for higher U content and non-equilibrium γ ratio (C range = 2.48 ± 0.08 - 28 ± 0.2 ppm; γ range = 0.862 ± 0.007 – 1.16 ± 0.02). More role of buried ice in lake feeding is, more water in moraine-glacial lakes deflects from glacial melted water by corresponding C and γ values, which allows to determine main feeding sources. The latter testifies about lake instability state and increasing of its outburst probability. The presented method is confirmed by our inspection of five Kyrgyz lakes (Valyaev et al. 2008b): maximum C and γ deflections from the same values in meteoric waters were in Teztor-1 lake (C=23± 2 ppm; γ=0.93 ±0.01) and Atjailoo lake (C=1.69 ±0.05 ppm; γ=0.89 ±0.01). After that Teztor-1 had several outbursts; the last was in 2004. Atjailoo outburst was in 1997 and today it is in constantly growing outburst stage. Another three lakes are stable and their uranium-isotopic parameters are close to meteoric waters: for Teztor-2 lake C=1.14±0.03 ppm; γ=1.00 ±0.02; for Kashkasu and Tuuktor lakes C=1.39 ±0.05 ppm; γ=1.06 ±0.01.

Also we notice three variants of lake outbursts, connected with their origination:

1. Surface overflow. It is typical for lakes of obstructed type, much less possible for glacial and moraine lakes, and even less possible for moraine-glacial and moraine-nogging types of lakes.
2. Subterranean outburst along intra-glacial and intra-moraine tunnels. Tunnels bring out water beyond bounds of moraine-glacial complex down to a valley. This outburst is typical for lakes of glacial and moraine-glacial types, rarely for moraine-nogging and moraine types.
3. Compound outburst. Outburst starts subterranean way, and during a process of outburst underground canal of drain widens so much that its roofing doesn't bear load of overlying and descends. Outburst becomes surface; usually in this case volume of outburst greatly increases. The third variant of outburst is most typical for moraine-glacial and moraine-nogging lakes, rarely for obstructed lakes. These observations show more complex nature of lake outburst

Break-through water wave propagation

Let us consider the most catastrophic processes after mountain lake outburst, caused by the total dam destroy and the next generation of huge break-through water wave (BWW). At first BWW will create the intense shock mechanical response on all natural and artificial objects along its propagation and then it will be transformed in water space submergence zone. The evaluation of BWW parameters will be included the following: (a) maximum possible height and speed of break-through wave propagation; (b) estimated time of coming of wave crest (front) onto selected object or point of territory; (c) boundaries of possible submergence zone in the vicinity; (d) maximum depth of submergence for every definite locality ant time of its submergence; (e) to point out all main objects, that will be under wave response.

As for last case, the following explanations have to be done. Some objects may be only under response of break-through wave front for the shot time without the next submergence for long time. It will only result to mechanical total or partial destroy of these objects with next water wash-out of soil and artificial constructional elements. This situation will be analyzed in according to the results, caused damages and consequences.

For estimates of BWW parameters we use the computer modeling with taking into account the real profiles of local earth's crust and mountains valley (including its rock and soil materials), another water reservoirs, such as lakes, small rivers and other natural objects. When WO is a lake or another huge water reservoir and it has a river, flowing through or out of it, and one or few natural or man-made dams, separated this river from WO. Then the possible scenarios of examined catastrophic flooding, related with dam destroy, will be elaborated on the base of method of the geographic analogous (Malik et al. 1998). BWW height is determined as a sum of upper and lower waves of destructed dams, height of the sea-

sonal high-water (flood) according to data of Water Register in certain parts of rivers. This method allows to determine BWW parameters and consequences of damages under the various order of dam total or partial destroy or damage. The calculations results will be usually presented on the special map, which allows to determine the extensions of damage and to develop the measurements on prevention of the negative consequences in accordance with distinguished hazard zones.

In the case of the wave propagation will located at different industrial zones, liquid and water objects, such as tailing storages, heat sinks, artificial water reservoirs and others, that contained different hazard pollutants (toxins, radionulclides, heavy metals, toxins and others), we have to take into account the influence of these objects on wave propagation and their additional hazard response on environment after wave response. Our consideration will include the analysis of the possible scenes of realization of situations on pollutant migration from these objects, for example, from tailing storage: (a) constant pollutant migration without damage of tailing storage dams; (b) similar migration with the partial damage of tailing storage dams, for example, under landslide or earth flow; (c) pollutant migration under total dam destroy; (d) pollutant migration in result of: (1) partial flowage; (2) total one;

Under realization of last two scenarios it is possible two following cases of development of catastrophic situation: (1) all tailings are washed off by a river flow during few days; (2) all tailings are washed off by a river flow instantly. The last situation is the most extreme and dangerous, because it will cause the maximum pollution with maximum losses both for environment and population. For all cases it is necessary to take into account the following kinds of possible damages caused by: (1) people victims and hazards to human health; (2) pollution of wide scale territories with subsequent losses in forest, agricultural and fish industries; (3) wide pollution of buildings and constructions; (4) pollutant migration in basins of the large rivers. Under radiological risk assessments it is necessary to take into account the possible chemical nuclear reactions and transformations of pollutants in soil, water and air. For example, transport calculation will be done for decay chain $^{238}U > {}^{234}U > {}^{230}Th > {}^{226}Ra$.

Assessment of damages

We use our method for assessment of damages, which includes the following (Valyaev et al. 2008a, 2008b). Let us consider the common case of any object exploration for the fixed time interval under the following assumptions: (1) at initial state the object is in normal (non accidents) exploitation; (2) the different kinds of accidents may be occurred as noticed $i = 2, 3, \ldots, m$, where m is the total number of possible accidents ($m=1$ is corresponded to the normal regime); (3) every accident may create the different kinds of damages. Assuming that j is the kind of damage with a_j value. Then $j = 1,2, \ldots n$, where n is the total number of possible kinds of damages; (4) realization of i accident creates the damage of j kind with P_{ij}

probability, thus the matrix of risks (probabilities) is determined. Then the total vector of limited losses $\vec{a}_{\lim}$ may be determined on next formula (Tuzova 2006):

$$\vec{a}_{\lim} = P(1)\vec{a}_{1n} + \sum_{i=2}^{m} \hat{P}_{ij}\vec{a}_j \qquad (1)$$

where *P(1)* is the probability of damage formation under normal exploitation; $\vec{a}_{1n}$ is the vector of limited damages under regular exploitation. $P_{ij}a_j$ coordinate vector value in sum is equal the damage value of *j* kind under realization of *i* kind accident. Obviously that at normal mountain lake state *P(1) =0*. At extreme case of the lake outburst the possible economic damage may be assess as total material losses, caused by break-through water wave, resulted to numerous destroys of different agricultural and industrial constructions, pollution of vast territories and others. Assessment of this wave parameters and size of flooding territories have to be done for selected lake on the method, described above.

Here we pay some attention to mountain lakes of Kyrgyzstan. The main natural and manmade water objects are presented in Fig.1.

The total or partial destroys of their natural and artificial dams from above mentioned disasters or directed water terrorist acts may cause huge water wave and its great irreversible negative responses on environment and populations with wide scale global hazard pollution of vast and transboundary territories (in Uzbekistan, Tajikistan and others), including water basins of Syrdarya and Amurdarya main rivers in Central Asia (see Fig.1). The Petrov unique huge mountain lake is located at the moraine and glacial complex of Petrov large glacier, flowing from the western slope of Ak-Shyirak mountain range. The Kumkor river, tributary of Naryn river, flows out the lake. The maximum registered Kumkor river flow is

Fig.1. Map of Kyrgyzstan Republic.

66.2 m^3/s, its usual average value is varied from 2.9 to 25.2 m^3/s from June to September. Petrov lake parameters are the following: 3734 m height at sea level; 60.3 million m^3 water volume; the ice dam; 15- 24 m lake depth range; 19-21 km bottom width range The lake feeds on melting ice from the glacier. The total glacier area of is 69.8 km^2.

The recent detail geophysical and engineer –geologic studying of Petrov lake, including uranium isotope indicator for water dynamic, shows the growing of the lake outburst dangerous in result of its constant water volume increasing and current underground thermo caster processes (Tuzova 2006; Erohin 2006). This outburst will cause destroys and hazard pollution of Naryn river head with some dangerous for the operative mountain gold mines of Kumtor Operating Company. Also the outburst wave may stimulate the dam destroys at the huge water reservoirs of Naryn five high power operated HES, that supply energy for all Republic. The most Torkogul HES reservoir (Fig.1) has accumulated 20 billion m^3 water with the height of its dam ~ 200 m. Its dam destroy will have the global catastrophic consequences for all Central Asia.

Conclusion

Under consideration and analysis of high mountain lake outbursts we have deal with the large scale open non equilibrium chaotic system, exposed to numerous external natural and man – made factors. Most part of them is non controlled or non known yet as their actions on system. As for forecast and assessment of possible economic and ecological damages, caused by catastrophes and cataclysms, the most difficult problem is the assessment of elements for P_{ij} matrix of risks and damages in (1) formula. One of the main reasons here is connected with insufficient representative statistic on such dangerous objects or often it's full absent. The analysis of all calculations results will be taken into account for these lakes classification on their dangerous degrees, management of their risks, development of counter measures for prediction/prevention of the lakes catastrophes, some terrorist acts, management of risks, reducing and softening of their negative damages. It will promote to substation and safety development of vast regional and transboundary territories of many countries. This approach has the universal character and may be used for many dangerous natural and man- made objects and also in development of common system for emergency prevention/elimination.

References

A.N. Valyaev, S.V. Kazakov, A.A. H. D. Passell et. al (2008a). in NATO Science Series: Proc. of NATO Advanced Research Workshop: "Prevention, Detection and Response to Nuclear and Radiological Threat", May 2-7, 2007 Yerevan, Armenia, Editors: S. Apikyan et. al. Published House: Springer, Netherlands, 2008, pp. 281-299

A.N. Valyaev, S.V. Kazakov, A.A. H. D. Passell et. al (2008b). in NATO Science Series: Proc. of NATO Advanced Research Workshop: "Nuclear Risk in Central Asia", Kazakhstan, Almaty, June 20-22, 2006. Editors: B. Salbu and L. Skipperud, Published House: Springer Science +Business Media B.V. 2008, Netherlands, pp. 133-149.

Kazakov S.V., Utkin S.S., Linge I.I., Valyaev A.N. (2006) in Proc. of International Conference "Radioactivity after Nuclear Explosions and Accidents", v.3, pp. 402-407, (in Russian),December 5-6, Moscow, Publ. House: St. Peterburg, GIDROMETIZDAT.

H. Vandeenhove, I.Torgaev et. al. (2003) in Proc. ISEM 03: The 9-th Intern/ Conf. on Rdioactive Waste Management and Inviromental Remendation, September 21-25, 2003, Oxford, England, icem 03-4535.

Valyaev A.N., Kazakov S.V. et.al. (2003) in Proc. the First Intern. Conference "Earth from Space- the Most effective Solutions" (in Russian), Moscow, http://www.transparentworld.ru/conference/presentations/operative.htm valyaev_doclad.zip

Valyaev A.N., Kazakov S.V. Stepanets O.V. et. al. (2005) in Proc. the Second Intern. Conference "Earth from Space- the Most Effective Solutions" Section "Space Monitoring in Problems of Management of Territories"; Moscow, http://www.transparentworld.ru/conference/2005/thesis.pdf

T.V.Tuzova, S.A.Erokhin, et.al. (1994) Water sources, v.1, № 2, pp. 236-239.

T.V.Tuzova (2006) "Investigations of waters of the Issykkyl basin with the use of uranium isotopic method. Study of the Issyk-Kyl lake hydrodynamics with the use of isotopic methods". PartII. Institute of water problems and hydropower, NAS KR: ISTC Report.- Bishkek:Ilim, p. 132-140. ISBN 5-8355-1440-9.

Erohin S. A. (2006) «Outburst lake Petrov. In Part II. Institute of water problems and hydropower, NAS KR:ISTC Report, Bishkek:Ilim, ISBN 5-8355-1440-9, pp.132-140.

Malik L.K., Koronkevich N.I., Barabanova E.A. (1998) Moscow, VINITI, №2, pp. 67-79.

Valyaev A.N. and Yanushkevich V.A. (2003) in NATO Science Series II "Detection of Bulk Explosives: Advanced Techniques against Terrorism" (Mathematics, Physics and Chemistry), vol. 138, pp. 175 – 183, Kluwer Academic Publishers, Netherlands. Proc. of NATO Advanced Research Workshop, June 16-21, 2003 St. Petersburg, Russia.

Uranium-isotopic method using to determine sources of moraine-glacial lakes feeding and assess of its outburst danger

Alexander N. Valyaev[1], D.M. Mamatkanov[2], S.A. Erochin[2] and T.V. Tusova[2]

[1] Nuclear Safety Institute, RAS, Moscow, Russia
[2] Institute of Water Problems and Hydro Energy, NAS, Bishkek, Kyrgyz Republic

Abstract. Mountain moraine-glacial lakes are formed from atmospheric precipitates in melted snow water form, "young" ice of glacier beetling over lake (meteoric waters) and water from melted "aged" buried ice, lying in adjoining rocks of lake edges and bottom (waters, leached from rocks; Tuzova et al. 1994). Waters from first source are characterized by extremely low U content and balanced ratio of its even isotopes (C = (0,39± 0,02) ppm; γ =1,02±0,02) [2]. Waters from melted buried ice are noted for higher U content and non-equilibrium γ ratio (C range = 2,48 ± 0,08 - 28 ± 0, 2 ppm; γ range = 0,862 ± 0,007 - 1,16 ± 0,02). More role of buried ice in lake feeding is, more water in moraine-glacial lakes deflects from glacial melted water by corresponding C and γ values, which allows to determine main feeding sources. The latter testifies about lake instability state and increasing of its outburst probability. The presented method is confirmed by our inspection of five Kyrgyz lakes (Tuzova 2006): maximum C and γ deflections from the same values in meteoric waters were in Teztor-1 lake (C=23± 2 ppm; γ=0,93 ±0,01) and Atjailoo lake (C=1,69 ±0,05 ppm; γ=0,89 ±0,01). After that Teztor-1 had several outbursts; the last was in 2004. Atjailoo outburst was in 1997 and today it is in constantly growing outburst stage. Another three lakes are stable and their uranium-isotopic parameters are close to meteoric waters: for Teztor-2 lake C=1,14±0,03 ppm; γ=1,00 ±0,02; for Kashkasu and Tuuktor lakes C=1,39 ±0,05 ppm; γ=1,06 ±0,01.

References

T.V.Tuzova, S.A.Erokhin, et.al."Uranium and tritium in glacial lakes of Northern Tien-Shan. Water sources", v.1, № 2, 1994, p. 236-239.

T.V.Tuzova. "Investigations of waters of the Issykkyl basin with the use of uranium isotopic method. Study of the Issyk-Kyl lake hydrodynamics with the use of isotopic methods". PartII. Institute of water problems and hydropower, NAS KR: ISTC.- Bishkek:Ilim,2006, p. 132-140. ISBN 5-8355-1440-9

Impact of uranium mines water treatment on the uranium and radium behaviour

Charlotte Cazala[1]; Christian Andrès[2]; Jean-Louis Decossas[3]; Michel Cathelineau[4] and Chantal Peiffert[4]

[1] IRSN/DEI/SARG/BRN, BP 17, 92262 FONTENAY AUX ROSES, France
[2] AREVA/BUM ; 1 Avenue du Brugeaud, 87250 BESSINES SUR GARTEMPE, France
[3] Pe@rl, 83 rue d'Isle, 87000 LIMOGES, France
[4] CREGU, BP 23, 54501 VANDOEUVRE LES NANCY, France

Abstract Uranium has been mined in the Limousin area (France) until the end of the 90's. Nowadays mines are closed and environmental monitoring is conducted by the former operator (AREVA-NC) under the control of the French administration. In the year 2006, the French safety authority board has created a pluralist expert group (GEP) that enjoin experts, stake holders and government representatives, to improve the environment protection concerning the process of uranium mines closure and rehabilitation. A part of the work is devoted to the study of mines as radionuclides sources and to the transport of radionuclides in the environment. According to regulation, site waters must be collected, and when necessary treated, before being released into the environment. Those waters constitute the main vector of radionuclides transportation. Several previous studies revealed an accumulation of radionuclides in lake sediments downstream mines inputs. This phenomenon is illustrated on the Ritord watershed; in an artificial lake created only few kilometres downstream one of the main treated mine waters release. To identify the mechanisms of the radionuclides accumulation in sediments, the GEP has investigated, through the environmental survey database, the water treatment efficiency and the behaviour of ^{238}U and ^{226}Ra from mines to the river. It concluded that a part of particles containing ^{226}Ra produced in the water treatment station is not trapped but released to the river. The reduction of the water flow velocity where the stream enters the lake leads to the particles deposition. As a con-

sequence, the water treatment station has been modified to reduce the particle outflow. The uranium and radium content on particulate, colloidal and dissolve fractions were then investigated over a year all along the treatment process as well as downstream the water release point. Results of this specific study will be presented.

Introduction

Uranium has been mined in the Limousin area (France) until the end of the 90's. Nowadays mines are closed and restored. Rehabilitation operations were devoted to assure the stability of land and infrastructures as well as to the collection of mine's waters to keep under control the radionuclide release into watersheds. Environmental monitoring is conducted by the former operator (AREVA-NC) under the control of the French administration which defines the objectives of environmental and population protection against radiations. Concerning natural radionuclides from former uranium mining installations, the French Decree 90/222 indicates that dissolved ^{226}Ra and ^{238}U activities in water released into the environment must remain under the limits of 0.74 $Bq.l^{-1}$ and 22.4 $Bq.l^{-1}$, respectively. The waters flowing out the mines are collected and analysed to determine their ^{226}Ra and ^{238}U contents. When necessary, waters are treated before being released.

In the year 2006, the French safety authority board has created a pluralist expert group (GEP) that enjoin experts, stake holders and government representatives, to improve the environment protection concerning the process of uranium mines closure and rehabilitation. A part of its work is devoted to the study of mines as radionuclides sources and to the transport of radionuclides in the environment. The group have examined many documents dealing with the environmental monitoring and impact of former mines and focused on accumulation of radionuclides in lake sediments downstream mines inputs.

This phenomenon is illustrated on the Ritord watershed in an artificial lake created only few kilometres downstream mines. To identify the mechanisms of the radionuclides accumulation in sediments, the GEP has investigated, through the environmental survey database, the water treatment efficiency and recommended to the operator to conduct a complementary study to determine the speciation of ^{238}U and ^{226}Ra from mines to the lake. The work was conducted between October 2006 and October 2007. Results are presented conjointly with previous investigations hereafter and interpreted from the management options point of view.

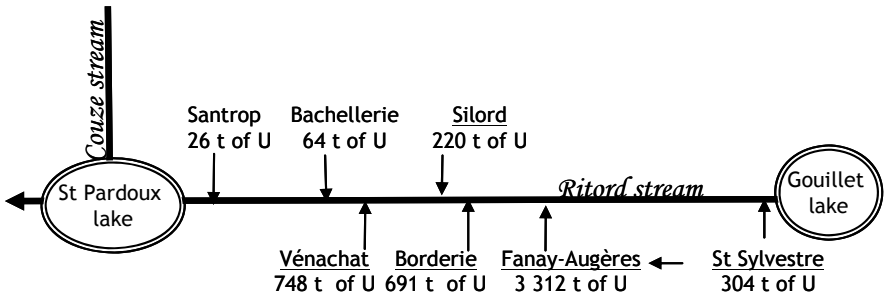

Fig.1. Production of uranium from mines in the Ritord watershed

Area

About 73 000 tons of uranium were extracted from the 200 French uranium mine sites. The Crouzille mining division (~ 300 km²) produced 24 000 tons of uranium from 24 underground and open mines. Seven watersheds compose the hydrological web of the Crouzille Division area. Among them, the Ritord basin (figure 1) was selected to illustrate the impact of mine's waters outflow. It corresponds to a small brook connecting two lakes. The upper one named "Gouillet" could be considered as not influenced by mines. Its outflow is the Ritord stream witch collects water from seven mine sites. Waters from St Sylvestre, Fanay-Augères and Silord are treated before being released into the environment due to their ^{226}Ra activity level higher than the authorized limit of 0.74 Bq.l^{-1}. Waters from Borderie and Vénachat do not require any treatment and no water flowing out the Bachellerie and Santrop sites was identified. It can be seen on figure 1 that in term of uranium production, the most important production comes from the Fanay-Augères site. The Ritord flows into the "Saint Pardoux" lake created in 1976 by the building of a dam on the river Couze flow about 1.5 km downstream the Couze/Ritord confluence.

Impact of mine's waters inflow to the Ritord

On the base of the survey operated by AREVA-NC under the control of the French administration (waters) or on itself decision (sediments), the impact of the mine's waters outflow in the Ritord brook was investigated in terms of radiological content.

Figure 2 presents, on its upper part, the dissolved ^{238}U (squares) and dissolved ^{226}Ra (lines) activities in waters from the Gouillet lake and all along the Ritord flow. On its lower part, ^{238}U, ^{226}Ra and ^{210}Pb activity levels in sediments are pre-

sented. The influence of each mine water inflow may be deduced from thecomparison of measurements conducted up and downstream the releasing point represented by dashed lines on figure 2. Waters were analysed monthly between 1990 and 2006; all data are reported except for the ones under the detection limit. The ^{238}U, ^{226}Ra and ^{210}Pb activity levels in sediments reported on figure 2 correspond to the mean values of measurements conducted near annually between 1992 and 2004.

Results on waters are analysed on the spatial and temporal dimensions. On the Gouillet lake, dissolved ^{238}U and dissolved ^{226}Ra activities fluctuate respectively around 0.01 $Bq.l^{-1}$ and 0.04 $Bq.l^{-1}$ with a more important variability for the ^{226}Ra. Downstream the St Sylvestre site, activity level increase slightly compared to the Gouillet lake. Downstream the Fanay-augères site activity levels reach the higher values measured on the Ritord stream. Then the Fanay-Augères site could be considered as the main source of radionuclides to the Ritord. This is confirmed by a mass balance along the Ritord flow which indicates that more than 90% of the ^{238}U and the ^{226}Ra entering the Saint Pardoux lake through the Ritord comes from the Fanay-Augères outflow. Influence of Silord, Borderie and Vénachat is limited compared to the Fanay-Augères one's. It can also be noted that the increase is

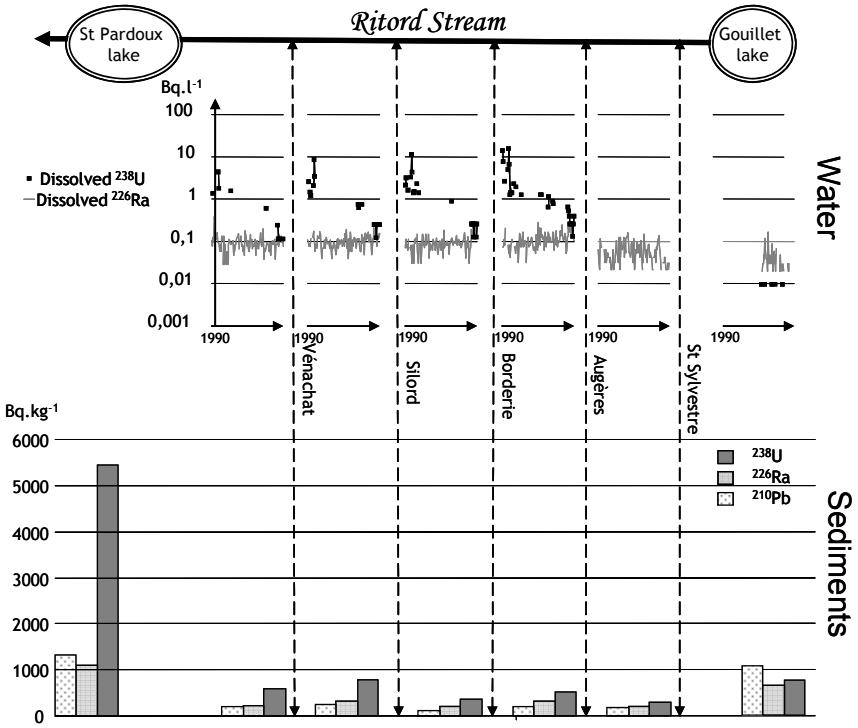

Fig.2. Influence of mine waters input on water and sediments radiological content in the Ritord stream and Saint Pardoux lake**.**

more important for the ^{238}U than for the ^{226}Ra. Considering the temporal variation higher activities correspond to the beginning of the 90's. They are contemporary with the restoration works on the Fanay-Augères site. Nowadays, dissolved ^{238}U and ^{226}Ra activity levels in the Ritord's water -downstream the Fanay-Augères water release point- are both around 0.1 $Bq.l^{-1}$ and the main influence remained linked to the uranium release.

Results on sediments show that activity level of the three radionuclides analysed is higher on lakes than on the Ritord. This could be linked to the size of sediment's grains which is bigger on rivers than on lakes. As the specific surface is inversely proportioned to the size of grain, specific activity increase when the particle size decrease. As a consequence, activity levels in sediments are higher in lakes than in rivers. Considering the two lakes, the comparison of activity levels in sediments shows an important increase up to down stream. Sediments from Saint Pardoux lake were sampled near the Ritord entrance into the lake and higher values were fund in the literature (up to 20 000 Bq.kg-1 of 238U were measured). The increase of the activity level in sediment may be linked to the input by mine waters.

The increase of activity level in water and sediments may be considered as a potential radiological hazard. Apart from this aspect, the French authority asked to AREVA-NC to work on treatments to keep ^{238}U activity level in sediments of Saint Pardoux lake under the value of 3 700 $Bq.kg^{-1}$.

Efficiency of Mine's water treatment

As more than 90% of uranium and radium come from the Fanay-Augères treatment station, the study focus on it. The actual regulation impose to AREVA-NC to keep dissolved ^{238}U and dissolved ^{226}Ra activity in water flowing out the station respectively under 22.4 $Bq.l^{-1}$ and 0.37 $Bq.l^{-1}$. Then chemical treatment applied by AREVA-NC focus on dissolved ^{226}Ra which is transformed as insoluble specie by $BaSO_4$ precipitation before to settle in retention basins.

Figure 3 shows the Fanay-Augères mine's water treatment efficiency between 1993 and 2006. The first graph presents the activity level of dissolved ^{226}Ra in water entering and exiting the water treatment station. The difference between the two corresponds to the efficiency of the transfer of dissolved ^{226}Ra on the particular form. The main yield over the duration of the study reaches 90%. Then the treatment seems very efficient. Nevertheless, the comparison between total ^{226}Ra entering and exiting the station shows that the total yield is 70%. That means a part of particles produced in the station does not settle in the basin and escape. They are released into the Ritord and may settle when they reach the lake. The last graph on the figure 3 presents activity levels of dissolved ^{238}U entering and exiting the treatment station. It shows that the chemical treatment applied is not efficient for uranium. In fact, as the dissolved ^{238}U activity level in water entering the station is under the legal limit of 22.4 $Bq.l^{-1}$ (annual mean), no treatment is deployed for uranium.

Nevertheless, as the objective is to reduce the ^{238}U activity level in sediments, developments were conducted to increase the settling in the basin and to remove uranium from water.

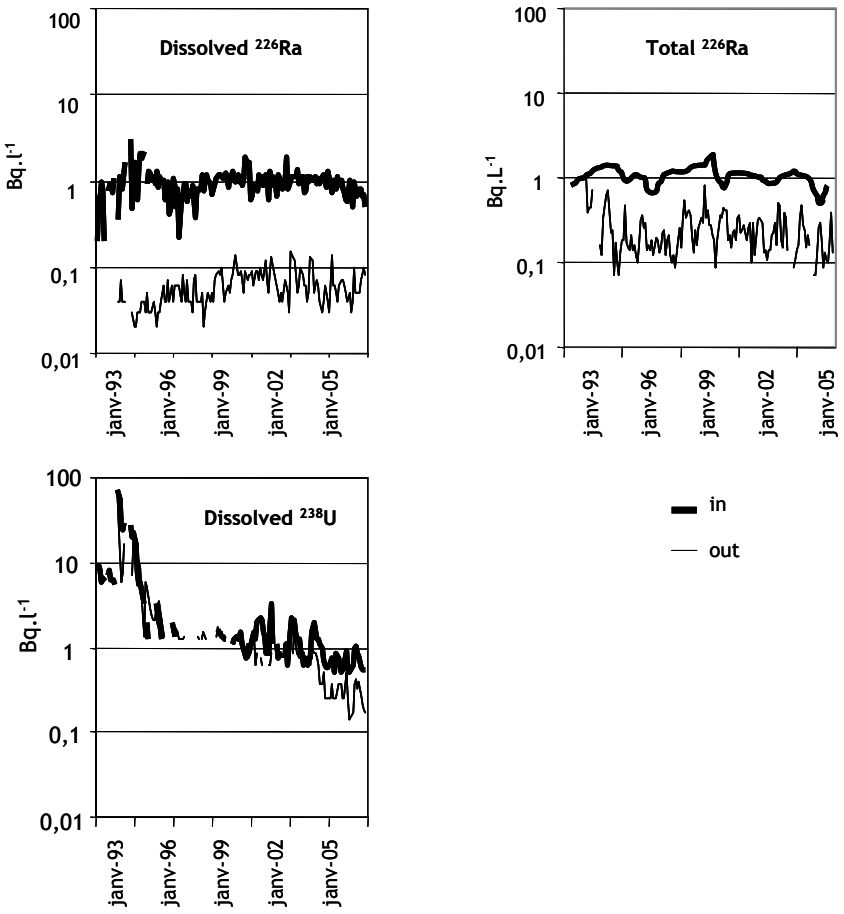

Fig.3. Fanay-Augères mine's water treatment efficiency

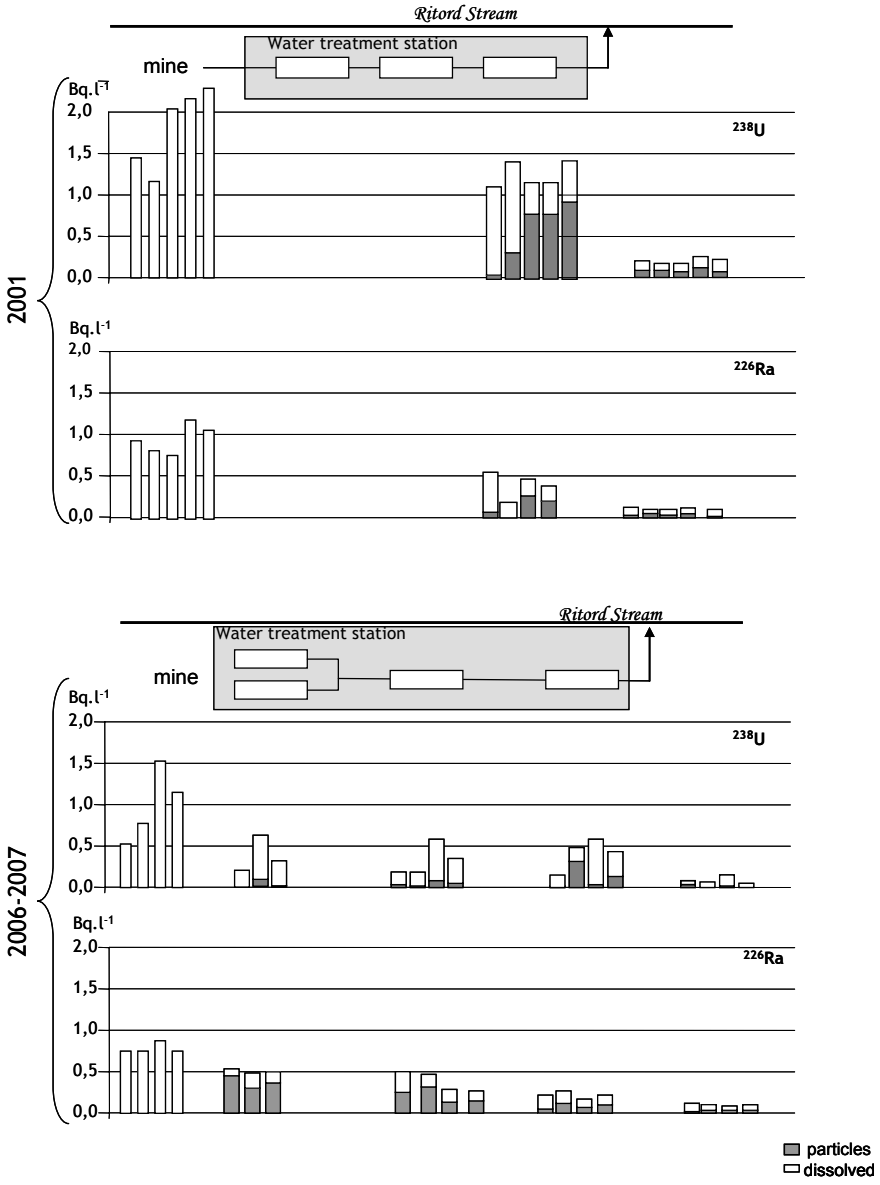

Fig.4. Distribution of ^{238}U and ^{226}Ra in water from mines and in the different water treatment steps before and after changes in the water treatment station.

Efficiency of developments in the Fanay-Augères water treatment station

Developments proposed by AREVA-NC consist in building a new settling basin, using new chemical agents, and optimising the flow in the station to increase the residence time in the station. Waters flowing out the mines are collected in a basin (not represented on figure 4) and convoyed to the treatment line where chemical agents are added in the flow. Then waters pass through four basins before being released in to the Ritord flow. Basins 1 and 2 work in parallel on waters exiting the chemical treatment line. Waters exiting theses basins are directed to basins 3 and 4 in series. The efficiency of developments was assessed through the measurement of ^{226}Ra and ^{238}U in dissolved and particulate fraction in waters entering the station, all along the treatment (basin 1+2; basin 3 and basin 4) and downstream the release point in the Ritord. Results are presented in figure 4 with ones of a similar previous study conducted in 2001. At this time waters flowing out the chemical treatment line flowed through three basins in series. Waters from mines, from the last basin and from the Ritord downstream the release point were analysed in 2001. Results are presented on figure 4.

Results show a strong decreasing of uranium in water from mines over time. This trend is weaker for the ^{226}Ra. Activities of ^{226}Ra measured on the basin 4 during the year 2007 are lower than ones obtained on basin 3 during the year 2001. That attests the improvement of the water treatment yield on the ^{226}Ra. Indeed, in water from mines ^{226}Ra is on the soluble form. As mentioned above, the chemical treatment produces particles able to catch the radium. It appears that changes on the flow in the basins are efficient to increase the settling of particles. Most of them are retained in basins 1 and 2, but some settled in basins 3 and 4. On the opposite, a small proportion of uranium is trapped during the treatment and most of uranium remained on a soluble form when it reaches the Ritord flow.

Between 2001 and 2007, the concentration in uranium is divided by 3.2 in exit of treatment. It reverberates by a content of uranium divided by 2.4 in the Ritord flow. For radium, the concentration also decrease and are divided by 2 in water at the exit of basin of treatment and by 1.2 in the Ritord. The water samples of Ritord downstream Augères effluents have intermediate characteristics between two poles: The diluting pole: water of refill (rainwater having more or less interacted with the granitic substratum, and the typical pole of water of mine which is characterized by contents relatively rich in Ca, Mg, U, SO_4 and Ba (Ba is an agent of treatment of the mining effluents). The proportion of the pole "mining water" in waters of Ritord remains weak and decreases in a significant way since 2001.

Conclusion

Dissolved ^{238}U and dissolved ^{226}Ra activities in natural waters of the Limousin region (France), vary respectively around 0.01 $Bq.l^{-1}$ and 0.04 $Bq.l^{-1}$. Corresponding activities in waters flowing out former mines are around 1 $Bq.l^{-1}$. As these waters

may, locally, constitute the main contribution of the flow, the radiological impact on the environment is monitored. In order to satisfy the French regulation chemical treatments are applied by the operator to limit the release of radionuclides.

That work indicates that activity levels in the environment depend on the flux released but also on the environment collecting and convoying flux. It shows the importance of lakes which presents the capability to trap radionuclides within their sediments. To limit the accumulation of "radioactives particles" in lakes, the functioning of the water treatment station was optimized. From the general point of view, the quality of the natural water of the Ritord increase. It results not only from changes operated in the station but also from the decrease of ^{238}U content in water flowing out the mines. Results of the monitoring of the Saint Pardoux Lake do not show a significant improvement in the radiological characteristics of the sediments, what demonstrates the efficiency limit of the chemical treatment.


Uranium Mining
and Hydrogeology

Changes of radium concentration in discharge waters from coal mines in Poland as a result of mitigation

Stanislaw Chałupnik and Małgorzata Wysocka

Laboratory of Radiometry, CENTRAL MINING INSTITUTE, 40-166 Katowice, Pl. Gwarkow 1, POLAND, s.chalupnik.@gig.katowice.pl

Abstract. Saline waters from underground coal mines in Poland often contain natural radioactive isotopes, mainly ^{226}Ra from the uranium decay series and ^{228}Ra from the thorium series. More than 70% of the total amount of radium remains underground as radioactive deposits due to spontaneous co-precipitation or water treatment technologies, but several tens of MBq of ^{226}Ra and even higher activity of ^{228}Ra are released daily into the rivers along with the other mine effluents from all Polish coal mines. Different technical measures such as inducing the precipitation of radium in gobs, decreasing the amount of meteoric inflow water into underground workings etc., have been undertaken in several coal mines, and as a result of these measures the total amount of radium released to the surface waters has diminished significantly during the last 15 years.Mine waters can have a severe impact on the natural environment, mainly due to its salinity. Additionally high levels of radium concentration in river waters, bottom sediments and vegetation were also observed. Sometimes radium concentrations in rivers exceeded 0.7 kBq/m^3, which was the permitted level for waste waters under Polish law. The investigations described here were carried out for all coal mines and on this basis the total radium balance in effluents has been calculated several times within last 20 years. Measurements in the vicinity of mine settling ponds and in rivers have given us an opportunity to study radium behaviour in river waters and to assess the degree of contamination.

Introduction

Very often human activity, connected with the exploitation of mineral resources, leads to the contamination of the natural environment. Sometimes natural radionuclides are released or concentrated as waste material. In Poland the main source of waste and by-products with enhanced concentration of natural radionuclides is power industry, based on the coal exploitation and combustion. In hard coal mining industry 50 million tons of different waste materials are produced annually. As a result of coal combustion in power plants, the area of fly ash and sludge piles is increased by several km^2 per year (Michalik et al., 1995).

Upper Silesian Coal Basin (USCB) is located in the Southern-West part of Poland. Presently there are 35 underground coal mines there extracting approximately 100 mln tons of coal per year. The depth of mine workings is from 350 to 1050 m. Upper Silesia is characterized by a very complicated and differentiated geological structure with numerous faults and other tectonic dislocations. Additionally, the area is very affected by mining

Two hydrological regions of the Coal Basin have been distinguished. First region is located in southern and western Silesia with thick strata of sediments covering carboniferous formation. This overlay is built mainly by Miocene clays and silts. The thickness of this rocks is up to 700 m. Such strata make almost impossible migration of water an gases. In the second region Miocene clays do not occur. Carboniferous strata are covered by and Quaternary sediments, slightly compacted.

The oldest formations of this area form isolated sediments of Permian or Triassic limestone strongly fissured. There are numerous outcrops of coal seams. These formations enable very easy migration of water and gases.

An additional and unexpected component of the radioactive contamination of the natural environment, and different from that usually associated with this kind of industry, is caused by underground coal exploitation. In many of coal mines, located in Upper Silesian Coal Basin waters with enhanced radium content occur (Lebecka et al., 1986). Sometimes in radium-bearing brines barium ions are also present, in concentrations up to 2 g/l. Such waters were classified as radium-bearing type A waters. On the other hand, in the second kind of waters, which have been called type B, no barium can be found but radium and sulphate ions are present.

In the area of Upper Silesian Coal Basin (USCB) operate of about 35 underground coal mines. The total water outflow from these mines is about 750 000 m^3/day. The salinity of these brines is far higher than that of ocean water. The total amount of salt (total dissolved solids - TDS) carried with mine waters to the rivers is about 10 000 tonnes/day. The commonest ions in these brines are Cl^- and Na^+ with concentrations up to 70 g/l and 40 g/l respectively, additionally brines usually contain several grams per litre of Ca^{2+} and Mg^{2+} and significant amounts of other ions (Tomza & Lebecka, 1981). Waters with high radium concentration occur mainly in the southern and central part of the coal basin, where coal seams are overlaid by a thick layer of impermeable clays (Rozkowski & Wilk, 1992).

These saline waters cause severe damage to the natural environment, owing mainly to their high salinity (sometimes > 200 g/l), but also their high radium concentration, reaching 390 kBq/m^3 (Skubacz et al., 1990).

The presence of barium in waters is the most important factor for the further behaviour of radium isotopes in mine galleries or on the surface. From type A waters radium and barium always co-precipitate as sulphates, when such waters are mixed with any water containing sulphate ions. As a result of the precipitation, barium sulphate deposits with highly enhanced radium concentrations are formed (Lebecka et al., 1986, Michalik et al., 1999). The total activity of radium isotopes in these sediments may sometimes reach 400 kBq/kg. In comparison, average radium content in soil is 25 Bq/kg (UNSCEAR, 1982). In case of radium-bearing type B waters, no precipitation occurs due to the lack of the barium carrier, and that is why the increase of radium content in sediments is much lower that ones originated from type A waters.

Applied methods and instrumentation

Radioactivity of waters from coal mines is mostly from radium isotopes - ^{226}Ra from the uranium series and ^{228}Ra from the thorium. A method of chemical separation of radium, developed by Goldin (Goldin, 1961), has been modified for liquid scintillation counting (Chalupnik & Lebecka, 1990; Chalupnik & Lebecka, 1993). Radium is co-precipitated with barium in form of sulphates and this precipitate is mixed with liquid gelling scintillator. The prepared samples were measured by a low background liquid scintillation spectrometer (QUANTULUS, PerkinElmer). This counter is equipped in alpha/beta separation and anti-coincidence shield, which enables measurements of ^{226}Ra concentration above 3 Bq/m^3 with simultaneous measurements of ^{228}Ra (LLD = 30 Bq/m^3) and ^{224}Ra (LLD = 50 Bq/m^3). In addition, the procedure enables the simultaneous preparation of ^{210}Pb, which can separated from radium isotopes at the last stage of analysis and also measured in the LS spectrometer with a detection limit of 20 Bq/m^3.

System of monitoring in the vicinity of coal mines

In the mining industry in Poland, monitoring of the radioactivity of mine waters, precipitates as well as gamma doses was obligatory since 1989 till 2003.

Monitoring of radioactive contamination caused by effluents and tailings from coal mines must be done since 1986 (Guidelines, 1986). Due to these regulations the following measurements must be done in mine's vicinity:

I. The concentration of ^{226}Ra and ^{228}Ra in effluent from the settlement pond, in river above and below the discharge point, in water supplies nearby discharge point.

II. The concentrations of natural radionuclides in solid samples, dumped onto the piles.

Such complex monitoring system gives an opportunity to obtain a complete picture of the influence of a certain mine on the underground and surface employees as well as on inhabitants of adjoining areas.

Concentration of radium isotopes in original water samples from different coal mines varies in a very wide range - from 0 to 110 kBq/m^3 for ^{226}Ra and from 0 to 70 kBq/m^3 for ^{228}Ra (Report, 2004). In 80's waters with radium concentration above 1.0 kBq/m^3 were found in 43 out of 65 coal mines in Upper Silesian Coal Basin. The highest concentrations of radium were measured in highly mineralised waters from deeper levels in radium-bearing waters type A. The ratio of ^{226}Ra to ^{228}Ra in radium-bearing waters type A was in average of about 2:1. Contrary in radium-bearing waters type B there were more ^{228}Ra than ^{226}Ra, the ratio ^{226}Ra: ^{228}Ra was from 1:2 up to 1:3. Concentration of ^{226}Ra in these waters reached 20 kBq/m^3, while maximum concentration of ^{228}Ra was as high as 32 kBq/m^3. These values justify the statement that Upper Silesian radium-bearing waters belong to the waters with highest known radium concentration.

Original waters flowing into mine workings from the rocks from different aquifers are collected in gutters in underground galleries, brought together from different parts of the mine, clarified and pumped out to the surface. Radium concentration in these mixed waters was lower than in original water and did not exceed 25 kBq/m^3 of ^{226}Ra and 14 kBq/m^3 of ^{228}Ra (Report, 2004).

Basing on the results of measurements of radium concentration in the original waters inflows into the mine workings and on data on the flow rates of water provided by the mine hydrologists, the total activities of both radioisotopes of radium flowing with water to different parts of mines and to different mines were calculated. This results were compared with values obtained using radium concentrations in mixed waters taken from the drainage system (from gutters) from different parts of mines and corresponding flow rates obtained from the mines. The difference is indicating the activity of radium remaining in underground mine workings due to spontaneous precipitation of radium and barium sulphates or due to applied purification of water. The calculated activity of radium remaining in underground mine workings as deposits in all Upper Silesian coal mines is 580 MBq/day of ^{226}Ra and 530 MBq/day of ^{228}Ra. These values can not be considered as very accurate, since the uncertainty of measurements of flow rates of small inflows is rather large. The approximate amount of ^{226}Ra in **water inflows in coal mines** in USCB have been calculated as high as 650 MBq/day (i.e. 230 GBq per year) while for ^{228}Ra this value is of about 700 MBq/day or 255 GBq per year. Although radium concentrations in waters type B were usually lower than in waters type A the total inflows to mines where radium-bearing waters type B occur were much higher. As a result the total activity of radium carried with water type B was higher. The highest values for a single mine (with waters type B) were: 78 MBq per day of ^{226}Ra and 145 MBq per day of ^{228}Ra.

In comparison corresponding values of inflows of radium with saline waters in 4 copper mines in Poland were: 31 MBq of ^{226}Ra and 3 MBq of ^{228}Ra per day.

Assessment of radium balance in discharge waters

One of the biggest advantages of the monitoring system in Upper Silesia region is a possibility to make an assessment of radium balance in discharge waters periodically. For instance in years 1987, 1995, 2003 and 2006 such assessments have been prepared. For the calculations of about 300 results of mine waters have been taken as well as 40 analyses of river waters have been done. The term „mine waters" means not only mine waters but also river waters close to the discharge points. Term "river waters" is used for the samples taken at the sampling points of regional monitoring system of water quality. All the data are included in the mine waters database in the Laboratory of Radiometry as the element of the radiation hazard monitoring and environmental monitoring. A comparison of assessment results in chosen periods is shown in table 1.

The assessment of the total activity of radium released from coal mines in Upper Silesia with waste water is based on:

- results of determination of radium isotopes in waters released by collieries;
- data on amount of water released by individual mines.

We have also made an estimation of total activity of radium which remains in underground workings in a form of deposit precipitated out of radium-bearing waters either due to unintended mixing of natural waters of different chemical composition or due to the purification of radium-bearing waters. This estimation has been done basing on:

- results of determination of radium isotopes in original waters inflowing to the underground mine workings from the rocks;
- rough estimation of the amounts of water inflows from different sources or parts of mines;
- calculated value of the total activity of radium pumped out from underground mine workings with waste waters by individual mines.

Much more accurate were the results of calculations of the total activities of radium present in water pumped out from individual mines. These values were calculated basing on the radium concentration determined in these waters and on data of amount of water provided by mines.

Samples of discharged waters were taken from settling ponds. In outflows from thses ponds in 87 % mines ^{226}Ra concentration exceeds 0.008 kBq/m^3, in 25% ^{226}Ra concentration is higher than 0.1 kBq/m^3 and in 8 % exceeded permissible level - i.e. 0.7 kBq/m^3 (Decree, 1989).

In rivers enhanced concentrations of radium can be observed many kilometres down from the discharge points. This is mainly true for radium-bearing waters type B, because out of these waters radium is not easily precipitated. The highest value of ^{226}Ra concentration was as high as 1.3 kBq/m^3 - it was found in a small stream near it's conjunction with Vistula river.

Table 1. Comparison of radium balance assessment in rivers from Upper Silesia region

Catchment area	Total activity **1995** [MBq/day]		Total activity **2003** [MBq/day]		Total activity **2006** [MBq/day]	
	^{226}Ra	^{228}Ra	^{226}Ra	^{228}Ra	^{226}Ra	^{228}Ra
Inflows into "OLZA" pipeline from 11 mines	9.8	6.7	6.8	6.8	6.5	6.5
Olza River – discharge of „Olza" pipeline	1.6	1.4	2.5	1.8	2.3	1.6
Ruda-Nacyna Rivers (3 mines)	2.2	1.4	0.7	0.7	1.2	1.1
Bierawka River (5 mines)	1.6	1.2	2.7	3.2	1.8	1.4
Bytomka River (5 mines)	0.4	0.5	1.5	3.0	1.2	1.9
Kłodnica River (7 mines)	2.6	2.9	2.6	3.7	2.8	2.9
Rawa River (4 mines)	0.2	0.2	1.2	2.7	0.6	2.1
Brynica River (4 mines	0.7	0.7	1.4	2.4	1.2	1.8
Przemsza River (2 mines)	0.4	0.4	2.3	5.6	1.2	2.4
Bobrek River (3 mines)	0.2	0.2	0.3	1.2	0.8	1.5
Black Przemsza River (4 mines)	1.6	3.1	1.3	2.3	1.5	2.8
Gostynka River (3 mines)	133.9	248.1	61.1	147.6	52.4	128.5
Mleczna River (2 mines)	1.3	2.4	1.5	3.3	1.5	3.3
Upper-Vistula (4 mines)	73.0	117.2	42.9	84.2	8.9	19.8
Total: 35 active mines 30 abandoned	219.1	380.1	120.1	258.2	77.4	169.5

The significant decrease of daily discharge of radium was observed in the period 1987 -1995. Very first assessment of radium ^{226}Ra in mine affluents has been done in 1987, giving the value of the daily release at level 400 MBq. At that time no results of ^{228}Ra measurements were available. Results of another assessment, prepared in 1995 showed a significant decrease of radium activity in mine waters, released into natural environment, roughly by factor 2. There were two reason of this effect. Firstly, the purification of A type mine waters has been started in sev-

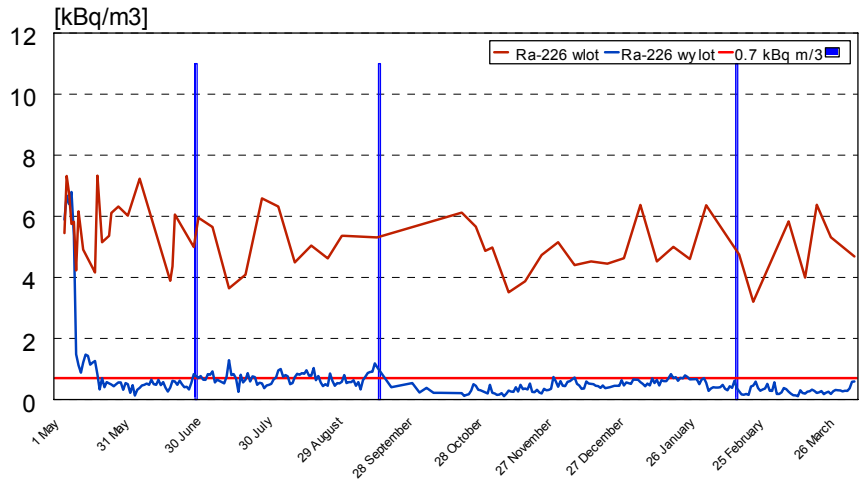

Fig.1. Results of water treatment in Piast Mine in years 1999-2000.

eral coal mines in catchment areas of Olza river and Upper Vistula. The another reason was due to economical changes in the mining industry – dewatering of deep mines was more and more expensive and hydro-technical solutions have been applied in numerous mines to reduce water inflows into underground galleries, with special emphasis on brines.

In the last decade the decrease of radium activity in discharge waters is mainly due to the purification of B type brines in Piast Colliery (started in 1999) and construction of another treatment station in the year 2006 in Ziemowit Mine. In Piast Mine the implementation of the treatment technology on deeper of the horizons in the mine caused the decrease of radium release from the mine at level 150 MBq/day – 60 MBq/day of ^{226}Ra and 90 MBq/day of ^{228}Ra. Additionally, purification system for second horizon of Piast mine is under designing, and it will solve most of the problems with radium contamination of river waters in Upper Silesia region.

The process of water treatment is based on the dissolutionof barium chloride and immediate co-precipitation of barium and radium ions sulphates. This reaction is possible due to the surplus of sulphate ions in brines (30-50 times more than required for steichiometric reaction). This reaction is shown below:

$$BaCl_2 \rightarrow Ba^{2+} + 2Cl^- \text{ (dissolution of barium chloride)}$$

$$Ba^{2+} + Ra^{2+} + 2SO_4^{2-} \rightarrow BaRa(SO_4)_2 \text{ (co-precititation)}$$

$$Ba^{2+} + SO_4^{2-} \rightarrow BaSO_4\downarrow$$

The solubility of barium sulphate is roughly 0.002 g/l, and presence of sulphate ions in the water makes the dissolution of barium sulphate impossible. Moreover,

the solubility of radium sulphate is two orders of magnit ude lower, therefore sediments are stable, and no back leaching is predicted.

In 90's enhanced radium concentrations were mainly observed in the Vistula river, into which most of the radium is discharged with B type waters - approximately 200 MBq of ^{226}Ra and 350 MBq of ^{228}Ra per day. Concentration of ^{226}Ra (0.035 kBq/m^3) was observed in Vistula in Cracow - 70 km downstream from Upper Silesia. Some of these waters were not discharged directly to Vistula river, but to it's tributaries. The influences of singular inflows were very clearly. Moreover, waters from first mine were A type and the difference of radium behaviour (fast precipitation) in comparison with other 3 mines (waters B type) was very evident. Different situation was observed in the vicinity of Oder river, where in coal mines occur mainly waters type A. The amount of radium discharged into this river was much lower - 20 MBq per day of ^{226}Ra and 25 MBg/day of ^{228}Ra. As a result concentrations of radium in Oder *were below 0.01 kBq/m^3*.

At the beginning of new century a treatment of mine waters (type B – without barium) has been started in underground galleries of Piast mine (1999). The total activity of radium isotopes in discharge waters decreased significantly, but still concentrations of radium isotopes in some rivers in Upper Silesia were clearly enhanced as compared with natural levels. In comparison with data from other locations, concentrations of radium isotopes in rivers in USCB are significantly higher. Enhanced concentrations of radium in river waters in Upper Silesia are caused solely by the influence of mine waters.

One of the collieries, releasing radium isotopes into surface settling pond and finally into Vistula River was Ziemowit Mine. In this mine saline brines are very common, and the total inflow into mine galleries exceeds 20 m^3/min. Radium concentration in these brines is as high as 12 kBq/m^3 for ^{226}Ra and 20 kBq/m^3 for ^{228}Ra. Due to the lack of barium in brines (type B waters) from Ziemowit Mine the spontaneous coprecipitation of radium was negligible and only small part of radium remained underground as a result of adsorption on bottom sediments in underground water galleries. Therefore Ziemowit Colliery was the main source of the contamination of small brook, called Potok Golawiecki, a tributary of Vistula River and Vistula itself. In 2003 almost 50% of total activity released from all mines in USCB was dumped into surface waters from Ziemowit. Of about 60 MBq of ^{226}Ra and 100 MBq of ^{228}Ra was released daily, despite the fact, that concentrations of radium isotopes in effluents from Ziemowit Mine weren't very high, reaching 1.3 kBq/m^3 in case of ^{226}Ra and for ^{228}Ra - 2.5 kBq/m^3.

The ecological effect of the purification is the most important issue. At the outflow from the purification system, at the level -650m the removal efficiency is above 95%. On the surface the efficiency is lower, due to mixing with untreated waters from level -500m, But at the inflow of saline waters into the settling pond, as well as at the outflow from that pond, concentrations of radium isotopes are approximately 80-85% lower than before purification. It corresponds to the decrease of about 40 MBq for ^{226}Ra and 60 MBq for isotope ^{228}Ra of daily release from the Ziemowit Mine. It means, that the total amount of radium, discharged into the Potok Golawiecki and Vistula rivers is much lower, by a value 100 MBq/day (see fig.2.).

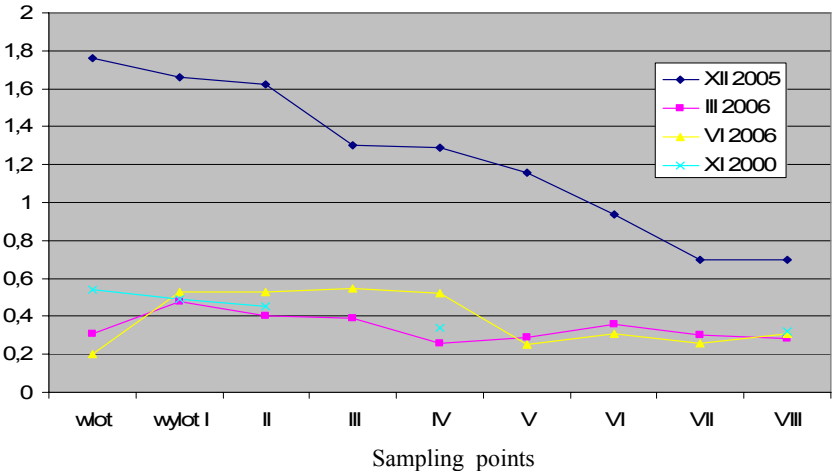

Fig. 2. Changes of radium concentration (kBq/m^3) in Potok Golawiecki as a result of water treatment in Ziemowit Mine.

Due to release of radium-bearing mine waters from coal mines there is a contamination of river waters. As a result radium concentration in some small rivers exceeds permissible level for radioactive wastes. Therefore development and application of purification methods is justified and further efforts should be done to reduce the contamination of rivers, particularly of Vistula River and it's tributaries.

On the other hand we must take into account, the exploitation of deeper coal seams will cause more problems with inflows of radium-bearing brines into underground workings, even in these mines where no radium problems exist right now. Therefore periodical monitoring of discharge waters is necessary. Another legal problem must be also solved - responsibility for monitoring of waters, released from abandoned mines

Summary

- Coal mining may cause significant pollution of the natural environment due to release of waste waters with enhanced concentrations of natural radionuclides (mainly radium isotopes. This phenomenon is well known not only in Upper Silesian Coal Basin but also in other regions of underground exploitation of coal (Ruhr Basin), oil and gas or other resources.
- Due to mitigation measures, undertaken by mines, the significant improvement can be observed during last two decades. In most cases radium concentrations in discharge waters are low and surface waters are not contaminated. Moreover,

further decrease of radium release is predicted as a result of underground mine water purification in two collieries.

- Monitoring system of natural radionuclides in waste waters and river waters is an important element of the prevention against the pollution of the natural environment. Moreover, it is a source of data for optimization of ground reclamation of previously contaminated areas (mainly settling ponds) of abandoned coal mines.

Of course, further improvement of the system is required as well as solution of important legal problems, related with liquidation of coal mines, harmonization with EU regulations etc.

References

Zgadzaj J., Skubacz K., Chałupnik S.: The influence of radon and it's progeny emitted from the exhaust shafts of coal mines on the contamination of the outdoor air. International Conference "Technologically enhanced natural radiation caused by non-uranium mining", Katowice, Główny Instytut Górnictwa 1996.

Lebecka J., i inni: Monitoring of Radiation Exposure from Different Natural Sources in Polish Coal Mines. International Conference on Occupational Safety in Mining, Vol.2, Toronto, Canadian Nuclear Association 1985.

Skubacz K., Lebecka J., Chałupnik S., Wysocka M.: Possible changes in radiation background of the natural environment caused by coal mines activity. International Symposium on Nuclear Techniques in Exploration and Exploitation of Energy and Mineral Resources, IAEA-SM-308, Vienna, IAEA 1990.

KOSTER H.W., MARWITZ P.A., BERGER G.W., VAN WEERS A.W., HAGEL P.: ^{210}Po, ^{210}Pb, ^{226}Ra in Aquatic Ecosystems and Polders, Anthropogenic Sources, Distribution and Enhanced Radiation Doses in the Netherlands. The Natural Radiation Environment, Nuclear Technology Publishing, Vol. 45, No. 1-4, 1992.

KHADEMI A., ALEMI A.,A., NASSERI A.: Transfer of radium of soil to plants in an area of high natural radioactivity in Ramsar, Iran. Conference on Natural Radiation Environment III, US DOE Report CONF-780422, Bethseda, Maryland, 1980.

Rajaretnam G., Spitz, H.B.: Effect of Leachability on Environmental Risk Assessment for Naturally Occurring Radioactivity Materials in Petroleum Oil Fields. Health Physics, vol. 78 (2), 2000.

PEIC T., i inni: Formation waters from oil and natural gas production: potential polluting source by Radium-226. International Symposium on the Natural Radiation Environment (NRE-VI), w: Environment International, vol. 22, supl. 1, Pergamon Press 1996.

GUCAŁO L.K.: Characteristics of radium distribution in underground waters of Dnieprowsko-Donieckoj Basin. Gieochimja, vol. 12, 1964.

DICKSON B. L.: Evaluation of the Radioactive Anomalies Using Radium Isotopes in Groundwaters. Journal of Geochemical Exploration, Vol. 19, 1966.

Gans I., i inni: Radium in waste water from coal mines and other sources in FRG. Second Symposium on Natural Radiation Environment, Bombay, India, Bethseda, DOE Symposium Series 1981.

Paschoa A.S., Nobrega A.W.: Non-nuclear mining with radiological implications in Araxa. International Conference On Radiation Hazards in Mining, Golden, Colorado, American Institute of Mining, Metallurgical, and Petroleum Engineers Inc., 1981.

Rogoż M., Posyłek E.: Górnicze i geologiczne metody ograniczania zrzutów słonych wód z kopalń węgla kamiennego (Geological and technical methods of brines release limitation from coal mines). „Kierunki zagospodarowania zasolonych wód z kopalń węgla kamiennego", Główny Instytut Górnictwa, Katowice 1991 (in Polish).

LEBECKA J., i inni: Influence of Mining Activity on Distribution of Radium in the Natural Environment. 4th Working Meeting Isotopes in Nature, Leipzig, Academy of Sciences of the GDR 1987.

LEBECKA J., SKUBACZ K., CHAŁUPNIK S., WYSOCKA M.: Skażenia promieniotwórcze środowiska naturalnego na Górnym Śląsku powodowane przez wody kopalniane i promieniotwórcze osady (Radioactive pollution of the natural environment in Upper Silesia, caused by mine waters and sediments).- Wiadomości Górnicze, no. 6, Katowice 1991 (in Polish).

LEBECKA J., CHAŁUPNIK S., WYSOCKA M.: Radioactivity of Mine Waters in Upper Silesian Coal Basin, and its Influence on Natural Environment. 5th International Mine Water Congress, Nottingham, International Mine Water Association 1994.

LEBECKA J., CHAŁUPNIK S., ŚLIWKA M.: Wyniki badań zachowania się radu podczas transportu słonych wód rurociągami (na przykładzie kolektora wód słonych OLZA). (Results of investigations of radium behaviour in pipelines on example of OLZA pipeline) Wiadomości Górnicze 5/92, Katowice 1992 (in Polish).

Tomza I., Lebecka J.: Radium-bearing waters in coal mines: occurrence, methods of measurements and radiation hazard. International Conference On Radiation Hazards in Mining, Golden, Colorado, American Institute of Mining, Metallurgical, and Petroleum Engineers Inc., 1981.

Ministerstwo Górnictwa i Energetyki: Wytyczne kontroli skażeń promieniotwórczych środowiska naturalnego powodowanych przez kopalnie węgla kamiennego (Guidelines for the monitoring of radioactive contamination of the natural environment, caused by coal mines – Ministry of Mining and Energy). MGiE Katowice 1986 (in Polish).

CHAŁUPNIK S., WYSOCKA M.: Removal of radium from mine waters – the experience from the coal mine. 7th International Mine Water Association Congress, 2000, ed. Silesian University.


Uranium Mining
and Hydrogeology

Radium transfer from solid into liquid phase – a theoretical approach to its behaviour in aquifers

Stanislaw Chalupnik

Laboratory of Radiometry, CENTRAL MINING INSTITUTE, 40-166 Katowice, Pl. Gwarkow 1, POLAND, s.chalupnik.@gig.katowice.pl

Abstract. In the paper, a theoretical approach to the problem of radium presence in mineralized mine water, is presented. Two main types of radium-bearing waters have been found in Polish coal mines. In type A waters, radium isotopes are present together with barium, while concentrations of sulphate ions are very low. Additionally, in these waters a ratio of ^{226}Ra:^{228}Ra activity is usually higher than 1. In type B waters, no barium can be fund, but radium together with sulphate ions. Contrary, in such waters the isotopic ratio of radium ^{226}Ra:^{228}Ra is below 1, and activities of both isotopes of radium are lower as in type A waters. No other differences in chemical composition of mine waters have been observed. Analysis shows, that the activity ratio of radium isotopes is related to the dynamics of radium adsorption on the grains of solid phase in the aquifer. During analysis must be taken into account, that the radium build up in formation water due to recoil effect, is stable in time. Additionally, no correlation with elevated concentrations of uranium and thorium in rocks, have been observed. Therefore the enhanced radium content in formation waters must be caused by its mineralization. The relatively short half life of ^{228}Ra (6 years) shows, that the process of radium transfer from solid into liquid phase is a short term process for geological scale. Therefore radium content in mine waters must be related to the concentration of natural radionuclides in the close vicinity of the aquifer or the water reservoir.

Introduction

Enhanced levels of gamma radiation were discovered in Polish coal mines during the early 1960's by Saldan (1965) who concluded that this resulted from uranium mineralisation. More detailed investigations were initiated by Tomza & Lebecka (1981), and subsequently undertaken on a regular basis by the Laboratory of Radiometry in the Central Mining Institute, Katowice, Poland. Investigations are focused on the enhanced concentrations of radium isotopes in brines and in precipitates from radium-bearing waters. The results of the investigations show, that scales of barium and radium sulphates had been mis-identified as uranium mineralisation by Saldan(1965). No elevated concentration of either uranium or thorium have been found in coal seams or the Carboniferous host rocks (Michalik et al., 1986; Wysocka and Skowronek, 1990) or in the brines (Pluta, 1988).

Similar phenomena in underground non-uranium mines in other countries have been described by other scientists. For instance in the Ruhr Basin, enhanced radium concentrations in brines were reported by Gans et. al. (1981). Other investigators reported only the presence of barium in mine waters from coal mines, for instance Younger in the UK (1994) or Martel and co-workers in Canada (2001). Reports of inflows of saline waters with elevated barium concentration came from a diamond mine in Russia (Kipko et al., 1994). Based upon our experience (e.g. Lebecka et al., 1991) the presence of barium in mine water is likely to be correlated with enhanced radium concentration. High radium concentrations in formation waters from oil fields is widely, reported by scientists from USA, Romania, Ukraine or Norway (Tanner, 1964, Peic et al., 1995, Gucalo, 1964, Sidhu, 2002). All these reports confirm the thesis, that the phenomenon of radium presence in brines is rather common, especially in confined aquifers, isolated from the influence of meteoric waters by impermeable layers, like clays or other deposits with low porosity (Tomza & Lebecka, 1981, Klessa, 2001) or even a thick permafrost layer.

In Polish coal mines two types of radium-bearing brines have been distinguished (Lebecka et. al., 1994). The first type, called type A radium-bearing waters, contain radium and barium ions, but no sulphates. Type B waters, contain radium and sulphate ions but no barium. The presence of barium in brines is a very important factor controlling the behaviour of radium, because barium acts as a carrier. Therefore radium can be easily co-precipitated on barium from type A waters as scales of barium/radium sulphate. This chemical reaction leads to the formation of highly radioactive deposits in underground galleries and surface settling ponds and rivers. In type B brines no carrier for radium exist and the main processes, leading to the decrease of the concentration of radium isotopes are adsorption on bottom sediments in settling ponds and rivers and dilution. Radioactivity of sediments in the vicinity of mines, discharging B type radium-bearing waters into environment, is not very high but often clearly enhanced.

The results, show little differences in the dissolved solids fractions of the two brines. The major difference is the absence of sulphate ions in type A and no barium in the B type water. Another significant difference is in the isotopic ratio of

radium in both brines. Typically, in A type waters radium 226Ra concentration is higher than the 228Ra content – typically this ratio is about 2:1. In B type water the opposite can be seen - 226Ra to 228Ra ratio can be as low as 1:2 but sometime even 1:3.

In table 1 typical chemical analyses of the two different radium-bearing brines are presented.

The occurrence of radium-bearing waters in different coal mines in the Upper Silesian Coal Basin, the range of radium concentrations in brines, and its' influence on the natural environment have been investigated since the 70's and is well recognised. On the other hand, the origins and difference between the two types of is still a problem without adequate explanation.

Table 1. Comparison of chemical composition of brines A and B types.

		type A	type B
Conductivity	[μS/cm]	151000	91000
pH	[-]	7.25	7.53
TDS at 378K	[mg/dm^3]	124300	85300
^{226}Ra	[Bq/dm^3]	**62.76**	**3.449**
^{228}Ra	[Bq/dm^3]	**34.67**	**5.10**
Cations			
Ca^{2+}	[mg/dm^3]	6500	1840
Mg^{2+}	[mg/dm^3]	3750	1980
Na^{+}	[mg/dm^3]	34720	28050
K^{+}	[mg/dm^3]	299	268
Fe	[mg/dm^3]	<0.05	<0.05
Mn^{2+}	[mg/dm^3]	<0.05	<0.05
Ba^{2+}	[mg/dm^3]	1480	-
Total	[mg/dm^3]	46740	32140
Anions			
Cl^{-}	[mg/dm^3]	77350	50830
SO_4^{2-}	[mg/dm^3]	0.0	2140
CO_3^{2-}	[mg/dm^3]	0.0	0.0
HCO_3^{-}	[mg/dm^3]	24.4	67.1
SiO_4^{4-}	[mg/dm^3]	2.00	3.45
Br^{-}	[mg/dm^3]	241	155
J^{-}	[mg/dm^3]	10.9	11.2
Total	[mg/dm^3]	77630	53210

Radium transfer and migration with water

The process of radium transfer from solid phase into water consists of three phases (Starik, 1964):

- transfer of radium from the crystalline lattice into capillaries or pores in the mineral or rock, caused by the alpha-recoil effect resulting from the decay of parent nuclei, respectively 230Th for 226Ra; and 232Th for 228Ra;
- in pores an equilibrium between radium in solution and radium adsorbed on the surface of the mineral phase is established.

Starik furthermore stated that most of the radium seems to be adsorbed on surfaces;

- when mineral grains are in contact with flowing water, some of the radium may diffuse out of pores and capillaries (if a concentration gradient exists), but simultaneously part of radium can be desorbed from surfaces to balance the concentration.

Aqueous radium migration studies have been carried out by numerous scientists, but mainly for groundwater aquifers (Davidson & Dickson, 1986, Morse et. al., 2000, Benes, 1990). One of the most important investigations has been performed by Krishnaswami and co-workers (1982) who assessed the adsorption/desorption ratio for radium and estimated the retardation factors for radium migration in the ground.

The simplified model of radium migration is based of the assumption of equilibrium between the concentration of radium in the liquid phase and that adsorbed on surfaces of solid phase (Frissel and Koster, 1990). In this model the factor Kd describes the ratio of radium concentrations in solid and liquid phases according to:

$$K_d = Cs/Cw \quad (1)$$

where:
Cs – concentration in solid phase (Bq/kg);
Cw – concentration in water (Bq/l)

This factor can be used to assess the migration velocity in the ground, which is defined as (Dickson, 1990):

$$V_{Ra} = V_{H20}*/(1 + \rho K_d/\theta) \quad (2)$$

where:
Cs – concentration in solid phase;
Cw – concentration in water;
ρ - density of solid phase;
θ - moisture content of the ground;
V_{H20} – velocity of water movement in the aquifer (measured in m/year).

The radium movement in the aquifer is retarded significantly in comparison with water movement, and the retardation depends strongly on the Kd value.

During one half-life of 226Ra (ca. 1600 y) the transport distance can be estimated as a maximum of several meters only. The effect of retardation is more im-

portant for 228Ra due to its relatively short half-live - 6 years only. Within this period radium might be transported only several centimetres. It seems to be a certain limitation for the possible volume of the solid phase, influencing radium concentration in formation water.

However, the consideration of radium migration in aquifers is far more complex. Numerous data confirm (Nathwani and Phillips, 1979), that Kd values depend on the concentration of other ions in the liquid phase, and this makes it useless for analysis of radium transport in brines.

Another method that can be considered is based on the idea of cation exchange capacity – CEC. Cations in an aquifer compete for adsorption on a limited and stable number of adsorption centres, given by the CEC. This problem is relatively simple if only two types of cations are present in water. Otherwise, as in saline mine waters, several different cations can be found in the brine (see table 1). The analytical solution of such complex equations is very difficult, only a numerical approach is possible (Frissel and Reiniger, 1974). The main limitation for this approach is that exchange factors are not stable, but depend on the total concentration of cations and chemical composition of dissolved solids.

The author would like to present a simple, mathematical approach to the problem of adsorption and desorption of radium in aquifers. The results for the simulation of changes in the radium isotopic concentration in water are compared with the results of long-term monitoring of radium content in different brines. That problem is not necessarily specific to the Silesian Basin, because reports of similar brines in different underground mines, especially non-uranium ones, and also in deep aquifers, are common.

One, additional issue is very important. One of the most important ions in brines is barium, which has very similar geochemical properties to radium. It seems that a most important problem would be to explain the presence of barium in some brines and absence in others. It is known, that barium is relatively easy dissolved by some hydrothermal fluids. For instance Krishnaswami and Turekian (1982) found in such fluids within basalts in Galapagos region a similar ratio of 226Ra/Ba as in host rocks. Moreover, these scientists discovered similar values for this ratio in other volcanic areas. Of course, the mechanism of radium transfer into the liquid phase may be different, but the idea is supported by elevated barium contents in some saline waters.

Ion exchange kinetics:

Equations, describing the balance of radium in aquifers, are quoted from Dickson (1990). Equation (3) presents changes of radium activity in the liquid phase and (4) on the surface of the solid phase.

For the liquid phase:

$$N_{rec} + k_2 * Ns = \lambda * Nw + k_1 * Nw \quad (3)$$

For the solid phase:

$$k_1 Nw = \lambda * Ns + k_2 * Ns \quad (4)$$

where:
N_{rec} – production of radium due to recoil effect;
k_1 – adsorption coefficient;
k_2 – desorption factor;
Nw – radium concentration in water;
Ns – radium content in solid phase.

The ratio of the radium atoms in the solution Nw to the transfer velocity into water, as a result of recoil Nrec, can be described as:

$$Nw/ N_{rec} = (\lambda+k_2)/(\lambda+ k_1+ k_2) \quad (5)$$

Theoretically, the radium concentration in water could be calculated, taking into considerations measured or arbitrary chosen adsorption and desorption coefficients – different ones for A and B type of brines. During in-situ measurements parameters k1 and k2 must be measured for each aquifers. Data for in-situ investigations of these parameters are scare (Taskaev et al., 1978, Shangde et al, 2000). Dickson (1972) showed, that measured values of adsorption/desorption coefficients often were not reliable. Therefore such an approach, based on the kinetics of ion exchange, may lead to wrong conclusions, if the above mentioned parameters are not well known.

It is proposed that a simplified, mathematical approach to this problem be used and the results compared with the actual results for Polish mines. One could consider this phenomenon as a product of the normal decay of the radionuclide (radium) in the liquid phase with additional exchange with solid surfaces (adsorption and desorption). Consider the Bateman equation for radium in the formation water in a modified form (Dickson, 1972), because only a part of radium atoms is transferred into water from solid phase. Assuming, that the recoil efficiency is denoted as e, the decay constant of the parent isotope (230Th) is l and N is the number of parent isotope atoms in the volume unit, then the number of radium atoms, recoiling into liquid phase, can be calculated as:

$$N_{rec} = N * \lambda * \varepsilon = A * \varepsilon \quad (6)$$

Consider first the case of simple decay with possible adsorption, while desorption is omitted (Semkow et al., 1996). On such an assumption, the equation, describing changes in the radium content in the liquid phase, as follows:

$$dN_{Ra}/dt = N_{rec} - \lambda * N_{Ra} – k_1 * N_{Ra} \quad (7)$$

When desorption is also taken into account along with another assumption; that the number of atoms in the liquid phase is similar to those adsorbed on solid surfaces, the final formula is different:

$$dN_{Ra}/dt = N_{rec} - \lambda * N_{Ra} – k_1 * N_{Ra} + k_2 * N_{Ra} \quad (7a)$$

where:
$\lambda * N_{Ra}$ – this part describes the radioactive decay of radium in the solution, λ is the decay constant of radium and N_{Ra} is numer of radium atoms in liquid phase;

$k_1 * N_{Ra}$ – the adsorption on the solid phase, k_1 is the adsorption coefficient;
$k_2 * N_{Ra}$ – the desorption into liquid phase, k_2 is the desorption coefficient.
The solution of equation (8) is:

$$N_{Ra}(t) = N_{rec}/(\lambda+k_1)*(1-\exp(-(\lambda+k_1)*t)) \quad (8)$$

or, for the case with desorption:

$$N_{Ra}(t) = N_{rec}/(\lambda+k_1-k_2)*(1-\exp(-(\lambda+k_1-k_2)*t)) \quad (8a)$$

Some conclusions can be drawn from these equations. Firstly, the dynamic equilibrium in the liquid phase seems to depend mainly on adsorption and desorption rates. The main reason is that decay the constants of 226Ra and 228Ra isotopes are much lower than the adsorption/desorption coefficients. The decay constant of 228Ra is $3.7*10^{-9}$ s^{-1} only and l for 226Ra is even lower, while the estimate of the adsorption rate for groundwaters gave values within the range 0.5 - 10^{-6} s^{-1} (Dickson, 1990). It means, that the equilibrium level of radium in the liquid phase should be controlled by other processes, not the decay. On the other hand, the adsorption and desorption rates of radium must depend on the solutes in the formation water and especially the presence of barium ions.

From the above equations it is clear that adsorption and desorption processes affect the level of radium concentration in liquid phase. The ratio of equilibrium concentrations for cases without and with adsorption/desorption is 1/((+k1-k2). Taking into consideration the assumption, that k1-k2 » l, the activity ratio is about 1/(k1-k2). This effect should be more important for the isotope with the lower decay constant - 226Ra. Although usually concentrations of radionuclides from uranium and thorium series in the solid phase are similar, the situation in the liquid phase should be different. If adsorption and desorption rates for both isotopes are the same, than the activity ratio in the solution should be A226/A228 = 6/1600 ≈ 0.004. Such low ratios are not usually observed in aquifers, if at all. It means, that another explanation is required.

Radium in mine waters

Any theory must explain the observed different effects found in brines in coal mines. As mentioned earlier, the ratio of radium concentrations in A type brines (226Ra/228Ra) is higher than 1. It might be explained as a combination of the low adsorption rate, resulting in longer time needed to reach equilibrium in the liquid phase, and the higher concentrations of radium in A type waters.

In B type waters the lack of barium leads to the higher adsorption rate and slower desorption. The main effect is that there is a shorter time required to reach equilibrium in the liquid phase. Additionally, the activity ratio 226Ra: 228Ra should be below 1, as observed.

Assuming that recoil is the only mechanism of radium transfer into the liquid phase and that no adsorption occurs, the build up of activity can be described as:

$$A_{Ra}(t) = (N_{rec}/\lambda)*(1-\exp(-\lambda*t)) = (A*\varepsilon/\lambda)*(1-\exp(-\lambda*t)) \quad (9)$$

where N_{rec}/λ is the maximum activity of radium in water.

By considering the following parameters for the host rock in the aquifer: – the concentrations of uranium and thorium isotopes are each 25 Bq/kg, the density of the rocks is 2000 kg/m3, the recoil coefficient e»10% (Semkov et al., 1998), and a porosity of 10 %, than the calculated maximum radium activity in the liquid phase should be 50 kBq/m3. However in Polish coal mines, much higher values have been measured, up to 400 kBq/m3 (Lebecka et. al., 1993). It is understandable, because often concentrations of radionuclides in rock body are higher, up to 200 Bq/kg. The fact, that the radium 226Ra concentrations are higher than those of 228Ra has been explained by Dickson (Dickson, 1990) to be the result of the previously mentioned recoil and adsorption of 230Th on the surface of solid phase. It is possible that the recoil dissolution of 226Ra may be more effective than 228Ra, since the parent 232Th is probably entirely embedded in the lattice. It is necessary to stress again, that such high radium concentrations in water are not connected with uranium or thorium mineralization.

Comparing equation (9) for the two isotopes of radium, 226Ra from the uranium series and 228Ra from thorium chain, and making the assumption that the recoil coefficient is similar for both radionuclides and that no adsorption occurs, the ratio of their activities in the liquid phase is as follows:

$$A_{226}/A_{228} = (\lambda_{228}/\lambda_{226})A_U*\{1-\exp(-\lambda_{226}*t)\}/\ A_{Th}*\ \{1-\exp(-\lambda_{228}*t)\} \quad (10)$$

Taking into account the adsorption and desorption (equation 8a), the activity ratio can be denoted as:

$$A_{226}/A_{228} = (A_U/A_{Th}) * \{\lambda_{228}/(\lambda_{226}+k_1-k_2) * (1-\exp(-(\lambda_{226}+k_1-k_2)*t))\} / \{\lambda_{226}/(\lambda_{228}+k_1-k_2) * (1-\exp(-(\lambda_{228}+k_1-k_2)*t))\} \quad (11)$$

If the adsorption coefficient is significantly higher than the decay constant of both radium isotopes, then equation (11) can be simplified further (taking into account a longer time for water contact with the solid phase):

$$A_{226}/A_{228} = (A_U/A_{Th}) * \{\lambda_{228}/(\lambda_{226}+k_1-k_2)\} / \{\lambda_{226}/(\lambda_{228}+k_1-k_2)\} \quad (12)$$

If we assume a much higher value for the adsorption coefficient in comparison with desorption, a final equation is simpler:

$$A_{226}/A_{228} = (A_U/A_{Th})(\lambda_{228}/\lambda_{226}) \quad (13)$$

The conclusion from the last equation is important. Such a big difference of activity ratio is not observed in mine waters. It means that adsorption and desorption coefficients in saline water aquifers are similar, rather low and comparable with the decay constants of radium isotopes. Therefore the equation (13) cannot be used for the prediction of radium concentrations in brines.

The use of the concept of an effective adsorption coefficient keff, obtained from the subtraction of adsorption and desorption factors (keff= k1 - k2), for numerical simulation of the build-up of radium isotope concentrations in the liquid phase in aquifer is proposed. Such simulation has been made for different values

of effective adsorption coefficients and results are presented in fig.1. The activities (concentrations) of radium isotopes are relative values and have been normalised to enable comparison of the increase of these values with time. The uranium:thorium ratio in the solid phase has been chosen as 1, which is close to actuality.

The results of these approximate estimations seems to be a little surprising. First of all – the effective adsorption of radium from brines is a very slow process. For A type waters value of this coefficient must be close to zero and adsorption simply does not occur. The activity ratio 226Ra:228Ra is of about 1, equal to the chosen activity ratio in the solid phase. The observed higher values, up to 2, can be explained, accordingly to Dickson (Dickson, 1990), by the higher recoil rate for 226Ra as a result of a previous recoil of parent isotope 230Th. The recoil ratio of radium isotopes has been calculated by Dickson as 2:1 and this value is in a good agreement with experimental data.

For the effective adsorption coefficient, equal to the decay constant of 226Ra (keff = $1{,}4*10^{-11}$ s^{-1}), the activity ratio was calculated above as 1:2, and this is close to the activity ratio measured for B type waters. In such waters the adsorption prevails over desorption, but the process appears to be very slow. The reason is that the presence of sodium and calcium ions in the liquid phase, compete with radium ions for the CECs.

Higher values of effective adsorption coefficient seem to be too high for aquifers with saline waters. For instance, the activity ratio, calculated for the keff $=1{,}4*10^{-11}$ s^{-1}, corresponding to period of 160 years (1/10th of 226Ra half-life),

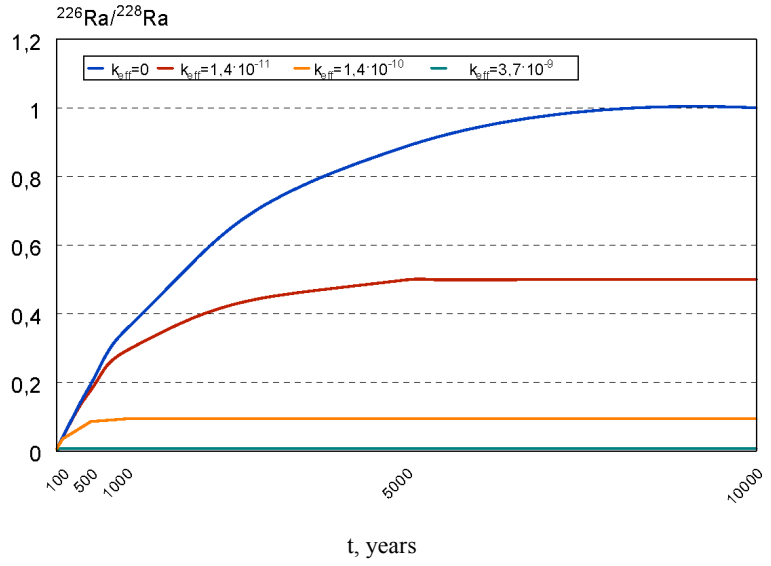

Fig.2. Simulation of the changes of activity ratio of radium isotopes in groundwater as a function of the effective adsorption coefficient; t- time, years

give the value of activity ratio = 0.1. (Results of radium ingrowth in liquid phase are shown in fig.2.) In Polish coal mines such an activity ratio has not been observed. Again, this conclusion supports strongly the thesis that the ionic exchange of radium with solid phase is an extremely slow process.

On the other hand, we have to remember, that all conclusions are related to the effective adsorption coefficient, which describes the difference between adsorption and desorption. Physically, both processes are fast and there have been numerous investigations on this subject, each giving clear evidence that desorption could take place within hours or even minutes (Chalupnik, 2003).

The problem needs further analyses and in-situ measurements to investigate brines and deep aquifers. One of the best possible sites is a colliery in southern part of Upper Silesian Coal Basin, where both types of radium bearing brines are present.

Summary

An approach to the problem of radium transfer from solid into liquid phase in aquifers is described in the paper, with special emphasis to brines that occur in coal mines. The main process, controlling the radium concentration in water, is adsorption of radium on the surfaces of solid phase. However the adsorption coefficient strongly depends on the dissolved solid content of the brines, and primarily on the barium presence in saline waters.

The migration length of radium isotopes in an aquifer is rather short, several meters for 226Ra and less than 1 meter for 228Ra. Therefore investigations of the stratum in the close vicinity of mine galleries should give important information of the uranium and thorium content in the solid phase as well as other parameters of the aquifer such as porosity, Eh, pH etc. All these results will be essential for the further investigations of radium behaviour in deep aquifers.

The results of simulation, based on the mathematical approach to the radium changes in the liquid phase, revealed that effective adsorption rate of radium from brines is very low, either comparable with the decay constant of 226Ra or even lower. Differences of adsorption coefficient, mainly due to the presence of barium ions in A type brines, lead to the significant differences in the activity ratio of radium isotopes. It means, that one of the most important features is the reason for barium occurrence in some aquifers. From that point of view, the change in radium concentration is a secondary problem.

Further research is required, mainly in-situ experiments directly within aquifers. The best possible sites seem to be deep underground mines, like collieries, with easy access to different aquifers. In one of coal mines in Poland both types of radium-bearing waters are present (A & B), therefore we would like to use this mine during future investigations.

References

Benes P. – Radium in continental surface water - Technical Report "The environmental behaviour of radium", IAEA, Vienna, STI/DOC/10/310, 1990.

Centeno L., et.al., – Radium-226 in coal-mine effluent, Perry County, Ohio – Proc. of Geological Society of America Annual Meeting, Boston, 2001.

Chałupnik S. – Purification of mine water of radium – IAEA-Tecodc-1271, Vienna 2002.

Chałupnik S. – Investigation of radium leaching from mine sediments – Kwartalnik Głównego Instytutu Górnictwa, no.3, 2003 (in Polish).

Davidson M.R., Dickson B.L. – A porous flow model for steady-state transport of radium in groundwater - Water Resources Journal, vol.22, 1986.

de Jezus A.S.M. - Behaviour of Radium In Waterways and Aquifers – IAEA Tecdoc 301, Vienna 1984.

Dickson B. L., et.al., - Evaluation of the Radioactive Anomalies Using ^{226}Radium Isotopes in Groundwaters - J. of Geochemical Exploration, Vol. 19, 1972.

Dickson B.L. – Radium in groundwater - Technical Report "The environmental behaviour of radium", IAEA, Vienna, STI/DOC/10/310, 1990.

Dickson B.L. – Radium isotopes in saline seepages, south-western Yilgarn, Western Australia – Geochimica and Cosmochemica Acta, vol. 49, 1985.

Frissel M.J., Koster H.W. – Radium in soil - Technical Report "The environmental behaviour of radium", IAEA, Vienna, STI/DOC/10/310, 1990.

Frissel M.J., Reiniger P. – Simulation of accumulation and leaching in soils – PUDOC, Wageningen, Netherlands, 1974.

Sidhu R. – Radium in formation waters from oil fields in Norway – Int. Conference ENOR III, Dresden 2003.

Gans I., et.al., - Radium in waste water from coal mines and other sources in FRG - Second Symposium on Natural Radiation Environment, Bombay, India, 1981.

Gucalo L.K. - O niekotorych zakonomiernostiach raspredielenija radia w podziemnych wodach sredniej czasti Dnieprowsko-Donieckoj Wpadliny - Gieochimja, vol. 12, 1964.

Humphreys, C.L. - Factors controlling uranium and radium isotopic distributions in groundwaters of the west-central Florida phosphate district. - In Graves, B., ed. Radon, Radium and other Radioactivity in Groundwaters, Lewis Publishers, 1987.

Kipko E.Y., et.al. – Environmental Projection during mining of diamond deposits of Yakutiya – Proc. Of 5th Int. Mine Water Congress, Quorn Repro Ltd., Loughgorough, England, 1994.

Klessa D. – Availabilities of radionuclides and non-radiological contaminants in sediments - Mine Water and the Environment, Uniwersytet Śląski, Katowice, 2001.

Koster H.W., et.al. - ^{210}Po, ^{210}Pb, ^{226}Ra in Aquatic Ecosystems and Polders, Anthropogenic Sources, Distribution and Enhanced Radiation Doses in the Netherlands - The Natual Radiation Environment, Nuclear Technology Publishing, Vol. 45, Nos. 1-4, (1992).

Kraemer T.F., Reid D.F. – The occurrence and behaviour of radium in saline formation water of the U.S. Gulf Coast region – Isotope Geoscience, vol. 2, 1984.

Krishnaswami S., et.al. – Radium, thorium and radioactive lead isotopes in groundwater – Water Resources Research, vol. 18, 1982.

Krishnaswami S., Turekian K.K. – U-238, Ra-226 and Pb-210 in some vent waters of the Galapagos spreading center – Geophysical Research Letters, vol. 9, 1982.

Langmuir D., Riese A.C. – The thermodynamic properties of radium – Geochemical and Cosmochemical Acta, vol. 49, 1985.

Lebecka J. et.al. - Radioactive contamination of Upper Silesia as a result of release of brines and deposits from coal mines - Wiadomości Górnicze, 6/91, Katowice 1991 (in Polish).

Lebecka J., et.al - Influence of Mining Activity on Distribution of Radium in the Natural Environment - Proc. of 4th Working Meeting Isotopes in Nature, Leipzig, 1986.

Lebecka J., et.al. - Methods of Monitoring of Radiation Exposure in Polish Coal Mines - Nukleonika Vol 38, 1993.

Martel A.T., et.al. - Brines in the Carboniferous Sydney Coalfield, Northern Canada – Applied Geochemistry, vol. 16, 2001.

Martin R., Akber R.A.– Radium isotopes as indicator of adsorption-desorption interactions and barite formation in groundwater – J. of Environmental Radioactivity, vol. 46, 1999.

Michalik B., Chałupnik S., Skowronek J. – Występowanie naturalnych izotopów promieniotwórczych w węglach na terenie GZW - metodyka i wstępne wyniki badań – Zeszyty Naukowe Politechniki Śląskiej, Seria : Górnictwo, z. 149, Gliwice 1986.

Moise T., et.al. – Ra isotopes and Rn in brines and groundwaters of the Jordan-Dead Sea Rift Valley: enrichment, retardation and mixing – Geochemica and Cosmochemica Acta, vol. 64, 2000.

Nathwani J.S., Phillips C.R. - Adsorption of Ra-226 by soils in the presence of Ca^{2+} ions – Chemosphere, vol. 5, 1979

Paridaens J., Vanmarcke H – Radium contamination of the Laak rivers bank as a consequence of phosphate industry in Belgium – IAEA-Tecdoc-1271, Vienna 2002.

Paschoa A.S., Nobrega A.W. - Non-nuclear mining with radiological implications in Araxa - Int. Conf. On Radiation Hazards in Mining, Golden, Co, 1981.

Peic T., et.al. - Formation waters from oil and natural gas production: potential polluting source by Radium-226 - International Symposium on the Natural Radiation Environment (NRE-VI), Montreal, 1995.

Pluta I. – Uranium in waters from Carboniferous aquifers in southern part of USCB – Zeszyty Naukowe Politechniki Śląskiej, seria Górnictwo, z. 172, 1988 (in Polish).

Pluta I., Zuber A. – Uranium and radium-226 and origin of brines in Upper Silesian Coal Basin – Prace Naukowe Instytuttu Geotechniki Politechniki Wrocławskiej, nr. 58, 1989 (in Polish).

Sałdan M. – Uranium origin in Carboniferous strata in USCB - Biuletyn Instytutu Geologicznego, Warszawa, vol. 5, 1965 (in Polish).

Shangde L., et.al. – In-situ radionuclide transport and preferential groundwater flow at Idaho – Geochemica and Cosmochemica Acta, vol. 65, 2000.

Starik I.E. – Principles of Radiochemistry – U.S. Atomic Energy Commission Report, AEC-tr-6314, 1964.

Tanner A.B. – Radium migration In the ground: a review – Natural Radiation Environment Conference, University of Chicago Press, Chicago, 1964.

Taskayev A. I., et al. – Forms of radium-226 in soil horizons containing its high concentrations – Pochvovedenie, vol. 2, 1978.

Tomza I., Lebecka J., - Radium-bearing waters in coal mines: occurrence, methods of measurements and radiation hazard - Int. Conf. On Radiation Hazards in Mining, Golden, Co, 1981.

Wysocka M. et.al. – Radium in mine waters in Poland: occurrence and impact on rivers – International Conference "Ecological Aspects of Coal Mining", Katowice, 1997.

Wysocka M., Skowronek J. - Analysis of natural radioactivity of coals from Upper Silesian Basin in aspects of geological structure - Int. Symp. On Nuclear techniques in the Exploration and Exploitation of Energy and mineral resources. IAEA-SM-308 Vienna, IAEA 1990.

Younger P.L., et.al. – Application of geochemical mineral exploitation techniques to the cataloguing of discharges from abandoned mines in north east England - Proc. Of 5th Int. Mine Water Congress, Quorn Repro Ltd., Loughgorough, England, 1994.


Uranium Mining
and Hydrogeology

Distribution of Ra-226 downstream a uranium mining site

Holger Dienemann[1,2], Claudia Dienemann[2] and E. Gert Dudel[2]

1Staatliche Umweltbetriebsgesellschaft, Bitterfelder Straße 25, 04849 Bad Düben
[2]TU Dresden, Institut für Allgemeine Ökologie und Umweltschutz, Pienner Straße 8, 01737 Tharandt

Abstract. Radioactive contaminated leachate waters emerging from small abandoned uranium mining sites are still a problem. At a particular location (Neuensalz, Germany), vascular plant litter and sediments were investigated focusing on Ra-226. Especially at leachate exit points, where iron-hydroxide coatings were found, extremely high specific activities of Ra-226 were measured.Vascular plant litter could function as an active surface, precipitating hydroxides and co-precipitating Ra-226.

Introduction

Many small uranium mines developed in Saxony and Thuringia after World War II up to 1960. Today, leachates contaminated with radionuclides still emerge from the respective dumps and tailings. Specific activities of Ra-226 are rather low (Benes 1990). At the investigation sites of Lengenfeld and Neuensalz (Saxony, Germany) they vary around 100 $mBq*L^{-1}$ and lower (Dienemann et al. 2002; Schöpe et al 2002).

Dissolved Ra-226 may be enriched in the solid phase by co-precipitation of barium-sulphate and other processes like sorption onto iron- and manganese-hydroxides and ion-exchange as shown in various laboratory experiments (Molinari and Snodgrass 1990; Burghardt 2006).

Under natural conditions, accumulation and dissolution processes (e.g. reduction processes causing dissolution and changes of metal hydroxides) happen parallel. So the question arose, how Ra-226 is distributed in sediments, vascular plant litter and how it is possibly transferred. A special focus lay on the background contamination of the sediment.

Material and Methods

The investigation site – Neuensalz – is located in Saxony (Germany) (see Fig.1). Uranium mining commenced in the late 1940s and ceased several years later. Dumps were established in the former valley of the Forellenbach (the Forellenbach (a small stream) is also known as Haarbach, Wismut 1999). The Forellenbach emerges west of the former dump. All dumps have mostly been removed, leaving only a caldera. At the eastern edge of the caldera leachates rich of iron hydroxide emerge.

For estimating the background activity clay was taken from the erosion zone of the Forellenbach (stream). Also, at the Forellenteich (a former fish pond currently containing no fishable fish at all) drilling was performed and material from 0-6 m depth investigated.

Dump material with and without influence of leachate water was collected directly at the exit point of the Forellenbach at the dump's slope to examine particulate inputs.

Of Forellenbach (stream) and Forellenteich (pond) and the eastern leachate exit points the upper 0-5 cm of the sediment were sampled and air-dried.

During fall season, samples of vascular plant litter were carefully removed from the water. Some samples were washed and assorted into their components. All samples were dried at 60 °C.

Samples for analysing Fe and Mn by atomic absorption spectrometry (AAS) (Fa. Unicam Solar MZ) were microwave-digested (Fa. CEM, MDS 2000) and measured at $\lambda = 248.3$ nm and 279.5 nm, respectively.

Samples for gammaspectrometry (n-type-Ge-detector, formerly Silena, now MATEC) were filled into polypropylene containers and vacuum-heat-sealed with poly-ethylene.

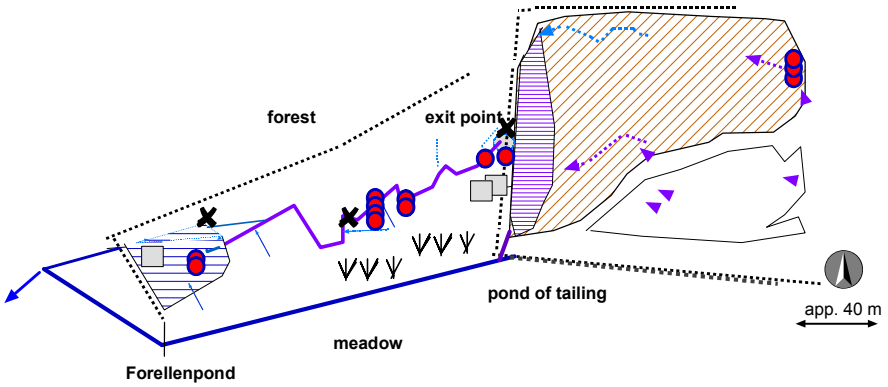

Fig.1. Investigation area with sampling points: crosses – background activity sampling, circles – sediment sampling, squares – plant litter sampling

Table 1. Specific activities of U-238, Ra-226 and Pb-210 of clay samples from the erosion zone of the Forellenbach (stream)

U-238	Ra-226	Pb-210	K-40
Bq g^{-1}	Bq g^{-1}	Bq g^{-1}	Bq g^{-1}
0.33 ± 0.05	0.062 ± 0.005	0.068 ± 0.007	0.88 ± 0.03

Results and Discussion

Background activity and specific activity of dump material

Table 1 shows selected specific activities of clay samples from the erosion zone of the Forellenbach (stream).

Specific activities of U-238 are in radioactive imbalance, possibly caused by different sorption capacities and different specific activities in the water. The range of the specific activity of Ra-226 is confirmed by the results of the drilling in the Forellenteich (pond) (Fig. 2).

Within the first 1 m the influence of uranium mining is distinct. Since specific activities of Th-234 are out of balance with those of Ra-226 it is assumed that human impacts may have caused the peak. Specific activities of Ra-226 are relatively balanced and range around 100 mBq*g^{-1}.

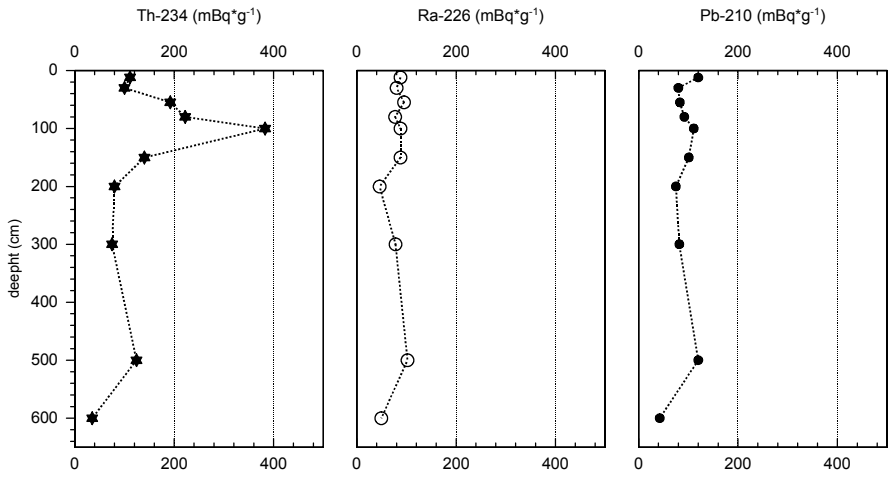

Fig.2. Specific activities of material from the drilling in the Forellenteich (pond)

Table 2. Specific activities of U-238, Ra-226 and Pb-210 (Bq*g^{-1}) of dump material with and without significant influence of leachate waters

	With influence of leachate waters Bq g^{-1}	Without influence of leachate waters Bq g^{-1}
U-238	<0.3	0.33 ± 0.07
Ra-226	1.83 ± 0.06	0.17 ± 0.02
Pb-210	0.23 ± 0.025	0.19 ± 0.012
colour	Black/greyish black	Greyish-brown

Ra-226 may be washed out from dump material into the sediment. Table 2 shows specific activities of dump material with and without influence of leachate waters.

Differences concerning the influence of leachate waters are specifically evident with Ra-226. Samples with influence of leachate waters additionally show a distinct radioactive imbalance of Ra-226 : U-238. However, U-238 and Pb-210 are radioactively balanced. Assuming the loss of volatile Rn to be negligible, Ra-226 would be selectively fixed and washed-off particles would cause the increase of specific activity at the exit point of the Forellenbach (stream).

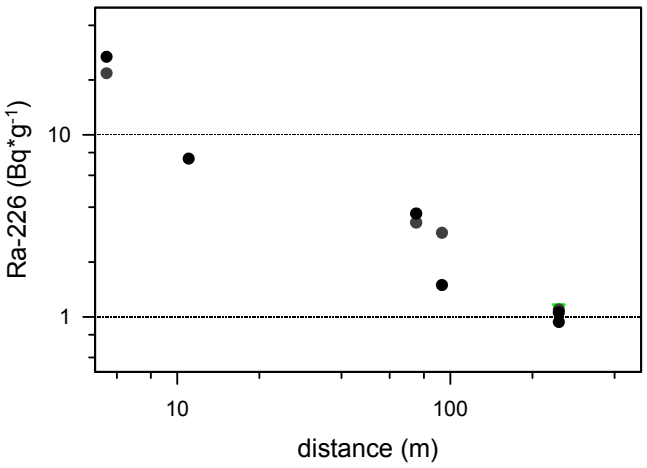

Fig.3. Specific activities of Ra-226 in sediments along the flow path (n=12);–log scaling

Table 3. Selected specific activities in sediments rich of iron-hydroxide, eastern slope of the dump, Neuensalz

	Exit point	3 m	5 m
	Bq g^{-1}	Bq g^{-1}	Bq g^{-1}
Th-234	1.32 ± 0.06	0.87 ± 0.02	0.67 ± 0.08
Ra-226	9.5 ± 0.19	8.2 ± 0.13	4.4 ± 0.087

Sediments

Fig. 3 shows highest specific activities of Ra-226 directly at the exit point of the Forellenbach (stream) (>20 Bq*g^{-1}), which are significantly higher than those of leachate influenced dump material (1.8 Bq*g^{-1}).

Fig. 3 suggests a correlation between the distance from the leachate exit point and the specific activity of Ra-226 (exponential decrease of specific activities). Accepting this assumption would also explain the comparable small specific activities found in the sediments of Czech uranium mining sites (Hansliket al. 2005).

The gradient of the specific Ra-226 activity may be caused by precipitation of metal-hydroxides sorbing Ra-226. Directly at the exit point of the stream, rocks and partially even leaves with ochre to black coatings were found. No such coatings were found in the pond.

In the eastern area of the investigation site iron-hydroxide-containing waters lead to rust coloured sediments with similar high specific Ra-226 activities.

As already seen in Fig. 3 a decrease of the specific activities with increasing distance from the leachate exit point is obvious. Differences could be due to different ages of the precipitates (varying around 100 d, see Dienemann et al. 2006). As they harden in the process of aging, this might cause changes in their structure.

Fluorescence-microscopic analysis of the sediment showed numerous microorganisms (diatoms, bacteria), so Ra-226 is possibly rather bound onto living components and released by microbial metabolic activities and/or death.

Vascular plant litter

Table 4, 5 and 6 illustrate specific activities of U-238, Ra-226 and Pb-210 of vascular plant litter (mostly from alder trees).

At all three sampling sites unwashed leaves show higher specific activities than unwashed twigs. Ra-226/Pb-210-ratios are generally shifted towards Ra-226, suggesting Ra-226 and U-238 to originate neither from primary ore particles nor from dump material. Accordingly a selective enrichment of U-238 and Ra-226 should be expected, as both have a high affinity to metal hydroxides (Fe and Mn).

Table 7 shows metal contents (Fe, Mn) for two of the aforementioned sampling sites (tables 4 and 5).

Mn- and Fe-contents of the samples are significantly higher than average contents of leaves and twigs, which may be caused by hydroxides precipitated at the surface. No relation between Fe- and Mn-contents and specific-Ra-226-activity could be confirmed by these results, although hydroxide coatings are prerequisites for high specific activities. Simple washing removed most of the Ra-226. Possibly the structure (thickness) of the coatings as well as the bacteria involved have a main influence on the specific Ra-226-activity.

Table 4. Selected specific activities in washed and unwashed plant litter samples from the exit point of the stream (Forellenbach), n.n. = below detection limit

	Leaves Washed Bq g^{-1}	Leaves Unwashed Bq g^{-1}	Twigs Washed Bq g^{-1}	Twigs Unwashed Bq g^{-1}
U-238	13.2 ± 0.9	10.8 ± 0.3	1.72 ± 0.22	1.67 ± 0.22
Ra-226	4.8 ± 0 .25	8.5 ± 0.3	1.75 ± 0.08	2.24 ± 0.085
Pb-210	n.n.	0.34 ± 0.041	n.n.	n.n.

Table 5. Selected specific activities of washed and unwashed plant litter samples taken 11 m downstream the Forellenbach (stream) exit point, n.n. = below detection limit

	Leaves Washed Bq g^{-1}	Leaves Unwashed Bq g^{-1}	Twigs unwashed Bq g^{-1}
U-238	17.5 ± 0.8	15.1 ± 0.4	1.44 ± 0.2
Ra-226	1.83 ± 0 .25	5.6 ± 0.3	1.2 ± 0.065
Pb-210	n.n.	n.n.	n.n.

Table 6. Selected specific activities of washed and unwashed plant litter samples taken 250 m downstream the Forellenbach (stream) exit point, n.n. = below detection limit

	Leaves Washed Bq g^{-1}	Leaves Unwashed Bq g^{-1}	Twigs Unwashed Bq g^{-1}
U-238	1.1 ± 0.085	1.08 ± 0.055	0.24 ± 0.07
Ra-226	0.285 ± 0 .03	0.39 ± 0.03	0.09 ± 0.004
Pb-210	n.n.	0.075 ± 0.01	n.n.

Table 7. Fe- and Mn-contents in samples of sedimented vascular plant litter (dry matter, mainly from alder trees); (w.)=washed, (uw.)=unwashed

Component	Distance from exit point (stream) m	Mn mg g^{-1}	Fe mg g^{-1}
Twigs (w.)	0	7.9	0.5
Twigs (uw.)	0	9.9	1.2
Twigs (uw.)	11	31.4	0.36
Leaves (w.)	0	31.8	7.65
Leaves (uw.)	0e	65.5	14.1
Leaves (w.)	11	29.9	0.5
Leaves (uw.)	11	103.6	2.5

Conclusions

Close to leachate exit points vascular plant litter and sediments may display very high activity concentrations of Ra-226. It seems advisable to make these relatively small sites – especially when they are located near communities – inaccessible for the public.

While planning passive treatment of waters containing Ra-226 arrangements concerning dumps and dump material should be considered as well as sediment settling ponds. Besides stability and clogging, seasonal variations of the water quantity have to be regarded.

Acknowledgments

This work was financed by the Saxon State Authority of Environment and Geology.

Many thanks to K. Klinzmann, M. Förster, L. Keydel and M. Pilz for assistance with sampling, sample preparation and AAS measurements, and also to Dr. J. Rotsche and C. Brackhage for gamma-spectrometry measurements. Thanks to Dr. A. Jahn for most interesting discussions on the subject.

References

Benes P (1990) Radium in (continental) surface water. The environmental behaviour of radium. Vienna, IAEA (International Atomic Energy Agency). 1: 373-418

Burghardt, D (2006) Ermittlung geochemischer, geomikrobiologischer und geotechnischer Grundlagen zur In-Situ-Immobilisierung von Arsen, Uran und Radium durch eine "reaktive Zone". Cottbus, Technische Universität Cottbus. Dissertation: 100

Dienemann C, Dudel EG, Dienemann H and Stolz L (2002) Retention of Radionuclides and Arsenic by Algae Downstream of U Mining Tailings. Uranium Mining and Hydrogeology III. B J Merkel, B Planer-Friedrich and C Wolkersdorfer: Springer-Verlag Berlin Heidelberg New York, 605-614

Dienemann H, Dienemann C, Brackhage C, Dudel EG, Rotsche J and Weiske A (2006) Ra-226 und U-238 in Sedimenten im Abstrom einer Uranbergbauhinterlassenschaft Abschätzungen der Perspektiven und Grenzen von Sedimentationsgräben. 57. Berg- und Hüttenmännischer Tag: Behandlungstechnologien für bergbaubeeinflusste Wässer. GIS – Geowissenschaftliche Anwendungen und Entwicklungen. Wissenschaftliche Mitteilungen 31. B. Merkel, H. Schaeben, C. Wolkersdorfer and A. Hasche-Berger. Freiberg, TU Bergakademie Freiberg: 79-85

Hanslik E, Kalinova E, Brtova M, Ivanovova D, Sedlarova B, J Svobodova J, V Jedinakova-Krizova V, Rider M, Medek J, Forejt K, Vondrak L, Jahn K and Jusko J. (2005) Radium isotopes in river sediments of Czech Republic. Limnologica - Ecology and Management of Inland Waters 35(3): 177-184

Molinari, J and Snodgrass WJ (1990) The chemistry and radiochemistry of Radium and other elements of the uranium and thorium natural decay series. The environmental behaviour of radium. Vienna, IAEA (International Atomic Energy Agency). 1: 11-55

Schöpe M, Hähne R, Tunger B and Löser R (2002) Remediation of uranium milling site Lengenfeld/Vogtland, needs and objectives. Uranium Mining and Hydrogeology III. J. Merkel, B. Planer-Friedrich and C. Wolkersdorfer. Springer-Verlag Berlin Heidelberg New York,: 861-870

Wismut (1999) Chronik der Wismut. Chemnitz, Wismut GmbH

Uranium and its decay products in radioactive anomalies of the oxidized brown coals (the western part of the Kansko-Achinsk brown coal basin)

Mikhail M. Melgunov, Vsevolod M. Gavshin and Elena V. Lazareva

Institute of Geology and Mineralogy of Russian Academy of Sciences, Siberian Brunch, Novosibirsk, Russia

Abstract. Vertical distribution of uranium and its decay products (^{226}Ra and ^{210}Pb) in the uppermost layers of the oxidised brown coals was studied for some deposits and natural outcrops of the Western part of the Kansko-Achinsk brown-coal basin. Abnormal accumulation of the mentioned radioactive elements is observed in all studied sites. Several types of radioactive anomalies are differed by the ratio of activities of ^{238}U and ^{226}Ra: 1) Equilibrium; 2) Radium; 3) Uranium. The depletion of ^{210}Pb in the radioactive horizons of some sites indicates an active emanation of ^{222}Rn in the underlying coal layers.

Introduction

Jurassic brown coals of the Kansko-Achinsk coal basin (Jurassic depositions of the southern edge of the Western-Siberian plate and the Siberian platform) are the actual source of combustible for thermal power stations and for house use by local population of the Western Siberia. This coal basin is unique due to its immense dimensions and giant reserves of brown coal suitable for opencast mining. Its reserves down to 1800 m depth were estimated as 1220 billion tons (Burtsev, 1961; Grigor'ev, 1968; Gavrilin and Ozerskiy, 1996). The Lower-Middle Jurassic coal-bearing formations in the western part of the basin formed a great syncline with gently sloping northern and southern limbs (Fig. 1). The thickness of the coal layers reaches 60-80 m. From West to East nine great coal deposits are distinguished: Tisul', Uryup, Barandat, Beryezovo, Kibiten', Altat, Nasarovo (southern limb of syncline), Itat, Bogotol (northern limb of syncline). The coal layers lay almost horizontally. Everywhere they are recoated by quaternary sediments. Coal deposits

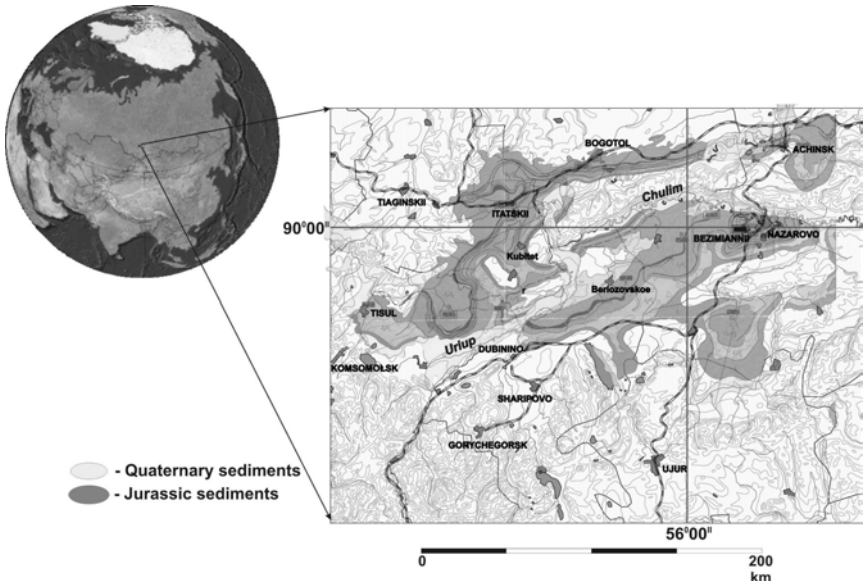

Fig.1. Location map of coal-bearing Jurassic formation in West Siberia (the western part of the Kansko-Achinsk brown coal basin).

here are very convenient for an opencast mining. The typical unaltered coals are characterized by low trace elements content and has, correspondingly, a low radioactivity. According to literary data average contents of uranium in unaltered coals for various deposits of the western part of the Kansko-Achinsk basin vary from 1 up to 11 ppm (12-140 Bq/kg). Ash content of such coals is 6-16% (Gavrilin and Ozerskiy 1996; Arbuzov et al. 2003; Arbuzov and Ershov 2007; Yudovich and Ketris 2006). Usually the upper part of the coal layers directly under quaternary sediments is oxidized. The uppermost horizons of coal (0.5-1.5 m) are most oxidated. They often become friable and have sooty structure. Ash content increases here up to 25-35%. Oxidized and especially “sooty” coals are often strongly enriched by uranium and its decay products (Gavrilin and Ozerskiy 1996; Arbuzov et al. 2003; Gavshin and Miroshnichenko 2000). Uranium content in “sooty” coals can reach 2100 ppm (26000 Bq/kg).

The radioactive anomalies connected with oxidized ("sooty") coals localized in some brown coal deposits of the western part of the Kansko-Achinsk coal basin are studied in this work.

Sampling and analyses

Distribution of uranium and its daughter products (^{226}Ra and ^{210}Pb) was studied in the uppermost horizons of the oxidized brown coals which are lying down straight

under recoating quarternary sediments. Sampling of the oxidized brown coals was carried out in the southwest part of the Kansko-Achinsk basin in active coal opencast mines (Berezovsky, Novoaltatsky and Itatsky), and in natural outcrops at Glinka village (Fig. 2). Presence and the scope of radioactive anomalies were preliminarily investigated by means of the field radiometry followed by selection of representative samples for the laboratory gamma spectrometry analysis. In the absence of signs of radioactive anomalies the sampling was carried out in arbitrary points. Representative samples of coal were taken down to the depth of 0.5 - 2.5 m from the contact with overlying rocks with the steps 5, 10 or 20 cm.

Definition of ^{238}U, ^{226}Ra and ^{210}Pb contents in studied samples was carried out in laboratory using a high-resolution semiconductor gamma-spectrometry technique. Low-energy gamma lines were used as analytical signal: 46.5 keV - for ^{210}Pb, 63.3 and 92 keV - ^{238}U (by ^{234}Th) and 186.1 keV - ^{226}Ra. The procedure was adapted for measuring 10 cm^3 samples in the HPGe well-type detector (Melgunov et al. 2003; Gavshin et al. 2005). Limits of detection of specified radioisotopes for 10 cm^3 sample were not worse then 3 Bq\kg at the counting time equal to 24 hours.

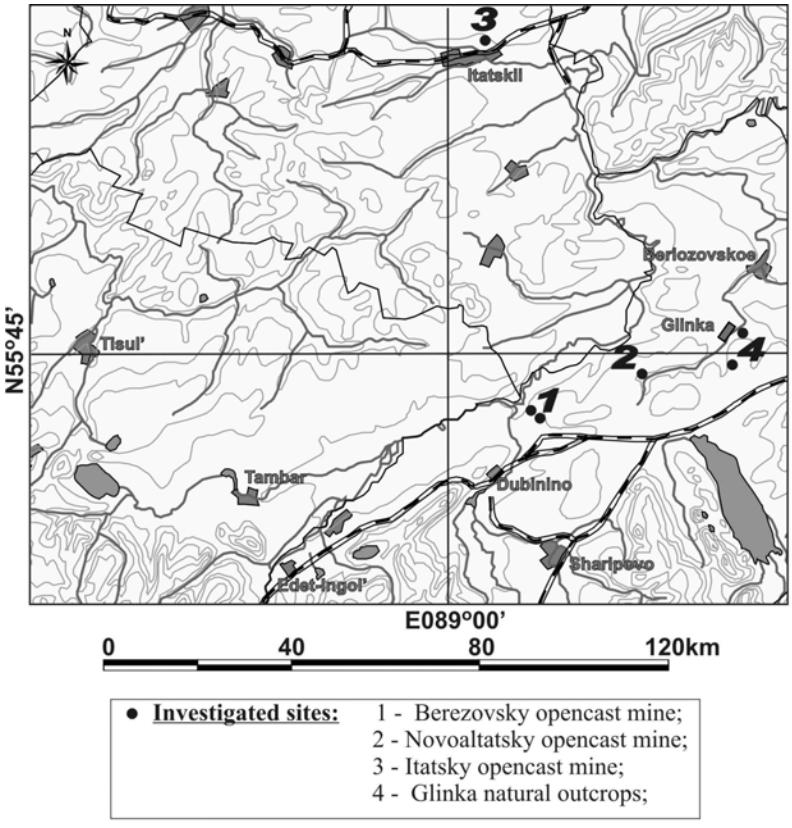

Fig.2. Location of the sampling sites of the oxidized brown coals.

Results and discussion

Background radioactivity

The background radioactivity has no precise determination. As it was mention earlier, average contents of uranium in unaltered brown coals of the Kansko-Achinsk basin vary in the range of 12-140 Bq/kg. In this study we take the value of 100 Bq\kg as the upper limit of the background for brown coals. For the background in a specific point we shall accept such level, below which the value of radioactivity is stabilized downward into the coal beds. Excess over a background is qualified as anomalies of a radioactivity.

Radioactivity anomalies in the oxidized brown coals

In this section the results characterizing distributions of ^{238}U, ^{226}Ra and ^{210}Pb in the uppermost horizons of the oxidized brown coals are presented. In all studied points the abnormal contents of the specified isotopes are fixed in a zone of "sooty-" (the uppermost, near contact layers) and oxidized coals. Diagrams characterized the distributions of ^{238}U, ^{226}Ra and ^{210}Pb are presented for two selected sites of the Berezovsky opencast mime (Fig. 3),the Novo-Altatsky opencast mime (Fig. 4), the Itatsky opencast mime (Fig. 5) and for the natural outcrops near the Glinka village (Fig. 6).

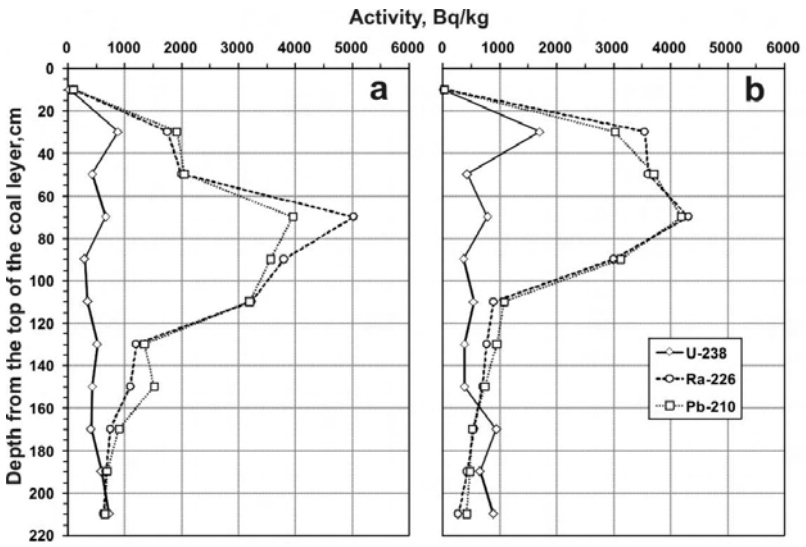

Fig.3. Radioactive anomalies in the oxidized brown coals. Selected sites (a and b) of Berezovsky opencast mine.

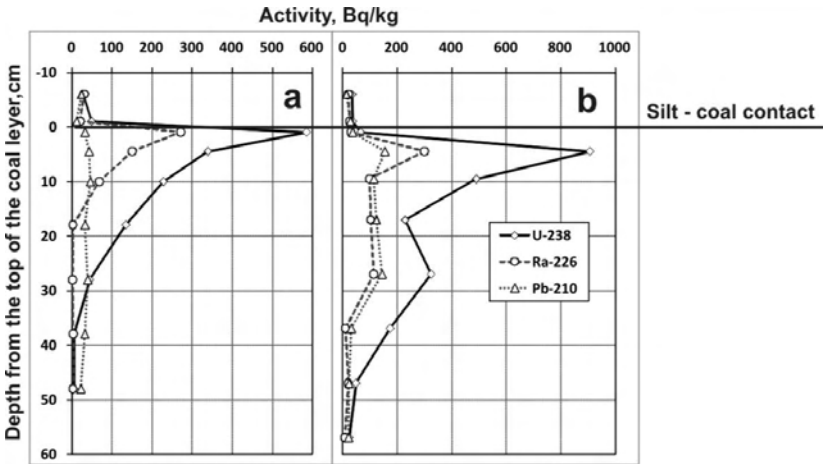

Fig.4. Radioactive anomalies in the oxidized brown coals. Selected sites (a and b) of Novo-Altatsky opencast mine.

The analysis of data of figures 3-6 shows that three types of radioactive anomalies can be distinguished differed by the ratio of activities of ^{238}U and ^{226}Ra: 1) Equilibrium; 2) Radium; 3) Uranium.

"Equilibrium"-type anomaly is observed in the natural outcrops near the Glinka village (Fig. 6). Such anomalies are characterized by presence of the quasi radioactive equilibrium between ^{238}U and ^{226}Ra. This is the evidence of the absence of any modern significant geochemical processes which can lead to separation of U and its decay products.

For "Radium"-type anomalies a considerable excess of Ra is observed. The strongest disequilibrium in the uranium family with significant deficiency of ^{238}U was found in the Berezovsky opencast mine (Fig.3). Signs of the "Radium"-type anomaly are visible in Itatsky opencast mine site (Fig. 5). Here underneath the uranium excess peak the second, radium one, can be seen. It is safe to say here about presence of some geochemical processes leading to removal of U already after accumulation of its decay products.

In "Uranium"-type anomalies ^{238}U prevails over its daughter products. It is the case of quite recent uranium migration and its enrichment relative to Ra, likewise in the Novo-Altatsky (Fig. 4) and Itatsky (Fig. 5) opencast mines. Sign of "Uranium"-type anomaly is presented in the lowest studied coal horizons in the Berezovsky opencast mine (Fig. 3, b)

Disequilibrium caused by natural Rn emanation in coals is observed in the Glinka village sites (Fig. 6) and in the upper horizons of the Novo-Altatsky opencast mine sites (Fig. 4). It was fixed by depletion of ^{210}Pb resulted from migration of its predecessor - heavy ^{222}Rn outside the U-Ra anomaly.

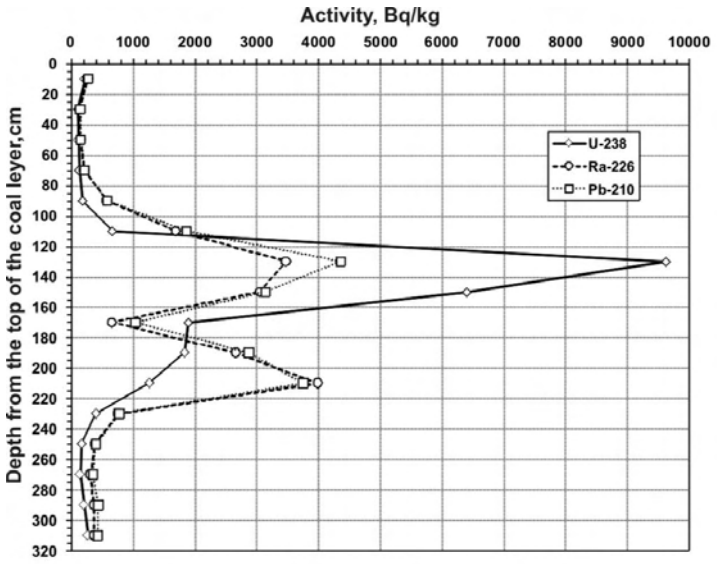

Fig.5. Radioactive anomalies in the oxidized brown coals. Selected site of Itatsky opencast mine.

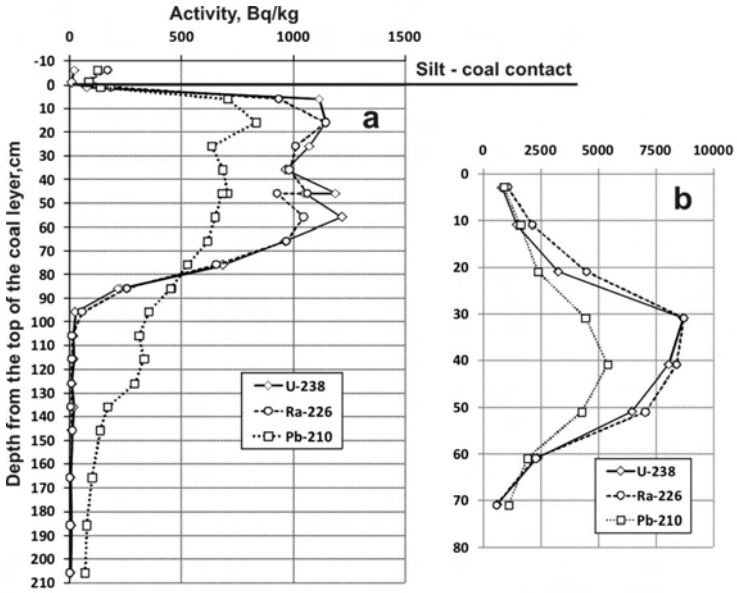

Fig.6. Radioactive anomalies in the oxidized brown coals. Selected sites (a and b) of Glinka natural outcrop.

References

Arbuzov S.I., Ershov V.V. (2007) Geochemistry or rare elements in coals of Siberia. Tomsk D-Print: 468 (In Russian)

Arbuzov S.I., Ershov V.V., Rikhvanov L.P et al. (2007) Rare-metal potential of Minusinsk basin coals. Novosibirsk: publ SB RAS Branch Geo: 347 (In Russian)

Burtsev M.P. (1961) Kansk-Achinsk coal basin. Geology and coal-bearing potential. Sov. Sci. Acad. Press Moscow: 138 (In Russian)

Gavshin V.M., Miroshnichenko L.V. (2000) Uranium concentration in altered brown coal located under burnt rocks from the Kansk-Achinsk basin, West Siberia. Geostandards Newsletter 14(2): 241-246

Gavshin V.M., Melgunov M.S., Sukhorukov F.V., Bobrov V.A. et al. (2005) Disequilibrium between uranium and its progeny in the Issyk-Kul system (Kyrgyzstan) under a combined effect of natural and manmade processes. J Env. Radioact. 83: 61-74.

Gavrilov K.V., Ozersky A.Yu. (1996) Kansk-Achinsk coal basin. Nedra Moscow: 271 (In Russian)

Grigor'ev K.N. (1968) Kansk-Achinsk coal basin. Nedra Moscow: 184 (In Russian)

Melgunov M.S., Gavshin V.M. Sukhorukov F.V., et al. (2003) Radioactivity anomalies on the southern coast of Lake Issyk Kul (Kyrgyzstan). Himiya v Interesah Ustoichivogo Razvitiya (Chem. for Sustainable Development) 11: 869-880 (In Rusian)

Yudovich Ya.E., Ketris M.P. Valuable trace elements in coal. Ekaterinburg: UrO RAN 2006: 538 (In Russian)


Uranium Mining
and Hydrogeology

Assessment of radiological impact of mining and processing low grade uranium ores on the environment and monitoring strategies

Amir Hasan Khan and Raja Ramanna Fellow

Environmental Assessment Division, Bhabha Atomic Research Centre, Trombay, Mumbai-400085, India, E-mail: ahkhan@barc.gov.in

Abstract. Low grades of uranium ores are mined by underground and opencast methods in many countries for several decades. Environmental considerations have assumed increasing importance during the recent times. Uranium mining results in generation of large quantities of waste rocks, sub-ores and mill tailings with low radioactive content. These, in turn, result in emanation and atmospheric dispersal of radon and its progeny in the vicinity of the mines and the tailings facilities. Mine water, runoff water from ore and waste rock stockpiles and that from the tailings facility even after treatment have the potential to carry small amounts of radioactivity in to the nearby aquatic system. Assessment of radiological impact of the operations on the environment is, therefore, important before undertaking mining and processing of uranium ores. Regulatory bodies require these assessments to be made and have issued guidelines.

With the exception of a few mines in some countries, most uranium ores mined in different countries have average grades between <0.05 to 0.3 % U_3O_8. This paper aims to evaluate the radiological impact of mining and processing of an ore with average grade of 0.1 % U_3O_8, so that for a particular grade of ore the values may be scaled appropriately. The waste rocks, ore heaps and tailing piles have the potential of low level gamma radiation exposure only in the immediate vicinity. Radon emanating from these materials has the potential to disperse in the atmosphere but is likely to get diluted to natural background levels with in short distances. The regulatory requirements, preoperational impact assessment and monitoring strate-

gies such as baseline surveys, in-operation monitoring of gamma radiation, radon and its progeny and natural radioactivity in aquatic systems are discussed. The estimates indicate that radiological impact of mining and processing low grade uranium ores is only marginal and confined to immediate vicinity of the operations. For example, radon emanation rate from the tailings emerging from an ore containing 0.1 % U_3O_8 is estimated at 5.6 $Bq.m^{-2}.s^{-1}$. This is reasonably comparable to the radon emanation rate of 1.3 $Bq.m^{-2}.s^{-1}$ from Olympic Dam tailings emerging from an ore of 0.08 % U_3O_8 and 1.53 $Bq.m^{-2}.s^{-1}$ reported for Indian uranium tailings emerging from ores below 0.07 % U_3O_8. The difference may be due to varying moisture content of the tailings. An area source of 10^5 m^2 is unlikely to contribute more than 0.3 $Bq.m^{-3}$at 1 km to the natural background radon concentration of 10-15 $Bq.m^{-3}$.

Introduction

India has an impressive plan of increasing its nuclear share of electricity from the present level of about 3 % to 10% by 2022 (McDonald 2008). Natural uranium being the basic fuel for its first phase of nuclear power programme, an increase in the momentum of prospecting, mining and processing of uranium is inevitable. The country has moderate reserve of uranium in the form of low grade ore spread over different parts of the country. Uranium ore deposit sites in India are shown in Figure-1 (Bhasin 1997). Currently there are four underground uranium mines operating at Jaduguda, Bhatin, Narwapahar and Turamdih in Singhbhum East in eastern state of Jharkhand. One underground mine at Bagjata and an opencast mine at Banduhurang are at different stages of development in the same state. Work on the development of another underground uranium mine with low grade of ore is in progress at Tumalpalle in the southern state of Andhra Pradesh. Mining and processing at the other low grade deposit sites at Mahuldih in Jharkhand, Lambapur-Peddagattu in Andhra Pradesh and at Killung (Kaul et al 1990) in the northeastern state of Meghalaya is to be taken up after completion of the regulatory processes (Gupta 2004). The deposits at Lambapur and Killung are amenable to opencast mining. In addition to those at Jaduguda and Turamdih, uranium mills will be constructed at the other ore mining sites.

While underground mining gives rise to relatively small quantities of solid waste, the opencast mines generate large quantities of solid wastes in the form of waste rock and overburden with a small potential for radiation exposure in the environment. In view of the low ore grades, the processing operations generate large quantities of mill tailings requiring adequate treatment and confinement. The mill

tailings also have potential for exposure in the environment from the gamma radiation and radon emanation. The wastes from low grade uranium ore mining and processing are very visible features of the industry inviting public attention. Hence, management of the wastes from the uranium mining and ore processing industry requires not only adequate treatment and confinement to meet regulatory constraints but also need a proactive campaign to address public concerns.

India has a long experience of radiological safety at workplace and in the environment. To meet growing environmental concerns all over the world and emerging regulatory norms, the industry has responded by detailed preoperational environmental impact assessment, baseline surveys by independent agencies, public information and societal participation in the monitoring programme. This paper gives an outline of the programme related to radiological safety in the environment of uranium mining industry in India.

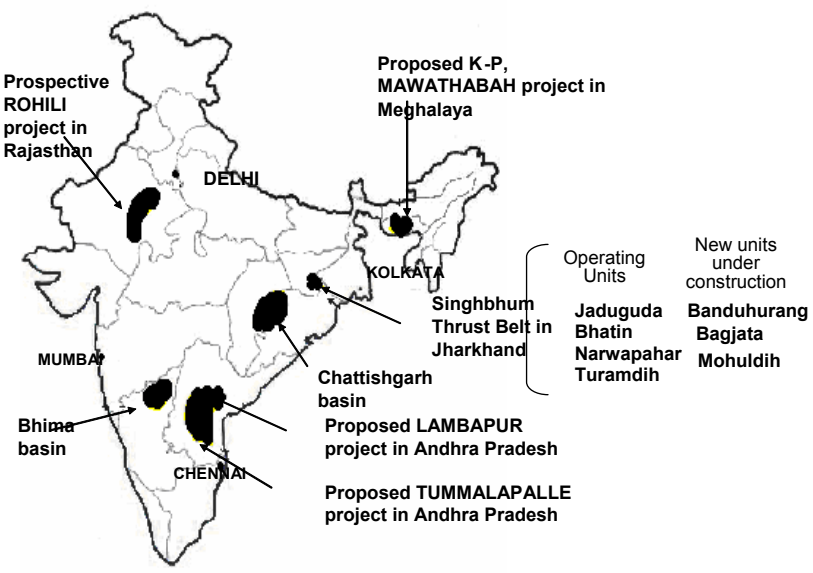

Fig.1. Uranium mining centres in India.

Environmental impact

The environmental impact of mining and ore processing arise from the storage of overburden, waste rock, ores in the stack yard, mill tailings, release of liquid effluents from mining, milling and tailings confinement facility and gaseous release from exhausts, waste rocks and ore storage and tailings surface. The radiological impacts of uranium mining in the environment are mainly identified as:

a. gamma radiation
b. radon and its progeny
c. ore and tailings dust
d. radioactivity in the effluents from mine, mill and tailings facility
e. pickup of radioactivity by vegetation and plants

Environmental impact assessment

Along with the production of ore, the mining operations generate significant quantities of overburden, waste rock and water from the mine strata or that used in drilling, dust suppression and backfilling (stowing). The waste rock is stored on surface with appropriate sloping and soil cover either permanently or as an interim measure so that some of these could later be filled back in mine cavities. Similarly, ore produced is either stored near mine site or near the mill as buffer stock. Some ore is always available in the ore bins of the milling plant. The large volume of mill tailings emerging after recovery of uranium is partly filled back in the mines and partly stored permanently in engineered facility for permanent storage and confinement.

To assess the environmental impact from a proposed mine, following assumptions are made:

Average ore grade	: 0.10% U_3O_8
Cut off grade (over burden/waste rock grade	: <0.02 % U_3O_8
Over burden storage area	: 10 hectare (ha)
Stockpile of ore at the mine	: 75 00 tonne
Fine ore bin stock (mill)	: 5 000 tonne
Tailings surface area	: 10 hectare (ha)
Mine backfill area exposed at a time	: 1 hectare (ha)

The radiological impact of the waste rock and over burden, ore storage and tailings system have three components, namely, gamma radiation, radon and long-lived radioactivity in the airborne ore dust. Since the long-lived radioactivity of the ore dust for grades below 1% U_3O_8 is considered insignificant (IAEA1989), only the gamma radiation and radon component are considered.

Gamma radiation

Radiation dose and radon emanation from the ore, over burden and the tailings pile depend on the radium content of the material and other factors like porosity and moisture. Assuming radioactive equilibrium, the radium-226 content of the ore and the mill tailings for an average ore grade of 0.10% U_3O_8 work out to be 10.4 $Bq.g^{-1}$. The gamma radiation at 1 m from the waste or over burden stockpile may be computed from the relation (IAEA, 1992 a),

$$\text{Gamma dose rate } (\mu Gy.h^{-1}) = 0.48\ C_{Ra}\ (Bq.g^{-1}),$$

where C_{Ra} is radium content ($Bq.g^{-1}$).

Similarly, radium-226 content of the over burden and waste rocks with cut off grade <0.02% U_3O_8 will be <2.0 $Bq.g^{-1}$, though average radium-226 content of the over burden will be much lower, as it will also contain soil and rocks with very low radium. The radium in over burden may typically be taken as 1.0 $Bq.g^{-1}$. Due to self attenuation, only a few meters of the outer layer of the waste rock or ore stockpile may contribute to environmental gamma radiation. Hence, gamma radiation near the source at different storage areas may work out as,

At 1 m from over burden and waste rock pile : 0.48 – 0.96 $\mu Gy.h^{-1}$
At 1 m from the ore storage area : 5.0 $\mu Gy.h^{-1}$
At 1 m above the tailings pile : 5.0 $\mu Gy.h^{-1}$
At 1 m above the mine backfill area : 5.0 $\mu Gy.h^{-1}$

As the intensity of gamma radiation reduces rapidly with the distance, it is expected to reduce to the background level of about 0.10 $\mu Gy.h^{-1}$at a distance of about 30 m. Hence, gamma radiation attributable to mining activities will be confined to small distances within the plant premises with negligible impact in the environment; beyond about 30-50 m. Similarly, the impact of tailings pond and the back filled mines on the gamma radiation field will also be limited to a distance of about 30 - 50 meter.

Radon emanation from ore

Radon emanation from rocks depends to a large extent on radium-226 content, porosity and exposed surface area, reducing with increasing porosity beyond about 20%. With a conservative value of 0.25 as radon emanation coefficient (E) for ore and waste rock pieces as that of fine tailings, the radon production rate from the ore stockpile may be computed as (IAEA, 1992 b),

Rn ($Bq.s^{-1}$) = Quantity of ore (T) x 10^6 g $.T^{-1}$ x C_{Ra} ($Bq.g^{-1}$) x λ_{Rn} (2.06 x 10^{-6} s^{-1}) x E

Radon from ore stock pile of 7500 tonne at the mine : 4.0 x 10^4 $Bq.s^{-1}$
Radon from 5000 tonne stock in mill fine ore bin : 2.7 x 10^4 $Bq.s^{-1}$

Although rate of radon released to the atmosphere is expected to be much lower than its production rate due to decay within the ore volume, the entire radon produced per second is taken as the radon released to the atmosphere, as a conservative approach.

Radon emanation from tailings and backfilled mine surfaces

Radon emanation from uranium tailings is known to be only from an effective thickness of the top 2 to 3 metres layer, as radon produced in lower layers decays before reaching the surface. The radon flux from uncovered tailings is given by the relation (IAEA, 1992 b),

$$F_t\,(Bq.m^{-2}.s^{-1}) = C_{Ra}\,\rho\,E\,(\lambda D_t)^{1/2}$$

where F_t is radon flux or emanation rate

C_{Ra} is radium-226 content ($Bq.kg^{-1}$)
E is emanation coefficient (0.25)
ρ is the material bulk density ($kg.m^{-3}$) (~1.5×10^3 $kg.m^{-3}$)
D_t is diffusion coefficient ($m^2.s^{-1}$) (1×10^{-6})
λ is decay constant of radon (2.06×10^{-6} s^{-1})

The radon emanation rate from surfaces of the tailings and back filled mine works out to be 5.6 $Bq.m^{-2}.s^{-1}$. In field, it is likely to be much lower because of moisture content of tailings. For example, the measured radon emanation rate from the Olympic dam tailings in Australia from an ore of grade 0.08% U_3O_8, comparable to the value of 0.1 % U_3O_8, is 1.3 $Bq.m^{-2}.s^{-1}$ (IAEA, 1992). The measured radon emanation rates at Jaduguda tailings from an ore grade of 0.06% range from 0.11 and 6.23 U_3O_8, with an at 1.53 $Bq.m^{-2}.s^{-1}$ (Khan 2000, Jha et al 2001).

The estimated radon emanation rates and total concentration from all sources are summarised in Table 1.

All the sources of radon considered above will be area sources located about a km or more away from each other. Considering the largest radon source term of 5.6×10^5 $Bq.s^{-1}$ contributed by the uncovered tailings pond and using the atmospheric dilution factor of 9.7×10^{-7} $Bq.m^{-3}$ per $Bq.s^{-1}$ (UNSCEAR 2000), the contribution to the atmospheric radon at a distance of 0.5 km will be 0.54 $Bq.m^{-3}$. At 1 km, 2 km and 5 km this contribution will reduce to 0.30 $Bq.m^{-3}$, 0.14 $Bq.m^{-3}$ and 0.03 $Bq.m^{-3}$, respectively. The dilution factors for 1, 2 and 5 km are 5.3×10^{-7}, 2.5×10^{-7} and 7.1×10^{-8} $Bq.m^{-3}$ per $Bq.s^{-1}$, respectively. The radon contribution will in fact be much lower as the full tailings pond and backfilled mine surfaces will not be in use at a single point of time. This works out be an insignificant addition to the atmospheric radon, which has a natural background level of 10 – 15 $Bq.m^{-3}$.

With the dose conversion factor of 6×10^{-6} $mSv.h^{-1}$ per $Bq.m^{-3}$ of radon [UNSCEAR 2000; Chambers et al. 2001] the annual dose from radon and its progeny at a distance of 0.5 km from the source is estimated as 0.028 $mSv.y^{-1}$for full year of continuous exposure. This is about 3 % of the annual dose limit of 1 $mSv.y^{-1}$ for members of public (IAEA 1996; ICRP 1991). At distances of 1 and 2 km the annual doses from radon and progeny will be 0.016 $mSv.y^{-1}$ and 0.007 $mSv.y^{-1}$, respectively.

Table.1. Radon emanation rates and output from different sources.

Source	Emanation rate ($Bq.m^{-2}.s^{-1}$)	Area Hectare (ha)	Total radon output ($Bq.s^{-1}$)
Mine ore stock	-----	----	4.0×10^4
Mill ore stock	-----	-----	2.7×10^4
Backfilled mine surface	5.6	1	5.6×10^4
Tailings surface*	5.6	10	5.6×10^5
Over burden / Waste rock*	0.5 – 1.0	10	$0.5\text{-}1.0 \times 10^5$

*The emanating surfaces will be subsequently covered with overburden and soil

Particulate dust

Longlived radioactivity from ore and tailings dust is significant only for ores grades above 1 % U_3O_8. Control measures of water spray and dust extraction at the mine and mill sites and proper soil and vegetation cover over the waste rocks and tailings surfaces will further reduce the potential for generation and dispersal of dust.

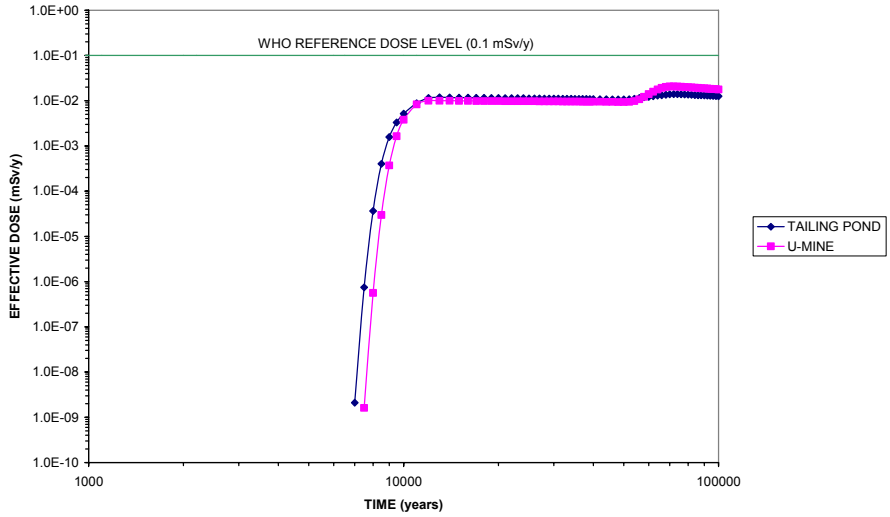

Fig.2. Total Effective dose to the members of the public due to consumption of groundwater at 1 km distance

Radiological impact of backfilled mine and tailings pond on ground water

At the proposed mining sites, the bottom of the back filled opencast mine will be in the hard rock and tailings management envisages providing appropriate lining with effective permeability of 10^{-9}- 10^{-8} $m.s^{-1}$. In view of this, seepage of water containing radionuclides will be very low and consequently the change of uranium concentration in ground water due to ingress from the tailings deposit will also be extremely slow and low. Modelling exercises are underway to estimate the impact of backfilled mines and the tailings repository on the nearby ground water. Figure-2 gives an estimate of the dose due to uranium and its decay products to members of the public from consumption of ground water at 1 km from the sites. The study indicates that only a trivial impact may be seen, that too after about 8000 years.

The maximum dose of 0.01 mSv/y may occur through ground water consumption only after about 10000 years. This is 1 % of the prescribed dose limit to members of the public and about $1/10^{th}$ of the present WHO reference level (WHO, 2004). Similar projections are available for McClean mine tailings where the processed ore grade is much higher (Rowson 2000).

Environmental management

Environmental safety aspects of uranium mining as also for other mining industries come under the purview of both state and central governments. The industry submits detailed environmental management plan including mining and processing methodologies and management of solid, liquid and gaseous wastes from the industry. The likely impact on the environment, including socio-economic impact and benefits to the community, safety measures and emergency plans are submitted to the state pollution control board which reviews and, depending on the size of the project, puts it up for public hearing. Comments received during the hearing are addressed and discussions are held with technical committees before giving clearance. Thereafter the project is reviewed by the appropriate authorities of the central government like the Ministry of Forest and Environment and the Atomic Energy regulatory Board. Only after a detailed review at different levels the project may proceed further. It will be subject to periodic review by the regulatory authorities. Effluent treatment plants and environmental monitoring are the integral parts of environmental management plan.

The current practice of managing the waste or treated mill tailings is to fill the coarse fraction of the tailings in to the underground mine cavities and store the finer portion in engineered containment system. For the proposed opencast mines one alternative for tailings management envisaged is to fill it in the worked out portion of the mine while continuing mining activity progressively in other portions. This way relatively smaller area may be required for the confinement of the remaining tailings. The tailings, whether backfilled in the worked out opencast mine or in the separately engineered confinement facility, are proposed to be covered with suitable layer of waste rocks and soil and plantation of vegetation after appropriate contouring to facilitate quick drainage of rain water with little scope for percolation in to the tailings.

Baseline surveys

The industry is required to carry out a baseline survey comprising of radiological as well as conventional pollutants present in the environment; in air, water and soil. Radioactivity and trace metal contents of the local vegetation and food items are also studied. Demographic and health status surveys are also undertaken. The recent trend is to get the baseline studies conducted through educational and re-

search institutions of repute. Initial baseline gamma radiation levels obtained at one of the proposed sites are summarized in Table 2 (Khan 2004).

Gamma radiation levels monitored using environmental TLDs gave results comparable to those observed using the radiation survey meters (Chougaonkar et al 2004).

Initial data on radioactivity levels in surface waters and soil near one of the proposed opencast mining sites in a high rainfall region are presented in Table 3 and Table 4.

Table.2. Natural background gamma radiation around the proposed uranium mining site at Killung, Meghalaya state**:**

Sl. No	**Location**	**Radiation Level $\mu Gy.h^{-1}$**	
		Range	**Average**
1	Killung ore block	0.11 – 0.23	0.17
2	Starting of Killung block	0.19 –0.36	0.25
3	Around Lambajrain village	0.11 – 0.22	0.15
4	1 to 2 km from Killung	0.13 – 0.15	0.14
5	Phot Killung (stream) crossing	0.33 – 0.36	0.35
6	Killung stream, in contact with ore out crop	1.10 – 1.20	1.16
7	Killung stream 1 m above ore out crop	0.75 – 0.85	0.80
8	Phot Killung (stream), U/S	0.19 - 0.26	0.23
9	Mawpynden (Wah Kharae stream)	0.12 – 0.15	0.14
10	~100 m SE of Mawpynden	0.13 – 0. 24	0.19
11	~3 km from Killung, (Domiasiat village)	0.14 – 0.17	0.16
12	Domiasiat village, near a hut	0.10 – 0.15	0.12
14	~10 km from Killung	0.10 –0.14	0.12
15	Wahkaji (about 13-14 km from Killung)	0.10 – 0.15	0.12
16	Mariyam village (~8 km from Wahkaji)	0.21 - 0.25	0.23
17	Jakrem crossing, 48 km from Wahkaji	0.20 - 0.38	0.33
18	Near Jakrem hot spring	0.43 – 0.47	0.45
19	Shillong city	0.09 – 0.14	0.13

Table.3. Background uranium and radium in surface waters around Killung mining site.

Sl. No	Location	U(Nat) $mg.m^{-3}$	^{226}Ra $Bq.m^{-3}$
1	Killung stream U/S	<0.5	27.8
2	Killung stream D/S	<0.5	< 3.5
3	Photrongam stream U/S	<0.5	48.2
4	Photrongam stream D/S	2.8	< 3.5
5	Umsophew river U/S	<0.5	8.8
6	Umsophew river D/S	<0.5	28.5
7	Wah Phodthra river U/S	<0.5	9.9
8	Wah Phodthra river D/S	<0.5	< 3.5
9	Jadukata river U/S	<0.5	< 3.5
10	Jadukata river M/S	<0.5	< 3.5
11	Jadukata river D/S	<0.5	3.9
	Derived Limit	**60**	**300**

Table.4. Uranium and radium in soil around Killung ore deposit.

Sl. No	Location of Sample	U(Nat) $mg.kg^{-1}$	^{226}Ra $Bq.kg^{-1}$
1	Within the Killung block	3.0	28.8
2	Outside the Killung block	2.7	35.8
3	Within the Rongam block	3.1	19.1
4	Outside the Rongam block	2.4	29.8
5	Proposed Tailings pond site	2.8–7.8	8.4-13.8

The above data are presented as an example of the baseline surveys. Detailed surveys are being carried out through the North Eastern Hill University, which is a reputed educational and research institution in the region. The detailed surveys include measurement of natural radioactivity, trace metals and other chemical pollutants in different environmental matrices and pickup of radioactivity by different plant species. The demographic and health status survey is also a part of the baseline studies.

Monitoring strategy

Radiological safety and environmental survey laboratories are established to carry out regular monitoring of the workplace and the environment at every uranium mining and ore processing site. The environmental survey laboratories are generally outside the administrative control of the mining industry. The regular environmental monitoring program includes periodical sampling and analysis of effluents from the mine, mill and the tailings system, surface and ground waters, soil, vegetation, edible vegetables, aquatic biota and foodstuff. Environmental levels of dust and radon are also monitored. Besides spot surveys for the natural radiation levels and atmospheric radon, thermoluminiscent dosimeters and passive radon monitoring systems are deployed at appropriate locations around the facility. On-line radiation and radon monitoring instruments are being developed for monitoring around the facility. The results would be accessible to the industry as well as the regulatory body.

Societal monitoring

As a confidence building measure, a concept of societal monitoring is being developed to encourage participation of local community of teachers, students and village representative to carry out environmental monitoring. This requires providing training to the participants in use of simple monitoring instruments.

Public awareness

Public awareness programmes are organised at the existing and proposed mining sites to inform the representative section of the society about radiation and radioactivity from natural and industrial sources, their impact and control measures adopted. Student community, local stakeholders, village representative and media personnel are the target groups for these public awareness programmes.

Conclusion

The preoperational assessments made indicate that with appropriate control measures from beginning of the operations, the radiological impact on the environment from mining of low grades of uranium ore will be only marginal.

Acknowledgement

The support provided by "DAE-BRNS Raja Ramanna Fellowship" is gratefully acknowledged. Thanks are due to Mr. H.S. Kushwaha, Director, Health Safety &Environment and Mr. V. D. Puranik, Head, Environmental Assessment Division, Bhabha Atomic Research Centre for the support provided. Cooperation received from my colleague Mr. Sunil Kumar Sahoo in preparing the manuscript is appreciated. Assistance received from Ms Indumati of EAD is also acknowledged.

References

Bhasin, J. L. (1998) Mining and milling of uranium ore: Indian scenario, IAEA Techdoc-1244 (2001), Impact of new regulations on uranium exploration, mining, milling and management of its waste, proceedings of Technical Committee meeting held in Vienna, 14-17 September 1998, pp. 189-200.

Chambers D.B, Lowe L.M and Stager R.H (1998), Long term population dose due to radon (Rn-222) released from uranium mill tailings, IAEA-Techdoc-1244 (2001), Impact of new environmental and safety regulations on uranium exploration, mining, milling and management of its waste, proceedings of Technical Committee meeting held in Vienna, 14-17 September 1998 pp. 9 – 27.

Chougaonkar, M. P., Walling, I. M., Khan, A. H., Hoda, S. Q. and Puranik, V. D. (2004), Preliminary results of the preoperational radiation survey carried out in the environs of Domiasiat, Meghalaya, India, using TLD Technique, Proceedings of Thirteenth National Symposium on Environment, June 5-7, 2004, North Eastern Hill University, Shillong, India

Gupta (2004), Uranium mining and environment management – The Indian scenario, Proceedings of Thirteenth National Symposium on Environment, June 5-7, 2004, North Eastern Hill University, Shillong, India

IAEA (1989), Radiation monitoring in the mining and milling of radioactive ores, Safety Series No. 95.

IAEA (1996), International Basic Safety Standards for Protection against Ionizing Radiation and for Safety of Radiation Sources, Safety Series no. 115.

IAEA (1992 a), Current Practices for the management and confinement of uranium mill tailings, Technical Report Series No-335.

IAEA (1992 b), Measurement and calculation of radon releases from uranium mill tailings, Technical Report Series No-333.

ICRP (1990), Recommendations of the International Commission on Radiological Protection, ICRP Publication No. 60 (1991).

ICRP (1993), Protection against Radon-222 at home and at work. ICRP Publication no. 65.

Jha, S., Khan A. H. and Mishra, U. C., A study of the technologically modified sources of ^{222}Rn and its environmental impact in an Indian U mineralised belt, Journal of Environmental Radioactivity, 53 (2001), pp. 183-197.

Kaul R and Verma H.M (1990), Geological evaluation and genesis of the sand stone type uranium deposit in Domiasiat, West Khasi Hills, District Meghalaya, India, Exploration and Research for Atomic minerals, Vol. 3, 1-16, 1990.

Khan, A.H., Basu, S.K., Jha, V.N., Jha, S. and Kumar, R., (2000), Assessment of Environmental Impact of Mining and Processing of Uranium Ore at Jaduguda, IAEA International Symposium on the Uranium Production Cycle and the Environment at Vienna, Oct. 2 – 6, 2000.

Khan A. H., Sahoo, S. K., Jha, V .N., Tripathi, R. M., Nair, R.N., Shukla, V. K., Seshadri, M .and Puranik V.D.(2004), A report on assessment of radiological impact of the proposed uranium mining operations at Domiasiat, West Khasi Hills, Meghalaya.

McDonald, A., Nuclear power: Global status, IAEA Bulletin, Vol. 49-2, March 2008, pp.45-48.

Rowson J, 2000, Tailings management at COGEMA resources inc.'s McClean lake operation, IAEA International Symposium on the Uranium Production Cycle and the Environment at Vienna, Oct. 2 – 6, 2000.

UNSCEAR, (2000), Sources and effects of ionising radiation, United Nations, Vol. 1, 2000.

WHO 2004, Guidelines for drinking water, Vol.1, 2004.


Uranium Mining
and Hydrogeology

Method of reducing radon levels in buildings

Rashid A. Khaydarov[1], Renat R. Khaydarov[1] and Seung Y. Cho[2]

[1]Institute of Nuclear Physics, Tashkent, Uzbekistan
[2]Yonsei University, Seoul, South Korea

Abstract. The paper deals with examination of the method of chemical treatment of walls, floor, ceiling, roof, etc for prevention of radon seeping into buildings. The mixture of organic compounds and catalyst are used to fill micropores inside the concrete or other constructive materials against radon, as well as other gases, and water molecules. The method allows reducing the coefficient of gas (air, Ar and ^{222}Rn) permeability 200 – 400 times. The consumption of the chemicals is 0.2 L/m^2 for gypsum and 0.3-0.4 L/m^2 for concrete and cement and it depends on porosity of the materials.

Introduction

Radon is a naturally occurring gas seeping into homes and underground structures (buildings, tunnels, hangars, garages, etc.) from the surrounding soil through walls, floor, etc. and emanating from construction materials such as concrete, granite, etc (Brooklins 1990). It is known that radon concentration is particularly great in regions with the heightened content of uranium in soil and water and with geological breaks of the earth crust (Chernik et al. 1997).

The purpose of this work was to develop a method to reduce concentration of radon gas in buildings and underground structures. This task can be solved by using special chemicals, which fill microcrevices and minute pores inside the concrete or other building materials against gases, as well as water molecules (Khaydarov et al. 2006). The layer with filled pores stops the diffusion of molecules of gases and income through the slab, as well as the walls, floors and ceilings. And in addition, it blocks the other gases pathway – water migration.

There are many chemicals preventing water diffusion in concrete and other building materials, but they do not change gas permeability of concrete and gases including radon migrates through them easily. The chemicals intended for prevention of gas seeping through constructive materials meet following requirements: low price and consumption, high efficiency with reducing the gas permeability

400-500 times, wide range of operation temperature from 1-2^{0}C to 40-50^{0}C and air humidity from 2-5% to 95-98%, low water consumption.

Materials and methods

The following organic compounds have been tested: polyethylhydrosiloxane (PEHS) and its aqueous emulsion, mixture of PEHS and benzene in the ratio 1:1, 25% solution of alkyltriethoxysilane (ATES) in isopropanol (25%ATES), mixture of PEHS and 25% solution of ATES in isopropanol. Sn-, Ti-, and Cu- organic compounds were tested as the catalysts.

Tested samples of concrete, cement and gypsum had the height and the diameter of 15-20 mm and 30 mm, respectively. The samples in a vertical position were treated by chemicals by means of spray.

The device for examination of gas permeability of concrete samples has been constructed. The device consists of compressor 1, receiver 2 with manometer 3, gates 4,5, holder 6 of concrete samples 7, flow meter of air 8 and vessel with gas 9 (Fig.1). The gate 5 adjusted the value of the gas pressure. In all experiments the pressure of gases in the receiver was chosen to be 110 kPa. The air, Ar and ^{222}Rn with concentration of 100 pCu/L in air were used as the gases.

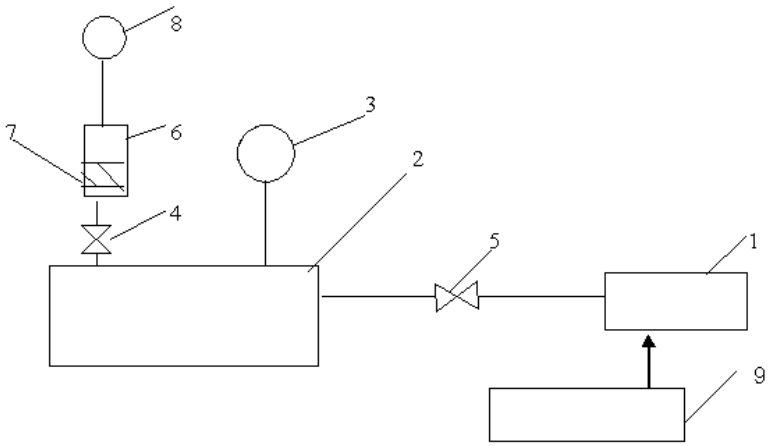

Fig.1. The scheme of the device for examination of radon permeability through building samples: compressor 1, receiver 2 with manometer 3, gates 4,5, holder 6 of building samples 7, flow meter of air 8, vessel with gas 9.

The coefficient of gas permeability K was determined by the following formula

$$K = \Delta V\ d / S\ \Delta t\ \Delta p, \quad (1)$$

where Δt is the time of passing the gas through the sample, ΔV is the volume of gas passed through the sample, Δp is a pressure drop of gas in the sample, S is an area of the sample, d is a thickness of the sample. In these experiments we have measured relations R between the coefficients of gas permeability for chemically non- treated samples K_0 and treated samples K:

$$R = K_0/K. \quad (2)$$

The gas permeability of concrete after the treatment by chemicals was examined. Influence of types of cement and sand, preliminary treatment by different chemicals including silicoorganic compounds, time periods between treatments, moisture of concrete, time between preparation of chemicals and treatment of concrete (aging of chemicals), time between treatment of concrete and testing (aging of treated concrete) were investigated. Concentration of ^{222}Rn in air was determined by radon measurement detector. The detector allows realizing continuous radon monitoring. It consists of electronic unit and scintillation cell. The electronic unit contains power supply, amplifier, discriminator, timer, counter, and indicator. The scintillation cell contains the zinc sulfide scintillator, photomultiplier, preamplifier, high voltage power supply and chamber with a volume of 200 mL over the scintillator. This chamber is intended to fill with gas to be analyzed. Air is either pumped or diffuses into the scintillation cell. Scintillation count is processed by electronics, and radon concentrations for predetermined intervals are stored in the memory of the device.

Results and discussion

In the system ATES - isopropanol a retherification of following type takes place:

$$AlkSi(OEt)_3 + (3\text{-}n)ROH \rightarrow AlkSi(OEt)_n(OR)_{3-n} + (3\text{-}n)EtOH$$

where n = 0-2, R is C_3H_7 . $AlkSi(OR)_3$, $AlkSi(OEt)(OR)_2$, $AlkSi(OEt)_2(OR)$ are the products of the retherification.

Products of this reaction are easily hydrolyzed even by air moisture

$$AlkSi(OR)_3 + 3\ H_2O \rightarrow AlkSi(OH)_3 + 3ROH$$

with formation of intermediate compounds $AlkSi(OR)_2OH$, $AlkSi(OR)(OH)_2$. When PEHS is introduced in the hydrolyzed solution, polymeric networks of linear, cyclical and ramified structures with different properties are formed, for example:

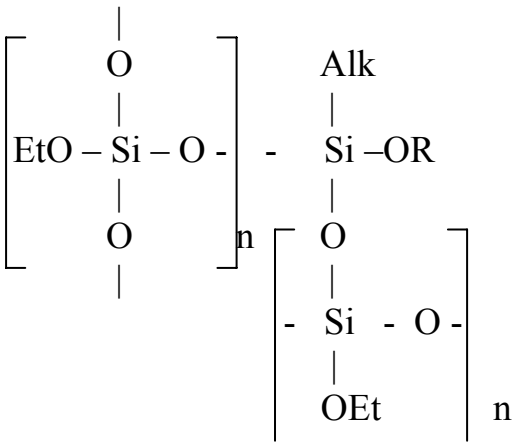

Hydrolysis of PEHS in early stages also takes place. Then the products of hydrolysis interact with ATES. The preferable formation of polymeric network type depends on methods of mixture preparation, treatment of concrete etc. Besides the reaction with $Ca(OH)_2$ takes plays and as the result the polymer is fixed strongly on the treated concrete.

Experiments have shown the following results. The depth of penetration of the organic compound without catalysts is about 10-14 cm. But polymerization time is large (about 2-3 days) and consumption of the compound is significant (about 1-2 L/m^2). The use of catalysts reduces duration of the polymerization process down to 1-3 hours. In this case the depth of penetration of chemicals into building materials is about 5-6 mm and as the result consumption of the organic compounds decreases. The treated materials have hydrophobic properties, relation R does not depend on humidity of the surface of materials.

Dependence of the relation R against the number of layers is given in Table 1. The best type of catalyst is the Sn-organic compound. The relation R for concrete increases slowly after the first layers and very fast after the 4^{th} and 5^{th} layer. It is explained by high porosity of concrete. In case of cement and gypsum R increases fast after the 2^{nd} layer. Total consumption of chemicals is about 0.4 L/m^2 for concrete (but depends on type of concrete), 0.3-0.4 L/m^2 and 0.2-0.3 L/m^2 for cement and gypsum, respectively. There is no a big difference between air, Ar and radon values of permeability.

Dependence of the relation R against the time after chemical treatment of construction materials is given in Table 2. After the 4^{th} day the relation R increases very slowly, about 5% within 7 months.

Table 1. Dependence of R vs. the number of layers.

Gas	Building material	Type of organic compound catalyst	Number of layers				Total consumption of chemicals, L/m^2
			2	3	4	6	
Air	Concrete	Sn-	2.1	3.5	110	420	0.402
		Ti-	2.0	3.1	80	320	0.560
		Cu-	1.2	2.4	45	100	0.610
	Cement	Sn-	2.5	47	120	>500	0.360
		Ti-	2.3	34	98	390	0.410
		Cu-	1.8	12	59	160	0.520
	Gypsum	Sn-	2.8	90	410	>500	0.270
		Ti-	2.6	49	380	440	0.330
		Cu-	2.2	35	280	360	0.410
Ar	Concrete	Sn-	2.0	3.4	105	400	0.400
	Cement	Sn-	2.3	45	115	>500	0.350
	Gypsum	Sn-	2.7	86	400	>500	0.260
^{222}Rn in air	Concrete	Sn-	2.1	3.5	110	430	0.400
	Cement	Sn-	2.4	46	120	>500	0.340
	Gypsum	Sn-	2.7	88	420	>500	0.260

Table 2. Dependence of R vs. time after chemical treatment of construction materials

Gas	Building material	Time after treatment, days					
		4	18	28	62	154	210
Ar	Concrete	420	420	430	430	440	440
	Cement	>500	>500	>500	>500	>500	>500
	Gypsum	>500	>500	>500	>500	>500	>500
^{222}Rn	Concrete	430	440	440	450	450	450
	Cement	>500	>500	>500	>500	>500	>500
	Gypsum	>500	>500	>500	>500	>500	>500

The authors have treated the floor, walls and ceiling of 5 specially chosen basements of buildings in 2007. This procedure has reduced the radon concentration in the premises of the first floor from 400 - 600 Bq/m^3 to the background value of 17-20 Bq/m^3.

Conclusion

The test results of these investigations demonstrate the efficacy of the described method of chemical treatment of walls, floor, ceiling, roof, etc. to prevent gas seeping into buildings. The method allows reducing the coefficient of gas (air, Ar and ^{222}Rn) permeability 200 – 400 times. Consumption of the chemicals is 0.2 L/m^2 for gypsum and 0.3-0.4 L/m^2 for concrete and cement and depends on poros-

ity of the materials. This method can be used for prevention of seeping radon through the constructive materials.

References

Brooklins D. (1990) The indoor radon problem, Columbia University Press

Chernik DA, Titov VK, Venkov VA (1997) ^{222}Rn in buildings and the underlying bedrock, Atomic energy, 82 :4, pp. 308-310

Khaydarov RA, Khaydarov RR and Gapurova OU (2006) in Medical Treatment of Intoxications and Decontamination of Chemical Agent in the Area of Terrorist Attack, NATO Security through Science Series, Springer Netherlands, v.1, pp. 219-224

Water tight Radon / Thoron probs and monitors without influence of high humidity, air pressure and temperature

T. Streil and V. Oeser

SARAD GmbH, Wiesbadener Str. 10, D-01159 Dresden, streil@sarad.de, http://www.sarad.de

Abstract. To measure Radon and Thorn simultaneously is only possible using the Alpha spectrometry. Pulse ionisation chambers are not very use full because of the bad energy resolution. The only effective method for a sufficient energy resolution is the charge collection of the Radon / Thoron daughters on the surface of a Semiconductor detector. But till now all existing monitors with this measuring principle has the disadvantage of a high influence of the humidity and temperature on the measuring values. All this devices used till now a correction algorithm or a drying tube.

With a Optimised high voltage chamber with electrostatic focus (Ion optics) like in the device RTM 1688-2 is it possible to collect nearly all short living Radon/ Thoron daughters inside the chamber at the surface of a semiconductor detector. This high electric field is special designed that the flight time of the Ions is so short that the Ion neutralisation process in chamber is negligible. Therefore the device has:

- No changes of the sensitivity due to the ambient humidity
- Usage of a drying tube or similar equipment is NOT required!
- High sensitivity at low chamber volume (approx. 3* 32,5 ml=130 ml)

Special attention was paid for the issue of quality assurance. Each stored data record contains a complete Alpha spectrum, which shows the error-free operation

of the instrument for each single integration interval. Any number of measurement series may be created by starting/stopping the data acquisition. PC can read the data stored within the instrument even if a measurement is in progress. As a matter of course the instrument is equipped with sensors for temperature, humidity and barometric pressure. An integrated tilt detector will give a signal if the instrument has been removed from its original position during the measurement.

Radon entry paths can be discovered by the “sniffing” mode. Soil gas sampling as well as Radon in water measurements is simple because of the built in pump.

The operation of the instrument is realised by only one button. A serial printer may be connected to the interface of the RTM1688-2 to present a protocol directly on site.

The instrument can be directly connected to a modem (analogue, ISDN, GSM) for remote data transmission. The Radon Vision Software (included in delivery) handles the telephone connection as simple as a direct cable link.

Further exist a watertight version with a fast gas transfer entrance window (diffusion time lower 1 min) and watertight housing. With 4 built in measuring chambers is the main application Radon /Thoron monitoring in Uranium mines or other places with high humidity or in aggressive environment. The version RTM1688 Geo consists of the watertight water soil probe (76 mm diameter) and the watertight electronic part including GSM-Modem for geological applications like (soil gas or water borehole measurements) and easy data transfer. Other versions are the watertight Analogous Radon Indoor sensor or the Analogous water/ soil probe with 0-1 V or 4.20 mA analogue output. This device can be integrated in existing SBS control system or combined with Data Acquisition systems like MEDAS.

Continuous Measurement of geo-chemical parameters in aggressive environment

T. Streil, V. Oeser and M. Ogena *)

SARAD GmbH, Wiesbadener Str. 10, D-01159 Dresden, streil@sarad.de, http://www.sarad.de
*) PNOC Energy Development Corp. PNPC Complex, Merritt Road, Fort Bonifacio, Makati City 1201, ogena@energy.com.ph

Abstract. To measure precise longtime data from geochemical parameters for studies of deep fluid streams in volcanic areas, hydro geological studies and reservoir management in geothermal fields robust and high reliable measuring systems are necessary.

A progress in this field is presented in this paper with the development of a new versatile measuring system called MEDAS (MEDAS – Modular Environmental Data Acquisition System) based on experiences and recent results from different research groups. MEDAS is an innovative multi-parameter station, which can continuously record as a function of time up to more than 100 geochemical and physical parameters suitable for many applications. A microcomputer system inside the MEDAS handles data exchange, data management and control and it is connected to a modular sensor system. The number of sensors and modules can be selected according to the needs at the measuring sites.

The main problem was the shielding of the system against the aggressive environment and to develop sensors, which survive in extreme acidic gases like in geothermal fields or in fumaroles.

In the presentation the system will be described the technical solutions for this big problem

With this system it was possible to measure Radon and Thoron gas concentrations over longtime in from deep reservoirs directly with high time resolution.

A MEDAS has been installed in four production wells in the Mahanagdong production sector of the Leyte Geothermal Production Field located in the island of Leyte, central Philippines. This field is chosen because: 1) it is the largest geothermal field in the Philippines with five separate power plants with total installed capacity of about 700 MW, and 2) the area is bisected by the Philippine Fault, a major left-lateral transcurrent fault similar to the San Andreas fault.

Results of long time measurement on Radon, Thoron and CO2 concentrations; gas flow, temperature and humidity; water temperature and pH; the Redox potential and conductivity will be presented. These parameters will be correlated with the historical and current data from the PNOC EDC established monitoring set-up for seismicity, micro-gravity and precise levelling surveys, wellhead pressure trends and well bore chemistry changes from monthly production sampling.

Efficient and sustainable production of geothermal energy requires constant monitoring of changes occurring in the reservoir. These changes, which may result from mass extraction for production, waste fluid injection for disposal and pressure support, and from natural geologic processes, are usually manifested in the chemistry and physical characteristics of the wells. Experience has also shown that these changes are related to the structure of the reservoir—the faults that transect the field as well as smaller fractures contained in the reservoir rocks. Identification and evaluation of chemical changes, and their correlation with the structural features, require among others the constant analysis of hot brine and gases discharged by the wells.

Changes in water and gas chemistry, for example, can indicate: 1) lowering in the water level of the reservoir, 2) invasion of cold and degassed re-injection fluids, 3) entry of shallow acidic steam condensates and deep corrosive volcanic-related fluids, 4) precursor of an earthquake, etc. Any of these changes can significantly alter the short- and long-term viability of the geothermal operation. Hence, it is critical that up-to-date collection and analysis of water and gases be undertaken. However, since almost all of the production wells are connected to the power plant, it is rarely possible to disconnect the wells in order to collect samples for

analysis because such disconnection will result to shortfall in power generation. In addition, the process is time-consuming and significant lapse is achieved from sample collection to the availability of the information. There is therefore a pressing need for a continuous and on-line system of measuring chemical parameters in the field.


Uranium Mining
and Hydrogeology

Thermodynamical Data of uranyl carbonate complexes from Absorption Spectroscopy

Christian Götz, Gerhard Geipel and Gert Bernhard

Forschungszentrum Dresden-Rossendorf, Institute of Radiochemistry,
P.O. Box 510 119, 01314 Dresden, Germany

Abstract. Aquatic uranyl carbonate complexes play an important role in the hydrogeology of uranium mining areas and nuclear waste disposals. Many publications are available for the stability of uranyl carbonate complexes, but thermodynamical data like the enthalpy or entropy are rare. We determined thermodynamical data from spectroscopic studies for the uranyl carbonate complex $UO_2(CO_3)_3^{4-}$ in the temperature range from 5 °C to 70 °C. The reaction enthalpy the reaction entropy were determined to be -36.25 ± 4.31 kJ/mol and 297.082 ± 13.839 J/(K·mol), respectively.

Introduction

The distribution of uranium in the environment is strongly dependent on the mobility. Soluble uranium species can be distributed within aquatic systems, so the solubility of the dominant species is a good indicator for the mobility of the uranium. Aquatic systems in the environment contain carbonate species if they are in contact with air or with carbonate containing minerals. If the pH is above 7 the uranium(VI) carbonate complexes are the predominant uranium species in such aquatic systems. For a better understanding of the mobility of uranium, solubility data and stability constants are the most important factors. Since the 1950´s many investigations were done by several groups and the results are reviewed (Grenthe et al. 1992). But for the modeling of environmental behavior, with different temperatures and pressures, also other thermodynamical data are useful. Such data are reaction enthalpies, reaction entropies, heat capacity and more. Some of these data were already reported in the 1980´s (Grenthe et al. 1984; Schreiner et al. 1985; Ullman and Schreiner 1988). Most of them have been determined out by calorimetric methods. But there is a lack of investigations with spectroscopic methods. The absorption spectroscopy is a good method for the investigation of chemical equili-

bria (Perkampus 1992). Vercouter (2005) et al. showed that thermodynamical data of actinide carbonate complexes can be determined by optical spectroscopy.

Theoretical background

The absorbance is given by the law of Bouguer-Lambert-Beer as the product of the concentration of the compound P, the path length of the cuvette and the molar decadic absorption coefficient at the wavelength λ.

$$A(\lambda) = d \cdot \varepsilon(\lambda) \cdot [P] \tag{2}$$

The absorption coefficient ε is temperature independent. Only the concentrations of the components can be temperature dependent.

For an example reaction xE + yF ⇆ zP the equilibrium constant follows equation (3). The equilibrium constant is associated with the Gibbs free energy of the reaction by equation (4), which is temperature dependent according to equation (5). The plot of Δ_RG against the absolute temperature should be a straight line. The intercept of the line equals the reaction enthalpy and the slope corresponds to the reaction entropy. The Gibbs free energies can be calculated by combining the equations (3) and (4) to equation (6).

$$K = \frac{[P]^z}{[E]^x \cdot [F]^y} \tag{3}$$

$$\Delta_R G = -R \cdot T \cdot \ln K \tag{4}$$

$$\Delta_R G = \Delta_R H - T \cdot \Delta_R S \tag{5}$$

$$\Delta_R G(T) = -R \cdot T \cdot \frac{[P]^z}{[E]^x \cdot [F]^y} \tag{6}$$

Experimentals

Solutions containing 10^{-2} M and $5 \cdot 10^{-4}$ M uranium(VI) and 0.1 M carbonate ions were prepared by adding 50 or 1000 µl of the 0.1 M uranyl perchlorate stock solution to the given sodium carbonate solution (1 ml of 1 M sodium carbonate stock solution and 8.95 or 8.0 ml Milli-Q water). The total uranium concentrations of the solutions were determined via ICP-MS.

The spectra were recorded with a Varian Cary 5G UV/VIS Spectrometer. A quartz cuvette with 1 cm path length was filled with Milli-Q water for the reference beam. A further quartz cuvette was used for the measurements. This cuvette

was first filled with Milli-Q water and set into a cuvette holder for recording a background. The cuvette holder is connected to a heating and cooling thermostat (LAUDA Ecoline Staredition RE105). After recording the background the quartz cuvette was emptied, cleaned, washed with the sample and filled with the sample for the measurements. Then the cuvette was set into the cuvette holder and the spectra were recorded in the temperature range from 5 °C to 70 °C in 5 K steps. The wavelength ranged from 300 nm to 600 nm and 0.1 nm steps were used.

Results

Figure 1 shows the recorded spectra of the solution with 0.01 M uranium(VI) at various temperatures. The main species should be the uranyl(tris-)carbonato complex $UO_2(CO_3)_3^{4-}$.

For the maximal absorbance a linear dependency on the temperature was found (Fig.2). With increasing the temperature dissolved carbon dioxide passes into gaseous carbon dioxide according to equation (7). This leads to a decrease of the amount of the solved carbon dioxide. It follows that also the amount of carbonate ions decrease in the following change in the equilibrium between solved carbon dioxide and carbonate ions (8). In the last step the uranyl(tris-)carbonato complex $UO_2(CO_3)_3^{4-}$ passes into other species with fewer carbonate content. The chemical equation for the formation of the uranyl(tris-)carbonato complex is given in equation (9).

$$CO_2(aq) \xrightarrow{\Delta T} CO_2(g) \tag{7}$$

$$2\ H^+ + CO_3^{2-} \leftrightarrows H_2O(l) + CO_2(aq) \tag{8}$$

$$UO_2^{2+} + 3\ CO_3^{2-} \leftrightarrows UO_2(CO_3)_3^{4-} \tag{9}$$

$$K_{103} = \frac{\left[UO_2(CO_3)_3^{4-}\right]}{\left[UO_2^{2+}\right] \cdot \left[CO_3^{2-}\right]^3} \tag{10}$$

The single component spectrum of the uranyl(tris-)carbonato complex $UO_2(CO_3)_3^{4-}$ (Fig.3) was determined by the dependence of the absorption spectra on concentration and pH. The band positions and the maximal molar decadic absorption coefficient ε_{max} of 30.50 ± 1.42 l·mol^{-1}·cm^{-1} are in agreement with literature data (29.0 ± 0.7 l·mol^{-1}·cm^{-1}; Meinrath 1996). From this single component spectrum the concentration of the complex was calculated according to equation (2).

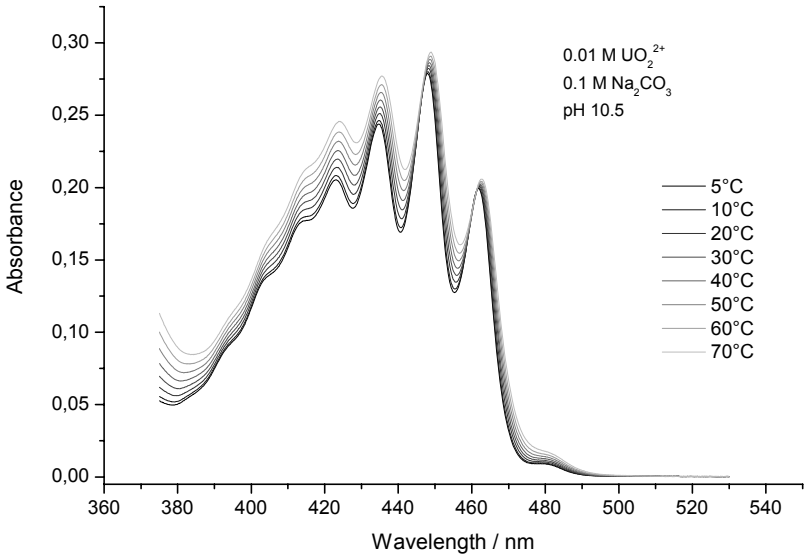

Fig.1. Absorption spectra of the uranyl carbonate solution at various temperatures.

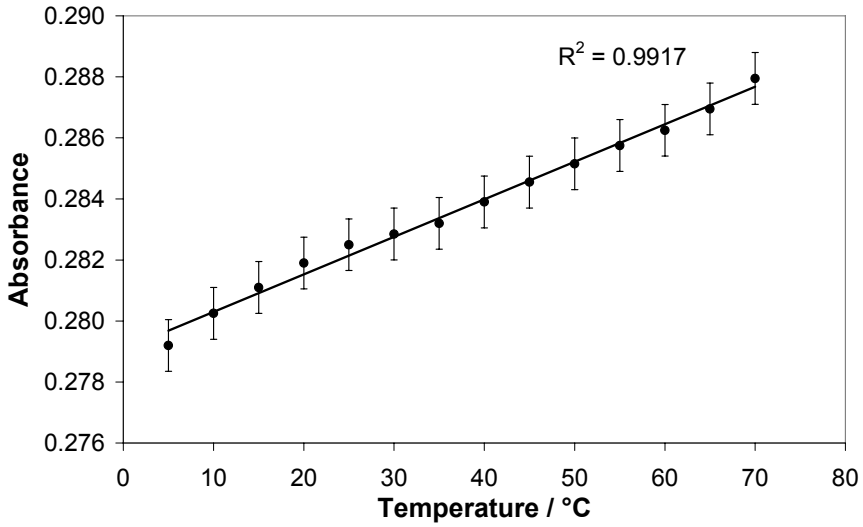

Fig.2. Temperature dependence of the absorbance at 447.8 nm.

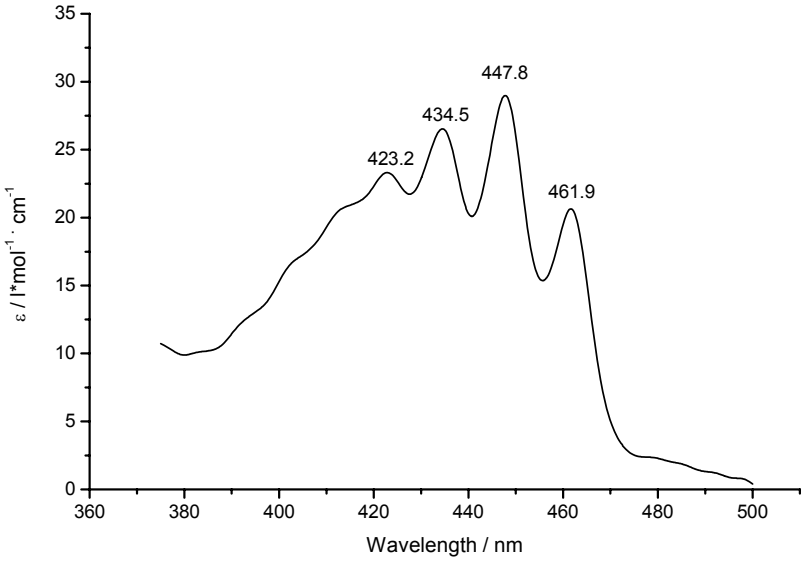

Fig.3. Single component spectrumof the uranyl(tris-)carbonato complex.

Only the spectra from solution containing about 0.01M uranium were evaluated, because the change in the absorbance is small. The concentrations of the free uranyl and carbonate ions were calculated with EQ3/6 (Wolery 1992). The equilibrium constant K_{103} for reaction (9) was then calculated for every temperature according to equation (10). The Gibbs free energies for every temperature were determined using equation (4). Table 1 shows the determined complex concentrations and the Gibbs free energies. The plot of the Gibbs free energies against the absolute temperatures (Fig.4) can be fitted by a straight line. The reaction enthalpy $\Delta_R H_{103}$ was derived from the intercept of this line and the reaction entropy $\Delta_R S_{103}$ from the slope, respectively. The Gibbs free energy for standard conditions $\Delta_R G^\circ_{103}$ was determined using equation (5) and the standard temperature $T^\circ = 298.15$ K. From this value the equilibrium constant K_{103} at standard conditions was calculated. A correction to infinite dilution with Specific ion Interaction Theory (Guillaumont et al. 2003) results in the complex stability constant β_{103}. Table 2 gives an overview of the results in comparison with literature data. Furthermore an estimated value for the formation Gibbs free energy is given, based on equation (11) and the values $\Delta_f G^\circ(UO_2^{2+}) = -989.5$ kJ /mol and $\Delta_f G^\circ(CO_3^{2}) = -528.0$ kJ/mol (Boughriet et al. 2000).

$$\Delta_f G^\circ_{103} = \Delta_f G^\circ(UO_2^{2+}) + 3 \cdot \Delta_f G^\circ(CO_3^{2-}) - \Delta_R G^\circ_{103} \qquad (11)$$

Table 1. Determined complex concentrations at various temperatures and resulting values for the equilibrium constant (shown as natural logarithm) and the Gibbs free energy

Temperature °C	$[UO_2(CO_3)_3^{4-}]$ M	ln K_{103}	$\Delta_R G_{103}$ kJ / mol
5	$(9.174 \pm 0.039)\cdot10^{-3}$	51.759 ± 0.004	-119.702 ± 0.010
10	$(9.210 \pm 0.042)\cdot10^{-3}$	51.313 ± 0.005	-120.804 ± 0.011
15	$(9.239 \pm 0.045)\cdot10^{-3}$	50.910 ± 0.005	-121.972 ± 0.012
20	$(9.269 \pm 0.051)\cdot10^{-3}$	50.548 ± 0.006	-123.206 ± 0.014
25	$(9.285 \pm 0.045)\cdot10^{-3}$	50.225 ± 0.005	-124.506 ± 0.012
30	$(9.295 \pm 0.042)\cdot10^{-3}$	49.937 ± 0.005	-125.869 ± 0.011
35	$(9.308 \pm 0.045)\cdot10^{-3}$	49.684 ± 0.005	-127.297 ± 0.012
40	$(9.331 \pm 0.045)\cdot10^{-3}$	49.465 ± 0.005	-128.792 ± 0.013
45	$(9.354 \pm 0.048)\cdot10^{-3}$	49.276 ± 0.005	-130.348 ± 0.014
50	$(9.374 \pm 0.048)\cdot10^{-3}$	49.115 ± 0.005	-131.963 ± 0.014
55	$(9.390 \pm 0.042)\cdot10^{-3}$	48.980 ± 0.004	-133.636 ± 0.012
60	$(9.410 \pm 0.048)\cdot10^{-3}$	48.867 ± 0.005	-135.362 ± 0.014
65	$(9.433 \pm 0.048)\cdot10^{-3}$	48.778 ± 0.005	-137.141 ± 0.014
70	$(9.466 \pm 0.048)\cdot10^{-3}$	48.708 ± 0.005	-138.969 ± 0.015

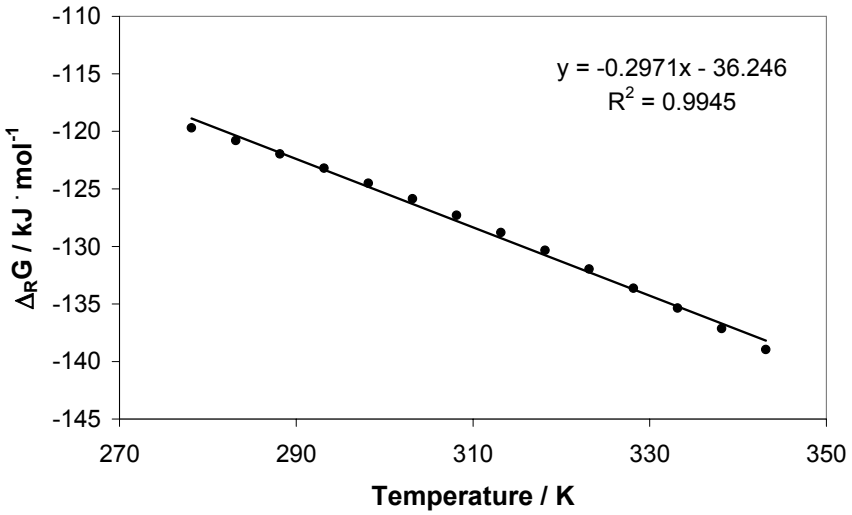

Fig.4. Plot of the Gibbs free energies against the used temperatures.

Table 2. Overview of the thermodynamical data of the uranyl(tris-)carbonato complex. Short names for the references were used.

	Value	Uncertainty	Ref.	Note
$\Delta_R H_{103}$ / kJ·mol^{-1}	-36.25	4.31	This work	
	-35.9	0.8	Grenthe 1984	
	-57.5	1.5	Schreiner 1985	Based on UO_2SO_4
	-42.1	1.3	Ullman 1988	
	-39.2	4.1	Guillaumont 2003	Weighted Mean
$\Delta_R S_{103}$ / J·K^{-1}·mol^{-1}	297.082	13.839	This work	
	312		Grenthe 1984	
	286.646	13.773	Guillaumont 2003	Weighted Mean
$\Delta_R G^\circ_{103}$ / kJ·mol^{-1}	-124.820	8.434	This work	
	-129		Grenthe 1984	
	-124.664	0.228	Guillaumont 2003	Weighted Mean
log K_{103}	21.867	1.478	This work	I ~ 0.2 M
log β_{103}	21.716	1.478	This work	
	21.74	0.22	Meinrath 1996	
	21.840	0.040	Guillaumont 2003	Weighted Mean
$\Delta_f G^\circ_{103}$ / kJ·mol^{-1}	-2248.7	8.4	This work	
	-2660.9	2.1	Guillaumont 2003	$\Delta_f G(UO_2^{2+})$ = -952.5

The determined values are in good agreement with literature data except the formation Gibbs free energy which is only estimated in this work as well as in literature. The uncertainty of the Gibbs free energy is a result of the uncertainties in the enthalpy and entropy according equation (5). Therefore it is higher than the uncertainty in the review from Guillaumont in 2003, where the Gibbs free energy was calculated from stability constants. This fact also applies to the determined stability constant.

Thermodynamical data of other uranium species should be determined in further studies by spectroscopic methods.

Acknowledge

We thank U. Schaefer for the ICP-MS measurements and C. Eckardt for the measurements of Total Inorganic Carbon.

References

Boughriet A et al. (2000) Generation of uranyl/carbonate/hydroxide “coatings” at vaterite surface. PHYS. CHEM. CHEM. PHYS. 2: 1059-1068

Grenthe I et al. (1984) Studies of Metal Carbonate Equilibria.9. Calorimetric Determination of the Enthalpy and Entropy Changes for the Formation of Uranium(IV and VI) Carbonate Complexes at 25-Degrees-C in a 3 M (Na,H)ClO4 Ionic Medium. INORG. CHIM. A-F-BLOCK 95: 79-84

Grenthe et al. (1992) Chemical Thermodynamics of Uranium. Elsevier, North-Holland Elsevier B.V., Amsterdam

Guillaumont R et al. (2003) Update on the Chemical Thermodynamics of Uranium, Neptunium, Plutonium, Americium and Technetium. Elsevier B.V., Amsterdam

Meinrath G et al. (1996) Direct spectroscopic speciation of uranium(VI) in carbonate solutions. Radiochim. Acta 74: 81-86

Perkampus HH (1992) UV-VIS Spectroscopy and Its Applications. Springer, Berlin

Schreiner F et al. (1985) Microcalorimetric Measurement of Reaction Enthalpies in Solutions of Uranium and Neptunium Compounds. J. Nucl. Mater. 130: 227-233

Ullman WJ, Schreiner F (1988) Calorimetric Determination of the Enthalpies of the Carbonate Complexes of U(VI), Np(VI) and Pu(VI) in Aqueous Solution at 25°C. Radiochim. Acta 43: 37-44

Volery TJ (1992) EQ3/6 A software package for the geochemical modeling of aqueous system. Report UCRL-MA-110662 part 1, Lawrence Livermore National Laboratory, California, USA

Vercouter T et al. (2005) Stabilities of the aqueous complexes Cm(CO3)33- and Am(CO3)33- in the temperature range 10-70 degrees C. Inorg. Chem. 44: 5833-5843

Digital elevation model created by airborne laser scanning in the field of mines areas

Sven Jany

Milan Flug GmbH, Büro Schwarze Pumpe, Schäfereistraße 24, 03130 Spremberg OT Schwarze Pumpe, Germany

Abstract. The Airborne laser scanning technology earned a permanent position worldwide in the generation of digital elevation models (DEM) in the last 10 years.

The technique of airborne laser scanning (altimetric) provides the data for the planning criteria in the mining industry, in water management, road construction and urban development and in many other sectors. Due to the extraordinary ability of the airborne laser scanning technology to penetrate the vegetation cover, two separate but consistent digital elevation models can be generated:

- The DSM (digital surface model) surface model with vegetation and building structures
- The DTM (digital terrain model) terrain model without vegetation and building structures

The laser scanning devices(systems) are firmly integrated into the aircraft or helicopter. Today they are able to transmit and receive up to 100.000 measured laser data per second. Generally the measured laser data is used to create a geometrical raster with variable screen ruling (1 m-100 m).


Uranium Mining
and Hydrogeology

Numerical simulation of groundwater flow and particle tracking around the proposed Uranium mine site, Andhra Pradesh, India

Lakshmanan Elango

Department of Geology, Anna University, Chennai 600025, India, elango@annauniv.edu, elango34@hotmail.com

Abstract. Groundwater modelling by numerical methods has been widely used around the world to study and understand the various aquifer systems. Modelling techniques has been successfully used to study the groundwater flow patterns and migration of particles along with flow in a number of mining sites. The present study was carried out to develop a groundwater model and study the groundwater flow regime in and around the proposed Uranium mine site at Lambapur – Peddagattu area in Nalagonda district, Andhra Pradesh with the following objective of predicting the movement of groundwater and particles in the region during next 15 years. Lambapur - Peddagattu deposit lie along the north- western margin of Cuddapah basin. The computer code MODFLOW that numerically approximates this equation by finite-difference method was used to simulate the groundwater flow in the study area. The pre and post processor developed by the United States Department of Defence Groundwater Modelling System was used to give input data and process the model output. Groundwater modelling study of Nalagonda region indicates that the groundwater occurring in the weathered rocks flow towards the Nagarjuna Sagar reservoir. The simulation carried out until the year 2017 suggests that there is not much change in the groundwater flow regime, with the assumed condition of no change in the groundwater pumping during mining activity. As groundwater is expected to move towards the reservoir, it takes more than 15 years for the particles from the proposed mine sites at Peddagattu to reach the boundary (reservoir) of the modelled area. However. the simulation assuming

constant head of 264m at Paddagattu mine sites indicate that the particles have moved to only to some distance by the end of the year 2017 at Mine II and no migration of particles from Mine I. The mineralised zone at Peddagattu occurring below the shale (30-50m thick) may not be in saturated condition, except for small quantity of water available in the fractures. Hence, with the proper dewatering strategy and the lined surface drainage to reduce the recharge, the migration of uranium with the groundwater may be prevented at the Mine II. In the case of Lambapur region as the formation is devoid of groundwater as predicted by the model, there will not be any groundwater problem due the mining. Hence, with the proper management dewatering strategy the migration of uranium with the groundwater may be prevented at Mine II.

Assessment of Uranyl Sorption Constants on Ferrihydrite – Comparison of Model Derived Constants and Updates to the Diffuse Layer Model Database

John J. Mahoney and Ryan T. Jakubowski

MWH Americas, Inc., Steamboat Springs, Colorado, USA

Abstract. Surface complexation constants for uranyl (UO_2^{+2}) sorption onto hydrous ferric oxide (HFO) using a diffuse layer model (DLM) developed with the Dzombak and Morel correlation are demonstrated to provide poor fits to two independently derived laboratory datasets. Alternative surface complexation reactions based upon geochemical modeling provided better matches to the data and still follow the underlying principles of the DLM as used in databases associated with several geochemical modeling programs.

Introduction

In 1990, David Dzombak and Francois Morel (D&M) (Dzombak and Morel, 1990) published a compilation of surface complexation reactions for hydrous ferric oxide (HFO). In their seminal work, previously published data sets were re-evaluated and surface complexation reactions were defined assuming that a diffuse layer model (DLM) best described the charge potential relationships on the surface. The model developed from their effort presupposed a series of well defined parameters such as surface site densities, and surface area assumptions. The database that was developed from these significant efforts has been used in numerous programs including MINTEQA2 (Allison et al. 1991), PHREEQC (Parkhurst and Appelo 1999) and Geochemist's Workbench (Bethke 1996). Because the USEPA provides MINTEQA2 to outside users, that program and its associated databases have developed a perceived or tacit approval by many regulatory agencies.

As part of the efforts to increase the number of components in the database, D&M developed a linear free energy relationship (LFER) to estimate surface complexation reaction constants for several species that were not evaluated using laboratory developed data, these included uranyl, tin, palladium, plutonium (as

PuO_2^{+2}) and manganese. The authors developed a relationship between the formation constant for various metal hydroxides ($MeOH^+$), and known surface complexation constants for strong (Hfo_sOH) and weak (Hfo_wOH) sites. Then new constants were developed for surface complexes not evaluated using experimentally derived measurements. Using the LFER and a log K of 8.2 for the $UO_2(OH)^+$ complex, D&M calculated log K values for $Hfo\_sOUO_2^+$ (log K^1_{int} of 5.2) and $Hfo\_wOUO_2^+$ (log K^2_{int} of 2.8). Unfortunately, comparison of the estimated surface complexation constants to two independent experimentally derived datasets indicates that the constants overestimate the extent of adsorption, particularly at low pH conditions.

The primary purpose of this work is to provide corrections to the DLM database for uranyl adsorption, while maintaining the basic conditions, such as surface site densities, with those presented by D&M in 1990. Work using EXAFS (Payne 1999) suggests that the uranyl surface complexes are of a bidendate nature. This paper assumes that the surface complexes are monodendate for consistency with the other surface complexes in the DLM database.

Comparison to experimental data

Experimental data from different published sources were used. Fits were prepared using PHREECQ. The method was primarily trial and error, where visual fits were compared between experimental and modeled data. Goodness of fit was evaluated by a root mean square type objective function.

Prior to performing the fitting calculations, an evaluation of the published uranyl complexation reactions in solution was undertaken. The evaluation indicated that the WATEQ4f.dat database, included in the PHREEQC distribution package, was consistent with generally accepted complexes and their stability constants. Figure 1 shows the distribution of UO_2^{+2}, uranyl hydroxide and uranyl carbonate complexes developed from this database.

Figure 2 shows data prepare by Hsi (Hsi 1981, Hsi and Langmuir 1985), and compares it to a model using the original LFER derived constants. Examination of Figure 2 indicates that the original DLM constants have a tendency to over-predict the extent of adsorption, in some cases by a factor of 10. The data developed by Hsi used an initial U(VI) concentration of $1x10^{-5}$ m and 1 g/L amorphous ferric hydroxide, total carbonate was zero. The second set of lined data (open diamonds) show the final fit using two surface complexation reactions:

$$Hfo\_sOH + UO_2^{+2} = Hfo\_sOUO_2^+ + H^+ \qquad \log K_1^{int} = 4.15$$

$$Hfo\_wOH + UO_2^{+2} = Hfo\_wOUO_2^+ + H^+ \qquad \log K_2^{int} = 2.05$$

The problem with the D&M constants becomes more evident when compared to other datasets. Failure to match one dataset may be related to experimental technique. Failure to match two independent datasets suggests a problem with the LFER estimation method. Figure 3 shows the model compared to experimental da-

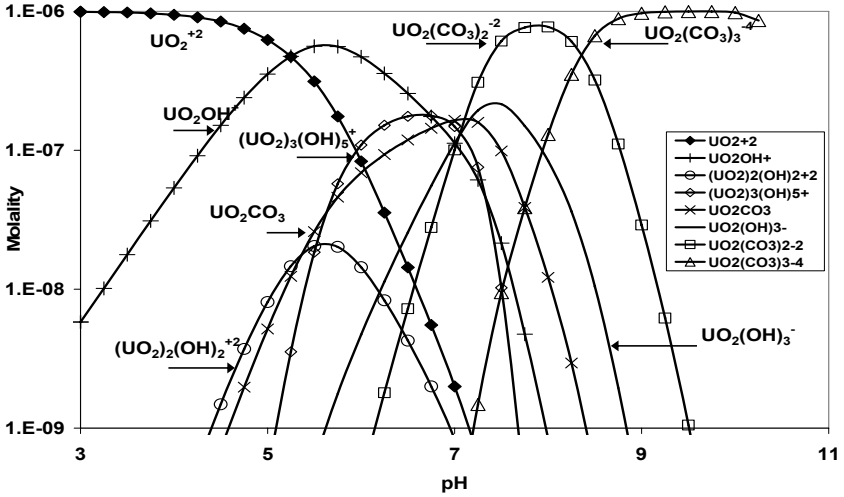

Fig.1. Distribution of uranyl species for a solution containing 10^{-6} M U(VI) and a carbon dioxide pressure of $10^{-3.5}$ atmospheres.

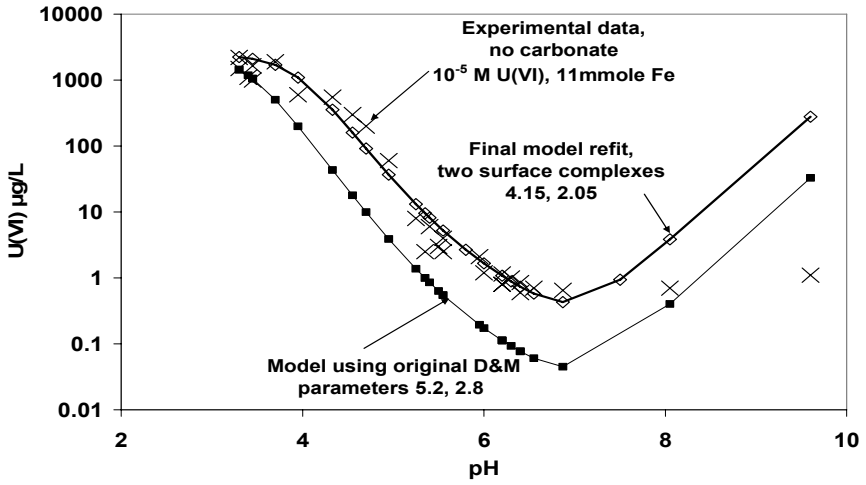

Fig.2. Comparison Hsi's (1981) of experimentally derived measurements of uranyl uptake onto amorphous ferric hydroxide (X's) to DLM calculations using LFER derived constants presented by D&M (thin line and small filled square) and our model fit (thicker line open diamonds).

ta developed by T. E. Payne for 10^{-6} m U(VI) onto 1 mmole Fe (precipitated as HFO). The experiments were open to the atmosphere; consequently, the partial pressure of carbon dioxide was set to $10^{-3.5}$ atmospheres. Again, the LFER derived values tend to over estimate adsorption at low pH values. The model also tends to underestimate adsorption at high pH conditions.

To obtain his fits, Payne modified several tenets of the D&M DLM. He increased the surface site density from 0.2 moles of weak sites/mole Fe to 0.875 moles/mole Fe. In the original model D&M assigned a site density for strong sites of 0.005 moles/mole Fe, Payne decreased it to 0.0018 moles/mole Fe. The overall increase in surface site concentrations impacts the surface charge/surface potential features of the model. Payne noted that his modifications required subsequent adjustments of other reactions, notable the surface ionization reactions involving the K_{a1}^{int} and K_{a2}^{int} constants. These changes limit the ability to apply his model to systems that contain other competing cations such as nickel or zinc. In general, the effects are small but can raise questions about internal consistency. One final feature of the Payne model is its assumption that the strong sites could form uranyl carbonate surface complexes. Uranyl carbonate complexes are either neutral or negatively charged. The original rationale for including strong sites in the DLM was to provide a means to model high affinity cation adsorption, which generally took place under low pH conditions. Because these assumptions changed the underlying assumptions of the D&M DLM we decided to recalculate uranyl sorption in accordance with the original requirements stated in D&M (1990).

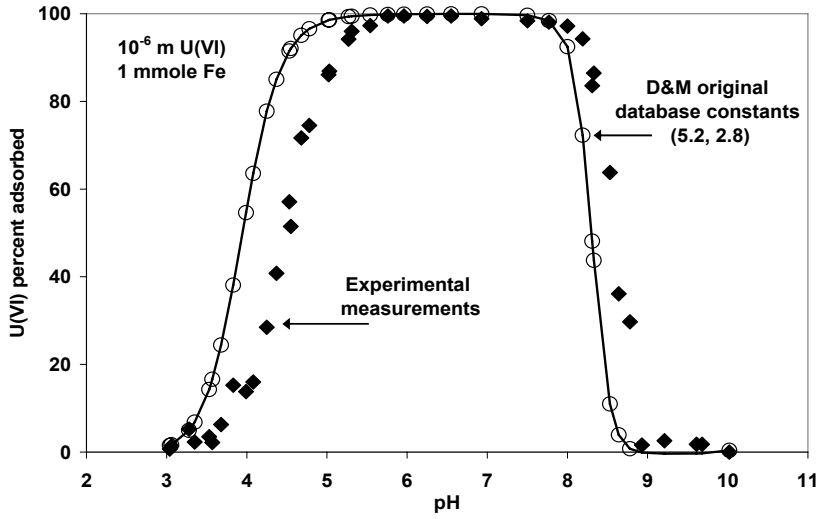

Fig.3. Comparison of Payne's (1999) experimental data (filled diamonds) to model based upon D&M uranyl surface complexation reaction (open circles with line); based upon 10^{-6} m U(VI) sorbed onto 1mmole of HFO in a 0.1 $NaNO_3$ solution, CO_2 at $10^{-3.5}$ atmospheres.

To refit the Payne experimental data, our work used the surface site density assumptions in the D&M version of the DLM (proportions of 0.2 and 0.005). Initially a third reaction was added to allow for a uranyl carbonate surface complex. The added reaction was:

$$Hfo\_wOH + UO_2^{+2} + CO_3^{-2} = Hfo\_wOUO_2CO_3^{-} + H^{+} \quad \log K^{int}_{Hfo\_wOUO2CO3-} = 10.05$$

Figure 4 compares Payne's experimental data at a U(VI) concentration of 10^{-6} m, and 1 mmole of Fe to three different model fits. The first fit was the simplest and included the three uranyl surface complexes described above. Based upon the values obtained from the Hsi data (Figure 3), we selected a log K_1^{int} value of 4.15, log K_2^{int} of 2.05 and a log $K^{int}_{Hfo\_wOUO2CO3-}$ of 10.05.

The original DLM database, as presented in PHREEQC, did not include surface complexation reactions between surface sites and carbonate, consequently the first models did not include surface complexation reactions with carbonate. Appelo et al. (2002) reported surface complexation reaction constants for carbonate suitable for the D&M database. The reactions are defined below.

$$Hfo\_wOH + CO_3^{-2} + H^{+} = Hfo\_wOCO_2^{-} + H_2O \qquad \log K^{int}_{Hfo\_wOCO2-} = 12.78 \pm 0.48$$

$$Hfo\_wOH + CO_3^{-2} + 2H^{+} = Hfo\_wOCO_2H + H_2O \qquad \log K^{int}_{Hfo\_wOCO2H} = 20.37 \pm 0.20$$

These reactions in addition to the uranyl surface complexation reactions were

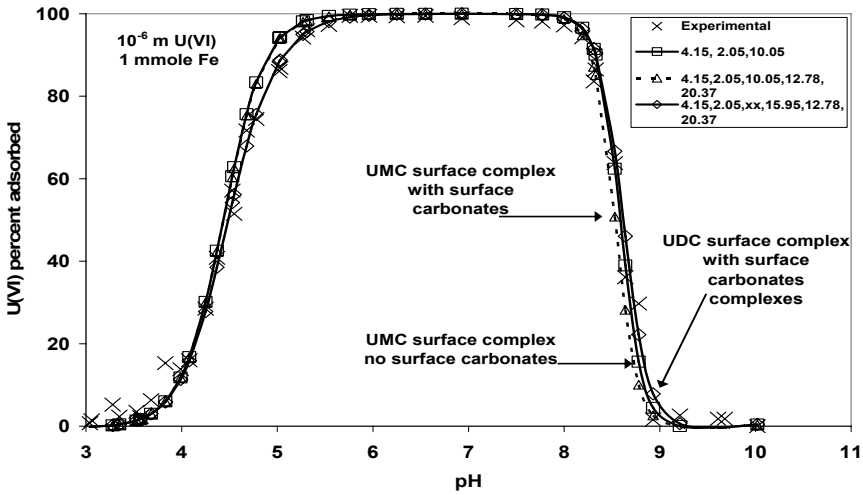

Fig.4. Comparison of Payne's (1999) experimental data (X's) with DLM fit assuming three surface complexation reactions for uranyl (line with squares); based upon 10^{-6} m U(VI) sorbed onto 1mmole of HFO in a 0.1 $NaNO_3$ solution with a partial pressure of CO_2 of $10^{-3.5}$ atmospheres. The figure also includes another model with two surface carbonate complexes (dashed line with triangles). A final model (line with diamonds) replaced the uranyl monocarbonate (UMC) surface complex (2nd model) with a uranyl dicarbonate (UDC) surface complex.

included in a second set of model calculations. Several simulations indicated that the impact of the carbonate surface complexes was minimal.

Finally, a third model was developed that included a uranyl dicarbonate (UDC) surface complex. The UDC surface complexation reaction was defined as:

$$Hfo\_wOH + UO_2^{+2} + 2CO_3^{-2} = Hfo\_wOUO_2(CO_3)_2^{-3} + H^+ \quad Log\ K^{int}_{UDC} = 15.95$$

The third model replaced the uranyl monocarbonate (UMC) surface complex with a uranyl dicarbonate (UDC) surface complex. The final model included the simple carbonate surface complexes. A value of 15.95 was selected as the best value for the log $K^{int}_{Hfo\_wOUO2(CO3)2\text{-}3}$. The constant was adjusted primarily to improve the fit in the higher pH range, but replacing the UMC surface complex with the UDC complex also resulted in a better fit in the lower pH ranges (4.5 to 6.0).

Figure 5 shows the distribution of uranyl surface complexes for two of the models shown in Figure 4. Under low pH conditions, the strong site is the dominant retainer of U(VI). The selection of either the UMC or UDC surface complex significantly impacts the distribution of the two uranyl surface complexes.

Payne expanded his experimental work to other conditions by increasing the amount of sorbent phase or increasing the initial concentration of uranium. Figure 6, shows the fit when the amount of U remains at 10^{-6} m, and the iron is increased to 20 mmole. These experiments have the lowest loadings of U. The log K_1^{int} value of 4.15, and log K_2^{int} of 2.05 remained the same, but for the first model the log $K^{int}_{Hfo\_wOUO2CO3\text{-}}$ was adjusted to 11.05 for this data set. For the model with the

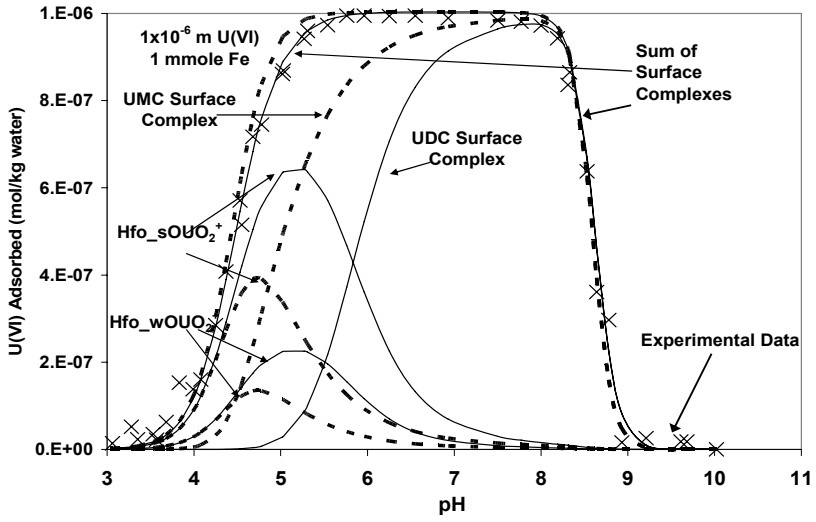

Fig.5. Distribution of uranyl-bearing surface complexes. The UMC model surface complexes are represented by thick dashed lines. The UDC model based surface complexes are represented by thin solid lines; experimental data from Payne (1999).

UDC surface complex, the selected log $K^{int}_{Hfo\_wOUO2(CO3)2-3}$ value was 16.4.

The effects of increasing the uranyl concentration to 10^{-5} or 10^{-4} m, while retaining HFO at 1mmole, are shown on Figures 7 and 8.

In both models, we have preserved the log K_2^{int} value at 2.05. For the 10^{-5} m

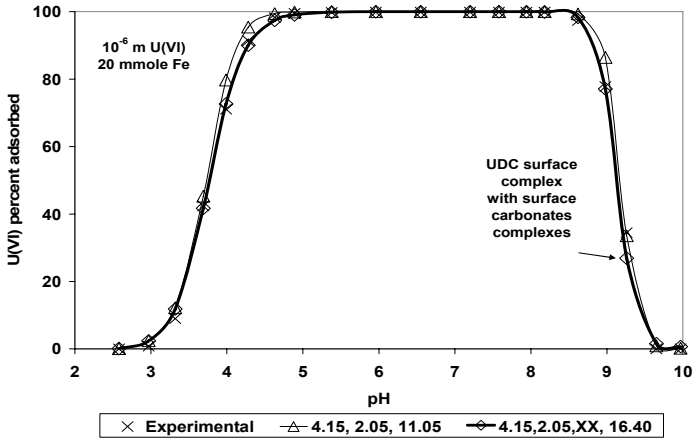

Fig.6. Comparison of experimental data (X's) comparing UMC and UDC surface complexes DLM fits. The model with UMC surface complex is represented by thin line with triangles. The UDC surface complex model also included carbonate surface complexes (thick line with diamonds). Experimental conditions from Payne (1999), based upon 10^{-6} m U(VI) sorbed onto 20 mmole of HFO in a 0.1 $NaNO_3$ solution CO_2 at $10^{-3.5}$ atmospheres.

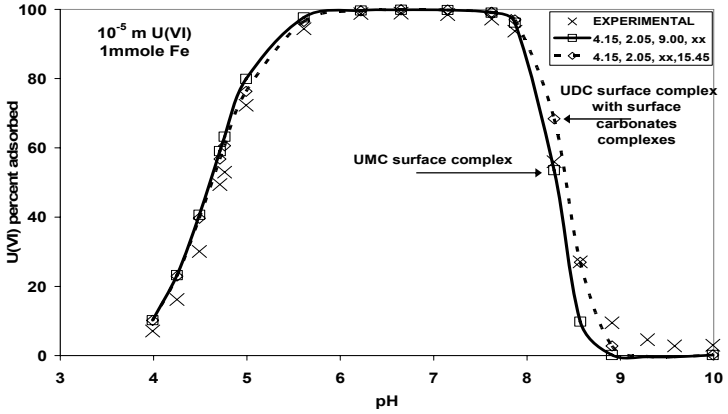

Fig. 7. Comparison of experimental data (X's) with two DLM simulations. The model fit with the UMC surface complex is represented by a solid line with squares. The fit with the UDC surface complex model also included carbonate surface complexes (dashed line with diamonds). Experimental conditions from Payne (1999) based upon 10^{-5} m U(VI) sorbed onto 1 mmole of HFO in a 0.1 $NaNO_3$ solution, CO_2 at $10^{-3.5}$ atmospheres.

U(VI) measurements we have retained both the log K_1^{int} and the K_2^{int} values at 4.15 and 2.05, respectively.

At a loading of 10^{-4} m U(VI) (Figure 8), the final constants were 3.70 for log K_1^{int}, 2.05 for the log K_2^{int} value and log $K^{int}_{Hfo\_wOUO2CO3-}$ was adjusted to 8.2. The model with the UDC surface complex used a log $K^{int}_{Hfo\_wOUO2(CO3)2-3}$ value of 15.0. The change in the log K_1^{int} for these experimental conditions is not surprising. At the 10^{-4} m loading, the less than 5 percent of U(VI) is sorbed onto strong sites (Figure 8) the model is not sensitive to the parameter, therefore a difference of nearly half a log unit is not unexpected. The role of the strong and weak uranyl surface complexes is reversed when compared to lower loadings (Figure 4).

Figure 8 also included another model that used the log $K^{int}_{Hfo\_wOUO2(CO3)2-3}$ developed from the 10^{-6} U(VI) 20 mmole Fe dataset, that value was 16.4 (see Figure 6). This simulation was run to demonstrate that acceptable fits can be obtained using the largest value for the UDC surface complex. Although the comparison to the higher pH range is not as good as models that use a smaller value, the 16.4 value actually improves the fit from pH 5.5 to 7.0.

Table 1 summarizes the model conditions and selected surface complexation

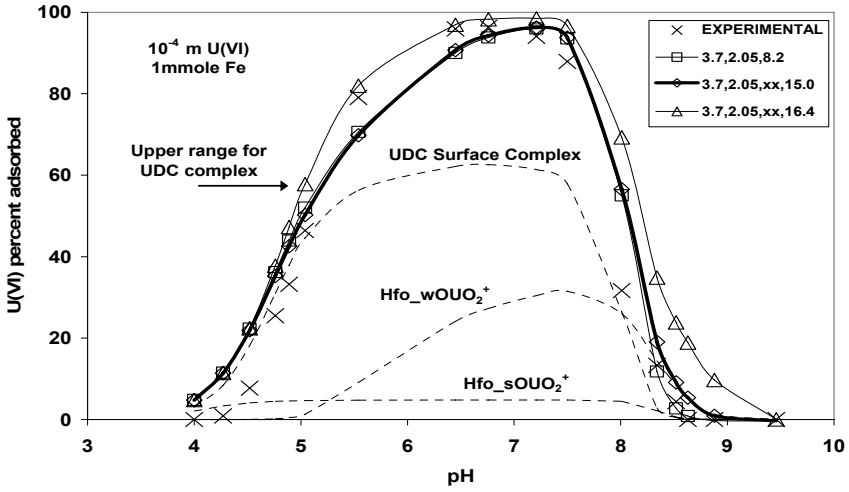

Fig.8. Comparison of experimental data (X's) with DLM fits assuming three surface complexation reactions for uranyl. The fit with the UMC surface complex is represented by a thin line with squares. The UDC surface complex model also included carbonate surface complexes (thick line with diamonds), the distribution of uranyl bearing surface complexes (thin dashed lines) for the UDC model is also included. A model using the maximum value for the UDC surface complex (line with triangles) was included to show sensitivity of model. Experimental conditions (Payne, 1999) based upon 10^{-4} m U(VI) sorbed onto 1 mmole of HFO in a 0.1 NaNO_3 solution CO_2 at $10^{-3.5}$ atmospheres.

constants derived from this study. Of greatest concern is the variation in log $K^{int}_{Hfo\_wOUO2CO3-}$ as the proportion of available U(VI) to sorption sites changes. The UMC surface complex models have a spread of 2.85 log units. Initially, it was thought that some of this variation could be explained by including the surface carbonate complexes. However, their inclusion had no effect on the selected values. A strong correlation between the log of the site loading value, defined as U(VI) as moles/mmoles Fe, to the selected log $K^{int}_{Hfo\_wOUO2CO3-}$ value was noted. The variation in the value of the UMC surface complex was the reason that the additional models with the UDC surface complex were prepared. Replacement of the UMC with the UDC surface complex reduced the spread to about 1.4 log units. Figure 8 demonstrates that the variation in the UDC surface complex does not have a significant effect on the overall fit, and that an average value of about 15.7 would provide a good starting point for most models.

Table 1. Summary of initial model parameters, experimental conditions and final surface complexation constants.

Data Source	U(VI) mol/L	Fe mmoles	Carb.	Log K_1^{int}	Log K_2^{int}	Log K^{int}_{UMD}	Log K^{int}_{UDC}
D&M LFER	NA	NA	NA	5.2	2.8	NA	NA
Hsi, 1981	1.E-5	11 (1gm/L)	Ct = 0.0	4.15	2.05	NA	NA
	1.E-6	20	$10^{-3.5}$ atms	4.15	2.05	11.05	16.40
Payne, 1999	1.E-6	1	$10^{-3.5}$ atms	4.15	2.05	10.05	15.95
	1.E-5	1	$10^{-3.5}$ atms	4.15	2.05	9.0	15.45
	1.E-4	1	$10^{-3.5}$ atms	3.7	2.05	8.2	15.0

Conclusions

This work has demonstrated that the constants for uranyl adsorption onto HFO (or ferrihydrite) provided in the D&M diffuse layer database are in error and tend to over estimate the extent of uranyl sorption particularly for low pH conditions. Furthermore, D&M did not consider the importance of uranyl carbonate surface complexes in their initial compilation. The original intent of this work was to develop a set of simple surface complexation constants to describe uranyl adsorption using the DLM. This has been partially accomplished. New constants have been provided (Table 1), but the role of the uranyl carbonate surface complexes has not been fully resolved. Satisfactory models can be constructed with either the UMC or UDC surface complex. We favor the model that uses the UDC surface complex, but we are performing more simulations to better resolve this issue.

These corrections will improve applications such as solute transport calculations. The errors in the previously published values were as much as an order of magnitude in the amount predicted to be adsorbed. The failure to include carbo-

nate complexation reactions was also a major shortcoming of the original work. The corrections will result in significant differences among the predicted mobility of uranium in solute transport models. Under low pH, carbonate-free conditions, which are common in some acid rock drainage environments, the calculated distribution coefficient of uranyl will be reduced in some cases by nearly a factor of 10. These new constants indicate less sorption of U(VI) than previously indicated and consequently these new estimates will under certain conditions tend to be more protective of the environment.

Future work will refine these fits using an alternative solver/fitting program such as UCODE (Poeter et al. 2005) and provide better estimates of errors. The additional work will re-evaluate the relationships involving the behavior of the uranyl surface carbonate surface complex. Also surface complexation models based upon the bidendate surface complexes identified by Payne will be developed, but will use the site density conventions of the original diffuse layer model. The bidendate models may provide a better means to handle the variations in the uranyl carbonate complexation constants.

References

Allison, J.D., Brown, D.S., and Novo-Gradac, K.J., 1991, MINTEQA2/PRODEFA2, a geochemical assessment model for environmental systems, Version 3.0 User's Manual: U.S. Environmental Protection Agency Report EPA/600/3-91/021, 106 p.

Appelo, C.A.J., Van der Weiden, M.J.J., Tournassat, C. and Charlet, L., 2002, Surface complexation of ferrous iron and carbonate on ferrihydrite and the mobilization of arsenic. Environ. Sci. Technol. V. 36, p. 3096 -3103.

Bethke, C.M., 1996, Geochemical Reaction Modeling: Oxford University Press, New York, 397 p.

Dzombak, D.A., and Morel, F.M.M., 1990, Surface complexation modeling - hydrous ferric oxide: New York, John Wiley and Sons, 393 p.

Hsi, C.-K.D., 1981, Sorption of Uranium (VI) by iron oxides. Ph.D. Dissertation, Colorado School of Mines, pp. 154.

Hsi, C.-K.D. and Langmuir, D. 1985, Adsorption of uranyl onto ferric oxyhydroxides: applications of a surface complexation site binding model. Geochimica et Cosmochimica Acta, 49, p. 2423-2432.

Parkhurst, D.L., and Appelo, C.A.J., 1999, User's guide to PHREEQE (version 2) - a computer program for speciation, batch-reaction, one-dimensional transport, and inverse geochemical calculations. U.S. Geological Survey Water Resources Investigation Report 99-4259, 312 p.

Payne, T.E. (1999), Uranium (VI) interactions with mineral surfaces: controlling factors and surface complexation modeling, Ph.D. Dissertation, University of New South Wales, pp. 332.

Poeter, E.P., Hill, M.C., Banta, E.R., Mehl, S., and Christensen, S., 2005. UCODE_2005 and six other computer codes for universal sensitivity analysis, calibration and uncertainty evaluation. USGS Techniques and Methods 6-A11. Reston, Virginia.

Surface complexation of U(VI) by Fe and Mn (hydr)oxides

David M. Sherman, Chris G. Hubbard and Caroline L. Peacock

Department of Earth Science, University of Bristol, Bristol BS8 1RJ UK.

Abstract. Sorption of U(VI) to iron and manganese (hydr)oxides is a fundamental control on the mobility of uranium in oxic soil and groundwater. Surface complexation models for these sorption reactions are needed to enable reactive transport simulations of U in the environment. We have been investigating the sorption of U(VI) to iron and manganese (hydr)oxide minerals using classical batch sorption experiments, EXAFS spectroscopy and first-principles (quantum mechanical) calculations of the structures and energetics of U surface complexes. EXAFS spectra of U surface complexes are complicated by multiple scattering and the poor resolution of U-carbonate complexes. We argue that previous models for surface complexation need to be reassessed. Instead, we show that on goethite (α-FeOOH) and ferrihydrite ($Fe_{10}O_{14}(OH)_2$), we can model both our EXAFS and our sorption experiments using three surface complexes, $(>FeOH)_2UO_2(H_2O)_3$, $>FeOCO_2UO_2$, and $(>FeOH)_2UO_2CO_3$. Using these complexes, we fit our batch sorption experiments to a surface complexation models for U on goethite and ferrihydrite with a 1pK model for surface protonation, an extended Stern model for surface electrostatics and inclusion of all known UO_2-OH-CO_3 aqueous complexes in the current thermodynamic database. The models give an excellent fit to our sorption experiments done in both ambient and reduced CO_2 environments at surface loadings of 0.02-2.0 wt. % U. We find that we can model the EXAFS and batch sorption experiments of U(VI) on birnessite as an inner-sphere $(>Mn_2O)_3UO_2^{++}$ and $(>Mn_2O)_3UO_2CO_3$ complexes over vacancy sites. In the

environment, U(VI) and its carbonate complexes will be preferentially sorbed by iron(III) (hydr)oxides over manganese(IV) oxides.

Differential equations of a U-Ra-Pb system accounting for a diffusion of components

I.S. Brandt, S.V. Rasskasov and S.B. Brandt

Institute of the Earth Crust, RAS, 664033 Irkutsk, Russia,e-mail: bra@crust.irk.ru

Abstract. Decay series are considered in textbooks on isotopy. Here we bring solutions of equations for a process dissipated in space, which is characteristic for contamination.. As to our knowledge, the differential equations below are original and were never published.

If the isotope of the first substance has a concentration N_1 and decays into an isotope of the second substance with a concentration N_2 and the second substance decays finally into a third substance with a concentration N_3 assuming a diffusion of components as possible then a one-dimensional model would be completely determined by a system of differential equations

$$\frac{\partial N_1}{\partial t} = D_1 \frac{\partial^2 N_1}{\partial x^2} - \lambda_1 N_1$$

$$\frac{\partial N_2}{\partial t} = D_2 \frac{\partial^2 N_2}{\partial x^2} - \lambda_2 N_2 + \lambda_1 N_1 \qquad (1)$$

$$\frac{\partial N_3}{\partial t} = D_3 \frac{\partial^2 N_3}{\partial x^2} + \lambda_2 N$$

This situation is realized in a system **U-Ra-Pb,** with

$$N_1 = {}^{238}U$$
$$N_2 = Ra$$
$$N_3 = {}^{206}Pb$$
$$D_1 = D_3 = 0$$

Only Ra *is* suggested as diffusing and the following differential equation becomes valid (due to a small lifetime of ***Ra*** the system fast reaches a stationary regime):

$$D_2 \frac{\partial^2 Ra}{\partial x^2} - \lambda_2 Ra + \lambda_1 {}^{238}U = 0 \qquad (2)$$

-h/2<x<h/2

Solving this equation we obtain a formula for the ***Ra***-concentration

$$Ra = \frac{\frac{-\lambda_1}{\lambda_2} {}^{238..}U}{ch\frac{h}{2}\sqrt{\frac{\lambda_{..2}}{D_{.2}}}} chx\sqrt{\frac{\lambda_2}{D_2}} + \frac{\lambda_1}{\lambda_2} {}^{238}U \qquad (3)$$

A coefficient of Ra losses is obtained if we determine the derivative of ***Ra*** at the boundary and multiply it by D_2

$$k = \frac{2}{h}(th\frac{h}{2}\sqrt{\frac{\lambda_2}{D_2}})\sqrt{\frac{D_2}{\lambda_2}} \qquad (4)$$

Or, in a more conveniant form

$$a = 2\sqrt{\frac{D_2}{h^2\lambda_2}} \qquad k = ath\frac{1}{a}$$

For the Pb-concentration the following formula is obtained.

$$^{206}Pb = {}^{238}U_0(1-e^{\lambda_1 t})\left(1-\frac{ch\frac{2x}{ha}}{ch\frac{1}{a}}\right) \quad (5)$$

The total quantity of residual ***Pb*** is given by

$$Pb=U_0(1-\exp\lambda_1 t)(1-k) \quad (6)$$

Where k is given by (4).

These formula can be used for estimates of dissipated unfavorable quantities of the ***U-Ra-Pb*** system.


Uranium Mining
and Hydrogeology

The use of kinetic modeling as a tool in the understanding of the geochemical processes at a uranium mine site

Mariza Franklin[1] and Horst Monken Fernandes[2]

[1]Institute of Radiation Protection and Dosimetry, Av Salvador Allende S/N – Recreio, Rio de Janeiro, Brazil.
[2] International Atomic Energy Agency, Wagramer Strasse 5, A-1400 Vienna, Austria

Abstract. Release of acid drainage from mining-waste disposal areas is a problem found in many mine sites all around the world. An understanding of waster flow and the geochemical processes within mining-waste is important to the long-term prediction of contaminant loading to the environment. This is the second of two papers and describes how useful it is the use of kinetic models in the evaluation of the geochemical processes in one of the waste rock piles of the first uranium-mining site in Brazil. The model chosen (STEADYQL v.4) predicts the steady-state composition of the drainage resulting from the interactions between the aqueous and solid phases being this interaction subjected to a combination of kinetic and equilibrium reactions (homogeneous and heterogeneous). The obtained results show that the concentrations of SO_4, K e F were underestimated by 2%, 13% e 5% respectively if compared to the average concentrations of these elements in the drainage waters. On the other hand Al concentrations were overestimated by in 19%. The model was not able to reproduce the concentrations of U and Fe satisfactorily. But, in a general way it can be affirmed that the simulations allow a coherent representation of the monitored conditions within the waste rock pile.

Introduction

Acid Mine Drainage (AMD) represents a significant environmental and financial liability for the mining industry (Sracek et al. 2004). It is happen when sulphide minerals (mainly pyrite) contained in mine waste are exposed and reacts with oxygen from the air and water to form sulfuric acid and dissolved iron. These minerals are not in equilibrium with the oxidizing environment and almost immediately begin weathering and mineral transformations. The reactions are analogous to "geologic weathering" which takes place over extended periods of time (i.e., hundreds to thousands of years) but the rates of reaction are orders of magnitude greater than in "natural" weathering systems. In the case of the first uranium production center in Brazil It was estimated that acid drainage generation will last for 600 and 200 years from waste rock piles and tailings dam, respectively (Fernandes and Franklin 2001). Due to the long timescale involved in these processes permanent solutions should be preferable to having to collect, treat, and discharge mine water, as it is done today by the operator of the mine. Our study focus on generation of AMD from one of the waste rock piles (WRP-4) of the Brazilian uranium mine site. It has been estimated that about US$ 200,000 are spent annually to treat the acid waters originated only from the waste-rock piles (Fernandes and Franklin 2001).

The environmental impact of this mine site can be reduced if the risks associated with sulphidic mine waste are managed adequately. Mainly in the current phase of the mine site (decommissioning phase) where effective remediation strategies will be chosen for will be put in place.

The chemical composition of the acid drainage is controlled by the pyrite oxidation rate, which is a function of temperature, pH, oxygen concentration, composition and amount of infiltrating water and the population of micro-organisms (Ritchie 1994). For long-term predictions, the rate of oxygen influx from the ground surface is therefore a controlling factor (Cathles and Apps 1975). The oxygen can be transported through diffusion in the gas phase, and by thermal or wind-induced convective transport (Lefebvre et al. 2001). Diffusive transport tends to be the dominant gas transport mechanism in large waste rock piles (Ritchie 1994). As the diffusion rate of oxygen in water is several order of magnitude less than in air, the rate of oxygen diffusion will vary throughout the pile depending on the local water content (Molson et al. 2005).

AMD production in waste rock piles take place in multiphase systems and involves numerous coupled geochemical and transfer processes, the interplay of the processes is difficult to understand and quantify (Morin et al. 1991, Lefebvre et al. 2001). Most of the waste rock geochemical studies analyze the chemical composition of drainage water at the toe of the waste rock pile. However, this information does not provide a clear picture of geochemical processes within the pile (Ritchie, 1994). On the other hand, it has been recognized that the obtaining of the data on water chemistry within the unsaturated zone of waste rock pile is technically difficult because of low water content and correspondingly high suction values (Ritchie, 1994).

Geochemical reactions in the unsaturated zone (as waste rock piles) occur primarily at the interfaces between the solid, air and aqueous phases; the rates at which these reactions occur are controlled by the transport (or trapping) of constituents to and across the interfaces. Rate controlling mechanisms are important since they determine the rate at which the various mass transfer processes proceed. The more important geochemical processes that are expected to control the rates of AMD inside the WRP-4 are precipitation/dissolution, chemical diffusion and superficial chemical reactions. One key reaction causing AMD should be pyrite oxidative dissolution.

Geochemical model techniques can provide valuable understanding of the geochemical processes leading to the production of AMD in waste rock piles. However, in function of the geochemical reactions involved in this system be dominated by kinetic processes, the use of equilibrium codes can take to unreal results. The STEADYQL code (Furrer et al. 1989, 1990) was chosen because it combines kinetic with equilibrium processes and it has been used widely to assess AMD starting from mine wastes (Stromberg and Banwart 1994, Brown and Lowson, 1997).

The purpose of this paper will be to show the successful application of a kinetic model to assessing the potential release of contaminants from the waste rock pile of the first uranium mine in Brazil.

Study Area

The studied waste-rock pile is part of the uranium mine and mill site located on the Poços de Caldas plateau, in the southeast region of Brazil. The alkaline complex corresponds to a circular volcanic structure formation of which began in the upper Cretaceous (87 ma) and evolved in successive steps until 60 ma. This intrusion is rounded by the leveling of bed rocks, consisting of granites and gneisses. These rocks are frequently cut by diabase dykes, amphibolites and gneisses. These igneous-policyclic activities, of alkaline nature, associated to intense metassomatic processes and a strong weathering, gave rise to a variety of rock types belonging to the Nepheline-Syenite family and to uranium mineralization.

The mining and milling facilities began commercial operation in 1982. After 13 years of intermittent operation, the mining activities were suspended definitively in 1995. The cumulative uranium production was 1,242 tons of U_3O_8. In the development of the mine 44.8 x 10^6 m^3 of rocks were removed. From this amount, 10 million tons were used as building material (roads, ponds, etc). The rest was disposed into two major rock piles, waste rock pile 8 (WRP-8) and 4 (WRP-4). Both piles are located at areas close to the mine pit. The WRP-4 was chosen as a study object because almost all the drainage coming from the pile is collected in only one holding pond, facilitating mass balance calculations. It is to be mentioned that a huge database from monitoring program carried out by the mine operator is available.

Geochemical Characterization of the Pile

The strategy of the inverse modelling developed by Plummer et al. (1983) and Plummer (1984) was used to characterize the principal geochemical processes that occur inside of the WRP-4, and to calculate the distribution of the chemical species in the drainages of the pile. The geochemical model of mass balance PHREEQC v.2 (Parkhust, 1995) was used to accomplish the inverse modeling and the speciation calculations. These calculations were based on data obtained from environmental and effluent monitoring programs conducted by the operator of the mine.

The inverse modeling revealed the sequence of important geochemical processes in WRP-4. The dominant processes in WRP-4 are: K-feldspar and albite dissolution, kaolinite dissolution, pyrite oxidation, barite solubility equilibrations, silica precipitation, goethite precipitation, manganese oxide dissolution, and fluorite and calcite dissolution. The result from inverse modeling is shown in table 1.

The speciation calculations were made to determine the distribution of the species, the saturation indexes, and redox potential. Aluminium species occur mainly in the form of fluoride. The iron almost all occur as Fe+2 (99,92%), being the occurrence of Fe+3 about of (0,08%). That is explained by the acidic pH value of the drainage waters. Fe+2 occurs fundamentally as a free species (~70%) followed for the ferrous sulphate. On the other hand, Fe+3 occurs fundamentally as sulphate. The uranium due to the redox potential of the solution occurs in its oxidized form (U+6) distributed basically between two species: uranila sulphate and free uranila. The potassium and the barium occur almost totally as free species. The calcium occurs mainly as free species followed by sulphates species.

Table 1. Mass balance and mass transfer results computed with the model. Values are in mol/kg of substance dissolved (positive) or precipitated (negative values)

Phase		Mole transfer (mol/kg)
K-Feldspar	$KAlSi_3O_8$	1.56×10^{-1}
Kaolinite	$Al2Si_2O_5(OH)_4$	2.06
Fluorite	CaF_2	2.09
Barite	$BaSO_4$	-3.2×10^{-3}
UO2	UO_2	2.74×10^{-2}
O2(g)	O2	21.0
Goethite	FeOOH	-5.80
Quartz	SiO_2	-4.01
MnO2	MnO_2	1.33
Pyrite	FeS_2	5.81
Redox mole transfer		
	Fe(2)	5.78×10^{-3}
	S(-2)	1.16×10^{-2}
	U(4)	2.74×10^{-5}

Conceptual model of the WRP-4

For the WRP-4 geochemical system, the assumption of local equilibrium is not fulfilled and a kinetic description is necessary. Based on this the conceptual model for the geochemical system of WRP-4 was based on equilibrium and kinetic reactions. The reactive system was completely defined by specifying chemical reactions and accounting the total number of chemical species involved in the reactions. Standard equilibrium expressions (with suitable equilibrium constants) were used to represent all fast reactions, such as the aqueous complexation and precipitation of secondary phases. The slow reactions were represented by kinetic expressions and associated rate constants to address the dissolution reactions of key minerals present in the pile, including Fe+2 oxygenation. The reaction network that describes the evolution of the geochemical system is defined in table 2.

All dissolution reactions require an estimate of the surface area of the minerals involved in the reactions. Values for mineral surface areas were derived using the methodology proposed in (Strömberg and Banwart1994), i.e. the surface area of an individual mineral was determined based on the assumption that its contribution to the surface area of the rock is proportional to its relative volume in the rock. The average measured physical surface area of the waste rock was approximately constant per volume of rock and independent of the particle size distribution (i.e. 1 ± 0.4 m^2/g) (Strömberg and Banwart1994). A surface area of 9.09×10^5 m^2 per m^{-3} for WRP-4 was estimated using average values of porosity (45%) and specific density (2.02 g/cm^3). The resulting value is in agreement with other estimates for waste-rock material (Strömberg and Banwart1994) and (Linklater et al. 2005).

Simulation of the WRP-4

The initial chemical composition of the rainfall that infiltrated WRP-4 was assumed to be mildly acid water and a concentration 6.3×10^{-6}M $[H^+]$ and $[SO_4^{2-}]$ was used. This relatively simple approach was considered adequate to model the overall behavior of the waste pile, and to calculate the long-term evolution of seepage effluent compositions.

Table 2. The reaction network used in STEADYQL. (a) Kinetic reactions and rate expressions, (b) Equilibrium reactions and their equilibrium constant.

(a) SLOW REACTION – (KINETIC EXPRESSIONS AND ASSOCIATED RATE CONSTANT)	
Reaction and Empirical Rate Law	
The mineral dissolution	
$Al(OH)_3$ (Gibbsite) + $3H^+ \leftrightarrow Al^{+3} + 3H_2O$	
R=-SA×[3.07×10^{-10}×[H^+]$^{0.992}$	[a]
Fe_2O_3(Hematite) + $6H^+ \leftrightarrow 2Fe^{+3} + 3H_2O$	
R=-SA×[6.33×10^{-12}×[H^+]^1	[a]
Fe_3O_4 (Magnetita) + $8H^+ \leftrightarrow Fe^{+2} + 2Fe^{+3} + 4H_2O$	
R=-SA×[2.91×10^{-11}×[H^+]$^{0.279}$	[a]
FeS_2 (Pyrite) + $8H_2O$ + $14Fe^{+3} \leftrightarrow 15Fe^{+2} + 2\,SO_4^{-2} + 16H^+$	
R=-SA×(2.56×10^{-8})×[Fe^{+3}]$^{0.93}$×[Fe^{+2}]$^{-0.40}$	[b]
$2FeS_2$ (Pyrite) + $7O_2$ (gas) + $2H_2O \leftrightarrow 2Fe^{+2} + 4H^+ + 4SO_4^{-2}$	
R=-S_{max}	[c]
$2FeS_2$ (Pyrite) + $7/2O_2$ (aq) + $H_2O \leftrightarrow Fe^{+2} + 2H^+ + 2\,SO_4^{-2}$	
R=-SA×(1.94×10^{-10})×{[O_2(aq)]$^{0.5}$×[H^+]$^{-0.11}$}	[b]
UO_2 (uraninita) $\leftrightarrow U^{+4} + 2H_2O$ - $4H^+$	
R=-SA×[1.30×10^{-10}]	[a]
$Al_2Si_2O_5(OH)_4$ (Kaolinite) + $6H^+ \leftrightarrow 2Al^{+3} + H_4SiO_4 + H_2O$	
R=-SA× [7.59×10^{-14}×[H^+]$^{0.777}$	[a]
$KAlSi_3O_8$ (K-feldspar) + $8H_2O \leftrightarrow K^+ + Al(OH)_4^- + 3H_4SiO_4$	
R=-SA× [1.23×10^{-12}×[H^+]$^{0.5}$	[a]
CaF_2 (Fluorite) $\leftrightarrow Ca^{+2} + 2F^-$	
R=-SA×[1.18×10^{-9}×[H^+]^1	[a]
$KAl_3Si_3O_{10}(OH)_2$ (Muscovite) + $10H^+ \leftrightarrow K^+ + 3Al^{+3} + 3\,H_4SiO_4$	
R=-SA×[1.63×10^{-14}×[H^+]$^{0.37}$	[a]
Fe^{+2} oxygenation	
$Fe^{2+} + 1/4O_2$(aq) + H^+ - $1/2H_2O \leftrightarrow Fe^{3+}$	
R=(9.63×10^{-8})× [Fe^{+2}]×[O_2(aq)]	[d]

(b) FAST REACTIONS – (EQUILIBRIUM EXPRESS WITH EQUILIBRIUM CONSTANT)	
Reaction	**Reaction Co**
Aqueous Complexation Reactions	
H_2O(aq) $\leftrightarrow H^+ + OH^-$	$Log_{10}K$ = -1
$Al^{+3} + F^- \leftrightarrow AlF^{+2}$	$Log_{10}K$ = 7.8
$Al^{+3} + 2F^{-1} \leftrightarrow AlF_2^+$	$Log_{10}K$ = 12
$Al^{+3} + SO_4^{-2} \leftrightarrow AlSO_4^+$	$Log_{10}K$ = 3.9
$Al^{+3} + 2SO_4^{-2} \leftrightarrow Al(SO_4)_2^-$	$Log_{10}K$ = 5.9
$Al^{+3} + 3F^- \leftrightarrow AlF_3$(aq)	$Log_{10}K$ = 16
$Ca^{+2} + SO_4^{-2} \leftrightarrow CaSO_4$(aq)	$Log_{10}K$= 2.3
$Fe^{+2} + SO_4^{-2} \leftrightarrow FeSO_4$(aq)	$Log_{10}K$ = 2.2
$Fe^{+3} + SO_4^{-2} \leftrightarrow FeSO_4^+$	$Log_{10}K$ = 4.2
$Fe^{+3} + F^- \leftrightarrow FeF^{+2}$	$Log_{10}K$ = 6.2
$Fe^{+3} + 2SO_4^{-2} \leftrightarrow Fe(SO_4)_2^-$	$Log_{10}K$ = 5.3
$Fe^{+3} + H_2O - H^+ \leftrightarrow FeOH^{+2}$	$Log_{10}K$ = -2.
$K^+ + SO_4^{-2} \leftrightarrow KSO_4^-$	$Log_{10}K$ = 0.8
$H^+ + SO_4^{-2} \leftrightarrow HSO_4^-$	$Log_{10}K$ = 1.9
$UO_2^{+2} + SO_4^{-2} \leftrightarrow UO_2SO_4$	$Log_{10}K$ = 3.1
$UO_2^{+2} + 2SO_4^{-2} \leftrightarrow UO_2(SO_4)_2^{-2}$	$Log_{10}K$ = 4.1
$UO_2^{+2} + F^- \leftrightarrow UO_2F^+$	$Log_{10}K$ = 5.0
SiO_2(Silica) + $2H_2O \leftrightarrow H_4SiO_4$	$Log_{10}K$ = -2.
Precipitation of secondary phases	
$Ba^{+2} + SO_4^{-2} \leftrightarrow BaSO_4$ (Barite)	$Log_{10}K$ = 9.9
$Fe^{+3} + 2H_2O$ - $3H^+ \leftrightarrow$ FeOOH (Goethite)	$Log_{10}K$ = 1.0

Notes: SA is the reactive surface area of the mineral concerned (m^2 per m^3 media); [ ] denotes a concentration in units of mol per dm^3 of water, and S_{max}= the maximum reaction rate. Sulfide oxidation was assumed to be the only process consuming significant amounts of O_2 so that the measured O_2 consumption rates can be used to determine the sulfide oxidation rates The S_{max} value used in the simulation was 2.00×10^{-6}Kg(S) $m^{-3}.d^{-1}$. [a] Palandri and Kharaka 2004; [b] Williamson and Rimstidt 1994; [c]Fernandes and Franklin, 2001; [d] Wehrli, 1990. The thermodynamic data base was based on Hummel et al. (2002).

Table 3. Estimated and measured concentrations of chemical species in the WRP-4 drainage.

Species	*Estimated (mg/L)*	*Measured (mg/L)*
SO_4^{-2}	1018.99	1039.47
Al	138.55	117.05
U	14.95	6.51
F	95.43	99.56
Fe	16.99	1.78
K	7.16	8.07
pH	3.49	3.03

Results and Discussions

The equilibrium speciation model and the stoichiometry and rate laws for slow kinetic processes are given in table 2. The choice of the components (equilibrium reactions) and the kinetic processes were based on composition of the outflow of the pile and the results of the inverse modeling described previously.

The inflow corresponds to the annual average precipitation at the site, and with an assumed corresponding acid deposition load.

Most of the rates of mineral dissolution used in our study were based on compilation of rate parameters published by USGS (Palandri and Kharaka 2004). Once the mechanism of pyrite oxidation is a key aspect in the generation of AMD, we opted to use in the simulations the three different mechanisms of pyrite oxidation (pyrite being oxidized by O_2aq, O_2 gas and Fe+3). We use the rates law suggested by Williamson and Rimstidt (1994), which determined the pyrite oxidation by the ferric Iron (Fe+3) in the presence of oxygen (situation found in the field) and by the dissolved oxygen (O_2aq). To describe the rate of pyrite oxidation by O_2 gas, we used the rate measured in laboratory with material of the pile suggested by Fernandes and Franklin (2001).

The reactive surface area of the WRP-4 was treated as a dependent variable. This means that it was used as calibration parameter to arrive at a chemical composition of the drainage that corresponds to site measurements. We assumed that 0.6% of the surface area of all minerals was reactive. The same strategy was adopted for by Strömberg and Banwart 1994 and Linklater et al. 2005.

Rates constants (k) were corrected with the Arrhenius expression to estimated average pile temperature of 30^{o}C, except for pyrite oxidation. The rate constant k for the oxidation of pyrite by O_2aq and Fe+3 was corrected to 40^{o}C, but not the k for oxidation by O_2 gas since this parameter was measured in the laboratory.

Table 3 shows the comparison of the chemical composition of the drainage as measured at the site and estimated with the model.

The results show that the relative rates of sulphide mineral and alkalinity production from the dissolution of primary silicate minerals were simulated reasonably well with the model. Differences between the measured and estimated values for the pH never exceeded 15%.

The estimated equilibrium concentrations for SO_4, Al, K and F were very close to those we actually observed. These results suggest that the dissolution of primary minerals that compose the waste rock was well simulated with the model. The production of K and Al was mainly controlled by K-feldspar dissolution and to a lesser extent by kaolinite and muscovite dissolution. The production of F furthermore resulted from the dissolution of fluorite. If we assume that all sulphate concentration is due to pyrite oxidation, it would be possible to verify that the key processes of AMD generation were also well described. However, the model overestimated the U concentrations by a factor of 2.3, and the Fe concentration by one order of magnitude. Similar results for Fe were observed by Strömberg and Banwart (1994). The author explained the results by the fact that the overall rate of ferrous iron oxidation within the pile was much faster than that given by abiotic kinetics (as used in the modeling). The oxidation of Fe^{+2} by bacteria (biotic oxidation) hence should be considered in the simulation. Calculated U concentrations show a need to recalculate the adopted parameters. For example, the rate constant used in the simulation was determined experimentally under neutral conditions. Since the pH of the drainage water from the pile was approximately 3, this parameter should be corrected for acid conditions.

The initial chemical composition of the rainfall that infiltrated WRP-4 was assumed to be mildly acid water and a concentration 6.3×10^{-6}M $[H^+]$ and $[SO_4^{2-}]$ was used. This relatively simple approach was considered adequate to model the overall behavior of the waste pile, and to calculate the long-term evolution of seepage effluent compositions.

Conclusion

The obtained results suggest that the dissolution of the principal minerals presents in the composition of the waste rock were well represented by the model, i.e. the dissolution of K-feldspar, that supports the production of K and Al; the dissolution of the fluorite, that supports the production of F; and, the oxidative dissolution of pyrite, that supports the sulphate concentration (the key process in the AMD generation). However, the model was not able to reproduce the concentrations of U and Fe satisfactorily. In the case of uranium this was due to a lack of information regarding the dissolution rate applicable to the simulation conditions. In the case of Fe that was due to the fact that only abiotic process was taken into account.

In a general way it can be affirmed that the kinetic model STEADYQL was successfully used to reproduce measured data for WRP-4. This suggests that the most important geochemical processes (the network of reactions accounting for both equilibrium and kinetic processes) at the site were properly considered in the model.

However, it should be emphasized that the phenomenon of AMD can be adequately simulated only by coupling variably-saturated water flow with the most relevant geochemical processes. The approach used in our study (explored in two different papers of this conference) allowed considerable insight in the processes controlling ARD generation and will serve as an initial step to the application of more realistic coupled models.

References

Brown, P. L., Lowson, R. T. (1997), The use of kinetic modeling as a tool in the assessment of contaminant release during rehabilitation of a uranium mine. Journal of Contaminant Hydrology, v.26, pp. 27–34.

Cathles, L. M. e Apps, J. A. (1975) A model of the dump leaching process that incorporates oxygen balance, heat balance, and air convection. Metallurgical Transaction B, v. 6b, pp. 617-624.

Hummel W., Berner, U., Curti, E., Pearson, F.J. Thoenen, T. (2002).The Nagra/PSI Chemical Thermodynamic Data Base 01/01. Paul Scherrer Institut (PSI/SNL).

Fernandes, H.M., Franklin, M.R. (2001) Assessment of acid rock drainage pollutants release in the uranium mining site of Poços de Caldas – Brazil. *J. of Environmental radioactivity*, 54, 5 – 25.

Furrer, G. and Westall, J. (1989) The Study of soil chemistry through quasi-steady-state models: I. Mathematical definition of the model. *Geochimica et Cosmochimica Acta.* 53, 595 - 601.

Furrer, G., Sollins, P., Westall, J.C. (1990) The Study of Soil Chemistry through Quasi-Steady-State Models: II. Acidity of Soil Solution. Geochimica Cosmochimica Acta. Vol 54, pp. 2263 - 2374.

Linklater, C.M., Sinclair, D.J., Brown, P.L. (2005) Coupled chemistry and transport modeling of sulphidic waste rock dumps at the Aitik mine site, Sweden. *Appl. Geochem*. 20, 275– 293.

Lefebvre R., Hockley D., Smolensky J., Gélinas P. (2001) Multiphase transfer processes in waste rock piles producing acid mine drainage 1 : conceptual model and system characterization. J Contam. Hydrol. 52, 137-164.

Molson, J. W.; Fala, O.; Aubertin, M. E Bussiere, B. (2005) Numerical simulations of pyrite oxidation and acid mine drainage in unsaturated waste rock piles. J Contam. Hydrol, v.78, n.4, pp. 343-371.

Morin, K. A., Gerencher, E., Jones, C. E., Konasewich, D.E. (1991) Critical literature review of acid drainage from waste rock. Prepared for CANMET, Department of Energy, Mines and Research Canada under MEND (NEDEM) Project No. 1.11.1, 175p.

Palandri, J.L., Kharaka, Y.K. (2004) A Compilation of Rate Parameters of Water-Mineral Interaction Kinetics for Application to Geochemical Modeling, USGS Open File Report 2004-1068. Menlo Park, California, 64p.

Parkhurst, D.L. (1995) User's Guide to PHREEQC--A Computer Program for Speciation, Reaction-Path, Advective Transport and Inverse Geochemical Calculations, U.S. Geological Survey Water-Resources Investigations Report 95-4227, 143 p.

Plummer, L.N., Parkhurst, D.L., Thorstenson, D.C. (1983) Development of reaction models for groundwater systems. *Geochim. Cosmochim. Acta*. 47, 665-686pp

Plummer, L. N. (1984) Geochemical Modeling: A comparison of forward and inverse methods. In: Proceedings First Canadian/American Conference on Hydrogeology, Practical applications of ground water geochemistry. National Water Well Association, Worthington, Ohio, pp. 149-177

Ritchie, A. I. M. (1994) Sulfide oxidation mechanisms: Controls and rates of oxygen tranport. In: Environmental geochemistry of sulphide mine wastes - Short Course Handbook.vol. 22, Jambor, J. L. and Blowes, D. W. (Ed.), Min Soc, Canada, pp.201–244.

Sracek, O.; Choquette, M.; Gelinas, P.; Lefebvre, R., Nicholson, R. V. (2004) Geochemical characterization of acid mine drainage from a waste rock pile, Mine Doyon, Quebec, Canada. Journal of Contaminant Hydrology, v.69, n.1-2, pp. 45-71.

Strömberg B., Banwart S. (1994) Kinetic modelling of geochemical processes at the Aitik mining waste rock site in northern Sweden. *Appl.Geochem*., 9,583 –595.

Williamson M.A., Rimstidt J.D. (1994) The kinetics and electrochemical rate-determining step of aqueous pyrite oxidation. *Geochim. Cosmochim. Acta* 58, 5443-5454.

Wehrli, B. (1990) Redox reactions of metal ions at mineral surfaces. In W. Stumm (ed.) Aquatic Chemical Kinetics; Reaction Rates of Processes in Natural Waters. Chapter 11, pp. 311-336. John Wiley & Sons. (Interscience).

Origin and oxidation processes of the Oklo uranium ore, Gabon: Reactive transport modelling

Joaquin Salas[1], Carlos Ayora[2] and Jesus Carreras[2]

[1]AmphosXXI Consulting S.L., Passeig de Rubí 29-31, E08197 Valldoreix, Barcelona (Spain), e-mail: Joaquin.Salas@amphos21.com
[2]Institute of Earth Sciences "Jaume Almera" (CSIC), Lluís Solé i Sabarís s/n. E08028 Barcelona, (Spain).

Abstract. In 1972, a series of isotopic anomalies was discovered in uranium samples originating in the Oklo mine district, Gabon. The only explanation was the natural fission of the isotope ^{235}U during the Paleoproterozoic, about $2 \cdot 10^9$ years ago. This hypothesis has been corroborated with geochemical and petrographical evidences. As a consequence of the fissiogenic products preservation, the deposits have been intensely studied as a natural analogue of a nuclear waste disposal site.

Previous studies have described the geological environment and some mineralogical and geochemical aspects of the Oklo site. However, the genetic processes have not been strictly treated; topics as the uranium source or the hydrologic mechanisms have not been numerically studied. In this way, the objective of this work is to verify the feasibility of the conceptual mechanisms proposed by different authors and to propose our own theory by means of a 3D-model (Fig. 1). The overall goal of this study has been to advance our understanding of the uranium ore formation through numerical modelling of coupled groundwater flow, heat transport and reactive solute transport. Other specific research questions have been evaluated, as the factors lead to the observed location of the uranium deposits and other mineral paragenesis.

The Okélobondo uranium deposit is part of the Oklo district. Actually, it is located at a depth of about 300 m, and is affected by oxidation and dissolution of urani-

nite. The presence of oxidising conditions at depth is unusual and, if repeated elsewhere, may affect the stability of uranium oxide under repository conditions. Therefore, it is important to determine whether the processes leading to this situation are specific of Okélobondo or they might represent a common phenomenon. In order to identify the geochemical processes which control the water composition, reactive transport modelling has been applied. The high Mn/Fe ratio and the high pH-Eh values of the water sampled in the lower part of the Okélobondo system are attributed to the interaction of the recharge with rhodochrosite and manganite deposits. Three key factors have been identified to obtain the chemistry of this water: a fast dissolution of a Mn-phase, a slower dissolution of a Fe-phase and a continuous source of alkalinity. However, in spite of the presence of Mn-carbonate deposits is uncommon in the Earth surface, it is necessary evaluate its abundance and distribution in the recharge area of hydrological systems, when evaluating the location of a nuclear waste repository.

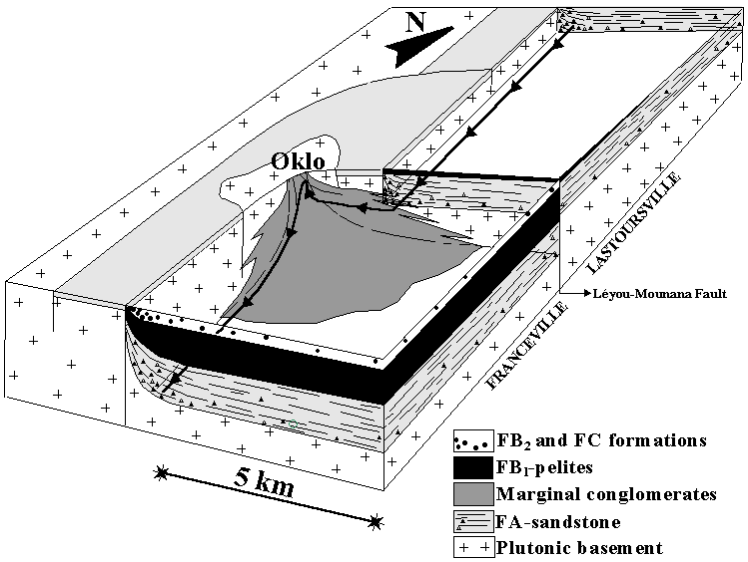

Fig.1. Geological schema of the basal Francevilian formations in the Oklo area. With a black line, the trace of the modelled streamline has been rebounded.

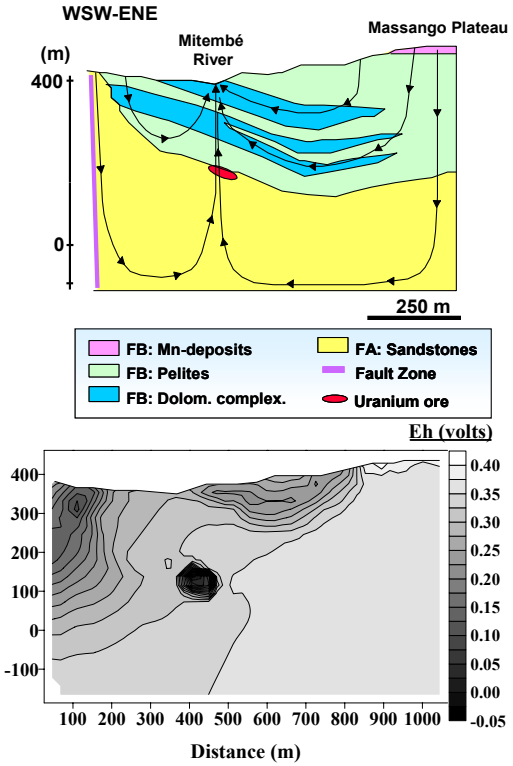

Fig.2. Geological schema and local groundwater flow system around of the Okélobondo area. Calculated redox distribution affecting the uranium ore, at a depth of 300 m.


Uranium Mining
and Hydrogeology

Study of uranium sorption by bentonite

V. M. Kadoshnikov, B. P. Zlobenko and S. P. Bugera

Institute of Environmental Geochemistry, National Academy of Sciences and Ministry for Emergency Situations of Ukraine (Kyiv, Ukraine).

Abstract. The concept of geological disposal in Ukraine is similar to that considered in other countries, being based on a system of multiple barriers consisting of the geological environment and the EBS. Bentonite clays are considered an important component for EBS due to properties: a marked swelling and the high sorption characteristics. Since uranium is an important nuclide in the radioactive waste management, the prediction of its sorption behavior is one of the major tasks in safety assessments. The aim of this study is to analyze the differences in sorption behavior of uranium onto bentonite clays.

Uranium sorption was studied on bentonite clay from Cherkasy deposit of bentonite and *palygorscite* clays (Ukraine). Sorption investigation was carried under medium pH equal 2.0 and 8.0 and ionic force of disperse medium $Ca(ClO_4)_2$ – $10^{-3} \div 10^{-1}$ M/l, and under uranium concentration up to 10^{-4} M/l.

Analysis of obtained sorption isotherms showed that under uranium concentration in the equilibrium solution below 10^{-5} M/l its sorption by bentonite has linear character and can be described by Freundlich isotherm. But under higher concentrations uranium sorbtion sharply increases and cannot be further described neither Freundlich equation nor *Lengmore* one.

Tacking into account, that in electrolyte solution negatively charged clay particles have double electrical layer, analogous to liophobic colloids, we suppose that sorption of uranium ob bentonite clay in electrolyte-containing medium and under low uranium concentrations (up to 10^{-5} M/l) is determined by processes of nucleophilic exchange of positively charged uranium ions with ions of clay particle dif-

fuse layer. When the uranium concentration in disperse medium is higher than 10^{-5} M/l, increased uranium sorption by clay is determined, possibly, by partial changes in structure and composition of clay particle anti-ion layer due to introduction in this layer of positively charged uranium complexes. In this case uranium-clay bonding occurs not only due to electrovalence interaction of positively charged uranium ions with negatively charged centers, which are located on the surface of clay particles, but also due to formation of complex coordination bonds between uranium and active centers of clay matrix.

Index